THE JOURNAL
OF
CHEMICAL PHYSICS

VOLUME 33, NUMBER 5 NOVEMBER, 1960

This issue of The Journal of Chemical Physics is in honor of John Gamble Kirkwood

John Gamble Kirkwood 1907–1959

GEORGE SCATCHARD

Department of Chemistry, Massachusetts Institute of Technology, Cambridge 39, Massachusetts

JOHN Gamble Kirkwood was born in Gatebo, Oklahoma, on May 30, 1907. Two years later his parents moved to Wichita, Kansas, where he obtained his education through the third year of high school. While visiting in California in the summer of 1923, he became much interested in the California Institute of Technology. On the advice of A. A. Noyes, he skipped the senior year of high school and entered the Institute that fall. After two years, apparently as a compromise between his ideas and his father's as to what a boy should get out of college, he transferred to the University of Chicago, from which he graduated with the degree S.B. in December, 1926. From February, 1927 to June, 1929 he was a graduate student at the Massachusetts Institute of Technology. His Ph.D. research was directed by Frederick G. Keyes.

In 1929–30, Kirkwood was National Research Fellow with Keyes at MIT and with Slater at Harvard. In 1931–32, he was International Research Fellow with Debye in Leipzig and with Sommerfeld in Munich. In 1930–31 and 1932–34, he was Research Associate at MIT. He married the former Miss Gladys Danielson in 1930; their son, John Millard Kirkwood, was born in 1935; they were divorced in 1951. He became Assistant Professor at Cornell University in 1934 and Associate Professor at Chicago in 1937. He returned to Cornell as Todd Professor of Chemistry in 1938, and went to California Institute of Technology as Arthur A. Noyes Professor in 1947. In 1951 he became Sterling Professor of Chemistry and Head of the Department of Chemistry at Yale University. In 1956 he also became Director of Science of the University. In 1958 he married the former Miss Platonia Kaldes. He was Visiting Professor at Princeton in 1946 and was Visiting Professor at Chicago and Lorentz Visiting Professor at Leiden in 1959. He was Chairman of the Division of Physical and Inorganic Chemistry and Vice President of the American Chemical Society in 1940–41, and Foreign Secretary of the National Academy of Sciences, 1955–58. He was associate editor of many scientific journals, and scientific consultant to several industrial companies and many government laboratories and offices, and a member of several committees. He died of cancer on August 9, 1959.

Kirkwood received the American Chemical Society Award in Pure Chemistry, at that time called the Langmuir Prize, in 1936, the Theodore William Richards Medal of the Northeastern Section of the American Chemical Society in 1950, and the Gilbert Newton Lewis Medal of the California Section in 1953. He received a Meritorious Civilian Service Award in 1945 from the U.S. Navy and a Presidential Certificate of Appreciation in 1947. He received the Honorary Doctor of Science Degree from Chicago University in 1954 and from the Free University in Brussels in 1959.

More than a hundred sixty journal articles have appeared with Kirkwood as author or coauthor. They will not be listed here because there is not enough space,

Copyright © 1960 by the American Institute of Physics

because more papers are still appearing, and because the number of papers to which he has contributed greatly is much larger than the number which carry his name. It is important to note that there are sixty-four coauthors, mostly younger men who had received a part of their education from him.

There are many who might have written this biographical sketch and up to this point the sketches would all have been nearly the same. For the rest they should be very different, for none of us can cover Kirkwood's whole career more than superficially. This sketch will concentrate on the part I know best. He was my student in a course entitled "Solutions," but the fifteen years difference in our ages was forgotten by both of us before we wrote our joint paper two years later. I introduced him to Edwin Cohn and to Debye. Our joint paper in 1932 was Kirkwood's first venture in liquids, in solutions, in electrolytes, and in proteins. It was also the first case in which he used his special skills to solve a problem which was baffling another worker; and it started a train which determined the direction of much of his work.

There is a distinct pattern in Kirkwood's career of return to a university where he had been a student or a staff member of lower rank. In his research there is a similar pattern of return to a field after some years with a more advanced or a more general treatment. His thesis and first two journal articles with Keyes were on the measurement of the dielectric constants of two polar gases, carbon dioxide and ammonia, as functions of the temperature and density. The last paper on the measurement of dielectric constant which I have seen appeared twenty-six years later. The fourth paper, with Slater, started a long series on the pressures of gases, polar and nonpolar, as functions of temperature and density.

Our joint paper had two purposes: to prove that the Debye limiting law depended in no way on the distribution of charges within the molecule, and to determine at what concentrations the effect of charge distribution might appear. We chose an extreme model, two spheres held a fixed distance apart by a bond which did not interfere with the distribution of other molecules, which we called the "dumb-bell model." It was too extreme to describe the properties of amino acids very well, and the late Edwin Cohn used to pronounce it in a way which implied that the adjective might be extended to the authors. This was taken by Kirkwood as a challenge and, now entirely independently, he derived the equations for the effects of dielectric constant and of salt concentration on a spherical molecule with any distribution of charges. The next challenge came immediately when a referee, misled by a misunderstanding of fluctuation theory, said that, since the very basis of the Debye theory was in doubt, there was no use in publishing an extension of it. This challenge led to the paper on the theory of strong electrolytes of which Debye said after the Langmuir Prize Award that it is not right to call it the "Debye theory" because it was only the "Debye guess" until *Kirkwood came along and put it on a firm foundation.* No one else would have been so grossly unfair to Debye, but the last phrase, which I have italicized, is an apt description of an important aspect of Kirkwood's research—of research done after the remark was made even more than of that done before.

The spherical model served very well for the simple amino acids. Kirkwood also made many calculations of multiply-charged molecules which might serve as models for proteins, but the possible charge distributions were too many for a definite and satisfactory answer. Four years later he treated an ellipsoid of revolution with any distribution of charges or dipoles of infinitesimal length along the axis-of-rotation in order to treat the influence of substituents on the dissociation constants of organic acids; and in 1957 he returned to the spherical model for the smaller protein molecules in which the distribution of charges was by then better known.

Electrolytes, even the complicated proteins, are special cases of solutes which have all the properties of nonelectrolyte solutes plus something else. A firm foundation for electrolytes required a fundamental treatment of nonelectrolytes. This was begun in 1935, and continued in the Langmuir Award address and in a long series of later papers.

With World War II came the realization that we were woefully ignorant of the nature of explosions and many of our best scientists were enlisted in increasing our knowledge. Kirkwood made very significant contributions to the theory of shock and detonation waves in air and in water, and he was a very valuable consultant to several experimental groups. Much of his work in these fields was published after the war in a series of ten papers.

In 1941, Kirkwood published a suggestion that proteins might be fractionated in a narrow perpendicular cell by differential electrophoresis across the cell combined with separative convection due to a thermal gradient. When he could return to this idea in 1946, he found that the density difference due to the change in concentrations by electrophoresis was sufficient for separation, and that a thermal gradient would even have been detrimental by preventing series operation. The theoretical and experimental development and the application of electrophoresis-convection are described

in about twenty papers; and a closely related method, diffusion-convection, was also devised.

If there are several groups on a protein molecule with approximately the same ionization constant and about half the groups are ionized, some molecules have more than the average charge, some less, and the fluctuations are large. They can be determined from macroscopic properties. The variation in position of the ionized sites in a single molecule, the effect on both number and position of these sites of the field of another molecule or an external field, and the importance of such changes in the chemical properties of large molecules are more subtle problems which intrigued Kirkwood in the latter years, probably long before his first publication on the subject in 1952.

A paper with Harkins on surface viscosity is the only one of Kirkwood's papers before 1940 not dealing with equilibrium, but after 1945 more than half his publications deal with transport or with nonequilibrium states. His life was by then too complicated to trace a single origin of any line of thought. His formal teaching, papers heard in seminar, discussions with friends, the interests of the young people who came to work with him, all had directive influence on his thinking. Either the war research on explosions or the electrophoresis-convection studies would have required a search for a firm foundation for the theory of transport processes. It is still too early to judge, but it is very possible that the series of papers on "The Statistical Mechanical Theory of Transport Processes" and the related papers will constitute Kirkwood's greatest contribution to science.

The fields which I have sketched include almost nine-tenths of Kirkwood's publications and illustrate the range of his work. The remaining tenth, however, show the variety of subjects which he put on a firm foundation.

The final challenge came in the spring of 1958 when he was told that he had about a year more of life. He determined to make as much as possible of that life normal and to make all of it full. Toward the end, the weakness of his body interfered with the transmission of his thoughts, but neither the weakness nor the suffering could distract his thinking. It was as though his will had erected a barrier between body and mind.

Kirkwood's standards were extremely high and he was really irritated by mediocrity in a contemporary or an older man; however, he was very patient with any younger person who came to him for instruction. At every meeting. he was the center of a cluster of former students and associates anxious to renew the inspiration. Since I cannot list all sixty, I have carefully deleted from this sketch the name of every younger co-worker. This is unfair to some, but not so unfair as stopping anywhere else. It is these younger people, and those still to come who will be inspired by them and by reading Kirkwood's papers, who will mitigate our loss in his tragic death at the height of his powers; in them he will continue to live.

THE JOURNAL OF CHEMICAL PHYSICS VOLUME 33, NUMBER 5 NOVEMBER, 1960

Theory of the Diffuse Double Layer*

FRANK H. STILLINGER, JR.† AND JOHN G. KIRKWOOD‡

Sterling Chemistry Laboratory, Yale University, New Haven, Connecticut

(Received December 9, 1959)

The charge moment expansion for potentials of mean force acting between the ions of an electrolyte is reviewed in a form applicable to surface phases. An integral equation is in this manner derived for approximate determination of the average charge distribution near a planar electrode. The solution of the linearized equation is constructed for an electrolyte consisting of charged hard spheres suspended in a dielectric continuum. For very dilute solutions, the predictions of the linearized Poisson-Boltzmann equation are verified; at higher concentrations, the average space charge in the neighborhood of the electrode tends to alternate in sign as a result of local latticelike ion arrangement imposed effectively by short range ion repulsions. Predicted values of the ζ potential relative to those of the linear Poisson-Boltzmann theory are reported.

I. INTRODUCTION

THE understanding of the molecular basis of the diffuse, or Gouy, double layer provides insight into a number of phenomena of interest to electrochemists. In particular, it is possible to analyze the several electrokinetic phenomena (e.g., electrophoretic migration velocities and streaming potentials) to predict the stability of lyophobic colloids toward added salt, and to interpret the capacitance of metal electrodes in contact with electrolytic solutions. Theoretical determination of average ion distributions in diffuse double layers typically has employed, in the past, the Poisson-Boltzmann equation as adapted to the surface region. Recent developments for the planar interface are concerned either with solution of the Poisson-Boltzmann equation retaining nonlinear terms,[1–3] or, assuming this equation as a basis, with introduction of complicating *ad hoc* physical models to account for such electrolyte parameters as ion size and degree of hydration.[4–6]

Although such extensions are interesting and perhaps intuitively appealing, it is nevertheless true that the Poisson-Boltzmann equation can give at best only an approximate description of the molecular situation. The linear terms in the average electrostatic potential (with the Poisson-Boltzmann equation in expanded form) are alone consistent with a rigorous integrability condition satisfied by the excess electrostatic free energy.[7]

The viewpoint adopted in the following analysis involves determination of local ion densities in the double layer region from the well-developed fundamental theory of molecular distribution functions. Specifically, a moment expansion in increasing orders of charge for a particular ion is derived for the potential of mean force acting in a set of particles (including the chosen ion). This is the diffuse double layer version of a similar treatment of bulk electrolytes which has been carried to some length by Kirkwood and Poirier.[8] An alternative approach to our present problem would introduce a conditionally convergent Mayer cluster expansion appropriate to the interfacial region; in order to obtain finite results for the ionic distribution functions, it would be necessary, as is well known, to select certain sets of clusters for partial summation.[9]

By way of illustrating the profound effect that finite ion size can have upon the average charge distribution in the double layer, our distribution function technique is formulated in approximate fashion to deal extensively with an idealized electrolyte. The electrolyte is regarded as consisting of charged rigid spheres suspended in a dielectric continuum, and a planar, uniformly charged electrode produces the double layer in this model fluid. It is in fact then possible to establish that both the ion-exclusion volumes and the electrostatic charges are instrumental in determining even the qualitative features of the distributions of ions. For sufficiently large dilutions, the usual linear Poisson-Boltzmann result is obtained, but as the electrolyte concentration is allowed to increase, the short-range ion-ion repulsions tend to set up a local latticelike structure with alternating layers of positive and negative charge. Numerical computations for the reduced ζ potential clearly reflect the ionic ordering at distances further from the electrode than would be predicted by the linear Poisson-Boltzmann theory.

II. MOMENT EXPANSION

The molecular system to be discussed consists of a large set of N particles of species $1\cdots\eta$, some of which are electrostatically charged (ions). These particles will be enclosed within a volume v. The surface of this

* Based upon part of a doctoral thesis submitted by Frank Stillinger, Jr. to the Graduate School Faculty at Yale University.

† Present address: Bell Telephone Laboratories, Murray Hill, New Jersey.

‡ Deceased.

[1] D. C. Grahame, Chem. Rev. **41**, 441 (1947).

[2] B. Breyer and F. Gutmann, J. Chem. Phys. **21**, 1323 (1953).

[3] J. R. Macdonald and M. K. Brachman, J. Chem. Phys. **22**, 1314 (1954).

[4] Freise, Z. Elektrochem. **56**, 822 (1952).

[5] R. Schlögl, Z. Physik **202**, 379 (1954).

[6] J. J. Bikerman, Phil. Mag. **33**, 384 (1942).

[7] R. H. Fowler and E. A. Guggenheim, *Statistical Thermodynamics* (The MacMillan Company, New York, 1956), p. 387.

[8] J. G. Kirkwood and J. C. Poirier, J. Phys. Chem. **58**, 591 (1954).

[9] In this connection, see F. P. Buff and F. H. Stillinger, Jr., J. Chem. Phys. **25**, 312 (1956).

volume may be regarded as a mathematical surface of discontinuity in the sense that it may be crossed by none of the particles. It might, for example, be represented by an infinitely steep and high potential barrier. It is necessary to have a certain portion of the containing surface (such as one face of a rectangular solid volume v) correspond to a charged electrode, which induces the Gouy double layer by creating an appropriate external force field.

Each of the N particles comprising our electrolyte is therefore subject to forces arising either from the charged electrode or from the other fluid particles. The total potential of interaction accordingly is split into single-particle, and particle-pair contributions, attributable to these two sources, respectively,

$$V_N(1\cdots N)=\sum_{i=1}^{N}V_{\alpha_i}{}^{(1)}(i)+\sum_{i<j=1}^{N}V_{\alpha_i\alpha_j}{}^{(2)}(ij),$$

$$\alpha_i,\alpha_j=1\cdots\eta. \tag{1}$$

Here, α_i and α_j denote the species of particles i and j. Each of the singlet and pair potentials, furthermore, may be separated into parts of electrostatic (e), and short-range (s) character.

$$V_{\alpha_i}{}^{(1)}(i)=V_{\alpha_i}{}^{(1,s)}(i)+\xi_iV_{\alpha_i}{}^{(1,e)}(i),$$

$$V_{\alpha_i\alpha_j}{}^{(2)}(ij)=V_{\alpha_i\alpha_j}{}^{(2,s)}(ij)+\xi_i\xi_jV_{\alpha_i\alpha_j}{}^{(2,e)}(ij). \tag{2}$$

We have, for the sake of convenience, introduced charging parameters ξ_i for each of the particles in the ionic fluid, such that the charge on i will be ξ_ie ($-e$ is the electronic charge). For neutral solvent species, ξ_i will of course vanish.

Specifically, the electrostatic interactions $V^{(1,e)}$ and $V^{(2,e)}$ will be written (including a dielectric constant appropriate to the fluid medium)

$$V_{\alpha_i}{}^{(1,e)}(i)=V^{(1,e)}(x_i)=-(2\pi\sigma e/D)x_i+A, \tag{3}$$

$$V_{\alpha_i\alpha_j}{}^{(2,e)}(ij)=V^{(2,e)}(r_{ij})=e^2/Dr_{ij}. \tag{4}$$

The singlet and pair electrostatic interactions therefore are species independent. The potential $V^{(1,e)}$ has been chosen as that for a uniformly charged (σ esu/cm^2) planar electrode, with distance x_i measured normal to its surface and directed inward toward the solution. The value of the additive constant A depends upon the choice of a zero of potential energy; its magnitude can in no way affect the ionic distributions.

The probability of observing a set of n particles such as $1\cdots n$ (the first particle is species α, $\cdots$, the nth particle is species ν) in a given set of positions $\mathbf{r}_1\cdots\mathbf{r}_n$ in the system, is conveniently expressed in terms of a molecular correlation function $g_{\alpha\cdots\nu}{}^{(n)}(1\cdots n)$. $g^{(n)}$ is normalized to unity when each member of the set $1\cdots n$ is far both from other members of the set, and from the double layer region. $g^{(n)}$ may be written as a phase space integral of the normalized canonical distribution, over the configurations of the remaining $N-n$ particles, correct to terms of order N^{-1},

$$g_{\alpha\cdots\nu}{}^{(n)}(1\cdots n)=\exp[-\beta W_{\alpha\cdots\nu}{}^{(n)}(1\cdots n)]$$

$$=\frac{v^n\int_v\cdots\int_v\exp[-\beta V_N(1\cdots N)]dv_{n+1}\cdots dv_N}{\int_v\cdots\int_v\exp[-\beta V_N(1\cdots N)]dv_1\cdots dv_N},$$

$$\beta=(kT)^{-1}, \tag{5}$$

where $W^{(n)}$ is the potential of mean force for the n particle set.

When each of $1\cdots n$ is microscopically far from the double layer region, $g^{(n)}$ assumes a value $g^{(n,b)}$ typical only of the bulk structure of the electrolytic fluid, and hence completely independent of the nature (shape, charge distribution) of the surface of the system. In particular, the pair correlation function $g^{(2,b)}$ depends only on the radial distance r separating a pair of particles.

The quantities of dominant interest for the double layer development are the singlet distributions, $g_\alpha{}^{(1)}(\mathbf{r})$. In the interior of the fluid they are unity, but deviations occur near the electrode on account of nonvanishing average force acting on a single particle there. For a position $\mathbf{r}$ within the Gouy double layer, the mean electrostatic charge density ρ_{el} may be expressed trivially in terms of the several $g_\alpha{}^{(1)}$,

$$\rho_{el}(\mathbf{r})=\sum_{\alpha=1}^{\eta}c_\alpha\xi_\alpha eg_\alpha{}^{(1)}(\mathbf{r}). \tag{6}$$

c_α is the bulk concentration of the αth species, and does not differ significantly from the reciprocal volume per α particle computed for the entire system volume v. This charge density ρ_{el} vanishes when $\mathbf{r}$ is within the bulk fluid; here, then, one has a bulk electroneutrality condition

$$\sum_{\alpha=1}^{\eta}c_\alpha\xi_\alpha=0. \tag{7}$$

If our system includes the uniformly charged planar electrode giving rise to the potential (3), a second electroneutrality condition may be formulated. The average charge residing in the double layer must precisely neutralize the charge density σ

$$-\sigma=\int_l^u\rho_{el}(x)dx. \tag{8}$$

The limits of integration on x, the normal distance to the electrode, must span the region over which excess space charge attributable to the ionic fluid is sensibly different from zero. These limits will be, respectively, just within the electrode (l), and well inside the electrolyte bulk (u).

The distribution of charge both on the electrode and induced within the electrolyte as the diffuse double

layer produces an average electric field. On account of the complete and exact shielding of the electrode charge, as illustrated by condition (8), this mean field will be nonzero only within the Gouy layer. By integration, the field defines an average potential $\psi(\mathbf{r})$ at a point $\mathbf{r}$ in the double layer relative to the bulk liquid. The value of $\psi(\mathbf{r})$ for the present situation (planar, uniformly charged electrode) will depend only on the coordinate x. Simple electrostatics suffices to provide the result

$$\psi(x) = (4\pi/D)\int_x^u (x-y)\rho_{el}(y)\,dy. \tag{9}$$

Once again the upper integration limit u on y must be sufficiently large that ρ_{el} is substantially zero. The value of ψ at the electrode surface defines the ζ potential.

The correlation function definitions (5) may be manipulated to yield finally a power series expansion of each $W^{(n)}$ in the charging parameter ξ_j for one of the set $1\cdots n$ (we shall choose ξ_1). In order to do so, first rewrite the total potential V_N in the form,

$$V_N(1\cdots N;\xi_1) = \xi_1[V^{(1,e)}(1)+\sum_{j=2}^{n}\xi_j V^{(2,e)}(1j)+V_{1,N-n}{}^{(2,e)}] + V_N(1\cdots N;\xi_1=0),$$

$$V_{1,N-n}{}^{(2,e)} = \sum_{k=n+1}^{N}\xi_k V^{(2,e)}(1k), \tag{10}$$

which specifically emphasizes the dependence of this quantity on the charge of particle 1. If (10) is inserted in (5), the correlation functions may be transformed to

$$g_{\alpha\cdots\nu}{}^{(n)}(1\cdots n;\xi_1) = \exp\{-\beta W_{\alpha\cdots\nu}{}^{(n)}(1\cdots n;\xi_1=0) - \beta\xi_1[V^{(1,e)}(1)+\sum_{j=2}^{n}\xi_j V^{(2,e)}(1j)]\} \times \frac{\langle\exp\{-\beta\xi_1 V_{1,N-n}{}^{(2,e)}\}\rangle_{\xi_1=0}{}^{(n)}}{\langle\exp\{-\beta\xi_1[V^{(1,e)}(1)+V_{1,N-1}{}^{(2,e)}]\}\rangle_{\xi_1=0}{}^{(0)}}. \tag{11}$$

The angular brackets denote averages in a canonical ensemble in which particle 1 has been discharged (i.e., $\xi_1=0$),

$$\langle f\rangle_{\xi_1=0}{}^{(j)} = \frac{\int_v\cdots\int_v f\exp[-\beta V_N(\xi_1=0)]\,dv_{j+1}\cdots dv_N}{\int_v\cdots\int_v \exp[-\beta V_N(\xi_1=0)]\,dv_{j+1}\cdots dv_N}. \tag{12}$$

The process of removing, as in Eq. (12), the electrostatic charge from a single ion in an electrolyte has no physically operational meaning. From the standpoint of the correlation functions $g^{(n)}$, it is often convenient to regard a discharged ion as corresponding qualitatively to a noble gas atom (isoelectronic with the original ion) dissolved in the electrolyte. Since a discharged ion can interact with the electrode and other ions only through the short-range functions $V^{(1,e)}(\mathbf{r}_1)$ and $V^{(2,e)}(r_{12})$, the correlation functions $g_\alpha{}^{(1)}(\mathbf{r}_1;\xi_1=0)$ and $g_{\alpha\beta}{}^{(2)}(\mathbf{r}_1,\mathbf{r}_2;\xi_1=0)$ can differ significantly from unity only when x_1 and r_{12} are small enough to bring these potentials into play. This behavior contrasts sharply with the correlations acting between fully charged ions, which extend over many molecular diameters on account of the long-range nature of electrostatic forces.

By taking logarithms in (11), and expanding the averaged exponential functions, the nth order potential of mean force becomes expressed as a contribution remaining when ion 1 is discharged, plus correction terms, which may be exhibited as the desired power series,

$$W_{\alpha\cdots\nu}{}^{(n)}(1\cdots n;\xi_1) = W_{\alpha\cdots\nu}{}^{(n)}(1\cdots n;\xi_1=0)+\xi_1[V^{(1,e)}(1)+\sum_{j=2}^{n}\xi_j V^{(2,e)}(1j)] - \beta^{-1}\log\Big[\sum_{s=0}^{\infty}\frac{(-\beta\xi_1)^s}{s!}M_s\Big]+\beta^{-1}\log\Big[\sum_{s=1}^{\infty}\frac{(-\beta\xi_1)^s}{s!}\bar{M}_s\Big]$$

$$= W_{\alpha\cdots\nu}{}^{(n)}(1\cdots n;\xi_1=0)+\xi_1[V^{(1,e)}(1)+\sum_{j=2}^{n}\xi_j V^{(2,e)}(1j)] + \sum_{s=1}^{\infty}\frac{(-\beta)^{s-1}}{s!}[\Lambda_s(1\cdots n)-\bar{\Lambda}_s]\xi_1{}^s. \tag{13}$$

M_s and $\bar{M}_s$ are moments of the electrostatic interactions involving particle 1

$$M_s = \langle[V_{1,N-n}{}^{(2,e)}]^s\rangle_{\xi_1=0}{}^{(n)},$$
$$\bar{M}_s = \langle[V_{1,N-1}{}^{(2,e)}+V^{(1,e)}(1)]^s\rangle_{\xi_1=0}{}^{(0)}, \tag{14}$$

and are related to the cumulants Λ_s, $\bar{\Lambda}_s$ by the relations[10]

$$M_s = \sum_{r=1}^{s}\binom{s-1}{r-1}\Lambda_r M_{s-r},$$
$$\bar{M}_s = \sum_{r=1}^{s}\binom{s-1}{r-1}\bar{\Lambda}_r \bar{M}_{s-r},$$
$$M_0=\bar{M}_0=1. \tag{15}$$

On solving for the cumulants, one easily finds:

$$\Lambda_1 = M_1,$$
$$\Lambda_2 = M_2-(M_1)^2,$$
$$\Lambda_3 = M_3-3M_2M_1+2(M_1)^3,$$
$$\Lambda_4 = M_4-4M_3M_1-3(M_2)^2+12M_2(M_1)^2-6(M_1)^4; \tag{16}$$

[10] H. Cramér, *Mathematical Methods of Statistics* (Princeton University Press, Princeton, New Jersey, 1946), p. 185.

precisely the same relations (16) hold for the barred quantities.

The power series (13) allows one, at least in principle, to compute each nth order potential of mean force in ascending orders of ionic charge. In practice, the integral equations arising in this task require knowledge of higher order W's, and so in this sense are coupled to each other in complicated fashion. The following section proposes a scheme for circumventing some of these difficulties.

III. APPROXIMATE DOUBLE-LAYER IONIC DISTRIBUTIONS

Having outlined the general moment method for ionic correlations, we now proceed to apply these ideas specifically to the diffuse double layer region. The terms of increasing ξ_1 order in the complete expansion (13) rapidly become more and more complicated to evaluate, even for the single-particle distributions. We shall adopt the viewpoint, for the present, that retention of only those terms linear in ξ_1 will yield a sufficiently accurate description of the double layer.[11] In the interests of concreteness, furthermore, the electrolyte (chosen to be a single component salt solution) will be described as consisting of uniformly charged, spherically symmetric particles which are suspended in a dielectric continuum. The ions (anions and cations may have different short-range forces) can penetrate neither one another extensively on account of strong core repulsions, nor can they penetrate the planar electrode appreciably. The latter will act essentially as a rigid charged "wall," and for convenience the coordinate system may be chosen to locate it near $x=0$.[12]

It is a fairly simple matter to include the molecular nature of the solvent medium in the following development if these latter particles interact with central forces. However, the results of this generalization differ only slightly from those to be obtained with the dielectric continuum, and hence do not seem to merit the extra notational complication. Attention, then, will be focused only on particles of ionic nature, and since we wish to consider only a single electrolyte, the relevant charge parameters ξ_1 can assume only two values, ξ_+ (cations) and ξ_- (anions).

In the linear ξ_1 approximation, the singlet potentials of mean force are written

$$W_\alpha^{(1)}(\mathbf{r}_1;\xi_1)=W_\alpha^{(1)}(\mathbf{r}_1;\xi_1=0)+\xi_1[V^{(1,e)}(x_1)+\langle V_{1,N-1}^{(2,e)}\rangle_{\xi_1=0}^{(1)}-\langle V_{1,N-1}^{(2,e)}+V^{(1,e)}(1)\rangle_{\xi_1=0}^{(0)}],\quad \alpha=+,-. \tag{17}$$

As anticipated earlier, the additive constant A has no effect on these expressions for the $W_\alpha^{(1)}$; it cancels in the combination

$$V^{(1,e)}(x_1)-\langle V^{(1,e)}(1)\rangle_{\xi_1=0}^{(0)}. \tag{18}$$

One may immediately make certain simplifying observations concerning relations (17). Because of the symmetry of our problem about the electrode normal direction, the singlet mean-force potentials $W_\alpha^{(1)}$ will depend only on the x_1 coordinate, as do $V^{(1,e)}$ and $V^{(1,s)}$. In addition, the second of the two average value quantities in (17) is just a constant, independent of $\mathbf{r}_1$. In view of the fact that the electrostatic potential $V^{(1,e)}$ is a simple linear function of x_1, a considerable reduction in complexity is achieved by performing a twofold x_1 differentiation on both members of (17)

$$d^2\phi_\alpha(x_1)/dx_1^2=(D/2\pi e\sigma)\,(d^2/dx_1^2)\,\langle V_{1,N-1}^{(2,e)}\rangle_{\xi_1=0}^{(1)}. \tag{19}$$

ϕ_α is a reduced electrostatic single-particle average potential for the species α,

$$W_\alpha^{(1)}(x_1;\xi_1)-W_\alpha^{(1)}(x_1;0)=(2\pi e\sigma\xi_\alpha/D)\phi_\alpha(x_1). \tag{20}$$

The quantities ϕ_α therefore carry the long-range electrostatic correlation of the diffuse double layer.

By utilizing the definitions (5), the averaged potential remaining in Eq. (19) may be expressed in terms of the singlet and pair correlation functions for the discharged particle 1

$$\frac{d^2\phi_\alpha(x_1)}{dx_1^2}=\frac{e}{2\pi\sigma}\frac{d^2}{dx_1^2}\int_v\frac{d\mathbf{r}_2}{r_{12}}\left[c_+\xi_+\frac{g_{\alpha+}^{(2)}(\mathbf{r}_1,\mathbf{r}_2;0)}{g_\alpha^{(1)}(x_1;0)}+c_-\xi_-\frac{g_{\alpha-}^{(2)}(\mathbf{r}_1,\mathbf{r}_2;0)}{g_\alpha^{(1)}(x_1;0)}\right]. \tag{21}$$

The integration in this last expression is over all configurations $\mathbf{r}_2$ of a second ion inside the containing volume v.

When x_1 is sufficiently large, the $g_\alpha^{(1)}(\mathbf{r}_1;0)$ do not differ sensibly from unity, and the pair correlations $g_{\alpha\beta}^{(2)}(\mathbf{r}_1,\mathbf{r}_2;0)$ may be replaced by the product of a bulk pair correlation, and the long-range singlet correlation for charged ion 2,

$$g_{\alpha\beta}^{(2)}(\mathbf{r}_1,\mathbf{r}_2;0)\to g_{\alpha\beta}^{(2,b)}(r_{12};0)\,g_\beta^{(1)}(x_2). \tag{22}$$

This replacement is the analog, for the double-layer theory, of the superposition approximation used extensively in the molecular theory of bulk liquids. For the present purposes, it should be noted we find it necessary to use (22) only for large x_1, rather than over the entire range of values for this variable.

[11] Reference to Eqs. (13) shows immediately that this approximation is equivalent to replacing the moments M_s and $\bar{M}_s$ by $(M_1)^s$ and $(\bar{M}_1)^s$.

[12] The exact position of the electrode is not critical; we wish only to imply here that for x decreasing through zero, the short-range electrode potential $V^{(1,e)}(x)$ becomes rapidly very large (strong repulsion).

In view of the reduction (22), one is led to the integrodifferential equation, valid if x_1 is not too small,

$$d^2\phi_\alpha(x_1)/dx_1^2=(e/2\pi\sigma)[d^2I(x_1)/dx_1^2],$$

$$I(x_1)=\int_v(d\mathbf{r}_2/r_{12})[c_+\xi_+g_{\alpha+}^{(2,b)}(r_{12};0)g_+^{(1)}(x_2)+c_-\xi_-g_{\alpha-}^{(2,b)}(r_{12};0)g_-^{(1)}(x_2)]. \quad (23)$$

Three contributions to $I(x_1)$ may be distinguished:

$$I(x_1)=I_1(x_1)+I_2(x_1)+I_3(x_1),$$

$$I_1(x_1)=\int_v(d\mathbf{r}_2/r_{12})\{c_+\xi_+g_{\alpha+}^{(2,b)}(r_{12};0)\times[g_+^{(1)}(x_2)-1+(2\pi\sigma e\xi_+/DkT)\phi_+(x_2)]+c_-\xi_-g_{\alpha-}^{(2,b)}(r_{12};0)\times[g_-^{(1)}(x_2)-1+(2\pi\sigma e\xi_-/DkT)\phi_-(x_2)]\},$$

$$I_2(x_1)=\int_v(d\mathbf{r}_2/r_{12})[c_+\xi_+g_{\alpha+}^{(2,b)}(r_{12};0)+c_-\xi_-g_{\alpha-}^{(2,b)}(r_{12};0)],$$

$$I_3(x_1)=-(2\pi\sigma e/DkT)\int_v(d\mathbf{r}_2/r_{12})\times[c_+\xi_+^2g_{\alpha+}^{(2,b)}(r_{12};0)\phi_+(x_2)+c_-\xi_-^2g_{\alpha-}^{(2,b)}(r_{12};0)\phi_-(x_2)]. \quad (24)$$

The square-bracketed quantities in I_1 represent the nonlinear (in the ϕ_α) portions of the singlet correlations in the double layer, as well as the nonelectrostatic ($\xi_3=0$) correlation; these differ significantly from zero only in the immediate vicinity of the electrode. When x_1 is large, therefore, the only contribution to the integral I_1 occurs when r_{12} is large, so that each $g_{\alpha\beta}^{(2,b)}(r_{12};0)$ is essentially just unity. As a result, then, $I_1(x_1)$ represents (for x_1 large) the potential energy of a uniform and somewhat diffuse sheet of charge density $\rho^*(\mathbf{r}_2)$,

$$\rho^*(\mathbf{r}_2)=c_+\xi_+[g_+^{(1)}(x_2)-1+(2\pi\sigma e\xi_+/DkT)\phi_+(x_2)]+c_-\xi_-[g_-^{(1)}(x_2)-1+(2\pi\sigma e\xi_-/DkT)\phi_-(x_2)]. \quad (25)$$

This amounts to concluding that $I_1(x_1)$ is asymptotically a linear function of x_1 similar to (3).

Since the pair correlations $g_{\alpha\beta}^{(2,b)}(r_{12};0)$ settle down rapidly to unity, the integrand of $I_2(x_1)$ differs from zero only when particle 2 is near 1. As a result, again valid for large x_1, the $\mathbf{r}_2$ integration may be extended over all space. It is established therefore that $I_2(x_1)$ is asymptotically constant.

On account of the double x_1 differentiation in Eq. (23), only $I_3(x_1)$ will survive in the large x_1 limit. After performing the requisite differentiations, and carrying out integrations parallel to the electrode surface, the ϕ_α are found asymptotically to satisfy linear homogeneous integrodifferential equations

$$d^2\phi_\alpha(x_1)/dx_1^2=\tfrac{1}{2}\int_0^\infty[\kappa_+^2k_{\alpha+}(x_1-x_2)\phi_+(x_2)+\kappa_-^2k_{\alpha-}(x_1-x_2)\phi_-(x_2)]dx_2,$$

$$k_{\alpha\beta}(x_1-x_2)=(d/dx_1)g_{\alpha\beta}^{(2,b)}(x_1-x_2;0),$$

$$\kappa_\alpha^2=4\pi c_\alpha(\xi_\alpha e)^2/DkT. \quad (26)$$

In the large x_1 region, (26) is entirely independent of the lower x_2 integration limit, since the $k_{\alpha\beta}$ decay rapidly to zero. The origin has been chosen as this lower limit, since it has been made roughly to coincide with the electrode surface. The pair correlation functions $g_{\alpha\beta}^{(2,b)}$ have been defined in (26) as odd functions of their distance variable, so that the kernels $k_{\alpha\beta}$ are even. The well-known Debye-Hückel parameter κ, appropriate to our electrolytic fluid, is related to κ_+ and κ_- by

$$\kappa^2=\kappa_+^2+\kappa_-^2. \quad (27)$$

Since Eqs. (26) were derived under the supposition that x_1 was not small, the ϕ_α can be given exactly over the entire range $0\leq x_1<\infty$ by adding suitable inhomogeneous functions h_α to (26),

$$d^2\phi_\alpha(x_1)/dx_1^2=h_\alpha(x_1)+\tfrac{1}{2}\int_0^\infty[\kappa_+^2k_{\alpha+}(x_1-x_2)\phi_+(x_2)+\kappa_-^2k_{\alpha-}(x_1-x_2)\phi_-(x_2)]dx_2. \quad (28)$$

The h_α are essentially designed to correct for the fact that the local density of β ions, in the environment of a discharged α ion at $\mathbf{r}_1$ near the electrode, is not precisely given by the expression

$$c_\beta g_{\alpha\beta}^{(2,b)}(r_{12};0)[1-(2\pi\sigma e\xi_\beta/DkT)\phi_\beta(x_2)]. \quad (29)$$

It is of course necessary only that each h_α differ from zero near $x_1=0$, since outside this small region (26) and (28) are identical. These inhomogeneous functions contain contributions arising through short-range force electrode interface correlations, through deviations from superposability of the actual pair function $g_{\alpha\beta}^{(2)}$ near the electrode [in terms of the approximation $g_{\alpha\beta}^{(2,b)}(r_{12})g_\alpha^{(1)}(x_1)g_\beta^{(1)}(x_2)$], and finally through the nonlinear ϕ_α terms neglected in the integral $I_1(x_1)$.

It is rather instructive to examine the form of Eqs. (28) under a simplifying assumption regarding the bulk correlations $g_{\alpha\beta}^{(2,b)}(r_{12};0)$. In particular, suppose that each pair of ions, one of which is discharged, will be correlated only to the extent of exhibiting a sphere of exclusion, or impenetrability, of radius a (the same for all pairs). Accordingly,

$$g_{\alpha\beta}^{(2,b)}(r_{12};0)=0 \qquad 0\leq r_{12}\leq a,$$
$$=1 \qquad r_{12}>a. \quad (30)$$

Since the derivative of this unit step is a Dirac delta

function, the kernels all have the common form

$$k_{\alpha\beta}(x)=\delta(x+a)+\delta(x-a). \tag{31}$$

Now when $x_1>a$, the integral in (28) is trivial, and leads to a differential-difference equation satisfied by ϕ_α,

$$d^2\phi_\alpha(x_1)/dx_1^2=h_\alpha(x_1)+\tfrac{1}{2}\{\kappa_+^2[\phi_+(x_1+a)+\phi_+(x_1-a)] +\kappa_-^2[\phi_-(x_1+a)+\phi_-(x_1-a)]\}. \tag{32}$$

If the ionic diameter a is allowed now to vanish, ϕ_+ and ϕ_- satisfy the same second-order differential equation for x_1 sufficiently large. Since the difference $\phi_+-\phi_-$ tends to zero as x_1 increases, both ϕ_+ and ϕ_- must asymptotically be equal to $\exp(-\kappa x_1)$ times a common constant. These rather naive assumptions therefore lead to the exponential decay solutions characteristic of the Poisson-Boltzmann theory. It will become apparent in the following section that retention of a finite ion size, even by means of the rather crude postulate (30), gives rise to solutions ϕ_α, and hence singlet correlations, which are qualitatively different from this monotonic decay function.

The pair of linear coupled Eqs. (28) may be formally solved by standard integral transform methods. It is desirable for this purpose to extend the definition of $\phi_\alpha(x_1)$ to negative x_1, as the solution of (28) for these values of the variable; we set $h_\alpha(x_1)$ identically equal to zero on the negative axis. The functions $\phi_\alpha(x_1)$ may now be separated into two parts, $\phi_\alpha^{(n)}(x_1)$ and $\phi_\alpha^{(p)}(x_1)$, which are the negative axis, and positive axis parts of ϕ_α, respectively,

$$\begin{aligned}&\phi_\alpha(x_1)=\phi_\alpha^{(n)}(x_1)+\phi_\alpha^{(p)}(x_1),\\ &\phi_\alpha^{(p)}(x_1)=0 \qquad x_1<0,\\ &\phi_\alpha^{(n)}(x_1)=0 \qquad x_1>0.\end{aligned} \tag{33}$$

As a consequence, (28) is equivalent to

$$(d^2/dx_1^2)[\phi_\alpha^{(n)}(x_1)+\phi_\alpha^{(p)}(x_1)] =h_\alpha(x_1)+\tfrac{1}{2}\int_{-\infty}^{+\infty}[\kappa_+^2k_{\alpha+}(x_1-x_2)\phi_+^{(p)}(x_2) +\kappa_-^2k_{\alpha-}(x_1-x_2)\phi_-^{(p)}(x_2)]dx_2. \tag{34}$$

In Fourier transform space, the integral equations (34) become a pair of simultaneous linear algebraic equations whose solution is elementary:

$$\Phi_+^{(p)}(z) =1/D(z)\begin{vmatrix}-H_+(z)-z^2\Phi_+^{(n)}(z) & \tfrac{1}{2}\kappa_-^2K_{+-}(z)\\ -H_-(z)-z^2\Phi_-^{(n)}(z) & z^2+\tfrac{1}{2}\kappa_-^2K_{--}(z)\end{vmatrix},$$

$$\Phi_-^{(p)}(z) =1/D(z)\begin{vmatrix}z^2+\tfrac{1}{2}\kappa_+^2K_{++}(z) & -H_+(z)-z^2\Phi_+^{(n)}(z)\\ \tfrac{1}{2}\kappa_+^2K_{-+}(z) & -H_-(z)-z^2\Phi_-^{(n)}(z)\end{vmatrix}; \tag{35}$$

$$D(z)=\begin{vmatrix}z^2+\tfrac{1}{2}\kappa_+^2K_{++}(z) & \tfrac{1}{2}\kappa_-^2K_{+-}(z)\\ \tfrac{1}{2}\kappa_+^2K_{-+}(z) & z^2+\tfrac{1}{2}\kappa_-^2K_{--}(z)\end{vmatrix}; \tag{36}$$

$$[\Phi_\alpha^{(\mu)}(z),H_\alpha(z),K_{\alpha\beta}(z)] =\int_{-\infty}^{+\infty}\exp(izx)[\phi_\alpha^{(\mu)}(x),h_\alpha(x),k_{\alpha\beta}(x)]dx, \qquad \alpha,\beta=+,-, \qquad \mu=n,p.$$

The inversion integrals are

$$\phi_\alpha^{(p)}(x_1)=(1/2\pi)\int_{-\infty}^{+\infty}\exp(-ix_1z)\Phi_\alpha^{(p)}(z)dz, \tag{37}$$

where the results (35) are to be inserted for $\Phi_\alpha^{(p)}(z)$. The contour of integration for (37), when x_1 is positive, may be closed along the infinite, lower half-plane semicircle; subsequently, $\phi_\alpha(x_1)$ may be evaluated in terms of the poles z_j of the transform $\Phi_\alpha^{(p)}(z)$, lying below the real axis

$$\phi_\alpha(x_1)=\sum_{j=1}^{\infty}A_{j,\alpha}\exp(-iz_jx_1). \tag{38}$$

The multiplicative constants $A_{j,\alpha}$ are related in the usual way to the residues at these poles

$$A_{j,\alpha}=i\lim_{z\to z_j}[(z-z_j)\Phi_\alpha^{(p)}(z)]. \tag{39}$$

These constants must naturally be such to make ϕ_+ and ϕ_- real functions of the real variable x_1.

Computation of the $A_{j,\alpha}$ by (39) clearly requires knowledge of $\Phi_\alpha^{(n)}(z)$. This transform must have the property of making the inversion integral (37) vanish identically for every negative x_1. In practical cases, this condition may be met in either of two ways. If only a finite number m of terms in the entire series (38) would suffice to provide an adequate description of the double layer structure, each of the two integrals (37) could be equated to zero for m distinct negative values of x_1, to provide a sufficient number of conditions for unique determination of the coefficients. Alternatively, (37) may be cast in the role of a pair of coupled integral equations on the negative axis for complete determination of the $\phi_\alpha^{(n)}(x_1)$; these solutions in turn would provide the entire set of $A_{j,\alpha}$ through (35) and (39).[13]

It should be remarked that the poles z_j may in general arise either as roots of the denominator $D(z)$, or as poles of the $K_{\alpha\beta}(z)$ or $H_\alpha(z)$ occurring in the determinental numerators of (35). Since $\phi_\alpha^{(n)}(x_1)$ decays rapidly to zero with decreasing x_1 on the negative axis, the transforms $\Phi_\alpha^{(n)}(z)$ cannot have poles in the lower-half z plane; therefore, these two functions are effective only in determining the exact values of the multiplicative constants $A_{j,\alpha}$, rather than in providing z_j's

[13] The use of these integral equations actually corresponds to allowing m to increase to infinity.

for the solution (38). Furthermore, it should be noted at this juncture that since the $h_\alpha(x_1)$ decay rapidly to zero on the positive axis, the set of z_j contributed as poles of the $H_\alpha(z)$ lie well below the real axis; the corresponding terms in $\phi_\alpha(x_1)$ therefore themselves decay very rapidly with increasing x_1.

If all of the kernels $k_{\alpha\beta}(x_1)$ as well as the inhomogeneous functions $h_\alpha(x_1)$ were zero for all x_1 greater than some fixed positive constant, then the transforms $K_{\alpha\beta}$ and H_α would be analytic in the entire z plane. As a result, each z_j would necessarily be a root,

$$D(z_j)=0. \tag{40}$$

The series expressions (38) for ϕ_+ and ϕ_- under these circumstances would differ only insofar as the exact numerical values of the coefficients $A_{j,\alpha}$ are concerned, since the same exponential functions must appear for both anions and cations.

IV. SIMPLIFIED RIGID-SPHERE MODEL

To clarify the way in which the formalism of the preceding sections leads to predictions concerning the detailed nature of the double layer, we are now in a position to deduce the properties of a simple, though informative, model. We choose to investigate that system of equal-sized rigid spherical ions which led to the differential-difference Eqs. (32). For the sake of simplicity also, we shall wish to disregard the effect of the inhomogeneous functions $h_\alpha(x_1)$; it has already been noted in this connection that such an assumption can have no effect on the asymptotic (large x_1) equations determining the ionic distributions. The nonelectrostatic effect of the planar electrode may be taken as that of a completely impenetrable "wall." By locating the surface of this wall at $x_1=-a/2$ (a distance from the origin equal to the ion radii), the single particle potentials $V_\alpha^{(1,\alpha)}$ are just

$$\begin{aligned} V_\alpha^{(1,\alpha)}(x_1) &= +\infty \qquad x_1 \leq 0, \\ &= 0 \qquad\quad x_1 > 0. \end{aligned} \tag{41}$$

On account of the pair correlations (30) being identical for any species pair, we have already emphasized that the kernels $k_{\alpha\beta}$ are identical, as indicated by Eq. (31). As a result of the foregoing idealizations, one has to deal with only a single homogeneous integro-differential equation,

$$d^2\phi(x_1)/dx_1^2=\tfrac{1}{2}\kappa^2\int_0^\infty k(x_1-x_2)\phi(x_2)\,dx_2,$$

$$\phi_+(x_1)=\phi_-(x_1)=\phi(x_1), \qquad k_{\alpha\beta}(x)=k(x). \tag{42}$$

The unpretentious double-layer picture described by the solution of (42) is probably a reasonable approximation to the actual physical state of affairs if the density of ion spheres is not too near the close-packed density; i.e.,

$$c_+ + c_- \ll 2^{\frac{1}{2}}a^{-3}. \tag{43}$$

The inversion integral for the solution to (42) may now be written down with the help of Eqs. (35)–(37)

$$\phi(x_1)=-(1/2\pi)\int_{-\infty}^{+\infty}\frac{z^2\exp(-ix_1z)\Phi^{(n)}(z)}{z^2+\kappa^2\cos(az)}\,dz \quad (x_1>0)$$

$$=\sum_{j=1}^{\infty}A_j\exp(-iz_jx). \tag{44}$$

In accordance with previous remarks, the z_j are precisely the roots of the transcendental equation

$$z^2+\kappa^2\cos(az)=0. \tag{45}$$

Consequently, the constants A_j may be displayed as

$$A_j=-\frac{iz_j^2\Phi^{(n)}(z_j)}{2z_j-\kappa^2a\sin(az_j)}. \tag{46}$$

For small values of the dimensionless parameter κa, the transcendental Eq. (45) has two roots $\pm z_1$, which may be expanded about $\kappa a=0$

$$y_j=iaz_j,$$

$$y_1=\kappa a[1+\tfrac{1}{4}(\kappa a)^2+\tfrac{1}{96}(\kappa a)^4+\tfrac{25}{1920}(\kappa a)^6+\cdots]. \tag{47}$$

The leading term in the series (44) corresponding to the root $+z_1$ produces a $\phi(x_1)$ of the form

$$\phi(x_1)\sim\exp(-\kappa x_1) \tag{48}$$

in the limit of zero electrolyte concentration. It is in this manner that the predictions of the linear Poisson-Boltzmann equation of the Debye-Hückel electrolyte theory are verified, even for finite ion sizes. It is possible to show that this result is in no way dependent upon the special form of the short-range ion-ion forces chosen for our simple model.

There is a second pair of pure imaginary roots $\pm z_2$ which, again for κa sufficiently small, may be represented by an asymptotic series

$$y_2=\log[2/(\kappa a)^2]+2\log\log[2/(\kappa a)^2]+\cdots. \tag{49}$$

It is evident that in dilute solutions, the z_2 contribution to $\phi(x_1)$ damps to zero extremely fast.

The remaining roots of (45) in the small κa region are all complex, and occur in quadruples

$$y_j=\pm\alpha_j\pm i\beta_j. \tag{50}$$

Numerical analysis shows that as κa increases from zero, the roots z_1 and z_2 move toward each other on the negative imaginary axis. They finally merge at $\kappa a=1.03$, and thereupon move away from the imaginary axis as complex conjugates. The values of the roots nearest the origin $z=0$ are exhibited in Table I for selected values of κa.

Even if only the first two terms in the complete sum (44) corresponding to z_1 and z_2 are retained as an approximation to the actual statistical state, it is clear that the ion size, or excluded volume, is capable of exerting a profound influence upon the charge density

in the double layer. Although for small κa, in this two-term approximation, ϕ is a sum of damped exponentials,

$$\phi(x_1) = A_1 \exp[-y_1(x_1/a)] + A_2 \exp[-y_2(x_1/a)], \quad (51)$$

this sum becomes a damped sinusoid when $\kappa a > 1.03$, and y_1 and y_2 are complex conjugates. On account of the resultant sign changes in ϕ, the average double-layer charge density likewise alternates in sign. This behavior denotes, in an average sense, that planar layers of anions and cations are held against, and parallel to, the electrode surface. This local structure is somewhat similar to the situation in ionic crystals where also alternate planes of positive and negative ions are encountered.

A detailed study of even the two roots z_1 and z_2 alone therefore provides insight into the transition from very dilute solutions, where the distribution of ions may be deduced from consideration of electrostatic forces alone, to concentrated solutions in which short-range forces are important. These latter begin to cause interference between the ions at moderate density, and to relieve this situation, the ions must begin to settle into locally ordered arrangements, the extreme case of which would be the long-range regularity of the ionic crystal. Only for very low electrolyte concentrations, therefore, is it reasonable to neglect exclusion volumes in deducing double layer structures.

The special kernel (31) gives the functional Eq. (42) for $\phi(x_1)$ three distinct forms in three different intervals

$$\begin{aligned} d^2\phi(x_1)/dx_1^2 &= 0 && x_1 < -a, \\ &= \tfrac{1}{2}\kappa^2\phi(x_1+a) && -a < x_1 < a, \\ &= \tfrac{1}{2}\kappa^2[\phi(x_1-a)+\phi(x_1+a)] && x_1 > a. \end{aligned} \quad (52)$$

In the first of these intervals, ϕ obviously must be the linear function

$$\phi(x_1) = B_1 x_1 + B_0 \qquad x_1 < -a, \quad (53)$$

with the constants B_1 and B_0 having values to provide a smooth fit onto $\phi(x_1)$ for $x_1 > -a$. Repeated use of (52) shows that ϕ has simple discontinuities in its second derivative at $-a$ and $+a$, in its fourth derivative at 0 and $2a$, and in the $2n$th derivative ($n>2$) at na. This series of discontinuities propagated down the x_1 axis arises solely by use of singular short-range ion interactions, and has no fundamental physical basis. It is of course possible to eliminate them by using differentiable functions $V_a^{(1,s)}$ and $V_a^{(2,s)}$.

A single restriction to which the constants A_j must conform is provided by the double layer electroneutrality condition (8). One might attempt further to determine the A_j for the present model by substitution into the integrodifferential equation (42), or equivalently, into the relations (52). When $x_1 > a$, no information is provided since each member of the sum (44) separately satisfies the condition imposed. However, the set of admissible values A_j is restricted by insisting that (44) satisfy (42) or (52) in the interval $-a < x_1 < a$. Demanding that $\phi(x_1)$ be a solution for this entire finite interval provides sufficient constraint to fix all the A_j. This finite interval procedure has a distinct advantage over the more general integral equation subsidiary problem of Sec. III, in which case the function $\phi_a^{(n)}$ would have to be determined over the entire negative axis, $x_1 < 0$.[14]

TABLE I. Roots of the transcendental equation $y^2 - (\kappa a)^2 \cosh y = 0$ near $y=0$ in the complex plane; $y_j = \alpha_j + i\beta_j$.

κa	α_1	β_1	α_2	β_2	α_3, α_4	$\beta_3, -\beta_4$
0.100	0.100	0	9.88	0	11.11	14.42
0.500	0.536	0	5.48	0	7.70	14.75
0.900	1.22	0	3.28	0	6.48	14.89
1.00	1.62	0	2.56	0	6.26	14.90
1.03	2.07	0	2.07	0	6.19	14.91
1.06	2.03	0.45	2.03	−0.45	6.14	14.93
1.15	1.92	0.89	1.92	−0.89	5.97	14.95
1.50	1.53	1.62	1.53	−1.62	5.43	15.02
2.00	1.06	2.08	1.06	−2.08	4.84	15.07

For the purposes of numerical computation, the two term representation (51) of $\phi(x_1)$ discussed previously, will suffice. Since the terms to be neglected correspond to z_j's with large negative imaginary parts, the predicted ion distributions will be in error only very near the electrode.

If the electrode surface charge is not too large, the double-layer electroneutrality condition adapted to the present example may be linearized with respect to ϕ to yield

$$2/\kappa^2 = \int_0^\infty \phi(x_1)\,dx_1. \quad (54)$$

The corresponding linearized result for the ζ potential, as expressed in (9) for $x=0$, becomes

$$\zeta(\sigma) = (2\pi\kappa^2\sigma/D)\int_0^\infty x_1\phi(x_1)\,dx_1. \quad (55)$$

The second condition on A_1 and A_2 in (51) to be utilized simultaneously with condition (54) results from the demand that the second of Eqs. (52) be satisfied at $x_1 = 0$,

$$d^2\phi(x_1=0)/dx_1^2 = \tfrac{1}{2}\kappa^2\phi(x_1=a); \quad (56)$$

this is precisely the center of the interval over which the second form in (52) is valid.

When the two term approximation (51) is inserted in each of (54) and (56), there is obtained a pair of independent linear equations in A_1 and A_2. One thus readily finds

$$A_1 = [2a/(\kappa a)^2]y_1y_2\left[\frac{\exp y_2}{y_2\exp y_2 - y_1\exp y_1}\right],$$

$$A_2 = [2a/(\kappa a)^2]y_1y_2\left[-\frac{\exp y_1}{y_2\exp y_2 - y_1\exp y_1}\right]. \quad (57)$$

[14] Such simplification was inherent in the rigid-sphere model by using step-function pair correlations.

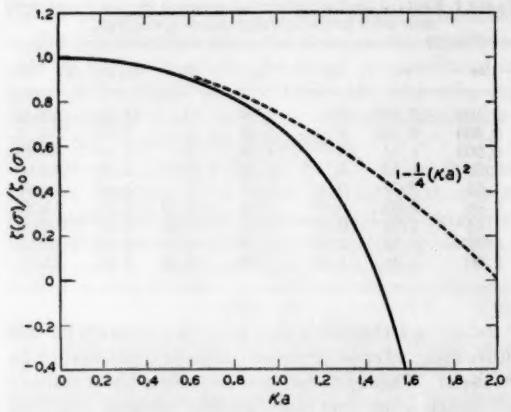

FIG. 1. Computed values of the ζ potential ratio (solid line), with the limiting parabolic behavior (dotted line) shown explicitly.

The results (57) reduce to

$$A_1=2/\kappa, \qquad A_2=0, \tag{58}$$

as κa approaches zero, to yield the correct Debye-Hückel result anticipated earlier:

$$\phi_0(x_1)=(2/\kappa)\exp(-\kappa x_1). \tag{59}$$

The ζ potential predicted on the basis of (59) follows from (55)

$$\zeta_0(\sigma)=4\pi\sigma/\kappa D, \tag{60}$$

a well-known result.

The ζ potential for finite κa may be exhibited in the following reduced form:

$$\zeta(\sigma)/\zeta_0(\sigma)=(\kappa a/y_1)\left[\frac{1-(y_1/y_2)^2\exp(y_1-y_2)}{1-(y_1/y_2)\exp(y_1-y_2)}\right]. \tag{61}$$

Reference to the asymptotes (47) and (49) for y_1 and y_2 show that the lowest order deviation (in κa) from ζ_0 is in the direction of decreasing ζ potential. In particular,

$$\zeta(\sigma)/\zeta_0(\sigma)=1-\tfrac{1}{4}(\kappa a)^2, \qquad \kappa a\ll 1. \tag{62}$$

As noted earlier, y_1 and y_2 have a common value when $\kappa a=1.03$. At this point, both A_1 and A_2 diverge, but ϕ in fact remains finite

$$\phi(x_1)=(c_1x_1+c_0)\exp[-y_1(x_1/a)], \qquad \kappa a=1.03. \tag{63}$$

Likewise, the ζ potential ratio as written in (61) is indeterminate, but may be properly evaluated as a limiting value as κa approaches 1.03 from either side.

When $\kappa a>1.03$, the complex conjugates $y_1=\alpha+i\beta$ and $y_2=\alpha-i\beta$ yield the ratio,

$$\zeta(\sigma)/\zeta_0(\sigma)=\kappa a/(\alpha^2+\beta^2)\left[\frac{(\alpha^2-\beta^2)\sin\beta+2\alpha\beta\cos\beta}{\alpha\sin\beta+\beta\cos\beta}\right]. \tag{64}$$

The ζ potential ratio has been computed on the basis of Eqs. (61) and (64) using the tabulated y_1 and y_2 values. The results are shown in Fig. 1. The low κa behavior is a parabolic decrease from unity in accord with (62). The ratio then decreases at an even more rapid rate, finally changing sign near $\kappa a=1.46$.[15] Since ζ_0 is always positive, therefore, we find that at a certain finite concentration, the ζ potential due to the diffuse Guoy layer (and, therefore, the Gouy layer reciprocal capacitance) becomes precisely zero. It is of interest to observe in addition that there is no break in the ζ potential curve at the singular value $\kappa a=1.03$, although the nature of the mean charge density, ρ_{el}, changes rapidly there.

[15] In water, at room temperature, this corresponds to about 0.8 moles/liter for a uniunivalent electrolyte with a equal to 5×10^{-8} cm.

Diffusion of Weak Electrolytes

W. H. STOCKMAYER

Department of Chemistry, MIT, Cambridge 39, Massachusetts

(Received August 11, 1960)

An expression is obtained by standard irreversible thermodynamics for the diffusion coefficient of a weak electrolyte in rapid equilibrium with an arbitrary number of species. The general result reduces to a simple form if all mobilities are independent of concentration.

VERY recently Creeth and Stokes[1] have discussed approximately the diffusion coefficient of an incompletely dissociated unibivalent electrolyte. The writer some time ago obtained the general expression for a single weak electrolyte of any valence type, and it seems worth while to communicate the result at this time.

Consider the weak electrolyte $A_{\nu_A}B_{\nu_B}$ at volume-formal concentration c. Let the ith solute species produced by dissociation or polymerization (or both) of this electrolyte have the formula $A_{p_i}B_{q_i}$, with algebraic charge z_i and molar concentration c_i. These quantities are subject to the conservation laws:

$$c=\nu_A^{-1}\sum_i p_i c_i=\nu_B^{-1}\sum_i q_i c_i,$$

$$z_i=p_i z_A+q_i z_B,$$

$$\sum_i c_i z_i=0,$$

$$\nu_A z_A+\nu_B z_B=0. \tag{1}$$

The flow of species i is given[2] by

$$J_i=-\sum_k \Omega_{ik}\nabla(\mu_k+z_k F\psi) \tag{2}$$

in the usual[2] symbolism. In a pure diffusion experiment, the electric current vanishes ($\sum_i z_i J_i=0$) and therefore

$$-F\nabla\psi=\sum_j z_j^{-1}t_j\nabla\mu_j, \tag{3}$$

where we have introduced the electric transport numbers

$$t_j\equiv z_j\sum_k z_k\Omega_{jk}/\sum_i\sum_k z_i z_k\Omega_{ik}. \tag{4}$$

If we now use (3) in (2), the flux becomes

$$J_i=-\sum_k(\Omega_{ik}-z_k^{-1}t_k\sum_j z_j\Omega_{ij})\nabla\mu_k. \tag{5}$$

By introduction of the specific conductance

$$L=F^2\sum_i\sum_k z_i z_k\Omega_{ik}, \tag{6}$$

the above result may be given the more symmetrical form

$$J_i=-\sum_k L_{ik}\nabla\mu_k;$$

$$L_{ik}\equiv\Omega_{ik}-(t_i t_k L/z_i z_k F^2). \tag{7}$$

Now all the chemical reactions are assumed to be locally at equilibrium, so that the chemical potentials satisfy the relations

$$\mu_k=p_k\mu_A+q_k\mu_B; \qquad \mu=\nu_A\mu_A+\nu_B\mu_B, \tag{8}$$

where μ_A, μ_B are the potentials of the ion constituents A, B; and μ without subscript is that of the component electrolyte. After introducing (8) into (7) and using (1) and (4), we find the flow of the solute component to be

$$J=\nu_A^{-1}\sum_i p_i J_i=\nu_B^{-1}\sum_i q_i J_i=-\Omega\nabla\mu, \tag{9}$$

where

$$\Omega=\nu_A^{-2}\sum_i\sum_k p_i p_k L_{ik}=\nu_A^{-1}\nu_B^{-1}\sum_i\sum_k p_i q_k L_{ik}. \tag{10}$$

Clearly Ω can be written in two other forms obtained by interchanging p, q and ν_A, ν_B or in any convenient linear combination of these forms. The coefficients of diffusion is, of course, defined by

$$D\equiv -J/\nabla c=\Omega(\partial\mu/\partial c)_{T,P}. \tag{11}$$

Since we have not appealed to the symmetry of the matrix Ω_{ik} our result does not depend on the frame of reference chosen. The only restrictions on the result are (a) that the solute can be treated as a single component, which excludes acid salts like $KHSO_4$ or salts which hydrolyze extensively; and (b) that the rates of all the chemical reactions are sufficiently rapid for the application of relations (8). A more quantitative statement of restriction (b) would depend on the particular system and experimental details. If the departures from local chemical equilibrium were small but not totally negligible, the general procedure of Kirkwood and Crawford[3] could be used to formulate the continuity equations, but their detailed solution would be complicated. In the case of a simple symmetrical weak electrolyte the correction terms would be measured by $\tau\Delta D/a^2$, where τ is the relaxation time[2] of the reaction, ΔD the difference in diffusivity of ionized and unionized forms, and a the dimension of the diffusion apparatus.

[1] J. M. Creeth and R. H. Stokes, J. Phys. Chem. **64**, 946 (1960).

[2] See H. S. Harned and B. B. Owen, *The Physical Chemistry of Electrolytic Solutions* (Reinhold Publishing Corporation, New York, 1958) 3rd ed.

[3] J. G. Kirkwood and B. L. Crawford, Jr., J. Phys. Chem. **56**, 1048 (1952).

For ideal dilute solutions, we may put

$$\Omega_{ik}^{0}=\delta_{ik}c_k D_k^{0}/RT, \tag{12}$$

where D_k^0 is the ideal diffusivity of species k. We then easily recover the previously[1] published special cases. In this connection, it is amusing to exhibit the general result in yet another form. If we introduce the transference numbers of the ion constituents,

$$t_A/z_A=\sum_i z_i^{-1}l_i p_i, \qquad t_B/z_B=\sum_i z_i^{-1}l_i q_i, \tag{13}$$

we find

$$\Omega=\frac{-Lt_A t_B}{F^2\nu_A\nu_B z_A z_B}+\frac{1}{\nu_A\nu_B}\sum_i\sum_k p_i q_k\Omega_{ik}, \tag{14}$$

where the first term is seen at a glance to reduce at infinite dilution to the familiar Nernst limit. As an example, we apply (12) and (14) to cadmium iodide, considering the species I^- and $CdI_n^{2-n}(0\leqslant n\leqslant 4)$, and obtaining

$$\Omega=\frac{Lt_A t_B}{4F^2}+\frac{1}{2RT}\sum_n nc_n D_n^{0}, \tag{15}$$

where the index n refers to the complex ion species.

The application of (10) or (14) to real solutions containing more than two ion species will involve all the difficulties of the relaxation effect.[4] It should perhaps also be noted that for uncharged species the quantity t_i/z_i need not vanish if charged species are present, although in sufficiently dilute solution the resulting terms must be negligible.

ACKNOWLEDGMENTS

This work originated in a conversation with J. L. Oncley and was greatly stimulated by discussions with the late John G. Kirkwood.

[4] L. Onsager and S. K. Kim, J. Phys. Chem. **61**, 215 (1957).

THE JOURNAL OF CHEMICAL PHYSICS VOLUME 33, NUMBER 5 NOVEMBER, 1960

New Type of Freezing-Point Apparatus. Freezing Points of Dilute Lanthanum Chloride Solutions*

G. SCATCHARD, B. VONNEGUT, AND D. W. BEAUMONT

Department of Chemistry, Massachusetts Institute of Technology, Cambridge 39, Massachusetts

(Received May 11, 1960)

A new type of freezing-point apparatus is described that reduces the errors of previous types. The freezing-point depressions of aqueous lanthanum chloride solutions up to 0.04 m are adequately expressed by the Debye-Hückel approximation for ions with $a=6.15$ A plus a very small linear term. The "higher terms" are computed by combining the equations of Mayer and Kirkwood, using the tables of Poirier, and are found to be very small in this case.

The parameters for the calculation of the activity of water from freezing point depressions, for the Debye-Hückel theory, and for the Kirkwood parameter B_{ik} are redetermined, and the more general use of B_{ik} is discussed.

APPARATUS

THE freezing point measurements reported from this laboratory were all measured in a single apparatus.[1] When this apparatus wore out, we decided to build one of entirely new design, in order to utilize even more fully the great accuracy of the differential equilibrium method of measuring freezing points. We made this apparatus as nearly adiabatic as possible because heat leaks decrease the accuracy of measurement, and because the greater heat leak into the vessel containing solution in the customary apparatus soon makes the amount of ice in this vessel less than in the other, and may decrease the advantages of twin vessels. We reduced the height of ice-liquid interface to about 4 cm and stirred the system by flowing the liquid gently to and fro, because the pressure corresponding to 1-cm head of water makes a difference of 8×10^{-6}°C in the freezing point. We evacuated the vessels because each atmosphere of nitrogen or air causes a decrease of about 10^{-3}°C in the freezing point of water or of an aqueous solution.

Each freezing-point vessel has an ω-shaped cross section and may be described as a right section of a cylindrical surface generated by translating an ω-shaped curve perpendicularly to the plane of the curve. The two vessels are mounted with a common axis, and the stirring is caused by rocking the vessels in unison 30° each side of horizontal about this common axis at

* Based on the Ph.D. theses of B. Vonnegut (1939) (present address: Arthur D. Little, Inc., Cambridge, Massachusetts) and D. W. Beaumont (1942), deceased. The final computations and correlation were supported financially by the U.S. Atomic Energy Commission.

[1] The last paper in the series is G. Scatchard and M. A. Benedict, J. Am. Chem. Soc. **58**, 837 (1936).

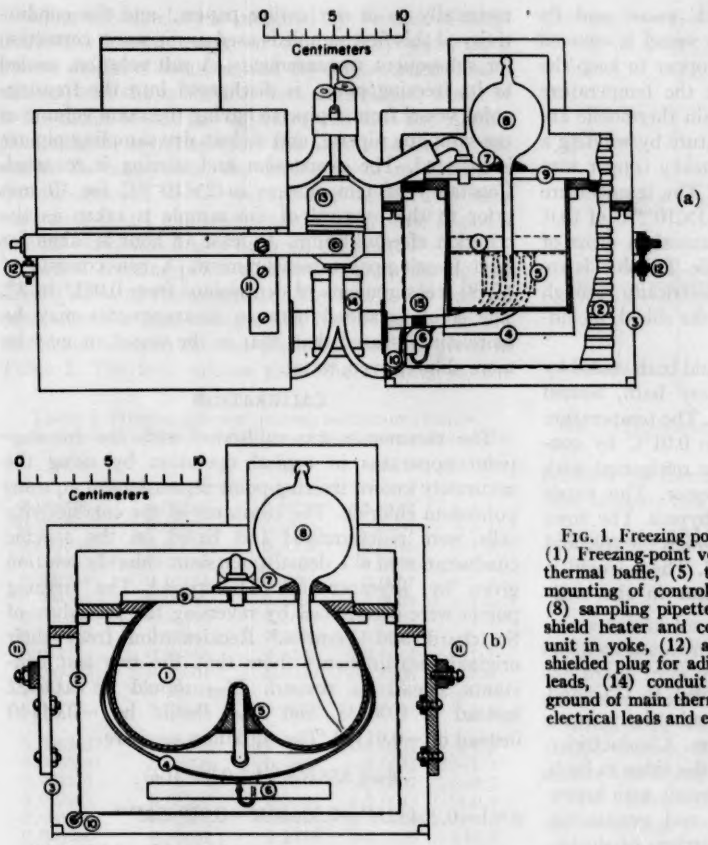

FIG. 1. Freezing point apparatus: (a) front view, (b) end view. (1) Freezing-point vessel, (2) adiabatic shield, (3) housing, (4) thermal baffle, (5) thermopiles mounted in Wood's metal, (6) mounting of control thermopile on shield, (7) vacuum cups, (8) sampling pipette, (9) glass cover, (10) leads to adiabatic-shield heater and control thermopile, (11) swivel supports of unit in yoke, (12) adjustable point of suspension of unit, (13) shielded plug for adiabatic-shield heater and control thermopile leads, (14) conduit for main thermopile leads, (15) thermal ground of main thermopile wire to adiabatic shield, (16) flexible electrical leads and evacuation tubes.

the rate of 6–12 cycles/min. Most of the liquid flows from the rising cup over the central ridge of the ω, but the ice is retained. The junctions of the differential thermopile are embedded in Wood's metal on the under side of the central ridge.

The vessel is planned to operate with approximately equal volumes of ice and solution, covering the central ridge with about 1 cm of liquid. The shape of the vessel is carefully planned so that this head remains nearly constant as the vessel is rocked. At the end of each cycle, much of the liquid has drained from the interstices of the ice in the upper cup, and there is a layer of liquid below the ice in the lower one.

The details of the vessels are shown in front view in Fig. 1(a) and in side view in Fig. 1(b). Each vessel (1) is surrounded by a thermal shield (2) in the form of a copper box which is maintained at a temperature close to that of the vessel by electrical heating. This thermal shield is surrounded by insulation and another box of metal (3). This system is immersed in a stirred air bath which is surrounded by a liquid bath, accurately regulated at a temperature slightly below that of the colder vessel.

The vessels are of "rolled gold plate," an alloy of 75% gold and 25% copper about 0.05 mm thick, welded to a backing of high copper brass, 0.13 mm thick on the curved portions and 0.20 mm on the flat ends. The vessels were fabricated with 14-carat gold solder. Frames of 6-mm brass were fastened to the tops of the vessels externally with soft solder. They were ground flat to receive the covers of plate glass (9). Each cover is pierced with two holes, one for the tube through which the vessel is evacuated and one for the pipette (8) in which is taken the sample to be analyzed. The tube and the pipette are held in position by small suction cups (7), designed to fasten small objects to an automobile windshield.

The main thermopile (5) is a pair of independent copper-constantan piles, each of 64 junctions, and each with an extra lead to its center. The pile can be used as 32, 64, 96, or 128 junctions. For test purposes the first pile can be opposed to the second, or either half of the first opposed to either half of the second. The junctions are immersed in a mass of Wood's metal which occupies the middle portion of the grooves formed by the ridges of the ω's. In addition to the main pile, there is a

five-junction pile (6) between each vessel and its thermal shield. The bottom of each vessel is covered by a thermal baffle (4) of 0.8-mm copper to keep the thermopile as nearly as possible at the temperature of the contents. The leads of the main thermopile are brought more closely to this temperature by winding a section of the insulated wires with heavy copper wire (15) soldered to the thermal shield. The temperature of the thermal shield is kept within 3×10^{-4}°C of that of the vessel. A difference of 1° causes an error of 2×10^{-3}° in the reading of the main pile. The shields are cooled by the air bath and heated electrically through resistant windings on the outside of the shield, including the cover, with manual control.

The air bath is surrounded by a liquid bath cooled by circulating the liquid from a primary bath, heated electrically and controlled to 0.001°C. The temperature of the primary bath is controlled to 0.01°C by controlling the rate of evaporation of the refrigerant with continuous operation of the compressor. The vapor line contains a solenoid valve and a bypass. The flows are controlled so that the bath cools when the solenoid is open, and warms when it is closed. The solenoid is operated through a mercury regulator in the well-stirred primary bath.[2]

PROCEDURE

The freezing-point vessels are cooled to 0°C and filled to the level of the ridges with conductivity water ice cracked to pieces of about 1 cm. Conductivity water is added to a level 1 cm above the ridge in both vessels. The covers are sealed to the vessels with heavy lubricant, the pipettes are inserted and evacuating tubes attached, and the removable portions of shields and housing are put in place. The stirring is started and the vessels are evacuated to the triple point. Next the heating currents to the shields are adjusted. The electromotive force of the thermopile is measured on a Leeds and Northrup "White" potentiometer with steps of 1 μv. Fractions of a microvolt are determined by deflection of a Leeds and Northrup high-sensitivity galvanometer measured on an illuminated scale 6 m distant. The Vernier scale designed by one of us[3] made possible reading to 0.1 mm. The reading of the thermopile was usually a few tenths of a microvolt, which was deducted from all measurements in that series. The rocking is stopped and a sample is withdrawn from one side by admitting air to the vessel.[4] The contents of the pipette are analyzed conductimetrically as in our earlier papers,[1] and the conductivity of this first sample is used as the water correction for subsequent measurements. A salt solution, cooled to its freezing point, is discharged into the freezing-point vessel from a pipette having the same volume as the sampling pipette, and a clean dry sampling pipette is inserted. The evacuation and stirring is resumed. Constancy of temperature to 2×10^{-5}°C for 10 min prior to the removal of the sample is taken as the criterion of equilibrium. At least an hour is taken for each freezing-point measurement. A run consists of 15–30 measurements of depressions from 0.001° to 3°. The solution added between measurements may be more concentrated than that in the vessel, or may be more dilute, even water.

CALIBRATION

The thermopile was calibrated with the freezing-point apparatus in typical operation by using the accurately known freezing-point depressions of aqueous potassium chloride. The constants of the conductivity cells were redetermined and based on the specific conductance of 0.1 demal potassium chloride solution given by Bremner and Thompson.[5] The freezing points were determined by reversing the procedure of Scatchard and Prentiss.[6] Recalculation from their original measurements show that the two last constants should be revised. D'_{222} should be 0.06922 instead of 0.06935, and E'_{222} should be -0.01140 instead of -0.01144. The equations used are

$$\theta=1.858M\phi/(1+0.001M\phi),$$

$$\phi=1-0.26432M^{\frac{1}{2}}+0.32640M-0.27975M^{3/2}+0.13844M^{2}-0.02850M^{5/2},$$

and

$$\theta=AE+BE^{2}+CE^{3},$$

in which θ is the freezing point depression, M the total molality, νm, m is the salt molality, ν is the number of ions formed from one molecule of salt, ϕ the osmotic coefficient, E the electromotive force and A, B, and C are coefficients characteristic of the thermopile.

MEASUREMENT WITH LANTHANUM CHLORIDE

The freezing points of dilute aqueous solutions of lanthanum chloride were measured. A quantity of $LaCl_3\cdot7H_2O$ was purified by crystallizing three times from conductivity water.[7] The concentration of a stock solution of salt in conductivity water was determined by gravimetric silver chloride analysis.[8] Several series

[2] We are very grateful for the friendly help of the following firms in the construction of this apparatus: The Gorham Company, Providence, Rhode Island; The General Plate Company, Attleboro, Massachusetts; and Harmon and Handy Company, Hartford, Connecticut.

[3] Bernard Vonnegut, Rev. Sci. Instr. **12**, 335 (1941).

[4] A very small amount of air is admitted while the vessel is tipped so that the pipette is out of the liquid, and then air is admitted to atmospheric pressure while the tip is immersed. This prevents the liquid from coming into contact with the cap of the pipette.

[5] R. W. Bremner and T. G. Thompson, J. Am. Chem. Soc. **59**, 2372 (1937).

[6] G. Scatchard and S. S. Prentiss, J. Am. Chem. Soc. **56**, 2320 (1934).

[7] Dr. C. M. Mason, at the time Associate Professor of Chemistry at the University of New Hampshire, kindly furnished us with an ample supply of the starting material.

[8] All weights were corrected to vacuum using the densities determined by G. Jones and C. F. Bickford, J. Am. Chem. Soc. **56**, 608 (1934).

of dilute solutions were prepared by successive additions of a known weight of conductivity water to a known weight of solution, and the conductance of each solution and the ratio m/L were determined, where m is the moles of salt per kg water and L is the specific conductance corrected for the conductance of the water. To interpolate, the deviations of m/L from a quartic equation in $(L)^{\frac{1}{2}}$ were plotted against $(L)^{\frac{1}{2}}$ on a scale such that 1 mm represented 0.02% of m/L, and a smooth curve was drawn between the points.

Several freezing-point runs were made during the development of the apparatus. The results for the two runs after the final changes and for the more concentrated solutions in the last preceding run are given in Table I. The first column gives the molality m, the second is the freezing point depression in centigrade degrees θ, the third is ϕ defined by Eq. (1), the fourth is $\Delta\phi$, the deviation of the measured value from that calculated by Eq. (2), and the fifth is the corresponding deviation in the depression θ. The values of $\Delta\phi$ are plotted against $(I/2)^{\frac{1}{2}}$ in Fig. 2. The two broken lines represent $\Delta\phi$ corresponding to 2×10^{-5}°C or 10^{-3} θ, whichever is the larger.

TABLE I. Freezing points of aqueous lanthanum chloride.

m	θ	ϕ	$\Delta\phi$	$\Delta\theta\times10^5$
0.0002566	0.00186_0	0.9770	+0.0167	+3.1
0.0005793	0.00406_8	0.9432	−0.0004	−0.2
0.001034	0.00710_4	0.9238	−0.0046	−3.3
0.001683	0.01140	0.9106	−0.0030	−3.4
0.002751	0.01834	0.8962	−0.0007	−1.3
0.004451	0.02915	0.8802	+0.0009	+2.6
0.006506	0.04190	0.8656	+0.0007	+2.9
0.009865	0.06241	0.8504	+0.0013	+8.1
0.01357	0.08468	0.8388	+0.0013	+11.1
0.01954	0.12001	0.8256	+0.0006	+7.2
0.01380	0.19180	0.8108	±0.0000	±0.0
0.04272	0.25541	0.8037	−0.0001	−2.6
0.0002657	0.00188_1	0.9516	−0.0081	−1.5
0.0005841	0.00408_6	0.9403	−0.0031	−1.3
0.001133	0.00779_0	0.9251	−0.0007	−0.7
0.002222	0.01502	0.9086	+0.0043	+6.5
0.003676	0.02431	0.8889	+0.0024	+4.8
0.005986	0.03882	0.8717	+0.0026	+10.9
0.008654	0.05518	0.8571	+0.0030	+16.5
0.01369	0.08546	0.8393	−0.0004	−3.4
0.01904	0.11729	0.8281	+0.0022	+25.6
0.02876	0.17422	0.8143	+0.0008	+13.9
0.03719	0.22339	0.8074	+0.0005	+11.2

The osmotic coefficient (see Appendix) is defined as

$$\phi=\theta/(1.860-0.001\theta)4m. \quad (1)$$

As shown by Table I and Fig. 2, our results are fitted within their scatter by the equation

$$\phi=1-1.6992Z_2-0.06m, \quad (2)$$

in which Z_2 is the Debye-Hückel function for $\kappa a=2(I/2)^{\frac{1}{2}}$ (see Appendix). Except for a small correction arising from the heat of dilution and the difference between the freezing points of the solution and of the pure solvent, this corresponds to

$$\ln\gamma=-3.3984(I/2)^{\frac{1}{2}}/[1+2(I/2)^{\frac{1}{2}}]-0.12m. \quad (3)$$

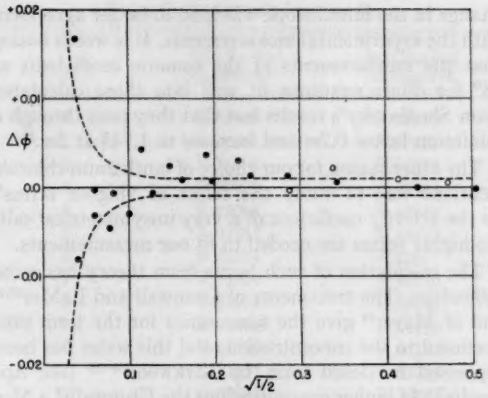

FIG. 2. Deviations for lanthanum chloride freezing points.

DISCUSSION

One reason for choosing lanthanum chloride for our first measurements was that Shedlovsky and MacInnes[9] had found from measurements of the emf of cells with transference and the transference numbers that the limiting slope was only about two-thirds that of the Debye theory. Shedlovsky[10] later recalculated their results and found agreement with the theory.[11]

The measurements of the osmotic coefficient have the advantage over those of activity coefficients of the solute that the value at infinite dilution is known. The intercept in Fig. 2 must be zero. It is clear that no

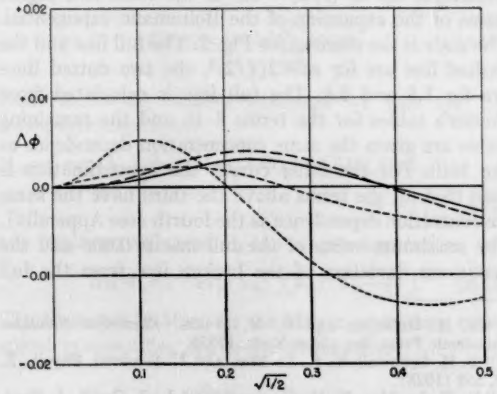

FIG. 3. Deviations for higher terms.

[9] T. Shedlovsky and D. A. MacInnes, J. Am. Chem. Soc. **61**, 200 (1939).

[10] T. Shedlovsky, J. Am. Chem. Soc. **72**, 3680 (1950).

[11] Publication of our results were delayed first by the press of war work, then to permit prior publication by Shedlovsky, by death of one author, and again by the press of other work.

change in the initial slope will lead to better agreement with the experimental measurements. It is worth noting that the measurements of the osmotic coefficients at 25° for dilute solutions fit well into those calculated from Shedlovsky's results but that they pass through a minimum below $0.2m$ and increase to 1.748 at $2m$.[12]

The other reason for our choice of lanthanum chloride solutions was to study the effect of "higher terms" on the activity coefficient of a very unsymmetrical salt. No higher terms are needed to fit our measurements.

The calculation of such terms from theory has some difficulties. The treatments of Gronwall and LaMer[13,14] and of Mayer[15] give the same series for the term proportional to the concentration, and this series has been expressed in closed form by Kirkwood[16–18] (see Appendix). At higher concentrations the Gronwall-La Mer treatment gives difficulties because of nonintegrability, and the Mayer treatment neglects triple interactions. The theory has been extended by Friedman,[19] but not yet in a form suitable for our purposes. The Gronwall-LaMer theory also has the practical disadvantage that their calculations are made only for the third and fourth terms and only to $\kappa\alpha=0.4$ For a 3–1 electrolyte with $\kappa\alpha=2(I/2)^{\frac{1}{2}}$, a $0.04m$ solution corresponds to $\kappa\alpha=1.0$, and the maximum value of the coefficient of m comes only with the eighth term. Since Poirier[20] has computed the Mayer expression through the 16th term, we have used his tables and assumed that the difference between the Kirkwood expression and that of the first 16 terms in the expansion has the same concentration dependence as the 16th term.[18] Although the eighth term is about twice the complete series, the 16th term is only about a sixth, and the sum of the remaining terms is about a ninth of the total.

Figure 3 shows the contributions to ϕ of a 3–1 electrolyte up to $(I/2)^{\frac{1}{2}}=0.5$ of the third and higher terms of the expansion of the Boltzmann exponential. The scale is the same as for Fig. 2. The full line and the dashed line are for $\kappa\alpha=2(I/2)^{\frac{1}{2}}$, the two dotted lines are for 1.5 and 2.5. The full line is calculated from Poirier's tables for the terms 3–16 and the remaining terms are given the same concentration dependence as the 16th. For the other curves the approximation is used that all the terms above the third have the same concentration dependence as the fourth (see Appendix). The maximum value of the full line is 0.003 and the maximum deviation of the broken line from the full one is 0.001. We trust that the approximation is also good for the other sizes.

An attempt to include the effect of these higher terms in an equation of the type of Eq. 2 would lead to a slightly larger value for a and a more negative coefficient of m. The value of this coefficient cannot be used to determine the correct size because there are also nonelectrostatic terms, such as that due to hydration, in the coefficient of m. The fit would be limited to concentrations below the inflection points in Fig. 3, but it is quite possible that the inflections are caused by the limitation of the Mayer equation to binary encounters.

For potassium chloride solutions we found $\kappa\alpha=1.5(I/2)^{\frac{1}{2}}$. If we use 1.5 for the chloride ion, additivity of radii leads to 2.5 for the lanthanum ion. The Debye-Hückel term is unchanged, the third term is changed slightly but in a complicated way. The higher terms are reduced but the relative effect decreases with increasing concentration. We have not made the much more tedious computation of the effect for ions of different sizes, but we are convinced that the effect is still very small. Moreover, as pointed out by Mayer and by Friedman, it is not necessary that the ionic radii be additive. We will therefore be satisfied with the indication of the calculation for equal sizes that theory, like experiment, indicates sufficiency of the Debye-Hückel approximation for lanthanum chloride in water.

APPENDIX

Osmotic Coefficients from Freezing Points

The osmotic coefficients from freezing points may be defined by the relation

$$\phi_f=\theta_f/(\lambda_0+\lambda_1\theta_f+\lambda_2\theta_f^2+\lambda_3\theta_f^3+\cdots)\nu m, \qquad \text{(A1)}$$

in which θ_f is the freezing point depression, ν the number of particles from one molecule of solute, and m the molality, so that νm is the osmolality of the solution. The λ's are parameters calculable from the specific heat of fusion and heat capacities of ice and water. At our request Dr. Rossini[21] correlated the National Bureau of Standards measurements of the heat capacities[22,23] and induced Dr. Osborne[24] to revise the heat of fusion of ice. Dr. Rossini calculated λ_0 as 1.860 (1.8599±0.0011, now reduced to 1.8598 by changing T_0 from 273.16 to 273.15), and we determine the other coefficients as $\lambda_1=-9.49\times10^{-4}$, $\lambda_2=9.32\times10^{-6}$, $\lambda_3=7.25\times10^{-8}$. For depressions less than 10°, 0.1% accuracy is assured by the much simpler form

$$\phi=\theta/(1.860-0.001\theta)\nu m. \qquad \text{(A2)}$$

[12] R. A. Robinson and R. H. Stokes, *Electrolyte Solutions* (Academic Press, Inc., New York, 1955).
[13] T. H. Gronwall, V. K. La Mer, and K. Sandved, Physik. Z. **29**, 558 (1928).
[14] V. K. La Mer, T. H. Gronwall, and L. J. Greiff, J. Phys. Chem. **35**, 2245 (1931).
[15] J. E. Mayer, J. Chem. Phys. **18**, 1426 (1950).
[16] J. G. Kirkwood, Chem. Revs. **19**, 275 (1936).
[17] G. Scatchard and L. F. Epstein, Chem. Revs. **30**, 211 (1942).
[18] G. Scatchard, Natl. Bur. Standards Circ. **524**, 185 (1953).
[19] H. Friedman, Mol. Phys. **2**, 23, 190, 436 (1959); J. Chem. Phys. **32**, 1134 1351 (1960).
[20] J. C. Poirier, J. Chem. Phys. **21**, 965, 972 (1953).
[21] F. D. Rossini (private communication, October 18, 1939).
[22] H. C. Dickinson and N. S. Osborne, Natl. Bur. Standards, Sci. Paper 248, (1915).
[23] N. S. Osborne, H. F. Stimson, and D. C. Ginnings, J. Research Natl. Bur. Standards **23**, 197 (1939).
[24] N. S. Osborne, J. Research Natl. Bur. Standards **23**, 643 (1939).

Guggenheim and Turgeon[25] obtained the same value for λ_0, and $-1.860\times4.8\times10^{-4}$ for λ_1.

Debye-Hückel Osmotic Coefficient

If

$$\ln\gamma_{\pm}=z_+z_-A(I/2)^{\frac{1}{2}}/[1+a'(I/2)^{\frac{1}{2}}], \quad \text{(A3)}$$

$$\phi-1=z_+z_-AZ_{a'}/a', \quad \text{(A4)}$$

in which

$$Z_{a'}=[(1+\kappa a)-1/(1+\kappa a)-2\ln(1+\kappa a)]/(\kappa a)^2. \quad \text{(A5)}$$

$\kappa a=a'(I/2)^{\frac{1}{2}}$. $Z_{a'}$ is not easy to compute for dilute solutions, but it may easily be interpolated from the tables of Z as a function of $\kappa a/(1+\kappa a)$ given by Scatchard and Epstein.[17] We have computed the Debye-Hückel parameters from the dielectric constant measurements of Malmburg and Maryott[26] and the universal constants of Cohen, Diamond, Layton, and Rollett[27] to give A of Eqs. (A3) and (A4) as

$$A=1.1328[1+0.1369(t/100)+0.0669(t/100)^2+0.0073(t/100)^3], \quad \text{(A6)}$$

$$10^{-8}\kappa/(I/2)^{\frac{1}{2}}=0.3250[1+0.0447(t/100)+0.0039(t/100)^2+0.0021(t/100)^3]. \quad \text{(A7)}$$

$I/2$ is the ionic strength in moles per kg of water.

Kirkwood Function, B_{ik}

For spherically symmetrical, rigid, nonpolarizable ions in a continuous medium of uniform dielectric constant, the electrostatic contribution to the term proportional to the concentration arising from powers of b_{ik} higher than b_{ik}^3 in the expansion of $\exp(b_{ik})$ is

$$\phi_K=-\frac{2\pi N\rho_0}{1000}\sum_{k=\alpha}^{\omega}\sum_{i=\alpha}^{\omega}m_im_ka_{ik}^3b_{ik}^3B_{ik}\Big/\sum_{l=\alpha}^{\omega}m_l, \quad \text{(A8)}$$

in which N is Avogadro's number, ρ_0 the density of the solvent, m_i the concentration of species i in moles per kg, a_{ik} the collision diameter of i and k, $b_{ik}=-z_iz_ke^2/DkTa_{ik}$, and B_{ik} is the Kirkwood function

$$B_{ik}=\int_0^{b_{ik}}t^{-4}(e^t-1-t-t^2/2-t^3/6)\,dt$$

$$=\{b_{ik}^3[Ei(b_{ik})-\ln|b_{ik}|-C_0]-\exp(b_{ik})(2+b_{ik}+b_{ik}^2)+(2+3b_{ik}+3b_{ik}^2+11b_{ik}^3/6)\}/6b_{ik}^3, \quad \text{(A9)}$$

in which $Ei(b_{ik})$ is the exponential integral

$$\int_{-\infty}^{b_{ik}}t^{-1}e^t\,dt,$$

and C_0 is Euler's constant. This expression is exact for the foregoing model.

We have found the Kirkwood function so useful that Allen Gee recomputed more accurately the values in the range of the tables for the exponential integral, which is -15 to $+15$. The results are recorded in Table II as $\log(B_{ik}/b_{ik})$, which is a convenient function for interpolation.

TABLE II. Kirkwood's function B_{ik}.

$\lvert b_{ik}\rvert$	$\log(B_{ik}/b_{ik})$ b_{ik} positive	$\log(B_{ik}/b_{ik})$ b_{ik} negative
0	$\bar{8}.61979$	$\bar{8}.61979$
1	$\bar{8}.66607$	$\bar{8}.57882$
2	$\bar{8}.71888$	$\bar{8}.54228$
3	$\bar{8}.87979$	$\bar{8}.50932$
4	$\bar{8}.85058$	$\bar{8}.47946$
5	$\bar{8}.93352$	$\bar{8}.45192$
6	$\bar{9}.03104$	$\bar{8}.42671$
7	$\bar{9}.14569$	$\bar{8}.40329$
8	$\bar{9}.27974$	$\bar{8}.38148$
9	$\bar{9}.43489$	$\bar{8}.36110$
10	$\bar{9}.61190$	$\bar{8}.34193$
11	$\bar{9}.81051$	$\bar{8}.32385$
12	0.02951	$\bar{8}.30683$
13	0.26703	$\bar{8}.29052$
14	0.52909	$\bar{8}.27510$
15	0.78995	$\bar{8}.26038$

For values of b_{ik} more negative than -10, very precise values may be obtained from the expression

$$B_{ik}=0.20936-\tfrac{1}{6}\ln|b_{ik}|+\tfrac{1}{2}b_{ik}+\tfrac{1}{2}b_{ik}^2+\tfrac{1}{3}b_{ik}^3. \quad \text{(A10)}$$

For values of b_{ik} more positive than 15, the exponential integral may be obtained from the asymptotic expansion

$$Ei(x)=(e^x/x)\sum_{n=0}^{\infty}n!/x^n. \quad \text{(A11)}$$

With somewhat smaller precision we can use the asymptotic expansion

$$B_{ik}=[\exp(b_{ik})/b_{ik}^4]\{1+(4/b_{ik})+[(4\times5)/b_{ik}^2]+\cdots\} \quad \text{(A12)}$$

and for larger values of b_{ik} the simpler expression

$$B_{ik}=[b_{ik}^{-4}\exp(b_{ik})][b_{ik}/(b_{ik}-4)]. \quad \text{(A13)}$$

The Gronwall-LaMer and the Mayer expansions correspond to expanding B_{ik} as the power series

$$B_{ik}=\sum_{n=4}^{\infty}[b_{ik}^n/n!(n-3)]. \quad \text{(A14)}$$

The success of our approximation using the concentration dependence of the fourth term in Fig. 4 depends upon the facts that most of the coefficient comes from the interaction of pairs of trivalent cations, for

[25] E. A. Guggenheim and J. C. Turgeon, Trans. Faraday Soc. **51**, 747 (1958).
[26] G. C. Malmberg and A. A. Maryott, J. Research Natl. Bur. Standards **56**, 1 (1956).
[27] E. R. Cohen, J. W. Diamond, T. W. Layton, and J. S. Rollett, Revs. Modern Phys. **27**, 363 (1955).

which the series is alternating, and that the concentration dependence varies smoothly and rather slowly as a function of n.

For cation-anion interaction, for which all the terms are negative, or for a symmetrical salt, for which the odd terms vanish, the best approximation should be to use the concentration dependence for n nearest b_{ik}. This would permit the use of Poirier's tables up to $b_{ik}=16$. For 0°C this corresponds to $-Da_{ik}/z_iz_k$ of about 40, or to a dielectric constant of about 7 for univalent ions 6A in diam. For larger values of b_{ik} the best approximation is to consider the contribution to the osmotic coefficient as minus half the association constant. For these large values of b_{ik}, the Q of Bjerrum[28] approaches B_{ik}, so that this method is essentially that of Bjerrum. A fair measure of the approximation of this method is the ratio of the contribution of pairs of ions of like charge to that of pairs of unlike charge. The proposal of Scatchard and Epstein to include the effect of pairs of like charge in the association constant for pairs of unlike charge may be regarded as a very crude method of determining the concentration dependence which we would now replace with the use of Poirier's tables outlined in the foregoing.

[28] N. Bjerrum, Kgl. Danske Videnskab. Selskab Mat. fys. Medd. **I**, No. 9 (1926).

For small values of the dielectric constant, the value of K calculated from B_{ik} or from Q is[29]

$$K=(4\pi N/1000)a_{ik}^3\exp(b_{ik})/b_{ik}. \qquad \text{(A15)}$$

Our use of K does not necessarily imply a distinction between bound and unbound ions, particularly as contributing to conductance. This step requires a use of intuition, which we are very willing to accept. However, it does appear that Fuoss[30] has taken a step backward in preferring to the Bjerrum treatment that of Denison and Ramsay[31] which makes $K=\exp b_{ik}$ and so ignores the spatial factors. The modification of Gilkerson[32] would include the $4\pi N/1000$ in the nonelectrostatic factor of the constant. It has the disadvantage, however, that it gives only relative values instead of an absolute calculation for the electrostatic contribution of the model chosen. It also omits the factor $1/b_{ik}$, which is relatively small but certainly belongs in the electrostatic osmotic coefficient and should not be dropped from the derived quantities without good reason.

[29] R. M. Fuoss and C. A. Kraus, J. Am. Chem. Soc. **55**, 1019 (1933).

[30] R. M. Fuoss, J. Am. Chem. Soc. **79**, 3301 (1957).

[31] J. T. Denison and J. B. Ramsay, J. Am. Chem. Soc. **77**, 2615 (1955).

[32] W. R. Gilkerson, J. Chem. Phys. **25**, 1199 (1956).

Contribution of Lattice Vibrations to the Order-Disorder Transformation in Alloys*

PETER J. WOJTOWICZ† AND JOHN G. KIRKWOOD‡

Sterling Chemistry Laboratory, Yale University, New Haven, Connecticut

(Received May 16, 1960)

The lattice vibrational partition function for a binary crystal is constructed from the normal mode frequencies in the classical nearest-neighbor harmonic approximation. The set of frequencies is computed as a function of the short-range order parameter by the use of the Born-von Karman analysis and second-order perturbation theory. The resulting form of the lattice vibrational partition function closely resembles that of the static configurational partition function so that a reexamination of the statistical thermodynamics, including lattice vibrational effects, proves to be straightforward. The derived thermodynamic quantities are compared with experiment for the case of β-brass. The theoretical heat capacity discontinuity as calculated by the method of Bethe and Kirkwood is increased from $1.7R$ to $6.1R$ by the inclusion of the lattice vibrational contribution. The agreement with the experimental value of about $5R$ is now satisfactory.

INTRODUCTION

THE statistical mechanical theory of the order-disorder transformation in the alloys has been examined by many investigators.[1,2] Of the several techniques devised to approximate the configurational partition function the most fruitful within the context of the alloy problem are the method of local configurations,[3] the method of moments,[4] and the quasi-chemical method.[5] The theory at this stage of development[6] affords a good qualitative description of the ordering process including the prediction of a transformation temperature and a heat capacity discontinuity. Quantitatively, however, several serious discrepancies between theory and experiment still remain. The most pronounced is the disagreement between the predicted and observed magnitudes of the heat capacity discontinuities.

Characteristic of these techniques is the assumption that the lattice vibrations, and consequently the vibrational partition function, are independent of the degree of order. The vibrational factor in the partition function can then be neglected, and the minimization of the configurational free energy alone serves to establish the equilibrium degree of order. Experimental evidence,[1,7–9] however, shows that the elastic constants, and hence the lattice vibrations, depend on the degree of order to a significant extent. A more complete theoretical treatment of the order-disorder problem must therefore include the vibrational free energy in the determination of the equilibrium properties of the system.

The perturbing effects of the lattice vibrations on the transformation have been recognized for some time, and several attempts at formulating the more correct theory have been made.[1] The most recent of such computations is the treatment of Booth and Rowlinson[10] in which the lattice vibrations are accounted for within the Einstein approximation. That is, the atoms are considered to perform independent simple harmonic oscillations, the coupling of vibrations being neglected completely. With this simple model Booth and Rowlinson have succeeded in demonstrating that the lattice vibrational effects considerably alter the details of order-disorder phenomena. In applying their theory to the specific case of β-brass, however, these authors find that the predicted value of the heat capacity discontinuity still falls significantly short of the experimental magnitude.

In this communication we wish to describe the influence of the lattice vibrations on the order-disorder transformation in terms of a more realistic model of a binary alloy. The recent theoretical work of Stripp and Kirkwood[11] (henceforth to be denoted by S-K) concerning the influence of lattice defects on the vibrational spectrum of a crystal has not only suggested that the vibrational contribution to ordering processes may by important, but has provided a powerful method for

* Contribution No. 1621 from the Sterling Chemistry Laboratory. This work is based on part of a dissertation presented to the Graduate School of Yale University by P.J.W. for the degree of Doctor of Philosophy.

† National Science Foundation Predoctoral Fellow, 1953–1956; now at RCA Laboratories, Princeton, New Jersey.

‡ Deceased.

[1] For a review of the current theoretical situation including many further references see T. Muto and Y. Takagi, Solid State Phys. **1**, 193 (1955).

[2] For a review of the current experimental situation see L. Guttman, Solid State Phys. **3**, 145 (1956).

[3] H. A. Bethe, Proc. Roy. Soc. (London) **A150**, 552 (1935).

[4] J. G. Kirkwood, J. Chem. Phys. **6**, 70 (1938).

[5] E. A. Guggenheim, Proc. Roy. Soc. (London) **A169**, 304 (1938); R. H. Fowler and E. A. Guggenheim, Proc. Roy. Soc. (London) **A174**, 189 (1940).

[6] Further improvements in the theory of the general cooperative (Ising) problem have been made but not specifically applied to the alloys. See for instance, G. H. Wannier, Revs. Modern Phys. **17**, 50 (1945); G. F. Newell and E. W. Montroll, *ibid.* **25**, 353 (1953); M. Kurata, R. Kikuchi, and T. Watari, J. Chem. Phys. **21**, 434 (1953); J. Hijmans and J. DeBoer, Physica **22**, 408 (1956); and further references contained therein.

[7] J. S. Reinhart, Phys. Rev. **58**, 365 (1940).

[8] W. A. Good, Phys. Rev. **60**, 605 (1941).

[9] R. A. Artman, J. Appl. Phys. **23**, 475 (1952).

[10] C. Booth and J. S. Rowlinson, Trans. Faraday Soc. **51**, 463 (1955).

[11] K. F. Stripp and J. G. Kirkwood, J. Chem. Phys. **22**, 1579 (1954), denoted by S-K in the text.

evaluating the vibrational free energy as a function of the degree of order. The lattice vibrational partition function for a binary crystal undergoing an order-disorder transformation is constructed from the normal mode frequencies in the classical nearest-neighbor harmonic approximation. The coupling of vibrations is explicitly included. The set of normal mode frequencies is determined as a function of the short-range order parameter by the use of the Born-von Karman analysis and second-order perturbation theory. The resulting form of the vibrational partition function closely resembles that of the static configurational partition function so that a re-examination of the statistical thermodynamics of the transformation, including lattice vibrational effects, proves to be quite straightforward. Indeed, the vibrational terms can be suitably incorporated into the configurational partition function so that the conventional static treatments are sufficient to complete the analysis. The combinatory approximation so adopted for alteration is the method of local configurations of Bethe[3] as modified by Bethe and Kirkwood[12,13] (henceforth to be denoted by B-K). The derived thermodynamic quantities are compared with the earlier theoretical work and with experiment. The agreement between the theory and experiment for the case of β-brass is now more satisfactory.

EQUATIONS OF MOTION

We begin with a body-centered cubic crystal containing x_1N atoms of type 1 and x_2N atoms of type 2 on N lattice sites, half of which may be designated cube corners, and the remaining half, cube centers. Each site is characterized by a vector

$$\mathbf{R}_j=n_1\mathbf{a}_1+n_2\mathbf{a}_2+n_3\mathbf{a}_3, \qquad 0\leqslant n_i<N^{\frac{1}{3}}, \tag{1}$$

where the $\mathbf{a}_i$ are the primitive lattice vectors, and where the subscript j is odd for corners and even for centers. For convenience $|\mathbf{a}_i|=a$ is chosen as the unit of length. In the classical, nearest neighbor, harmonic approximation, the potential energy may be written as

$$U=\tfrac{1}{2}\sum_{j}^{N}\sum_{j'}^{N}\lambda_{jj'}\{\eta_j\eta_{j'}(V_{11}+\alpha_{11}\Omega_{jj'})+\rho_j\rho_{j'}(V_{22}+\alpha_{22}\Omega_{jj'})$$
$$+(\eta_j\rho_{j'}+\eta_{j'}\rho_j)(V_{12}+\alpha_{12}\Omega_{jj'})\},$$
$$\Omega_{jj'}=\tfrac{1}{2}(\mathbf{r}_j-\mathbf{r}_{j'})\cdot\mathbf{R}_{jj'}\mathbf{R}_{jj'}\cdot(\mathbf{r}_j-\mathbf{r}_{j'}), \tag{2}$$

where V_{kl} are the indicated minimum interatomic pair potentials, the α_{kl} their second derivatives at the minimum (Hooke's law force constants), $\mathbf{R}_{jj'}$ is the vector distance between the sites j and j' at equilibrium, $\mathbf{r}_j$ is the vector displacement of an atom from equilibrium at site j. The matrix $\lambda_{jj'}$ is the nearest-neighbor selector factor defined to be unity if j and j' are nearest neighbors, and zero otherwise. The η_j and ρ_j are occupation variables defined as:

$$\eta_j=\begin{cases}1, & \text{if site } j \text{ is occupied by an atom of type 1,}\\ 0, & \text{otherwise.}\end{cases}$$
$$\rho_j=\begin{cases}1, & \text{if site } j \text{ is occupied by an atom of type 2,}\\ 0, & \text{otherwise.}\end{cases} \tag{3}$$

These variables satisfy the following relationships

$$\eta_j+\rho_j=1; \qquad \sum_{j}^{N}\eta_j=x_1N; \qquad \sum_{j}^{N}\rho_j=x_2N, \tag{4}$$

$$\sum_{j}^{N}\lambda_{jj'}=\sum_{j'}^{N}\lambda_{jj'}=z, \tag{5}$$

where z is the coordination number of the lattice. The kinetic energy is given by

$$T=\tfrac{1}{2}\sum_{j}^{N}(\eta_jm_1+\rho_jm_2)\,\mathbf{r}_j'\cdot\mathbf{r}_j', \tag{6}$$

where m_1 and m_2 are the masses of atom types 1 and 2, respectively. The Lagrangian composed of Eqs. (2) and (6) gives the equations of motion of the N atoms:

$$m(d^2\mathbf{r}_j/dt^2)+\sum_{j'}^{N}\lambda_{jj'}\mathbf{R}_{jj'}\mathbf{R}_{jj'}\cdot(\mathbf{r}_j-\mathbf{r}_{j'})$$
$$\times\{\eta_j\eta_{j'}\alpha_{11}+\rho_j\rho_{j'}\alpha_{22}+(\eta_j\rho_{j'}+\eta_{j'}\rho_j)\alpha_{12}\}=0,$$
$$(j=1\cdots N). \tag{7}$$

For simplicity we have assumed that the masses m_1 and m_2 are almost equal so that $(\eta_jm_1+\rho_jm_2)$ can be replaced by the mean mass, m. The equations of motion will now be rearranged so that the perturbation theory can be applied to their solution.

To properly utilize the perturbation scheme in S-K it is first necessary to choose a suitable unperturbed crystal, the solutions of whose equations of motion we may presume to know. Since it is the presence of the occupation variables that effectively prevents the formal solution of Eq. (7), the equations of motion of the unperturbed system clearly should not contain occupation variables. Furthermore, the unperturbed crystal should be as close an approximation as possible to the system of actual interest so that the perturbation series will have a reasonable convergence. The most convenient choice of unperturbed system is the "virtual crystal" approximation to the disordered or random alloy. According to this approximation, the disordered crystal is replaced by an equivalent ordered crystal in which each site is occupied by the same type of hypothetical atom called the "virtual atom." The properties of the virtual crystal are uniquely defined by the composition. The Hooke's law force constant α_R is taken to be the average (averaged over the composition) of

[12] H. A. Bethe and J. G. Kirkwood, J. Chem. Phys. 7, 578 (1939), denoted by B-K in the text.
[13] J. G. Kirkwood, J. Chem. Phys. 8, 623 (1940).

the force constants for the actual nearest-neighbor pairs

$$\alpha_R = x_1^2\alpha_{11} + x_2^2\alpha_{22} + 2x_1x_2\alpha_{12}. \tag{8}$$

Since we have already approximated the masses of real atoms with the mean mass, the mass of the virtual atom will also be the (constant) mean mass, m.

The quantity

$$\sum_{j'}^{N} \lambda_{jj'}\mathbf{R}_{jj'}\mathbf{R}_{jj'} \cdot (\mathbf{r}_j - \mathbf{r}_{j'})\alpha_R \tag{9}$$

is now added to both sides of Eq. (7). After suitable rearrangement and use of Eq. (4) we obtain the equations of motion in the following form:

$$(d^2\mathbf{r}_j/dt^2) - \sum_{j'}^{N} \mathbf{H}_{jj'} \cdot (\mathbf{r}_j - \mathbf{r}_{j'}) = -\sum_{j'}^{N} \mathbf{K}_{jj'} \cdot (\mathbf{r}_j - \mathbf{r}_{j'}),$$

$$\mathbf{H}_{jj'} = -m^{-1}\lambda_{jj'}\mathbf{R}_{jj'}\mathbf{R}_{jj'}\alpha_R,$$

$$\mathbf{K}_{jj'} = -m^{-1}\lambda_{jj'}\mathbf{R}_{jj'}\mathbf{R}_{jj'}\{(\eta_j\eta_{j'} - x_1^2)(\alpha_{12} - \alpha_{11}) + (\rho_j\rho_{j'} - x_2^2)(\alpha_{12} - \alpha_{22})\}. \tag{10}$$

The left-hand side of Eq. (10) corresponds to the equations of motion of the virtual crystal while the right-hand side represents the difference in potential energy between the virtual crystal and the true binary crystal in an arbitrary state of short-range order. The terms on the right-hand side of Eq. (10) will therefore be treated as perturbations acting on the virtual crystal, the normal mode frequencies of which can be found in terms of α_R.

The nonvanishing terms on the right-hand side of Eq. (10) implicitly contain two different kinds of perturbation terms. The first kind act on the virtual crystal correcting for the fact that there really are two types of atoms with three different force constants in a random alloy; the second kind then correct the equations of motion of the random alloy when short-range order is introduced. The contribution of terms of the first kind might be expected to be large since it is known that the vibrational spectrum of the real random alloy is quite different from that of the virtual crystal. However, in a later section we shall find that the contribution of the first kind of perturbation to the logarithm of the partition function is actually quite small, beginning to appear only in the second order of perturbation. The reason for this is as follows: For a random crystal (disordered with respect to the short-range order; the average composition of nearest neighbors is the same as the macroscopic composition), the average Hooke's law force constant is α_R while the products of the occupation variables average out to the values,

$$\eta_j\eta_{j'} \rightarrow x_1^2, \qquad \rho_j\rho_{j'} \rightarrow x_2^2. \tag{11}$$

Thus, in the state of disorder, the right-hand side of Eq. (10) vanishes *on the average*, leaving the equations of motion for the virtual crystal. The average normal mode frequency of the random alloy will therefore very nearly equal that for the virtual crystal. Since taking the logarithm of the classical vibrational partition function is equivalent to taking the average of the normal mode frequencies [see Eq. (26) to follow], it is then not surprising that the vibrational partition functions of the random alloy and the virtual crystal are nearly equal. We note also that it is the low frequency or long wavelength modes that contribute most heavily to the partition function. The long-wavelength modes, however should be insensitive to the specific arrangement of the atoms among the lattice sites. The frequencies of such modes should depend on the average force constants between the various pairs of atoms and on the average masses. These are just the quantities on which the virtual crystal approximation is based.

The contribution of the perturbation terms of the second kind will, of course, be more important. The convergence of the perturbation treatment for these terms will depend on the degree of short-range order introduced. Since our interest is primarily confined to the thermodynamic functions at or near the transformation temperature where the degree of short range order is small, a perturbation expansion based on the random alloy should prove adequate.

FORMAL PERTURBATION THEORY

Following the formal perturbation treatment in S-K, we impose periodic boundary conditions, and the normal mode analysis of the unperturbed lattice (virtual crystal) can be carried out conveniently in terms of the running waves[14]

$$\mathbf{r}_j = \mathbf{A}_j(\zeta, \mathbf{k}) \exp[-i\omega_0(\zeta, \mathbf{k})t],$$

$$\mathbf{A}_j(\zeta, \mathbf{k}) = N^{-\frac{1}{2}}\boldsymbol{\varepsilon}(\zeta, \mathbf{k}) \exp[i\mathbf{k}\cdot\mathbf{R}_j], \tag{12}$$

where $\omega_0(\zeta, \mathbf{k})$ is the frequency of the wave with wave-number vector $\mathbf{k}$, $\boldsymbol{\varepsilon}(\zeta, \mathbf{k})$ is a unit polarization vector, and ζ takes the values 1, 2, 3 to distinguish the three directions of polarization associated with each $\mathbf{k}$. The wave-number vector has the N values

$$\mathbf{k} = (2\pi/N^{\frac{1}{3}})(k_1\mathbf{b}_1 + k_2\mathbf{b}_2 + k_3\mathbf{b}_3),$$

$$-\tfrac{1}{2}N^{\frac{1}{3}} < k_i \leqslant \tfrac{1}{2}N^{\frac{1}{3}}, \tag{13}$$

where the $\mathbf{b}_i$ are the primitive vectors in reciprocal space. The following important relationships obtain for the polarization and amplitude vectors of Eq. (12):

$$\boldsymbol{\varepsilon}(\zeta, \mathbf{k}) \cdot \boldsymbol{\varepsilon}(\zeta', \mathbf{k}) = \delta_{\zeta\zeta'},$$

$$\sum_{\zeta} \boldsymbol{\varepsilon}(\zeta, \mathbf{k})\boldsymbol{\varepsilon}(\zeta, \mathbf{k}) = \mathbf{1},$$

$$\sum_{\zeta} \mathbf{A}_j^*(\zeta', \mathbf{k}') \cdot \mathbf{A}_j(\zeta, \mathbf{k}) = \delta_{\zeta\zeta'}\delta_{\mathbf{k}\mathbf{k}'}, \tag{14}$$

[14] M. Born and M. G. Mayer, *Handbuch der Physik* edited by E. Flügge (Springer-Verlag, Berlin, 1935), 2nd ed., Vol. 24, Part 2, p. 623 ff.

where δ is the Kronecker delta symbol, and where $\mathbf{1}$ is the unit dyad. By substitution of Eq. (12) into Eq. (10) without perturbation ($\mathbf{K}_{jj'}=0$), the following equation is obtained:

$$\omega_0^2(\zeta,\mathbf{k})\,\boldsymbol{\varepsilon}(\zeta,\mathbf{k})+\sum_{j'}^{N}\mathbf{H}_{jj'}\cdot\boldsymbol{\varepsilon}(\zeta,\mathbf{k}) \times\{1-\exp[i\mathbf{k}\cdot\mathbf{R}_{jj'}]\}=0. \quad (15)$$

Equation (15) represents the eigenvalue problem which determines the unperturbed frequencies and polarization vectors. It will be found that the detailed solution of Eq. (15) is not required for the present problem.

The normal mode analysis of the perturbed system (lattice of intermediate order) is carried out in terms of solutions of the form

$$\mathbf{r}_j=\mathbf{B}_j\exp[-i\omega t],$$

where the $\mathbf{B}_j$ and ω are the perturbed amplitudes and frequencies. Substitution in Eq. (10) yields the perturbed counterpart of Eq. (15),

$$\omega^2\mathbf{B}_j+\sum_{j'}^{N}\mathbf{H}_{jj'}\cdot(\mathbf{B}_j-\mathbf{B}_{j'})=\sum_{j'}^{N}\mathbf{K}_{jj'}\cdot(\mathbf{B}_j-\mathbf{B}_{j'}), \quad (16)$$

to which perturbation theory shall be applied. Since the unperturbed waves are highly degenerate, the degenerate perturbation method must be used. The $3N$ unperturbed amplitudes are grouped into S degenerate sets $s(s=1, 2, \cdots, S)$ in order of increasing frequency $\omega_0(s)$. The members of each set are suitably numbered:

$$\mathbf{A}_j(n,s), \qquad (n=1,\cdots,\sigma_s),$$

where σ_s is the number of waves in the set s; $\sum_s\sigma_s=3N$. The perturbed amplitudes are written to first order in perturbation corrections:

$$\mathbf{B}_j(t,s)=\mathbf{B}_j^0(t,s)+\mathbf{B}_j^1(t,s)+\cdots, \quad (17)$$

$$\mathbf{B}_j^0(t,s)=\sum_{n=1}^{\sigma_s}\alpha_{tn}(s)\mathbf{A}_j(n,s); \qquad (t=1,\cdots,\sigma_s), \quad (18)$$

$$\mathbf{B}_j^1(t,s)=\sum_{s'\neq s}^{S}\sum_{n=1}^{\sigma_{s'}}\beta_{tn}(s,s')\mathbf{B}_j^0(n,s), \quad (19)$$

where the $\mathbf{B}_j^0(t,s)$ are the proper unperturbed amplitudes (linear combinations of the degenerate plane waves). The perturbed frequencies are written to second order in perturbation corrections:

$$\omega^2(t,s)=\omega_0^2(s)+\omega_{\mathrm{I}}^2(t,s)+\omega_{\mathrm{II}}^2(t,s)+\cdots. \quad (20)$$

The proper zero-order amplitudes, Eq. (18), are found to be equally good solutions for the "virtual crystal" and satisfy the equation

$$\omega_0^2(s)\mathbf{B}_j^0(t,s)+\sum_{j'}^{N}\mathbf{H}_{jj'}\cdot[\mathbf{B}_j^0(t,s)-\mathbf{B}_{j'}^0(t,s)]=0.$$

Substitution of Eqs. (17) through (20) into Eq. (16), and use of the standard perturbation method[15] yields:

$$\omega_{\mathrm{I}}^2(t,s)=F(t,s;t,s), \quad (21)$$

$$0=F(n,s;t,s); \qquad n\neq t, \quad (22)$$

$$\beta_{tn}(s,s')=F(n,s';t,s)/[\omega_0^2(s)-\omega_0^2(s')], \quad (23)$$

$$\omega_{\mathrm{II}}^2(t,s)=\sum_{s'\neq s}^{S}\sum_{n=1}^{\sigma_{s'}}\frac{F(n,s';ts)\,F(t,s;n,s')}{\omega_0^2(s)-\omega_0^2(s')}, \quad (24)$$

in terms of the matrix elements,

$$F(n,s';t,s)=\sum_{j}^{N}\sum_{j'}^{N}\mathbf{B}_j^0(n,s') \cdot\mathbf{K}_{jj'}\cdot[\mathbf{B}_j^0(t,s)-\mathbf{B}_{j'}^0(t,s)]. \quad (25)$$

The $\sigma_s(\sigma_s-1)$ conditions, Eq. (22), plus the σ_s normalization conditions,

$$\sum_{n=1}^{\sigma_s}\alpha_{tn}^*(s)\alpha_{tn}(s)=1, \qquad (t=1,\cdots,\sigma_s),$$

serve to determine the coefficients, α_{tn}, of Eq. (18). Since we are interested in obtaining only the vibrational partition function, rather than the individual normal modes, we shall find that the explicit determination of the α_{tn} is not necessary.

VIBRATIONAL PARTITION FUNCTION

The classical vibrational partition function is given in terms of the $3N$ normal mode frequencies as[16]

$$Q_V=(kT/\hbar)^{3N}\prod_{s=1}^{S}\prod_{t=1}^{\sigma_s}\omega^{-1}(t,s), \quad (26)$$

where T is the thermodynamic temperature, and where k and $\hbar$ are Boltzmann's constant, and Planck's constant divided by 2π, respectively. When the perturbed frequencies are expressed as

$$\omega^2(t,s)=\omega_0^2(s)\left[1+\frac{\omega_{\mathrm{I}}^2(t,s)}{\omega_0^2(s)}+\frac{\omega_{\mathrm{II}}^2(t,s)}{\omega_0^2(s)}+\cdots\right]$$

the logarithm of the partition function can be expanded in the form,

$$\ln Q_V=\ln Q_V^0+\ln Q_V^{\mathrm{I}}+\ln Q_V^{\mathrm{II}}+\cdots, \quad (27)$$

where

$$\ln Q_V^0=3N\ln(kT/\hbar)-\tfrac{1}{2}\sum_{s=1}^{S}\sum_{t=1}^{\sigma_s}\ln\omega_0^2(s) \quad (28)$$

is the logarithm of the vibrational partition function of the unperturbed "virtual crystal", and where $\ln Q_V^{\mathrm{I}}$ and $\ln Q_V^{\mathrm{II}}$ are the first and second-order perturbation

[15] R. Courant and D. Hilbert, *Methods of Mathematical Physics*, (Interscience Publishers, Inc., New York, 1953), Vol. I, pp. 343–348.

[16] J. E. Mayer and M. G. Mayer, *Statistical Mechanics* (John Wiley & Sons, Inc., New York, 1940), p. 240.

corrections:

$$\ln Q_V^{\mathrm{I}} = -\tfrac{1}{2}\sum_{s=1}^{S}\sum_{t=1}^{\sigma_s}[\omega_1^2(t,s)/\omega_0^2(s)], \qquad (29)$$

$$\ln Q_V^{\mathrm{II}} = -\tfrac{1}{2}\sum_{s=1}^{S}\sum_{t=1}^{\sigma_s}\left\{\frac{\omega_{\mathrm{II}}^2(t,s)}{\omega_0^2(s)} - \tfrac{1}{2}\frac{\omega_1^4(t,s)}{\omega_0^4(s)}\right\}. \qquad (30)$$

Substitution of Eq. (21) into Eq. (29) provides the first-order correction to the partition function in terms of the matrix elements of the perturbation treatment

$$\ln Q_V^{\mathrm{I}} = -\tfrac{1}{2}\sum_{s=1}^{s}\sum_{t=1}^{\sigma_s}\omega_0^{-2}(s)\,F(t,s;t,s). \qquad (31)$$

The summation over t in the above equation is the trace of the degenerate submatrix of the set s, and as such is invariant to the similarity transformation, Eq. (18). Hence, it may be replaced by the sum of the analogous matrix elements formed from the plane waves of the set. By regrouping the sums in Eq. (31), the first-order correction becomes

$$\ln Q_V^{\mathrm{I}} = -\tfrac{1}{2}\sum_{\zeta}^{3}\sum_{\mathbf{k}}^{N}\omega_0^{-2}(\zeta,\mathbf{k})\,F(\zeta,\mathbf{k};\zeta,\mathbf{k}). \qquad (32)$$

Substitution of Eqs. (22) and (24) into Eq. (30) provides the second-order correction

$$\ln Q_V^{\mathrm{II}} = -\tfrac{1}{2}\sum_{s=1}^{S}\sum_{t=1}^{\sigma_s}\left\{-\tfrac{1}{2}\left[\frac{F(t,s;t,s)}{\omega_0^2(s)}\right]^2 + \sum_{s'\neq s}^{S}\sum_{n=1}^{\sigma_{s'}}\frac{F(n,s';t,s)\,F(t,s;n,s')}{\omega_0^2(s)[\omega_0^2(s)-\omega_0^2(s')]}\right\}. \qquad (33)$$

The "resonance denominator" of the second term of Eq. (33) may be removed as follows: the restriction on the s' summation may be removed by including the factor $(1-\delta_{ss'})$. Further, the second term will not be altered if the roles of s and s' were interchanged in the development leading to Eq. (33). Adding one-half of these two versions then gives the following for this term:

$$\tfrac{1}{4}\sum_{s}^{S}\sum_{s'}^{S}\sum_{t}^{\sigma_s}\sum_{n}^{\sigma_{s'}}\frac{F(n,s';t,s)\,F(t,s;n,s')}{\omega_0^2(s)\omega_0^2(s')}(1-\delta_{ss'}). \qquad (34)$$

But now, the first term of Eq. (33) contains just those terms missing from Eq. (34) because of the factor $(1-\delta_{ss'})$. Combining these terms then yields the following simplified form for the second-order correction

$$\ln Q_V^{\mathrm{II}} = \tfrac{1}{4}\sum_{s,s'}^{S}\sum_{t,n}^{\sigma_s}\omega_0^{-2}(s)\omega_0^{-2}(s')\,F(t,s;n,s')\,F(n,s';t,s). \qquad (35)$$

Here again, the t and n summations are traces invariant to the transformation, Eq. (18), so that just as in the case of $\ln Q_V^{\mathrm{I}}$, we obtain

$$\ln Q_V^{\mathrm{II}} = \tfrac{1}{4}\sum_{\zeta,\zeta'}^{3}\sum_{\mathbf{k}\mathbf{k}'}^{N}\omega_0^{-2}(\zeta,\mathbf{k})\omega_0^{-2}(\zeta',\mathbf{k}')\,F(\zeta,\mathbf{k};\zeta',\mathbf{k}')\times F(\zeta',\mathbf{k}';\zeta,\mathbf{k}) \qquad (36)$$

in terms of the original plane wave matrix elements. The plane wave matrix elements are obtained from Eq. (25) by replacing the $\mathbf{B}_j^0$ with the $\mathbf{A}_j$ of Eq. (12)

$$F(\zeta,\mathbf{k};\zeta',\mathbf{k}') = N^{-1}\sum_{j}^{N}\sum_{j'}^{N}\exp[i(\mathbf{k}-\mathbf{k}')\cdot\mathbf{R}_j]\times\boldsymbol{\varepsilon}(\zeta,\mathbf{k})\cdot\mathbf{K}_{jj'}\cdot\boldsymbol{\varepsilon}(\zeta',\mathbf{k}')\{1-\exp[i\mathbf{k}'\cdot\mathbf{R}_{jj'}]\}. \qquad (37)$$

Thus, we have obtained the first- and second-order perturbation corrections to the logarithm of the vibrational partition function in terms of matrix elements composed of the original unperturbed plane waves, Eq. (12). By computing only the partition function we have been able to utilize the invariance property of traces of matrices. The degeneracy may therefore be ignored in computing the partition function, and, as shown in S-K, the virtually impossible calculation of the coefficients, Eq. (18), can be avoided.

EVALUATION OF PERTURBATION TERMS

This section is devoted to the evaluation of the first- and second-order perturbation corrections to the vibrational partition function for the body-centered cubic lattice. Combining Eqs. (32) and (37) and using the definitions in Eq. (10), the first-order correction assumes the form

$$\ln Q_V^{\mathrm{I}} = (2mN)^{-1}\sum_{\mathbf{k}}^{N}\sum_{j}^{N}\sum_{j'}^{N}\lambda_{jj'}\mathbf{R}_{jj'}\cdot\mathbf{M}^{-1}(\mathbf{k})\mathbf{R}_{jj'}\times\{(\eta_j\eta_{j'}-x_1^2)(\alpha_{12}-\alpha_{11})+(\rho_j\rho_{j'}-x_2^2)(\alpha_{12}-\alpha_{22})\}\times[1-\exp(i\mathbf{k}\cdot\mathbf{R}_{jj'})], \qquad (38)$$

where we have defined the dyad

$$\mathbf{M}^{-1}(\mathbf{k}) = \sum_{\zeta}^{3}\boldsymbol{\varepsilon}(\zeta,\mathbf{k})\,\boldsymbol{\varepsilon}(\zeta,\mathbf{k})\,\omega_0^{-2}(\zeta,\mathbf{k}). \qquad (39)$$

Before evaluating the first-order correction generally, it is instructive to examine Eq. (38) for a certain simple special case where the evaluation of $\ln Q_V^{\mathrm{I}}$ proves to be quite straightforward. For this special case we assume that all *like* nearest-neighbor pairs have their intersite separation vectors, $\mathbf{R}_{jj'}$ uniformly distributed over the z possible directions. It then becomes possible to replace the products of the occupation variables with their mean values

$$\eta_j\eta_{j'}\rightarrow 2v/Nz, \qquad \rho_j\rho_{j'}\rightarrow 2w/Nz, \qquad (40)$$

where v and w are the total number of 1–1 and 2–2 nearest-neighbor pairs, respectively, defined by

$$v = \tfrac{1}{2}\sum_{jj'}\lambda_{jj'}\eta_j\eta_{j'},$$

$$w = \tfrac{1}{2}\sum_{jj'}\lambda_{jj'}\rho_j\rho_{j'}, \qquad (41)$$

and where $Nz/2=\sum_{jj'}\lambda_{jj'}$ is the total number of all nearest-neighbor pairs in the lattice. Substitution of Eq. (40) into Eq. (38) permits the removal of j and j'

dependent terms from the braces of Eq. (38). The j' summation may then be conveniently performed using the unperturbed equations of motion, Eq. (15), in the rearranged form,

$$m^{-1}\sum_{j'}^{N}\lambda_{jj'}\epsilon(\zeta,\mathbf{k})\cdot\mathbf{R}_{jj'}\mathbf{R}_{jj'}\cdot\epsilon(\zeta,\mathbf{k})[1-\exp(i\mathbf{k}\cdot\mathbf{R}_{jj'})] =\omega_0^2(\zeta,\mathbf{k})\alpha_R^{-1}. \quad (42)$$

By combining Eqs. (38), (40), and (42), the first-order correction reduces to

$$\ln Q_V^{\mathrm{I}}=(2N)^{-1}\sum_{\mathbf{k}}^{N}\sum_{j}^{N}\sum_{\zeta}^{3}\alpha_R^{-1}\{[(2v/Nz)-x_1^2](\alpha_{12}-\alpha_{11}) +[(2w/Nz)-x_2^2](\alpha_{12}-\alpha_{22})\}.$$

The remaining summations are elementary, yielding the following final result

$$\ln Q_V^{\mathrm{I}}=3\alpha_R^{-1}\{([v/z)-\tfrac{1}{2}x_1^2N](\alpha_{12}-\alpha_{11}) +[(w/z)-\tfrac{1}{2}x_2^2N](\alpha_{12}-\alpha_{22})\}. \quad (43)$$

Although the preceding expression was obtained under rather special assumptions for illustrative purposes, this result will be found later to be generally valid.

In evaluating the first-order correction, Eq. (38) for the general case we shall make use of important results obtained in S-K concerning the dyad $\mathbf{M}^{-1}(\mathbf{k})$. We shall not reproduce the entire argument here since it is presented in complete detail in S-K. The matrix inverse,

$$\mathbf{M}(\mathbf{k})=\sum_{\zeta}\epsilon(\zeta,\mathbf{k})\epsilon(\zeta,\mathbf{k})\omega_0^2(\zeta,\mathbf{k})$$

is obtained from Eq. (15), use of Eq. (14), and replacement of the nearest-neighbor sum by the appropriate surface integral. $\mathbf{M}^{-1}(\mathbf{k})$ is then obtained by matrix inversion in the form of a power series in $|\mathbf{k}|$. Summations over $\mathbf{k}$ are replaced by integrations in k-space over equal spherical volumes. The pertinent result from S-K, but with force constants appropriate to this problem, may be stated as follows:

$$N^{-1}\sum_{\mathbf{k}}^{N}\mathbf{M}^{-1}(\mathbf{k})\exp(i\mathbf{k}\cdot\mathbf{R})=(30m/\alpha_R z)\{\mathbf{1}X(R) +(\mathbf{RR}/R^2)Y(R)\}, \quad (44)$$

$$X(R)=\sum_{i=0}^{3}X_i(R),$$

$$Y(R)=\sum_{i=0}^{3}Y_i(R). \quad (45)$$

The exact forms of the X_i and Y_i for the body-centered cubic lattice are given in the Appendix (these had to be computed explicitly since the results in S-K pertain specifically to the face-centered cubic lattice alone). Applying the result indicated in Eq. (44) to Eq. (38), the first-order correction to the partition function becomes

$$\ln Q_V^{\mathrm{I}}=(30/\alpha_R z)\sum_{jj'}^{N}\tfrac{1}{2}\lambda_{jj'}\mathbf{R}_{jj'} \cdot\{\mathbf{1}X(R_{jj'})+(\mathbf{R}_{jj'}\mathbf{R}_{jj'}/R_{jj'}^2)Y(R_{jj'})\} \cdot\mathbf{R}_{jj}\{(\eta_j\eta_{j'}-x_1^2)(\alpha_{12}-\alpha_{11})+(\rho_j\rho_{j'}-x_2^2)(\alpha_{12}-\alpha_{22})\}. \quad (46)$$

Summation over j and j' and use of Eq. (41) yields

$$\ln Q_V^{\mathrm{I}}=\alpha_R^{-1}\{[(v/z)-\tfrac{1}{2}x_1^2N](\alpha_{12}-\alpha_{11}) +[(w/z)-\tfrac{1}{2}x_2^2N](\alpha_{12}-\alpha_{22})\} \times 30\{X(0)-X(1)+Y(0)-Y(1)\}. \quad (47)$$

Using the definitions in Eq. (45) and in Eqs. (A1) through (A4), numerical computation gives

$$X(0)=0.167743, \qquad X(1)=0.044357,$$
$$Y(0)=0.000000, \qquad Y(1)=0.023876. \quad (48)$$

Substitution of Eq. (48) into Eq. (47) yields as a final result a form for $\ln Q_V^{\mathrm{I}}$ entirely similar to that of Eq. (43), but differing by the numerical factor 2.9853/3. From this we may conclude that Eq. (43) is also generally valid, and that the result of S-K, Eq. (44) is essentially correct in the context of the order-disorder problem as well.

The second-order correction term will now be considered. It will be found to depend on the interaction of pairs of atoms whether nearest neighbors or not. Combining Eqs. (36) and (37), and using the definitions in Eq. (9), the second-order term, after some algebraic manipulation, can be expressed as:

$$\ln Q_V^{\mathrm{II}}=(4m^2)^{-1}\sum_{jj'}^{N}\sum_{ll'}^{N}\sum_{\mathbf{k}\mathbf{k}'}^{N}\Phi_{jj'}\Phi_{ll'}\frac{\mathbf{R}_{ll'}}{R_{ll'}} \cdot N^{-1}\mathbf{M}^{-1}(\mathbf{k})[\exp(i\mathbf{k}\cdot\mathbf{R}_{lj})-\exp(i\mathbf{k}'\cdot\mathbf{R}_{jl'})]\cdot\frac{\mathbf{R}_{jj'}\mathbf{R}_{jj'}}{R_{jj'}^2} \cdot N^{-1}\mathbf{M}^{-1}(\mathbf{k}')[\exp(i\mathbf{k}\cdot\mathbf{R}_{jl})-\exp(i\mathbf{k}'\cdot\mathbf{R}_{lj'})]\cdot\frac{\mathbf{R}_{ll'}}{R_{ll'}}, \quad (49)$$

where we have defined the matrix

$$\Phi_{jj'}=\lambda_{jj'}\{(\eta_j\eta_{j'}-x_1^2)(\alpha_{12}-\alpha_{11}) +(\rho_j\rho_{j'}-x_2^2)(\alpha_{12}-\alpha_{22})\}. \quad (50)$$

It is clear from Eq. (50) that only $j-j'$ and $l-l'$ must be nearest-neighbor pairs in Eq. (49): higher-order neighbor pairs of other combinations of j, j', l and l' are not excluded by $\lambda_{jj'}$ and $\lambda_{ll'}$. Employing Eq. (44) again for the $\mathbf{k}$ and $\mathbf{k}'$ summations in Eq. (49) we

obtain:

$$\ln Q_V^{II}=\frac{900}{4\alpha_R^2 z^2}\sum_{jj'}^{N}\sum_{ll'}^{N}\Phi_{jj'}\Phi_{ll'}\frac{\mathbf{R}_{ll'}}{R_{ll'}}\cdot\left\{\mathbf{1}[X(R_{lj})-X(R_{jl'})]\right.$$
$$\left.+\frac{\mathbf{R}_{lj}\mathbf{R}_{lj'}}{R_{lj}^2}Y(R_{lj})-\frac{\mathbf{R}_{jl'}\mathbf{R}_{jl'}}{R_{jl'}^2}Y(R_{jl'})\right\}\cdot\frac{\mathbf{R}_{jj'}\mathbf{R}_{jj'}}{R_{jj'}^2}$$
$$\cdot\left\{\mathbf{1}[X(R_{jl})-X(R_{lj'})]+\frac{\mathbf{R}_{jl}\mathbf{R}_{jl}}{R_{jl}^2}Y(R_{jl})\right.$$
$$\left.-\frac{\mathbf{R}_{lj'}\mathbf{R}_{lj'}}{R_{lj'}^2}Y(R_{lj'})\right\}\cdot\frac{\mathbf{R}_{ll'}}{R_{ll'}},\quad(51)$$

which shall be evaluated for several cases of interest.

First we consider the case of self-interaction. This arises from those terms in Eq. (51) for which j' and l' pertain to the same atom. Neglecting the occupation variables and atom fractions in the factors Φ, it is possible to evaluate these terms from Eq. (51) using the crystal geometry and the entries in Table I of the Appendix, with the result

$$\ln Q_V^{I}(\text{self})=\sum_{j'l'}0.3574/\alpha_R^2 z.$$

The numerical constant actually obtained is 0.3539 which we have increased by the factor $(3/2.985)^2$ in view of the behavior of the $\mathbf{k}$ summation, Eq. (44), in the evaluation of $\ln Q_V^{I}$.

In considering the self-interaction terms of Eq. (51) without the neglect of the Φ factors, some members of the 64 terms of $\ln Q_V^{I}(\text{self})$ will vanish. The vanishing terms will depend not only on the degree of local order, but also on the orientation of the various types of nearest-neighbor pairs about the particular site, $j'=l'$ being considered. It has been shown in S-K, however, that the orientation effect is small. Thus, it is permissible to assume that the value of the terms in question will decrease linearly with the number of vanishing terms (this is the principle of "linear decrease" described and applied in S-K). The general self-interaction term can then be evaluated to yield the following final result:

$$\ln Q_V^{II}(\text{self})=(0.3574/\alpha_R^2)$$
$$\times\left\{(\alpha_{12}-\alpha_{11})^2\left[\frac{2(v+w)}{z}-Nx_2-(2v/z)x_1^2+Nx_1^4\right]\right.$$
$$+(\alpha_{12}-\alpha_{22})^2\left[\frac{2(v+w)}{z}-Nx_1-(2w/z)x_2^2+Nx_2^4\right]$$
$$+(\alpha_{12}-\alpha_{11})(\alpha_{12}-\alpha_{22})[2Nx_1^2x_2^2$$
$$\left.-(2v/z)x_2^2-(2w/z)x_1^2]\right\}.\quad(52)$$

The next case of interest is that for which j' and l' are nearest-neighbor sites in Eq. (51). With neglect of the Φ factors we find by the use of crystal geometry and the entries in Table I of the Appendix that this term compares with the self-interaction term in the ratio 0.0421/0.3574. Use of the "linear decrease" principle of S-K in the evaluation of these terms without neglect of the factors provides the following result for the nearest-neighbor contribution:

$$\ln Q_V^{II}(nn)=(0.0421/\alpha_R^2)\left\{(\alpha_{12}-\alpha_{11})^2\right.$$
$$\times[Nx_1^4-2x_1^2(v/z)+(2v/Nz^2x_1)(2v+2w-Nzx_2)]$$
$$+(\alpha_{12}-\alpha_{11})^2[Nx_2^4-2x_2^2(w/z)$$
$$+(2w/Nz^2x_2)(2v+2w-Nzx_1)]$$
$$+(\alpha_{12}-\alpha_{11})(\alpha_{12}-\alpha_{22})\left[2Nx_1^2x_2^2-2x_1^2(w/z)-2x_2^2(v/z)\right.$$
$$\left.\left.+\left(1-\frac{2w+2v}{Nz}\right)\left(N-\frac{v+w}{zx_1x_2}\right)\right]\right\}.\quad(53)$$

Further terms in Eq. (51) arising from interactions between higher-order neighbor pairs will not be considered here. Neglect of these contributions should not produce too large an error in view of the asymptotic behavior derived in S-K (contributions from distant pairs are found to fall off with their separation as R^{-6}). Actually, we shall not even include the nearest-neighbor contribution in the remaining statistical mechanics, taking Eqs. (43) and (52) to be the entire corrections to the vibrational partition function. The nearest-neighbor contribution, unlike Eqs. (43) and (52), contains terms which are nonlinear in the order parameters v and w. Such terms cannot be conveniently incorporated into the combinatorial portion of the alloy problem. The simplicity obtained through their neglect, however, certainly outweighs any errors that may be introduced. Indeed, we estimate that the neglect of the terms in Eq. (53) introduces an error of only about 3 to 4% in the important parameter θ to be defined later.

As mentioned in an earlier section, two kinds of perturbations act to correct the logarithm of the vibrational partition function. The separate contributions may be distinguished by examining the correction terms, Eqs. (43), (52) and (53) in the limit of disappearing short-range order $v\to\frac{1}{2}Nzx_1^2, w\to\frac{1}{2}Nzx_2^2$. Examination of Eq. (43) shows that the first-order correction to the partition function vanishes in this limit. This term therefore contains contributions only from the second kind of perturbation (that representing the introduction of finite short-range order). Thus, to within the first order of perturbation theory, the vibrational partition functions of the random alloy and the virtual crystal are identical. Passing to the limit of complete randomness in Eqs. (52) and (53) we find the following nonvanishing contributions to the second-order

corrections:

$$\ln Q_V^{II}(\text{self}) = 0.3574\alpha_R^{-2}N(x_1-x_2) \times[x_1(\alpha_{12}-\alpha_{11})^2-x_2(\alpha_{12}-\alpha_{22})^2],$$

$$\ln Q_V^{II}(nn) = 0.0421\alpha_R^{-2}N(x_1-x_2)[x_1^2(\alpha_{12}-\alpha_{11})^2 -x_2^2(\alpha_{12}-\alpha_{22})^2+(x_2-x_1)(\alpha_{12}-\alpha_{11})(\alpha_{12}-\alpha_{22})].$$

These expressions represent the first appearance of perturbation terms of the first kind correcting the virtual crystal approximation of the random alloy. There will be no need to consider these terms further, however. Since they are constants independent of the short-range order parameters they cannot influence the ordering contributions to the thermodynamic functions.

A case of very special interest is the lattice composed of equal numbers of atoms of types 1 and 2. For the equiatomic composition $x_1=x_2=\frac{1}{2}$, and $v=w$. Furthermore, it becomes possible to use the single traditional short-range order parameter[4] p

$$p=(2/Nz)\sum_j\sum_{j'}\lambda_{jj'}\eta_j\eta_{j'}, \tag{54}$$

so that from Eq. (41), $p=4v/Nz=4w/Nz$. The short-range order parameter is thereby equal to zero when the lattice is perfectly ordered, and equal to $\frac{1}{2}$ when the lattice is disordered. The perturbation corrections for the equiatomic lattice may be expressed most simply in terms of p

$$\ln Q_V^{I}=1.5N(\tfrac{1}{2}-p)\alpha_0\alpha_D^{-1},$$

$$\ln Q_V^{II}=0.3574N(\tfrac{1}{2}-p)(\tfrac{1}{2}\alpha_0^2-\alpha_s^2)\alpha_D^{-2}, \tag{55}$$

where α_D is the average force constant for the equiatomic virtual crystal,

$$\alpha_D=\tfrac{1}{4}(\alpha_{11}+\alpha_{22}+2\alpha_{12}), \tag{56}$$

and where we have also defined

$$\alpha_0=\tfrac{1}{2}(\alpha_{11}+\alpha_{22}-2\alpha_{12}),$$

$$\alpha_s^2=(\alpha_{12}-\alpha_{11})^2+(\alpha_{12}-\alpha_{22})^2. \tag{57}$$

Collecting results, Eqs. (27) and (55), the vibrational partition function for an equiatomic binary lattice in a state of short-range order p can be written as

$$Q_V(p)=Q_V^0\exp[\tfrac{1}{2}Nz(\tfrac{1}{2}-p)\theta], \tag{58}$$

$$\theta=(2/z)\{1.5\alpha_0\alpha_D^{-1}+0.3574(\tfrac{1}{2}\alpha_0^2-\alpha_s^2)\alpha_D^{-2}\}. \tag{59}$$

The parameter θ depends only on the force constants α_{kl}, and is a valid expression only for the body-centered cubic lattice with atoms of approximately equal masses. When the lattice is disordered, $p\to\frac{1}{2}$, and all perturbation terms vanish leaving $Q_V=Q_V^0$. When $\alpha_{11}=\alpha_{22}=\alpha_{12}$ the perturbations also vanish; if the force constants are all the same the lattice vibrational spectrum cannot be influenced by varying degrees of short-range order.

ORDER-DISORDER THEORY

In this section the theory of the order-disorder transformation will be reformulated to include the lattice vibrational terms computed in the previous sections. The particular version of the theory to be examined is that of Bethe and Kirkwood as described in B-K.[12,13]

The static configurational partition function for an equiatomic binary lattice in a state of short-range order p has been shown[4] to have the form

$$Q_c(p)=Q_c^0\exp[\tfrac{1}{2}Nz(\tfrac{1}{2}-p)V/kT], \tag{60}$$

where Q_c^0 is the corresponding function for a disordered lattice ($p=\frac{1}{2}$), and where V is the following combination of the minimum interatomic potentials of Eq. (2)

$$V=\tfrac{1}{2}(V_{11}+V_{22}-2V_{12}). \tag{61}$$

The complete partition function for the lattice in a state of order p is then the product of Eqs. (58) and (60). It is found more convenient, however, to examine the statistical thermodynamics of the transformation in terms of the long-range order parameter $s=x_1^A-x_1^B$, where x_1^A and x_1^B are the fractions of type 1 atoms located at the corner and center sites, respectively, of our body-centered cubic lattice. The parameter s ranges in value from zero to ±1. The complete partition function for the lattice in the state of long-range order s is

$$Q(s)=\sum_p Q_c(p)Q_V(p),$$

$$Q(s)=Q_c^0Q_V^0\sum_p\exp\{\tfrac{1}{2}Nz(\tfrac{1}{2}-p)[\theta+(V/kT)]\}, \tag{62}$$

where the summation extends over all values of p consistent with a given value of s.

The exact solution of the combinatory problem implied in Eq. (62) has not yet been obtained. Several methods of approximation have been derived for the evaluation of (62) for $\theta=0$, however.[1,3-6] It will be found possible to utilize any one of the "static" approximations of the type developed in references 3–5, and in B-K for the case of finite θ after a suitable redefinition of the quantities appearing in Eq. (62). We define a new potential function,

$$\tilde{V}=V+kT\theta \tag{63}$$

equal to the former V plus an apparent temperature dependent potential $kT\theta$. Substituting in Eq. (62),

$$Q(s)=Q_c^0Q_V^0\sum_p\exp[\tfrac{1}{2}Nz(\tfrac{1}{2}-p)\tilde{V}/kT], \tag{64}$$

where the partition function now has the same form as previously considered in the static theories. Thus, through the definition, Eq. (63), the perturbation corrections for the lattice vibrations may be formally regarded as part of the static configurational partition function. The static theories for the statistical thermodynamics may then be used, but now implicitly including the lattice vibrational effects because of the

dependence of $\bar{V}$ on θ. This does not mean to say, however, that such an incorporation of the vibrational effects into the configurational problem will always be possible or valid. The procedure described here is possible only because of the approximations adopted both in computing $\ln Q_V$ and in deriving the theory in B-K. The present treatment would require considerable further development if one were to attempt a more complete analysis of the general vibrational-configurational interaction. In order to treat the lattice vibrations within the framework of the methods of Kurata *et al.*,[6] and Hijmans and DeBoer,[6] for instance, one would have to make at least the following improvements in the perturbation calculation: abandon the "linear decrease" principle in S-K and take account of the orientation of like- neighbor pairs in the summations; define short-range order parameters for triplets and higher multiplets of atoms to account for the orientation effects; compute terms in Eq. (51) arising from pairs more distance than nearest neighbors. Improvements such as these are of doubtful value in the alloy problem, however; errors introduced by the model itself are far more significant.

Apart from the constant factors outside the p summation, the partition function $Q(s)$ reduces to the total number of configurations consistent with the specified s for vanishing α,

$$\alpha=\bar{V}/kT. \tag{65}$$

Hence, a function $G(\alpha, s^2)$, vanishing for vanishing α, may be defined by

$$Q(s)=[\tfrac{1}{2}(1+s)]^{-\frac{1}{2}N(1+s)}[\tfrac{1}{2}(1-s)]^{-\frac{1}{2}N(1-s)} \cdot\exp[Nz G(\alpha, s^2)], \tag{66}$$

where the form of $G(\alpha, s^2)$ will be different for the different approximations to the combinatory problem, Eqs. (62) or (64). For the approximation reported in B-K,

$$\begin{aligned} G(\alpha, s^2)&=G_0(\alpha)+s^2G_1(\alpha)+s^4G_2(\alpha)+\cdots,\\ G_0(\alpha)&=\tfrac{1}{2}\ln\tfrac{1}{2}[1+\exp(-\alpha)],\\ G_1(\alpha)&=\tfrac{1}{4}[1-\exp(-\alpha)],\\ G_2(\alpha)&=(1/24)[1-\tfrac{3}{2}\exp(-\alpha)+\tfrac{1}{2}\exp(-3\alpha)]. \end{aligned} \tag{67}$$

The corresponding Helmholtz free energy equal to $-kT\ln Q$ is expressed as follows:

$$-A/NkT=zG(\alpha, s^2)-\tfrac{1}{2}(1+s)\ln\tfrac{1}{2}(1+s) -\tfrac{1}{2}(1-s)\ln\tfrac{1}{2}(1-s). \tag{68}$$

The equilibrium value of the long-range order s is found by minimization of A with respect to s at constant temperature. Differentiation with respect to s provides the following transcendental equation which determines s as a function of α or of the temperature:

$$(\partial A/\partial s)_\alpha=0, \tag{69}$$

$$\ln[(1+s)/(1-s)]=4zs[\partial G(\alpha, s^2)/\partial s^2]_\alpha. \tag{70}$$

For a phase change of the second order Eq. (70) has no real solutions other than $s=0$ for values of α less than a certain critical value α_c satisfying the equation

$$2zG_1(\alpha_c)=1. \tag{71}$$

For values of $\alpha>\alpha_c$, there exist two nonvanishing real solutions, $\pm s$, yielding a unique equilibrium value of s^2. Combining Eqs. (67) and (71),

$$\alpha_c=\ln[z/(z-2)]. \tag{72}$$

For the body-centered cubic lattice $z=8$ and $\alpha_c=0.288$. Equations (53), (65), and (72) then give

$$T_c=V/k(\alpha_c-\theta)=V/k(0.288-\theta) \tag{73}$$

for the theoretical critical temperature above which all the long-range order disappears ($s=0$). When θ is set equal to zero in Eq. (73) the former "static" result is regained.

Along with the prediction of the critical temperature the theory also attempts to predict the magnitude of the heat capacity discontinuity at the critical temperature. The internal energy is obtained from Eq. (68) by differentiation with respect to temperature

$$E=\left(\frac{\partial A/T}{\partial 1/T}\right)_v,$$

where the differentiation with respect to T proceeds as follows:

$$(\partial/\partial T)_v=(d\alpha/dT)(\partial/\partial\alpha)_s+(ds/dT)(\partial/\partial s)_\alpha, \tag{74}$$

since A/T is an explicit function of α and s. Performing the indicated differentiations and utilizing Eqs. (63), (65), and (69),

$$E=-R(\alpha-\theta)Tz(\partial G/\partial\alpha)_s, \tag{75}$$

where $R=Nk$ is the universal gas constant. The heat capacity at constant volume is given by $C_v=(\partial E/\partial T)_v$. Performing the differentiation of Eq. (75) with the aid of Eq. (74), and using Eq. (70) to determine ds/dT, the following is obtained after suitable algebraic manipulation:

$$C_v=R(\alpha-\theta)^2\left\{z\left(\frac{\partial^2 G}{\partial\alpha^2}\right)_s+\frac{z^2(\partial^2G/\partial\alpha\partial s)^2}{[(1-s^2)^{-1}-z(\partial^2G/\partial s^2)_\alpha]}\right\}. \tag{76}$$

Equation (76) is found to be discontinuous at $\alpha=\alpha_c$, $s=0$. Taking the limit of C_v as $s\to 0$ from both above and below the critical temperature and subtracting we obtain the theoretical heat capacity discontinuity

$$\Delta C_v=\frac{6R[z(\alpha_c-\theta)(dG_1/d\alpha)_{\alpha=\alpha_c}]^2}{1-12zG_2(\alpha_c)}. \tag{77}$$

Again, the static result reported in B-K may be regained by setting $\theta=0$ in the above equation. This property may be utilized to recast the above equation into the following simple and interesting form:

$$\Delta C_v=(\alpha_c-\theta)^2\alpha_c^{-2}[\Delta C_v]_{\text{static}}, \tag{78}$$

where the quantity in brackets is the theoretical result obtained in the static approximation ($\theta=0$). For $z=8$ the static theory in B-K gives $[\Delta C_v]_{\text{static}}=1.70R$, so that combining with Eq. (72) and (78),

$$\Delta C_v=1.70R(1-3.47\theta)^2. \tag{79}$$

Equations (73), (75), and (78) show that the qualitative effects of the lattice vibrations on the transformation depend on the sign of the parameter θ. If θ is positive, T_c will be raised and ΔC_v will be depressed while if θ is negative T_c will be lowered and ΔC_v increased. The energy of the transformation, however, is independent of the lattice vibrations; setting $T=T_c$, $\alpha=\alpha_c$ in Eq. (75) and using Eq. (73) it can be seen that the energy of transformation, $E(T_c)-E(0)$ is independent of θ.

COMPARISON WITH EXPERIMENT: β-BRASS

The β phase of brass satisfies most of the requirements imposed by the simplifications introduced into the theory. The composition of this phase is very nearly 50-50 in copper and zinc, and the body-centered cubic structure is exhibited. Moreover, the masses of copper and zinc atoms are almost equal, the mass ratio being $63.54/65.38=0.972$. We shall therefore undertake the approximate computation of the parameter θ for this system for the purpose of comparing the experimental and theoretical results.

Reasonable estimates of the Hooke's law force constants, α_{kl} can be obtained from the appropriate macroscopic elastic constants through the use of relations derived by de Launay.[17] Adopting a simplified model for the cubic metallic elements, and utilizing the Born-von Karman lattice dynamics, de Launay has shown that

$$\alpha=\gamma a c_{44}, \tag{80}$$

where α is the desired force constant, c_{44} is the indicated elastic constant, and a is the lattice parameter; γ is a constant, $\frac{3}{2}$ for the body-centered cubic lattice and 1 for the face-centered cubic lattice.

Computation of α_{11} from data on copper: The elastic constant, c_{44} at room temperature has the value[18] 7.56×10^{11} d/cm^2. The lattice constant of the face-centered cubic unit cell is [19] 3.615 A. Use of Eq. (80) with $\gamma=1$ yields $\alpha_{11}=2.73\times10^4$ d/cm.

Computation of α_{12} from room temperature data on β-brass: Since β-brass is essentially all ordered at room temperature all the nearest-neighbor pairs are Cu-Zn or 1–2 pairs. Thus the macroscopic c_{44} is a measure of α_{12} (since the masses are nearly the same we assume that de Launay's formula holds for this case also). The elastic constant c_{44} for β-brass at 25°C has the value[20] 7.44×10^{11} d/cm^2. The lattice constant of the body-centered cubic unit cell is[21] 2.948 A. Use of Eq. (80) with $\gamma=\frac{3}{2}$ yields $\alpha_{12}=3.29\times10^4$ d/cm.

Computation of α_{22}: The computation of α_{22} is not as straightforward as that for the previous two force constants. In order to obtain a reliable estimate of α_{22} we have used two independent sets of elastic constant data: (i) that for Zn at room temperature and (ii) that for disordered β-brass. (i): Since Zn crystallizes in the hexagonal close packed structure the formula of de Launay, [Eq. (80)] need not be correct in this case. Since both the *hcp* and *fcc* lattices have $z=12$, however, we shall assume that Eq. (80) is at least approximately correct for Zn. The elastic constant c_{44} for Zn has the value[22] 3.78×10^{11} d/cm^2 while the a parameter is[23] 2.659 A. Use of Eq. (80) with $\gamma=1$ yields $\alpha_{22}=1.00\times10^4$ d/cm. (ii): At temperatures higher than T_c, β-brass is completely disordered so that a c_{44} determined in this range should be a measure of the average force constant α_D, Eq. (56). The lattice constant of β-brass at high temperatures has not been measured; we shall assume that it has increased only about 1% from room temperature having a value of 2.97 A. Artman[9] has measured the elastic moduli, E_{hkl} of β-brass as a function of temperature through the entire transformation, but unfortunately these do not alone determine the desired elastic constants. Good,[8] on the other hand, measured the elastic constants directly over the same temperature range. Good's data, however, is not in agreement with that of Artman and Thompson[9,20] at lower temperatures. In fact, it appears as if Good's results are off by simple scale factors. On the assumption that this is so, we have computed the scale factors from the two sets of low-temperature data and used them to correct Good's results at 506°C. Good's direct observations for the elastic coefficients s_{11}, s_{12} and s_{44} are 5.06, -1.99, and 0.739×10^{-12} cm^2/d, respectively. The corrected values are 5.35, -2.48, and 1.72×10^{-12} cm^2/d, respectively. To check the correctness of these coefficients we have computed the elastic moduli from them and compared these with Artman's observations. The computed[24] E_{100}^{-1}, E_{110}^{-1}, and E_{111}^{-1} are 5.35, 1.86 and 0.700×10^{12} cm^2/d, respectively, while the observed[9] values are 5.270, 1.864, and 0.729×10^{12} cm^2/d, re-

[17] J. de Launay, J. Chem. Phys. **21**, 1975 (1953).
[18] D. Lazarus, Phys. Rev. **76**, 545 (1949).
[19] *American Institute of Physics Handbook* (McGraw-Hill Book Company, Inc., New York, 1957), p. 2-48.
[20] R. A. Artman and D. O. Thompson, J. Appl. Phys. **23**, 470 (1952).
[21] F. W. Jones and C. Sykes, Proc. Roy. Soc. (London) **A161**, 440 (1937).
[22] Footnote reference 19, p. 3-82.
[23] Footnote reference 19, p. 2-52.
[24] The required formulas may be found in footnote reference 20, p. 472.

spectively. The agreement here is rather good so that we may confidently use the corrected value of 1.72×10^{12} cm²/d for the s_{44} of disordered β-brass. The desired c_{44} equal to s_{44}^{-1} is then 5.81×10^{11} d/cm². Using Eq. (80) with $\gamma=\frac{3}{2}$ yields $\alpha_D=2.59\times10^4$ d/cm. Substituting the computed values of α_{11}, α_{12} and α_D in Eq. (56) yields $\alpha_{22}=1.05\times10^4$ d/cm in close agreement with that computed in (i).

Equations (56), (57), and (59) provide the formulas for computing the parameter θ from the force constants. Using the values for α_{11} and α_{12} computed before and the value of α_{22} computed in (i) we obtain $\theta=(2/z)(-0.826-0.243)=-0.267$. Using the value of α_{22} computed in (ii) we obtain $\theta=(2/z)(-0.811-0.231)=-0.260$. Not only do the two values of θ agree, but the first- and second-order contributions separately are found to be in close correspondence. Note also that the second-order terms contribute only about a fourth of the total effect; the convergence of our perturbation series is therefore demonstrated to be quite good. For the purpose of computing the thermodynamic properties we shall use the value, $\theta=-0.26$.

Substitution into Eq. (73) gives the theoretical critical temperature:

$$T_c=1.82V/k. \tag{81}$$

The critical temperature is thus reduced to approximately a half of that predicted by the static theory. It is not possible to compare Eq. (81) with experiment, however, as unambiguous values of V are unobtainable at present.

Substitution of the computed value of θ into Eq. (79) yields the predicted heat-capacity discontinuity

$$\Delta C_v=1.70R(3.62)=6.1R. \tag{82}$$

Thus the lattice vibrations increase the heat capacity discontinuity by a factor of about three and a half. In the theory of Booth and Rowlinson,[10] the heat capacity discontinuity is also increased but only to a value of $2.6R$. The experimentally determined[25] value for C_p is about $5R$. The agreement between theory and experiment now appears to be quite satisfactory. The greater increase in ΔC_v obtained in this research over that computed by Booth and Rowlinson is most certainly due to our more realistic treatment of the lattice vibrational effects through use of the Born-von Karman model.

A more stringent test of the theory consists of a comparison of the entire course of theoretical and experimental heat capacity curves. Substitution of the numerical solutions of Eq. (70) into Eqs. (67) and (76) provides the theoretical heat capacity curves for both $\theta=0$ and $\theta=-0.26$. These results, along with the experimental[25] curve, are plotted in Fig. 1 as functions of the reduced temperature T/T_c. The solid line is the experimental C_p curve of Sykes and Wilkinson,[25] the dotted line is the result without lattice vibrations (theory in B-K, $\theta=0$), and the dashed line represents the present results with lattice vibrations included, $\theta=-0.26$. The results in Fig. 1 demonstrate that a significant improvement has been obtained through the addition of the lattice vibrational contribution. The lattice vibrational effects raise the heat capacity in the regions immediately above and below T_c while lowering it at the low-temperature end. The general shape of the theoretical curve has also been brought into closer correspondence with experiment. The thermal anomaly is still too broad, however, producing too large an increment in the entropy of the ordering process. On combining Eqs. (68), (72), and (75), the entropy change on ordering, $S(T_c)-S(0)$, is calculated to be $1.1R$. The experimental value[25] is $0.51R$ or only about half this amount.

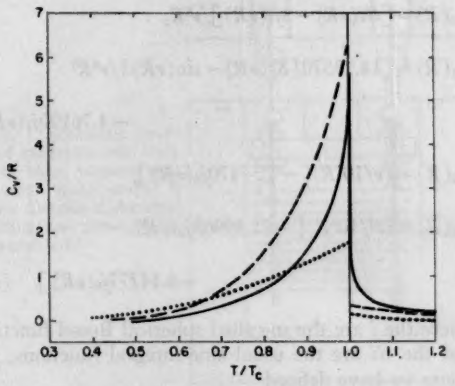

FIG. 1. Theoretical and experimental heat capacity curves for β-brass (CuZn). The solid line is the experimental C_p of footnote reference 25. The dotted line is theoretical, $\theta=0$, while the dashed line represents the results of the present calculation, $\theta=-0.26$.

APPENDIX

The functions X_i and Y_i for the body-centered cubic lattice are given as follows:

$$X_0(R)=[2Si(\nu R)+j_1(\nu R)]/\nu^3R,$$

$$X_1(R)=[10.71429j_1(\nu R)-4.76190\{Si(\nu R)-\sin(\nu R)\}/\nu^2R^2]/10^2\nu R,$$

$$X_2(R)=(\nu/10^4R)[11.36937j_1(\nu R)-7.05468j_3(\nu R)],$$

$$X_3(R)=(\nu^3/10^6R)[13.1468j_1(\nu R)-6.74496j_3(\nu R)+1.92714j_5(\nu R)], \tag{A1}$$

[25] C. Sykes and H. Wilkinson, J. Inst. Metals 61, 223 (1937).

$$Y_0(R)=[Si(\nu R)-3j_1(\nu R)]/\nu^3R,$$

$$Y_1(R)=[14.28570\{Si(\nu R)-\sin(\nu R)\}/\nu^2R^2 -4.76190j_1(\nu R)],$$

$$Y_2(R)=(\nu/10^4R)[-1.57470j_3(\nu R)],$$

$$Y_3(R)=(\nu^3/10^6R)[-21.49968j_3(\nu R) +6.14277j_5(\nu R)], \quad \text{(A2)}$$

where the j are the so-called spherical Bessel functions and the Si are the usual sine integral functions, and where we have defined

$$\nu=(6\Delta\pi^2)^{\frac{1}{3}}, \quad \text{(A3)}$$

Δ being the volume of the primitive cell in reciprocal space ($\frac{3}{4}\sqrt{3}$ for the *bcc* lattice). A convenient tabulation of the j may be found in *Table of Spherical Bessel Functions* (Columbia University Press, New York, 1947). For $R=0$ the preceding functions reduce to:

$$X_0(0)=2.33333\nu^{-2},$$

$$X_1(0)=3.04233\times10^{-2},$$

$$X_2(0)=3.78978\times10^{-4}\nu^2,$$

$$X_3(0)=4.47156\times10^{-6}\nu^4,$$

$$Y_i(0)=0, \quad (i=0, 1, 2, 3). \quad \text{(A4)}$$

TABLE I. Values of $X(R)$ and $Y(R)$ for the body-centered cubic lattice.

R	$X(R)$	$Y(R)$
0	0.167743	0.000000
1	0.044357	0.023876
$2(1/3)^{\frac{1}{2}}$	0.030482	0.023801
$2(2/3)^{\frac{1}{2}}$	0.020242	0.015015
2	0.023158	0.008884
$(11/3)^{\frac{1}{2}}$	0.022905	0.009836
$(19/3)^{\frac{1}{2}}$	0.016768	0.008179
3	0.012009	0.007951

THE JOURNAL OF CHEMICAL PHYSICS VOLUME 33, NUMBER 5 NOVEMBER, 1960

Dielectric Constants of Imperfect Gases. I. Helium, Argon, Nitrogen, and Methane

D. R. JOHNSTON, G. J. OUDEMANS, AND R. H. COLE

Metcalf Chemical Laboratories, Brown University, Providence, Rhode Island

(Received May 16, 1960)

Measurements from 1 to 100 atm have been made at one or more temperatures between −30° and 70°C by a special transformer ratio arm bridge operating at 10 kc; derived values of the Clausius-Mossotti function are of sufficient precision (0.1%) to justify comparison with theoretical pair fluctuation, polarizability and multipole moment interaction effects at higher densities. Helium shows a decrease of 0.3% and argon an increase of 0.1% in C-M at 100 atm, while nitrogen and methane show somewhat larger positive effects, especially at lower temperatures. A decreased effective polarizability of atom pairs at small distances is discussed as a possible explanation of the data for helium and argon, while the effect in nitrogen is consistent with quadrupole-induced dipole moments of pairs. A theory of octupole-induced dipole interactions is shown to be capable of explaining the methane results with plausible estimated values of the octupole moment.

THE dielectric constants of imperfect gases are determined by both the properties of the isolated molecules and the effects of molecular interactions. At relatively low densities, the variations of dielectric constant with density should be calculable from theories which take account only of pair interactions. The classic calculation by Lorentz[1] of the average field at a molecule due to identically polarized neighbors in a structure of cubic symmetry leads to the Clausius-Mossotti expression for nonpolar molecules that

$$\text{C-M}=(\epsilon-1)/(\epsilon+2)n/V=4\pi N_0\alpha/3,$$

where ϵ is the dielectric constant, n/V the molar density, N_0 is Avogadro's number, and α the polarizability of the isolated molecule, assumed to be independent of interactions with neighbors.

One of Kirkwood's first theoretical contributions[2] was his calculation of the effect of fluctuating molecular fields for a pair of molecules, with the result that a small increase of C-M proportional to density is predicted. His assumption that the amount induced in a molecule by the field of a neighbor could be represented by a constant polarizability was modified by Jansen and Mazur's perturbation calculation[3] of the moments of

[1] H. A. Lorentz, *The Theory of Electrons* (Dover Publications, Inc., New York, 1952).

[2] J. G. Kirkwood, J. Chem. Phys. **4**, 592 (1936).

[3] L. Jansen and P. Mazur, Physica **21**, 193 (1955).

a pair of interacting molecules in an external field: This treatment predicts a further increase of C-M with density; the estimated magnitude for atoms and simple molecules is comparable with the Kirkwood-Yvon translational fluctuation effect. Still another kind of contribution for molecules can result from the moments induced by permanent multipole moments of a neighbor, which have a net effect when an external field makes orientations of low energy favorable. Zwanzig,[4] Buckingham and Pople,[5] and Jansen[6] have made calculations for quadrupole moments, and a similar octupole treatment for tetrahedral molecules such as methane is presented in the discussion section of this paper.

If the multipole effect can be distinguished and used to estimate higher multipole moments with any degree of accuracy, one has a means of obtaining a useful index of electron distribution in nonpolar molecules. Thus, studying dielectric constant variations with density offers possibilities in this direction, as well as in testing the present theories of the other interaction effects.

The experimental problem is difficult because dielectric constants of simple gases in the theoretically tractable pair density range differ from unity by amounts ranging from 100 parts per million to 1% at most, and these differences must be determined with considerable accuracy if any reliable conclusions are to be drawn about the interaction effects.

One of the earliest experimental studies was by Kirkwood in collaboration with Keyes and Uhlig[7]; these revealed definite changes with density of the Clausius-Mossotti function for several nonpolar gases. A considerable number of subsequent investigations have been adequate to show a significant *decrease* of C-M with density at pressures above 100 atm and approximate constancy or small positive deviations in the range 1 to 100 atm. In most of these studies, however, random and systematic errors have been too large at the lowest densities to permit satisfactory estimates of the theoretically interesting "dielectric second virial" coefficient B in the equation

$$\text{C-M}=A+B(n/V). \qquad (1)$$

Results of different investigators have, moreover, often been in rather poor agreement as to the values both of B and of $A=4\pi N_0\alpha/3$, the isolated molecule contribution to C-M. The present work was undertaken to determine values of sufficiently improved accuracy at pressures below 100 atm to justify comparison with the various interaction theories. In this report, a new method and results for helium, argon, nitrogen, and methane are presented.

[4] R. W. Zwanzig, J. Chem. Phys. **25**, 211 (1956); **27**, 821 (1957).
[5] A. D. Buckingham and J. A. Pople, Trans. Faraday Soc. **51**, 1029 (1957).
[6] L. Jansen, Phys. Rev. **112**, 434 (1958).
[7] H. H. Uhlig, J. G. Kirkwood, and F. G. Keyes, J. Chem. Phys. **1**, 155 (1933).

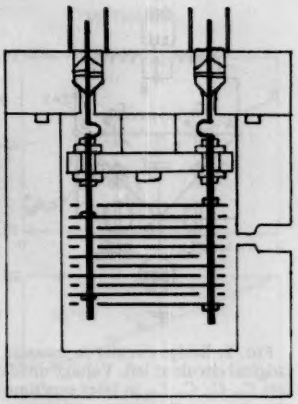

FIG. 1. Schematic drawing of capacitor cell. Only one of three support rods for each plate stack is shown. Details of electrical shielding and pressure fittings omitted.

I. EXPERIMENTAL METHODS

Dielectric constants were measured by a transformer bridge method,[8] in which the capacitance difference between two identically constructed capacitors, one containing the gas and the other evacuated, was balanced by calibrated variable capacitances or capacitance networks. By the use of closely coupled transformer windings as ratio arms, only direct capacitances between ungrounded electrodes of the cells are measured, as effects from shielded lead or other capacitances to ground are eliminated to a very high degree of approximation by the guard circuit action such ratio arms provide. Variations in such residual capacitances with pressure have probably caused much of the random and systematic deviations in resonance substitution methods used in several of the earlier investigations.

The sample and reference cells contained parallel plate capacitors of construction patterned after standard air capacitor designs and shown schematically in Fig. 1. Their mounting in the pressure vessels was designed to ensure that the parts determining the measured direct capacitances were subjected to hydrostatic pressure with a minimum of distortion from pressure-induced stresses elsewhere. A variety of tests with modifications of the lead connections and internal shielding gave no indications of any measurable errors from such effects. The cells were constructed of stainless steel with quartz insulation except for Teflon and soapstone washers in the pressure seals for the connecting leads; their vacuum capacitances were 80.5 pf and were matched to 0.05 pf.

The bridge circuit for measuring the differences is shown in Fig. 2. The generator, ratio arms, and phase sensitive detector circuits were all contained in a special General Radio type 1605-AS3 impedance comparator, modified by the manufacturer to give ten times higher sensitivity than the standard model. An external indicating meter (Doelcam "Magnetik" Null indicator)

[8] R. H. Cole and P. M. Gross, Jr., Rev. Sci. Instr. **20**, 252 (1949).

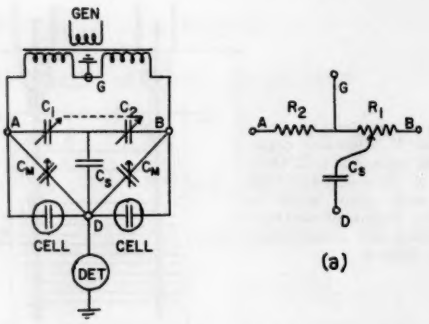

FIG. 2. Bridge circuits to measure cell capacitance differences. Original circuit at left. Voltage divider circuit (a) replaced capacitors C_1, C_2, C_s, C_m in later experiments.

with minor circuit changes further increased the usable sensitivity to one scale division for a capacitance difference of two parts per million.

In most of the experiments, the capacitance network $C_1C_2C_s$ of Fig. 2 was used to balance capacitance differences, C_1 and C_2 being variable 20–70 pf air capacitors driven in opposition and C_s any one of three fixed standards adjusted to give full scale ranges of 0.5, 5, and 50 pf. The nearly linear variation of C_1 and C_2 to cover these ranges was indicated by a 500-division dial, readable to 0.1 division, which was calibrated by iteration. For helium, variable capacitors C_m were used in which a grounded micrometer head between two fixed parallel electrodes varied the direct capacitance between them; the linear range of 0.08 pf was covered in 400 divisions readable to 0.1 division. In later experiments on argon and methane, the network of Fig. 2(a) was used in which R_1 is a 500-ohm precision 10-turn air-core potentiometer (Helipot type 7703) readable and linear to 0.02% of full scale. The variable voltage at the tap then supplies a variable capacitative current to the detector through capacitor C_s (0.05, 0.5, 5, or 50 pf). For these values at the 10-kc operation frequency, inductive and resistive phase errors are negligibly small and with the phase sensitive detector used need not be balanced. Resistor R_2 is a dummy 500-ohm load across the other ratio arm as a precaution to minimize small errors from unbalanced loads. Estimated reading and calibration errors give a 0.07% standard deviation of the Clausius-Mossotti function calculated from a single reading.

Gas densities were determined from pressure measurements and *PVT* data. Pressures above 30 atm were measured by a Budenberg dead weight gauge supplied with piston and weights certified to 0.03%, which was connected to the gas apparatus by a mercury separator. A correction of 0.08% converted the indicated pressures to standard atmospheres. Pressures below 2 atm were measured by a conventional mercury manometer and cathetometer. Two procedures were used for series of measurements at different densities. The first, of taking readings at directly measured pressures starting with the initial highest available pressure, had the disadvantage of increased errors from dead weight gauge insensitivity in the 2- to 40-atm range. The second procedure was to use the Burnett expansion method, in which the initial high-pressure gas was repeatedly expanded into a smaller previously evacuated vessel thus producing the same fractional density decrease (25%) at each expansion. Initial high and final low pressures were determined and the corresponding densities computed from *PVT* data: from these data all the intermediate densities could then be calculated.

Expansion ratios obtained in this way were very consistent: for example, density ratios, after ten expansions of nitrogen, argon, and methane at −30°C agreed to 0.03%. Various comparisons showed no significant differences in results from the two methods when sufficient care was taken to ensure thermal equilibrium and freedom from contamination. A number of further spot measurements were made to test reproducibility. The capacitor cells and expansion vessel were mounted in a liquid thermostat bath controlled to 0.1°C or better. Temperatures near −30°C were produced by a conventional refrigeration unit.

The helium used was obtained from the U. S. Navy, argon from Air Reduction Company, and nitrogen and helium from Matheson. Stated impurities of the helium and argon, used without further purification, were less than 0.2 and 0.4%, principally nitrogen. The nitrogen used was the prepurified grade; measurements with oil-pumped nitrogen were less reproducible and are not reported. The C.P. methane was dried by passage through a high pressure line in a dry ice trap before being admitted to the cell.

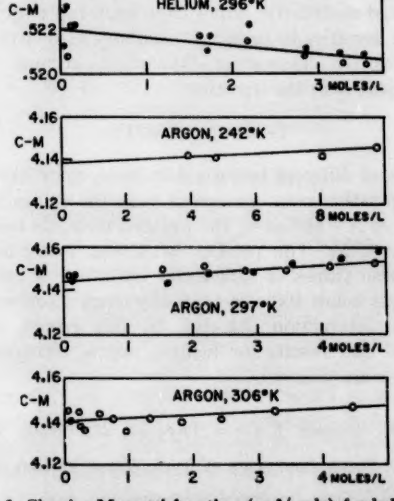

FIG. 3. Clausius-Mossotti function (cm³/mole) for helium and argon vs density (moles/liter). Results of different runs indicated by open and filled circles.

II. RESULTS

Values of the Clausius-Mossotti function in cm³/mole calculated from the dielectric constant density data are plotted against density in moles/liter in Figs. 3–5. The plots for the four gases and different temperatures suggest what more detailed analysis shows, that there is in no case evidence for anything more complicated than a linear variation of C-M with density over the ranges covered. Table I lists the values of the intercept A (cm³/mole) and slope B (cm⁶/mole²), with standard deviation estimates in parentheses. The table also lists the sources of PVT data used to convert measured pressures to densities. Some doubt was originally felt about the use of Kvalnes and Gaddy's PVT data[9] for methane at −30°C because their data at higher temperatures do not agree too well with values of Michels and Nederbrag[10] and of Keyes and Burks.[11] However, these data gave excellent expansion ratio agreement as mentioned before, which we take to be good evidence for their use (conversely, we could have taken the ratio as known from results for other gases and computed densities from it with the same result).

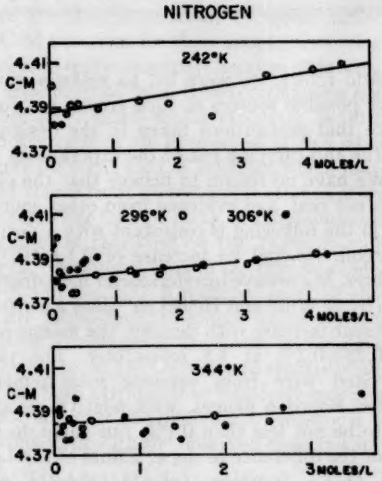

FIG. 4. Clausius-Mossotti function (cm³/mole) for nitrogen vs density (moles/liter). Results of different runs indicated by open and filled circles.

The precision of the data can be indicated by the standard deviation of single measurements from mean values corresponding to the constants in Table I. This averages about 0.15% at pressures below 10 atm, 0.1% for higher pressures, and for no run does it exceed 0.2%. These figures are not much greater than the 0.07% estimate from possible capacitance reading and calibration errors; the differences could easily result from small variations in temperature, cell geometry, and the like.

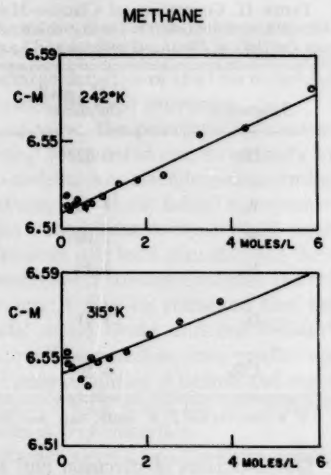

FIG. 5. Clausius-Mossotti function (cm³/mole) for methane vs density (moles/liter).

A partial check on accuracy of the present results can be obtained by comparison with precise atmospheric pressure results obtained from various microwave, radio-frequency resonance, and refractive index measurements. For helium, argon, and nitrogen, our values of A agree with averages calculated from reference data cited by Maryott and Buckley[12] to 0.2% or less, and lie within the range of values selected by them as a basis for their estimates of the best values. This comparison is reassuring, as many earlier results for compressed gases show rather large differences and uncertainties in extrapolation to the limiting value A for low densities, which makes estimates of the virial term B correspondingly uncertain.

TABLE I. Values of A and B of the Clausius-Mossotti function. Standard deviations are listed in parentheses. Sources of density data cited by letters (a), (b), and (c).

Gas	T°K	A (cm³/mole)	B (cm⁶/mole²)
He[a]	296	0.5221 (0.0004)	−0.6 (0.2)
	296	0.5219 (0.0004)	−0.4 (0.3)
A[b]	242	4.138 (0.004)	0.6 (0.7)
	296	4.145 (0.002)	1.6 (0.6)
	306	4.140 (0.002)	1.0 (0.7)
N_2[b]	242	4.389 (0.003)	4.2 (1.0)
	296	4.381 (0.002)	2.0 (1.0)
	306	4.384 (0.002)	1.8 (1.0)
	344	4.382 (0.001)	0.0 (0.8)
	344	4.380 (0.002)	1.5 (2.5)
CH_4[c]	242	6.518 (0.001)	9.0 (0.4)
	315	6.543 (0.003)	7.3 (1.8)

[a] A. Michels and H. Wouters, Physica 8, 923 (1941).
[b] Natl. Bur. Standards Circ. 564 (1955).
[c] See footnote references 9 and 10.

[9] H. M. Kvalnes and V. L. Gaddy, J. Am. Chem. Soc. 53, 394 (1931).
[10] A. Michels and G. W. Nederbragt, Physica 3, 569 (1936).
[11] F. G. Keyes and H. G. Burks, J. Am. Chem. Soc. 49, 1403 (1927).
[12] A. A. Maryott and F. G. Buckley, Natl. Bur. Standards Circ. 537 (1953).

TABLE II. Comparison of Clausius-Mossotti functions for ideal gas and liquid states. Liquid dielectric constant (ϵ) and density (d) data used are listed in the last columns; dielectric constants are from tabulations by Maryott and Smith,[a] densities from the *American Institute of Physics Handbook* and Landolt-Bornstein.

Substance	C-M (gas) cm³/mole	C-M (liq) cm³/mole	T (liq) °K	ϵ (liq)	d (liq) g/cm³
He	0.522	0.504	4.19	1.0480	0.125
		0.509	3.09	1.0540	0.139
A	4.14	(4.25)	87.4	1.538	1.39
H_2	2.04	2.01	20.4	1.228	0.0710
N_2	4.39	4.32	75.0	1.440	0.8297
		4.36	68.0	1.460	0.854
O_2	3.97	3.88	90.2	1.483	1.142
		3.90	84.9	1.507	1.183
CH_4	6.52	(7.00)	111.7	1.68	0.424

[a] A. A. Maryott and E. R. Smith, Natl. Bur. Standards Circ. 514 (1951).

Our estimates of precision and accuracy have been discussed at some length, because conclusions about density effects are sensitive to small errors. Space limitations prevent listing the original data and details of calibrations, tests for residual effects, and analysis of errors; these are presented more fully in doctoral theses, copies of which are available.

As far as we know, the work here is the most precise application so far made of a bridge method to measure dielectric constants of gases. The precision and accuracy compare quite favorably with those reported for radio-frequency and microwave resonance methods. Problems of lead capacitance and inductance and of frequency stability in radio-frequency resonance circuits are absent and the relatively simple electrical circuitry has been quite reliable. The low operating frequency of 10 kc ensures that static values are measured in any ordinary case.

III. DISCUSSION

The results for helium show a small but consistent decrease of the Clausius-Mossotti function with increasing density, which amounts to about 0.3% at 4 moles/liter (approx 90 amagat). The only other data for a comparable range of densities[13] show much larger random deviations (3%) and systematically lower values (10%) than precise atmospheric density results, with which the present values agree well. (In such comparison, it should be noted that we have applied a positive correction of 0.0024 to all measured C-M values. This is the result of the calculated geometric capacitance decrease of the cell by compression of the steel electrodes and spacers.)

This decrease was surprising to us at first, because Jansen's analysis[6] of polarizability and fluctuation effects, predicted a much smaller positive density effect, of about 0.02%. Because the measured effect is deduced from very small dielectric constant differences ($\epsilon-1=65\times10^{-6}$ at 20°C and 1 atm) and so is vulnerable to systematic errors, we were led to make a variety of tests for possible sources of such errors, but found no evidence that precautions taken in the design of the apparatus and carrying out of the experiments were at fault. We have no reason to believe that the observed effect is not real, and evidence from other sources discussed in the following is consistent with a decrease.

In argon, we find an increase of $0.1\pm0.07\%$ at 4 moles/liter. Microwave interferometer measurements at 1.29 cm by de Wijm and Heineken[14] show a considerably larger linear increase with density, the measured effect being $0.25\pm0.2\%$ at 1.8 moles/liter. The principal errors cited were from pressure measurements by calibrated Bourdon gauges, with relative inaccuracies stated to be not less than 0.1%, but these do not account for the difference in slope. Values of the Lorentz-Lorenz (L-L) function $(n^2-1)/(n^2+2)V/n$ from measurements of refractive indices n by Michels and Botzen[15] are inconclusive at densities below 4 moles/liter, but show a significant decrease at higher densities.

The sum of pair interaction effects in argon calculated by Jansen[6] at a density of 4 moles/liter gives a predicted increase of 0.5%. Our results are thus consistently lower for both helium and argon, and we were led to look for evidence of other density effects of compressed helium and argon which might throw light on the discrepancies.

Nonpolar gases of simple molecules generally show significant decreases of the L-L and C-M functions above 100–200 amagat; in particular this has been found for both argon and nitrogen. In discussing this effect, Kirkwood[2] observed that such decreases might result from suppression of fluctuation effects as liquid densities are approached. If there is in addition a negative effect, such as a decreased effective polarizability of "compressed" atoms, which is not suppressed, then one could expect that values of the C-M function at liquid densities would be smaller than for the dilute gases.

[13] A. Clay and E. van der Maesen, Physica **15**, 467 (1949).

[14] H. W. de Wijn and F. W. Heineken, Physica, **25**, 615 (1959).

[15] A. Michels and A. Botzen, Physica **15**, 769 (1949).

To test this conjecture, values of the C-M function derived from gas and liquid data for dielectric constants and densities are given in Table II; more than one value is listed for the liquid if alternative data are not in very good agreement. A real decrease of 2% or more is indicated for helium, and somewhat smaller decreases for hydrogen, nitrogen, and oxygen. The indicated increase for argon is suspect, as it depends on the single liquid dielectric constant value found by McLennan, Jacobsen, and Wilhelm,[16] and their measurements for liquid nitrogen under quite similar experimental conditions give a C-M function 4.8% larger than the value from other work. This disagreement also casts doubt on the comparison for ethane, which also depends on their liquid data.

There are thus suggestions of significantly smaller liquid C-M functions for these simple molecules but the conclusion is quite uncertain because of inconsistencies of the experimental data. Redeterminations and values for other inert gases would evidently be interesting; such measurements are in progress at this laboratory.

A quite different kind of evidence which may well be relevant comes from spectroscopic studies of frequency shifts on adding foreign gases of simple molecules. Recent studies of this kind on the 21-cm line of atomic hydrogen,[17] rotational lines in the first overtone band of HCl,[18,19] and the 2537 A mercury line[20] all show shifts which are increasingly to longer wavelengths for more polarizable foreign gases. However, for helium and to a lesser extent neon, the shifts are to shorter wavelengths, which has been attributed to relatively more important repulsive effects.[18] The qualitative behavior is evidently not inconsistent with the observed dielectric interaction effects.

From the theoretical point of view, the most likely direction in which to look for an explanation of the dielectric behavior seems to be in the evaluation of the effective induced moment of a molecule interacting with one or more neighbors. This problem of calculating the average induced moments of a pair of molecules was first considered by Jansen and Mazur[3]; these writers showed that for a harmonic oscillator model there is no change with intermolecular distance, but that for more realistic wave functions of the separated molecules a net increase of effective polarizabilities results. As Dr. Mazur has pointed out to us in discussion, the calculations are most appropriate at relatively large separations for which the intermolecular potential is attractive and internal electron displacements "softer" than for harmonic oscillators. At close separations, however, product wave functions for the atoms become less suitable, and one might well expect a decreased polarizability as the electron charge densities of the two molecules are increasingly confined by their proximity.

From this point of view, the polarizability calculations ought, as Jansen[6] has pointed out, to be made by considering the two molecules as a single system, rather than by using intermolecular "local fields" to represent the interaction. That a significant decrease could result for increased pair densities is at least plausible, but there appears to be no theoretical treatment available and the difficulties are obvious. It may be remarked that the "caged atom" model of de Groot and ten Seldam[21] more relevant to liquidlike densities does predict appreciably decreased polarizabilities of helium and argon atoms, but the accuracy with which the model represents exclusion effects is very uncertain.

The results for nitrogen show a small positive density effect, which at a density of 4 moles/liter is $0.4\pm0.1\%$ at 242°K and somewhat less at 300 and 344°K. Several other investigations of nitrogen have been made, but the evidence is not very consistent. Michels and Michels[22] found no significant density effect for pressures to 1500 atm, while de Wijn and Heineken's results show an increase of $0.36\pm0.2\%$ at 1.8 moles/liter. Data of Keyes and Oncley[23] indicate an increase at 100°C of 0.2% at 4 moles/liter which is not inconsistent with our results at lower temperatures.

Density variations of the Lorentz-Lorenz refractive index function are of interest here but not directly comparable because the quadrupole-induced dipole orientation effects make no net contributions to polarization at optical frequencies. The data of Michels, Lebesque, and de Groot[24] show no density effect exceeding 0.1% below 300 atm and a decrease of about 1% in the range 300 to 2000 atm (240 to 580 amagat).

Jansen has calculated that polarizability and fluctuation effects give an increase of 0.37% at 4 moles/liter, and the quadrupole effect a further increase of 0.08% at 316°K. The total of 0.45% is larger than, but not far from, our observed values. Even this partial agreement is suspect, however, in view of the discrepancies for inert gas atoms, the smaller or negative effects indicated by the refractive index data, and the necessarily more approximate nature of the polarizability calculations for molecules.

The data for nitrogen are not inconsistent with the existence of a quadrupole-induced dipole interaction of the predicted magnitude, but they clearly offer little hope at present of a quantitative test comparison or of estimating the molecular quadrupole moment. The considerably larger effects for such molecules as CO_2,

[16] J. McLennan, R. Hoyt, and J. Wilhelm, Trans. Roy. Soc. Can. **24**, 37 (1930).
[17] L. W. Anderson, F. M. Pipkin, and J. C. Baird, Bull. Am. Phys. Soc. Ser. II **4**, 418 (1959).
[18] M. A. Hirshfeld, J. H. Jaffe, and S. Kimel, J. Chem. Phys. **32**, 297 (1960).
[19] D. H. Rank, W. B. Birtley, D. P. Eastman, and T. A. Wiggins, J. Chem. Phys. **32**, 296 (1960).
[20] C. Füchtbauer, G. Joos, and O. Dinkelacker, Ann. Phys. **71**, 204 (1923).
[21] S. R. de Groot and C. J. ten Seldam, Physica **18**, 905, 910 (1952).
[22] A. Michels and C. Michels, Proc. Roy. Soc. (London) **A153**, 201 (1935); **A160**, 348 (1937).
[23] F. G. Keyes and J. L. Oncley, Chem. Rev. **19**, 195 (1936).
[24] A. Michels, H. L. Lebesque and S. R. de Groot, Physica **13**, 337 (1947).

ethylene, and propane are more promising in this respect; results for these will be reported later, together with an analysis of the quadrupole effect for molecules lacking axial symmetry.

In the case of methane, there is evidence from the data of a temperature dependent contribution to the second virial coefficient. As molecules of tetrahedral symmetry have no permanent quadrupole moment, the first possible multipole contribution is from the octupole moment. An analysis like that for quadrupole interactions is outlined in the Appendix, and shows that for molecules with isotropic polarizability α the contribution B_ω to the second virial term in Eq. (1) is given by

$$B_\omega = 320\pi^2 N_0^2 \alpha^2 \omega^2 \langle R^{-10} \rangle_0 / 9kT,$$

where the molecular octupole moment $\omega = \sum_i e_i x_i y_i z_i$ is summed over positions of nuclear and electronic charges and the average $\langle R^{-10} \rangle_0$ is over internuclear distances with a radial pair distribution function in the absence of an external field. The predicted temperature dependence is principally from the factor T^{-1} and to a lesser extent from the R^{-10} average.

Use of a Lennard-Jones 6-12 potential $W(r) = E[(a/R)^{12} - (a/R)^6]$, with $E/k = 597°$K and $a = 3.82$ A obtained from the PVT second virial coefficient, gives $B_\omega = 0.6(10^{-34}\omega)^2$ cm^6/mole^2 at 242°K for $\alpha = 2.58 \times 10^{-24}$ cm^3. As an indication of sensitivity of the result to variations in the intermolecular potential used, an empirical 7–∞ potential, $W(r) = -E(a/R)^7$ for $R > a$, $= \infty$ for $R < a$, was also used. The principal reason for the choice was expediency, perhaps justified to some extent as a simulation of R^{-6} polarizability and R^{-7} octupole terms in a better potential. With $E/k = 610°$K and $a = 3.58$ A to fit second virial data, the result is $B_\omega = 2.4(10^{-34}\omega)^2$.

Crude point charge calculations by placing two electrons on the C—H bond lines of length 1.09 A show the extreme sensitivity of the calculated octupole moments to electron charge distribution: for the pair midway between the nuclei, $10^{34}\omega = 3.6$ esu cm^3, but the moment is zero for the pair at 0.87 A from the carbon nucleus. If the entire virial coefficient B for methane is attributed to the octupole term, the necessary value of ω to give the observed effect is $1.7\text{–}3.4 \times 10^{-34}$ esu cm^3, which is not unreasonable. Results of valence bond calculations with sp^3 and Slater orbitals in progress should be of some interest for comparison, but these too are of dubious accuracy.[25]

IV. CONCLUSION

The Clausius-Mossotti function for the nonpolar atomic and simple molecular gases studied changes remarkably little in pair interaction ranges of density. The near constancy is not so much a justification of the Lorentz field without complicating factors as it is an indication that the resultant effect of pair interactions are very small for these gases, and to the extent the local field approach is useful must result from approximate compensation of the separately treated effects.

The conjecture that the negative deviation for helium and small positive effect in argon reflect a relatively larger repulsion or "compressed atom" effect for the former ought to be further examined. Dielectric constant data for compressed xenon and for liquefied gases should be of considerable interest in this and related connections; such measurements are under way or planned.

There is some evidence for nitrogen and methane of the multipole field-induced dipole effects predicted by interaction theories, but the differences are too small and too obscured by other uncertainties to give quantitative results. The small temperature effect in methane is not inconsistent with plausible values of octupole moment, but can hardly be considered to give an experimental determination of this quantity. Again, further measurements may help to clarify the situation and permit more definite conclusions.

The several complicating factors indicated by theory and experiment for nonpolar gases must also be present in dielectric behavior of polar gases and mixtures. While their effects may be small in comparison with those of interactions involving permanent dipoles, there is no reason to think that they can always, or even usually, be neglected in only moderately precise comparisons of theory and experiment.

ACKNOWLEDGMENTS

This research was supported in large part by a National Science Foundation grant. Discussions with Dr. P. Mazur and Dr. J. Ross were very helpful in developing the point of view adopted to interpret the results. One of us (DRJ) wishes to thank the Monsanto Chemical Company for award of a fellowship in 1959–60.

APPENDIX

Octupole-Induced Dipole Interaction

The problem is to evaluate the mean moment which the field of the octupole moment of one molecule induced in a neighbor of isotropic polarizability when both are part of a spherical sample subjected to an external field E_0. For simplicity, only molecules of tetrahedral symmetry will be considered. The axes of the one molecule may be arbitrarily fixed in space relative to the field E_0 of external charges if the moment induced in a neighbor by the octupole field is averaged over all relative positions of the neighbor. A convenient orientation of the tetrahedral axes is along the four body diagonals of a cube with edges parallel to axes x, y, z, with E_0 parallel to x. The only nonvanishing quadrupole

[25] *Note added in proof.* Since this paper was submitted, Professor R. G. Parr has informed us of a calculation of ω, using a one-center wave function with Slater orbitals, which gives the value 2.6×10^{-34} esu cm^3 for ω as here defined. This calculation was reported in a paper by Turner, Saturno, and Parr read at the New York ACS meeting in September, 1960.

moment element is then $\omega=\sum e_i x_i y_i z_i$, where charges e_i are at distances x_i, y_i, z_i relative to the cube center, and the field component $(E_\omega)_z$ at a point $R(x, y, z)$ is

$$(E\omega)_z=-(15\omega/R^5)(yz/R^2)(1-7x^2/R^2). \quad \text{(A1)}$$

The mean moment along x and E_0 of a molecule at R is then $\langle m_z\rangle=\alpha\langle E_{\omega z}\rangle$, where the brackets indicate averaging with the Boltzmann factor $\exp(-W/kT)$, and we take $W=W(R)-\alpha E_{\omega z}E_0$, thus neglecting angular correlations of the pair energy in the absence of E_0. Expanding in the normal way to obtain the linear term in E_0 gives

$$\langle m_z\rangle=\alpha^2\langle E_{\omega z}^2\rangle_0 E_0/kT,$$

where the subscript zero denotes averaging with $W(r)$ for $E_0=0$. Inserting $E_{\omega z}$ from Eq. (A1) and averaging over products of direction cosines (x/R), (y/R), and (z/R) gives

$$\langle m_z\rangle=80\pi\alpha^2\omega^2 E_0\langle R^{-10}\rangle_0/kT. \quad \text{(A2)}$$

The contribution B_ω to the second virial term in the C-M function is given by

$$B_\omega(n/V)^2=4\pi N^2\langle m_z\rangle E_0/3(\epsilon+2)EV.$$

Inserting $E_0=(\epsilon+2)E/3$ for the spherical sample and $N=N_0 n$ where N_0 is Avogadro's number, gives the desired result.

THE JOURNAL OF CHEMICAL PHYSICS VOLUME 33, NUMBER 5 NOVEMBER, 1960

Statistical Mechanics of Transport Processes. XIV. Linear Relations in Multicomponent Systems*

JOHN G. KIRKWOOD
Sterling Chemistry Laboratory,† Yale University, New Haven, Connecticut
AND
DONALD D. FITTS
Department of Chemistry, University of Pennsylvania, Philadelphia 4, Pennsylvania

(Received May 11, 1960)

A classical treatment of the time dependence of a phase-space distribution function for a system near equilibrium is presented. The nonequilibrium distribution function is expressed as a stationary zero-order function plus a perturbation term and is used to obtain the diffusion and heat fluxes by averaging the appropriate dynamical variables. When only terms linear in the gradients of the local temperature, the chemical potentials, and the velocity of the local centers of mass are retained, the usual linear relations result and explicit expressions for the phenomenological coefficients are obtained. These expressions agree with the results of Mori and of Green and are shown to obey the Onsager reciprocal relations.

WITH the use of the statistical-mechanical theory of transport processes as developed by Kirkwood,[1] Irving and Kirkwood[2] have derived the macroscopic equations of transport for one-component systems from the equations of molecular dynamics. Their results have been generalized to multicomponent systems by Bearman and Kirkwood.[3] Thus, macroscopic quantities such as the stress tensor and fluxes of matter and heat are expressed as averages over nonequilibrium molecular distribution functions.

The next objective of the statistical-mechanical theory of transport processes is the determination of the time dependence of a deviation of the phase space distribution function from its equilibrium form. Since the decay of this deviation gives rise to transport phenomena, an evaluation of its time dependence determines the various transport coefficients in terms of molecular variables. These transport coefficients may then be calculated for particular systems. We attempt here to fulfill part of this objective.

In this article we develop a method for treating the time dependence of a distribution function for a system near equilibrium. We restrict our discussion to classical systems, although the same treatment could be developed quantum mechanically by replacing the probability density in phase space with the Wigner distribution function.[4,5] The temporal development of the nonequilibrium distribution function is governed by Liouville's equation. We express this distribution function as a zero-order function plus a perturbation term. Upon introducing a specific zero-order function

* The work presented in this article was started when both authors were at Yale University. A preliminary report was given by Professor Kirkwood at the International School of Physics of the Italian Physical Society in June, 1959 and published in *Nuovo cimento Supplemento* [16, (1960)]. This article was prepared by D.D.F. after the death of Professor Kirkwood.

† Contribution No. 1611.

[1] J. G. Kirkwood, J. Chem. Phys. **14**, 180 (1946).

[2] J. H. Irving and J. G. Kirkwood, J. Chem. Phys. **18**, 817 (1950).

[3] R. J. Bearman and J. G. Kirkwood, J. Chem. Phys. **28**, 136 (1958).

[4] E. Wigner, Phys. Rev. **40**, 749 (1932).

[5] J. H. Irving and R. W. Zwanzig, J. Chem. Phys. **19**, 1173 (1951).

and neglecting all terms except those linear in the macroscopic parameters which determine the deviations from equilibrium,[6] we obtain explicit expressions for the phenomenological coefficients which appear in the linear relations for the heat flux and for the diffusion current densities of the various components in the system. These expressions involve time integrals of temporal correlation functions of dynamical variables and are independent of our choice for the zero-order distribution function. The phenomenological coefficients are shown to obey the Onsager reciprocal relations.[7] We do not attempt here to calculate numerical values of these coefficients for specific systems.

In Sec. I we consider the general first-order perturbation theory for the nonequilibrium distribution function. In Sec. II, we introduce a specific zero-order local-equilibrium distribution function and linearize it. Section III treats the linear relations for the diffusion fluxes, while Sec. IV deals with the heat flux. In Sec. V we prove the Onsager reciprocal relations for the phenomenological coefficients that appear in the linear relations obtained in Secs. III and IV. Section VI is devoted to a brief discussion of our results and to a comparison of our treatment with those of Mori[8] and of Green.[9]

I.

We consider a ν component nonequilibrium system containing N molecules which are not chemically reacting. Each component is labeled by the index α, which runs from 1 to ν. There are N_α molecules of species α; the individual molecules of each component α are numbered 1, 2, $\cdots$, N_α. Each molecule is assumed for simplicity to have only three degrees of translational freedom and no others. The position and momentum of molecule i of component α may, therefore, be denoted by the vectors $\mathbf{R}_{\alpha i}$ and $\mathbf{p}_{\alpha i}$, respectively. We may occasionally let $\mathbf{R}$ denote the set of N vectors $\mathbf{R}_{11}, \mathbf{R}_{12}, \cdots, \mathbf{R}_{\nu N_\nu}$, and $\mathbf{p}$ the set $\mathbf{p}_{11}, \mathbf{p}_{12}, \cdots, \mathbf{p}_{\nu N_\nu}$.

We shall be concerned with a time-smoothed probability distribution function $\bar{f}^{(N)}(\mathbf{R}, \mathbf{p}, t)$ for the nonequilibrium N-particle system. For a temporal coarse graining,[1] we may consider a uniformly weighted average over an interval τ,

$$\bar{f}^{(N)}(\mathbf{R}, \mathbf{p}, t) = \tau^{-1}\int_0^\tau f^{(N)}(\mathbf{R}, \mathbf{p}, t+s)ds, \quad (1.1)$$

where $f^{(N)}(\mathbf{R}, \mathbf{p}, t)$ is the probability density in phase space at time t of an appropriate statistical ensemble. The interval τ is determined by the time resolution of the instruments employed in the measurement of the macroscopic observable. We discuss the interval τ further in Sec. VI.

[6] In this regard, our treatment is similar to the Chapman-Enskog treatment of the Boltzmann equation.
[7] L. Onsager, Phys. Rev. **37**, 405; **38**, 2265 (1931).
[8] H. Mori, Phys. Rev. **112**, 1829 (1958).
[9] M. S. Green, J. Chem. Phys. **22**, 398 (1954).

This temporal averaging of the distribution function does not need to be uniformly weighted in time; another possible temporal coarse graining is

$$\bar{f}^{(N)}(\mathbf{R}, \mathbf{p}, t) = \tau^{-1}\int_0^\infty \exp(-s/\tau) f^{(N)}(\mathbf{R}, \mathbf{p}, t+s)ds. \quad (1.2)$$

In general, this coarse graining in time may be expressed as

$$\bar{f}^{(N)}(\mathbf{R}, \mathbf{p}, t) = \int_{-\infty}^{\infty} w(s) f^{(N)}(\mathbf{R}, \mathbf{p}, t+s)ds, \quad (1.3)$$

where $w(s)$ is a normalized weighting function. In an experimental measurement, the observed result should be independent of $w(s)$ if the characteristic width τ of $w(s)$ is short relative to the relaxation times τ_r for the transport processes occurring in the system. Therefore, we shall adopt here the simple Kirkwood form (1.1).

The molecules in the system are assumed to obey the laws of classical mechanics. Consequently,[1] the time-smoothed probability distribution function $\bar{f}^{(N)}(\mathbf{R}, \mathbf{p}, t)$ for the nonequilibrium system at a time t obeys the Liouville equation

$$L\bar{f}^{(N)} + i(\partial \bar{f}^{(N)}/\partial t) = 0, \quad (1.4)$$

where i is the imaginary unit and L is the self-adjoint Liouville operator,

$$L = i\sum_{\alpha=1}^{\nu}\sum_{l=1}^{N_\alpha}[(\mathbf{p}_{\alpha l}/m_\alpha)\cdot\nabla_{\mathbf{R}_{\alpha l}} + (\mathbf{X}_{\alpha l}+\mathbf{F}_{\alpha l})\cdot\nabla_{\mathbf{p}_{\alpha l}}]. \quad (1.5)$$

In Eq. (1.5) m_α is the molecular mass of component α, $\mathbf{X}_{\alpha l}$ is the external force acting on molecule l of species α, and $\mathbf{F}_{\alpha l}$ is the intermolecular force exerted on this molecule by the other $(N-1)$ molecules.

We assume that the intermolecular force $\mathbf{F}_{\alpha l}$ has a pairwise additive form,

$$\mathbf{F}_{\alpha l} = \sum_{\substack{\beta=1 \\ \alpha l \neq \beta j}}^{\nu}\sum_{j=1}^{N_\beta}\mathbf{F}_{\beta j \alpha l}, \quad (1.6)$$

where $\mathbf{F}_{\beta j \alpha l}$ is the force acting on molecule l of species α due to molecule j of species β. The notation of $\alpha l \neq \beta j$ indicates that there is no term corresponding to $l=j$ when $\alpha=\beta$. The force $\mathbf{F}_{\beta j \alpha l}$ may be expressed in terms of the mutual potential energy $V_{\alpha\beta}$ of a pair of molecules of species α and β,

$$\mathbf{F}_{\beta j \alpha l} = -\nabla_{\mathbf{R}_{\alpha l}} V_{\alpha\beta}(R_{\beta j \alpha l}), \quad (1.7)$$

where $V_{\alpha\beta}$ is a function only of the magnitude of the vector distance

$$\mathbf{R}_{\beta j \alpha l} = \mathbf{R}_{\alpha l} - \mathbf{R}_{\beta j} \quad (1.8)$$

between the centers of masses of the two molecules.

The nonequilibrium system under consideration has gradients of temperature T, of the velocity $\mathbf{u}$ of the

local centers of mass, and of the chemical potentials μ_α of the ν chemical components.[10] The deviation from equilibrium is measured by r such parameters, which we write as γ_k where k runs from 1 to r. As each of the parameters γ_k approaches zero, the system approaches equilibrium.

We assume that the nonequilibrium system is sufficiently close to equilibrium that we may discard terms in the distribution function $\bar{f}^{(N)}$ higher than those linear in γ_k. Under this assumption we write $\bar{f}^{(N)}$ as the sum of a zero-order distribution function $\bar{f}_0^{(N)}$ and a perturbation term $\bar{f}_1^{(N)}$,

$$\bar{f}^{(N)}=\bar{f}_0^{(N)}(\gamma_1, \cdots, \gamma_r)+\bar{f}_1^{(N)} \tag{1.9}$$

with

$$\bar{f}_1^{(N)}=\sum_{k=1}^{r}\gamma_k\bar{f}_{1k}^{(N)}. \tag{1.10}$$

The zero-order distribution function $\bar{f}_0^{(N)}$ may be taken from a wide variety of possible choices. It must, of course, reduce to the equilibrium distribution function $f_{eq}^{(N)}$ when each of the parameters γ_k vanishes. Otherwise, convenience is the only criterion in the selection of $\bar{f}_0^{(N)}$. However, we choose $\bar{f}_0^{(N)}$ to be stationary, i.e., $\bar{f}_0^{(N)}$ is not an explicit function of time.

The quantities $\bar{f}_{1k}^{(N)}$ are not functions of the parameters γ_k. Therefore, the perturbation term $\bar{f}_1^{(N)}$ contains all those terms, linear in the γ_k, which are not included in $\bar{f}_0^{(N)}$. In principle, it is possible for $\bar{f}_0^{(N)}$ to contain all the linear terms and for $\bar{f}_1^{(N)}$ to vanish. However, if we select $\bar{f}_0^{(N)}$ to be stationary, then $\bar{f}_1^{(N)}$ may not be zero at all times.

Since we wish to retain in $\bar{f}^{(N)}$ only terms which are linear in the γ_k, we expand $\bar{f}_0^{(N)}$ in a Taylor series about equilibrium and discard quadratic and higher terms in γ_k. As a result, $\bar{f}_0^{(N)}$ has the form

$$\bar{f}_0^{(N)}=f_{eq}^{(N)}+\sum_{k=1}^{r}\gamma_k(\partial\bar{f}_0^{(N)}/\partial\gamma_k)_{eq} \tag{1.11}$$

and Eq. (1.6) becomes

$$\bar{f}^{(N)}=f_{eq}^{(N)}+\sum_{k=1}^{r}\gamma_k(\partial\bar{f}_0^{(N)}/\partial\gamma_k)_{eq}+\bar{f}_1^{(N)}. \tag{1.12}$$

When Eq. (1.9) is substituted into the Liouville equation (1.4), we obtain

$$L\bar{f}_0^{(N)}+L\bar{f}_1^{(N)}+i(\partial\bar{f}_1^{(N)}/\partial t)=0 \tag{1.13}$$

The term $\partial\bar{f}_0^{(N)}/\partial t$ vanishes because $\bar{f}_0^{(N)}$ is stationary. Now the quantity $L\bar{f}_0^{(N)}$ may be expressed in the form

$$L\bar{f}_0^{(N)}=-i\sum_{k=1}^{r}\gamma_kB_k\bar{f}_0^{(N)}=-iB\bar{f}_0^{(N)}, \tag{1.14}$$

where B is defined by

$$B(\mathbf{R}, \mathbf{p})=\sum_{k=1}^{r}\gamma_kB_k(\mathbf{R}, \mathbf{p}). \tag{1.15}$$

The actual form of the coefficients B_k depends on the choice of the zero-order distribution function $\bar{f}_0^{(N)}$. Substitution of Eq. (1.14) into Eq. (1.13) yields a differential equation for the perturbation term $\bar{f}_1^{(N)}$ in the nonequilibrium distribution function,

$$(\partial\bar{f}_1^{(N)}/\partial t)-iL\bar{f}_1^{(N)}-B\bar{f}_0^{(N)}=0. \tag{1.16}$$

We take as the origin of time ($t=0$) that instant when the perturbation $\bar{f}_1^{(N)}$ to the distribution function $\bar{f}^{(N)}$ is turned on. Prior to the time $t=0$, we assume that the system is maintained in a steady state with a distribution function $\bar{f}_0^{(N)}$ by the application of appropriate external forces and heat reservoirs. These fictitious external forces are not to be confused with the real external forces $\mathbf{X}_{\alpha l}$ acting on the system. The maintenance of such a steady state by this method has been discussed in detail by McLennan[11] and therefore will not be elaborated on here. At the time $t=0$, we remove these fictitious external forces and heat reservoirs and allow the system to approach equilibrium; i.e., we allow the parameters γ_k to decay to zero. During this decay process, the distribution function $\bar{f}^{(N)}$ for the system is represented by Eq. (1.9), which defines $\bar{f}_1^{(N)}$ when $\bar{f}_0^{(N)}$ is given. Since $\bar{f}_0^{(N)}$ is stationary in time, $\bar{f}_1^{(N)}$ decays to its equilibrium value $(f_{eq}^{(N)}-\bar{f}_0^{(N)})$ with a relaxation time τ_r.

With the boundary condition that $\bar{f}_1^{(N)}$ vanishes for negative values of time t, the solution of the differential equation (1.16) is

$$\bar{f}_1^{(N)}(t)=\int_0^t \exp[-i(s'-t)L]B(\mathbf{R}_{s'}, \mathbf{p}_{s'})f_{eq}^{(N)}ds', \tag{1.17}$$

where $\bar{f}_0^{(N)}$ has been replaced by $f_{eq}^{(N)}$ in order to avoid quadratic and higher terms in γ_k. We have also introduced the convention that $\mathbf{R}_t$, $\mathbf{p}_t$ are the values of $\mathbf{R}$, $\mathbf{p}$ at time t if $\mathbf{R}_0$, $\mathbf{p}_0$ are their values at time $t=0$, i.e., $\mathbf{R}_t=\mathbf{R}(\mathbf{R}_0, \mathbf{p}_0, t)$ and $\mathbf{p}_t=\mathbf{p}(\mathbf{R}_0, \mathbf{p}_0, t)$. The homogeneous solutions of Eq. (1.16) vanish upon application of the boundary condition. If we introduce the variable of integration $s=2s'-t$ into Eq. (1.17), we obtain

$$\bar{f}_1^{(N)}(t)=\tfrac{1}{2}\int_{-t}^{t}\exp[-i(s-t)L/2]B(\mathbf{R}_{(s+t)/2}, \mathbf{p}_{(s+t)/2})f_{eq}^{(N)}ds. \tag{1.18}$$

[10] When these gradients are sufficiently small, it is reasonable to regard the system as possessing local equilibrium character. Arbitrary initial gradients of the temperature and of the chemical potentials of the various components would imply a gradient in the hydrodynamic pressure, as may be seen from the Gibbs-Duhem equation. Consequently, acoustic waves would propagate across the system as time progresses. The Gibbs-Duhem equation may be employed, on the other hand, to provide a restriction on the initial gradients to suppress acoustic waves. In the general situation, however, the diffusion and heat currents defined in Secs. III and IV refer to flows *relative* to the local acoustic motion of the fluid medium.

[11] J. A. McLennan, Jr., Phys. Rev. **115**, 1405 (1959).

If ϕ is any function of $\mathbf{R}(t)$ and $\mathbf{p}(t)$, but is not an explicit function of time (i.e., $\partial\phi/\partial t=0$), then the total time derivative of $\phi(\mathbf{R}_t, \mathbf{p}_t)$ is

$$d\phi/dt=\sum_{\alpha=1}^{\nu}\sum_{i=1}^{N_\alpha}[(d\mathbf{R}_{\alpha i}/dt)\cdot\nabla_{\mathbf{R}_{\alpha i}}\phi+(d\mathbf{p}_{\alpha i}/dt)\cdot\nabla_{\mathbf{p}_{\alpha i}}\phi]$$
$$=-iL\phi, \tag{1.19}$$

where the Liouville operator is given by Eq. (1.5) and does not contain the fictitious external forces or the effects of the heat reservoirs discussed previously. Integration of Eq. (1.19) from a time t to a time $t+s$ yields

$$\phi(\mathbf{R}_{t+s}, \mathbf{p}_{t+s})=\exp(-isL)\phi(\mathbf{R}_t, \mathbf{p}_t), \tag{1.20}$$

where the operator $\exp(-isL)$ is defined by the relation

$$\exp(-isL)=\sum_{n=0}^{\infty}\frac{(-is)^n}{n!}L^n. \tag{1.21}$$

On applying Eq. (1.20) to Eq. (1.18), we obtain

$$\bar{f}_1^{(N)}(t)=\tfrac{1}{2}\int_{-t}^{t}B(\mathbf{R}_s, \mathbf{p}_s)f_{\mathrm{eq}}{}^{(N)}ds. \tag{1.22}$$

We may integrate over negative values of t in Eq. (1.22) if we acknowledge that $\mathbf{R}$ and $\mathbf{p}$ are extrapolated backward in time by Eq. (1.20) to values which they would have had in the absence of the fictitious external forces and heat reservoirs, since these effects are not contained in the operator L. Since the equilibrium distribution function by definition does not change with time (neither explicitly nor implicitly), it is not affected by the various time transformations which were made.

The expectation value G_{obs} of any dynamical variable $G(\mathbf{R}, \mathbf{p})$ at the time t may be expressed as $\langle G; \bar{f}^{(N)}\rangle$, where, by definition,

$$\langle G;\bar{f}^{(N)}\rangle=\iint G(\mathbf{R}, \mathbf{p})\,\bar{f}^{(N)}(\mathbf{R}, \mathbf{p}, t)d\mathbf{R}d\mathbf{p}. \tag{1.23}$$

In Eq. (1.23) the product $G\bar{f}^{(N)}$ is integrated over all of phase space. The distribution function $\bar{f}^{(N)}$, correct to first-order terms in the γ_k, is given in Eq. (1.12), so that in this linear approximation G_{obs} is:

$$G_{\mathrm{obs}}=G^{(0)}+G_{\mathrm{I}}{}^{(1)}+G_{\mathrm{II}}{}^{(1)},$$
$$G^{(0)}=\langle G; f_{\mathrm{eq}}{}^{(N)}\rangle,$$
$$G_{\mathrm{I}}{}^{(1)}=\sum_{k=1}^{r}\gamma_k\langle G; (\partial\bar{f}_0^{(N)}/\partial\gamma_k)_{\mathrm{eq}}\rangle, \tag{1.24}$$
$$G_{\mathrm{II}}{}^{(1)}=\langle G;\bar{f}_1^{(N)}\rangle.$$

In view of Eq. (1.22), $G_{\mathrm{II}}{}^{(1)}$ becomes

$$G_{\mathrm{II}}{}^{(1)}=\tfrac{1}{2}\int_{-t}^{t}\langle G(\mathbf{R}_t, \mathbf{p}_t)B(\mathbf{R}_s, \mathbf{p}_s); f_{\mathrm{eq}}{}^{(N)}\rangle ds. \tag{1.25}$$

For any given dynamical variable $G(\mathbf{R}, \mathbf{p})$, the values of $G^{(0)}$, $G_{\mathrm{I}}{}^{(1)}$, $G_{\mathrm{II}}{}^{(1)}$ depend upon the choice of the zero-order distribution function $\bar{f}_0^{(N)}$; some of these quantities may vanish.

II.

We now introduce a pseudocanonical zero-order distribution function $\bar{f}_0^{(N)}$ for the nonequilibrium system under consideration,

$$\bar{f}_0^{(N)}=A\exp\Bigg[-\sum_{\beta=1}^{\nu}\sum_{j=1}^{N_\beta}\frac{(\mathbf{p}_{\beta j}-m_\beta\mathbf{u}_{\beta j})^2}{2m_\beta kT_{\beta j}}$$
$$-\sum_{\alpha=1}^{\nu}\sum_{\beta=1}^{\nu}\sum_{i=1}^{N_\alpha}\sum_{j=1}^{N_\beta}{}'\frac{V_{\alpha\beta}(R_{\beta j\alpha i})}{k(T_{\alpha i}+T_{\beta j})}-\sum_{\beta=1}^{\nu}\sum_{j=1}^{N_\beta}\frac{\phi_{\beta j}}{kT_{\beta j}}\Bigg], \tag{2.1}$$

where k is the Boltzmann constant and A is a normalizing factor. This form of $\bar{f}_0^{(N)}$, analogous to the equilibrium canonical distribution, is consistent with our assumption of small gradients of T, $\mathbf{u}$, and μ_α and hence, of local equilibrium.

The first term in the exponential of Eq. (2.1) represents a velocity distribution which is Gaussian about the local hydrodynamic velocity. The local temperature and the local hydrodynamic velocity at the position in ordinary three-dimensional space of molecule j of species β are $T_{\beta j}$ and $\mathbf{u}_{\beta j}$, respectively. Thus, $T_{\beta j}$ and $\mathbf{u}_{\beta j}$ are abbreviations for $T(\mathbf{R}_{\beta j})$ and $\mathbf{u}(\mathbf{R}_{\beta j})$. The temperature $T_{\alpha i}$ is related to $T_{\beta j}$ by

$$T_{\alpha i}=T_{\beta j}+\mathbf{R}_{\beta j\alpha i}\cdot\nabla T, \tag{2.2}$$

where $\mathbf{R}_{\beta j\alpha i}$ is the vector defined in Eq. (1.8) and ∇T is the gradient of $T(\mathbf{r}, t)$ with respect to the position vector $\mathbf{r}$ in ordinary three-dimensional space. Similarly, $\mathbf{u}_{\alpha i}$ is related to $\mathbf{u}_{\beta j}$ by

$$\mathbf{u}_{\alpha i}=\mathbf{u}_{\beta j}+\mathbf{R}_{\beta j\alpha i}\cdot\nabla\mathbf{u}. \tag{2.3}$$

In the third term, $\phi_{\beta j}$ is the potential of a fictitious external force acting on molecule j of species β. As we mentioned in Sec. I, it is these fictitious forces and heat reservoirs which keep the system in a steady state before the time $t=0$. In order to prevent diffusive flow in this stationary state, the potential $\phi_{\beta j}$ of the pseudoforce on molecule j of component β must be the negative of the chemical potential of species β at the position $\mathbf{R}_{\beta j}$. Therefore, the desired form for $\bar{f}_0^{(N)}$ is

$$\bar{f}_0^{(N)}=A\exp\Bigg[-\sum_{\beta=1}^{\nu}\sum_{j=1}^{N_\beta}\frac{(\mathbf{p}_{\beta j}-m_\beta\mathbf{u}_{\beta j})^2}{2m_\beta kT_{\beta j}}$$
$$-\sum_{\alpha=1}^{\nu}\sum_{\beta=1}^{\nu}\sum_{i=1}^{N_\alpha}\sum_{j=1}^{N_\beta}{}'\frac{V_{\alpha\beta}(R_{\beta j\alpha i})}{k(T_{\alpha i}+T_{\beta j})}+\sum_{\beta=1}^{\nu}\sum_{j=1}^{N_\beta}\frac{\mu_{\beta j}}{kT_{\beta j}}\Bigg], \tag{2.4}$$

where $\mu_{\beta j}$ is an abbreviation for $\mu_\beta(\mathbf{R}_{\beta j})$.

In order to determine the coefficients B_k in Eq. (1.14), we operate on $\bar{f}_0^{(N)}$ given in Eq. (2.4) with the Liouville operator L and then discard all terms which are of higher order than linear in $\nabla\mathbf{u}$, $\nabla\ln T$, and $\nabla\mu_\alpha$. When Eqs. (2.2) and (2.3) are substituted into the expres-

sion for $L\bar{f}_0^{(N)}$, Eqs. (1.6) and (1.7) are used to cancel two terms, and only linear terms are retained, we obtain:

$$B=(kT)^{-1}\{\mathbf{S}:\nabla\mathbf{u}-\mathbf{Q}\cdot\nabla\ln T$$
$$-\sum_{\alpha=1}^{\nu}\sum_{l=1}^{N_\alpha}(\mathbf{p}_{\alpha l}'/m_\alpha)\cdot[T\nabla(\mu_\alpha/T)-\mathbf{X}_\alpha]\delta(\mathbf{R}_{\alpha l}-\mathbf{r})\},\tag{2.5}$$

where

$$\mathbf{S}=-\sum_{\alpha=1}^{\nu}\sum_{l=1}^{N_\alpha}(\mathbf{p}_{\alpha l}'\mathbf{p}_{\alpha l}'/m_\alpha)\delta(\mathbf{R}_{\alpha l}-\mathbf{r})$$
$$+\tfrac{1}{2}\sum_{\alpha=1}^{\nu}\sum_{\beta=1}^{\nu}\sum_{l=1}^{N_\alpha}\sum_{j=1}^{N_\beta}{}'\mathbf{R}_{\beta j\alpha l}\nabla_{\mathbf{R}_{\alpha l}}V_{\alpha\beta}(R_{\beta j\alpha l})\delta(\mathbf{R}_{\alpha l}-\mathbf{r}),$$
$$\mathbf{Q}=\sum_{\alpha=1}^{\nu}\sum_{l=1}^{N_\alpha}(\mathbf{p}_{\alpha l}'/m_\alpha)\cdot[(p_{\alpha l}'^2/2m_\alpha)\mathbf{1}+\tfrac{1}{2}\mathbf{\Lambda}_{\alpha l}]\delta(\mathbf{R}_{\alpha l}-\mathbf{r}),\tag{2.6}$$
$$\mathbf{\Lambda}_{\alpha l}=\sum_{\beta=1}^{\nu}\sum_{j=1}^{N_\beta}{}'[V_{\alpha\beta}(R_{\beta j\alpha l})\mathbf{1}-\mathbf{R}_{\beta j\alpha l}\nabla_{\mathbf{R}_{\alpha l}}V_{\alpha\beta}(R_{\beta j\alpha l})].$$

In Eqs. (2.5) and (2.6), $\delta(\mathbf{R}_{\alpha l}-\mathbf{r})$ in the Dirac delta function, $\mathbf{1}$ is the unit dyadic, and $\mathbf{p}_{\alpha l}'$ represents the momentum of the molecule relative to the hydrodynamical motion of the local center of mass; thus

$$\mathbf{p}_{\alpha l}'=\mathbf{p}_{\alpha l}-m_\alpha\mathbf{u}.\tag{2.7}$$

III.

Now that we have an expression for B for our choice of the zero-order distribution function $\bar{f}_0^{(N)}$, we may determine some of the transport properties for the nonequilibrium system through the use of Eqs. (1.24) and (1.25). We shall use the conclusions of Bearman and Kirkwood[3] to determine the diffusion current density of species α and the heat current density for our nonequilibrium system. In this section we consider the diffusion fluxes. Section IV deals with the heat flux.

The flow pattern of the system is determined by specifying the local mean velocity $\mathbf{u}_\alpha$ of each component α. The velocity $\mathbf{u}$ of the local center of mass is given by

$$\rho\mathbf{u}=\sum_{\alpha=1}^{\nu}\rho_\alpha\mathbf{u}_\alpha,\tag{3.1}$$

where ρ_α is the partial mass density of species α and ρ is the total mass density,

$$\rho=\sum_{\alpha=1}^{\nu}\rho_\alpha.\tag{3.2}$$

The diffusion current density of component α is defined by the relation

$$\mathbf{j}_\alpha=(\rho_\alpha/m_\alpha)(\mathbf{u}_\alpha-\mathbf{u}).\tag{3.3}$$

The diffusion fluxes $\mathbf{j}_\alpha$ are not all independent, for

$$\sum_{\alpha=1}^{\nu}m_\alpha\mathbf{j}_\alpha=0,\tag{3.4}$$

from Eqs. (3.1) and (3.3).

According to Bearman and Kirkwood,[3] the diffusion flux $\mathbf{j}_\alpha$ is given in terms of microscopic variables by

$$\mathbf{j}_\alpha(\mathbf{r})=\Big\langle\sum_{i=1}^{N_\alpha}(\mathbf{p}_{\alpha i}'/m_\alpha)\delta(\mathbf{R}_{\alpha i}-\mathbf{r});\bar{f}^{(N)}\Big\rangle.\tag{3.5}$$

Therefore, the dynamical variable G to be used in calculating $\mathbf{j}_\alpha$ from Eqs. (1.24) is

$$G(\mathbf{R}_t,\mathbf{p}_t)=\sum_{i=1}^{N_\alpha}(\mathbf{p}_{\alpha it}'/m_\alpha)\delta(\mathbf{R}_{\alpha it}-\mathbf{r}).\tag{3.6}$$

The term $G^{(0)}$ immediately integrates to zero, since G in Eq. (3.6) is odd in $\mathbf{p}_{\alpha i}$ and $f_{\text{eq}}^{(N)}$ is even in $\mathbf{p}_{\alpha i}$. For similar reasons, the term $G_{\text{I}}^{(1)}$ also vanishes. The term $G_{\text{II}}^{(1)}$, however, does not vanish. Substituting Eq. (3.6) into Eq. (1.25) and using Eq. (2.5) for the quantity B, we obtain:

$$\mathbf{j}_\alpha(\mathbf{r})=-\mathbf{\Omega}_{\alpha 0}\cdot\nabla\ln T-\sum_{\beta=1}^{\nu}\mathbf{\Omega}_{\alpha\beta}\cdot[T\nabla(\mu_\beta/T)-\mathbf{X}_\beta],\tag{3.7}$$

where

$$\mathbf{\Omega}_{\alpha 0}=(2kT)^{-1}\int_{-t}^{t}\langle\sum_{i=1}^{N_\alpha}(\mathbf{p}_{\alpha it}'/m_\alpha)\mathbf{Q}_s\delta(\mathbf{R}_{\alpha it}-\mathbf{r});f_{\text{eq}}^{(N)}\rangle ds,$$
$$\mathbf{\Omega}_{\alpha\beta}=(2kT)^{-1}\int_{-t}^{t}\langle\sum_{i=1}^{N_\alpha}\sum_{j=1}^{N_\beta}(\mathbf{p}_{\alpha it}'/m_\alpha)(\mathbf{p}_{\beta js}'/m_\beta)$$
$$\times\delta(\mathbf{R}_{\alpha it}-\mathbf{r})\delta(\mathbf{R}_{\beta js}-\mathbf{r});f_{\text{eq}}^{(N)}\rangle ds.\tag{3.8}$$

The quantity $\mathbf{Q}_s$ is an abbreviation for $\mathbf{Q}(\mathbf{R}_s,\mathbf{p}_s)$. The coefficient of the force $\nabla\mathbf{u}$ vanishes because the integrand of the phase integral is an odd function of $\mathbf{p}_{\alpha i}$. This result is to be expected from Curie's theorem[12] that tensor forces do not cause vector fluxes.

The phenomenological coefficients in Eqs. (3.8) may be somewhat simplified by carrying out the indicated summations:

$$\mathbf{\Omega}_{\alpha 0}=\frac{N_\alpha}{2m_\alpha kT}\int_{-t}^{t}\langle\mathbf{p}_{\alpha 1t}'\mathbf{Q}_s\delta(\mathbf{R}_{\alpha 1t}-\mathbf{r});f_{\text{eq}}^{(N)}\rangle ds,\tag{3.9}$$

$$\mathbf{\Omega}_{\alpha\beta}=\frac{N_\alpha N_\beta}{2m_\alpha m_\beta kT}\int_{-t}^{t}\langle\mathbf{p}_{\alpha 1t}'\mathbf{p}_{\beta 1s}'\delta(\mathbf{R}_{\alpha 1t}-\mathbf{r})\delta(\mathbf{R}_{\beta 1s}-\mathbf{r});$$
$$\times f_{\text{eq}}^{(N)}\rangle ds\quad(\alpha\neq\beta),\tag{3.10}$$

$$\mathbf{\Omega}_{\alpha\alpha}=\frac{N_\alpha(N_\alpha-1)}{2m_\alpha^2kT}\int_{-t}^{t}\langle\mathbf{p}_{\alpha 1t}'\mathbf{p}_{\alpha 2s}'\delta(\mathbf{R}_{\alpha 1t}-\mathbf{r})\delta(\mathbf{R}_{\alpha 2s}-\mathbf{r});$$
$$\times f_{\text{eq}}^{(N)}\rangle ds+\frac{N_\alpha}{2m_\alpha^2kT}\int_{-t}^{t}\langle\mathbf{p}_{\alpha 1t}'\mathbf{p}_{\alpha 1s}'\delta(\mathbf{R}_{\alpha 1t}-\mathbf{r})$$
$$\times\delta(\mathbf{R}_{\alpha 1s}-\mathbf{r});f_{\text{eq}}^{(N)}\rangle ds.\tag{3.11}$$

[12] P. Curie, J. phys. 3, 393 (1894); *Oeuvres de Pierre Curie* (Gauthier-Villars, Paris, 1908), p. 118–141.

Since the forces $\nabla \ln T$, $[T\nabla(\mu_\beta/T)-\mathbf{X}_\beta]$ are independent of one another, substitution of Eq. (3.7) into Eq. (3.4) gives

$$\sum_{\alpha=1}^{\nu} m_\alpha \mathbf{\Omega}_{\alpha 0}=0, \qquad \sum_{\alpha=1}^{\nu} m_\alpha \mathbf{\Omega}_{\alpha\beta}=0. \tag{3.12}$$

These relations also follow from Eqs. (3.9)–(3.11), since the linear momentum of the system is conserved.

IV.

We now determine the heat current density for the nonequilibrium system. Since there exists some arbitrariness in the definition of the heat flux,[13] a number of heat fluxes may be defined; they differ from one another by functions of position $\mathbf{r}$ only. The heat flux $\mathbf{q}$ to be considered here must satisfy the relationship[7,14]

$$\Phi=-\sum_{\alpha=1}^{\nu} \mathbf{j}_\alpha\cdot[T\nabla(\mu_\alpha/T)-\mathbf{X}_\alpha]-\mathbf{q}\cdot\nabla \ln T, \tag{4.1}$$

where Φ/T is the rate per unit volume of the internal entropy production in the nonequilibrium system. Only if $\mathbf{q}$ satisfies Eq. (4.1) may we expect the Onsager reciprocal relations to hold. The heat flux $\mathbf{q}$ as determined by Eq. (4.1) is identical with the conduction current density of the internal energy.[15]

According to Bearman and Kirkwood,[3] this heat flux $\mathbf{q}$ is given in terms of microscopic variables by

$$\mathbf{q}(\mathbf{r})=\langle \mathbf{Q}; \bar{f}^{(N)}\rangle, \tag{4.2}$$

where $\mathbf{Q}$ is defined in Eqs. (2.6). When the dynamical variable $\mathbf{Q}_t$ is substituted for $G(\mathbf{R}_t, \mathbf{p}_t)$ in Eqs. (1.24), $G^{(0)}$ and $G_1^{(1)}$ integrate to zero because their integrands are odd functions of $\mathbf{p}_{\alpha i}$. Substitution of $\mathbf{Q}_t$ and Eq. (2.5) into Eq. (1.25) yields

$$\mathbf{q}=-\mathbf{\Omega}_{00}\cdot\nabla \ln T-\sum_{\alpha=1}^{\nu}\mathbf{\Omega}_{0\alpha}\cdot[T\nabla(\mu_\alpha/T)-\mathbf{X}_\alpha], \tag{4.3}$$

where

$$\mathbf{\Omega}_{00}=\frac{1}{2kT}\int_{-t}^{t}\langle \mathbf{Q}_t\mathbf{Q}_s; f_{\mathrm{eq}}^{(N)}\rangle ds, \tag{4.4}$$

$$\mathbf{\Omega}_{0\alpha}=\frac{N_\alpha}{2m_\alpha kT}\int_{-t}^{t}\langle \mathbf{Q}_t\mathbf{p}_{\alpha 1s}'\delta(\mathbf{R}_{\alpha 1s}-\mathbf{r}); f_{\mathrm{eq}}^{(N)}\rangle ds. \tag{4.5}$$

In Eq. (4.3) the term linear in $\nabla\mathbf{u}$ integrates to zero in accord with Curie's theorem.

It should be noted that the phenomenological coefficients $\mathbf{\Omega}_{\alpha 0}$, $\mathbf{\Omega}_{\alpha\beta}$, $\mathbf{\Omega}_{00}$, $\mathbf{\Omega}_{0\alpha}$ in Eqs. (3.9)–(3.11), (4.4), and (4.5) are *not* functions of position $\mathbf{r}$, even though Dirac delta functions involving $\mathbf{r}$ occur in these expressions. Since the equilibrium distribution function is not dependent on position, these delta functions integrate to unity in the integration over phase space.

V.

We now show that the phenomenological coefficients given in Eqs. (3.9), (3.10), and (4.5) obey the Onsager reciprocal relations,[7] i.e.,

$$\mathbf{\Omega}_{0\alpha}=\mathbf{\Omega}_{\alpha 0} \qquad (\alpha=1, 2, \cdots, \nu), \tag{5.1}$$

$$\mathbf{\Omega}_{\alpha\beta}=\mathbf{\Omega}_{\beta\alpha} \qquad (\alpha, \beta=1, 2, \cdots, \nu). \tag{5.2}$$

We consider first the coefficients $\mathbf{\Omega}_{\alpha 0}$ given in Eq. (3.9). The phase space integral which appears in $\mathbf{\Omega}_{\alpha 0}$ is

$$\langle \mathbf{p}_{\alpha 1t}'\delta(\mathbf{R}_{\alpha 1t}-\mathbf{r})\mathbf{Q}_s; f_{\mathrm{eq}}^{(N)}\rangle.$$

Since the microscopic variables taken at time s are related to the same variables taken at time t by

$$\phi(\mathbf{R}_s, \mathbf{p}_s)=\exp[-i(s-t)L]\phi(\mathbf{R}_t, \mathbf{p}_t), \tag{5.3}$$

this phase space integral becomes

$$\langle \mathbf{p}_{\alpha 1t}'\delta(\mathbf{R}_{\alpha 1t}-\mathbf{r})\exp[-i(s-t)L]\mathbf{Q}_t; f_{\mathrm{eq}}^{(N)}\rangle.$$

If the operator $\exp[-i(s-t)L]$ is expanded according to Eq. (1.21), the nth term in the summation is

$$n!^{-1}[-i(s-t)]^n\langle \mathbf{p}_{\alpha 1t}'\delta(\mathbf{R}_{\alpha 1t}-\mathbf{r})L^n\mathbf{Q}_t; f_{\mathrm{eq}}^{(N)}\rangle.$$

When n is odd, the integrand here is odd in the momentum of each molecule and therefore integrates to zero. When n is even, however, the phase space integral does not vanish. Consequently, the original phase space integral is an even function of $(s-t)$ and may be written as

$$\langle \mathbf{p}_{\alpha 1t}'\delta(\mathbf{R}_{\alpha 1t}-\mathbf{r})\exp[-i(t-s)L]\mathbf{Q}_t; f_{\mathrm{eq}}^{(N)}\rangle.$$

This phase space integral may be regarded as a function of the dynamical variables at time t, averaged over an equilibrium distribution at that time. However, the equilibrium distribution is stationary by definition, so that it does not matter whether we take such an average at time t or at some other time, say s. Under this translation of the time scale, the phase space integral which appears in $\mathbf{\Omega}_{\alpha 0}$ becomes

$$\langle \mathbf{p}_{\alpha 1s}'\delta(\mathbf{R}_{\alpha 1s}-\mathbf{r})\mathbf{Q}_t; f_{\mathrm{eq}}^{(N)}\rangle.$$

This phase space integral, however, is exactly that which appears in $\mathbf{\Omega}_{0\alpha}$ in Eq. (4.5). As a result, the Onsager relations (5.1) are proved.

To prove the Onsager reciprocal relations for $\mathbf{\Omega}_{\alpha\beta}$, which are given in Eq. (3.10), we repeat exactly the same procedure as before, except that we replace $\mathbf{Q}$ by $\mathbf{p}_{\beta 1}'\delta(\mathbf{R}_{\beta 1}-\mathbf{r})$. The relations (5.2) follow in a straightforward manner.

VI.

By developing a perturbation theory for the nonequilibrium distribution function, we have obtained the linear relations for diffusion and heat flow in a multicomponent system without chemical reactions. In order to obtain these linear relations, we have neglected

[13] J. G. Kirkwood and B. Crawford, Jr., J. Phys. Chem. **56**, 1048 (1952).

[14] S. R. deGroot, *Thermodynamics of Irreversible Processes* (North-Holland Publishing Company, Amsterdam, 1952), pp. 6–7.

[15] Footnote reference 14, pp. 94–100.

terms in the distribution function which are of higher order than linear in the parameters γ_k, i.e., in $\nabla \ln T$, $\nabla \mathbf{u}$, and $\nabla \mu_\alpha$. The analysis presented here is valid whenever the parameters γ_k are sufficiently small that quadratic and higher terms in γ_k may be neglected. However, from this treatment we are not able to draw any conclusions regarding the situations under which this linear description is adequate.

The time integrals of the temporal correlation functions which appear in the phenomenological coefficients Ω_{00}, $\Omega_{0\alpha}$, $\Omega_{\alpha 0}$, $\Omega_{\alpha\beta}$ may be expressed in a different, but equivalent form. By making the substitution $s=t+s''$ in Eq. (1.25), we obtain

$$G_{II}^{(1)} = -\tfrac{1}{2}\int_0^{-2t} \langle G(\mathbf{R}_t, \mathbf{p}_t) B(\mathbf{R}_{t+s''}, \mathbf{p}_{t+s''}); f_{eq}^{(N)} \rangle ds''. \tag{6.1}$$

Now the time correlation function

$$\langle G(\mathbf{R}_t, \mathbf{p}_t) B(\mathbf{R}_{t+s''}, \mathbf{p}_{t+s''}); f_{eq}^{(N)} \rangle$$

has a value which is not zero in the neighborhood of $s''=0$. However, when s'' has reached a certain value τ_e, this correlation function vanishes. Therefore, we may cut off the integral in Eq. (6.1) at τ_e and obtain

$$G_{II}^{(1)} = -\tfrac{1}{2}\int_0^{\tau_e} \langle G(\mathbf{R}_t, \mathbf{p}_t) B(\mathbf{R}_{t+s''}, \mathbf{p}_{t+s''}); f_{eq}^{(N)} \rangle ds''. \tag{6.2}$$

Equation (6.2) may be used in place of Eq. (1.25) to determine the phenomenological coefficients for diffusion and heat transport. In a theory of irreversible processes based on regression of fluctuations in an equilibrium system,[16] Fixman has also obtained expressions for transport coefficients involving time correlation functions similar to Eq. (6.2).

At the time $t=0$, the fictitious external forces and heat reservoirs which maintain the system in a stationary state are removed. The system then rapidly attains local equilibrium character. By local equilibrium we mean that equilibrium exists in regions whose linear extents are large compared with the mean free path of the molecules in the system, but are small compared with the linear extent of the entire system. The time interval required for the system to attain local equilibrium is τ_0. The relaxation time for the entire system to reach equilibrium is τ_r. Since τ_r increases with the size of the system, while τ_0 is independent of the size, we have $\tau_0 \ll \tau_r$ for a large system.

We now consider the time smoothing of the distribution function over an interval τ as stated by Eq. (1.1) and the time correlation over an interval τ_e as given by Eq. (6.2). As indicated in Eqs. (1.1) and (6.2), we choose a time t after the system has attained local equilibrium and before it has reached thermodynamic equilibrium. In the case of Eq. (1.1), we then average $f^{(N)}$ over an interval τ from the time t to the time $(t+\tau)$. For the time correlation function in Eq. (6.2), we average over an interval τ_e from time t to time $(t+\tau_e)$. In order that the temporal coarse graining of the distribution function $f^{(N)}$ be independent of the interval τ, it is necessary that

$$\tau_e \ll \tau \ll \tau_r. \tag{6.3}$$

As a consequence of these inequalities, the value of $G_{II}^{(1)}$ in Eq. (6.2) remains unchanged if we replace τ_e in the limit of integration by the coarse-graining time interval τ. Our notation for the four time intervals discussed here is the same as that of Mori,[8] who also discusses the relationships expressed in Eq. (6.3).

By a quantum-mechanical correlation function method which is similar to the classical procedure used here, Mori[8] has derived the linear relations for diffusion and heat transport and has obtained explicit expressions for the phenomenological coefficients in these linear relations. When we transform Mori's equations for diffusion and heat flow to our choice of diffusion fluxes $\mathbf{j}_\alpha$ and heat flux $\mathbf{q}$ and then take the classical limit of these equations, his expressions for the phenomenological coefficients are the same as our expressions for these coefficients obtained with the use of Eq. (6.2) instead of Eq. (1.25).

The method presented here differs from that of Mori in several respects. The averages in our classical treatment are formed with the canonical ensemble, whereas in Mori's quantum-mechanical theory, they are computed with the grand canonical ensemble. Moreover, we provide a physical basis for what Mori calls the coarse graining of the distribution function at the origin of time, i.e., for the boundary condition on $\bar{f}_1^{(N)}$.

In Mori's treatment, the temporal coarse graining of the distribution function is taken over an interval of time τ starting with the origin of time $(t=0)$. Thus, during at least part of the interval τ, the system has not yet attained local equilibrium. Consequently, Mori is forced to extend the interval τ so that $\tau \gg \tau_0$ in order to obtain results which are independent of τ. This procedure may lead to difficulties as, for example, in the case of a dense rigid sphere fluid.[17] For such a fluid in which only binary collisions are considered, the time interval τ must be taken as infinitesimally small, so that successive binary collisions are not included. During this short interval, the system would not yet have attained local equilibrium. Therefore, we prefer to wait until after the time interval τ_0 before carrying out the time smoothing of $f^{(N)}$.

In an approach which differs from both Mori's method and the treatment presented here, Green[9] has also derived the linear relations for diffusion and heat flow and has obtained expressions for the phenomeno-

[16] M. Fixman, J. Chem. Phys. **26**, 1421 (1957); **28**, 397 (1958).

[17] S. A. Rice, J. G. Kirkwood, J. Ross, and R. W. Zwanzig, J. Chem. Phys. **31**, 575 (1959).

logical coefficients which appear therein. In Green's classical treatment, averages are taken in the microcanonical ensemble with fixed momentum and energy. Although Mori has claimed that Green's expression for the thermal conductivity Ω_{00} is not in accord with his theory, Green[18] has recently shown that his expression for Ω_{00} differs from that of Mori only by quantities which are completely negligible for large systems. We may conclude, therefore, that our results are also in agreement with those of Green.

[18] M. S. Green, Phys. Rev. **119**, 829 (1960).

ACKNOWLEDGMENTS

One of us (D.D.F.) would like to thank Dr. Frank Stillinger for many stimulating and helpful discussions during the course of this work and for a critical reading of the manuscript. He would also like to thank Dr. Eugene Helfand for several suggestions for improving the presentation of this work.

THE JOURNAL OF CHEMICAL PHYSICS VOLUME 33, NUMBER 5 NOVEMBER, 1960

Quantum Corrections for Transport Coefficients*

SANG-IL CHOI AND JOHN ROSS†

Metcalf Chemical Labratories, Brown University, Providence, Rhode Island

(Received May 12, 1960)

The equation of motion of a quantum-mechanical two-particle system is solved without approximation in an expansion in Planck's constant. First-order quantum corrections comprising all contributions to the coefficient of $\hbar^2$ in the expansion are derived for the differential scattering cross section and the kinetic-theory transport coefficients. Numerical results are obtained for a simple model of molecular interactions, and lack of agreement is found with work based on the WKB solution of the Schrödinger equation.

INTRODUCTION

THE equation of motion of a quantum-mechanical two-particle system with centrosymmetric forces is solved, without approximation, in an expansion in powers of Planck's constant. We choose the phase space transformation function for the description of the dynamics of the system and solve the time-dependent Wigner equation obeyed by that function. The classical limit of the transformation function is a Dirac δ function which expresses the contact transformation of classical dynamics.[1] With this solution we derive the first order quantum corrections, i.e., all contributions to the coefficient of $\hbar^2$ in the expansion, for the following: the differential scattering cross section, the kinetic-theory transport cross sections, and hence the transport coefficients. Quantum corrections for these quantities are calculated for a simple model of the potential energy of interaction. The results do not agree with computations based on the solution of the Schrödinger equation by the WKB method.

Quantum corrections for elastic scattering problems and transport coefficients have been evaluated by means of a WKB solution for the phase shifts of the Schrödinger wave function.[2] The quantum-mechanical differential scattering cross section is

$$\sigma_{qu}=(4k^2)^{-1}\,|\sum_{l=0}^{\infty}(2l+1)[\exp(2i\eta_l)-1]P_l(\cos\chi)\,|^2, \tag{1}$$

where η_l is the phase shift for the lth partial wave. Three approximations are frequently introduced: (a) the WKB solution for the one-dimensional Schrödinger equation is applied to the radial Schrödinger equation in which $l(l+1)$ is replaced by $(l+\frac{1}{2})^2$; (b) the Legendre polynomials P_l are replaced by their asymptotic values for large l; (c) integration is substituted for summation in Eq. (1). These approximations do indeed lead to the classical differential scattering cross section in the limit as $\hbar$ approaches zero.[1a] Necessary modifications of these approximations for higher-order WKB developments have not been discussed, even though they are required for the evaluation of quantum corrections to the scattering cross sections.

Ford and Wheeler confined their study of scattering phenomena to deductions from the equation of the

* This work was supported in part by the U.S. Air Force through the Air Force Office of Scientific Research of the Air Research Development Command.

† John Simon Guggenheim Fellow, 1959–1960.

[1] We could have chosen alternatively the Green's function of the density matrix for which the classical limit is the appropriate Fourier transform of the classical transformation function.

[2] (a) N. F. Mott and H. S. W. Massey, *The Theory of Atomic Collisions* (Oxford University Press, New York, 1952), 2nd ed., Chap. VII, p. 120; (b) L. D. Landau and E. M. Lifshitz, *Quantum Mechanics—Non-Relativistic Theory* (Addison-Wesley Publishing Company, Inc., Reading, Massachusetts, 1958), Chap. XIV, p. 414; (c) H. A. Kramers, Z. Physik **39**, 828 (1926); (d) B. Kahn, doctoral dissertation, Utrecht, 1938; (e) J. de Boer and R. B. Bird, Physica **20**, 185 (1954); (f) J. A. Wheeler and K. W. Ford, Ann. Phys. **7**, 259 (1959).

first-order WKB solution for the phase shifts within the limits of the above approximations. A distinction must be drawn between the first-order WKB solutions and its consequences and first-order quantum corrections, proportional to $\hbar^2$, to the various cross sections, as there does not exist a one-to-one correspondence.

De Boer and Bird calculated phase shifts for centrosymmetric molecules with a repulsive potential proportional to the inverse 12th power of the intermolecular distance and obtained quantum corrections to the transport coefficients. They applied the one-dimensional WKB solution to the radial Schrödinger equation and considered the first- and second-order WKB result for the phase shifts, retaining thereof contributions to the quantum corrections of order $\hbar^2$. The calculations were restricted to a monotonic potential because of difficulties encountered in WKB computations if more than one classical turning point occurs. They did so, nevertheless, in the hope that a repulsive potential might suffice as an appropriate model, at least for helium at higher temperatures. The depth of the potential well for the Lennard-Jones potential for helium is only $10°k$ (k is Boltzmann's constant).

SOLUTION OF THE EQUATION OF MOTION

In relative coordinates, with the three component vectors $\mathbf{R}$ for configuration space and $\mathbf{p}$ for momentum space, the Wigner equation for the phase space transformation function of a quantum-mechanical two-particle system is[3]

$$(\partial K/\partial s)+(\mathbf{p}/\mu)\cdot\nabla_{\mathbf{R}}K+\Theta\cdot K=0. \tag{2}$$

The function $K(\mathbf{R}, \mathbf{p}; t+s \mid \mathbf{R}_0, \mathbf{p}_0; t)$ represents the conditional probability of transition from the coordinates $(\mathbf{R}_0, \mathbf{p}_0)$ at time t to $(\mathbf{R}, \mathbf{p})$ at time $t+s$. The symbol s denotes a time interval and the Θ operator can be written:

$$\Theta\cdot K(\mathbf{R}, \mathbf{p}; t+s \mid \mathbf{R}_0, \mathbf{p}_0; t)$$
$$=(i/\hbar)(1/\hbar\pi)^3\iint[V(\mathbf{R}-\mathbf{x})-V(\mathbf{R}+\mathbf{x})]$$
$$\times\exp[(2i/\hbar)(\mathbf{p}-\mathbf{p}')\cdot\mathbf{x}]K(\mathbf{R}, \mathbf{p}'; t+s \mid \mathbf{R}_0, \mathbf{p}_0; t)$$
$$\times d\mathbf{p}'d\mathbf{x}. \tag{3}$$

If the intermolecular potential $V(\mathbf{R})$ admits a Taylor series expansion at each point, then an alternative form of the Θ operator is

$$\Theta\cdot K=-(2/\hbar)\sin[(\hbar/2)\nabla_{\mathbf{R}}\cdot\nabla_{\mathbf{p}}]V(\mathbf{R})K, \tag{4}$$

in which $\nabla_{\mathbf{R}}$ operates on $V(\mathbf{R})$ only. Initial conditions for Eq. (2) at $s=0$ are

$$K(\mathbf{R}, \mathbf{p}; t \mid \mathbf{R}_0, \mathbf{p}_0; t)=\delta(\mathbf{R}-\mathbf{R}_0)\delta(\mathbf{p}-\mathbf{p}_0). \tag{5}$$

[3] (a) E. P. Wigner, Phys. Rev. **40**, 749 (1932); (b) J. E. Moyal, Proc. Cambridge Phil. Soc. **45**, 99 (1949); (c) J. H. Irving and R. W. Zwanzig, J. Chem. Phys. **19**, 1173 (1951); (d) J. Ross and J. Kirkwood, J. Chem. Phys. **22**, 1094 (1954).

We seek a solution of the equation

$$(\partial K/\partial s)+(\mathbf{p}/\mu)\cdot\nabla_{\mathbf{R}}K$$
$$=\sum_{j=1}^{\infty}\frac{(-)^{j+1}\hbar^{2j-2}}{(2j-1)!2^{2j-2}}(\nabla_{\mathbf{R}}\cdot\nabla_{\mathbf{p}})^{2j-1}V(\mathbf{R})K \tag{6}$$

in the form

$$K=\sum_{n=0}^{\infty}\hbar^{2n}K_n, \tag{7}$$

and find on substitution the set of differential equations as coefficients of $\hbar^{2n}$:

$$(\partial K_n/\partial s)+(\mathbf{p}/\mu)\cdot\nabla_{\mathbf{R}}K_n$$
$$=\sum_{j=1}^{n+1}\frac{(-)^{j+1}}{(2j-1)!2^{2j-2}}(\nabla_{\mathbf{R}}\cdot\nabla_{\mathbf{p}})^{2j-1}V(\mathbf{R})K_{n+1-j}. \tag{8}$$

For $n=0$ we obtain the Liouville equation for the classical motion of the two-particle system,

$$(\partial K_0/\partial s)+(\mathbf{p}/\mu)\cdot\nabla_{\mathbf{R}}K_0-\nabla_{\mathbf{R}}V(\mathbf{R})\cdot\nabla_{\mathbf{p}}K_0=0, \tag{9}$$

with solution:

$$K_0(\mathbf{R}, \mathbf{p}; t+\tau \mid \mathbf{R}_0, \mathbf{p}_0; t)$$
$$=\delta(\mathbf{R}(-\tau)-\mathbf{R}_0)\delta(\mathbf{p}(-\tau)-\mathbf{p}_0)$$
$$\mathbf{R}(-\tau)=\mathbf{R}+\Delta\mathbf{R}(-\tau)=\mathbf{R}+\int_0^{-\tau}[\mathbf{p}(s)/\mu]ds$$
$$\mathbf{p}(-\tau)=\mathbf{p}+\Delta\mathbf{p}(-\tau)=\mathbf{p}-\int_0^{-\tau}\nabla_{\mathbf{R}}V(\mathbf{R})ds \tag{10}$$

or

$$K_0(\tau)=\exp(-\tau L)K_0(0),$$
$$L=(\mathbf{p}/\mu)\cdot\nabla_{\mathbf{R}}-\nabla_{\mathbf{R}}V(\mathbf{R})\cdot\nabla_{\mathbf{p}}; \tag{11}$$

these express the contact transformation.

The first quantum correction containing only, but all, terms contributing to the coefficient of $\hbar^2$ is obtained as a solution of the equation for $n=1$,

$$(\partial K_1/\partial s)+LK_1+\tfrac{1}{24}(\nabla_{\mathbf{R}}\cdot\nabla_{\mathbf{p}})^3V(\mathbf{R})K_0=0, \tag{12}$$

namely,

$$K_1(\mathbf{R}, \mathbf{p}; t+\tau \mid \mathbf{R}_0, \mathbf{p}_0; t)$$
$$=-\tfrac{1}{24}\int_0^{\tau}\exp[(s-\tau)L](\nabla_{\mathbf{R}}\cdot\nabla_{\mathbf{p}})^3V(R)K_0(s)ds. \tag{13}$$

The operator L changes a function of the phase space coordinates according to the rule

$$\exp(\tau L)\phi[\mathbf{R}(t), \mathbf{p}(t)]=\phi[\mathbf{R}(t+\tau), \mathbf{p}(t+\tau)] \tag{14}$$

along the classical trajectory. The transformation function is invariant to translation on the time axis and obeys the relation of dynamic reversibility,

$$K(\mathbf{R}, \mathbf{p} \mid \mathbf{R}_0, \mathbf{p}_0; \tau)=K(\mathbf{R}_0, \mathbf{p}_0 \mid \mathbf{R}, \mathbf{p}; -\tau). \tag{15}$$

With these aids we can rewrite Eq. (13) for a transition

from $(\mathbf{R}_0, \mathbf{p}_0)$ to $(\mathbf{R}, \mathbf{p})$ in an interval of τ,

$$K_1(\mathbf{R}, \mathbf{p} \mid \mathbf{R}_0, \mathbf{p}_0; \tau)$$

$$= \tfrac{1}{24}\int_0^\tau D(s)\, V[\mathbf{R}_0(s)]\, K_0(\mathbf{R}_0, \mathbf{p}_0 \mid \mathbf{R}, \mathbf{p}; -\tau)\, ds \quad (16)$$

$$D(s) \equiv [\nabla_{\mathbf{R}_0(s)} \cdot \nabla_{\mathbf{p}_0(s)}]^3, \quad (17)$$

in which the subscripts zero indicate the origin of the running coordinates. But these subscripts will be dropped for brevity since there will be no confusion.

The operator D can be simplified in spherical polar coordinates $(R, \theta, \phi, p_R, p_\theta, p_\varphi)$ since the differentiations in configuration space act only on the potential energy function, assumed to be spherically symmetric,

$$D(s)\, V[R(s)] = \frac{d^3V(R)}{dR(s)^3}\frac{\partial^3}{\partial p_R(s)^3} + 3\left[R(s)\frac{d^2V}{dR(s)^2} - \frac{dV}{dR(s)}\right] \times \left[\frac{\partial^3}{\partial p_R(s)\partial p_\theta(s)^2} + \frac{dV}{\partial p_R(s)\partial p_\varphi(s)^2}\right]. \quad (18)$$

We observe here, then, the essential mathematical difficulty of the present problem: The differential operators are to act on explicit functions of $\mathbf{R}(s)$ and $\mathbf{p}(s)$, $0 \le s \le \tau$, the coordinates of the classical trajectory after an interval s. The operand, however, is an explicit function of $\mathbf{R}(\tau) = \mathbf{R}_f$, $\mathbf{p}(\tau) = \mathbf{p}_f$, the coordinates at one end point of the trajectory. Hence the operators must be altered by a classical canonical transformation from the variables $[\mathbf{R}(s), \mathbf{p}(s)]$ to $[\mathbf{R}(\tau), \mathbf{p}(\tau)] = [\mathbf{R}_f, \mathbf{p}_f]$. This procedure is outlined in Appendix A.

From Eq. (16) we draw the conclusion that the quantum corrections appear as simple operations on the entire classical trajectory, as is to be expected from the perturbation solution. Although the classical motion occurs in a plane, the quantum corrections constitute a three-dimensional problem.

DIFFERENTIAL SCATTERING CROSS SECTION

Further development is facilitated by establishing the relation of the phase-space transformation function to the differential scattering cross section. The conditional probability of transition from the coordinates $(\mathbf{R}_0, \mathbf{p}_0)$ at time t to $(\mathbf{R}, \mathbf{p})$ at time $t+\tau$ is given by the transformation function $K(\mathbf{R}, \mathbf{p} \mid \mathbf{R}_0, \mathbf{p}_0; \tau)$ and hence the conditional probability of transition in momentum space is the integral of K over its configuration coordinates[4]:

$$W(\mathbf{p} \mid \mathbf{p}_0; \tau) = (1/2\pi\hbar)^3 \iint K(\mathbf{R}, \mathbf{p} \mid \mathbf{R}_0, \mathbf{p}_0; \tau)\, d\mathbf{R}_0 d\mathbf{R}. \quad (19)$$

[4] The factor $(2\pi\hbar)^{-3}$ in Eq. (18) is a result of δ-function normalization and is replaced by V^{-1} in box normalization.

The differential scattering cross section for the solid angle element $d\Omega$ is then simply given by the expression

$$\lim_{\tau\to\infty} \tau^{-1} W(\mathbf{p} \mid \mathbf{p}_0; \tau)\, d\mathbf{p} = [1/(2\pi\hbar)^3](p_0/\mu)\, \sigma(p_0, \Omega)\, \delta(E_p - E_{p_0})\, d\Omega\, dE_p; \quad (20)$$

the symbols E_p, E_{p_0} denote the energy of the system prior to, and after the collision, and the δ function is included as a representation of the conservation of energy.[5]

The details for the classical mechanical case are as follows: For the phase-space transformation function, we have

$$K(\mathbf{R}, \mathbf{p} \mid \mathbf{R}_0, \mathbf{p}_0; \tau) = \delta(\mathbf{R} - \Delta\mathbf{R}_0(\tau) - \mathbf{R}_0) \cdot \delta(\mathbf{p} - \Delta\mathbf{p}_0(\tau) - \mathbf{p}_0), \quad (10)$$

and the transition probability for the momentum vector $\mathbf{p}_0$ into the solid angle element $d\Omega$, in a spherical coordinate system with polar axis $\mathbf{p}_0$, is

$$d\Omega \times (1/2\pi\hbar)^3 \iint \delta(\mathbf{p} - \Delta\mathbf{p}_0(\tau) - \mathbf{p}_0)\, d\mathbf{R}_0 p^2 dp, \quad (21)$$

where the vector $\mathbf{p}$ is specified by (p, χ, ϕ) in the integration and the vector $\mathbf{p}_f = \mathbf{p}_0 + \Delta\mathbf{p}_0(\tau)$ by (p_f, χ_f, ϕ_f). The remaining integration in configuration space is performed in a cylindrical coordinate system (b, ϵ, z) with z axis antiparallel to $\mathbf{p}_0$; for a monotonic potential the differential volume element which contributes uniquely to the transition is in the limit of large τ

$$d\mathbf{R}_0 = b\,db\,d\epsilon\,dz = b\,db\,d\epsilon\,(p_0/\mu)\tau. \quad (22)$$

The transition probability of the momentum vector $\mathbf{p}_0$ into the solid angle element $d\Omega$, per unit time and unit flux, is defined as the classical differential scattering cross section σ_{Cl},

$$\sigma_{Cl}(p_0, \Omega) = \iiint \frac{\delta(p - p_f)}{p^2} p^2 \frac{\delta(\chi - \chi_f)\,\delta(\phi - \phi_f)}{\sin\chi} dp\, b\, db\, d\epsilon. \quad (23)$$

The values of (b, ϵ, z) are related to (p_f, χ_f, ϕ_f) through the equation of motion and for a spherically symmetric potential we may set $\epsilon = \phi_f$. Again, if the potential function is monotonic, then the scattering angle is a single-valued function of the impact parameter b for a given initial momentum $\mathbf{p}_0$; therefore, we may write

$$b\,db\,d\epsilon = b \mid db/d\chi_f \mid d\chi_f d\phi_f. \quad (24)$$

Final integration over the δ functions leads to the well-known result

$$\sigma_{Cl}(p_0, \Omega) = (b/\sin\chi) \mid db/d\chi \mid. \quad (25)$$

[5] (a) B. A. Lippmann and J. Schwinger, Phys. Rev. **79**, 469 (1950); (b) M. Gell-Mann and M. L. Goldberger, Phys. Rev. **91**, 398 (1953).

For nonmonotonic potentials different regions of the impact parameter b, labeled with the subscript i, may contribute to the scattering into a given angle; the analysis is parallel to the foregoing and the differential scattering cross section is a sum over these regions

$$\sigma_{Cl}(p_0,\Omega)=(\sin\chi)^{-1}\sum_i b_i\,|\,db_i/d\chi\,|. \tag{26}$$

The first quantum correction to the differential cross section can now be derived straightforwardly. We define the first quantum correction to $W(\mathbf{p}\,|\,\mathbf{p}_0;\tau)$ by $\hbar^2W_1$,

$$W_1(\mathbf{p}\,|\,\mathbf{p}_0;\tau)=\left(\frac{1}{2\pi\hbar}\right)^3\iint K_1(\mathbf{R},\mathbf{p}\,|\,\mathbf{R}_0,\mathbf{p}_0;\tau)\,d\mathbf{R}d\mathbf{R}_0 \tag{27}$$

$$K_1(\mathbf{R},\mathbf{p}\,|\,\mathbf{R}_0,\mathbf{p}_0;\tau)=\tfrac{1}{24}\int_0^\tau D(s)\,V[R(s)]K_0(\mathbf{R}_0,\mathbf{p}_0\,|\,\mathbf{R},\mathbf{p};-\tau)\,ds. \tag{15}$$

The properties of the classical transformation function have been discussed and the desired form of the differential operator D is listed in Appendix A. The integration over the configuration coordinate $\mathbf{R}$ can be done at once and the coordinate system chosen for the integration over $\mathbf{R}_0$ is the same as just used, namely,

$$d\mathbf{R}_0=bdbdedz, \tag{21}$$

cylindrical coordinates with z axis antiparallel to $\mathbf{p}_0$. Next, we form the integral

$$\int W_1(\mathbf{p}\,|\,\mathbf{p}_0;\tau)\,p^2dp$$

$$=\tfrac{1}{24}(2\pi\hbar)^{-3}\int_0^\tau\iint D(s)\,V[R(s)]\frac{\delta(p-p_f)}{p^2}p^2\frac{\delta(\chi-\chi_f)}{\sin\chi_f}\times\delta(\phi-\phi_f)\,dpbdbdedzds, \tag{28}$$

and note that due to the integration over the radial component of the momentum vector all terms in the differential operator D (Appendix A) with remaining derivatives with respect to a radial component of momentum vanish, since the operand becomes independent of p_f.

We obtain therefore after an integration by parts and use of Eq. (24) or Eq. (26):

$$\frac{V}{2\pi}\iint W_1(\mathbf{p}\,|\,\mathbf{p}_0;\tau)\,p^2dpd\phi$$

$$=\tfrac{1}{24}\int dz\Big\{-(\partial/\partial\chi)\Big[\int_0^\tau V_3G_1ds\sigma_{Cl}\sin\chi\Big]+(\partial^2/\partial\chi^2)\Big[\int_0^\tau V_3G_2ds\sigma_{Cl}\sin\chi\Big]-(\partial^3/\partial\chi^3)\Big[\int_0^\tau V_3G_3ds\sigma_{Cl}\sin\chi\Big]$$

$$-(\partial/\partial\chi)\Big[3\int_0^\tau(R(s)V_2-V_1)G_4ds\sigma_{Cl}\sin\chi\Big]+(\partial^2/\partial\chi^2)\Big[3\int_0^\tau(R(s)V_2-V_1)G_5ds\sigma_{Cl}\sin\chi\Big]-(\partial^3/\partial\chi^3)\Big[3\int_0^\tau(R(s)V_2-V_1)G_6ds\sigma_{Cl}\sin\chi\Big]$$

$$-(\partial/\partial\chi)\Big[3\int_0^\tau(R(s)V_2-V_1)G_7ds\sigma_{Cl}\sin\chi\Big]+(\partial^2/\partial\chi^2)\Big[3\int_0^\tau(R(s)V_2-V_1)G_8ds\sigma_{Cl}\sin\chi\Big]\Big\}(\sin\chi)^{-1}, \tag{29}$$

where V_n is the nth derivative of the potential energy

$$V_n\equiv d^nV/dR(s)^n, \tag{30}$$

and the quantities G_1–G_8 are listed in Appendix B. The presence of the δ functions makes the integrated terms in the integration by parts equal to zero if the scattering angle χ is not 0 or π.[6] The contributions from these regions to the transport cross section is negligible.

From the relation of the scattering cross section to the probability of transition in momentum space, Eq. (19), we obtain the first quantum correction to the differential scattering cross section, $\hbar^2\sigma_1$:

$$\hbar^2\sigma_1(\chi)=-\frac{\hbar^2}{24}(\sin\chi)^{-1}\Big\{(\partial/\partial\chi)\Big[\int_{-\infty}^\infty V_3G_1ds\sigma_{Cl}\sin\chi\Big]-(\partial^2/\partial\chi^2)\Big[\int_{-\infty}^\infty V_3G_2ds\sigma_{Cl}\sin\chi\Big]+(\partial^3/\partial\chi^3)\Big[\int_{-\infty}^\infty V_3G_3ds\sigma_{Cl}\sin\chi\Big]$$

$$+(\partial/\partial\chi)\Big[3\int_{-\infty}^\infty(R(s)V_2-V_1)G_4ds\sigma_{Cl}\sin\chi\Big]-(\partial^2/\partial\chi^2)\Big[3\int_{-\infty}^\infty(R(s)V_2-V_1)G_5ds\sigma_{Cl}\sin\chi\Big]+(\partial^3/\partial\chi^3)\Big[3\int_{-\infty}^\infty(R(s)V_2-V_1)G_6ds\sigma_{Cl}\sin\chi\Big]$$

$$+(\partial/\partial\chi)\Big[3\int_{-\infty}^\infty(R(s)V_2-V_1)G_7ds\sigma_{Cl}\sin\chi\Big]-(\partial^2/\partial\chi^2)\Big[3\int_{-\infty}^\infty(R(s)V_2-V_1)G_8ds\sigma_{Cl}\sin\chi\Big]\Big\}. \tag{31}$$

[6] This follows from the property of the δ function:

$$\int f(x)\,(d/dx)\delta(x-a)dx=-[(d/dx)f(x)]_{x=a}.$$

The evaluation of the various quantities appearing in this equation requires explicit solution of the classical two-particle problem. These are well known and the essential points are outlined in Appendix C.

TRANSPORT COEFFICIENTS

The system under consideration is a gas at low density; the de Broglie wavelength approaches the size of the molecules and the description of the elementary event, a binary collision, by classical mechanics is not adequate. However, the density of the gas is such that the mean distance between molecules exceeds the de Broglie wavelength, and consequently the effects of quantum statistics (Bose-Einstein or Fermi-Dirac) are absent. This is consistent with the binary collision approximation. For convenience we do not consider the influence of the identity of the particles on the cross section itself.

If we are prepared to accept the proposition that the transport coefficients for such a system can be derived from the Chapman-Enskog theory[7] for a classical mechanical system merely by substitution of the quantum-mechanical differential scattering cross section for the corresponding classical quantity, then the transport coefficients for the quantum mechanical gas can be written as follows:

$$Q^{(l)}(g)=2\pi\int_0^{\pi}(1-\cos^l\chi)\sigma(g,\chi)\,\sin\chi d\chi \quad (32)$$

$$\Omega^{(l,m)}(T)=(kT/2\pi\mu)^{\frac{1}{2}}\int_0^{\infty}\exp(-\gamma^2)\gamma^{2m+3}Q^{(l)}(g)d\gamma \quad (33)$$

$\gamma^2\equiv\mu g^2/2kT$

$g\equiv p/\mu$, initial relative speed

$\mu\equiv$reduced mass

$T\equiv$temperature

$\eta\equiv$viscosity coefficient

$$\eta=5kT/8\Omega^{(2,2)}. \quad (34)$$

The expansion for the differential scattering cross section in powers of Planck's constant may be substituted in the preceding equations and corresponding expansions of the kinetic theory transport cross sections are obtained. Although small angle scattering is poorly described by a near-classical development, the contribution of these collisions to the transport cross section is small because of the suppressing factor $(1-\cos^l\chi)\sin\chi$ in Eq. (31). Such a development is also not too well suited for a treatment of collisions of low relative speed, of course; but here again, the statistical factors in Eq. (33) restrict the range of integration over relative speeds effectively to the thermal range of the order of $(2kT/\mu)^{\frac{1}{2}}$. This indicates also that the thermal de Broglie wavelength is a useful measure of the degree of quantization. The expansion of the transport cross sections in powers of $\hbar^2$ is appropriate, therefore, if the differential scattering cross section is adequately represented by such an expansion for scattering angles not in the neighborhood of zero or π and for relative energies of the order of the thermal energy of the gas. For the temperature dependent transport cross sections we thus have

$$\Omega^{(l,m)}(T)=\Omega_{Cl}^{(l,m)}(T)+\hbar^2\Omega_1^{(l,m)}(T)+\cdots \quad (35)$$

and hence the viscosity coefficient, for instance, is

$$\eta=5kT[8\Omega_{Cl}^{(2,2)}(T)]^{-1}\{1-\hbar^2\Omega_1^{(2,2)}/\Omega_{Cl}^{(2,2)}(T)+\cdots\}. \quad (36)$$

CALCULATIONS AND DISCUSSION

The calculations of the quantum corrections derived in the last section are complex for realistic models of molecular interactions and can only be done by resort to lengthy numerical integrations. A simple form of potential function is adopted and the quantum corrections are calculated. The results enable one to make an immediate comparison with analogous calculations based on the WKB development as used by de Boer and Bird. Unfortunately, the equations themselves are not directly comparable.

If the potential energy of interaction corresponds to repulsion and has the analytic form

$$V=a^2/R^2, \quad (37)$$

then the quantum correction for the viscosity transport cross section $Q^{(2)}(g)$ is

$$\hbar^2Q_1^{(2)}(g)=-0.78\,\pi\hbar^2/(\mu g)^2. \quad (38)$$

For this model of interaction the equations used by de Boer and Bird yield

$$\hbar^2Q_1^{(2)}(g)=-0.50\,\pi\hbar^2/(\mu g)^2. \quad (39)$$

There is agreement in sign but not in numerical value. It should be remembered at this point that de Boer and Bird obtained a positive quantum correction to the viscosity transport cross section for a repulsive potential varying as the twelfth power of the distance.

The analysis of available experimental results on the viscosity of helium, hydrogen, and deuterium at low temperatures shows that the quantum corrections to the kinetic theory cross sections are negative.[8] This implies that an increase in the thermal de Broglie wavelength has the apparent effect of decreasing the

[7] (a) S. Chapman and T. G. Cowling, *The Mathematical Theory of Nonuniform Gases* (Cambridge University Press, New York, 1953), 2nd ed., Chap. XVII, p. 300; (b) J. O. Hirschfelder, C. F. Curtiss, and R. B. Bird, *Molecular Theory of Gases and Liquids* (John Wiley & Sons, Inc., New York), Chap. X, p. 671.

[8] (a) J. M. J. Coremans, A. van Itterbeek, J. J. M. Beenakker, H. F. P. Knaap, and P. Zandbergen, Physica **24**, 557 (1958); (b) A. O. Rietveld, A. van Itterbeek, and C. A. Velds, *ibid.* **25**, 205 (1959).

range of certain potential functions, with an attendant decrease in the cross sections. A similar behavior is encountered in the quantum corrections to the second virial coefficient.

It is not strange, therefore, that the model of the potential, with long range interactions, also leads to negative quantum corrections, as the above phenomena can, and does occur. It is interesting to note, is conclusion, that a repulsive potential can produce positive or negative quantum corrections depending on the steepness and range of the potential.

Numerical calculations of the quantum corrections for the transport coefficients derived in the present communication for realistic models of potential interactions are in progress.

ACKNOWLEDGMENTS

Professor J. G. Kirkwood and Dr. W. F. Brooks have considered the problem of the solution of the Wigner equation in a power series expansion in Planck's constant, and we are grateful for the benefit of a number of conversations. Our gratitude is due Dr. H. Mori for his constant interest and sound advice.

APPENDIX A

Let the coordinates of relative motion of the two-particle system be $\mathbf{R}_0$, $\mathbf{p}_0$ at a given initial time prior to collision; the coordinates after an interval s be $\mathbf{R}$, $\mathbf{p}$; and the final coordinates after the collision and a time interval τ, $\mathbf{R}_f$, $\mathbf{p}_f$. The canonical transformation of the operator D, Eqs. (16–18), to the final coordinates $[\mathbf{R}(\tau), \mathbf{p}(\tau)]\equiv[\mathbf{R}_f, \mathbf{p}_f]$ will be listed here. Choose the spherical coordinate system with polar axis in the direction of $\mathbf{p}_0$; the radial component of the momentum vector $\mathbf{p}_f$ is denoted by p_f and the two angles by χ_f, ϕ_f. A spherical coordinate system is also chosen for the vector $\mathbf{R}$ with polar axis parallel to the constant angular momentum vector of the motion. The classical motion occurs in a plane, therefore, perpendicular to the polar axis, and if the angles are denoted here by θ, ϕ, then we set $\varphi=\pi/2$, $p_\varphi=0$. The required transformations are:

$$\frac{\partial^3}{\partial p_R{}^3}=\frac{\partial^3 p_f}{\partial p_R{}^3}\frac{\partial}{\partial p_f}+3\frac{\partial p_f}{\partial p_R}\frac{\partial^2 p_f}{\partial p_R{}^2}\frac{\partial^2}{\partial p_f{}^2}+\frac{\partial^3\chi_f}{\partial p_R{}^3}\frac{\partial}{\partial\chi_f}+\left(\frac{\partial p_f}{\partial p_R}\right)^3\frac{\partial^3}{\partial p_f{}^3}+3\left(\frac{\partial p_f}{\partial p_R}\right)^2\left(\frac{\partial p_f}{\partial p_R}\right)\frac{\partial^3}{\partial\chi_f\partial p_f{}^2}$$

$$+3\left\{\frac{\partial^2 p_f}{\partial p_R{}^2}\frac{\partial\chi_f}{\partial p_R}+\frac{\partial p_f}{\partial p_R}\frac{\partial^2\chi_f}{\partial p_R{}^2}\right\}\frac{\partial^2}{\partial\chi_f\partial p_f}+3\left(\frac{\partial p_f}{\partial p_R}\right)\left(\frac{\partial\chi_f}{\partial p_R}\right)^2\frac{\partial^3}{\partial\chi_f{}^2\partial p_f}+3\frac{\partial^2\chi_f}{\partial p_R{}^2}\frac{\partial\chi_f}{\partial p_R}\frac{\partial^2}{\partial\chi_f{}^2}+\left(\frac{\partial\chi_f}{\partial p_R}\right)^3\frac{\partial^3}{\partial\chi_f{}^3}+\text{operators on }\phi_f. \tag{A1}$$

$$\frac{\partial}{\partial p_R\partial p_\theta{}^2}=\frac{\partial^3 p_f}{\partial p_R\partial p_\theta{}^2}\frac{\partial}{\partial p_f}+\left\{2\frac{\partial^2 p_f}{\partial p_R\partial p_\theta}\frac{\partial p_f}{\partial p_\theta}+\frac{\partial^2 p_f}{\partial p_\theta{}^2}\frac{\partial p_f}{\partial p_R}\right\}\frac{\partial^2}{\partial p_f{}^2}+\left(\frac{\partial p_f}{\partial p_\theta}\right)^2\left(\frac{\partial p_f}{\partial p_R}\right)\frac{\partial^3}{\partial p_f{}^3}+\frac{\partial^3\chi_f}{\partial p_R\partial p_\theta{}^2}\frac{\partial}{\partial\chi_f}$$

$$+\left\{2\frac{\partial^2\chi_f}{\partial p_R\partial p_\theta}\frac{\partial\chi_f}{\partial p_\theta}+\frac{\partial\chi_f}{\partial p_R}\frac{\partial^2\chi_f}{\partial p_\theta{}^2}\right\}\frac{\partial^2}{\partial\chi_f{}^2}+\left\{2\frac{\partial^2 p_f}{\partial p_R\partial p_\theta}\frac{\partial\chi_f}{\partial p_\theta}+2\frac{\partial^2\chi_f}{\partial p_R\partial p_\theta}\frac{\partial p_f}{\partial p_\theta}+\frac{\partial p_f}{\partial p_R}\frac{\partial^2\chi_f}{\partial p_\theta{}^2}+\frac{\partial\chi_f}{\partial p_R}\frac{\partial^2 p_f}{\partial p_\theta{}^2}\right\}\frac{\partial^2}{\partial p_f\partial\chi_f}$$

$$+\left\{2\frac{\partial p_f}{\partial p_R}\frac{\partial p_f}{\partial p_\theta}\frac{\partial\chi_f}{\partial p_\theta}+\left(\frac{\partial p_f}{\partial p_\theta}\right)^2\left(\frac{\partial\chi_f}{\partial p_R}\right)\right\}\frac{\partial^3}{\partial p_f{}^2\partial\chi_f}+\left\{2\frac{\partial\chi_f}{\partial p_R}\frac{\partial p_f}{\partial p_\theta}\frac{\partial\chi_f}{\partial p_\theta}+\frac{\partial p_f}{\partial p_R}\left(\frac{\partial\chi_f}{\partial p_\theta}\right)^2\right\}\frac{\partial^3}{\partial p_f\partial\chi_f{}^2}+\frac{\partial\chi_f}{\partial p_R}\left(\frac{\partial\chi_f}{\partial p_\theta}\right)^2\frac{\partial^3}{\partial\chi_f{}^3}+\text{operators on }\phi_f. \tag{A2}$$

$$\frac{\partial^3}{\partial p_R\partial p_\varphi{}^2}=\frac{\partial^3 p_f}{\partial p_R\partial p_\varphi{}^2}\frac{\partial}{\partial p_f}+\left\{2\frac{\partial^2 p_f}{\partial p_R\partial p_\varphi}\frac{\partial p_f}{\partial p_\varphi}+\frac{\partial^2 p_f}{\partial p_\varphi{}^2}\frac{\partial p_f}{\partial p_R}\right\}\frac{\partial^2}{\partial p_f{}^2}+\left(\frac{\partial p_f}{\partial p_\varphi}\right)^2\left(\frac{\partial p_f}{\partial p_R}\right)\frac{\partial^3}{\partial p_f{}^3}+\frac{\partial^3\chi_f}{\partial p_R\partial p_\varphi{}^2}\frac{\partial}{\partial\chi_f}$$

$$+\left\{2\frac{\partial^2\chi_f}{\partial p_R\partial p_\varphi}\frac{\partial\chi_f}{\partial p_\varphi}+\frac{\partial\chi_f}{\partial p_R}\frac{\partial^2\chi_f}{\partial p_\varphi{}^2}\right\}\frac{\partial^2}{\partial\chi_f{}^2}+\left\{2\frac{\partial^2 p_f}{\partial p_R\partial p_\varphi}\frac{\partial\chi_f}{\partial p_\varphi}+2\frac{\partial^2\chi_f}{\partial p_R\partial p_\varphi}\frac{\partial p_f}{\partial p_\varphi}+\frac{\partial p_f}{\partial p_R}\frac{\partial^2\chi_f}{\partial p_\varphi{}^2}+\frac{\partial\chi_f}{\partial p_R}\frac{\partial^2 p_f}{\partial p_\varphi{}^2}\right\}\frac{\partial^2}{\partial p_f\partial\chi_f}$$

$$+\left\{2\frac{\partial p_f}{\partial p_R}\frac{\partial p_f}{\partial p_\varphi}\frac{\partial\chi_f}{\partial p_\varphi}+\left(\frac{\partial p_f}{\partial p_\varphi}\right)^2\left(\frac{\partial\chi_f}{\partial p_R}\right)\right\}\frac{\partial^3}{\partial p_f{}^2\partial\chi_f}+\left\{2\frac{\partial p_f}{\partial p_R}\frac{\partial p_f}{\partial p_\varphi}\frac{\partial\chi_f}{\partial p_\varphi}+\frac{\partial p_f}{\partial p_R}\left(\frac{\partial\chi_f}{\partial p_\varphi}\right)^2\right\}\frac{\partial^3}{\partial p_f\partial\chi_f{}^2}+\frac{\partial\chi_f}{\partial p_R}\left(\frac{\partial\chi_f}{\partial p_\varphi}\right)^2\frac{\partial^3}{\partial\chi_f{}^3}+\text{operators on }\phi_f. \tag{A3}$$

Owing to the selection of the coordinate systems, the following identities hold:

$$\begin{aligned}(\partial p_f/\partial p_\varphi)_{p_\varphi=0}&=0\\(\partial^2 p_f/\partial p_R\partial p_\varphi)_{p_\varphi=0}&=0\\(\partial\chi_f/\partial p_\varphi)_{p_\varphi=0}&=0\end{aligned} \tag{A4}$$

so that Eq. (A3) can be reduced to

$$\left(\frac{\partial^3}{\partial p_R \partial p_\varphi^2}\right)_{p_\varphi=0} = \left(\frac{\partial^3 p_f}{\partial p_R \partial p_\varphi^2}\right)_{p_\varphi=0} \frac{\partial}{\partial p_f} + \left(\frac{\partial^2 p_f}{\partial p_\varphi^2}\right)_{p_\varphi=0} \left(\frac{\partial p_f}{\partial p_R}\right) \frac{\partial^2}{\partial p_f^2} + \left(\frac{\partial^3 \chi_f}{\partial p_R \partial p_\varphi^2}\right)_{p_\varphi=0} \frac{\partial}{\partial \chi_f} + \left(\frac{\partial \chi_f}{\partial p_R}\right) \left(\frac{\partial^2 \chi_f}{\partial p_\varphi^2}\right)_{p_\varphi=0} \frac{\partial^2}{\partial \chi_f^2}$$

$$+ \left\{\frac{\partial p_f}{\partial p_R} \frac{\partial^2 \chi_f}{\partial p_\varphi^2} + \frac{\partial \chi_f}{\partial p_R} \frac{\partial^2 p_f}{\partial p_\varphi^2}\right\}_{p_\varphi=0} \frac{\partial^2}{\partial p_f \partial \chi_f} + \text{operators on } \phi_f. \tag{A5}$$

The terms remaining in the final equations for the quantum corrections are listed in Appendix B.

APPENDIX B

The functions appearing in Eq. (31) are the remaining terms from the operator D and are denoted as follows:

$$G_1 = [\partial^3 \chi_f / \partial p_R(s)^3]_{\chi_f = \chi}$$

$$G_2 = 3\{[\partial^2 \chi_f / \partial p_R(s)^2][\partial \chi_f / \partial p_R(s)]\}_{\chi_f = \chi}$$

$$G_3 = [\partial \chi_f / \partial p_R(s)]^3_{\chi_f = \chi}$$

$$G_4 = [\partial^3 \chi_f / \partial p_R(s) \partial p_\theta(s)^2]_{\chi_f = \chi}$$

$$G_5 = \{2[\partial^2 \chi_f / \partial p_R(s) \partial p_\theta(s)][\partial \chi_f / \partial p_\theta(s)] + [\partial \chi_f / \partial p_R(s)][\partial^2 \chi_f / \partial p_\theta(s)^2]\}_{\chi_f = \chi}$$

$$G_6 = \{[\partial \chi_f / \partial p_R(s)][\partial \chi_f / \partial p_\theta(s)]^2\}_{\chi_f = \chi}$$

$$G_7 = [\partial^3 \chi_f / \partial p_R(s) \partial p_\varphi(s)^2]_{\chi_f = \chi, P_\varphi = 0}$$

$$G_8 = \{[\partial \chi_f / \partial p_R(s)][\partial^2 \chi_f / \partial p_\varphi(s)^2]_{\chi_f = \chi, p_\varphi = 0}.$$

The relation of these differentials to the equation of motion is given in Appendix C.

APPENDIX C

The necessary relations for the evaluation of the quantities $G_1 - G_8$ appearing in the final equation for the quantum corrections, Eq. (31), are established in this Appendix. For two particles interacting with centrosymmetric forces, the equations of conservation of energy and momentum are

$$p_0^2 = p_R^2 + p_\theta^2/R^2 + 2\mu V(R) \tag{C1}$$

$$p_{\theta 0} = b p_0 = \mu R^2 \dot{\theta}(s). \tag{C2}$$

The symbols denote:

$\mu \equiv$ reduced mass

$b \equiv$ impact parameter

$R, \theta, p_R, p_\theta \equiv$ polar coordinates and conjugate momenta at s

$s \equiv$ time interval.

The scattering angle for completed collisions is related to the angle of the spherical coordinate system for the relative momentum after the collision, χ_f (see Appendix A), by the equations

$$\chi_f = (2n+1)\pi - \theta(\infty) \quad \text{if} \quad 2n\pi \le \theta(\infty) \le (2n+1)\pi$$

$$= \theta(\infty) - (2n+1)\pi \quad \text{if} \quad (2n+1)\pi \le \theta(\infty) \le (2n+2)\pi \tag{C3}$$

$$\theta(\infty) = 2\int_{R_m}^{\infty} p_\theta [p_\theta^2 - p_0^2/R^2 - 2\mu V(R)]^{-\frac{1}{2}} dR/R^2 \tag{C4}$$

$$p_0^2 - p_\theta^2/R_m^2 - 2\mu V(R_m) = 0, \tag{C5}$$

where $n = 0, 1, 2, \cdots$. For monotonic potential functions the scattering angle $\theta(\infty)$ is limited to the range $0 \le \theta(\infty) \le \pi$ and we consider this case in further detail.

If the relative motion is approaching the point of minimum separation of the particles, then the angle χ_f is

$$\chi_f = \pi - \theta - p_\theta \int_{R_m}^{R} [p_0^2 - p_\theta^2/y^2 - 2\mu V(y)]^{-\frac{1}{2}} dy/y^2 - p_\theta \int_{R_m}^{\infty} [p_0^2 - p_\theta^2/y^2 - 2\mu V(y)]^{-\frac{1}{2}} dy/y^2; \tag{C6}$$

but if the relative motion is receding from closest approach, then we have

$$\chi_f = \pi - \theta - p_\theta \int_{R}^{\infty} [p_0^2 - p_\theta^2/y^2 - 2\mu V(y)]^{-\frac{1}{2}} dy/y^2. \tag{C7}$$

Differentiation of χ_f with respect to p_R and p_θ is possible in these equations and the quantities G_1 through G_6 can be computed if the potential energy of interaction is specified.

The evaluation of the derivatives of χ_f with respect to p_φ requires an additional development. The coordinate systems originally chosen (see Appendix A) describe the classical motion confined to a plane; the component of momentum perpendicular to this plane, p_φ, is therefore zero. Now consider the virtual motion in a new plane with finite value of p_φ. The original and new plane possess in common the radial vector $\mathbf{R}$ and form an angle denoted by ξ. The momentum vector of the virtual motion in the new plane is

$$\mathbf{p}_v(s) = \hat{\imath}_R p_R + \hat{\imath}_\theta p_\theta / R + \hat{\imath}_\varphi p_\varphi / R, \tag{C8}$$

where $\mathbf{1}_R$ is the unit vector along $\mathbf{R}$, $\mathbf{1}_\theta$ is the unit vector perpendicular to $\mathbf{R}$ in the original plane, and $\mathbf{1}_\varphi$ a unit vector perpendicular to the original plane (see Fig. 1). In Fig. 1, the original plane of motion is taken to be the YZ plane, and the new plane is shown shaded. The angle ξ between the planes is given by the equations

$$\cos\xi = p_\theta/(p_\theta^2+p_\varphi^2)^{\frac{1}{2}}. \tag{C9}$$

For χ_f^v, the angle between the initial momentum vector $\mathbf{p}_0$ and the final virtual momentum vector, we have (see Fig. 2)

$$\cos\chi_f^v = \cos(\pi-\theta)\ \cos\Delta\theta + \cos(\pi/2-\theta)\ \cos\gamma. \tag{C10}$$

The relation

$$\cos\gamma = \sin(\Delta\theta)\ \sin(\pi/2-\xi) \tag{C11}$$

and simple trigonometric identities lead to

$$\cos\chi_f^v = -\cos\theta\cos(\Delta\theta) + \sin\theta\sin(\Delta\theta)\,p_\theta/(p_\theta^2+p_\varphi^2)^{\frac{1}{2}}. \tag{C11}$$

The angle $\Delta\theta$ between the radial vector $\mathbf{R}$ and the final momentum in the virtual plane of motion can of course be expressed in terms of polar coordinates of $\mathbf{R}$

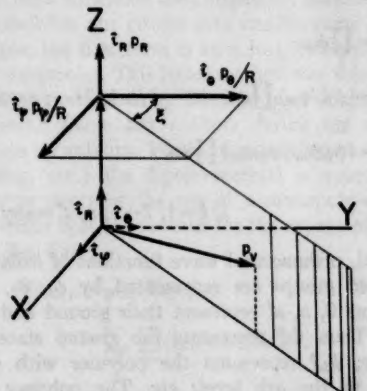

FIG. 1. Relation between the original plane of motion (YZ plane) and the new plane of virtual motion (shaded plane). The initial momentum vector $\mathbf{p}_0$ is not shown above; the final momentum of the virtual motion is $\mathbf{p}_v$.

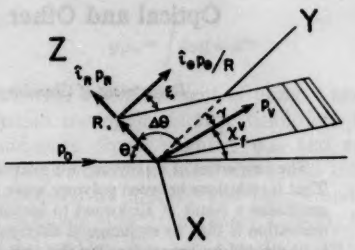

FIG. 2. The relation among $\mathbf{R}$, the radial vector at time s; the initial momentum $\mathbf{p}_0$ in the YZ plane; and the final momentum $\mathbf{p}_v$ in the plane of virtual motion (shaded). $\Delta\theta$ is the angle traversed by the radial vector in the latter plane since the time s; χ_f^v is the virtual scattering angle.

and their conjugate momenta; if the relative motion approaches the scattering center we have

$$\Delta\theta = -\int_R^{R_m}(p_\theta^2+p_\varphi^2)^{\frac{1}{2}}\,[p_v^2-(p_\theta^2+p_\varphi^2)/y^2-2\mu V(y)]^{-\frac{1}{2}}dy/y^2 + \int_{R_m}^{\infty}(p_\theta^2+p_\varphi^2)^{\frac{1}{2}}\times[p_v^2-(p_\theta^2+p_\varphi^2)/y^2-2\mu V(y)]^{-\frac{1}{2}}dy/y^2, \tag{C12}$$

but if the relative motion recedes from the scattering conter, then $\Delta\theta$ is given by the expression

$$\Delta\theta = -\int_R^{\infty}(p_\theta^2+p_\varphi^2)^{\frac{1}{2}}\,[p_v^2-(p_\theta^2+p_\varphi^2)/y^2-2\mu V(y)]^{-\frac{1}{2}}dy/y^2. \tag{C13}$$

From the foregoing equations we can determine the remaining derivatives of the scattering angle χ_f in the plane of the actual motion for which $\varphi=\pi/2$ and $p_\varphi=0$. The quantities G_7 and G_8 are

$$G_7 = -(\partial/\partial p_R)(\partial^2\Delta\theta/\partial p_\varphi^2)_{p_\varphi=0} - (\sin^2\theta/p_\theta^2)\ \mathrm{cosec}^2\chi(\partial\chi_f/\partial p_R)_{\chi_f=\chi} \tag{C14}$$

$$G_8 = (\partial\chi_f/\partial p_R)_{\chi_f=\chi}\{-(\partial^2\Delta\theta/\partial p_\varphi^2)_{p_\varphi=0} + (\sin^2\theta/p_\theta^2)\ \cot\chi = (\sin\theta/p_\theta^2)\ \cos\theta\} \tag{C15}$$

where $\Delta\theta$ is given by Eqs. (C12) and (C13).

Optical and Other Electronic Properties of Polymers*

IGNACIO TINOCO, JR.

Department of Chemistry, University of California, Berkeley 4, California

(Received May 13, 1960)

The properties of a polymer are related to the properties of its constituent groups and to its geometry. That is, relations between polymer wave functions and group wave functions are obtained. The equations generalize a result of Kirkwood to include the effect of time-average fields. The main assumption in the derivation is that no exchange of electrons between groups occurs. The usefulness of these wave functions is illustrated by expressions for the absorption coefficient, polarizability, optical rotation, dipole moment, and stability of a polymer.

INTRODUCTION

IN 1937 John G. Kirkwood[1] derived a theory of optical activity. He related the optical rotation of a molecule to the optical properties (polarizabilities) of groups in the molecule. In so doing he obtained wave functions for the molecule that were a function of the group wave functions. Moffitt, Fitts, and Kirkwood[2] in 1957 rederived these wave functions explicitly including degenerate states, i.e., polymers. In this paper we will derive once again these wave functions, but we will include the previously neglected effect of static fields. To show the usefulness of these wave functions we will relate the absorption coefficient, polarizability, optical rotation, dipole moment, and stability of a polymer to the properties of the individual groups in the polymer. A consistent treatment of these various optical and electrical properties has many advantages. The best group parameters to use can be determined from comparison of polymer property A with the calculated value. Then prediction of property B can be made with some confidence. For example, the optical rotation might be calculated from the much more easily measured absorption curve.

WAVE FUNCTIONS

A polymer is considered to be made up of groups of electrons and nuclei. The groups are chosen, if possible, so that there is negligible exchange of electrons between groups. If this choice is not possible, then the present treatment can not be applied. We can consider polystyrene or polyamides, for example, but not polyphenyls.

The total electronic Hamiltonian for the polymer is

$$\mathcal{H}=\sum_{i}^{\text{groups}}\mathcal{H}_i+\sum_{i}^{\text{groups}}\sum_{j>i}V_{s_i,t_j}$$

$$V_{s_i,t_j}=e^2\sum_{s}^{\text{particles}}\sum_{t}^{\text{particles}}(Z_s{}^iZ_t{}^j/r_{s_it_j}). \qquad (1)$$

The electronic charge is e; $Z_s{}^i$ is the charge on the sth particle in the ith group, where at least one of the charges is an electron; r is the distance between two particles in different groups. The $\mathcal{H}_i$ specify the kinetic energy of the electrons in group i and that part of their potential energy which involves only the other electrons and nuclei of the group. The potential energy of interaction between particles in different groups is given by the second term. We will treat this term as a perturbation.

The solutions of the zero-order polymer Hamiltonian are represented by zero-order polymer wave functions ψ^0:

$$\psi_0{}^0=\prod_i\phi_{i0}$$

$$\psi_{ja}{}^0=(\phi_{ja}/\phi_{j0})\prod_i\phi_{i0} \qquad j=1, 2\cdots;\ a=\text{any a}$$

$$\psi_{ja,ka'}{}^0=(\phi_{ja}\phi_{ka'}/\phi_{j0}\phi_{k0})\prod_i\phi_{i0}$$

$$j, k=1, 2\cdots;\ a, a'=\text{any } a. \qquad (2)$$

The real, orthonormal wave functions of isolated, unperturbed groups are represented by ϕ_i, ϕ_j, ϕ_k; the subscripts 0, a, a' represent their ground and excited states. Thus, $\psi_0{}^0$ represents the ground state of the polymer; $\psi_{ja}{}^0$ represents the polymer with group j excited to the ath level; etc. The polymer excited states will be N-fold degenerate. The number N can be 1 or any number up to the total number of groups in the polymer. We are, of course, considering a general polymer not necessarily composed of identical groups. The wave functions to use for these N-fold degenerate states in any further calculation are appropriate linear combinations:

$$\psi_{AK}{}^0=\sum_{i=1}^{N}C_{iaK}\psi_{ia}{}^0 \qquad K=1, 2\cdots N$$

$$\sum_{i=1}^{N}C_{iaK}C_{iaK}{}^*=1$$

$$\sum_{K=1}^{N}C_{iaK}C_{jaK}{}^*=0. \qquad (3)$$

* This work was supported in part by a research grant from the National Institute of Arthritis and Metabolic Diseases, Public Health Service, and by an unrestricted grant from Research Corporation.

[1] J. G. Kirkwood, J. Chem. Phys. **5**, 479 (1937).

[2] W. Moffitt, D. D. Fitts, and J. G. Kirkwood, Proc. Natl. Acad. Sci. U.S. **43**, 723 (1957).

We choose the zero-order polymer excited-state functions in Eq. (2) as a complete set for the expansion of the first-order functions[3]:

$$\psi_0^1=\psi_0^0-\sum_i\sum_{j\neq i}\sum_a[(V)_{ia;j0}\psi_{ia}^0/h\nu_{j0a}]$$
$$-\sum_i\sum_{j>i}\sum_a\sum_{a'}[(V)_{ia;ja'}\psi_{ia,ja'}^0/h(\nu_{j0a}+\nu_{j0a'})];$$

$$\psi_{AK}^1=\sum_{i=1}^{N}C_{iaK}\{\psi_{ia}^0-\sum_{j\neq i}\sum_{a'\neq a}[(V)_{ia;ja'}\psi_{ja'}^0/h(\nu_{j0a'}-\nu_{0a})]$$
$$-\sum_{j\neq i=1}\sum_{a'\neq a}[(V)_{iaa';j0}\psi_{ia'}^0/h(\nu_{0a'}-\nu_{0a})]$$
$$+\sum_{j\neq i}[(V)_{ia;j0}\psi_a^0/h\nu_{0a}]\}. \quad (4)$$

The (V) represents the perturbation term integrated over the appropriate zero-order wave functions. For example,

$$(V)_{ia;ja'}=\int\psi_{ia}^0V_{s_i,t_j}\psi_0^0d\tau. \quad (5)$$

To perform the integration we use either of two methods. First, we expand V in a multipole expansion. Then, if we choose our groups electrically neutral, the first nonzero term after integration is a dipole-dipole term; this is the term Kirkwood used originally. Alternatively, we can subdivide our groups into smaller parts having net charges; the first term is now just Coulomb's law for these monopoles. This latter method was introduced by London[4] and used by Moffitt[5] and Haugh and Hirschfelder.[6] These last authors derive the method and discuss its validity. For localized electrons (sigma, nonbonding, etc.) the dipole method is appropriate, while for pi electrons the use of a monopole at each nucleus seems best. The results for the expansion coefficients in Eq. 4 are:

$$(V)_{ia;j0}=\boldsymbol{\mu}_{i0a}\cdot\mathbf{T}_{ij}\cdot\boldsymbol{\mu}_{j00}$$

or

$$=\sum_s\sum_t(\rho_{s0a}{}^i\rho_{t00}{}^j/R_{s_it_j}),$$

$$(V)_{ia;ja'}=\boldsymbol{\mu}_{i0a}\cdot\mathbf{T}_{ij}\cdot\boldsymbol{\mu}_{j0a'}$$

or

$$=\sum_s\sum_t(\rho_{s0a}{}^i\rho_{t0a'}{}^j/R_{s_it_j}),$$

$$(V)_{iaa';j0}=\boldsymbol{\mu}_{iaa'}\cdot\mathbf{T}_{ij}\cdot\boldsymbol{\mu}_{j00}$$

or,

$$=\sum_s\sum_t(\rho_{saa'}{}^i\rho_{t00}{}^j/R_{s_it_j}). \quad (6)$$

For all groups

$$\sum_s\rho_{s0a}{}^i\mathbf{r}_{s_i}=\boldsymbol{\mu}_{i0a} \quad \text{and} \quad \sum_s\rho_{s0a}{}^i=0,$$

where

$$\boldsymbol{\mu}_{i0a}=\int\phi_0\boldsymbol{\mu}_i\phi_ad\tau$$

is the transition dipole moment of group i and $\rho_{s0a}{}^i$ is the transition monopole. Similar definitions hold for the ground-state dipole moment $\boldsymbol{\mu}_{i00}$ and monopole $\rho_{s00}{}^i$. The proper decomposition of a group into monopoles is discussed by Moffitt[5] and Haugh and Hirschfelder.[6] The dipole interaction tensor $\mathbf{T}_{ij}=(1/R_{ij}{}^3)(1-3\mathbf{R}_{ij}\mathbf{R}_{ij}/R_{ij}{}^2)$. The R's are the distances between either the point dipoles or monopoles.

With the wave functions defined by Eqs. (4) and (6) we can obtain the electronic properties of a polymer molecule.

Energy Level

The shifts in energy levels of a monomer on forming a polymer[7–9] and the analogous shifts when gas molecules are dissolved in a solvent[10] or form a molecular crystal[11,12] have received the most attention and are the most difficult to calculate. The difficulty arises from the vibrational structure, which we have ignored in the previous section. As Simpson and Peterson[12] have pointed out, for a crystal one does not know whether to apply the Born-Oppenheimer approximation to the crystal as a whole (strong coupling) or to the individual molecules in the crystal (weak coupling). An analogous problem occurs in a polymer, of course. The calculated shifts in energy levels depend completely on the assumption about strong or weak coupling, and it is very difficult to make the right choice *a priori*. In many systems intermediate coupling occurs, which makes the calculation of energy levels even more difficult. Happily, this problem of coupling strength does not occur in the calculation of intensities and other electronic properties considered in succeeding sections. The vibrational structure, of course, governs the shape of the absorption and optical rotation curves, but it does not affect the total oscillator and rotational strengths.

We will only outline the calculation of energy levels in a polymer relative to the energy levels in the isolated groups. The shift in energy of any level in the polymer is just the perturbing potential [second term of Eq. (1)] averaged over the corresponding wave functions [Eq. (4)]:

$$\Delta E_0=\int\psi_0{}^{0*}V\psi_0{}^1d\tau,$$

$$\Delta E_{AK}=\int\psi_{AK}{}^{0*}V\psi_{AK}{}^1d\tau. \quad (7)$$

[3] In the equation following we have omitted the $\psi_{ia,ja'}{}^0$ term from the expansion of $\psi_{AK}{}^1$, as it does not contribute in first order to any of the calculated electronic properties.

[4] F. London, J. Phys. Chem. **46**, 305 (1942).

[5] W. Moffitt, Proc. Natl. Acad. Sci. U.S. **42**, 10 (1956).

[6] E. F. Haugh and J. O. Hirschfelder, J. Chem. Phys. **23**, 1778 (1955).

[7] G. S. Levinson, W. T. Simpson, and W. Curtis, J. Am. Chem. Soc. **79**, 4314 (1957).

[8] D. S. McClure, Can. J. Chem. **36**, 59 (1958).

[9] E. G. McRae and M. Kasha, J. Chem. Phys. **28**, 721 (1958).

[10] E. G. McRae, J. Phys. Chem. **61**, 562 (1957).

[11] D. P. Craig, J. Chem. Soc. **1955**, 2302.

[12] W. T. Simpson and D. L. Peterson, J. Chem. Phys. **26**, 588 (1957).

The polymer transition frequency corresponding to the isolated group frequency ν_{0a} is

$$\nu_{0AK}=\nu_{0a}+(\Delta E_{AK}-\Delta E_0)/h. \quad (8)$$

Instead of explicitly writing down the algebra indicated by Eq. (7) we discuss the various contributions to the change in transition frequency on polymerization.

There is a term for the energy needed to produce a dipole in group i which is in the time-average field of the rest of the polymer. This can be represented by

$$\sum_i(\boldsymbol{\mu}_{iaa}-\boldsymbol{\mu}_{i00})\cdot\mathbf{E}_j. \quad (9)$$

It is just the potential energy change in removing a ground state dipole at group i and introducing an excited-state dipole. There are corresponding terms for dipole-induced dipole and London forces between groups. Usually, the most important contribution to the polymer transition frequency comes from the interaction among degenerate groups, however. This term is

$$\Delta E_{AK}(\text{deg})=\sum_{i=1}^{N}\sum_{j\neq i=1}^{N}C_{iaK}{}^{*}C_{jaK}(V)_{ia;ja}. \quad (10)$$

If one assumes weak coupling, the electronic transition moments appearing in $(V)_{ia;ja}$ must be replaced by the much smaller vibronic transition moments. For example, we replace $\boldsymbol{\mu}_{0a}$ by $\boldsymbol{\mu}_{00ab}$, where

$$\boldsymbol{\mu}_{0a}=\int E_0{}^{*}\boldsymbol{\mu}E_a d\tau,$$

$$\boldsymbol{\mu}_{00ab}=\int E_0{}^{*}\boldsymbol{\mu}E_a d\tau\int V_{00}{}^{*}V_{ab}d\tau, \quad (11)$$

and the E, V are electronic and vibrational wave functions, respectively. As the vibrational integral is much smaller than unity, the calculated splitting of a degenerate level becomes negligible when weak coupling is assumed.

For the intensity calculations, the transition moment will always appear squared, and we will be interested in sums over vibrational states. It is easy to show that the sum of squares of vibronic transition moments equals the square of the electronic transition moment:

$$\sum_b\mu_{00ab}{}^2=\mu_{0a}{}^2\sum_b\left[\int V_{00}{}^{*}V_{ab}d\tau\right]^2,$$

$$V_{00}=\sum_b C_bV_{ab},$$

$$\sum_b\left[\int V_{00}{}^{*}V_{ab}d\tau\right]^2=\sum_b C_b{}^2=1. \quad (12)$$

This means that the subsequent intensity equations will be independent of assumptions about coupling strength.

Polymer Stability

The conformation and stability of a polymer will depend on the forces between its constituent groups. In addition to bonding forces and short-range repulsive forces, there will be other longer range forces. Pitzer and Catalano[13] have written for the heat of formation of a hydrocarbon

$$\Delta H_f(0^\circ\text{K})=\Delta H_B+\Delta E_S+\Delta E_Z+\Delta E_0. \quad (13)$$

The various energies are ΔH_B, the sum of bond energies of the molecule; ΔE_S, the strain energy or short-range repulsion energy; ΔE_Z, the zero-point energy; and ΔE_0, the energy of the polymer relative to the isolated groups, as defined in Eq. (7) (the correlation energy).[13] For polymers, this equation will be most useful in predicting the relative stability of different conformations. The problem of helix-coil transitions in polypeptides and polynucleotides and the relative stability of right- and left-handed helices of enantiomers can be considered. For these problems, ΔE_B and ΔE_Z will be essentially identical for the two conformations. Whether ΔE_S or ΔE_0 is the dominant factor in the stability will depend on each individual system; however, ΔE_0 will, in general, be an important term.

Performing the integration in Eq. (7), we find

$$\Delta E_0=\sum_i\sum_{j>i}(V)_{i0;j0}-\sum_i\sum_a\Big[\sum_{j\neq i}(V)_{ia;j0}\Big]^2/h\nu_{i0a}$$

$$-\sum_i\sum_{j>i}\sum_a\sum_{a'}[(V)_{ia;ja}{}^2/h(\nu_{i0a}+\nu_{j0a'})];$$

$$(V)_{i0;j0}=\boldsymbol{\mu}_{i00}\cdot\mathbf{T}_{ij}\cdot\boldsymbol{\mu}_{j00} \quad (14)$$

or

$$\sum_s\sum_t[\rho_{s00}{}^i\rho_{t00}{}^j/R_{s_it_j}].$$

The first term is the interaction between permanent dipoles in the molecule; the second term is the dipole-induced dipole term; and the last term is the London force between groups in the molecule. Although permanent dipole forces are often negligible compared to London forces for gas-phase molecules, in a rigid polymer these forces may be quite important. In using Eq. 14, it is convenient to include ΔE_0 for bonded groups in the bond energies and only sum over nonbonded groups.

Permanent Dipole Moment

Equations for relating the permanent dipole moment of a molecule to its bond dipoles are well known.[14,15] We include the equation obtained by the use of the present wave functions mainly for completeness. The

[13] K. S. Pitzer and E. Catalano, J. Am. Chem. Soc. **78**, 4844 (1956).

[14] C. P. Smyth, *Dielectric Behavior and Structure* (McGraw-Hill Book Company, Inc., New York, 1955), p. 235.

[15] R. P. Smith, T. Ree, J. L. Magee, and H. Eyring, J. Am. Chem. Soc. **73**, 2263 (1951).

dipole moment of the polymer is

$$\boldsymbol{\mu}_{00}=\int\psi_0{}^{1*}\boldsymbol{\mu}\psi_0{}^{1}d\tau,$$

$$\boldsymbol{\mu}_{00}=\sum_i\boldsymbol{\mu}_{i00}-2\sum_i\sum_{j\neq1}\sum_a[(V)_{ia;j0}\boldsymbol{\mu}_{i0a}/h\nu_{i0a}]. \quad (15)$$

If we use the first definition of $(V)_{ia;j0}$ in Eq. (6), we can write Eq. (15) in terms of polarizabilities. As the static polarizability is

$$\boldsymbol{\alpha}_i=2\sum_a[\boldsymbol{\mu}_{i0a}\boldsymbol{\mu}_{i0a}/h\nu_{0ia}], \quad (16)$$

we can write

$$\boldsymbol{\mu}_{00}=\sum_i\boldsymbol{\mu}_{i00}-\sum_i\sum_{j\neq i}\boldsymbol{\alpha}_i\cdot\mathbf{T}_{ij}\cdot\boldsymbol{\mu}_{j00}. \quad (17)$$

That is, the total dipole moment of the polymer is the sum of the group permanent and induced moments.

Optical Properties

We mentioned in the Introduction that similar wave functions (minus the time-average field terms) had been used previously to calculate the optical rotation of polymers.[16–18] They have also been used to discuss the light absorption of polymers; in particular, an explanation of hypochromism in polynucleotides has been presented.[19] The inclusion of the static field terms, however, should be an improvement. Also, we will write the equation both in terms of the tensor quantities for the molecules (the polarizability tensor, the optical-rotation tensor, etc.) and in terms of the values averaged over all directions in the molecule. Rigid polymers are relatively easy to orient, making the measurements of direction-dependent properties possible. Other differences in the application of these wave functions become apparent in succeeding sections.

The quantities of interest for the optical properties are polymer transition moments such as $\boldsymbol{\mu}_{OA}$ and $\mathbf{m}_{OA}$, the electric and magnetic moments, respectively. We can write a general transition property $\mathbf{q}_{OA}$ for a polymer as follows:

$$\mathbf{q}_{OA}=\int\psi_0{}^{1*}\mathbf{q}\psi_A{}^{1}d\tau. \quad (18)$$

For a property which can be written as a sum of group properties we have

$$\mathbf{q}_{OA}=\int\psi_0{}^{1*}\sum_i\mathbf{q}_i\psi_A{}^{1}d\tau. \quad (19)$$

Therefore:

$$\mathbf{q}_{OA}=\sum_{k=1}^{N}\sum_{i=1}^{N}C_{iaK}\Bigg\{\mathbf{q}_{i0a}-\sum_{j\neq i}\sum_{a'\neq a}\frac{(V)_{ia;ja'}}{h}\times\left[\frac{\mathbf{q}_{j0a'}}{\nu_{j0a'}-\nu_{0a}}+\frac{\mathbf{q}_{ja'0}}{\nu_{j0a'}+\nu_{0a}}\right]-\sum_{j\neq i=1}^{N}\frac{(V)_{ia;ja}\mathbf{q}_{ja0}}{2h\nu_{0a}}-\sum_{j\neq i}\frac{(V)_{ia;j0}(\mathbf{q}_{iaa}-\mathbf{q}_{i00})}{h\nu_{0a}}-\sum_{j\neq i}\sum_{a'\neq a}\frac{(V)_{ia';j0}\mathbf{q}_{j0a'}}{h(\nu_{0a'}-\nu_{0a})}-\sum_{j\neq i}\sum_{a'\neq a}\frac{(V)_{ia';j0}\mathbf{q}_{iaa'}}{h\nu_{0a'}}\Bigg\}. \quad (20)$$

The last term will in general be small compared to the other terms because of its denominator; we drop it in subsequent equations.

Absorption Coefficient and Refractive Index

The absorption of plane-polarized light by a molecule depends on the magnitude and direction of the electric dipole transition moment. The integrated intensity of absorption can be characterized by an oscillator strength tensor defined as

$$\mathbf{f}_{OA}=(8\pi^2m\nu_{OA}/he^2)\,\boldsymbol{\mu}_{OA}\boldsymbol{\mu}_{AO}=(6909mc^2/\pi e^2N_0)\int\boldsymbol{\epsilon}_{OA}d\omega. \quad (21)$$

The $\boldsymbol{\epsilon}_{OA}$ is the absorption coefficient tensor in 1/ mole and ω is the frequency in cm^{-1}. If we average the absorption over all directions in the molecule we get the more familiar expressions

$$f_{OA}=(8\pi^2m\nu_{OA}/3he^2)\,\boldsymbol{\mu}_{OA}\cdot\boldsymbol{\mu}_{AO}=(2303mc^2/\pi e^2N_0)\int\epsilon_{OA}d\omega. \quad (22)$$

We can write the polarizability tensor for the polymer and the corresponding average polarizability as

$$\boldsymbol{\alpha}=(2/h)\sum_A[\nu_{OA}\boldsymbol{\mu}_{OA}\boldsymbol{\mu}_{AO}/(\nu_{OA}{}^2-\nu^2)]$$

$$\alpha=(2/3h)\sum_A[(\nu_{OA}\boldsymbol{\mu}_{OA}\cdot\boldsymbol{\mu}_{AO})/(\nu_{OA}{}^2-\nu^2)]. \quad (23)$$

We should add an empirical damping factor to the denominator of both expressions to indicate that the actual polarizability does not become infinite at $\nu=\nu_{OA}$. The exact shape of the α vs ν curve near ν_{OA} and the magnitude of ν_{OA} depends on the vibrational structure of the polymer; we do not try to predict them.

[16] D. D. Fitts and J. G. Kirkwood, Proc. Natl. Acad. Sci., U. S. **43**, 12 (1957).
[17] W. Moffitt, J. Chem. Phys. **25**, 467 (1956).
[18] I. Tinoco, Jr. and R. W. Woody, J. Chem. Phys. **32**, 461 (1960).
[19] I. Tinoco, Jr., J. Am. Chem. Soc. (to be published).

The value of $\mathfrak{y}_{OA}\cdot\mathfrak{y}_{AO}$, which characterizes the absorption and refractive index of the polymer, can be obtained from Eq. (20). If the A level is N-fold degenerate in zero order, we sum over all N levels:

$$\mathfrak{y}_{OA}\cdot\mathfrak{y}_{AO}=N\mathfrak{y}_{0a}\,\mathfrak{y}_{a0}$$
$$-\sum_{i=1}^{N}\sum_{j\neq i}\sum_{a'\neq a}\frac{4(V)_{ia;ja'}\,\mathfrak{y}_{i0a}\cdot\mathfrak{y}_{j0a'}\nu_{j0a'}}{h(\nu_{j0a'}^2-\nu_{0a}^2)}$$
$$-\sum_{i=1}^{N}\left[\sum_{j\neq i=1}^{N}\frac{(V)_{ia;ja}\,\mathfrak{y}_{i0a}\cdot\mathfrak{y}_{j0a}}{h\nu_{0a}}\right.$$
$$\left.-2\sum_{j\neq i}\frac{(V)_{ia;j0}\,\mathfrak{y}_{i0a}\cdot(\mathfrak{y}_{iaa}-\mathfrak{y}_{i0})}{h\nu_{0a}}\right]$$
$$-2\sum_{i=1}^{N}\sum_{j\neq i}\sum_{a'\neq a}\frac{(V)_{iaa';j0}\,\mathfrak{y}_{i0a}\cdot\mathfrak{y}_{j0a'}}{h(\nu_{0a'}-\nu_{0a})}. \quad (24)$$

If the A level is not degenerate, we set $N=1$. The first term is just the property of the unperturbed group. The next two terms represent the interaction of the group transition moment with the transition moments in other groups. The last two terms include the interactions with the static field of the polymer. The denominators in the terms show that significant contributions to the interaction come only from ν_{0a} or transitions with frequencies ν_{0a}' near the frequency under consideration ν_{0a}.

Equation (24) explicitly relates the absorption and refractive index of a polymer to measurable properties of its constituent groups and to the geometry of the polymer. It therefore provides for changes in polarizability and oscillator strength with conformation. Both the average properties and the tensor (direction-dependent) properties are determined by the configuration of the polymer. This is different from the usual discussions of molecular polarizabilities, which assume that the group polarizabilities are simply additive.[20,21] As Pitzer[22] has pointed out, this assumption may be approximately valid for the average polarizability, but not for the polarizability tensor.

Discussion of the absorption spectrum of polymers has usually been confined to wavelength shifts.[7-9] The experimentally observed changes of 25% to 50% in the absorption coefficients of polypeptides[23] and polynucleotides[24] owing to conformational changes have been considered in the present context.[10]

[20] R. P. Smith and E. M. Mortensen, J. Chem. Phys. **32**, 502 (1960).
[21] C. G. LeFevre and R. J. W. LeFevre, Revs. Pure and Appl. Chem. (Australia) **5**, 261 (1955).
[22] K. S. Pitzer, *Advances in Chemical Physics*, Vol. II, (Interscience Publishers, Inc., New York, 1959), p. 59.
[23] K. Imahori and J. Tanaka, J. Mol. Biol. **1**, 359 (1959).
[24] P. Doty, H. Boedtker, J. R. Fresco, R. Hazelkorn, and M. Litt, Proc. Natl. Acad. Sci. U.S. **45**, 482 (1959).

Optical Rotation

The rotation of plane-polarized light by a molecule can be characterized by the following equations[25]:

$$[m]=(3/n^2+2)[\alpha]M/100;$$

and

$$[m]=\frac{144N_0\nu^2}{\hbar c}\left(\frac{e}{2mc}\right)\sum_A\frac{Im\,\mathfrak{y}_{OA}\times(\mathbf{pr})_{OA}}{\nu_{OA}^2-\nu^2}. \quad (25)$$

The specific optical-rotation tensor $[\alpha]$ is in deg/dm g/cm^3. M = molecular weight, and n = refractive index of the solvent. The $\mathbf{pr}=\sum_i\mathbf{p}_i\mathbf{r}_i$ tensor is the sum of the position $\mathbf{r}$ and momentum $\mathbf{p}$ vectors of all the electrons in the molecule. In using this equation, we must remember that to find the optical rotation in a particular direction we need to dot in the propagation vector of the light instead of the electric vector. If we again average over all directions in the molecule we obtain

$$[m]=-(48N_0\nu^2/\hbar c)\sum_A\mathrm{Im}[(\mathfrak{y}_{OA}\cdot\mathbf{m}_{OA})/(\nu_{OA}^2-\nu^2)]. \quad (26)$$

We have made the substitution

$$\mathbf{m}_{OA}=(e/2mc)(\mathbf{r}\times\mathbf{p})_{OA} \quad (27)$$

and interchanged the dot and the cross after averaging. Before we can use Eq. (20) we must write the transition magnetic moment of the molecule as a sum of group properties[1,2]

$$\mathbf{m}_{OA}=(e/2mc)\sum_i\mathbf{R}_i\times\mathbf{p}_{iOA}+\sum_i\mathbf{m}_{iOA}. \quad (28)$$

R_i is the distance from an arbitrary center to group i. We can now specifically write out an expression for the average optical rotation of the molecule. This equation is very long and cumbersome; it is more useful to consider special cases.

The optical rotation will depend on the transition electric and magnetic dipole moments for the groups. It can be shown[27] that if an isolated group possesses a point or plane of symmetry either the electric or magnetic moment must be zero for every transition (including vibrations). This is equivalent to the statement that an isolated group with a point or plane of symmetry is not optically active. Therefore, each transition in the polymer can be classified as either electric dipole forbidden by local (group) symmetry or magnetic dipole forbidden by local symmetry.[28] The resulting equations

[25] The optical-rotation equations also need a damping term in the denominator. A discussion of the shape of α vs ν, $[m]$ vs ν and ϵ vs ν curves in an absorption band is given by Moffitt and Moscowitz.[26]
[26] W. Moffitt and A. Moscowitz, J. Chem. Phys. **30**, 3 (1959).
[27] H. Eyring, J. Walter, and G. E. Kimball, *Quantum Chemistry* (John Wiley & Sons, Inc., New York, 1944), p. 346.
[28] We can always choose our group to have a point or plane of symmetry except for the case of an asymmetric group of π electrons such as phenanthrophenanthrene.[29]
[29] M. S. Newman and D. Lednicer, J. Am. Chem. Soc. **78**, 4765 (1956).

are:

Electric dipole forbidden ($\boldsymbol{\mu}_{i0a}=O$):

$$\boldsymbol{\mu}_{OA}\cdot\mathbf{m}_{OA}=-\sum_{i=1}^{N}\sum_{j\neq i}\sum_{a'\neq a}\frac{2V_{ia;ja'}\boldsymbol{\mu}_{j0a'}\cdot\mathbf{m}_{i0a}\nu_{j0a'}}{h(\nu_{j0a'}^2-\nu_{0a}^2)}$$
$$-\sum_{i=1}^{N}\sum_{j\neq i}\frac{V_{ia;j0}(\boldsymbol{\mu}_{iaa}-\boldsymbol{\mu}_{i00})\cdot\mathbf{m}_{i0a}}{h\nu_{0a}}$$
$$-\sum_{i=1}^{N}\sum_{j\neq i}\sum_{a'\neq a}\frac{V_{iaa';j0}\boldsymbol{\mu}_{i0a'}\cdot\mathbf{m}_{i0a}}{h(\nu_{0a'}-\nu_{0a})}. \quad (29)$$

Magnetic dipole forbidden ($\mathbf{m}_{i0a}=0$):

$$\boldsymbol{\mu}_{OA}\cdot\mathbf{m}_{OA}=(2\pi i/c)\sum_{i=1}^{N}\sum_{j\neq i}\sum_{a'\neq a}$$
$$\times\frac{(V)_{ia;ja'}\nu_{i0a}\nu_{j0a'}(\mathbf{R}_i-\mathbf{R}_j)\cdot(\boldsymbol{\mu}_{i0a}\times\boldsymbol{\mu}_{j0a'})}{h(\nu_{j0a'}^2-\nu_{0a}^2)}$$
$$-\sum_{i=1}^{N}\sum_{j\neq i}\sum_{a'\neq a}\frac{V_{iaa';j0}\boldsymbol{\mu}_{i0a}\cdot\mathbf{m}_{i0a'}}{h(\nu_{0a'}-\nu_{0a})}$$
$$-\sum_{i=1}^{N}\sum_{j\neq i}\sum_{a'\neq a}\frac{2V_{ia;ja'}\boldsymbol{\mu}_{i0a}\cdot\mathbf{m}_{j0a'}\nu_{0a}}{h(\nu_{j0a'}^2-\nu_{0a}^2)}. \quad (30)$$

In this last equation we have set terms involving the permanent magnetic moment of a group $\mathbf{m}_{i00}$ equal to zero. In general, $\mathbf{m}_{i00}$ is equal to zero, and in any case there will be no correlation between $\mathbf{m}_{i00}$ and $\boldsymbol{\mu}$.[30] We have also made use of the identity

$$-\mathbf{p}_{i0a}=(i2\pi m\nu_{i0a}/e)\,\boldsymbol{\mu}_{i0a}. \quad (31)$$

In Eq. (29) we must use the transition monopole definition of $(V)_{ia;ja'}$, etc., to get a nonzero value for the rotation from a transition that is electric dipole forbidden by local symmetry. However, these definitions plus the static field terms (last two terms) in Eq. (29) remove one of the objections to Kirkwood's original calculation of optical rotation. The objection was that his treatment did not include the effect of electric-dipole forbidden transitions. Since these types of transitions ($n\rightarrow\pi^*$, for example) contribute to the optical rotation of many common compounds, this was a serious lack. It remains to be seen, of course, whether Eq. (29) can quantitatively account for the optical rotation of this class of compounds.

The first two terms of Eq. (30) have been used in the past for calculation of optical rotation.[1,16–18] They can be written in terms of polarizabilities if desired.

There is one more difference in the proposed use of the present equations for the calculation of optical rotation. It concerns the previously suggested[2,5,17] special frequency dependence of the optical-rotation contribution from degenerate levels. Moffitt proposed the following treatment of degenerate levels. The contribution to the rotation from a set of levels A which are degenerate in zero order is

$$[m]_A=\nu^2\sum_{K=1}^{N}[R_{AK}/(\nu_{AK}^2-\nu^2)]. \quad (32)$$

R_{AK} is the rotational strength of the Kth degenerate level and ν_{AK} is the corresponding frequency of that level. This expression is expanded in a Taylor's series about ν_A with the following results:

$$[m]_A=\left[\nu^2\sum_{K=1}^{N}R_{AK}/(\nu_A^2-\nu^2)\right]$$
$$-2\nu_A\nu^2\left[\sum_{K=1}^{N}R_{AK}(\nu_{AK}-\nu_A)/(\nu_A^2-\nu^2)^2\right]+\cdots. \quad (33)$$

The second term is the unique frequency-dependent contribution from the degenerate level, which Moffitt proposed should be compared with experiment. In order to use Eq. (33), however, we need to be able to calculate ν_{AK}, which depends on the vibrational structure and is therefore very difficult to obtain. We know that neither Eq. (32) nor Eq. (33) is useful near the absorption band, yet the large differences between a $(\nu_A^2-\nu^2)^{-1}$ and a $(\nu^2-\nu^2)^{-2}$ dependence will occur only near this band. For these reasons we have written Eqs. (28) and (29) as total rotational contributions from a particular level (degenerate or not). The frequency dependence will be of the general Drude type $(\nu_A^2-\nu^2)^{-1}$, but the exact shape of the curve is not predicted.

DISCUSSION

Before summarizing the possible uses of the polymer wave functions presented in this paper, we must discuss their validity. The fundamental assumption in the derivation is that electrons can be assigned to a particular group. That is, we neglect (a) exchange of electrons between groups in the ground state and (b) transfer of electrons from one group to another in excited states. Therefore, we must choose our groups in the polymer so that this neglect is valid. The other approximations made in the present equations are mainly for computational convenience. Examples of this type of approximation are (a) use of first-order perturbation theory only, (b) neglect of interactions involving three groups at a time, and (c) the multipole expansion of the perturbation potential with the retention of only the first term. Consideration of all these conditions leads one to the conclusion that the present equations should be most useful for molecular crystals and conformational effects in polymers. In both systems there will be significant interactions between non-nearest neighbors; these effects will be mainly of the type discussed here. Previously, the main use of equations of this type has been in these fields.

Polymers seem particularly interesting because in-

[30] J. H. Van Vleck, *Electric and Magnetic Susceptibilities* (Oxford University Press, New York, 1932), p. 272.

formation can be obtained about their configuration in solution. Polynucleotides, polysaccharides, polypeptides, and proteins, for example, undergo changes in conformation upon variation of temperature, *p*H, solvent, etc. These changes, in general, do not involve any differences in primary chemical bonding, but they do give rise to changes in optical properties. These changes can be interpreted with the present equations. Differences between stereospecific and random synthetic polymers can also be treated. We should not ignore small molecules completely, however, one can make qualitative and perhaps quantitative predictions of the effect of substituents on the spectra of simple molecules also.

Other properties of a molecule which depend on the electron distribution can be considered from the present point of view. For all calculations, the information needed is the geometry of the molecule plus the dipole moment and transition moments of its constituent groups of electrons.

ACKNOWLEDGMENTS

We wish to thank Dr. H. Devoe and R. W. Woody for many helpful suggestions.

THE JOURNAL OF CHEMICAL PHYSICS VOLUME 33, NUMBER 5 NOVEMBER, 1960

Ensemble Method in the Theory of Irreversibility

ROBERT ZWANZIG

National Bureau of Standards, Washington 25, D. C.

(Received May 16, 1960)

We describe a new formulation of methods introduced in the theory of irreversibility by Van Hove and Prigogine, with the purpose of making their ideas easier to understand and to apply. The main tool in this reformulation is the use of projection operators in the Hilbert space of Gibbsian ensemble densities. Projection operators are used to separate an ensemble density into a "relevant" part, needed for the calculation of mean values of specified observables, and the remaining "irrelevant" part. The relevant part is shown to satisfy a kinetic equation which is a generalization of Van Hove's "master equation to general order." Diagram summation methods are not used. The formalism is illustrated by a new derivation of the Prigogine-Brout master equation for a classical weakly interacting system.

INTRODUCTION

THIS article is the first of several to be devoted to the study, from a unified point of view, of various topics in the statistical mechanical theory of irreversibility.

Since the appearance in 1946 of Kirkwood's pioneering work in this field, activity has been intense and varied.

In the last few years significant advances have been made by Van Hove[1] and by Prigogine and his coworkers.[2] The work to be presented here originated in an effort to understand the methods introduced by these authors and to see their interrelations. In the course of this study it became evident that the Van Hove-Prigogine (VHP) methods can be made easier to understand and to use if a new point of view is taken. The initial formulation of this point of view is the main subject of this article. Future articles will deal with further developments.

We shall begin with a rough characterization of the VHP methods: (a) the initial state of a many-body system is specified; (b) the evolution of this state is followed by means of a many-body perturbation theory, involving expansion, rearrangement, approximation, and resummation of infinite series in powers of a perturbation; and (c) kinetic equations describing special features of this evolution are shown to be valid in an asymptotic (long-time) sense, for certain kinds of initial states.

An important feature of the VHP methods is that coarse-graining or time-smoothing is not needed. Random phase assumptions are not introduced except in specifying the initial state.

The examples worked out in detail by VHP are concerned with situations where a small parameter ξ (which may be a coupling strength, a density, etc.) characterizes the interaction responsible for irreversible behavior. They demonstrate the validity of kinetic equations in the limit t(time)$\to\infty$, $\xi\to 0$, and ξt is held constant. The formulation to be given in this article allows a simpler and more precise treatment of such weak interaction problems, but does not add anything substantially new to their results.

When the interaction parameter ξ is not small, the VHP methods become exceedingly complicated. The emphasis that has to be given to algebraic detail tends

[1] L. Van Hove, Physica **21**, 517 (1955); **25**, 268 (1959).

[2] I. Prigogine and R. Balescu, Physica **25**, 281, 302 (1959) and references given therein; R. Brout and I. Prigogine, *ibid.* **22**, 621 (1956).

to obscure issues of a more physical kind. As a result it is hard to apply their methods and to assess the validity of their conclusions. The formulation to be presented here avoids some technical difficulties in the VHP methods. We hope that it will be useful in problems where ξ is not small, but at present no new results have been obtained in such problems.

Our reformulation of the VHP methods is characterized by extensive use of Gibbsian ensembles (in which we differ from Van Hove, whose concern with the evolution of initial pure quantum states is more in the Boltzmann tradition).

Projection operators in the space of all possible ensemble densities[3] are used to separate an ensemble density into a "relevant" part, required for the calculation of ensemble averages of specified quantities, and the remaining "irrelevant" part. This is a generalization of the common separation of a density matrix into diagonal and nondiagonal parts, as used for example in Van Hove's derivation of the Pauli equation.

The projected or relevant part of an ensemble density will be shown to satisfy a special kinetic equation. This equation is in some respects a generalization of Van Hove's "master equation to general order." If the initial ensemble density lies entirely within the subspace defined by the projection operator, our kinetic equation takes on a particularly useful form. It becomes a closed equation for the projected ensemble density; it describes the decay of this density; and it is not Markoffian.[4] This equation is of fundamental importance in the theory of irreversibility.

As an illustration of our formalism we shall present another derivation of a master equation, first derived by Prigogine and Brout,[2] for a weakly interacting system in classical mechanics.

DERIVATION OF A KINETIC EQUATION

Liouville's equation is the natural starting point of any theory of time-dependent processes in statistical mechanics. In this section it will be used in the derivation of a useful kinetic equation.

In order to avoid duplication, we shall introduce a notation which can be used simultaneously for both the classical and the quantum mechanical theory.

The ensemble density (phase space distribution function or density matrix) at time t is $f(t)$. The average of a dynamical variable α (function, matrix or operator) at time t is $\langle \alpha; f(t) \rangle$. The Hamiltonian function or operator is called H.

In classical statistical mechanics, Liouville's equation is conveniently written

$$i[\partial f(t)/\partial t] = i[H, f(t)] \equiv Lf(t), \tag{1}$$

where $[A, B]$ denotes the Poisson bracket of A and B. This equation defines the operator L, which is Hermitian by virtue of the imaginary unit i. Equation (1) has the formal solution

$$f(t) = \exp(-itL) f(0). \tag{2}$$

The operator $\exp(-itL)$, introduced by Von Neumann and used by Kirkwood, is defined by Eq. (2). It has the property of displacing a function in time along a trajectory in phase space.

In quantum statistical mechanics Liouville's equation takes the form

$$i[\partial f(t)/\partial t] = \hbar^{-1}[H, f(t)] \equiv Lf(t), \tag{3}$$

where $[A, B]$ is the commutator $AB-BA$. This equation defines a Hermitian operator L. Equation (3) has the formal solution

$$f(t) = \exp(-itL) f(0), \tag{4}$$

which is actually equivalent to

$$f(t) = \exp(-itH/\hbar) f(0) \exp(+itH/\hbar). \tag{5}$$

The solution in the form of Eq. (4) is preferred because of its analogy with the classical case. (Fano[5] has shown how to construct the quantum mechanical L explicitly).

In the rest of this section we shall not distinguish between the classical and quantum mechanical interpretations of this notation.

Now we introduce an operator P. We have in mind specifically a projection operator, but its projection property will not be used until later. P is used to divide an ensemble density $f(t)$ into a "relevant" part $f_1(t) = Pf(t)$ and an "irrelevant" part $f_2(t) = (1-P)f(t)$,

$$f(t) = f_1(t) + f_2(t). \tag{6}$$

We require that P be a linear operator and time independent so that we can commute P and $\partial/\partial t$. Liouville's equation can then be written as a pair of equations,

$$P[i(\partial f/\partial t)] = i(\partial f_1/\partial t) = PL(f_1+f_2), \tag{7a}$$

$$(1-P)[i(\partial f/\partial t)] = i(\partial f_2/\partial t) = (1-P)L(f_1+f_2). \tag{7b}$$

The second of these equations can be solved formally for $f_2(t)$ in terms of $f_2(0)$ and $f_1(t)$. In this solution we require the operator $\exp[-i(1-P)Lt]$ which is defined by the formal solution of

$$i(\partial G/\partial t) = (1-P)LG; \tag{8}$$

$$G(t) = \exp[-it(1-P)L] G(0). \tag{9}$$

The solution of Eq. (7b) is

$$f_2(t) = \exp[-it(1-P)L] f_2(0) - i\int_0^t ds \exp[-is(1-P)L](1-P)Lf_1(t-s). \tag{10}$$

[3] "Ensemble density" is used to denote either a quantum mechanical density matrix or a classical phase space distribution function.

[4] A kinetic equation is called Markoffian if it involves properties of an ensemble density only at a single time.

[5] U. Fano, Revs. Modern Phys. 29, 74 (1957).

When this is substituted in Eq. (7a) we obtain

$$i[\partial f_1(t)/\partial t]=PL\exp[-it(1-P)L]f_2(0)+PLf_1(t)$$
$$-i\int_0^t ds PL\exp[-is(1-P)L](1-P)Lf_1(t-s). \quad (11)$$

This is a generalization of Van Hove's "master equation to general order in the perturbation." It corresponds to his equation when (a) the Hamiltonian is separated into an unperturbed part and a perturbation, (b) we use the matrix representation in which the unperturbed Hamiltonian is diagonal, and (c) the projection operator selects the diagonal part of any matrix in this representation. Van Hove's interference terms are contained in $f_2(0)$.

Equation (11) is of particular value when $f_2(0)=0$, since it then becomes a closed equation for $f_1(t)$. The assumption $f_2(0)=0$ is equivalent to $Pf(0)=f(0)$. The projection operator P specifies a class of initial ensemble densities for which the assumption is valid.

The physical significance of the characterization $f_2(0)=0$ of a class of initial states will be discussed in a future article. We shall then describe a method of expanding an ensemble density in terms of a complete set of functions in Hilbert space. The basis functions are found by orthogonalizing a set of observables with respect to a microcanonical density. This method is an extension of one developed by Fano.[5] It may be used for the construction of initial ensemble densities in terms of prescribed information.

In Van Hove's derivation of the master equation, the assumption $f_2(0)=0$ is the same as discarding interference terms. It corresponds to an initial phase-randomization.

Equation (11) [henceforth with $f_2(0)=0$] has a number of interesting properties.

It is a closed equation for the projected ensemble density, giving correctly the time dependence of that part $f(t)$ which lies in the P-subspace, but giving no other information. If P projects onto the subspace of functions of dynamical invariants, then $\partial f_1(t)/\partial t=0$.

Equation (11) contains a memory, represented by the convolution in time. It describes a non-Markoffian process.

Another feature of Eq. (11) is its "irreversibility." Roughly speaking, the total ensemble density, initially in a certain subspace, "leaks" out of this subspace so that information is lost.

It is interesting to see the form taken by Eq. (11) under Fourier transformation. The transform of $f_1(t)$ is defined by

$$g(\omega)=\int_0^\infty dt\exp[i(\omega+i\epsilon)t]f_1(t), \quad (12)$$

where the frequency is given a positive imaginary part, $\epsilon>0$, to insure convergence. At the end of a calculation the limit $\epsilon\to 0^+$ should be taken. We consider the particular but typical case where the Hamiltonian separates into an unperturbed part H_0 and a perturbation H_1, and the operator L separates into L_0+L_1. Furthermore, we assume that the projection operator commutes with L_0, which is a common situation in practice. Then Eq. (11) can be written in terms of a "scattering operator" $T(\omega)$,

$$(\omega+i\epsilon)g(\omega)=if_1(0)+P(L_0+T(\omega))g(\omega), \quad (13)$$

where $T(\omega)$ satisfies an equation of the Lippmann-Schwinger[6] type,

$$T(\omega)=L_1+L_1(\omega+i\epsilon-L_0)^{-1}(1-P)T(\omega). \quad (14)$$

The kinetic theory of gases can be formulated using Eqs. (13) and (14), together with a binary collision expansion of $T(\omega)$. This will be reserved for a future article.

ILLUSTRATION

As an illustration of how the preceding formalism can be applied, we shall derive the Prigogine-Brout master equation in the limit of weak interaction.

We consider a classical system of N particles in a volume V. The Hamiltonian is

$$H=\sum_{j=1}^N(p_j^2/2m)+\tfrac{1}{2}\lambda\sum_{j=1}^N\sum_{\substack{k=1\\k\neq j}}^N U(r_{jk}), \quad (15)$$

where the jth particle has momentum p_j, position r_j, and mass m. The potential energy of interaction of the pair (jk) is $U(r_{jk})$ and depends only on their separation. The parameter λ determines the strength of the interaction.

The corresponding Liouville operator is

$$L=L_0+\lambda L_1,$$
$$L_0=-i\sum_{j=1}^N(p_j/m)\cdot(\partial/\partial r_j),$$
$$L_1=-(i/2)\sum_{j\neq k}\sum F_{jk}\cdot[(\partial/\partial p_j)-(\partial/\partial p_k)], \quad (16)$$

where

$$\lambda F_{jk}=-\lambda[\partial U(r_{jk})/\partial r_j] \quad (17)$$

is the force on j due to k.

The master equation is concerned with the momentum dependence of a phase space distribution function $f(r, p; t)$. We introduce the projection operator

$$P\equiv(V^N)^{-1}\int_V d^{3N}r, \quad (18)$$

which has the effect of removing all position dependence from f,

$$Pf(r, p; t)=f_1(p; t). \quad (19)$$

We shall consider only initial states which are spatially homogeneous, so that $Pf(0)=f(0)$ and $f_2(0)=$

[6] B. Lippman and J. Schwinger, Phys. Rev. 79, 469 (1950).

0. Then Eq. (11) becomes a closed equation for the spatially homogeneous part of the entire $f(t)$. The projected function $f_1(t)$ gives correct averages of all functions of momentum.

It is easy to show that the term $PLf_1(t)$ in Eq. (11) vanishes. The contribution from L_0 vanishes because f_1 is independent of position. The L_1 part is

$$PL_1f_1=-\tfrac{1}{2}i\sum_{j\neq k}\sum(V^N)^{-1}\int_V d^{3N}\tau F_{jk}\times[(\partial/\partial p_j)-(\partial/\partial p_k)]f_1(p;t). \quad (20)$$

This is zero because the integral of a force over all positions is zero. The same argument serves to eliminate a term $PLf_1(t-s)$ from Eq. (11). We are left with the exact kinetic equation

$$\partial f_1(t)/\partial t=-\int_0^t ds PL\exp[-is(1-P)L]Lf_1(t-s). \quad (21)$$

Next we use $Lf_1=\lambda L_1f_1$, since $L_0f_1=0$. We also note that (for arbitrary G)

$$PLG=\lambda PL_1G \quad (22)$$

because P removes the contribution from L_0. This gives

$$\partial f_1(t)/\partial t=\lambda^2\int_0^t dsK(s;\lambda)f_1(t-s), \quad (23)$$

where $K(s;\lambda)$ is an operator in momentum space,

$$K(s;\lambda)=-PL_1\exp[-is(1-P)L]L_1. \quad (24)$$

Equation (23), which is still exact, can be simplified further in the limit of weak interaction and long time. We introduce the new time scale,

$$\tau=\lambda^2t \quad (25)$$

and replace $f_1(t)$ by $\rho(\tau)$. Equation (23) becomes

$$\partial\rho(\tau)/\partial\tau=\int_0^{\tau/\lambda^2}dsK(s;\lambda)\rho(\tau-\lambda^2s). \quad (26)$$

We assume that the memory of $K(s;\lambda)$ extends only over a finite interval of time $0<s<T$ in the original time scale, or

$$K(s;\lambda)\cong 0 \quad \text{if} \quad s>T. \quad (27)$$

In actual cases the memory extends roughly over the time required for a particle of momentum p to traverse the distance over which the interaction does not vanish.

Now we can take the limit $\lambda\to 0$ at fixed $\tau>0$. In this limit we obtain

$$\partial\rho(\tau)/\partial\tau=\int_0^\infty dsK(s;0)\rho(\tau) \quad (28)$$

which is a Markoffian equation. The memory operator in the limit is

$$K(s;0)=-PL_1\exp(-isL_0)L_1 \quad (29)$$

because

$$(1-P)L=L_0+\lambda L_1-PL; \quad (30)$$

and PL is of order λ because of Eq. (22). Equations (28) and (29) are, in rather condensed notation, exactly the Prigogine-Brout master equation.

ACKNOWLEDGMENT

I am indebted to Dr. R. J. Rubin for many useful discussions.

THE JOURNAL OF CHEMICAL PHYSICS VOLUME 33, NUMBER 5 NOVEMBER, 1960

On Molecular Chaos and the Kirkwood Superposition Hypothesis*

HAROLD GRAD

Institute of Mathematical Sciences, New York University

(Received July 11, 1960)

We consider properties which are possessed by typical functions of very many variables such as the n-particle molecular distribution function of a dynamical system. We show that such a function "selected at random" will in all likelihood approximately satisfy the molecular chaos condition and, to a better approximation, will very likely satisfy the Kirkwood superposition relation.

1. INTRODUCTION

WE consider distribution functions $f(x_1\cdots x_n)$ which are nonnegative, symmetric in all the variables $x_1\cdots x_n$, and normalized

$$\int f(x_1\cdots x_n)dx_1\cdots dx_n=1. \tag{1}$$

For the purposes of this paper, it is immaterial whether the variable x_i is a single variable or an abbreviation for several (such as the six coordinates specifying the state of a point molecule). Also, whether the range of integration is finite or infinite (as in the case of velocity coordinates) is unimportant. For simplicity, we therefore take x_i to be a single real variable with the unit interval as its range

$$0\leq x_i\leq 1. \tag{2}$$

When convenient, we shall use x for $(x_1\cdots x_n)$ and dx for $dx_1\cdots dx_n$. To call attention to the number of independent variables in $f(x)$ we may use the notation $f^{(n)}(x)$.

Reduced or marginal distributions (also nonnegative, symmetric, and normalized) are defined by

$$f_1(x_1)=\int f(x_1\cdots x_n)dx_2\cdots dx_n$$

$$f_m(x_1\cdots x_m)=\int f(x_1\cdots x_n)dx_{m+1}\cdots dx_n. \tag{3}$$

In probabilistic terminology, the random variables $x_1\cdots x_n$ are said to be independent (for brevity, f *is independent*) if

$$f(x_1\cdots x_n)=f_1(x_1)f_1(x_2)\cdots f_1(x_n). \tag{4}$$

We say that f *is chaotic* if

$$f_2(x_1, x_2)=f_1(x_1)f_1(x_2). \tag{5}$$

This is a weaker condition than independence.

We would like to formulate properties of sequences of functions $f^{(n)}(x)$ with n tending to infinity and, in particular, one that for most such sequences (properly defined) the chaos condition becomes more accurately satisfied as n becomes large. More precisely, take a given sequence $f^{(n)}(x)$ for which the one-particle distribution is fixed for all n,

$$f_1(x_1)=\int f^{(n)}(x_1\cdots x_n)dx_2\cdots dx_n \tag{6}$$

The two-particle reduced distributions will, in general, depend on n,

$$f_2^{(n)}(x_1, x_2)=\int f^{(n)}(x_1\cdots x_n)dx_3\cdots dx_n; \tag{7}$$

(here the superscript denotes the number of variables in the base function). We wish to consider conditions under which the difference, $f_2^{(n)}(x_1, x_2)-f_1(x_1)f_1(x_2)$, becomes small for large n. Clearly, this cannot be true of all sequences $f^{(n)}(x)$, since it is easy to construct a sequence for which the reduced distribution $f_2^{(n)}$ as well as f_1 is arbitrary. On the other hand, if one restricts the class of functions $f^{(n)}(x)$ too much, one can prove the theorem too easily! For example, if the functions $f^{(n)}(x)$ are taken to be uniformly bounded independent of n, $f^{(n)}(x)<M$, then one can show that for every such bounded sequence $f^{(n)}(x)$, the reduced distributions $f_1^{(n)}(x_1)$ and $f_2^{(n)}(x_1, x_2)$ can only converge to the constant 1. In order to obtain a reduced distribution $f_1(x_1)$ which is somewhat arbitrary, $f^{(n)}(x)$ must be allowed to become unbounded exponentially in n. Within the class of such rather ill-behaved functions $f^{(n)}$, we shall find that the ones which are not chaotic behave even more poorly. It should be emphasized that the symmetry of $f^{(n)}$ is crucial for this result.

Aside from its purely mathematical interest, a theorem of this type is of significance to kinetic theory. The chaos property has long been known to be vital for the derivation of the Boltzmann equation.[1] Moreover, this requirement is found to enter in two distinct ways. In an elementary formal analysis, the chaos condition (actually, a somewhat weakened condition which is irrelevant for our purposes) is required to hold for all time. The basic philosophy of a dynamical analysis is that, whatever may be assumed to hold initially, the

* The molecular chaos results contained in theorems 1 and 2 of this paper were described in an address at State College, Pennsylvania, July, 1953; Phys. Rev. **91**, 1031 (1953).

[1] For example, see (a) P. and T. Ehrenfest, Encykl. Math. Wiss. **4**, 2 (1911); (b) J. G. Kirkwood, J. Chem. Phys. **15**, 72 (1947); (c) H. Grad, *Handbuch der Physik* (Springer-Verlag, Berlin, 1958), Vol. 12, p. 205.

equations of motion alone should determine the subsequent behavior. It is not our purpose to discuss here the question of the propagation of chaos in time, granted it initially.[2] Our problem is whether a physical system, "randomly prepared" at the initial constant, will be found to be chaotic. If, indeed, we could not convince ourselves that this is so, this would imply the existence of an independent hitherto unannounced law of nature (possibly the existence of Maxwell's demons).

This matter is a statistical one, concerning functions of many variables. In the application of a mathematical result of a statistical type to nature, there always remains a gap. All that a theorem can state is that in a certain sense a specified result will be observed "almost always." It usually remains a matter of the reader's conviction whether the measure that is used to separate likely from unlikely is the proper one. This well-known point is underlined here, because the criterion that is found to distinguish unlikely choices in the present context is a rather unusual and unconventional one.

The error by which chaos is not satisfied is, under certain conditions, seen to be of the order $1/n$. Estimating more closely, it is found that the Kirkwood superposition condition, viz.,

$$f_3(x_1, x_2, x_3) = \frac{f_2(x_1, x_2) f_2(x_1, x_3) f_2(x_2, x_3)}{f_1(x_1) f_1(x_2) f_1(x_3)}, \tag{8}$$

is satisfied with a smaller error of the order $1/n^2$. Again, this is a mathematical result which is somewhat difficult to interpret physically. A distribution function occurring in nature cannot be said to be random. On the other hand, we are familiar in statistical mechanics with situations in which the equations of motion may be powerless to contradict a result that is based purely on the very large number of particles. One might be tempted to adopt such statistical results in cases when it is not evident that they *must* be violated (as is clearly the case of the chaos requirement for small intermolecular distances $x_2 - x_1$ where correlations are known to be strong).

2. COARSE-GRAINED DISTRIBUTIONS

The basic difficulty in investigating the limit of large n is to compare functions of a different number of variables. We would like to be able to say that a sequence $f^{(n)}(x)$ approaches a limit in some sense as n tends to infinity, or that two functions $f^{(n)}(x_1 \cdots x_n)$ and $f^{(m)}(x_1 \cdots x_m)$ define approximately the same probability distribution. To do this it is necessary to use a coarse-grained distribution and to make very strong use of the symmetry of f.

The unit interval $0 \leq x_i \leq 1$ is subdivided into r equal intervals (the n-dimensional unit cube into r^n cubes), and these intervals are labelled by the index ξ_i which takes integral values $\xi_i = 1, 2 \cdots r$ $(i = i, 2 \cdots n)$. The n-dimensional cubes are thus indexed by the set $\xi = (\xi_1 \cdots \xi_n)$; i.e., the continuous variable x is replaced by the discrete variable ξ. We denote integration over the cube ξ by $\int_\xi (\ )\, dx$ and define the coarse-grained distribution

$$f_\xi = \int_\xi f dx, \tag{9}$$

which has the normalization

$$\sum_\xi f_\xi = 1. \tag{10}$$

Note that $\int_\xi$ represents integration over a single cube identified by ξ, while $\sum_\xi$ is summed over all values of ξ (all cubes).

For a given cube $\xi = (\xi_1 \cdots \xi_n)$, we count the number of indices ξ_i which are equal to s and call this number k_s; (k_s takes the values $0, 1 \cdots n$). By the symmetry of $f(x_1 \cdots x_n)$, the value of f_ξ is the same for all cubes ξ which are represented by the same value of $k = (k_1 \cdots k_r)$. Consequently, f_ξ can be considered to be a function of k, and it should cause no confusion if we represent this function by the same symbol $f(k)$. By use of the symmetry of f, we have obtained a function $f(k)$ of r variables in place of the function f_ξ of n variables. This offers the possibility of investigating the limit $n \to \infty$ in a fixed space. The variables k are not independent but satisfy the relation

$$\sum_{s=1}^{r} k_s = n. \tag{11}$$

The proper k-space is therefore an $(r-1)$-dimensional hyperplane.

This mapping of ξ into k is not one-one; the number of points ξ which map into a given point k is the multinomial coefficient

$$\binom{n}{k} = \frac{n!}{k_1! \cdots k_r!}. \tag{12}$$

The normalization of $f(k)$ is therefore given by

$$\sum_\xi f_\xi = \sum_k \binom{n}{k} f(k) = 1. \tag{13}$$

We now introduce the function

$$F(k) = \binom{n}{k} f(k), \tag{14}$$

which has the normalization

$$\sum_k F(k) = 1 \tag{15}$$

and claim that this correctly represents the coarse-grained equivalent in k-space of the original distribution $f(x_1 \cdots x_n)$. To verify this, we consider a symmetric

[2] The significance of this problem was first noted by Kirkwood, footnote reference 1b; for a discussion of this point see footnote reference 1c.

phase function $\phi(x_1 \cdots x_n)$ and its mean value

$$\langle \phi \rangle = \int \phi(x) f(x) dx. \tag{16}$$

The mean value of ϕ (with respect to volume) on a cube ξ is denoted by

$$\bar{\phi}_\xi = r^n \int_\xi \phi dx = r^n \phi_\xi. \tag{17}$$

By symmetry, $\bar{\phi}_\xi$ is a function of k which, without confusion, can be denoted by $\bar{\phi}(k)$. If ϕ is a step function with a constant value on each cube ξ, we have the exact formula

$$\langle \phi \rangle = \sum_\xi \bar{\phi}_\xi f_\xi = \sum_k \bar{\phi}(k) F(k). \tag{18}$$

More generally, we can interpret this formula as a coarse-grained approximation to $\langle \phi \rangle$ obtained by replacing ϕ by its volume average on each cube ξ. It should be remarked that, although ϕ and f appear symmetrically in (16) as do $\bar{\phi}$ and F in (18), the volume element r^{-n} and the multiplicity

$$\binom{n}{k}$$

have been combined with ϕ and f respectively to obtain the average $\bar{\phi}$ and the normalized function F. When convenient, superscripts will be attached to $F^{(n)}$ to indicate the parameter n.

It now remains to identify the reduced distributions $f_1(x_1)$, etc., in coarse-grained form. To do this, we write

$$f_1(x_1) = \int \delta(y_1 - x_1) f(y) dy = \int n^{-1} \sum_i \delta(y_i - x_1) f(y) dy. \tag{19}$$

In other words, $f_1(x_1)$ is just the mean value of the symmetric phase function

$$\phi(y) = n^{-1} \sum_i \delta(y_i - x_1); \tag{20}$$

x_1 is a parameter in ϕ. We now replace ϕ by its coarse-grained average,

$$\bar{\phi}_\xi = (r^n/n) \sum_i \int_\xi \delta(y_i - x_1) dy. \tag{21}$$

Fixing ξ and assuming that the coordinate x_1 lies in the interval $s (s = 1, 2 \cdots r)$, we see that

$$\int_\xi \delta(y_i - x_1) dy_1 \cdots dy_n = \begin{cases} 0 \text{ if } \xi_i \neq s \\ \\ 1/r^{n-1} \text{ if } \xi_i = s. \end{cases} \tag{22}$$

Thus the summation in (21) merely counts the number of indices ξ_i which are equal to s, viz., k_s, and we obtain

$$\bar{\phi}(k) = (r/n) k_s. \tag{23}$$

It is convenient to change the normalization by dropping the factor r; thus, taking $\bar{\phi} = k_s/n$ we obtain the reduced distribution

$$F_1(s) = (1/n) \langle k_s \rangle. \tag{24}$$

Here F_1 is a function of the discrete variable $s = 1, 2 \cdots r$ instead of the continuous variable x_1 of $f_1(x_1)$. The factor r was dropped from (23) in order to have the normalization

$$\sum_s F_1(s) = 1; \tag{25}$$

$1/r$ is merely the step size that was removed to obtain a summation from 1 to r of s instead of an integration from 0 to 1 of x_1.

In exactly the same way we write

$$f_2(x_1, x_2) = \int \delta(y_1 - x_1) \delta(y_2 - x_2) f(y) dy$$

$$= \int [n(n-1)]^{-1} \sum_{i \neq j} \delta(y_i - x_1) \delta(y_j - x_2) f(y) dy, \tag{26}$$

identify the appropriate phase function

$$\phi(y) = [n(n-1)]^{-1} \sum_{i \neq j} \delta(y_i - x_1) \delta(y_j - x_1), \tag{27}$$

and compute the coarse-grained average

$$\bar{\phi}(k) = [r^2/n(n-1)] \begin{cases} k_s k_t & \text{if } s \neq t \\ \\ k_s(k_s - 1) & \text{if } s = t. \end{cases} \tag{28}$$

Here s is the interval containing x_1 and t the interval containing x_2. For the same reason as before, we drop the factor r^2 and obtain the reduced distribution

$$F_2(s, t) = [n(n-1)]^{-1} \begin{cases} \langle k_s k_t \rangle & \text{if } s \neq t \\ \\ \langle k_s(k_s - 1) \rangle & \text{if } s = t. \end{cases} \tag{29}$$

Finally, a simple computation yields the result

$$F_3(s, t, u) = [n(n-1)(n-2)]^{-1} \begin{cases} \langle k_s k_t k_u \rangle & \text{if } s \neq t \neq u \\ \\ \langle k_s(k_s - 1) k_u \rangle & \text{if } s = t \neq u \\ \\ \langle k_s(k_s - 1)(k_s - 2) \rangle & \text{if } s = t = u. \end{cases} \tag{30}$$

The interpretation of F_1 as given in formula (24) is very simple. For a given cube ξ we have a set $(k_1 \cdots k_r)$ which we plot as a step function, k_s as a function of s. This is a frequency count (i.e., an approximate coarse-grained reduced distribution) assigned to the cube ξ. F_1 is the average of this local distribution over all cubes ξ.

For F_2 the interpretation is equally simple. Before averaging over cubes ξ, the expressions in the brace in (29) represent the number of combinations of pairs of particles, one being in s and one in t.

We conclude this section with a simple example, the special case of strict independence, $f(x_1\cdots x_n)=f_1(x_1)\cdots f_1(x_n)$. We denote the coarse-grained integral of $f_1(x_1)$ over the interval s by p_s,

$$\int_s f_1(x_1)dx_1=p_s. \tag{31}$$

From the multinomial expansion

$$(p_1+p_2+\cdots+p_r)^n=\sum_k\binom{n}{k}p_1^{k_1}\cdots p_r^{k_r} \tag{32}$$

we read off

$$F(k)=\binom{n}{k}p_1^{k_1}\cdots p_r^{k_r}. \tag{33}$$

The following elementary results,

$$\begin{aligned}
&\langle k_s\rangle=np_s\\
&\langle k_sk_t\rangle=n(n-1)p_sp_t, && s\neq t\\
&\langle k_s(k_s-1)\rangle=n(n-1)p_s^2\\
&\langle k_sk_tk_u\rangle=n(n-1)(n-2)p_sp_tp_u, && s\neq t\neq u\\
&\langle k_s(k_s-1)k_t\rangle=n(n-1)(n-2)p_s^2p_t, && s\neq t\\
&\langle k_s(k_s-1)(k_s-2)\rangle=n(n-1)(n-2)p_s^3,
\end{aligned} \tag{34}$$

allow one to verify that

$$\begin{aligned}
F_1(s)&=p_s\\
F_2(s,t)&=p_sp_t\\
F_3(s,t,u)&=p_sp_tp_u.
\end{aligned} \tag{35}$$

It is amusing to note that this roundabout method of computing the distributions F_1, F_2, and F_3 involves correlation expressions such as $k_s(k_s-1)$ in (29) which become uncorrelated only after averaging with respect to k.

3. THE GENERATING FUNCTION

We wish to consider the behavior of the discrete-valued function $F^{(n)}(k)$ for fixed r as n tends to infinity. First we introduce the variable

$$y_s=k_s/n, \qquad \sum_s y_s=1, \tag{36}$$

which has the property that $0\leq y_s\leq 1$. We use the same symbol for F as a function of y, $F^{(n)}(k)=F^{(n)}(ny)\to F^{(n)}(y)$. The behavior of $F^{(n)}$ as n tends to infinity is, of course, not well defined until the remaining variables in $F^{(n)}$ are suitably restricted. Since we wish to fix the function F_1 as n is varied, and since $F_1(s)=\langle y_s\rangle$ [Eq. (24)], we conclude that the proper question to ask is the behavior of $F^{(n)}$ with y rather than k held fixed.

The simplest possible example is $f(x_1\cdots x_n)=1$ which yields

$$F^{(n)}(k)=\binom{n}{k}r^{-n}.$$

The function $F^{(n)}$ does not approach a limit as n becomes large (either as a function of k or of y). What it does is become peaked and approach a δ function in the neighborhood of $y_s=1/r$. It is evident that the same result follows from any function $f(x_1\cdots x_n)$ which is uniformly bounded independent of n; the situation is dominated by the factor

$$\binom{n}{k}$$

which becomes peaked. The choice of an independent $f(x_1\cdots x_n)=f_1(x_1)\cdots f_1(x_n)$ yields a different but similar result; the distribution $F^{(n)}$ [see Eq. (33)] is again peaked but this time in the neighborhood of an arbitrarily assigned point, $y_s=p_s$. We can now assign the one-particle distribution $F_1(s)$ arbitrarily. The function $f(x_1\cdots x_n)$, as the product of n equal factors, behaves exponentially in n.

Perhaps the simplest way to ameliorate this singular behavior is to consider the limit $[F^{(n)}(y)]^{1/n}$. This is equivalent to the common expedient for obtaining thermodynamic quantities, viz., to take the logarithm and then divide by n. On using Sterling's formula for the factorial, we obtain the perspicuous result

$$\lim\binom{n}{k}^{1/n}=[y_1^{y_1}\cdots y_r^{y_r}]^{-1}$$

or

$$\lim[n^{-1}\log\binom{n}{k}]=-\sum_s y_s\log y_s. \tag{37}$$

For the case of independence, Eq. (33), we obtain

$$\lim[n^{-1}\log F^{(n)}]=\sum_s y_s\log(p_s/y_s)\equiv\log\psi^*(y). \tag{38}$$

These remarks lead us to consider a more general class of functions $F^{(n)}(y)$ for which the uniform limit

$$\lim[F^{(n)}(y)]^{1/n}=\psi(y) \tag{39}$$

exists. We call such a sequence *r-convergent* ($F^{(n)}$ and ψ are functions of r variables) and call the function $\psi(y)$ the *generating function* of the sequence $F^{(n)}$. Except for certain mild restrictions on $\psi(y)$ to allow $F^{(n)}(y)$ to be normalized (this will be discussed later), any nonnegative continuous function $\psi(y)$ can be used to generate a sequence $F^{(n)}(y)$ and thus a sequence of coarse-grained functions $f^{(n)}(x_1\cdots x_n)$. It is easy to show that $F^{(n)}$ is *asymptotically* independent for large n only if it is generated by ψ^*. Thus the class of generated functions is without question wider than the class of independent functions in that the special functions $\psi^*(y)$ of (38) are replaced by arbitrary functions. It is

this class of generated functions which we shall investigate. It will be seen that the chaos property is also special in this class, but it is much more widespread than independence and is even, in some sense, almost universal in the class of generated functions.

There is an intermediate class of functions which may be worth mentioning. A generating function $\psi(y_1\cdots y_r)$ which is a product, $\psi(y_1)\psi(y_2)\cdots\psi(y_r)$, has the property that $\log F^{(n)}$ is a sum function which, in the limit of large r, can be written as an integral. In the special case of independence, this is Boltzmann's H function, cf., (37).

There is an immediate generalization of this concept of r convergence to simply convergence. A sequence $f^{(n)}(x_1\cdots x_n)$ is said to *converge* if it is r-convergent for each of a sequence of increasing $r=r_1, r_2, \cdots$ to an appropriate function $\psi(y_1\cdots y_r)$. This is a rather complicated concept, and it will not be discussed further.

It is worth remarking that for the case of independence, the approximation $F^{(n)}\sim c_n(\psi^*)^n$ (the contant c_n is required for normalization) is better than the more conventional approximation to the binomial (or multinomial) distribution by a normal distribution. The normal approximation is valid only within a range of order $n^{-\frac{1}{2}}$ of the peak, whereas the power approximation is much better over a wider range.

4. MOLECULAR CHAOS

In terms of the variable $y=k/n$, Eq. (24) and (29) become

$$F_1(s)=\langle y_s\rangle \tag{40}$$

$$F_2^{(n)}(s,t)=(1-1/n)^{-1}\begin{cases}\langle y_s y_t\rangle & s\neq t\\ \langle y_s^2\rangle-(1/n)\langle y_s\rangle, & s=t.\end{cases} \tag{41}$$

The problem is to determine the behavior of $F_2^{(n)}(s,t)$ in the limit of large n while keeping $F_1(s)$ fixed. The answer is almost immediate. From (41) we obtain

$$F_2^n(s,t)-F_1(s)F_1(t)=\langle y_s y_t\rangle-\langle y_s\rangle\langle y_t\rangle+O(1/n) \tag{42}$$

which is valid for $s=t$ as well as $s\neq t$. We recognize the difference $\langle y_s y_t\rangle-\langle y_s\rangle\langle y_t\rangle$ as the covariance matrix of the distribution $F^{(n)}(y)$. We conclude that a necessary and sufficient condition for chaos to hold in the limit of large n is that the covariance matrix of $F^{(n)}(y)$ approach zero. The latter evidently implies that $F^{(n)}(y)$ becomes peaked and approaches a δ-function.

Theorem 1: A necessary and sufficient condition that $F_2^{(n)}(s,t)$ become chaotic as n becomes large is that the sequence $F^{(n)}(y)$ become peaked in this limit. The location of the peak is given by the prescribed mean values $\langle y_s\rangle=F_1(s)$.

This theorem has been very easily proved and makes no use of the complications in the previous section involving generating functions; however, it is not very intuitive. It is not clear, at first glance, whether peaking is a property to be expected in general or one to be surprised at. This is clarified by the following theorem.

Theorem 2: If the generating function $\psi(y)$ for a sequence $F^{(n)}(y)$ attains its maximum at a single point y^0, then $F^{(n)}(y)$ becomes peaked in the limit of large n.

The proof of this theorem for continuous $\psi(y)$ is quite easy. It is convenient to consider the function $F^{(n)}(y)$ as a step function defined for continuous y rather than only at the discrete points $y_i=0, 1/n, 2/n, \cdots, 1$. Replacing $F^{(n)}(y)$ by $n^rF^{(n)}(y)$, we can now integrate with respect to y rather than sum; this provides an easier comparison with the limiting function $[\psi(y)]^n$. Now, choose an arbitrary spherical (or cubical) neighborhood of y^0, $|y-y^0|<\eta$. We wish to show that the sum of $F^{(n)}$ (or integral of $n^rF^{(n)}$) outside this sphere can be made arbitrarily small compared to the sum inside the sphere by choosing n sufficiently large. By hypothesis, $\psi(y^0)-\psi(y)>0$ for $y\neq y^0$. We write $\psi(y^0)=\psi_0$; (we shall see later that $\psi_0=1$, but this is unimportant). Outside the sphere we have $\psi_0-\psi(y)>\alpha\psi_0>0$ for some α. A small subsphere of volume V can be found within the η sphere such that $\psi_0-\psi(y)<\frac{1}{2}\alpha\psi_0$. Within the η sphere we have

$$\int_\eta [\psi(y)]^n dy>\psi_0^n(1-\tfrac{1}{2}\alpha)^n V;$$

outside the η-sphere we have

$$\int_{\eta'} [\psi(y)]^n dy<\psi_0^n(1-\alpha)^n.$$

Now, by the definition of ψ as a generating function, for any small ϵ we have {using the uniform convergence of $[F^{(n)}]^{1/n}$ to ψ}

$$(1-\epsilon)^n\psi^n<F^{(n)}<(1+\epsilon)^n\psi^n,$$

for all sufficiently large n. We choose $\epsilon=\frac{1}{4}\alpha$ and observe that

$$\int_\eta n^rF^{(n)}(y)dy>n^r\psi_0^n(1-\tfrac{3}{4}\alpha+\tfrac{1}{8}\alpha^2)^n V,$$

$$\int_{\eta'} n^rF^{(n)}(y)dy<n^r\psi_0^n(1-\tfrac{3}{4}\alpha-\tfrac{1}{4}\alpha^2)^n.$$

By inspection we see that the outer integral can be made arbitrarily small compared to the inner integral by choosing n large.

The two theorems combine to give the result that a sequence $F^{(n)}$ is asymptotically chaotic if the generating function $\psi(y)$ attains its maximum at a single point. We now contend that this situation is very likely among functions $\psi(y)$ chosen "at random." It is possible that this question can be formalized by introducing, say, the Wiener measure over the space of continuous functions, but we shall be content to examine it intuitively. It is very difficult to draw intuitive conclusions about merely continuous functions; we shall therefore examine

smooth functions with, for example, continuous second derivatives. For simplicity of language, consider y to be a single variable. First we dismiss as unlikely the random occurrence of a function $\psi(y)$ with a linear segment; in other words, the maximum is not attained on a whole segment. If the maximum is attained at an infinity of points, one of them must be a point of accumulation, and it is easily seen that the second derivative as well as the first derivative vanishes at this point. The vanishing of both these functions simultaneously we interpret as being unlikely. Finally, consider the case of a finite number of isolated maxima. If y^0 is one such point, it would seem exceedingly unlikely, on intuitive grounds, that $\psi(y)$ would return to exactly the same height at another local maximum $\psi(y^1)$.

These arguments are, of course, rather arbitrary and subjective, but we shall not pursue the matter here.

It may be profitable to briefly discuss the physical relevance of the theorems which were proved. It is, of course, true that the concept of generating function and the maximum properties of a randomly chosen function are quite artificial and possibly even unnatural. On the other hand, the existence of any theorem at all of this general types removes some of the mystery inherent in the apparent tendency of natural systems to be observed when chaotic. Also, there may very well exist much more powerful theorems of this type.

5. FURTHER PROPERTIES OF PEAKED DISTRIBUTIONS

If the generating function $\psi(y)$ has continuous second derivatives, the behavior of the peaked distribution $[\psi(y)]^n$ can be studied in some detail. In particular, we can study the dispersion about the mean (which is small of order $1/n$). It is well known that in a neighborhood of the maximum, $\psi(y^0)=\psi_0$, one can use the approximation

$$[\psi(y)]^n \sim \psi_0^n \exp[-(n/2)\sum_{i,j} a_{ij}(y_i-y_i^0)(y_j-y_j^0)] \tag{43}$$

where

$$a_{ij}=-\psi_0^{-1}(\partial^2\psi/\partial y_i \partial y_j)\,|_{y^0}; \tag{44}$$

(a_{ij} is assumed to be positive definite). This approximation is sufficiently accurate for purposes of integration; outside its range of validity, which is $y-y^0=O(n^{-\frac{1}{2}})$, the value of ψ^n is very small. To this approximation, one need only know the point y^0 at which ψ is largest and the matrix of second derivatives at this point. The remainder of the function $\psi(y)$ is unessential.

To obtain $F^{(n)}(y)$ it is necessary to normalize the distribution (43)

$$F^{(n)}(y) \sim A^{\frac{1}{2}}(n/2\pi)^{r/2} \times \exp[-(n/2)\sum a_{ij}(y_i-y_i^0)(y_j-y_j^0)] \sim \psi_0^{-n} A^{\frac{1}{2}}(n/2\pi)^{r/2}[\psi(y)]^n; \tag{45}$$

here A is the determinant of a_{ij}. In order for this normalized $F^{(n)}$ to be generated by ψ, $[F^{(n)}]^{1/n}\to\psi$, we must take $\psi_0=1$.

From the normal approximation to $F^{(n)}$, (45), we easily compute (with an error which has the order $1/n^2$)

$$\langle y_s\rangle = y_s^0$$

$$\langle y_s y_t\rangle = y_s^0 y_t^0 + (1/n) b_{st}$$

$$\langle y_s y_t y_u\rangle = y_s^0 y_t^0 y_u^0 + (1/n)(b_{st}y_u^0 + b_{su}y_t^0 + b_{tu}y_s^0), \tag{46}$$

where the matrix b_{st} is the reciprocal of a_{ij}. We see that the second moments of $F^{(n)}$ are closely related to the matrix of second derivatives of ψ. Thus the statement that the essentials of ψ are contained in y^0 and a_{ij} alone is reflected in the statement that $F^{(n)}$ is adequately described by its first and second moments, or alternatively, by its first two marginal distributions $F_1(s)$ and $F_2(s,t)$. By the way of contrast, for the independent distribution, ψ is (precisely) determined by the maximizing coordinate y^0, and $F^{(n)}$ is to sufficient accuracy known in terms of the single marginal distribution, F_1. Of course, *to lowest order*, even the arbitrary peaked distribution is within an error $1/n$ fully determined by F_1.

We have just observed that, for a smooth function $\psi(y)$ with a single maximum, we required $\psi_0=1$ to allow $F^{(n)}$ to be normalized. It is easy to verify that this is always so; the maximum value of ψ must be unity no matter what the point set on which it is attained. The proof is trivial, and we shall omit it. Moreover, we saw that it was necessary to introduce a normalization constant c_n such that

$$F^{(n)}=c_n[\psi(y)]^n. \tag{47}$$

To obtain the exact independent distribution (33), we must even take c_n to be a function of y. The sequence $F^{(n)}$ is, of course, not uniquely defined by $\psi(y)$. It *is* unique provided we restrict c_n to be a constant; but, in general, we can construct many sequences $F^{(n)}$ from a given generating function by choosing $C_n(y)$.

An interesting problem arises if $\psi(y)$ takes its maximum at exactly two points, y^0 and y^1. The distribution is doubly peaked with comparable contributions from each maximum provided that the second derivatives are not degenerate. However, if, for example, $\psi(y)$ has a corner at $y=y^1$, then the normalization at this point is $c_n\sim n^r$ instead of $c_n\sim n^{r/2}$ at the smooth point. In this case, the distribution $F^{(n)}$ would be peaked around y^0 even though ψ has two equal maxima.

6. SUPERPOSITION

To easily study refinements of the low-order chaos result, we restrict our attention to the case of smooth $\psi(y)$ for which the normal approximation (45) is

valid. We recall (40) and (41) and introduce $y=k/n$ into (30) to obtain

$$F_3(s,t,u)=[(1-1/n)(1-2/n)]^{-1}$$
$$\times\begin{cases}\langle y_s y_t y_u\rangle, & s\neq t\neq u\\ \langle y_s^2 y_u\rangle - n^{-1}\langle y_s y_u\rangle, & s=t\neq u.\\ \langle y_s^3\rangle - (3/n)\langle y_s^2\rangle + (2/n^2)\langle y_s\rangle, & s=t=u.\end{cases} \quad (48)$$

It is an easy computation to obtain from (46)

$$\langle y_s y_t\rangle = \langle y_s\rangle\langle y_t\rangle + O(1/n), \quad (49)$$

$$\langle y_s y_t y_u\rangle = \frac{\langle y_s y_t\rangle\langle y_s y_u\rangle\langle y_t y_u\rangle}{\langle y_s\rangle\langle y_t\rangle\langle y_u\rangle} + O(1/n^2). \quad (50)$$

Substitution of these values into (41) and (48) immediately yields the superposition formula (8), ignoring only terms of order $1/n^2$. It is worth remarking that substitution into (46) and then (41) of the exact expressions b_{st} for the independent distribution (33), viz.,

$$b_{st}=Y_{st}-\langle y_s\rangle\langle y_t\rangle, \quad (51)$$

where Y_{st} is the diagonal matrix

$$Y=\begin{pmatrix}\langle y_1\rangle & & & \\ & \langle y_2\rangle & & \\ & & \cdots & \\ & & & \langle y_r\rangle\end{pmatrix}, \quad (52)$$

yields chaos only when terms $O(1/n^2)$ are dropped. The reason is that the multinomial distribution is approximated by the normal distribution only to this order.

The application of these probabilistic results to statistical mechanics is not clear. There is, of course, the possibility mentioned earlier that the statistics overwhelm the dynamics thereby yielding results of very widespread validity. More precisely, in any situation which is approximately chaotic and in which the deviation has the order $1/n$, it would be very surprising if the superposition formula did not hold. There are many cases in equilibrium statistical mechanics which do not exhibit a distant correlation of this magnitude. On the other hand, it may be that stronger statistical results can be proved. In any event, we have seen that the superposition hypothesis has a purely mathematical significance, possibly independent of its use in statistical mechanics.

Theory of "Melting" of the Helical Form in Double Chains of the DNA Type*

BRUNO H. ZIMM†

Department of Chemistry, Yale University, New Haven, Connecticut

(Received May 13, 1960)

Previous theoretical treatments of the transition between the helical and random forms of the desoxyribose nucleic acid (DNA) molecule are extended to include formally the explicit consideration of the dissociation into two separate chains and the consideration of the effects of the ends of the chains. An approximate form for the fraction of base pairs that are bonded is obtained in terms of two parameters, a stability constant for base pairing and a constant representing the interaction of adjacent base pairs. The matrix method of statistical mechanics proves to be adaptable to this problem. Some numerical examples are worked out for very long molecules, for which case it is found that the effect of concentration is small.

SINCE Watson and Crick[1] established that the native molecule of desoxyribose nucleic acid (DNA) is a double-chain helix, it has been commonly supposed that the denaturation induced by heat or other agents corresponds to the breakdown of the helical structure followed by the separation of the two chains.[2] Several theoretical treatments of the first part of this process have already appeared.[3–5] These theories are restricted to long chains, the effects of the ends being neglected. In this paper the matrix method of statistical mechanics[6–9] is adapted to the DNA problem, reproducing the previous results in a more rigorous manner and including the end effects. We have already used the matrix method successfully on the simpler helix-coil transition of polypeptide chains.[10,11] The extension to the DNA case requires going to very large, practically infinite, matrices because of the long-range effects present in DNA, and the demonstration that the use of such matrices does not lead to impossible complications may be of some interest in itself.

The native DNA molecule appears to consist of two complementary chains of the same length, each in turn consisting of a sequence of mononucleotides. The heterocyclic bases of the nucleotides of one chain are presumed to be hydrogen bonded to the complementary bases of the other chain.[1] There are four different bases, adenine, thymidine, guanine, and cytidine, and the analytical and structural evidence suggests that adenine bonds effectively only to thymidine and guanine only to cytidine. Hence, unless the opposing bases of the two chains are matched properly, the bonding does not occur. (In this respect native DNA differs from its synthetic analogs, where all the bases of one chain are the same.) We shall assume that the two chains can be matched in only one way, with each base in register with the complementary base of the other chain. Our problem is then that of the formation of n bonded pairs from two complementary chains of n bases each.

We assume, for simplicity, that all base pairs are bonded with hydrogen bonds of the same strength. (This assumption is not quite correct, since Marmur and Doty[12] have shown that the melting temperatures of the pure adenine-thymidine and guanine-cytidine polymers appear to differ by about 50°C. Consequently there must be a small difference between the bond energies of the two forms.)

In this paper an explicit treatment of the molecule as a polyelectrolyte is not contemplated. To a considerable extent, the energetic interactions of the negative charges on the phosphate groups can be lumped together with the other interactions between the bases into one stability parameter for pairing, which then becomes dependent upon the ionic strength of the solution. The titration curve of the bases is affected by these interactions, but as its discussion involves several unclear points concerning the attachment of the hydrogen ions, and as Steiner has recently published[13] a substantial investigation of it, further mention here is omitted. Electrostatic interactions probably play only a minor role in the stability of the helix in solutions with substantial concentrations of added salt.[14]

We assume that the base pairs can exist in any of three states, bonded in the helix, unbonded in free chains, or in unbonded sequences between two helical portions. In the latter state the sequence of j unbonded

* Contribution No. 1620 from the Sterling Chemistry Laboratory, Yale University, New Haven, Connecticut.

† Visiting Professor at Yale in the spring of 1960. Permanent address, School of Science and Engineering, University of California, La Jolla, California.

[1] J. D. Watson and F. H. C. Crick, Nature **171**, 738 (1953).

[2] See, for example, the review by E. P. Geiduschek and A. Holtzer, Advances in Biol. and Med. Phys. **6**, 490 (1958).

[3] S. A. Rice and A. Wada, J. Chem. Phys. **29**, 233 (1958).

[4] J. H. Gibbs and E. A. DiMarzio, J. Chem. Phys. **30**, 271 (1959).

[5] T. L. Hill, J. Chem. Phys. **30**, 383 (1959).

[6] H. A. Kramers and G. H. Wannier, Phys. Rev. **60**, 252, 263 (1941).

[7] E. W. Montroll, J. Chem. Phys. **9**, 706 (1941).

[8] E. N. Lasettre and J. P. Howe, J. Chem. Phys. **9**, 747 (1941).

[9] T. L. Hill, *Statistical Mechanics* (McGraw-Hill Book Company, Inc., New York, 1956).

[10] B. H. Zimm and J. K. Bragg, J. Chem. Phys. **28**, 1246 (1958); **31**, 526 (1959).

[11] B. H. Zimm, P. Doty and K. Iso, Proc. Natl. Acad. Sci (U.S.) **45**, 1601 (1959).

[12] J. Marmur and P. Doty, Nature **183**, 1427 (1959).

[13] R. F. Steiner, J. Chem. Phys. **32**, 215 (1960).

[14] This is not true in solutions of low ionic strength. See, for example, L. F. Cavalieri, M. Rosoff and B. H. Rosenberg, J. Am. Chem. Soc. **78**, 5239 (1956).

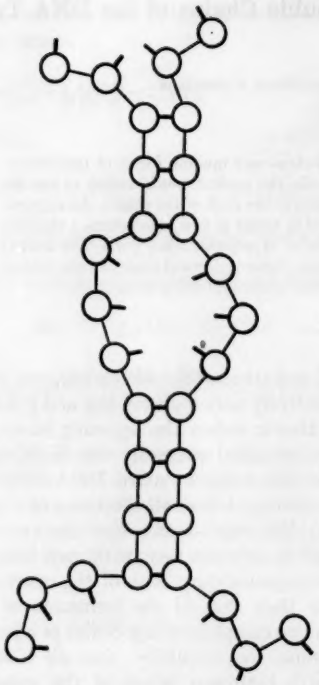

FIG. 1. Schematic representation of a state of the DNA molecule, showing the free chains at the ends, the helical portions (represented as untwisted ladderlike structures for simplicity), and the unbonded bases between helical portions.

base pairs forms a ring of $2j+2$ links, that portion of a chain between two successive bases being considered as a link. By "free chains" we mean complementary portions of the complete double molecule that are either unattached to each other, or are attached at one end only, so that the internal degrees of freedom of the unbonded base pairs are unrestricted by the bonding of the other pairs. See Fig. 1.

The two complementary chains may be unattached to each other except by the bonding of the base pairs, so that when the latter is dissolved the chains separate completely. It is also possible in some cases that an occasional bond of a more permanent nature holds the two together even when the base pairs are not themselves bonded.[15] It is very little extra work to enlarge the formalism to consider examples of both cases. In the first case the results depend on the concentration of the solution, since a bimolecular reaction is involved. We first set up the formalism for handling this case.

Consider a solution of DNA chains of two complementary types, a and b, but of equal length, and which can pair to form double-stranded molecules, ab. Let the molar concentrations be c_a, c_b and c_{ab}, respectively. Then the equilibrium constant K for the pairing reaction is

$$K=c_{ab}/c_ac_b. \tag{1}$$

(The solution is assumed to be sufficiently dilute so that interactions between the molecules, other than pairing, are negligible.) Let the concentrations of a and b be equal, and let the total concentration, free and paired, of a or b be equal to c,

$$c=c_{ab}+c_a=c_{ab}+c_b. \tag{2}$$

Then we have

$$c_a=c_b=[-1+(1+4Kc)^{\frac{1}{2}}]/2K. \tag{3}$$

If θ be the fraction of bases in the ab molecules that are paired, and Θ the fraction of all bases that are paired, we have

$$\Theta=c_{ab}\theta/c=\theta[2Kc+1-(1+4Kc)^{\frac{1}{2}}/2Kc]. \tag{4}$$

Our problem is to derive an expression for the equilibrium constant, K, and the fraction, θ, in terms of elementary quantities. By a well-known result of statistical mechanics,[16] K is related to the partition functions Q_a, Q_b, Q_{ab} of the molecules a, b, and ab by the expression

$$K=VQ_{ab}/Q_aQ_b. \tag{5}$$

Moreover, we shall see that the quantity θ can be derived from Q_{ab} if the dependence of the latter on the free energy of a bonded base pair is known. Hence our problem becomes that of deriving the partition functions. For this we proceed in the following way, which is an extension of the matrix method.

We consider now a single pair of complementary chains in a volume V of solvent, and call the partition function of this pair $\mathbf{Q}$, including both the paired states and the unpaired (unbonded) states. We can write $\mathbf{Q}$ formally as follows to display the distinction between the two kinds of states,

$$\mathbf{Q}=[1+(us/V)\sum_i w_i]Q_aQ_b. \tag{6}$$

Here the second term represents the paired states, so that

$$Q_{ab}=(us/V)\sum_i w_iQ_aQ_b, \tag{7}$$

while the quantity $(us/V)Q_aQ_b$ is the partition function of the two chains bonded at one pair of bases only, and the w_i are the statistical weights of states i of two chains bonded at more than one base pair. The exact meaning of *state* in this connection will be explained shortly, as will the symbols u and s.

The matrix method as commonly used involves the construction of a vector whose components are the statistical weights of the various states of a small group of segments of the chain. An operator, represented by

[15] Usually the molecular weight is unchanged on denaturation. It is only very recently that clear evidence has been obtained for the complete separation of the two chains. See M. Meselson and F. Stahl, Proc. Natl. Acad. Sci. (U.S.) **44**, 671 (1958); P. Doty, J. Marmur, J. Eigner and C. Schildkraut, *ibid.* **46**, 461 (1960).

[16] See, for example, J. E. Mayer and M. G. Mayer, *Statistical Mechanics*, (John Wiley & Sons, Inc., New York, 1940), Chap. 9.

a matrix, operates on this vector and computes the statistical weights of a new group formed by adding one segment to one end of the previous group and removing one from the other end. When this operator is used repeatedly a sufficient number of times it generates the statistical weights of all states of the whole chain, the sum of which is the partition function. In our case the group of segments must be as large as the largest rings that can be formed by unbonded sections of the two chains between bonded sections, since the free energy of a ring depends nonlinearly on the number of segments in the ring (see the following). We therefore take the size of our group to be n, the number of bases in each chain, each homologous base pair being considered to be the segment.

Since the number n is large, it might be thought that nothing is gained by applying the matrix method to this case; however, we show that it still yields a valuable result. Specifically, we find a representation of the partition function in terms of the eigenvalues of the operator, and find an equation for these eigenvalues, the secular equation, whose form is fairly simple.

Returning to the problem of defining the states of the double molecule, we find that a state is sufficiently defined if we specify only which of the base pairs are bonded and which are unbonded. Thus if we let the symbol 0 stand for an unbonded pair and the symbol 1 for a bonded pair, a state can be represented by a binary number with n digits which we call the state index. For example, the number 000$\cdots$000 represents the state in which none of the base pairs are bonded, the number 000$\cdots$001 that in which only the nth pair is bonded, and so on. (It is assumed that we have numbered the base pairs in order from one end to the other.)

We now write down a set of rules establishing the values of the statistical weights of the various states. These rules embody our model of the molecule, which is the same as T. L. Hill's[5]; we assume that the free energy of bonded base pairs involves interactions with no more than the nearest neighbors, while that of rings of unbonded base pairs depends only on the size of the ring. We use as references for the free energy those unbonded base pairs that lie in sections of chains that are "free," i.e., bonded at no more than one end, and we assume that the free energies of all such unbonded base pairs in free chains are the same, having the standard of value of zero. The free energies as such do not enter the calculation, but only exponentials of differences of them divided by kT; these are the equilibrium constants of certain elementary processes. The necessary rules for the statistical weights follow.

The statistical weight of a state whose index is a given binary number of n digits is Q_aQ_b times the product of the following factors:

(1) The factor unity for every zero that appears in the state index.

(2) The factor s to the power of the number of ones in the state index.

(3) The additional factor u/V when any ones at all appear in the state index.

(4) A factor designated by σ_j for every ring of j segments, i.e., a sequence of j zeros bounded by ones at both ends.

Some comments on these rules may be helpful. Rule (1) expresses the fact that the free energy of an unbonded segment in a free chain is taken as zero. Rule (2) implies that the free energy of a sequence of bonded segments is proportional to the number of bonded segments, except for the effects of the ends of the sequences, which are taken care of by the next two rules. The quantity s is essentially the equilibrium constant for the process of increasing a bonded sequence by one segment taken from an adjoining sequence of free segments; we shall call it the *stability constant* for bonding. Rule (3) recognizes that a great deal of freedom is lost when the two chains are first bonded together at one base pair. According to a simple interpretation of equilibrium constants,[16] u can be thought of as the volume of configuration space available to the center of mass of one member of a bonded base pair while the center of mass of the other is held fixed, and reduced further by any necessary restrictions on the internal degrees of freedom of the base when it enters the bonded state. Rule (4) admits the fact that the free energy of a ring is less than that of a free chain of the same number of segments.

In the following discussion, s is thought of as the primary independent thermodynamic variable. The factors u and σ_j are parameters that depend on the structure of the model.

We shall now explain the formal operations that produce the partition function. These do not differ in fundamentals from those commonly used in the matrix method, but because the "small" group is now as large as the entire chain, some change in point of view is necessary.

The statistical weight vector is an array of 2^n components, each of which is the statistical weight, computed according to the foregoing rules, of one of the possible states of the chain molecule of n segments, including the completely unbonded, or 000$\cdots$000 state. Consider now a sequence of such vectors, the last of which is the vector of the complete chain as already described, while the preceding ones refer to the chain increased in length by the addition of up to n hypothetical segments before first segment of the real chain. We designate these additional segments by the numbers $-n+1$ to 0, while the real segments are designated by the numbers 1 to n. The first vector of the sequence is the statistical weight vector of the segments $-n+1$ to 0; the second vector refers to segments $-n+2$ to 1; the third refers to $-n+3$ to 2, and so on up to the last, which refers to segments 1 to n.

The successive vectors are produced each from the preceding by the operation of a matrix, M, which expresses the rules (1) through (4) set down above. Since M is of the size $2^n \times 2^n$ it is hardly profitable to attempt to write it down, nor shall we find that this is necessary. The required elements are readily found from the basic rules (1) through (4) as needed.

Since the added segments are completely hypothetical, some freedom is available to us in defining their properties. This freedom allows us to choose the appropriate boundary conditions for the ends of the chain of real segments; in this article we discuss three possibilities. In the first, I, we assume that the two chains, a and b, are not connected to each other except through base pairing; this requires that the added segments be always unbonded. In the second, II, we assume that the two chains are connected by a permanent bond at one end; this is represented by requiring that the zeroth segment be always bonded. In the third, III, we assume permanent bonds at both ends; this likewise requires that the zeroth segment be bonded, as well as a further modification at the nth segment.

The statistical weight vector of the added segments, which is the initial vector of the sequence, is then the following for the three cases:

$$\text{I} \qquad (1, 0, 0, \cdots 0, 0, 0) Q_a Q_b \tag{8a}$$

$$\text{II} \qquad (0, 1, 0, \cdots 0, 0, 0) Q_a Q_b \tag{8b}$$

$$\text{III} \qquad (0, 1, 0, \cdots 0, 0, 0) Q_a Q_b. \tag{8c}$$

(Note that the first component of the vector refers to the state whose index has the value zero, i.e., 000$\cdots$ 000, while the second refers to the state whose index has the value one, i.e., 000$\cdots$001, and so on.) The scalar fractors Q_a and Q_b are to be understood as multiplying each component.

The statistical weight vector of the real segments is formed by operating n successive times with the matrix M on the initial vector as given by Eqs. (8a), (8b), or (8c). The partition function Q is the sum of those components of the statistical weight vector that are consistent with the boundary condition at n; for cases I and II these are all the elements, while for case III, in which the nth segment is required to be bonded always, the appropriate components are those whose index is odd. Thus in the three cases $\mathbf{Q}$ is given by the following matrix-vector products:

I

$$\mathbf{Q} = (1, 1, 1, \cdots 1, 1, 1) M^n (1, 0, 0, \cdots 0, 0, 0)^\dagger Q_a Q_b \tag{9a}$$

II

$$\mathbf{Q} = (1, 1, 1, \cdots 1, 1, 1) M^n (0, 1, 0, \cdots 0, 0, 0)^\dagger Q_a Q_b \tag{9b}$$

III

$$\mathbf{Q} = (0, 1, 0, \cdots 1, 0, 1) M^n (0, 1, 0, \cdots 0, 0, 0)^\dagger Q_a Q_b. \tag{9c}$$

Here the dagger sign † transposes a vector from a row to a column.

From here on the formal operations are familiar. We assume that M can be diagonalized by matrices composed of its eigenvectors. Then

$$M^n = V \cdot \Lambda^n \cdot (U \cdot V)^{-1} \cdot U, \tag{10}$$

where V is the matrix whose columns are the right-hand[17] eigenvectors of M, U the matrix whose rows are the left-hand eigenvectors of M, and Λ is the diagonal matrix whose diagonal elements are the eigenvalues of M.[17] If the eigenfunctions and eigenvalues are available, the evaluation of Eqs. (9a), (9b) and (9c) then offers little difficulty.

A right-hand eigenvector v satisfies the eigenvalue equation

$$M \cdot v^\dagger = \lambda v^\dagger, \tag{11}$$

where λ is the corresponding eigenvalue. Since the equation is homogeneous, the vector may be multiplied by an arbitrary constant; we choose this constant such that the first element of the eigenvector is unity:

$$v_{000\cdots0} = 1. \tag{12}$$

According to Eq. (11) the operator M merely multiplies each component of the eigenvector by λ. According to our previous interpretation of M its operation is more complex; it removes the first digit of the state indices and adds a new digit on the end, simultaneously synthesizing the appropriate statistical weight for each new state. By confronting these two interpretations of M with each other we determine the components of the eigenvector and derive an equation (the secular equation) for the eigenvalue. For example, the state 000$\cdots$0 is obtained from the two states 000$\cdots$0 and 100$\cdots$0 by removing the first digit and adding 0 at the end. According to rule (1), adding a 0 to the state index multiplies the corresponding statistical weight component by unity. Hence if

$$v' = M \cdot v, \tag{13}$$

then

$$v'_{000\cdots0} = v_{000\cdots0} + v_{100\cdots0}. \tag{14}$$

But by Eq. (11) v' is just λv, and $v_{000\cdots0}$ is unity by Eq. (12), hence

$$v_{100\cdots0} = \lambda - 1. \tag{15}$$

In exactly the same way we get the equation,

$$v'_{000\cdots01} = (us/V) v_{000\cdots00} + \sigma_{n-1} s v_{100\cdots00} \tag{16}$$

from which we derive $v_{000\cdots01}$:

$$v_{000\cdots01} = [(us/V) + \sigma_{n-1} s(\lambda - 1)]\lambda^{-1}. \tag{17}$$

Many of the remaining components may now be evaluated at sight by the use of the appropriate rule.

[17] We are assuming that the matrix M is unsymmetrical so that its left- and right-hand eigenvectors are different. In simple cases it is possible to symmetrize M, but there appears to be very little advantage in doing so.

For example, $v_{100\cdots01}$ is $\sigma_{n-2}s$ times $v_{100\cdots00}$, or $\sigma_{n-2}s(\lambda-1)$. With this result we can now evaluate $v_{000\cdots010}$ from $v_{000\cdots001}$ and $v_{100\cdots001}$. By repeating this process we can get the general formula for all components with a single unity and no more than $n-2$ zeros following it in the state index; this is

$$v_{0\cdots1\cdots0}=[(u/V)+(\lambda-1)\sum_{j=n-k-1}^{j=n-1}\sigma_j\lambda^{n-j-1}]s\lambda^{-k-1}, \quad (18)$$

where k is the number of zeros following the one, k less than or equal to $n-2$.

Finally, we have

$$\lambda v_{100\cdots0}=v_{110\cdots0}+v_{010\cdots0}, \quad (19a)$$

or

$$\lambda(\lambda-1)=s(\lambda-1)+[(u/V)+(\lambda-1)\sum_{j=1}^{j=n-1}\sigma_j\lambda^{n-j-1}]s\lambda^{-n+1}, \quad (19b)$$

which may be simplified to

$$(\lambda-s)(\lambda-1)=s(\lambda-1)\sum_{j=1}^{j=n-1}\sigma_j\lambda^{-j}+us/V\lambda^{n-1}. \quad (20)$$

This last is the secular equation, the solution of which gives λ. Thus we have found all the components of the right-hand eigenvector as well as the secular equation.

The left-hand eigenvector may be treated in a similar way. The eigenvalue equation is

$$u\cdot M=\lambda u. \quad (21)$$

The operation of M to the left adds a digit to the front of the state index and removes one from the back; it also introduces a factor into the statistical weight corresponding to the interaction of the factor removed and those preceding it in the state index. All components with state numbers ending in one have the same value; this follows from the fact that there are no direct interactions between digits following a one and the digits preceding it according to the rules (1) through (4). We choose the value of these components to be unity. We have, by confronting the interpretation of M with Eq. (21), the following relation:

$$\lambda u_{111\cdots11}=su_{111\cdots11}+u_{111\cdots10}. \quad (22)$$

Since $u_{111\cdots11}$ is unity, then

$$u_{111\cdots10}=\lambda-s. \quad (23)$$

All other components with state numbers ending in 10 have this same value.

In general we find that

$$u_{\cdots100\cdots0}=(\lambda-s)\lambda^{k-1}-s\sum_{j=1}^{j=k-1}\sigma_j\lambda^{k-j-1}, \quad (24)$$

where k is the number of zeros following the last unity. This formula also holds for $u_{000\cdots0}$, with k replaced by n. Alternatively, we have

$$\lambda u_{000\cdots0}=(us/V)u_{000\cdots01}+u_{000\cdots00}, \quad (25)$$

which in conjunction with Eq. (24) yields again the the secular equation, Eq. (20).

The sets of left-hand and right-hand eigenvectors are biorthogonal, that is, the product of a left-hand and right-hand eigenvector belonging to different eigenvalues vanishes. We shall need the product of the two eigenvectors belonging to the same eigenvalue. This can be written in several alternative ways, but most compactly as follows:

$$u\cdot v^{\dagger}=\lambda^{n-1}(\lambda-1)(\partial\ln\lambda/\partial\ln s)^{-1}, \quad (26)$$

where the derivative is to be evaluated from the secular Eq. (20).

We shall need certain sums over the components of v. Combinations of the relations of the type of Eqs. (14) through (19) yield the following results[18]:

$$\sum v_i=\lambda^n \quad \text{(sum over all state indices)} \quad (27)$$

$$\sum v_i=\lambda^{n-i} \quad \text{(sum over all state indices divisible by 2)} \quad (28)$$

$$\sum v_i=\lambda^{n-i-1}(\lambda-1). \quad \text{(sum over all state indices ending in } i0\text{'s)}. \quad (29)$$

We are now prepared to give the final expressions for the partition function, $\mathbf{Q}$. As a shorthand, we designate the components of the eigenvectors belonging to the kth eigenvalue, λ_k, by ${}_ku_j$ and ${}_kv_j$. Then by the use of Eqs. (10) and (26), Eq. (9a) for the case of the chains with both ends free, case I, becomes

$$\mathbf{Q}/Q_aQ_b=\sum_{k=0}^{n}\lambda_k{}^n\,{}_ku_0\sum_{j=0}^{n}{}_kv_j \quad (30a)$$

$$=(us/V)\sum_{k=0}^{n}[\lambda_k{}^{n+1}/(\lambda_k-1)^2](\partial\ln\lambda_k/\partial\ln s). \quad (30b)$$

For case II, one end tied, we have from Eq. (9b)

$$\mathbf{Q}/Q_aQ_b=\sum_{k=0}^{n}\lambda_k{}^n\,{}_ku_1\sum_{j=0}^{n}{}_kv_j \quad (31a)$$

$$=\sum_{k=0}^{n}[\lambda_k{}^{n+1}/(\lambda_k-1)](\partial\ln\lambda_k/\partial\ln s). \quad (31b)$$

For case III, both ends tied, we have from Eq. (9c)

$$\mathbf{Q}/Q_aQ_b=\sum_{k=0}^{n}\lambda_k{}^n\,{}_ku_1\sum_{j\ \text{odd}}{}_kv_j \quad (32a)$$

$$=\sum_{k=0}^{n}\lambda_k{}^n(\partial\ln\lambda_k/\partial\ln s). \quad (32b)$$

[18] We have as yet found no compact derivation of these formulas, although their simplicity suggests that one should exist.

We may note that in all cases when the chain length n is large,

$$\ln \mathbf{Q} = n \ln \lambda_0, \tag{33a}$$

where λ_0 is the largest eigenvalue. This is the result obtained by previous authors[3-5] by other methods. We shall show later that the largest eigenvalue is always greater than unity when the parameters are such that the double-chain helix is stable. In this case we may neglect the last term of Eq. (20) and let the limit of the summation index go to infinity; the equation that results is identical with that obtained by Hill[5] by the so-called method of the maximum term.[19] Thus the equation for the nth root of the partition function, obtained by the maximum term method, is actually a close approximation to the secular equation of the appropriate matrix, the n eigenvalues of which give the partition function exactly.[20]

The melting of the polypeptide helices previously discussed[4,5,10] may be treated as a special case of the foregoing. We merely let all the σ_j be the same quantity σ for j greater than or equal to a certain minimum value μ. We let us/V equal this quantity also. Then the secular equation becomes

$$(\lambda - s)(\lambda - 1) = \sigma s\left[(\lambda - 1)\sum_{j=\mu}^{n-1} \lambda^{-j} + \lambda^{-n+1}\right]$$

$$= \sigma s \lambda^{-\mu+1}. \tag{33b}$$

This is identical with that previously obtained.[10]

We now turn to an attempt to evaluate the partition function in terms of quantities that may be related to experiment. This attempt must be admitted to be preliminary, as we have not had time to investigate thoroughly the smaller eigenvalues, roots of Eq. (20), which play a significant role when n is small, and at the present time insufficient information exists about the flexibility of the chains to allow anything but a rough guess concerning the values of the σ_j for small j. We hope, however, that even a preliminary attempt may have some value as the basis of future advances.

Following Rice and Wada[3] and Gibbs and DiMarzio,[4] we estimate the σ_j with the use of the theory of rings of random-flights chains, as first applied by Jacobson and Stockmayer.[21] According to the latter, the partition function of a ring of m links differs from that of a chain of m links by a factor that depends on m as $m^{-\frac{1}{2}}$. Consider then the following two structures, x and y:

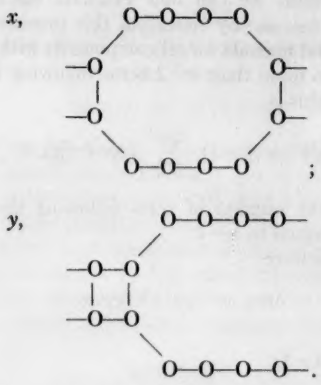

In x we have a ring of ten links (the two bonds between the chains are assumed to be rigid), while in y we have a ring of two links and two free chains with a total of eight links. The contribution of x to the statistical weight is $\sigma_4 s^2$; that of y, s^2. According to Jacobson and Stockmayer, however, the ratio of the contributions of the two structures is $(10/2)^{-\frac{1}{2}}$, or $5^{-\frac{1}{2}}$. In general, then σ_j should contain the factor $(j+1)^{-\frac{1}{2}}$. In addition, the two cross-bonds, i.e., base pairs, in y are in contact, while in x they are separated; this suggests that we should introduce another factor, σ_0, related to the free energy of stacking the base pairs on top of each other, ϵ.

$$\sigma_0 = \exp(-\epsilon/kT). \tag{34}$$

The quantity σ_j is then approximated by

$$\sigma_j = \sigma_0 (j+1)^{-\frac{1}{2}}. \tag{35}$$

We say "approximated" since the links in DNA contain at the most five flexible bonds while the Jacobson-Stockmayer formula applies rigorously only when the number of bonds is large; furthermore, we have neglected the effects of the considerable size of the base pairs themselves. Hence, this approximation is of questionable validity for small values of j. For large values of j, however, where the number of links becomes large, the approximation should be quite good.

The secular equation now assumes the form

$$(\lambda - s)(\lambda - 1)$$

$$= \sigma_0 s\left[(\lambda - 1) g_{n-1}(\lambda) + (us/V)\lambda^{-n+1}\right], \tag{36}$$

where

$$g_{n-1}(\lambda) = \sum_{j=1}^{n-1} \left[(j+1)^{\frac{1}{2}} \lambda^j\right]^{-1}. \tag{37}$$

This equation frequently has a root λ_0 greater than unity. In this case the last term on the right of Eq. (36) may be neglected, and $g_{n-1}(\lambda)$ replaced by $g_\infty(\lambda)$, where the upper limit of the summation index has been allowed to go to infinity. Then the secular equation

[19] We refer to Hill's Eq. (21). To make the identification, we may equate the symbols in the following way, Hill's first and ours second, $z^2 = \sigma_1$, $p^2 = \lambda^{-1}$, $q = s/\lambda$, $x_{ii} = \sigma_{i+1}/\sigma_1$, $y = 1$. The quantity q is the solution of his Eq. (20) that we obtain by letting $j_a = 1$, $s^2 = s$.

[20] Note however, that the approximate form of Eq. (20) obtained by omitting the last term is good only for the largest eigenvalue, since if λ is equal to or less than one the last term is not negligible.

[21] H. Jacobson and W. Stockmayer, J. Chem. Phys. **18**, 1600 (1950).

appears as

$$\lambda - s = \sigma_0 s g_\infty(\lambda). \tag{38}$$

The function $g_\infty(\lambda)$ is related to certain functions discussed by C. Truesdell,[22] $\phi(x, s)$. In fact, $g_\infty(\lambda) = \lambda\phi(\lambda^{-1}, \frac{3}{2}) - 1$. The functions $\phi(x, s)$ are tabulated by Truesdell, and limiting forms at small and large x are given. From these we get the following:

$$g_\infty(\lambda) = 1.612 - 3.545(\lambda-1)^{\frac{1}{2}} + 4.072(\lambda-1) + \cdots$$

$$g_\infty(\infty) = 0. \tag{39}$$

The left- and right-hand sides of Eq. (38) are plotted schematically in Fig. 2. We can see at once that the equation has a remarkable behavior; there is a root greater than unity only when the parameter s is greater than a certain critical value, s_c, given by

$$s_c = 1/(1+1.612\sigma_0). \tag{40}$$

Therefore Eq. (38) is a good approximation only if s is greater than s_c.

Let us assume for the moment that s is greater than s_c and λ_0 is appreciably greater than any of the other roots, so that $\mathbf{Q}$ is effectively given for long chains by λ_0 alone according to Eq. (33). Then θ, the fraction of base pairs that are hydrogen bonded, is given by[4,5,10]

$$\theta = \partial \ln\lambda_0/\partial \ln s = 1/[1 - \sigma_0 s g'(\lambda_0)], \tag{41}$$

where $g'(\lambda)$ is the derivative of $g_\infty(\lambda)$ with respect to λ, and is given by the formula

$$g'(\lambda) = \phi(\lambda^{-1}, \tfrac{3}{2}) - \phi(\lambda^{-1}, \tfrac{1}{2}). \tag{42}$$

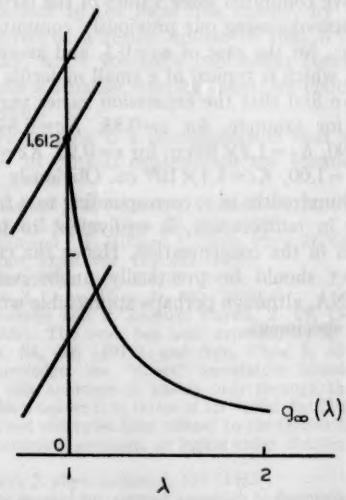

FIG. 2. The two sides of the approximate form of the secular equation, $(\lambda - s)/\sigma_0 s = g_\infty(\lambda)$. The three straight lines representing the left side of this equation are, reading in order from the top down, for the cases of $s < s_c$, $s = s_c$, and $s > s_c$.

[22] C. Truesdell, Ann. Math. **46**, 144 (1945).

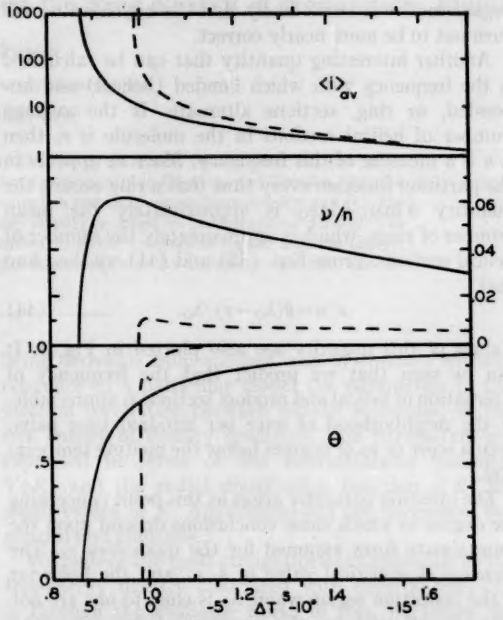

FIG. 3. The dependence of θ, the fraction of the base pairs hydrogen-bonded, of ν/n, the frequency of alternation of helical and unbonded sections, and of $\langle i \rangle_{Nl}$, the mean number of base pairs unbonded at each end, upon s and upon temperature. The temperature is expressed as the difference between the temperature in question and the temperature at which s is unity and is measured in °C. See text. Solid lines, $\sigma_0 = 0.1$; dashed lines, $\sigma_0 = 0.01$.

We have evaluated λ_0 graphically from plots of the type of Fig. 2 for two values of σ_0. The fraction θ was then obtained from Eqs. (41) and (42); the results are shown in Fig. 3 as a function of s. We have also tentatively related s to temperature, assuming that

$$d \ln s/dT = \Delta H/RT^2, \tag{43}$$

analogous to the polypeptide case.[10,11] The heat of melting per base pair has been measured by Sturtevant, Rice and Geiduschek[23]; they find that it is a function of the temperature, but we may take a rough mean value as 5 kcal per base pair.

It can be seen that the sharpness of the transition depends markedly on the value of the "stacking parameter," σ_0. The experimentally observed transitions in good DNA samples seem to occur within one or two degrees centigrade, or intermediate between our two curves. This would imply that the stacking energy, ϵ, from Eq. (34), is between 1.5 and 3 kcal per base pair. Since the experimental curves have become continually sharper as more homogeneous preparations of DNA have been obtained from simpler and simpler

[23] J. M. Sturtevant, S. A. Rice, and E. P. Geiduschek, Discussions Faraday Soc. **25**, 138 (1958).

organisms,[12,24] it seems likely that the higher value will turn out to be more nearly correct.

Another interesting quantity that can be calculated is the frequency with which bonded (helical) and unbonded, or ring, sections alternate. If the average number of helical sections in the molecule is ν, then ν/n is a measure of this frequency. Since σ_0 appears in the partition function every time that a ring occurs, the quantity $\partial \ln\lambda_0/\partial \ln\sigma_0$ is approximately the mean number of rings, which is approximately the number of helical sections. From Eqs. (38) and (41) we then find that

$$\nu/n=\theta(\lambda_0-s)/\lambda_0. \tag{44}$$

Values of this quantity are also plotted in Fig. 3. It can be seen that we predict that the frequency of alternation of helical and random sections is appreciable, in the neighborhood of once per hundred base pairs, even a score or so of degrees below the melting temperature.

The question naturally arises at this point concerning the degree to which these conclusions depend upon the approximate form assumed for the quantities σ_j. The presence of a critical value of s, s_c, and the behavior in the transition region where λ_0 is close to one are not seriously affected by the approximations, since the function $g_\infty(\lambda)$ in this region is determined mainly by the terms with large j, for which the approximations are good. However, when θ approaches unity the mean size of the rings becomes small, so that the result depends upon the small values of j for which the approximations are quantitatively poor.[25]

It is interesting to consider also the situation at the free ends of a long double chain. If the chain is long enough, the relative statistical weights of any state are proportional to the values of the corresponding components of the right-hand eigenvector associated with λ_0. Since the sum of all these components is λ_0^n, the probability of any state is the value of the component divided by λ_0^n. For example, we find from Eq. (29) that the total probability of all states that end in just i0's is

$$P(i,0)=(\lambda_0-1)\lambda_0^{-i-1}. \tag{45}$$

The mean number of unbonded base pairs at the end of the long molecule $\langle i\rangle_{\infty}$, is

$$\langle i\rangle_{\infty}=\sum_{i=1}^{\infty} iP(i,0)=1/(\lambda_0-1). \tag{46}$$

Since λ_0 is close to one in the transition region, this mean number of free bases at the end may be quite appreciable. Its dependence on s is shown in Fig. 3.

The foregoing discussion of the end effect also applies to the polypeptide case, for which a less accurate discussion was given earlier.[4,10] The previous treatments were equivalent to replacing λ_0 in the above formulas by s, its approximate value at large s.

Finally we return to the question of the effect of concentration on the dissociation of the two chains. What follows applies only to case I, in which it is actually possible for the chains to separate completely. We have seen that general considerations tell us that **Q** must be of the form of Eq. (6) for this case; that is, it must contain both a term independent of volume and one that varies as $1/V$. Since we have seen that λ_0 is independent of V, the first term of the expression for **Q** in terms of the eigenvalues, Eq. (30b), varies as $1/V$. Thus we have by Eq. (7) an expression for Q_{ab} that is good as long as the smaller eigenvalues can be neglected,

$$Q_{ab}=Q_aQ_b(us/V)\lambda_0^{n+1}(\lambda_0-1)^{-2}d\ln\lambda_0/d\ln s. \tag{47}$$

From this we immediately find that the dimensionless quantity, Kc, is

$$Kc=cus\lambda_0^{n+1}(\lambda_0-1)^{-2}d\ln\lambda_0/d\ln s. \tag{48}$$

We have computed some values of the latter part of this expression, using our previously computed values of λ_0, etc., for the case of $\sigma_0=0.1$, and assuming that $n=1000$, which is typical of a small molecule of native DNA. We find that the expression varies very rapidly with s; for example, for $s=0.88$, $Kc=0.84\times10^6$ cu; for $s=0.90$, $Kc=1.2\times10^9$cu; for $s=0.95$, $Kc=1.3\times10^{22}$ cu; for $s=1.00$, $Kc=1.1\times10^{38}$ cu. Obviously a change of a few hundredths in s, corresponding to a fraction of a degree in temperature, is equivalent to factors of thousands in the concentration. Hence the concentration effect should be practically unobservable with native DNA, although perhaps appreciable with highly degraded specimens.

[24] P. Doty, J. Marmur and N. Sueoka, in *Structure and Function of Genetic Elements*, Brookhaven Symposia in Biology, **12**, (1959).

[25] The value of σ_0 depends also on the validity of the Stockmayer-Jacobson approximation for the ring of two links, since all other rings are compared to this as a standard.

THE JOURNAL OF CHEMICAL PHYSICS VOLUME 33, NUMBER 5 NOVEMBER, 1960

Density Correlations, Critical Opalescence, and the Free Energy of Nonuniform Fluids

MARSHALL FIXMAN

Mellon Institute, Pittsburgh, Pennsylvania

(Received April 1, 1960)

We show the equivalence of three prior approaches to the theory of critical opalescence: (a) the direct study of the long range behavior of the radial distribution function, due to Ornstein and Zernike, (b), the indirect approach by Rocard, who obtained the local pressure in a system of nonuniform density, and (c), the indirect approach by Debye, who obtained the free-energy density in a system of nonuniform density. The molecular aspects of the theory are relieved to some extent from the confines of regular solution theory. The consequences of the Kirkwood superposition approximation, and its necessary revision, are examined.

I. INTRODUCTION

IN the recently revived literature[1-6] dealing with the free energy of nonuniform systems, studies have been made of nucleation problems, by Cahn and Hilliard, and of critical opalescence, by Debye. The regular solution theory has been used to evaluate the energy associated with density or concentration gradients, while the contribution of the latter to the entropy has been neglected, a neglect in accord with the formulas of regular solution theory. The statistical mechanical approach has not been such that it could easily be relieved of the restrictions of this particular model.

Discussions of critical opalescence have been based on an integral equation for the radial distribution function by Ornstein and Zernike,[7] on the contribution of the Laplacian of the density to the local pressure, as a device to evaluate the energy, by Rocard,[8] and on the contribution of the square of the density or concentration gradient to the local free energy, by Debye.[6] Debye arrived at a result similar to that of Ornstein and Zernike, while Rocard's conclusion (erroneously derived from a sensible starting point, we believe) was quite different.[9]

What we propose is a demonstration that all three approaches to critical opalescence are identical, one being derivable from another, and to evaluate without reference to a particular model the parameters in the position correlation between distant molecules, or the free energy of density gradients. The parameters are expressed in terms of the intermolecular potential $V(R)$ and the radial distribution function $g(R)$ for small values of R. Approximations are necessary, but general and plausible.

We believe the most straightforward approach to the free-energy density associated with density gradients is through the available work; in this, we follow the spirit of Rocard's calculation. In turn, the available work is computed by integrating the equations of motion of the fluid.

In Sec. II we obtain the equations of motion of the fluid, the point of view being macroscopic. In Secs. III and IV, it is shown that the description of distant correlations by the radial distribution function is identical with the description of density variations in macroscopically nonuniform systems. In Sec. V, the free-energy density is evaluated. In Sec. VI, the intensity of critical opalescence is computed.

II. SINGLET METHOD

The rate of change with time of the mean velocity $\mathbf{u}_1$ of a particle located at $\mathbf{R}_1$ is given, with neglect of terms in $\mathbf{u}^2$, by[10,11]

$$m\rho_1(\partial\mathbf{u}_1/\partial t)+\nabla_1(\rho_1 kT)+\int\rho_{12}\nabla_1 V_{12}d\mathbf{R}_2=F_1, \qquad (1)$$

where $\mathbf{F}_1$ is an external force acting on unit volume at $\mathbf{R}_1$ and will be suppressed until Sec. IV; ρ_1 and ρ_{12} are the singlet and pair distribution functions, respectively. The intermolecular potential V_{12} is taken to be a function only of $|\mathbf{R}_1-\mathbf{R}_2|$. We will develop Eq. (1) in a fashion similar to that used by other authors,[10,11] albeit with changes which allow a more convenient introduction of the necessary approximations.

We have taken the temperature T to be constant at all points and all t, and the variation in the distribution

[1] J. W. Cahn and J. E. Hilliard, J. Chem. Phys. **28**, 258 (1958).
[2] J. W. Cahn, J. Chem. Phys. **30**, 1121 (1959).
[3] J. W. Cahn and J. E. Hilliard, J. Chem. Phys. **31**, 688 (1959).
[4] E. W. Hart, Phys. Rev. **113**, 412 (1959).
[5] E. W. Hart, Phys. Rev. **114**, 27 (1959).
[6] P. Debye, J. Chem. Phys. **31**, 680 (1959).
[7] L. S. Ornstein and F. Zernike, Physik. Z. **19**, 134 (1918); **27**, 761 (1926). The work has been extended by L. Goldstein [Phys. Rev. **84**, 466 (1951), and Ann. Phys. **1**, 33 (1957)]. To our knowledge, the "direct" correlation function which enters into this approach is known only through the integral equation which defines it in terms of the radial distribution function. It has not otherwise been related to the intermolecular potential or canonical averages, or higher-order distribution functions.
[8] Y. Rocard, J. phys. radium **4**, 165 (1933).
[9] In a very general and elegant approach to fluctuation correlations, M. J. Klein and L. Tisza [Phys. Rev. **76**, 1861 (1949)] demonstrate that both the Ornstein-Zernike and Rocard starting points follow from the general equations of Klein and Tisza. With less justification, they assert that different approximations are involved and accept Rocard's conclusion that different formulas for critical opalescence follow.
[10] H. S. Green, *The Molecular Theory of Fluids* (Interscience Publishers, Inc., New York, 1952), p. 131.
[11] J. H. Irving and J. G. Kirkwood, J. Chem. Phys. **18**, 817 (1950).

functions, or ultimately the pressure, will be ascribed only to variations in density ρ_1. That is, isothermal conditions are supposed. In the event that these equations should be applied to some problem where adiabatic conditions are more appropriate, as to a discussion of macroscopic sound waves, the change can easily be made at the end of the calculation by replacing the operator $(\partial/\partial\rho)$, with constant T understood, by $(\partial/\partial\rho)_S$, where S is the entropy. If neither of these extreme conditions, isothermal or adiabatic, is applicable, an explicit discussion of energy transport by heat conduction is required. We shall further neglect viscous processes in the discussion of Eq. (1). For our primary interest in equilibrium calculations, such processes are irrelevant rather than neglected, but one may imagine problems, as a dynamical theory of nucleation, where the addition of a viscous stress to that which we compute would be desirable.

Equation (1) may be carried further with another definition,

$$\rho_{13}=\rho_1\rho_3 g(1,3), \tag{2}$$

where $g(1,3)$ is the radial distribution function. What is desirable now is an investigation of the difference between the equilibrium g for constant ρ_1, and the equilibrium g for ρ_1 varying with $\mathbf{R}_1$, an investigation which might be carried out precisely by ascertaining the simultaneous influence on ρ_1 and ρ_{13} of an external conservative force.[12a,b] However, to obtain the nth distribution function in the presence of such a potential requires the $(n+1)$th in the absence of the potential. For our purposes a very plausible approximation, which gives the usual pressure contribution to the local stress correctly, and is detached from any model, should suffice. We assume that

$$g(1,3)=g[13,\rho(\mathbf{R}_1+R_{13}/2)], \tag{3}$$

that is, the radial distribution function appropriate to uniform density is used, but the density is evaluated at the mid-point of the two molecules.[13]

The presence of $V(13)$ in Eq. (1) makes small values of R_{13} pertinent, and so even though ρ_1 may differ greatly from its system average ρ, $\rho=N/V$, it should still be a good approximation to write

$$g(1,3)=g(13,\rho_1)+[\partial g(13,\rho_1)/\partial\rho_1][\rho(\mathbf{R}_1+\mathbf{R}_{13}/2)-\rho_1]+\cdots \tag{4}$$

and neglect higher-order terms.

For a precise examination of the influence of variable ρ_1 on the local stress, under the approximations already employed, a Fourier resolution of ρ_1 is a more powerful tool than the Taylor expansion which we now employ. But so long as the pertinent wavelengths entering into a Fourier expansion of ρ_1 are large compared to the value of R at which $V(R)$ becomes negligibly small, as holds for the light scattering application in this work, the equivalent Taylor series converges very rapidly.

In Eqs. (2) and (4), put

$$\rho_3=\rho(\mathbf{R}_1+\mathbf{R}_{13})=\sum_0^\infty\frac{(\mathbf{R}_{13}\cdot\nabla_1)^i}{i!}\rho_1 \tag{5}$$

$$\rho(\mathbf{R}_1+\mathbf{R}_{13}/2)=\sum_0^\infty\frac{1}{2^i i!}(\mathbf{R}_{13}\cdot\nabla_1)^i\rho_1. \tag{6}$$

Terms of order higher than $i=3$ will be suppressed in Eqs. (5) and (6). With Eqs. (4), (5), and (6), the integral in Eq. (1) becomes

$$\int\rho_{13}\nabla_1 V(13)\,d\mathbf{R}_3=-\rho_1\int V'(R)\mathbf{e}[\sum_0^\infty(i!)^{-1}(\mathbf{R}\cdot\nabla_1)^i\rho_1]\times[g(R,\rho_1)+(\partial g(R,\rho_1)/\partial\rho_1)\sum_1^\infty(2^i i!)^{-1}(\mathbf{R}\cdot\nabla_1)^i\rho_1]\,d\mathbf{R}, \tag{7}$$

where

$$\mathbf{R}=R\mathbf{e}$$

$$V'(R)=\partial V(R)/\partial R. \tag{8}$$

An average over the orientation of $\mathbf{R}$, that is, over $\mathbf{e}$, is as far as Eq. (7) can be carried without specific approximations to the short-range behavior of $g(R)$. We require

$$\langle\mathbf{e}\rangle=0,$$

$$\langle\mathbf{ee}\rangle=\mathbf{e}_i\mathbf{e}_i/3=\mathbf{1}/3,$$

where the $\mathbf{e}_i$ are unit vectors along three Cartesian axes, and $\mathbf{1}$ is the idemfactor, and summation over repeated indices, $i=1, 2, 3$ is implied. Also

$$\langle\mathbf{eee}\rangle=0,$$

$$\langle\mathbf{eeee}\rangle=(\mathbf{e}_i\mathbf{e}_i\mathbf{e}_j\mathbf{e}_j+\mathbf{e}_i\mathbf{e}_j\mathbf{e}_i\mathbf{e}_j+\mathbf{e}_i\mathbf{e}_j\mathbf{e}_j\mathbf{e}_i)/15.$$

The nonvanishing operators in Eq. (7) consequently have the following averages:

$$\langle\mathbf{e}(\mathbf{e}\cdot\nabla_1)\rangle=\tfrac{1}{3}\nabla_1,$$

$$\langle\mathbf{e}(\mathbf{e}\cdot\nabla_1)^3\rangle=\tfrac{1}{5}\nabla_1\nabla_1^2, \tag{9}$$

and therefore

$$\int\rho_{13}\nabla_1 V(13)\,d\mathbf{R}_3=-(\rho_1/3)\int RV'[g+(\rho_1/2)\partial g/\partial\rho_1]\,d\mathbf{R}\nabla_1\rho_1-(\rho_1/3!5)\int R^3V'[g+(\rho_1/8)\partial g/\partial\rho_1]\,d\mathbf{R}\nabla_1\nabla_1^2\rho_1+\cdots, \tag{10}$$

[12] (a) J. K. Percus and G. J. Yevick, Phys. Rev. **110**, 1 (1958). (b) J. Yvon, Nuovo cimento Suppl. **9**, 144 (1958).

[13] An alternative approximation would be to choose the density in Eq. (3) as $(\rho_1+\rho_2)/2$. The only effect on the calculation would be to change slightly the definition of β in Eq. (27); the coefficient of $\rho(\partial g/\partial g)$ in the numerator would be changed from $\frac{1}{8}$ to $\frac{1}{3}$.

with suppression of higher-order derivatives and terms in $(\partial g/\partial\rho)\nabla(\nabla\rho)^2$, which enter only into the correction to the usual pressure term. As the correction terms are completely consistent only when the fractional variation of ρ_1 from ρ is small, we shall take the coefficient of $\nabla_1\nabla_1^2\rho_1$, in Eq. (10), to be independent of $\mathbf{R}_1$.

The first term on the right-hand side of Eq. (10) may be written more simply with the molecular expression for the local pressure P_1, the pressure in a uniform system of density[14] ρ_1:

$$P_1=\rho_1 kT-(\rho_1^2/6)\int RV'g\,d\mathbf{R}, \tag{11}$$

$$\partial P_1/\partial\rho=kT-(\rho_1/3)\int RV'[g+(\rho_1/2)\partial g/\partial\rho_1]\,d\mathbf{R}. \tag{12}$$

This substitution makes the first term on the right-hand side of (10)

$$[\partial(P_1-\rho_1 kT)/\partial\rho_1]\nabla_1\rho_1=\nabla_1(P_1-\rho_1 kT). \tag{13}$$

Substitution of (10) and (13) into (1) yields

$$m\rho_1(\partial\mathbf{u}_1/\partial t)$$
$$+\nabla_1\left\{P_1-(\rho/30)\int R^3V'[g+(\rho/8)\partial g/\partial\rho]\,d\mathbf{R}\nabla_1^2\rho_1\right\}=0. \tag{14}$$

Further discussion of (14) will be postponed until a corresponding development of the pair distribution function is made.

III. DOUBLET METHOD

Here we will keep in mind only an application to critical opalescence, to which end the radial distribution function in a stationary fluid with uniform singlet density is required. The radial distribution function is related to the triplet correlation function $g^{(3)}(1, 2, 3)$ through[14]

$$kT\nabla_1\ln g(12)+\nabla_1V(12)$$
$$+(\rho/g(12))\int g^{(3)}(1,2,3)\nabla_1V(13)\,d\mathbf{R}_3=0. \tag{15}$$

Application of the Kirkwood superposition approximation,[14]

$$g^{(3)}(1,2,3)=g(12)g(23)g(13), \tag{16}$$

to Eq. (15), gives a closed equation for $g(R)$. Let us anticipate, however, a result we find, that the superposition approximation will not yield an infinite compressibility at the critical point [or, more precisely, Eqs. (12) and (31), both valid if the correct $g(R)$ is used, will under the superposition approximation be in explicit conflict at the critical point]. In order to see what changes in Eq. (16) are indicated, we point out that the great increase in the intensity of scattered light which occurs at the critical point is not to be ascribed to a great increase in $g(R)$ for small R, such being prevented by the repulsive core of the intermolecular potential,[15] but to the great extension of the range of R in which $[g(R)-1]$ is sensibly nonvanishing. Therefore, let us put $g(12)$ equal to its asymptotic value plus a perturbation $s(12)$ which may be regarded as small in magnitude but, possibly, large in range. Numerical considerations in Sec. IV will substantiate the hypothesis that $s(12)$ is small for the significant values of R_{12}. The presence of $V(13)$ in the integral in (15) makes the pertinent values of R_{13} small (to make our lexicon somewhat more precise, the values of R_{13} are small compared to λ, the wavelength of light in the medium, while the values of R_{12} cannot be taken small compared to λ). Consequently we can assume $s(23)$ to be small in

$$g(23)=1+s(23), \tag{17}$$

but $g(13)$ must be known at small R_{13}.

We now modify Eq. (16) in a way suggested by the development in Sec. II. The presence of a molecule fixed at $\mathbf{R}_2$ causes a nonuniform density in the vicinity of $\mathbf{R}_1$ and $\mathbf{R}_3$, even in the absence of a specification of the positions of molecules 1 and 3. We assume, then, that $g(13)$ is not to be evaluated at the constant density, but at the density at $(\mathbf{R}_1+\mathbf{R}_3)/2$, presumed to be

$$\rho g\{[(\mathbf{R}_1+\mathbf{R}_3)/2]-\mathbf{R}_2\}=\rho+\rho s(\mathbf{R}_{12}-\mathbf{R}_{13}/2). \tag{18}$$

Thus we suggest using in Eq. (15), not Eq. (16), but, in general[16] in Eq. (15),

$$g^{(3)}(1,2,3)=g(12)g(23)\{g(13)+\rho(\partial g(13/\partial\rho)$$
$$\times[g(\mathbf{R}_{12}-\mathbf{R}_{13}/2)-1]\},$$

or, for R_{12} large,

$$g^{(3)}(1,2,3)=[1+s(12)][1+s(23)]$$
$$\times\{g(13)+\rho(\partial g(13/\partial\rho)s(\mathbf{R}_{12}-\mathbf{R}_{13}/2)\}. \tag{19}$$

The consequences of the usual assumption may be ascertained at the end of the calculation by setting equal to zero terms containing a factor $\partial g/\partial\rho$. With (19) and with neglect of $V(12)$ in (15), as R_{12} is large, (15) becomes

$$kT\nabla_1 s(12)+\rho\int\nabla_1V(13)[1+s(23)][g(13)$$
$$+\rho(\partial g(13)/\partial\rho)s(\mathbf{R}_{12}-\mathbf{R}_{13}/2)]\,d\mathbf{R}_3=0. \tag{20}$$

[14] T. L. Hill, *Statistical Mechanics* (McGraw-Hill Book Company, Inc., New York, 1956).

[15] This remark on the nature of $g(R)$ near the critical point is due to B. H. Zimm [J. Chem. Phys. **19**, 1019 (1951)].

[16] The possibility that Eq. (19) might yield a significant improvement in the equation of state resulting from the superposition approximation is under investigation.

We now expand s, a function only of the magnitude of its argument, around R_{12}. Put $\mathbf{R}_{12}=\mathbf{r}$; $\mathbf{R}_{13}=\mathbf{R}$.

$$s(23)=s(\mathbf{R}_{12}-\mathbf{R}_{13})=\sum_0^\infty (i!)^{-1}(\mathbf{R}\cdot\nabla_1)^i s(r), \quad (21)$$

$$s(\mathbf{R}_{12}-\mathbf{R}_{13}/2)=\sum_0^\infty (2^i i!)^{-1}(\mathbf{R}\cdot\nabla_1)^i s(r). \quad (22)$$

The substitution of the expansions into Eq. (20), and an average over the orientations of $\mathbf{R}$ as in Sec. II, yields for the integral term in (20)

$$-(\rho/3)\int RV'[g+(\rho/2)(\partial g/\partial\rho)]d\mathbf{R}\nabla_1 s(r)$$

$$-(\rho/3!5)\int R^3V'[g+(\rho/8)(\partial g/\partial\rho)]d\mathbf{R}\nabla_1\nabla_1^2 s(r)+\cdots. \quad (23)$$

The use of Eq. (12) in (23), and substitution of the result into Eq. (20) yields

$$\nabla_1\Big\{(\partial P/\partial\rho)s(r)-(\rho/30)\int R^3V' \times[g+(\rho/8)(\partial g/\partial\rho)]d\mathbf{R}\nabla_1^2 s(r)\Big\}=0, \quad (24)$$

where P is the pressure at a density ρ.

IV. COMPARISON

A. Comments

It is seen from a comparison of Eq. (24) and Eq. (14) that the macroscopic concepts embodied in Eq. (12) produce the same equation as does a direct examination of the radial distribution function. To make the similarity between Eqs. (24) and (14) complete (with $\partial\mathbf{u}/\partial t=0$ for the equilibrium application), one needs only to expand P_1, in Eq. (14), in the deviation of ρ_1 from ρ,

$$P_1=P+(\partial P/\partial\rho)(\rho_1-\rho)+\cdots$$

to first order, and identify the fluctuation $\rho_1-\rho$ with the density fluctuation caused by a molecule acting on the fluid at a distant point R_2, that is, $\rho_1-\rho=\rho s(r)$. Thus one point is established, that there is no difference in principle between the Ornstein-Zernike approach to critical opalescence via the radial distribution function, and Rocard's modification of the local pressure to take into account density gradients. The difference in results we ascribe to a spurious summation by Rocard of the energies of all modes of density fluctuation, rather than just those modes which actually scatter light at the given wavelength and angle of scattering. Debye's treatment,[6] also based on semimacroscopic considerations of the energy associated with a density or concentration gradient, and also somewhat intuitive on the surface, did not involve this error and yielded results quite similar to those of Ornstein and Zernike.

If we had used the superposition approximation, Eq. (24) would be changed to the extent of elimination of $\partial g/\partial\rho$; see Eq. (12). The magnitude of the consequent error in the vicinity of the critical point can be gauged from Eq. (12). Under critical conditions, denoted by a subscript "c," $\partial P/\partial\rho$ vanishes and

$$kT_c=(\rho_c/3)\int RV'[g+(\rho_c/2)(\partial g/\partial\rho_c)]d\mathbf{R}. \quad (25)$$

Elimination of the first part of the integral with Eq. (11) yields

$$(\rho_c/2)\int RV'(\partial g/\partial\rho_c)d\mathbf{R}\Big/\int RV'g d\mathbf{R} =2(1-P_c/\rho_c kT_c)]^{-1}-1. \quad (26)$$

Since, in practice,[14] $(P_c/\rho_c kT_c)\approx 0.3$, the $\partial g/\partial\rho$ term in $\partial P/\partial\rho$ is about 30% of the g term, and has opposite sign.

B. Evaluation of $g(r)$

Now let us follow Ornstein-Zernike and Debye, and define a short-range correlation length:

$$l^2\equiv\frac{\int R^3V'[g+(\rho/8)\partial g/\partial\rho]d\mathbf{R}}{\int RV'[g+(\rho/2)\partial g/\partial\rho]d\mathbf{R}}, \quad (27)$$

where, from Eq. (12), the denominator is $(3/\rho)(kT-\partial P/\partial\rho)$. Of course, l^2 is by no means an "average" of R^2, and even a modification of the original approximation[13] to make $[g+(\rho/2)(\partial g/\partial\rho)]$ occur in both integrands in Eq. (27) would not make l^2 an average, because V' is negative at small R and positive at large R. For the vicinity of the critical point it does seem extremely probable that l is real and about equal to the usual range of intermolecular forces, because the range of R corresponding to molecular attraction, $V'>0$, must dominate if $\partial P/\partial\rho$ vanishes; see Eq. (12). We shall, at any rate, proceed on this supposition.

An integration of Eq. (24), and introduction of l^2 yields

$$(\partial P/\partial\rho)s(r)-(kT-\partial P/\partial\rho)(l^2/10)\nabla^2 s(r)=0 \quad (28)$$

or

$$\nabla^2 s(r)-\kappa^2 s(r)=0, \quad (29)$$

where

$$\kappa^2\equiv 10(\partial P/\partial\rho)/l^2(kT-\partial P/\partial\rho). \quad (30)$$

The intermolecular potential terms which are missing from Eq. (29) by virtue of our restriction to large r, could be used, in principle, to provide a source in Eq. (29). However, we will follow the simpler and probably

more reliable course of Ornstein and Zernike and evaluate the arbitrary coefficient of the solution by demanding that $(\partial P/\partial\rho)$ be correctly given in the fluctuation theory expression[14]

$$\partial P/\partial\rho = kT \Big/ \left\{1+\rho\int[g(R)-1]d\mathbf{R}\right\}. \quad (31)$$

The feasibility of this procedure is ensured by having the correct $(\partial P/\partial\rho)$ in Eq. (30). The formula (31), evaluated near the critical point, is extremely sensitive to the long-range behavior of $g(r)$.

The spherically symmetric solution of Eq. (29), appropriate to an infinite fluid, is

$$s(r) = ae^{-\kappa r}/r, \quad (32)$$

which, with Eq. (17), may be introduced into Eq. (31) to give

$$\partial P/\partial\rho = kT/(1+4\pi a\rho/\kappa^2) \quad (33)$$

and, with Eq. (30), the value of the constant a,

$$a = 5/(2\pi\rho l^3). \quad (34)$$

This value provides some justification for our assumption that $s(r)$ is small compared to unity, for[14] $\rho_c \simeq 1/l^3$, and therefore $a \simeq l$, so that $s(r)$ rapidly becomes small, though of course not negligible, as r increases.

V. ENERGY OF NONUNIFORM FLUIDS

Here we show that the contribution of a $\nabla^2\rho$ term to the pressure is equivalent to the supposition of a $|\nabla\rho|^2$ term in the free-energy density. This will be done by finding the Lagrange density for which the equation of motion, Eq. (14), is the Euler equation.[17] For small density variations to which we will now restrict ourselves, Eq. (14) appears, in the notation of Secs. III and IV, as

$$m(\partial\mathbf{u}/\partial t)+(\partial P/\partial\rho)\nabla[s(r)-\kappa^{-2}\nabla^2 s(r)]=0, \quad (35)$$

where $s(r)$ is the fractional density fluctuation.

Equation (35) differs from the usual description of compressional waves only by the presence of the $\nabla^2 s$ term. Consequently we follow, with modifications, the Lagrange formulation of compressional waves. To this end, we require the equation of mass conservation

$$\partial\rho_1/\partial t = -\nabla_1\cdot\rho_1\mathbf{u}_1$$

or

$$\partial s(r)/\partial t = -\nabla\cdot\mathbf{u}. \quad (36)$$

Upon taking the divergence of Eq. (35), we obtain, with (36), a restatement of the equation of motion,

$$-m\ddot{s}+(\partial P/\partial\rho)\nabla^2[s-\kappa^{-2}\nabla^2 s]=0. \quad (37)$$

It will be convenient to introduce a scalar potential ψ by

$$\mathbf{u}=\nabla\psi \quad (38)$$

which, being substituted into Eq. (36), gives

$$\dot{s}=-\nabla^2\psi$$

or

$$s=-\nabla^2\psi. \quad (39)$$

A suitable statement of Hamilton's principle, appropriate to the conservative forces present here, is

$$\delta\int[T(\mathbf{r},t)-\bar{U}(\mathbf{r},t)]d\mathbf{r}dt=0, \quad (40)$$

where, in the Lagrange density $(T-\bar{U})$, T is the kinetic-energy density and $\bar{U}$ the potential-energy density (actually a free-energy density in this application). The kinetic-energy density is, from Eq. (38)

$$T=\tfrac{1}{2}\rho m u^2=\tfrac{1}{2}\rho m|\nabla\psi|^2. \quad (41)$$

The usual free-energy density, for small density variations, is

$$\rho(\partial P/\partial\rho)(s^2/2).$$

However, to account for the $\nabla^2 s$ term in Eq. (35), we shall instead hypothesize

$$\bar{U}=\tfrac{1}{2}\rho(\partial P/\partial\rho)[s^2+\kappa^{-2}|\nabla s|^2], \quad (42)$$

and verify that the correct equation of motion, Eq. (37), results. We have, beginning with a variation of the kinetic energy,

$$\delta\int T d\mathbf{r}dt=\rho m\int\nabla\psi\cdot\nabla(\delta\psi)d\mathbf{r}dt$$

$$=\rho m\int\nabla^2\psi(\delta\psi)d\mathbf{r}dt$$

after integrating by parts over both $\mathbf{r}$ and t, with nonvarying boundary conditions. Or, with Eq. (39),

$$\delta\int T d\mathbf{r}dt=-\rho m\int\ddot{s}(\delta\psi)d\mathbf{r}dt; \quad (43)$$

next,

$$\delta\int\bar{U}d\mathbf{r}dt=\rho(\partial P/\partial\rho)\int[s(\delta s)+\kappa^{-2}\nabla s\cdot\nabla(\delta s)]d\mathbf{r}dt$$

$$=\rho(\partial P/\partial\rho)\int(s-\kappa^{-2}\nabla^2 s)(\delta s)d\mathbf{r}dt,$$

after an integration by parts. Substitution of Eq. (39) for δs, and an application of Green's theorem yields

$$\delta\int\bar{U}d\mathbf{r}dt=-\rho(\partial P/\partial\rho)\int[\nabla^2(s-\kappa^{-2}\nabla^2 s)](\delta\psi)d\mathbf{r}dt. \quad (44)$$

Subtracting Eq. (44) from Eq. (43), and setting the coefficient of the arbitrary variation $\delta\psi$ equal to zero, we recover Eq. (37).

The verification of the free-energy density, Eq. (42), completes our demonstration of the mathematical

[17] P. M. Morse and H. Feshbach, *Methods of Theoretical Physics* (McGraw-Hill Book Company, Inc., New York, 1953), Chap. 3.

equivalence of the approaches of Ornstein-Zernike, Rocard, and Debye.

VI. LIGHT SCATTERING

Whether the usual light scattering theory[18,19] is completely adequate in the presence of long-range correlations is a question we have not been able to answer satisfactorily. There is no doubt that as the critical point is approached sufficiently closely multiple scattering and extinction must be computed for the particular experimental geometry. But so far as we have been able to ascertain,[20] no revision of the *molecular* theory is required. The conventional formula for Rayleigh's ratio, for unpolarized incident light, and a nonpolarized detector, is

$$\mathfrak{T}=\frac{k_0^4}{(4\pi)^2}\left(\frac{\partial n^2}{\partial \rho}\right)^2\left(\frac{1+\cos^2\theta}{2}\right)\int\langle\delta_1\delta_2\rangle\frac{\sin wR}{wR}4\pi R^2dR \qquad (45)$$

for light of wavelength $(2\pi/k_0)$ in vacuum, an index of refraction n, and scattering angle θ.

$$w\equiv 2nk_0\sin(\theta/2).$$

The correlation between density fluctuations δ_1 and δ_2 at $\mathbf{R}_1$ and $\mathbf{R}_2$ [$R_{12}=R$ and

$$\delta_1=\sum\delta(\mathbf{R}_1-\mathbf{R}_i)-\rho,$$

where $\delta(\ )$ is a Dirac δ function and the sum goes over all molecules in the system], is

$$\langle\delta_1\delta_2\rangle=\rho\{\delta(\mathbf{R})+\rho[g(R)-1]\}.$$

With $s(R)=g(R)-1=(a/R)\exp(-\kappa R)$, the parameters being given in Eqs. (30) and (34),

$$\int\langle\delta_1\delta_2\rangle\frac{\sin wR}{wR}4\pi R^2dR=\rho\left[1+\frac{10}{l^2(\kappa^2+w^2)}\right]. \qquad (46)$$

In form, this result, with Eq. (45), is the same as was obtained by Ornstein-Zernike, and Debye. We have followed the more straightforward derivation of the former.

As regards the experimental test[21–23] of Eq. (46), which has not been entirely confirmatory, we would only suggest that a rejection[23] of Eq. (46) is premature in the absence of a quantitative study of multiple scattering for the experimental geometry.

[18] A. Einstein, Ann. Physik **25**, 205 (1908).
[19] M. Fixman, J. Chem. Phys. **23**, 2074 (1955).
[20] The integral (33) in footnote reference 19, which is the lowest order in the polarizability that might furnish a correction term, has been found to be negligible compared to the usual term, Eq. (45) here, even at the critical point.

[21] B. H. Zimm. J. Phys. & Colloid Chem. **54**, 1306 (1950).
[22] Chow Quantie, Proc. Roy. Soc. (London) **A224**, 90 (1954).
[23] R. Fürth and C. L. Williams, Proc. Roy. Soc. (London) **A224**, 104 (1954).

THE JOURNAL OF CHEMICAL PHYSICS VOLUME 33, NUMBER 5 NOVEMBER, 1960

Ultrasonic Attenuation in the Critical Region

MARSHALL FIXMAN

Mellon Institute, Pittsburgh, Pennsylvania

(Received April 1, 1960)

The interaction of forced sound waves with critical density fluctuations is discussed quantitatively. The nonlinear equations of motion are analyzed to distinguish three contributions to the instantaneous density and temperature variation: (1) the spontaneous fluctuations that are defined as the solution to an initial value problem, (2) the macroscopically observed sound wave which oscillates with harmonic time dependence, and (3) the result of an interaction between (1) and (2). The three contributions satisfy three equations, which are discussed separately. A completely general combination of these equations to compute ultrasonic absorption and attenuation is avoided, as the requisite thermodynamic and transport coefficients are inadequately known. Because, however, a thermal relaxation mechanism has previously been treated on the basis of an oversimplified multiphase picture of spontaneous fluctuations, the present calculations are carried to completion on the assumption that only the local heat capacity is affected by the density fluctuations. The sound wave together with the fluctuating heat capacity produce temperature fluctuations, whose relaxation is the source of the absorption.

I. INTRODUCTION

IN THE critical region a variety of systems, both simple[1] and complex,[2–8] absorb ultrasonic waves to a much greater extent than the classical loss due to viscosity or heat conductivity.[3] Neither can an explanation of the intense absorption be based on relaxation of intramolecular motions.[1] Probably the absorption is caused, in a sense to be elucidated, by the large density or composition fluctuations in a system near its critical point.

One's first thought, that the ultrasonic absorption is a scattering process, similar to critical opalescence,[9,10] is quickly rejected. The absorption of sound due to scattering from fixed inhomogeneities,[11–13] resembles the absorption of light, and varies inversely as the fourth power of wavelength when the wavelength is much greater than the size of the inhomogeneities. This condition holds for the sound waves to within controllable temperature intervals around the critical point, but the fourth-power dependence is not observed.

The anomalous absorption has been ascribed, in a qualitative way, to a time lag in the adjustment of the long-range density correlation to the variations of temperature and density induced by the sound wave, a particular application of the idea of structural relaxation.[1,14,15] Also, qualitative and quantitative treatments have been based on the possibility of heat exchange in an inhomogeneous system; the system is assumed to consist of spheres, having one set of properties, imbedded in a uniform medium of different properties.[16,17]

Except for the scattering calculations, there seem to have been no attempts to treat the interaction between fluctuations and forced sound waves in any way which is free from objections to an oversimplified pictorial model of the fluctuations. We will attempt to remedy this lack.

There are two classes of things that must be known before a calculation of the interaction between fluctuations and sound can be made. First is needed a description of the static and dynamic behavior of long wavelength fluctuations in the absence of a forced sound wave. Secondly there is needed a description of the interaction between fluctuations and sound. This division of labors, though apparently arbitrary, is extremely useful and perhaps even necessary. In the (nonlinear) equations of motion and energy transport which describe the instantaneous propagation of density and temperature variations through a fluid, there is not at first sight any distinction as to how a density or temperature variation arose, whether by spontaneous fluctuation, or at the urging of an oscillating crystal, or by an "interaction." We are free, however, to impose such a distinction, if any simplification results. Therefore, we divide the density variation,

[1] A. G. Chynoweth and W. G. Schneider, J. Chem. Phys. **20**, 1777 (1952).
[2] A. G. Chynoweth and W. G. Schneider, J. Chem. Phys. **19**, 1566 (1951).
[3] G. F. Alfrey and W. G. Schneider, Discussions Faraday Soc. No. 15, 218 (1953).
[4] D. Atack and W. G. Schneider, J. Phys. Chem. **55**, 532 (1951).
[5] V. F. Nozdrev, Soviet Phys. Acoust. **1**, 249 (1955).
[6] V. F. Nozdrev, Soviet Phys. Acoust. **2**, 209 (1956).
[7] V. F. Nozdrev and V. D. Sobolev, Soviet Phys. Acoust. **2**, 408 (1956).
[8] B. I. Kal'ianov and V. F. Nozdrev, Soviet Phys. Acoust. **4**, 198 (1958).
[9] L. S. Ornstein and F. Zernike, Physik. Z. **19**, 134 (1918); **27**, 761 (1926).
[10] M. Fixman, J. Chem. Phys. **33**, 1357 (1960), preceding article.
[11] L. Liebermann, J. Acoust. Soc. Am. **23**, 563 (1951).
[12] P. J. Westervelt, J. Acoust. Soc. Am. **29**, 199 (1957).
[13] A. B. Bhatia, J. Acoust. Soc. Am. **31**, 16 (1959).
[14] D. Sette, J. Chem. Phys. **21**, 558 (1953).
[15] K. F. Herzfeld and T. A. Litovitz, *Absorption and Dispersion of Ultrasonic Waves* (Academic Press, Inc., New York, 1959).
[16] A. B. Pippard, Phil. Mag. **42**, 1209 (1951); this concerns liquid He I slightly above the λ transition.
[17] A. Odajima, Research Inst. Appl. Elec. Hokkaido Univ., Bull. **5**, 61 (1953). We have seen only Chem. Abstracts [**48**, 7370d (1954); see also Research Inst. Appl. Elec. Hokkaido Univ., Monograph Ser. No. 4, 125 (1954); Chem. Abstracts **48**, 13305f (1954).

($\delta\rho$) say, into three parts: (a) ρ_1 the macroscopic density variation, which is ($\delta\rho$) averaged over all values of the spontaneous fluctuations. We may reasonably assume that ρ_1 is a plane spatially damped wave, as is permitted by the final equation for ρ_1. (b) ρ_0 the fluctuation in the absence of ρ_1, that is, the spontaneous fluctuation. Although ρ_0 must satisfy the equations of motion, ρ_0 is not (unlike ρ_1), periodic in time. Rather, at one time, and one time only, ρ_0 is treated as a random variable subject to a known probability distribution. At subsequent times ρ_0 must be expressed in terms of the initial conditions. (c) ρ_2 the "interaction." ρ_2 is quite simply whatever is left over in the equations of motion after there has been subtracted from the latter an equation for the periodic solution, ρ_1, and for the solution, ρ_0, to the initial value problem.

Our aims, then, will be first to arrive at equations that describe each of these three types of variation of temperature and density, and second, by an explicit evaluation of the correlations between the spontaneous fluctuations and the "interaction," as this correlation occurs in the equation for ρ_1, to obtain explicitly the absorption and dispersion. This second aim will be realized only in part. Two simplifications will be made. The fluctuations will be treated as static, and of the various thermodynamic quantities in the equations of motion which fluctuate with the local density or temperature, only the heat capacity will actually be allowed to do so. The second simplification could be eliminated fairly readily, though present knowledge of thermodynamic and macroscopic transport properties in the critical region does not seem extensive enough to warrant the work. The first simplification will be justified to some extent. Actually to use time dependent correlations would not, unless the equations hold latent surprises, involve conceptual or mathematical difficulties, but the required computations seem severe.

II. INITIAL CORRELATIONS

Here we discuss the correlation between density fluctuations at $\mathbf{R}_1$ and $\mathbf{R}_2$, of which both are observed at the same time, say $t=0$. We will also examine the correlation between the Fourier components of the density fluctuation.

Let

$$\rho(R_1)=\sum\delta(\mathbf{R}_1-\mathbf{R}_i) \tag{1}$$

be the local number density; the sum of δ functions goes over the positions of all molecules in the system. Let ρ be the average number density. Then

$$\langle[\rho(\mathbf{R}_1)-\rho][\rho(\mathbf{R}_2)-\rho]\rangle=\rho\delta(\mathbf{R}_{12})+\rho^2[g(R_{12})-1], \tag{2}$$

where $g(R_{12})$ is the radial distribution function. Now let

$$\rho(\mathbf{R})-\rho=\int\rho^{\mathbf{k}}\exp(i\mathbf{k}\cdot\mathbf{R})d\mathbf{k}, \tag{3}$$

$$\rho^{\mathbf{k}}=(2\pi)^{-3}\int[\rho(\mathbf{R})-\rho]\exp(-i\mathbf{k}\cdot\mathbf{R})d\mathbf{R} \tag{4}$$

be the Fourier resolution of the fluctuations. Equations (4), (3), and (2) give

$$\langle\rho^{\mathbf{k}}\rho^{\mathbf{k}'}\rangle=(2\pi)^{-3}\delta(\mathbf{k}+\mathbf{k}')\Big\{\rho+\rho^2\int[g(R)-1]\exp(i\mathbf{k}\cdot\mathbf{R})d\mathbf{R}\Big\}. \tag{5}$$

We have concluded,[10] in agreement with Ornstein and Zernike,[9] that the long-range density correlations that exist in the critical region may be described by

$$g(R)-1=a\exp(-\kappa R)/R, \tag{6}$$

where, in the critical region,

$$\kappa^2\approx(4\pi a\rho_c/k_BT_c)(\partial P/\partial\rho)_T, \tag{7}$$

$$a=5/(2\pi\rho_c l^3). \tag{8}$$

The critical point is indicated by a subscript c, and k_B is Boltzmann's constant. Both a and l are small distances, of the order of the range of the intermolecular potential, while κ^{-1} is an "indirect" correlation length which becomes infinitely large at the critical point.

A correlation of the same form as (6) describes composition fluctuations in the critical mixing region of a binary system,[18] and light scattering studies[18,19] give values of κ. As an order of magnitude useful in qualitative thinking, $\kappa^{-1}\approx10^{-5}$ cm if $(T-T_c)\approx1°$. Also, Eq. (7) yields the conclusion $\kappa^2\propto(T-T_c)$, for the gas phase.

From Eqs. (5) and (6), we obtain

$$\langle\rho^{\mathbf{k}}\rho^{\mathbf{k}'}\rangle=(2\pi)^{-3}\delta(\mathbf{k}+\mathbf{k}')\{\rho+4\pi a\rho^2/(k^2+\kappa^2)\} \tag{9}$$

$$\cong\delta(\mathbf{k}+\mathbf{k}')\rho^2a[2\pi^3(k^2+\kappa^2)]^{-1}. \tag{10}$$

Thus we neglect the first term on the right-hand side of Eq. (9). This neglect would be illegitimate only if κ^2 were large, so that the system is far from the critical point, or k were large, a region of k space which is used to describe small values of the argument in $g(R)$. Neither circumstance will be of interest here.

III. TIME-DEPENDENT CORRELATIONS

The present problem is: Given the magnitude of a spontaneous fluctuation at time zero, say $\rho^{\mathbf{k}}(0)\exp i\mathbf{k}\cdot\mathbf{R}$, what is the magnitude of the fluctuation, $\rho^{\mathbf{k}}(t)\exp i\mathbf{k}\cdot\mathbf{R}$, at time t? The correlation which

[18] P. Debye, J. Chem. Phys. **31**, 680 (1959).
[19] B. H. Zimm, J. Phys. & Colloid Chem. **54**, 1306 (1950).

finally enters into a time dependent problem is $\langle \rho^k(t)\rho^{k'}(0)\rangle$, or its Fourier transform over t.

Van Hove[20] has discussed precisely this problem in connection with his general treatment of slow neutron diffraction. Although our qualitative conclusion, that the relaxation time of a spontaneous fluctuation becomes infinitely large at the critical point, is the same as Van Hove's, we conclude that his arguments, derived from Landau and Placzek,[21,22] are largely irrelevant to the problem.

Let us first state the essential result of the Landau-Placzek- Van Hove treatment: A spontaneous density fluctuation decays at the same rate as does a macroscopic temperature variation allowed to relax at constant pressure. The origin of this statement seems to be the observation that, under some conditions,[23] the linearized equations of motion and energy transfer possess two approximately independent types of wave motion: (a) variations in pressure P at constant entropy S, and (b) variations in entropy (or temperature), at constant pressure. This observation, and one more, that fluctuations of S at constant P become very large at the critical point, while fluctuations of P at constant S remain small, constitute the chain of argument which is to yield the result stated.

It is, however, difficult to see how the result or the argument can be correct. The notion that a mass fluctuation must relieve itself by a process of heat conduction, or that a composition fluctuation near the critical mixing point, to which the arguments of the preceding paragraph are as readily applied, must decay by heat conduction rather than diffusion, is not a notion to command intuitive assent.

Let us, therefore, reexamine the equations governing the relaxation process. The essential point which must be kept carefully in mind is that we have an initial value problem: Given the initial temperature, velocity, and density distribution in an infinite fluid, what values do these quantities assume at $t>0$? An examination of only harmonic variations can be misleading.

We have previously[10] arrived at an equation of motion which described an isothermal, undamped, density variation in the critical region,

$$-\ddot{s}(R,t)+C_T^2\nabla^2[s(R,t)-\kappa^{-2}\nabla^2 s(R,t)]=0, \quad (11)$$

where, with m equal to the molecular mass,

$$C_T^2=m^{-1}(\partial P/\partial\rho)_T,$$
$$\delta\rho=\rho s, \quad (12)$$

and $\dot{s}=(\partial s/\partial t)$. More generally, if there is a temperature variation $\delta T=T_0(R,t)$, it will contribute to the pressure an increment $(\partial P/\partial T)_\rho T_0$. Also the viscous damping causes an acceleration of $s(R,t)$equal[24] to $-(4\eta/3\rho m)\nabla^2\dot{s}$, where η is the shear viscosity (η may be redefined to include a volume viscosity, with no change in the form of the equations). Consequently we generalize Eq. (11) (or we may say instead that we generalize the usual linearized equation of motion by the addition of the $\kappa^{-2}\nabla^2 s$ term) to

$$-\ddot{s}+\nabla^2\{C_T^2[s-\kappa^{-2}\nabla^2 s]+(1/\rho m)(\partial P/\partial T)_\rho T_0\}$$
$$+(4\eta/3\rho m)\nabla^2\dot{s}=0. \quad (13)$$

The independent variables are $s(R,t)$ and $T_0(R,t)$. The linearized equation of energy transfer states that the entropy increase of a volume element is equal to the amount of heat energy that has flowed into the volume element,

$$(H/T)\nabla^2 T_0=\rho(\partial S/\partial\rho)_T\dot{s}+(\partial S/\partial T)_\rho\dot{T}_0, \quad (14)$$

where H is the heat conductivity. Now examine the decay of a particular Fourier component $s(\mathbf{R},t)=s^k(t)\exp(i\mathbf{k}\cdot\mathbf{R})$; $T_0(\mathbf{R},t)=T_0^k(t)\exp(i\mathbf{k}\cdot\mathbf{R})$. Equations (13) and (14) become

$$+\ddot{s}^k+k^2C_T^2(1+k^2/\kappa^2)s^k+k^2(4\eta/3\rho m)\dot{s}^k$$
$$+(k^2/\rho m)(\partial P/\partial T)_\rho T_0^k=0 \quad (15)$$

and

$$(\partial S/\partial T)_\rho\dot{T}_0^k+k^2(H/T)T_0;+\rho(\partial S/\partial\rho)_T\dot{s}^k=0. \quad (16)$$

If it were necessary to know quantitatively $s^k(t)$ and $T_0^k(t)$ for all $t>0$, the course of solution would clearly be to suppose that all t-dependent quantities in Eqs. (15) and (16) vary as $\exp(-i\omega t)$. A combination of Eqs. (15) and (16) would then give a cubic equation for ω, having roots $\omega_l(l=1,2,3)$, say. The solution would then be of the form

$$s^k(t)=\sum_{l=1}^{3}a_l\exp(-i\omega_l t), \quad (17)$$

where, after imposition of the initial conditions, the a_l become complicated functions of the ω_l, but *linear* functions of the three initial values: $s^k(0)$, $\dot{s}^k(0)$, and $T_0^k(0)$. Because the result is so different from, and more complicated than, Van Hove's treatment, we shall not be able to carry out a quantitative analysis similar to his. However, with the conclusions already drawn here regarding the general solution, and an explicit solution for $T_0^k(t)$ in terms of $s^k(t)$, we can learn quite a bit about the initial modes of decay of a density fluctuation.

Equation (16) is a linear first-order inhomogeneous equation in $T_0^k(t)$ and t. The solution of the initial

[20] L. Van Hove, Phys. Rev. **95**, 249 (1954).
[21] L. Landau and G. Placzek, Physik. Z. Sowjetunion **5**, 172 (1934).
[22] J. Frenkel, *Kinetic Theory of Liquids* (Oxford University Press, New York, 1946), p. 244 ff.
[23] These are discussed precisely by C. Truesdell [J. Rat. Mech. Anal. **2**, 643 (1953)].
[24] P. M. Morse and H. Feshback, *Methods of Theoretical Physics* (McGraw-Hill Book Company, Inc., New York, 1953), p. 162.

value problem is readily obtained as

$$T_0^{\mathbf{k}}(t) = T_0^{\mathbf{k}}(0)\exp(-\gamma t) - \beta\exp(-\gamma t)\int_0^t \exp(\gamma t)\dot{s}^{\mathbf{k}}(t)\,dt, \quad (18)$$

where

$$\gamma = k^2 H/T(\partial S/\partial T)_\rho,$$
$$\beta = \rho(\partial S/\partial\rho)_T/(\partial S/\partial T)_\rho. \quad (19)$$

We now use Eq. (15) to examine the decay of $s^{\mathbf{k}}(t)$, and take the $T^{\mathbf{k}}(t)$ term in (15) to be given by Eq. (18). Because our major interest is in $\langle s^{\mathbf{k}}(t)s^{\mathbf{k}}(0)\rangle$, it is reasonable to consider only those parts of the t-dependent solution that are correlated with $s^{\mathbf{k}}(0)$ through the linear dependence of the coefficients a_l, in Eq. (17), on the initial conditions. Now the contribution of the initial velocity to the initial energy of the fluctuations is[10] solely to the kinetic energy, while $s^{\mathbf{k}}(0)$ appears solely in the potential energy. Since the probability of the initial state of fluctuations is proportional to the exponential of the total energy, it follows that $s^{\mathbf{k}}(0)$ and $\dot{s}^{\mathbf{k}}(0)$ are distributed independently, and no conclusion about $\langle s^{\mathbf{k}}(t)s^{\mathbf{k}}(0)\rangle$ would be altered if we put $\dot{s}^{\mathbf{k}}(0)=0$; we therefore do so.

Next, consider $T_0^{\mathbf{k}}(0)$. In the equation for the initial energy of the fluctuations,[10] we have not put down any contribution from a temperature fluctuation, and it would indeed be an innovation in the theory of spontaneous critical-point fluctuations to suppose that such a contribution were necessary. However, the question of a possible correlation between the initial density and initial temperature fluctuations is crucial in this context, and so it may be worthwhile to state clearly why no such correlation exists. Note first that if there were such a correlation,[25] the density fluctuations would not become abnormally large in the critical region, because the T fluctuations, correlated to the ρ fluctuations, would make the energy of the fluctuation state large. Beyond this, at a molecular level of description, there is only a narrowly circumscribed part of phase space that might be described by temperature fluctuations. The probability that a system be in a small element of phase space is a product of f_K giving the velocity distribution, and f_e, the configurational distribution

$$f_e \propto \exp(-V/k_B T_{en}), \quad (20)$$

where V is the intermolecular potential energy, a function only of the positions of the molecules, and we have been careful to give a full designation to the ensemble temperature T_{en} (previously called T). An integration of f_e over the coordinates, subject to an assigned singlet density distribution $\rho(\mathbf{R})$ (or, conceivably, subject to higher multiplet assignments), produces a probability density for $\rho(\mathbf{R})$,

$$\int f_e d\mathbf{R}_1\cdots d\mathbf{R}_N = \exp\{-A_e[(\rho(\mathbf{R})), T_{en}]/k_B T_{en}\},$$

where the configurational free energy A_e is a functional of $\rho(\mathbf{R})$, but a function only of T_{en}, the ensemble temperature. A specification of the coordinate probabilities exhausts the constraints which may be imposed on a coordinate integration; there is no room here for a fluctuating temperature.

This is the essential justification of the neglect of initial temperature fluctuations in a calculation of the initial probable magnitude of density fluctuations, for whatever use is made of the kinetic energy to define the initial temperature fluctuations, no correlation of them with $\rho(R, t)\mid_{t=0}$, can be induced. The question to what extent the kinetic energy is adequately described by a velocity which is the gradient of a scalar potential (implicit in our equations), is referred to other sources.[26-28]

Formal calculations of temperature fluctuations[29] present, in the result, the equilibrium heat capacity of the system. Since the remarks of the preceding paragraph permit the conclusion that the temperature fluctuations depend only on T_{en}, k_B, and m (nothing more appears in the kinetic energy), a reconciliation of the points of view is required and is given at the end of this section.

We now return to consideration of Eqs. (15) and (18); take $\dot{s}^{\mathbf{k}}(0)=T_0^{\mathbf{k}}(0)=0$. An initial density fluctuation produces a nonvanishing acceleration $\ddot{s}^{\mathbf{k}}(0)$, and so the density decay begins as the spreading of an isothermal wave. The next effect which is felt in Eq. (15), is a viscous damping due to the growing velocity ($\dot{s}^{\mathbf{k}}\propto t$). Thirdly, there appears, as a result of the work done during the displacement, a temperature variation ($T^{\mathbf{k}}(t)\propto t^2$). Now the initial acceleration in Eq. (15) is $[-k^2C_T^2(1+k^2/\kappa^2)]$, and therefore the smaller is C_T^2, or the closer the critical point, the smaller will be the acceleration, the slower the decay.[30] This qualitative conclusion will have to suffice, for although the qualitative explanation is, relative to previous discussions, quite simple, namely that large fluctuations arise only when their energy is small, and therefore the decelerating force small, a full quantitative treatment is much more complicated.

Perhaps greater quantitative progress could be made in a study of diffusional relaxation in the critical region, as there it seems reasonable to neglect both inertial

[25] One might imagine the correlation to be induced by a term $(\partial^2 A/\partial T\partial\rho)\rho(R)T(R)$ in the energy; A is the Helmholtz free energy.

[26] D. Ter Haar, *Introduction to the Physics of Many-Body Systems* (Interscience Publishers, Inc., New York, 1958).

[27] F. London, *Superfluids* (John Wiley & Sons, Inc., New York, 1954), Vol. II, p. 107.

[28] Footnote reference 24, p. 302.

[29] R. M. Mazo, Physica 25, 57 (1959).

[30] Unless $k\gg\kappa$. But such values of k seem relatively improbable. [See Eq. (10).] This conclusion should be treated with some reserve, as relaxation processes in other parts of the calculation, Sec. IV, may pick out $k\gg\kappa$.

and induced temperature terms in the equation of motion.

We can now see the meaning of the calculations of T fluctuations given in phenomenological fluctuation theory.[29] A closed system, aged in a temperature bath, will have when removed and isolated an energy different from the ensemble average energy. However, that part of the energy fluctuation which may reasonably be described as due to an initial temperature fluctuation, involves no property of the intermolecular potential and is independent of the local density fluctuations. *After* the isolated system is allowed to age, the processes of viscous flow and heat conduction (and their molecular analogs), will throw *all* the initial energy fluctuation into a uniform temperature increment. The latter we regard as the object of phenomenological fluctuation theory.

IV. PASSAGE OF SOUND WAVE

The passage of a plane sound wave through a medium may induce a variety of secondary processes. There may be ordinary scattering, in which the primary wave is scattered from fixed obstacles and the secondary wave propagates away with the macroscopic sound speed. As previously mentioned however, the sound wavelength is considerably greater than the correlation length of the fluctuations at the observed $(T-T_c)$, and the absorption will be proportional to ω^4, a dependence which is not observed. If the relaxation times of the fluctuations are not so large that the fluctuations may be taken as static, the sound wave, which varies as $\exp(i\omega t)$, will leak energy into a spectrum of other frequencies. It would be quite possible to maintain the possibility of such relaxation until the final stage of the ensuing calculations. Then, however, in

$$\langle s^k(t)s^{k'}(0)\rangle=\langle s^k(0)s^{k'}(0)\rangle\sum_{l=1}^{3}b_l(k)\exp[-i\omega_l(k)t],$$

an explicit knowledge of the functions $b_l(k)$, $\omega_l(k)$ is required, so that functions of b_l and ω_l can be integrated over k. We have seen that the ω_l approach zero as the critical point is approached, and so we have grounds other than practicality—which would suffice—for our subsequent neglect of fluctuation relaxation. We may finally distinguish a thermal relaxation. If the heat capacity of the medium varies from point to point because of the density fluctuations, there will be a secondary temperature variation imposed on that of the sound wave, and a consequent heat flow and loss of energy from the sound wave.

Because this last process seems intuitively to be at least as important as any other that can be simply distinguished, because it is tractable, and because it has already been treated on the basis of an unrealistic picture of critical fluctuations, we will examine the thermal relaxation process in detail. It will be appreciated, as we proceed, that the process of discarding terms which do not seem to originate in this mechanism is arbitrary.

Suppose that the acoustic wave induces an entropy increment per volume of $S_a(R,t)$, a number density increment $\rho_a(R,t)$, and temperature increment $T_a(R,t)$ Suppose also that at any point the medium may be characterized by a quantity x (density or composition), that differs from its mean value $\bar{x}$: $x-\bar{x}=X(\mathbf{R})$, presumed static. Then, with S the entropy per volume, an equilibrium function of its arguments,

$$S_a=(\partial S(x)/\partial\rho)_T\rho_a+(\partial S(x)/\partial T)_\rho T_a, \quad (21)$$

$$(\partial S(x)/\partial\rho)_T=(\partial S/\partial\rho)_T+(\partial^2 S/\partial\rho\partial\bar{x})X, \quad (22)$$

$$(\partial S(x)/\partial T)_\rho=(\partial S/\partial T)_\rho+(\partial^2 S/\partial T\partial\bar{x})X. \quad (23)$$

The arguments of S are the mean values, if the contrary is not made explicit.

To provide a rationale of Eq. (21), and to explain further the meaning of the symbols, let us see to what extent it can be derived from a Taylor series expansion of the entropy. For a one-component system, with $(\delta\rho)$ the *total* density increment (spontaneous plus forced), (δT) the total temperature increment, and ΔS the total increment at $\mathbf{R}$ of the entropy density,

$$\Delta S=(\partial S/\partial\rho)_T(\delta\rho)+\tfrac{1}{2}(\partial^2 S/\partial\rho^2)_T(\delta\rho)^2+(\partial S/\partial T)_\rho(\delta T)+\tfrac{1}{2}(\partial^2 S/\partial T^2)_\rho(\delta T)^2+(\partial^2 S/\partial T\partial\rho)(\delta T)(\delta\rho)+\cdots. \quad (24)$$

Now divide the temperature and density variations into parts $\rho_0(R,t)$ and $T_0(R,t)$ which are functionals of the spontaneous density fluctuation at $t=0$, and would represent the density and temperature variations if there were no forced acoustic wave, and ρ_a and T_a, the "induced" density and temperature variation:

$$(\delta\rho)=\rho_0(R,t)+\rho_a(R,t), \quad (25)$$

$$(\delta T)=T_0(R,t)+T_a(R,t). \quad (26)$$

By a reduction of the energy fed into the system, ρ_a and T_a can be made as small as desired. Therefore, when Eqs. (25) and (26) are substituted into Eq. (24), nonlinear terms in ρ_a and T_a can be discarded.

$$\Delta S=(\partial S/\partial\rho)_T(\rho_0+\rho_a)+(\partial S/\partial T)_\rho(T_0+T_a)+\tfrac{1}{2}(\partial^2 S/\partial\rho^2)_T(\rho_0^2+2\rho_0\rho_a)+\tfrac{1}{2}(\partial^2 S/\partial T^2)_\rho(T_0^2+2T_0T_a)+(\partial^2 S/\partial T\partial\rho)(\rho_0T_0+\rho_0T_a+\rho_aT_0)+\cdots. \quad (27)$$

Let $\Delta S=S_0+S_a$, with the same interpretation of the subscripts. To avoid extraneous complications, suppose nonlinear effects in the heat conduction to be neglected. Then

$$\Delta\dot{S}=\Delta\dot{S}_0+\Delta\dot{S}_a=(H/T)\nabla^2T_0+(H/T)\nabla^2T_a. \quad (28)$$

As ρ_0 and T_0 are, by supposition, the proper solutions to the initial value problem, Eq. (27) breaks up into

two equations:

$$\Delta S_0=(\partial S/\partial\rho)_T\rho_0+(\partial S/\partial T)_\rho T_0+\tfrac{1}{2}(\partial^2 S/\partial\rho^2)_T\rho_0^2 +\tfrac{1}{2}(\partial^2 S/\partial T^2)_\rho T_0^2+(\partial^2 S/\partial T\partial\rho)\rho_0 T_0+\cdots,$$

$$\Delta\dot{S}_0=(H/T)\nabla^2 T_0; \tag{29}$$

$$\Delta S_a=(\partial S/\partial\rho)_T\rho_a+(\partial S/\partial T)_\rho T_a+(\partial^2 S/\partial\rho^2)_T\rho_0\rho_a +(\partial^2 S/\partial T^2)_\rho T_0 T_a+(\partial^2 S/\partial T\partial\rho)(\rho_0 T_a+\rho_a T_0)+\cdots;$$

$$\Delta\dot{S}_a=(H/T)^2 T_a. \tag{30}$$

Equation (29), with the deletion of its nonlinear terms, reduces to Eq. (14). We have supposed, and will continue to suppose, that Eq. (14) constitutes a good first approximation to the description of spontaneous fluctuations. [See the discussion preceding Eq. (36).] It is, of course, true that terms which have been retained in Eq. (30) must by our hypotheses (linearization with respect to ρ_a, T_a), be smaller than terms which have been rejected from Eq. (29). But this implies no inconsistency in the terms retained; it is possible to measure the absorption and dispersion of the forced waves, even though they are small.

Equation (30) may be specialized with $\rho_0\equiv X$ and the hypothesis of static fluctuations, so that $T_0(R,t)=T_0(R,0)=0$. Equation (21) results.

If the restriction, previously mentioned, that only the heat capacity is affected by the fluctuations of x, be introduced, we have from Eq. (21)

$$T\dot{S}_a=H^2 T_a=T(\partial S/\partial\rho)_T\dot{\rho}_a+C_V\dot{T}_a+(\partial C_V/\partial\bar{x})X\dot{T}_a, \tag{31}$$

where C_V is the heat capacity per volume at constant volume. The induced temperature and density variations can be written as their averages (over the fluctuations), plus a secondary variation that arises from an interaction of the induced variations with the spontaneous fluctuations,

$$T_a=T_1+T_2; \qquad T_1=\langle T_a\rangle,$$
$$\rho_a=\rho_1+\rho_2; \qquad \rho_1=\langle\rho_a\rangle. \tag{32}$$

The assumption of a thermal relaxation process is further delimited to require that ρ_2 be negligible in Eq. (31); that is, the interaction of the sound wave and spontaneous fluctuation induces a heat flow, but not a mass flow. Equation (31) becomes

$$H\nabla^2(T_1+T_2)=T(\partial S/\partial\rho)_T\dot{\rho}_1+C_V(\dot{T}_1+\dot{T}_2) +(\partial C_V/\partial\bar{x})X(\dot{T}_1+\dot{T}_2). \tag{33}$$

Take now the average of Eq. (33):

$$H\nabla^2 T_1=T(\partial S/\partial\rho)_T\dot{\rho}_1+C_V\dot{T}_1+(\partial C_V/\partial\bar{x})\langle X\dot{T}_2\rangle\cong 0. \tag{34}$$

The last equation of (34) follows from the fact that the wavelength of the mean (or macroscopically observed) sound wave is itself too large for appreciable heat conduction from $H\nabla^2 T_1$ to result.

The essential computation, then, is of $\langle X\dot{T}_2\rangle$. On subtraction of Eq. (34) from Eq. (33), there results

$$H\nabla^2 T_2=C_V\dot{T}_2+(\partial C_V/\partial\bar{x})[X\dot{T}_1+X\dot{T}_2-\langle X\dot{T}_2\rangle]. \tag{35}$$

On two grounds we neglect $[X\dot{T}_2-\langle X\dot{T}_2\rangle]$ in Eq. (35). There is first the argument that T_2 is much smaller than T_1 and therefore both XT_2 and $\langle XT_2\rangle$ are negligible, to a first approximation, in Eq. (35). Second, XT_2, being the product of two fluctuations, will be much less sensitive to fluctuations (of the sign of X, say), than XT_1, and consequently XT_2 will be largely canceled by $\langle XT_2\rangle$.

To suppose that T_2 is much smaller than T_1 raises a question regarding Eq. (30). Why did we not retain terms of "order" $T_1\rho_0^2$, which would be of the same "order" as $T_2\rho_0$? A few remarks may add to the plausibility of the treatment. First, if $[\rho_0(R)]^2$ is to be actually used in a calculation, there is required a preliminary average of ρ_0 over a volume element containing many molecules. Such a procedure smooths out the δ function singularities in $\rho_0(R)$, and thereby keeps $[\rho_0(R)]^2$ finite, and even small. For even if the volume element contained, on the average, only ten molecules, the repulsive cores would keep the maximum number that has any appreciable probability below, say, 20, and this even at the critical point. It is not $[\rho_0(R)]^2$ that becomes abnormally (infinitely) large at the critical point, but the range of the correlation. Thus $\int\rho_0(R_1)\rho_0(R_2)d\mathbf{R}_2$ has an infinite expectation at the critical point. One hopes that $\rho_0 T_2$ may be much more significant than $\rho_0^2 T_1$, because, in the former term, $T_2(R_1)$ may through heat conduction correlate $\rho_0(R_1)$ with distant fluctuations.

Equation (35) becomes

$$H\nabla^2 T_2=C_V\dot{T}_2+(\partial C_V/\partial\bar{x})X\dot{T}_1 \tag{36}$$

and is readily solved by a Fourier resolution.

In addition to Eqs. (34) and (36), an equation of motion is required to allow determination of ρ_1, T_1. In view of the restricted model we have adopted, this equation will be the usual linearized equation of motion, say Eq. (13), in which $\kappa^{-2}\nabla^2 s$ and $\eta\nabla^2\dot{s}$ are neglected because the wavelength of ρ_1 is so large. With $\rho_1=\rho s$, Eq. (13) becomes

$$-\ddot{\rho}_1+m^{-1}(\partial P/\partial\rho)_T\nabla^2\rho_1+m^{-1}(\partial P/\partial T)\rho\nabla^2 T_1=0. \tag{37}$$

V. SOLUTION FOR THERMAL PROCESS

We begin by solving Eq. (36) for T_2. The mean forced wave, ρ_1 and T_1, and therefore also T_2, are taken to have time dependence $\exp(-i\omega t)$. Further, let

$$X(\mathbf{R})=\int X^{\mathbf{k}}\exp(i\mathbf{k}\cdot\mathbf{R})d\mathbf{k}, \tag{38}$$

$$T_2(\mathbf{R},t)=\exp(-i\omega t)\int T_2^{\mathbf{k}}\exp(i\mathbf{k}\cdot\mathbf{R})d\mathbf{k}. \tag{39}$$

The range over which the correlations extend, although abnormally large in the critical region, is much less than the wavelength of T_1, so we shall suppose that the evaluation of $\langle XT_2\rangle$ may be completed without taking account, in intermediate stages, of the dependence of T_1 on R. Then substitution of Eq. (38) into Eq. (36) gives

$$T_2^{\mathbf{k}}=-i\omega(\partial C_V/\partial\bar{x})X^{\mathbf{k}}T_1'/(i\omega C_V-k^2H) \quad (40)$$

for the $\mathbf{k}$ component of T_2; $T_1=T_1'\exp(-i\omega t)$. From Eqs. (38) and (40),

$$\langle X(\mathbf{R})T_2(\mathbf{R},t)\rangle$$

$$=\exp(-i\omega t)\int\langle X^{\mathbf{k}'}T_2^{\mathbf{k}}\rangle\exp[i(\mathbf{k}+\mathbf{k}')\cdot\mathbf{R}]d\mathbf{k}d\mathbf{k}' \quad (41)$$

$$=-i\omega(\partial C_V/\partial\bar{x})T_1\int\frac{\langle X^{\mathbf{k}'}X^{\mathbf{k}}\rangle\exp[i(\mathbf{k}+\mathbf{k}')\cdot\mathbf{R}]}{(i\omega C_V-k^2H)}d\mathbf{k}d\mathbf{k}'. \quad (42)$$

For either a density of composition fluctuation [see Eq. (10)],

$$\langle X^{\mathbf{k}'}X^{\mathbf{k}}\rangle=A\delta(\mathbf{k}+\mathbf{k}')/(k^2+\kappa^2), \quad (43)$$

where A is independent of k, and, relative to κ, insensitive to $(T-T_c)$ in the critical region. Let

$$Q\equiv-i\omega C_V^{-1}(\partial C_V/\partial\bar{x})^2A\int[(i\omega C_V-k^2H)(k^2+\kappa^2)]^{-1}d\mathbf{k}. \quad (44)$$

Then

$$\langle XT_2\rangle=QT_1C_V/[\partial C_V/\partial\bar{x}], \quad (45)$$

and may be substituted in Eq. (34),

$$T(\partial S/\partial\rho)_T\dot{\rho}_1+C_V\dot{T}_1(1+Q)=0. \quad (46)$$

Having completed the computation of the correlations in Eqs. (45) and (46), we reinstate the dependence of T_1 on R in the quantity T_1Q. An evaluation of Q will be deferred until it is shown how Q enters into the absorption and dispersion.

Substitution of T_1, from Eq. (46), into Eq. (37) gives

$$-\ddot{\rho}_1+\{m^{-1}(\partial P/\partial\rho)_T-T(\partial P/\partial T)_\rho\times(\partial S/\partial\rho)_T[mC_V(1+Q)]^{-1}\}\nabla^2\rho_1=0. \quad (47)$$

Let the macroscopic wave ρ_1 be a plane wave propagating along the y axis,

$$\rho_1=e^{ik_1y-i\omega t}. \quad (48)$$

The real and complex parts of k_1 yield, respectively, the dispersion and absorption,

$$\mathrm{Re}(k_1)=\omega/c, \quad (49)$$

$$\mathrm{I}(k_1)=\alpha, \quad (50)$$

where c is the speed of sound at the frequency ω, and α is the absorption. Substitution of Eq. (48) into (47) gives

$$\omega^2=k_1^2\{c_a^2+(c_a^2-c_T^2)[(1+Q)^{-1}-1]\}, \quad (51)$$

where c_a is the adiabatic speed of sound,

$$c_a^2=m^{-1}(\partial P/\partial\rho)_T-T(\partial P/\partial T)_\rho(\partial S/\partial\rho)_T(mC_V)^{-1}, \quad (52)$$

and c_T is the isothermal speed of sound, $c_T^2=m^{-1}(\partial P/\partial\rho)_T$. It has been assumed in the derivation of Eq. (51) that Q gives a small correction to adiabatic propagation, and consequently the subsequent equations are linearized with respect to Q. From Eq. (51),

$$k_1=(\omega/c_a)[1+Q(c_a^2-c_T^2)/c_a^2] \quad (53)$$

and

$$\alpha=\mathrm{I}(k_1)=\omega c_a^{-3}(c_a^2-c_T^2)\mathrm{I}(Q). \quad (54)$$

An absorption per wavelength α_λ, where λ is the wavelength and α_λ is dimensionless, may be defined as

$$\alpha_\lambda=\alpha\lambda. \quad (55)$$

Because Q has been supposed small, it is a sufficiently good approximation in Eq. (55) to neglect the dispersion in λ vs ω; $\lambda\cong 2\pi c_a/\omega$. Consequently

$$\alpha_\lambda=2\pi(1-c_T^2/c_a^2)\mathrm{I}(Q). \quad (56)$$

From Eqs. (49) and (53), we obtain

$$c=c_a[1-(1-c_T^2/c_a^2)\,\mathrm{Re}(Q)]. \quad (57)$$

Returning now to Q, we evaluate the integral in Eq. (44) by a residue integration:

$$\int[(i\omega C_v-k^2H)(k^2+\kappa^2)]^{-1}d\mathbf{k}$$

$$=(-2\pi/H)\int_{-\infty}^{+\infty}[k^2-i(\omega C_V/H)]^{-1}[k^2+\kappa^2]^{-1}k^2dk \quad (58)$$

$$=[(-2\pi^2/H)/(\kappa^4+4f^4)]\{if[\kappa^2+2f(f-\kappa)]+[2f^3-\kappa^2(f-\kappa)]\}, \quad (59)$$

where

$$f\equiv(\omega C_V/2H)^{\frac{1}{2}}. \quad (60)$$

Consequently,

$$Q=4\pi^2A(\partial\ln C_V/\partial\bar{x})^2f^2(\kappa^4+4f^4)^{-1}\times\{i[2f^3-\kappa^2(f-\kappa)]-f[\kappa^2+2f(f-\kappa)]\}. \quad (61)$$

The real and imaginary parts of Q have been separated and may be substituted into Eqs. (56) and (57).

Although we will not attempt a detailed comparison of the results with experiment, a few comments are in order. Both the dispersion and absorption due to the selected mechanism remain finite at the critical point. Thus, as $\kappa\to 0$,

$$Q\to 2\pi^2A(\partial\ln C_V/\partial\bar{x})^2f(i-1). \quad (62)$$

The predicted linear increase of c with $\omega^{\frac{1}{2}}$ seems to be a fair approximation to the xenon results,[1] although the latter are sufficiently systematic to indicate linear dependence on a slightly lower power of ω. Moreover, the predicted ratio

$$\alpha_\lambda = 2\pi(c-c_a)/c_a \tag{63}$$

is approximately correct for the one frequency at which α_λ was measured.

As far as the absolute magnitude of Q: If we assume $(\partial \ln C_V/\partial \ln\rho)_T \simeq 1$ (as the van der Waals equation indicates), $H \simeq C_V c_a l_H$, where l_H is a mean free path of a few angstroms, and $a \simeq 10$ A [Eq. (6)], it turns out that α_λ is about 0.05 at the critical point and $\omega = 10^9$. This is too small by a factor of ten, but the estimate can hardly be taken seriously, either pro or con the result.

A more detailed discussion, and an evaluation of those contributions to α_λ and c which we have arbitrarily discarded, we regard as a fruitless labor in the absence of precise knowledge of the thermodynamic properties, the transport coefficients, and the angular dissymmetry of light scattering, for a simple system in its critical region.

THE JOURNAL OF CHEMICAL PHYSICS VOLUME 33, NUMBER 5 NOVEMBER, 1960

Dielectric Relaxation of Polar Liquids*

SIVERT H. GLARUM†

Metcalf Research Laboratories, Brown University, Providence, Rhode Island

(Received October 8, 1959)

The statistical theory of the dielectric relaxation of polar liquids is developed using the fluctuation-dissipation approach to linear dissipative phenomena, and an expression is derived relating the complex dielectric constant to a time-dependent microscopic correlation function. It is found that a finite number of microscopic relaxation times leads to an equal number of macroscopic decay times, and, in the case of a single relaxation time τ_0, the decay time is given by

$$T_0=[3\epsilon_0/(2\epsilon_0+\epsilon_\infty)]\tau_0,$$

ϵ_0 being the static dielectric constant, and ϵ_∞ being the high frequency dielectric constant. Relaxation times are also determined for systems having two decay times, and for systems characterized by the circular-arc and skewed-arc distribution functions.

I. INTRODUCTION

THE statistical mechanics of the behavior of systems comprised of polar molecules in time-independent fields has been frequently discussed, and is reasonably well understood, although various theories have differed in their representations of the effects of induced polarization.[1–3] Treating induced moments as displacements of isotropic, regularly spaced harmonic oscillators, Cole has shown that for pure polar liquids[3]

$$\epsilon_0-\epsilon_\infty=[9\epsilon_0/(2\epsilon_0+\epsilon_\infty)][(\epsilon_\infty+2)/3]^2(4\pi N/9kTV)\langle\boldsymbol{\mu}_0\cdot\mathbf{m}\rangle_0. \quad (1)$$

Here ϵ_0 is the static dielectric constant, ϵ_∞ is the high frequency dielectric constant due to induced moments, N/V is the number of molecules per unit volume, and $\mathbf{m}$ is the vector sum of the permanent dipole moments in a microscopic spherical region surrounding the permanent moment $\boldsymbol{\mu}_0$ when immersed in a medium of dielectric constant ϵ_0. The brackets $\langle\cdots\rangle_0$ indicate a phase space average using $\exp[-H^0(p,q)/kT]$ as a weighting factor, $H^0(p,q)$ being the Hamiltonian of the system when undisturbed by external fields.

The statistical theory of dielectric polarization in time-dependent fields has not been previously developed because of complications arising from its nonequilibrium nature. When the electric field polarizing a dielectric is abruptly removed, the polarization does not vanish instantly, but requires a measurable period of time in which to disappear. Frequently the decay of polarization is exponential in time and may be described by a single decay time, while in other cases this decay may be represented by a linear superposition or distribution of decay times. These times are a measure of the time required for a system of dipoles to pass from a polarized equilibrium configuration to a nonpolarized equilibrium configuration, and therefore depend upon the rates of molecular reorientation.

When the applied electric field is monochromatic and of the form

$$\mathbf{E}=\mathbf{E}_0\exp(i\omega t), \quad (2)$$

ω being the angular frequency of the field, the resulting polarization is, in general, not in equilibrium with the field, but differs in phase and amplitude from its equilibrium value. The relationship between the field and the polarization $\mathbf{P}$ is formally expressed by means of the complex dielectric constant ϵ^* through the expression

$$\mathbf{P}=[(\epsilon^*-1)/4\pi]\mathbf{E},$$

where $\mathbf{E}$ is the average macroscopic field existing within the dielectric.

In the limiting case of very weak molecular interactions, Debye has shown that[4]

$$T_0=[(\epsilon_0+2)/(\epsilon_\infty+2)]\tau_0.$$

Here τ_0 is a molecular *relaxation* time, and T_0 is the corresponding macroscopic *decay* time.[5] According to this equation these times may differ by nearly two orders of magnitude for highly polar media, but it is usually supposed that T_0 and τ_0 are nearly equal, the difference being attributed to the inadequacy of the Lorentz local field employed by Debye.

* This research was supported in part by the U. S. Air Force through the Air Force Office of Scientific Research of the Air Research and Development Command.

† Present address: Bell Telephone Laboratories, Inc., Murray Hill, New Jersey.

[1] J. G. Kirkwood, J. Chem. Phys. 7, 911 (1939).

[2] H. Frohlich, *Theory of Dielectrics* (Oxford University Press, New York, 1949); F. E. Harris and B. J. Alder, J. Chem. Phys. 21, 1031 (1953); A. D. Buckingham, Proc. Roy. Soc. (London) A238, 235 (1956).

[3] R. H. Cole, J. Chem. Phys. 27, 33 (1957).

[4] P. Debye, *Polar Molecules* (Dover Publications, Inc., New York, 1945).

[5] Throughout this paper we shall refer to times characteristic of molecular reorientation as relaxation times, whereas times describing the decay of the dielectric polarization of a macroscopic body will be called decay times. As measured decay times depend upon the geometric form of the dielectric considered because of sample dependent boundary conditions, we shall reserve the symbol T for decay times which would be found using a dielectric-filled parallel plate condenser if the applied voltage were a step function.

Several attempts have been made to extend Eq. (1) to the case of dielectric relaxation, thereby taking into account all molecular correlations.[6] One method has been to replace ϵ_0 in Eq. (1) by ϵ^*, and to multiply the right-hand side of this expression by $(1+i\omega\tau_0)^{-1}$. The resulting equation is quadratic in ϵ^*, and cannot be described in terms of a single decay time or, in fact, even by a distribution of decay times.

Powles has taken a different approach to the problem of relating τ_0 and T_0.[7] Assuming an expression for the effective field acting on a molecule due to external charges, he finds that

$$T_0=[3\epsilon_0/(2\epsilon_0+\epsilon_\infty)]\tau_0, \tag{3}$$

if there is to be only one decay time. Of the various expressions proposed connecting τ_0 and T_0, that of Powles has been found to correlate most successfully measured values of T_0 with assumed values of τ_0.[8]

In this paper we shall seek a relationship between the observed macroscopic behavior of a system and its microscopic relaxation behavior. Starting from a statistical expression for the decay function in terms of a time-dependent macroscopic correlation function, we shall ultimately obtain an equation relating this function to a microscopic correlation function which depends on the behavior of a relatively small number of molecules. Two basic problems arise in the formulation of a theory of dielectric relaxation. One is that of relating observed macroscopic behavior to the actual rates of molecular reorientation, while the other involves predicting these rates *a priori*. It is exclusively with the former problem that we shall be concerned.

II. RELAXATION FUNCTIONS

Dielectric relaxation may be described in terms of either the complex dielectric constant, the decay function characterizing the decay of polarization upon the removal of a previously constant electric field, or the distribution of decay frequencies (reciprocal decay times). All three descriptions may be conveniently related by means of Laplace transforms. The logarithmic distribution of decay frequencies $F(\alpha)$ is defined in terms of the decay function $\Phi(t)$ by the expression

$$\Phi(t)=\int_0^\infty \exp(-\alpha t)\,F(\alpha)\,(d\alpha/\alpha),$$

so that

$$-d\Phi(t)/dt=\mathfrak{L}[F(\alpha)],$$

where the operator $\mathfrak{L}$ indicates that the Laplace transform of $F(\alpha)$ is to be taken. Similarly, it follows from the superposition integral that

$$(\epsilon^*-\epsilon_\infty)/(\epsilon_0-\epsilon_\infty)=-\int_0^\infty \exp(-i\omega t)[d\Phi_0(t)/dt]dt$$
$$=\mathfrak{L}[-d\Phi_0(t)/dt]=\mathfrak{L}^2[F_0(\alpha)], \tag{4}$$

subscripts referring to the decay and distribution functions for dielectric polarization in a parallel plate condenser. Laplace transforms provide a useful connection between the complex dielectric constant, the decay function, and the distribution function, for the many available tables of these transforms and their inverses often make it a comparatively simple matter to pass from one of these functions to another.

III. STATISTICAL THEORY

In a recent article Kubo has presented a general statistical theory of linear dissipative phenomena which is readily applied to the case of dielectric relaxation.[9] From his results it follows that the moment of an isotropic dielectric specimen in a time-dependent field parallel to the z axis is given by

$$M(t)=\langle M_z\rangle_0-\frac{\langle \mathbf{M}(0)\cdot\mathbf{M}(0)\rangle_0}{3kT}\int_{-\infty}^{t}E(t')\cdot[d\Phi(t-t')/dt]dt'$$

$$\Phi(t)=\langle \mathbf{M}(0)\cdot\mathbf{M}(t)\rangle_0/\langle \mathbf{M}(0)\cdot\mathbf{M}(0)\rangle_0. \tag{5}$$

Here $\mathbf{M}(t)$ is the vector sum of all molecular dipole moments, permanent and induced, at time t, and M_z is the z component of this vector. The first of these expressions is equivalent to the superposition integral, while the latter expresses the decay function in terms of a time-dependent correlation function for an equilibrium system free from external fields.

Let us now consider a dielectric sphere of volume V suspended in space in an otherwise uniform electric field given by Eq. (2). The moment of this sphere, representing its uniform polarization by the field, may be shown to be

$$\mathbf{M}(t)=[(\epsilon^*-1)/(\epsilon^*+2)](3V/4\pi)\mathbf{E}_0\exp(i\omega t),$$

and the function $\Phi(t)$ describes the decay of this polarization when a previously constant electric field is removed. Thus we find that

$$(\epsilon^*-1)/(\epsilon^*+2)=[(\epsilon_\infty-1)/(\epsilon_\infty+2)]$$
$$+(4\pi/9kTV)\langle \mathbf{M}(0)\cdot\mathbf{M}(0)\rangle_0\mathfrak{L}[-d\Phi(t)/dt], \tag{6}$$

ϵ_∞ being the value of ϵ^* for fields of infinite frequency.

The problem we wish to consider in the formulation of the statistical theory of dielectric relaxation is that of relating the macroscopic correlation function $\langle \mathbf{M}(0)\cdot\mathbf{M}(t)\rangle_0$ to the time-dependent behavior of a microscopic region within a dielectric. In the limiting case of negligible intermolecular correlations, this function

[6] R. H. Cole, J. Chem. Phys. **6**, 385 (1938); H. C. Bolton, *ibid.* **16**, 486 (1948); J. Ph. Poley, Appl. Sci. Research **B4**, 337 (1954); M. Mandel, Bull. soc. chem. Belges **60**, 301 (1951); J. J. O'Dwyer and R. Sack, Australian J. Sci. Research **A5**, 647 (1952).

[7] J. G. Powles, J. Chem. Phys. **21**, 633 (1953).

[8] R. C. Miller and C. P. Smyth, J. Am. Chem. Soc. **79**, 3310 (1957); N. E. Hill, Proc. Roy. Soc. (London) **A240**, 101 (1957).

[9] R. Kubo, J. Phys. Soc. Japan **12**, 570 (1957).

reduces to $N\langle \boldsymbol{\mu}_0(0)\cdot\boldsymbol{\mu}_0(t)\rangle_0$, and Debye's results follow.

To evaluate more rigorously $\langle \mathbf{M}(0)\cdot\mathbf{M}(t)\rangle_0$, we shall neglect induced polarization for the present, assuming that $\epsilon_\infty=1$. Then, because of the equivalence of all molecules, this correlation function reduces to $N\langle \boldsymbol{\mu}_0(0)\cdot\mathbf{M}(t)\rangle_0$. Following an approach suggested by Kirkwood, we shall divide the moment $\mathbf{M}(t)$ of our macroscopic sphere into two components. One, $\mathbf{m}(t)$, is that of a microscopic spherical region surrounding the moment $\boldsymbol{\mu}_0$, while the other represents the sum of all moments outside this small sphere. The size of the microscopic region must be sufficiently great that its interaction with the outer region corresponds to its interaction with a body possessing macroscopic dielectric behavior.

The moment $\mathbf{m}(t)$ induces an ordering of dipoles in the outer region through long-range dipole-dipole forces, and, as $\mathbf{m}(t)$ varies both in direction and magnitude with time, this ordering also varies, attempting to follow the changes of $\mathbf{m}(t)$. If the dynamic behavior of all molecules in the outer region could be exactly expressed in terms of the interaction of the moment $\mathbf{m}(t)$ with a dielectric continuum, then, from a knowledge of the past history of $\mathbf{m}(t)$, it would be possible to determine $\mathbf{M}(t)$ exactly. However, it is necessary to consider the existence of spontaneous fluctuations in the outer region, and, if these are supposed random in nature, they cannot be predicted from a knowledge of $\mathbf{m}(t)$ by macroscopic arguments. We shall therefore assume that the moment of this region is given by the sum of two terms: one, $\mathbf{M}_\infty(t)$, is equivalent to the result found by the interaction of $\mathbf{m}(t)$ with a true continuum possessing macroscopic dielectric behavior; the other, $\boldsymbol{\Delta}(t_1, t_2)$, represents the resultant vector of polarization in the outer region at time t_2 due to all random events occurring in the interval of time between t_1 and t_2. Thus

$$\mathbf{M}(t)=\mathbf{m}(t)+\mathbf{M}_\infty(t)+\boldsymbol{\Delta}(-\infty, t).$$

The moment $\mathbf{M}_\infty(t)$, corresponding to a homogeneous polarization of the macroscopic sphere due to a field produced by the external boundary of this sphere, may be thought of as the sum of moments previously excited by $\mathbf{m}(t)$ and subsequently decayed. We shall characterize the excitation and decay of this polarization by the function $\Phi(t)$, which also describes the behavior of a uniform polarization when produced by an external electric field. Assuming a linear superposition of after effects, it follows that

$$\mathbf{M}_\infty(t)=-\int_{-\infty}^{t}\mathbf{M}_\infty^{0}(t')[d\Phi(t-t')/dt]dt',$$

where $\mathbf{M}_\infty^{0}(t')$ is the moment which would be induced in a true dielectric continuum if the moment $\mathbf{m}(t')$ were held fixed at time t'. This moment has been shown to equal[1]

$$-\frac{2(\epsilon_0-1)^2}{(2\epsilon_0+1)(\epsilon_0+2)}\mathbf{m}(t')=-A(\epsilon_0)\mathbf{m}(t'). \qquad (7)$$

The total moment of the macroscopic sphere may be written as

$$\mathbf{M}(t)=\mathbf{m}(t)+[\mathbf{M}_\infty(0)+\boldsymbol{\Delta}(-\infty,0)]\Phi(t)+A\int_0^t\mathbf{m}(t')[d\Phi(t-t')/dt]dt'+\boldsymbol{\Delta}(0,t),$$

for at an arbitrary time $t=0$ the system may be taken to be in an equilibrium configuration, and consequently the decay of the total polarization then existing in the outer region can be described by $\Phi(t)$. In the above expression the fluctuation term has been separated into two components, one, $\boldsymbol{\Delta}(-\infty, 0)$, representing the sum of all random events at time $t=0$ due to earlier fluctuations, and the other, $\boldsymbol{\Delta}(0, t)$, representing the sum of such effects at time t due to random events occurring between $t=0$ and $t=t$. The correlation function $\langle \boldsymbol{\mu}_0(0)\cdot\mathbf{M}(t)\rangle_0$ is therefore given by

$$\langle \boldsymbol{\mu}_0(0)\cdot\mathbf{M}(t)\rangle_0=\langle \boldsymbol{\mu}_0(0)\cdot\mathbf{m}(t)\rangle_0+\langle \boldsymbol{\mu}_0(0)\cdot[\mathbf{M}_\infty(0)+\boldsymbol{\Delta}(-\infty,0)]\rangle_0\Phi(t)+A\int_0^t\langle \boldsymbol{\mu}_0(0)\cdot\mathbf{m}(t')\rangle_0[d\Phi(t-t')/dt]dt'+\langle \boldsymbol{\mu}_0(0)\cdot\boldsymbol{\Delta}(0,t)\rangle_0.$$

As all fluctuations after $t=0$ are random and uncorrelated with $\boldsymbol{\mu}_0(0)$, the last term on the right-hand side of this expression vanishes. The second term on this side may be evaluated by noting that at $t=0$ the system is assumed to be in an equilibrium configuration. Using Kirkwood's results we therefore find that

$$\langle \boldsymbol{\mu}_0(0)\cdot[\mathbf{M}_\infty(0)+\boldsymbol{\Delta}(-\infty,0)]\rangle_0=-A\langle \boldsymbol{\mu}_0(0)\cdot\mathbf{m}(0)\rangle_0,$$

and consequently

$$\langle \boldsymbol{\mu}_0(0)\cdot\mathbf{M}(t)\rangle_0=\langle \boldsymbol{\mu}_0(0)\cdot\mathbf{m}(t)\rangle_0-A\langle \boldsymbol{\mu}_0(0)\cdot\mathbf{m}(0)\rangle_0\Phi(t)+A\int_0^t\langle \boldsymbol{\mu}_0(0)\cdot\mathbf{m}(t')\rangle_0[d\Phi(t-t')/dt]dt'.$$

Defining a microscopic relaxation function $\phi(t)$ as

$$\phi(t)=\langle \boldsymbol{\mu}_0(0)\cdot\mathbf{m}(t)\rangle_0/\langle \boldsymbol{\mu}_0(0)\cdot\mathbf{m}(0)\rangle_0, \qquad (8)$$

it follows from Eqs. (5) and (8) that

$$\Phi(t)=\phi(t)+A\int_0^t\phi(t')[d\Phi(t-t')/dt]dt'.$$

This integral equation expresses the relationship between the macroscopic decay function $\Phi(t)$ and the microscopic or molecular relaxation function $\phi(t)$

for a system of rigid dipoles. Its solution in terms of Laplace transforms is found to be

$$\mathfrak{L}[-d\Phi(t)/dt]=\mathfrak{L}[-\dot{\phi}(t)]/\{(1-A)+A\mathfrak{L}[-\dot{\phi}(t)]\}.$$

Equation (6) shows that

$$\mathfrak{L}[-d\Phi(t)/dt]=[(\epsilon^*-1)/(\epsilon^*+2)][(\epsilon_0+2)/(\epsilon_0-1)],$$

as we have assumed that $\epsilon_\infty=1$. Upon rearranging terms and introducing the value of A given by Eq. (7), we obtain

$$(\epsilon^*-1)/(\epsilon_0-1)$$
$$=\mathfrak{L}[-d\Phi_0(t)/dt]=\frac{(2\epsilon_0+1)\mathfrak{L}[-\dot{\phi}(t)]}{3\epsilon_0-(\epsilon_0-1)\mathfrak{L}[-\dot{\phi}(t)]},$$

$\Phi_0(t)$ being the decay function for dielectric polarization in a parallel plate condenser [cf. Eq. (4)].

At this point is is convenient to introduce a high-frequency dielectric constant ϵ_∞ into our expressions, supposing that high-frequency polarization, in effect, relaxes instantly. Defining new relaxation and decay functions to describe the behavior of noninstantly relaxing components of polarization through the equations

$$\mathfrak{L}[-\dot{\phi}(t)]=a+(1-a)\mathfrak{L}[-\dot{\phi}'(t)]$$
$$\mathfrak{L}[-d\Phi_0(t)/dt]=b+(1-b)\mathfrak{L}-d\Phi_0'(t)/dt$$
$$b=(\epsilon_\infty-1)/(\epsilon_0-1),$$

we find that

$$(\epsilon^*-\epsilon_\infty)/(\epsilon_0-\epsilon_\infty)=\frac{(2\epsilon_0+\epsilon_\infty)\mathfrak{L}[-\dot{\phi}'(t)]}{3\epsilon_0-(\epsilon_0-\epsilon_\infty)\mathfrak{L}[-\dot{\phi}'(t)]}. \quad (9)$$

Strictly speaking, according to our derivation this expression is only valid when the instantly relaxing component of polarization is due to permanent dipole moments. As, however, ϵ^* is not dependent on the frequencywise behavior of this polarization, but only on its magnitude as represented by ϵ_∞, we shall assume that Eq. (9) is correct regardless of the origins of the high-frequency polarization. Thus, if ϵ_∞ takes into account only induced polarization, then $\phi'(t)$ describes the reorientation of the permanent moments in a microscopic region. Equations (1) and (9) combine to yield

$$\epsilon^*-\epsilon_\infty=\frac{3(2\epsilon_0+\epsilon^*)}{2\epsilon_0+\epsilon_\infty}\left(\frac{\epsilon_\infty+2}{3}\right)^2\frac{4\pi N}{9kTV}\langle\mu_0\cdot\mathbf{m}\rangle_0$$
$$\times\mathfrak{L}[-\dot{\phi}'(t)]. \quad (10)$$

This expression is the dynamic analog of Eq. (1). It can readily be seen that it is not obtained by replacing ϵ_0 in Eq. (1) by ϵ^*, as proposed by others, for the right-hand side of this equation contains terms involving both ϵ_0 and ϵ^*.

Finally we note that if the microscopic relaxation function is characterized by a finite number of relaxation times, i.e.,

$$\mathfrak{L}[-\dot{\phi}'(t)]=\sum_{j=1}^{N}\frac{a_j}{1+i\omega\tau_j},$$

then it follows from Eq. (9) that

$$\mathfrak{L}[-d\Phi_0'(t)/dt]=\sum_{j=1}^{N}\frac{b_j}{1+i\omega T_j},$$

and, consequently, the number of decay times equals the number of relaxation times. In general, however, the relationship between the a_j, b_j, τ_j, and T_j is a quite complicated one.

IV. DECAY AND RELAXATION TIMES

A. One Relaxation Time

The simplest case of dielectric relaxation involves only one relaxation time τ_0, and therefore

$$\mathfrak{L}[-\dot{\phi}'(t)]=1/(1+i\omega\tau_0).$$

Substitution of this expression in Eq. (9) shows that there is also only one macroscopic decay time, and this is given by

$$T_0=[3\epsilon_0/(2\epsilon_0+\epsilon_\infty)]\tau_0. \quad (11)$$

This equation indicates that, as is usually supposed, the macroscopic decay time and the microscopic relaxation time do not greatly differ, and, in fact, Eq. (11) corresponds to Powles' expression [Eq. (3)].

B. Two Relaxation Times

For this particular case it has already been shown that there are also two macroscopic decay times. Thus we may write

$$\mathfrak{L}[-\dot{\phi}'(t)]=[a/(1+i\omega\tau_1)]+[(1-a)/(1+i\omega\tau_2)]$$
$$\mathfrak{L}[-d\Phi_0'(t)/dt]=[b/(1+i\omega T_1)]+[(1-b)/(1+i\omega T_2)]$$
$$b=(\epsilon_1-\epsilon_\infty)/(\epsilon_0-\epsilon_\infty),$$

the last of these equations defining a limiting high-frequency dielectric constant ϵ_1 for the low-frequency dispersion. The relationships between the three parameters characterizing each function may be found by substituting these expressions in Eq. (9). To see more easily how the macroscopic and microscopic functions differ, let us suppose that $\tau_2\gg\tau_1$. Then we find that

$$a/b=3\epsilon_0/(2\epsilon_0+\epsilon_1)$$
$$T_2/\tau_2=3\epsilon_0/(2\epsilon_0+\epsilon_1)$$
$$T_1/\tau_1=(2\epsilon_0+\epsilon_1)/(2\epsilon_0+\epsilon_\infty). \quad (12)$$

The first of these equations shows that the high-frequency macroscopic dispersion is always smaller than the corresponding microscopic dispersion. Both decay

times, on the other hand are always somewhat longer than their corresponding relaxation times.

C. Circular-Arc Function

In some studies of dielectric relaxation it has been found that relaxation cannot be described in terms of a finite number of decay times, but that it is necessary to consider a distribution of such times. In the frequently encountered case of the circular-arc function,[10]

$$\mathfrak{L}[-d\Phi_0'(t)/dt]=1/[1+(i\omega T_0)^{1-\alpha}]. \quad (13)$$

The logarithmic distribution of decay times characterizing this function is symmetric about the most probable decay time T_0, α being a measure of the width of the distribution. Substitution of the foregoing equation in Eq. (9) leads to an expression identical with Eq. (13) for $\mathfrak{L}[-\phi'(t)]$, except that T_0 is replaced by the most probable relaxation time τ_0, given by

$$T_0=[3\epsilon_0/(2\epsilon_0+\epsilon_\infty)]^{1/(1-\alpha)}\tau_0. \quad (14)$$

Consequently, the distribution of relaxation times is of the same form as that of decay times, but is symmetric about τ_0 instead of T_0.

D. Skewed-Arc Function

Another frequently occurring case involving a distribution of decay times is described by the skewed-arc function.[11] For this function

$$\mathfrak{L}[-d\Phi_0'(t)/dt]=1/(1+i\omega T_0)^\beta,$$

and the corresponding microscopic distribution function may be shown to be

$$F(\tau)=\left\{\frac{\sin\beta\pi}{\pi}\left(\frac{\tau}{T_0-\tau}\right)^\beta\right\}\left(\frac{3\epsilon_0}{2\epsilon_0+\epsilon_\infty}\right)\Big/\left\{\left[\left(\frac{\epsilon_0-\epsilon_\infty}{2\epsilon_0+\epsilon_\infty}\right)\times\left(\frac{\tau}{T_0-\tau}\right)^\beta+1\right]^2-2\left(\frac{\epsilon_0-\epsilon_\infty}{2\epsilon_0+\epsilon_\infty}\right)\left(\frac{\tau}{T_0-\tau}\right)^\beta(1-\cos\beta\pi)\right\}$$

$$\tau<T_0$$

$$=0 \qquad \tau>T_0. \quad (15)$$

The first bracketed term on the right-hand side of this expression corresponds to the distribution function for macroscopic decay times. As τ approaches T_0 this term becomes infinite. In contrast, the latter terms vanish at such a rate as τ approaches T_0 that

$$\lim_{\tau\to T_0}F(\tau)=0.$$

Both the macroscopic and microscopic distributions are asymmetric, however, and both have a low frequency cutoff at T_0.

ACKNOWLEDGMENTS

The author wishes to express his appreciation to Professor Robert H. Cole for many helpful discussions and suggestions concerning this work, and gratefully acknowledges fellowship grants from the Bell Telephone Laboratories, Inc.

[10] K. S. Cole and R. H. Cole, J. Chem. Phys. **9**, 341 (1941).
[11] D. W. Davidson and R. H. Cole, J. Chem. Phys. **19**, 1484 (1951).

Some Further Remarks on the Coefficient of Self-Diffusion in Simple Dense Fluids*

STUART A. RICE†

Department of Chemistry and Institute for the Study of Metals, University of Chicago, Chicago 37, Illinois

(Received February 26, 1960)

The self-diffusion coefficient in a simple dense fluid is calculated from the autocorrelation function of the momenta. If the randomization of momentum is rapid, the resultant diffusion coefficient differs from that first suggested by Kirkwood, Buff and Green by only $(2/\pi)^{\frac{1}{2}}$. The physical basis of this result is considered. A very simple method of demonstrating the necessity for molecular correlations in the approach to equilibrium is discussed.

I. INTRODUCTION

THE theory of transport in dense fluids has developed slowly over the past 15 years. If we temporarily put aside the fundamental question of the "nature of irreversibility," it must be recognized that the most successful line of attack is due to Kirkwood.[1,2] The central idea of this approach is that the average force exerted on a given molecule or a given pair of molecules by the rest of the system is analogous to the frictional force exerted by a fluid on a Brownian particle of semimacroscopic dimensions. Although this force may be expected to fluctuate rapidly in time, the implication of the above identification is that there exists a time scale on which the basic dynamical event may be considered to be independent of both prior and future events. The time evolution of the distribution function is then described only in coarse grained intervals of length τ, where τ is to be chosen by the criterion of independence stated. Within this framework Kirkwood was able to derive a generalized Fokker-Planck equation for the evolution of the distribution function. The friction constant which appears in this equation is formally related to the autocorrelation function of the intermolecular force acting on the molecule or group of molecules. In the subsequent theoretical development wherein the transport coefficients are related to integrals over the perturbation to the equilibrium distribution function,[3] the friction constant appears as a parameter. A power series solution of formal structure was obtained by Kirkwood for the autocorrelation representation of the friction constant but its numerical evaluation is much too difficult for practical use. Kirkwood, Buff, and Green[4] on the basis of a dimensional analysis suggested the relation

$$\zeta_0^2=(Nm/3v)\int\nabla^2 V g_0^{(2)}(R)d^3R, \tag{1}$$

with $g_0^{(2)}(R)$ the equilibrium pair correlation function, and V the pair interaction potential. More recently Rice and Kirkwood[5] have derived Eq. (1) by assuming that diffusion in a dense fluid proceeds by a series of displacements each small compared to the interatomic spacing. The analysis proceeds by time smoothing the force along this diffusive trajectory and using a distribution function which is Maxwellian about the local mean velocity and temperature in momentum space and at local equilibrium in configuration space. Collins and Raffel[6] have also derived Eq. (1) by a totally different method which utilizes the assumption that the initial curvature of a decay trajectory (of say the momentum of a "hot" molecule) is equal and opposite in sign to the curvature at later times. Due to assumptions made in the analyses neither of the above derivations constitutes a precise determination of the frictional coefficient in terms of the intermolecular forces. It is the purpose of this brief note to obtain a relationship for the frictional coefficient without the use of time smoothing or an explicit distribution function. It will, of course, be necessary to characterize the irreversibility of the motion in some suitable manner. We shall see in a particularly transparent manner that it is the nature of the intermolecular correlations which define the approach to equilibrium, and that in the absence of correlations between pairs of particles the diffusion coefficient is undefined.

II. SELF-DIFFUSION COEFFICIENT

The starting point of the development of this paper is the Liouville equation

$$Lf^{(N)}=-\partial f^{(N)}/\partial t \tag{2}$$

$$L=\sum_{j=1}^{N}[(\mathbf{p}_j/m)\cdot\nabla_{R_j}+\mathbf{F}_j\cdot\nabla_{p_j}], \tag{3}$$

* This work was suggested to the author by the late Professor J. G. Kirkwood when the latter was a visiting professor at The University of Chicago, February, 1959.

† Alfred P. Sloan Fellow.

[1] J. G. Kirkwood, J. Chem. Phys. **14**, 180 (1946).

[2] J. H. Irving and J. G. Kirkwood, J. Chem. Phys. **18**, 817 (1950).

[3] See, for example, R. W. Zwanzig, J. G. Kirkwood, K. Stripp, and I. Oppenheim, J. Chem. Phys. **21**, 2050 (1953); R. W. Zwanzig, J. G. Kirkwood, I. Oppenheim, and B. J. Alder, J. Chem. Phys. **22**, 783 (1954).

[4] J. G. Kirkwood, F. P. Buff, and M. Green, J. Chem. Phys. **17**, 988 (1949).

[5] S. A. Rice and J. G. Kirkwood, J. Chem. Phys. **31**, 901 (1959).

[6] F. C. Collins and H. Raffel, J. Chem. Phys. **29**, 699 (1958).

and the autocorrelation function definition of the self-diffusion coefficient

$$D=(3m^2)^{-1}\int_0^\infty \langle \mathbf{p}_1(t)\cdot\mathbf{p}_1(t+s)\rangle ds. \tag{4}$$

As usual $\mathbf{p}_j$, $\mathbf{R}_j$, and m are the momentum, position, and mass of molecule j, $f^{(N)}$ is the N-body distribution function, and $\mathbf{F}_j$ is the force exerted on molecule j by the $N-1$ other molecules of the system. Equation (4) is equivalent to the more familiar Einstein relation in which D is dependent upon the mean square displacement in a semimacroscopic time interval τ. To evaluate the integral in Eq. (4) it is convenient to use the formal properties of the Liouville operator. If $A(\mathbf{p}^{(N)}, \mathbf{R}^{(N)})$ is a dynamic variable, the evolution of A in time is governed by

$$A(t+s)=e^{sL}A(t), \tag{5}$$

whereupon Eq. (4) may be written

$$D=(3m^2)^{-1}\int_0^\infty \langle \mathbf{p}_1(t)\cdot e^{sL}\mathbf{p}_1(t)\rangle ds. \tag{6}$$

In both Eqs. (4) and (6) the average is to be performed over an equilibrium ensemble. The integral in Eq. (6) is most conveniently handled if use is made of the series expansion

$$\langle \mathbf{p}_1(t)\cdot e^{sL}\mathbf{p}_1(t)\rangle=\sum_{n=0}^\infty \langle \mathbf{p}_1(t)\cdot L^n\mathbf{p}_1(t)\rangle (s^n/n!). \tag{7}$$

There are two cases in which the evaluation may be performed without excessive difficulty. Since these two cases will correspond to interesting physical situations we restrict attention to them and consider no others.

It is instructive to proceed as far as possible with a general analysis before introducing a simplification. To this end, define the dyadic $\mathbf{A}_{2n}(l,k)$ by the relation

$$\mathbf{A}_{2n}(l,k)=\langle \mathbf{p}_l L^{2n}\mathbf{p}_k\rangle_{m0m}, \tag{8}$$

where the average is taken over the equilibrium momentum distribution. Now

$$L^{2n}=L^{2n-2}L^2 \tag{9}$$

and

$$L^2\mathbf{p}_k=\sum_{j_1=1}^N (\mathbf{p}_{j_1}/m)\cdot(\partial/\partial\mathbf{R}_{j_1})\mathbf{F}_k, \tag{10}$$

so that by substitution

$$\mathbf{A}_{2n}(l,k)=m^{-1}\sum_{j_1=1}^N \mathbf{A}_{2n-2}(l,j_1)\cdot(\partial/\partial\mathbf{R}_{j_1})\mathbf{F}_k. \tag{11}$$

If this procedure is repeated until a total of n operations have been carried out, it is seen that

$$\mathbf{A}_{2n}(l,k)=(1/m^n)\sum_{j_n=1}^N\cdots\sum_{j_1=1}^N \mathbf{A}_0(l,j_n)\cdot(\partial/\partial\mathbf{R}_{j_n})\mathbf{F}_{j_{n-1}}\cdot\cdots\cdot(\partial/\partial\mathbf{R}_{j_1})\mathbf{F}_k. \tag{12}$$

The diffusion coefficient depends not upon the dyadic $\mathbf{A}_{2n}(l,k)$ but rather upon the scalar $\mathrm{Tr}\langle \mathbf{A}_{2n}(k,k)\rangle_{\mathrm{conf}}$, where the dyadic is averaged over the equilibrium configurational distribution function. On using the well-known relation

$$\mathbf{A}_0(l,j_n)=3mkT\mathbf{1}, \tag{13}$$

and defining scalar coefficients B_{2n} by

$$3mkTB_{2n}=\mathrm{Tr}\langle \mathbf{A}_{2n}(k,k)\rangle_{\mathrm{conf}}, \tag{14}$$

we again easily find

$$B_{2n}=\mathrm{Tr}\{[(-)^n/m^n]\sum_{l_1\neq l}\sum_{l_2\neq l_1}^N\cdots\sum_{l_n\neq l_{n-1}}\times\langle(\nabla_{R_k}\nabla_{R_k}V_{l_1k})\cdot\cdots\cdot(\nabla_{R_k}\nabla_{R_k}V_{l_nk})\rangle\}. \tag{15}$$

Due to the nature of the average over an equilibrium ensemble, all odd terms in Eq. (7) vanish and we have as our final formal result,

$$\langle \mathbf{p}_k\cdot e^{sL}\mathbf{p}_k\rangle=\sum_{n=0}^\infty [s^{2n}/(2n)!]B_{2n}(k,k). \tag{16}$$

Case I

Consider now the simplification introduced if the ordered products of $\nabla\nabla V$ are considered uncorrelated. Each factor of $\nabla\nabla V$ then makes the same contribution and thereby from Eq. (15)

$$\tfrac{1}{3}B_{2n}=(-)^n[N\langle\nabla^2V\rangle/3m]^n. \tag{17}$$

The substitution of Eq. (17) into Eq. (16) and summation of the series gives

$$\langle \mathbf{p}_k\cdot e^{sL}\mathbf{p}_k\rangle=9mkT\cos[(N\langle\nabla^2V\rangle/3m)s], \tag{18}$$

clearly showing that D is undefined in this case. Thus the correlations between pairs of molecules are required for the approach to equilibrium.

Case II

If the frequency of dynamical events is very large, then we may anticipate that $\langle \mathbf{p}_1(t)\cdot\mathbf{p}_1(t+s)\rangle$ will vanish after a short time, and a suitable approximation to Eq. (6) will be obtained by retaining only the first few terms in the power series expansion. Thus,

$$\begin{aligned}\langle \mathbf{p}_1\cdot e^{sL}\mathbf{p}_1\rangle&=\langle \mathbf{p}_1\cdot\mathbf{p}_1\rangle+\langle \mathbf{p}_1\cdot L\mathbf{p}_1\rangle s+\langle \mathbf{p}_1\cdot L^2\mathbf{p}_1\rangle\tfrac{1}{2}s^2+\cdots\\&=3mkT[1-(N\langle\nabla^2V\rangle/6m)s^2+\cdots]\\&=3mkTf(s),\end{aligned} \tag{19}$$

since

$$\langle p_1^2\rangle=3mkT$$

$$\langle \mathbf{p}_1\cdot L\mathbf{p}_1\rangle=0$$

$$\langle \mathbf{p}_1\cdot L^2\mathbf{p}_1\rangle=kT\langle\nabla_{R_1}\cdot\mathbf{F}_1\rangle=-kT\sum_{j=2}^N\langle\nabla_{R_j}{}^2V_{1j}\rangle. \tag{20}$$

In order that the neglect of higher-order terms be valid, it is sufficient that $s^2 \ll 2m^2/\zeta_0^2$ with ζ_0^2 defined by Eq. (1). For the case of dense fluids this is likely to be satisfied. A suitable correlation function which reproduces the terms displayed in Eq. (19) and has the property of making the momenta independent after a short time interval is

$$f(s) = \exp[-(N\langle\nabla^2 V\rangle/6m)s^2], \tag{21}$$

a form similar to that used by Longuet-Higgins and Pople[7] in their study of the dense rigid-sphere fluid. The use of Eq. (21) leads to

$$D = (kT/2m)(6\pi m/N\langle\nabla^2 V\rangle)^{\frac{1}{2}}, \tag{22}$$

or

$$\zeta^2 = (2Nm/3\pi v)\int \nabla^2 V g_0^{(2)}(R)d^3R. \tag{23}$$

III. DISCUSSION

The purpose of this note has been to derive Eq. (23) without the explicit use of time smoothing and second to explore briefly the nature of the approach to equilibrium. We note that Eqs. (1) and (23) differ by the factor $2/\pi$. The calculated diffusion coefficient for liquid argon at 90°K is, from Eq. (1), 2.60×10^{-5} cm^2/sec,[5,6] and from Eq. (23), 3.25×10^{-5} cm^2/sec. The experiments of Corbett and Wang[8] give $D=2.06\times10^{-5}$ cm^2/sec. The worsening of the agreement suggests that we examine the nature of the approximations leading to Eq. (23). To obtain the specific form displayed we must have $s^2 \ll 2m^2/\zeta_0^2$. For the case of liquid argon $\zeta_0 = 4.8\times10^{-10}$ g/sec, whereupon s must be less than 10^{-13} sec to make the second term in Eq. (19) less than 20% of the lead term. For the case of the dense rigid sphere fluid Harris and Rice[9] have recently calculated the longest relaxation time for the return to equilibrium of a distribution perturbed in momentum space but always at equilibrium in configuration space. In the gas phase the time required corresponded to approximately four collisions. However at liquid densities, the time required corresponded to only one collision. Now, in a real fluid transfer of energy occurs continuously through the potential energy of interaction. Although no meaning can be assigned to the concept of a collision under these conditions, it is clear that significant energy exchanges must occur at a rate equal to or greater than that corresponding to the collision rate of the rigid sphere fluid at the same density. By extrapolation, we are led to the conclusion that the relaxation time in a real fluid should be equal to or less than the relaxation time for a rigid sphere fluid of the same density. Such a conclusion appears reasonable but requires detailed analytic verification. If correct, the truncation of the power series is justified.

We interpret the lack of agreement between calculation and experiment to mean that the assumed Gaussian form for the autocorrelation function is erroneous. In fact, the physical picture to which Eq. (1) conforms is one in which the selected molecule on the average moves quasi-randomly in the time τ. In a dense medium one would anticipate that a motion carrying the molecule away from the center of its "cell" and towards its near neighbors would be more likely to be followed by a motion with some nonvanishing component in the direction back towards the center of the "cell." Under these circumstances the autocorrelation function would oscillate about zero before asymptotically vanishing. The use of the Gaussian approximation implies that no such negative correlations exist and that each displacement is random relative to all other displacements. Since the diffusion coefficient is effectively determined by the area of the decaying autocorrelation function, the use of a Gaussian form for the envelope must lead to a value of the frictional coefficient which is too small. In the case of the hard sphere fluid the fact that relaxation in momentum space occurs after only a very few collisions makes the Gaussian approximation quite good in several respects. In the real fluid although the autocorrelation function may vanish after a very short time interval, negative correlations can never be neglected.

Of greater theoretical interest is the simple demonstration of the well-known fact that interactions are necessary for an approach to equilibrium. The model fluid to which the uncorrelated products of $\nabla\nabla V$ correspond is related to an Einstein model for the solid. That is, the lack of correlation is representative of a model in which the particle is assumed to move in a manner independent of all other molecules except for a simple coupling to the medium. Direct examination of Eq. (6) for more general "independent particle" models (i.e., a normal mode representation of the crystalline state) shows, in agreement with our previous arguments,[10] that interaction (anharmonicity) is required to permit the diffusive process to become dissipative. This result displays in a particularly simple manner some of the arbitrary assumptions ordinarily invoked in calculations of transport coefficients from simple models of the fluid state.

IV. ACKNOWLEDGMENT

The problem discussed in this short note and some of the preliminary calculations were suggested to the author by the late Professor J. G. Kirkwood. It was originally intended that this work be a joint publication, but Professor Kirkwood's untimely death prevented collaboration. The author alone is responsible for all the opinions and calculations contained herein.

[7] H. C. Longuet-Higgins and J. Pople. J. Chem. Phys. **25,** 884 (1956).
[8] J. W. Corbett and J. H. Wang, J. Chem. Phys. **25,** 422 (1956).
[9] R. A. Harris and S. A. Rice. (to be published).
[10] S. A. Rice and H. L. Frisch, J. Chem. Phys. **32,** 1026 (1960).

Scaled Particle Theory of Fluids

E. HELFAND, H. REISS, AND H. L. FRISCH
Bell Telephone Laboratories, Murray Hill, New Jersey
AND
J. L. LEBOWITZ*
Graduate School of Mathematical Sciences, Yeshiva University, New York, New York

(Received April 14, 1960)

A statistical thermodynamic theory has been developed employing distance scaling as a coupling procedure. This is an extension to real fluids of the technique applied by Reiss, Frisch, and Lebowitz to rigid-sphere systems. One considers molecules interacting with pair potential $u(r)$, except for one particle which interacts with potential $u(r/\lambda)$. This single particle, essentially a scaled version of a normal molecule, is termed a λ-cule. It is convenient to restrict discussion to potentials with rigid cores at $r=a$ and cutoffs at γa. Attention is focused on a function, $\Theta(\lambda, \rho, T)$, which reduces to G of footnote reference 1 in the case of rigid spheres. The pressure, chemical potential, and work of expanding a λ-cule are simply related to Θ. One can write Θ exactly for $\lambda<1/2\gamma$ and simple connection conditions hold at $\lambda=1/2\gamma$. An integral condition and $\lambda=\infty$ condition on Θ also exist. While Θ is not completely specified, the foregoing conditions determine much of its behavior.

1. INTRODUCTION

RESEARCH in the statistical mechanics of classical fluids, including the liquid state, has centered around the free volume-cell theories and the radial distribution-function method. These theories have been moderately successful in predicting thermodynamic properties. Recently Reiss, Frisch, and Lebowitz[1] (hereinafter referred to as I) have taken a somewhat new approach to the theory of rigid sphere systems and have been able to make striking quantitative predictions of the thermodynamic properties of such fluids. Reiss, Frisch, Helfand, and Lebowitz[2] have employed that method to allow calculation of certain select properties of real fluids.

The present work is another effort to extend to the treatment of real fluids the technique of I which we shall show is essentially the use of distance scaling as a coupling parameter. We shall concentrate on a function, Θ, which reduces in the rigid sphere limit to the G function of I. The Θ function can be made to play a role of central importance in the statistical thermodynamics of fluids. It is also closely related to several microscopic, nonthermodynamic quantities.

In the following section the Θ function will be defined and its relation to statistical thermodynamics and molecular processes will be elaborated. Under certain special, but no prohibitively restrictive conditions, it will be possible to display explicitly the expression for $\Theta(\lambda)$ when the argument λ, the distance scaling parameter, is small. We will then wish to say a bit about the analytical properties of Θ to aid in the extension of Θ to higher λ values. For λ very large, some exact conditions which the function must satisfy can be developed. Finally, there exists an integral condition which may aid in extrapolation.

In Sec. 5 a relation between the Θ function and the customary particle correlation functions will be developed.

2. DEFINITION OF THE Θ FUNCTION

Consider the statistical thermodynamics of a single component fluid in terms of the radial distribution function. Employing either the virial theorem[3] or the volume scaling method of Born and Green[3,4] the equation for the pressure may be written as

$$p/\rho kT=1-(\rho/6kT)\int_0^\infty r[du(r)/dr]g(r)4\pi r^2dr, \quad (2.1)$$

where p is the pressure, ρ the particle number density, k the Boltzmann constant, T the temperature, $u(r)$ the two-particle intermolecular potential, and $g(r)$ the radial distribution function normalized to unity at infinite r.

There are several methods of determining the chemical potential. An interesting technique which we shall focus attention on is the reversible coupling of a single particle to an equilibrium system of $(N\text{-}1)$ particles. Kirkwood[5] has employed the depth of the potential well as a coupling constant. This procedure has also been used partially by Reiss, Frisch, Helfand and Lebowitz[2] in the extension of I to the description of real fluids.

The rigid-sphere theory of I employs the sphere diameter as a coupling parameter. This is an example of a distance scaling coupling. Thus, the total potential energy of the fluid may be written as

$$U_N(\mathbf{r}_1, \cdots, \mathbf{r}_N; \lambda)=U_{N-1}(\mathbf{r}_2, \cdots, \mathbf{r}_N)+\sum_{i=2}^{N}u(r_{1i}/\lambda), \quad (2.2)$$

* Supported by the Air Force Office of Scientific Research.

[1] H. Reiss, H. L. Frisch, and J. L. Lebowitz, J. Chem. Phys. **31**, 369 (1959); *Proceedings of the 10th International Conference on Refrigeration, Copenhagen, August, 1959* (to be published).

[2] H. Reiss, H. L. Firsch, E. Helfand, and J. L. Lebowitz, J. Chem. Phys. **32**, 119 (1960).

[3] J. O. Hirschfelder, C. F. Curtiss, and R. B. Bird, *Molecular Theory of Gases and Liquids* (John Wiley & Sons, Inc., New York, 1954), p. 134.

[4] M. Born and H. S. Green, Proc. Roy. Soc. (London) **A191**, 168 (1947).

[5] J. G. Kirkwood, J. Chem. Phys. **3**, 300 (1935).

where $r_{1i} = |\mathbf{r}_i - \mathbf{r}_1|$. When $\lambda = 1$ particle 1 is fully coupled. When $\lambda = 0$ the potential u has argument ∞ for all values of r_{1i} so that u always is zero and particle 1 is fully decoupled. For other values of λ particle 1 is a scaled version of the other molecules. Such a scaled particle we shall term a λ-cule. The λ-cule may be regarded as a single solute particle and the remainder of the fluid as the solvent. Since the intermolecular potential has the functional form $u(r) = \epsilon\phi(r/a)$ we see that $u(r/\lambda) = \epsilon\phi(r/a\lambda)$. The λ-cule is thus to be pictured as a particle with characteristic distance λa rather than a but the same potential-well depth and ϕ function.

The coupling procedures for determining the chemical potential, μ, are based on the fact that

$$\mu = (\partial A/\partial N)_{V,T} = A(N, V, T) - A(N-1, V, T)$$
$$= kT \ln N\Lambda^3 - kT \ln(Z_N/Z_{N-1}), \quad (2.3)$$

where A is the Helmholtz free energy, N the number of particles (assumed large), V the volume, $\Lambda = h(2\pi mkT)^{-\frac{1}{2}}$, and Z is the configuration integral

$$Z(\lambda) = \int_V \cdots \int \exp[-U_N(\lambda)/kT] d\mathbf{r}_1 \cdots d\mathbf{r}_N, \quad (2.4)$$

with $Z(1) = Z_N$ and $Z(0) = VZ_{N-1}$. Equation (2.3) may be written as

$$\mu = kT \ln\rho\Lambda^3 - kT \int_0^1 \frac{\partial \ln Z(\lambda)}{\partial\lambda} d\lambda,$$

$$\frac{\partial \ln Z(\lambda)}{\partial\lambda} = -[kTZ(\lambda)]^{-1} \sum_{i=2}^{N} \int \frac{\partial u(r_{1i}/\lambda)}{\partial\lambda}$$
$$\times \left[\int \cdots \int \exp[-U_N(\lambda)/kT] \cdot \prod_{j=2, \neq i}^{N} d\mathbf{r}_j\right] d\mathbf{r}_i d\mathbf{r}_1. \quad (2.5)$$

We may write

$$\frac{\partial u(r/\lambda)}{\partial\lambda} = \frac{\partial(r/\lambda)}{\partial\lambda} \frac{\partial u(r/\lambda)}{\partial(r/\lambda)} = -(r/\lambda^2) u'(r/\lambda). \quad (2.6)$$

(N.B. The prime on u denotes differentiation with respect to the argument r/λ, not merely r.) The radial distribution function, $g(r, \lambda)$, defined by

$$\rho^2 g(r_{12}, \lambda) = [N(N-1)/Z(\lambda)] \int \cdots \int$$
$$\times \exp[-U_N(\lambda)/kT] d^3\mathbf{r}_3 \cdots d^3\mathbf{r}_N, \quad (2.7)$$

has the physical significance that $\rho g(r, \lambda)$ is the density of molecules at a distance r from a λ-cule. Combining these results we have for the chemical potential

$$\mu = kT \ln\rho\Lambda^3 - \rho a^3 \int_0^1 \lambda^2 d\lambda \int_0^\infty (r/\lambda) u'(r/\lambda) g(r, \lambda)$$
$$(4\pi r^2 dr/\lambda^3 a^3). \quad (2.8)$$

These results may be unified if we define a function $\Theta(\lambda, \rho, T)$ by

$$\Theta(\lambda, \rho, T) = -\int_0^\infty (r/\lambda) \frac{u'(r/\lambda)}{kT} g(r, \lambda) \frac{r^2 dr}{\lambda^3 a^3}. \quad (2.9)$$

The Θ function depends on the variable λ as well as the thermodynamic state specified by ρ and T. In this paper the T dependence will never explicitly be employed so that we shall not usually write it out. Frequently the ρ dependence will also be left implicit. The pressure and chemical potential may now be written in terms of Θ as

$$p/\rho kT = 1 + \tfrac{2}{3}\pi\rho a^3 \Theta(1, \rho), \quad (2.10)$$

and

$$\mu = kT \ln\rho\Lambda^3 + 4\pi\rho a^3 kT \int_0^1 \lambda^2 \Theta(\lambda, \rho) d\lambda. \quad (2.11)$$

Equations (2.10) and (2.11) are identical in form with equations appropriate to rigid sphere systems[1] with the contact distribution function $G(\lambda) = g(\lambda a+, \lambda)$ of I replaced by Θ.

Let us look further into the physical significance of the Θ function. In Eq. (2.11) for μ the ideal term $kT \ln\rho\Lambda^3$ accounts for the translational free energy and the entropy of mixing. The integral term is the work of adding the molecule at a fixed position. More generally, the average work of adding a λ-cule at a given position is

$$W(\lambda, \rho) = 4\pi\rho a^3 kT \int_0^\lambda \lambda'^2 \Theta(\lambda', \rho) d\lambda' \quad (2.12)$$

so that the work of expanding the λ-cule's characteristic distance from λa to $(\lambda + d\lambda)a$ at constant density is

$$dW(\lambda, \rho) = 4\pi\rho a^3 kT\lambda^2 \Theta(\lambda, \rho) d\lambda. \quad (2.13)$$

This relates Θ to the expansion work by

$$\Theta(\lambda, \rho) = (1/4\pi\rho a^3 kT\lambda^2)[\partial W(\lambda, \rho)/\partial\lambda]_\rho. \quad (2.14)$$

One reason for it being convenient to introduce the function W becomes clear upon examining the Mayer and Montroll[6] expression for this expansion work function. Referring again to Eqs. (2.2–4) it is seen that W may be written in terms of an activity coefficient $\Gamma(\lambda)$ as

$$W(\lambda, \rho) = -kT \ln[Z(\lambda)/Z(0)] = -kT \ln\Gamma(\lambda), \quad (2.15)$$

and that $Z(\lambda)/Z(0)$ may be expanded as

$$\Gamma(\lambda) = Z(\lambda)/Z(0)$$
$$= (VZ_{N-1})^{-1} \int \exp[-U_{N-1}(\mathbf{r}_2, \cdots, \mathbf{r}_N)kT]$$
$$\times \prod_{i=2}^{N} \exp[-u(r_{i1}/\lambda)/kT] d\mathbf{r}_1 \cdots d\mathbf{r}_N. \quad (2.16)$$

[6] J. E. Mayer and E. Montroll, J. Chem. Phys. 9, 2 (1941).

If the Mayer f function

$$f(s)=\exp(-u(s)/kT]-1 \tag{2.17}$$

is introduced and the product under the integral in Eq. (2.1) expanded in terms of the f's, and one integration is performed, we find

$$\Gamma(\lambda)=1+\sum_{m=1}^{N}(\rho^m/m!)\Phi_m(\lambda) \tag{2.18}$$

$$\Phi_1=\int f(r_{12}/\lambda)d\mathbf{r}_{12} \tag{2.19}$$

$$\Phi_m=\int\left[\prod_{i=2}^{m+1}f(r_{1i}/\lambda)\right]g^{(m)}(\mathbf{r}_2,\cdots,\mathbf{r}_{m+1})d\mathbf{r}_{12}\cdots d\mathbf{r}_{1,m+1} \tag{2.20}$$

where $g^{(m)}$ is the m particle correlation function[7] defined in the absence of the λ-cule.

Performing a change of variables, we may express Φ_1 in terms of the second virial coefficient:

$$\Phi_1=-2\lambda^3B=-(\tfrac{4}{3})\pi a^3\lambda^3B^*, \tag{2.21}$$

where

$$B=-\tfrac{1}{2}\int f(s)d\mathbf{s}=\tfrac{2}{3}\pi a^3B^* \tag{2.22}$$

and B^* is the second virial coefficient reduced by the value of the second virial coefficient of a rigid sphere system.

To gather further insight into Θ we shall consider its significance in the case of several types of molecular interactions.

3. MODEL POTENTIALS

Rigid Spheres

As previously stated the present development is a generalization of the rigid sphere theory of Reiss, Frisch, and Lebowitz.[1] In the rigid sphere case the potential has the form

$$u(r)=\begin{cases}\infty & r<a,\\ 0 & r>a.\end{cases} \tag{3.1}$$

Using the standard technique[1,7] for evaluating the integral involved in the definition of Θ, Eq. (2.9), we find

$$\Theta(\lambda,\rho)=g(\lambda a+,\lambda)\equiv G(\lambda a,\rho) \tag{3.2}$$

where G is the symbol used in I. The derivations employed here therefore serve as an alternative to the probability arguments used there.

Square Wells

The square well is among the simplest potentials capable of qualitatively exhibiting real fluid behavior,

[7] T. L. Hill, *Statistical Mechanics* (McGraw-Hill Book Company, Inc., New York, 1956), Chap. 6.

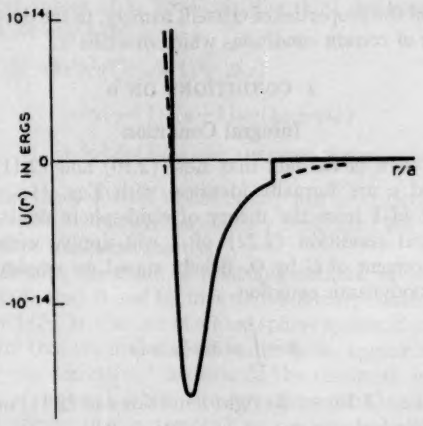

FIG. 1. Comparison of the finite range potential —— with the Lennard-Jones 6-12 potential ------ for argon.

e.g., a vapor-liquid transition. Therefore, we shall frequently specialize to this case in order to avoid undue complications in illustrating techniques. For a potential of the form

$$u(r)=\begin{cases}\infty, & r<a,\\ -\epsilon, & a<r<\gamma a,\\ 0, & \gamma a<r,\end{cases} \tag{3.3}$$

we find that the Θ function in terms of radial distribution functions is

$$\Theta(\lambda,\rho)=g(\lambda a+,\lambda)-\gamma^3\omega g(\gamma\lambda a+,\lambda), \tag{3.4}$$

where $\omega=[\exp(\epsilon/kT)-1]$.

Finite Range Potential

While we are discussing potential models, let us introduce one which will be quite useful in the subsequent discussion, and which is capable of quantitatively emulating real fluids. This potential has the form (cf., Fig. 1)

$$u(r)=\begin{cases}\infty, & r<a,\\ v(r), & a<r<\gamma a,\\ 0, & \gamma a<r,\end{cases} \tag{3.5}$$

where $v(r)$ is any suitable function, e.g., the Lennard-Jones 6–12. In such a case the rigid core cutoff might be chosen where $v(r)=0$. It will not strain matters too severely if we restrict γ to be less than 2. More general conditions are tractable but in places lead to a slightly more complicated formalism.

Hitherto we have discussed Θ primarily in terms of radial distribution functions. Our aim was to develop a physical description in terms of a quantity which has long been familiar. We will now proceed to a considera-

tion of the properties of Θ itself, namely, to the development of certain conditions which describe it.

4. CONDITIONS ON Θ

Integral Condition

In view of the fact that Eqs. (2.10) and (2.11) for p and μ are formally identical with Eqs. (1.1) and (2.9) of I from the theory of rigid-sphere fluids, the integral condition (2.22) of I will apply, with the replacement of G by Θ. Briefly stated we employ the thermodynamic equation

$$p=\int_0^\rho \rho(\partial\mu/\partial\rho)_T d\rho \tag{4.1}$$

with Eq. (2.10) on the right-hand side and (2.11) on the left. We find

$$\tfrac{2}{3}\pi\rho^2\Theta(1,\rho)=\rho^2\int_0^1 4\pi\lambda^2\Theta(\lambda,\rho)d\lambda - \int_0^\rho \rho' d\rho' \int_0^1 4\pi\lambda^2\Theta(\lambda,\rho')d\lambda \tag{4.2}$$

as an exact condition. This equation does not have a unique solution. Nevertheless it is evident that Eq. (4.2) strongly restricts the possible shape of the Θ function. In addition it is capable of telling us quite a bit about the density dependence of Θ when its dependence on λ is known. (Note the indefinite limit on the ρ integration as opposed to the definite limit on the λ integration.)

As in I it is possible to derive an integral equation for Θ with definite λ limits by considering the statistical mechanics of mixtures. Development of this point will be postponed until Sec. 5.

Value for Small λ

The exact expression for the Θ function may be determined for a range of small values of λ. This possibility arises as a consequence of the finite upper cutoff possessed by the intermolecular potential function [$u(r)=0$ for $r>\gamma a$]. There are several approaches to this calculation and we shall present two of them. The first is based on Eqs. (2.14)–(2.20).

According to the definition of the Mayer f function, f vanishes when u vanishes; i.e., $f(r/\lambda)=0$ for $r\geq\gamma\lambda a$. On the other hand it is a property of the radial distribution function that $g(r_{12})=0$ for $r_{12}<a$. Examining Eq. (2.20) for Φ_2 we see that for values of $\lambda<1/(2\gamma)$ there is no configuration of particles 1 and 2 such that the radial distribution function or one or the other of the f functions in the product does not vanish. The same argument applies to all higher order Φ_m, so that

$$\Phi_m(r,\lambda<1/2\gamma)=0 \qquad \text{for} \quad m\geq 2. \tag{4.3}$$

$\Theta(\lambda<1/2\gamma,\ \rho)$ may thus be expressed in terms of Φ_1 (i.e., the second virial coefficient) only, and by Eqs. (2.14), (2.15), (2.18), and (2.21), one finds

$$\Gamma(\lambda<1/2\gamma)=1-(\tfrac{4}{3})\pi\rho a^3\lambda^3 B^*, \tag{4.4}$$

$$\Theta(\lambda<1/2\gamma)=B^*/[1-(\tfrac{4}{3})\pi\rho a^3\lambda^3 B^*]. \tag{4.5}$$

Equation (4.5) may also be obtained directly from the definition of the Θ function, Eq. (2.9), by studying the radial distribution function $g(r,\lambda)$. The effective range of integration in (2.9) is $r<\gamma\lambda a$ where the potiential does not vanish. For values of $\lambda<1/2\gamma$ the λ-cule may be in interaction with but one molecule at a time. This is brought out in Fig. 2 where a molecule and λ-cule (with $\lambda<1/2\gamma$) are pictured as being in interaction. One notes that when the center of molecule 2 is inside the potential range of the λ-cule no other molecule can approach within $(\gamma\lambda a)$ of the λ-cule because of the rigid core sphere of exclusion of molecule 2. Thus the radial distribution function between molecules and λ-cules has the r dependence of a Boltzmann factor, $\exp[-u(r/\lambda)/kT]$. The prefactor, however, is not unity and to determine it, it is necessary to discuss the problem in a quantitative fashion.

The radial distribution function is defined to order $1/N$ by [cf. Eqs. (2.2), (2.4), and (2.7)]

$$g(r_{12},\lambda)=[V^2/Z(\lambda)]\int \exp[-U_{N-1}(\mathbf{r}_2,\cdots,\mathbf{r}_N)/kT] \times\prod_{i=2}^{N}\exp[-u(r_{1i}/\lambda)/kT]d\mathbf{r}_3\cdots d\mathbf{r}_N. \tag{4.6}$$

For the given range of r and λ particle 1 (the λ-cule) can interact only with particle 2, as was just explained, so that in the product which appears in the integrand only the $i=2$ term differs from unity. By expressing all distances relative to $\mathbf{r}_2$ we may write

$$g(r_{12},\lambda)=\{\exp[-u(r_{12}/\lambda)/kT]\}/\Gamma(\lambda). \tag{4.7}$$

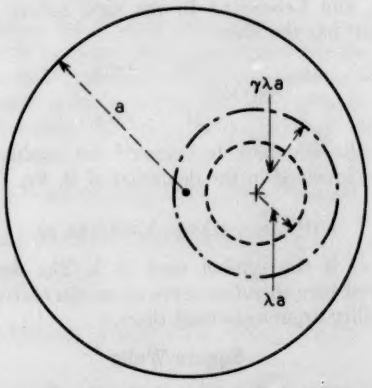

FIG. 2. A λ-cule with $\lambda<1/2\gamma$ in interaction with a molecule. Note that no other molecule can enter sphere of interaction of the λ-cule. + center of the λ-cule, · center of the molecule, ——— sphere of exclusion of molecule, ——— — range of interaction of λ-cule, — — — sphere of exclusion of λ-cule.

Using Eq. (4.4) for $\Gamma(\lambda)$ and inserting g into Eq. (2.9), we obtain

$$\Theta(\lambda<1/2\gamma) = -(a^3kT)^{-1}[1-(\tfrac{4}{3})\pi\rho a^3\lambda^3B^*] \times\int_0^\infty su'(s)e^{-u(s)/kT}s^2ds. \quad (4.8)$$

The integral on the right-hand side may be written as

$$-kT\int_0^\infty s^3\{d[e^{-u(s)/kT}-1]/ds\}ds,$$

so that an integration by parts yields Eq. (4.5) for $\Theta(\lambda<1/2\gamma)$.

Continuity Conditions

It is possible to study the analytic properties of Θ as a function of λ at $\lambda=1/2\gamma$, and in particular the continuity of Θ and its derivatives. The chain of reasoning we shall use will be to show that the first discontinuous derivative of $\mathbf{y}(\lambda)$ at $1/2\gamma$ is the third, which implies, by Eq. (2.15), that $W(\lambda)$ and its first two derivatives are continuous. This, in turn, leads one, by Eq. (2.14), to the conclusion that Θ and its first derivative are continuous at $\lambda=1/2\gamma$.

As seen previously, up to $\lambda=1/2\gamma$ the function $\mathbf{y}(\lambda)$ is given in terms of $\Phi_1(\lambda)$ which has been evaluated in Eq. (2.21) and which is continuous. At $\lambda=1/2\gamma$ the function Φ_2 enters Γ since now two f's can be simultaneously nonzero (Φ_m, $m\geq3$ still vanishes). Thus we may concentrate on a study of the continuity properties of Φ_2.

To simplify the discussion let us restrict consideration, at first, to the square well model. For such a potential it is possible to greatly simplify Φ_2; viz., all but one of the sixfold integrations may be performed. One finds that[8]

$$\Phi_2 = -8\pi^2\{(\omega+1)^2L(\lambda,\lambda)-2(\omega+1)\omega[L(\gamma,\gamma\lambda) - L(-\gamma,\gamma\lambda)]+\omega^2L(\gamma\lambda,\gamma\lambda)\}, \quad (4.9)$$

where $\omega=\exp(\epsilon/kT)-1$, ϵ is the depth of the well, and L is the integral

$$L(u,v) = -(\tfrac{1}{2}\gamma)a^6\int_0^{u+v} sg(sa) \times[s^4-6s^2(u^2+v^2)+8s(u^3+v^3)-3(u^2-v^2)^2]ds. \quad (4.10)$$

In this form the derivatives may be explicitly taken and examined. One finds that Φ_2, $d\Phi_2/d\lambda$, and $d^2\Phi_2/d\lambda^2$ are continuous *for all values of* λ. The third derivative $d^3\Phi_2/d\lambda^3$ has a discontinuity at $\lambda=1/2\gamma$ (recall that this is the first point for which $\Phi_2\not\equiv0$) as well as at many greater values of λ. Explicitly the third derivative is given for any λ by

$$d^3\Phi_2/d\lambda^3 = 8\pi^2\lambda^3a^6[8(\omega+1)^2g(2\lambda a) -\gamma(\gamma+1)^4(\omega+1)\omega g(\lambda a+\gamma\lambda a) +8\gamma^6\omega^2g(2\gamma\lambda a)]+\text{continuous part}, \quad (4.11)$$

so that the points of discontinuity are determined by those of the radial distribution function. We shall return to this point shortly.

Following the chain of reasoning outlined earlier we conclude that Θ and its first derivative are continuous at $\lambda=1/2\gamma$. In the case of a hard sphere system it can be shown[1] that the first discontinuities in Φ_m appear in the $(2m-1)$ derivative.[9] Because of the similarity in the type of integral which appears for square well and hard sphere one is tempted to conjecture that this result applies also to the more general potential. If this is the case then one would have that Θ and its first derivative are continuous for all λ.

By means of a change of variables in Eq. (2.20) for Φ_m one can shift points of view on this continuity problem. Thus, write

$$\Phi_m=\lambda^m\int\left[\prod_{i=2}^{m+1}f(z_{1i})\right] \times g^{(m)}(\lambda z_{12},\cdots,\lambda z_{1,m+1})dz_{12}\cdots dz_{1,m+1}, \quad (4.12)$$

from which it is seen that the analytic properties of Φ_m are totally related to the analytic properties of $g^{(m)}$.

While attention has been confined to the square well in this section the results are actually quite general. The discontinuities in the f function are what lead to discontinuous Θ derivatives. Whether f is flat between discontinuities or not is unimportant. As a matter of fact if f were completely analytic Θ would be analytic. However, if f undergoes drastic changes in short, but finite distance, as it is known to do physically, Θ would also change drastically in nature with a small, but finite, increment of λ.

Infinity Condition

When the λ-cule becomes very large it is possible to consider its effects from the point of view of macroscopic thermodynamics. In the case of a rigid-sphere potential (footnote reference 1) the λ-cule behaves like a rigid wall. Θ for hard spheres is related to the density of molecules at the wall, while this density, in turn, is directly proportional to the pressure. The infinity condition for a more general potential is not as simple, but one still can be found. Once again the salient features of the derivation are brought out most clearly when discussion is restricted to the square well potential. Let us consider a system with a very large λ-cule in its interior. The volume of the system, V, may be

[8] The calculation is quite extensive, although for the most part straightforward. Converting to bipolar coordinates renders three of the variables of integration redundant. Two more of the variables appear only in the limits of integration. One proceeds further by inverting the order of integration to make the $s=r_{23}$ integration the last. Extensive use may be made of symmetry if one defines $g(-s)=g(+s)$.

[9] Φ_m corresponds to the function $(-1)^mF_m$ of I.

divided into three regions. Part 1, of volume $V_1 = V - (\frac{4}{3})\pi\lambda^3 a^3$, is outside the sphere of interaction of the λ-cule. Volume 2, $V_2 = \frac{4}{3}\pi(\gamma^3-1)\lambda^3 a^3$, is within the well of the λ-cule. Region 3 is the exclusion sphere of the λ-cule. For the present discussion we will consider the total system to be infinite. The λ-cule is now also taken as approaching infinity but with $(V_2+V_3)/V \to 0$. In this way the over-all density is unaffected by its presence. The work of expanding the λ-cule is related to the Helmholtz free energy of the system A by

$$dW = dA = -\sum_{i=1}^{3} p_i dV_i + \sum_{i=1}^{3} \tilde{\mu}_i dN_i + \text{surface of } \lambda\text{-cule terms.} \quad (4.13)$$

The summations are over the three regions. The surface terms are of higher order in $1/\lambda$ and may be neglected here. The pressure p_3 is zero since no particles can get inside 3. The important volume changes may be related to $d\lambda$ by the expressions in the earlier part of this paragraph. The total chemical potentials, $\tilde{\mu}_i$, include the effect of the λ-cule's field, and must be equal in the equilibrium condition. There are no molecules in region 3 so $dN_3 = 0$, and therefore $dN_1 = -dN_2$. On using these facts with Eq. (2.13) we may write

$$dW = 4\pi\lambda^2\rho_1 a^3 kT\Theta(\infty, \rho_1)d\lambda,$$
$$= 4\pi\lambda^2 a^3\gamma^3 p_1 d\lambda - 4\pi\lambda^2 a^3(\gamma^3-1)p_2 d\lambda. \quad (4.14)$$

The pressures may be expressed in terms of Θ functions by Eq. (2.10) so that one obtains as a condition relating $\Theta(\infty)$ to $\Theta(1)$

$$\rho_1\Theta(\infty, \rho_1) = \gamma^3[\rho_1 + \tfrac{2}{3}\pi a^3\rho_1^2\Theta(1, \rho_1)]$$
$$= (\gamma^3-1)[\rho_2 + \tfrac{2}{3}\pi a^3\rho_2^2\Theta(1, \rho_2)]. \quad (4.15)$$

This equation is actually somewhat complex in that ρ_2 is a function of ρ_1. A relation between these two densities arises from the condition

$$0 = \tilde{\mu}_2 - \tilde{\mu}_1 = (\mu_2 - \epsilon) - \mu_1, \quad (4.16)$$

which yields, by Eq. (2.11),

$$\epsilon/kT = \ln(\rho_2/\rho_1) + 4\pi a^3\int_0^1 \lambda^2[\rho_2\Theta(\lambda, \rho_2) - \rho_1\Theta(\lambda, \rho_1)]d\lambda, \quad (4.17)$$

to be considered simultaneously with Eq. (4.15).

The case of hard spheres may be obtained by specializing to $\gamma = 1$ with finite ϵ, or by letting $\epsilon = 0$. In either limit Eq. (3.14) reduces to

$$\Theta_{HS}(\infty, \rho) = G(\infty, \rho) = p/\rho kT,$$

where G is the notation of I.

5. A MORE GENERAL INTEGRAL EQUATION FROM THE MIXTURE VIEWPOINT

In footnote reference 1 the possibility of writing a determinate integral equation for G by considering dilute mixtures of λ-cules in molecules was exploited. It is easily shown that the parallelism between Θ and G applies here and one may write the same equation for real fluids; viz.,

$$Q(\lambda, \rho) = -\rho a^3(\partial/\partial\rho)\{\rho\int_0^\lambda 4\pi\lambda^2\Theta(\lambda, \rho)d\lambda\} + \tfrac{4}{3}\pi\rho a^3\lambda^3\Theta(\lambda, \rho), \quad (5.1)$$

where

$$Q(\lambda, \rho) = -\tfrac{2}{3}\pi a^3\rho^2[\partial\Theta(1, \rho)/\partial\rho_\lambda]_{\rho_\lambda \to 0}. \quad (5.2)$$

With the definition of Θ, Eq. (2.9), we obtain

$$Q(\lambda, \rho) = \tfrac{2}{3}\pi\rho^2\int_0^\infty ru'(r)[\partial g_{mm}(r, \rho, \rho_\lambda)/\partial\rho_\lambda]_{\rho_\lambda \to 0} r^2 dr, \quad (5.3)$$

where $g_{mm}(r, \rho, \rho_\lambda)$ is the molecule-molecule radial distribution function in a mixture with molecule density ρ and λ-cule density ρ_λ.

In order to develop further insight into the Q function it is of interest to find another expression for it in terms of correlation functions. The ρ_λ derivative of g_{mm} may be written as

$$V^{-1}[\partial g_{mm}/d\rho_\lambda]_{\rho_\lambda \to 0} = [\partial g_{mm}/\partial N_\lambda]_{N_\lambda \to 0}$$
$$= g_{mm}(N_\lambda = 1) - g_{mm}(N_\lambda = 0), \quad (5.4)$$

where N_λ is the number of λ-cules. Now if the presence of a single λ-cule is reflected in g_{mm} by specification of the value of λ, i.e., $g_{mm}(\lambda)$, then

$$V^{-1}[\partial g_{mm}/\partial\rho_\lambda]_{\rho_\lambda \to 0} = g_{mm}(\lambda) - g_{mm}(0)$$
$$= \int_0^\lambda [\partial g_{mm}(\lambda')/\partial\lambda']d\lambda'. \quad (5.5)$$

The molecule correlation function $g_{k_1,\cdots,k_n}^{(n)}(\mathbf{r}_{k_1}, \cdots, \mathbf{r}_{k_n}, \lambda)$ ($g_{mm}^{(2)}$ is the radial distribution function g_{mm}) may be expressed to order $1/(N-n)$ as

$$g_{k_1\cdots k_n}^{(n)}(\lambda) = [V^n/Z(\lambda)]\int_V \cdots \int_V \times \exp[-U_N(\lambda)/kT] \prod_{j=1,\neq k_1\cdots k_n}^{N} d\mathbf{r}_j, \quad (5.6)$$

where the λ-cule is particle 1. Differentiating $\ln g_{23}^{(2)}(r_{23}, \lambda)$ with respect to λ, multiplying by $g_{23}^{(2)}(\lambda)$, and introducing higher-order correlation functions yields, after some manipulations,

$$\frac{\partial g_{23}^{(2)}(\lambda)}{\partial\lambda} = \frac{(N-3)}{kTV^2}\iint\frac{\partial u(r_{14}/\lambda)}{\partial\lambda} \times [g_{14}^{(2)}(\lambda)g_{23}^{(2)}(\lambda) - g_{1234}^{(4)}(\lambda)]d\mathbf{r}_1 d\mathbf{r}_4 + \frac{2}{kTV}\int\frac{\partial u(r_{12}/\lambda)}{\partial\lambda} \times [g_{12}^{(2)}(\lambda)g_{23}^{(2)}(\lambda) - g_{123}^{(3)}(\lambda)]d\mathbf{r}_1. \quad (5.7)$$

Employing (5.4), (5.5), and (2.6), we arrive at

$$[\partial g_{23}^{(2)}/\partial\rho_\lambda]_{\rho_\lambda\to 0}=[(N-3)/kT]\int_0^\lambda \lambda'^2 d\lambda' \iint (r_{14}/\lambda')u'(r_{14}/\lambda')[g_{1234}^{(4)}(\lambda')-g_{14}^{(2)}(\lambda')g_{23}^{(2)}(\lambda')](d\mathbf{r}_1 d\mathbf{r}_4/\lambda'^3)$$

$$+(2/kT)\int_0^\lambda \lambda'^2 d\lambda' \int (r_{12}/\lambda')u'(r_{12}/\lambda')[g_{123}^{(3)}(\lambda')-g_{12}^{(2)}(\lambda')g_{23}^{(2)}(\lambda')](d\mathbf{r}_1/\lambda'^3), \quad (5.8)$$

which may be substituted immediately into Eq. (5.3) for Q. It is to be noted that important contributions to both integrals of Eq. (5.8) come only from the region where the λ-cule, particle 1, is near the pair 2,3. In the second integral this is evident from the short range nature of $u(r_{12}/\lambda)$. In the first integral the potential $u(r_{14}/\lambda)$ requires that 1 be near 4. Thus when 1 is far from 2, 3, so is 4. The particles are then correlated only in pairs so that $g_{1234}^{(4)}=g_{14}^{(2)}g_{23}^{(2)}$ and the integrand vanishes.

It will be convenient to examine certain properties of Q by referring to the hard sphere case. In this instance Eq. (5.3) becomes

$$Q_{HS}(\lambda,\rho)=-\tfrac{3}{8}a^3\rho^2\left[\frac{\partial g_{23}^{(2)}(r_{23}=a,\lambda)}{\partial\rho_\lambda}\right]_{\rho_\lambda\to 0}. \quad (5.9)$$

Let us consider the value of Q for $\lambda\leq\frac{1}{2}$. In the first integral of Eq. (5.8), because of the $\delta(r_{14}-\lambda a)$ nature of $u'(r_{14}/\lambda)$, the λ-cule must be wholly inside of particle 4 for a nonvanishing integrand. In this case the λ-cule cannot be in contact with, or in any way influence, any particle except 4, so that

$$g_{1234}^{(4)}(\lambda)=g_{14}^{(2)}(\lambda)g_{234}^{(3)}(\lambda), \qquad \lambda<\tfrac{1}{2}. \quad (5.10)$$

The first integral may be written, for $\lambda<\frac{1}{2}$, as

$$[(N-3)/kT]\int_0^\lambda (d\lambda'/\lambda'^2)\int r_{14}u'(r_{14}/\lambda')g_{14}^{(2)}(\lambda')d\mathbf{r}_{14}\{\int[g_{234}^{(3)}(\lambda')-g_{23}^{(2)}(\lambda')]d\mathbf{r}_4\}. \quad (5.11)$$

By definition of the correlation function, Eq. (5.6), the expression in { } vanishes. In the second integral on the right-hand side of (5.8) the λ-cule must be totally inside of particle 2 so that

$$g_{123}^{(3)}(\lambda)=g_{12}^{(2)}(\lambda)g_{23}^{(2)}(\lambda), \quad \lambda<\tfrac{1}{2}, \quad (5.12)$$

and this term also vanishes. Thus, for $\lambda<\frac{1}{2}$ in the hard sphere case we have $Q_{HS}(\lambda<\frac{1}{2},\rho)=0$, a result already obtained in I in a different manner.

Similar results may be demonstrated for the general case of a potential with core at a and cutoff at γa. In this instance we have

$$Q(\lambda,\rho)=0, \qquad \lambda\leq 1/2\gamma. \quad (5.13)$$

It is easily shown that the $\Theta(\lambda<1/2\gamma)$ of Eq. (4.5) is a solution of Eq. (4.1) when $Q=0$.

Kinetic Theory of Dense Gases*

HENRY B. HOLLINGER† AND C. F. CURTISS

University of Wisconsin Theoretical Chemistry Laboratory, Madison, Wisconsin

(Received April 6, 1960)

The Boltzmann equation is found to be determined to arbitrary order in the density as a consequence of the molecular chaos assumption. A three-body collision approximation is given explicitly and shown to be identical to that implied by the Bogolyubov assumptions; the relation between the molecular chaos assumption and the Bogolyubov assumptions is discussed. It is shown that the Enskog modification of the Boltzmann equation for dense gases composed of rigid spheres is correct, subject to the molecular chaos assumption. The current disagreement over the correct form for this equation is discussed.

I. INTRODUCTION

THE kinetic theory of dense gases has been based largely on a modified Boltzmann equation proposed by Enskog[1] in 1922 as an equation for rigid spheres. The Enskog theory has been found to be good for dense gases composed of rigid spheres as studied by high-speed computing techniques,[2] and it has been useful in the development of semiempirical formulas for transport coefficients in real gases.

In recent years the role of statistical mechanics in kinetic theory has been emphasized and various attempts have been made to derive the Boltzmann equation and its Enskog modification from the Liouville equation. Derivations of the dilute-gas Boltzmann equation appeared[3–6] in 1946 and stimulated interest in the use of the latter to obtain equations such as the Enskog equation for dense gases.

It was found by Born and Green that the "molecular chaos" assumption used by Boltzmann in his intuitive derivation of the dilute-gas equation is a sufficient assumption in the derivation of the Boltzmann equation from the Liouville equation. An approximation is involved in the derivation, the binary-collision approximation, but it is shown in this paper that correction terms for higher order collisions may be included. The correction term for dense gases in the binary-collision approximation was considered by Green[7] and the kinetic theory of dense gases has been developed to this approximation[8]; the results are consistent with the Enskog theory.

In a theory proposed by Bogolyubov[5,6] a hierarchy of ensemble distribution functions is considered and each function is assumed to be a functional of the one-particle distribution function f. Additional assumptions are introduced and an equation for f is obtained. In the binary-collision approximation this theory gives essentially the same Boltzmann equation as that obtained by Born and Green. A formulation of this theory has recently been given by Choh and Uhlenbeck.[9,10] Thus a kinetic theory to the ternary-collision approximation is available and dependent on the ternary-collision dynamics.

The time-smoothing technique introduced by Kirkwood[3] in his derivation of the dilute-gas Boltzmann equation has been used in a derivation of an equation for dense gases composed of rigid spheres.[11] The results obtained are not consistent with any of the aforementioned results and are of considerable interest at the present time because a number of papers have recently been presented in support of the Enskog modification of the Boltzmann equation.[12–14] There is, then, some controversy over the form of this equation and the issue is not the proper use of the molecular chaos assumption but rather is the proper form of the inhomogeneous equation of change for the one-particle distribution function before any assumptions are introduced. It is felt by the authors that the issue has been settled[10,12–14]; further discussion of this problem is given below.

In the present paper the molecular chaos assumption is used to derive a Boltzmann equation for dense gases from the Liouville equation; the derivation is carried explicitly to the ternary-collision approximation where

* This research was carried out under the National Science Foundation at the University of Wisconsin Theoretical Chemistry Laboratory and is based in part on a thesis submitted by Henry B. Hollinger to the University of Wisconsin in partial fulfillment of the requirements for the Ph.D. degree.

† Present address: Department of Chemistry, Lebanon Valley College, Annville, Pennsylvania.

[1] D. Enskog, Kgl. Svenska Vetenskaps akad. Handl. **63**, No. 4 (1922).

[2] I. Prigogine, editor, *Proceedings of the International Symposium on Transport Processes in Statistical Mechanics* (Interscience Publishers, Inc., New York, 1958). See the article by B. J. Alder and T. Wainwright.

[3] J. G. Kirkwood, J. Chem. Phys. **14**, 180 (1946).

[4] M. Born and H. S. Green, *A General Kinetic Theory of Liquids* (Cambridge University Press, New York, 1949).

[5] N. N. Bogolyubov, J. Phys. (U.S.S.R), **10**, 256 (1946).

[6] N. N. Bogolyubov, *Problemy Dinamicheskoi Teorii v Statistichestoi Fisike* (Technical Press, Moscow, 1946).

[7] H. S. Green, *Molecular Theory of Fluids* (North Holland Publishing Company, Amsterdam, 1952).

[8] R. F. Snider and C. F. Curtiss, Phys. Fluids **1**, 122 (1958).

[9] G. E. Uhlenbeck, "The Boltzmann equation," University of Michigan publication, Navy Theoretical Physics (1957).

[10] S. T. Choh, dissertation, University of Michigan, 1958.

[11] S. A. Rice, J. G. Kirkwood, J. Ross, and R. W. Zwanzig, J. Chem. Phys. **31**, 575 (1959).

[12] J. T. O'Toole and J. S. Dahler, J. Chem. Phys. **32**, 1487 (1960).

[13] C. F. Curtiss, University of Wisconsin Theoretical Chemistry Laboratory publication, WIS-NSF-14 (1959).

[14] H. B. Hollinger, dissertation, University of Wisconsin, 1959.

it is found to be consistent with the Bogolyubov theory as formulated by Choh and Uhlenbeck. The gas considered is not confined to a fixed space by the presence of walls; the interaction potential is continuous except at the origin. The rigid-sphere case is considered by regarding the rigid potential as the limit of a sequence of continuous potentials and the Enskog form of the Boltzmann equation is obtained. The case of a discontinuous interaction potential is discussed elsewhere[14] and the Enskog form obtained directly from the Liouville theorem.

In Sec. II the model is described and the Liouville theorem is expressed in the form of equations on spaces smaller than phase space. In Sec. III a Boltzmann equation is derived by introducing the molecular chaos assumption. In Sec. IV the Enskog equation for rigid spheres is obtained; in Sec. V the alternative form of this equation mentioned above is discussed. In Sec. VI the relation between the present work and that of Bogolyubov, Uhlenbeck, and Choh is discussed.

II. THE LIOUVILLE THEOREM

In this section the Liouville theorm is expressed in various forms and the model considered is described using a notation due largely to Uhlenbeck and Choh.[9,10] We consider a dynamical system containing N particles for which the Hamiltonian is

$$H=(2m)^{-1}\sum_{i=1}^{N}p_i^2+\Phi(\mathbf{r}_1, \mathbf{r}_2, \cdots, \mathbf{r}_N).$$

The potential Φ is a sum:

$$\Phi=\sum_{i=1}^{N}\sum_{j=1}^{i-1}\phi_{ij},$$

where $\phi_{ij}=\phi(|\mathbf{r}_i-\mathbf{r}_j|)$ is the two-body interaction potential; $\phi(r)$ and its first two derivatives are continuous on $0<r<\infty$ so that particle trajectories and their first partial derivatives may be continuous functions of initial points; $\phi\to\infty$ as $r\to 0$ so that two particles in a system of finite energy may never coalesce. At an initial time t the system is contained in a definite volume $V(t)$ but is not required to remain there.

The following notation is used:

$$x_i=(\mathbf{r}_i, \mathbf{p}_i)$$

$$\mathbf{r}^s=(\mathbf{r}_1, \mathbf{r}_2, \cdots, \mathbf{r}_s)$$

$$x^s=(x_1, x_2, \cdots, x_s)$$

$$dx_i=d\mathbf{r}_i d\mathbf{p}_i$$

$$dx^s=dx_1 dx_2\cdots dx_s$$

$$dx^{N-s}=dx_{s+1}dx_{s+2}\cdots dx_N$$

$$r_{ij}=|\mathbf{r}_i-\mathbf{r}_j|$$

$$p_{ij}=|\mathbf{p}_i-\mathbf{p}_j|.$$

The phase space $X^{(s)}$ is a domain in the $6s$-dimensional Euclidean space of x^s defined by: x^s is in $X^{(s)}$ means $r_{ij}>0$ for every pair $(i, j\neq i)\leq s$. The interval T is $-\infty<t<\infty$. The $6s+1$-dimensional space of (x^s, t), x^s in $X^{(s)}$ and t in T, is denoted $X^{(s)}\cdot T$.

For an ensemble of systems with the given $H(x^N)$, V, and with energies distributed over a bounded interval, we let $f^{(N)}$ be the function defined on $X^{(N)}\cdot T$, which gives the density of points, representing systems in the ensemble, which are in an element dx^N containing x^N at time t. Two types of conditions are to be satisfied by $f^{(N)}$; conditions which are called "requirements" may be interpreted as restrictions on the ensemble at an initial time; conditions which are called "properties" are implied by requirements.

The function $f^{(N)}$ is required to be continuous on $X^{(N)}$ at time t; it will be shown that $f^{(N)}$ is continuous on $X^{(N)}\cdot T$. Thus the integral $\int dx^{N-s}f^{(N)}$ exists and has the same property on $X^{(s)}\cdot T$. The function $f^{(N)}$ is required to satisfy the arbitrary normalization condition

$$\int dx^N f^{(N)}=\alpha_N. \tag{1}$$

Since the momenta in the ensemble are bounded, $f^{(N)}$ satisfies the boundary condition

$$f^{(N)}\to 0 \quad \text{as} \quad |\mathbf{p}_i|\to\infty. \tag{2}$$

Since $V(t)$ is finite, $f^{(N)}$ satisfies the boundary condition

$$f^{(N)}\to 0 \quad \text{as} \quad |\mathbf{r}_i|\to\infty, \tag{3}$$

which remains as a property on T by virtue of the bound on the momenta in the ensemble. The conditions (2, 3) together with the Liouville theorem imply that α_N in (1) is a constant on T. The function $f^{(N)}$ is required to satisfy the symmetry condition

$$f^{(N)}(x_1, x_2, \cdots, x_i, x_j, \cdots, x_N, t) = f^{(N)}(x_1, x_2, \cdots, x_j, x_i, \cdots, x_N, t), \tag{4}$$

which remains as a property on T by virtue of Liouville's theorem.

The transformation $e^{\tau\kappa_s}$ on $X^{(s)}$ is defined by

$$e^{\tau\kappa_s}x_i=y_i(x^s, \tau), \tag{5}$$

where $y_i(x^s, \tau)$ is the point in the space of x_i reached by particle i in time τ if s interacting particles are placed at x^s and allowed to carry out the classical motion prescribed by κ_s. The Liouville theorem may be expressed in the form

$$f^{(N)}(x^N, t+\tau)=e^{-\tau\kappa_N}f^{(N)}(x^N, t)=f^{(N)}(e^{-\tau\kappa_N}x^N, t). \tag{6}$$

We now show that $f^{(N)}$ is continuous on $X^{(N)}\cdot T$. The interval T' is $-\infty<\tau<\infty$; the function $e^{\tau\kappa_s}x^s$ is continuous on $X^{(s)}\cdot T'$ by virtue of the form of Hamilton's equations of motion. Since a continuous function

of a continuous function of τ, fixed $x^{(N)}$, is itself continuous in τ, the continuity of $f^{(N)}$ in time is clearly implied by (6). The continuity of $f^{(N)}$ on $X^{(N)}$ at arbitrary $t+\tau$ is similarly implied by (6), for if $f^{(N)}$ is continuous on $X^{(N)}$ at the initial time t, then for arbitrary $\epsilon>0$ we can find $\delta(\epsilon)>0$ so that $|x^N-\bar{x}^N|<\delta$ implies $|f^{(N)}(x^N, t)-f^{(N)}(\bar{x}^N, t)|<\epsilon$ and using $y^N=e^{-\tau\kappa_N}x^N$ we may find $\delta'(\epsilon)>0$ so that $|x^N-\bar{x}^N|<\delta'$ implies $|y^N-\bar{y}^N|<\delta$ and hence $|f^{(N)}(x^N, t+\tau)-f^{(N)}(\bar{x}^N, t+\tau)|=|f^{(N)}(y^N, t)-f^{(N)}(\bar{y}^N, t)|<\epsilon$.

The distribution functions $f^{(s)}$ are defined on $X^{(s)}\cdot T$ by

$$\int dx^s f^{(s)}=\alpha_s \tag{7}$$

$$f^{(s)}=(\alpha_s/\alpha_N)\int dx^{N-s}f^{(N)}, \tag{8}$$

where α_s is a normalization constant. The Liouville theorem may be expressed in the form

$$\begin{aligned}f^{(s)}(x^s, t+\tau)&=(\alpha_s/\alpha_N)\int dx^{N-s}e^{-\tau\kappa_N}f^{(N)}(x^N, t)\\&=(\alpha_s/\alpha_N)\int dx^{N-s}\{[e^{-\tau\kappa_N}-\exp(-\tau\kappa_{N-1})]\\&\quad+[\exp(-\tau\kappa_{N-1})-\exp(-\tau\kappa_{N-2})]+\cdots\\&\quad+[\exp(-\tau\kappa_{s+1})-e^{-\tau\kappa_s}]+e^{-\tau\kappa_s}\}f^{(N)}(x^N, t)\\&=\exp(-\tau\kappa_s)f^{(s)}(x^s, t)\\&\quad+(\alpha_s/\alpha_{s+1})\int dx_{s+1}[\exp(-\tau\kappa_{s+1})-\exp(-\tau\kappa_s)]\\&\quad\times f^{(s+1)}(x^{s+1}, t)+\cdots\\&\quad+(\alpha_s/\alpha_N)\int dx^{N-s}[e^{-\tau\kappa_N}-\exp(-\tau\kappa_{N-1})]f^{(N)}(x^N, t).\end{aligned} \tag{9}$$

For the purpose of finding analogs of (9) into which a binary-collision approximation may be introduced we show that $f^{(N)}$ satisfies the Liouville equation and obtain familiar integrals of this equation over parts of phase space.

The Liouville operator on $X^{(s)}$ is

$$\kappa_s=m^{-1}\sum_{i=1}^{s}\mathbf{p}_i\cdot(\partial/\partial\mathbf{r}_i)-\sum_{i=1}^{s}[(\partial/\partial\mathbf{r}_i)(\sum_{j=1}^{s}\sum_{k=1}^{j-1}\phi_{jk})]\cdot(\partial/\partial\mathbf{p}_i),$$

which will also be written

$$\kappa_s=m^{-1}\sum_{i=1}^{s}\mathbf{p}_i\cdot(\partial/\partial\mathbf{r}_i)-\sum_{i=1}^{s}\Omega_i, \tag{10}$$

where

$$\Omega_i=\sum_{j=1}^{i-1}\theta_{ij}$$

$$\theta_{ij}=(\partial\phi_{ij}/\partial\mathbf{r}_i)\cdot(\partial/\partial\mathbf{p}_i)+(\partial\phi_{ij}/\partial\mathbf{r}_j)\cdot(\partial/\partial\mathbf{p}_j). \tag{11}$$

Finally,

$$\kappa_s=-\sum_{i=1}^{s}\omega_i, \tag{12}$$

where

$$\omega_i=\Omega_i-m^{-1}\mathbf{p}_i\cdot(\partial/\partial\mathbf{r}_i). \tag{13}$$

The Liouville equation is

$$(\partial/\partial t)F+\kappa_N F=0. \tag{14}$$

We require that the momentum and position partial derivatives of $f^{(N)}$ be continuous on $X^{(N)}$ at time t. The partial derivatives of $y^s(x^s, -\tau)=e^{-\tau\kappa_s}x^s$ are continuous on $X^{(s)}\cdot T'$ by virtue of the form of Hamilton's equations of motion, subject to the restrictions on ϕ; if x^N is fixed in $X^{(N)}$, then the time-derivative of $f^{(N)}(x^N, t+\tau)$ is

$$\begin{aligned}(\partial/\partial\tau)f^{(N)}(x^N, t+\tau)&=(\partial/\partial\tau)f^{(N)}[y^N(x^N, -\tau), t]\\&=-\kappa_N(y^N)f^{(N)}(y^N, t)\\&=e^{-\tau\kappa_N}\kappa_N(x^N)f^{(N)}(x^N, t),\end{aligned} \tag{15}$$

which is continuous on $X^{(N)}\cdot T'$ for fixed t. Since the x-partial derivatives of $y^{(N)}$ are continuous on $X^{(N)}\cdot T'$, the x-partial derivatives of $f^{(N)}(x^N, t+\tau)=f^{(N)}(y^N, t)$ are continuous on $X^{(N)}\cdot T'$ for fixed t; since the inverse of $e^{-\tau\kappa_s}$ exists on T' we may show that (15) is

$$[(\partial/\partial\tau)+\kappa_N]f^{(N)}(x^N, t+\tau)=0 \tag{16}$$

by using

$$(\partial/\partial\tau)e^{\tau\kappa_N}e^{-\tau\kappa_N}f^{(N)}(x^N, t)=0$$

and introducing

$$y^N=e^{-\tau\kappa_N}x^N$$

$$z^N=e^{\tau\kappa_N}x^N$$

$$g(x^N, t, \tau)=e^{-\tau\kappa_N}f^{(N)}(x^N, t)=f^{(N)}(y^N, t)$$

to obtain

$$\begin{aligned}(\partial/\partial\tau)e^{\tau\kappa_N}e^{-\tau\kappa_N}f^{(N)}(x^N, t)&=(\partial/\partial\tau)g[z^N(x^N, \tau), t, \tau]\\&=\kappa_N(z^N)g+(\partial g/\partial\tau)\,|_{z^N=e^{\tau\kappa_N}\kappa_N(x^N)e^{-\tau\kappa_N}f^{(N)}}\\&\quad+e^{\tau\kappa_N}(\partial/\partial\tau)e^{-\tau\kappa_N}f^{(N)}\\&=e^{\tau\kappa_N}(\kappa_N e^{-\tau\kappa_N}-e^{-\tau\kappa_N}\kappa_N)f^{(N)}=0,\end{aligned} \tag{17}$$

from which the equivalence of (15) and (16) follows. We conclude that the partial derivatives of $f^{(N)}$, as well as $f^{(N)}$ itself, are continuous on $X^{(N)}\cdot T$ and we may obtain equations on $X^{(s)}\cdot T$ by integrating (16) over parts of $X^{(N)}\cdot T$.

The equation obtained by integrating (16) over the space of $x_{s+1}, x_{s+2}, \cdots x_N$ and using (1), (7), (8), and (12) is

$$\begin{aligned}&[(\partial/\partial t)+\kappa_s]f^{(s)}\\&\quad=\sum_{k=1}^{N-s}(\alpha_s/\alpha_{s+k})\int dx_{s+1}dx_{s+2}\cdots dx_{s+k}\omega_{s+k}f^{(s+k)}.\end{aligned} \tag{18}$$

The conditions (2) and (4) may be used to express (18) in the form

$$[(\partial/\partial t)+\kappa_s]f^{(s)}=\gamma_s\int dx_{s+1}\omega_{s+1}f^{(s+1)}, \quad (19)$$

where

$$\gamma_s=(\alpha_s/\alpha_{s+1})(N-s).$$

This hierarchy of equations was derived independently by Bogolyubov[5,6] Born and Green,[4] Kirkwood,[3] and Yvon.[15] Following Uhlenbeck and Choh[9,10] we will refer to the hierarchy as the BBGKY equations. The operator ω_i in (18, 19) may be replaced by Ω_i since their difference $(1/m)\mathbf{p}_i\cdot\partial/\partial\mathbf{r}_i$ integrates to zero by the boundary condition (3).

The desired analogs of (9) are found by using (19) to obtain

$$(\partial/\partial\tau)[e^{\tau\kappa_s}f^{(s)}(x^s, t+\tau)]$$
$$=e^{\tau\kappa_s}[(\partial/\partial\tau)+\kappa_s]f^{(s)}(x^s, t+\tau)$$
$$=\gamma_s e^{\tau\kappa_s}\int dx_{s+1}\omega_{s+1}f^{(s+1)}(x^s, t+\tau) \quad (20)$$

and consequently,

$$f^{(s)}(x^s, t+\tau)=e^{-\tau\kappa_s}\left[f^{(s)}(x^s, t)+\gamma_s\int_0^\tau d\tau_1\exp(\tau_1\kappa_s)\int dx_{s+1}\omega_{s+1}f^{(s+1)}(x^{s+1}, t+\tau_1)\right] \quad (21)$$

or, by repetition,

$$f^{(s)}(x^s, t+\tau)=e^{-\tau\kappa_s}\left[f^{(s)}(x^s, t)+\sum_{k=1}^{N-s}b_{s+k}{}^{(s)}\int dx_{s+1}dx_{s+2}\cdots dx_{s+k}Q_{s+k}{}^{(s)}(\tau)f^{(s+k)}(x^{s+k}, t)\right], \quad (22)$$

where

$$b_{s+k}{}^{(s)}=\gamma_s\gamma_{s+1}\cdots\gamma_{s+k-1}$$

$$Q_{s+k}{}^{(s)}(\tau)=\int_0^\tau d\tau_1\int_0^{\tau_1}d\tau_2\cdots\int_0^{\tau_{k-1}}d\tau_k W_{s+1}(\tau_1)W_{s+2}(\tau_2)\cdots W_{s+k}(\tau_k)$$

$$W_{s+l}(\tau_l)=\exp(\tau_l\kappa_{s+l-1})\omega_{s+k}\exp(-\tau\kappa_{s+l}). \quad (23)$$

In the next section (21) and the molecular chaos assumption are used to obtain a Boltzmann equation.

III. MOLECULAR CHAOS ASSUMPTION

We consider a fluid composed of N structureless particles which form a dynamical system of the type described in Sec. II. The potential ϕ has a range $r_0>0$; thus $\phi=0$ on $r_0\leq r<\infty$, since $d\phi/dr$ is continuous at r_0, $d\phi/dr=0$ on $r_0\leq r<\infty$.

In this section we derive a Boltzmann equation for f

$$[(\partial/\partial t)+m^{-1}\mathbf{p}_1\cdot(\partial/\partial\mathbf{r}_1)]f=J(f) \quad (24)$$

by using the molecular chaos assumption to express $f^{(2)}$ as a functional of $f^{(1)}$, inserting the result into the first BBGKY equation,

$$[(\partial/\partial t)+m^{-1}\mathbf{p}_1\cdot(\partial/\partial\mathbf{r}_1)]f^{(1)}=\gamma_1\int dx_2\theta_{12}f^{(2)}, \quad (25)$$

identifying f with $f^{(1)}$, and thus finding a formula for the collision integral $J(f^{(1)})$ in (24). The molecular chaos assumption, as used here, may be described as follows: if a group of noninteracting particles has always been a group of noninteracting particles, then the momenta of the particles are not correlated. For the purpose of expressing this assumption in a form that can be used in the present calculation it is convenient to introduce several new definitions.

The space $Y^{(s)}(r_0)$ is a part of $X^{(s)}$ in which $r_{ij}<r_0$ for at least one pair $(i, j\neq i)\leq s$. The surface $G^{(s)}$ is defined by: x^s is on $G^{(s)}$ means $r_{ij}=r_0$ for at least one pair $(i, j\neq i)\leq s$ and $r_{ij}\geq r_0$ for every pair $(i, j\neq i)\leq s$. The function $\tau_s(x^s)$ is defined on $Y^{(s)}$ as follows. If s interacting particles are placed at x^s and their trajectory followed backwards in time, then τ_s is the time required for the point initially at x^s to reach $G^{(s)}$. Because $d\phi/dr=0$ at $r=r_0$, it will not be necessary to define τ_s on $G^{(s)}$, and it will not be necessary to consider other surfaces analogous to $G^{(s)}$ explicitly in the following discussion. The surface $G^{(s)}$ exists if r_0 does, the question of whether τ_s exists will be considered later.

The molecular chaos assumption will now be stated for x^2 in $Y^{(2)}$. If τ_2 exists, then for $\tau\geq\tau_2$,

$$e^{-\tau\kappa_2}f^{(2)}(x^2, t-\tau)=\beta_2 e^{-\tau\kappa_2}f^{(1)}(x_1, t-\tau)f^{(1)}(x_2, t-\tau), \quad (26)$$

where β_2 is constant. The motivation for this assumption may be described as follows. If two particles are interacting, then the momentum of each has been changed in the immediate past because of the presence of the other. Under these circumstances the value of $f^{(2)}(x_1, x_2, t)$ may be quite different from the value of

[15] J. Yvon, *Actualities Scientifiques et Industrielles* (Hermann & Cie, Paris, 1935).

$f^{(1)}(x_1, t)f^{(1)}(x_2, t)$ because the effect of the presence of a second particle has been "smeared out" into a global effect in $f^{(1)}$ while this effect remains local in $f^{(2)}$. If the particles are outside of interaction range, however, and more important, if the particles are on straight-line trajectories that will bring them into a collision, then their momenta are not correlated by this collision. In the more distant past, of course, two particles will have collided with others and may have collided with each other; but since this assumption is a statement about the value of $f^{(2)}$ rather than $f^{(k)}$, $k>2$, these effects that arise from the presence of other particles are somewhat "smeared out."

There remains a global difference between $f^{(2)}$ and $f^{(1)}f^{(1)}$ which arises from their definitions. For example, if this factorization were valid everywhere in $X^{(2)}$, then

$$\beta_2=\frac{\int dx^2 f^{(2)}(x^2, t)}{\int dx^2 f^{(1)}(x_1, t)f^{(1)}(x_2, t)}=\frac{\alpha_2}{{\alpha_1}^2}.$$

The molecular chaos assumption with β_2 constant may be improved by taking β_2 to be a function defined on $X^{(2)}$; then the assumption (26) is replaced by the assumption used to determine β_2. This modification will be considered, following Enskog, in the section on rigid spheres where β_2 must provide the entire effect of the presence of a third particle on the form of J, but it will not be considered here.

The time dependence in (26) is not significant for the molecular chaos assumption, but we are committed to this time, for fixed t, by the absence of the container. The position dependence in (26) is important because it determines the extent of momentum correlation and also the density, for fixed r_0, at which the binary collision approximation may be expected to be sufficient. For example, if particles at (x_1, x_2) are not interacting but are on straight-line trajectories directed from a past collision, then the momenta are correlated by that collision, and the correlation should be recognized over greater distances in more dilute gases. This assumption, which was introduced by Boltzmann, is evidently successful because of the importance of momentum correlation, which in dilute gases is permitted to extend out to the point at which a binary collision begins even if $r_0\to\infty$.

The intuitive basis for (26) is not changed if $s>2$ is considered provided the time τ_s is replaced by a possibly longer time T_s required for s particles to be taken back along collision trajectories so far that the trajectories become permanent straight lines. A new problem arises, however, because the existence of T_s becomes difficult to establish with $s>2$. It is possible that such an assumption may be useful even if T_s does not exist on a sufficiently small part of $X^{(s)}$; and modifications of (26) may be considered which involve shorter times than T_s. Before considering this new problem further, we will state the assumption in various forms and indicate how it may be used to find J.

The molecular chaos assumption will now be stated for $f^{(s)}$ on $X^{(s)}$. The function

$$T_s^{(1,k)(k+1,s)}\equiv T_s^{(1,2,\cdots k)(k+1,k+2\cdots s)}$$

is defined on $X^{(s)}$ as follows. If s interacting particles are placed at x^s and their trajectories followed backwards in time, then $T_s^{(1,k)(k+1,s)}$ is the time required for the group initially at x^k to become permanently free from interactions with the other particles initially at x_j, $k+1\leq j\leq s$. If this function exists, then for $\tau\geq T_s^{(1,k)(k+1,s)}$,

$$e^{-\tau\kappa_s}f^{(s)}(x^s, t-\tau)=\beta_s^{(1,k)(k+1,s)}e^{-\tau\kappa_s}f^{(k)}(x^k, t-\tau)f^{(s-k)}(x_{k+1}\cdots x_s, t-\tau). \tag{27}$$

This statement may be regarded as the basic form of the molecular chaos assumption in the present discussion, although only special forms of it will be used explicitly.

The function T_s is defined on $X^{(s)}$ by

$$T_s=\max_{i\leq s} T_s^{(i)(1,2,\cdots,i-1,i+1,\cdots,s)}.$$

This function may be expressed in other forms; for example,

$$T_3(x^3)=T_3^{(12)(3)}(x^3)+\exp(-T^{(12)(3)}\kappa_3)\,T_2(x^2).$$

Finally, the molecular chaos assumption will be stated in the form to be used explicitly in the calculation following. The space $Z^{(s)}$ is defined by: $Z^{(2)}$ is $Y^{(2)}$, and x^{s+1} is in $Z^{(s+1)}$ if and only if x^s is in $Z^{(s)}$ and $r_{i,s+1}<r_0$ for at least one $i\leq s$. Thus x^s is in $Y^{(s)}$ if at least two of the s particles placed at x^s are interacting, and x^s in $Y^{(s)}$ is in $Z^{(s)}$ if the s particles may not be divided into two noninteracting groups. If $\tau\geq T_s$ then $f^{(s)}$ on $Z^{(s)}$ satisfies

$$e^{-\tau\kappa_s}f^{(s)}(x^s, t-\tau)=\beta_s e^{-\tau\kappa_s}\prod_{j=1}^{s}f^{(1)}(x_j, t-\tau). \tag{28}$$

The constants β_s and $\beta_s^{(1,k)(k+1,s)}$ are not independent.

We now proceed to the calculation of J in (24). For this purpose we will insert a parameter λ in the BBGKY Eqs. (19), which then become

$$[(\partial/\partial t)+\kappa_s]f^{(s)}=\lambda\gamma_s\int dx_{s+1}\Omega_{s+1}f^{(s+1)}. \tag{29}$$

The form of (21) is changed to

$$f^{(s)}(t+\tau)=e^{-\tau\kappa_s}\left[f^{(s)}(t)+\lambda\gamma_s\int_0^\tau dt_1\exp(t_1\kappa_s)\int dx_{s+1}\Omega_{s+1}f^{(s+1)}(t+t_1)\right], \tag{30}$$

where the dependence of $f^{(k)}$ on x^k is suppressed from the notation. The parameter λ will be used for collecting terms; its value is unity and the statement, $f=\mathcal{O}(\lambda^n)$, that a function f is n-order in λ, will mean that it has been expressed as a polynomial of order λ^n by using (30) and that the coefficients in this polynomial will not again be altered by using (30). Thus λ is used for convenience in describing the calculation; all λ-dependence could be made explicit.

If we replace τ by $-\tau$ in (30) we obtain

$$f^{(s)}(t-\tau)=e^{\tau\kappa_s}\left[f^{(s)}(t)-\lambda\gamma_s\int_0^\tau dt_1\exp(-t_1\kappa_s)\int dx_{s+1}\Omega_{s+1}f^{(s+1)}(t-t_1)\right]. \tag{31}$$

The inverse of $e^{\tau\kappa_s}$ exists on $X^{(s)}$ so that (31) may be solved to obtain

$$f^{(s)}(t)=e^{-\tau\kappa_s}f^{(s)}(t-\tau)+\lambda\gamma_s\int_0^\tau dt_1\exp(-t_1\kappa_s)\int dx_{s+1}\Omega_{s+1}f^{(s+1)}(t-t_1). \tag{32}$$

We intend to express $f^{(2)}$ and J as polynomials in λ by using (28, 29, 31, 32):

$$f^{(2)}=\sum_{k=0}^{N-2}\lambda^k F_k \tag{33}$$

$$J=\sum_{k=1}^{N-1}\lambda^k J_k, \tag{34}$$

where x^2 is in $V^{(2)}$, and the F_n are functions of $\tau\geq\tau_2$ and r_0, as well as (x^2, t).

If x^2 is in $V^{(2)}$ and $\tau\geq\tau_2$ then (28, 31, 32) may be used to obtain $f^{(2)}$ in the form

$$\begin{aligned}
f^{(2)}(t)&=e^{-\tau\kappa_2}f^{(2)}(t-\tau)+\lambda\gamma_2\int_0^\tau dt_1 e^{-t_1\kappa_2}\int dx_3(\theta_{13}+\theta_{23})f^{(3)}(t-t_1)\\
&=\beta_2 e^{-\tau\kappa_2}f^{(1)}(x_1, t-\tau)f^{(1)}(x_2, t-\tau)+\cdots\\
&=\beta_2 e^{-\tau\kappa_2}e^{\tau\kappa_1(1)}e^{\tau\kappa_1(2)}\left[f^{(1)}(x_1, t)-\lambda\gamma_1\int_0^\tau dt_1 e^{-t_1\kappa_1(1)}\int dx_2\theta_{13}f^{(2)}(x_1, x_3, t-t_1)\right]\\
&\qquad\cdot\left[f^{(1)}(x_2, t)-\lambda\gamma_1\int_0^\tau dt_1 e^{-t_1\kappa_1(2)}\int dx_3\theta_{23}f^{(2)}(x_2, x_3, t-t_1)\right]+\cdots\\
&=\beta_2 e^{-\tau\kappa_2}e^{\tau\kappa_1(1)}e^{\tau\kappa_1(2)}f^{(1)}(x_1, t)f^{(1)}(x_2, t)+\mathcal{O}(\lambda).
\end{aligned} \tag{35}$$

Following Choh and Uhlenbeck,[10] we introduce the transformation $\mathcal{S}^{(s)}(\tau)_{1,2,\cdots,s}$ on $X^{(s)}$ defined by

$$\mathcal{S}^{(s)}(\tau)_{1,2,\cdots,s}=e^{-\tau\kappa_s}\exp\left[\tau\sum_{i=1}^{s}\kappa_1(i)\right]. \tag{36}$$

The function $\mathcal{S}^{(s)}(\tau)_{1,2,\cdots,s}x^s$ is constant on $T_s<\tau<\infty$, and when $\mathcal{S}^{(s)}(\tau)_{1,2,\cdots,s}$ is written as $\mathcal{S}_{1,2,\cdots,s}{}^{(s)}$ then it is understood that $\tau\geq T_s$. Finally, for F_0 in (33) we have

$$F_0=\beta_2\mathcal{S}_{12}{}^{(2)}f^{(1)}(x_1, t)f^{(1)}(x_2, t). \tag{37}$$

The function f is now identified with $f^{(1)}$ and the collision integral J in (24) is obtained from (29) in the form:

$$J=\lambda\gamma_1\int dx_2\theta_{12}f^{(2)}(x^2, t). \tag{38}$$

Thus we have

$$J_1=\beta_2\gamma_1\int dx_2\theta_{12}\mathcal{S}_{12}{}^{(2)}f(x_1, t)f(x_2, t). \tag{39}$$

In the binary collision approximation this result is essentially the same as that given by Green.[7] The same result (39) was given by Choh and Uhlenbeck,[10] following a proposal by Bogolyubov, in a calculation that is apparently different from the one used here; this calculation will be discussed in Sec. V. In order to identify the Eq. (24), in which the assumed form for J is (39), with the Boltzmann equation for dilute gases near equilibrium, we will assume that the spatial dependence of f is not important in (39) but is important on the left side of (24). This is equivalent to the assumption that $f(r_2, p_2, t)$ may be expanded in a Taylor series abour $\mathbf{r}_2=\mathbf{r}_1$, that only the first derivative need be kept either because r_0 is small enough or because the higher derivatives are small enough, and that even the first derivative is negligible compared to f but not compared to $\partial f/\partial t$. Thus we may ignore the difference between $\mathcal{S}_{12}{}^{(2)}\mathbf{r}_i$ and $\mathbf{r}_i$ so that

$$\mathcal{S}_{12}{}^{(2)}f(x_1, t)f(x_2, t)=f(\mathbf{r}_1, \mathbf{P}_1, t)f(\mathbf{r}_1, \mathbf{P}_2, t), \tag{40}$$

where the $\mathbf{P}_i(x^2, \tau)$ are the momenta of particles imagined to be at x^2 before they enter into the collision

being described. Because $d\phi/dr=0$ on $r\geq r_0$, $(\partial/\partial\tau)\,\mathbf{P}_i=0$ on $\tau_2\leq\tau<\infty$ and consequently,

$$(\partial/\partial\tau)\,e^{-\tau\kappa_2}\mathbf{p}_i=-\kappa_2 e^{-\tau\kappa_2}\mathbf{p}_i$$
$$=[\theta_{12}-m^{-1}\mathbf{p}_1\cdot(\partial/\partial\mathbf{r}_1)-m^{-1}\mathbf{p}_2\cdot(\partial/\partial\mathbf{r}_2)]e^{-\tau\kappa_2}\mathbf{p}_i=0.$$

Thus $\theta_{12}f(\mathbf{r}_1,\mathbf{P}_1,t)f(\mathbf{r}_1,\mathbf{P}_2,t)$ may be replaced in (39) by

$$m^{-1}[\mathbf{p}_1\cdot(\partial/\partial\mathbf{r}_1)+\mathbf{p}_2\cdot(\partial/\partial\mathbf{r}_2)]f(\mathbf{r}_1,\mathbf{P}_1,t)f(\mathbf{r}_1,\mathbf{P}_2,t), \tag{41}$$

where $\mathbf{r}_1$ in f, but not in $(\mathbf{P}_1,\mathbf{P}_2)$, is held constant in the r_i differentiation. Since the $\mathbf{P}_i$ depend on $\mathbf{r}_j$ only through $\mathbf{r}_{21}$, the Boltzmann equation is obtained in the form:

$$[(\partial/\partial t)+m^{-1}\mathbf{p}_1\cdot(\partial/\partial\mathbf{r}_1)]f(\mathbf{r}_1,\mathbf{p}_1,t)=(\beta_2\gamma_1/m)\int d\mathbf{p}_2\int d\mathbf{r}_{21}[\mathbf{p}_{21}\cdot(\partial/\partial\mathbf{r}_{21})]f(\mathbf{r}_1,\mathbf{P}_1,t)f(\mathbf{r}_1,\mathbf{P}_2,t). \tag{42}$$

If the $\mathbf{r}_{21}$ integration in (42) is carried out in cylindrical coordinates (ρ,φ,z) with the z axis in the $\mathbf{p}_{21}$ direction and the other coordinates introduced arbitrarily, then (42) becomes

$$[(\partial/\partial t)+m^{-1}\mathbf{p}_1\cdot(\partial/\partial\mathbf{r}_1)]f_1=(\beta_2\gamma_1/m)\int_0^{r_0}d\rho\rho\int_0^{2\pi}d\varphi\int d\mathbf{p}_2 p_{21}(f_1'f_2'-f_1f_2), \tag{43}$$

where f_i' is evaluated at $\mathbf{p}_i'$, the momentum of particle i before the collision which changes $\mathbf{p}_i'$ into $\mathbf{p}_i$. The $\mathbf{p}_i'$ are functions of the p_i, ρ, and φ. In (43) the limit $r_0\to\infty$ may be considered.

Clearly, this approximation is not well defined if we consider the dilute-gas Boltzmann equation to have been derived for a general potential from (39). For fixed r_0 and density, the approximation becomes better in gases closer to equilibrium. For fixed spatial inhomogeneity in f and fixed density, it becomes better in gases with smaller r_0. These two cases have well-defined limits, namely, equilibrium and the ideal gas of point rigid spheres, although in the latter case the formulation requires modification. For fixed inhomogeneity and r_0, however, it is not clear how this approximation becomes better in gases at lower density. The result (43), however, has been successful in dilute-gas kinetic theory for gases not far removed from equilibrium. The binary-collision approximation with density correction terms derived from (39) has also been formulated[8]; numerical results for the transport coefficients have not yet been obtained.

Continuing to the calculation of the second order collision integral J_2 we have, from (35),

$$\lambda^{-1}(f^{(2)}(t)-F_0(t))=\gamma_2\int_0^t dt_1\int dx_3(\theta_{13}+\theta_{23})f^{(3)}(t-t_1)-\beta_2\gamma_1 S_{12}^{(2)}\int_0^t dt_1\int dx_3[e^{-t_1\kappa_1(1)}\theta_{13}f^{(2)}(x_1,x_3,t-t_1)f^{(1)}(x_2,t)$$
$$+e^{-t_1\kappa_1(2)}\theta_{23}f^{(2)}(x_2,x_3,t-t_1)f^{(1)}(x_1,t)]. \tag{44}$$

From (28, 31, 32) we have

$$f^{(2)}(x_i,x_3,t-t_1)=\beta_2 S_{i3}^{(2)}\exp\{t_1[\kappa_1(i)+\kappa_1(3)]\}\,f(x_i,t)f(x_3,t)+\mathcal{O}(\lambda)$$
$$f^{(3)}(x^3,t-t_1)=\beta_3 S_{123}^{(3)}\exp[t_1\sum_{j=1}^{3}\kappa_1(j)]\prod_{\nu=1}^{3}f(x_\nu,t)+\mathcal{O}(\lambda). \tag{45}$$

Thus F_1 is obtained in the form

$$F_1=\int dx_3\int_0^\tau dt_1 u(t_1)\prod_{\nu=1}^{3}f(x_\nu,t), \tag{46}$$

where

$$u(t_1)=\beta_3\gamma_2 e^{-t_1\kappa_2}(\theta_{13}+\theta_{23})S_{123}^{(3)}\exp[t_1(K_1+K_2+K_3)]-\beta_2^2\gamma_1 e^{-\tau\kappa_2}\{e^{(\tau-t_1)K_1}e^{\tau K_2}\theta_{13}S_{13}^{(2)}\exp[t_1(K_1+K_3)]$$
$$+\exp[(\tau-t_1)K_2]\exp(\tau K_1)\theta_{23}S_{23}^{(2)}\exp[t_1(K_2+K_3)]\} \tag{47}$$

and $K_i=\kappa_1(i)$. The upper limit τ in the t_1-integration is $\tau_2(x^2)$, in the present case. The x_3 integration receives contributions only from $Z^{(3)}$ with x^2 in $Z^{(2)}$ since $\theta_{i3}=0$ if $r_{i3}\geq r_0$, $i=1,2$. Thus (28) was needed only on $Z^{(3)}$ in the calculation of (46, 47). The calculation may be extended by repetition to higher order in λ. From (46) we obtain J_2 in the form

$$J_2=\gamma_1\int dx_2\theta_{12}\int_0^{\tau_2(x^2)}dt_1\int dx_3 u(t_1)\prod_{\nu=1}^{3}f(x_\nu,t). \tag{48}$$

The function F_1 (46, 47) with $\tau=\tau_2$ may be described as follows. In the evaluation of F_1, the two-body collision used to obtain F_0 is reconsidered, and the three-body collisions which would have interfered with this two-body collision at each point along the collision trajectories provide a contribution that is added to $f^{(2)}-F_0$, while the two-body collisions in the presence of a third particle provide a contribution that is subtracted from $f^{(2)}-F_0$. Thus F_1 may be interpreted as a correction to F_0 which arises from three-body collisions.

We now consider whether $F_0+\lambda F_1$ provides a J which is a ternary-collision approximation. It is clear that F_0 provides a binary-collision approximation since $f^{(2)}=F_0$, subject to the molecular chaos assumption, if no ternary or higher collisions are occurring in the ensemble. In order to obtain a ternary-collision approximation, however, it is necessary to let $\tau\to\infty$ in (35). Otherwise the three-body collisions which contribute to F_1 are only those which have $r_{12}<r_0$ for each x_3 in the range of the x_3 integration of (46). Thus correction terms for the binary-collision approximation have been obtained by the use of the molecular chaos assumption on $Z^{(3)}$, but in order to modify these terms so that successively higher order collision approximations are obtained, it is necessary to use the assumption on $Y^{(3)}$.

For the purpose of determining F_1 with $\tau\to\infty$ we use (28) with $Y^{(s)}$ in place of $Z^{(s)}$ and consider F_1 in the form

$$F_1=\int_0^\tau dt_1 M(x^2, t_1, \tau), \tag{49}$$

where

$$M(x^2, t_1, \tau)=\sum_{i=1}^{2}\Big[\beta_3\gamma_2 e^{-t_1\kappa_2}\int_{R_i} dx_3\theta_{i3}S_{123}^{(3)}\exp(t_1\sum_{l=1}^{3}K_l)\prod_{\nu=1}^{3}f(x_\nu, t)$$
$$-\beta_2^2\gamma_1\exp(-\tau\kappa_2)\exp(\tau K_j)\exp[(\tau-t_1)K_i]\int_{R_i} dx_3\theta_{i3}S_{i3}^{(2)}\exp[t_1(K_1+K_3)]\prod_{\nu=1}^{3}f(x_\nu, t)\Big], \tag{50}$$

and $(i, j\neq i)\leq 2$, $\tau\geq T_2$. The space $R_i(x_i)$ is the part of the space of x_3 in which $r_{i3}<r_0$ for fixed x_i; the operator θ_{i3} is zero unless x_3 is in R_i, and R_i is placed under the symbols of integration in (50) to indicate explicitly the range of integration.

First we consider the question of whether or not M vanishes for sufficiently large t_1. For fixed x_3 and $\tau>t_1>\tau_2$, θ_{i3} vanishes in both terms inside the bracket in (50) whenever it vanishes in either term. This is due to the equality

$$\begin{aligned}\exp(-t_1\kappa_2)h(x_i)&=\exp(-\tau_2\kappa_2)\exp[-(t_1-\tau_2)K_i]h(x_i)\\&=\exp(-\tau\kappa_2)\exp[-(t_1-\tau)K_i]h(x_i)\\&=\exp(-\tau\kappa_2)\exp(\tau K_j)\exp[(\tau-t_1)K_i]h(x_i),\end{aligned} \tag{51}$$

where $h(x_i)$ is an arbitrary function[16] of x_i. Thus (49) may be written in the form

$$M(x^2, t_1, \tau)=\sum_{i=1}^{2}\int_{\exp(-t_1\kappa_2)R_i} dx_3[e^{-t_1\kappa_2}\theta_{i3}](K_{i3}-\bar{K}_{i3})\prod_{\nu=1}^{3}f(x_\nu, t), \tag{52}$$

where

$$\begin{aligned}K_{i3}&=\beta_3\gamma_2\exp[-t_1\kappa_2(1, 2)]S_{123}^{(3)}\exp[t_1(K_1+K_2+K_3)]\\&=\beta_3\gamma_2\exp[-t_1\kappa_2(1, 2)]\exp(-T_3\kappa_3)\exp[(T_3+t_1)(K_1+K_2+K_3)],\end{aligned} \tag{53}$$

and

$$\begin{aligned}\bar{K}_{i3}&=\beta_2^2\gamma_1\exp[-\tau\kappa_2(1, 2)]\exp(\tau K_j)\exp[(\tau-t_1)K_i]S_{i3}^{(2)}\exp[t_1(K_i+K_3)]\\&=\beta_2^2\gamma_1\exp[-\tau\kappa_2(1, 2)]\exp(\tau K_j)\exp[(\tau-t_1)K_i]\exp[-T_2(x_i, x_3)\kappa_2(i, 3)]\exp[(T_2+t_1)(K_i+K_3)].\end{aligned} \tag{54}$$

In order that these terms cancel for $i=1$ or 2 it is sufficient that

$$\beta_3\gamma_2=\beta_2^2\gamma_1 \tag{55}$$

and

$$\exp(-T_3'\kappa_3)\exp[T_3'(K_1+K_2+K_3)]=\exp[-T_2'(i, 3)\kappa_2(i, 3)]\exp[T_2'(K_i+K_3)], \tag{56}$$

where $T_s'=\exp[-t_1\kappa_2(1, 2)]T_s$. We may express (56) in the form

$$\begin{aligned}\exp[-t_1\kappa_2(1, 2)]T_2(x_i, x_3)&=\exp[-t_1\kappa_2(1, 2)]T_3(x^3)\\&=\exp[-t_1\kappa_2(1, 2)][T_3^{(i3)(j)}+\exp(-T_3^{(i3)(j)}\kappa_3)T_2(x_i, x_3)].\end{aligned}$$

[16] A product of transformations like that in (51) is applied from left to right; thus, for example,
$\exp(-\tau\kappa_2)\exp(\tau\kappa_1)h(x_1)=h[\exp(\tau\kappa_1)\exp(-\tau\kappa_2)x_1]$.

It is sufficient, therefore, that

$$\exp[-t_1\kappa_2(1,2)]T^{(i3)(j)}(x^3)=0. \tag{57}$$

The condition (57) holds for some t_1 if and only if both particles i and 3, which at $\exp[-t_1\kappa_2(1,2)]x_i$ and x_3 in $\exp(-t_1\kappa_2^{(1,2)})R_i$ are separated from particle j at $e^{-\tau_1\kappa_3}x_j$, had no previous collisions with particle j, and in addition, do not remain in an $(i,3)$ collision up to the present time when $r_{21}<r_0$.

There are, therefore, two situations in which F_1 may not become constant in τ for sufficiently large τ. In the first place, F_1 with $\tau\to\infty$ includes not only the contributions of three-body collisions occurring at the present time, but also contributions from two-body collisions $(i,3)$ that were completed in the indefinite past and contributed a particle to the presently occurring binary collision $(1,2)$. Secondly, if the potential is such that an $(i,3)$ collision begun in the indefinite past continues up to the present time when particles 1 and 2 interact, then this is a three-body collision and contributes to F_1.

The second difficulty may be avoided by restricting the potential so that stable molecules are not formed. The first difficulty may be avoided by adopting a modified molecular chaos assumption such as the one considered below.

Let x^s be in $Y^{(s)}$ and let $\tau\geq\tau_s$ (not T_s if $s>2$). The modified molecular chaos assumption is

$$e^{-\tau\kappa_s}f^{(s)}(x^s,t-\tau)=\beta_s e^{-\tau\kappa_s}\prod_{i=1}^{s}f^{(1)}(x_i,t-\tau). \tag{58}$$

This assumption is poorer than (28) from an intuitive point of view. Particles placed at x^s are followed backwards in time until all of them are separated, and then it is assumed that their momenta are not correlated. Thus previous collisions among the s particles are ignored. The possible success of this assumption would arise from the fact that F_n is an integral over the space of $x_3, x_4, \cdots x_{n+2}$, and hence the effects of these previous collisions are somewhat "smeared out."

We conclude that for some potentials the molecular chaos assumption in the form (28) on $Y^{(s)}$ determines J_n in such a way that $\sum_{i=1}^{n}J_i$ may be regarded as an $(N+1)$-order collision approximation, but that J_n includes effects of past correlations unless the modified assumption (58) is used. We will not attempt to appraise the contributions of these past collisions.

The important question raised in this section is the question of whether T_s, or at least τ_s, exists on a sufficient part of $Y^{(s)}$, or at least $Z^{(s)}$, so that the molecular chaos assumption, or at least its modification, may be used as a tool in kinetic theory. It is clear that T_s exists on $Z^{(s)}$ for strictly repulsive potentials, but T_s will be τ_s there only for $s\leq 3$. It seems possible that T_s exists on all but an insignificant part of $Y^{(s)}$ for the same potentials. It is also clear that τ_s exists on $Y^{(s)}$ for repulsive potentials, and it seems possible that τ_s exists on $Y^{(s)}$ for mildly attractive potentials.

In the next section it will be shown that the molecular chaos assumption in a simple form is all that is required to obtain the Enskog theory of rigid spheres from the Liouville equation, and in Sec. VI it is shown that this assumption is all that is required to obtain the Bogolyubov theory, as formulated by Choh and Uhlenbeck, to the ternary collision approximation.

IV. BOLTZMANN EQUATION FOR RIGID SPHERES

In this section we consider a dynamical system of N rigid spheres of diameter σ. As in Sec. III, the goal is to obtain the collision integral $J(f^{(1)})$ in the Boltzmann equation by invoking the molecular chaos assumption and using the Liouville theorem as an aid. In Sec. III this theorem was used for two distinct purposes. In the first place, the first BBGKY equation was used to obtain the form of J in terms of $f^{(2)}$. Then the Liouville theorem was used again to express the value of $f^{(2)}$ at (x_1, x_2, t) in terms of $f^{(2)}$ at a different point $(\exp-\tau\kappa_2 x_1, \exp-\tau\kappa_2 x_2, t-\tau)$ together with corrections interpreted as contributions from higher-order collisions. In the present case, however, the Liouville theorem is used only to provide the form of J in terms of $f^{(2)}$. We cannot express $f^{(2)}$ as a series in which various terms may be interpreted as the effects of higher-order collisions because the rigid-sphere collision goes to completion in zero time. Thus an attempt to follow two colliding particles back along their trajectories to the points at which the collision began results in a zero displacement, and the correction terms which provide the effects of higher-order collisions during this displacement are zero.

This derivation of a Boltzmann equation for rigid spheres is based on the calculation of

$$[(\partial/\partial t)+m^{-1}\mathbf{p}_1\cdot(\partial/\partial\mathbf{r}_1)]f^{(1)}=\lim_{\tau\to+0}\tau^{-1}[f^{(1)}(t+\tau)-f^{(1)}(t)+(1-e^{-\tau\kappa_1})f^{(1)}(t)] \tag{59}$$

from (22). The replacement of $e^{-\tau\kappa_1}$ by the operator $\sum_n(-\tau\kappa_1)^n/n!$ does not require the existence of all of the derivatives of ϕ because κ_1 does not involve the potential.

From (22) and (59) we obtain

$$J^{(1)}=[(\partial/\partial t)+m^{-1}\mathbf{p}_1\cdot(\partial/\partial\mathbf{r}_1)]f^{(1)}$$
$$=\lim_{\tau\to+0}\tau^{-1}\sum_{k=1}^{N-1}b_{k+1}^{(1)}e^{-\tau\kappa_1}\int dx_2\cdots dx_{k+1}Q^{(1)}(\tau)_{k+1}f^{(k+1)}$$
$$=J_1^{(1)}+J_2^{(1)}+\lim_{\tau\to+0}\tau^{-1}\sum_{k=3}^{N-1}b_{k+1}^{(1)}e^{-\tau\kappa_1}\int dx_2\cdots dx_{k+1}Q^{(1)}(\tau)_{k+1}f^{(k+1)}, \tag{60}$$

where

$$J_1^{(1)}=\gamma_1\lim_{\tau\to+0}\tau^{-1}e^{-\tau\kappa_1}\int_0^\tau d\tau_1 e^{\tau_1\kappa_1}\int dx_2\omega_2 e^{-\tau_1\kappa_2}f^{(2)} \tag{61}$$

and

$$J_2^{(1)}=\gamma_1\gamma_2\lim_{\tau\to+0}\tau^{-1}e^{-\tau\kappa_1}\int_0^\tau d\tau_1 e^{\tau_1\kappa_1}\int dx_2\omega_2 e^{-\tau_1\kappa_2}\int_0^{\tau_1}d\tau_2 e^{\tau_2\kappa_2}\int dx_3\omega_3\exp(-\tau_1\kappa_3)f^{(3)}. \tag{62}$$

The term $J_2^{(1)}$ may be integrated by parts to obtain

$$J_2^{(1)}=\gamma_1\gamma_2\lim_{\tau\to+0}\tau^{-1}\int_0^\tau d\tau_1\int dx_2[e^{-(\tau-\tau_1)\kappa_2}-e^{-(\tau-\tau_1)\kappa_1}]\int dx_3\omega_3\exp(-\tau_1\kappa_3)f^{(3)}. \tag{63}$$

No matter how rigid the potential becomes, the integral over $\mathbf{r}_2$ in (63) receives contributions only from a region with volume proportional to $(\tau-\tau_1)\,|\,\mathbf{p}_{21}\,|$ for small τ. Thus the x_2-integral is $\Theta(\tau-\tau_1)$ which integrates to $\Theta(\tau^2)$ and $J_2^{(1)}=0$. The higher terms in (60) also vanish.

The evaluation of $J_1^{(1)}$ must be carried out in some detail. Let $R_1(\mathbf{r}_1)$ be the part of the space of x_2 in which $r_{21}<r_0$. Let $C_1(\mathbf{r}_1)$ be the complement of R_1. The transformation $\exp[(\tau/m)\mathbf{p}_1\cdot(\partial/\partial\mathbf{r}_2)]$ on $X^{(2)}$ is defined by

$$\exp[(\tau/m)\mathbf{p}_1\cdot(\partial/\partial r_2)](\mathbf{r}_1,\mathbf{p}_1,\mathbf{p}_2)=(\mathbf{r}_1,\mathbf{p}_1,\mathbf{p}_2)$$
$$\exp[(\tau/m)\mathbf{p}_1\cdot(\partial/\partial\mathbf{r}_2)](\mathbf{r}_2)=(\mathbf{r}_2+m^{-1}\mathbf{p}_1\tau), \tag{64}$$

and hence

$$(\partial/\partial\tau)\{\exp[(\tau/m)\mathbf{p}_1\cdot(\partial/\partial\mathbf{r}_2)]f^{(2)}(\mathbf{r}_1,\mathbf{r}_2)\}=(\partial/\partial\tau)f^{(2)}(\mathbf{r}_1,\mathbf{r}_2,+m^{-1}\mathbf{p}_1\tau)$$
$$=m^{-1}\mathbf{p}_1\cdot(\partial/\partial\mathbf{r}_2)\{\exp[(\tau/m)\mathbf{p}_1\cdot(\partial/\partial\mathbf{r}_2)]f^{(2)}(\mathbf{r}_1,\mathbf{r}_2)\}. \tag{65}$$

If F is a function defined on $X^{(2)}$, then

$$e^{\tau\kappa_1}\int_{R_1}dx_2F=\int dx_2e^{\tau\kappa_1}F=\int_{R_1}dx_2\exp[(\tau/m)\mathbf{p}_1\cdot(\partial/\partial\mathbf{r}_2)]e^{\tau\kappa_1}F$$
$$\exp(\tau\kappa_1)R_1$$

although

$$e^{\tau\kappa_1}\int_{R_1+C_1}dx_2F=\int_{R_1+C_1}dx_2e^{\tau\kappa_1}F. \tag{66}$$

In (66) R_1 and C_1 have been placed under the integral signs to indicate explicitly the range of integration.

The integral $J_1^{(1)}=J^{(1)}$ is

$$J^{(1)}=\lim_{\tau\to+0}\tau^{-1}\gamma_1e^{-\tau\kappa_1}\int_0^\tau d\tau_1e^{\tau_1\kappa_1}\left[\int_{R_1}dx_2[\theta_{12}-m^{-1}\mathbf{p}_2\cdot(\partial/\partial\mathbf{r}_2)]e^{-\tau_1\kappa_2}f^{(2)}-\int_{C_1}dx_2m^{-1}\mathbf{p}_2\cdot(\partial/\partial\mathbf{r}_2)e^{-\tau_1\kappa_2}f^{(2)}\right]. \tag{67}$$

The first term in (67) is

$$\lim_{\tau\to+0}\tau^{-1}\gamma_1e^{-\tau\kappa_1}\int_0^\tau d\tau_1\left[\int_{R_1}dx_2(\partial/\partial\tau_1)\{e^{\tau_1\kappa_1}\exp[(\tau_1/m)\mathbf{p}_1\cdot(\partial/\partial\mathbf{r}_2)]e^{-\tau_1\kappa_2}\}f^{(2)}-e^{\tau_1\kappa_1}\int_{R_1}dx_2m^{-1}\mathbf{p}_1\cdot(\partial/\partial\mathbf{r}_2)e^{-\tau_1\kappa_2}f^{(2)}\right], \tag{68}$$

where (64–66) have been used. The first term in (68) is

$$\lim_{\tau\to+0}\tau^{-1}\gamma_1e^{-\tau\kappa_1}\int_{R_1}dx_2[e^{\tau\kappa_1}\exp[(\tau/m)\mathbf{p}_1\cdot(\partial/\partial\mathbf{r}_2)]e^{-\tau\kappa_2}-1]f^{(2)}. \tag{69}$$

In the rigid sphere limit if $r_{ij}<r_0\to\sigma$, then $f^{(2)}\to 0$ and as a consequence,

$$\int_{R_1} dx_2 f^{(2)}\to 0.$$

Since $e^{\tau\mathfrak{L}_1}\exp[(\tau/m)\mathbf{p}_1\cdot(\partial/\partial\mathbf{r}_2)]r_{21}=r_{21}<r_0$ and $e^{-\tau\mathfrak{L}_2}|\mathbf{p}_i|\to\infty$ for $r_{21}<r_0\to\sigma$, the function $e^{\tau\mathfrak{L}_1}\exp[(\tau/m)\mathbf{p}_1\cdot(\partial/\partial\mathbf{r}_2)]e^{-\tau\mathfrak{L}_2}f^{(2)}$ is evaluated at very large momenta, as $r_0\to\sigma$, in the first term of (69). The momenta in the ensemble are bounded, however, and we conclude that (69) will not contribute to (67) in the rigid-sphere limit. Finally, we have

$$J^{(1)}=\lim_{\tau\to+0}\tau^{-1}\gamma_1 e^{-\tau\mathfrak{L}_1}\int_0^\tau d\tau_1 e^{\tau_1\mathfrak{L}_1}\left[\int_{R_1} dx_2 m^{-1}\mathbf{p}_1\cdot(\partial/\partial\mathbf{r}_2)e^{-\tau_1\mathfrak{L}_2}f^{(2)}+\int_{C_1} dx_2 m^{-1}\mathbf{p}_2\cdot(\partial/\partial\mathbf{r}_2)e^{-\tau_1\mathfrak{L}_2}f^{(2)}\right]. \tag{70}$$

The second integral in the bracket of (70) is

$$\int_{R_1+C_1} dx_2\cdots-\int_{R_1} dx_2\cdots$$

so that $J^{(1)}$ may be expressed in the form

$$J^{(1)}=(\gamma_1/m)\lim_{\tau\to+0}\tau^{-1}e^{-\tau\mathfrak{L}_1}\int_0^\tau d\tau_1 e^{\tau_1\mathfrak{L}_1}\left[\int_{R_1} dx_2[\mathbf{p}_{21}\cdot(\partial/\partial\mathbf{r}_2)]e^{-\tau_1\mathfrak{L}_2}f^{(2)}-\int_{R_1+C_1} dx_2[\mathbf{p}_2\cdot(\partial/\partial\mathbf{r}_2)]e^{-\tau_1\mathfrak{L}_2}f^{(2)}\right]$$

$$=(\gamma_1\sigma^2/m)\lim_{\tau\to+0}\tau^{-1}e^{-\tau\mathfrak{L}_1}\int_0^\tau d\tau_1 e^{\tau_1\mathfrak{L}_1}\int d\mathbf{p}_2\int d\mathbf{k}_{21}(\mathbf{p}_{21}\cdot\mathbf{k}_{21})e^{-\tau_1\mathfrak{L}_2}f^{(2)}, \tag{71}$$

in which the integral over R_1+C_1 vanishes by virtue of (3). In more detail, this is

$$J^{(1)}=(\gamma_1\sigma^2/m)\lim_{\tau\to+0}\tau^{-1}\int_0^\tau d\tau_1\int d\mathbf{p}_2\int_{(\mathbf{p}_{21}\cdot\mathbf{k}_{21})>0} d\mathbf{k}_{21}(\mathbf{p}_{21}\cdot\mathbf{k}_{21})f^{(2)\prime}(\tau_1)$$

$$+(\gamma_1\sigma^2/m)\lim_{\tau\to+0}\tau^{-1}\int_0^\tau d\tau_1\int d\mathbf{p}_2\int_{(\mathbf{p}_{21}\cdot\mathbf{k}_{21})<0} d\mathbf{k}_{21}(\mathbf{p}_{21}\cdot\mathbf{k}_{21})f^{(2)\prime\prime}(\tau_1) \tag{72}$$

where

$$f^{(2)\prime}(\tau_1)=f^{(2)}(\mathbf{r}_1-[(\tau-\tau_1)/m]\mathbf{p}_1-\tau_1\mathbf{p}_1',\ \mathbf{r}_1+\mathbf{k}_{21}\sigma-[(\tau-\tau_1)/m]\mathbf{p}_1-\tau_1\mathbf{p}_1',\ \mathbf{p}_1',\ \mathbf{p}_2',\ t\} \tag{73}$$

$$f^{(2)\prime\prime}(\tau_1)=f^{(2)}\{\mathbf{r}_1-(\tau/m)\mathbf{p}_1,\ \mathbf{r}_1+\mathbf{k}_{21}\sigma-(\tau_1/m)\mathbf{p}_2-[(\tau-\tau_1)/m]\mathbf{p}_1,\ \mathbf{p}_1,\ \mathbf{p}_2,\ t\} \tag{74}$$

and

$$\mathbf{p}_i'=\lim_{\tau\to+0}e^{-\tau\mathfrak{L}_2}\mathbf{p}_i.$$

The momenta in the arguments of the functions (73, 74) have already been changed by the rigid collision which occurs even though $\tau\to 0$, so that the τ_1-integration is merely a position average. Finally, we have

$$J^{(1)}=(\gamma_1\sigma^2/m)\int d\mathbf{p}_2\int_{(\mathbf{p}_{21}\cdot\mathbf{k}_{21})>0} d\mathbf{k}_{21}(\mathbf{p}_{21}\cdot\mathbf{k}_{21})f^{(2)}(\mathbf{r}_1,\ \mathbf{r}_1+\mathbf{k}_{21}\sigma,\ \mathbf{p}_1',\ \mathbf{p}_2',\ t)$$

$$+(\gamma_1\sigma^2/m)\int d\mathbf{p}_2\int_{(\mathbf{p}_{21}\cdot\mathbf{k}_{21})<0} d\mathbf{k}_{21}(\mathbf{p}_{21}\cdot\mathbf{k}_{21})f^{(2)}(\mathbf{r}_1,\ \mathbf{r}_1+\mathbf{k}_{21}\sigma,\ \mathbf{p}_1,\ \mathbf{p}_2,\ t)$$

$$=(\gamma_1\sigma^2/m)\int d\mathbf{p}_2\int_{(\mathbf{p}_{21}\cdot\mathbf{k}_{21})>0} d\mathbf{k}_{21}(\mathbf{p}_{21}\cdot\mathbf{k}_{21})[f^{(2)}(\mathbf{r}_1,\ \mathbf{r}_1+\mathbf{k}_{21}\sigma,\ \mathbf{p}_1',\ \mathbf{p}_2',\ t)-f^{(2)}(\mathbf{r}_1,\ \mathbf{r}_1-\mathbf{k}_{21}\sigma,\ \mathbf{p}_1,\ \mathbf{p}_2,\ t)]. \tag{75}$$

The same form for J may be obtained directly from (9) (with $s=1$) by a similar calculation; each term in the series (9) becomes $J^{(1)}/(N-1)$ in this limit so that the series sums to (75). This form has also been obtained, without using a time-displacement, directly from (19).[14]

In order to obtain an equation for $f^{(1)}$ it is necessary to introduce an assumption. The molecular chaos assumption will now be stated for rigid spheres. Let x^2 be in the part of $X^{(2)}$ where $r_{12}=\sigma$ and $(\mathbf{p}_{21}\cdot\mathbf{k}_{21})<0$. Then we will assume that

$$f^{(2)}(x^2,t)=Y(x^2)f^{(1)}(x_1,t)f^{(1)}(x_2,t), \tag{76}$$

where $Y(x^2)$ must at least compensate for the global difference between $f^{(2)}$ and $f^{(1)}f^{(1)}$ which arises from their definition. If Y is taken to be a function of one space vector and is evaluated midway between the positions of particles 1 and 2, then the insertion of (76) into (75) gives the modified Boltzmann equation proposed by Enskog. The assumption (76) is not a binary-collision approximation and does not depend on the prior introduction of such an approximation; thus the burden on Y is greater than that on β_2 in (26), for Y must supply the entire effect of the presence of a third particle. A more detailed discussion of the relation of the Enskog theory to the Liouville equation is given elsewhere.[14]

By itself the Liouville equation can provide no more than the inhomogeneous equation (75), to which it is equivalent in the case of rigid spheres. No attempt is made here to improve on the added statement (76). There is, however, disagreement concerning the form of the right side of (75) itself; in the next section a comparison is made between the form (75) and its analog derived by Rice, Kirkwood, Ross, and Zwanzig.[11]

V. ENSKOG EQUATION AND TIME-SMOOTHING

In this section, we present another derivation of (75), the modification of the Boltzmann equation proposed by Enskog, subject to the molecular chaos assumption. This derivation is related to the derivation of Rice *et al.*[11] based on the introduction of time-smoothed distribution functions,

$$\bar{f}^{(s)}(t)=\tau^{-1}\int_0^\tau d\tau_1 f^{(s)}(t+\tau_1)$$

The time-smoothed form of the first BBGKY equation [(19) with $s=1$] is

$$[(\partial/\partial t)+m^{-1}\mathbf{p}_1\cdot(\partial/\partial\mathbf{r}_1)]\bar{f}^{(1)}(t)=(\lambda\gamma_1/\tau)\int dx_2\int_0^\tau d\tau_1\theta_{12}f^{(2)}(t+\tau_1)=\bar{J} \tag{77}$$

By using (30), the binary collision approximation may be separated from the time-smoothed collision integral to obtain

$$\bar{J}=-(\lambda\gamma_1/\tau)\int_0^\tau d\tau_1\int dx_2(\kappa_2-\kappa_2^0)[e^{-\tau_1\kappa_2}f^{(2)}(t)+\mathcal{O}(\lambda)], \tag{78}$$

where θ_{12} has been expressed as

$$\theta_{12}=-(\kappa_2-\kappa_2^0) \tag{79}$$

in terms of κ_2 the Liouville operator of the pair and

$$\kappa_2^0=K_1+K_2=m^{-1}[\mathbf{p}_1\cdot(\partial/\partial\mathbf{r}_1)+\mathbf{p}_2\cdot(\partial/\partial\mathbf{r}_2)]$$

the Liouville operator for a "noninteracting pair." The effect of $\exp(-\tau\kappa_2^0)$ is to transform the particles along straight-line trajectories with constant momenta.

If the time τ over which the distribution functions are time-smoothed is taken to be arbitrarily small, we find from (78) that

$$\lim_{\tau\to+0}\bar{J}=J=-\gamma_1\int dx_2(\kappa_2-\kappa_2^0)f^{(2)}. \tag{80}$$

This is simply the right side of first BBGKY equation with θ_{12} expressed in terms of κ_2 and κ_2^0; all effects of the time-smoothing are entirely eliminated. Nevertheless, it is convenient to express the collision integral J, as given by (80) in the form,

$$J=\lim_{\tau\to+0}(\gamma_1/\tau)\int dx_2[\exp(-\tau\kappa_2)-\exp(-\tau\kappa_2^0)]f^{(2)}. \tag{81}$$

Clearly, this formal trick is possible for any potential with continuous derivatives. (A justification in this treatment of rigid spheres is obtained by considering the rigid sphere potential as the limit of a sequence of continuous potentials.) Using, for the position $\mathbf{r}_2$, spherical coordinates with origin at $\mathbf{r}_1$, we obtain from (81), the expression

$$J=\lim_{\tau\to+0}(\gamma_1/\tau)\int d\mathbf{p}_2\int d\mathbf{k}_{21}\int_0^\infty dr\, r^2[\exp(-\tau\kappa_2)-\exp(-\tau\kappa_2^0)]f^{(2)}. \tag{82}$$

We now consider the limit in which the potential becomes rigid and $e^{-\tau\kappa_2}$ takes into account rigid collisions. In this case (82) is the entire collision integral; there are no contributions to J from higher-order collisions.

The integration in (82) over the two hemispheres of $\mathbf{k}_{21}=\mathbf{k}$ may be carried out separately. Let us first consider the integration over the hemisphere on which $\mathbf{k}\cdot\mathbf{p}>0$, where

$$\mathbf{p}=\mathbf{p}_2-\mathbf{p}_1$$

If $r>\sigma+(\tau/m)(\mathbf{k}\cdot\mathbf{p})$ there is no contribution to J since then the natural and straight-line trajectories backwards in time are identical. If $\sigma+(\tau/m)(\mathbf{k}\cdot\mathbf{p})>r>\sigma$ a contribution arises from the first term since the natural trajectory carries the point back through a collision to a point outside the collision sphere and with the pre-collision momenta $\mathbf{p}_1'$ and $\mathbf{p}_2'$. No contribution to J arises from the second term, since the straight-line trajectory carries the point inside the collision sphere and $f^{(2)}$ is zero inside in the rigid sphere limit. If $r<\sigma$, the transformation back along a natural trajectory leads in the limit of rigid spheres to infinite momenta. Thus since $f^{(2)}$ is zero for infinite values of the momenta the first term does not contribute to the integral. Also if $r<\sigma$, the transformation back along a straight-line trajectory (a short distance) leads to a point inside the collision sphere. Then since $f^{(2)}$ is zero inside the collision sphere, the second term does not contribute to the integral. The total contribution to J of the integration over this hemisphere is thus

$$(\gamma_1\sigma^2/m)\int d\mathbf{p}_2\int d\mathbf{k}(\mathbf{k}\cdot\mathbf{p})\qquad(\mathbf{k}\cdot\mathbf{p})>0$$
$$f^{(2)}(\mathbf{r}_1,\mathbf{r}_1+\sigma\mathbf{k},\mathbf{p}',\mathbf{p}_2',t). \quad (83)$$

The contribution of the integration over the hemisphere on which

$$\mathbf{k}\cdot\mathbf{p}<0$$

is considered in a similar manner. If $r>\sigma$, the natural trajectory backwards in time is identical with the straight-line trajectory and hence the two terms in the integral of Eq. 82 are identical and there is no contribution to J. If $r<\sigma$, the transformation backwards along a natural trajectory leads to infinite momenta in the limit of rigid spheres and hence (since $f^{(2)}$ is zero for infinite momenta) the first term does not contribute to J. On the other hand, if $\sigma<r<\sigma+(\tau/m)(\mathbf{k}\cdot\mathbf{p})$, the transformation back along straight-line trajectories leads to a point outside the collision spheres and the second term contributes

$$(\gamma_1\sigma^2/m)\int d\mathbf{p}_2\int d\mathbf{k}(\mathbf{k}\cdot\mathbf{p})f^{(2)}(\mathbf{r}_1,\mathbf{r}_1+\sigma\mathbf{k},\mathbf{p}_1,\mathbf{p}_2,t)\qquad(\mathbf{k}\cdot\mathbf{p})<0 \quad (84)$$

to the collision integral. Finally, if $r<\sigma+(\tau/m)(\mathbf{k}\cdot\mathbf{p})$ the transformation back along straight-line trajectories leads to a point inside the collision spheres. Thus since $f^{(2)}$ is zero inside the collision sphere the second term does not contribute to J in this range of values of r.

The collision integral J is the sum of contributions given by (83, 84). In these two integrals the value of $f^{(2)}$ at x^2 with $r=\sigma$ is the limit obtained by considering a sequence of points in which $r\to\sigma$. Finally,

$$J=(\gamma_1\sigma^2/m)\int d\mathbf{p}_2\int d\mathbf{k}(\mathbf{k}\cdot\mathbf{p})f^{(2)}(\mathbf{r}_1,\mathbf{r}_1+\sigma\mathbf{k},\mathbf{p}_1',\mathbf{p}_2',t)\qquad(\mathbf{k}\cdot\mathbf{p})>0$$
$$+(\gamma_1\sigma^2/m)\int d\mathbf{p}_2\int d\mathbf{k}(\mathbf{k}\cdot\mathbf{p})f^{(2)}(\mathbf{r}_1,\mathbf{r}_1+\sigma\mathbf{k},\mathbf{p}_1,\mathbf{p}_2,t), \quad (85)\qquad(\mathbf{k}\cdot\mathbf{p})<0$$

in which $\mathbf{k}$ appears only explicitly in the second term, which can be transformed to obtain

$$J=(\gamma_1\sigma^2/m)\int d\mathbf{p}_2\int d\mathbf{k}(\mathbf{k}\cdot\mathbf{p})[f^{(2)}(\mathbf{r}_1,\mathbf{r}_1+\sigma\mathbf{k},\mathbf{p}_1',\mathbf{p}_2',t)-f^{(2)}(\mathbf{r}_1,\mathbf{r}_1-\sigma\mathbf{k}.\,\mathbf{p}_1,\mathbf{p}_2,t)]. \quad (86)\qquad(\mathbf{k}\cdot\mathbf{p})>0$$

If we adopt (76), then (86) becomes identical to the collision integral of the Boltzmann equation for a dense gas of rigid spheres proposed by Enskog.

The integral (86) differs from that developed by Rice, Kirkwood, Ross, and Zwanzig[11] and Dahler[17] in the sign of $\mathbf{k}$ in the argument of the function in the second term. This difference is equivalent to a difference in the hemisphere over which the second integral in (86) is integrated.

The origin of the differences between the present results and those of Dahler[17] are clear; Dahler neglected all the contributions to (82) from values of $r<\sigma$. He thus obtained no contribution from the hemisphere on which $(\mathbf{k}\cdot\mathbf{p})<0$. In evaluating the integral over the hemisphere on which $(\mathbf{k}\cdot\mathbf{p})>0$, Dahler assumed that $f^{(2)}$ was finite inside the collision sphere and continuous with the function outside. Recently O'Toole and Dahler[12] have pre-

[17] J. S. Dahler, J. Chem. Phys. **30**, 1447 (1959).

sented another derivation of J. Using arguments similar to those considered in the present paper, they conclude that the Enskog collision integral is correct, subject to the molecular chaos assumption.

The origin of the differences between the Enskog result and the result of Rice, Kirkwood, Ross, and Zwanzig lies deeper in the formalism. These authors use the binary-collision approximation in (78) in the form

$$\bar{J}=(\gamma_1/\tau)\int_0^\tau d\tau_1\int dx_2\int d\hat{x}_2\theta_{12}\delta(\hat{x}^2-e^{-\tau_1\mathfrak{L}_2}x^2)f^{(2)}(x^2,t) \tag{87}$$

and make use of the factorization

$$\delta(\hat{x}^2-e^{-\tau_1\mathfrak{L}_2}x^2)=\delta(\hat{\mathbf{r}}^2-e^{-\tau_1\mathfrak{L}_2}\mathbf{r}_2)\,\delta(\hat{\mathbf{p}}^2-e^{-\tau_1\mathfrak{L}_2}\mathbf{p}^2)$$

to obtain

$$\begin{aligned}\theta_{12}\delta(\hat{x}^2-e^{-\tau_1\mathfrak{L}_2}x^2)&=[(\partial/\partial\tau_1)+\kappa_2{}^0]\delta(\hat{x}^2-e^{-\tau_1\mathfrak{L}_2}x^2)\\&=\delta(\hat{\mathbf{r}}^2-e^{-\tau_1\mathfrak{L}_2}\mathbf{r}^2)\,(\partial/\partial\tau_1)\,\delta(\hat{\mathbf{p}}^2-e^{-\tau_1\mathfrak{L}_2}\mathbf{p}^2)+R,\end{aligned}$$

where the remainder

$$R=\delta(\hat{\mathbf{p}}^2-e^{-\tau_1\mathfrak{L}_2}\mathbf{p}^2)\,(\partial/\partial\tau_1)\,\delta(\hat{\mathbf{r}}^2-e^{-\tau_1\mathfrak{L}_2}\mathbf{r}_1)+\kappa_2{}^0\delta(\hat{x}^2-e^{-\tau_1\mathfrak{L}_2}x^2)$$

is ignored. Thus J is obtained as

$$\bar{J}=(\gamma_1/\tau)\int_0^\tau d\tau_1\int dx_2\int d\hat{x}_2\delta(\hat{\mathbf{r}}^2-e^{-\tau_1\mathfrak{L}_2}\mathbf{r}^2)\,(\partial/\partial\tau_1)\,\delta(\hat{\mathbf{p}}^2-e^{-\tau_1\mathfrak{L}_2}\mathbf{p}^2)f^{(2)}(x^2,t). \tag{88}$$

Assuming that in the limit $\tau\to+0$ the τ_1-dependence of $\delta(\hat{\mathbf{r}}^2-e^{-\tau_1\mathfrak{L}_2})\,\mathbf{r}$ is negligible, (88) is finally expressed as

$$\begin{aligned}\bar{J}&=\lim_{\tau\to+0}(\gamma_1/\tau)\int_0^\tau d\tau_1\int dx_2\int d\hat{x}_2(\partial/\partial\tau_1)\,\delta(\hat{x}^2-e^{-\tau_1\mathfrak{L}_2}x^2)f^{(2)}(x^2,t)\\&=\lim_{\tau\to+0}(\gamma_1/\tau)\int dx_2(e^{-\tau\mathfrak{L}_2}-1)f^{(2)}(x^2,t).\end{aligned} \tag{89}$$

A comparison of (89) with (81) shows that the approximations used to obtain (89) are equivalent to the replacement of $\exp(-\tau\kappa_2{}^0)$ by unity in (81).

The analog of (86) obtained by Rice *et al.*[11] from (89) is

$$\bar{J}=(\gamma_1\sigma^2/m)\int d\mathbf{p}_2\int d\mathbf{k}(\mathbf{k}\cdot\mathbf{p})[f^{(2)}(\mathbf{r}_1,\,\mathbf{r}_1+\sigma\mathbf{k},\,\mathbf{p}_1',\,\mathbf{p}_2',\,t)-f^{(2)}(\mathbf{r}_1,\,\mathbf{r}_1+\sigma\mathbf{k},\,\mathbf{p}_1,\,\mathbf{p}_2,\,t)]. \tag{90}$$

It seems clear that the values of $f^{(2)}$ in the two terms of the integrand in (90) are equal and (90) is $J=0$, for if this were not the case then the distribution functions would change discontinuously with time.

VI. MOLECULAR CHAOS ASSUMPTION AND THE BOGOLYUBOV THEORY

In previous sections we have attempted to show that the molecular chaos assumption is capable of determining a Boltzmann equation to any order in the density for some potentials, including the rigid-sphere potential. It remains to be seen, of course, whether this assumption can provide a successful kinetic theory for soft potentials, but the success of the Enskog theory of dense gases composed of rigid spheres provides some encouragement.

In the present section we raise the question of whether this assumption, which is as old as the Boltzmann equation, is the only substantial tool that has been used in the development of kinetic theory from a statistical-mechanical point of view. This question is discussed elsewhere[14]; here we wish to indicate the relation between this assumption and the Bogolyubov assumptions which have been used by Uhlenbeck and Choh to formulate a kinetic theory explicitly to the ternary-collision approximation.[10] For the purpose of discussing this relation we will describe part of the formal development.

The assumptions of Bogolyubov may be described as follows. It is assumed that $f^{(s)}$ depends on time only through $f^{(1)}$. Thus $f^{(s)}$ is a functional of $f^{(1)}$. This is a much more general statement than the molecular chaos assumption, in which it is assumed that $f^{(s)}$ is a particular functional of $f^{(1)}$ on at least part of $X^{(s)}$. On the other hand, the Bogolyubov assumption is used in an essential way on the whole of $X^{(s)}$. Secondly, it is assumed that $f^{(s)}$, $s\geq 2$, admits an expansion in v where $v=V/N$, the ratio of the total volume of the gas to the total number of particles (this parameter is held

fixed while the size of the system becomes infinite to remove the walls). Thus

$$f^{(s)}[x^s \mid f^{(1)}(t)] = \sum_{n=0}^{\infty} (1/v)^n f_n^{(s)}. \tag{91}$$

The absence of v dependence in $f^{(1)}$ at a fixed time t is important; in the initial value problem $f^{(1)}$ acquires v dependence, but the problem considered here is that of finding a Boltzmann equation at a fixed time t. Finally, it is assumed that

$$\lim_{\tau\to\infty} e^{-\tau\kappa_s} f^{(s)}[x^s \mid e^{\tau\kappa_1} f^{(1)}(t)] = \lim_{\tau\to\infty} e^{-\tau\kappa_s} \exp(\tau \sum_{i=1}^{s} K_i) \prod_{\nu=1}^{s} f^{(1)}(x_\nu, t) \tag{92}$$

which is, in view of (91)

$$\lim_{\tau\to\infty} e^{-\tau\kappa_s} f_0^{(s)}[x^s \mid e^{\tau\kappa_1} f^{(1)}(t)] = \lim_{\tau\to\infty} e^{-\tau\kappa_s} \exp(\tau \sum_{i=1}^{s} K_i) \prod_{\nu=1}^{s} f^{(1)}(x_\nu, t) \tag{93}$$

$$\lim_{\tau\to\infty} e^{-\tau\kappa_s} f_n^{(s)}[x^s \mid e^{\tau\kappa_1} f^{(1)}(t)] = 0, \qquad n > 0. \tag{94}$$

The boundary condition $f^{(N)} \to 0$ as $|x_i| \to \infty$ is adopted, and since

$$\lim_{\tau\to\infty} e^{-\tau\kappa_s} |x_i| = \infty,$$

this condition requires that the left side, but not the right side, of (93) vanish unless $f_0^{(s)}$ depends on x_i, as well as t, only through $f^{(1)}$. The logical difficulty here is overcome by forcing this property on $f_0^{(s)}$ in a way that will be described in the following.

The derivatives of $f^{(1)}$ are functions of v and the first BBGKY equation (19) is used in the form

$$(\partial/\partial t) f^{(1)} = A[x_1 \mid f^{(1)}(t)] = \sum_{n=0}^{\infty} (1/v)^n A_n. \tag{95}$$

Thus A is immediately defined in terms of $f^{(2)}$, but is immediately determined only to zero order:

$$A_0 = -(1/m)\, \mathbf{p}_1 \cdot (\partial/\partial \mathbf{r}_1) f^{(1)}. \tag{96}$$

The A_n are functionals of $f^{(1)}$.

The higher BBGKY equations are

$$[(\partial/\partial t) + \kappa_s] f_n^{(s)} = \epsilon_s \int dx_{s+1} \Omega_{s+1} f_{n-1}^{(s+1)} \tag{97}$$

where ϵ_s is $v\gamma_s$ in our notation. We may take $\epsilon_s = 1$ which fixes all the ratios among the normalization constants α_i. In particular we have

$$[(\partial/\partial t) + \kappa_s] f_0^{(s)} = 0. \tag{98}$$

The time derivative of $f^{(s)}$ is obtained by formally differentiating the formula for $f^{(s)}$ with respect to each $f^{(1)}$, multiplying by $(\partial/\partial t) f^{(1)}$, and summing these functionals. The result is a linear functional of $(\partial/\partial t) f^{(1)} = A$, and hence a new functional of $f^{(1)}$. The BBGKY equations, therefore, are regarded as functional equations for $f^{(1)}$ which are to be determined in a stepwise manner. The symbol for the linear functional of $(\partial/\partial t) f^{(1)}$ just described is

$$\left[\frac{\delta f^{(s)}(x^s \mid f^{(1)})}{\partial f^{(1)}}, \frac{\partial f^{(1)}}{\partial t}\right] = \left[\frac{\partial f^{(s)}}{\partial f^{(1)}}, A\right] = \frac{\partial f^{(s)}}{\partial t}. \tag{99}$$

Expanding (99) in $(1/v)$ we obtain

$$\left[\frac{\delta f_0^{(s)}(x^s \mid f^{(1)})}{\partial f^{(1)}}, A_0(x^s \mid f^{(1)})\right] + \kappa_s f_0^{(s)}(x^s \mid f^{(1)}) = [(\partial/\partial t) + \kappa_s] f_0^{(s)} = 0, \tag{100}$$

which may be solved for $f_0^{(s)}$.

The difficulty inherent in (93) is overcome by replacing (100) by

$$\left[\frac{\partial f_0^{(s)}(x^s \mid e^{\tau\kappa_1} f^{(1)})}{\delta e^{\tau\kappa_1} f^{(1)}}, A_0(x^s \mid e^{\tau\kappa_1} f^{(1)})\right] + \kappa_s f_0^{(s)}(x^s \mid e^{\tau\kappa_1} f^{(1)}) = 0, \tag{101}$$

which is not equivalent to (100) unless $f_0^{(s)}$ depends on x_i only through $f^{(1)}$. Thus the equivalence of the two initial value problems based on (100) and (101) with a common initial value is an additional assumption in the Bogolyubov theory which evidently restricts the general nature of the other postulates.

Since (101) is

$$[(\partial/\partial\tau) - \kappa_s] f_0^{(s)}(x^s \mid e^{\tau\kappa_1} f^{(1)}) = 0,$$

we have

$$f_0^{(s)}(x^s \mid e^{\tau\kappa_1} f^{(1)}) = e^{\tau\kappa_s} f_0^{(s)}(x^s \mid f^{(1)}). \tag{102}$$

The inverse of $e^{\tau\varepsilon_0}$ is applied to (102) to obtain

$$f_0^{(s)}(x^s \mid f^{(1)}) = e^{-\tau\varepsilon_s} f_0^{(s)}(x^s \mid e^{\tau\varepsilon_1} f^{(1)}), \quad (103)$$

in which the limit $\tau \to \infty$ is taken to make use of (93). The result is the zero-order molecular chaos assumption:

$$f_0^{(s)} = \lim_{\tau\to\infty} e^{-\tau\varepsilon_s} \exp(\tau \sum_{i=1}^{s} K_i) \prod_{r=1}^{s} f^{(1)}(x_r, t). \quad (104)$$

The calculation of $f_1^{(2)}$ must be preceded by the determination of A_1 from $f_0^{(2)}$, which is immediately given by the form of the first BBGKY equation:

$$A_1 = \int dx_2 \theta_{12} \mathcal{S}_{12}^{(2)} f^{(1)}(x_1, t) f^{(1)}(x_2, t). \quad (105)$$

The calculation of higher $f_n^{(2)}$ and A_n is more complicated; the formula obtained by Choh and Uhlenbeck for $f_1^{(2)}$ is

$$f_1^{(2)} = \int_0^\infty d\tau e^{-\tau\varepsilon_2} \int dx_3 [(\theta_{13}+\theta_{23}) \mathcal{S}_{123}^{(3)} - \mathcal{S}_{12}^{(2)} (\theta_{13}\mathcal{S}_{13}^{(2)} + \theta_{23}\mathcal{S}_{23}^{(2)})] \exp(\tau \sum_{i=1}^{3} K_i) \prod_{r=1}^{3} f^{(1)}(x_r, t). \quad (106)$$

In order to show that (104–106) are given by the molecular chaos assumption without other important assumptions, we repeat the calculation of Sec. III with the following changes. The $f^{(s)}$, $s>1$, are assumed to be expanded in $(1/v)$, with choices of α_i which satisfy $\gamma_s = 1/v$; the statement (28) on $Y^{(3)}$ with $\beta_s = 1$ is assumed, and it is assumed that ϕ is sufficiently short range and repulsive that T_s exists on $Y^{(s)}$. From (32) we obtain

$$f^{(s)}(t) = e^{-\tau\varepsilon_s} f^{(s)}(t-\tau) + v^{-1} \int_0^\tau dt_1 e^{-t_1\varepsilon_s} \int dx_{s+1} \Omega_{s+1} f^{(s+1)}(t-t_1), \quad (107)$$

in which the molecular chaos assumption is used to obtain

$$f^{(s)}(t) = e^{-\tau\varepsilon_s} \prod_{r=1}^{s} f^{(1)}(x_r, t-\tau) + \mathcal{O}(1/v). \quad (108)$$

The functions $f^{(1)}$ in (108) are replaced by

$$f^{(1)}(t-\tau) = e^{\tau\varepsilon_1} \left[f^{(1)}(t) - v^{-1} \int_0^\tau dt_1 e^{-t_1\varepsilon_1} \int dx_2 \Omega_2 f^{(2)}(t-t_1) \right] \quad (109)$$

from (31). As is expected, (109) shows that $f^{(1)}$ may be independent of v only at a fixed time t. Taking $\tau \geq \tau_s$, of course, and expanding $f^{(s)}$ we have

$$f^{(s)}(t) = e^{-\tau\varepsilon_s} \exp(\tau \sum_{i=1}^{s} K_i) \prod_{r=1}^{s} f^{(1)}(x_r, t) + \mathcal{O}(1/v)$$

or

$$f_0^{(s)}(t) = e^{-\tau\varepsilon_s} \exp(\tau \sum_{i=1}^{s} K_i) \prod_{r=1}^{s} f^{(1)}(x_r, t) \quad (110)$$

which is (104). The formula (105) follows immediately, as it does in the Bogolyubov theory.

Expanding $f^{(s)}$ in $1/v$ in the calculation that ends at (46) we obtain $f_1^{(2)}$ in the form

$$f_1^{(2)}(t) = \int_0^t dt_1 e^{-t_1\varepsilon_2} \int dx_3 [(\theta_{13}+\theta_{23}) \mathcal{S}_{123}^{(3)} - e^{-(\tau-t_1)\varepsilon_3} e^{(\tau-t_1)K_1} e^{\tau K_2} \theta_{13} \mathcal{S}_{13}^{(2)} e^{-t_1 K_2} - e^{-(\tau-t_1)\varepsilon_3} e^{(\tau-t_1)K_2} e^{\tau K_1} \theta_{23} \mathcal{S}_{23}^{(2)} e^{-t_1 K_1}]$$

$$\times \exp(t_1 \sum_{i=1}^{3} K_i) \prod_{r=1}^{3} f^{(1)}(x_r, t) \quad (111)$$

where, as in Sec. III,

$$\mathcal{S}_{1,2,\cdots,s}^{(s)}=\mathcal{S}_{1,2,\cdots,s}^{(s)}(\infty)=\mathcal{S}_{1,2,\cdots,s}^{(s)}(\tau)$$

$$=e^{-\tau L_s}\exp(\tau\sum_{i=1}^{s}K_i),\qquad \tau\geq T_s.$$

If we let $\tau\to\infty$ in (103) with $s=2$, then $f_0^{(2)}$ becomes constant at $\tau=\tau_2$, when the molecular chaos assumption is introduced, and $f_1^{(2)}$ is determined by

$$f_1^{(2)}=\int_0^\infty d\tau e^{-\tau L_2}\int dx_3[(\theta_{13}+\theta_{23})\mathcal{S}_{123}^{(1)}$$

$$-\mathcal{S}_{12}^{(2)}(\theta_{13}\mathcal{S}_{13}^{(2)}+\theta_{23}\mathcal{S}_{23}^{(2)})]$$

$$\times\exp(\tau\sum_{i=1}^{3}K_i)\prod_{\nu=1}^{3}f^{(1)}(x_\nu,t),\quad(112)$$

where the integration variable t_1 in (111) has been replaced by τ, and the transformations $\mathcal{S}_{23}^{(2)}$ and $e^{-\tau L_i}$ $(i,j\neq i)\leq 2$, have been commuted. For fixed (x_1,x_2,x_3), the τ integral receives no contributions on $T_3<\tau<\infty$. as was shown in Sec. III.

Since (112) is (106), we conclude that the form of J determined by the molecular chaos assumption as used in Sec. III is the same to the ternary collision approximation as the J determined by the Bogolyubov assumptions. It seems possible that the generality of the Bogolyubov assumption concerning the nature of the functional $f^{(s)}$ is reduced by the compensation of logical errors in (93) and (101). We speculate that the Bogolyubov theory is given by the molecular chaos assumption, but we have not obtained the complicated induction which would reveal this equivalence in higher order.

On the Theory of the Critical Point of a Simple Fluid

MELVILLE S. GREEN

National Bureau of Standards, Washington 25, D. C.

(Received July 28, 1960)

The consequences of a new system of integral equations for the theory of the critical point are discussed. Reasons are given for believing that the fundamental assumption of the Ornstein-Zernicke theory about the direct correlation function is incorrect.

IT would be impossible to carry out a modern investigation in the statistical theory of fluids without building in a hundred ways on ideas, concepts, and lines of approach, contributed by Professor Kirkwood. In this issue of the *Journal of Chemical Physics* devoted to his honor, it is appropriate to mention specifically those of Professor Kirkwood's contributions upon which the present work is founded. The first of these is the idea that reduced distribution functions, and in particular the pair distribution function, are important and useful mathematical objects in the theory of dense gases and liquids.[1] The second is that in dense gases and liquids, the pair distribution function may be better determined implicitly through the solution of an integral equation rather than explicitly from its defining formula or from a series expansion.[2] The third, finally, is the idea that mathematical singularities in the integral equation are to be interpreted as phase transitions.[3]

Although these ideas of Kirkwood have motivated the present investigation, they are carried out, as is perhaps natural, rather differently than in Kirkwood's own work. The integral equation for the pair distribution with which we will be concerned is neither the one developed by Kirkwood nor the very similar one of Born-Green,[4] but a system of three integral equations for three parts of the pair distribution which have recently been derived by Van Leeuwen, Groeneveld, and DeBoer, and independently by Meeron, and by the author.[5] These equations are derived by summation of infinite subclasses of terms in the Mayer density expansion for the pair distribution function, and insofar as the rearrangements are mathematically justified, these equations involve no approximations.

If we define the pair correlation function $G(R)$ by the formula

$$f_2(\mathbf{X}_1\mathbf{X}_2)=\rho^2[G(R_{12})+1], \tag{1}$$

where $f_2(\mathbf{X}_1\mathbf{X}_2)$ is the pair distribution function, ρ the number density, and $R_{12}=|\mathbf{X}_1-\mathbf{X}_2|$ and write

$$G(R)=S(R)+P(R)+B(R)-\beta V(R), \tag{2}$$

where $S(R)$, $P(R)$, and $B(R)$ are the three parts of the pair correlation function referred to above, $V(R)$ is the intermolecular pair potential, and $\beta=1/kT$, the three equations in question are

$$T(R)=\exp[-\beta V(R)+S(R)+B(R)]-S(R)-1 \tag{3}$$

$$s(k)=[\rho t^2(k)]/[1-\rho t(k)] \tag{4}$$

$$B(R)=\sum_{n=2}^{\infty}(\rho^n/n!)\sum_{\substack{1,2\\ \text{all wider-sense}\\ \text{irreducible graphs}}}\int\Pi G(R_{ij})\,d(3)\cdots d(n+2)$$
$$=\Phi_1[R,G(R)]. \tag{5}$$

In Eq. (3)

$$T(R)=P(R)+B(R)-\beta V(R), \tag{6}$$

and in Eq. (4)

$$kt(k)=4\pi\int RT(R)\,\sin kR\,dR \tag{7}$$

$$ks(k)=4\pi\int RS(R)\,\sin kR\,dR \tag{8}$$

[$t(k)$ and $s(k)$ are, respectively, the Fourier transforms of $T(R)$ and $S(R)$]. In Eq. (5), $B(R)$ is defined by an infinite series of a form very similar to the Mayer density series for the pair distribution function. Each term in the integrand is associated with a Mayer graph consisting of the points 1 and 2, a number of other points, together with a number of lines joining them. For every line joining the points, say, ij, a factor $G(R_{ij})$ appears in the integrand of the corresponding term. The sum on the right in Eq. (5) includes all terms corresponding to the class of graphs which we have called 1, 2 wider-sense irreducible. This class is the subclass of the irreducible Mayer graphs for the potential of average force whose members contain no ij subgraph.[6] An ij subgraph consists of i, j, and at least one other point, does not contain both 1 and 2, and has only i and j in common with the remainder of the graph.

[1] J. G. Kirkwood, J. Chem. Phys. **3**, 300 (1935).
[2] J. G. Kirkwood, J. Chem. Phys. **7**, 919 (1939).
[3] J. G. Kirkwood and E. Monroe, J. Chem. Phys. **8**, 845 (1940).
[4] M. Born and H. S. Green, *A Kinetic Theory of Liquids* (Cambridge University Press, New York, 1949).
[5] J. M. J. Van Leeuwen, J. Groeneveld, and J. DeBoer, Physica **25**, 792 (1959); E. Meeron, Phys. Fluids **1**, 246 (1958), J. Math. Phys. **1**, 192 (1960). M. S. Green, Hughes Aircraft Company Rept., September, 1959.
[6] E. Meeron, Phys. Fluids **1**, 139 (1958).

It has been pointed out by R. W. Zwanzig that Eqs. (3)–(5) [together with definitions Eqs. (2) and (6)–(8)] can be replaced by a single equation for the pair correlation function which is very similar in form to both the Kirkwood and the Born-Green integral equations based on the superposition approximation. The equation is

$$\log[G(R)+1]$$

$$=-\beta V(R)+\rho\int T(|\mathbf{R}-\mathbf{X}|)g(|\mathbf{X}|)d\mathbf{X}+B(R), \quad (9)$$

where

$$T(R)=-\beta V+G(R)-\log[G(R)+1]+B(R), \quad (10)$$

and $B(R)$ is given in terms of $G(R)$ through Eq. (5).

With respect to the third idea mentioned, the present work will consider the liquid-vapor transition rather than the liquid-solid transition considered by Kirkwood. Perhaps the most interesting feature of the equations we have described is that the vanishing of the denominator in Eq. (4) for $k=0$ is rigorously associated with an infinite compressibility. This can be seen by noting that $g(k)$, the Fourier transform of $G(R)$ can be written by Eqs. (2) and (6) as

$$g(k)=s(k)+t(k)=t(k)/[1-\rho t(k)]. \quad (10a)$$

If the denominator in Eq. (10a) vanishes for $k=0$, $g(0)$ is infinite. $g(0)$, however, is nothing else than

$$\int G(R)d\mathbf{R}.$$

This integral is related to the compressibility κ by a well-known formula

$$\kappa=\rho kT[1+\rho g(0)], \quad (11)$$

and κ is infinite when $g(0)$ is infinite.[7]

Now the only stable point in the thermodynamic phase plane of a simple liquid which has an infinite compressibility is the critical point. These integral equations are thus especially suited to the study of the critical point and since the critical point is in effect the beginning of the distinction between liquid and vapor, we can expect them to yield information also about the liquid-vapor transition. In fact, one of the equations has long been used in the theory of the critical point. Eq. (10a) is nothing else than the expression in Fourier transform language of an equation used by Ornstein and Zernicke in their 1917 phenomenological theory of critical opalescence.[8] Their equation is a relation between the pair correlation function $G(R)$, and what they call the direct pair correlation function, $T(R)$. From their phenomenological considerations, it was reasonable for them to assume that whereas the correlation function becomes extremely long range at the critical point, which fact is responsible for critical opalescence, the range of the direct correlation function remains finite and of the order of the range of intermolecular forces. If this last supposition is interpreted mathematically to mean that $T(R)$ has all moments, or in Fourier language, that $t(k)$ has a Taylor expansion in powers of k^2, Eq. (10a) together with the assumption of short rangedness of $T(R)$ are by themselves sufficient to give a quite explicit form for $G(R)$ near the critical for large R. The Ornstein-Zernicke theory gives

$$G(R)\sim(\exp-\alpha R)/R \quad \text{for large } R, \quad (12)$$

and

$$g(k)\sim(\alpha^2+k^2)^{-1} \quad \text{for small } k, \quad (13)$$

α is small near, and zero at the critical point. Other authors, starting from different, but evidently equivalent assumptions arrive at the same result.[9]

Equations (3)–(5), however, contain more information about $T(R)$ and $G(R)$ than is contained in Eq. (10a) and indeed, if it were possible to determine the behavior of the solutions for values of ρ and T for which the denominator of Eq. (5) is zero or small for $k=0$, we should not need to make suppositions about $T(R)$, near the critical. We have not succeeded in doing this, but it has been possible to make a rather complete analysis near a singularity of the system of two equations relating $S(R)$ and $T(R)$ which results from setting $B(R)=0$. From this solution, the somewhat surprising fact emerges that the range of the direct correlation, $T(R)$ for the approximate equations, does not remain finite at the critical in the sense that all its moments exist although it is shorter ranged than $G(R)$ itself. The solution requires that

$$T(R)\sim 1/R^4 \quad (14)$$

$$G(R)\sim 1/R^2 \quad (15)$$

$$g(k)\sim 1/k, \quad (16)$$

for large R at the critical. In the last section of the paper, an attempt is made to analyze the effect of the various terms of $B(R)$ leading to the conclusion that the right-hand sides of Eqs. (14) and (15) should each be multiplied by some function of R which is of order less than any positive and greater than any negative power. This conclusion is in direct conflict with the conclusion of the classical theory.

Although our conclusions are based on the very inadequate treatment of the infinite series of terms $B(R)$, they are derived from a more complete system of equations than the classical theory. At the very least, they cast doubt on the basic assumptions of the classical theory. Since $g(k)$ is a rather directly available datum

[7] J. O. Hirschfelder, C. Curtiss, and R. Bird, *Molecular Theory of Gases and Liquids*, (John Wiley & Sons., Inc., New York, 1954), pp. 127, 128.

[8] L. S. Ornstein and F. Zernicke, Proc. Acad. Sci. Amsterdam, **17**, 793 (1914); Z. Physik. **27**, 761 (1926); see also L. Rosenfeld, *Theory of Electrons* (North-Holland Publishing Company, Amsterdam, 1951).

[9] P. Debye, J. Chem. Phys. **31**, 680 (1959); M. Fixman, J. Chem. Phys. **33**, 1357, 1363 (1960), this issue.

in light, x-ray and neutron scattering from liquids in the critical region, an effective test of the classical theory is possible.[10]

The derivation of Eqs. (3)–(5) by summing infinite subclasses of terms has been given by Van Leeuwen, Groeneveld, and DeBoer.[5] In Sec. I we show how they may be derived from a variation principle and show that the function which is varied is the Helmholtz free energy expressed as a functional of $S(R)$, $P(R)$,[11] $B(R)$. In Sec. II, we discuss the relation of the roots of the denominator in Eq. (4) to the liquid vapor phase transition. In Sec. III, we exhibit a solution of the approximate equations. In Sec. IV, we discuss this solution.

I. VARIATIONAL PRINCIPLE FOR THE INTEGRAL EQUATIONS

We consider the following functional of $S(R)$, $P(R)$, $B(R)$:

$$\Psi[S(R),T(R),B(R)]=\tfrac{1}{2}[1/(2\pi)^3]\int\{\log[1-\rho t(k)]^{-1}-\tfrac{1}{2}[\rho^2 t^2(k)]-\rho t(k)\}d\mathbf{k}$$

$$+\tfrac{1}{2}\rho^2\int\{\exp[-\beta V(R)+S(R)+B(R)]-\tfrac{1}{2}\{[-\beta V(R)+S(R)+B(R)]^2-\beta^2V^2(R)\}$$

$$-S(R)-B(R)-1\}d\mathbf{R}-(\rho^2/2)\int\{P(R)S(R)+P(R)B(R)+\tfrac{1}{2}B^2(R)\}d\mathbf{R}$$

$$+(\rho V)^{-1}\sum(\rho_n/n!)\sum_{\substack{\text{all wider-sense}\\ \text{irreducible graph}\\ \text{of } 1\cdots n}}\int\Pi G(R_{ij})d(1)\cdots d(n). \quad (17)$$

In Eq. (17), the term wider-sense irreducible graph means an irreducible graph which contains no $i-j$ subdiagrams other than the simple bond.

To compute the functional derivatives of Ψ with respect to S, P, and B, we need $\delta\Phi/\delta G(R)$ where $\Phi[G(R)]$ represents the last group of terms on the right in Eq. (17). This is simply $\frac{1}{2}\rho^2\Phi_1[R,G(R)]$. The variation of a particular contribution to Φ is

$$V^{-1}(\rho^n/n!)\sum_{kl}\int d(k)d(l)\,\delta G(R_{kl})\int\prod_{ij\neq kl}G(R_{ij})d(1)\cdots d(h-1)d(h+1)\cdots d(l-1)d(l+1)\cdots d(n). \quad (18)$$

The second product is taken over all lines of the wider-sense irreducible cluster to which the contribution corresponds except the line kl, while the sum is over all pairs kl corresponding to lines of the graph. Now a wider-sense irreducible graph with one line removed is a 1, 2-wider-sense irreducible graph. Thus every contribution to the variation of $\Phi[G(R)]$ corresponds to a term in $\Phi_1[R,G(R)]$. Assigning a factor ρ to each of the n-2 internal points and taking account of the $n!/2!\times(n-2)!$ ways of assigning labels, our statement is verified.

Taking the variation with respect to $S(R)$, we have $[\phi=-\beta V(R)]$

$$\delta\Psi/\delta S(R)=\tfrac{1}{2}\rho^2[\exp(\phi+S+B)-(\phi+S+B)-1]-\tfrac{1}{2}\rho^2[P(R)+B(R)]+\tfrac{1}{2}\rho^2\Phi_1[R,G(R)]. \quad (19)$$

Similarly, taking the variation with respect to $P(R)$, we obtain

$$\delta\Psi/\delta P(R)=\tfrac{1}{2}\rho^2[1/(2\pi)^3]\int\{\rho t^2(k)/[1-\rho t(k)]\}\exp(i\mathbf{k}\cdot\mathbf{R})dk-\tfrac{1}{2}\rho^2(S+B)+\tfrac{1}{2}\rho^2\Phi_1[R,G(R)]. \quad (20)$$

[10] The most extensive experimental test of the Ornstein-Zernicke theory of critical opalescence has been carried out in binary solutions. Three investigations which apply modern methods to the test of the theory are those of B. H. Zimm [J. Phys. Coll. Chem. **54**, 1306 (1950)], Chow Quantie [Proc. Roy. Soc. (London) **A224**, 90 (1954)], and P. Debye, H. Coll, and D. Woermann [J. Chem. Phys. **32**, 939 (1960)]. The most serious difficulty with this type of experiment is multiple scattering which is large because of the large turbidities encountered especially near the critical point. Zimm (private communication) has adjusted his data for multiple scattering and has found confirmation of the O.Z. theory. On the other hand, his corrections were quite large near the critical point and the author feels that for a completely satisfactory test multiple scattering should be minimized by using small scattering volumes and small refractive index differences. The author has replotted the data of R. L. Wild [J. Chem. Phys. **18**, 1627 (1950)] on x-ray scattering near the critical point of nitrogen and has found significant deviations from the O.Z. theory. For an extensive bibliography and discussion on critical opalescence, see F. D. Rossini, *Thermodynamics and Physics of Matter* (Princeton University Press, Princeton, New Jersey, 1955), article by O. K. Rice.

[11] $P(R)$ is defined by the equation $T(R)=P(R)+B(R)-\beta V(R)$.

Finally,

$$\delta\Psi/\delta B(R)=\tfrac{1}{2}\rho^2[1/(2\pi)^3]\int\{\rho t^2(k)/[1-\rho t(k)]\}\ \exp(i\mathbf{k}\cdot\mathbf{R})dk+\tfrac{1}{2}\rho^2\exp(\phi+S+B)-(\phi+S+B)-1$$

$$-\tfrac{1}{2}\rho^2(S+P+B)+\tfrac{1}{2}\rho^2\Phi_1[R,G(R)]. \quad (21)$$

The right-hand sides of Eqs. (19)–(21) vanish as a consequence of Eqs. (3)–(5). Similarly, if $\delta\Psi/\delta B(R)$, $\delta\Psi/\delta S(R)$, and $\delta\Psi/\delta B(R)$ are all zero, Eqs. (3)–(5) follow.

We complete this section by showing that the functional Ψ is the excess Helmholtz free energy over that of a perfect gas. To do this, it is convenient to introduce dimensionless variables. We set $x=R\rho^{\frac{1}{3}}$, $\kappa=k\rho^{-\frac{1}{3}}$, $\mathfrak{S}(x)=S(R)$, $\mathcal{P}(x)=P(R)$, $\mathfrak{B}(x)=B(R)$, $\phi(x)=-\beta V(R)$, $\mathfrak{I}(x)=T(R)$, and $\mathfrak{s}(\kappa)=\rho s(k)$, $\mathfrak{p}(\kappa)=\rho p(k)$, $\mathfrak{b}(\kappa)=\rho b(k)$, $\mathfrak{t}(\kappa)=\rho t(k)$, $\mathcal{G}(x)=G(R)$. We have, then,

$$\Psi[S(R),P(R),B(R)]=\rho\psi[\mathfrak{S}(x),\mathcal{P}(x),\mathfrak{B}(x)], \quad (22)$$

where

$$\psi[\mathfrak{S}(x),\mathcal{P}(x),\mathfrak{B}(x)]=\tfrac{1}{2}[1/(2\pi)^3]\int\log[1-\mathfrak{t}(\kappa)]^{-1}-\tfrac{1}{2}[\mathfrak{t}^2(\kappa)]-\mathfrak{t}(\kappa)d\boldsymbol{\kappa}+\tfrac{1}{2}\int(\exp\phi(x)+\mathfrak{S}(x)+\mathfrak{B}(x)$$

$$-\tfrac{1}{2}\{[\phi(x)+\mathfrak{S}(x)+\mathfrak{B}(x)]^2-\phi(x)^2\}-\mathfrak{S}(x)-\mathfrak{B}(x)-1)d\mathbf{x}-\tfrac{1}{2}\int[\mathcal{P}(x)\mathfrak{S}(x)+\mathcal{P}(x)\mathfrak{B}(x)+\mathfrak{S}(x)\mathfrak{B}(x)+\tfrac{1}{2}\mathfrak{B}^2(x)]d\mathbf{x}$$

$$+(\rho V)^{-1}\sum(n!)^{-1}\sum_{\substack{\text{all wider-sense}\\ \text{irreducible graphs}}}\int\prod\mathcal{G}(x_{ij})d\mathbf{x}_1\cdots d\mathbf{x}_n. \quad (23)$$

We note that ψ does not contain ρ explicitly (the last group of terms is only apparently dependent on ρ since every term contains a factor $\int dx_1=\rho V$ which cancels the factor $1/\rho V$). Moreover, the functional derivatives $\delta\psi/\delta\mathfrak{S}(x)$, $\delta\psi/\delta\mathcal{P}(x)$, $\delta\psi/\delta\mathfrak{B}(x)$ all vanish if Eqs. (3)–(5) are satisfied. Thus, the derivatives of the right-hand side of Eq. (22) with respect to ρ and β can be computed without taking account of the implicit dependence of $\mathfrak{S}(x)$, $\mathcal{P}(x)$, $\mathfrak{B}(x)$ on these variables. Thus,

$$\rho(\partial\psi/\partial\rho)=\rho\int[\delta\psi/\delta\phi](\partial\phi/\partial\rho)dx, \quad (24)$$

and

$$\partial\psi/\partial\beta=\int[\delta\psi/\delta\phi(x)](\partial\phi/\partial\beta)dx. \quad (25)$$

Now

$$\delta\psi/\delta\phi(x)=\tfrac{1}{2}[1/(2\pi)^3]\int\{\mathfrak{t}^2(\kappa)/[1-\mathfrak{t}^2(\kappa)]\}$$

$$\times\exp(i\boldsymbol{\kappa}\mathbf{x})d\mathbf{x}+\tfrac{1}{2}\{\exp[\phi(x)+\mathfrak{S}(x)+\mathfrak{B}(x)]$$

$$-\mathfrak{S}(x)\mathfrak{B}(x)+\tfrac{1}{2}\Phi_1[x,\mathcal{G}(x)]\}, \quad (26)$$

where $\Phi_1[x,\mathcal{G}(x)]$ is the functional derivative with respect to $\mathcal{G}(x)$ of the last group of terms in Eq. (23). By Eqs. (3) –(5), the right-hand side of Eq. (26) is simply $\frac{1}{2}[\mathcal{G}(x)+1]=\frac{1}{2}[G(R)+1]$. Since $\rho\partial\psi/\partial\rho=(\beta/3)R(\partial V/\partial R)$ and $\partial\psi/\partial\beta)=-V(R)$, we have

$$\rho(\partial\psi/\partial\rho)=\tfrac{1}{6}(\beta\rho^2)\int R(\partial V/\partial R)[G(R)+1]d\mathbf{R} \quad (27)$$

and

$$(\partial/\partial\beta)\Psi=-\tfrac{1}{2}\rho^2\int V(R)[G(R)+1]d\mathbf{R}. \quad (28)$$

On using the well-known formulas relating the pair-distribution function to the pressure and internal energy of a fluid, these equations may be written

$$\rho^2(\partial/\partial\rho)\Psi=p_e \quad (29)$$

$$\rho(\partial/\partial\beta)\Psi=-\epsilon_e, \quad (30)$$

where p_e is the excess pressure and ϵ_e the density of excess internal energy over that of a perfect gas.[12] Equations (29) and (30) identify Ψ_e as the excess free energy per particle.

II. PHASE TRANSITIONS AND THE LOCUS OF SINGULARITIES

We have presented reasons for suggesting that the vanishing of the denominator in Eq. (4) is associated with the liquid-vapor critical point. Since there are two independent variables ρ and β and only one relation

$$1-\rho t(0,\rho,\beta)=0, \quad (31)$$

the locus of singularities is, by a simple count of variables and conditions, not a point but a line in the ρ, t plane. Before we can give a picture of the behavior of the pair correlation function and the thermodynamic functions, we must give an interpretation to this locus and its relation to the liquid-vapor transition.

[12] T. L. Hill, *Statistical Mechanics* (McGraw-Hill Book Company, Inc., New York, 1956), pp. 189–190.

We suppose that the locus is, in fact, a line and that on this line T as a function of ρ has a single maximum (Fig. 1). For isotherms above this maximum, there are no roots of Eq. (31). For isotherms below the maximum there are no roots of Eq. (31). For isotherms below the maximum (BB in the figure), there are two roots while the isotherm corresponding to the maximum has a double root. In a PV plane, the locus of roots is supposed to have the form indicated in Fig. 2. The isotherm CC and the isotherm BB must meet the locus horizontally because as we remarked before, the compressibility must be infinite on the locus.

In the PV plane the locus of singularities looks very similar to the boundary between the two-phase and the single-phase region. They cannot be the same since the PV isotherms do not in general meet the curve horizontally. In actual fact, as a number of authors have pointed out, a theory such as the present, which does not take into account the volume dependence of the cluster integrals, does not show any remarkable behavior near the boundary of the two-phase region.[13]

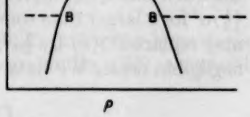

FIG. 1. Locus of singularities in the temperature-density plane.

There is, however, a well-known thermodynamic construction, the so-called double-tangent construction by which the boundaries of the two-phase region may be determined from the Helmholtz free energy.[14] It is not unreasonable to suppose that a rigorous theory of the liquid-vapor phase transition would yield this construction. Figure 3 represents a plot of the Helmholtz free energy against volume. The isotherm BB, BB, has a double tangent $B'B''$. The slope of the isotherm for these two points is the same. Moreover, we have

$$p' = -(\partial A/\partial V)' = -(A''-A')/(V''-V') = p'' = -(\partial A/\partial V)'',$$

where p', A', V', and p'', A'', V'' are the pressure, Helmholtz free energy, and volume at the points B' and B'', respectively, and

$$A''+p''V''=A'+p'V'. \tag{32}$$

Thus, for B' and B'', the temperature, pressure, and Gibbs free energy, are in equilibrium according to the usual rules of thermodynamics.

As has been tacitly indicated in the figures, it is the opinion of the author that Eqs. (3)–(5) do not have a physically meaningful solution within the area bounded by the locus of singularities. As opposed to the Maxwell or equal-area construction,[14] the double-tangent construction does not require information about the isotherms from within this region. Thus, through Eq. (17) the Helmholtz free energy can be determined completely enough to define the boundary of the two-phase region (the line B'–B'' in Figs. 2 and 3). We suppose that this boundary meets every isotherm below the critical isotherm in two points which approach each other as the isotherm approaches the critical isotherm. Since these two points have the same pressure but different volumes, it is natural to suppose that when they coincide at the critical isotherm, the derivative of the pressure with respect to volume is zero. In other words, the boundary of the two-phase region meets the critical isotherm in a point for which the compressibility is zero, i.e., which lies on the locus of singularities. We suppose therefore, that the boundary of the two-phase region surrounds the locus of singularities meeting it in a single point, the critical point. The figures have been drawn to agree with this supposition. From the point of view of the present theory, the critical point is the point of maximum temperature on the locus of singularities. The remainder of the locus of singularities lies within the boundary of the two-phase region.

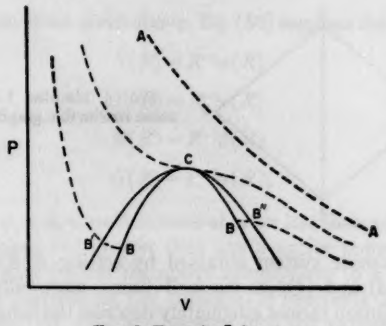

FIG. 2. Equation of state.

III. SOLUTION OF THE APPROXIMATE EQUATIONS ON THE LOCUS OF SINGULARITIES

It has not been possible to analyze the solution of the complete Eqs. (3)–(5) on the locus of singularities. Such an analysis has been made, however, of the

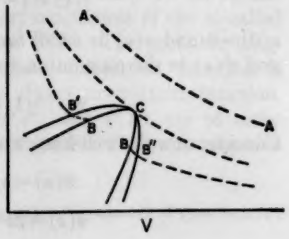

FIG. 3. Double tangent construction.

[13] T. L. Hill, footnote reference 12, p. 413, *et seq.*

[14] J. O. Hirschfelder, C. Curtiss, and R. Bird, footnote reference 7, pp. 363–367.

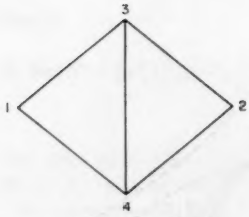

FIG. 4. Simplest 1-2 wider-sense irreducible graph.

approximate system obtained by setting $B(R)=0$ in Eqs. (3) and (4). As we shall discuss more fully later, this solution cannot adequately describe the behavior of thermodynamic and other experimental quantities near the critical point. Nevertheless, it may very well represent a significant part of the truth. Moreover, the analysis of the approximate equations will certainly suggest ways in which the complete equations can be attacked. For these reasons, we present this solution here.

It is convenient to introduce the dimensionless variables which were used in Sec. II. In terms of these variables, Eqs. (3)–(5), become

$$\mathfrak{Z}(x) = \exp\phi(x)+\mathfrak{S}(x)+\mathfrak{B}(x)-\mathfrak{S}(x)-1 \tag{33}$$

$$\mathfrak{s}(\kappa)=\mathfrak{t}^2(\kappa)/[1-\mathfrak{t}(\kappa)] \tag{34}$$

$$\mathfrak{B}(x)=\sum_{n=2}^{\infty}(\rho^n/n!)\sum_{\substack{\text{all 1-2 wider-sense}\\ \text{irreducible bridges}}}\int\Pi\mathfrak{G}(x_{ij})d(3)\cdots d(n+2). \tag{35}$$

On setting $\mathfrak{B}(x)=0$ in Eqs. (3) and (4), we obtain the approximate equations with which we will work:

$$\mathfrak{Z}(x) = \exp[\phi(x)+\mathfrak{S}(x)]-\mathfrak{S}(x)-1 \tag{36}$$

$$\mathfrak{s}(\kappa)=\mathfrak{t}^2(\kappa)/[1-\mathfrak{t}(\kappa)]. \tag{37}$$

We attempt to determine the behavior of $\mathfrak{Z}(x)$, $\mathfrak{S}(x)$ for large values of x and of $\mathfrak{t}(\kappa)$, $\mathfrak{s}(\kappa)$ for small values of κ. Since $\phi(x)$ is assumed to be short-ranged, it can be neglected for large x. Moreover, $\mathfrak{S}(x)$ must be assumed to approach zero for large x so that for considerations of long-range behavior, the exponential may be expanded in a power series. Taking only the first non-vanishing term, Eq. (3) becomes

$$\mathfrak{Z}(x)=\tfrac{1}{2}\mathfrak{S}^2(x) \tag{38}$$

according to our assumption $\mathfrak{t}(0)=1$. So that if we write

$$\mathfrak{t}(\kappa)=1-\tau(\kappa), \tag{39}$$

$\tau(0)=0$ and $\tau(\kappa)$ is small for small κ. Neglecting $\tau(\kappa)$ and $\tau^2(\kappa)$ in the numerator, we have for small κ

$$\mathfrak{s}(\kappa)=1/\tau(\kappa). \tag{40}$$

Consider now the well-known pair of Fourier transforms:

$$\mathfrak{S}(x)=\alpha/x^2 \tag{41}$$

$$\mathfrak{s}(\kappa)=2\pi^2\alpha/\kappa. \tag{42}$$

We investigate whether this pair can provide a solution of Eqs. (38) and (40) with an appropriate choice for α. Since $\mathfrak{t}(\kappa)$ and $\mathfrak{Z}(x)$ are related as Fourier transforms

$$\mathfrak{t}(\kappa)=(4\pi/\kappa)\int_0^\infty \sin\kappa x\mathfrak{Z}(x)x dx. \tag{43}$$

Also, since $t(0)=1$, we have

$$1=4\pi\int x^2\mathfrak{Z}(x)dx. \tag{44}$$

On subtracting Eq. (43) from Eq. (44),

$$\tau(\kappa)=1-\mathfrak{t}(\kappa)=4\pi\int_0^\infty\left(x^2-\frac{x\sin\kappa x}{\kappa}\right)\mathfrak{Z}(x)dx,$$

or

$$\tau(\kappa)=4\pi\kappa\int_0^\infty\left(\frac{\kappa x-\sin\kappa x}{\kappa^3x^3}\right)x^4\mathfrak{Z}(x)d(\kappa x). \tag{45}$$

Now the first factor in the integral in Eq. (45) has a length scale which becomes larger and larger as $\kappa\to 0$, and the region where it is different from zero occupies a larger and larger portion of the positive real axis. On the other hand, the factor $x^4\mathfrak{Z}(x)$ approaches a constant $(\frac{1}{2})\alpha^2$ for x larger than some fixed x_0. Thus for small κ we may replace $x^4\mathfrak{Z}(x)$ by $\frac{1}{2}\alpha^2$ for all $x>0$ making thereby a negligible error. We have therefore

$$\tau(\kappa)=\tfrac{1}{2}(4\pi)\alpha^2\kappa\int_0^\infty\frac{x-\sin x}{x^3}dx=\tfrac{1}{2}\pi^2\alpha^2\kappa. \tag{46}$$

On the other hand, by Eqs. (40) and (42),

$$\tau(\kappa)=\kappa/2\pi^2\alpha. \tag{47}$$

Evidently, Eqs. (41) and (42) provide a solution with

$$\alpha=\pi^{-4/3} \tag{48}$$

$$\tau(\kappa)=\kappa/2\pi^{2/3},\ \mathfrak{t}(\kappa)=1-(\kappa/2\pi^{2/3}),\ \mathfrak{s}(\kappa)=2\pi^{2/3}/\kappa \tag{49}$$

$$\mathfrak{S}(x)=(\pi^{(4/3)}x^2)^{-1},\qquad \mathfrak{Z}(x)=(2\pi^{(8/3)}x^4)^{-1}, \tag{50}$$

Eqs. (49) give the behavior of $\mathfrak{t}(\kappa)$ and $\mathfrak{s}(\kappa)$, for small κ, Eq. (50), the behavior of $\mathfrak{Z}(x)$ and $\mathfrak{S}(x)$ for large x. For small x we may expect that $\mathfrak{S}(x)$ and $\mathfrak{Z}(x)$ deviate from Eqs. (50) and, in particular, have features determined by $\phi(x)$ for x corresponding to the range of intermolecular forces. Since $\mathfrak{G}(x)=\mathfrak{S}(x)+\mathfrak{Z}(x)$, the long-range behavior of $\mathfrak{G}(x)$ is the same as that of $\mathfrak{S}(x)$. It may be remarked that while $\mathfrak{Z}(x)$ has a zeroth moment, it has no second or higher moments contrary to the assumption of the Ornstein-Zernicke theory.

IV. DISCUSSION

In order to discuss the validity of the asymptotic solution, Eqs. (49) and (50), to Eqs. (36) and (37), we consider first the simplest term in $B(R)$. This is given by the graph, Fig. 4. The integral associated

with this graph is

$$B_1(R_{12})$$

$$=\tfrac{1}{2}\int G(R_{13})G(R_{14})G(R_{23})G(R_{24})G(R_{34})d(3)d(4). \quad (51)$$

We are interested in the asymptotic form of Eq. (51) when R_{12} is large, given the asymptotic form of $G(R)$. Suppose first of all that the form of $G(R)$ is such that the integral

$$C=\int G(R_{34})G(R_{3i})G(R_{4i})d(3)d(4), \quad (52)$$

where $i=1, 2$, converges. Then the significant contributions to Eq. (51) come from a configuration in which points 3 and 4 are both close to 1 or both close to 2. In the first case, $G(R_{13})G(R_{14})$, and in the second, $G(R_{23})G(R_{24})$ can be set equal to $G^2(R_{12})$ and we have

$$B_1(R)\sim CG^2(R). \quad (53)$$

If we expand the exponential in Eq. (3) and neglect $\phi(R)$, $B^2(R)$, and $B(R)S(R)$, but not $B(R)$, we have

$$T(R)=B(R)+\tfrac{1}{2}S^2(R). \quad (54)$$

Since $G(R)\sim S(R)$ for large R, under the hypothesis of the convergence of the integral in Eq. (52), we would have

$$T(R)=(C+\tfrac{1}{2})S^2(R). \quad (55)$$

Our analysis of the singularity would go through the same way and result in an asymptotic form $G(R)\sim \alpha/R^2$ with, however, a new value for α. If $G(R)\sim \alpha R^{-2}$, however, the integral, Eq. (52), does not converge for large R, but rather diverges logarithmically. An indication that this is so can be gotten by dimensional considerations since if all R's are the same order of magnitude, the integrand is of order R^{-6}, while the dimensions of volume element $d(3)d(4)$ are R^6. Integration over all but one R gives an integral $\int dR/R$. The upper limit in this integral is $\max(R_{34}, R_{3i}, R_{4i})$. If any one of these distances is large compared to R_{12}, we may no longer set $R_{3j}, R_{4j}=R_{12}$ and the additional factors $G(R_{3j})G(R_{4j})$ will make $B_1(R)$ converge. Thus we may expect

$$B_1(R)\sim R^{-4}\log R. \quad (56)$$

This is confirmed by a more rigorous analysis.

Equation (56) shows that we have not been justified in neglecting $B(R)$ near the locus of singularities for large R, since the first correction to $T(R)$ is larger than the expression for $T(R)$ given by Eq. (50). Nevertheless, the fact that our considerations have missed being correct by an integral which diverges only logarithmically suggests that the correct asymptotic forms for the pair correlation function and its parts are not too different from those given above. Eq. (56) suggests the forms:

$$S(R)=R^{-2}\sigma(R)$$
$$T(R)=R^{-4}\tau(R)$$
$$B(R)=R^{-4}\beta(R)$$
$$G(R)=R^{-2}\gamma(R), \quad (57)$$

where $\sigma, \tau, \beta, \gamma$ are functions of order less than any positive power and greater than any negative power of R.

We may submit the above assumptions to a further test by considering the question: If functions $G(R)$ of the form Eq. (57) are inserted into the various terms of $B(R)$, do any terms larger than $R^{-4}\beta(R)$ result? It is, of course, not possible to analyze rigorously the various terms of $B(R)$ especially since the form of $\beta(R)$ is not known. It is, however, possible to apply the naive dimensional considerations used to analyze $B_1(R)$. The most significant topological property of the 1, 2 wider-sense irreducible graphs making up $B(R)$ is the fact that the index[15] $I(j)$ of every point j of the graph except points 1 and 2 must be at least 3. $I(1)$, $I(2)$ must be at least 2. The dimensional considerations used above suggest that the asymptotic order of magnitude of the contribution of any graph to $B(R)$ is $R^{-2l+3k}\alpha(R)$ where l is the number of lines and $2+k$ is the number of points of the graph, and $\alpha(R)$ is of order less than any positive and greater than any negative power. Since every line of the graph impinges on two points, we have

$$\sum_{j=1}^{2+k} I(j)=2l.$$

If we replace every index I on the left by its smallest possible value we obtain

$$4+3k\leqslant 2l,$$

or

$$-2l+3k\leqslant -4. \quad (58)$$

Thus, according to this naive analysis, no term in $B(R)$ is of order greater than $\alpha(R)R^{-4}$, where $\alpha(R)$ is as before. The graphs which give the largest contribution are those for which the indices of points 1 and 2 are both 2 while those of all other points are 3.

We may summarize the conclusions of the foregoing analysis in the following way: A very considerable doubt is cast on the validity of the Ornstein-Zernicke theory of critical opalescence, especially on the fundamental assumption of short-rangedness of the so-called direct correlation function $T(R)$. The probable long-range behavior of the direct correlation function is $G(R)\sim R^{-2}\gamma(R)$, of the direct correlation function, $T(R)\sim R^{-4}\tau(R)$ when $\gamma(R)$ and $\tau(R)$ are of order less than any positive and greater than any negative power of R.

[15] The index of a point of a graph is the number of lines incident upon it.

Effect of Binding of Ions and Other Small Molecules on Protein Structure. VIII. On Isomerization of Serum Albumin in Acidic Media*

JOHN R. CANN

Department of Biophysics, Florence R. Sabin Laboratories, University of Colorado Medical Center, Denver, Colorado

(Received May 10, 1960)

The complex electrophoretic patterns of BSA in 0.02*M* NaCl-HCl are due to reaction boundaries arising from a set of rapidly established isomerization equilibria and a slow, apparently irreversible reaction. The slow reaction is of only minor importance for electrophoresis in acetate buffer, although a second irreversible process occurs in this solvent at protein concentrations of 0.2% and lower. This latter reaction accounts for the bimodality of the patterns obtained at low field strength with 0.2% BSA in acetate buffer. Resolution of those peaks corresponding to the rapidly established isomerization equilibria is a consequence of changes in either *p*H or conductance in the reaction boundary during nonideal electrophoresis. Equilibrium constants can, nevertheless, be computed from extrapolated values of the various electrophoretic mobilities without recourse to area measurements. Our observations suggest the following set of consecutive isomerization equilibria:

$$N+nH^+ \rightleftharpoons F$$

$$F+mH^+ \rightleftharpoons I$$

where, as in the reaction scheme of Aoki and Foster, the *F* form of the protein has a larger electrophoretic mobility than the *N* form, whereas that of the *I* form is intermediate between those of the *N* and *F* forms.

INTRODUCTION

BOVINE serum albumin (BSA) undergoes two electrophoretically distinguishable types of reaction in acidic media.[1,2] The first, [1–7] which is also shown by ovalbumin, bovine γ-pseudoglobulin and oxidized ribonuclease, is observed only in the presence of acetate or other carboxylic acid buffers. The various peaks shown by the electrophoretic patterns obtained in these media constitute a reaction boundary which arises as a result of the reversible binding of undissociated buffer acid by the protein. The equilibrium constant for the binding of acetic acid by BSA has been evaluated from the various electrophoretic mobilities without recourse to area measurements.[3] Comparison of the equilibrium constants for the binding of several different buffer acids by ovalbumin suggests that binding occurs via formation of a single, heterologous hydrogen bond in which the acid acts as the proton donor.

The second reaction is exhibited by BSA but not ovalbumin and involves hydrogen-ion mediated configurational changes. The superposition of this reaction on the electrophoretic pattern due to the interaction of protein with undissociated carboxylic acid generally confers a fine structure upon the rising boundary of the latter reaction.[2,8] This second type of interaction was first described by Aoki and Foster[9–13] who found that the electrophoretic patterns of 0.2% BSA in 0.02*M* NaCl-HCl show two (and sometimes three) peaks whose relative areas depend upon *p*H. They interpreted their observations in terms of a reversible, *p*H-dependent transformation (isomerization[14]) of BSA between two states in which the protein molecule has different electrophoretic mobilities. Although their general picture of a strongly *p*H-dependent isomerization reaction is undoubtedly correct, the patterns possess certain curious features which would seem to complicate their quantitative interpretation and have prompted us to reinvestigate this reaction.

EXPERIMENTAL

The electrophoresis experiments were carried out in the standard 11cc Tiselius cell using the Spinco Model H electrophoresis-diffusion instrument. The BSA was Armour's crystallized bovine plasma albumin, Lot No.

* Supported in part by the National Institute of Allergy and Infectious Diseases of the National Institutes of Health, Public Health Service, and in part by the Damon Runyon Fund and the American Cancer Society. The author wishes to thank Stanley Fisher for his technical assistance.

[1] J. R. Cann. J. Am. Chem. Soc. **80**, 4263 (1958).
[2] J. R. Cann, J. Biol. Chem. (to be published).
[3] R. A. Phelps and J. R. Cann, J. Am. Chem. Soc. **78**, 3539 (1956).
[4] J. R. Cann and R. A. Phelps, J. Am. Chem. Soc. **79**, 4672 (1957).
[5] R. A. Phelps and J. R. Cann, J. Am. Chem. Soc. **79**, 4677 (1957).
[6] J. R. Cann and R. A. Phelps, J. Am. Chem. Soc. **81**, 4378 (1959).
[7] J. R. Cann, J. Phys. Chem. **63**, 210 (1959).

[8] The large bracket ⌐ in Figs. 3(a) and 6 designates the reaction boundary arising from the interaction of BSA with acetic acid. The brace — indicates the fine structure of the reaction boundary attributable to the isomerization reaction. The small bracket in Fig. 6 indicates fine structure arising from an irreversible modification of BSA which occurs in acetate buffer at low protein concentrations.
[9] K. Aoki and J. F. Foster, J. Am. Chem. Soc. **78**, 3538 (1956).
[10] K. Aoki and J. F. Foster, J. Am. Chem. Soc. **79**, 3385 (1957).
[11] K. Aoki and J. F. Foster, J. Am. Chem. Soc. **79**, 3393 (1957).
[12] J. F. Foster and K. Aoki, J. Phys. Chem. **61**, 1369 (1957).
[13] J. F. Foster and K. Aoki, J. Am. Chem. Soc. **80**, 1117 (1958).
[14] In two of our early papers[4,5] the term, "isomerization," was used incorrectly to describe the interaction of serum albumin, ovalbumin, and γ-pseudoglobulin with undissociated buffer acid.

T6820 UO1. For experiments in buffered systems, samples of protein were dissolved in buffer and then dialyzed vs buffer in the cold for 17 to 24 hr with one change of dialyzate. In the case of unbuffered systems, samples of protein in 0.02*M* NaCl were adjusted to the desired *p*H with HCl and then dialyzed in the cold vs 0.02*M* NaCl-HCl of the same *p*H with one change of dialyzate. In all Schlieren patterns shown in the figures, the apparent mobilities, μ, were positive. Values of $10^5 \times \mu$ cm^2 sec^{-1} v^{-1} are given in many of the figures.

RESULTS AND DISCUSSION

Rates of Isomerization Reactions

Previous experiments[2] in which 0.4% BSA in 0.02*M* NaCl-HCl was subjected to prolonged electrophoresis with back compensation indicate that at *p*H 4.0 the protein migrates as a reaction boundary in which the gradient does not become zero between any two peaks.

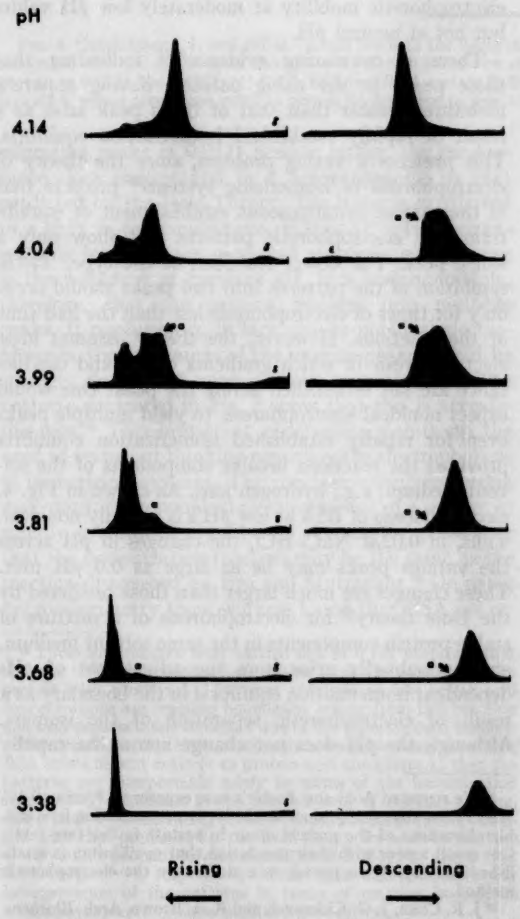

FIG. 1. Electrophoretic patterns of 0.2% BSA in 0.02*M* NaCl-HCl. Electric field strength, about 4 v cm^{-1}.

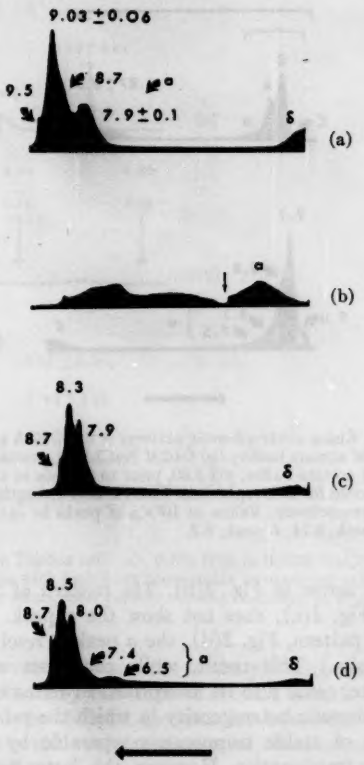

FIG. 2. Rising electrophoretic patterns in 0.02*M* NaCl-HCl: (a) 0.4% BSA at *p*H 3.80; (b), same as (a) after prolonged electrophoresis with back compensation, vertical arrow indicates the narrow region of the channel in which the gradient becomes zero; (c) fraction described in text, *p*H 3.79, protein concentration, 0.11%; (d) 0.12% BSA, *p*H 3.80. Electric field strength, about 8 v cm^{-1}.

Although the electrophoretic patterns of 0.02% protein at various *p*H values, Fig. 1, are entirely consistent with this view, there is something curious about the slow-moving *a* peak shown by many of the patterns. It occurred to us that this peak might correspond to an unstable protein component which transforms slowly into faster-migrating components which, in turn, participate in rapidly established isomerization equilibria. This idea found support in the following observations: (a) the relative area of the *a* peak in the rising pattern of 0.4% BSA at *p*H 3.8, Fig. 2(a), varies from experiment to experiment and ranges from 23 to 45% (average of 14 experiments, 34.4±5.8%); (b) On prolonged electrophoresis with back compensation at this *p*H, the gradient of protein concentration usually becomes zero in the region between the *a* peak and the faster-moving ones, Fig. 2(b). The significance of the latter observation was established by electrophoretic analysis of the material obtained by withdrawing from the Tiselius cell the protein disappearing across the broad multi-modal reaction boundary to the left of the

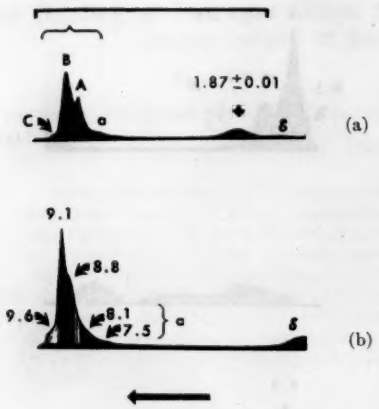

FIG. 3. Rising electrophoretic patterns of 0.4% BSA at *p*H 3.80; (a) 0.02*M* acetate buffer; (b) 0.02*M* NaCl-HCl, protein dialyzed vs 0.02*M* acetate buffer, *p*H 3.80, prior to dialysis vs the solvent medium used for electrophoresis. Electric field strength, 12 and 8 v cm^{-1}, respectively. Values of $10^5 \times \mu$ of peaks in (a): *A* peak, 8.27; *B* peak, 8.74; *C* peak, 9.2.

vertical arrow in Fig. 2(b). The pattern of this material, Fig. 2(c), does not show the *a* peak. (In the control pattern, Fig. 2(d), the *a* peak is resolved into two peaks.) This result, while consistent with our postulate, could also be interpreted in terms of a true electrophoretic heterogeneity in which the protein is a mixture of stable components separable by electrophoretic fractionation. However, this latter possibility was eliminated by the results of the following experiments which were based on the fundamental finding that, whereas the relative area of the *a* peak ranges from 23 to 45% in 0.02*M* NaCl-HCl, *p*H 3.8, it is consistently only 8% in 0.02*M* acetate buffer of the same *p*H, Fig. 3(a).[8]

In the first set of experiments, a solution of BSA was dialyzed vs 0.02*M* NaCl-HCl before dialysis vs the 0.02*M* acetate buffer which served as the solvent medium for electrophoresis. The resulting patterns were identical to that shown in Fig. 3(a) for BSA which had not been exposed to NaCl-HCl prior to electrophoresis in acetate buffer. In contrast, exposure of the protein to acetate buffer prior to electrophoresis in NaCl-HCl has a pronounced effect on the proportion of the *a* peak. In one experiment, BSA was first dialyzed vs 0.02*M* acetate buffer; then vs 0.02*M* sodium acetate, *p*H 7.3; and finally vs 0.02*M* NaCl. The dialyzed protein solution was then adjusted to *p*H 3.80 with HCl, dialyzed vs 0.02*M* NaCl-HCl of the same *p*H and subjected to electrophoresis. The resulting pattern, Fig. 3(b), shows only 12% of the *a* peak. The same results were obtained in experiments in which a solution of BSA, previously equilibrated vs 0.02*M* acetate buffer, was dialyzed directly vs many changes of the 0.02*M* NaCl-HCl used in electrophoresis. These experiments clearly demonstrate that the *a* peak corresponds to one or two unstable protein components which transform, apparently irreversibly, into faster-moving components. In 0.02*M* NaCl-HCl, *p*H 3.80, the transformation reaction proceeds rapidly to about 55 to 75% of completion after which it proceeds at a much slower rate, while in 0.02*M* acetate buffer it proceeds rapidly to about 92% of completion. Despite the apparent irreversibility of the transformation it has no effect on the electrophoretic behavior of the protein at neutral *p*H. Thus, the electrophoretic pattern and mobility of BSA exposed to acetate buffer at *p*H 3.8, prior to electrophoresis in 0.1 ionic strength phosphate buffer, *p*H 7, are the same within experimental error (±0.02 mobility units) as those of BSA never exposed to low *p*H. One of the many possible interpretations of this observation is that the transformation reaction involves the shedding by the protein of small, unchanged molecules such as decanol. The binding of a neutral molecule by the protein could conceivably modify the ionization of its carboxyl groups thereby changing its electrophoretic mobility at moderately low *p*H values but not at neutral *p*H.

There is convincing evidence[10,15] indicating that those peaks in the rising patterns having apparent mobilities greater than that of the *a* peak arise as a result of rapidly established isomerization equilibria. This presents a vexing problem, since the theory of electrophoresis of isomerizing systems[16] predicts that in the case of instantaneous establishment of equilibrium, the electrophoretic patterns will show only a single peak. For slower reactions of the type, $A \rightleftharpoons B$, resolution of the patterns into two peaks should occur only for times of electrophoresis less than the half-time of the reactions. However, the theory assumes ideal electrophoresis in which gradients of *p*H and conductance are not established across the peak. One would expect nonideal electrophoresis to yield multiple peaks even for rapidly established isomerization equilibria provided the reactions involve components of the solvent medium, e.g., hydrogen ions. As shown in Fig. 4, electrophoresis of BSA at low *p*H's is actually nonideal. Thus, in 0.02*M* NaCl-HCl, the changes in *p*H across the various peaks may be as large as 0.6 *p*H unit. These changes are much larger than those predicted by the Dole theory[17] for electrophoresis of a mixture of stable protein components in the same solvent medium, and undoubtedly arise from the adjustment of *p*H-dependent isomerization equilibria in the boundary as a result of electrophoretic separation of the isomers. Although the *p*H does not change across the rapidly

[15] We repeated Aoki and Foster's rate experiment[10] using 0.4% BSA rather than 0.2%, since at the lower concentration irreversible alterations of the protein occur in acetate buffer (see text). Our result agrees with their conclusion that equilibrium is established too rapidly to permit rate studies by the electrophoretic method.

[16] J. R. Cann, J. G. Kirkwood, and R. A. Brown, Arch. Biochem. Biophys. **72**, 37 (1957).

[17] V. P. Dole, J. Am. Chem. Soc. **67**, 1119 (1945).

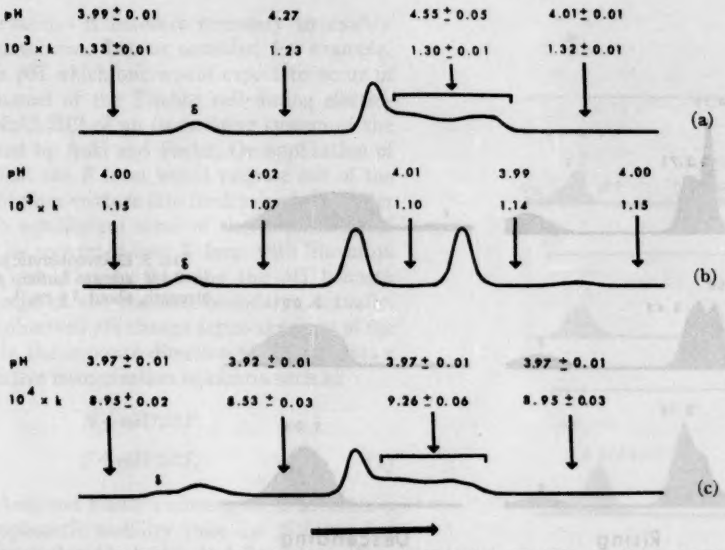

FIG. 4. Conductance, k, and pH at various levels in the rising channel of the Tiselius cell: (a), 0.4% BSA in 0.02M NaCl-HCl; (b) computed with aid of the Dole theory for a 1:1 mixture of two stable proteins with mobilities comparable to observed values, 0.4% protein in 0.02M NaCl-HCl; (c) 0.4% BSA in 0.02M acetate buffer. The very small, most rapidly moving boundary in B is a "false" boundary whose area is too small to permit its detection in practice.

migrating peaks in 0.02M acetate buffer, the conductance does change and in a sense opposite to that predicted by the Dole Theory. The latter is attributed to a shift in the equilibrium, $HAc \rightleftharpoons Ac^- + H^+$, accompanying hydrogen-ion mediated reactions which occur in the boundary at constant pH. It is understandable, therefore, that the pattern resolves into multiple peaks. If resolution is, in fact, due to nonideal electrophoresis, then the areas of the various peaks should be strongly dependent upon protein concentration. The patterns presented in Fig. 5 show that this is actually the case.[18] This important observation points up the need to revise our thinking regarding the electrophoresis of isomerizing systems. The conclusion that resolution may result from nonideal electrophoresis of a system in rapidly established equilibrium revives the possibility that the isomerization reaction may be the same as the reaction discovered by Bro and Sturtevant.[19] On using microcalorimetry these workers found that BSA undergoes a reversible transition in the pH range 4.5 to 3.5, characterized by half-time of about 2 min. It has previously been difficult to visualize how such a rapid reaction could cause resolution of the electrophoretic patterns.[20]

Effect of Field Strength

The electrophoretic behavior of an isomerizing system might depend upon the electric field strength. In particular, the Schlieren pattern obtained at a sufficiently low field strength might show only a single peak, if for no other reason than the merging of several peaks because of diffusion. In 0.02M acetate buffer, where the slow transformation reaction described above is of minor importance,[21] a single peak is obtained at low field strength when the protein concentration is 0.4%, Fig. 6(b), but not when it is 0.2%, Fig. 6(c). As first observed by Aoki and Foster,[13] two peaks are obtained at the lower protein concentration. These peaks

[18] These experiments were carried out in 0.1M acetate buffer in order to avoid complications arising from the reaction of the protein with acetic acid. Patterns obtained at low acetic acid concentrations are reaction boundaries arising from this reaction and may possess a fine structure due to the superimposed isomerization reaction. At high acetic-acid concentrations, however, BSA exists almost entirely as protein-acid complexes so that the patterns are interpretable solely in terms of the isomerization reaction.[3] The increase in the relative area of the fast-moving, rising peak with increasing protein concentration is almost identical with that predicted by the Dole theory for a 20-80 mixture of two stable proteins having mobilities of 3.18×10^{-4} and 2.89×10^{-4} $cm^2 sec^{-1} v^{-1}$, respectively. This does not invalidate our interpretation of the patterns in terms of reaction boundaries which are expected to show modified Dole effects.

[19] P. Bro and J. M. Sturtevant, J. Am. Chem. Soc. **80**, 1789 (1958).

[20] (a) J. F. Foster, Compt. rend. trav. lab. Carlsberg, Sér. chim. **31**, 351 (1960); (b) Foster has proposed a mechanism of protein isomerization capable of providing for a rapid approach to equilibrium upon changing pH even though interconversion of equilibrium species may be very slow during their electrophoretic separation. However, it is difficult to reconcile his mechanism with our observations. Thus, for example, the changes in pH or conductance which occur in the Tiselius cell indicate that the various isomeric forms of BSA do, in fact, interconvert during electrophoresis.

[21] Two well defined peaks were obtained on electrophoresis of 0.4% BSA in 0.02M NaCl-HCl, pH 4.0, at a field strength of 1 v cm^{-1}. Unpublished experiments of the author show that the failure to give a single peak at this low field strength is attributable, in large part at least, to the slow transformation reaction which plays a major role in the electrophoresis of BSA in 0.02M NaCl-HCl.

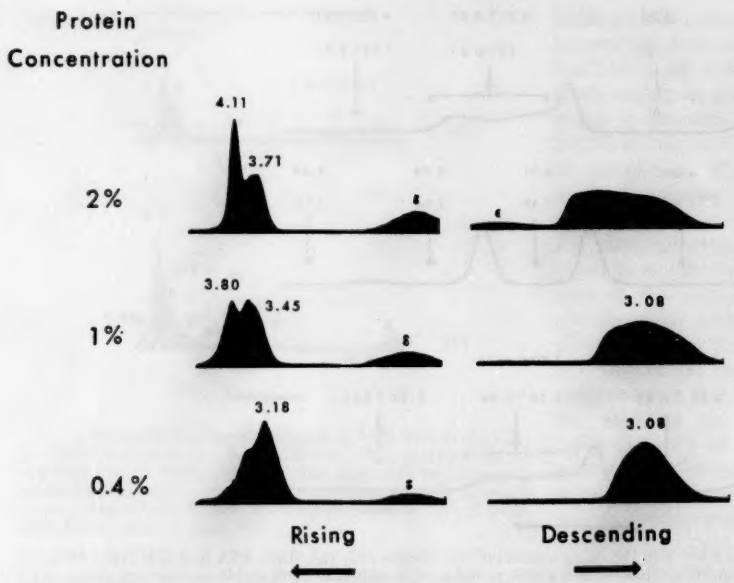

FIG. 5. Electrophoretic patterns of BSA in 0.1*M* acetate buffer, *p*H 4.10. Field strength, about 3 v cm^{-1}.

are indicated by a small bracket rather than by a brace[8] in order to emphasize that they arise not as a result of isomerization but rather from an irreversible modification of the protein which occurs in acetate buffer at low but not high protein concentrations. The validity of this latter assertion has been demonstrated by experiments based on the finding that the proportion of the faster moving of the two peaks approximately doubles when the 0.2% protein solution is aged for 48 hr at 3°C before electrophoresis at low field strength. Two solutions of BSA in acetate buffer, one at a protein concentration of 0.2% and the other at 0.1%, were aged for 48 hr at 3°C before dialysis vs water followed by lyophilization. These materials were then subjected to low field strength electrophoresis in acetate buffer, *p*H 4.0, at a protein concentration of 0.4%. The resulting patterns, Figs. 6(d) and 6(e), show two major peaks (indicated by small bracket) which is in sharp contrast to the single peak obtained with BSA which had not been aged in acetate buffer at low protein concentration [Fig. 6(b)]. Furthermore, the pattern of the material aged at 0.1% protein concentration is more complex than that of the material aged at 0.2%. (A greater proportion of the faster moving peak was obtained when the 0.2% solution of aged protein was dialyzed vs phosphate buffer at *p*H 7 before dialysis vs water and lyophilization.) Ageing not only modifies the electrophoretic behavior of the protein at low *p*H but also at *p*H 7. Thus, while protein aged at a concentration of 0.2% still showed a single peak at *p*H 7, its mobility was about 4% greater than that of BSA never exposed to low *p*H (mobility difference of 0.23±0.05 units). Clearly, BSA undergoes irreversible modification when exposed at sufficiently low concentrations to acetate buffer of *p*H 4. The modification reaction involves subtle structural changes as evidenced by the fact, that, whereas it has a profound effect on electrophoretic behavior, it does not affect the sedimentation behavior of the protein significantly as determined by ultracentrifugation at *p*H 4. The curious concentration dependence of the reaction and the fact that in 0.2% protein, an increase in both the mean positive electrophoretic mobility at *p*H 4 and in the negative mobility at *p*H 7 occurs suggest the following possibilities: a reaction of the protein with some trace contaminant of the solvent; a reaction which is inhibited at high protein concentrations by a contaminant whose concentration is insufficient to inhibit effectively at low protein concentration; or a configurational alteration which is inhibited by high protein concentration *per se*, i.e., a protective colloid phenomenon, rather than simply a slow desorption of small bound ions.

It must be emphasized that the foregoing findings in no way invalidate our previous experiments on the interaction of BSA with acetic acid which were carried out at protein concentrations of 0.4 to 1% nor do they invalidate the experiments of Aoki and Foster on the isomerization of 0.2% BSA in 0.02*M* NaCl-HCl. These workers have shown that the protein does not undergo irreversible changes under the latter conditions.[10]

Nature of Isomerization Equilibria

Aoki and Foster[10] have interpreted their findings in terms of the isomerization equilibrium, $N+3H^+ \rightleftharpoons F$, where the F form of the protein has a larger electrophoretic mobility than the N form. In order to account

for our observations it becomes necessary to modify their reaction scheme. Let us consider, for example, the change in pH which one would expect to occur in the rising channel of the Tiselius cell during electrophoresis in NaCl-HCl of an isomerizing system of the type postulated by Aoki and Foster. On application of the electric field the F form would migrate out of the original equilibrium mixture into fresh solvent. In order to reestablish equilibrium some of the F form would immediately be converted into N form with liberation of hydrogen ions, thereby lowering the pH beneath the leading edge of the reaction boundary. Actually, however, the observed pH change across the front of the boundary is in the opposite direction which suggests a set of consecutive isomerization equilibria such as

$$N + nH^+ \rightleftharpoons F$$
$$F + mH^+ \rightleftharpoons I, \qquad (1)$$

where, as in Aoki and Foster's scheme, the F form has a larger electrophoretic mobility than the N form; but the I form is postulated to have a mobility intermediate between those of the N and F forms. (The three forms are assumed to differ in both net charge and frictional coefficient.) Now, when the electric field is applied the F form migrates out of the original equilibrium mixture into fresh solvent where, in order to reestablish equilibrium, it is necessary not only for some of the F form to convert into the N form with the liberation of hydrogen ions, but also for other F macroions to react with hydrogen ions to yield the I form. When macroions of the I form, in turn, migrate out of the original solution into the overlying, freshly generated equilibrium mixture, reequilibration occurs once again with further change in hydrogen ion concentration. Consequently, the reaction boundary might show three peaks with a gradient of pH across each. Depending upon the values of n, m and the equilibrium constants, the net result could very well be the generation of a solution in the boundary having an average pH greater than that of the overlying solvent as in Fig. 4(a). Similar reasoning leads one to conclude that electrophoresis in a buffered solvent could generate a solution in the boundary having an average conductance greater than that of the overlying solvent, Fig. 4(c). (A hydrogen-ion mediated reaction occurring at constant pH would shift the equilibrium, $HAc \rightleftharpoons Ac^- + H^+$, in the forward direction thereby increasing the acetate ion concentration and, consequently, the conductivity of the solution.)

Reaction scheme (1) is consistent not only with observed pH and conductance changes and multiplicity of peaks in the reaction boundary, but also with variation in the areas of the peaks with variation in the pH of the solvent medium. Superficial examination of Figs. 1, 3(a), and 6(a) suggests that a peak of intermediate mobility grows at the expense of faster- and slower-moving ones when the pH is lowered from a value of about 4.1 to about 3.7. To confirm this notion, the

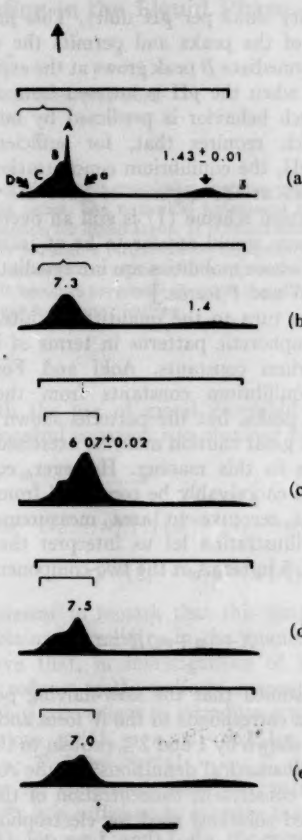

FIG. 6. Rising electrophoretic patterns of BSA in 0.02M acetate buffer, pH 3.97; (a) 0.4% protein at a field strength of 12 v cm^{-1}; (b), 0.4% protein, field strength of 0.9 v cm^{-1}; (c) 0.2% protein, field strength of 0.90 v. cm^{-1}; (d) 0.4% protein at 0.87 v cm^{-1}, material aged for 48 hr in acetate buffer at a protein concentration of 0.2% prior to electrophoresis at the higher concentration (see text for details); (e) 0.4% protein at 0.87 v cm^{-1}, material aged for 48 hr in acetate buffer at a protein concentration of 0.1% prior to electrophoresis at the higher concentration (see text for details). Times of electrophoresis: (a), 125 min.; (b), 1507 min.; (c) 1709 min.; (d) 1521 min.; (e) 1507 min. Values of $10^8 \times \mu$ of peaks in (a): A peak, 6.61; B peak, 6.85; C peak, 7.4; D peak, 8.1.

various peaks shown by 0.4% protein in 0.02M acetate buffer, pH 4.1 to 3.8, were arbitrarily designed in order of increasing apparent mobility as (a), (b), (c), and (d), Figs. 3(a) and 6(a), and their apparent mobilities plotted vs pH.[22] Each peak gave a typical mobility-pH curve about which the data scattered with a surprisingly small standard deviation, 2 to 3%, considering the small pH range involved and the large slope of the mobility-pH curves (average value of about 9

[22] The patterns obtained at pH 3.97 and 3.80 were extremely reproducible. At intermediate pH values the B and C peaks were sometimes well resolved while in other experiments they were poorly resolved. This is not surprising considering the narrow pH range involved.

to 14 mobility units per pH unit). This justifies our designation of the peaks and permits the conclusion that the intermediate B peak grows at the expanse of all other peaks when the pH is lowered from a value of 4 to 3.8. Such behavior is predicted by our reaction scheme which requires that, for sufficiently large changes in pH, the equilibrium concentration of the I form increases at the expense of both the N and F forms. [Reaction scheme (1) is still an oversimplification since there would appear to be at least two isomeric forms whose mobilities are intermediate between those of the N and F forms.]

Finally, we turn to the quantitative interpretation of the electrophoretic patterns in terms of isomerization equilibrium constants. Aoki and Foster have computed equilibrium constants from the relative areas of the peaks, but the patterns shown in Fig. 5 indicate that great caution must be exercised in treating the data in this manner. However, equilibrium constants can conceivably be computed from mobility data without recourse to area measurements. For purposes of illustration let us interpret the patterns shown in Fig. 5 in terms of the two-component equilibrium,

$$N+(n+m)H^+ \rightleftharpoons I. \qquad (2)$$

It will be assumed that the slow-moving peak in all three patterns corresponds to the N form and the fast-moving peak shown by 1 and 2% protein to the I form. From the mathematical definitions[23] of the constituent mobility and constituent concentration of the protein in the dialyzed solutions used for electrophoresis, the following expression can be derived for the equilibrium constant, K, of reaction (2):

$$K=[1/(H^+)^{n+m}]\cdot[(\mu_N-\bar{\mu}_P)/(\bar{\mu}_P-\mu_I)]=K'/(H^+)^{n+m}, \qquad (3)$$

where μ_N and μ_I are the mobilities of the N and I forms, respectively, and $\bar{\mu}_P$, the constituent mobility of the protein. Since the mobility of the descending boundary is the same at 0.4% as at 1% protein concentration, its value 3.08×10^{-5} cm^2 sec^{-1} v^{-1}, was taken as $\bar{\mu}_P$. The values of μ_N and μ_I, 2.89×10^{-5} and 3.18×10^{-5}, respectively, were obtained by extrapolating the apparent rising mobilities to infinite dilution of the protein.[24] The computed value, 1.9, of K' should be compared with values obtained from area measurements: 1.4 at 2% protein; 0.96 at 1% protein; 0.3 or 0.1 at 0.4% protein depending upon whether or not the composite area of the two fast peaks is taken as the relative concentration of the I form. Clearly, values of the equilibrium constants computed from pattern areas at low protein concentrations may be in error by as much as an order of magnitude. The disagreement between the values obtained from area measurements at different protein concentrations arises from the nonideality of the electrophoretic process. On the other hand, the value computed from mobility data is subject to the uncertainty as to whether the mobilities of the peaks in the reaction boundaries can be identified with the mobilities of the various isomeric forms of the protein.[25] Another complication is that the extrapolated mean mobility of the rising pattern is not the same as the mean descending mobility.

[23] E. B. Dismukes and R. A. Alberty, J. Am. Chem. Soc. 76, 191 (1954).

[24] An approximately linear extrapolation was obtained by plotting the reciprocal of the apparent mobility of the slow-moving peak vs the square root of the protein concentration. The same relationship was assumed for extrapolation of the apparent mobilities of the fast peak shown by 1 and 2% protein.

[25] G. A. Gilbert and R. C. Ll. Jenkins, Proc. Royal Soc. (London) A253, 420 (1959).

Some Tests of the Superposition Approximation in the Liquid Phase

FRANK P. BUFF AND R. BROUT*

Department of Chemistry, University of Rochester, Rochester, New York

(Received June 22, 1960)

The statistical mechanical theory of the concentration dependence of the pair correlation function provides a delicate test of the superposition approximation in the liquid phase. The numerical assessment is carried out directly with use of the experimental x-ray scattering function for liquid argon. It is found that the utilization of superposition in the theoretical expression produces too high a concentration dependence of the first coordination sphere of the radial distribution function. Although the superposition approximation fails for integrals possessing a pure density fluctuation origin, it becomes progressively more useful in applications in which the superposition error is damped by short-range force contributions.

I.

THE pair correlation function of the theory of homogeneous liquids varies with the distance between the pair and also depends on the thermodynamic variables characterizing the state of the fluid. It is the purpose of this paper to study the concentration dependence of the pair correlation function. This examination leads in a natural way to a delicate assessment of the validity of the Kirkwood superposition approximation[1] in the condensed liquid phase. It will be seen subsequently that the structure of the basic equation provides this test of the approximation by the direct use of experimental x-ray scattering data rather than the utilization of approximate theoretical distribution functions. The motivation for the present investigations arose from our previous general statistical mechanical formulation of the thermodynamic functions encountered in solution theory.[2] This theory was based on generalized fluctuation theory in the grand ensemble, or, alternatively, on the use of the expressions for the chemical potential and temperature derivatives of the number densities of open systems. It was observed that, for one-component systems, the formula for $(\partial E/\partial V)_{T,N}$, sometimes designated as the internal pressure, was relatively simple. Although the present investigation is concerned with the detailed numerical assessment of this formula, the conclusions as to the applicability of the superposition approximation were already briefly summarized in our earlier paper.

The starting point for the desired concentration dependence of the correlation functions is provided by the chemical potential derivative of the distribution function $\rho^{(n)}$. $\rho^{(n)}(1,\cdots n;\ T,\ \beta\mu)$ is the generic number density of sets of n molecules located at the points $\mathbf{R}_1,\cdots,\mathbf{R}_n$, at absolute temperature T and chemical potential μ. $\beta=1/kT$, where k is the Boltzmann constant. With the use of grand ensemble theory, the following integral equation was obtained by one of us.[3]

$$[\partial\rho^{(n)}(1,\cdots n)/\partial\beta\mu]_{T,1,\cdots n}$$
$$=n\rho^{(n)}(1,\cdots n)+\int[\rho^{(n+1)}(1,\cdots n+1)$$
$$-\rho^{(n)}(1,\cdots n)\rho^{(1)}(n+1)]dv_{n+1}. \quad (1)$$

It is of interest to remark that this simple recursion formula retains its validity in the quantum case. We also observe that, in investigations of homogeneous fluids, $\rho^{(1)}$ reduces to the uniform concentration c and that it is thus convenient to introduce n tuplet correlation functions $g^{(n)}(1,\cdots n;\ T,\ \beta\mu)$ by the relation $\rho^{(n)}(1,\cdots u;\ T,\ \beta\mu)=c^n g^{(n)}(1,\cdots n;\ T,\ \beta\mu)$. Since we shall only be concerned with the pair correlation function $g^{(2)}$, it is sufficient to examine the implications of Eq. (1) for $n=1$ and 2. In the former case, for homogeneous fluids, Eq. (1) simply reduces to

$$(\partial c/\partial\beta\mu)_T=c+c^2\int(g^{(2)}-1)dv_{12}. \quad (2)$$

The left-hand side may be simplified by an elementary thermodynamic identity so that Eq. (2) leads to the well-known expression[4] for the coefficient of isothermal compressibility κ,

$$ckT\kappa-1=c\int(g^{(2)}-1)dv_{12}. \quad (3)$$

In the second case it is convenient to combine the expression for $n=1$ and 2 in the following form:

$$\left\{\frac{\partial\log[\rho^{(2)}(12)/\rho^{(1)}(1)\rho^{(1)}(2)]}{\partial\beta\mu}\right\}_T$$
$$=\int\{[\rho^{(3)}(123)/\rho^{(2)}(12)]-[\rho^{(2)}(13)/\rho^{(1)}(1)]$$
$$-[\rho^{(2)}(23)/\rho^{(1)}(2)]+\rho^{(1)}(3)\}dv_3. \quad (4)$$

* Present Address: Department of Physics, Cornell University, Ithaca, New York.

[1] J. G. Kirkwood, J. Chem. Phys. 3, 300 (1935).

[2] F. P. Buff and R. Brout, J. Chem. Phys. 23, 458 (1955).

[3] F. P. Buff, J. Chem. Phys. 23, 419 (1955).

[4] J. Yvon, *Actualités scientifiques et industrielles* (Hermann & Cie, Paris, France, 1937), p. 40.

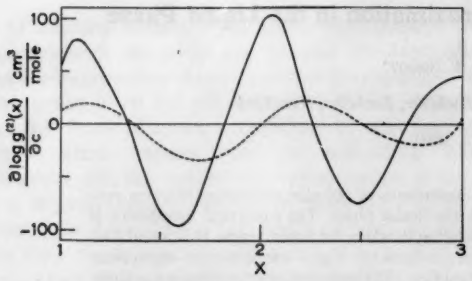

FIG. 1. Concentration derivative of $\log g^{(2)}(x)$. Solid line, theoretical calculation with superposition and $\kappa = 2\times10^{-4}$ atm^{-1}. Dotted line, hard-sphere calculation with $\lambda = 27.4$. Both at 91.8°K and 2 atm.

Upon introducing correlation functions and using Eqs. (2) and (3), the required formula for the concentration dependence of $g^{(2)}$ is obtained

$$[\partial \log g^{(2)}(R_{12})/\partial c]_T$$
$$= (ckT\kappa)^{-1}\left\{\int [g^{(2)}(R_{13})-1][g^{(2)}(R_{23})-1]dv_3 + \int\left[\frac{g^{(3)}(R_{12},R_{13},R_{23})}{g^{(2)}(R_{12})} - g^{(2)}(R_{13})g^{(2)}(R_{23})\right]dv_3\right\};$$
$$R_{ij} = |\mathbf{R}_i - \mathbf{R}_j|. \qquad (5)$$

We now turn to two applications of this expression, the calculation of $(\partial E/\partial V)_{T,N}$ and of the pressure dependence of κ, $(\partial\kappa/\partial p)_T$. We consider a classical fluid with pairwise spherically symmetric potential of intermolecular force. Its energy $\bar{E}$, per molecule, is given by the familiar relation

$$\bar{E} = \bar{E}^*(T) + \tfrac{1}{2}c\int V(R_{12})g^{(2)}(R_{12})dv_{12}. \qquad (6)$$

$V(R)$ is the potential of intermolecular force between two isolated molecules separated by the distance R, and $\bar{E}^*(T)$ is the energy per molecule of an ideal gas. Differentiation of Eq. (6) and use of Eq. (5) directly yields the statistical mechanical expression for $(\partial E/\partial V)_{T,N}$,

$$(\partial E/\partial V)_{T,N} = -c^2(\partial\bar{E}/\partial c)_T = c\bar{E}_{vap}{}^* + \Delta, \qquad (7)$$

where

$$\Delta = -\tfrac{1}{2}c^2\int V(R_{12})g^{(2)}(R_{12})[\partial \log g^{(2)}(R_{12})/\partial c]_T dv_{12}. \qquad (8)$$

$\bar{E}_{vap}{}^*$ is the energy of vaporization per molecule of liquid into an ideal gas and Δ, by Eq. (5), is the exact correction to the van der Waals estimate, $c\bar{E}_{vap}{}^*$. Here it is of interest to recall that Hildebrand,[6] in his study of regular solutions, has shown that, for representative simple liquids, the estimate $c\bar{E}_{vap}{}^*$ for $(\partial E/\partial V)_{T,N}$ is usually within 10% of experimental results.

The calculation of $(\partial\kappa/\partial p)_T$, or equivalently, the thermodynamic evaluation of the analog of the third virial coefficient in the liquid phase, follows from the differentiation of Eq. (3) and use of Eq. (5). The result may be exhibited in the following form

$$I_{superpos} + J = -1 + 3ckT\kappa - (ckT\kappa)^2 + (ckT)^2(\partial\kappa/\partial p)_T, \qquad (9)$$

where

$$I_{superpos} = c^2\iint [g^{(2)}(R_{12})-1][g^{(2)}(R_{23})-1] \times [g^{(2)}(R_{13})-1]dv_2dv_3$$

$$J = c^2\iint [g^{(3)}(R_{12},R_{13},R_{23}) - g^{(2)}(R_{12})g^{(2)}(R_{13})g^{(2)}(R_{23})]dv_2dv_3.$$

Further applications to problems such as the alternative formula[6] for κ and the high-temperature quantum corrections to the equation of state will not be considered.

II.

The utilization of Eq. (5) illustrates a familiar difficulty in the theory of liquids. As in Kirkwood's[1] pioneering coupling parameter integral equation and that of Born and Green,[7] it involves both the pair and triplet correlation functions. These two sequences of integral equations are conventionally terminated by the use of the Kirkwood[1] superposition approximation $g^{(3)}(123) = g^{(2)}(R_{12})g^{(2)}(R_{23})g^{(2)}(R_{13})$. Although this approximation possesses no *a priori* justification, it leads to equations which can be solved by numerical means. It is known that, for imperfect gases, it leads to errors beginning with the fourth virial coefficient.[8] The magnitude of this error depends on, which otherwise rigorous, basic formula is used in the calculation of the equation of state. In the case of solutions of strong electrolytes, by charge expansions[9] or diagram summation techniques,[10] it can be shown to be exact for the linearized term which leads to the Debye-Hückel limiting law. In the most important case of the liquid phase, the evidence for its applicability is not readily available. The simple form of Eq. (5) does, however, provide a direct delicate test for the range of applicability of the superposition approximation in the liquid state. With use of superposition, the substitution of Eq. (5) into Eqs. (8) and (9) leads to a triangular

[6] J. H. Hildebrand and R. L. Scott, *The Solubility of Non-Electrolytes* (Reinhold Publishing Corporation, New York, 1950), 3rd ed.

[6] Footnote reference 2, Eq. (63).

[7] M. Born and H. S. Green, Proc. Roy. Soc. (London) **A188**, 10 (1946).

[8] See, for example, B. R. A. Nijboer and L. Van Hove, Phys. Rev. **85**, 777 (1952).

[9] J. G. Kirkwood and J. C. Poirier, J. Phys. Chem. **58**, 591 (1954).

[10] See, for example, F. P. Buff and F. H. Stillinger, Jr., J. Chem. Phys. **25**, 312 (1956).

diagram which can be readily evaluated by the Fourier transform technique.

$$v^{-1}\iiint H_1(R_{12})H_2(R_{23})H_3(R_{13})\,dv_1dv_2dv_3 = (2\pi^2)^{-1}\int_0^\infty \prod_{i=1}^{3} h_i(s)\,s^2\,ds;$$

$$h_i(s) = 4\pi\int_0^\infty (\sin sR/sR)H_i(R)R^2dR. \qquad (10)$$

It is, however, more instructive to employ this technique also for the direct evaluation of $(\partial \log g^{(2)}/\partial c)_T$. With use of superposition, it reduces to the form

$$[\partial \log g^{(2)}(R)/\partial c]_T = (2\pi^2c^3kT\kappa)^{-1}\int_0^\infty [si(s)]^2 \times (\sin sR/sR)ds, \qquad (11)$$

where

$$i(s) = 4\pi c\int_0^\infty R^2[g^{(2)}(R)-1](\sin sR/sR)dR. \qquad (12)$$

Since liquid argon satisfies the assumptions inherent in Eq. (6), the calculations to be discussed will refer to this substance at 91.8°K and 2 atm. The function $i(s)$ appearing in Eq. (11) is directly available from the careful x-ray scattering investigation of Eisenstein and Gingrich[11] on liquid argon in the thermodynamic region of interest. We note that Eq. (12) in conjunction with Eq. (3) leads to the relation

$$i(0) = -1+ckT\kappa. \qquad (13)$$

In the experimentally difficult region of low angle scattering, an extrapolation of the Eisenstein-Gingrich data to zero scattering angle led to a value of κ equal to 2 to 3×10^{-4} atm^{-1}, which is to be compared with the thermodynamic value of $\kappa=2\times10^{-4}$ atm^{-1}, obtained from an extrapolation of Bridgman's melting point data.[12] This agreement is to be contrasted with the direct computation of $i(0)$ from theoretical[13] values of $g^{(2)}$ only. This approach implies the value 7.67×10^{-3} atm^{-1} for κ, which is too high by a factor of 35.

On the basis of these considerations, the evaluation of the integral in Eq. (11) has been carried out with the use of the Eisenstein-Gingrich data.[14] The computations were carried out with the help of IBM equipment making use of the National Bureau of Standards punched cards for $\sin sR/sR$. The solid line of Fig. 1 summarizes the results of this calculation on a reduced basis.

[11] A. Eisenstein and N. S. Gingrich, Phys. Rev. **62**, 261 (1942).
[12] P. W. Bridgman, Trans. Am. Acad. **70**, 1 (1935).
[13] R. W. Zwanzig, J. G. Kirkwood, K. F. Stripp, and I. Oppenheim, J. Chem. Phys. **21**, 1268 (1953).
[14] We are indebted to Professor Gingrich for supplying us with the original experimental data.

TABLE I.

	$g^{(2)}_{\text{E.G.}}$	$g_L^{(2)}(x)$	$g_L^{(2)}(\xi x)$; $\xi=1.023$
Δ_{superpos}(atm)	1680	1910	1870

$\Delta_{\text{exp}} = (\partial E/\partial v)_{T,N}^{\text{exp}} - c\bar{E}_{\text{vap}} = (2130\pm100) - 1930 = 200 \pm 100$ atm

In addition to $(\partial \log g^{(2)}/\partial c)_T$, the evaluation of the integral in Eq. (8) requires knowledge of the radial distribution function $g^{(2)}$. As the Eisenstein-Gingrich radial distribution function $g_{\text{E.G.}}^{(2)}$ is not as reliable as its experimentally determined Fourier transform $i(s)$, we have tested the sensitivity of the integral in Eq. (8) by also employing Kirkwood's theoretical distribution function $g_L^{(2)}(\lambda=27.4)$.[13] For the potential of intermolecular force, we use the Lennard-Jones form

$$V(R) = 4\epsilon[(1/x^{12})-(1/x^6)]; \qquad x=R/a, \qquad (14)$$

where[15]

$$\epsilon = 1.653\times10^{-14}\text{ erg},$$
$$a = 3.405\times10^{-8}\text{ cm}.$$

In order to compensate partially for the arbitrary form of the potential, Eq. (14), and the approximate nature of $g_L^{(2)}(x)$, we have also employed the function $g_L^{(2)}(\xi x)$, where the scale parameter ξ has been adjusted so as to give the correct value for $\bar{E}_{\text{vap}}{}^*$, i.e., ξ is determined from the equation

$$\bar{E}_{\text{vap}}{}^* = -2\pi a^3 c\int_0^\infty V(x)g_L^{(2)}(\xi x)x^2\,dx. \qquad (15)$$

Table I summarizes the results of the calculation of Eqs. (5) and (8), subject to the superposition approximation, for liquid argon at 91.8°K and 2 atm. The theoretical value of the quantity

$$\Delta_{\text{superpos}} = (\partial E/\partial V)_{T,N}^{\text{superpos}} - c\bar{E}_{\text{vap}}{}^*$$

is thus found to be quite insensitive to the choice of the radial distribution. In view of this observation and the carefully determined Eisenstein-Gingrich data, we feel that our numerical estimate of Δ_{superpos} is reliable. At this thermodynamic condition, the somewhat uncertain value $\Delta_{\text{exp}}=200\pm100$ atm applies. It is obtained from the relation $(\partial E/\partial V)_{T,N} = (T\alpha/\kappa)-p$, with coefficient of thermal expansion[16] $\alpha=4.65\ 10^{-3}$ deg^{-1} and $\kappa=2\times10^{-4}$ atm^{-1}, and the experimental value of 1930 atm for $c\bar{E}_{\text{vap}}{}^*$.[17,18] The discrepancy between theory and experiment must be ascribed to the

[15] A. Michels, H. Wijker, and H. Wijker, Physica **15**, 627 (1949).
[16] E. C. C. Baly and F. G. Donnan, Trans. Chem. Soc. **81**, 907 (1902).
[17] A. Frank and K. Clusius, Z. physik Chem. (Leipzig) **B42**, 395 (1939).
[18] E. Mathias, H. K. Onnes, and C. A. Crommelin, Comm. Kamerlingh Onnes Lab. Univ. Leiden **12**, No. 131a (1912).

TABLE II.

	$g_L^{(2)}(x)$	$g_L^{(2)}(\xi x)$; $\xi=1.023$	$g_{h.s.}^{(2)}(x)$	$g_{h.s.}^{(2)}(\xi x)$; $\xi=1.012$
$\Delta_{h.s.}$(atm)	470	460	390	370

failure of the superposition approximation. The large value of Δ_{superpos} arises from the fact that superposition induces too large a concentration dependence on $g^{(2)}$, the effect of which is primarily restricted to the first peak in this calculation.

We now turn to a more favorable illustration of the superposition approximation. We contrast the preceding calculation with the available concentration dependence of theoretical distribution functions, the determination of which entails the use of superposition in integrals which are damped by the potential of intermolecular force. In the thermodynamic region of interest we have had to resort to the $g_{h.s.}^{(2)}$ calculated on the basis of a hard-sphere interaction.[19,20] The dotted curve in Fig. 1 summarizes $(\partial \log g_{h.s}^{(2)}/\partial c)_T$ on a reduced basis, obtained by interpolation from the available tabulations of the theoretically calculated $g_{h.s.}^{(2)}$. The corresponding $\Delta_{h.s.}$ is defined by the relation

$$\Delta_{h.s.}=-2\pi a^3 c^3 \int_0^\infty V(x) g^{(2)}(x) (\partial \log g_{h.s.}^{(2)}/\partial c)_T x^2 dx. \tag{16}$$

For $g^{(2)}$ we have employed $g_L^{(2)}(\lambda=27.4)$ and, for the sake of completeness, $g_{h.s.}^{(2)}(\lambda=27.4)$; we have also employed scale parameters to give agreement with the experimental E_{vap}^* again using for our interaction potential the Lennard-Jones form, Eq. (14), for both $g_L^{(2)}$ and $g_{h.s.}^{(2)}$. The results of this calculation for liquid argon at 91.8°K and 2 atm are shown in Table II. These values compare much more favorably with Δ_{exp}. It is to be expected that the use of distribution functions, determined by the utilization of superposition in integrals damped by the interaction potential, would improve the agreement between theory and experiment. However, the necessary use of $g_{h.s.}^{(2)}$ to obtain the concentration dependence of the radial distribution function casts some doubt on the precision of the resulting numerical values.

As a final application of Eq. (5), we consider the numerical evaluation of Eq. (9). When the superposition approximation is employed, $J=0$. The remaining integral I_{superpos} may be entirely evaluated with use of Eq. (10) and the Eisenstein-Gingrich $i(s)$. By this procedure it is found that $I_{\text{superpos}}=0.33$. This is to be contrasted with the thermodynamic right-hand side of Eq. (9). With the estimate[21] $(\partial\kappa/\partial p)_T=-6\times10^{-6}$ atm^{-2}, it possesses the value -0.85, which differs in sign with I_{superpos}.

These tests of the superposition approximation which are carried out with reliable experimental input for the sensitive part of the calculation lead to the following conclusions. The usefulness of Kirkwood's suggestion depends on the application that is desired. It fails in connection with integrals having the pure density fluctuation origin of the generalized virial coefficients of the liquid phase. It appears more favorable in those cases in which, either through its original mode of computation or in its final application, the error is damped by the presence of contributions arising from short-range intermolecular forces. It becomes a particularly powerful tool in the recent exact analysis[22] of solution theories involving small perturbations from ideality. Here a triangular diagram is encountered, two sides of which possess short-range character only. The results of a calculation based on superposition confirm the successful Prigogine[23]—Scott[24] two-fluid model.

[19] J. G. Kirkwood, E. K. Mann, and B. J. Alder, J. Chem. Phys. **18**, 1040 (1950).
[20] J. G. Kirkwood, V. A. Levinson, and B. J. Alder, J. Chem. Phys. **20**, 929 (1952).
[21] P. W. Bridgman, Trans. Am. Acad. **49**, 1 (1913).
[22] F. P. Buff and F. M. Schindler, J. Chem. Phys. **29**, 1075 (1958).
[23] I. Prigogine, *The Molecular Theory of Solutions* (Interscience Publishers, Inc., New York, 1957).
[24] R. L. Scott, J. Chem. Phys. **25**, 193 (1956).

Structure of Transport Equations

S. TAMOR

General Electric Research Laboratory, Schenectady, New York

(Received July 11, 1960)

The problem of inventing irreversible equations which in some sense approximate the Liouville equation is examined. First a class of solutions of the Liouville equation is defined which have the property of weak convergence to equilibrium. A modified Liouville equation is then constructed which is inherently irreversible and whose solutions constitute an asymptotic approximation to the Liouville equation for those systems which decay to equilibrium. The approximation involves replacing the force term in the Liouville equation by an operator involving the prehistory of the system for a small but finite time. It is found that solutions of this modified equation exist only for time-smoothed distribution functions, and that the smoothing interval must increase slowly with time. This smoothing procedure is essentially the repeated time-smoothing method of Kirkwood.

I. INTRODUCTION

WHILE the motion of an assemblage of classical point particles with prescribed interactions is completely specified by the equations of Hamiltonian dynamics, actual solution of these equations is quite impractical for all but the simplest systems. Since one is never interested in the extremely detailed description provided by particle dynamics it is reasonable to seek some more tractable approximate equations of motion at the expense of losing some information. The process of throwing away information changes the character of the solutions from multiply periodic reversible motions to an irreversible motion. The most familiar examples of such irreversible equations (we will call them transport equations) are the Boltzmann and Fokker-Planck equations. While these statistical descriptions of the motion have proven to be of great utility, the formal structure of these equations is so different from classical dynamics, particularly with regard to irreversibility, that the relation between them has long been obscure. In recent years, mainly through the work of Kirkwood,[1] Bogoliubov,[2] Prigogine,[3] and others[4–7] considerable progress has been made in clarifying this question. It is now possible to provide a mathematical formulation of the underlying physical features of the very many body problem and more or less deductively arrive at an irreversible equation of motion as an approximation to classical dynamics.

The several studies referred to proceed by developing various approximate methods of integrating the Liouville equation (based either upon power series expansions or upon the BBGKY scheme) and then showing that for large particle numbers and long times the solutions are obtainable from a transport equation. The final result of all these analyses is that the motion of the phase point is no longer given by the instantaneously acting forces, but by some operator (like a collision operator) involving an integration over a finite part of the history of the system. The derivation of a transport equation appropriate to a given class of systems involves approximations of an essentially statistical nature appropriate to the limit of the particle number, N, tending to infinity as well as an approximate treatment of the dynamics of the system which determines the actual form of the collision operator. It is of interest to attempt to separate these two aspects of the problem as completely as possible, and this paper is devoted to the first of them.

More specifically, we inquire into the following question: In what mathematical sense, if any, can the motion of a system of point particles be approximated by an essentially irreversible description? The fundamental point behind the answer is, of course, well known. Although the phase point of a bounded N particle system describes a multiply periodic orbit, the recurrence time grows enormously rapidly with increasing N, so that to a first approximation it may be considered infinite compared to the duration of any laboratory experiment. Or, in mathematical terms, the study of the approach to equilibrium involves a double limiting process in which first $N\to\infty$ and then $t\to\infty$. Observance of the correct order of limits is crucial.

For the purpose of the following discussion it is convenient to introduce a distinction between the concepts of "approach to equilibrium" and "irreversibility." In the limit $N\to\infty$ there indeed exists a class of solutions of the Liouville equation which, in an appropriate sense, relax to equilibrium. This approach to equilibrium is, however, a property only of this limiting class of solutions and not a general property of the equations of motion. Furthermore, even those systems which do relax to equilibrium do so by such an enormously complicated path that solution of the Liouville equation is still completely impractical and we are

[1] J. G. Kirkwood, J. Chem. Phys. **14**, 180 (1946); **15**, 72 (1947).
[2] N. N. Bogoliubov, J. Phys. (U.S.S.R) **10**, 265 (1956), and "Problems of a dynamical theory in statistical physics," translated by E. K. Gora, ASTIA Document No. AD-213317.
[3] I. Prigogine and F. Henin, Physica **23**, 345 (1957), and I. Prigogine and R. Balescu, Physica **25**, 281, 302 (1959).
[4] R. Brout, Physica **22**, 509 (1956).
[5] M. S. Green, J. Chem. Phys. **25**, 386 (1956).
[6] J. Ross, J. Chem. Phys. **24**, 375 (1956).
[7] Proceedings of the International Symposium on Transport Processes in Statistical Mechanics I. Prigogine, Editor (Interscience Publishers, Inc., New York, 1958). See particularly Parts I and II.

led to seek other approximate descriptions of the motion. These descriptions generally have the property of irreversibility, since the approach to equilibrium is an essential property of the equations of motion.

It is clear that for those systems which do not actually relax to equilibrium an irreversible description makes no sense at all. Our first task, to which the next section is devoted, is then to characterize those solutions of the Liouville equation which do relax to equilibrium. Having done this, our problem is to discover whether the temporal evolution of such systems can be approximated by the solutions of an irreversible equation. In Sec. III a quite simple procedure is proposed for the construction of a class of irreversible equations. The method involves exact integration of the Liouville equation over a short interval of time and then assuming that during that time the configuration of the system has not actually changed very much. This introduces explicitly the "forgetting mechanism" which leads to irreversibility. It is found, however, that meaningful solutions exist only if a time-smoothing operation is performed which is analogous to the Kirkwood smoothing procedure.

While the present approach to the theory of irreversibility may seem somewhat artificial, its motivation came from a study of the nonuniform gas described in the following paper.[8] This paper is concerned only with the formal structure of transport equations, while the next outlines an application to a particular class of dynamical systems. Much of the following development would benefit in both rigor and generality by use of the tools of measure theory. We will be content, however, with more elementary methods since the principal objective is to present a new point of view rather than a fully developed mathematical theory.

II. SYSTEMS WHICH DECAY TO EQUILIBRIUM

Hamilton's equations for the motion of the phase point of an N particle system may be written in the form of a Liouville equation

$$(\partial/\partial t)\rho_N\{x, p; t\} = -[H\{x, p\}, \quad \rho_N\{x, p; t\}]$$
$$= -L\{x, p\}\rho_N\{x, p; t\}. \qquad (1)$$

H is the total Hamiltonian of the system and the distribution function ρ_N is a delta function in the $6N$ dimensional $\{x, p\}$ space whose singularity is at the locus of the phase point at time t. (Singular distribution functions are introduced to simplify the exposition. Since we shall be concerned with integral properties of ρ this singularity causes no difficulty.) The curly bracket is used to denote collectively all coordinates and/or momenta, but explicit reference to these coordinates will be omitted except when required for clarity. The "Liouville operator" L is defined by

$$L = \sum_{\mu=1}^{3N}[(\partial H/\partial p_\mu)(\partial/\partial x_\mu) - (\partial H/\partial x_\mu)(\partial/\partial p_\mu)]. \quad (2)$$

The Hamiltonian is assumed to be a known time independent function of $\{x, p\}$. The wall forces, if any, are included in H, but need not be referred to explicitly except to note that they serve to guarantee the boundedness of the system in space. For systems with finite energy ρ also vanishes with increasing p, so that with respect to these distribution functions L is an anti-Hermitian operator. Hence the eigenvalues of L are purely imaginary and Eq. (1) describes a multiply periodic motion.

Let $F_N\{x, p\}$ be an arbitrary integrable function of the phase point and consider quantities of the form

$$F_N(t) = \int F_N\{x, p\}\rho_N\{x, p; t\}d\{x\}d\{p\}. \qquad (3)$$

We write the solutions of Eq. (1) in the form

$$\rho_N\{x, p; t\} = \sum_n \phi_N\{x, p; \omega_n\} \exp(i\omega_n t). \qquad (4)$$

Since ρ_N is a delta function the series (4) does not converge, but since the ϕ_N are $0(\omega_n^{-1})$ for all $F_N\{x, p\}$ such that $F_N(0)$ exists

$$F_N(t) = \sum_n \exp(i\omega_n t)\int F_N\{x, p\}\phi_N\{x, p; \omega_n\}d\{x\}d\{p\} \qquad (5)$$

which does converge. Considering a sequence of systems with increasing N such that

$$\lim_{N\to\infty} F_N(0)$$

exists, the frequencies ω_n become dense and we may replace the summation over n by an integration. The limiting forms of F_N, ϕ_N and ρ_N as $N\to\infty$ are indicated by merely dropping the subscript. Note, however, that the normalization integral is time independent implying a delta-like singularity in $\phi(\omega)$ at $\omega=0$. To remove this singularity we define

$$f(t) = F(t) - \lim_{T\to\infty} T^{-1}\int_{-T}^{T} \theta(t, t')F(t')dt', \qquad (6)$$

where

$$\theta(t, t') = \begin{cases} 1 \text{ if } t \text{ and } t' \text{ have like signs} \\ 0 \text{ if } t \text{ and } t' \text{ have opposite signs,} \end{cases}$$

and let

$$f(t) = \int \exp(i\omega t)\psi(\omega)d\omega. \qquad (7)$$

Definitions (6) and (7) ensure that $\psi(\omega)$ is finite at $\omega=0$. The step function $\theta(t, t')$ is introduced to accommodate the possibility (here not excluded) that $F(t)$ converges to different limits as t tends to plus or minus

[8] P. L. Auer and S. Tamor, J. Chem. Phys. 33, 1423 (1960).

infinity. The existence of the limit in Eq. (6) and its independence of the origin of t is assured by Birkhoff's theorem.[9] For bounded $|\psi|$ we apply the Riemann-Lebesgue lemma[10] and have

$$\lim_{|t|\to\infty} f(t)=0, \tag{8}$$

so that all $F(t)$ have well-defined limits as $|t|\to\infty$.[11] This is in effect a statement that $\rho\{x, p; t\}$ has the property of weak convergence as $|t|\to\infty$.

The functions $F(t)$ represent all intensive variables of the limiting class of systems as functions of time, while the $f(t)$ represent their deviations from the equilibrium values. These are to be considered as approximations to the corresponding quantities for a large but finite system. Whether or not these limiting solutions are appropriate to an actual physical system depends upon whether or not the density of the ω_n is large compared with the time required to perform a measurement. Since the spectral density varies with the size of the system roughly as N^N, it is generally much larger than this time even for moderately large systems. Under these conditions the ω summation can indeed be replaced by an integration.

It is to be emphasized that this development does not prove anything about the conditions under which a real physical system approaches equilibrium. Instead, it serves to characterize the class of distribution functions with which we shall be concerned in the subsequent argument and to define precisely the sense in which such systems can be said to approach equilibrium. The relaxation to equilibrium is not a manifestation of true irreversibility since the frequencies, ω, are always real.

III. IRREVERSIBILITY

Let the Hamiltonian be written as the sum of two terms, $H=H_0+H_1$, and correspondingly $L=L_0+L_1$. The rule for separating H into two parts is left unspecified and will in general be determined by physical considerations, although a restriction will appear later in the development. We write the formal solution of the Liouville equation for the N body problem in terms of the propagator $U^{(N)}\{x, p; t\}$ so that

$$\rho_N\{x, p; t\}=U^{(N)}\{x, p; t-t'\}\rho_N\{x, p; t'\}, \tag{9}$$

where

$$(\partial/\partial t)U^{(N)}\{x, p; t\}=-L\{x, p\}U^{(N)}\{x, p; t\};$$
$$U^{(N)}\{x, p; 0\}=1. \tag{10}$$

The Liouville equation may now be written

$$(\partial/\partial t)\rho_N(t)=-L_0\rho_N(t)-L_1U^{(N)}(t-t')\rho_N(t'), \tag{11}$$

where the variables $\{x, p\}$ have been suppressed.

Let τ be a fixed but macroscopically small time interval, and rewrite Eq. (11),

$$(\partial/\partial t)\rho_N(t)=-L_0\rho_N(t)-L_1U_N(\tau)\rho_N(t-\tau). \tag{12}$$

While this equation is identical with the Liouville equation, we have introduced explicitly the operator $U(\tau)$ which involves the trajectory of the phase point for a finite but small time. Suppose, now, that τ is small enough that in some sense ρ has not changed very much during this time. We are then led to examine the solutions of the equation

$$(\partial/\partial t)\rho_N^*(t)=-L_0\rho_N^*(t)-L_1U^{(N)}(\tau)\rho_N^*(t) \tag{13}$$

subject to the initial conditions $\rho_N(0)=\rho_N^*(0)$. At present it is only a guess that the solutions ρ_N^* are in some way approximations to ρ_N, and it is this connection which will now be examined.

First observe that any time independent solution of the Liouville equation also satisfies Eq. (13) so that their "equilibrium" solutions are identical. Also, as $\tau\to 0$, Eq. (13) reduces to the Liouville equation so that we expect the difference between ρ_N and ρ_N^* to be of order τ. While clearly for short times the error in approximating ρ_N by ρ_N^* is small, the important point is whether or not this error grows in time. If it can be verified, at least in the limit $N\to\infty$, that for all $F(t)$ the error in replacing ρ by ρ^* is bounded and tends to zero at $t\to\infty$, then Eq. (13) is a useful approximation to the Liouville equation.

It is suggestive to rewrite Eq. (13)

$$(\partial/\partial t)\rho_N^*(t)=-[L_0+L_1\exp(-L\tau)]\rho_N^*(t)$$
$$=-\Lambda\rho_N^*(t) \tag{14}$$

which defines the modified Liouville operator Λ. To study the time dependence of ρ^* we examine the spectral decomposition of the operator Λ. To illustrate the essential points we first consider the simple, but rather academic, choice $H_0=0$, $H_1=H$. In this case the operators L and Λ commute and for every eigenfunction $\phi\{x, p\}$ such that $-L\phi=i\omega_n\phi$ we have $-\Lambda\phi=i\omega_n\exp(i\omega_n\tau)\phi$. Since the eigenvalues of Λ are complex, the solutions of Eq. (14) are neither multiply periodic nor reversible. In terms of the eigenfunctions of Eq. (1), we have

$$\rho_N^*(t)=\sum_n \exp[i\omega_n t\exp(i\omega_n\tau)]\phi_N\{x, p;\omega_n\}. \tag{15}$$

Let N tend to infinity by the same sequence of systems as in the previous section and we compare the limiting forms of Eqs. (4) and (15). The error in $f\{x, p\}$ is given by

$$\Delta f(t)=\int f\{x, p\}[\rho\{x, p; t\}-\rho^*\{x, p; t\}]d\{x\}d\{p\}$$
$$=\int\{e^{i\omega t}-\exp[i\omega t\exp(i\omega\tau)]\}\psi(\omega)d\omega. \tag{16}$$

[9] A. I. Kinchin, *Mathematical Foundations of Statistical Mechanics* (Dover Publications, New York, 1949), p. 19.

[10] E. T. Whittaker and G. N. Watson, *Modern Analysis* (Cambridge University Press, New York, 1946), p. 172.

[11] A similar method was applied to a model of an ideal gas by H. L. Frisch, Phys. Rev. **109**, 22 (1958).

One important property of Λ is at once evident. The real part of its eigenvalues is given by $-\omega \sin\omega\tau$, so that for $|\omega\tau| \lesssim 1$ these modes decay in time. Hence all low frequency motions are driven to equilibrium by Eq. (14) and do not simply relax by phase mixing. For large ω, however, the real part oscillates in sign and the integral in Eq. (16) does not actually exist. To suppress this divergence at high frequencies we consider not the instantaneous $f(t)$, but its time-smoothed value defined by

$$\bar{f}(t) = \frac{1}{\epsilon(\pi)^{\frac{1}{2}}} \int_{-\infty}^{\infty} \exp[-(t-t')^2/\epsilon^2] f(t')\,dt'. \quad (17)$$

While this time smoothing guarantees that $\overline{\Delta f}(t)$ exists for all t it is still not sufficient since the error grows without bound as $t \to \infty$ due to the violent oscillation of the integrand when $|\omega\tau| \gg 1$ and $t > \omega\epsilon^2$ are simultaneously satisfied. It is therefore necessary to make ϵ itself a function of t. Choosing a constant time interval $\delta > \tau$, we let $\epsilon^2 = t\delta$ giving finally

$$\overline{\Delta f}(t) = \int \exp(-\omega^2 t\delta/4) \times \{\exp(i\omega t) - \exp[i\omega t \exp(i\omega\tau)]\}\psi(\omega)\,d\omega. \quad (18)$$

It is not difficult to verify by explicit calculation that for small τ and large t

$$\overline{\Delta f}(t) = 0(\tau/t\delta). \quad (19)$$

Before discussing the physical meaning of this procedure, we return to examination of the general case of arbitrary L_0 and L_1. Here Λ and L do not in general commute and the situation is much more complicated. To first order in τ, however, the frequency shift may be obtained by a perturbation procedure. In a representation in which L is diagonal the first-order frequency shift is given by the diagonal elements of the operator $L_1(1-e^{-L\tau})$, or $(1-e^{i\omega\tau})$ times the diagonal elements of L_1. The diagonal elements of L_1 are purely imaginary and the previous argument can again be carried through if we can verify that they have the same sign as ω.

Let the exact solution of the N body problem be written in terms of the action and angle variables J_i and Q_i, where $H = \sum_i \omega_i J_i$ so that $\dot{J}_i = 0$ and $\dot{Q}_i = \omega_i$. The most general solution of the Liouville equation is of the form

$$\rho_N(t) = \rho_N\{J, \chi\} \sum_{\{m_i\}} \exp\{i m_i[Q_i + \omega_i t - \chi_i]\}, \quad (20)$$

where the summation is carried out over all possible sets of integer values of the $\{m_i\}$. The summand in Eq. (20) is an eigenfunction of Eq. (1) of frequency $\omega_n = \sum_i m_i\omega_i$, which is, of course, equal to the diagonal element of L. We need, now, the diagonal element of

$$L_1 = (\partial H_1/\partial J)(\partial/\partial Q) - (\partial H_1/\partial Q)(\partial/\partial J).$$

The diagonal element of the second term vanishes. We must now verify that for all choices of $\{m_i\}$

$$0 < \operatorname{diag}(L_1)/\operatorname{diag}(L) = \frac{\sum_i m_i \operatorname{diag}(\partial H_1/\partial J)}{\sum_i m_i \operatorname{diag}(\partial H/\partial J)} \lesssim 1. \quad (21)$$

We see from Eq. (20) that the diagonal element of an operator is simply its average over the phases $\{Q\}$. Hence the diagonal elements of L and L_1 are the first-order changes in the average values of H_1 and H, respectively, when all action variables $\{J_i\}$ are changed by m_i. For Eq. (21) to hold for all $\{m_i\}$ we require the phase average $(H_1)_N$ and $(H)_N$ to satisfy

$$0 < \delta(H_1)_N/\delta(H)_N \lesssim 1 \quad (22)$$

for any pair of neighboring orbits of the N body system.

Equation (22) constitutes a constraint on the possible choices of H_0 and H_1 for which the time-smoothing procedure works. Since the averages must be taken over the exact trajectories of the N body system, it is not very useful in this form. It unfortunately does not seem possible to find the corresponding condition in an arbitrary representation. That this is at least physically reasonable may be seen from a simple illustration. Consider a gas confined in a fixed volume and let H_0 be the kinetic energy and H_1 the interparticle interactions. (The wall interaction may be included in either term without affecting the argument.) If the forces are repulsive a positive increment in the kinetic energy permits the particles to penetrate more deeply into each other's force field thereby increasing the average value of H_1. When the forces are attractive, on the other hand, deep penetration is highly probable but when the average kinetic energy is increased the particles spend less time in interaction. In either case a change in the average H_0 produces a change of the same sign in H_1 so that Eq. (22) is satisfied. A more quantitative statement of this condition is obtained if it is assumed that in the limit $N \to \infty$ the motion becomes ergodic. We may then replace phase averages by averages over the canonical distribution. Denoting this average by $\langle\rangle$, we can easily show that Eq. (22) reduces to

$$0 < \frac{\delta\langle H_1\rangle}{\delta\langle H\rangle} = \frac{\langle (H_1 - \langle H_1\rangle)(H - \langle H\rangle)\rangle}{\langle (H - \langle H\rangle)^2\rangle} = \tfrac{1}{2}\left[1 + \frac{\langle (H_1 - \langle H_1\rangle)^2\rangle - \langle (H_0 - \langle H_0\rangle)^2\rangle}{\langle (H - \langle H\rangle)^2\rangle}\right] \lesssim 1. \quad (23)$$

Condition (22) is somewhat more useful in this form and is, at least in principle, verifiable in particular cases. One interesting and particularly simple case is found by letting H_0 and H_1 depend upon different sets of variables (say one depends upon coordinates and the other on momenta). In this case Eq. (23) is always satisfied. We point out, finally, that it is always possible to choose H_0 and H_1 so that Eq. (23) is satisfied since

if it fails we need only interchange their roles to restore the correct sign.

When Eq. (22) is satisfied the eigenvalues of Eq. (13) have to first order in τ a negative real part so that, again, all low frequencies decay while the high frequencies are suppressed by the time smoothing. Therefore with very minor modifications the analysis leading to Eq. (19) proceeds as before.

IV. SUMMARY AND CONCLUSIONS

The result of this development may be summarized as follows. We consider those solutions of the Liouville equation which relax to equilibrium in the sense described in Sec. II. Equation (13) shares with the Liouville equation the same time independent solutions, but in general solutions do not exist unless they are time smoothed. If the smoothing interval is chosen proportional to t^3 we find that solutions of Eqs. (1) and (13) are asymptotically equivalent in the sense that all time-smoothed observables as computed from these two equations differ only in order $\tau/t\delta$, and they both converge to precisely the same equilibrium state as $t\to\infty$.

It may seem at first glance that these results are trivial since by having the smoothing interval increase with time we artificially force the dominance of the zero-frequency component of ρ^*. That this is not the case may be seen rather simply. Suppose for some system we wish to describe some property which decays to its equilibrium value with characteristic time τ_0. The major contribution to the integral, Eq. (7), then arises from frequencies satisfying $|\omega\tau_0| \lesssim 1$. On the other hand the smoothing suppresses frequencies $\omega^2 > (t\delta)^{-1}$. No ω satisfy both inequalities until $t > \tau_0^2/\delta$. Hence, if $\tau_0/\delta \gg 1$ the time-smoothed description is useful for times much longer than the relaxation time for that property. Another way of stating this result is that the "forgetting mechanism" artificially introduced in going from Eqs. (12) to (13) causes high-frequency divergence which had to be suppressed by the time smoothing, but the frequencies involved are much higher than those of physical interest. The utility of this method ultimately rests upon the choice of τ and δ, which in turn is determined by dynamical considerations. For example, in the following paper[8] it is found that for a dense gas an appropriate choice of τ is the duration of a binary collision. Under gas kinetic conditions this is typically of the order of 10^{-13} sec. Choosing $\delta = 10^{-10}$ sec, we see that for properties decaying in, say, 1 μsec the time smoothing introduces no error until about 10^4 relaxation times, long after one has lost interest in the problem.

The choice of a smoothing function whose width increases as t^3 is strongly reminiscent of the repeated time smoothing of Kirkwood. Since our transport equation is linear in ρ the smoothing permits a variety of equally valid physical interpretations. We may decide in advance what interval to use and smooth the initial distribution function; we may say that our instruments have finite time resolution so that the smoothing is done at the time of observation, or, following Kirkwood, we may envisage a stepwise integration of the equation of motion smoothing at each stage with a Gaussian smoothing function with ϵ^2 equal to δ multiplied by the time step.

Essentially no assumptions have been made concerning the actual form of H. Also, both ρ and ρ^* are distribution functions in the complete phase space; reduced distribution functions are not needed. Indeed the analysis could not have been carried out for the reduced distributions since the linearity of the equations of motion is essential. The price paid for this generality is that Eq. (13) as it stands is no more tractable than the Liouville equation. However, with formal questions concerning irreversibility out of the way, it is now possible to examine the dynamics of a particular system and seek approximations to $U(\tau)$ which lead to further simplification. The following paper is devoted to the further reduction of Eq. (13) for the nonuniform gas. In that problem it is possible to choose τ small enough that the smoothing procedure is appropriate, but still sufficiently large that the collision operator $L_1 U(\tau)$ takes on a simple form.

ACKNOWLEDGMENTS

The author wishes to thank Dr. P. L. Auer for his helpful criticism and suggestions, and Professor I. Prigogine for several stimulating conversations.

Statistical Mechanics of the Nonuniform Gas

P. L. AUER AND S. TAMOR

General Electric Research Laboratory, Schenectady, New York

(Received July 11, 1960)

The method of the previous paper is applied to the derivation of a transport equation for the nonuniform dense gas. The required short time propagator is computed by an approximation scheme based upon the assumption that the duration of a binary collision is small compared to the mean free time between collisions. A transport equation for the phase space distribution function is obtained in which the "collision operator" satisfies a simple integral equation. The collision operator is nonlocal in the coordinate space and hence contains interference effects between collisions and the streaming motion. The limit of infinite dilution is examined by means of a moment expansion in which case the collision operator reduces to the Boltzmann collision integral. In this limit one obtains the master equation for the nonuniform gas.

I. INTRODUCTION

IN THE preceding paper[1] it was shown how properly time-smoothed solutions of the Liouville equation are approximated by the solutions of an inherently irreversible equation of motion. This analysis provides a formal framework for the construction of transport equations, but makes no reference to the dynamics of any particular system. For our purposes the important part of the dynamics is contained in the short time propagator for the system, denoted by $U(\tau)$. The problem is now to find approximate methods of evaluating this operator which are appropriate to the class of systems under consideration. In this effort we are aided by the availability of the parameter τ, which can be chosen to simplify the calculation as much as possible. In the present paper this method is applied to the study of the nonuniform dense gas.

We consider an assemblage of particles interacting through known pairwise forces of finite range so that the duration of a typical binary encounter may be characterized by a time τ_c. The class of systems to be considered is defined by the requirement that τ_c be small compared with the mean free time between collisions, τ_f. Strictly speaking this limits us to forces which are repulsive, or at least not too strongly attractive so that there are no collisions of extremely long duration (bound states). Note, however, that the assumption $\tau_c/\tau_f \ll 1$ does not necessarily imply the gas is dilute; for example, for hard spheres which are not actually close packed, $\tau_c/\tau_f = 0$. To first order in this expansion parameter it is possible to choose a τ such that $U(\tau)$ is quite simple. One obtains by this method a "binary Liouville equation" which still describes a reversible multiply periodic motion but takes advantage of the fact that the motion proceeds mainly via two-body encounters. If this approximate form of $U(\tau)$ is inserted into the result of Part I, we obtain a transport equation which is similar to that of Bogoliubov.[2] Further simplification is achieved in the limit of infinite dilution where an obvious extension of the Kac master equation is obtained. The collision operator is the usual Boltzmann collision integral, but is expressed as the solution of an integral equation which, if solved by iteration, generates the coupling constant expansion of Prigogine and Henin.[3]

The development outlined here and in the preceding paper constitutes a formalization of the program pointed out long ago by Kirkwood.[4] He suggested solution of the Liouville equation by integrating for a time somewhat longer than τ_c, neglecting the effects of collision more complex than binary encounters, and then piecing these together to obtain a complete history of the system.[5]

II. NOTATION AND FORMALISM

The notation of Part I will be carried over with elaborations as indicated in the following. Our main object of consideration is the propagator $U(t)$ defined by $\rho(t) = U(t-t_1)\rho(t_1)$. If the distribution function satisfies the Liouville equation then the propagator must satisfy

$$(\partial/\partial t)\, U(t-t_1) = -LU(t-t_1), \tag{1}$$

subject to the initial condition

$$U(0) = 1. \tag{2}$$

Particles are assumed to interact via two-body potentials ϕ_{ij}, which are of finite range but otherwise arbitrary. Latin indices i, j run from 1 to N and enumerate the particles of the system. Components of vectors attached to the particles (such as momentum components) are denoted by Greek indices μ, ν running from 1 to $3N$. Let the total Hamiltonian be written as a sum of separable and nonseparable parts

$$H = H_0 + H_1, \tag{3a}$$

[1] S. Tamor, J. Chem. Phys. **33**, 1418 (1960), to be referred to as I.

[2] N. N. Bogoliubov, J. Phys. (U.S.S.R) **10**, 265 (1946).

[3] I. Prigogine and F. Henin, Physica **24**, 214 (1958); Bull. Classe Sci. Acad. roy. Belg (December, 1957).

[4] J. G. Kirkwood, J. Chem. Phys. **14**, 180 (1946); **15**, 72 (1947).

[5] This point of view is stated explicitly in *The Molecular Theory of Gases and Liquids* by J. O. Hirschfelder, C. F. Curtiss, and R. B. Bird (John Wiley & Sons, Inc., New York, 1954), pp. 449 et. seq.

where H_0 contains the kinetic energy and wall forces and H_1 the energy of interaction. It will be assumed that the wall potential is sufficiently steep that no collision occurs involving particles simultaneously interacting with the walls; consequently, its contribution to the propagator will be neglected in what follows. Explicitly, we write

$$H_0=\sum_\mu p_\mu^2/2m_i,$$
$$H_1=\sum_{i<j}\phi_{ij}. \tag{3b}$$

The corresponding Liouville operator may be written

$$L=L_0+L_1, \tag{4a}$$
$$L_0=\sum_\mu(\partial H_0/\partial p_\mu)(\partial/\partial x_\mu)=\sum_\mu v_\mu(\partial/\partial x_\mu), \tag{4b}$$
$$L_1=\sum_{i<j}L_{ij}=\sum_{i<j}\sum_\mu\left(\frac{\partial\phi_{ij}}{\partial p_\mu}\frac{\partial}{\partial x_\mu}-\frac{\partial\phi_{ij}}{\partial x_\mu}\frac{\partial}{\partial p_\mu}\right). \tag{4c}$$

We emphasize that the ϕ_{ij} and L_{ij} are known functions of $\{x, p\}$ and are independent of time. The operator L_0 is the free particle drift operator so that $(\partial/\partial t)+L_0$ is the Stokes operator in the phase space.

It is convenient to remove the free streaming motion by a contact transformation so that the distribution function is time independent in the absence of interactions. We transform to the interaction representation by

$$\bar\rho(t)=\exp(L_0t)\rho(t), \tag{5a}$$

so that the transformed Liouville equation is

$$\partial\bar\rho(t)/\partial t=-\mathfrak{L}(t)\bar\rho(t),$$
$$\mathfrak{L}(t)=\exp(L_0t)L_1\exp(-L_0t), \tag{5b}$$

and correspondingly

$$(\partial/\partial t)\mathfrak{U}(t,t_0)=-\mathfrak{L}(t)\mathfrak{U}(t,t_0), \tag{5c}$$
$$\bar\rho(t)=\mathfrak{U}(t,t_0)\bar\rho(t_0);$$
$$\mathfrak{U}(t,t_0)=\exp(L_0t)U(t-t_0)\exp(-L_0t_0). \tag{5d}$$

The Liouville operator in the interaction representation depends explicitly upon t, while the propagator depends upon both t and t_0 and not only upon the interval $t-t_0$. The essential property of the operator $\exp(L_0t)$ is that it is a finite translation operator (and hence a contact transformation) such that operating upon an arbitrary function $f\{x, p; t\}$ we have

$$\exp(L_0t)f\{x, p; t\}=f\{x+vt, p; t\}. \tag{6}$$

Since the operator $\mathfrak{L}$ depends upon the coordinates, we have

$$\mathfrak{L}_{ij}(t)=L_{ij}\{x+vt, p\}$$
$$=\sum_\mu\left(\frac{\partial\phi_{ij}\{x+vt, p\}}{\partial p_\mu}\frac{\partial}{\partial x_\mu}-\frac{\partial\phi_{ij}\{x+vt, p\}}{\partial x_\mu}\frac{\partial}{\partial p_\mu}\right). \tag{7}$$

Equation (7) may be verified by explicit calculation, but follows at once from the invariance of the Poisson bracket under contact transformations.

Two more definitions will be found useful in the subsequent discussion. Consider an operator function of the coordinate of particles $i, j, k, \cdots$. Two such operators (clusters) will be called *disjoint* if they have no particle indices in common and hence operate in orthogonal subspaces of the complete phase space. A cluster is said to be *elementary* if it cannot be nontrivially factored into disjoint clusters.

III. THE τ EXPANSION

We now seek to develop an approximation scheme for the solution of Eq. (5c) by decomposing $\mathfrak{U}$ into a series of operators which are expressible in terms of the coordinates of single particles, pairs, triples, etc. Write

$$\mathfrak{U}^{(N)}(t,t_0)=1+\sum_{n=1}^{N}R^{(n)}(t,t_0), \tag{8}$$

where

$$R^{(n)}(t,t_0)=\sum_{i_1<i_2<\cdots<i_n}\mathfrak{U}_{i_1\cdots i_n}(t,t_0);\quad R^{(n)}(t,t)=0. \tag{9}$$

The operator $\mathfrak{U}_{i_1\cdots i_n}$ is defined in the phase space of particles $i_1\cdots i_n$. $R^{(n)}$ is obtained by permitting the indices $i_1\cdots i_n$ to run from 1 to N. These equations do not uniquely define a decomposition scheme, but the definition may be completed by requiring each $\mathfrak{U}_{i_1\cdots i_n}$ to satisfy an equation homogeneous in the particle indices. We then obtain

$$-(\partial/\partial t)\mathfrak{U}_{i_1\cdots i_n}(t,t_0)=\sum_{p<q}\mathfrak{L}_{p,q}(t)\mathfrak{U}_{i_1\cdots i_n}(t,t_0)$$
$$+\sum_{p<i_r}\mathfrak{L}_{p,i_r}(t)\mathfrak{U}_{i_1\cdots i_{r-1}\,i_{r+1}\cdots i_n}(t,t_0)$$
$$+\sum_{i_r<i_s}\mathfrak{L}_{i_r,i_s}(t)\mathfrak{U}_{i_1\cdots i_{r-1},i_{r+1}\cdots i_{s-1},i_{s+1}\cdots i_n}(t,t_0); \tag{10}$$

where the indices p, q, i_r, i_s run over the $i_1\cdots i_n$. The character of Eq. (10) is that only the coordinate of a particular subset of particles appears and that each equation in the sequence expresses an n particle propagator in terms of $n-1$ and $n-2$ particle propagators. It is easily verified by direct substitution that Eqs. (8), (9), and (10) combine to reproduce the Liouville equation, Eq. (5c).

The first few equations of the sequence, Eq. (10), are

$$(\partial/\partial t)\mathfrak{U}_i(t,t_0)=0 \tag{10a}$$
$$-(\partial/\partial t)\mathfrak{U}_{ij}(t,t_0)=\mathfrak{L}_{ij}(t)[1+\mathfrak{U}_{ij}(t,t_0)] \tag{10b}$$
$$-(\partial/\partial t)\mathfrak{U}_{ijk}(t,t_0)=[\mathfrak{L}_{ij}(t)+\mathfrak{L}_{ik}(t)+\mathfrak{L}_{jk}(t)]\mathfrak{U}_{ijk}(t,t_0)$$
$$+[\mathfrak{L}_{ij}(t)+\mathfrak{L}_{ik}(t)]\mathfrak{U}_{jk}(t,t_0)+[\mathfrak{L}_{ij}(t)+\mathfrak{L}_{jk}(t)]\mathfrak{U}_{ik}(t,t_0)$$
$$+[\mathfrak{L}_{ik}(t)+\mathfrak{L}_{jk}(t)]\mathfrak{U}_{ij}(t,t_0). \tag{10c}$$

The last equation in the sequence is given by $n=N$ and all particles in the system are represented. Terminating at some smaller n gives the exact propagator for the smaller system of particles $i_1 \cdots i_n$. In particular the operator $1+\mathfrak{U}_{ij}(t, t_0)$ is the exact propagator for the isolated two-body problem for particles i and j. [Equation (10a) is simply an expression of the fact that in the absence of external forces an isolated particle has nothing with which to interact.]

We now show how expansion (8) is in effect an expansion in powers of the time interval, $t-t_0$. To illustrate the essential point, first consider the Liouville equation

$$(\partial/\partial t)\mathfrak{U}(t, t_0) = -\sum_{i<j}\mathfrak{L}_{ij}(t)\mathfrak{U}(t, t_0), \tag{11}$$

and count the number of nonvanishing terms in the summation over i, j. $\mathfrak{L}_{ij}$ is nonzero only if particles i and j happen to be interacting at time t. Hence on the average, the number of terms contributing to the sum in Eq. (11) is of order $N\tau_c/\tau_f$, and the rate of change of $\bar{p}$ per *degree of freedom* is proportional to τ_c/τ_f. The factor N expresses the trivial fact that $\bar{p}$ changes in time via the deflections suffered by N particles.

Similarly, if we integrate Eq. (10b) from t_0 to $t_0+\tau$, the number of nonvanishing terms per degree of freedom is proportional to τ/τ_f. The generalization to more complex operators is straightforward. Let an arbitrary operator be factored into a product of elementary disjoint clusters. The τ dependence of the operator is the product of the τ dependences of its elementary factors. But an elementary cluster referring to n particles is of order $(\tau/\tau_f)^{n-1}$.

Applying this scheme to the right-hand side of Eq. (10), we find by induction that in this sense each $R^{(n)}$ is of order $(\tau/\tau_f)^{n-1}$. The rate of convergence of this expansion therefore depends upon the choice of τ and is rapid if $t-t_0=\tau \ll \tau_f$.

For small τ, therefore, we replace Eq. 8 by its binary approximation obtained by terminating the expansion at $n=2$ and obtain

$$\mathfrak{L}(t)\mathfrak{U}(t, t_0) = \sum_{i<j}\mathfrak{L}_{ij}(t)[1+\mathfrak{U}_{ij}(t, t_0)]. \tag{12}$$

In this approximation we have the "binary Liouville equation"[6] in the interaction representation

$$\partial\bar{p}(t)/\partial t = -\sum_{i<j}\Lambda_{ij}(t; \tau)\bar{p}(t-\tau), \tag{13}$$

where we have defined

$$\Lambda_{ij}(t; \tau) = \mathfrak{L}_{ij}(t)[1+\mathfrak{U}_{ij}(t, t_0)]_{t_0=t-\tau} = -\frac{\partial\mathfrak{U}_{ij}(t, t_0)}{\partial t}\bigg|_{t_0=t-\tau}. \tag{14}$$

[6] R. Brout, Physica **22**, 509 (1956). The equation to which Brout gives this title is based upon the same physical approximations, but is formally somewhat different since ternary collisions are completely excluded.

Discussion of this equation will be postponed to a later portion of this section.

Equation (14) reduces to a simple integral equation if we choose $\tau \geq \tau_c$. For every i, j, $\Lambda_{ij} \neq 0$ only if at time t, $\mathfrak{L}_{ij}(t) \neq 0$. But since $t_0 \leq t-\tau_c$, the interaction could not yet have begun at t_0 so that $\mathfrak{U}_{ij}(t, t_0)$ is unchanged if t_0 is decreased. To take advantage of this property rewrite Eq. (14),

$$\Lambda_{ij}(t; \tau) = \mathfrak{L}_{ij}(t)\left[1+\int_{t_0}^{t}\frac{\partial\mathfrak{U}_{ij}(t', t_0)}{\partial t'}dt'\right]_{t_0=t-\tau}, \tag{14a}$$

and since $\tau > \tau_c$, we may without error let $t_0 \to -\infty$ giving

$$\Lambda_{ij}(t) = \mathfrak{L}_{ij}\left[1-\int_{-\infty}^{t}\Lambda_{ij}(t')dt'\right]. \tag{15}$$

So long as $\tau > \tau_c$, $\Lambda_{ij}(t; \tau)$ is independent of the particular choice of τ so that this variable has been suppressed. It is important to remember, however, that τ still appears in the transformation to the interaction representation. In order not to lose sight of this we write explicitly

$$\Lambda_{ij}(t) = \exp(L_0 t)\Lambda_{ij}\{x, p\}\exp[-L_0(t-\tau)] \tag{16}$$

and

$$\Lambda_{ij}\{x, p\} = L_{ij}\{x, p\}\left[1-\int_{-\infty}^{0}\Lambda_{ij}\{x+vt, p\}dt\right]. \tag{17}$$

We now have the binary Liouville equation in the desired form

$$\partial\bar{p}/\partial t = -\sum_{i<j}\exp(L_0 t)\Lambda_{ij}\exp[-L_0(t-\tau)]\bar{p}(t-\tau) \tag{18}$$

or

$$Dp/Dt = [(\partial/\partial t)+L_0]p(t) = -\sum_{i<j}\Lambda_{ij}\{x, p\}p(t-\tau). \tag{19}$$

Equation (19) is now in the same form as Eq. (I, 12) where $\mathfrak{U}(\tau)$ has been evaluated to lowest order in τ/τ_f. Inserting this approximate form of U into Eq. (I, 13), we obtain finally

$$Dp^*(t)/Dt = -\sum_{i<j}\Lambda_{ij}\{x, p\}p^*(t), \tag{20}$$

where Λ_{ij} is the solution of Eq. (17) and $p^*(t)$ is the time-smoothed distribution function as defined in I. In what follows we delete the asterisk when referring to the smoothed distribution.

Before proceeding with further reduction of Eq. (20) it is profitable to insert a few remarks concerning its derivation. It is important to note that the two approximations needed to obtain Eq. (20), namely the binary approximation and the time smoothing, are independent and can be made in either order. Indeed, it is not difficult to show that the solutions of the binary Liouville equation, Eq. (19), have the same periodicity and time reversibility properties as the full Liouville equation. This is also true to any order in the

expansion scheme, Eq. (10). The binary approximation is therefore purely a trick for solving a dynamical problem and has nothing to do with irreversibility. The transition to irreversible motion lies in the time smoothing which was discussed in I.

It should also be emphasized that while Eqs. (18) and (20) describe a motion which proceeds primarily through binary encounters more complicated collisions are not ignored, but are treated in an approximate way. For example, it is clearly possible for Λ_{ij} and Λ_{ik} to be simultaneously nonzero so that even in the description provided by Eqs. (19) and (20) ternary collisions do occur. Physically, however, the approximation made is that the force between i and j at time t is to be computed from the configuration at time $t-\tau$ by integrating forward in time as if particle k were absent, and similarly for i, k, etc. Those events which do happen to be binary encounters are, of course, described exactly. It is clear, therefore, that Eq. (19) and its irreversible counterpart Eq. (20) contain a quite detailed description of the motion of the system including excluded volume and more complicated correlation effects.

With some changes in notation Eq. (20) can be put into a form which permits comparison with the Bogoliubov equation.[2] With the aid of Eqs. (14) and (17) and the definition of L, Eq. (20) may be written

$$D\rho(t)/Dt=-\lim_{T\to\infty}\sum_{i<j}[\phi_{ij},\exp(L_0t)(1+\mathfrak{U}_{ij}(t,t-T))\times\exp(-L_0(t-T))\rho(t)]. \quad (21)$$

Since $1+\mathfrak{U}_{ij}(t,t-T)$ is the exact two-body propagator in the interaction representation, when operating upon $\bar{\rho}(t-T)$ it gives $\bar{\rho}(t)$ in the binary approximation. Since $\rho(t)$ is constant along a trajectory the quantity $\exp(L_0t)[1+\mathfrak{U}_{ij}(t,t-T)]\exp[L_0(t-T)]\rho\{x,p;t\}$ is equal to $\rho\{x',p';t\}$ where x', p' is to be found by starting from x, p and following the exact two-body trajectory backward for time T, and then extrapolating forward to time t along free particle orbits. In terms of the generators of the one- and two-body orbits, denoted by Bogoliubov as $S_T^{(1)}$ and $S_T^{(2)}$ Eq. (21) becomes

$$(D/Dt)\rho\{x,p;t\}=-\lim_{T\to\infty}\sum_{i<j}[\phi_{ij},\rho\{S_T^{(1)}S_{-T}^{(2)}\{x,p\};t\}]. \quad (22)$$

This equation is the same as Bogoliubov's result but for the nontrivial difference that here ρ refers to the complete phase space (time-smoothed) distribution function.

IV. REDUCTION TO THE MASTER EQUATION

One expects that in the limit of infinite dilution the effects of the finite range of interaction disappear and Λ_{ij} reduces to a point operator related to the collision cross section. To study this property it is convenient to relate Λ to a transition probability per unit time giving the rate of change of $\rho\{x,p\}$ in terms of $\rho\{x',p'\}$. This can be done by a simple change of representation but the calculation is rather long and is carried out in the appendix. One finds, as expected, that in the limit of zero-range forces Λ_{ij} vanishes except when $x_i=x_j$ and is essentially the collision cross section. In this limit one finds

$$\begin{aligned}(D/Dt)\rho\{\mathbf{x},\mathbf{p};t\}&=\sum_{i<j}\int d\{\mathbf{x}'\}d\{\mathbf{p}'\}\prod_{k\neq i,j}\delta(\mathbf{x}_k-\mathbf{x}_k')\delta(\mathbf{p}_k-\mathbf{p}_k')\\&\cdot\delta(\mathbf{R}_{ij}-\mathbf{R}_{ij}')[\delta(\mathbf{x}_{ij})\mid v_{ij}'\mid\sigma(\mathbf{p}_i,\mathbf{p}_j;\mathbf{p}_i',\mathbf{p}_j')\\&\cdot\delta(\mathbf{x}_{ij}')\rho\{\mathbf{x}',\mathbf{p}';t\}-\delta(\mathbf{x}_{ij}')\mid v_{ij}\mid\sigma(\mathbf{p}_i',\mathbf{p}_j';\mathbf{p}_i,\mathbf{p}_j)\\&\cdot\delta(\mathbf{x}_{ij})\rho\{\mathbf{x},\mathbf{p};t\}]. \quad (23)\end{aligned}$$

Here we have introduced vector notation for simplicity. $\mathbf{R}_{ij}$ is the coordinate of the center of mass of the colliding pair, $\mathbf{x}_{ij}$ their relative coordinate, $\mid v_{ij}\mid$ their relative speed, and $\sigma(\mathbf{p}_i,\mathbf{p}_j;\mathbf{p}_i',\mathbf{p}_j')$ the cross section for scattering from initial momenta $\mathbf{p}_i'$, $\mathbf{p}_j'$ to $\mathbf{p}_i$, $\mathbf{p}_j$. While σ is generally a function only of the relative momenta we do not take advantage of this property here. Equation (22) is the obvious extension of the Kac master equation[7] to nonuniform systems. In effect we have merely justified adding the streaming term to the left-hand side while on the right the $\delta(\mathbf{x}_{ij})$ guarantees that only particles which happen to be close to one another contribute to the collision integral. If it is further assumed that the distribution function is factorable to the singlet the Boltzmann equation is recovered.

In the derivation of Eq. (23) it is shown that $\mid v_{ij}\mid$ times the scattering cross section is given by the matrix element of $\langle\Lambda_{ij}\rangle$ between the appropriate initial and final momentum states, where $\langle\Lambda_{ij}\rangle$ is obtained by integrating Λ_{ij} over coordinates. Equation (15) may be solved by iteration and averaged over $\{x\}$ term by term to obtain an expansion of the cross section in powers of a coupling parameter. The even-order terms of this expansion are precisely those of Prigogine and Henin.[3] That they do not obtain the odd-order terms is accounted for by the fact that their matrix elements contain factors of the form

$$\int_{-\infty}^{0}\exp(i\omega t)dt=\pi\delta(\omega)+iP(1/\omega)$$

and they neglect the principal value. While this contribution does indeed vanish in second order, in general, it gives a finite contribution. On the other hand the delta function part vanishes in odd orders. Except for this point the two expansions are indeed the same.

ACKNOWLEDGMENT

This work is in large part an outgrowth of a very stimulating series of lectures given by Professor I. Prigogine at the General Electric Research Laboratory during the summer of 1957.

[7] *Proceedings of the Third Berkeley Symposium on Mathematical Statistics and Probability* (University of California Press, Berkeley, California, 1956), p. 171.

APPENDIX

The purpose of this section is to recast Eq. (20) into the form of a Chapman-Kolmogoroff equation and then examine the transition probability in the limit of zero-range forces, thereby extracting the Boltzmann collision operator. Unfortunately, the notation tends to become rather unwieldy, so that to keep already long formulas from becoming still more complicated some notational short cuts will be used. These should cause no confusion, however.

Equation (20) may be written

$$(D/Dt)\rho\{\mathbf{x},\mathbf{p};t\}=-\sum_{i<j}\int d\{\mathbf{x}'\}d\{\mathbf{p}'\}d\{\mathbf{x}''\}d\{\mathbf{p}''\}$$
$$\times\delta\{\mathbf{x}-\mathbf{x}''\}\delta\{\mathbf{p}-\mathbf{p}''\}\Lambda_{ij}\{\mathbf{x}'',\mathbf{p}''\}\delta\{\mathbf{p}''-\mathbf{p}'\}\delta\{\mathbf{x}''-\mathbf{x}'\}\rho\{\mathbf{x}',\mathbf{p}';t\}. \quad \text{(A1)}$$

After the integration over $\{\mathbf{x}'',\mathbf{p}''\}$ has been carried out, the resulting coefficient of $\rho\{\mathbf{x}',\mathbf{p}';t\}$ may be interpreted as the transition probability per unit time for carrying the phase point of the system from $\{\mathbf{x}',\mathbf{p}'\}$ to $\{\mathbf{x},\mathbf{p}\}$. Since a collision causes the momenta of the participating particles to undergo a finite momentum change, Λ is a finite displacement operator in the momentum space. During a collision the spatial cordinates are also displaced from their unperturbed values so that Λ couples together points $\{\mathbf{x}\}$ and $\{\mathbf{x}'\}$ which are a finite distance apart. This nonlocal character disappears, however, as the range of the forces decreases.

By defining a transition probability W, Eq. (A1) may be put into standard form

$$(D/Dt)\rho\{\mathbf{x},\mathbf{p};t\}=\int d\{\mathbf{x}'\}d\{\mathbf{p}'\}[W\{\mathbf{x},\mathbf{p};\mathbf{x}',\mathbf{p}'\}\rho\{\mathbf{x}',\mathbf{p}';t\}-W\{\mathbf{x}',\mathbf{p}';\mathbf{x},\mathbf{p}\}\rho\{\mathbf{x},\mathbf{p};t\}], \quad \text{(A2)}$$

where

$$W\{\mathbf{x},\mathbf{p};\mathbf{x}',\mathbf{p}'\}=-\sum_{i<j}\int\delta\{\mathbf{x}-\mathbf{x}''\}\delta\{\mathbf{p}-\mathbf{p}''\}\Lambda_{ij}\{\mathbf{x}'',\mathbf{p}''\}\delta\{\mathbf{p}''-\mathbf{p}'\}\delta\{\mathbf{x}''-\mathbf{x}'\}d\{\mathbf{x}''\}d\{\mathbf{p}''\}. \quad \text{(A3)}$$

The second term in the integral (A2) is identically zero since Λ_{ij}, is a divergence operator in the phase space (probability is conserved). This term is added to cancel explicitly the diagonal term $\{\mathbf{x},\mathbf{p}\}=\{\mathbf{x}',\mathbf{p}'\}$. We now fix our attention upon a particular pair of particles and carry out the integrations over the space of these two, the rest being trivial. If the potentials are invariant under Galilean transformations the operator Λ_{ij} depends only upon the relative coordinates and momenta of particles i and j. Therefore let $\mathbf{R}_{ij}$ be the center of mass coordinates of the particle pair and $\mathbf{x}_{ij}$ their relative coordinate. The integral over $\mathbf{R}_{ij}''$ gives simply a factor $\delta(\mathbf{R}_{ij}-\mathbf{R}_{ij}')$.

To take advantage of the short range of the forces we introduce a representation of the delta function in terms of the biorthogonal set

$$u_n(x)=[(-1)^n/n!]\delta^{(n)}(x), \qquad u_n{}^+(x)=x^n, \quad \text{(A4)}$$

and can easily verify, by partial integration,

$$\int u_m{}^+(x)u_n(x)dx=\delta_{mn}; \qquad \sum_n u_n{}^+(x)u_n(x')=\delta(x-x'). \quad \text{(A5)}$$

The superscript (n) indicates n fold differentiation with respect to the argument. Equations (A4) and (A5) have been written in one dimension to simplify the notation, but the correct extension to three dimensions is evident. The property, Eq. (A5), is a formal way of writing Taylor's theorem since for any expandable $f(x)$

$$f(x)=\sum_n[(x-x_0)^n/n!]f^{(n)}(x_0)=\sum_n[(-1)^n(x-x_0)^n/n!]\int\delta^{(n)}(x'-x_0)f(x')dx'.$$

Expanding the spatial delta functions in this representation, we have

$$W\{\mathbf{x},\mathbf{p};\mathbf{x}',\mathbf{p}'\}=\sum_{i<j}\prod_{k\neq i,j}\delta(\mathbf{p}_k-\mathbf{p}_k')\delta(\mathbf{x}_k-\mathbf{x}_k')\delta(\mathbf{R}_{ij}-\mathbf{R}_{ij}')\sum_{m,n}\delta^{(m)}(\mathbf{x}_{ij})W_{mn}[\mathbf{p}_i,\mathbf{p}_j;\mathbf{p}_i'\mathbf{p}_j']\delta^{(n)}(\mathbf{x}_{ij}'), \quad \text{(A6)}$$

where

$$W_{mn}=-[(-1)^{m+n}/m!n!]\int d\mathbf{x}_{ij}''d\mathbf{p}_i''d\mathbf{p}_j''\delta(\mathbf{p}_i-\mathbf{p}_i'')\delta(\mathbf{p}_j-\mathbf{p}_j'')$$
$$\times(\mathbf{x}_{ij}'')^m\Lambda_{ij}(\mathbf{x}_{ij}'';\mathbf{p}_i'',\mathbf{p}_j'')(\mathbf{x}_{ij}'')^n\delta(\mathbf{p}_i''-\mathbf{p}_i')\delta(\mathbf{p}_j''-\mathbf{p}_j'). \quad \text{(A7)}$$

The complete transport equation may now be written in terms of the W_{mn}

$$(D/Dt)\rho\{\mathbf{x},\mathbf{p};t\}=\sum_{i<j}\int d\{\mathbf{x}'\}d\{\mathbf{p}'\}\prod_{k\neq i,j}\delta(\mathbf{x}_k-\mathbf{x}_k')\delta(\mathbf{p}_k-\mathbf{p}_k')\delta(\mathbf{R}_{ij}-\mathbf{R}_{ij}')$$
$$\times\sum_{m,n}\{\delta^{(m)}(\mathbf{x}_{ij})W_{mn}[\mathbf{p}_i,\mathbf{p}_j;\mathbf{p}_i',\mathbf{p}_j']\delta^{(n)}(\mathbf{x}_{ij}')\rho\{\mathbf{x}',\mathbf{p}';t\}$$
$$-\delta^{(m)}(\mathbf{x}_{ij}')W_{mn}[\mathbf{p}_i',\mathbf{p}_j';\mathbf{p}_i,\mathbf{p}_j]\delta^{(n)}(\mathbf{x}_{ij})\rho\{\mathbf{x},\mathbf{p};t\}\}. \quad \text{(A8)}$$

The physical meaning of Eq. (A8) is actually quite simple. In momentum space W_{mn} is the transition probability per unit time for scattering from momenta $\mathbf{p}'$ to $\mathbf{p}$. In coordinate space it relates the rate of change of the mth coefficient of the Taylor expansion of ρ in power of $\mathbf{x}_{ij}$ to the nth coefficient. As the range of forces decreases we see from Eq. (A7) that the W_{mn} are rapidly decreasing functions of m and n. Keeping only the leading term, we obtain the master equation

$$(D/Dt)\rho\{\mathbf{x},\mathbf{p};t\}=\sum_{i<j}\int d\{\mathbf{x}'\}d\{\mathbf{p}'\}\prod_{k\neq i,j}\delta(\mathbf{x}_k-\mathbf{x}_k')\delta(\mathbf{p}_k-\mathbf{p}_k')$$
$$\times\delta(\mathbf{R}_{ij}-\mathbf{R}_{ij}')\{\delta(\mathbf{x}_{ij})W_{00}[\mathbf{p}_i,\mathbf{p}_j;\mathbf{p}_i',\mathbf{p}_j']\delta(\mathbf{x}_{ij}')\rho\{\mathbf{x}',\mathbf{p}';t\}$$
$$-\delta(\mathbf{x}_{ij}')W_{00}[\mathbf{p}_i',\mathbf{p}_j';\mathbf{p}_i,\mathbf{p}_j]\delta(\mathbf{x}_{ij})\rho\{\mathbf{x},\mathbf{p};t\}\}; \quad \text{(A9)}$$

while Eq. (A7) reduces to

$$W_{00}[\mathbf{p}_i,\mathbf{p}_j;\mathbf{p}_i',\mathbf{p}_j']=-\int d\mathbf{p}_i''d\mathbf{p}_j''\delta(\mathbf{p}_i-\mathbf{p}_i'')\delta(\mathbf{p}_j-\mathbf{p}_j'')\langle\Lambda_{ij}(\mathbf{p}_i'',\mathbf{p}_j'')\rangle\delta(\mathbf{p}_i''-\mathbf{p}_i')\delta(\mathbf{p}_j''-\mathbf{p}_j'), \quad \text{(A10)}$$

where

$$\langle\Lambda_{ij}(\mathbf{p}_i,\mathbf{p}_j)\rangle=\int d\mathbf{x}_{ij}\Lambda_{ij}(\mathbf{x}_{ij},\mathbf{p}_i,\mathbf{p}_j). \quad \text{(A11)}$$

Finally, there remains the task of establishing the connection between W_{00} and the scattering cross section. That such a connection must exist is clear from the fact that the binary Liouville equation is exact for the two-body system. To make the connection more apparent we do the $\mathbf{x}_{ij}$ integration in cylindrical coordinates with axis along $\mathbf{v}'_{ij}$ and denote the perpendicular component by $\mathbf{r}$. Changing variables from dz to $|v_{ij}|dt$, we have

$$W_{00}=-|v_{ij}|\int d\mathbf{r}dtd\mathbf{p}_i''d\mathbf{p}_j''\delta(\mathbf{p}_i-\mathbf{p}_i'')\delta(\mathbf{p}_j-\mathbf{p}_j'')\Lambda_{ij}(\mathbf{r},z+v_{ij}t,\mathbf{p}_i'',\mathbf{p}_j'')\delta(\mathbf{p}_i''-\mathbf{p}_i')\delta(\mathbf{p}_j''-\mathbf{p}_j'). \quad \text{(A12)}$$

A mathematical formulation of the two-body problem may be given in two equivalent forms; either in terms of the Λ operator or in terms of the particle trajectories. Suppose that at $t=t_0$ the trajectories pass through the point $\{\mathbf{x}_0,\mathbf{p}_0\}$. The whole trajectory is given by $\mathbf{x}(t)=\mathbf{x}_t\{\mathbf{x}_0,\mathbf{p}_0\}$; $\mathbf{p}(t)=\mathbf{p}_t\{\mathbf{x}_0,\mathbf{p}_0\}$. Since ρ is constant along a trajectory

$$\rho\{\mathbf{x},\mathbf{p};t\}=\int\delta\{\mathbf{x}-\mathbf{x}_t\{\mathbf{x}_0,\mathbf{p}_0\}\}\delta\{\mathbf{p}-\mathbf{p}_t\{\mathbf{x}_0,\mathbf{p}_0\}\}\rho\{\mathbf{x}_0,\mathbf{p}_0;t_0\}d\{\mathbf{x}_0\}d\{\mathbf{p}_0\}$$
$$=-\int_{t_0}^{t}\Lambda\{\mathbf{x}+\mathbf{v}t',\mathbf{p}\}\rho\{\mathbf{x},\mathbf{p};t_0\}dt'. \quad \text{(A13)}$$

A scattering cross section describes the result of the following experiment. At time t_0 we prepare a beam of particles of momentum $\mathbf{p}_0$ uniformly distributed in a plane $z=$const. At some much later time we measure the total number of particles in the system with momentum $\mathbf{p}$. The differential cross section for scattering from $\mathbf{p}_0$ to $\mathbf{p}$ is the area of the plane $z=$const through which passed those particles whose final momenta lay between $\mathbf{p}$ and $\mathbf{p}+d\mathbf{p}$. To compute this from Eq. (A13) we use the initial distribution function $\delta(z-z_0)\delta(\mathbf{p}-\mathbf{p}_0)$ and integrate both sides over $\mathbf{r}$. This gives

$$-\int_{t_0}^{t}dt'\int d\mathbf{r}\Lambda_{ij}(\mathbf{r},z_0+vt';\mathbf{p}_i,\mathbf{p}_j)\delta(\mathbf{p}_i-\mathbf{p}_{i0})\delta(\mathbf{p}_j-\mathbf{p}_{j0})=\int d\mathbf{r}\delta\{\mathbf{p}-\mathbf{p}_t\{\mathbf{r},z_0,\mathbf{p}_0\}\}. \quad \text{(A14)}$$

For t large and positive and t_0 large and negative both sides become independent of z_0 and comparing with Eq. (A12) we obtain

$$W_{00}\{\mathbf{p},\mathbf{p}'\}=|v_{ij}|\int d\mathbf{r}\delta\{\mathbf{p}-\mathbf{p}_t\{\mathbf{r},\mathbf{p}'\}\} \quad \text{(A15)}$$

which is precisely $|v_{ij}|$ times the differential cross section for scattering from $\mathbf{p}'$ to $\mathbf{p}$.

THE JOURNAL OF CHEMICAL PHYSICS VOLUME 33, NUMBER 5 NOVEMBER, 1960

Statistical Mechanical Theory of the Viscosity Coefficients of Binary Liquid Solutions

RICHARD J. BEARMAN AND PETER F. JONES*

Department of Chemistry, University of Kansas, Lawrence, Kansas

(Received May 13, 1960)

The method of the pair space linear relations is used to develop a formula for the coefficient of viscosity of a binary liquid solution from statistical mechanics. When the solution is regular a statistical-mechanical analog of the Stokes-Einstein equation is obtained in which the product of the self-diffusion coefficient and the viscosity is expressed as a composition independent average over the radial distribution function for unlike pairs. The relationship between the present theory and the results of experimental measurements of viscosity and diffusion coefficients is discussed at some length, and the Gordon equation for the mutual diffusion coefficient is derived.

I. INTRODUCTION

THE viscosity of liquid solutions has been the subject of considerable study since the end of the first half of the nineteenth century.[1] Over the years, a multitude of relations have been put forth to predict the viscosity of mixtures. Most of these are frankly empirical while the remainder are based upon the free volume model, or similar models, of the structure of the liquid state and of the nature of the flow process.

In the present article we treat the subject from the statistical mechanical viewpoint in a continuation of our current series on a unified theory of the transport properties of simple liquid solutions.[2-7] Starting with the Liouville equation, we derive the exact equations of hydrodynamics, including the partial equations of motion of the components, and obtain expressions for the transport parameters as averages over nonequilibrium distribution functions. The usual phenomenological relations for the heat and matter fluxes and the stress tensor arise when perturbations to the equilibrium distribution are taken to be linear functions of the relative velocities and gradients of temperature and velocity. Under these conditions the average frictional force on a molecule is likewise linearly related through friction coefficients to the mean velocities of the components. To permit the explicit evaluation of transport coefficients in terms of equilibrium microscopic parameters, we suppose that the same linear relation holds for the force in pair configuration space, provided that the appropriate velocity of the molecule is introduced. This takes into account the difference between the gross velocity of a species and the average velocity of a molecule in a pair, but ignores the possible dependence of the pair friction coefficients on intermolecular separation. From our hypothesis we find, with the use of rigorously derived pair space equations of continuity, differential equations for the distribution-function perturbations in terms of the radial distribution functions. The solutions of these when introduced into the aforementioned nonequilibrium averages lead to expressions for the heat of transport, thermal diffusion factor, thermal conductivity coefficient, and diffusion coefficient ratios, which we have discussed previously[2,4,5,7] and the coefficients of shear and bulk viscosity now to be considered.

We find that for a binary mixture each of the viscosity coefficients may be expressed as the sum of three integrals representing, respectively, the interactions of like and unlike pairs of molecules. Our result reduces in the limit of infinite dilution to that found by Kirkwood, Buff, and Green[8] and Zwanzig, Kirkwood, Stripp, and Oppenheim[9] for pure substances. These authors carried out extensive numerical calculations for the case of liquid argon. We shall not here attempt to extend that work to include solutions, partly because of the lack of adequate data concerning pair potentials and distribution functions in mixtures and partly because the qualitative conclusions would not be expected to be appreciably different. Rather, we focus our attention on the concentration dependence of the viscosity coefficients. With this object, we introduce the assumption of the theory of regular solutions of Hildebrand[10] that radial distribution functions are independent of composition. This enables us to discover a statistical mechanical analog of the Stokes-Einstein equation in which the product of the coefficients of self-diffusion and shear viscosity is expressed precisely as a composition independent average over the radial distribution function for pairs of unlike mole-

* Carnegie Foundation Undergraduate Scholar, Present Address: Department of Chemistry, University of Chicago, Chicago, Illinois.

[1] For a partial bibliography of work through 1950, the reader is referred to J. R. Partington, *An Advanced Treatise on Physical Chemistry* (Longmans, Green, and Company, London, 1951), Vol. 2, p. 120. Reviews by E. U. Franck and W. Jost, [Z. Electrochemie **62**, 1054 (1958)] and P. A. Johnson and A. L. Babb [Chem. Rev. **56**, 387 (1956)] are useful for further references.

[2] R. J. Bearman, J. G. Kirkwood, and M. Fixman, Advances in Chem. Phys. **1**, 1 (1958).

[3] R. J. Bearman and J. G. Kirkwood, J. Chem. Phys. **28**, 136 (1958).

[4] R. J. Bearman, J. Chem. Phys. **29**, 1278 (1958).

[5] R. J. Bearman, J. Chem. Phys. **30**, 835 (1959).

[6] R. J. Bearman, J. Chem. Phys. **31**, 751 (1959).

[7] R. J. Bearman, J. Chem. Phys. **32**, 1308 (1960).

[8] J. G. Kirkwood, F. P. Buff, and M. S. Green, J. Chem. Phys. **17**, 988 (1949).

[9] R. W. Zwanzig, J. G. Kirkwood, K. F. Stripp, and I. Oppenheim, J. Chem. Phys. **21**, 2050 (1953).

[10] J. H. Hildebrand and R. L. Scott, *The Solubility of Nonelectrolytes* (Reinhold Publishing Corporation, New York, 1950), 3rd ed., Chap. VII.

cules. We conclude with a discussion of the relationship of our theoretical results to the empirical observations of several authors. In particular, we derive the well-known Gordon equation for the mutual diffusion coefficient.

II. PHENOMENOLOGICAL THEORY

The law of conservation of mass at an element of a nonreacting fluid system of ν components is expressed through the equations of continuity,

$$(\partial c_\alpha/\partial t)+\nabla\cdot c_\alpha \mathbf{u}_\alpha=0, \qquad \alpha=1\cdots\nu, \tag{2.1}$$

where t is time, c_α is the concentration of species α, and $\mathbf{u}_\alpha$ is the velocity of α.

The movement of the fluid element is described by the equation of motion,

$$\begin{aligned}(\partial\rho\mathbf{u}/\partial t)&=\nabla\cdot(\mathfrak{d}-\rho\mathbf{u}\mathbf{u})+c\mathbf{X},\\ \rho\mathbf{u}&=\sum_\alpha \rho_\alpha\mathbf{u}_\alpha,\\ c\mathbf{X}&=\sum_\alpha c_\alpha\mathbf{X}_\alpha,\\ \rho_\alpha&=m_\alpha c_\alpha,\end{aligned} \tag{2.2}$$

where ρ_α is the density of α, m_α is the molecular weight, $c_\alpha\mathbf{X}_\alpha$ is the external force density, ρ is the overall density, $\mathbf{u}$ is the velocity of the local center of mass, and $\mathfrak{d}$ is the stress tensor. If in addition the fluid is Newtonian, then the stress tensor is given by the phenomenological relation,

$$\begin{aligned}\mathfrak{d}&=-[p+(\tfrac{2}{3}\eta-\phi)\nabla\cdot\mathbf{u}]\mathbf{1}+2\eta\dot{\epsilon},\\ \dot{\epsilon}&=\operatorname{sym}\nabla\mathbf{u}=\tfrac{1}{2}[(\nabla\mathbf{u})+(\nabla\mathbf{u})^{\text{transpose}}],\end{aligned} \tag{2.3}$$

where p is the local equilibrium pressure, $\mathbf{1}$ is the unit tensor, $\dot{\epsilon}$ is the rate of strain tensor, η is the coefficient of shear viscosity, and ϕ is the coefficient of bulk viscosity. Our objective in the following section will be to calculate η and ϕ from the statistical mechanical theory of transport processes.

III. STATISTICAL MECHANICAL THEORY

The statistical mechanical ensemble averages representing the coefficients of shear and bulk viscosity contain parameters, initially unspecified, which measure the departure of the pair correlation function from its equilibrium value. In this section our objective is to determine the perturbation parameters in terms of equilibrium functions and self-diffusion coefficients, and thereby enable explicit evaluation of the viscosity coefficients. To this end, we observe that the mean frictional forces acting on the molecules of the system are related, on the one hand, to the gradients of local thermodynamic properties and, on the other hand, to the relative mean velocities of the components. From these relationships, derived in detail, and from the equations of continuity, we find differential equations, the solutions of which are the desired perturbation parameters.

Mean Intermolecular Forces and the Partial Equations of Motion

We consider a two component system containing N_1 molecules of species 1 and N_2 molecule of species 2. The molecules are assumed to obey the laws of classical mechanics, so that we may denote the position of the center of mass of molecule i of species α by the vector $\mathbf{R}_{\alpha i}$ and its momentum by $\mathbf{P}_{\alpha i}$. When the contribution of internal degrees of freedom may be neglected, the time-smoothed probability distribution function

$$\bar{f}^{(N)}(\mathbf{R}_{11}\cdots\mathbf{R}_{1N_1},\ \mathbf{R}_{21}\cdots\mathbf{R}_{2N_2},\ \mathbf{P}_{11}\cdots\mathbf{P}_{1N_1},\ \mathbf{P}_{21}\cdots\mathbf{P}_{2N_2};\ t)$$

at a time t in a statistical ensemble obeys the Liouville equation

$$(\partial\bar{f}^{(N)}/\partial t)+\sum_{\beta=1}^{2}\sum_{i=1}^{N_\beta}(\mathbf{P}_{\beta i}/m_\beta)\cdot\nabla_{R_{\beta i}}\bar{f}^{(N)} -\sum_{\beta=1}^{2}\sum_{i=1}^{N_\beta}\nabla_{R_{\beta i}}U\cdot\nabla_{P_{\beta i}}\bar{f}^{(N)}=0, \tag{3.1}$$

where U is the potential energy of the entire system.

If the intermolecular contributions to the potential energy may be represented as the sum of pair potentials $V_{\alpha\beta}(r)$, dependent upon the nature of the two molecules of species α and β located at $\mathbf{r}_1$ and $\mathbf{r}_2$ and upon the magnitude r of their relative position $\mathbf{r}\equiv\mathbf{r}_2-\mathbf{r}_1$, but not upon their absolute positions or orientations, then the mean force $\bar{\mathbf{F}}_\alpha^{(1)}$ on a molecule is the sum of two terms[3,4],

$$\begin{aligned}c_\alpha\bar{\mathbf{F}}_\alpha^{(1)}&=c_\alpha\bar{\mathbf{F}}_\alpha^{(1)*}+\tfrac{1}{2}\nabla_{r_1}\\ &\cdot\sum_\beta c_\alpha(\mathbf{r}_1)c_\beta(\mathbf{r}_1)\int(\mathbf{r}\mathbf{r}/r)(dV_{\beta\alpha}/dr)g_{\beta\alpha}^{(2)}(\mathbf{r}_1,\mathbf{r})d^3\mathbf{r},\end{aligned} \tag{3.2}$$

$$\begin{aligned}c_\alpha\bar{\mathbf{F}}_\alpha^{(1)*}&=\tfrac{1}{2}\sum_\beta c_\alpha(\mathbf{r}_1)c_\beta(\mathbf{r}_1)\int(\mathbf{r}/r)(dV_{\beta\alpha}/dr)\\ &\times[g_{\alpha\beta}^{(2)}(\mathbf{r}_1,\mathbf{r})-g_{\beta\alpha}^{(2)}(\mathbf{r}_1,\mathbf{r})]d^3\mathbf{r},\end{aligned} \tag{3.2}$$

where $g_{\alpha\beta}^{(2)}$ is the nonequilibrium pair correlation function. The partial equation of motion of component α, derivable from the Liouville equation,[3,4] contains each of these terms,

$$\begin{aligned}\partial\rho_\alpha\mathbf{u}_\alpha/\partial t&=\nabla_{r_1}\cdot[\mathfrak{d}_\alpha-\rho_\alpha(\mathbf{u}_\alpha\mathbf{u}+\mathbf{u}\mathbf{u}_\alpha-\mathbf{u}\mathbf{u})]\\ &\quad+c_\alpha\bar{\mathbf{F}}_\alpha^{(1)*}+c_\alpha\mathbf{X}_\alpha,\\ \mathfrak{d}_\alpha&=(\mathfrak{d}_\alpha)_v+(\mathfrak{d}_\alpha)_k,\\ (\mathfrak{d}_\alpha)_v&=\tfrac{1}{2}\sum_\beta c_\alpha c_\beta\int(\mathbf{r}\mathbf{r}/r)(dV_{\beta\alpha}/dr)g_{\beta\alpha}^{(2)}(\mathbf{r}_1,\mathbf{r})d^3\mathbf{r}.\end{aligned} \tag{3.3}$$

In Eq. (3.3), $\mathfrak{d}_\alpha$ is the partial stress tensor, the sum of the intermolecular force contribution $(\mathfrak{d}_\alpha)_v$ and a kinetic contribution $(\mathfrak{d}_\alpha)_k$ defined more fully in the references.

We write the forces acting on a molecule in a given state to be the sum of their values $\mathbf{F}_\alpha^{(1,0)}$ and $\mathbf{F}_\alpha^{(1,0)*}$ in an equilibrium state with the same nonuniform concentration distribution (enforced by the presence of external fields) and the frictional forces $\mathbf{F}_\alpha^{(1,1)}$ and $\mathbf{F}_\alpha^{(1,1)*}$,

$$\mathbf{F}_\alpha^{(1)}=\mathbf{F}_\alpha^{(1,0)}+\mathbf{F}_\alpha^{(1,1)},$$
$$\mathbf{F}_\alpha^{(1)*}=\mathbf{F}_\alpha^{(1,0)*}+\mathbf{F}_\alpha^{(1,1)*}. \tag{3.4}$$

In a like manner the pair correlation function and the partial stress tensor may be written as the sum of equilibrium and perturbation terms,[3]

$$g_{\alpha\beta}^{(2)}=g_{\alpha\beta}^{(2,0)}+g_{\alpha\beta}^{(2,1)},$$
$$\mathfrak{d}_\alpha=-p_\alpha\mathbf{1}+\mathfrak{d}_\alpha^{(1)},$$
$$p_\alpha=c_\alpha kT-\tfrac{1}{6}\sum_\beta c_\alpha c_\beta\int r(dv_{\alpha\beta}/dr)\,g_{\alpha\beta}^{(2,0)}d^3\mathbf{r}, \tag{3.5}$$

where $g_{\alpha\beta}^{(2,0)}$ is the well-known radial distribution function of equilibrium statistical mechanics, p_α is the local equilibrium partial pressure of species α, k is the Boltzmann constant, and T is absolute temperature.

Quasi-Phenomenological Relations

We shall now transform the partial equations of motion with the object of obtaining expressions for the forces in terms of the gradients of local thermodynamic properties. Substituting the equations of continuity, Eq. (2.1), and the overall equations of motion, Eq. (2.2), into the partial equations, Eq. (3.3), we find when external forces are absent,

$$c_\alpha\mathbf{F}_\alpha^{(1)*}=m_\alpha(\partial\mathbf{j}_\alpha/\partial t)+m_\alpha[\nabla_{r_1}\cdot(\mathbf{j}_\alpha\mathbf{u}+\mathbf{u}\mathbf{j}_\alpha)-\mathbf{u}\nabla_{r_1}\cdot\mathbf{j}_\alpha]$$
$$+(\rho_\alpha/\rho)\nabla_{r_1}\cdot\mathfrak{d}-\nabla_{r_1}\cdot\mathfrak{d}_\alpha,$$
$$\mathbf{j}_\alpha=c_\alpha(\mathbf{u}_\alpha-\mathbf{u}), \tag{3.6}$$

where $\mathbf{j}_\alpha$ is the diffusion flux of component α relative to the center of mass. With the neglect of the inertial term, of cross terms of order $\mathbf{j}_\alpha\nabla\cdot\mathbf{u}$ and of terms of order $\nabla^2\mathbf{u}$, Eqs. (2.3), (3.5), and (3.6) then yield the following expression for $\mathbf{F}_\alpha^{(1)*}$ in terms of the local equilibrium gradients of total and partial pressures:

$$c_\alpha\mathbf{F}_\alpha^{(1)*}=\nabla_{r_1}p_\alpha-(\rho_\alpha/\rho)\nabla_{r_1}p. \tag{3.7}$$

In addition, from Eq. (3.7) and the definitions of p_α in Eq. (3.5) and of $\mathbf{F}_\alpha^{(1)*}$ in Eq. (3.2) we find

$$c_\alpha\mathbf{F}_\alpha^{(1)}=\nabla_{r_1}c_\alpha kT-(\rho_\alpha/\rho)\nabla_{r_1}p. \tag{3.8}$$

At equilibrium, the diffusion fluxes and the gradients of velocity vanish, and the external force $\mathbf{X}_\alpha$ equals the gradient of chemical potential $\nabla_{r_1}\mu_\alpha$, so that we may determine expressions for the forces directly from Eq. (3.3),

$$c_\alpha\mathbf{F}_\alpha^{(1,0)*}=\nabla_{r_1}p_\alpha-c_\alpha\nabla_{r_1}\mu_\alpha,$$
$$c_\alpha\mathbf{F}_\alpha^{(1,0)}=\nabla_{r_1}kTc_\alpha-c_\alpha\nabla_{r_1}\mu_\alpha. \tag{3.9}$$

The components of the mean pair space force associated with pairs of molecules of species α at $\mathbf{r}_1$ and β at $\mathbf{r}_2$ are the force on the first molecule, $\mathbf{F}_{\alpha\beta,1}^{(2)}(\mathbf{r}_1,\mathbf{r}_2)$, and the force on the second $\mathbf{F}_{\alpha\beta,2}^{(2)}(\mathbf{r}_1,\mathbf{r}_2)$. Relations for these forces, similar to Eqs. (3.8) and (3.9), may be derived by multiplying the Liouville equation by $(\mathbf{P}_{\alpha j}\oplus\mathbf{P}_{\beta k})\delta(\mathbf{R}_{\alpha j}-\mathbf{r}_1)\delta(\mathbf{R}_{\beta k}-\mathbf{r}_2)$, where δ denotes the Dirac delta function, and integrating over coordinates and momenta. With the use of the definition of temperature and upon neglect of inertial terms, save for that portion required to bring about the asymptotic equality of the pair and singlet forces, we have

$$c_{\alpha\beta}^{(2)}\mathbf{F}_{\alpha\beta,1}^{(2)}=\nabla_{r_1}kTc_{\alpha\beta}^{(2)}-(m_\alpha c_{\alpha\beta}^{(2)}/\rho)\nabla_{r_1}p,$$
$$c_{\alpha\beta}^{(2)}\mathbf{F}_{\alpha\beta,2}^{(2)}=\nabla_{r_2}kTc_{\alpha\beta}^{(2)}-(m_\beta c_{\alpha\beta}^{(2)}/\rho)\nabla_{r_2}p,$$
$$c_{\alpha\beta}^{(2)}=c_\alpha(\mathbf{r}_1)c_\beta(\mathbf{r}_2)g_{\alpha\beta}^{(2)}(\mathbf{r}_1,\mathbf{r}_2), \tag{3.10}$$

where $c_{\alpha\beta}^{(2)}$ is the density in pair configuration space. At equilibrium,

$$c_{\alpha\beta}^{(2,0)}\mathbf{F}_{\alpha\beta,1}^{(2,0)}=\nabla_{r_1}kTc_{\alpha\beta}^{(2,0)}-c_{\alpha\beta}^{(2,0)}\nabla_{r_1}\mu_\alpha,$$
$$c_{\alpha\beta}^{(2,0)}\mathbf{F}_{\alpha\beta,2}^{(2,0)}=\nabla_{r_2}kTc_{\alpha\beta}^{(2,0)}-c_{\alpha\beta}^{(2,0)}\nabla_{r_2}\mu_\beta. \tag{3.11}$$

The phenomenological equations for diffusion and the Newtonian stress tensor arise when the perturbations to the radial distribution functions are linear functions of the relative velocities and velocity gradient in an isothermal nonequilibrium system,[3,6]

$$g_{\alpha\beta}^{(2,1)}/g_{\alpha\beta}^{(2,0)}=\psi_{\alpha\beta}^{(1)}(r)(\mathbf{r}/r)\cdot[\mathbf{u}_\beta(\mathbf{r}_1)-\mathbf{u}_\alpha(\mathbf{r}_1)]$$
$$+\psi_{\alpha\beta}^{(0)}(r)\nabla_{r_1}\cdot\mathbf{u}+\psi_{\alpha\beta}^{(2)}(r)[(\mathbf{r}\cdot\dot{\boldsymbol{\epsilon}}^*\cdot\mathbf{r}/r^2],$$
$$\dot{\boldsymbol{\epsilon}}^*=\dot{\boldsymbol{\epsilon}}-\tfrac{1}{3}\mathbf{1}\nabla_{r_1}\cdot\mathbf{u}. \tag{3.12}$$

The first term, a first-order spherical harmonic in the polar and azimuthal angles defining the direction of the vector $\mathbf{r}$, contributes only to $\mathbf{F}_\alpha^{(1,1)*}$ while the second and third terms, zero and second order harmonics, respectively, contribute to $(\mathfrak{d}_\alpha)_v$. Higher order harmonics, which contribute neither to the frictional force nor to the stress tensor, we here leave unspecified.

From Eq. (3.12) for the perturbations and from Eqs. (3.2)–(3.5), we find that the forces $\mathbf{F}_\alpha^{(1,1)*}$ are proportional to the relative velocities and that the partial stress tensors are of Newtonian form,[3]

$$\mathbf{F}_\alpha^{(1,1)*}=-\sum_\beta\zeta_{\alpha\beta}(\mathbf{u}_\alpha-\mathbf{u}_\beta),$$
$$\mathfrak{d}_\alpha^{(1)}=(\phi_\alpha-\tfrac{2}{3}\eta_\alpha)\mathbf{1}\nabla_{r_1}\cdot\mathbf{u}+2\eta_\alpha\dot{\boldsymbol{\epsilon}}, \tag{3.13}$$

with friction coefficients $\zeta_{\alpha\beta}$ and partial coefficients of shear and bulk viscosity, η_α and ϕ_α, defined by the relations

$$\zeta_{\alpha\beta}=\tfrac{1}{6}\int\frac{dV_{\alpha\beta}}{dr}[\psi_{\alpha\beta}^{(1)}+\psi_{\beta\alpha}^{(1)}]g_{\alpha\beta}^{(2,0)}d^3\mathbf{r}$$
$$\eta_\alpha=\tfrac{1}{30}\sum_\beta c_\alpha c_\beta\int r\frac{dV_{\alpha\beta}}{dr}\psi_{\alpha\beta}^{(2)}g_{\alpha\beta}^{(2,0)}d^3\mathbf{r},$$
$$\phi_\alpha=\tfrac{1}{6}\sum_\beta c_\alpha c_\beta\int r\frac{dV_{\alpha\beta}}{dr}\psi_{\alpha\beta}^{(0)}g_{\alpha\beta}^{(2,0)}d^3\mathbf{r}. \tag{3.14}$$

In Eq. (3.14), a kinetic contribution to the coefficient of shear viscosity, dominant in gases but small in liquids, has been neglected in accordance with the findings of Kirkwood, Buff, and Green.[8]

It follows from Eqs. (3.13) and the definitions of the frictional forces and the partial stress tensor that to within terms of order $\nabla^2\mathbf{u}$,

$$\mathbf{F}_\alpha^{(1,1)}=\mathbf{F}_\alpha^{(1,1)*}=-\sum_\beta c_\beta\zeta_{\alpha\beta}(\mathbf{u}_\alpha-\mathbf{u}_\beta). \tag{3.15}$$

It is the generalization of Eq. (3.15) to the space of molecular pairs which comprises the principal hypothesis of our unified theory of transport parameters in liquid solutions.[4,7] Stated verbally, the assumption is that the mean frictional force $\mathbf{F}_{\alpha\beta}^{(2,1)}$ in the configuration space of molecular pairs, defined as the six-dimensional sum, $\mathbf{F}_{\alpha\beta,1}^{(2)}\oplus\mathbf{F}_{\alpha\beta,2}^{(2)}$, of the mean frictional forces acting on the first and second molecules, is linearly related to the pair space velocity $\mathbf{u}_{\alpha\beta}^{(2)}(\mathbf{r}_1,\mathbf{r}_2)$ through the same friction coefficients that appear in Eq. 3.15. In mathematical terms, we assume

$$\mathbf{F}_{\alpha\beta}^{(2,1)}=-\tfrac{1}{2}\sum_\gamma\sum_\sigma\zeta_{\alpha\beta;\gamma\sigma}\cdot\{\mathbf{u}_{\alpha\beta}^{(2)}-[\mathbf{u}_\gamma(\mathbf{r}_1)\oplus\mathbf{u}_\sigma(\mathbf{r}_2)]\},$$

$$\mathbf{F}_{\alpha\beta}^{(2,1)}\equiv\mathbf{F}_{\alpha\beta}^{(2)}-\mathbf{F}_{\alpha\beta}^{(2,0)}=(\mathbf{F}_{\alpha\beta,1}^{(2)}-\mathbf{F}_{\alpha\beta,1}^{(2,0)})$$

$$\oplus(\mathbf{F}_{\alpha\beta,2}^{(2)}-\mathbf{F}_{\alpha\beta,2}^{(2,0)})=\mathbf{F}_{\alpha\beta,1}^{(2,1)}\oplus\mathbf{F}_{\alpha\beta,2}^{(2,1)},$$

$$\mathbf{u}_{\alpha\beta}^{(2)}\equiv\mathbf{u}_{\alpha\beta,1}^{(2)}\oplus\mathbf{u}_{\alpha\beta,2}^{(2)},$$

$$\zeta_{\alpha\beta;\gamma\sigma}=c_\gamma\zeta_{\alpha\gamma}\mathbf{1}_1\oplus c_\sigma\zeta_{\beta\sigma}\mathbf{1}_2, \tag{3.16}$$

where $\mathbf{1}_1$ and $\mathbf{1}_2$ are the unit tensors at $\mathbf{r}_1$ and $\mathbf{r}_2$, respectively.

Pair Space Equation of Continuity

Integration of the Liouville equation over all coordinates except those of two molecules of species α and β located at $\mathbf{r}_1$ and $\mathbf{r}_2$ and over all momenta yields the exact pair space equation of continuity,

$$(\partial/\partial t)c_{\alpha\beta}^{(2)}+\nabla_{r_1}\cdot\mathbf{j}_{\alpha\beta,1}^{(2)}+\nabla_{r_2}\cdot\mathbf{j}_{\alpha\beta,2}^{(2)}=0,$$

$$\mathbf{j}_{\alpha\beta,1}^{(2)}=c_{\alpha\beta}^{(2)}\mathbf{u}_{\alpha\beta,1}^{(2)},\quad \mathbf{j}_{\alpha\beta,2}^{(2)}=c_{\alpha\beta}^{(2)}\mathbf{u}_{\alpha\beta,2}^{(2)}, \tag{3.17}$$

where $\mathbf{j}_{\alpha\beta,1}^{(2)}$ and $\mathbf{j}_{\alpha\beta,2}^{(2)}$ are the pair space fluxes of the two molecules. Eq. (3.17) may be combined with the singlet space equations of continuity, Eq. (2.1), and linearized to give

$$-c_\alpha c_\beta(\partial g_{\alpha\beta}^{(2,0)}/\partial t)-c_\alpha c_\beta[\mathbf{u}_\beta(\mathbf{r}_2)-\mathbf{u}_\alpha(\mathbf{r}_1)]\cdot\nabla_r g_{\alpha\beta}^{(2,0)}$$

$$=-\nabla_r\cdot(\mathbf{j}_{\alpha\beta,1}^{(2)}-c_{\alpha\beta}^{(2,0)}\mathbf{u}_\alpha)$$

$$+\nabla_r\cdot(\mathbf{j}_{\alpha\beta,2}^{(2)}-c_{\alpha\beta}^{(2,0)}\mathbf{u}_\beta). \tag{3.18}$$

Coefficients of Viscosity

Substitution of Eqs. (3.8)–(3.11) and (3.15) into Eq. (3.16) results in the following expression for the pair space fluxes[2,4]:

$$\mathbf{j}_{\alpha\beta,1}^{(2)}-c_{\alpha\beta}^{(2,0)}\mathbf{u}_\alpha=\frac{c_\alpha c_\beta kT}{\zeta_\alpha}g_{\alpha\beta}^{(2,0)}\nabla_r\frac{g_{\alpha\beta}^{(2,1)}}{g_{\alpha\beta}^{(2,0)}},$$

$$\mathbf{j}_{\alpha\beta,2}^{(2)}-c_{\alpha\beta}^{(2,0)}\mathbf{u}_\beta=-\frac{c_\alpha c_\beta kT}{\zeta_\beta}g_{\alpha\beta}^{(2,0)}\nabla_r\frac{g_{\alpha\beta}^{(2,1)}}{g_{\alpha\beta}^{(2,0)}},$$

$$\zeta_\alpha=\sum_\gamma c_\gamma\zeta_{\alpha\gamma}\qquad\alpha=1,2. \tag{3.19}$$

In the derivation of Eq. (3.19) we have used the definition of the distribution function perturbation $g_{\alpha\beta}^{(2,1)}$ to eliminate $g_{\alpha\beta}^{(2)}$ and have shifted independent variables from $\mathbf{r}_1$ and $\mathbf{r}_2$ to $\mathbf{r}_1$ and $\mathbf{r}$ in the first equation and to $\mathbf{r}_2$ and $\mathbf{r}$ in the second, neglecting second-order terms.

For the case of purely viscous flow, the diffusion fluxes vanish and the velocities of the components at a point are equal to each other and to the center of mass velocity. Under these conditions, we find from Eqs. (3.18) and (3.19) differential equations for the perturbations to the distribution functions,[11]

$$c_\alpha c_\beta[(\partial g_{\alpha\beta}^{(2,0)}/\partial\ln c_1)+(\partial g_{\alpha\beta}^{(2,0)}/\partial\ln c_2)]\nabla_{r_1}\cdot\mathbf{u}$$

$$-c_\alpha c_\beta(\mathbf{r}\cdot\nabla_{r_1}\mathbf{u})\cdot\nabla_r g_{\alpha\beta}^{(2,0)}$$

$$=-c_\alpha c_\beta(D_\alpha+D_\beta)\nabla_r\cdot g_{\alpha\beta}^{(2,0)}\nabla_r(g_{\alpha\beta}^{(2,1)}/g_{\alpha\beta}^{(2,0)}), \tag{3.20}$$

$$D_\alpha=kT/\zeta_\alpha,$$

$$\partial g_{\alpha\beta}^{(2,0)}/\partial t$$

$$=-[(\partial g_{\alpha\beta}^{(2,0)}/\partial\ln c_1)+(\partial g_{\alpha\beta}^{(2,0)}/\partial\ln c_2)]\nabla_{r_1}\cdot\mathbf{u},$$

$$\mathbf{u}_\beta(\mathbf{r}_2)-\mathbf{u}_\alpha(\mathbf{r}_1)=\mathbf{r}\cdot\nabla\mathbf{u}, \tag{3.20}$$

where D_α is the self-diffusion coefficient of species α in the mixture. The form of the distribution function perturbation is given by Eq. (3.12),

$$\frac{g_{\alpha\beta}^{(2,1)}}{g_{\alpha\beta}^{(2,0)}}=\psi_{\alpha\beta}^{(0)}\nabla_{r_1}\cdot\mathbf{u}+\psi_{\alpha\beta}^{(2)}\frac{\mathbf{r}\cdot\dot{\boldsymbol{\epsilon}}^*\cdot\mathbf{r}}{r^2}. \tag{3.21}$$

Differential equations for the perturbation parameters $\psi_{\alpha\beta}^{(0)}$ and $\psi_{\alpha\beta}^{(2)}$ result when Eq. (3.21) is inserted into Eq. (3.20) and surface spherical harmonics of the same

[11] The careful reader may notice at this point that the singlet space forces and the gradients of thermodynamic properties become second-order terms. This permits some simplification in the derivation, which we have, however, avoided for the sake of maintaining a uniform pattern of presentation throughout our series of papers.

order are separately equated,

$$g_{\alpha\beta}^{(2,0)}\frac{d^2\psi_{\alpha\beta}^{*(0)}}{dr^2}+\left(\frac{dg_{\alpha\beta}^{(2,0)}}{dr}+\frac{2}{r}g_{\alpha\beta}^{(2,0)}\right)\frac{d\psi_{\alpha\beta}^{*(0)}}{dr}$$
$$=\frac{1}{3}r\frac{dg_{\alpha\beta}^{(2,0)}}{dr}-\left(\frac{\partial g_{\alpha\beta}^{(2,0)}}{\partial \ln c_1}+\frac{\partial g_{\alpha\beta}^{(2,0)}}{\partial \ln c_2}\right),$$

$$g_{\alpha\beta}^{(2,0)}\frac{d^2\psi_{\alpha\beta}^{*(2)}}{dr^2}+\left(\frac{dg_{\alpha\beta}^{(2,0)}}{dr}+\frac{2}{r}g_{\alpha\beta}^{(2,0)}\right)\frac{d\psi_{\alpha\beta}^{*(2)}}{dr}$$
$$-\frac{6g_{\alpha\beta}^{(2,0)}}{r^2}\psi_{\alpha\beta}^{*(2)}=r\frac{dg_{\alpha\beta}^{(2,0)}}{dr},$$

$$\psi_{\alpha\beta}^{*(0)}=(D_\alpha+D_\beta)\psi_{\alpha\beta}^{(0)},$$
$$\psi_{\alpha\beta}^{*(2)}=(D_\alpha+D_\beta)\psi_{\alpha\beta}^{(2)}. \qquad (3.22)$$

Boundary conditions may be obtained by the method of Kirkwood, Buff, and Green.[8] These seem to be somewhat controversial,[12] and, as they are not required in the following, we shall here omit their explicit formulation.

From known radial distribution functions and diffusion coefficients, we may in principle solve Eqs. (3.22) for the perturbation parameters. Expressions for the coefficients of viscosity then follow from Eq. (3.14) and the condition that the partial equations of motion combine to give the overall equation for the fluid element,

$$\phi=\frac{c_1^2}{12D_1}\int r\frac{dV_{11}}{dr}\psi_{11}^{*(0)}g_{11}^{(2,0)}d^3\mathbf{r}$$
$$+\frac{c_1c_2}{3(D_1+D_2)}\int r\frac{dV_{12}}{dr}\psi_{12}^{*(0)}g_{12}^{(2,0)}d^3\mathbf{r}$$
$$+\frac{c_2^2}{12D_2}\int r\frac{dV_{22}}{dr}\psi_{22}^{*(0)}g_{22}^{(2,0)}d^3\mathbf{r},$$

$$\eta=\frac{c_1^2}{60D_1}\int r\frac{dV_{11}}{dr}\psi_{11}^{*(2)}g_{11}^{(2,0)}d^3\mathbf{r}$$
$$+\frac{c_1c_2}{15(D_1+D_2)}\int r\frac{dV_{12}}{dr}\psi_{12}^{*(2)}g_{12}^{(2,0)}d^3\mathbf{r}$$
$$+\frac{c_2^2}{60D_2}\int r\frac{dV_{22}}{dr}\psi_{22}^{*(2)}g_{22}^{(2,0)}d^3\mathbf{r},$$
$$\phi=\sum_\alpha\phi_\alpha, \qquad \eta=\sum_\alpha\eta_\alpha. \qquad (3.23)$$

When the species are identical or when the concentration of one of them vanishes, Eqs. (3.22) and (3.23) reduce to those obtained by Kirkwood, Buff, and Green.[8,13] With the use of equations for the friction coefficient ratios developed in our paper on diffusion,[7] it is possible in principle to calculate numerically from known equilibrium distribution functions the product of the viscosity coefficients and either of the two self-diffusion coefficients. This has been carried out for the limiting case of a single component.[8,9]

IV. DISCUSSION

We now turn our attention to the composition dependence of the viscosity, considering in particular the coefficient of shear viscosity which has been the subject of many experiments and omitting the parallel arguments concerning the coefficient of bulk viscosity which is less well known.

The changes of η, or more precisely $D_1\eta$, with composition are governed by the corresponding changes in the radial distribution functions, which, for arbitrary mixtures, are of complex form, not amenable to simple treatment. For the present, therefore, we shall content ourselves with a study of solutions, regular in behavior, with additive volumes and composition independent radial distribution functions.[10] Under these conditions $\psi_{\alpha\beta}^{*(2)}$ is also constant, so that Eq. (3.23) for η may be rewritten

$$(x_1^2v_1^2/D_1)[D_1\eta-D_1^0\eta_1]+2x_1x_2v_1v_2\eta$$
$$+(x_2^2v_2^2/D_2)[D_2\eta-D_2^0\eta_2]$$
$$=\tfrac{1}{15}[x_1x_2/(D_1+D_2)]\int r(dV_{12}/dr)\psi_{12}^{*(2)}g_{12}^{(2,0)}d^3\mathbf{r}, \qquad (4.1)$$
$$v=x_1v_1+x_2v_2,$$
$$D_i^0\eta_i=(60v_i^2)^{-1}\int r(dV_{ii}/dr)\psi_{ii}^{*(2)}g_{ii}^{(2,0)}d^3\mathbf{r} \qquad i=1,2, \qquad (4.1)$$

where x_1 and x_2 are the mole fractions of 1 and 2, respectively, v_1 and v_2 are the volumes per molecule of pure 1 and 2, v is the mean molecular volume of the mixture, D_i^0 is the self-diffusion coefficient of pure species i, and η_i is the viscosity coefficient of pure i, not to be confused with the partial coefficient of viscosity of the previous section. Under the same hypotheses, we have already found[7] that the ratio of the self-diffusion coefficients at any composition is in the inverse ratio of the molar volumes $D_1/D_2=v_2/v_1$, and hence

$$(x_1/x_2)v_1^2[D_1\eta-D_1^0\eta_1]+2v_1v_2D_1\eta$$
$$+(x_2/x_1)v_2^2[D_1\eta-D_1^\infty\eta_2]$$
$$=\tfrac{1}{15}[v_2/(v_2+v_1)]\int r(dV_{12}/dr)\psi_{12}^{*(2)}g_{12}^{(2,0)}d^3\mathbf{r}, \qquad (4.2)$$

where D_1^∞ is the self-diffusion coefficient at infinite dilution (that is, the coefficient of species one in pure two). The right-hand side of Eq. (4.2) must be independent of composition. For the case of most physical interest wherein the volumes are unequal and $D_1\eta$ is

[12] R. Eisenschitz and A. Suddaby, *Proceedings of the Second International Congress on Rheology* (Academic Press, Inc., New York, 1950).

[13] Apparently because of a misprint, the coefficient of ψ_2 in Eq. (6) of Zwanzig, Kirkwood, Stripp, and Oppenheim[9] is too large by a factor of two.

analytic in the mole fraction, the only solution to Eq. (4.2) is that $D_1\eta$ is independent of composition, whence[14]

$$D_1\eta=[30(v_2+v_1)v_1]^{-1}\int r(dV_{12}/dr)\psi_{12}^{*(2)}g_{12}^{(2,0)}d^3\mathbf{r}. \quad (4.3)$$

This equation may be regarded as a statistical mechanical analog of the Stokes-Einstein equation for two-component systems. The constancy of $D_1\eta$ has been verified by Carman and Stein for the system *n*-butyl iodide–ethyl iodide.[15]

According to our theory of diffusion,[7] when the radial distribution function is independent of composition, then the mutual diffusion coefficient D is simply related to the self-diffusion coefficient D_1,

$$D=D_1[1+(\partial \ln f_1/\partial \ln c_1)_{T,p}], \quad (4.4)$$

where f_1 is the activity coefficient on the concentration basis. Multiplying both sides by η and replacing $D_1\eta$ by $D_1^{\infty}\eta_2$, we find

$$D\eta=D_1^{\infty}\eta_2[1+(\partial \ln f_1/\partial \ln c_1)_{T,p}]. \quad (4.5)$$

The self-diffusion coefficient D_1^{∞} is equal to the mutual diffusion coefficient D^{∞} at infinite dilution of species one,[4] so that Eq. (4.5) may be written

$$D\eta=D^{\infty}\eta_2[1+(\partial \ln f_1/\partial \ln c_1)_{T,p}]. \quad (4.6)$$

A similar relationship has been proposed by Gordon[16] for electrolytic solutions. Equation (4.6) has been tested in its present form for nonelectrolyte solutions by Gosting and co-workers[17] and by Sandquist and Lyons[18] who found it valid to two significant figures. If the solution is very nearly ideal—that is, if the activity coefficient f_1' on the mole fraction basis is nearly unity—then $(\partial \ln f_1/\partial \ln c_1)_{T,p}$ is proportional to the mole fraction, provided that the molar volumes of the two components are not equal. In this circumstance, we would expect $D\eta$ to be linear in the mole fraction and this has been verified by Caldwell and Babb for several systems.[19] The theories of Eyring and co-workers,[20] and of Hartley and Crank[21,22] similarly suggest that for ideal solutions $D\eta$ should be linear in the mole fraction, although the physical basis of their reasoning is rather different from ours. It has also been proposed that $D\eta \div (\partial \ln x_1 f_1'/\partial \ln x_1)$ is linear in the mole fraction for nonideal solutions.[20,22] For solutions deviating strongly from ideality, this does not seem to be generally the case.[23] Hammond and Stokes[22] tested the proposal for a relatively simple system, carbon tetrachloride–cyclohexane, with fair success. Our Eq. (4.6) fits their data rather better and can be used to predict $D\eta$ to three significant figures except in the limit of pure solute.

We cannot fail to remark that it would be surprising, indeed, if the simple equations derived in the present section were obeyed exactly by the very accurate mutual diffusion and viscosity data currently available, for we have employed some rather restrictive assumptions concerning the nature of the intermolecular forces and of the radial distribution functions.[7] However, it should prove possible to correlate deviations from our formulas with the departure of the thermodynamic properties of mixtures from those predicted by the theory of regular solutions. Thus, the present treatment provides the groundwork for systematic experimentation parallel to that which is now being carried out on equilibrium systems.

Further insight of a more qualitative nature into the significance of Eq. (4.3) for $D_1\eta$ can be achieved by introducing the very crude approximation that $\psi_{12}^{*(2)}$ can be taken to be a constant, $\bar{\psi}$, independent of temperature, pressure, and the nature of species two. Equation (4.3) then reduces to[5]

$$D_1\eta=\tfrac{1}{5}\bar{\psi}\{(kT/2v_1)-p[v_2/(v_1+v_2)]\},$$

$$\int r(dV_{12}/dr)g_{12}^{(2,0)}d^3\mathbf{r}=\{[(v_1+v_2)kT/2v_1v_2]-p\}6v_1v_2. \quad (4.7)$$

The first term, $kT/2v_1$, in this expression for $D_1\eta$ is far larger at ordinary pressures and temperatures than the second, so that $D_1\eta/T$ should be approximately independent of temperature. Such constancy has been noted experimentally.[15] In contrast to the Stokes-Einstein equation, Eq. (4.7) predicts that $D_1\eta$ is pressure dependent. If a series of measurements of $D_1\eta$ are taken at constant temperature and pressure with a variety of different solvents (species two), then by Eq. (4.7), a plot of $D_1\eta$ vs (v_2/v_1+v_2) should be a straight line with slope and intercept simply related to the temperature and pressure. Hammond and Stokes[24] carried out a set of measurements, obtaining, in our notation, $D_1^{\infty}\eta_2$ for carbon tetrachloride in a number of solvents, the most interesting of which are benzene, cyclohexane, tetralin, and decalin. They found empirically that $D_1^{\infty}\eta_2$ vs v_2 is

[14] If the volumes are identical, then $D_1\eta$ may be a linear or quadratic function of the mole fraction. In view of the limited self-diffusion data available, it does not seem necessary at this time to consider this possibility, although it may prove important in connection with a full discussion of Eq. (4.6).

[15] P. C. Carman and L. H. Stein, Trans. Faraday Soc. **52**, 619 (1956).

[16] A. R. Gordon, J. Chem. Phys. **5**, 522 (1937).

[17] (a) L. J. Gosting and M. S. Morris, J. Am. Chem. Soc. **21**, 1998 (1949); (b) L. J. Gosting and D. F. Akeley, *ibid.* **74**, 2059 (1952).

[18] C. L. Sandquist and P. A. Lyons, J. Am. Chem. Soc. **76**, 4641 (1954).

[19] C. S. Caldwell and A. L. Babb, J. Phys. Chem. **60**, 51 (1956).

[20] (a) W. E. Roseveare, R. E. Powell, and H. Eyring, J. App. Phys. **12**, 669 (1941); (b) S. Glasstone, K. J. Laidler, and H. Eyring, *The Theory of Rate Processes* (McGraw-Hill Book Company, New York, 1941), p. 536.

[21] G. S. Hartley and J. Crank, Trans. Faraday Soc. **45**, 801 (1949).

[22] B. R. Hammond and R. H. Stokes, Trans. Faraday Soc. **52**, 781 (1956).

[23] D. K. Anderson, J. R. Hall, and A. L. Babb, J. Phys. Chem. **62**, 404 (1958).

[24] B. R. Hammond and R. H. Stokes, Trans. Faraday Soc. **51**, 1641 (1955).

linear. However, a plot with abscissa $v_2/(v_1+v_2)$ fits as well, although the ratio of slope to intercept is not at all close to the predicted value. Thus, as one might expect, Eq. (4.7) must not be taken too literally.

Evidently, when $D_1\eta$ is constant over the entire composition range, it obeys a particularly simple form of the law of corresponding states. For arbitrary solutions, however, the law does not seem to follow in a simple way from Eq. (3.23). The statistical mechanical foundation for the theorem of corresponding states in the case of thermodynamic properties lies in the possibility of defining a pseudopotential such that the partition function of one of the pure components at an appropriate reduced temperature is equal to that of the mixture.[25] However, the radial distribution function and therefore the perturbation parameters are not determined by the partition function, and hence it is by no means obvious that $D_1\eta$ for the mixture will equal that of the pure species at the reduced temperature. These remarks may have some bearing on the interesting papers of Thomaes and Van Itterbeek[26] and Bak and Anderson.[27]

We end our discussion by observing that it is possible to derive one rule for predicting η without going into extended arguments concerning the distribution functions and perturbation parameters. We merely assume that $(1/v^2)\int r(dV_{\alpha\beta}/dr)\psi_{\alpha\beta}^{(2)}g_{\alpha\beta}^{(2,0)}d^3\mathbf{r}$ is independent of composition. Then Eqs. (3.14) and (3.23) become

$$\eta=x_1^2\eta_1+2x_1x_2\eta_{12}+x_2^2\eta_2,$$
$$\eta_{12}=(30v^2)^{-1}\int r(dV_{12}/dr)\psi_{12}^{(2)}g_{12}^{(2,0)}d^3\mathbf{r}, \quad (4.8)$$

where η_1 and η_2 are the viscosities of pure species one and two, respectively, and η_{12} is to be derived from experimental measurements. This formula for the viscosity has been suggested by Sachanov and Rjachowsky[28] and more recently by Hind, McLaughlin, and Ubbelhode.[29]

[25] P. J. Wojtowicz, Z. W. Salsburg, and J. G. Kirkwood, J. Chem. Phys. **27**, 505 (1957).
[26] G. Thomaes and J. Van Itterbeek, Mol. Phys. **2**, 372 (1959).
[27] T. A. Bak and K. Anderson, Acta Chem. Scand. **12**, 1367 (1958).
[28] A. Sachanov and N. Rjachowsky, Z. Phys. Chem. **86**, 529 (1914).
[29] R. K. Hind, E. McLaughlin, and A. R. Ubbelhode, Trans. Faraday Soc. **56**, 328 (1960).

THE JOURNAL OF CHEMICAL PHYSICS VOLUME 33, NUMBER 5 NOVEMBER, 1960

Studies in Molecular Dynamics. II. Behavior of a Small Number of Elastic Spheres

B. J. ALDER AND T. E. WAINWRIGHT

Lawrence Radiation Laboratory, University of California, Livermore, California

(Received May 23, 1960)

The equation of state and the collision rate for systems ranging in size from four to 500 particles are described. The dependence of the results on the number of particles is qualitatively discussed and in this way insight is gained as to what is required of more accurate analytical theories. By comparing the results to various analytical theories now available their region of validity is established. The number of particles necessary at various densities to obtain a quantitative description of the equilibrium properties is delineated. Whether a first-order phase transition exists for hard spheres remains open until larger systems are investigated.

INTRODUCTION

IN the previous paper[1] a program for digital computers has been described which reproduces the detailed motions of a system of interacting classical particles. In this paper some of the results of such a calculation as applied to a relatively small number of hard sphere molecules is presented. The aim of such a study was to learn how many particles are required to adequately represent the equilibrium behavior of a real system.

In order to answer this question it is necessary to study the dependence of the results on the number of particles. Thus, systems as small as four particles and as large as 500 particles are reported on. The four-particle system was studied in the hope that it would reproduce the two-state behavior at a density near 1.5 times close-packing noted previously[2-5] for larger systems. If this were the case then it would have been worthwhile to attempt an analytical solution for the four-particle system, and determine from it what the proper average behavior between the two states is at that density. Since a larger number of particles than four were required to bring about a two-state behavior, analytical treatment is out of the question; even dealing with three independent particles would have been a hard task (three particles are placed relative to the fourth). This also means that any analytic treatment to even qualitatively describe the behavior near this density would be extremely difficult.

The larger systems were studied in the hope that the two states would eventually coexist. Only then can one be sure that hard spheres have a first-order phase transition between a fluid and a solid state. The fact that this was not achieved with systems as large as 500 particles is not surprising. The best hope of getting the two phases to coexist for a small number of particles is in two-dimensional systems, since fewer particles are perturbed by the boundary. In two-dimensional systems the same two-state behavior was found as in three-dimensional systems and a study is now under way to determine whether a 1000- or a 2000-particle system does have the two phases coexisting.

Before it can be said that a large enough number of particles have been used to adequately represent an infinite system, the boundary conditions used should not influence the results. This has by no means been achieved with a 500-particle system. Periodic boundary conditions have been used throughout for the systems presented in this report in the belief that they give the most realistic results. They are certainly natural boundary conditions in condensed or solid systems where the structure is periodic. They also can be shown to cause the least error in the equilibrium properties at low density. Other boundary conditions have been studied also, and will be reported on subsequently. Although qualitatively the results are the same, they differ quantitatively and they will continue to do so until the number of particles on the surface is a small fraction of the total number of particles. In the more favorable situation of two-dimensional systems this will not occur until systems containing more than 10 000 particles can be handled. This is, however, quite feasible with the latest generation of computers.

With a system so large that boundary conditions do not significantly influence the results, it would be possible to represent an arbitrary number of particles at solid densities provided the system is run long enough to rearrange itself to the state of lowest free energy from some arbitrary initial configuration. In the fluid region the number of particles does not affect the results as long as there are enough particles to establish the proper local order. For solids, however, long-range order can only be obtained for a small number of particles if the order extends across the boundaries of the system. In the case of periodic boundary conditions this means that the particles on one side of the cell have to be perfectly arranged relative to the other side of the cell. For large systems, however, fairly long-range order can be established within a given cell and even if the boundaries do not match, this does not seriously influence the results. Thus a crystal can form

[1] B. J. Alder and T. E. Wainwright, J. Chem. Phys. **31**, 459 (1959).
[2] B. J. Alder and T. E. Wainwright, J. Chem. Phys. **27**, 1208 (1957).
[3] T. E. Wainwright and B. J. Alder, Nuovo cimento Suppl. **9**, Ser. 10, 116 (1958).
[4] W. W. Wood and J. D. Jacobson, J. Chem. Phys. **27**, 1207 (1957).
[5] W. W. Wood, R. R. Parker and J. D. Jacobson, Nuovo cimento Suppl. **9**, Ser. 10, 133 (1958).

TABLE I. Equation of state and the collision rate for four particles.

v/v_0	$(pv/NkT)-1$	Γ/Γ_0	R[a]	C[b]
1.250	13.35	5.03	0.89	2
1.400	8.88	3.73	0.89	2
1.500	7.41	3.36	0.89	7
1.525	7.12	3.27	0.89	5
1.550	6.86	3.23	0.90	3
1.600	6.40	3.08	0.89	5
1.700	5.76	2.93	0.88	2
1.800	5.28	2.88	0.90	2
1.850	5.09	2.87	0.91	5
1.900	4.99	2.83	0.88	5
2.000	4.61	2.80	0.90	2
2.100	4.33	2.73	0.89	5
2.200	4.20	2.74	0.88	2
2.300	3.94	2.74	0.90	5
2.400	4.00	2.87	0.88	5
2.500	3.68	2.82	0.91	2
3.000	3.02	2.72	0.89	2

[a] R is the ratio of the experimental to theoretical collision rate, if the latter is calculated from the Enskog theory with the machine determined equation of state.
[b] C is the number of 1000 collisions the problem has been run.

in any direction relative to the boundary, which is not the case in the smaller systems. However, there are still serious problems in large systems with respect to the calculating time involved to transform an arbitrary initial state to the final equilibrium state. Just as in real systems, glasses can be stable for very long times, so an arbitrary initial configuration can be metastable for as long a time as one cares to calculate.

For small systems it is thus necessary to study that precise number of particles which fit exactly into the cell in order to represent a solid as realistically as possible. This number of particles also has to be placed into the chosen lattice positions; otherwise it has been found that the system will not convert to the state of lowest free energy in reasonable calculating time.

TABLE II. Equation of state and the collision rate for eight particles.

v/v_0[a]	$(pv/NkT)-1$	Γ/Γ_0	R[b]	C[c]
1.500(s)	7.56	3.59	0.94	0–5.0
1.525(s)	7.37	3.61	0.95	0–5.0
1.550(s)	7.07	3.50	0.95	0–20.0
1.570(s)	6.88	3.46	0.95	0–7.5
1.580(s)	6.82	3.46	0.95	0–6.6
1.580(f)	9.90	4.14	0.79	6.6–10.0
1.590(s)	6.78	3.41	0.94	0–5.0
1.600(s)	6.67	3.42	0.95	0–1.4
1.600(f)	9.72	4.14	0.79	1.4–5.0
1.610(s)	6.56	3.36	0.95	0–10.0
1.620(s)	6.50	3.40	0.96	0–5.0
1.650(s)	6.34	3.37	0.96	0–10.0
1.700(s)	5.99	3.28	0.96	0–7.6
1.800(s)	5.55	3.17	0.94	0–10.0
2.000(s)	4.71	3.09	0.97	0–1.3
2.000(f)	5.16	3.34	0.96	1.3–5

[a] The brackets symbolize the solid (s) and the fluid (f) branch, respectively.
[b] As defined in Table I.
[c] C stands for the range in units of 1000 collisions the problem has run in each branch.

Although only the two close-packed lattices for hard spheres were studied and they both, as expected, gave the same results, it is believed that they yield the state of lowest free energy at least at the highest densities. If metastability is a problem, the most efficient way to avoid long calculations is to study various initial states and select the one of lowest free energy at various densities. This has not as yet been done extensively. Thus a body-centered crystal should be examined in the two-state region.

It is, however, possible even in small systems to slightly change the number of particles studied and still get a solid with long-range order. One example of this is given when a perfect solid with one imperfection, namely with one missing particle, is described. Of course, not too many such holes could be introduced in small systems or they would lose their long-range character.

TABLE III. Equation of state and the collision rate for 16 particles.

v/v_0[a]	$(pv/NkT)-1$	Γ/Γ_0	R[a]	C[a]
1.500	7.71	3.77	0.97	0–5.0
1.525(s)	7.49	3.72	0.97	0–8.6, 9.0–10.0
1.525(f)[b]	...	...	...	8.6–9.0
1.550	7.31	3.74	0.97	0–10.0
1.600(s)	6.98	3.67	0.97	0–1.9, 2.0–10.0
1.600(f)[b]	...	...	...	1.9–2.0
1.650(s)	6.63	3.57	0.97	2.5–6.0, 8.6–10.0
1.650(f)	9.0	4.84	0.97	0–2.5, 6.0–8.6

[a] The symbols have been defined in the previous tables.
[b] For the cases $v/v_0=1.525$ and 1.600, the fluid branch existed for too few collisions to determine the pressure adequately.

RESULTS

Since the machine is made to calculate the actual motion of each particle, this program has been principally designed to study the transport properties of systems. Some preliminary results[6] of these have been previously given. In this report, however, attention is focused on the equilibrium properties because these are much better understood and hence confidence in the method can be established, especially since direct comparison with the Monte Carlo results[4,5] can be made.

The thermodynamic properties of a hard sphere system are completely described by the pressure since the internal energy is that of a perfect gas. The pressure is calculated by a direct application of the virial theorem which states that

$$(pv/NkT)-1=(1/Nu^2)(d\Xi/dt), \qquad (1)$$

where u^2 is the mean square velocity,

$$\Xi=\sum_{\text{collisions}} b_{ij},$$

[6] B. J. Alder and T. E. Wainwright, *Transport Processes in Statistical Mechanics, I. Prigogine* (Interscience Publishers, New York, 1958), p. 97.

TABLE IV. Equation of state and the collision rate for 32 particles.

v/v_0[a]	$(pv/NkT)-1$	rmsd[b]	Γ/Γ_0	R[a]	C[a]
1.03139	97.2	0.21	34.1	1.01	0–2.0
1.25000	13.62		5.72	1.00	0–10.0
1.40000	9.33	0.16	4.37	0.99	0–11.0
1.50000	8.12		4.06	0.99	0–42.0
1.52500(s)	7.92		4.04	0.99	0–29.0, 30.0–93.0, 106.0–107.0, 204.0–205.0
1.52500(f)	10.51		5.42	1.00	29.0–30.0, 93.0–106.0, 107.0–204.0, 205.0–263.0
1.53000(s)	7.88		4.03	0.99	0–76.0
1.53000(f)	10.47		5.41	1.00	76.0–200.0
1.53125(s)	7.90		4.04	0.99	0–4.2
1.53125(f)	10.54		5.41	0.99	4.2–28.0
1.53250(s)	7.84		4.00	0.99	0–9.0
1.53250(f)	10.45		5.35	0.99	9.0–52.0
1.53500(s)	7.78		4.01	1.00	0–2.5
1.53500(f)	10.30		5.28	0.99	2.5–52.0
1.54000(s)	7.72		4.01	1.00	0–0.4
1.54000(f)	10.23		5.26	0.99	0.4–47.0
1.55000(s)	7.63	0.77	3.95	0.99	0–5.0, 6.5–25.0, 179.0–180.0
1.55000(f)	10.02		5.19	0.99	5.0–6.5, 25.0–179.0, 180.0–220.0
1.60000(s)	7.57		4.02	0.98	0–5.0
1.60000(f)	9.06		4.87	1.00	5.0–53.0
1.65000	8.41	0.82	4.63	0.99	0–50.0
1.70000	7.83	0.37	4.40	0.98	0–15.0
1.75000	7.13	0.47	4.19	1.00	0–15.0
1.80000	6.59	0.88	3.99	1.00	0–15.0
2.00000	4.89	0.50	3.28	1.00	0–5.0
3.00000	2.09		2.07	0.98	0–39.0
9.00000	0.409		1.23	0.99	0–9.0
10.00000	0.343		1.17	1.01	0–1.5
14.14214	0.249		1.05	0.97	0–3.0

[a] The symbols have been defined in the previous tables.
[b] rmsd stands for the root-mean-square deviation in $(pv/NkT)-1$.

and $b_{ij}=r_{ij}\cdot u_{ij}$ has been defined previously[1] as the scalar product of the relative positions and relative velocities of particles i and j which are involved in a collision. The pressure is graphically determined from the slope of a plot Ξ vs t, and can for a sufficiently long run be obtained within an accuracy of 1% in pv/NkT.

The only property involving the time which shall be discussed here is the collision rate Γ. According to the theory of Enskog,[7] Γ is intimately related to the equation of state,

$$\Gamma/\Gamma_0=(pv/NkT-1)/(B/v), \qquad (2)$$

where B is the second virial coefficient and Γ_0 is the collision rate at infinite dilution

$$\Gamma_0=2N(N-1)\sigma^2(\pi u^2/3)^{\frac{1}{2}}. \qquad (3)$$

N is the number of particles per unit volume. Since finite systems are dealt with, it is strictly speaking necessary to use the value of B for finite systems also. Hence the expression given in Sec. E was used for B. σ is the diameter of the particles. The collision rate and the equation of state are tabulated at various compressions expressed in terms of v/v_0, where v_0 is the volume of the system at close packing.

[7] D. Enskog, Kgl. Svenska Ventenskapsakad. Handl. **64**, No. 4 (1922).

(A) Intermediate Densities

The results are presented in Tables I through XI and in graphs 1 through 4. Figure 1 shows the results for various sized systems in the intermediate density region where the two-state behavior is found. As the

TABLE V. Equation of state and the collision rate for 96 particles.

v/v_0[a]	$(pv/NkT)-1$	Γ Γ_0	R[a]	C[a]
1.0306	99.55	34.4	1.00	0–2.0
1.1000	31.54	11.90	1.02	0–2.9
1.1600	20.27	7.85	0.99	0–2.0
1.2500	13.66	5.75	1.00	0–3.0
1.3448	10.53	4.83	1.01	0–2.0
1.4200	9.22	4.36	0.99	0–2.0
1.5000	8.41	4.25	1.00	0–7.0
1.6000(s)	7.77	4.18	1.00	0–2.6
1.6000(f)	8.96	4.88	1.01	2.6–10.0
1.7000(s)[b]	...	...	...	0–1.0
1.7000(f)	7.54	4.25	0.98	1.0–6.5
1.8000(s)	6.14	3.75	1.01	0–3.8
1.8000(f)	6.80	4.10	0.99	3.8–6.0
1.9000	5.44	3.50	1.00	0–4.0
2.0000	4.72	3.22	1.01	0–3.6
2.7220	2.63	2.31	0.96	0–3.0
14.1422	0.240	1.14	0.99	0–3.0

[a] The symbols have been defined in previous tables.
[b] The solid branch is too short to determine the pressure with any accuracy.

TABLE VI. Equation of state and the collision rate for 108 particles.

v/v_0[a]	$(pv/NkT)-1$	Γ/Γ_0	R[a]	C[a]
1.0306	99.02	34.3	1.00	0–5.0
1.2500	13.68	5.70	1.00	0–5.5
1.3448	10.65	4.89	1.02	0–4.6
1.4200	9.34	4.48	1.01	0–2.6
1.5000	8.36	4.24	1.01	0–13.9
1.5500(s)	8.20	4.31	1.01	0–3.0
1.5500(f)	9.84	5.09	1.00	3.7–29.7
1.6000(s)[b]	8.13	4.36	1.00	0–1.9
1.6000(f)	8.87	4.67	0.98	2.2–34.0
1.6500(s)[b]	7.73	4.01	...	0–0.7
1.6500(f)	8.30	4.58	1.00	0.7–4.2
1.7000	7.61	4.35	1.00	0–33.0
1.7678	6.83	3.90	0.97	0–5.4

[a] The symbols have been defined in previous tables.
[b] The accuracy of the results at these densities is poor due to the short existence of these branches.

TABLE VII. Equation of state and the collision rate for 256 particles.

v/v_0[a]	$(pv/NkT)-1$	Γ/Γ_0	R[a]	C[a]
1.5000	8.34	4.12	0.98	0–3.0
1.6000(s)	7.52	3.98	0.99	0–2.5
1.6000(f)	8.96	4.87	1.01	4.9–9.5
1.7678(s)	6.37	3.87	1.02	0–3.7
1.7678(f)	6.88	4.09	1.00	5.0–9.2
2.0000	4.81	3.21	0.99	0–3.0

[a] The symbols have been defined in previous tables.

TABLE VIII. Equation of state and the collision rate for 500 particles.

v/v_0[a]	$(pv/NkT)-1$	Γ/Γ_0	R[a]	C[a]
1.6000(s)	7.68	4.07	0.98	0–6.2
1.6000(f)	8.91	4.82	1.00	11.0–22.5
1.6500	7.06	3.84	0.98	0–3.0
1.7000	6.67	3.79	0.99	0–3.2
1.7678	6.36	3.73	0.99	0–2.8

[a] The symbols have been defined in previous tables.

TABLE IX. Equation of state and the collision rate for 32 particles in the compressed-fluid region.

v/v_0	$(pv/NkT)-1$	Γ/Γ_0	R[b]	C[b]	$v/v_0-0.1506$
1.1546[a]	700	300	1.10	0–1.4	1.0040
1.1987	64.1	26.2	1.01	0–1.1	1.0481
1.2496	30.8	13.1	1.01	0–1.4	1.0990
1.2982	22.5	9.37	0.95	0–1.2	1.1476
1.3443	18.3	8.10	0.98	0–1.4	1.1937
1.4017	14.7	6.93	1.00	0–1.4	1.2511
1.4948	11.2	5.55	0.99	0–1.3	1.3442
1.5981	9.20	4.98	1.00	0–1.2	1.4475

[a] The system was carried to a density of $v/v_0=1.1546$, but $(pv/NkT)-1$ was so high that with the short run available the pressure could not be determined accurately.
[b] The symbols have been defined in previous tables.

TABLE X. Equation of state for 100 particles, initially always in a random configuration.

v/v_0	$(pv/NkT)-1$	C[a]	$(pv^b/NkT)-1$
1.2279	21.5	0–4.0	
1.3448	13.3	0–3.5	
1.7678	6.70	0–4.3	
2.0000	4.81	0–5.6	
2.722	2.47	0–1.9	
14.142	0.237	0–2.8	0.240
30.43	0.104	0–3.2	0.104
86.07	0.0359	0–1.9	0.0352

[a] The number of collisions in units of 1000 collisions the problem has been run.
[b] From the five-term virial expansion.

TABLE XI. Equation of state for 31 particles, initially in a face-centered lattice with one particle left out.

v/v_0	v/v_0[a]	pv_0/NkT	$(pv/NkT)-1$	C
1.2903	1.2500	11.4	13.75	0–2.0
1.4464	1.4012	7.28	9.53	0–7.2
1.5484(s)	1.5000	5.88	8.11	0–1.0
1.5484(f)	1.5000	7.23	10.19	3.0–7.0

[a] The value of v/v_0 if there were 32 particles present.

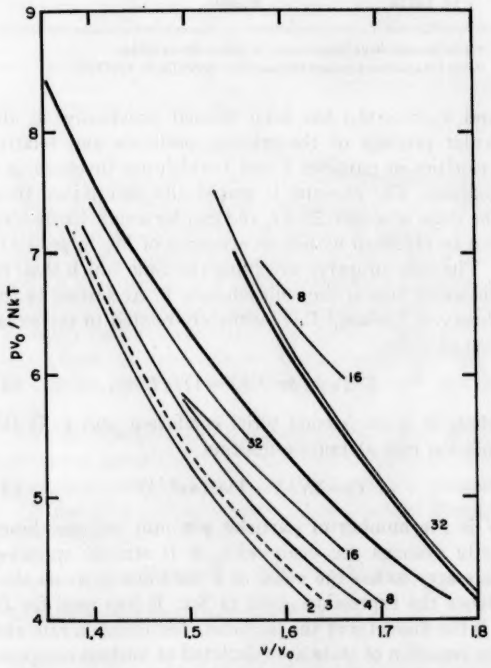

FIG. 1. Equation of state in the transition region. Both the fluid and solid branches are plotted for those numbers of particles where each was found. The curves are labeled by the number of particles. The heavy lines refer to systems which contain 96 or more particles.

cathode ray tube pictures displayed in paper I[1] clearly showed, the lower branch of the system is solidlike and the upper branch is fluidlike. It was found that the system stayed in the lower branch for quite a long calculating time, then suddenly jumped to the upper branch and stayed there for quite a long calculating time before jumping back to the solid branch again. The transition between the two branches occurs so infrequently that it was not possible to get enough statistics to establish the average time the system spends in each branch. Thus, each branch is plotted separately. Even if an average pressure could be established in this density region its significance would not be clear.

Thus, in these small systems it is not possible to have solid and fluid together in equilibrium, but the whole system is in either one phase or the other. The accessible region of phase space might be considered as consisting of two pockets, one solid, the other liquid, connected by a narrow passage. The narrow passage represents the relatively improbable cooperative motion among the particles necessary to let a particles escape out of its cell and turn a solid into a liquid. The reverse process also is improbable since a cooperative motion among a set of particles is required to form a small ordered region. For these small systems such processes are made more unlikely, because the solid has to crystallize in a particular orientation. For larger systems this is not necessary so that presumably the passage between the two pockets enlarges for this reason. On the other hand, the crystallites could be bigger so that more particles might be involved in the cooperative motion, causing a narrowing of the passage. If there is to be a first-order phase change, crystals must exist in equilibrium with the fluid; that means that the passage must not be choked off in larger systems. The passage can, however, be still quite narrow so that it might take a large amount of calculating time to establish equilibrium, but the system is large enough so that part of the system is in the solid phase and part in the liquid one.

The question of what actually happens is not settled yet, but can probably be settled by the study of large two dimensional systems. From the results presented in Table XII it appears that the passage widens as the number of particles increase. Table XII shows that as the number of particles increases it takes fewer and fewer collisions per particle to go from an initial solid state to the fluid state at a given density. These results are for a single run for all the different systems and hence large statistical fluctuations can be expected. Nevertheless the trend is clearly established. Table XII also shows the number of collisions necessary to go from the lower branch to the upper branch as judged by the interval from the point at which the pressure first increases to the point at which the pressure steadies down to the upper branch value. The fact that the transition region between these two states persists longer as the number of particles increases also indicates that the passage widens, because the systems spend more time in the partially melted state. Without referring to the picture just presented one can say that the partially melted region becomes more stable for larger systems, so that for large enough systems that state might become stable for very long times and a first-order phase transition would then exist.

Returning to the picture of phase space, as the density changes the pockets change relatively in size. Thus, at higher densities the solid pocket grows at the expense of the liquid pocket. This means that the system spends more time in the solid pocket and attempts fewer entries into the passage to the liquid side. At the same time, however, the passage also narrows, since a more improbable fluctuation is involved in turning a denser solid at least partially into a fluid. This picture is confirmed by the results in Table XIII, where the density dependence of the transition is studied for a set number of particles. At higher densities the transition from the solid to the fluid state requires many more collisions, until finally at v/v_0 of 1.50 it was impossible to cause the transition to take place. Since the passage is wider for larger systems, it can be expected that at higher densities than for smaller systems it will still be possible to reach the fluid state. Eventually, however, the passage should be choked off at high but finite densities, but, as will be seen, the liquid pocket can still persist as a metastable state. In any case these considerations are in accordance with the sensitive dependence of the results on density.

TABLE XII. Occurrence of the first transition from the solid to the fluid state at a given density ($v/v_0=1.60$) for various numbers of particles and the duration of the transition.

N	collisions/particle	duration[a] (collisions/particle)
8	350	
16	240	
32	310	
96	54	...
108	35	6
256	20	19
500	25	19

[a] For the small systems the duration of the transition is too short to be accurately determined, but they are of the order of one collision per particle.

TABLE XIII. Occurrence of the first major transition from the solid to the fluid state for a given number of particles (32) as a function of density.

v/v_0	collisions/particle
1.52500	5800
1.53000	4700
1.53125	260
1.53250	560
1.53500	150
1.54000	25
1.55000	310
1.60000	310

Figure 1 also demonstrates the systematic variation of the results with the number of particles. It is found that the larger systems have a higher pressure in the solid phase than the smaller systems, while in the fluid phase just the reverse is true. However, for systems greater than about 100 particles the pressure is no longer different within the accuracy of the results. These systems form the heavy curve drawn in Fig. 1. For 100 or more particles all the second neighbors of a given particle are in the same cell, while for 32 particles some of these second neighbors are in the adjacent cell. Because of the periodic boundary condition this means that these second neighbors are not all independent of each other in their motion, that is, some of them have identical histories. For systems with less than 32 particles even the nearest neighbors are not independent. This apparently causes the fairly large change in the results for very small systems. Once the first neighbors are correctly treated the results are close to the behavior of larger systems. Whether third neighbors are treated independently or not is apparently of not much quantitative significance except as far as the phase transition is concerned. There many particles are needed to represent a crystallite in equilibrium with a fluid.

The two-state behavior was found over a region of density of $1.5<v/v_0<1.7$. Above v/v_0 of about 1.7 the solid system which was initially set up almost immediately lost the ordered configuration, and hence did not stay on the lower pressure branch for an observable time. Systems with $v/v_0<1.525$ remained in the lower branch and in the original configuration for very long runs.

The results of the free volume theory[8] are given in Fig. 1 by the curve labeled 2. From the point of view of periodic boundary conditions one particle surrounded by its neighbors at fixed positions is generated by a two-particle system, the second particle representing all the neighbors. A one-particle-per-cell system with periodic boundary conditions leads to no collisions and hence a perfect gas equation of state. This free-volume theory uses the smeared-out neighbor approximation, that is, the central particle is confined to an equivalent sphere rather than the exact, but geometrically complex, region that is accessible in between the neighboring spheres when they are located on lattice positions. If the latter free volume is calculated[9] the pressure is raised but not nearly enough to bring it into agreement with the larger system results.

The dotted curve labeled 3 in Fig. 1 refers similarly to a free-volume theory, but one in which two particles are confined to a cell determined by their neighbors.[10] The curve is dotted because it is not the accurate result of such a calculation. Because of the complexity of the calculation some mathematical approximations had to be used in order to apply the theory to this region of density. Again the results are in the right direction from the two-particle theory but not large enough.

A characteristic of the free-volume theory and of very small periodic systems is that density fluctuations are suppressed. This could make the pressure too low as compared to an infinite system. Thus, if $P(\rho)$ is the pressure as a function of density, according to the free volume theory, then the effect of fluctuations can be calculated as a perturbation. Let ρ_0 be the average density and let $f(\rho)$ be the distribution of densities in the region of an atom. That is, $f(\rho)$ is related to the distribution of nearest-neighbor configurations or cell sizes which would be found in an infinite system. Then,

$$\bar{P}=\int_0^\infty P(\rho)f(\rho)\,d\rho.$$

Expanding $P(\rho)$ in a Taylor series about ρ_0 yields

$$\bar{P}=P(\rho_0)\int_0^\infty f(\rho)\,d\rho+(dP/d\rho)\,|_{\rho_0}\int_0^\infty(\rho-\rho_0)f(\rho)\,d\rho$$

$$+\tfrac{1}{2}(d^2P/d\rho^2)\,|_{\rho_0}\int_0^\infty(\rho-\rho_0)^2f(\rho)\,d\rho+\cdots,$$

and since

$$\int_0^\infty f(\rho)\,d\rho=1$$

and

$$\int_0^\infty \rho f(\rho)\,d\rho=\rho_0,$$

$$\bar{P}=P(\rho_0)+\tfrac{1}{2}(d^2P/d\rho^2)\,|_{\rho_0}\int_0^\infty(\rho-\rho_0)^2f(\rho)\,d\rho$$

$$+\text{ higher order terms.}$$

At very high densities where density fluctuations are inhibited, $f(\rho)$ is a delta function centered at ρ_0 so the integral in the above equation vanishes.

Thus, as can be seen from Fig. 1 and particularly from Fig. 3, at densities near close-packing, the free-volume theory calculates the pressure very accurately. At densities lower than that of close-packing, the integral is positive so that P is larger than $P(\rho_0)$ since $d^2P/d\rho^2$ is positive. The amount of fluctuation in density, that is the width of the function $f(\rho)$, grows with increasing system size so that the larger systems in this density range should show higher pressures.

The free-volume theory is a model applicable in the solid state in as much as the neighboring particles are strictly confined to a lattice. It is, therefore, not surprising that the two-state behavior is not found for this theory. The larger systems investigated on the calculating machine are akin to the cell theory, as previously implied, when periodic boundary condi-

[8] J. E. Lennard-Jones and A. F. Devonshire, Proc. Roy. Soc. (London) **A163,** 53 (1937).
[9] R. J. Buehler, R. H. Wentorf, J. O. Hirschfelder, and C. F. Curtiss, J. Chem. Phys. **19,** 61 (1951).
[10] J. de Boer, Physica **20,** 655 (1954); **21,** 137 (1955).

tions are used. For example, the same results for the equation of state are obtained when two particles are studied on a body-centered cubic lattice with periodic boundary conditions and when the free-volume theory for that situation is worked out. Thus larger systems are merely cell theories with more particles per cell. The question is, then, how many particles per cell are necessary to get away from an ordered state and create the opportunity to produce a disordered state. As Fig. 1 shows, the three-particle analytical theory did not show a disordered state; neither does the four-particle system worked out on the computer.

The four-particle system is the smallest cubic unit of a face-centered lattice. Since the system is so small, it was necessary in the calculation to anticipate collisions with a particle and also with its periodic continuations in neighboring boxes. This causes such small systems to be not nearly so fast to run on the computers as one might at first think. Nevertheless, quite long runs were made without finding a transition to a fluid-like state. However, a comparison of the positions of particles initially and after some collisions had taken place, showed that particles had switched positions for values of $v/v_0 \geq 1.80$ while they were still in their original order for $v/v_0 \leq 1.7-$ at the end of the run. This means that although particles are free to interchange, it is not possible to create any disorder in the system, because after the interchange the particles are again in a regular arrangement near lattice positions. The value of v/v_0 at which interchange can first take place is a reasonable one. Interchange can first occur roughly when two particles can slip past each other along the diagonal of the unit cube after a third one is placed on the corner. This means that the diagonal length ($\sqrt{3}$) has to be equal to 3σ or $v/v_0 = 1.837$. By cooperative motion of three particles a rotation of the three (equivalent to an interchange) can occur at slightly higher densities in agreement with the facts.

For systems containing eight or more particles the two-state behavior was obtained, though with eight-particle systems the fluid state was reached in only a few cases, and then after rather long runs. The eight-particle system consisted of two unit cubes containing four particles each placed next to each other. The resulting periodic space consisted of rectangular parallelopipeds. Similarly for the 16-particle system two of the eight-particle cells were placed next to each other. The 32-particle system again has a cubic cell when two of these 16-particle cells are combined. Figure 1 shows that the difference in the pressure for the two states is larger for the smaller systems. An explanation of why the fluid pressure is higher for the smaller system might be that when these systems get into the disordered state it is impossible to establish the proper local order. Because for the eight- and 16-particle systems the nearest neighbors are not independent, it is not possible to relax the position of one neighbor if the other neighbor is in a favorable position. In other words, there is

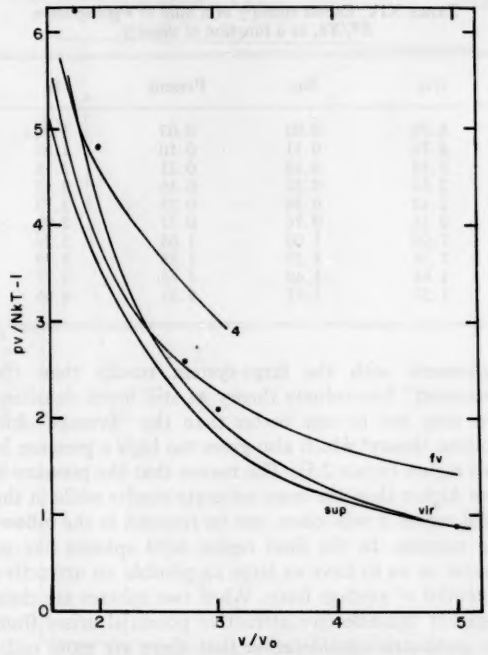

FIG. 2. Equation of state in the low-density region. The symbols labeling the curve mean: sup=superposition theory, vir=five-term virial expansion, fv=free-volume theory, 4=four-particle results, and the dots refer to the machine calculations for systems with 32 or more particles.

order among the correlated neighbors but the system overall is more jammed up than in larger systems because less flexibility is available. This jamming causes a higher pressure.[11] The very same reason caused a lower pressure in the solid branch. Less flexibility in the solid phase meant that the correlated neighbors were always the same distance apart so that if a particle collides with one member of a correlated set it will certainly be far away from some of the others. This effect was described previously as an inhibition of fluctuation in cell size.

(B) Low Densities

Figure 2 compares the molecular dynamics results with various analytical theories in the dense-gas region. The dots refer to the results for larger systems. The free-volume theory (labeled fv) is just not applicable in this region and results in pressures which are too high. Because the curves for small systems cross the curve for larger systems at different densities it misleadingly appears that the four-particle theory gives a worse result than the two-particle theory at low densities. The four-particle theory is probably in better

[11] See the next paragraph which explains the same phenomena in an equivalent way, namely, the inability of the system to form clusters.

TABLE XIV. Excess entropy of a fluid of rigid spheres, S^E/Nk, as a function of density.

v/v_0	Sup	Present	fv
8.38	0.03	0.03	1.36
4.74	0.11	0.10	1.81
3.48	0.23	0.21	2.16
2.83	0.37	0.36	2.45
2.42	0.56	0.55	2.73
2.15	0.76	0.77	2.98
1.94	1.00	1.04	3.24
1.78	1.23	1.35	3.49
1.64	1.49	1.76	3.77
1.53	1.77	2.21	4.05

agreement with the large-system results than the "smeared" free-volume theory at still lower densities, but may not be any better than the "average" free volume theory[9] which also gives too high a pressure in this region ($v/v_0 > 2.5$). The reason that the pressure is now higher than the more accurate results while in the solid region it was lower, can be restated in the following manner. In the fluid region hard spheres like to cluster so as to have as large as possible an attractive potential of average force. When two spheres are close together this effective attractive potential arises from the geometric consideration that there are more collisions forcing the two spheres together than forcing them apart. The cell theory prevents this clustering by confining the neighboring particles to their lattice positions; the effective attractive potential is hence less and the pressure higher.

The superposition theory of Kirkwood[12] treats the distribution of particles in a much more satisfactory manner, as can be seen by the better results in Fig. 2. (The curve labeled sup) In fact, it was the prediction of the superposition theory[13] that hard spheres have a solid-fluid-like phase transition at a v/v_0 of about 1.5 that lead originally to this investigation. That something unusual happens there is demonstrated in this report. We hope in a later report to make a more detailed comparison of the superposition theory with the present results for both the pair and triplet distribution function. This allows a direct checking of the validity of the Kirkwood approximation. It can be anticipated that the pair and triplet distribution functions compare almost quantitatively but that some finer details are left out in the superposition approximation. This can be ascribed to the fact[14] that the superposition approximation is equivalent to leaving out some of the highly linked cluster diagrams in the rigorous Mayer cluster expansion. It is because of these omitted terms that the pressure calculated from the theory for hard spheres is too low. These highly linked diagrams become relatively more important at high densities, so that at lower densities the theory is quantitatively correct. Unfortunately, however, in the interesting liquid-density region the theory is only semiquantitative, but still the best analytic theory available.

To carry the theory logically one step further by making the superposition approximation in the space of four molecules (the free-volume theory carries it out in the space of only two molecules[15]) is a formidable mathematical problem. Even if this were done, as the previous discussion showed, it would not yet lead to quantitative results. In order to get quantitative results the superposition approximation would have to be made in the space of 20 or so molecules. Even a solution of the equation resulting from the superposition approximation with four particles would require extensive use of computers, so it was felt best to try the present calculational approach to learn more about what is ultimately required of an analytical description of the classical many-body problem.

The study of the entropy clearly shows the superiority of the superposition theory over the free-volume theory. Table XIV makes such a comparison of the excess entropy, S^E, defined as follows,

$$S = -Nk \ln p + S^*(T) + S^E,$$

where

$$S^E/Nk = \int_\infty^{v/v_0} [(pv/NkT) - 1](v_0/v)\, d(v/v_0) + \ln(pv/NkT), \quad (4)$$

and

$$S^*(T) = \lim_{p \to 0} [S + Nk \ln p].$$

S^E is the excess entropy at constant pressure over that of an ideal gas. The free-volume theory gives much too low an entropy because the particles are ordered on lattice positions. However, when the free-volume theory is considered from the point view of a two-particle periodic boundary-condition problem then the entropy is considerably raised even though the equation of state is the same for the body-centered cubic lattice. We hope to discuss this more fully in a later paper. The excess entropy calculated from the superposition theory is in quite good agreement with the present results. Only at the highest density does any discrepancy appear.

Figure 2 also shows the pressure resulting from the five term virial expansion (labeled vir)

$$(pv/NkT) - 1 = (b/v) + 0.625(b/v)^2 + 0.287(b/v)^3 + 0.115(b/v)^4. \quad (5)$$

At low density perfect agreement with this expression is obtained as it must be (see Table X). At higher densities the expansion no longer converges; however further terms are hard to evaluate analytically. These further terms are also hard to get from the numerical results

[12] J. G. Kirkwood, J. Chem. Phys. **3**, 300 (1935).
[13] J. G. Kirkwood, E. K. Maun, and B. J. Alder, J. Chem. Phys. **18**, 1040 (1950).
[14] B. R. A. Nijboer and L. van Hove, Phys. Rev. **85**, 777 (1952).
[15] J. G. Kirkwood, J. Chem. Phys. **18**, 380 (1950).

because no effort has been made to obtain precise and more data points in the intermediate-density region. The precision required of the data is very high in order to say with confidence what the next virial coefficients are going to be. All that can be said with confidence with the available results is that the sixth and seventh virial coefficients are positive. The data can be empirically fitted up to the transition density adding a term $0.079(b/v)^5$ to Eq. (5). Only slight improvement can be obtained over this fit by adding two terms $0.046(b/v)^5+0.02(b/v)^6$. These terms may not have any relation to the theoretical higher virial coefficients.

The fact that all the known virial coefficients are positive has theoretical impact on the question of the divergence of the virial expansion for hard spheres. If they were all positive it would be of course impossible to get a flat pressure volume region or a van der Waals loop indicative of a first-order phase transition. If there then is a phase transition, with all the coefficients positive, the series either diverges at the phase transition or, what appears more likely, the series continues into a metastable fluid region. This region can be artifically generated on the calculator and will be discussed in the next section. The earlier Monte Carlo results[16] had indicated that some of the higher virial coefficients are negative. This was in error due to insufficiently long runs.[4]

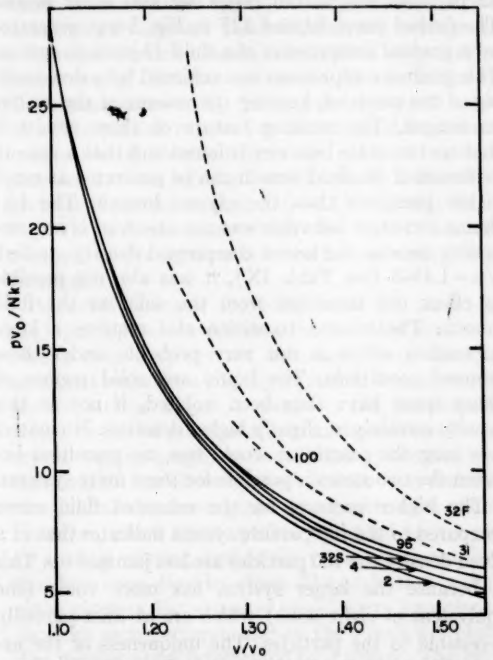

FIG. 3. Equation of state in the high-density region. The curves are labeled by the number of particles which were used. For 32 particles both the solid and fluid branch are graphed. The significance of the dotted lines is that these curves were obtained by using unusual initial configurations and hence these curves do not represent a usual equilibrium state of the system.

[16] M. N. Rosenbluth and A. W. Rosenbluth, J. Chem. Phys. **22**, 881 (1954).

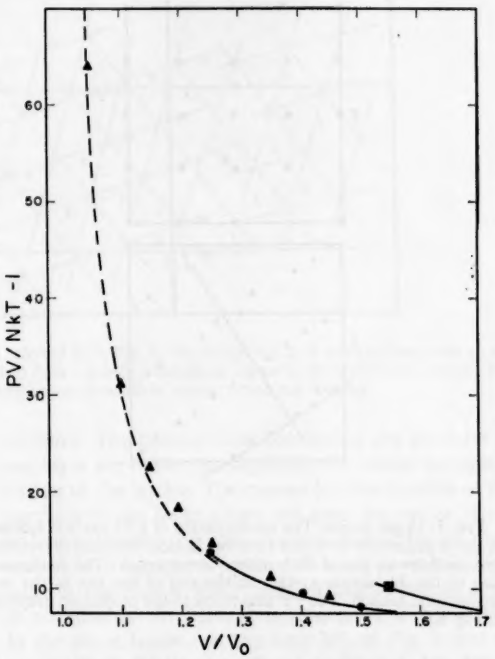

FIG. 4. Equation of state in the high-density region. The solid lines represent the data for the 32-particle system in the solid and fluid branches. The dashed line is calculated by the free-volume theory in the region where it is accurate. The triangles represent the equation of state for 32 particles in the extended fluid branch when that data has been corrected by subtracting an empirically determined constant from v/v_0 (Table IX). The dots represent the equation of state for 31 particles when their close-packed volume has been corrected to that of 32 particles. The square represents an uncorrected point on the fluid branch of the 31-particle system.

(C) High-Density Region

The high-density results for the equation of state are shown in Fig. 3. As mentioned before, there is a systematic trend in the pressure with the number of particles (solid lines) but the differences vanish at high enough densities. The 96-particle results are plotted explicitly although they do not significantly differ from the other large-system results. This is of interest because the 96-particle system was placed into a hexagonal closed-packed lattice with a rectangular parallelopiped box while all the other large systems were in a cubic box containing a face-centered crystal. These two lattices differ only in the arrangement of the third nearest neighbors of a particle. As has already been seen, these third neighbors do not significantly affect the results and hence it is not surprising that the hexagonal and face-centered lattice results agree over the entire density region.

The dotted curves in Fig. 3 demonstrate that in the

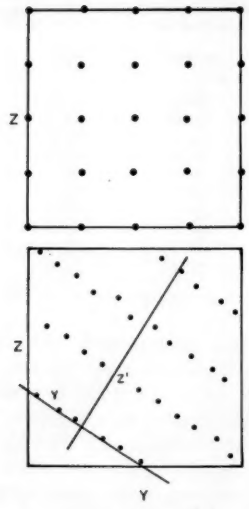

FIG. 5. Upper graph: The configuration of a 32-particle system in the yz projection for a face-centered lattice. Each dot represents two particles on top of each other. Lower graph: The configuration of the 32-particle system at the end of the run in the extended fluid branch. The $y'z'$ axis refers to the projection graphed in Fig. 6.

solid region for these small systems the results depend on the number of particles studied as well as their initial configuration. In the fluid phase these factors did not influence the pressure, as the results for 100 particles in Table X show. The 100 particles were initially placed in some random configuration, but one which allowed the spheres to be quite tightly packed, so that quite high densities could be achieved. The density could then be lowered by shrinking the diameter of the spheres, keeping the cubic box the same dimensions. At high densities the system could not rearrange itself to a perfect crystal as the higher pressure in Fig. 3 indicates. Even if this system were able to unjam itself it could not form a perfect crystal but only one with eight holes, since that is required by the periodic boundary conditions for a face-centered cubic lattice. However, when the density was lowered to that of a fluid, the system was able to rearrange itself to obtain the proper local order.

A system with an artifically introduced single hole was then set up to study its behavior in this region. The resultant 31-particle pressure is shown in Fig. 3, and it is again higher in the solid region, but not as high as the 100-particle system since it is much more ordered. However, again, as the square point in Fig. 4 shows, in the fluid region the pressure is the same as that of a 32-particle system. The results on the solid side can, however, be understood if it is considered that the hole is just an inaccessible region to the system, in other words, the 31-particle system behaves like a 32-particle system. Thus, if the close-packed volume, v_0, is converted to that of a 32-particle system, the dots in Fig. 4 result, yielding perfect agreement in the pressure with that of the perfect crystal. Actually the agreement should not be perfect since the particles surrounding the hole have a slightly larger volume accessible to them, so that the pressure should be slightly smaller than that of a perfect crystal. At high densities of the solid even this difference should disappear, since the particles surrounding the hole are completely locked in. Within the accuracy of the present results this difference could not be picked up even at the lowest solid densities.

It is of interest to check whether this hole has moved during a run from the point of view of diffusion theory. A mechanism of diffusion in solids is by means of a particle moving into the hole leaving a hole in its stead. Even if this did not take place it would not alter the above argument for changing v_0. An examination of the positions of the particles at the end of the rather short run at the lowest solid density showed that this phenomenon had not occurred. This is not surprising since such a motion would involve a highly cooperative movement of the particles surrounding the hole. Furthermore, the few particles used seriously restrict such fluctuations.

The extension of the fluid branch to solid volumes for 32 particles was accomplished by still other means. The dashed curve labeled 32F in Fig. 3 was generated by a gradual compression of a fluid 32-particle system. This gradual compression was achieved by a slow swelling of the particles, keeping the volume of the system unchanged. The striking feature of these results is that no two-state behavior is found and that a smooth extension of the fluid branch can be generated at much higher pressures than the crystal branch. The fact that a two-state behavior was not observed is not surprising since at the lowest compressed density studied, $v/v_0=1.4948$ (see Table IX), it was also not possible to effect the transition from the solid to the fluid branch. The reverse transition also requires a large fluctuation which is not very probable under these jammed conditions. The liquid and solid regions of phase space have thus been isolated, if not at this density certainly at slightly higher densities. No matter how long the calculator would run, no transition between the two states is possible for these finite systems.

The higher pressure for the extended fluid curve compared to the 100-particle system indicates that at a given density the 100 particles are less jammed up. This is because the larger system has more voids (the equivalent of eight holes) which are at least partially accessible to the particles. The uniqueness of the extended fluid branch has not been investigated, since only a single run has been made. It might be expected that there exists a fairly narrow band of curves extending the fluid branch depending on from what particular configuration the compression was started. The only relevant data on this was obtained by the Monte Carlo

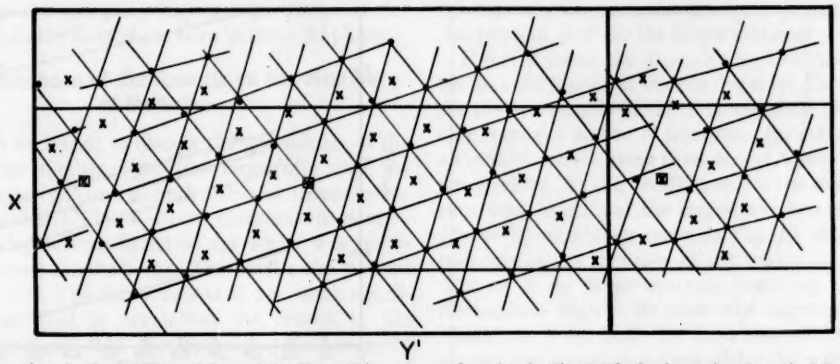

FIG. 6. The xy' projection of the positions of the 32-particle system referred to in Fig. 5. The horizontal and vertical lines refer to the repeat planes due to the periodic boundary conditions. The crosshatched lines connect positions of atoms in the lower layer (dots). The crosses represent positions of atoms in the layer above. The squares represent location of atoms which are missing.

method[17] using a similar procedure for 32 particles. The curves do differ in some detail but are over-all in substantial agreement.

Since it was possible to understand the behavior of the 31-particle system by correcting its close-packed volume, it should be possible to do the same thing for these other disordered systems except that the close-packed volume has to be found empirically. In other words, a free-volume type of theory should still work since the particles are localized, but the average free-volume per particle cannot be calculated from a crystal lattice model. The free volume could be calculated if the volume taken up by the imperfections were known. The close-packed volume for the extended fluid branch system was determined from the point at which the pressure became infinite (about $v/v_0=1.1506$). If the pressure is plotted against $v/v_0-0.1506$ (Table IX and Fig. 4) good agreement with the crystal branch is obtained in the region where the free-volume theory is accurate.

An examination of the positions of the particles at the highest density studied on the extended fluid branch reveals that they are not in a completely disordered array but rather in a slightly imperfect hexagonal close-packed lattice. Figure 5 compares the positions projected in the yz plane of a perfect face-centered cubic crystal (upper graph) to that found at the end of the compression run (lower graph). It is obvious that on an over-all basis the lower graph shows quite a bit of order. However, where the z' symbol is located on the graph an atom is missing, and in the plane above and below that hole some disorder exists. The projection in the xy' plane given in Fig. 6 makes this clearer. Two planes of particles each perpendicular to the z' axis are plotted. The missing atom is indicated by a square. The crystal does not repeat every cube in the y' direction but every three cubes as indicated by the heavy vertical line. However, in the x direction the repetition distance is the usual one of every cube as indicated by the horizontal lines. The crossed lines connecting the particles in one layer are drawn to emphasize the nearly hexagonal nature of the lattice. The crosses for the location of the particles in the layer above fall near the center of the triangles formed by the crosshatched lines as they should for a hexagonal lattice. There appears to be one fault in the crystal which might be described as a slip in addition to the hole. It is associated with the hole in the plane below (on the very left of Fig. 6 and repeated periodically just to the right of the heavy vertical line for purposes of clearer demonstration). The particles above the hole are quite regularly arranged as shown in the middle of the box in Fig. 6. The slip also appears very clearly again (about $\frac{3}{4}$ over in the box) in the upper layer of particles marked by crosses.

Undoubtedly these same imperfections would not appear each time such a compression was tried, as mentioned earlier. However, there are only a limited number of ways to have imperfections in such small systems. What would happen if the same thing were tried on larger systems is pure speculation. Very likely, however, a similar slightly disordered system would result if the fluid state compressed so fast that not enough time were allowed to reach the equilibrium state at each density. This behavior is quite analogous to cooling a liquid so fast that a glass forms. A glass is also believed to give a high degree of local order. Larger systems can, of course, have more complicated imperfections; however, it is the instantaneous local arrangements in the fluid that primarily determines what sort of faults are frozen in.

(D) Collision Rate

The results for the collision rate relative to the collision rate at infinite dilution for the various systems are given in Tables I through IX, and some of the results are graphically presented in Fig. 7. The collision rate ratio generally conforms to the behavior of the equation of state. Thus, as Fig. 7 shows, the collision rates for systems of less than 96 particles are low on the

[17] W. W. Wood, (private communication).

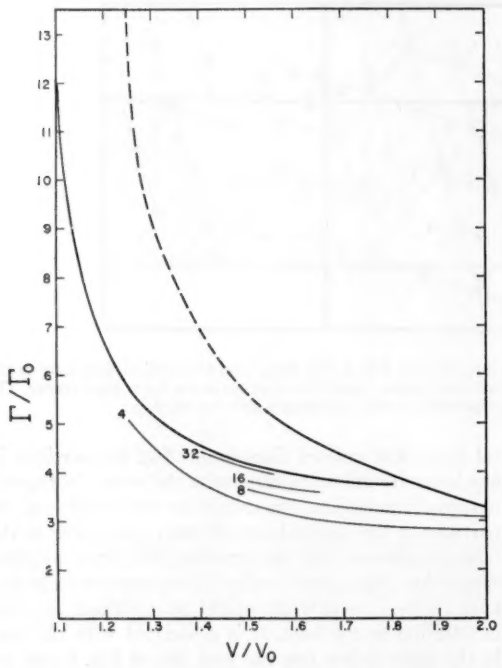

FIG. 7. Collision rate relative to the Boltzmann collision rate as a function of v/v_0. The fluid branch is represented by the upper curve for systems of 32 particles and larger. The dashed curve represents the extended fluid branch. The solid branch is represented by the heavy curve for systems of 96 particles and larger, and by the labeled curves for smaller systems.

solid branch just as the equation of state is. The collision rates for eight-particle systems in the fluid branch seem unusually low (Table II) although the pressures are high.

As Eq. (2) shows, the collision rate ratio is purely a function of the equation of state according to the theory of Enskog. The R column in Tables I through IX is the ratio of the experimental value of Γ/Γ_0 to the theoretical one. The theoretical one is determined by the use of the equation of state as obtained by the computer work for the same system. A striking confirmation of the Enskog theory of collision rates is obtained for systems larger than 32 particles, which shows that this ratio is unity within statistical significance at all densities. This in turn implies that the molecular chaos approximation made by the Enskog theory is a valid one insofar as the collision rate is concerned. The validity of this assumption[7] at solid densities is certainly doubtful. The result then probably means that the collision rate is insensitive to this approximation. However, when artificial velocity correlations are introduced among the nearest neighbors of a particle as in small systems, the experimental to theoretical collision rate does reflect this correlation. This ratio is less than unity and the deviation is the largest for the smallest system. It is remarkable that this deviation is independent of density within the accuracy of the results; although the eight-

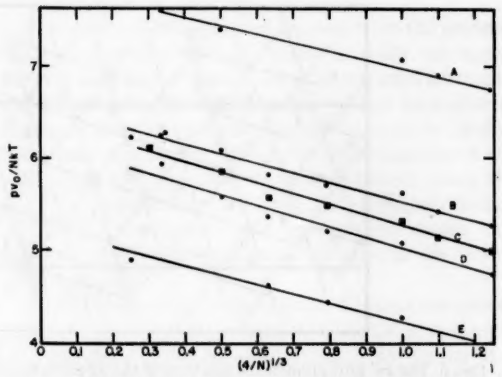

FIG. 9. Dependence of the equation of state on the number of particles at higher density. Curves A, B, C, D, and E refer to, respectively, $v/v_0=1.4$, 1.5, 1.525, 1.55, and 1.65 in the solid branch.

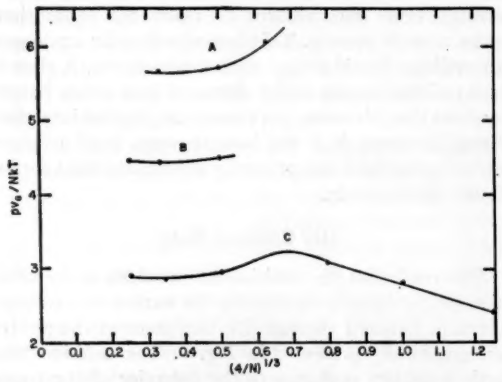

FIG. 8. Dependence of the equation of state on the number of particles at lower density. Curve A refers to $v/v_0=1.65$, curve B to $v/v_0=1.7678$ and curve C to $v/v_0=2.0$ in the fluid branch.

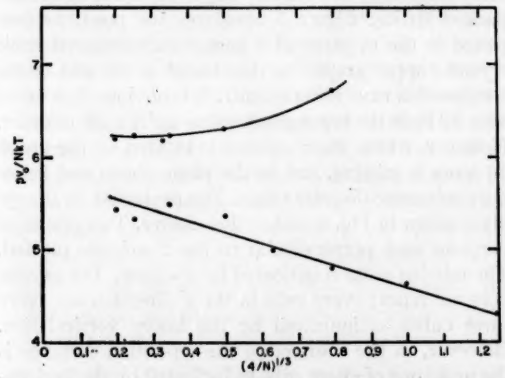

FIG. 10. Dependence of the equation of state on the number of particles for $v/v_0=1.60$ in both the fluid and solid branch.

particle case is a spurious exception, the deviation was much larger in the fluid phase than in the solid phase.

(E) Dependence of the Results on the Number of Particles

Although we intend to discuss the dependence of the results on the number of particles more fully when the study of larger systems in both two and three dimensions is completed, Figs. 8–10 are presented to demonstrate the dependence found so far which was previously discussed qualitatively. The results are plotted against $(4/N)^{\frac{1}{3}}$. The factor four is of not much significance except that it normalizes the results to the smallest cubic cell that can generate a face-centered lattice. The choice of the reciprocal one-third power of the number of particles which is characteristic of the linear dimensions of the system has been chosen empirically as the power which makes the graphs most nearly linear.

It is only at low density that it has been possible to investigate theoretically the dependence of the results on the number of particles. The first few virial coefficients for an infinite system (subscript ∞) of hard spheres are related to those of a finite periodic system[18] (subscript N) by

$$B_N = B_\infty(1-1/N)$$

$$C_N = C_\infty[1+(1/5N)-(6/5N^2)],$$

where B and C are the second and third virial coefficients. For one particle these expressions correctly reduce the virial coefficients to zero and for a system as small as 32 particles the corrections are already small. For dense gas systems the results are given in Fig. 8 and show that the pressure first increases as N increases and then decreases very slightly (curve C). At higher densities, but still in the fluid region, the pressure decreases monotonically as N increases (curves A and B). All curves show that the results have become pretty independent of N for the larger systems.

Figure 9 shows the dependence of the pressure on N for the solid branch at various densities. The lines drawn are the best ones to fit the data and show that the pressure increases as the N increases. An extrapolation to an infinite system along these straight lines is, however, not justified. At the densities where the most extensive runs were made and the largest systems were studied (curve B) and lower curve in Fig. 10, the results appear within the accuracy of the results to be independent of N for larger systems justifying the previous discussions. Figure 10 plots the dependence of the results on N for both the fluid and solid branch of a system and shows that even under the worst condition of extrapolation of the solid branch the pressure difference between the two branches does not vanish.

[18] I. Oppenheim and P. Mazur, Physica **23**, 197 (1957).

CONCLUSION

It appears that systems as small as 100 particles are sufficient to describe accurately the equilibrium behavior in the fluid region of hard spheres. In the two-state region four particles are insufficient to establish both states and 500 particles are insufficient to make the two states coexist. In the solid region for these small systems the initial state of the system and the number of particles must be selected so as to achieve the lowest free energy.

The Enskog theory for the collision rate is valid over the entire density region, while the free-volume theory is valid only at high densities and the superposition theory at low densities. In the intermediate-density region analytical theories for the equation of state have to take into account higher-order correlations between the particles.

ACKNOWLEDGMENTS

We wish to thank Dr. S. Fernbach for making a large amount of computing time available and M. Mansigh and S. Campbell for their coding help.

Surface Specific Heat of an Isotropic Solid at Low Temperatures*

MARC DUPUIS,† ROBERT MAZO,‡ AND LARS ONSAGER

Sterling Chemistry Laboratory,§ Yale University, New Haven, Connecticut

(Received May 12, 1960)

The effect of realistic boundary conditions on the computation of the specific heat of an isotropic solid at low temperatures is investigated. Two cases are considered: the surface free of stress and the surface rigidly clamped. The first of these is the one of physical interest. For both cases a term in the specific heat arises which is proportional to the surface area and to T^2 and appreciably higher than Montroll's result in the case of the free solid. The effect of approximations introduced during the computation is estimated. Available experimental data are not adequate for a critical test of the theory.

INTRODUCTION

THE Debye theory for the specific heat of a solid is usually presented using an elastic parallelopiped with boundary conditions either periodic or corresponding to perfectly reflecting faces as a model. Actually in his original paper[1] Debye took as a model a free elastic sphere, because the sphere is one of the few solids for which the equation of elastic motion can be integrated. However, in order to carry the calculation through he had to assume that the sphere was very large, which led him to the well-known frequency spectrum

$$g(\nu)=4\pi V[(2/c_t^3)+(1/c_l^3)]\nu^2,$$

where V is the volume of the solid, c_t and c_l the transverse and longitudinal sound velocities, and ν the frequency.

More generally Weyl[2] and Courant[3] have shown that in a continuous medium the distribution of the vibrations does not depend on the shape of the surface nor on the boundary conditions, if the wavelength is small with respect to the dimensions of the solid, that is if the solid is practically considered as infinite. It is interesting to know from M. Born himself[4] why he introduced in 1923 the model of the infinite crystal with cyclic boundary conditions: first, the natural surface is likely to be rough and not perfectly smooth and secondly, he was "not interested in properties of the surface, or in properties depending on the surface, but only in intrinsic properties of the matter forming the crystal."

However, the behavior of the atoms at the surface is certainly different from their behavior in the bulk and it seemed to us worthwhile to investigate their thermal energy, because the knowledge of this might be useful for the study of phenomena involving kinetic properties of surfaces.

Several authors have already undertaken such an investigation. Montroll[5] pointed out in 1950 a defect in the usual counting process of the normal modes of vibration and derived a corresponding correction term for the Debye frequency spectrum,

$$g_M(\nu)=(\pi/2)S[(2/c_t^2)+(1/c_l^2)]\nu$$

proportional to the area S of the solid. But it must be clearly realized that he used as a model a parallelopiped with perfectly reflecting faces, and that such boundary conditions are not realistic. It is well known that in the case of a free surface as well as in the case of a clamped surface, one cannot satisfy the boundary conditions by the simple superposition of an incident wave and of a reflected wave of the same kind; one must add a transverse reflected wave if the incident is longitudinal and vice versa. The surface "scrambles" the waves, so that one can no longer analyze the vibrations of the solid in terms of pure transverse and pure longitudinal modes.

Two authors actually considered the problem in this realistic situation, where the surface mixes up transverse and longitudinal waves: Brager and Schuchowitzky,[6] in 1946, only treated the simpler case of an incompressible medium. Stratton[7] in 1953 computed the densities of points in the wave number space and then derived the specific heat in the usual fashion.

In this paper we shall also compute the frequency spectrum in the case of these realistic boundary conditions. But we shall use a completely different mathematical method, which we shall now expose.

1. MODEL

As in the Debye theory, the solid is taken as an isotropic elastic continuum. Our model will be a rec-

* Based on dissertations presented to the Graduate School of Yale University in partial fulfillment of the requirements for the degree of Doctor of Philosophy in 1955 (RM) and 1959 (MD).

† Sheffield Scientific School Fellow, Present address: Section des Isotopes Stables, Centre d' Etudes Nucléaires de Saclay. Gif-sur-Yvette (S et O) France.

‡ National Science Foundation Predoctoral Fellow, 1952–55, Present address: Gates and Crellin Laboratories of Chemistry, California Institute of Technology, Pasadena, California.

§ Contribution No. 1626.

[1] P. Debye, Ann. Physik **39**, 789 (1912).

[2] H. Weyl, Math. Ann. **71**, 441, 1212 (1911).

[3] R. Courant, Math. Z. **7**, 1 (1920).

[4] M. Born, Proc. Phys. Soc. (London) **54**, 362 (1942).

[5] E. Montroll, J. Chem. Phys. **18**, 183 (1950).

[6] A. Brager and A. Schuckowitzky, Acta Physicochim. U.R.S.S. **21**, 1001 (1946).

[7] R. Stratton, Phil. Mag. **44**, 519 (1953).

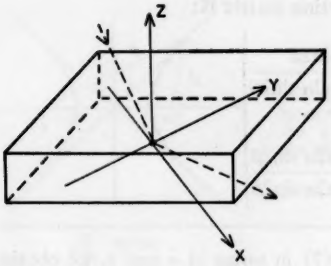

FIG. 1. Model used in the calculation, showing the rotated axes.

tangular plate of thickness l_3 and other dimensions l_1 and l_2. The faces parallel to the plane of the plate are supposed to be free of stresses, whereas we take periodic boundary conditions on the other faces.

The notation will be the following: the displacement vector is

$$\mathbf{s}=\mathbf{i}\xi+\mathbf{j}\eta+\mathbf{k}\zeta$$

at the point A determined by $\mathbf{r}=\mathbf{i}x+\mathbf{j}y+\mathbf{k}z$. The maximum amplitude of the displacement is $\mathbf{a}$, the wave number is $\mathbf{k}$, the frequency is ν. The indices t and l refer to the transverse and longitudinal waves. All the quantities with the superscript "prime" refer to "reflected quantities" whereas incident quantities will remain without superscript.

As was pointed out earlier, we cannot analyze the modes of vibration in pure transverse and pure longitudinal waves; therefore we construct a solution by superposing four coplanar plane waves: an incident transverse and its reflected, and an incident longitudinal and its reflected:

$$\mathbf{s}=\mathbf{s}_t+\mathbf{s}_t'+\mathbf{s}_l+\mathbf{s}_l', \tag{1}$$

where $\mathbf{s}=\mathbf{a}\exp[2\pi i(\mathbf{k}\cdot\mathbf{r}-\nu t)]$.

As will be seen later, the symmetry of the model introduces the components of the propagation vector only through the components parallel and perpendicular to the plane of the plate, which we shall from now on respectively call τ and σ. If we call k_1 and k_2 the components of τ parallel to the edges with dimension l_1 and l_2, the periodic boundary conditions immediately determine k_1 and k_2 and therefore τ,

$$k_1=\eta_1/l_1; \qquad k_2=\eta_2/l_2,$$

where n_1 and n_2 are any integer. For the rest of the problem the directions of the edges parallel to the plane of the plate do not play any role, so that we can without loss of generality adopt the following frame of reference: The faces parallel to the plane of the plate are the planes $z=0$ and $z=l_3$. We consider a point A of the face $z=0$ where the displacement is $\mathbf{s}$ given by (1). Ax will be the trace of the common plane of propagation on $z=0$ and Ay will be perpendicular to it in this plane (Fig. 1).

The longitudinal vibrations $\mathbf{s}_l$ are in the plane of propagation xAz but not the transverse vibrations $\mathbf{s}_t$. We shall decompose the latter into two polarized components. One is polarized in the plane of propagation and the other is polarized normally to it, along Ay. The normally polarized wave does not give rise to an extra wave after reflection, but gives rise to a Montroll surface correction, because we shall use the usual counting process for the wave number τ. We shall take care of this component later and forget about it for the time being. Thus, the problem we have now to solve is a problem, whose geometry is in a plane, namely the plane of propagation xAz (Fig. 2).

2. SECULAR EQUATION

If the face $z=0$ is free of stresses, then the three stress components σ_{xz}, σ_{yz}, σ_{zz} vanish identically with respect to x and y.

$$\sigma_{xz}(x,y,0)\equiv\mu[(\partial\zeta/\partial x)+(\partial\xi/\partial z)]_{z=0}=0$$

$$\sigma_{yz}(x,y,0)\equiv\mu[(\partial\zeta/\partial y)+(\partial\eta/\partial z)]_{z=0}=0$$

$$\sigma_{zz}(x,y,0)\equiv\{2\mu(\partial\zeta/\partial z)+\lambda[(\partial\xi/\partial x)+(\partial\eta/\partial y)+(\partial\zeta/\partial z)]\}_{z=0}=0. \tag{2}$$

If we define α and β as the angles of the propagation vectors $\mathbf{k}_t$ and $\mathbf{k}_l$ with the Az axis (see Fig. 2), and if we apply the conditions (2) to the wave solution (1), we obtain the following relations:

$$k_t\sin\alpha=k_l\sin\beta \tag{3}$$

$$[k_t^2\cos^2 2\alpha+k_l^2\sin 2\alpha\sin 2\beta]a_t'=[k_t^2\cos^2 2\alpha-k_l^2\sin 2\alpha\sin 2\beta]a_t+2k_tk_l\sin 2\beta\cos 2\alpha\, a_l \tag{4}$$

$$[k_t^2\cos^2 2\alpha+k_l^2\sin 2\alpha\sin 2\beta]a_l'=2k_tk_l\sin 2\alpha\cos 2\alpha\, a_t-[k_t^2\cos^2 2\alpha-k_l^2\sin 2\alpha\sin 2\beta]a_l, \tag{5}$$

in which λ and μ have been eliminated by using the well-known relations

$$c_t^2/c_t^2=k_t^2/k_l^2=(\lambda+2\mu)/\mu.$$

Equation (3) expresses the fact that the component of the wave number, which is parallel to the plane of the plate, is the same for both transverse and longitudinal vibrations. This common component was already called τ.

Equations (4) and (5) are linear with respect to the amplitudes a. We might do an identical computation at the face $z=l_{3a}$ and we would obtain the secular equation by expressing the fact that these four linear and homogeneous equations have a nontrivial solution. But a more instructive way to obtain the secular equation is to notice that one obtains the reflected amplitudes

a_t' and a_l' by operating on the incident amplitudes a_t and a_l with the reflection matrix $\mathbf{R}$:

$$\mathbf{R}\equiv\begin{pmatrix} \dfrac{k_t^2\cos^2 2\alpha - k_l^2\sin 2\alpha\sin 2\beta}{k_t^2\cos^2 2\alpha + k_l^2\sin 2\alpha\sin 2\beta} & \dfrac{2k_tk_l\cos 2\alpha\sin 2\beta}{k_t^2\cos^2 2\alpha + k_l^2\sin 2\alpha\sin 2\beta} \\ \dfrac{2k_tk_l\cos 2\alpha\sin 2\alpha}{k_t^2\cos^2 2\alpha + k_l^2\sin 2\alpha\sin 2\beta} & -\dfrac{k_t^2\cos^2 2\alpha - k_l^2\sin 2\alpha\sin 2\beta}{k_t^2\cos^2 2\alpha + k_l^2\sin 2\alpha\sin 2\beta} \end{pmatrix},$$

so that we can write

$$\mathbf{a}'=\mathbf{R}\mathbf{a},$$

where the vectors $\mathbf{a}'$ and $\mathbf{a}$ have for components a_t', a_l', and a_t, a_l.

When after a first reflection the waves travel from the face $z=0$ to the face $z=l_3$, the amplitudes a_t' and a_l' are transformed into a_t'' and a_l'', such that

$$a_t''=a_t'\exp(2\pi i k_t l_3\cos\alpha)$$

$$a_l''=a_l'\exp(2\pi i k_l l_3\cos\beta).$$

Thus we may define a second matrix $\mathbf{T}$,

$$\mathbf{T}=\begin{pmatrix} \exp(2\pi i k_t l_3\cos\alpha) & 0 \\ 0 & \exp(2\pi i k_l l_3\cos\beta) \end{pmatrix},$$

and when the waves are back to the face $z=0$, the amplitudes are a_t^{IV} and a_l^{IV} so that

$$\mathbf{a}^{\mathrm{IV}}=\mathbf{TRTR}\mathbf{a}.$$

But we must have

$$\mathbf{a}^{\mathrm{IV}}=\mathbf{a},$$

which requires for a nontrivial solution

$$|\,\mathbf{TRTR}-\mathbf{1}\,|=0. \tag{6}$$

This is the secular equation for the allowed frequencies, provided that it does not contain any extraneous root. This point will be examined in a moment.

Equation (6) is equivalent to

$$|\,\mathbf{R}+\mathbf{T}^{-1}\,||\,\mathbf{R}-\mathbf{T}^{-1}\,|=0. \tag{7}$$

By introducing the components τ and σ of the wave numbers

$$\tau=k_t\sin\alpha=k_l\sin\beta$$
$$\sigma_t=[(\nu^2/c_t^2)-\tau^2]^{\frac{1}{2}} \tag{8}$$
$$\sigma_l=[(\nu^2/c_l^2)-\tau^2]^{\frac{1}{2}}$$

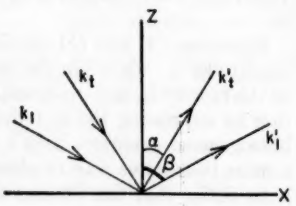

FIG. 2. Geometry of a reflection.

and by expressing (7) in terms of σ and τ, we obtain the equation

$$[(\sigma_t^2-\tau^2)^4+16\tau^4\sigma_t^2\sigma_l^2]\sin 2\pi\sigma_t l_3\sin 2\pi\sigma_l l_3$$
$$+8\tau^2\sigma_t\sigma_l(\sigma_t^2-\tau^2)^2(1-\cos 2\pi\sigma_t l_3\cos 2\pi\sigma_l l_3)=0. \tag{9}$$

This is the secular equation for the allowed frequencies if our technique has not introduced any extraneous roots, that is, roots which do not correspond to any real mode of vibration, because the corresponding total amplitude vanishes identically everywhere. Thus, in order to make sure that all the roots of (9) do correspond to real modes of vibration, we must now try to construct the total amplitude for every solution of (9). For brevity we shall not reproduce the details of this analysis, which is easily done by studying the systems of linear equations corresponding to the vectorial equalities

$$\mathbf{Ra}=\mathbf{Ta}$$

or

$$\mathbf{Ra}=-\mathbf{Ta}.$$

The results are the following: The only extraneous roots are the frequencies corresponding to $\sigma_t=0$ and $\sigma_l=0$. For these frequencies, it is impossible to construct a total amplitude which does not vanish identically everywhere unless we equate the wave numbers to zero, which corresponds to the case of a translation for the whole crystal. But we only consider the case of a solid large enough so that the number of the translational degrees of freedom is always negligible compared to the number of vibrational degrees of freedom.

Therefore we must divide (9) by $\sigma_t\sigma_l$ so that the true secular equation for the allowed frequencies of the normal modes for a given τ is

$$\Delta(\nu,l)\equiv[(\sigma_t^2-\tau^2)^4+16\tau^4\sigma_t^2\sigma_l^2]$$
$$\times(\sin 2\pi\sigma_t l_3/\sigma_t)(\sin 2\pi\sigma_l l_3/\sigma_l)$$
$$+8\tau^2(\sigma_t^2-\tau^2)^2(1-\cos 2\pi\sigma_t l_3\cos 2\pi\sigma_l l_3)=0, \tag{10}$$

where the frequencies are introduced through the relations (8).

3. COMPUTATION OF THE SPECIFIC HEAT

A. Method

The specific heat at constant volume is given by the

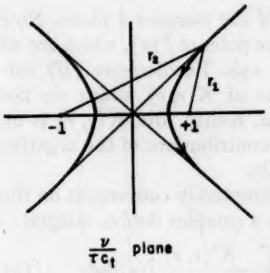

FIG. 3. Contour for the integration of Eq. (11) in the $\nu/\tau c_t$ plane, showing the elliptic coordinates.

well-known expression

$$C=k\sum_i(\beta\nu_i/\sinh\beta\nu_i),^2$$

where $\beta=h/2kT$. Since we shall have occasion to use subscripts on C to indicate various contributions to the specific heat, we denote the specific heat at constant volume by C instead of the more customary C_v. The problem now is to evaluate this sum over the frequencies given by (10).

To solve it, we shall use a well-known result of the theory of complex variables: If a function $g(\nu)$ is analytic within a contour (Γ), except at poles a of order m, and if we call b any one of its zeros of order n, and if $f(\nu)$ is another function analytic within (Γ) and on (Γ), then

$$(2\pi i)^{-1}\oint_{(\Gamma)}\frac{g'(\nu)}{g(\nu)}f(\nu)d\nu=\sum_b nf(b)-\sum_a mf(a).$$

Therefore the contribution of the modes with a wave number component parallel to the plane of the plate equal to τ is given by

$$I(\tau)=\frac{k}{2\pi i}\oint_{(\Gamma)}\frac{\beta^2\nu^2}{\sinh^2\beta\nu}d[\ln\Delta(\nu,\tau)],$$

where (Γ) is a contour surrounding all the roots of the secular equation $\Delta(\nu,\tau)=0$. This counting technique is analogous to one introduced by Wentzel in the context of meson field theory[8]; it has been used for varied purposes.

The summation over τ is then done in the usual manner by counting the number of points in the wave number τ lattice. If we remember to take into account the contribution C' of the transverse waves normally polarized to the plane of propagation, the total specific heat is

$$C=\int_0^\infty 2\pi l_1l_2\tau d\tau\frac{k}{2\pi i}\oint_{(\Gamma)}\frac{\Delta'(\nu,\tau)}{\Delta(\nu,\tau)}\frac{\beta^2\nu^2}{\sinh^2\beta\nu}d\nu+C', \qquad (11)$$

where the integration over τ is performed from zero to infinity, because we restrict ourselves to the low-temperature region. The reason for this restriction will be given in a moment.

[8] G. Wentzel, Helv. Phys. Acta 15, 111 (1942).

B. Simplification of the Secular Equation

The expression of Δ'/Δ is complicated and the major difficulty in applying this method is to evaluate the contour integral included in (11). However, this difficulty can be overcome in the following way. After a short manipulation the secular equation (10) can be rewritten as

$$\Delta(\nu,\tau)=\frac{[(\sigma_t^2-\tau^2)^2+4\tau^2\sigma_t\sigma_l]^2}{\sigma_t\sigma_l}\exp[-2\pi il_3(\sigma_t+\sigma_l)]$$
$$\times\Bigg(\{1-\exp[2\pi il_3(\sigma_t+\sigma_l)]\}^2-\left[\frac{(\sigma_t^2-\tau^2)^2-4\tau^2\sigma_t\sigma_l}{(\sigma_t^2-\tau^2)^2+4\tau^2\sigma_t\sigma_l}\right]^2$$
$$\times[\exp(2\pi il_3\sigma_t)-\exp(2\pi il_3\sigma_l)]^2\Bigg)=0, \qquad (12)$$

and we are going to show that we can find a contour of integration on which the expression

$$G(\nu,\tau)=\{1-\exp[2\pi il_3(\sigma_t+\sigma_l)]\}^2$$
$$-\left[\frac{(\sigma_t^2-\tau^2)^2-4\tau^2\sigma_t\sigma_l}{(\sigma_t^2-\tau^2)^2+4\tau^2\sigma_t\sigma_l}\right]^2[\exp(2\pi i\sigma_t l_3)-\exp(2\pi i\sigma_l l_3]^2$$

is very close to unity, so that its contribution to (11) can be neglected.

Although the contour integral included in (11) is to be evaluated in the ν plane, we shall work with the reduced variable $\nu/\tau c_t$ and introduce in the corresponding plane elliptic coordinates λ and μ

$$\lambda=\tfrac{1}{2}(r_1+r_2); \qquad \mu=\tfrac{1}{2}(r_1-r_2)$$

with respect to the centers $+1$ and -1 (Fig. 3).

In terms of these coordinates, a short calculation gives for the complex number σ_t/τ the following expression:

$$\sigma_t/\tau=\mu(\lambda^2-1)^{\frac{1}{2}}+i\lambda(1-\mu^2)^{\frac{1}{2}}.$$

Thus, if we choose for the path of integration a hyperbola (H) which has the points $\nu/\tau c_t=\pm1$ for foci, μ will be a constant and λ will never be less than unity. Therefore the imaginary part of σ_t/τ will have a lower limit over all the contour. If we choose for σ_t the determination, the argument of which remains between 0 and π so that the imaginary part of σ_t remains positive over all the contour, the terms which contain in (12) $\exp(2\pi il_3\sigma_t)$ decrease very rapidly as $\exp[-\lambda(1-\mu^2)^{\frac{1}{2}}\tau l_3]$ when we leave the intercepts of the hyperbola, where this factor reaches its upper limit.

It must be clearly realized that this hyperbola is not the only contour on which these terms become negligible: any contour on which the imaginary part of σ_t has a lower bound will be proper. In particular, the hyperbola has this property for the terms which contain $\exp(2\pi il_3\sigma_l)$.

Now we shall make the approximation that the terms which contain $\exp(2\pi il_3\sigma_t)$ and $\exp(2\pi il_3\sigma_l)$ are negligi-

ble over all the hyperbola, so that we take as a secular equation

$$K(\nu,\tau)=\frac{[(\sigma_t^2-\tau^2)^2+4\tau^2\sigma_t\sigma_l]^2}{\sigma_t\sigma_l}\exp[-2\pi i(\sigma_t+\sigma_l)l_3]=0.$$

This approximation introduces an error which will be shown later, in Sec. 4, to be negligible if the plate is not too thin.

C. Transformations of the Specific Heat Integral

With this simplifying approximation the problem is now to evaluate

$$C-C'=2\pi l_1l_2\int_0^\infty \tau d\tau(2\pi i)^{-1}\oint_{(H)}\frac{K'(\nu,\tau)}{K(\nu,\tau)}f(\nu)d\nu, \quad (13)$$

where

$$K'(\nu,\tau)=\partial K(\nu,\tau)/\partial\nu; \qquad f(\nu)=k\beta^2\nu^2/\sinh^2\beta\nu,$$

and (H) is a hyperbola of the complex ν plane. Note that (H) leaves outside the poles of $f(\nu)$, which are all located on the imaginary axis. Furthermore (H) surrounds the negative roots of $K(\nu,\tau)$ which do not correspond to any physical reality. But $K(\nu,\tau)$ is an even function, so that the contributions of the negative roots can be discarded easily.

If we note that (13) is absolutely convergent on the contour, we can write it as a complex double integral

$$C-C'=2\pi l_1l_2\int_0^\infty(2\pi i)^{-1}\oint_{(H)}\tau\frac{K'(\nu,\tau)}{K(\nu,\tau)}f(\nu)d\nu d\tau, \quad (14)$$

and use the rules valid for the real variable double integral, such as interchanging the order of the integrations. But before performing the integrations, we shall transform (14).

We notice that $K(\nu,\tau)$ may be written as a function of τ and $\xi=\nu/\tau$:

$$K(\nu,\tau)=\frac{\tau^6\{[(\xi^2/c_t^2)-2]^2+4[(\xi^2/c_t^2)-1]^{\frac{1}{2}}[(\xi^2/c_t^2)-1]^{\frac{1}{2}}\}^2}{[(\xi^2/c_t^2-1]^{\frac{1}{2}}[(\xi^2/c_t^2)-1]^{\frac{1}{2}}}\exp\left\{-2\pi i\tau l_3\left[\left(\frac{\xi^2}{c_t^2}-1\right)^{\frac{1}{2}}+\left(\frac{\xi^2}{c_l^2}-1\right)^{\frac{1}{2}}\right]\right\}$$

$$=\tau^6M(\xi)\exp\left\{-2\pi i\tau l_3\left[\left(\frac{\xi^2}{c_t^2}-1\right)^{\frac{1}{2}}+\left(\frac{\xi^2}{c_l^2}-1\right)^{\frac{1}{2}}\right]\right\}.$$

So we change the variables τ and ν into τ and $\xi=\nu/\tau$ and (14) is easily transformed into the following integral:

$$C-C'=2\pi l_1l_2\int_0^\infty(2\pi i)^{-1}\oint_{(H_1)}\tau f(\xi\tau)\left\{[M'(\xi)/M(\xi)]\right.$$

$$\left.-2\pi i\tau l_3\left[\frac{\xi}{c_t^2[(\xi^2/c_t^2)-1]^{\frac{1}{2}}}+\frac{\xi}{c_l^2[(\xi^2/c_l^2)-1]^{\frac{1}{2}}}\right]\right\}d\tau d\xi, \quad (15)$$

where (H_1) is the analogous hyperbola in the ξ plane.

The association in (15) of τ and ξ in $\xi\tau$ suggests the second change of τ and ξ into $\nu=\xi\tau$ and ξ, both complex. Now the path of integration for the ν integral will be half a straight line (L) issued from the origin with a slope depending on ξ. As a choice of the contour (H_1) shows that

$$|\text{ argument of }\xi\ |<\pi/2;$$

this half-straight line will be located in the right-half plane, the imaginary axis being included. Thus (15) becomes

$$C-C'=2\pi l_1l_2\int_{(L)}(2\pi i)^{-1}\oint_{(H_1)}\left\{\nu f(\nu)\frac{M'(\xi)}{\xi^2M(\xi)}-\frac{2\pi i l_3}{\xi^2}\right.$$

$$\left.\times\left[\frac{1}{c_t^2(\xi^2/c_t^2-1)^{\frac{1}{2}}}+\frac{1}{c_l^2(\xi^2/c_l^2-1)^{\frac{1}{2}}}\right]\nu^2f(\nu)\right\}d\xi d\nu. \quad (16)$$

Keeping ξ constant, we first perform the integration over ν; as ν varies on (L) from zero to infinity, the result of an integration performed between limits independent of ξ, will also be independent of ξ. It is now clear why we extended the range of variation of τ until infinity, restricting the solution to low temperatures. This restriction allows us to break down each double integral of (16) into a product of simple integrals.

D. Computation of the Volume Dependent Term

We first take care of the integral which in (16) depends on the volume $V=l_1l_2l_3$ and which gives the volume contribution C_D

$$C_D=-2\pi l_1l_2l_3\oint_{(H_1)}\frac{1}{\xi^2}\left[\frac{1}{c_t^2[(\xi^2/c_t^2)-1]^{\frac{1}{2}}}\right.$$

$$\left.+\frac{1}{c_l^2[(\xi^2/c_l^2)-1]^{\frac{1}{2}}}\right]d\xi\int_0^\infty\nu^2f(\nu)d\nu. \quad (17)$$

The contour integral over (H_1) is evaluated without any difficulty: Using Cauchy's theorem we may swing (H_1) down to the real axis, so that

$$\oint_{(H_1)}\frac{1}{\xi^2}\frac{d\xi}{c^2[(\xi^2/c^2)-1]^{\frac{1}{2}}}=-\frac{2}{c^2}\int_0^\infty\frac{d\xi}{\xi^2[(\xi^2/c^2)-1]^{\frac{1}{2}}}=-\frac{2}{c^3}.$$

(17) becomes

$$C_D=4\pi l_1l_2l_3\left(\frac{1}{c_t^3}+\frac{1}{c_l^3}\right)\int_0^\infty\frac{\beta^2\nu^4}{\sinh^2\beta\nu}d\nu.$$

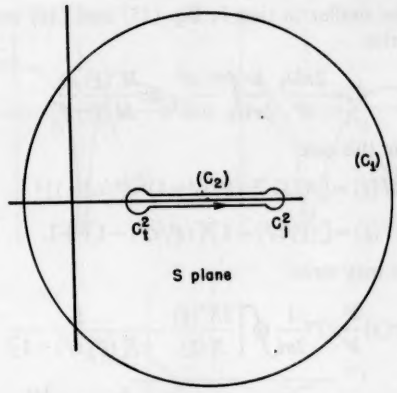

FIG. 4. Contour for the counting of the roots of $N_+(s)$ and $N_-(s)$.

If we add the contribution of the normally polarized transverse wave, we find the Debye result as expected

$$C_D=4\pi l_1 l_2 l_3\left(\frac{2}{c_t^3}+\frac{1}{c_l^3}\right)\int_0^\infty \frac{\beta^2\nu^4}{\sinh^2\beta\nu}d\nu=(12\pi^4/5)\,R(T/\theta)^3, \tag{18}$$

where θ is the Debye temperature.

E. Evaluation of the Surface Contribution

The other integral included in (16) proportional to the surface area $S=2l_1l_2$,

$$C_S=(2\pi i)^{-1}\oint_{(H_1)}(1/\xi^2)[M'(\xi)/M(\xi)]d\xi\pi S\int_0^\infty \nu f(\nu)d\nu,$$

requires more attention. We put

$$M(\xi)=\frac{\{[(\xi^2/c_t^2)-2]^2+4[(\xi^2/c_t^2)-1]^{\frac{1}{2}}[(\xi^2/c_l^2)-1]^{\frac{1}{2}}\}^2}{[(\xi^2/c_t^2)-1]^{\frac{1}{2}}[(\xi^2/c_l^2)-1]^{\frac{1}{2}}},\qquad \xi^2=s$$

in order to examine the quantity

$$N(s)\equiv[(s/c_t^2)-2]^2+4\{[(s/c_t^2)-1][(s/c_l^2)-1]\}^{\frac{1}{2}}.$$

$N(s)$ has two determinations

$$N_+(s)=[(s/c_t^2)-2]^2+4[(s/c_t^2)-1]^{\frac{1}{2}}[(s/c_l^2)-1)]^{\frac{1}{2}};$$

$$N_-(s)=[(s/c_t^2)-2]^2-4[(s/c_t^2)-1]^{\frac{1}{2}}[(s/c_l^2)-1]^{\frac{1}{2}},$$

the zeros of which are roots of the equation

$$F(s)=N_+(s)N_-(s)=[(s/c_t^2)-2]^4$$
$$-16[(s/c_t^2)-1][(s/c_l^2)-1]=0.$$

The roots of $F(s)=0$ are the trivial root $s=0$ and the roots of the equation

$$R(s)=s^3-8c_t^2s^2+8c_t^6[(3/c_t^2)-(2/c_l^2)]s$$
$$+16c_t^8[(1/c_l^2)-(1/c_t^2)]=0,$$

which is the well-known Rayleigh surface wave equation. An important problem now arises, that is to know to which determination which zero of $F(s)$ belongs. In order to solve it, we shall count the roots of $N_+(s)$ and $N_-(s)$ by using Cauchy's rule over the contour shown in Fig. 4. (C_1) is a very large circle and (C_2) surrounds the cut (c_t^2, c_l^2).

For brevity we shall only give the result. $N_-(s)$ has the root $s=0$ and the root $s=c_s^2$, which corresponds to the common Rayleigh surface wave. $N_+(s)$ has two roots, bigger than c_l^2 if real, or imaginary. But these last two roots obviously do not correspond to any surface wave and are just extraneous roots introduced by our technique. We shall discard them and perform the integration in the Riemann sheet corresponding to $N_-(s)$.

Thus we first integrate over ν and obtain

$$C_S=6\pi(k^3/h^2)\zeta(3)ST^2(2\pi i)^{-1}\oint_{(H_1)}\frac{1}{\xi^2}\frac{M'(\xi)}{M(\xi)}d\xi.$$

The evaluation of the ξ integral does not present any difficulty if we note that

$$\oint_{(H_1)}\frac{1}{\xi^2}\frac{N'(\xi)}{N(\xi)}d\xi=\oint_{(H_2)}s^{-1}\frac{N'(s)}{N(s)}ds=-2\pi i$$
$$\times(\text{residue at } s=0),$$

because the only pole outside the contour (H_2) in the s plane shown in Fig. 5 corresponding to (H_1) in the ξ plane, is the origin.

A limited development near the origin gives the residue and the final result is

$$C_S=6\pi\frac{k^3}{h^2}\zeta(3)\frac{c_t^4-c_t^2c_l^2+c_l^4}{(c_l^2-c_t^2)c_t^2c_l^2}ST^2. \tag{19}$$

To be complete we must add the Montroll correction to the specific heat for the normally polarized wave:

$$\frac{\pi S}{2c_t^2}\int_0^\infty \nu f(\nu)d\nu=\frac{3\pi}{c_t^2}\frac{k^3}{h^2}\zeta(3)\,ST^2. \tag{20}$$

Adding (19) and (20) we find the surface specific heat

$$C_S=3\pi\frac{k^3}{h^2}\zeta(3)\frac{2c_t^4-3c_t^2c_l^2+3c_l^4}{c_t^2c_l^2(c_l^2-c_t^2)}ST^2 \tag{21}$$

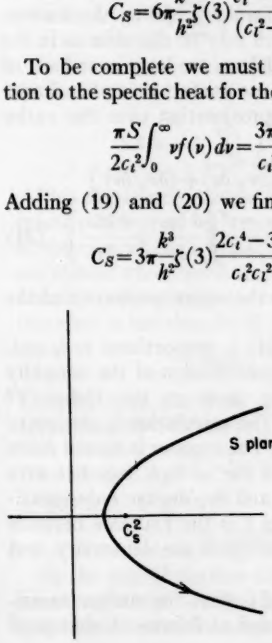

FIG. 5. Contour (H_2) in the s plane for the evaluation of C_S.

where $\zeta(3)$ is the value of the Riemann Zeta function for argument 3, namely, 1.202.

4. CLAMPED SOLID

Before attempting to estimate the error caused by the approximation of the secular equation in the previous section, we briefly give the treatment for a different set of boundary conditions, viz., the clamped solid. In this case we have

$$\xi=\eta=\zeta=0$$

for

$$z=0, \qquad z=l_3. \tag{22}$$

Periodic boundary conditions are imposed on the other faces, as in the free surface case. The clamped solid is not of great physical interest, since surface effects are expected to be experimentally measurable when the surface area of the sample is large, i.e., when the sample is a powder. It is hard to see how to clamp powder granules. Therefore we merely sketch the theory in this case.

As before transverse and longitudinal waves are "scrambled" on reflection, but a transverse wave polarized parallel to the surface is not affected. The secular equation can then be derived by straightforward application of the conditions (22) to the wave (1). It is

$$\Delta(\nu,\tau)=4\tau^2-[(\sigma_t\sigma_l+\tau^2)^2/\sigma_t\sigma_l]\cos(2\pi l_3(\sigma_l+\sigma_t))+[(\sigma_t\sigma_l-\tau^2)^2/\sigma_t\sigma_l]\cos(2\pi l_3(\sigma_l-\sigma_t))=0. \tag{23}$$

The extraneous roots $\sigma_l=0$, $\sigma_t=0$ have already been eliminated. From Eq. (23) $\Delta'(\nu,\tau)$ can easily be computed, but we shall not display it. Along the contour of integration chosen, which may be the same as in the previous section, $\mathrm{Im}\sigma_l$ and $\mathrm{Im}\sigma_t$ are large over most of the contour. Thus we may use the fact that when $\mathrm{Im}z\gg 1$, $\tan z\approx i$. Using this approximation over the entire contour

$$\Delta'(\nu,l)/\Delta(\nu,\tau)=\pm 2\pi i l_3[(\partial\sigma_l/\partial\nu)+(\partial\sigma_t/\partial\nu)]+\left[\frac{\sigma_t\sigma_l-\tau^2}{\sigma_t\sigma_l+\tau^2}\right]\left[\frac{\partial\ln\sigma_t}{\partial\nu}+\frac{\partial\ln\sigma_l}{\partial\nu}\right]. \tag{24}$$

The negative sign holds in the upper quadrant and the positive in the lower.

The first term in Eq. (24) is proportional to l_3 and, when combined with the contribution of the normally polarized transverse wave, leads to the Debye T^3 law for the specific heat. The calculation is similar to the derivation of Eq. (18). The contour is moved down to the real axis. Because of the $\pm$ sign, together with the branch cuts in $\partial\sigma_t/\partial\nu$ and $\partial\sigma_l/\partial\nu$, the only contribution to the integral over ξ is the real axis between $\xi=c_t$ or c_l and $\xi=\infty$. The integrals are elementary, and the Debye law follows.

The term independent of l_3 gives the surface contribution and may be evaluated as follows. A change of variables similar to that in Eq. (15) and (16) enables us to write

$$C_s=\frac{2\pi l_1 l_2}{\beta^2}\frac{k}{2\pi i}\int_0^\infty \frac{x^3}{\sinh^2 x}dx\frac{M'(\xi)}{M(\xi)}\frac{d\xi}{\xi^2}, \tag{25}$$

where, in this case

$$M(\xi)=[N(\xi)]^2/(\xi^2/c_t^2-1)^{\frac{1}{2}}(\xi^2/c_l^2-1)^{\frac{1}{2}}$$

$$N(\xi)=[(\xi^2/c_t^2)-1]^{\frac{1}{2}}[(\xi^2/c_l^2)-1]^{\frac{1}{2}}+1. \tag{26}$$

Thus we may write

$$C_s=6\pi\zeta(3)\frac{k^3}{h^2}ST^2\frac{1}{2\pi i}\oint\left[\frac{2N'(\xi)}{N(\xi)}-\frac{\xi}{c_t^2[(\xi^2/c_t^2)-1]}-\frac{\xi}{c_l^2[(\xi^2/c_l^2)-1]}\right]\frac{d\xi}{\xi^2} \tag{27}$$

where the contour surrounds the positive real axis. The last two terms in the integral in Eq. (27) contribute

$$-i\pi[(1/c_t^2)+(1/c_l^2)]$$

to the integral because of the poles. To evaluate the first part, we must take the determination of $N(\xi)$ corresponding to the negative square root, for this choice of the sheet of the Riemann surface corresponds to the choice of phases for σ_t and σ_l used in deriving the approximate secular equation. This being the case, the only pole of the resulting function outside the contour is at the origin. Evaluation of the pole there yields for the integral

$$-i\pi[(c_l^2-c_t^2)^2/c_l^2c_t^2(c_l^2+c_t^2)].$$

Adding to these results, together with the Montroll correction due to the normally polarized transverse wave, we obtain

$$C_S=-3\pi\zeta(3)(k^3/h^2)ST^2\{(2/c_t^2)+(1/c_l^2)+[(c_l^2-c_t^2)^2/c_l^2c_t^2(c_l^2+c_t^2)]\}. \tag{28}$$

Note that the Montroll correction is negative in this case.

5. ERROR INTRODUCED BY THE SIMPLIFICATION OF THE SECULAR EQUATION

By taking as the secular equation the approximate expression

$$K(\nu,\tau)\equiv\frac{[(\sigma_t^2-\tau^2)^2+4\tau^2\sigma_t\sigma_l]^2}{\sigma_t\sigma_l}\exp[-2\pi i l_3(\sigma_t+\sigma_l)],$$

we have neglected the contribution of the factor

$$G(\nu,\tau)\equiv\{1-\exp[2\pi i l_3(\sigma_t+\sigma_l)]\}^2-\left(\frac{(\sigma_t^2-\tau^2)^2-4\tau^2\sigma_t\sigma_l}{(\sigma_t^2-\tau^2)^2+4\tau^2\sigma_t\sigma_l}\right)^2[\exp(2\pi i l_3\sigma_t)-\exp(2\pi i l_3\sigma_l)]^2,$$

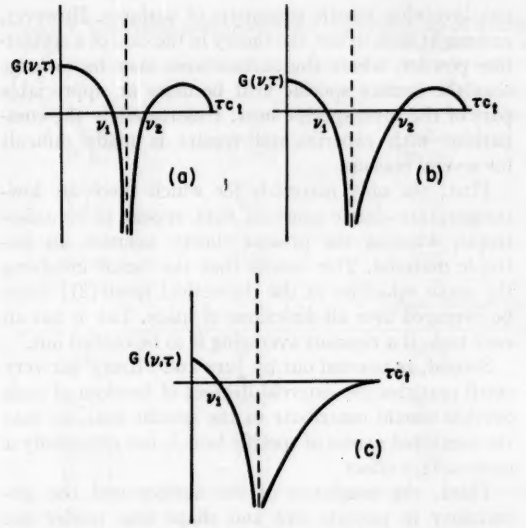

FIG. 6. $G(\nu, \tau)$ as a function of ν for various values of τl_3. The dotted line is $\nu = \tau c_S$. (a) τl_3 very large, (b) τl_3 large, (c) τl_3 small.

that is,

$$\Delta C = 2\pi l_1 l_2 \int_0^\infty \tau d\tau (2\pi i)^{-1} \oint_{(\Gamma)} \frac{G'(\nu,\tau)}{G(\nu,\tau)} \frac{k\beta^2\nu^2}{\sinh^2\beta\nu} d\nu. \quad (30)$$

We are now going to show that this error is completely negligible if the plate is not too thin.

The nature of the approximation is clear once we know the zeros of $G(\nu, \tau)$, which we rewrite as

$$G(\nu,\tau) = 4\exp[2\pi i(\sigma_t+\sigma_l)l_3]\{\sinh^2[-i\pi l_3(\sigma_t+\sigma_l)] - H^2\sinh^2[-i\pi l_3(\sigma_t-\sigma_l)]\},$$

where

$$H(\nu,\tau) \equiv [(\sigma_t^2-\tau^2)^2-4\tau^2\sigma_t\sigma_l]/[(\sigma_t^2-\tau^2)^2+4\tau^2\sigma_t\sigma_l].$$

We see that $G(\nu, \tau)$ has an infinite number of zeros larger than τc_l, but we shall only concentrate our attention on the low-frequency region, because at low temperatures the low frequencies are the only ones which appreciably contribute to the specific heat.

In this region a study of $G(\nu, \tau)$, which for brevity we shall not reproduce, gives the following result depending on the magnitude of τl_3 (Figs. 6a–6c).

Thus the nature of the approximation made is clear. Let us first examine the frequency interval $(0, \tau c_l)$. $G(\nu, \tau)$ has a double pole τc_S and two zeros ν_1 and ν_2. If τl_3 is large, the zeros are very close to the pole τc_S, the contribution to (30) of the double pole and of the two zeros will nearly cancel each other and the total contribution of $G(\nu, \tau)$ will be negligible. But if τl_3 is very small, the zeros ν_1 and ν_2 will become very different, so that their contribution to (30) will not cancel any more the contribution of the double pole.

As the presence of the pole τc_S arises from the fact that we have factored out the quantity $(\sigma_t^2-\tau^2)^2+4\tau^2\sigma_t\sigma_l$, we can say in other words that we have approximated the frequencies ν_1 and ν_2 by the frequency τc_S of the Rayleigh wave.

In the high-frequency region the approximation is of the same nature and is even more justified since the high frequencies do not contribute much to heat capacity at low temperatures.

The nature of the approximation made is now clear from the mathematical viewpoint; before giving the physical interpretation, we shall evaluate its order of magnitude.

For reasons of simplicity we shall rather estimate first the error in the free energy of the solid:

$$\delta A = 2\pi l_1 l_2 \int_0^\infty \tau d\tau \frac{kT}{2\pi i} \oint_{(\Gamma)} \frac{G'(\nu,\tau)}{G(\nu,\tau)} \times \log[1-\exp(-h\nu/kT)]d\nu, \quad (31)$$

where (Γ) is a contour surrounding the zeros of $G(\nu, \tau)$ but leaving outside the poles of $\log[1-\exp(-h\nu/kT)]$, namely,

$$\nu_E = 2\pi i n k T/h,$$

where n is an integer or zero.

By integrating by parts, (31) becomes

$$\delta A = -2\pi l_1 l_2 \int_0^\infty \tau d\tau \frac{h}{2\pi i} \oint_{(\Gamma)} \frac{\log G(\nu,\tau)}{\exp(h\nu/kT)-1} d\nu,$$

and remembering that a contour integral can be evaluated by using the poles which are outside the contour, we obtain

$$\delta A = 2\pi l_1 l_2 \int_0^\infty \tau d\tau \tfrac{1}{2} h \sum_{n=-\infty}^{\infty} \log G(\nu_E,\tau) \times \{\mathrm{Res}[\exp(h\nu/kT)-1]^{-1}\}_{\nu=\nu_E},$$

or

$$\delta A = \pi l_1 l_2 \sum_{n=-\infty}^{\infty} \int_0^\infty \tau \log G(\nu_E,\tau) d\tau.$$

This apparently simple result cannot be evaluated exactly. However, we can get the order of magnitude in the case where l_3 is not too small. An approximate calculation which we shall not reproduce shows that the error is proportional to $\exp[-4\pi l_3 kT/\hbar c_l]$ and that this error is less than 0.1% if

$$4\pi l_3 kT/\hbar c_l > 10.$$

That is, since the usual order of magnitude of c_l is approximately 5000 m/sec,

$$l_3 T > 3\times 10^{-6} \text{ cm deg.}$$

or 300 A at 1°K.

6. DISCUSSION

In the case of the free solid, by replacing the surface wave frequencies ν_1 and ν_2 by τc_S, we are just neglecting the interferences between surface waves of opposite

faces which transform the frequency of a single face surface wave τc_S into the frequencies ν_1 and ν_2. These interferences become important only if the plate becomes very thin. In this case we have seen that the frequency ν_1 becomes low enough to become a pending vibration.

A simple calculation gives for the specific heat associated with bending vibrations the following upper limit:

$$C_{\text{Bending}}<\sqrt{3}\zeta(2)[\rho(1-\sigma^2)/E]^{\frac{1}{2}}(k^2/h)(S/l_3)T,$$

where E is the Young modulus and σ the Poisson modulus. This expression shows that C_{Bending} becomes important if l_3 is very small: numerical estimations made in average cases ($c_t=3000$ m/sec, $c_l=5000$ m/sec) give indeed the following orders of magnitude:

$$C_D\approx 10^{-6}VT^3 \text{ cal/deg}$$

$$C_S\approx 10^{-12}ST^2 \text{ cal/deg}$$

$$C_{\text{Bending}}\approx 10^{-18}ST/l_3 \text{ cal/deg}.$$

Therefore in usual conditions C_{Bend} is absolutely negligible.

With this analysis of the approximation in mind, we can reasonably think that our result not only represents the surface specific heat of an isotropic plate, but generally represents the surface specific heat of a solid of total surface S, if this solid is not too small.

One might object that edge corrections would arise. But the edge correction, according to Bolt[9] and Maa[10] adds to the frequency spectrum the term

$$e(\nu)=\tfrac{1}{8}L[(2/c_t)+(1/c_l)],$$

and contributes to the specific heat at low temperatures an amount

$$C_{\text{Edge}}=[\zeta(2)/4](k^2/h)[(2/c_t)+(1/c_l)]LT,$$

where L is the total length of the edges. Its order of magnitude under usual conditions is the same as that of the bending vibrations. It is therefore completely negligible.

There is little point in spending much time in discussing the clamped case. We should just like to point out that the negative sign of the result is only to be expected, for it is well known that imposing addition restraints (in this case, clamping) on a vibrating system raises the frequencies and hence lowers the specific heat. The negative sign of the Montroll correction is due to the fact that propagation of a wave parallel to the clamped sides is forbidden by the boundary conditions. Hence the partial contribution of such waves, which is included in the usual Debye term, must be subtracted.

As was pointed out at the beginning of this paper, this investigation seemed worthwhile to us mainly in view of its possible application to the study of phenomena involving kinetic properties of surfaces. However, one might wish to test the theory in the case of a crystalline powder, where the surface area may be so large that the surface specific heat becomes an appreciable part of the total specific heat. Unfortunately the comparison with experimental results is made difficult for several reasons.

First, the only materials for which there are low-temperature elastic constant data appear to be anisotropic, whereas the present theory assumes an isotropic material. This means that the factor involving the wave velocities in the theoretical result (21) must be averaged over all directions of space. This is not an easy task, if a rigorous averaging is to be carried out.

Second, as pointed out by Jura and Pitzer,[11] for very small particles the external degrees of freedom of each particle should contribute to the specific heat, so that the measured excess of specific heat is not necessarily a pure surface effect.

Third, the roughness of the surface and the uncertainty in particle size and shape also render the interpretation of the results uncertain.

To compute numerically the theoretical result (21) in the case of anisotropic crystals, we averaged the sound velocities in the following way: since longitudinal sound velocities vary with direction much less than the transverse ones, we determined $\langle c_l\rangle_{Av}$ simply by averaging over the directions 100, 110, and 111 for which c_l can be computed easily from elastic constants. Then $\langle c_t\rangle_{Av}$ was determined by using the experimental Debye temperature. This method is certainly approximate, but should give reasonable results since at least both velocities are such that they give a correct Debye temperature.

The theoretical surface effect and the observed excess of specific heat have been compared for two sets of measurements. One has been done by Lien and Phillips[12] between 1.5 and 4° K on a sample of MgO powder with specific surface area of 166 m²/g. Their results can be expressed rather well by[13]

$$C=0.00459T^3+0.163T^2 \text{ mjoules/mole/deg},$$

where the T^3-term is the theoretical Debye contribution.

Theoretically, we find

$$C=0.00459T^3+0.043T^2 \text{ mjoules/mole/deg},$$

with $\langle c_t\rangle_{Av}=9692$ m/sec and $\langle c_l\rangle_{Av}=6071$ m/sec. Low-temperature elastic constants are from Durand,[14] and the density has been taken equal to 3.592 for the whole range of temperature.[15] It should be pointed out

[9] R. H. Bolt, J. Acoust. Soc. Am. **10**, 228 (1939).
[10] D. Y. Maa, J. Acoust. Soc. Am. **10**, 235 (1939).
[11] G. Jura and K. Pitzer, J. Am. Chem. Soc. **74**, 6030 (1952).
[12] W. H. Lien and N. E. Phillips, J. Chem. Phys. **29**, 1415 (1958).
[13] W. H. Lien and N. E. Phillips, private communication.
[14] M. Durand, Phys. Rev. **50**, 449 (1936).
[15] T. H. K. Baron, W. T. Berg, and J. A. Morrison, Proc. Roy. Soc. (London) **A250**, 70 (1959).

TABLE I. Theoretical surface effect and observed excess of specific heat for NaCl powder. [$\Delta C = C_P$ (particles), smoothed C_P (bulk crystal). Both C_P are observed values.[21]]

Sample 1—Specific surface area: 38 m^2/g

T (0° K)	$\langle c_t \rangle_{Av}$ (m/sec)	$\langle c_l \rangle_{Av}$ (m/sec)	C_P (particles) (cal/mole deg.)	ΔC (obs.) (cal/mole deg.)	C_s (theor.) (cal/mole deg.)
10.062	2653	4615	0.0343	0.0035	0.0017
12.160	2609	4539	0.0616	0.0041	0.0026
14.438	2551	4438	0.1083	0.0056	0.0038
16.591	2501	4351	0.1722	0.0074	0.0053
18.648	2459	4278	0.2565	0.0103	0.0069

Sample 3—Specific surface area: 59 m^2/g

T (0° K)	$\langle c_t \rangle_{Av}$ (m/sec)	$\langle c_l \rangle_{Av}$ (m/sec)	C_P (particles) (cal/mole deg.)	ΔC (obs.) (cal/mole deg.)	C_s (theor.) (cal/mole deg.)
10.165	2651	4612	0.0378	0.00605	0.0027
12.190	2608	4537	0.0661	0.0082	0.0041
14.804	2543	4424	0.1237	0.0121	0.0063
16.814	2496	4343	0.1887	0.0162	0.00845
18.791	2456	4273	0.2715	0.0187	0.0109

that both the theoretical and observed expressions suppose that the elastic constants of the crystal remain independent of temperature in the range considered. This assumption is probably correct, since the temperature is very low and the range is small. The uncertainty is rather in the value of the corresponding Debye temperature, which has been obtained by extrapolating high-temperature measurements: since the Debye temperature has not been measured below 9° K, the value extrapolated at 0° K, $\Theta = 946°$ K, was used.[15]

The observed effect appears to be 3.8 times larger than the theoretical surface effect. But the particle size was so small (cubes of 100 A edge) and the temperature so low that these measurements are at the limit of validity of our computation. Furthermore, a contribution of the particle motion may be expected.

Another set of measurements has been done by Morrison and Patterson[16,17] on samples of NaCl powder between 10° K and room temperature. The theoretical surface effect and the observed excess between 10 and 20° K are given in Table I. As the Debye temperature has been measured in this range of temperature,[18] we could estimate more accurately the theoretical surface effect. *Low*-temperature elastic constants are from Overton and Swim.[19] The correction $C_P - C_V$ has been neglected, and the density has been taken equal to 2.209 for the whole range of temperature.[20]

It appears that the observed ΔC is about 1.5 times larger than the theoretical surface effect for sample 1, and 2 times larger for sample 3. However, it should be noticed that the observed effects are not exactly proportional to surface areas. The authors attribute this nonproportionality to experimental errors.[18] Particle motion also may have contributed.

A third set of measurements has been done on lampblack graphite.[22] The interpretation of the observed excess is still being debated.[23] Even though a pure surface effect may exist, measurements of the surface areas of the samples were not made (only the mean size of the particles has been estimated), so that an accurate test of our theory is precluded.

To sum up, we can only conclude that the experimental data presently available, at least to our knowledge, are not adequate for a critical test of our theory.

This reasearch received support from the National Science Foundation by Grant NSF–1865, in addition to the Fellowship held by one of the authors.

[16] D. Patterson, J. A. Morrison, and F. Thompson, Can. J. Chem. **33**, 240 (1955).
[17] J. A. Morrison and D. Patterson, Trans. Faraday Soc. **52**, 1 (1956).
[18] J. A. Morrison, D. Patterson, and J. S. Dugdale, Can. J. Chem. **33**, 375 (1955).
[19] W. C. Overton and R. T. Swim, Phys. Rev. **84**, 758 (1951).
[20] R. M. Buffington and W. M. Latimer, J. Am. Chem. Soc. **48**, 2312 (1926).
[21] J. A. Morrison, (private communication).
[22] W. De Sorbo and G. E. Nichols, J. Phys. Chem. Solids **6**, 352 (1958).
[23] P. Flubacher, A. J. Leadbetter, and J. A. Morrison, J. Phys. Chem. Solids **13**, 160 (1960).

THE JOURNAL OF CHEMICAL PHYSICS VOLUME 33, NUMBER 5 NOVEMBER, 1960

Classical and Quantum Mechanical Hypervirial Theorems*

JOSEPH O. HIRSCHFELDER

University of Wisconsin Theoretical Chemistry Laboratory, Madison, Wisconsin

(Received August 1, 1960)

If W is a function of the coordinates and momenta, then in classical mechanics the time average of the Poisson bracket (H, W) is zero. In quantum mechanics it follows from the Heisenberg equation of motion that the expectation value of $(WH-HW)$ for *any* wave function, corresponding to a stationary energy state of the system, is zero. For each selection of W there is a dynamical relationship, in a time-average or space-average sense, which the system must obey. Two classes of W's are considered in detail: W as a function only of the coordinates, and W as a function of the coordinates times the first power of a momentum. For the first class, neither the classical mechanical nor the quantum mechanical results provide useful information. The usual virial theorem of Clausius is a special case of the second class of relations. The classical treatment should be useful for the determination of the equation of state of liquids. The use of the quantum-mechanical relations for determining the constants in an approximate wave function is discussed.

THE classical mechanical equation of motion in terms of Poisson brackets and the corresponding Heisenberg quantum-mechanical equation of motion provide a means for determining a wide variety of generalizations of the virial theorem. These relations determine all of the statistical moments required to make a detailed study of the average motion in each degree of freedom of a dynamical system and to determine the statistical correlations between the motions in different degrees of freedom. The classical treatment should be useful with respect to the determination of the equation of state of liquids. The quantum-mechanical treatment provides a set of integral conditions which might be used to determine the constants in an approximate wave function.

If W is a function of the coordinates and momenta, then in classical mechanics the time average of the Poisson bracket (H, W) is zero. In quantum mechanics, the expectation value of $(WH-HW)$ for *any* wave function, corresponding to a stationary energy state of the system, is zero. For each selection of W there is a dynamical relationship, in a time-average or space-average sense, which the system must obey. In the present paper, we first consider the class of relations which are obtained when W is taken to be a function only of the coordinates. For this case, neither the classical nor the quantum-mechanical relations are very useful. Next, we consider the class of relations obtained when W is taken to be a homogeneous function of the first degree in the momenta with arbitrary functions of the coordinates as coefficients. The usual virial theorem of Clausius is a special case resulting from this class of W functions. Clearly, this analysis could be extended to considerations of W's which involve the squares or higher powers of the momenta.

* This research is being reported under contract to the U. S. Atomic Energy Commission.

I. THE CLASSICAL HYPERVIRIAL THEOREM

Consider a mechanical system composed of N particles and having a Hamiltonian function H. The state of the system can be described in terms of the set of orthogonal generalized curvilinear coordinates q_1, q_2, $\cdots$, q_{3N} and their conjugate momenta p_1, p_2, $\cdots$, p_{3N}. Let W be a function of the generalized coordinates and momenta which is uniquely defined by the state of the system[1] and which remains finite for all configurations of the system consistent with the prescribed constants of motion and boundary conditions. Then the classical equation of motion in terms of Poisson brackets states that[2]

$$dW/dt=(H,W)=\sum_{j=1}^{3N}[(\partial H/\partial p_j)(\partial W/\partial q_j)-(\partial H/\partial q_j)(\partial W/\partial p_j)]. \quad (1)$$

And, of course, the canonical equations give $\partial H/\partial p_j=\dot{q}_j$ and $\partial H/\partial q_j=-\dot{p}_j$.

Let us take the time average of Eq. (1) by integrating the two sides of the equation from time $t=0$ to a time θ and dividing by θ. If the motion of the system is periodic, θ is taken to be the time required for the system to return to its original state. Otherwise, θ is allowed to approach infinity. Clearly, the time average of dW/dt is zero. Thus, indicating the time average by the brackets $\langle\ \rangle$ around the averaged function,

$$0=\langle(H,W)\rangle=\sum_{j=1}^{3N}\langle\dot{q}_j(\partial W/\partial q_j)-(\partial H/\partial q_j)(\partial W/\partial p_j)\rangle. \quad (2)$$

Because of its great generality, Eq. (2) is applicable to a wide variety of problems where the system has attained dynamical equilibrium.

[1] Note that angle variables are only defined to within a modulus. Thus, if q_3 were an angle variable, W could not be proportional to q_3. However, W could be proportional to $\sin(q_3)$.

[2] P. M. Morse and H. Feshbach, *Methods of Theoretical Physics* (McGraw-Hill Book Company, Inc., New York, 1955), Vol. I, p. 291.

If $W=f(q_1, q_2, \cdots, q_{3N})$ so that W has no dependence on the momenta, Eq. (2) gives the result

$$\sum_{j=1}^{3N}\langle(\partial f/\partial q_j)\dot{q}_j\rangle=\langle df/dt\rangle=0. \tag{3}$$

A very interesting class of relationships is obtained by restricting W to be a homogeneous function of degree one in the momenta. We call these relations the classical hypervirial theorem, since they correspond to a generalization of the usual virial theorem. For example, we might suppose that

$$W=p_k f(q_1, q_2, \cdots, q_{3N}). \tag{4}$$

In this case, Eq. (2) becomes

$$\sum_{j=1}^{3N}\langle\dot{q}_j(\partial f/\partial q_j)p_k\rangle=\langle f(\partial H/\partial q_k)\rangle. \tag{5}$$

If $f=q_k$ [see footnote (1)], Eq. (5) leads to the usual virial theorem of Clausius.

A simple example of the hypervirial theorem is obtained by setting $W=x_i^s p_{xi}$, where x_i is the cartesian x coordinate of the ith particle and p_{xi} is its momentum. If m_i is the mass of the ith particle, Eq. (2) or Eq. (5) becomes

$$sm_i\langle x_i^{s-1}\dot{x}_i^2\rangle=\langle x_i^s(\partial V/\partial x_i)\rangle. \tag{6}$$

Now let us suppose that the $3N$ generalized coordinates consist of the spherical coordinates r_i, θ_i, ϕ_i of the ith particle for $i=1, 2, \cdots, N$. Furthermore, let us restrict W to be equal to $r_i^s p_{ri}$. Then, with $p_{ri}=m_i\dot{r}_i$ and with T_i the total kinetic energy of the ith particle, Eq. (2) or Eq. (5) becomes

$$m_i(s-1)\langle r_i^{s-1}\dot{r}_i^2\rangle+2\langle r_i^{s-1}T_i\rangle=\langle r_i^s(\partial V/\partial r_i)\rangle. \tag{7}$$

When $s=1$, Eq. (7) is one of the frequently used forms of the Clausius virial theorem. For large values of s, one obtains information regarding the behavior of the system when r_i is large.

For a one-dimensional problem taking $W=m\dot{x}V^s$, we obtain, for $s=0, 1, 2, \cdots$, the relations

$$\langle V^s(\partial V/\partial x)\rangle=0.$$

There are many problems, such as the equation of state of liquids, where it is necessary to investigate the correlation between the motions of two particles having the same mass m. For this purpose, let $W=m\dot{r}_{12}r_{12}^s$. Here r_{12} is the separation between the two particles. Using this form of W in Eq. (2) and supposing that the potential energy of the system is a function of the relative distances between pairs of particles, we find

$$\langle m[(d\mathbf{r}_1/dt)-(d\mathbf{r}_2/dt)]^2 r_{12}^{s-1}\rangle+m(s-1)\langle\dot{r}_{12}^2 r_{12}^{s-1}\rangle$$
$$=2\langle r_{12}^s(\partial V/\partial r_{12})\rangle+\sum_{j=3}^{N}\left\langle r_{12}^{s-1}(\mathbf{r}_1-\mathbf{r}_2)\cdot\left[\frac{(\mathbf{r}_1-\mathbf{r}_j)}{r_{1j}}\frac{\partial V}{\partial r_{1j}}-\frac{(\mathbf{r}_2-\mathbf{r}_j)}{r_{2j}}\frac{\partial V}{\partial r_{2j}}\right]\right\rangle. \tag{8}$$

If W is a function only of the momenta, $W=S(p_1, p_2, \cdots, p_{3N})$, then Eq. (2) gives the result parallel to Eq. (3)

$$\sum_{j=1}^{3N}\langle(\partial S/\partial p_j)p_j\rangle=\langle dS/dt\rangle=0. \tag{3'}$$

Or, if W is equal to $q_k S(p_1, p_2, \cdots, p_{3N})$, Eq. (2) gives a result parallel to Eq. (5)

$$\sum_{j=1}^{3N}\langle q_k p_j(\partial S/\partial p_j)\rangle=-\langle\dot{q}_k S\rangle. \tag{5'}$$

For a one-dimensional simple harmonic potential $V=(k/2)x^2$, taking $W=x^s p^r$ we obtain *all* of the statistical moments of the coordinates and momenta. The only nonvanishing moments are

$$\langle(x/x_m)^{2s}(p/p_m)^{2r}\rangle=\frac{(2s)!(2r)!}{s!r!(s+r)!2^{2(s+r)}}.$$

If E is the total energy of the system, then $x_m=(2E/k)^{\frac{1}{2}}$ is the classical turning point and $p_m=(2mE)^{\frac{1}{2}}$ is the maximum momentum.

The hypervirial relations are not restricted to systems for which a potential energy function exists. Quite generally in these equations, $-\partial V/\partial q_j$ may be replaced by the generalized force F_{qj}. Thus, if $T(q, p)$ is the kinetic energy of the system expressed in terms of the generalized coordinates and momenta, in Eq. (2) we may set

$$(\partial H/\partial q_j)=(\partial T(q, p)/\partial q_j)-F_{qj}.$$

For systems in thermal equilibrium at a temperature T, there are considerable simplifications which can be made in the hypervirial relations. For thermal equilibrium distributions there is no statistical correlation between the coordinates and the momenta, so that

$$\langle f(q_1, \cdots)S(p_1, \cdots)\rangle=\langle f(q_1, \cdots)\rangle\langle S(p_1, \cdots)\rangle.$$

Furthermore, $\langle p_j\partial H/\partial p_j\rangle=kT$. Thus, for example, Eq. (6) becomes

$$skT\langle x_i^{s-1}\rangle=\langle x_i^s\partial V/\partial x_i\rangle. \tag{6'}$$

As W. W. Wood points out, such relations can also be obtained by integrating by parts the corresponding average of the canonical ensemble over phase space.

Applications of these relations to equations of state, and possibly to transport properties, will be given in a subsequent paper.

II. THE QUANTUM MECHANICAL HYPERVIRIAL THEOREM

The Heisenberg equation of motion is the quantum-mechanical equivalent of the classical equation of motion in terms of Poisson brackets. Take W to be an arbitrary function of the generalized coordinates and the (differential) operators for their conjugate momenta. Let ψ_m and ψ_n be eigenfunctions for the total

energy of the system, E_m and E_n, respectively. Then,[3]

$$\frac{d}{dt}\int\psi_m^*W\psi_n d\tau=-(i/\hbar)\int\psi_m^*[WH-HW]\psi_n d\tau$$

$$=(i/\hbar)(E_m-E_n)\int\psi_m^*W\psi_n d\tau. \quad (9)$$

If the expectation value of W for a stationary energy state n is not infinite, Eq. (9) gives

$$0=(i/\hbar)\int\psi_n^*[WH-HW]\psi_n d\tau. \quad (10)$$

Equation (10) is the quantum mechanical equivalent of Eq. (2) with spatial averaging (or integration) replacing the time averaging. Let us define the operator

$$J=(i/\hbar)[WH-HW]. \quad (11)$$

Then, Eq. (10) states that if ψ is any solution to the Schrödinger equation, the expectation value of J is equal to zero,

$$\int\psi^*J\psi d\tau=0. \quad (12)$$

Equation (12) is a powerful theorem since there is a wide variety of J operators.

Usually quantum-mechanical formulations are expressed in terms of a set of orthogonal generalized coordinates q_j which have the corresponding metric scale factors g_j defined by setting the square of an infinitesimal length equal to

$$\sum_{j=1}^{3N}g_j^2(dq_j)^2.$$

In these coordinates, the quantum mechanical operator for the momentum p_j is $(\hbar/i)\partial/\partial q_j$. The volume element is

$$d\tau=gdq_1dq_2\cdots dq_{3N}. \quad (13)$$

Here $g=g_1g_2\cdots g_{3N}$. The Hamiltonian for a set of particles each having the same mass m_i is then

$$H=-(\hbar^2/2m_i)\sum_{j=1}^{3N}g^{-1}(\partial/\partial q_j)[gg_j^{-2}(\partial/\partial q_j)]+V. \quad (14)$$

If $W=f(q_1, q_2, \cdots, q_{3N})$, so that W has no dependence on the momenta, and if the masses are all equal, it follows from Eqs. (11) and (14) that

$$J(f)=\frac{i\hbar}{2m_i}\sum_{j=1}^{3N}\left\{\frac{\partial f}{\partial q_j}g^{-1}\left[\frac{\partial}{\partial q_j}(gg_j^{-2})\right]+\left(\frac{\partial^2 f}{\partial q_j^2}\right)g_j^{-2}+2\frac{\partial f}{\partial q_j}g_j^{-2}\frac{\partial}{\partial q_j}\right\}. \quad (15)$$

Although this case was trivial with respect to classical mechanics, the quantum mechanical relations, Eqs. (9) and (12) using the J of Eq. (15), are very useful in evaluating the corrections to the Born-Oppenheimer approximation in the separation of variables, etc. To see the significance of Eq. (15), let us suppose that $f=r_i^s$ (the restriction that all of the particles have the same mass need not apply), so that J becomes

$$J(r_i^s)=(i\hbar/2m_i)[s(s+1)r_i^{s-2}+2sr_i^{s-1}(\partial/\partial r_i)]. \quad (16)$$

Substituting Eq. (16) into Eq. (11) leads to the result

$$\int\psi^*r_i^{s-1}(\partial\psi/\partial r_i)d\tau=-\tfrac{1}{2}(s+1)\int\psi^*r_i^{s-2}\psi d\tau. \quad (17)$$

Similarly, if $f=x_{ij}^s$ where x_{ij} is the jth cartesian coordinate of the ith particle (and the masses of the particles are not necessarily equal),

$$J(x_{ij}^s)=(i\hbar/2m_i)[s(s-1)x_{ij}^{s-2}+2sx_{ij}^{s-1}(\partial/\partial x_{ij})] \quad (18)$$

and

$$\int\psi^*x_{ij}^{s-1}(\partial\psi/\partial x_{ij})d\tau=-\tfrac{1}{2}(s-1)\int\psi^*x_{ij}^{s-2}\psi d\tau. \quad (19)$$

Another example of this sort results from setting $f=r_{12}^s$ where r_{12} is the distance between particles 1 and 2 which have different masses. For this case,

$$J(r_{12}^s)=i\hbar sr_{12}^{s-2}\left[\frac{s+1}{2}\left(\frac{1}{m_1}+\frac{1}{m_2}\right)+(\mathbf{r}_1-\mathbf{r}_2)\cdot\left(\frac{1}{m_1}\nabla_1-\frac{1}{m_2}\nabla_2\right)\right]. \quad (20)$$

In analogy with the classical treatment, we obtain the hypervirial relations by setting

$$W=(\hbar/i)f(\partial/\partial q_k). \quad (21)$$

Here we suppose that f is an arbitrary function of the generalized coordinates and the masses of all of the particles are equal. Then, making use of Eq. (14),

$$J(fp_k)=f\frac{\partial V}{\partial q_k}+\frac{\hbar^2}{2m_i}\sum_{j=1}^{3N}[A_j^{(1)}+A_j^{(2)}], \quad (22)$$

where

$$A_j^{(1)}=\left[-f\left(\frac{\partial g^{-1}}{\partial q_k}\right)\left(\frac{\partial(gg_j^{-2})}{\partial q_j}\right)-fg^{-1}\left(\frac{\partial^2(gg_j^{-2})}{\partial q_j\partial q_k}\right)\right]\frac{\partial}{\partial q_j}+\left[g^{-1}\left(\frac{\partial f}{\partial q_j}\right)\left(\frac{\partial(gg_j^{-2})}{\partial q_j}\right)+g_j^{-2}\left(\frac{\partial^2 f}{\partial q_j^2}\right)\right]\frac{\partial}{\partial q_k}$$

$$A_j^{(2)}=-f\left(\frac{\partial(g_j^{-2})}{\partial q_k}\right)\frac{\partial^2}{\partial q_j^2}+2g_j^{-2}\frac{\partial f}{\partial q_j}\frac{\partial^2}{\partial q_j\partial q_k}.$$

In Cartesian coordinates (and with arbitrary masses)

[3] L. I. Schiff, *Quantum Mechanics* (McGraw-Hill Book Company, Inc., New York, 1955), 2nd ed., p. 140.

Eq. (22) reduces to

$$J(fp_{xlk})=f\frac{\partial V}{\partial x_{lk}}+\sum_{i=1}^{N}\frac{\hbar^2}{2m_i}\sum_{j=1}^{3}\left[\frac{\partial^2 f}{\partial x_{ij}^2}\frac{\partial}{\partial x_{lk}}+2\frac{\partial f}{\partial x_{ij}}\frac{\partial^2}{\partial x_{ij}\partial x_{lk}}\right]. \quad (23)$$

An interesting example corresponds to setting $W=(\hbar/i)r_i^s(\partial/\partial r_i)$ and letting the particles have arbitrary masses. Then Eq. (22) gives

$$J(r_i^s p_{ri})=r_i^s(\partial V/\partial r_i)+(\hbar^2/2m_i)[2r_i^{s-1}\Delta_i+(s-1)r_i^{s-2}\{2r_i(\partial^2/\partial r_i^2)+(s+2)(\partial/\partial r_i)\}]. \quad (24)$$

Similarly, if $W=(\hbar/i)x_{ij}^s(\partial/\partial x_{ij})$, then

$$J(x_{ij}^s p_{xij})=x_{ij}^s(\partial V/\partial x_{ij})+(\hbar^2/2m_i)[s(s-1)x_{ij}^{s-2}(\partial/\partial x_{ij})+2sx_{ij}^{s-1}(\partial^2/\partial x_{ij}^2)]. \quad (25)$$

There are indeed a large number of examples which can be solved rather easily. However, it is best that these examples be considered in terms of specific applications.

III. QUANTUM MECHANICAL IMPLICATIONS

In Sec. II we found two sets of integral relationships which must be satisfied by ψ, an exact wave function for a stationary state of the system,

$$\int\psi^* J(f)\psi d\tau=0 \quad (26)$$

and

$$\int\psi^* J(fp)\psi d\tau=0. \quad (27)$$

The relations involving $J(f)$ are the quantum mechanical counterpart to the classical result $\sum_j(\partial f/\partial q_j)(\partial H/\partial p_j)=0$. The $J(f)$ operators do not involve the potential energy of the system and therefore the same set of relations, Eq. (26), must be satisfied by all wave functions (regardless of potential energy) which correspond to stationary energy-states of an arbitrary system. The satisfaction of the $J(f)$ relations is an inherent property of the Schrödinger Hamiltonian and the boundary conditions required for a physically acceptable wave function.

Let the kinetic energy operator be

$$\mathcal{K}=-\sum_{j=1}^{3}\sum_{i=1}^{N}(\hbar^2/2m_i)(\partial^2/\partial x_j{}^2). \quad (28)$$

Then regardless of the potential-energy function,

$$\int\psi^* J(f)\psi d\tau=(i/\hbar)\sum_{j=1}^{3}\sum_{i=1}^{N}(\hbar^2/2m_i)\int(\partial/\partial x_{ji})[\psi^*\psi(\partial f/\partial x_{ji})]d\tau. \quad (29)$$

Eq. (26) is then satisfied if ψ decreases at infinity faster than any negative power of the cartesian coordinates so that

$$\lim_{x_{ji}\to\pm\infty}\psi^*\psi(\partial f/\partial x_{ji})=0. \quad (30)$$

The Eq. (27) relations for the integrals of $J(fp)$ involve the potential energy and are specific to the dynamical problem under consideration. For example, if we again focus our attention on the radial coordinate of the ith particle, according to Eq. (24) we have the set of operators (expressed in atomic units);

$$J(r_i p_{ri})=r_i\partial V/\partial r_i+\Delta_i \quad (31)$$

$$J(r_i^2 p_{ri})=r_i^2\partial V/\partial r_i+r_i\Delta_i+2\partial/\partial r_i+r_i\partial^2/\partial r_i^2 \quad (32)$$

$$J(r_i^3 p_{ri})=r_i^3\partial V/\partial r_i+r_i^2\Delta_i+5r_i\partial/\partial r_i+2r_i^2\partial^2/\partial r_i^2 \quad (33)$$

$$\cdots=\cdots.$$

Equation (27) with the operator $J(r_i p_{ri})$ is the usual virial theorem of Clausius; the other operators lead to generalizations of the virial theorem. It is easy to show that if we take $\psi_1=\exp(-r_i)$ for the wave function, $V=-1/r_i$ and any of the operators $J(r_i p_{ri})$, $J(r_i^2 p_{ri})$, $J(r_i^3 p_{ri})$, $\cdots$, Eq. (27) is satisfied. Similarly Eq. (27) is satisfied if we take $\psi_2=\exp(-ar_i^2)$, $V=2a^2 r_i^2$ and any of these operators.

Other members of the $J(fp)$ family involve functions of more than one variable and second derivatives with respect to either one or two variables.

M. S. Wertheim showed the significance of the $J(fp)$ relations. Let ψ be real and decrease faster than any negative power of x_{ij} as x_{ij} approaches $\pm\infty$. Also, we assume that f does not increase faster than any positive power of x_{ij} as x_{ij} approaches $\pm\infty$. Then, integrating by parts, we obtain

$$\int\psi J(fp_{xlk})\psi d\tau=0=\int f\psi^2(\partial/\partial x_{lk})[H\psi/\psi]d\tau. \quad (34)$$

Since Eq. (34) is valid for arbitrary functions f, it follows that

$$(\partial/\partial x_{lk})[H\psi/\psi]=0. \quad (35)$$

Equation (35) integrates to give

$$H\psi=E\psi. \quad (36)$$

Thus, any function ψ which satisfies the complete set of $J(fp)$ relations is a solution to the Schrödinger equation corresponding to a stationary energy state. Similarly, one can show that the J relations involving higher powers of the momentum operators correspond to the vanishing of the higher derivatives of $[H\psi/\psi]$. No additional information could be obtained from such relations.

The $J(fp)$ relations can be used to determine a wave function. We might proceed as follows. Let ϕ_1, ϕ_2, $\cdots$ form a mathematically complete set of functions in the coordinate space which are everywhere continuous, have continuous first derivatives, are square integrable, and satisfy the boundary conditions imposed on the wave function. Now let us express the set of energy wave functions in the form

$$\psi=\sum_{j=1}^{\infty}C_j\phi_j. \tag{37}$$

Then substituting Eq. (37) into Eqs. (26) and (27) we obtain the sets of equations

$$\sum_{i,j}C_i^*J(fp)_{ij}C_i=0, \tag{38}$$

where the $J(fp)_{ij}$ are the matrix elements

$$J(fp)_{ij}=\int\phi_i^*J(fp)\phi_j d\tau. \tag{39}$$

It is possible to completely determine the wave function from these relations and there are a sufficient number of linearly independent operators to determine these constants. Of course, there would be an infinite number of sets of C_j corresponding to the various quantum states of the system. However, the quantum numbers corresponding to a particular solution would be very easy to recognize from the nodal structure of the wave function.

We shall use the $J(fp)$ relations to assist in the selection of an approximate wave function. Depending on the physical properties of the system which we are most interested in, we shall select the set of $J(fp)$ realtions which will be most sensitive to this property. For example, if we were interested in chemical binding, which requires that the wave functions be accurately determined at large separations from the nuclei, we might require the satisfaction of integral equations involving $J(r_i^sp_{ri})$ with large values of s.

ACKNOWLEDGMENT

The author wishes to express his gratitude to Robert G. Sachs for pointing out the similarity between the Heisenberg equation-of-state and the set of integral relations which the author had independently derived. He is also grateful to Michael S. Wertheim for pointing out the true significance of the quantum-mechanical $J(f)$ and $J(fp)$ relations. Thanks are due Charles F. Curtiss, Elizabeth S. Hirschfelder, George V. Nazaroff, and Thomas A. Bronikowski for many helpful suggestions.

THE JOURNAL OF CHEMICAL PHYSICS VOLUME 33, NUMBER 5 NOVEMBER, 1960

Cell Method in Grand Canonical Ensemble

J. M. RICHARDSON,
Hughes Research Laboratories, A Division of Hughes Aircraft Company, Malibu, California
AND
S. R. BRINKLEY, JR.,
Combustion and Explosive Research, Inc., Pittsburgh, Pennsylvania

(Received May 23, 1960)

A variational form of the cell theory of multicomponent liquids is formulated on the basis of the grand canonical ensemble. The method can in principle be extended to any desired level of accuracy. More explicit results are obtained for the case in which each cell can contain at most one particle and the correlation between cells is neglected. In addition, a higher order theory is presented in which correlations in the modes of occupancy of cells is treated to the second order. The relation between the radial distribution function and the results of the simpler cell theory is considered.

I. INTRODUCTION

THE cell (or free volume) theories of the liquid state developed by Eyring and Hirschfelder[1] and by Lennard-Jones and Devonshire[2] have been successful in approximately accounting for the thermodynamic properties of simple nonpolar liquids in terms of intermolecular forces. During the past several years numerous investigators[3–7] have devised improved versions of this type of theory. However, all of these efforts are limited by the fact that they are based upon a particular model in which the molecules are confined to cells in certain ways. Kirkwood[8] has published a critique showing how the cell theory can be put on a sounder conceptual basis by deriving it from the general formulation in the petit canonical ensemble with the aid of well-defined approximations. His paper shows that the physical model is identical with a particular approximation within the general formulation, and it suggests a way for devising higher approximations.

A more convenient general formulation can be obtained by employing the grand canonical ensemble. One can then speak of the states of cells (the numbers of various molecules in each cell and their positions) instead of the states of molecules, and with the aid of a general variational method[9] a cooperative theory of arbitrarily high accuracy can be constructed with the cells themselves playing the roles of the cooperative elements. The principal advantage of the grand canonical ensemble over the petit is that with vanishing intermolecular potentials, the cells are statistically independent. On the other hand, the restrictions on the total numbers of various types of molecules introduce a statistical dependence[10] in the petit ensemble.

The general formulation is presented in Sec. II. Section III is devoted to first-order theories in which statistical correlations among cells are neglected and the cell volume is optimized. In the beginning of this section we present the most general of the first-order theories. Next we neglect multiple occupancies obtaining a theory of which a special case is identical to the theory of Mayer and Careri.[11] We then introduce the spherical smoothing and singlewise displacement approximations giving finally a result that may be considered a generalization of the Lennard-Jones Devonshire theory. In Sec. IV, we specialize the last results to a one-component system and neglect vacancies, thereby obtaining a result identical to the Lennard-Jones Devonshire theory. Section V is devoted to the calculation of the radial distribution function within the framework of the first-order theories. In Sec. VI, we consider second-order theories in which pair correlations are approximately taken into account. It is hoped that a second-order theory will eventually prove successful in treating the case of a mixture of molecules involving large radius ratios—a case can be handled by a first-order theory only by allowing multiple occupancies and employing a larger cell size.

The communal entropy is given only brief consideration because it does not appear in a natural way. Kirkwood[8] has shown that the communal entropy may be regarded as a correction for the neglect of vacancies and multiple occupancies in a theory explicitly treating the cells as only singly occupied. It has nothing whatever to do with the interchange of identical molecules between cells, as is often assumed.[12] Although an ap-

[1] H. Eyring and J. O. Hirschfelder, J. Phys. Chem. **41**, 249 (1937); also, J. O. Hirschfelder, J. Chem. Ed. **16**, 540 (1939).
[2] J. E. Lennard-Jones and A. F. Devonshire, Proc. Roy. Soc. (London) **A163**, 53 (1937); *ibid.* **A165**, 1 (1938).
[3] P. Janssens and I. Prigogine, Physica **16**, 851 (1950).
[4] J. S. Rowlinson and C. F. Curtiss, J. Chem. Phys. **19**, 1519 (1951).
[5] S. Ono, Mem. Fac. Eng. Kyushu Univ. **10**, 190 (1947).
[6] F. Cernushi and H. Eyring, J. Chem. Phys. **7**, 547 (1939).
[7] J. Pople, Phil. Mag. **42**, 459 (1951).
[8] J. G. Kirkwood, J. Chem. Phys. **18**, 380 (1950). A further application of this formulation may be found in D. W. Salsburg and J. G. Kirkwood, J. Chem. Phys. **20**, 1538 (1952).
[9] J. M. Richardson, *A General Variational Method in Statistical Mechanics* (to be published).
[10] To be sure, this dependence is negligible when the numbers are large. Nevertheless, it is a conceptual and mathematical convenience to have this dependence vanish exactly.
[11] J. E. Mayer and G. Careri, J. Chem. Phys. **20**, 1001 (1952).
[12] See, R. H. Fowler and E. A. Guggenheim, *Statistical Thermodynamics* (Cambridge University Press, New York, 1939), p. 327.

proximation to the communal entropy is considered in Sec. IV, the authors hold the opinion that the problem of evaluating this quantity is a futile one since its evaluation depends on comparing a single occupancy theory with one treating more complicated modes of occupancy. Once the more accurate theory has been constructed, one then has all the physically significant answers one is seeking and there then seems to be little profit in considering the deviations from the less accurate theory.

The present paper emphasizes formal results. The results of numerical computation and comparisons with experiment will be presented in a sequel.

II. GENERAL THEORY OF CELL METHOD IN GRAND CANONICAL ENSEMBLE

Our model is an assemblage of classical molecules confined within a large container of volume V. We consider c types of molecules labeled by α, $\alpha=1, \cdots, c$. The mass of a molecule of type α is denoted by m_α. A pair of molecules, one of type α and the other of type α' (α may equal α'), separated by a distance r, has an interaction energy $\phi_{\alpha\alpha'}(r)$. Thus, our treatment is limited to molecules which, to an adequate degree of approximation, can be regarded as spherical.[13] If the system contains N_1 molecules of type 1, N_2 molecules of type 2, etc., then Hamiltonian is

$$H=\sum_\alpha (2m_\alpha)\sum_{s=1}^{N_\alpha} p_{\alpha s}{}^2+U, \tag{2.1}$$

where the potential energy U is given by

$$U=\tfrac{1}{2}\sum_{\alpha,\alpha'}\sum_{s=1}^{N_\alpha}\sum_{s'=1}^{N_{\alpha'}}\phi_{\alpha\alpha'}(r_{ss'})+\tfrac{1}{2}\sum_\alpha\sum_{\substack{s,s'=1\\ s\neq s'}}^{N_\alpha}\phi_{\alpha\alpha}(r_{ss'}), \tag{2.2}$$

and where $p_{\alpha s}=|\mathbf{p}_{\alpha s}|$ in which $\mathbf{p}_{\alpha s}$ is the momentum of the sth particle of type α.

The grand partition function can be expressed in the form

$$\exp(\beta\hat{p}V)=\mathcal{S}\exp[\beta(\sum_{\alpha=1}^{c}\mu_\alpha{}^*N_\alpha-U)], \tag{2.3}$$

where $\beta=1/kT$, $\hat{p}$ is the pressure, and $\mathcal{S}$ is the configurational summation operator in the grand canonical ensemble defined by

$$\mathcal{S}(\ )=\prod_{\alpha=1}^{c}\sum_{N_\alpha=0}^{\infty}[1/(N_\alpha)!]\int_V d\{N_\alpha\}(\ ), \tag{2.4}$$

in which $\int_V d\{N_\alpha\}\ (\ )$ is the operation of integration in the configuration space of N_α molecules of type α confined in a volume V. In the case of no molecules of type α, the integration written in Eq. (2.4) is to be replaced by unity. Apart from an additive constant, the quantity $\mu_\alpha{}^*$ is the chemical potential per molecule of type α. It is related to the absolute potential μ_α by the formulas

$$\mu_\alpha{}^*=\mu_\alpha-\beta^{-1}\log v_\alpha{}^0,$$
$$v_\alpha{}^0=(2\pi m_\alpha/h^2\beta)^{-\frac{3}{2}}, \tag{2.5}$$

where h is Planck's constant. The quantity $\mu_\alpha{}^*$ has the convenient property that at infinite dilution it approaches $\beta^{-1}\log C_\alpha$, where C_α is the average number density of molecules of type α.

The theory depends upon the important property of the summation operator $\mathcal{S}$, namely, that it can be factored into a product

$$\mathcal{S}=\prod_i \mathcal{S}_i, \tag{2.6}$$

in which the factor labeled by i sums over the states of cell i (with volume v_i in real space). These cells may be of any shape or size as long as they are nonoverlapping and collectively make up the total volume V,

$$\sum_i v_i=V. \tag{2.7}$$

Later we will find it convenient to require the cells to be identical. The factor $\mathcal{S}_i$ is defined by

$$\mathcal{S}_i(\ )=\prod_{\alpha=1}^{c}\sum_{n_{\alpha i}=0}^{\infty}[1/(n_{\alpha i})!]\int_{v_i} d\{n_{\alpha i}\}(\ ), \tag{2.8}$$

when $n_{\alpha i}$ is the number of molecules of type α contained in cell i. The operation $\int_{v_i} d\{n_{\alpha i}\}$ is the integration over the configuration space of $n_{\alpha i}$ molecules of type α contained in the volume v_i. It is apparent that the operator $\mathcal{S}_i$ has the same meaning as $\mathcal{S}$ except that it sums over the numbers and configurations of the molecules in the cell i instead of the total volume V.

Now we consider the variational principle corresponding to the grand canonical ensemble. This principle involves the maximization of the variational function

$$-\beta\hat{p}V=\mathcal{S}P(\log P-\beta\sum_{\alpha=1}^{c}\mu_\alpha{}^*N_\alpha+\beta U), \tag{2.9}$$

with respect to the distribution function P (dependent upon numbers as well as configurations) and subject to the constraints that the $\mu_\alpha{}^*$, β, and V are constant and that P is normalized,

$$\mathcal{S}P=1. \tag{2.10}$$

It can be shown that the maximum value of $\hat{p}$ is the pressure p given by Eq. (2.3) and that the functional form of P giving this maximum is

$$P=\exp[\beta(-pV+\sum_{\alpha=1}^{c}\mu_\alpha{}^*N_\alpha-U)], \tag{2.11}$$

which defines the grand canonical ensemble.

Now we will use the factorization property of the summation operator $\mathcal{S}$. According to the general variational method developed by one of the authors,[9] one can define cooperative elements as the entities whose states are summed over th the factors $\mathcal{S}_i$ of $\mathcal{S}$. In the present case the cells are the cooperative elements and we will

[13] It is not difficult, at least in principle, to extend the treatment to nonspherical molecules.

be concerned with the states of cells, interaction and correlation between cells, etc.

The general variational method provides an expansion of $\beta\hat{p}V$, defined by Eq. (2.9), in a series of terms containing progressively higher-order correlations. Now let the cells be identical (for example, they could be the unit cells of a face-centered cubic lattice). Let the distribution function be written

$$P=\prod_i \rho(i)\prod_{i,i'}{}' g_{ii'}(i,i')\prod_{i,i',i''}{}' g_{ii'i''}(i,i',i'')\cdots, \quad (2.12)$$

in which the letters i, i', $\cdots$in parentheses denote the dependence upon the *states* of cells i, i', $\cdots$, whereas i, i', $\cdots$appearing as subscripts denote the dependence upon the *labels* of the corresponding cells. For example, $\rho(i)$ depends only upon the state of cell i, and its dependence upon this state is independent of i regarded as a mere label. In other words, $\rho(i)$ is the same *function* for all cells. On the other hand, $g_{ii'}(i,i')$ depends upon both the states and labels of cells i and i'. However, we will require that the dependence upon the labels be such that only the distance between cells i and i' is involved. Obvious extensions pertain to the higher order g's. These statements amount to saying that the cells are statistically equivalent. The primes on the product operators in Eq. (2.12) are employed to denote the omission of factors in which the same cell appears more than once.

According to the general variational method, certain restrictions must be imposed upon the factors in Eq. (2.12). First, the factors $\rho(i)$ must be normalized,

$$\mathcal{S}_i\rho(i)=1. \quad (2.13a)$$

In addition there exists a sequence of compatibility conditions,

$$\mathcal{S}_i\rho(i)g_{ii'}(i,i')=1, \quad (2.13b)$$

$$\mathcal{S}_i\rho(i)g_{ii'}(i,i')g_{ii''}(i,i'')g_{ii'i''}(i,i',i'')=1. \quad (2.13c)$$

and so forth. In the present application we will not explicitly use compatibility conditions of order higher than the third. For example, condition (2.13b) ensures that if $\rho(i)\rho i')g_{ii'}(i,i')$ be the joint distribution for a pair of cells i and i', then $\rho(i)$ is the distribution for one cell.

Insertion of (2.12) and (2.9) using the normalization and compatibility conditions reduces the variational function to

$$\begin{aligned}-\beta\hat{p}v=&\mathcal{S}_i\rho(i)[\log\rho(i)-\beta\sum_{\alpha=1}^{r}\mu_\alpha{}^*n_\alpha+\beta U(i)]\\&+\tfrac{1}{2}\sum_{i'}{}'\mathcal{S}_i\mathcal{S}_{i'}\rho(i)\rho(i')g_{ii'}(i,i')[\log g_{ii'}(i,i')+\beta U_{ii'}(i,i')]\\&+(1/3!)\sum_{i'i''}{}'\mathcal{S}_i\mathcal{S}_{i'}\mathcal{S}_{i''}\rho(i)\rho(i')\rho(i'')g_{ii'}(i,i')g_{i'i''}(i',i'')\\&\cdot g_{i''i}(i'',i)g_{ii'i''}(i,i',i'')\log g_{ii'i''}(i,i',i'')+\cdots,\end{aligned} \quad (2.14)$$

in which v is the cell volume, $U(i)$ is the potential energy of a cell in state i (nonvanishing only if the cell is multiply occupied), and $U_{ii'}(i,i')$ is the interaction energy of cells i and i'. The primes on the $\sum$'s denote the omission of terms involving a cell more than once. The quantities $U(i)$ and $U_{ii'}(i,i')$, expressing U in terms of cells, can be readily obtained from Eq. (2.2) expressing U in terms of the molecular coordinates. This can be done by comparing

$$U=\sum_i U(i)+\tfrac{1}{2}\sum_{i,i'}{}'U_{ii'}(i,i') \quad (2.15)$$

with Eq. (2.2) for the states of a single cell, then for a pair of cells. For instance, if cell i contains no molecules or only one molecule, $U(i)=0$. If it contains two molecules, one of type α and the other of type α', then $U(i)=\phi_{\alpha\alpha'}(r)$, where r is the distance between the two molecules. If one or both of two cells, i and i', are vacant, then the interaction energy $U_{ii'}(i,i')$ vanishes. If cell i contains one molecule of type α at a vector distance $\mathbf{r}$ from its center and cell i' contains one molecule of type α' at a distance $\mathbf{r}'$ from its center, then $U_{ii'}(i,i')=\phi_{\alpha\alpha'}(|\mathbf{r}-\mathbf{r}'+\mathbf{R}|)$, where $\mathbf{R}$ is the vector distance between the cell centers. The states of higher occupancy can be treated by similar means.

The solution of our problem is obtained by maximizing the variational function, Eq. (2.14), with respect to $\rho(i)$, $g_{ii'}(i,i')$, etc., under the constraints (2.13a), (2.13b), etc., and holding β and the $\mu_\alpha{}^*$ fixed. If desired, v can be varied also. However, as long as the expression (2.14) is employed in its exact form, the maximum value is independent of v. If certain approximations are introduced into (2.14), the result will depend upon v and it may be advantageous to let v vary in the maximization.

Regardless of whether $\hat{p}$ is an exact or approximate functional, its maximum value p, the pressure, can be used for the computation of all of the thermodynamic quantities if its dependence on β and the $\mu_\alpha{}^*$ is known. The resulting quantities will be thermodynamically consistent, i.e., they will still conform to the general thermodynamic relations. The preservation of thermodynamic consistency when approximations are introduced is a convenient property of a variational procedure, since it provides directly a single function from which all the thermodynamic quantities can be derived. Another useful property is the fact that a first derivative of p (with respect to the parameters β or the $\mu_\alpha{}^*$) equals the same derivative of $\hat{p}$ holding the variables v, $\rho(i)$, etc., fixed if after differentiation these variables are assigned the values making $\hat{p}$ a maximum. Let the symbol γ represent the above variables (v, $\rho(i)$, etc.) and let γ_m represent the particular values making $\hat{p}$ a maximum. Obviously γ_m is dependent only upon β and the $\mu_\alpha{}^*$. We have

$$\hat{p}=\hat{p}(\beta,\mu_\alpha{}^*;\gamma), \quad (2.16)$$

$$p(\beta,\mu_\alpha{}^*)=\hat{p}(\beta,\mu_\alpha{}^*;\gamma_m), \quad (2.17)$$

$$\gamma_m=\gamma_m(\beta,\mu_\alpha{}^*), \quad (2.18)$$

where the maximum condition is given by

$$(\partial\hat{p}/\partial\gamma)_{\gamma=\gamma_m}=0. \tag{2.19}$$

Let us consider for example the derivative of p with respect to β. We obtain from Eqs. (2.16)–(2.18),

$$\partial p/\partial\beta=(\partial\hat{p}/\partial\beta)_{\gamma=\gamma_m}+(\partial\hat{p}/\partial\gamma)_{\gamma=\gamma_m}(\partial\gamma_m/\partial\beta). \tag{2.20}$$

By Eq. (2.19) the second term on the right vanishes, giving the desired result

$$\partial p/\partial\beta=(\partial\hat{p}/\partial\beta)_{\gamma=\gamma_m}. \tag{2.21}$$

Now let us consider more explicitly the evaluation of the thermodynamic functions. From Eq. (2.3), defining exactly the grand partition function, we obtain (holding the volume V fixed)

$$d(\beta pV)=\sum_\alpha\langle N_\alpha\rangle d(\beta\mu_\alpha{}^*)-\langle U\rangle d\beta, \tag{2.22}$$

where

$$\langle N_\alpha\rangle\equiv VC_\alpha=\mathcal{S}PN_\alpha, \tag{2.23}$$

and

$$\langle U\rangle=\mathcal{S}PU. \tag{2.24}$$

C_α is the average number density of molecules of type α and U is potential energy given by Eq. (2.2) [or Eq. (2.15)]. Eq. (2.22) is a somewhat disguised form of the well-known Gibbs-Duhem equation. From Eq. (2.5) we obtain

$$d(\beta\mu_\alpha{}^*)=d(\beta\mu_\alpha)-3d\beta/2\beta. \tag{2.25}$$

Insertion of Eq. (2.25) into (2.22) gives

$$d(\beta pV)=\sum_\alpha\langle N_\alpha\rangle d(\beta\mu_\alpha)-\langle H\rangle d\beta, \tag{2.26}$$

where

$$\langle H\rangle=E=\langle U\rangle+(3/2\beta)\sum_\alpha\langle N_\alpha\rangle \tag{2.27}$$

is the average total energy. Eq. (2.26) is the more familiar form of the Gibbs-Duhem equation. The entropy S may be defined by

$$S=-k_\beta(V\sum_\alpha\mu_\alpha C_\alpha-E-pV). \tag{2.28}$$

All of these relations are exact, and suffice for the calculation of S, E, p, and C_α in terms of β and μ (or $\mu_\alpha{}^*$). When p is an approximate function of β and the $\mu_\alpha{}^*$, we will keep Eq. (2.22) as the definition of $\langle N_\alpha\rangle$ and $\langle U\rangle$, and then use (2.25), (2.27), and (2.28) for the calculation of the other functions. In each particular case it must be determined whether or not the approximations used in $\hat{p}$ are consistent with Eqs. (2.23) and (2.24). For example, suppose we make the approximation of setting all the g's equal to unity in Eq. (2.14) and then calculate $\langle U\rangle$ from Eq. (2.22) with the aid of Eq. (2.21). Is this result the same as that obtained by introducing the same approximations into $\mathcal{S}PU$? In this particular case the answer is yes. However, it is hard to make general statements valid for all conceivable approximations.

After C_α and $\langle U\rangle$ have been calculated from p using (2.22) [or from $\hat{p}$ using (2.22) and (2.21)], and the modified entropy S^* defined by

$$S^*=k_\beta(V\sum_{\alpha=1}^{c}\mu_\alpha{}^*C_\alpha-\langle U\rangle-pV), \tag{2.29}$$

has been obtained, then E may be calculated from (2.27), μ_α from (2.5) and S from

$$S=S^*+kV\sum_{\alpha=1}^{c}C_\alpha(\tfrac{3}{2}-\log v_\alpha{}^0). \tag{2.30}$$

In these last computations we have regarded the independent variables to be β and the $\mu_\alpha{}^*$. However, it is more conventional to take the set β and the C_α. This set is usually more convenient mathematically because the solution of the variational problem usually yields the $\mu_\alpha{}^*$ expressed explicitly as functions of β and the C_α.

III. FIRST-ORDER THEORIES[14]

By the phrase "first order" we mean that only first-order factors in the product (2.12) are retained, the higher-order factors being approximated by unity. This approximation is equivalent in a formal sense to that used in the Bragg-Williams theory. The most general first-order theory is given by the following approximation to $-\beta\hat{p}v$ [defined exactly by Eq. (2.14)]:

$$-\beta\hat{p}v=\mathcal{S}_i\rho(i)[\log\rho(i)-\beta\sum_{\alpha=1}^{c}\mu_\alpha{}^*n_{\alpha i}+\beta U(i)]$$
$$+\tfrac{1}{2}\beta\sum_{i'}{}'\mathcal{S}_i\mathcal{S}_{i'}\rho(i)\rho(i')U_{ii'}(i,i') \tag{3.1}$$

in which cell i is any representative cell. We drop all of the compatibility conditions, Eqs. (2.13b), (2.13c), $\cdots$, and retain only the first-order normalization condition

$$\mathcal{S}_i\rho(i)=1, \tag{3.2}$$

which is now the only restraint on the variations of $\rho(i)$. It is permissible also to vary v in order to obtain the optimum cell size. As pointed out by Mayer and Careri,[11] if one does not impose an upper limit to the cell occupancy, the optimum cell size will equal the total volume in which case (3.1) becomes identical to the exact variational principle (2.9). If the method is to have any practical value we should allow an occupancy limit of one or perhaps two molecules per cell.

Let us confine our attention henceforth to the case of an upper limit of one molecule per cell. Let $\rho(i)$ take the more explicit form

$$\rho(i)=\left\{\begin{matrix}\rho_0\\ \rho_\alpha(\mathbf{r})\end{matrix}\right\}, \tag{3.3}$$

[14] The main part of this section was presented at the Washington Meeting of the American Physical Society, May 1952. J. M. Richardson and S. R. Brinkley, Jr., Phys. Rev. **87**, 199(A) (1952).

where ρ_0 is the probability of vacancy in cell i, and $\rho_\alpha(\mathbf{r})d\mathbf{r}$ is the probability that one molecule of type α is located in the volume element $d\mathbf{r}$ situated at a vector distance $\mathbf{r}$ from the cell center *and* that no other molecules are contained in the cell.

With these restrictions, Eq. (3.1) reduces to

$$-\beta\hat{p}v=\rho_0\log\rho_0+\sum_{\alpha=1}^{c}\int d\mathbf{r}\rho_\alpha(\mathbf{r})[\log\rho_\alpha(\mathbf{r})-\beta\mu_\alpha{}^*]$$

$$+\tfrac{1}{2}\beta\sum_{\alpha,\alpha'=1}^{c}\int_v d\mathbf{r}\int d\mathbf{r}'\rho_\alpha(\mathbf{r})\rho_{\alpha'}(\mathbf{r}')W_{\alpha\alpha'}(\mathbf{r}-\mathbf{r}'), \quad (3.4)$$

where

$$W_{\alpha\alpha'}(\mathbf{r}-\mathbf{r}')=\sum_{\mathbf{R}}{}'\phi_{\alpha\alpha'}(|\mathbf{r}-\mathbf{r}'-\mathbf{R}|). \quad (3.5)$$

In Eq. (3.4),

$$\int_v d\mathbf{r}$$

denotes the integration over the cell volume v. In Eq. (3.5), $\phi_{\alpha\alpha'}(\mathbf{r}-\mathbf{r}'-\mathbf{R})$ is the interaction energy between a molecule of species α at a position $\mathbf{r}$ in a cell and another molecule of species α' at a position $\mathbf{r}'$ in another cell whose center is located at a vector distance $\mathbf{R}$ from the center of the first cell. The prime on the summation over $\mathbf{R}$ in Eq. (3.5) denotes the exclusion of $\mathbf{R}=0$. The normalization condition $\$_i\rho(i)=1$ takes the explicit form

$$\rho_0+\sum_{\alpha=1}^{c}\int_v d\mathbf{r}\rho_\alpha(\mathbf{r})=1. \quad (3.6)$$

The variational function should be maximized with respect to v, ρ_0, and $\rho_\alpha(\mathbf{r})$ subject to the normalization condition Eq. (3.6). This operation yields the following subsidiary conditions

$$\log\rho_\alpha(\mathbf{r})=\log\rho_0+\beta[\mu_\alpha{}^*-w_\alpha(\mathbf{r})],$$

$$w_\alpha(\mathbf{r})=\sum_{\alpha'=1}^{c}\int_v d\mathbf{r}'\rho_{\alpha'}(\mathbf{r}')W_{\alpha\alpha'}(\mathbf{r}-\mathbf{r}'), \quad (3.7)$$

$$\beta\hat{p}v=1-\rho_0-\tfrac{1}{6}\beta\sum_{\alpha,\alpha'=1}^{c}\int_v d\mathbf{r}\int_v d\mathbf{r}'\rho_\alpha(\mathbf{r})\rho_{\alpha'}(\mathbf{r}')\bar{W}_{\alpha\alpha'}(\mathbf{r}-\mathbf{r}'),$$

$$\bar{W}_{\alpha\alpha'}(\mathbf{r}-\mathbf{r}')=\sum_{\mathbf{R}}{}'|\mathbf{r}-\mathbf{r}'-\mathbf{R}|\phi_{\alpha\alpha'}{}'(|\mathbf{r}-\mathbf{r}'-\mathbf{R}|). \quad (3.8)$$

Equation (3.7) arises from the variation of $\hat{p}$ with respect to the distribution functions. It is an integral equation for the determination of $\rho_\alpha(\mathbf{r})$ and must be supplemented by the normalization condition, Eq. (3.6). In the one-component case, it is identical to a result obtained by Mayer and Careri[11] by somewhat different methods and is similar to the integral equation Kirkwood[8] obtained under the constraint of single occupancy. Equation (3.8) arises from the variation of $\hat{p}$ with respect to the cell volume v and may be seen to conform to the kinetic theory definition of pressure. To obtain, in principle at least, the solution of the problem, we must solve Eqs. (3.6)–(3.8) along with Eq. (3.4) (with $\hat{p}$ replacing $\hat{p}$) for ρ_0, $\rho_\alpha(\mathbf{r})$, v, and $\hat{p}$. This unfortunately cannot be done exactly. It is necessary to resort to approximations (e.g., those used by Kirkwood).[8] One achieves greater logical coherence and the obvious preservation of thermodynamic consistency if one introduces the approximations into the expression for the functional $\hat{p}$ before taking the variations. We derive below a more approximate form of $\hat{p}$ and repeat the variational procedure.

Two additional approximations are desirable. The first is the treatment of the displacements of molecules from their cell centers in a singlewise fashion. More explicitly we set

$$\rho_\alpha(\mathbf{r})=\rho_\alpha\delta(\mathbf{r})+\psi_\alpha(\mathbf{r}) \quad (3.9)$$

in the interaction energy part of Eq. (3.4) and neglect terms that are quadratic in the $\psi_\alpha(\mathbf{r})$. The quantity ρ_α, which is not to be confused with $\rho_\alpha(\mathbf{r})$, is the occupation probability of molecules of type α and is defined by

$$\rho_\alpha=\int_v d\mathbf{r}\rho_\alpha(\mathbf{r}). \quad (3.10)$$

The second approximation is that of spherical smoothing. We require $\rho_\alpha(\mathbf{r})$ to be spherically symmetric and replace the cell by an equivalent sphere of radius r^* given by $4\pi/3\cdot r^{*3}=v$.

It will be convenient to separate the scale of the cell distribution from the shape. To do this, let

$$\rho_\alpha(\mathbf{r})=\rho_\alpha\theta_\alpha(\xi)/v,$$
$$\xi=r/r^*. \quad (3.11)$$

The normalization condition (3.6) can now be written

$$\rho_0+\sum_{\alpha=1}^{c}\rho_\alpha=1. \quad (3.12)$$

From Eq. (3.10) we obtain

$$\int_0^1 3\xi^2 d\xi\theta_\alpha(\xi)=1. \quad (3.13)$$

With the preceding approximations and definitions Eq. (3.4) assumes the form

$$-\beta\hat{p}v=\rho_0\log\rho_0+\sum_{\alpha=1}^{c}\rho_\alpha[\log(\rho_\alpha/v)$$

$$+\int_0^1 3\xi^2 d\xi\theta_\alpha(\xi)\log\theta_\alpha(\xi)]-\beta\sum_{\alpha=1}^{c}\rho_\alpha\mu_\alpha{}^*$$

$$+\tfrac{1}{2}\beta\sum_{\alpha,\alpha'}^{c}\rho_\alpha\rho_{\alpha'}\left[W_{\alpha\alpha'}(0)+2\int_0^1 3\xi^2 d\xi\theta_\alpha(\xi)\langle\Delta W_{\alpha\alpha'}\rangle_e\right] \quad (3.14)$$

where $W_{\alpha\alpha'}(0)$ is defined by Eq. (3.5) and $\langle\Delta W_{\alpha\alpha'}\rangle_{e'}$, the spherically-smoothed excess interaction energy

introduced by Lennard-Jones and Devonshire,[2] is given by

$$\langle \Delta W_{\alpha\alpha'} \rangle_e = (1/4\pi) \int d\mathbf{e} [W_{\alpha\alpha'}(r^* \xi \mathbf{e}) - W_{\alpha\alpha'}(0)], \quad (3.15)$$

where $\int d\mathbf{e}$ is integration over all orientations of the unit vector $\mathbf{e}$. Equation (3.15) is symmetrical in α and α'.

Our ultimate purpose is to maximize $\hat{p}$ at constant β and μ_α^* with respect to v, p_0, p_α and $\theta_\alpha(\xi)$, subject to the constraints (3.12) and (3.13). However, it is expedient to maximize $\hat{p}$ first with respect to $\theta_\alpha(\xi)$ subject to (3.13), keeping all of the other variables fixed. This operation leads to the expression

$$\theta_\alpha = 1/\Gamma_\alpha \cdot \exp(-\beta \sum_{\alpha'=1}^{c} \rho_{\alpha'} \langle \Delta W_{\alpha\alpha'} \rangle_e), \quad (3.16)$$

where

$$\Gamma_\alpha = \int_0^1 3\xi^2 d\xi \exp(-\beta \sum_{\alpha'=1}^{c} \rho_{\alpha'} \langle \Delta W_{\alpha\alpha'} \rangle_e). \quad (3.17)$$

The quantity Γ_α and its derivatives have been evaluated by Lennard-Jones and Devonshire[2] for the case of one component and single occupancy. Substitution of (3.16) and (3.14) yields

$$-\beta \hat{p} v = \rho_0 \log \rho_0 + \sum_{\alpha=1}^{c} \rho_\alpha \log(\rho_\alpha / v) - \log\Gamma - \beta \sum_{\alpha=1}^{c} \rho_\alpha \mu_\alpha^* + \tfrac{1}{2}\beta \sum_{\alpha,\alpha'=1}^{c} \rho_\alpha \rho_{\alpha'} W_{\alpha\alpha'}(0), \quad (3.18)$$

where

$$\log\Gamma = \sum_{\alpha=1}^{c} \rho_\alpha \log \Gamma_\alpha. \quad (3.19)$$

Here Γ is to be considered a function of v, β, and the ρ_α.

Now we maximize $\hat{p}$, given by (3.18) with respect to v and the ρ_α, using

$$\rho_0 = 1 - \sum_{\alpha=1}^{c} \rho_\alpha.$$

The variation with respect to v gives

$$\beta p v = 1 - \rho_0 + v(\partial/\partial v)(\log\Gamma - \tfrac{1}{2}\beta \sum_{\alpha,\alpha'=1}^{c} \rho_\alpha \rho_{\alpha'} W_{\alpha\alpha'}), \quad (3.20)$$

where p is given by (3.18) after replacing $\hat{p}$ by its maximum value p. On inspection one sees that this expression is an approximation to the kinetic-theory definition of pressure. The variation with respect to ρ_α gives

$$\beta \mu_\alpha^* = \log \rho_0 + \log(\rho_\alpha / v) - (\partial/\partial \rho_\alpha) \log\Gamma + \beta \sum_{\alpha'=1}^{c} \rho_{\alpha'} W_{\alpha\alpha'}(0), \quad (3.21)$$

an expression to be used for computing μ_α^*. Replacing $\hat{p}$ by p in (3.18) and substituting (3.21), we obtain

$$\beta p v = -\log \rho_0 - \beta(\partial/\partial\beta) \log\Gamma + \tfrac{1}{2}\beta \sum_{\alpha,\alpha'=1}^{c} \rho_\alpha \rho_{\alpha'} W_{\alpha\alpha'}(0). \quad (3.22)$$

We have used the identity

$$\sum_{\alpha=1}^{c} \rho_\alpha (\partial/\partial \rho_\alpha) \log\Gamma = \log\Gamma + \beta(\partial/\partial\beta) \log\Gamma \quad (3.23)$$

in deriving the last result.

If β and μ_α^* were the prescribed independent variables, our program would be to eliminate v and the ρ_α from Eqs. (3.20)–(3.22), thus obtaining p as a function of the prescribed independent variables. It is more convenient to choose β and the ρ_α as the independent variables. In this case we can determine v as a function of β and the ρ_α by using Eqs. (3.20) and (3.22). Then p is given by either (3.20) or (3.22) and μ_α^* by (3.21).

Applying Eqs. (2.21) and (2.22) of Sec. II, we obtain the potential energy density and the concentration of α, respectively, in the form

$$\langle U \rangle / V = 1/v \cdot [-(\partial/\partial\beta) \log\Gamma + \tfrac{1}{2} \sum_{\alpha,\alpha'=1}^{c} \rho_\alpha \rho_{\alpha'} W_{\alpha\alpha'}(0)] \quad (3.24)$$

and

$$C_\alpha = \rho_\alpha / v. \quad (3.25)$$

The question arises if these equations are consistent with Eqs. (2.23) and (2.24) of Sec. II. Eq. (3.25) is obviously consistent with Eq. (2.24), since when multiple occupancy is ignored, the average number of molecules of component α in a cell is equal to the probability ρ_α of single occupancy by a molecule of component α. Then division by v, of course, gives the concentration C_α. The consistency of (3.24) and (2.23) is not as obvious. However, we will assert without proof that if one starts with Eq. (2.23) and introduces the approximations of the present section (neglect of correlation, neglect of multiple occupancy, singlewise displacement in interaction energy, and spherical smoothing) into it, one obtains Eq. (3.24) after some manipulation.

From Eq. (2.29) we find the density of the modified entropy S^* to be given by

$$S^*/V = k/v \cdot [\rho_0 \log \rho_0 + \sum_{\alpha=1}^{c} \rho_\alpha \log(\rho_\alpha / v) + \beta^2 (\partial/\partial\beta) \beta^{-1} \log\Gamma]. \quad (3.26)$$

With this result together with Eqs. (3.24) and (3.25) we can compute E, μ_α, and S by Eqs. (2.27), (2.5),

and (2.30), respectively, which we now summarize:

$$E/V=\langle U\rangle/V+(3/2\beta)\sum_{\alpha=1}^{c}C_\alpha, \tag{3.27}$$

$$\mu_\alpha=\mu_\alpha^*+\beta^{-1}\log v_\alpha^0, \tag{3.28}$$

$$S/V=S^*/V+k\sum_{\alpha=1}^{c}C_\alpha(\tfrac{5}{2}-\log v_\alpha^0), \tag{3.29}$$

where

$$v_\alpha^0=(2\pi m_\alpha/h^2\beta)^{-\frac{3}{2}}. \tag{3.30}$$

IV. THEORY OF LENNARD-JONES AND DEVONSHIRE

It is possible to obtain the results of Lennard-Jones and Devonshire[2] from our previous results by specializing the variational function (3.18) to the one-component case and by imposing the further requirement that there be no vacancies. To specialize to the one-component case, the index α takes only one value: 1, say. The requirement of no vacancies means, of course, that the probability of vacancy ρ_0 vanishes and that the probability of occupancy (by one molecule of type 1) ρ_1 is equal to unity. Equation (3.18) reduces to

$$-\beta\hat{p}v=\log(v\Gamma)-\beta\mu_1^*+\tfrac{1}{2}\beta W_{11}(0), \tag{4.1}$$

where Γ is given by (3.19) reduced to the form

$$\log\Gamma=\log\Gamma_1. \tag{4.2}$$

Then Γ_1 is in turn given by the following simplified form of Eq. (3.17):

$$\Gamma_1=\int_0^1 3\xi^2 d\xi\,\exp(-\beta\langle\Delta W_{11}\rangle_e) \tag{4.3}$$

in which $\xi=r/r^*$, where r^* is the radius of the equivalent spherical cell. $\langle\Delta W_{11}\rangle_e$ is the spherically-smoothed excess interaction energy of a displaced molecule with the surrounding neighbors fixed at their cell centers, and is given by Eq. (3.15). $W_{11}(0)$ is the energy per molecule of a perfect crystalline array of molecules all at their cell centers, and is given by Eq. (3.5) with the argument $\mathbf{r}-\mathbf{r}'$ set equal to zero.

In Eq. (4.1) there is only one parameter left to vary: the cell volume v. The vanishing of the variation of $\hat{p}$ with respect to v yields[15]

$$\beta pv=1-\tfrac{1}{2}\beta v(\partial/\partial v)W_{11}(0)+v(\partial/\partial v)\log\Gamma \tag{4.4}$$

which is actually Eq. (3.20) specialized to the present case. This is the Lennard-Jones Devonshire equation of state in a different notation. From the viewpoint of our variational method, the best value of v for fixed β and μ_1^* is obtained by eliminating p from Eq. (4.4) and Eq. (4.1) (with p replacing $\hat{p}$).

If the best value of v is substituted into (4.1), we can set $\hat{p}$ equal to p and with a little rearrangement obtain an expression for the Helmholtz free energy A in the form

$$\beta(A/N)=\beta(\mu_1-pv)=\beta(\mu_1^*-pv)+\log v_1^0$$
$$=\tfrac{1}{2}\beta W_{11}(0)-\log(v\Gamma/v_1^0), \tag{4.5}$$

where N is the total number of molecules in the system and

$$v_1^0=(2\pi m_1/h^2\beta)^{-\frac{3}{2}}. \tag{4.6}$$

Here the cell volume v is the molecular volume equal to C_1^{-1}. The combination $v\Gamma$ may be regarded as the free volume v_β.[16]

In their original work, Lennard-Jones and Devonshire[2] used a larger number of approximations than are used in this derivation. We have shown in effect that their approximations are self-consistent by deriving the same results by introducing four obviously self-consistent approximations directly into the variational function. These approximations are: neglect of correlation, single occupancy, spherical smoothing, and single-wise displacements.

In order to correct for the neglect of vacancies and multiple occupancies, it is customary to add a term $-\log\sigma$ to the last member of Eq. (4.5). The expression $k\log\sigma$ is known as the communal entropy (per molecule). We make an approximate calculation of σ by comparing the present results obtained under the restriction of single occupancy with the corresponding results of the last section, where both vacancies and single occupancies were allowed. Neglecting the difference in entropy arising from the difference in the *shapes* of the cell distributions in the two cases, we obtain the result

$$\log\sigma=-\rho_0\log\rho_0/(1-\rho_0), \tag{4.7}$$

where ρ_0 is the probability of vacancy per cell in the case in which both vacancies and single occupancies are allowed. It is perhaps of interest to note that as ρ_0 increases from 0 to 1, σ increases monotonically from 1 to e, as pointed out by Kirkwood.[8]

V. THE RADIAL DISTRIBUTION FUNCTION

Knowing the distribution function for each cell makes it possible to compute the radial distribution function to a satisfactory degree of approximation. Recently, Dahler[17] has calculated the radial distribution function from a cell theory. Here, we accomplish essentially the same objective in the frame of the present theory. For this purpose let us confine our attention to a one-component system containing only molecules of type 1. First we consider a molecule (of type 1) in the cell whose center is at $\mathbf{R}=0$, and let this molecule be a distance $\mathbf{r}$ from the cell center. The average number

[15] Here Γ is to be regarded as a function of β and v. $W_{11}(0)$ is a function of v alone.

[16] The free volume is defined here with the potential energy (per molecule) of the perfect lattice playing the role of the energy zero. It is perhaps more conventional to use the average energy as the zero.

[17] J. S. Dahler, J. Chem. Phys. **29**, 1082 (1958).

density of molecules at a distance $\mathbf{x}$ from the first molecule is evidently

$$\sum_{\mathbf{R}}{}'\rho_1(\mathbf{x}+\mathbf{r}-\mathbf{R}), \tag{5.1}$$

where the prime on the summation denotes the omission of the term for $\mathbf{R}=0$. The discrete set of $\mathbf{R}$'s defines the lattice of cell centers. The *cell distribution functions ρ_1 are supposed to be defined so that they vanish when their arguments exceed the vector distance from the cell center to the cell wall.* The quantity (5.1) when averaged over the positions of the first molecule (in the cell whose center is at $\mathbf{R}=0$) becomes

$$(C_1v)^{-1}\int_v d\mathbf{r}\rho_1(\mathbf{r})\sum_{\mathbf{R}}{}'\rho_1(\mathbf{x}+\mathbf{r}-\mathbf{R}), \tag{5.2}$$

where

$$C_1=v^{-1}\int_v d\mathbf{r}\rho_1(\mathbf{r})$$

is the macroscopic number density. Averaging over the directions of $\mathbf{x}$ gives

$$(C_1v)^{-1}\int_v d\mathbf{r}\rho_1(\mathbf{r})\sum_{\mathbf{R}}{}'\langle\rho_1(\mathbf{e}x+\mathbf{r}-\mathbf{R})\rangle_e \tag{5.3}$$

where $x=|\mathbf{x}|$, $\mathbf{e}=\mathbf{x}/x$, and $\langle\ \rangle_e$ denotes the average (uniformly weighted) over the directions of $\mathbf{e}$. The radial distribution $g(x)$ is defined as the ratio of the average number density at a scalar distance x from a given molecule to the average number density calculated without this constraint (macroscopic number density). Evidently it is the ratio of (5.3) to C_1 so that

$$g(x)=C_1^{-2}v^{-1}\int_v d\mathbf{r}\rho_1(\mathbf{r})\sum_{\mathbf{R}}{}'\langle\rho_1(\mathbf{e}x+\mathbf{r}-\mathbf{R})\rangle_e, \tag{5.4}$$

which expresses g in terms of ρ_1.

Equation (5.4) can be recast in a form which is more convenient for calculation. First of all, we observe that in the identity,

$$\sum_{\mathbf{R}}{}'\rho_1(\mathbf{x}-\mathbf{R})=\sum_{\mathbf{R}}\rho_1(\mathbf{x}-\mathbf{R})-\rho_1(\mathbf{x}), \tag{5.5}$$

the complete sum $\sum_{\mathbf{R}}\rho_1(\mathbf{x}-\mathbf{R})$ is a function possessing the periodicity of the lattice and $\rho_1(\mathbf{x})$ is localized in the cell centered on $\mathbf{R}=0$. In accordance with this, we decompose g into two parts,

$$g(x)=g^{(0)}(x)-g^{(1)}(x), \tag{5.6}$$

where

$$g^{(0)}(x)=C_1^{-2}v^{-1}\int_v d\mathbf{r}\rho_1(\mathbf{r})\sum_{\mathbf{R}}\langle\rho_1(\mathbf{e}x+\mathbf{r}-\mathbf{R})\rangle_e \tag{5.7}$$

can be calculated most conveniently using a Fourier series representation, and where

$$g^{(1)}(x)=C_1^{-2}v^{-1}\int_v d\mathbf{r}\rho_1(\mathbf{r})\langle\rho_1(\mathbf{e}x+\mathbf{r})\rangle_e \tag{5.8}$$

can be handled most conveniently as it stands.

Now we consider more explicitly the calculation of $g^{(0)}(x)$. We first express the complete sum over $\mathbf{R}$ as a Fourier series

$$\sum_{\mathbf{R}}\rho_1(\mathbf{x}-\mathbf{R})=\sum_{\mathbf{K}}\rho_{\mathbf{K}}\exp(i\mathbf{K}\cdot\mathbf{x}), \tag{5.9}$$

$$\rho_{\mathbf{K}}=v^{-1}\int_v d\mathbf{r}\rho_1(\mathbf{r})\exp(-i\mathbf{K}\cdot\mathbf{r}), \tag{5.10}$$

in which the sum on the right-hand side of (5.9) extends over the discrete set of $\mathbf{K}$'s generated by the condition that $\mathbf{R}\cdot\mathbf{K}/2\pi$ be an integer. It can be shown that the set of $\mathbf{K}$'s forms a lattice and that except for the factor 2π, this lattice is reciprocal to the $\mathbf{R}$ lattice. From the fact that ρ_1 is real it follows that $\rho_{\mathbf{K}}{}^*=\rho_{-\mathbf{K}}$. If one is limited to the interior of the cell centered on $\mathbf{R}=0$, Eq. (5.9) can be used as a representation of $\rho_1(\mathbf{x})$. Inserting these results (with appropriate changes of the arguments) into Eq. (5.7), we obtain

$$g^{(0)}(x)=C_1^{-2}\sum_{\mathbf{K}}|\rho_{\mathbf{K}}|^2\langle\exp(i\mathbf{K}\cdot\mathbf{e}x)\rangle_e$$
$$=C_1^{-2}\sum_{\mathbf{K}}|\rho_{\mathbf{K}}|^2(\sin Kx/Kx), \tag{5.11}$$

where $K=|\mathbf{K}|$. It is to be expected that a sum over a relatively small number of K's neighboring the origin of the $\mathbf{K}$ lattice will give quite a good approximation to $g^{(0)}(x)$ when x is larger than the maximum cell diameter. The $\mathbf{K}=0$ term in (5.11) turns out to be equal to unity since

$$\langle\exp(i\mathbf{K}\cdot\mathbf{e}x)\rangle_e=\langle 1\rangle_e=1 \quad\text{and}\quad \rho_{\mathbf{K}}=C_1 \quad\text{when}\quad \mathbf{K}=0.$$

The coefficients $\rho_{\mathbf{K}}$ are given by Eq. (5.11) in the most exact verision of the first-order cell theory. Suppose we use as an approximation spherical cells and spherically-symmetric cell distributions as was done in Sec. III. In this case we obtain

$$\rho_{\mathbf{K}}=v^{-1}\int_0^{r^*}4\pi r^2dr\rho_1(r)(\sin Kr/Kr), \tag{5.12}$$

where $r^*=(3v/4\pi)^{\frac{1}{3}}$.

The term $g^{(1)}(x)$ is actually not very interesting and its calculation is rather troublesome. It can be shown that $g^{(1)}(x)$ vanishes for all x larger than the maximum cell diameter. Thus it contributes nothing to $g(x)$ in this range of x. For x less than the maximum cell diameter this theory of the radial distribution function is not very accurate. It is true that if $g^{(0)}$ and $g^{(1)}$ are computed precisely, $g(0)=0$; however, it will not approach zero as rapidly as one would expect for a repulsive potential that approaches infinity in the limit of zero

separation. As a practical matter it is probably worthwhile, considering g only for x larger than the maximum cell diameter, or in the case of the spherical approximation, larger than r^*, the diameter of the equivalent sphere.

Since the first-order cell method by its very nature introduces an artificial long-range order into a liquid, one expects the amplitude of undulation of g about the value unity to attenuate less rapidly than it should with increasing distance; in fact, the amplitude is inversely proportional to the distance when the distance is large. The more exact theories of the radial distribution function developed by Kirkwood,[18] Born and Green[19] and Yvon,[20] give attentuations which are more rapid than this.

It can be shown that if we calculate the pressure by the formula

$$\beta p/C_1=1-\tfrac{1}{6}\beta\int_0^\infty 4\pi x^3 g(x)[d\phi_{11}(x)/dx]dx, \quad (5.13)$$

using $g(x)$ given by Eq. (5.4), the result is identical to Eq. (3.8). This is of interest because it is sometimes contended that Eq. (5.13) belongs exclusively to the radial distribution function method and that the equation of state yielded by the cell method is quite unrelated to the preceding result. Similar considerations pertain to the average energy. If the singlewise displacement approximation is introduced into the calculation of $\rho_i(\mathbf{r})$ to be used in (5.4), certain difficulties arise. For example, in order to obtain a result with (5.13) which is identical to (3.20) appropriately specialized, we must retain the δ-function peak in ρ, in which case g will have a series of similar peaks corresponding to the perfect crystal. Thus, when g is suitable for thermodynamic purposes, it looks quite unlike the expected form.

It may be of interest to note here that Hill[21] has treated the inverse of the present problem; namely, the deduction of information concerning cells and holes from the radial distribution function.

VI. SECOND-ORDER THEORIES INCLUDING SECOND-ORDER CORRELATIONS

The first-order theories considered in previous sections suffer from the defect that correlations between cells are neglected. Even though the single-cell distribution functions are adjusted to give the best answer under this limitation, the error will be large if the fluctuations in the states of cells are large, but not too large, in a certain sense to be clarified later. One might expect that for a binary mixture a first-order theory of the type so far considered will be appreciably in error if the concentration ratio is 1:1 and that the error will be seriously aggravated if the molecular radius ratio is far from unity. The situation might be improved still keeping the basic framework of the first-order theories if we either increase the cell size and occupancy, or relax the restriction that the cells be statistically equivalent. The first modification is obviously impractical; however, the second might be quite workable if the concentration ratios are approximately ratios of small integers, in which case the theory would closely resemble certain treatments of order—disorder phenomena in alloys. In this section we try a more direct and generally applicable approach to the partial correction of the errors of the first-order theories. We simply extend the earlier theory to include second-order correlations. It will not be possible to do this exactly; however, we obtain explicit results with the aid of an approximation which should be fairly good under a wide range of conditions.

We reconsider the expansion of the variational function $\beta\hat{p}V$ discussed in Sec. II. Here we keep second-order correlations but neglect those of higher order giving us

$$-\beta\hat{p}v=\mathfrak{S}_i\rho(i)[\log\rho(i)-\beta\sum_{\alpha=1}^{c}\mu_\alpha^* n_\alpha+\beta U(i)]$$
$$+\tfrac{1}{2}\sum_{i'}{}'\mathfrak{S}_i\mathfrak{S}_{i'}\rho(i)\rho(i')g_{ii'}(i,i')[\log g_{ii'}(i,i')+\beta U_{ii'}(i,i')] \quad (6.1)$$

in which the notation has already been defined in Sec. II. The functions $\rho(i)$ and $g_{ii'}(i,i')$ must satisfy the constraints

$$\mathfrak{S}_i\rho(i)=1, \quad (6.2)$$

$$\mathfrak{S}_i\rho(i)g_{ii'}(i,i')=1, \quad (6.3)$$

expressing normalization and compatibility, respectively.

We first maximize $\hat{p}$ with respect to $g_{ii'}(i,i')$ with the constraint (6.3) and keeping all other variables fixed. We obtain

$$\log g_{ii'}(i,i')=-\beta C_{ii'}(i,i')+\lambda_{ii'}(i)+\lambda_{i'i}(i'), \quad (6.4)$$

where $\lambda_{ii'}(i)$ [and $\lambda_{i'i}(i')$] constitute a continuous set of Lagrange multipliers to be determined by the constraint (6.3). At this point a word about notation is in order: in $\lambda_{ii'}(i)$ the subscripts denote (as discussed in Sec. II) a dependence upon the relative positions of cells i and i' whereas the i in the parentheses denotes a dependence upon the state of cell i. Insertion of (6.4) into (6.3) yields the nonlinear integral equation

$$\mathfrak{S}_i\rho(i)\exp[-\beta U_{ii'}(i,i')+\lambda_{ii'}(i)]=\exp[-\lambda_{i'i}(i')]. \quad (6.5)$$

Substitution of (6.4) in (6.1) yields

$$-\beta\hat{p}v=\sum_i\mathfrak{S}_i\rho(i)[\log\rho(i)-\beta\sum_{\alpha=1}^{c}\mu_\alpha^* n_\alpha+\sum_{i'}\lambda_{ii'}(i)]. \quad (6.6)$$

[18] J. G. Kirkwood, J. Chem. Phys. **3**, 300 (1935).
[19] M. Born and H. S. Green, Proc. Roy. Soc. (London) **A189**, 103 (1947).
[20] J. Yvon, Actualitiés sci. et ind. (**1935**).
[21] T. L. Hill, J. Chem. Phys. **28**, 1179 (1958).

Thus, provided the integral equation (6.5) can be solved to a suitable degree of approximation, $\hat{p}$ is a functional of the same variables [$\rho(i)$ and v] as in the first-order theory discussed in Sec. II.

We obtain an approximate solution of (6.5) by a perturbation method. To start the procedure, let us take as a zero-order solution

$$\lambda_{ii'}(i)=\tfrac{1}{2}\kappa_{ii'}, \tag{6.7}$$

where $\kappa_{ii'}$ depends only upon the relative positions of cells i and i', and not upon their states. Let $\kappa_{ii'}$ be determined so that the resulting form of $g_{ii'}(i,i')$ given by Eq. (6.4) satisfies the second-order normalization condition

$$\mathfrak{S}_i\mathfrak{S}_{i'}\rho(i)\rho(i')g_{ii'}(i,i')=1. \tag{6.8}$$

We then obtain

$$\kappa_{ii'}=-\log\mathfrak{S}_i\mathfrak{S}_{i'}\rho(i)\rho(i')\exp[-\beta U_{ii'}(i,i')]. \tag{6.9}$$

Define the quantities

$$f_{ii'}(i,i')=\exp[-\beta U_{ii'}(i,i')+\kappa_{ii'}]-1 \tag{6.10a}$$

and

$$f_{ii'}(i')=\mathfrak{S}_i\rho(i)f_{ii'}(i,i'). \tag{6.10b}$$

It is evident that

$$f_{ii'}(i')=\mathfrak{S}_i\rho(i)\exp[-\beta U_{ii'}(i,i')+\kappa_{ii'}]-1 \tag{6.11a}$$

and

$$\mathfrak{S}_{i'}\rho(i')f_{ii'}(i')=0. \tag{6.11b}$$

On using these definitions and regarding $f_{ii'}(i,i')$ as a perturbation, we obtain from Eq. (6.5) the result

$$\lambda_{ii'}(i)=\tfrac{1}{2}\kappa_{ii'}+f_{ii'}(i)+f_{ii'}^2(i)+\mathfrak{S}_{i'}\rho(i')f_{ii'}(i')[f_{ii'}(i,i')-f_{ii'}(i')]+\cdots. \tag{6.12}$$

However, many of the terms in this expression drop out when averaged over the states of cell i

$$\mathfrak{S}_i\rho(i)\lambda_{ii'}(i)=\tfrac{1}{2}\kappa_{ii'}+\tfrac{1}{2}\mathfrak{S}_i\rho(i)f_{ii'}^2(i)+\cdots. \tag{6.13}$$

Thus in the variational function $\hat{p}$ given by (6.6) only the corrections of second and higher order will appear. As a reasonable approximation we may take only the zero order solution for $\lambda_{ii'}(i)$, namely, $\frac{1}{2}\kappa_{ii'}$. Then (6.6) reduces to

$$-\beta\hat{p}v=\mathfrak{S}_i\rho(i)[\log\rho(i)-\sum_{\alpha=1}^{c}\mu_\alpha^*n_{\alpha i}]+\tfrac{1}{2}\sum_{i'}\kappa_{ii'}, \tag{6.14}$$

where $\kappa_{ii'}$ is defined by Eq. (6.9).

Now we make the approximation that a cell is at most singly occupied and we introduce the more explicit notation defined in Sec. III. (The neglect of multiple occupancy is undoubtedly less serious here than it was in Sec. III because the introduction of the second-order correlations, although approximate, will reduce the optimum cell size, thereby further reducing multiple occupancy probabilities.) Following this plan, we obtain

$$-\beta\hat{p}v=\rho_0\log\rho_0+\sum_{\alpha=1}^{c}\int_v d\mathbf{r}\rho_\alpha(\mathbf{r})[\log\rho_\alpha(\mathbf{r})-\beta\mu_\alpha^*]+\tfrac{1}{2}{\sum_{\mathbf{R}}}'\kappa_{\mathbf{R}}, \tag{6.15}$$

where

$$\kappa_{\mathbf{R}}=-\log\Big[1+\sum_{\alpha,\alpha'=1}^{c}\int_v d\mathbf{r}\int_v d\mathbf{r}'\rho_\alpha(\mathbf{r})\rho_{\alpha'}(\mathbf{r}')Y_{\alpha\alpha'}\times(|\mathbf{r}-\mathbf{r}'+\mathbf{R}|)\Big], \tag{6.16}$$

in which

$$Y_{\alpha\alpha'}(r)=\exp[-\beta\phi_{\alpha\alpha'}(r)]-1. \tag{6.17}$$

These equations must be amended by the normalization constraint

$$\rho_0+\sum_{\alpha=1}^{c}\int d\mathbf{r}\rho_\alpha(\mathbf{r})=1. \tag{6.18}$$

It is interesting to digress from the main line of argument to consider the connection between our new form of $\hat{p}$ and the old form given by Eq. (3.4) of Sec. III. It can be shown that the new form reduces to the old form in two cases: (a) when the temperature is very high (more precisely, when $kT=\beta^{-1}$ is large compared with the average interaction energy between adjacent cells), and (b) when there is negligible fluctuation in the state of each cell. To treat either case we need only consider the term $\frac{1}{2}{\sum_{\mathbf{R}}}'\kappa_{\mathbf{R}}$, since this is the only part of the new form of $\hat{p}$ that differs from the old. In case (a) we have

$$Y_{\alpha\alpha'}(|\mathbf{r}-\mathbf{r}'+\mathbf{R}|)\simeq-\beta\phi_{\alpha\alpha'}(|\mathbf{r}-\mathbf{r}'+\mathbf{R}|) \tag{6.19}$$

for most values of $\mathbf{r}$ and $\mathbf{r}'$ if β is sufficiently small, so that we obtain

$$\begin{aligned}\tfrac{1}{2}{\sum_{\mathbf{R}}}'\kappa_{\mathbf{R}}&\simeq-\tfrac{1}{2}{\sum_{\mathbf{R}}}'\cdot\log\Big[1-\beta\sum_{\alpha,\alpha'=1}^{c}\int_v d\mathbf{r}\rho_\alpha(\mathbf{r})\int_v d\mathbf{r}\rho_{\alpha'}(\mathbf{r}')U_{\alpha\alpha'}(|\mathbf{r}-\mathbf{r}'+\mathbf{R}|)\Big]\\&\simeq\tfrac{1}{2}\beta\sum_{\alpha,\alpha'=1}^{c}\int_v d\mathbf{r}\int_v d\mathbf{r}'\hat{p}_\alpha(\mathbf{r})\rho_{\alpha'}(\mathbf{r}'){\sum_{\mathbf{R}}}'\phi_{\alpha\alpha'}(|\mathbf{r}-\mathbf{r}'+\mathbf{R}|),\end{aligned} \tag{6.20}$$

in agreement with the interaction terms of Eq. (3.4) recognizing that $W_{\alpha\alpha'}(\mathbf{r}-\mathbf{r}')$ in (3.4) is defined by (3.5).

In case (b) we dismiss the subcase of unit probability of vacancy as trivial and consider the distribution $\rho_0=0$, $\rho_1(\mathbf{r})=\delta(\mathbf{r})$, $\rho_\alpha(\mathbf{r})=0(\alpha>1)$, corresponding to the certainty of the presence of a particle of type 1 at

each cell center. We now obtain

$$\tfrac{1}{2}\sum_{\mathbf{R}}{}'\kappa_{\mathbf{R}}=-\tfrac{1}{2}\sum_{\mathbf{R}}{}'\log\{1+\exp[-\beta\phi_{11}(R)]-1\}$$
$$=\tfrac{1}{2}\beta\sum_{\mathbf{R}}{}'\phi_{11}(R), \tag{6.21}$$

obviously identical with the form to which the interaction terms of Eq. (3.4) reduce when the above distribution is assumed. Thus correlation becomes unimportant when one has a high degree of randomness arising from a high temperature or when the state of each cell is known with certainty.

It is also of interest to find the form that the new $\hat{p}$ takes in the limit of vanishing cell volume. For this case we let $\rho_\alpha(\mathbf{r})$ be independent of $\mathbf{r}$ and equal to C_α where C_α is the number density of component α. It is obvious that the spatial variation of $\rho_\alpha(\mathbf{r})$ in a cell will be of negligible magnitude when the cells are very small. Using the normalization condition, we set

$$\rho_0=1-v\sum_{\alpha=1}^{c}C_\alpha.$$

Inserting these relations into Eq. (6.15), dividing the result by v, and neglecting terms of the order of v, we obtain

$$-\beta\hat{p}=\sum_{\alpha=1}^{c}C_\alpha[\log C_\alpha-1-\beta\mu_\alpha{}^*]$$
$$-\tfrac{1}{2}\sum_{\alpha,\alpha'=1}^{c}C_\alpha C_{\alpha'}\int_0^\infty 4\pi r^2dr\,Y_{\alpha\alpha'}(r), \tag{6.22}$$

where $Y_{\alpha\alpha'}(r)$ is defined by Eq. (6.17). This expression is now to be extremalized with respect to C_α. When this is done, we find

$$\mu_\alpha{}^*=\beta^{-1}\log C_\alpha-\beta^{-1}\sum_{\alpha'=1}^{c}C_{\alpha'}\int_0^\infty 4\pi r^2dr\,Y_{\alpha\alpha'}(r). \tag{6.23}$$

Also we find that the maximum of $\hat{p}$, equal to the equilibrium pressure p, is given by

$$\beta p=\sum_{\alpha=1}^{c}C_\alpha-\tfrac{1}{2}\sum_{\alpha,\alpha'=1}^{c}C_\alpha C_{\alpha'}\int_0^\infty 4\pi r^2dr\,Y_{\alpha\alpha'}(r). \tag{6.24}$$

The reader will recognize that this is the correct equation of state for an imperfect gas mixture neglecting terms cubic in the concentrations. Thus, assuming that the optimum cell volume will approach zero sufficiently closely as the system approaches infinite dilution, our theory will agree with the rigorous theory of imperfect gases neglecting third- and higher-order virial coefficients.

Returning now to the main line of argument, we consider the general equations yielded by the maximization of $\hat{p}$ given by Eqs. (6.15) and (6.16). This process is to be performed with β and with $\mu_\alpha{}^*$ held fixed and with the normalization constraint expressed by Eq. (6.18). The variation with respect to $\rho_\alpha(\mathbf{r})$ yields the result

$$\log\rho_\alpha(\mathbf{r})=\log\rho_0+\beta\mu_\alpha{}^*$$
$$+\sum_{\mathbf{R}}{}'\exp(\kappa_{\mathbf{R}})\sum_{\alpha'=1}^{c}\int_v d\mathbf{r}'\rho_{\alpha'}(\mathbf{r}')\,Y_{\alpha\alpha'}(|\,\mathbf{r}-\mathbf{r}'+\mathbf{R}\,|) \tag{6.25}$$

and the variation with respect to v yields

$$\beta\hat{p}v=1-\rho_0$$
$$+\tfrac{1}{6}\sum_{\mathbf{R}}{}'\exp(\kappa_{\mathbf{R}})\sum_{\alpha'=1}^{c}\int_v d\mathbf{r}'\rho_{\alpha'}(\mathbf{r}')\,\tilde{Y}_{\alpha\alpha'}(|\,\mathbf{r}-\mathbf{r}'+\mathbf{R}\,|), \tag{6.26}$$

where

$$\tilde{Y}_{\alpha\alpha'}(r)=r(d/dr)\,Y_{\alpha\alpha'}(r). \tag{6.27}$$

Equations (6.25) and (6.26) are to be compared with Eqs. (3.7) and (3.8) of Sec. III.

In the second-order theory it is possible to employ the spherical smoothing and singlewise displacement approximations just as in the first-order theory. We introduce the modifications expressed by Eqs. (3.9)–(3.13). We finally obtain Eq. (6.15) in the form

$$-\beta\hat{p}v=\rho_0\log\rho_0+\sum_{\alpha=1}^{c}\rho_\alpha\log(\rho_\alpha/v)$$
$$+\sum_{\alpha=1}^{c}\rho_\alpha\int_0^1 3\xi^2d\xi\theta_\alpha(\xi)\,\log\theta_\alpha(\xi)$$
$$-\beta\sum_{\alpha=1}^{c}\rho_\alpha\mu_\alpha{}^*+\tfrac{1}{2}\sum_{\mathbf{R}}{}'\tilde{\kappa}_{\mathbf{R}}, \tag{6.28}$$

where $\tilde{\kappa}_{\mathbf{R}}$ is the modified form of $\kappa_{\mathbf{R}}$ and is given by

$$\tilde{\kappa}_{\mathbf{R}}=-\log G-2G^{-1}\sum_{\alpha,\alpha'=1}^{c}\rho_\alpha\hat{\rho}_{\alpha'}\int_0^1 3\xi^2d\xi\theta_\alpha(\xi)\,\langle\Delta Y_{\alpha\alpha'}\rangle_{\mathbf{e}}, \tag{6.29}$$

in which

$$G(R)=1+\sum_{\alpha,\alpha'=1}^{c}\rho_\alpha\rho_{\alpha'}Y_{\alpha\alpha'}(R) \tag{6.30}$$

and

$$\langle\Delta Y_{\alpha\alpha'}\rangle_{\mathbf{e}}=\frac{1}{4\pi}\int d\mathbf{e}[Y_{\alpha\alpha'}(\mathbf{e}r^*\xi+\mathbf{R})-Y_{\alpha\alpha'}(R)]. \tag{6.31}$$

The symbol $\int d\mathbf{e}$ denotes the integration over all orientations of the unit vector $\mathbf{e}$.

Following the same procedure as in Sec. III, we will maximize $\hat{p}$ with respect to the θ_α's subject to the condition

$$\int_0^1 3\xi^2d\xi\theta_\alpha(\xi)=1. \tag{6.32}$$

We obtain

$$\theta_\alpha(\xi)=1/\Theta_\alpha\cdot\exp(G^{-1}\sum_{\alpha'=1}^{c}\rho_{\alpha'}\langle\Delta Y_{\alpha\alpha'}\rangle_{\mathbf{e}}), \tag{6.33}$$

where

$$\Theta_\alpha = \int_0^1 3\xi^2 d\xi \exp[G^{-1}\sum_{\alpha'=1}^{c} \rho_{\alpha'} \langle \Delta Y_{\alpha\alpha'} \rangle_e]. \quad (6.34)$$

Finally, $\hat{p}$ is given by

$$-\beta\hat{p}v = \rho_0 \log\rho_0 + \sum_{\alpha=1}^{c} \rho_\alpha \log(\rho_\alpha/v) - \beta\sum_{\alpha=1}^{c} \rho_\alpha \mu_\alpha^* - \sum_{R}{}' (\tfrac{1}{2}\log G + \log\Theta), \quad (6.35)$$

where $\Theta = \Theta(R)$ is given by

$$\log\Theta = \sum_{\alpha=1}^{c} \rho_\alpha \log\Theta_\alpha. \quad (6.36)$$

We now maximize the new form of $\hat{p}$, just given, with respect to v and the ρ_α's using

$$\rho_0 = 1 - \sum_{\alpha=1}^{c} \rho_\alpha.$$

$$\beta p v = 1 - \rho_0 + \sum_{R}{}' v(\partial/\partial v)(\tfrac{1}{2}\log G + \log\Theta), \quad (6.37)$$

where p is given by (6.35) after replacing $\hat{p}$ by its maximum value p. The variation with respect to ρ_α gives

$$\beta\mu_\alpha^* = \log\rho_0 + \log(\rho_\alpha/v) - \sum_{R}{}' (\partial/\partial\rho_\alpha)(\tfrac{1}{2}\log G + \log\Theta). \quad (6.38)$$

The expressions (6.37) and (6.38) bear a close resemblance to Eqs. (3.20) and (3.21) of Sec. III. The computation of other thermodynamic functions can be simply carried through in much the same way as in Sec. III and will hence not be treated here.

VII. DISCUSSION

We have formulated a general cell method for a classical system which can be extended to any degree of accuracy. Two main classes of theories are treated in detail: first-order theories in which correlations between cells are neglected, and second-order theories in which second-order correlations are approximately taken into account. In both classes we introduce approximations (spherical smoothing and singlewise displacement) which lead to results on a practical computational level. On this level the second-order results are only slightly more complicated than the first order. The first-order results on this level, with a slight reduction of generality, are identical to the Lennard-Jones Devonshire theory. The problem of calculating the radial distribution function within the framework of the first order theories has been treated, and the results appear to be reasonable.

There are several questions that remain unanswered. One is: How much better is a second-order theory than the corresponding first-order theory in a given case? In the question we have appended the phrase "in a given case" because the second-order theory is not always better than the corresponding first-order theory. If we consider Coulomb forces, for example, we find that the most approximate form of the first-order theory gives a finite but wrong answer, whereas the corresponding second order theory gives a divergent answer, which is definitely worse.

The example of Coulomb forces brings us to the second question. Why does this type of theory fail for coulomb forces? The unsatisfactory results above do not arise from the additional approximations. In fact, the most refined first- and second-order theories still fail in much the same fashion. It was hoped that the methods of this paper might be first fully applied to strong electrolytes. However, it appears that the methods work only for nonionic, perhaps even nonpolar, liquids and solutions. If a clear insight into the reasons for this failure could be gained, it would be a valuable contribution to methodology of the theory of electrolytes.

THE JOURNAL OF CHEMICAL PHYSICS VOLUME 33, NUMBER 5 NOVEMBER, 1960

On Temporal Evolution of Isolated Dynamical Systems

S. GOLDEN† AND H. C. LONGUET-HIGGINS

Department of Theoretical Chemistry, University Chemical Laboratory, Lensfield Road, Cambridge, England

(Received June 1, 1960)

It is shown that if $\langle A(t)\rangle$ is the expectation value of a real observable A at time t, then for a finite closed dynamical system $\langle A(t)\rangle$ can converge to a limit as $t\to\infty$ only if $\langle A(t)\rangle$ is altogether independent of t. This conclusion is unaffected by time-smoothing or coarse-graining. On the other hand, for an infinite system whose energy levels form a purely continuous spectrum, $\langle A(t)\rangle$ tends to a limit as $t\to\infty$ under very general conditions. This conclusion does not depend on the introduction of either time-smoothing or coarse-graining.

1.

A CENTRAL problem in statistical mechanics is that of reconciling the tendency of any system towards equilibrium with the time-reversibility of the equations of motion. This difficulty is especially acute for isolated systems because, as a result of Liouville's theorem or its quantum-mechanical analog, the entropy cannot change with time.

In this paper we offer no complete solution to this problem, but merely prove certain theorems which are relevant to its discussion. Though our analysis ignores the radiation field we believe that it is of some value in indicating the manner in which the problem of irreversibility must be approached. The scheme of the paper is as follows:

In Sec. 2 we examine the long-term behavior of the expectation value $\langle A(t)\rangle$ of an arbitrary observable A which does not depend explicitly on the time. It is shown that for any finite closed mechanical system $\langle A(t)\rangle$ can only converge to a limit as $t\to\infty$ if it is constant for all values of the time. This conclusion is, moreover, unaffected by "time-smoothing" the statistical operator.

In Sec. 3 we consider an ensemble, the "equivalent asymptotic ensemble," which yields the time-average properties of the given system, i.e., the time-average expectation values of all its time-independent observables. It is shown that in a precise sense the temporal fluctuation of $\langle A(t)\rangle$ in a finite closed mechanical system can never exceed the dispersion of the observable A in the equivalent asymptotic ensemble, and will in general be smaller.

In Sec. 4 we extend our analysis to an infinite mechanical system, and find that the situation is essentially different. If the Hamiltonian has a purely continuous spectrum, $\langle A(t)\rangle$ will under very general conditions tend to a limit as $t\to\infty$, without necessarily being constant for all time. In Sec. 5 the implications of these results are examined.

2.

Consider a system of interacting particles confined within a finite box whose walls completely isolate the system, thermally and mechanically, from the outside world. The Hamiltonian H will be a function of the coordinates and momenta of all the particles, and the eigenvalues of H will constitute a discrete spectrum of energy levels.[1]

For expressing our knowledge of the state of the system we adopt von Neumann's statistical operator $\rho(t)$, whose temporal evolution is determined by

$$i\hbar(\partial\rho/\partial t)=H\rho-\rho H. \tag{2.1}$$

Since by hypothesis H depends on the coordinates and momenta but not on the time, we may integrate (2.1) immediately to obtain the formal result

$$\rho(t)=\exp(-iHt/\hbar)\rho(0)\exp(iHt/\hbar), \tag{2.2}$$

where $\rho(0)$ is the value of ρ at $t=0$. This result may be used to derive an expression for $\langle A(t)\rangle$, the expectation value at time t of any observable A which does not depend explicitly on the time

$$\langle A(t)\rangle=\operatorname{trace}[\rho(t)A]/\operatorname{trace}\rho(t)=\operatorname{trace}[\rho(t)A], \tag{2.3}$$

where we have used the fact that trace $\rho(t)$ is constant in time, and have for convenience normalized it to unity.

Now it is a matter of experience that large systems tend to a condition of equilibrium in the sense that many of their observable properties seem to approach limiting values after the lapse of a sufficiently long time. Though this statement should be qualified to allow for metastability, it prompts us to inquire under what circumstances an observable[2] can exhibit a limiting asymptotic behavior as $t\to\infty$.

Consider, then, the quantity

$$z\int_0^\infty dt e^{-zt}\langle A(t)\rangle=z\int_0^\infty dt e^{-zt}\operatorname{trace}[\rho(t)A], \tag{2.4}$$

where z is a positive real quantity. This expression is a weighted time average of the expectation value of A,

† Fulbright Scholar and Guggenheim Fellow, 1959–1960; Permanent address(Brandeis University, Waltham, Massachusetts).

[1] The discrete nature of its energy spectrum is the only special property of the system which we invoke; the number of degrees of freedom may be finite or infinite. Energies are measured from the lowest eigenvalue.

[2] Here and later it is to be understood that the only observables under discussion are those which do not involve the time *explicitly*.

and in the limit $z\to 0$ it becomes the ordinary time-average value of $\langle A(t)\rangle$. Hence *if* $\langle A(t)\rangle$ tends to a limit as $t\to\infty$, this limit must be the same as the limit of (2.4) when z tends to 0. To determine the latter limit it is convenient to evaluate the trace in a representation which diagonalizes H:

$$z\int_0^\infty dt e^{-zt}\,\mathrm{trace}[\rho(t)A]$$

$$=z\int_0^\infty dt e^{-zt}\sum_{nm}\rho_{nm}(0)\,\exp[i(E_m-E_n)t/\hbar]A_{mn} \tag{2.5}$$

$$=\sum_{nm}\rho_{nm}(0)A_{mn}\left[\frac{z}{z-i(E_m-E_n)/\hbar}\right]. \tag{2.6}$$

Since by hypothesis the eigenvalues E_n are discrete, the terms in (2.6) for which $E_m\neq E_n$ all vanish in the limit $z\to 0$, so that the time-average value of $\langle A(t)\rangle$ is just

$$\langle A\rangle_t\equiv\lim_{z\to 0} z\int_0^\infty dt e^{-zt}\langle A(t)\rangle=\sum_{E_m=E_n}\sum_{m}\sum_{n}\rho_{mn}(0)A_{nm}. \tag{2.7}$$

Now if $\langle A(t)\rangle$ were to tend to an asymptotic limit, this limit would have to be $\langle A\rangle_t$, and the expression

$$z\int_0^\infty dt e^{-zt}[\langle A(t)\rangle-\langle A\rangle_t]^2$$

$$=z\int_0^\infty dt e^{-zt}\left|\sum_{E_n\neq E_m}\sum_{n}\sum_{m}\rho_{nm}(0)\,\exp[i(E_m-E_n)t/\hbar]A_{mn}\right|^2$$

would vanish in the limit $z\to 0$. To examine the limit of this expression let us define the discontinuous function

$$g(\omega)=\sum_{(E_n=E_m-\hbar\omega)}\rho_{nm}(0)A_{mn}, \tag{2.8}$$

which vanishes unless $\hbar\omega$ is one of the possible values of E_m-E_n. Then

$$z\int_0^\infty dt e^{-zt}[\langle A(t)\rangle-\langle A\rangle_t]^2$$

$$=z\int_0^\infty dt e^{-zt}\Big|\sum_{\omega\neq 0}g(\omega)e^{i\omega t}\Big|^2$$

$$=\sum_{\omega\neq 0}\sum_{\omega'\neq 0}g(\omega)\bar{g}(\omega')\left[\frac{z}{z-i(\omega-\omega')}\right], \tag{2.9}$$

and in the limit $z\to 0$ all terms vanish for which $\omega\neq\omega'$. Hence

$$\lim_{z\to 0} z\int_0^\infty dt e^{-zt}[\langle A(t)\rangle-\langle A\rangle_t]^2=\sum_{\omega\neq 0}|g(\omega)|^2, \tag{2.10}$$

and the vanishing result is obtained only if $g(\omega)$ vanishes for *all* nonzero values of ω. Now in the notation of (2.8), (2.7) may be written

$$\langle A\rangle_t=g(0),$$

whereas the ensemble average value of A is initially

$$\langle A(0)\rangle=\mathrm{trace}[\rho(0)A]=g(0)+\sum_{\omega\neq 0}g(\omega).$$

Hence if the equality is to hold in (2.10) we must have $\langle A(0)\rangle=\langle A\rangle_t$; in other words, if $\langle A(t)\rangle$ tends to an asymptotic limit $\langle A\rangle_t$ it must already have had this value at $t=0$, i.e., at any arbitrary earlier time. We conclude, then, that unless the expectation value $\langle A(t)\rangle$ is constant for all time it cannot exhibit limiting asymptotic behavior as $t\to\infty$. Any observable whose expectation value is not constant all the time must therefore continue to fluctuate forever.

The question arises: Might this conclusion require revision if the properties of the ensemble are time-averaged? The idea here is that if the fluctuations in $\langle A(t)\rangle$ are of fairly short duration, they might be smoothed out by averaging over a short time interval, so that limiting asymptotic behavior might be recovered. The answer to this question is, however, in the negative, as will now be shown.

We define a "time-smoothed" statistical operator $R(t)$ by the equation

$$R(t)=\int_{-\infty}^{\infty}d\tau f(\tau)\rho(t+\tau), \tag{2.11}$$

where $f(x)$ is a nonnegative real function whose integral over all x is unity, Then, whatever the precise form of $f(x)$,

$$i\hbar(\partial R/\partial t)=i\hbar\int_{-\infty}^{\infty}d\tau f(\tau)[\partial(t+\tau)/\partial t]$$

$$=\int_{-\infty}^{\infty}d\tau f(\tau)\{H\rho(t+\tau)-\rho(t+\tau)H\}$$

$$=HR(t)-R(t)H, \tag{2.12}$$

showing that the equation of motion of a time-smoothed statistical operator is identical with that of a statistical operator which has not been time-smoothed. Consequently the theorem already established about the inevitability of ceaseless fluctuations in $\langle A(t)\rangle$ remains true even when the procedure of time-smoothing is applied. To put the matter differently, if the time-smoothing is made effective enough to abolish the fluctuations which might otherwise occur at very large values of t, then it will also obliterate any secular variation in $\langle A(t)\rangle$ for small values of t. The device of time-smoothing is therefore useless in attempts to ensure the asymptotic approach of any time-independent observable to a limiting value.

We may note in concluding this section that the arbitrariness of the observable A in the preceding analysis permits it to depend on a limited selection of the coordinates of the system. In these circumstances A may indeed represent an appropriately "coarse-grained" property of the system, or of a portion of the system. It is therefore evident that coarse-graining makes no

difference to the theorem that $\langle A(t)\rangle$ must fluctuate ceaselessly unless it is constant for *all* values of the time.

3.

The theorem established in the preceding section precludes the construction of asymptotically developing observables in any isolated dynamical system of finite extent, and seems to cast doubt on the validity of any theory of such systems which postulates the existence of such observables. One can, nevertheless, establish a further theorem which places an upper limit on the fluctuations which can occur for a very long time. To do this it is convenient to introduce the concept of the "equivalent asymptotic ensemble."

Suppose, as before, that at $t=0$ the original system is described, in a representation which diagonalizes H, by the statistical matrix $\rho_{mn}(0)$. Because the energy levels may be degenerate, such a representation is not necessarily unique. In these circumstances a representation which diagonalizes H may be chosen in which the blocks of the statistical matrix corresponding to degenerate energy levels are also diagonalized. Such a choice evidently involves no loss of generality. Then the equivalent asymptotic ensemble is defined as that ensemble whose Hamiltonian H is the same as that of the original system, but whose statistical operator ρ', in the aforementioned representation which diagonalizes H, is the *diagonal* part of $\rho_{mn}(0)$. Thus ρ' commutes with H, and is constant in time

$$\rho_{nm}'(t)=\rho_{nm}(0), \quad n=m; \quad \rho_{nm}'(t)=0, \quad n\neq m. \tag{3.1}$$

By (2.7), which may now be written

$$\langle A\rangle_t=\sum_n \rho_{nn}'A_{nn}=\operatorname{trace}(\rho'A),$$

the time-average of the expectation value of A in the original system is the same as the expectation value of A in the equivalent asymptotic ensemble at any time. It follows immediately, for instance, that

$$\langle A^2\rangle_t=\operatorname{trace}(\rho'A^2).$$

The useful feature of the equivalent asymptotic ensemble is a connection between the fluctuation of A in the original system and the dispersion of A in the equivalent asymptotic ensemble. We now show that this relation places a useful upper bound on the fluctuations in $\langle A(t)\rangle$.

First we note that for the original system, by Schwartz's inequality,

$$\langle A(t)\rangle^2\leq\langle A^2(t)\rangle. \tag{3.2}$$

Averaging over time gives

$$\langle\langle A(t)\rangle^2\rangle_t\leq\langle A^2\rangle_t=\operatorname{trace}(\rho'A^2). \tag{3.3}$$

Subtracting from this the equation

$$(\langle A\rangle_t)^2=[\operatorname{trace}(\rho'A)]^2, \tag{3.4}$$

we obtain

$$\langle\langle A(t)\rangle^2\rangle_t-(\langle A\rangle_t)^2\leq\operatorname{trace}(\rho'A^2)-[\operatorname{trace}(\rho'A)]^2, \tag{3.5}$$

which may be written in the alternative form

$$\langle\{\langle A(t)\rangle-\langle A\rangle_t\}^2\rangle_t\leq\operatorname{trace}(\rho'A^2)-[\operatorname{trace}(\rho'A)]^2, \tag{3.6}$$

showing that the fluctuation of $\langle A(t)\rangle$ in the original system cannot exceed the dispersion of A in the equivalent asymptotic ensemble. Equality of these two quantities can only occur if the equality holds in (3.2) for all values of the time. This in turn implies that A has no dispersion in the original system at any time, i.e., that the system is in a pure eigenstate of A all the time, so that $\langle A(t)\rangle$ is constant.

4.

The results obtained in Sec. 2 preclude the possibility of constructing observables which exhibit genuine asymptotic limits for finite dynamical systems, however large, and show also that even if time-smoothing or coarse-graining procedures are carried out they are of no avail in preventing the ceaseless fluctuations of any observable whose expectation value is not constant over the whole of time. This result may be regarded as an inescapable consequence of the ergodic theorem that a finite dynamical system must return arbitrarily close to its initial state of motion after a sufficiently long time; but it shows that the consideration of a time-smoothed or coarse-grained ensemble in no way affects the essentials of the situation. It may well be pointed out that this conclusion is of merely academic interest for very large systems; but this only underlines the necessity for considering the *macroscopic character* of a system as the essential requirement for effectively irreversible behavior.

The theorem established in Sec. 3 offers more promising prospects. It shows that though the fluctuations in $\langle A(t)\rangle$ can never die away, a useful upper bound can nevertheless be set on their magnitude. The larger the system under consideration, the smaller one would expect to be the relative dispersion of any macroscopic observable in the equivalent asymptotic ensemble. Hence if the initial deviation of $\langle A(t)\rangle$ from its time-average value is sufficiently great compared to the variance of A in the equivalent asymptotic ensemble, we can feel confident that $\langle A(t)\rangle$ must approach its time-average value and remain close to this value for very long periods of time. The considerations indicate clearly that the virtually infinite nature of macroscopic systems must be taken into account in any theory of irreversible processes; and to such systems we now turn. It transpires that their properties are radically different from those of the finite systems discussed previously.

Consider, then, an infinite mechanical system, whose Hamiltonian has a purely continuous spectrum.[3] In those cases where there is degeneracy the eigenstates $|E', \alpha'\rangle$ are characterized by the energy of the system E' and the values of some other set of properties of the system which are here represented by α'. The values taken on by α' may in general depend upon E'. It is convenient to normalize the eigenstates so that

$$\langle E', \alpha' \mid E'', \alpha''\rangle = \delta(E'-E')\delta_{\alpha'\alpha''}.$$

(The use of a discrete formalism for the α' values is entirely a matter of convenience.) In this representation, the statistical matrix is written as $\langle E', \alpha' \mid \rho \mid E'', \alpha''\rangle$ and the matrix elements of A as $\langle E', \alpha' \mid A \mid E'', \alpha''\rangle$. When there is no degeneracy the presence of α' may be suppressed.

We now suppose our knowledge of the system at $t=0$, expressed by $\langle E', \alpha' \mid \rho(0) \mid E'', \alpha''\rangle$, to be entirely based on the measurement of observables *at that time*, so that the expectation value of every observable at any later time is an even function of t; this is a necessay consequence of the time-reversibility of the equations of motion.

On measuring all energies from the lowest eigenvalue of H, we have

$$\langle A(t)\rangle = \int_0^\infty dE' \int_0^\infty dE'' \sum_{\alpha',\alpha''} \langle E', \alpha', \mid \rho \mid E'', \alpha''\rangle \times \langle E'', \alpha'' \mid A \mid E', \alpha'\rangle \exp[i(E''-E')t/\hbar], \quad (4.1)$$

which is to be an even function of t. The substitutions

$$x = \tfrac{1}{2}(E''+E'); \qquad y = \tfrac{1}{2}(E''-E') \quad (4.2)$$

yield

$$\langle A(t)\rangle = 2\int_{-\infty}^{+\infty} dy \int_{|y|}^\infty dx [\sum_{\alpha',\alpha''} \langle x-y, \alpha' \mid \rho \mid x+y, \alpha''\rangle \times \langle x+y, \alpha'' \mid A \mid x-y, \alpha'\rangle] \exp(2iyt/\hbar), \quad (4.3)$$

which may be written in the form

$$\langle A(t)\rangle = 2\int_{-\infty}^{+\infty} dy g(y) \exp(2iyt/\hbar), \quad (4.4)$$

where

$$g(y) = \int_{|y|}^\infty dx [\sum_{\alpha',\alpha''} \langle x-y, \alpha' \mid \rho \mid x+y, \alpha''\rangle \times \langle x+g, \alpha'' \mid A \mid x-y, \alpha'\rangle]. \quad (4.5)$$

[3] The continuous nature of its energy spectrum is the only special property of the infinite system which we invoke; the number of degrees of freedom may or may not be infinite.

This form shows that $g(y)$ must be purely real if $\langle A(t)\rangle$ is to be an even function of t. But,

$$\begin{aligned} g(-y) &= \int_{|y|}^\infty dx [\sum_{\alpha',\alpha''} \langle x+y, \alpha' \mid \rho \mid x-y, \alpha''\rangle \times \langle x-y, \alpha'' \mid A \mid x+y, \alpha'\rangle] \\ &= \int_{|y|}^\infty dx [\sum_{\alpha',\alpha''} \langle x+y, \alpha'' \mid \rho \mid x-y, \alpha'\rangle \times \langle x-y, \alpha' \mid A \mid x+y, \alpha''\rangle] \\ &= \int_{|y|}^\infty dx [\sum_{\alpha',\alpha''} \langle x-y, \alpha' \mid \rho \mid x+y, \alpha''\rangle \times \langle x+y, \alpha'' \mid A \mid x-y, \alpha'\rangle]^* \\ &= \bar{g}(y) \end{aligned} \quad (4.6)$$

in view of the Hermitean character of ρ and A. Hence $g(y)$ is not only real, but also an even function of y.

To obtain the time-average value of $\langle A(t)\rangle$ we write

$$\begin{aligned} \langle A\rangle_t &= \lim_{z\to 0} \int_0^\infty dt e^{-zt} \langle A(t)\rangle \\ &= 2\lim_{z\to 0} \int_0^\infty dt e^{-zt} \int_{-\infty}^{+\infty} dy g(y) \exp(2igt/\hbar). \end{aligned} \quad (4.7)$$

The time integration yields

$$\begin{aligned} \langle A\rangle_t &= 2\lim_{z\to 0} z\int_{-\infty}^\infty dy g(y) \left[\frac{1}{z-2iy/\hbar}\right] \\ &= 2\lim_{z\to 0} \int_{-\infty}^\infty dy g(y) \left[\frac{z^2}{z^2+4y^2/\hbar^2}\right], \end{aligned} \quad (4.8)$$

where we have used the fact that $g(y)$ is real. Now for $|y| \gg z$ the function $[z^2/(z^2+4y^2/\hbar^2)]$ is very small, whereas for $|y| \ll z$ this function is close to unity. Hence if $g(y)$ is nonsingular at $y=0$ the integral vanishes in the limit $z\to 0$, and $\langle A\rangle_t = 0$. Allowing, then, for the more general possibility that

$$g(y) = G\delta(y) + h(y), \quad (4.9)$$

where $h(y)$ is nonsingular, we obtain

$$\begin{aligned} \langle A\rangle_t &= \lim_{z\to 0} \int_{-\infty}^\infty dy G\delta(y) \left[\frac{2z^2}{z^2+4y^2/\hbar^2}\right] \\ &= \lim_{z\to 0} G(2z^2/z^2] = 2G. \end{aligned} \quad (4.10)$$

The time average value of $\langle A(t)\rangle^2$ may also be obtained from the form $G\delta(y)+h(y)$. Precisely,

$$\begin{aligned} \langle A(t)\rangle^2 &= \left| 2\int_{-\infty}^\infty dy g(y) \exp(2iyt/\hbar) \right|^2 \\ &= 4\int_{-\infty}^\infty dy \int_{-\infty}^\infty dy' g(y) g(y') \exp[2i(y-y')t/\hbar], \end{aligned} \quad (4.11)$$

so that

$$\langle\langle A(t)\rangle^2\rangle_t$$

$$=4\lim_{\varepsilon\to 0}\int_{-\infty}^{\infty}dy\int_{-\infty}^{\infty}dy'g(y)g(y')\left[\frac{z^2}{z^2+4(y-y')^2/\hbar^2}\right]. \quad (4.12)$$

The integration over y' gives zero unless $g(y')$ has a delta function singularity at $y'=y$. By hypothesis the only such singularity is $y'=0$, namely, $G\delta(y')$. Hence we obtain

$$\langle\langle A(t)^2\rangle_t=4\lim_{\varepsilon\to 0}\int_{-\infty}^{\infty}dyg(y)\left[\frac{Gz^2}{z^2+4y^2/\hbar^2}\right], \quad (4.13)$$

which in turn reduces to $4G^2$ upon integration over y. We conclude that

$$\langle\langle A(t)\rangle^2\rangle_t=4G^2=(\langle A\rangle_t)^2, \quad (4.14)$$

showing that the fluctuations in $\langle A(t)\rangle$ must eventually die away completely.

It is not out of the question, of course, that $g(y)$ might possess other singularities than $G\delta(y)$, for example that

$$g(y)=G\delta(y)+G_1\{\delta(y-y_1)+\delta(y+y_1)\}+h(y), \quad (4.15)$$

where $h(y)$ is again nonsingular. This assumption leads, as before, to $\langle A\rangle_t=2G$; but the calculation of $\langle\langle A(t)\rangle^2\rangle_t$ is modified. By (4.12), as before,

$$\langle A(t)\rangle^2_t$$

$$=4\lim_{\varepsilon\to 0}\int_{-\infty}^{\infty}dy\int_{-\infty}^{\infty}dy'g(y)g(y')\left[\frac{z^2}{z^2+4(y-y')^2/\hbar^2}\right].$$

But now the integration over y gives three distinct terms

$$\langle\langle A(t)\rangle^2\rangle_t$$

$$=4\lim_{\varepsilon\to 0}\int_{-\infty}^{\infty}dyg(y)\left[\frac{Gz^2}{z^2+4y^2/\hbar^2}+\frac{Gz^2}{z^2+4(y-y_1)^2/\hbar^2}\right.$$

$$\left.-\frac{Gz^2}{z^2+4(y-y_1)^2/\hbar^2}\right]. \quad (4.16)$$

In the integration over y, all three terms contribute to the result, and we obtain

$$\langle\langle A(t)\rangle^2\rangle_t=4(G^2+2G_1^2)\neq(\langle A(t)\rangle)^2. \quad (4.17)$$

Hence the presence of *any other* delta function singularities in $g(y)$ except $G\delta(y)$ leads to permanently fluctuating behavior in $\langle A(t)\rangle$. This should occasion no surprise, since the separated singularities at $\pm y_1$, would be expected to lead to periodic fluctuations in $\langle A(t)\rangle$ of frequency $y_1/2\pi\hbar$.

5.

Possibly the most striking result which we have obtained in this paper, is that there is a qualitative difference between the time-development of expectation values in finite and infinite systems. This result might seem paradoxical at first sight, since it is difficult to define an infinite system except as the limit of a sequence of finite systems of increasing size. The resolution of this paradox lies in the fact that two different limiting processes must be carried out in order to establish the long-time behaviour of any expectation value in an infinite system. The first of these is allowing the time to tend to infinity; this limiting process was given precedence in Sec. 2, which was concerned ostensibly with finite systems. But consideration of Eq. (2.9) shows that for a large finite system the times involved are exceedingly great—of the order of the Poincaré cycle—so that it is physically unrealistic to base a theory of irreversible behaviour upon such an analysis. For this reason the other limiting process—making the size of the system tend to infinity—should take precedence over the passage to infinite time, and in Sec. 4 we have taken cognizance of this necessity. We therefore feel that the results obtained in Sec. 2 merely demonstrate the danger of making the time tend to infinity before making the system infinite; it is the results of Sec. 4 which indicate the correct way of handling irreversible phenomena.

A word must be said about time-smoothing, and the bearing of our results upon theories of irreversibility which invoke time-smoothing as an essential device for obtaining irreversible behavior. We do not wish to claim that time-smoothing can never be helpful in the practical formulation of irreversible equations. We do, furthermore, recognize that a measurement takes a small finite time, so that a time-smoothed expectation value might correspond more faithfully to what is actually measured. On the other hand, the fact that irreversibility is manifested by infinite systems under very general conditions indicates that time-smoothing should not be regarded as essential to the irreversible character of many phenomena.

Finally, it is of interest to compare the results of Sec. 4 with the work of Van Hove.[4-7] Van Hove showed that a sufficient condition for limiting asymptotic behavior in an infinite system was that the perturbation-inducing-transitions between eigenstates of the unperturbed Hamiltonian should exhibit a diagonal singularity of the type discussed in Sec. 4. His analysis was couched in terms of perturbation theory, though he carried it to infinite order. In our paper we make no use of perturbation theory; we deal directly with the observable whose expectation value is to be determined. The function whose analytic properties are relevant to the time-development of the observable now involves both the statistical operator and the observable itself; the diagonal singularity condition on this func-

[4] L. Van Hove, Physica **21**, 901 (1955).
[5] L. Van Hove, Physica **22**, 343 (1956).
[6] L. Van Hove, Physica **23**, 441 (1957).
[7] L. Van Hove, *Proceedings of the International Symposium on Transport Processes in Statistical Mechanics* (Interscience Publishers, Inc., New York 1958), p. 219.

tion corresponds mathematically to that of Van Hove, but we find a converse result to that of Van Hove, namely, that our function shall be *non*singular *except* possibly on the diagonal. We feel that this conclusion adds to our knowledge of the necessary and sufficient conditions for irreversible behavior.

THE JOURNAL OF CHEMICAL PHYSICS VOLUME 33, NUMBER 5 NOVEMBER, 1960

Ensembles of Maximum Entropy

JOSEPH E. MAYER

*Enrico Fermi Institute for Nuclear Studies, University of Chicago, Chicago, Illinois**

(Received December 23, 1959)

A theorem is stated and proved. The theorem considers the various possible probability density functions, W_N, in the phase space of all the N molecules of a system, defined for an ensemble for which known mechanical properties require a given set of reduced probability densities, w_n, for *small* numbers of molecules $n<n_0$. The theorem states that the function, W_N, of maximum entropy is that with the simplest possible correlations between the molecules consistent with the restraint imposed by the fixed w_n, $n<n_0$. It is then shown that the course of the negative entropy flow in a real "isolated" system undergoing spontaneous change is a flow of negative entropy into the correlation functions of many molecules followed by the destruction of these negative entropy terms due to the random time dependent fluctuations at the container walls.

INTRODUCTION

IN this article a theorem is stated and proved. The mathematics of the proof are quite simple, and, indeed, after its statement is understood, one would intuitively believe, almost without proof, the correctness of the theorem. The statement of the theorem is less simple.

STATEMENT OF THE THEOREM

An ensemble of classical systems is mechanically defined in all detail by giving the probability density function, W_N, in the coordinate-momentum phase space of all the N molecules composing the systems. If we deal with an ensemble of open systems, the functions W_N must be given for all numbers, $N\geq 0$, of molecules.

There are, however, a much smaller set w_n, of less complicated probability density functions which completely describe the average mechanical properties of the systems of the ensemble. These are the "reduced" probability densities for $n=1, 2, 3, \cdots$ molecules, giving the probability densities in the phase space of n molecules for occupancy of the position in this phase space by n molecules simultaneously, independently of the positions and momenta of all others in the systems. Included in this set one may define the constant w_0, so defined as to always have the value unity.

In present practice no measurements have been devised which measure the probability density functions, w_n, for $n>2$, with any accuracy at all. In principle some measurements (i.e., low-energy neutron scattering) can be utilized to find w_n for $n=3$ and $n=4$. Conversely, no measurements are affected by the values of these functions w_n for large values of n, say for $n\geq n_0$, where n_0 is reasonably small and very much smaller than the total number, $N\sim 10^{23}$, in the macroscopic systems. The average mechanical properties of the systems of the ensemble are thus fully determined by the set of n_0 functions, $w_0\equiv 1, w_1, \cdots w_{n_0-1}$.

Now an infinite continuum of the probability density functions W_N, for all N molecules will lead to the same fixed set of functions, w_0 to w_{n_0-1}. We may, however, ask the following question. Which function, W_N, of this infinite continuum, has maximum entropy? The answer follows.

For a specified set of functions W_N, defined for $N\geq 0$, we may define a unique set of functions, ϕ_0 which is a constant, ϕ_1 which is dependent on the phase space of a single molecule, ϕ_2 on that of a pair, $\cdots$, ϕ_n on that of n molecules, $\cdots$, etc. These are so defined that $\ln W_N$ is the sum of these functions ϕ_n for $0\leq n\leq N$, one ϕ_n entering the sum for each of the $N!/(N-n)!n!$ subsets of n numbered molecules out of the total set of N numbered molecules. Our theorem is that the function W_N, which has maximum entropy consistent with a fixed set of n_0 reduced probability density functions, w_0, $w_1, \cdots, w_{n_0-1}$ is that function for which $\phi_n\equiv 0$ if $n\geq n_0$.

The functions w_n are obtained from the W_N by integration of W_N over the phase space of the remaining $N-n$ molecules. The condition $w_0=1$ is merely the normalization that the integral of the probability density must be unity. For given set $\phi_1^{(0)}, \phi_2^{(0)}, \cdots, \phi_{n_0-1}^{(0)}$, of functions, with $\phi_n^{(0)}\equiv 0$ for $n\geq n_0$, this equation determines a normalizing factor $\exp \phi_0^{(0)}$ in W_N. The other reduced probability densities, w_n are then determined by the appropriate sum of partial integrals.

* Present address: Department of Chemistry, School of Science and Engineering, University of California, La Jolla, California.

One may now assume any arbitrary set of functions $\phi_n(\lambda)$, dependent on a parameter λ, for $n \geq n_0$, but such that these functions are all identically zero for $\lambda=0$. The n_0 integral equations for $w_0, w_1, \cdots w_{n_0-1}$ may now be used to determine the n_0 functions $\phi_0(\lambda), \phi_1(\lambda) \cdots \phi_{n_0-1}(\lambda)$, with $\phi_n(\lambda=0)=\phi_n^{(0)}$, such that the reduced probability densities, w_n, for $0 \leq n \leq n_0-1$, remain unchanged for all values of λ. We prove in the next section that the entropy expression has an extremum at $\lambda=0$, and that the second derivative with respect to λ is negative: The entropy is maximum when the correlation functions ϕ_n for $n \geq n_0$ are all zero.

It is intuitively obvious that this is to be expected when one remembers that the entropy is maximized by the "smoothest" probability density consistent with given restraints. The function W_N for $\lambda \neq 0$ contains correlation functions, ϕ_n for $n \geq n_0$ giving detailed correlations in phase space between numbers n, of molecules. At $\lambda=0$ these correlations are wiped out but in such a way that their averaged effect is retained by altering the correlations, ϕ_n, for $n<n_0$, so as to retain the same physical characteristics of the ensemble in the unaltered w_n for $n<n_0$. The entropy is a maximum for the "smoothed" functions.

PROOF OF THE THEOREM

In the interests of generality we prove the theorem for a system containing any number of different components, a, b, $\cdots$. Let $\mathbf{N}=N_a, N_b$, and use

$$\mathbf{N}!=N_a!N_b!\cdots, \tag{1}$$

$$N=\sum_a N_a. \tag{2}$$

The symbol

$$\{\mathbf{N}\}=\mathbf{q}_1, \mathbf{p}_1 \cdots \mathbf{q}_N, \mathbf{p}_N \tag{3}$$

is used for the coordinate-momentum space of the set $\mathbf{N}$ of molecules, in such units that Planck's constant h is unity, and

$$d\{\mathbf{N}\}=d\mathbf{q}_1, d\mathbf{p}_1, \cdots, d\mathbf{p}_N \tag{4}$$

is used for the volume element.

We prefer to use the equations for an open system and introduce functions $W_N(V, \lambda, \{\mathbf{N}\})$, which depend on a parameter λ, and are defined as being proportional to the probability density in phase space of the set $\mathbf{N}$ of molecules, when that set *alone* is in the volume V of an open system. The proportionality factor is such that

$$P_N(V, \lambda,)=(\mathbf{N}!)^{-1}\iint\cdots\int W_N(V, \lambda, \{\mathbf{N}\})d\{\mathbf{N}\} \tag{5}$$

is the probability that exactly the set $\mathbf{N}$ of molecules occupies V. The sum of P_N over all number sets, $\mathbf{N}$, is necessarily unity, so that

$$w_0 \equiv 1=\sum_{\mathbf{N} \geq 0}(\mathbf{N}!)^{-1}\iint\cdots\int W_N(V, \lambda, \{\mathbf{N}\})d\{\mathbf{N}\}. \tag{6}$$

The reduced probability densities $w_n(V, \lambda\{\mathbf{n}\})$, for a set $\mathbf{n}=n_a n_b, \cdots$ of molecules are given by

$$w_n(V, \lambda\{\mathbf{n}\}) = \sum_{\mathbf{N} \geq 0}(\mathbf{N}!)^{-1}\iint\cdots\int W_{N+n}(V, \lambda, \{\mathbf{N}+\mathbf{n}\})d\{\mathbf{N}\} \tag{7}$$

which include Eq. (6) when $\mathbf{n}=0$. We have

$$\partial w_n/\partial\lambda=\sum_{\mathbf{N} \geq 0}(\mathbf{N}!)^{-1}\iint\cdots\int\frac{\partial W_{N+n}}{\partial\lambda}d\{\mathbf{N}\}, \tag{8}$$

$$\partial^2 w_n/\partial\lambda^2=\sum_{\mathbf{N} \geq 0}(\mathbf{N}!)^{-1}\iint\cdots\int\frac{\partial^2 W_{N+n}}{\partial\lambda^2}d\{\mathbf{N}\}, \tag{9}$$

and necessarily $\partial w_0/\partial\lambda=\partial^2 w_0/\partial\lambda^2=0$.

The correlation functions $\phi_n(V, \lambda\{\mathbf{n}\})$ are defined in terms of the W_m for $0 \leq \mathbf{m} \leq \mathbf{n}$ by

$$\phi_n(V, \lambda, \{\mathbf{n}\})=\sum_{m=0}^{m=n}\sum_{\{\mathbf{m}\}_n}(-)^{n-m}\ln W_m(V, \lambda, \{\mathbf{m}\}_n), \tag{10}$$

where, for a given number set $\mathbf{m}$, the sum runs over all $\mathbf{n}!/(\mathbf{n}-\mathbf{m})!\mathbf{m}!$ different subsets, $\{\mathbf{m}\}_n$, of numbered molecules of the numbered set $\mathbf{n}$.

With (10) one has

$$\ln W_n(V, \lambda, \{\mathbf{N}\})=\sum_{n=0}^{n=N}\sum_{\{n\}_N}\phi_n(V, \lambda\{\mathbf{n}\}_N), \tag{11}$$

which follows from Eq. (10) by observing that if Eq. (10) is used in Eq. (11) an identity is obtained.

The negative entropy divided by Boltzmann's constant $-S/k$ in the volume V, is given at equilibrium by the expression

$$-S/k=\sum_{\mathbf{N} \geq 0}\frac{1}{\mathbf{N}!}\iint\cdots\int W_N \ln W_N d\{\mathbf{N}\}, \tag{12}$$

and we use this as a general definition for any ensemble. Differentiation with respect to λ gives

$$(\partial/\partial\lambda)(-S/k) = \sum_{\mathbf{N} \geq 0}(\mathbf{N}!)^{-1}\iint\cdots\int\frac{\partial W_N}{\partial\lambda}[\ln W_N+1]d\{\mathbf{N}\},$$

$$(\partial^2/\partial\lambda^2)(-S/k)=\sum_{\mathbf{N} \geq 0}(\mathbf{N}!)^{-1}\iint\cdots\int\left[\frac{\partial^2 W_N}{\partial^2\lambda}[\ln W_N+1]+\left(\frac{\partial W_N}{\partial\lambda}\right)^2 W_N^{-1}\right]d\{\mathbf{N}\},$$

which with (8) and (9), and $\partial w_0/\partial\lambda=\partial^2 w_0/\partial\lambda=0$,

may be written as

$$(\partial/\partial\lambda)(-S/k)=\sum_{\mathbf{N}\geq 0}(\mathbf{N}!)^{-1}\iint\cdots\int(\partial W_{\mathbf{N}}/\partial\lambda)\times\ln W_{\mathbf{N}}d\{\mathbf{N}\},\quad(13)$$

$$(\partial^2/\partial\lambda^2)(-S/k)=\sigma+\sum_{\mathbf{N}\geq 0}(\mathbf{N}!)^{-1}(\partial^2 W_{\mathbf{N}}/\partial\lambda^2)\ln W_{\mathbf{N}}d\{\mathbf{N}\},\quad(14)$$

$$\sigma=\sum_{\mathbf{N}\geq 0}(\mathbf{N}!)^{-1}\iint\cdots\int[\partial\ln W_{\mathbf{N}}/\partial\lambda]^2 W_{\mathbf{N}}d\{\mathbf{N}\}.\quad(15)$$

We note here that since from its definition as a probability density $W_{\mathbf{N}}$ is necessarily positive, it follows that

$$\sigma\geq 0.\quad(16)$$

Use (11) in (13) and (14) for $\ln W_{\mathbf{N}}$. Use (8) and (9) for $\partial w_{\mathbf{n}}/\partial\lambda$ and $\partial^2 w_{\mathbf{n}}/\partial\lambda^2$. Noting that there are $\mathbf{N}!/(\mathbf{N}-\mathbf{n})!\mathbf{n}!$ different subsets, $\{\mathbf{n}\}_{\mathbf{N}}$, for each set $\mathbf{n}$ one finds,

$$(\partial/\partial\lambda)(-S/k)=\sum_{\mathbf{n}\geq 1}\frac{1}{\mathbf{n}!}\iint\cdots\int\phi_{\mathbf{n}}(\partial w_{\mathbf{n}}/\partial\lambda)d\{\mathbf{n}\},\quad(17)$$

$$(\partial^2/\partial\lambda^2)(-S/k)=\sigma+\sum_{\mathbf{n}\geq 1}(\mathbf{n}!)^{-1}\iint\cdots\int\phi_{\mathbf{n}}(\partial^2 w_{\mathbf{n}}/\partial\lambda^2)d\{\mathbf{n}\},\quad(18)$$

where we have dropped the terms $\phi_0\partial w_0/\partial\lambda$ and $\phi_0\partial^2 w_0/\partial\lambda^2$, since they are necessarily zero.

Now define

$$\phi_{\mathbf{n}}(V,\lambda=0,\{\mathbf{n}\})=\phi_{\mathbf{n}}^{(0)}\quad(19)$$

and let

$$\phi_{\mathbf{n}}^{(0)}\equiv 0\quad\text{for}\quad\mathbf{n}\geq\mathbf{n}_0.\quad(20)$$

Assume arbitrary functions $\phi_{\mathbf{n}}(V,\lambda\{\mathbf{n}\})$ for $\mathbf{n}\geq\mathbf{n}_0$ consistent with (20) that they all be identically zero at $\lambda=0$. We may then fix the functions $\phi_{\mathbf{n}}(V,\lambda,\{\mathbf{n}\})$ for $\mathbf{n}<\mathbf{n}_0$ so that[1]

$$\partial w_{\mathbf{n}}(V,\lambda\{\mathbf{n}\})/\partial\lambda\equiv\partial^2 w_{\mathbf{n}}(V,\lambda,\{\mathbf{n}\})/\partial\lambda^2\equiv 0,\quad\mathbf{n}<\mathbf{n}_0.\quad(21)$$

With (20) and (21) the sums displayed in (17) and (18) are both zero at $\lambda=0$, since $\phi_{\mathbf{n}}=0$ for $\mathbf{n}\geq\mathbf{n}_0$, and the derivatives are zero for $\mathbf{n}<\mathbf{n}_0$. Since (17) is zero at $\lambda=0$ the entropy is an extremum at $\lambda=0$. Since the sum in (18) is zero at $\lambda=0$, and σ is positive, Eq. (16), the entropy is seen to be a maximum at $\lambda=0$.

The demonstration would be the same for a closed system. All equations except (10) are then the same, except that only a single set $\mathbf{N}$ of molecules has a nonzero function $W_{\mathbf{N}}$. Since, however, in a closed system, and in the absence of some rule, $W_{\mathbf{N}}$ is not defined for all $\mathbf{N}$, Eq. (10) has no meaning. The functions $\phi_{\mathbf{n}}$ must then be defined implicitly by (11), which is not really unique, since, for instance ϕ_0/N could be added to each of the N functions ϕ_1, and ϕ_0 eliminated. This in no way alters the physical picture or the results, as given $\ln W_{\mathbf{N}}$ requires functions $\phi_{\mathbf{n}}$ in (11) up to some $\mathbf{n}<\mathbf{n}_0$; if functions $\phi_{\mathbf{n}}$ for $\mathbf{n}\geq\mathbf{n}_0$ are arbitrarily added they in turn could always be analyzed as sums of functions of smaller subsets, $\mathbf{n}<\mathbf{n}_0$. The use of the language of the open system permits us to define the $\phi_{\mathbf{n}}$ uniquely by Eq. (10) and thus obviates the necessity of this kind of awkward discussion.

SIGNIFICANCE OF THE THEOREM

The theorem has one use which may, or may not, be of some value in discussing equilibrium systems. If the reduced probability densities $w_0\equiv 1$, w_1 and w_2 are taken as known, one may ask what is known about the entropy of the ensemble. Green and Nettleton[2] have attempted an answer based on the (implicit) assumption that the Kirkwood superposition approximation holds for the higher reduced probability densities w_n. The answer they obtained was disappointingly complicated. It may be that the answer is simpler if one computes for the ensemble of highest entropy as defined here.

Probably more important seems to be the interpretation in connection with the entropy increase in a time dependent system. The usual transport problem involves a system described by thermodynamic variables at $t=0$, which, however, are generally such that the intensive variables are functions of the position in the system. The appropriate probability density function $W_{\mathbf{N}}$, for the ensemble representing the totality of all experimental systems prepared in this manner, is then that of local thermodynamic equilibrium at $t=0$. Equation (12) then gives the correct expression for the negative entropy divided by k, the same as the thermodynamic value, which in turn is higher than $(-S_{eq}/k)$ the value of the thermodynamic function at the equilibrium which the system will approach as $t\to\infty$. This $W_{\mathbf{N}}$ at $t=0$ has only the equilibrium correlations, which, for a sum of pair potentials, have $\phi_2=-u_{ij}(r_{ij})/kT$, and $\phi_{\mathbf{n}}=0$ for $\mathbf{n}>2$.

Now for an ensemble consisting of hypothetical completely isolated systems, all in containers having identical time independent Hamiltonians, the function $W_{\mathbf{N}}(V,t,\mathbf{N})$ is given for any t by the integration of the Liouville equation from the initial function $W_{\mathbf{N}}(V,t=0,\{\mathbf{N}\})$. The correlation functions $\phi_{\mathbf{n}}(V,t,\{\mathbf{n}\})$ for large sets $\mathbf{n}$, now grow with time. Indeed, if ρ is the number density in the systems, and if c is the sound

[1] The equations to do this are by no means readily solved. The general set of integral equations are given by the author [J. Chem. Phys. **15**, 187 (1947)]. These are somewhat generalized equations similar to those of J. Yvon, [*Statistique des Fluides* (Hermann and Cie, Paris, 1935)] or of Kirkwood, [John G. Kirkwood and Elizabeth Monroe, J. Chem. Phys. **9**, 514 (1941)].

[2] R. E. Nettleton and M. S. Green, J. Chem. Phys. **29**, 1365 (1958).

velocity, then nonzero correlation functions ϕ_n will appear at the time t for values of n of the order

$$n \simeq (4\pi/3)\rho(ct)^3. \quad (22)$$

Thus in an ordinary laboratory system correlation functions involving all the molecules of the system will be nonzero in about a millisecond.

It is also well known that with the $W_N(V, t, \{N\})$ computed for ideal isolation, the quantity $-S/k$ given by Eq. (12) does not change with time.

Actually, of course, the experimental systems are not so isolated. They must really be in containers which are in some contact with the remainder of the universe. Even extremely small time-dependent random fluctuations in the Hamiltonian due to the container walls will destroy these high-order correlation functions. However, *by definition*, if the systems behave like thermodynamically isolated systems, the mechanical properties will be those predicted for the strictly isolated systems: the functions $w_n(V, t, \{\mathbf{n}\})$ for $n<n_0$ will be those computed from the correlation functions $\phi_n(V, t, \{\mathbf{n}\})$ of the ensemble of strictly isolated systems. The actual correlation functions for large n will be wiped out by the fluctuations, but those for smaller n values, $n=0, 1, 2, \cdots$will be altered by this "smoothing," in such a way as to retain the w_n's of the isolated ensemble.

The course of the negative-entropy quantity $-S/k$ can thus be described as a flow into the high-number correlation functions, followed by a destruction there due to the otherwise trivial time dependent random fluctuations introduced at the walls.

THE JOURNAL OF CHEMICAL PHYSICS VOLUME 33, NUMBER 5 NOVEMBER, 1960

Boltzmann Equation and Inverse Collisions*

J. T. O'Toole† and J. S. Dahler

Department of Chemical Engineering, University of Minnesota, Minneapolis 14, Minnesota

(Received May 12, 1960)

The equations of change for the statistical distribution functions involved in the kinetic theory are examined for molecular species which interact with arbitrary central forces. It is shown that the notion of inverse encounters follows in a straightforward fashion from the fundamental Liouville equation. The analysis also establishes that it is not the usual singlet distribution function, but a particular modification thereof, which should satisfy an equation of the Boltzmann variety. Three body collision processes are briefly examined and the extension of the method to the domain of chemical kinetics discussed.

I. INTRODUCTION

In the modern kinetic theory the fluxes or currents of matter, momentum, and energy are expressed as moments of certain statistical distribution functions. The accuracy with which we can calculate these fluxes then depends only upon our ability to derive and to solve appropriate equations of change for the various distribution functions. The remarkable success of the Chapman-Enskog theory seems generally to be interpreted as almost conclusive evidence that at low densities the equation of change for the singlet distribution function is the one originally proposed by Maxwell and Boltzmann. Consequently, many attempts have been made to derive this equation from the fundamental theorem of Liouville. Particularly noteworthy are the investigations of Bogoliubov,[1] Kirkwood,[2] M. S. Green,[3] H. S. Green,[4] and Brout.[5] A common denominator of all these studies is their reliance upon some condition which artificially limits the system's memory of its dynamical history. Thus, in one or another of its forms the assumption of molecular chaos appears to be an unavoidable prerequisite to the establishment of the Boltzmann equation and, indeed, to the general development of the theory of irreversible processes. However, even when the inevitability of this hypothesis is accepted, the question of how to introduce it into the theory still remains. In the past investigators often have been so concerned with justifying the chaos condition that they have disregarded or actually erred in their identification of the dynamical states which appear in the "collision integral" of the Boltzmann equation. The inadequacy of this approach has occasionally tended to obscure the physical content of Boltzmann-like equations and even to discredit the interpretation of collision integrals in terms of direct

* This research was supported in part by a grant from the National Science Foundation.

† Formerly General Electric Fellow, Chemical Engineering Department, University of Minnesota: now National Science Foundation Fellow, Faculty of Science, University of Brussels, Belgium.

[1] N. Bogoliubov, J. Phys. (U.S.S.R) **10**, 256, 265 (1946).

[2] J. G. Kirkwood, J. Chem. Phys. **15**, 72 (1947).

[3] M. S. Green, J. Chem. Phys. **25**, 836 (1956).

[4] H. S. Green, *Molecular Theory of Fluids* (North Holland Publishing Company, Amsterdam, 1952).

[5] R. Brout, Physica **22**, 509 (1956).

and inverse encounters. The *practical* consequences of these errors are generally more pronounced at high densities where the mechanism of collisional transfer contributes significantly to transport phenomena. Thus, only the collisional transfer portions of the fluxes would be adversely affected in calculations based upon the erroneous Boltzmann-like equations proposed by Dahler[6] and by Rice, Kirkwood, Ross, and Zwanzig[7] for the case of rigid sphere molecules.

In a previous communication[8] we were able to establish that when the discontinuous nature of the rigid sphere interaction is treated carefully the resulting equation of change for the singlet distribution function agrees with that of Enskog and that the collision integral then becomes explicable in terms of direct and inverse encounters. These conclusions have been fully confirmed by the recent studies of Hollinger and Curtiss.[9] The purpose of this article is to illustrate how the methods previously developed for rigid spheres can be applied to a more general class of pair interaction potentials.

In the next section it will be shown how one can arrive at a Boltzmann equation for a modified singlet distribution function which is defined in terms of rather arbitrarily chosen regions of interaction. A similar approach has been employed, but in a less explicit manner, by M. S. Green[8] and by Hollinger and Curtiss.[9] In Sec. III the equation of change for an analogously defined pair distribution function is derived.

II. EQUATION OF CHANGE FOR SINGLET DISTRIBUTION FUNCTION

We consider a system of N identical molecules each of mass m and denote the position and momentum of the ith by $\mathbf{R}_i$ and $\mathbf{p}_i$, respectively. The probability of a particular state of the system is given by the corresponding value of the specific distribution function $D^{(N)}=D^{(N)}(\mathbf{R}_1, \mathbf{p}_1; \cdots; \mathbf{R}_N, \mathbf{p}_N; t)$. Conservation of system points in the $6N$-dimensional phase space on which $D^{(N)}$ is defined can then be expressed by the Liouville equation,

$$\partial D^{(N)}/\partial t+\sum_{i=1}^{N}[(\mathbf{p}_i/m)\cdot\nabla_{\mathbf{R}_i}+\mathbf{F}_i\cdot\nabla_{\mathbf{p}_i}]D^{(N)}=0. \quad (1)$$

Here $\mathbf{F}_i$, the force acting on the ith molecule, is assumed to equal the sum of the gradients of the $N-1$ pair potentials $\phi(R_{ij})$,

$$\mathbf{F}_i=-\nabla_{\mathbf{R}_i}\sum_{j\neq 1}^{N}\phi(R_{ij}). \quad (2)$$

We now find it convenient to define the sequence of regions and corresponding complements,

$$V_i:\{R_{ij}<\sigma, \quad j\neq i\}$$
$$V_i'=V-V_i, \quad (3)$$

where V denotes the volume in ordinary three-space accessible to the system. In the case of rigid spheres this division of the space into an interior and an exterior region is an intrinsic property of the pair interaction potential. For the moment we require only that the parameter σ be small in comparison with macroscopic dimensions and that $\nabla_{\mathbf{R}_i}\phi(R_{ij})$ be continuous on V_i'.

Let us next integrate Eq. (1) over all values of the momenta, $\mathbf{p}_2, \cdots, \mathbf{p}_N$, and over the range V_i' of the coordinates $\mathbf{R}_2, \cdots \mathbf{R}_N$. If the total energy of the system is to be finite, then the terms involving momentum gradients, $\{\nabla_{\mathbf{p}_j}; j>1\}$, must vanish upon integration with the result that

$$\frac{\partial}{\partial t}D_{(1)}{}^{(1)}+\frac{\mathbf{p}_1}{m}\cdot\int_{V_1'}\cdots\int_{V_1'}\nabla_{\mathbf{R}_1}D^{(N)}d\mathbf{R}^{N-1}d\mathbf{p}^{N-1}+\sum_{j=2}^{N}\iint_{V_1'}\frac{\mathbf{p}_j}{m}\cdot\nabla_{\mathbf{R}_j}D_{(1)j}{}^{(2)}d\mathbf{R}_jd\mathbf{p}_j=\sum_{j=2}^{N}\iint_{V_1'}[\nabla_{\mathbf{R}_1}\phi(R_{1j}]\cdot\nabla_{\mathbf{p}_1}D_{(1)j}{}^{(2)}d\mathbf{R}_jd\mathbf{p}_j, \quad (4)$$

where

$$D_{(1)}{}^{(1)}=\int_{V_1'}\cdots\int_{V_1'}D^{(N)}d\mathbf{R}^{N-1}d\mathbf{p}^{N-1}=\int_{V_1'}\cdots\int_{V_1'}D^{(N)}d\mathbf{R}_2d\mathbf{p}_2\cdots d\mathbf{R}_Nd\mathbf{p}_N$$

and

$$D_{(1)j}{}^{(2)}=\int_{V_1'}\cdots\int_{V_1'}D^{(N)}d\mathbf{R}^{N-2}d\mathbf{p}^{N-2}=\int_{V_1'}\cdots\int_{V_1'}D^{(N)}d\mathbf{R}_2d\mathbf{p}_2\cdots d\mathbf{R}_{j-1}d\mathbf{p}_{j-1}d\mathbf{R}_{j+1}d\mathbf{p}_{j+1}\cdots d\mathbf{R}_Nd\mathbf{p}_N$$

differ from the usual singlet and pair distribution functions in that molecule one is isolated from all others to an extent determined by the magnitude of σ.

[6] J. S. Dahler, J. Chem. Phys. **30**, 1447 (1959).
[7] S. A. Rice, J. G. Kirkwood, J. Ross and R. Zwanzig, J. Chem. Phys. **31**, 575 (1959).
[8] J. T. O'Toole and J. S. Dahler, J. Chem. Phys. **32**, 1097 (1960).
[9] H. Hollinger and C. F. Curtiss, J. Chem. Phys. **33**, 1386 (1960).

We now perform the transformation of variables

$$(\mathbf{R}_1, \nabla_{\mathbf{R}_1}; \mathbf{R}_j, \nabla_{\mathbf{R}j}, j=2, \cdots, N) \rightarrow (\mathbf{R}_1, \nabla_{\mathbf{R}_1} - \sum_{j=2}^{N} \nabla_{\mathbf{R}j1}; \mathbf{R}_{j1} = \mathbf{R}_j - \mathbf{R}_1, \nabla_{\mathbf{R}j1}, j=2, \cdots, N) \tag{5}$$

and proceed to the limit $N \rightarrow \infty$, $V \rightarrow \infty$, $N/V \rightarrow n$.[10] The second of these steps is unnecessary if we agree to omit from the equation of change contributions which arise from the surface of the container to which the system is confined. In either event the volume integral of a divergence conditioned only by the requirement that $R_{j1} > \sigma$ can be replaced by an integral extended over the boundary surface $R_{j1} = \sigma$. As a result of these manipulations, (4) becomes,

$$[(\partial/\partial t) + (\mathbf{p}_1/m) \cdot \nabla_{\mathbf{R}_1}] D_{(1)}{}^{(1)} = (\sigma^2/m) \sum_{j=2}^{N} \iint_{\{R_{j1}=\sigma\}} \hat{R}_{j1} \cdot (\mathbf{p}_j - \mathbf{p}_1) D_{(1)j}{}^{(2)} d\hat{R}_{j1} d\mathbf{p}_j - \sum_{j=2}^{N} \iint_{V_1'} [\nabla_{\mathbf{R}j1} \phi(R_{j1})] \cdot \nabla_{\mathbf{p}_1} D_{(1)j}{}^{(2)} d\mathbf{R}_{j1} d\mathbf{p}_j \tag{6}$$

where $\hat{R}_{j1} = \mathbf{R}_{j1}/|\mathbf{R}_{j1}|$.

Partition of the range of integration into the two regions $\hat{R}_{j1} \cdot (\mathbf{p}_j - \mathbf{p}_1) > 0$ and $\hat{R}_{j1} \cdot (\mathbf{p}_j - \mathbf{p}_1) \leq 0$ and a simple change of sign in one variable of integration then transforms the first integral of (6) into

$$(\sigma^2/m) \sum_{j=2}^{N} \iint_{\{\hat{R}_{j1} \cdot (\mathbf{p}_j - \mathbf{p}_1) \geq 0\}} \hat{R}_{j1} \cdot (\mathbf{p}_j - \mathbf{p}_1) [D_{(1)j}{}^{(2)}(\mathbf{R}_1, \mathbf{p}_1; \mathbf{R}_1 + \sigma \hat{R}_{j1}, \mathbf{p}_j; t) - D_{(1)j}{}^{(2)}(\mathbf{R}_1, \mathbf{p}_1; \mathbf{R}_1 - \sigma \hat{R}_{j1}, \mathbf{p}_j; t)] d\hat{R}_{j1} d\mathbf{p}_j. \tag{7}$$

We can now be somewhat more specific concerning the value of σ. The integrand of this last expression consists of two terms, the first describing pairs moving away from one another, the second, those headed toward one another. We desire to treat these pairs as being involved in binary collisions. For this purpose σ should be as small as possible. On the other hand, to be rid of the second integral in (6) σ must be chosen so large that the contribution of $\nabla_{\mathbf{R}_{j1}} \phi(R_{j1})$ in V_1' is negligible.

Although we have required $\phi(R_{j1})$ to be continuous for $R_{j1} > \sigma$ no restriction has been placed upon its behavior within this "collision sphere." Thus Eq. (6) remains valid for the rigid sphere potential in which case the obvious choice is to allow σ to approach the diameter of the sphere. The second set of integrals will then be identically zero and the distinction between the modified and usual distribution functions will vanish. Likewise all collisions will be binary and, since σ approaches the sphere diameter from greater values, no problems can arise from the discontinuity. With allowance for notational difference it may easily be verified that the result is identical to the rigorous equation obtained previously.[8]

For a more general choice of the pair potential the trajectory of a typical binary encounter will resemble that illustrated in Fig. 1. Corresponding to each of the post-collisional pair states $\{\mathbf{R}_1, \mathbf{p}_1; \mathbf{R}_1 + \sigma \hat{R}_{j1}, \mathbf{p}_j; t\}$ for which $\hat{R}_{j1} \cdot (\mathbf{p}_j - \mathbf{p}_1) \geq 0$ there is a unique precollisional state $\{\mathbf{R}_{10}, \mathbf{p}_{10}; \mathbf{R}_{10} + \sigma \hat{R}_{j10}, \mathbf{p}_{j0}; t - \tau_c\}$ for which $\hat{R}_{j10} \cdot (\mathbf{p}_{j0} - \mathbf{p}_{10}) \leq 0$. The relationships between these pre- and post-collisional states are easily found to be

$$\mathbf{R}_{10} = \mathbf{R}_1 - (\mathbf{p}_j + \mathbf{p}_1)\tau_c/2m + (\hat{R}_{j1} - \hat{R}_{j10})\sigma/2$$
$$\mathbf{p}_{10} - \mathbf{p}_1 = -(\mathbf{p}_{j0} - \mathbf{p}_j) = \hat{k}\hat{k} \cdot (\mathbf{p}_j - \mathbf{p}_1), \tag{8}$$

where

$$\hat{R}_{j1} = \hat{R}_{j1}(\theta, \varphi)$$
$$\hat{R}_{j10} = \hat{R}_{j10}(\pi - \theta - \chi, \varphi)$$

and

$$\hat{k} = \hat{k}[(\pi - \chi)/2, \varphi]$$

are unit vectors, the polar spherical angles of which are shown in Fig. 1. The collisional duration τ_c and the

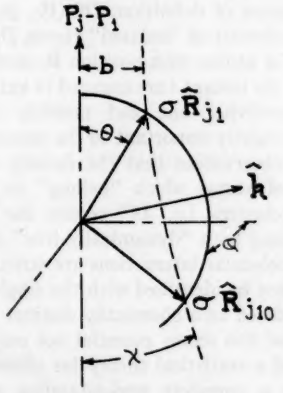

FIG. 1. Binary collision trajectory.

[10] Strictly, it is

$$\sum_{N \geq j > i \geq 1} \sum D_{(1)j}{}^{(2)} = \tfrac{1}{2} N(N-1) D_{(1)2}{}^{(2)}$$

and not $D_{(1)j}{}^{(2)}$ which converges in this limit.

scattering angle χ are given by

$$\tau_c = 2m\int_{r_m}^{\infty}[(\mathbf{p}_j-\mathbf{p}_1)^2(1+b^2/r^2)-4m\phi(r)]^{-\frac{1}{2}}dr$$

and

$$\chi=\pi-2\theta-2b\int_{r_m}^{\infty}[(1+b^2/r^2)-4m\phi(r)/(\mathbf{p}_j-\mathbf{p}_1)^2]^{-\frac{1}{2}}dr/r^2$$

where r_m is the greatest positive root of the radical appearing within each of these integrands.

Along the trajectories of these isolated binary encounters both the total number and density of phase points (in pair space) are conserved. Thus, when higher order collisional events are neglected the pair distribution functions in (7) referring to postcollisional states can be replaced with those referring to the precollisional configurations given by (8). Then, by choosing σ so that the terms involving $\phi(R_{j1})$ are negligible we find that

$$[(\partial/\partial t)+(\mathbf{p}_1/m)\cdot\nabla_{\mathbf{R}_1}]D_{(1)}{}^{(1)}(\mathbf{R}_1,\mathbf{p}_1;t)$$

$$=(\sigma^2/m)\sum_{j=2}^{N}\iint_{\{\hat{R}_{j1}\cdot(\mathbf{p}_j-\mathbf{p}_1)\geq 0\}}\hat{R}_{j1}\cdot(\mathbf{p}_j-\mathbf{p}_1)[D_{(1)j}{}^{(2)}(\mathbf{R}_{10},\mathbf{p}_{10};\mathbf{R}_{10}+\sigma\hat{R}_{j10},\mathbf{p}_{j0};t-\tau_c)$$

$$-D_{(1)j}{}^{(2)}(\mathbf{R}_1,\mathbf{p}_1;\mathbf{R}_1-\sigma\hat{R}_{j1},\mathbf{p}_j;t)]d\hat{R}_{j1}d\mathbf{p}_j. \quad (9)$$

It should be emphasized that the validity of this expression is dependent upon the extent to which the molecular collisions can be treated as isolated binary events. The error introduced by this approximation will be examined later.

The various contributions to the collision integral represented by the right-hand member of (9) are obviously separable into direct collisions which remove molecular pairs from states $(\mathbf{R}_1, \mathbf{p}_1, \mathbf{p}_j)$ and inverse events which project pairs into these very same states. Thus, we have succeeded in casting the equation of change for the modified singlet distribution function into a form such that there is a term-for-term counterpart with an identical physical interpretation in the familiar Boltzmann equation. There is significance in the fact that $D_{(1)}{}^{(1)}$ and not the usual singlet distribution function, $D^{(1)}$, appears on the left-hand side of (9). By its very manner of definition, $D^{(1)}(\mathbf{R}_1, \mathbf{p}_1; t)$ includes not only the density of "isolated" atoms, $D_{(1)}{}^{(1)}$, but also the density of atoms with position $\mathbf{R}_1$ and momentum $\mathbf{p}_1$ which at the instant t are engaged in various collision processes involving one and possibly many other atoms. Particularly important to the present investigation is the observation that the density $D^{(1)}$ will include that of atoms which "belong" to diatomic or polyatomic clusters, i.e., $D^{(1)}$ counts the members of molecules along with "dynamically free" atoms. Thus, unless the molecular interactions are strictly repulsive, $D^{(1)}$ should not be identified with the singlet density of atoms considered as a chemically distinct species. The recognition of this seems essential not only to the development of a statistical theory for chemical kinetics but also to a complete understanding of transport processes in chemically inert fluids. The latter remark appears to be justified by the accumulating evidence for the existence in inert gases of loosely bound atomic or molecular clusters.[11]

As a consequence of these observations we are pleased rather than dismayed to find that it is $D_{(1)}{}^{(1)}$ instead of $D^{(1)}$ which satisfies Eq. (9). In fact, a moment's reflection will convince one that the intuitive arguments upon which the traditional demonstration of the Boltzmann equation is based apply not to $D^{(1)}$ but to $D_{(1)}{}^{(1)}$ or some similarly defined partial density.

From our present point of view an error which is frequently incorporated within formal derivations of the Boltzmann equation can be described in the following manner: (1) the Liouville equation is first integrated over *all* values of the momenta *and* coordinates of $N-1$ molecules to yield the "streaming contribution" $(\partial/\partial t+(\mathbf{p}_1/m)\cdot\nabla_{\mathbf{R}_1})D^{(1)}$ and another term arising solely from the molecular interactions; (2) the second of these contributions is then approximated by neglecting all but "pre- and postcollisional pair states," i.e., integrals over V are replaced by the corresponding integrals over V_1'. One effect of this unsymmetrical procedure is precisely that which we have previously demonstrated for the case of rigid spheres, namely, that it is impossible to interpret the collisional integral of this unsymmetrical Boltzmann equation in terms of direct and inverse encounters. Also it will be observed that with a symmetrical development the "streaming terms" involve $D_{(1)}{}^{(1)}$ and not $D^{(1)}$.

Our use of binary collision dynamics in proceeding

[11] N. Bernardes and H. Primakoff, J. Chem. Phys. **30**, 691 (1959); D. E. Stogryn and J. O. Hirschfelder, *ibid.* **31**, 1531, 1545 (1959); A. Michels, H. de Kluiver, and C. A. ten Seldam, Physica **25**, 1321 (1959).

from (7) to (9) was based upon the assumption that during the course of their mutual collision neither molecule experienced interactions with any others. This precludes not only our usual conception of three-body collisions but also genuine molecule-atom encounters. In the remainder of this section our attention will be confined to the atom-atom collisional contribution to the equation of change for $D_{(1)}{}^{(1)}$ given by the right-hand member of (9). This procedure is adopted solely as a convenience and in no way implies that molecule-atom contributions are unimportant. Although an indication of how a more general equation of change can be obtained is given in Sec. III, we shall reserve for separate communication a presentation of the detailed theory.

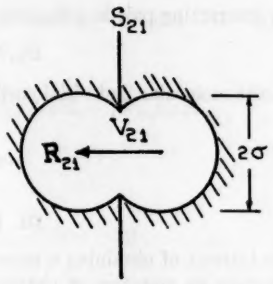

FIG. 2. Excluded region for an interacting pair.

Returning to (9) we see that both terms on the right-hand side refer to precollisional pair states. Therefore, it is reasonable to assume that there will be very little correlation between the individual molecular momenta and so

$$D_{(1)j}{}^{(2)}(\mathbf{R}_{10},\ \mathbf{p}_{10};\ \mathbf{R}_{10}+\sigma\hat{R}_{j10},\ \mathbf{p}_{j0};\ t-\tau_c)=\mathbf{X}(\mathbf{R}_{10},\ \sigma\hat{R}_{j10})D_{(1)}{}^{(1)}(\mathbf{R}_{10},\ \mathbf{p}_{10};\ t-\tau_c)D_{(j)}{}^{(1)}(\mathbf{R}_{10}+\sigma\hat{R}_{j10},\ \mathbf{p}_{j0};\ t-\tau_c)$$

$$D_{(1)j}{}^{(2)}(\mathbf{R}_1,\ \mathbf{p}_1;\ \mathbf{R}_1-\sigma\hat{R}_{j1},\ \mathbf{p}_j;\ t)=\mathbf{X}(\mathbf{R}_1,\ -\sigma\hat{R}_j)D_{(1)}{}^{(1)}(\mathbf{R}_1,\ \mathbf{p}_1;\ t)D_{(j)}{}^{(1)}(\mathbf{R}_1-\sigma\hat{R}_{j1},\ \mathbf{p}_j;\ t). \tag{10}$$

Here $\mathbf{X}$ is a spatial correlation which arises solely from the influence of the molecules constituting the environment of the colliding pair. An approximation to this function may be calculated from the equilibrium theory of the potential of the mean force. For a gas so dilute that isolated binary encounters are predominant $\mathbf{X}$ can safely be equated to unity. As we have stated in the introduction no mathematical verification for the chaos assumption, (10), will be attempted, since its introduction or that of some similar factorization seems to be a necessary hypothesis in the theory of irreversible phenomena.

When these arguments are used to reformulate (9) the result is

$$[(\partial/\partial t)+(\mathbf{p}_1/m)\cdot\nabla_{\mathbf{R}_1}]D_{(1)}{}^{(1)}$$
$$=(\sigma^2/m)\sum_{j=2}^{N}\iint_{\{\hat{R}_{j1}\cdot(\mathbf{p}_j-\mathbf{p}_1)\geq 0\}}\hat{R}_{j1}\cdot(\mathbf{p}_j-\mathbf{p}_1)[D_{(1)}{}^{(1)}(\mathbf{R}_{10},\ \mathbf{p}_{10};\ t-\tau_c)D_{(j)}{}^{(1)}(\mathbf{R}_{10}+\sigma\hat{R}_{j10},\ \mathbf{p}_{j0};\ t-\tau_c)$$
$$-D_{(1)}{}^{(1)}(\mathbf{R}_1,\ \mathbf{p}_1;\ t)D_{(j)}{}^{(1)}(\mathbf{R}_1-\sigma\hat{R}_{j1},\ \mathbf{p}_j;\ t)]d\hat{R}_{j1}d\mathbf{p}_j. \tag{11}$$

If the gas is dilute and we only wish to consider terms of the lowest order in the number density, the discrepancies in the positional and temporal arguments of the distribution functions can be ignored. This approximation then reduces (11) to the classical form of the Boltzmann equation.

As an estimate of what is meant by "dilute" the two singlet distribution functions may be related by a virial type expansion. The formal technique is presented by M. Green.[3]

Let us define a function

$$G_{ij}=\begin{cases}0; & R_{ij}>\sigma\\ -1; & R_{ij}\leq\sigma.\end{cases}$$

Then from (3) and (4) we find,

$$D_{(1)}{}^{(1)}=\int_V\cdots\int_V D^{(N)}\prod_{j=2}^{N}(1+G_{1j})d\mathbf{R}^{N-1}d\mathbf{p}^{N-1}$$
$$=D_1{}^{(1)}-\sum_{j=2}^{N}\iint_{V_1}D_{1j}{}^{(2)}d\mathbf{R}_jd\mathbf{p}_j+0(n^3)$$
$$=D_1{}^{(1)}-\sum_{j=2}^{N}\tfrac{4}{3}(n\pi\sigma^3/N)D_1{}^{(1)}+\sum_{j=2}^{N}\iint_{V_1}[D_1{}^{(1)}D_j{}^{(1)}-D_{1j}{}^{(2)}]d\mathbf{R}_jd\mathbf{p}_j+0(n^3). \tag{12}$$

For a weakly interacting pair in a fluid at equilibrium this reduces to,

$$D_{(1)}{}^{(1)} = D_1{}^{(1)}[1-2n(b_2+\tfrac{2}{3}\pi\sigma^3)+0(n^2)] \tag{13}$$

where $-b_2$ is the molecular 2nd virial coefficient,

$$b_2 = \tfrac{1}{2}\int \{\exp[-\phi(r)/kT]-1\}d\mathbf{r}.$$

III. PAIR DISTRIBUTION FUNCTION

Both in the interest of obtaining a more refined Boltzmann equation and of developing the kinetic theory for diatomic molecules an equation of change for the function $D_{ij}{}^{(2)}$ or some suitable modification thereof should prove useful. To proceed in this direction we define, analogous to (3) and (4), the regions

$$V_{ij} = V_i \cup V_j, \qquad V_{ij}' = V_i' \cap V_j'$$

or $V_{ij}' : \{R_{li} > \sigma,\ R_{lj} > \sigma;\ \forall\, l \neq i, j\}$
and the functions

$$D_{(12)3\cdots s}{}^{(s)} = \int_{V_{12}'} \cdots \int_{V_{12}'} D^{(N)} d\mathbf{R}^{N-s} d\mathbf{p}^{N-s}. \tag{14}$$

By proper choice of σ we may interpret $D_{(12)}{}^{(2)}$ as the distribution function (including internal coordinates) for interacting molecular pairs.

Integration of the Liouville equation (1) over all $\mathbf{p}_j$, $\mathbf{R}_j$ in V_{21}' for $j>2$ yields,

$$[(\partial/\partial t)+\nabla_{R_{21}}\phi(R_{21})\cdot(\nabla_{p_1}-\nabla_{p_2})]D_{(12)}{}^{(2)} = -\sum_{i=1}^{N} \int_{V_{12}'} \cdots \int_{V_{12}'} (\mathbf{p}_i/m)\cdot\nabla_{R_i} D^{(N)} d\mathbf{R}^{N-2} d\mathbf{p}^{N-2}$$

$$+\sum_{j=3}^{N} \iint_{V_{12}'} [\nabla_{R_1}\phi(R_{j1})\cdot\nabla_{p_1}+\nabla_{R_2}\phi(R_{j2})\cdot\nabla_{p_2}] D_{(12)j}{}^{(3)} d\mathbf{R}_j d\mathbf{p}_j. \tag{15}$$

By careful manipulation of this equation we hope to show that it, like its analog (4), may be separated into streaming terms and contributions arising from encounters between the pair and other molecules. To accomplish this we consider the function

$$\nabla_{R_1}\int_{V_{12}'} H d\mathbf{R}_j = \nabla_{R_1} \int_{\{R_{j1}>\sigma,\ \mathbf{R}_{j1}\cdot\hat{R}_{21}<R_{21}/2\}} H d\mathbf{R}_{j1} + \nabla_{R1} \int_{\{R_{j2}>\sigma,\ \mathbf{R}_{j2}\cdot\hat{R}_{21}<-R_{21}/2\}} H d\mathbf{R}_{j2}. \tag{16}$$

If $R_{21}>2\sigma$ the two halves of V_{21}' are distinct and independent of R_{21}. Otherwise, they are the regions on either side of a partial plane $S_{21}:\{R_{j1}=R_{j2}>\sigma;\ j>2\}$ shown in Fig. 2. With the indicated choice of variables only one component in each integral depends on $\mathbf{R}_1$. Thus[12]

$$\nabla_{R_1}\int_{V_{12}'} H d\mathbf{R}_j = \nabla_{R_1}\int_{-\infty}^{R_{21}/2} d(\mathbf{R}_{j1}\cdot\hat{R}_{21}) \int H d(\mathbf{R}_{j1}\times\hat{R}_{21}) + \nabla_{R_1}\int_{-R_{21}/2}^{\infty} d(\mathbf{R}_{j2}\cdot\hat{R}_{21}) \int H d(\mathbf{R}_{j2}\times\hat{R}_{21})$$

$$= -\tfrac{1}{2}\hat{R}_{21}\int_{S_{21}} H d(\mathbf{R}_{j1}\times\mathbf{R}_{21}) + \int_{\{R_{j2}>R_{j1}>\sigma\}} \nabla_{R_1} H d\mathbf{R}_{j1} - \tfrac{1}{2}\hat{R}_{21}\int_{S_{21}} H d(\mathbf{R}_{j2}\times\hat{R}_{21}) + \int_{\{R_{j1}>R_{j2}>\sigma\}} \nabla_{R_1} H d\mathbf{R}_{j2}. \tag{17}$$

[12] The symbol $d(\mathbf{R}_{ji}\times\hat{R}_{21})$ is used here to denote the differential of the two components of $\mathbf{R}_{ji}$ which are orthogonal to $\hat{R}_{21}$.

When we employ the transformations, $(\mathbf{R}_1, \nabla_{\mathbf{R}_1}; \mathbf{R}_{j1}, \nabla_{\mathbf{R}j1}) \rightarrow (\mathbf{R}_1, \nabla_{\mathbf{R}_1}+\nabla_{\mathbf{R}j}; \mathbf{R}_j, \nabla_{\mathbf{R}j})$ and $(\mathbf{R}_1, \nabla_{\mathbf{R}_1}; \mathbf{R}_{j2}, \nabla_{\mathbf{R}j2}) \rightarrow (\mathbf{R}_1, \nabla_{\mathbf{R}_1}; \mathbf{R}_j, \nabla_{\mathbf{R}j})$, (17) becomes

$$\nabla_{\mathbf{R}_1}\int_{V_{12}'} H d\mathbf{R}_j = -\hat{R}_{21}\int_{S_{12}} H d(\mathbf{R}_j \times \hat{R}_{21}) + \int_{\{R_{j2}>R_{j1}>\sigma\}} \nabla_{\mathbf{R}_j} H d\mathbf{R}_j + \int_{V_{12}'} \nabla_{\mathbf{R}_1} H d\mathbf{R}_j. \tag{18}$$

For the set of functions

$$H_j(\mathbf{R}_1, \mathbf{R}_2, \cdots, \mathbf{R}_j; \mathbf{p}_1, \mathbf{p}_2) = \int\cdots\int D_{(12)3\cdots j}^{(j)} d\mathbf{p}_3 \cdots d\mathbf{p}_j,$$

(18) implies the recurrence relationship

$$\nabla_{\mathbf{R}_1} H_{j-1} = -\hat{R}_{21}\iint_{S_{12}} D_{(12)j}^{(3)} d(\mathbf{R}_j \times \hat{R}_{21}) d\mathbf{p}_j + \iint_{\{R_{j2}>R_{j1}>\sigma\}} \nabla_{\mathbf{R}_j} D_{(12)j}^{(3)} d\mathbf{R}_j d\mathbf{p}_j + \int_{V_{12}'} \nabla_{\mathbf{R}_1} H_j d\mathbf{R}_j. \tag{19}$$

A similar expression can be derived for $\nabla_{\mathbf{R}_2} H_{j-1}$ and an iterative procedure then used to establish that

$$m^{-1}(\mathbf{p}_1\cdot\nabla_{\mathbf{R}_1}+\mathbf{p}_2\cdot\nabla_{\mathbf{R}_2}) D_{(12)}^{(2)} = m^{-1}\int_{V_{12}'}\cdots\int_{V_{12}'} (\mathbf{p}_1\cdot\nabla_{\mathbf{R}_1}+\mathbf{p}_2\cdot\nabla_{\mathbf{R}_2}) D^{(N)} d\mathbf{R}^{N-2} d\mathbf{p}^{N-2}$$

$$+\sum_{j=3}^{N}\left[\frac{\mathbf{p}_2-\mathbf{p}_1}{m}\cdot\hat{R}_{21}\iint_{S_{12}} D_{(12)j}^{(2)} d(\mathbf{R}_j\times\hat{R}_{21}) d\mathbf{p}_j + (\mathbf{p}_1/m)\cdot \iint_{\{R_{j2}>R_{j1}>\sigma\}} \nabla_{\mathbf{R}_j} D_{(12)j}^{(3)} d\mathbf{R}_j d\mathbf{p}_j \right.$$

$$\left. + (\mathbf{p}_2/m)\cdot \iint_{\{R_{j1}>R_{j2}>\sigma\}} \nabla_{\mathbf{R}_j} D_{(12)j}^{(3)} d\mathbf{R}_j d\mathbf{p}_j\right]. \tag{20}$$

The left-hand side of (20) is, however, just the streaming contribution to the time derivative of $D_{(12)}^{(2)}$ and so when (20) is added to (15) we find that

$$[(\partial/\partial t)+(\mathbf{p}_1/m)\cdot\nabla_{\mathbf{R}_1}+(\mathbf{p}_2/m)\cdot\nabla_{\mathbf{R}_2}+\nabla_{\mathbf{R}_{21}}\phi(R_{21})\cdot(\nabla_{\mathbf{p}_1}-\nabla_{\mathbf{p}_2})]D_{(12)}^{(2)}$$

$$= \frac{\partial_c D_{(12)}^{(2)}}{\partial t} + \sum_{j=3}^{N}\iint_{V_{12}'} [\nabla_{\mathbf{R}_1}\phi(R_{j1})\cdot\nabla_{\mathbf{p}_1}+\nabla_{\mathbf{R}_2}\phi(R_{j2})\cdot\nabla_{\mathbf{p}_2}] D_{(12)j}^{(3)} d\mathbf{R}_j d\mathbf{p}_j, \tag{21}$$

where

$$\partial_c D_{(12)}^{(2)}/\partial t = [(\mathbf{p}_2-\mathbf{p}_1)/m]\cdot\hat{R}_{21}\sum_{j=3}^{N}\iint_{S_{12}} D_{(12)j}^{(3)} d(\mathbf{R}_j\times\hat{R}_{21}) d\mathbf{p}_j + m^{-1}\sum_{j=3}^{N}\iint_{\{R_{j2}>R_{j1}>\sigma\}} (\mathbf{p}_1-\mathbf{p}_j)\cdot\nabla_{\mathbf{R}_j} D_{(12)j}^{(3)} d\mathbf{R}_j d\mathbf{p}_j$$

$$+ m^{-1}\sum_{j=3}^{N}\iint_{\{R_{j1}>R_{j2}>\sigma\}} (\mathbf{p}_2-\mathbf{p}_j)\cdot\nabla_{\mathbf{R}_j} D_{(12)j}^{(3)} d\mathbf{R}_j d\mathbf{p}_j. \tag{22}$$

Finally by again dividing V_{21}' into two regions and applying the divergence theorem we obtain

$$\int_{\{R_{j2}>R_{j1}>\sigma\}} \nabla_{\mathbf{R}_j} D_{(12)j}^{(3)} d\mathbf{R}_j = -\sigma^2 \int_{\{R_{j2}>R_{j1}=\sigma\}} \hat{R}_{j1} D_{(12)j}^{(3)} d\hat{R}_{j1} + \hat{R}_{21}\int_{S_{12}} D_{(12)j}^{(3)} d(\mathbf{R}_j\times\hat{R}_{21})$$

$$\int_{\{R_{j1}>R_{j2}>\sigma\}} \nabla_{\mathbf{R}_j} D_{(12)j}^{(3)} d\mathbf{R}_j = -\sigma^2 \int_{\{R_{j1}>R_{j2}=\sigma\}} \hat{R}_{j2} D_{(12)j}^{(3)} d\hat{R}_{j2} - \hat{R}_{21}\int_{S_{12}} D_{(12)j}^{(3)} d(\mathbf{R}_j\times\hat{R}_{21}), \tag{23}$$

where the integration ranges $\{R_{j2}>R_{j1}=\sigma\}$ and $\{R_{j1}>R_{j2}=\sigma\}$ refer to the two truncated spherical surfaces illustrated in Fig. 2. The substitution of these results into (22) then leads to the expression

$$\partial_c D_{(12)}{}^{(2)}/\partial t=(\sigma^2/m)\sum_{j=3}^{N}\Bigg[\iint_{\{R_{j2}>R_{j1}=\sigma\}}\hat{R}_{j1}\cdot(\mathbf{p}_j-\mathbf{p}_1)\,D_{(12)j}{}^{(3)}d\hat{R}_{j1}d\mathbf{p}_j+\iint_{\{R_{j1}>R_{j2}=\sigma\}}\hat{R}_{j2}\cdot(\mathbf{p}_j-\mathbf{p}_2)\,D_{(12)j}{}^{(3)}d\hat{R}_{j2}d\mathbf{p}_j\Bigg] \tag{24}$$

for the rate of change of $D_{(12)}{}^{(2)}$ due to collisions of molecules 1 and 2 with their environment. Actually if the gas is predominantly in an associated state it will be more convenient to replace $D_{(12)j}{}^{(3)}$ by

$$\iint_{V_{12}'} D_{(12)ji}{}^{(4)}\mathbf{dR}_i\mathbf{dp}_i$$

and interpret (24) in terms of diatom-diatom collisional events. In general, the integration of (21) followed by a factorization similar to (10) leads to an "extended Boltzmann equation" which includes within its collision integral contributions both from binary and from three-body encounters.

The relationships (6) and (21) may be identified as the first and second members of an infinite set which closely resembles the well-known Born-Green-Kirkwood-Yvon-Bogoliubov hierarchy of relationships between the conventionally defined distribution functions. Although no proof will be presented, the generalization of (6) and (21) to higher order molecular clusters is obvious. Thus, for a group of s molecules we would have

$$\Big[(\partial/\partial t)+\sum_{i=1}^{s}(\mathbf{p}_i/m)\cdot\nabla_{\mathbf{R}_i}+\sum_{i=1}^{s}\sum_{l\neq i}^{s}\nabla_{\mathbf{R}_{li}}\phi(R_{li})\cdot\nabla_{\mathbf{p}_i}\Big]D_{(1\cdots s)}{}^{(s)}$$
$$=(\sigma^2/m)\sum_{i=1}^{s}\sum_{j=s+1}^{N}\iint_{\{R_{jl}>R_{ji}=\sigma,\ \forall l\leq s,\ l\neq i\}}\hat{R}_{ji}\cdot(\mathbf{p}_j-\mathbf{p}_i)\,D_{(1\cdots s)j}{}^{(s+1)}d\hat{R}_{ji}d\mathbf{p}_j$$
$$+\sum_{i=1}^{s}\sum_{j=s+1\,j\neq}^{N}\iint_{V_{12\cdots s}'}\big[\nabla_{\mathbf{R}_i}\phi(R_{ji})\big]\cdot\nabla_{\mathbf{p}_i}D_{(1\cdots s)j}{}^{(s+1)}d\mathbf{R}_jd\mathbf{p}_j. \tag{25}$$

The relationship (21) and its higher order analog (25) seem particularly well adapted to the description of simple chemical kinetics. Thus, in cases where the pair potential permits the existence of bound diatomic or polyatomic species, $\partial_c D_{(12)}{}^{(2)}/\partial t$ can be decomposed into portions identifiable with the rate of production of bound pairs due to three body collisions, the stabilization of meta-bound pairs by the intervention of third bodies, the internal reorganization of energy in a bound pair accompanying its collision with some third molecule, and the corresponding conjugate processes of dissociation. These various events can be explicitly accounted for in terms of partial pair densities which represent the contributions to $D_{(12)}{}^{(2)}$ arising from bound, meta-bound, and unbound pairs. The details of this procedure will be presented in a separate communication. For the present we restrict ourselves to the observation that (24) may be written in the form,

$$\partial_c D_{(12)}{}^{(2)}/\partial t=(\sigma^2/m)\sum_{j=3}^{N}\Bigg[\iint_{\{R_{j2}>R_{j1}=\sigma\}}\hat{R}_{j1}\cdot(\mathbf{p}_j-\mathbf{p}_1)\,D_{(12)j}{}^{(3)\prime}d\hat{R}_{j1}d\mathbf{p}_j$$
$$+\iint_{\{R_{j2}>R_{j1}=\sigma\}}\hat{R}_{j1}\cdot(\mathbf{p}_j-\mathbf{p}_1)\,D_{(12)j}{}^{(3)}d\hat{R}_{j1}d\mathbf{p}_j+\iint_{\{R_{j1}>R_{j2}=\sigma\}}\hat{R}_{j2}\cdot(\mathbf{p}_j-\mathbf{p}_2)\,D_{(12)j}{}^{(3)\prime\prime}d\hat{R}_{j2}d\mathbf{p}_j$$
$$+\iint_{\{\hat{R}_{j1}>R_{j2}=\sigma\}}\hat{R}_{j2}\cdot(\mathbf{p}_j-\mathbf{p}_2)\,D_{(12)j}{}^{(3)}d\hat{R}_{j2}d\mathbf{p}_j\Bigg], \tag{26}$$

where the precursor states to $\{\mathbf{p}_1, \mathbf{p}_2, \mathbf{p}_j\}$ indicated by the primes are determined by dynamical considerations similar to those presented in Sec. II. Although the evaluation of these states is a practical possibility for only a few special cases, the information gained from a careful study of these should provide valuable insight into the dynamics of reactive processes, the relaxation of internal excitations, and the collisional events which contribute to transport behavior in moderately dense gases.

Note added in proof. It has recently (and somewhat belatedly) come to our attention that modified distribution functions such as $D_{(1)}{}^{(1)}$ have also been employed by H. Grad, *Handbuch der Physik* (Springer-Verlag, Berlin, 1958) Bd. XII, p. 208.

THE JOURNAL OF CHEMICAL PHYSICS VOLUME 33, NUMBER 5 NOVEMBER, 1960

Molecular Friction in Dilute Gases*

J. T. O'Toole† and J. S. Dahler

Department of Chemical Engineering, University of Minnesota, Minneapolis 14, Minnesota

(Received February 11, 1960)

General formulas have been derived for the molecular friction coefficients of a dilute gas. The velocity and temperature dependencies of these coefficients are examined in detail for several choices of the pair interaction potential. Also we have considered the frictional loss of kinetic energy and, for one special case, the dissipation of molecular internal angular momentum. The concepts of free path length and collision frequency are extended to nonrigid molecular models.

I. INTRODUCTION

A TOPIC of major importance in the theory of dissipative phenomena is the rate at which a molecule exchanges energy and momentum with its environment. One familiar approach to this problem is provided by the theory of Brownian motion where the dynamical behavior of a massive particle moving through a fluid composed of much lighter solvent molecules is assumed to be governed by the Langevin equation,

$$(d/dt)(m_i\mathbf{c}_i)+\zeta_i\mathbf{c}_i=\mathbf{G}_i. \tag{1}$$

Here m_i and $\mathbf{c}_i$ are the mass and velocity of the Brownian particle and $\mathbf{G}_i$, a rapidly fluctuating force due to collisions between the particle and solvent molecules. Over macroscopically small intervals of time the average of $\mathbf{G}_i$ is assumed to vanish so that the velocity of the massive particle decays exponentially with a relaxation time equal to m_i/ζ_i. The introduction into the Langevin equation of the dissipative force, $-\zeta_i\mathbf{c}_i$, is suggested by analogy between the motion of the massive particle and that of a macroscopic body moving through a continuous medium. Therefore, just as in the hydrodynamical case we should expect that the friction coefficient ζ_i will be independent of velocity for very slow motions but gradually increase with the speed of the Brownian particle.

In his classic paper on the statistical mechanical theory of transport processes Kirkwood[1] not only developed a molecular interpretation for this friction coefficient, but also succeeded in demonstrating that an equation analogous to that of Langevin could be associated with the average behavior of individual molecules in a fluid phase. An important feature of this theory is its use of a representative ensemble for the given dynamical system so constructed that at a particular time t the ith molecule (of the chemical species α) in each member of the ensemble lies at the point $\mathbf{r}_{i0}$ and has the velocity $\mathbf{c}_{i0}$. The (specific) ensemble distribution function conditioned by this precise characterization of the state of the ith molecule will be denoted by $D_{i\alpha}^{(N/1)}(\mathbf{Q}_0\mathbf{C}_0/\mathbf{r}_{i0},\mathbf{c}_{i0};t)$ where $\mathbf{Q}_0$ and $\mathbf{C}_0$ refer to the locations and velocities at the time t of the $N-1$ molecules other than i. During the interval from t to $t+\tau$ the ith molecule belonging to a particular member of the ensemble experiences a sequence of (dynamically reversible) collisional encounters uniquely determined by the state of the member system at time t. Thus, the resultant change of momentum,

$$\int_0^\tau \mathbf{F}_{i\alpha}(t+s)ds=\int_0^\tau \mathbf{F}_{i\alpha}[\mathbf{r}_i(t+s),\quad \mathbf{Q}(t+s)]ds,$$

will generally assume a different value for each member system of the ensemble. However, the statistical superposition of momentum-time histories represented by the average force,

$$^i\langle(\mathbf{F}_{i\alpha})_\tau\rangle=\int\cdots\int d\mathbf{Q}_0d\mathbf{C}_0D_{i\alpha}^{(N/1)}(\mathbf{Q}_0\mathbf{C}_0/\mathbf{r}_{i0},\mathbf{c}_{i0};t)\times(1/\tau)\int_0^\tau \mathbf{F}_{i\alpha}(t+s)ds \tag{2}$$

should conform to our intuitive belief that in the course of time molecule i will, on the average, adapt its motions to those of its fellows. For example, if the distribution of neighbor molecules at time t corresponds to statistical equilibrium, then we may anticipate that the ith molecule ultimately will be "thermalized," the memory of its initial direction of motion being obliterated and the magnitude of its mean velocity tending to zero. Proceeding from arguments of this sort Kirkwood proposed that the equation of motion for the ith molecule of the physical system under consideration be written in the manner,

$$(d/dt)(m_\alpha\mathbf{c}_i)-{}^i\langle(\mathbf{F}_{i\alpha})_\tau\rangle=\mathbf{F}_{i\alpha}-{}^i\langle(\mathbf{F}_{i\alpha})_\tau\rangle. \tag{3}$$

The right-hand member of (3) then closely resembles the fluctuating force $\mathbf{G}_i$ appearing in the Langevin equation, since the ensemble average of its integral over the interval τ vanishes. Thus, the analogy between Eqs. (1) and (3) will be complete if it can be demonstrated

* This research was supported in part by the National Aeronautics and Space Administration and in part by a grant from the National Science Foundation.

† Formerly General Electric Fellow, Department of Chemical Engineering, University of Minnesota; now National Science Foundation Fellow, Faculty of Sciences, University of Brussels, Belgium.

[1] J. G. Kirkwood, J. Chem. Phys. **14**, 180 (1946).

that the average force ${}^{i}\langle(\mathbf{F}_{i\alpha})_{\tau}\rangle$ has the form

$$ {}^{i}\langle(\mathbf{F}_{i\alpha})_{\tau}\rangle=-\zeta_{\alpha}(c_i)\mathbf{c}_i, \tag{4} $$

where $\zeta_{\alpha}(c_i)$ is a scalar whose value is independent of the averaging interval τ.

During the several years which have elapsed since Kirkwood's original investigation of this problem, numerous methods[2,3] have been invented for the purpose of calculating the friction coefficient $\zeta_{\alpha}(c_i)$. However, so far as we have been able to determine these techniques were developed primarily for use in dense gases or liquids, and so for those situations where the representative molecule is in a state of continuous collision with its neighbors.[4] In the present communication we have chosen the opposite extreme of physical conditions and derived explicit formulas for the friction coefficient in dilute gases where the collisional events are essentially discrete. Perhaps the most obvious feature of our calculation is its remarkable and in fact almost trivial simplicity. Because of this simplicity it is possible to proceed a step further than for the case of dense fluids and examine in complete detail the velocity dependence of the friction coefficient and its sensitivity with respect to the choice of intermolecular forces. It is worthy of note that our calculation of the friction coefficient for a dilute gas is really no more than a generalization of Jean's persistence of velocity study for rigid spheres.

II. FORMULAS FOR THE FRICTION COEFFICIENT AT LOW DENSITIES

If the intermolecular forces are assumed to be pair-additive, then the average force defined by (2) can be written as

$$ {}^{i}\langle(\mathbf{F}_{i\alpha})_{\tau}\rangle=\sum_{\beta=1}^{\nu}\sum_{j=1}^{N_\beta}\iint d\mathbf{r}_{j0}d\mathbf{c}_{j0}D_{\alpha\beta}^{(2/1)}(\mathbf{r}_{j0},\mathbf{c}_{j0}/\mathbf{r}_{i0},\mathbf{c}_{i0};t) $$

$$ \times(1/\tau)\int_0^{\tau}\mathbf{F}_{\alpha i}^{\beta j}(t+s)ds, \tag{5} $$

where $D_{\alpha\beta}^{(2/1)}$ is the conditional distribution function specific to two molecules, one of the species α and the other of species β. $\mathbf{F}_{\alpha i}^{\beta j}$ is the force upon the ith molecule due to its interaction with the jth of species β.

To simplify further this expression for ${}^{i}\langle(\mathbf{F}_{i\alpha})_{\tau}\rangle$, we now proceed in precisely the same manner as one does in constructing the collisional contributions to the Boltzmann equation.[5] Should molecules i and j fail to suffer a mutual collisional encounter during the interval $(t, t+\tau)$ then the momentum increment

$$ \int_0^{\tau}\mathbf{F}_{\alpha i}^{\beta j}(t+s)ds $$

will be identically equal to zero. However, in the event that molecules i and j experience a mutual collision which is begun and completed within this interval, then

$$ \int_0^{\tau}\mathbf{F}_{\alpha i}^{\beta j}(t+s)ds=\Delta(m_\alpha\mathbf{c}_i)=2\mu_{\alpha\beta}\mathbf{k}\mathbf{k}\cdot(\mathbf{c}_{j0}-\mathbf{c}_{i0}), \tag{6} $$

where $\mu_{\alpha\beta}=m_\alpha m_\beta/(m_\alpha+m_\beta)$ is the reduced mass of the pair and $\mathbf{k}$, the unit vector directed from i to j at the instant of their closest approach to one another. The situation will of course be much more complicated if during $(t, t+\tau)$ either or both of i and j happens to be involved not only in a mutual collision but also chances to interact with other molecules belonging to the system. To minimize the possibility of such events and yet to permit completion of isolated binary collisions we must therefore choose τ considerably larger than τ_c the mean duration of a binary event but less than τ_m the recurrence time for multiple encounters. Such a choice would be impossible for dense gases or liquids where the interval between and the duration of collisional events are comparable in magnitude. On the other hand these requirements are easily satisfied in a dilute gas if τ is taken to be of the order of the mean transit time for a free path length. To proceed further we now imagine the ith molecule to be the center of a "collision sphere" with radius equal to the effective range of the intermolecular forces. In this way the beginning of a collision between i and j can be characterized as the moment at which the center of j first pierces the collision sphere about i. The collision terminates when the center of j crosses this surface in the outward direction. The velocity of j relative to i is given by $\mathbf{c}_{ji0}=\mathbf{c}_{j0}-\mathbf{c}_{i0}$ and the miss distance and azimuthal angle (see Fig. 1) lie in the ranges $(b, b+db)$ and $(\phi, \phi+d\phi)$, respectively. Provided that it is not deflected from its path by other molecules, j can then penetrate the collision sphere of i if and only if its center does at time t lie somewhere within the region bounded by (1) the two planes parallel to $\mathbf{c}_{ji0}$ and passing through the center of i which are characterized by azimuthal angles ϕ and $\phi+d\phi$; (2) the cylinders with axes along $\mathbf{c}_{ji0}$ and of radii b and $b+db$; (3) the upper surface of the collision sphere about i; and, (4) the plane normal to $\mathbf{c}_{ji0}$ which lies at the distance $|\mathbf{c}_{ji0}|\tau$ above the surface element on the sphere. The volume of this region is clearly equal to $|\mathbf{c}_{ji0}|\tau bdbd\phi$.

If τ is chosen to be much larger than the duration of a representative collision then we may safely conclude that the measure of the precollision states previously described will far exceed that of collisions which are in progress at the time t. (This subject has already received the attention of Kirkwood[5] and will be con-

[2] J. G. Kirkwood, F. P. Buff, and M. S. Green, J. Chem. Phys. **17**, 988 (1949).

[3] F. C. Collins and Helen Raffel, J. Chem. Phys. **23**, 1454 (1955); F. C. Collins, Advances in Chem. Phys. **1**, 135 (1958).

[4] The one exception of which we are aware is the "persistence of velocity" calculation for rigid spheres, performed by J. H. Jeans [*The Dynamical Theory of Gases*, (Dover Publications, New York, 1954), 4th ed., Chap. X]. Jean's result has been confirmed by Collins and Raffel[3] and is discussed as aspecial case in Sec. IV of the present report.

[5] For example, see J. G. Kirkwood, J. Chem. Phys. **15**, 72 (1947).

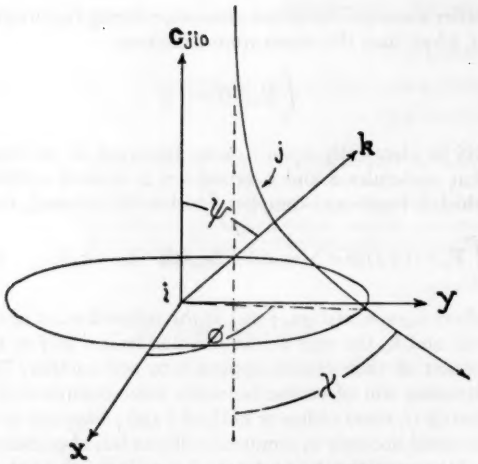

FIG. 1. Schematic diagram illustrating a collisional trajectory (repulsive) of molecule j relative to the position of i.

sidered from a different point of view in a forthcoming publication.) However, we must also require τ to be no greater than the mean transit time between successive collisions; for otherwise only a portion of the molecules in the element of volume $|\mathbf{c}_{ji0}|\tau bdbd\phi$ would actually succeed in reaching the collision sphere of molecule i. These two requirements upon τ can only be satisfied in a dilute gas.

Finally, if it be assumed that the velocities of the molecules are uncorrelated before collision (molecular chaos) and that the departure from equilibrium of the environmental distribution is negligible,[6] then the average force on an α species molecule may be expressed in the form[7]

$$\langle(\mathbf{F}_\alpha)_\tau\rangle=\sum_{\beta=1}^{\nu}2\mu_{\alpha\beta}\int\mathbf{dc}_\beta\int_0^\infty bdb\int_0^{2\pi}d\phi(\mathbf{kk}\cdot\mathbf{c}_{\beta\alpha})c_{\beta\alpha}f(c_\beta). \tag{7}$$

Here,

$$f(c_\beta)=n_\beta(m_\beta/2\pi kT)^{\frac{3}{2}}\exp(-m_\beta c_\beta^2/2kT)$$

is the equilibrium singlet distribution function, T the local thermodynamical temperature, and n_β the number density for β species molecules.

Integration over the azimuthal angles is easily performed with the result that

$$\langle(\mathbf{F}_\alpha)_\tau\rangle=\sum_{\beta=1}^{\nu}\mu_{\alpha\beta}\int\mathbf{dc}_\beta\mathbf{c}_{\beta\alpha}c_{\beta\alpha}Q_{\alpha\beta}^{(1)}(c_{\beta\alpha})\,f(c_\beta), \tag{8}$$

where

$$Q_{\alpha\beta}^{(1)}(c_{\beta\alpha})=4\pi\int_0^\infty\cos^2\psi bdb=2\pi\int_0^\infty(1-\cos\chi)bdb \tag{9}$$

is the cross section which appears in the Chapman-Enskog theory for the diffusion coefficients of a dilute gas mixture.[8] The angle of deflection $\chi=\pi+2\psi$ is related to the potential of the intermolecular forces $\phi_{\alpha\beta}(r)$, by the formula

$$\chi(b,c_{\beta\alpha})=\pi-2b\times\int_{r_m}^\infty(dr/r^2)[1-2\phi_{\alpha\beta}(r)/\mu_{\alpha\beta}c_{\beta\alpha}^2+b^2/r^2]^{-\frac{1}{2}}, \tag{10}$$

and r_m is the smallest positive root of the radical appearing within the integrand of (10).[9]

Next, by choosing a coordinate frame with its polar axis directed along $\mathbf{c}_\alpha$, one can readily verify that

$$\langle(\mathbf{F}_\alpha)_\tau\rangle=-\left\{\sum_{\beta=1}^{\nu}\zeta_{\alpha\beta}(c_\alpha)\right\}\mathbf{c}_\alpha=-\zeta_\alpha(c_\alpha)\mathbf{c}_\alpha, \tag{11}$$

with

$$\begin{aligned}\zeta_{\alpha\beta}(c_\alpha)&=-\mu_{\alpha\beta}\int\mathbf{dc}_\beta\mathbf{c}_\alpha\cdot\mathbf{c}_{\beta\alpha}c_{\beta\alpha}c_\alpha^{-2}Q_{\alpha\beta}^{(1)}(c_{\beta\alpha})f(c_\beta)\\&=(\pi\mu_{\alpha\beta}/c_\alpha)\left[\int_0^{c_\alpha}dc_\beta\int_{c_\alpha-c_\beta}^{c_\alpha+c_\beta}dc_{\beta\alpha}(1+c_{\beta\alpha}^2c_\alpha^{-2}-c_\beta^2c_\alpha^{-2})\times c_\beta c_{\beta\alpha}^2Q_{\alpha\beta}^{(1)}(c_{\beta\alpha})f(c_\beta)\right.\\&\left.+\int_{c_\alpha}^\infty dc_\beta\int_{c_\beta-c_\alpha}^{c_\alpha+c_\beta}(1+c_{\beta\alpha}^2c_\alpha^{-2}-c_\beta^2c_\alpha^{-2})c_\beta c_{\beta\alpha}^2Q_{\alpha\beta}^{(1)}(c_{\beta\alpha})f(c_\beta)\right].\end{aligned} \tag{12}$$

Interchange of the order of integration and substitution of the explicit form for $f(c_\beta)$ then leads to the result

$$\begin{aligned}\zeta_{\alpha\beta}(c_\alpha)&=n_\beta\mu_{\alpha\beta}(kT/2\pi m_\beta)^{\frac{1}{2}}c_\alpha^{-3}\times\exp(-m_\beta c_\alpha^2/2kT)\int_0^\infty dgg^2Q_{\alpha\beta}^{(1)}(g)\exp(-m_\beta g^2/2kT)\\&\times[(m_\beta c_\alpha g/kT+1)\exp(-m_\beta c_\alpha g/kT)+(m_\beta c_\alpha g/kT-1)\exp(m_\beta c_\alpha g/kT)].\end{aligned} \tag{13}$$

In a very few exceptional cases (see Sec. IV) $Q^{(1)}$ is so simple a function that the integration of (13) can be accomplished in closed form. However, in general the evaluation of $\zeta_{\alpha\beta}$ must be carried out numerically and so it proves useful to express this function in terms of tabulated integrals. To this end we therefore expand the

[6] These assumptions are by no means unique to the present investigation and have in fact been incorporated within most dense gas theories of the friction coefficient.

[7] For notational convenience all unnecessary subscripts on the symbols are here and henceforth suppressed.

[8] Cf. J. O. Hirschfelder, C. F. Curtiss, and R. B. Bird, *The Molecular Theory of Gases and Liquids* (John Wiley & Sons, New York, 1954), p. 525.

[9] Footnote reference 8, p. 51.

integrand of (13) in a Taylor series and obtain

$$\zeta_{\alpha\beta}(c_\alpha)=\left\{\frac{4\pi\sigma_{\alpha\beta}^2 n_\beta\mu_{\alpha\beta}}{(\pi m_\beta/2kT)^{\frac{1}{2}}}\right\}$$
$$\times\exp(-W_{\alpha\beta}^2)\sum_{s=1}^{\infty}\frac{2s(s+1)!}{(2s+1)!}(2W_{\alpha\beta})^{2s-2}\Omega_{\alpha\beta}^{(1,s)*}(T_{\alpha\beta}^*), \tag{14}$$

where $W_{\alpha\beta}^2=m_\beta c_\alpha^2/2kT$, $T_{\alpha\beta}^*=(\mu_{\alpha\beta}/m_\beta)(kT/\epsilon_{\alpha\beta})$, and $\sigma_{\alpha\beta}$ and $\epsilon_{\alpha\beta}$ are parameters with the dimensions of length and energy, respectively. $\Omega^{(1,s)*}$ is the reduced omega integral[10] defined by

$$\Omega_{\alpha\beta}^{(1,s)*}(T_{\alpha\beta}^*)=\left\{\frac{2(2\pi\mu_{\alpha\beta}/kT_{\alpha\beta})^{\frac{1}{2}}}{\pi\sigma_{\alpha\beta}^2(s+1)!}\right\}\Omega_{\alpha\beta}^{(1,s)}(T_{\alpha\beta}), \tag{15}$$

with

$$\Omega_{\alpha\beta}^{(1,s)}(T_{\alpha\beta})=(kT_{\alpha\beta}/2\pi\mu_{\alpha\beta})^{\frac{1}{2}}\int_0^\infty \times\exp(-\gamma^2)\gamma^{2s+3}Q_{\alpha\beta}^{(1)}(g)d\gamma, \tag{16}$$

and

$$T_{\alpha\beta}=(\mu_{\alpha\beta}/m_\beta)T, \qquad \gamma^2=\mu_{\alpha\beta}g^2/2kT_{\alpha\beta}.$$

From (14) it is easily verified that

$$\lim_{c_\alpha\to 0}\zeta_{\alpha\beta}(c_\alpha)=\zeta_{\alpha\beta}(0)$$
$$=\frac{8\pi\sigma_{\alpha\beta}^2 n_\beta\mu_{\alpha\beta}}{3(\pi m_\beta/2kT)^{\frac{1}{2}}}\Omega_{\alpha\beta}^{(1,1)*}(T_{\alpha\beta}^*), \tag{17}$$

so that

$$\zeta_{\alpha\beta}^*(W_{\alpha\beta})=\zeta_{\alpha\beta}(c_\alpha)/\zeta_{\alpha\beta}(0)$$
$$=\exp(-W_{\alpha\beta}^2)\sum_{s=1}^{\infty}h_s W_{\alpha\beta}^{2s-2}, \tag{18}$$

where

$$h_s=\frac{3s(s+1)!2^{2s-2}\Omega_{\alpha\beta}^{(1,s)*}(T_{\alpha\beta}^*)}{(2s+1)!\Omega_{\alpha\beta}^{(1,1)*}(T_{\alpha\beta}^*)}. \tag{19}$$

In Fig. 2 the temperature dependence of $\zeta_{\alpha\beta}(0)$, the low velocity limit of the friction coefficient, is shown for several choices of the pair interaction potential.

From (13) one finds that at very large velocities $\zeta_{\alpha\beta}^*$ is given by

$$\zeta_{\alpha\beta}^*(W_{\alpha\beta})\to\frac{3(\pi)^{\frac{1}{2}}}{8}W_{\alpha\beta}\left\{\frac{Q_{\alpha\beta}^{(1)*}(T_{\alpha\beta}^*W_{\alpha\beta})}{\Omega_{\alpha\beta}^{(1,1)*}(T_{\alpha\beta}^*)}\right\}, \tag{20}$$

where $Q^{(1)*}=Q^{(1)}/\pi\sigma_{\alpha\beta}^2$.

III. SOME RELATED QUANTITIES

The methods developed in the previous section for the purpose of calculating the systematic collisional degradation of momentum can also be used to investigate other dissipative processes. Especially interesting

[10] Footnote reference 8, p. 526.

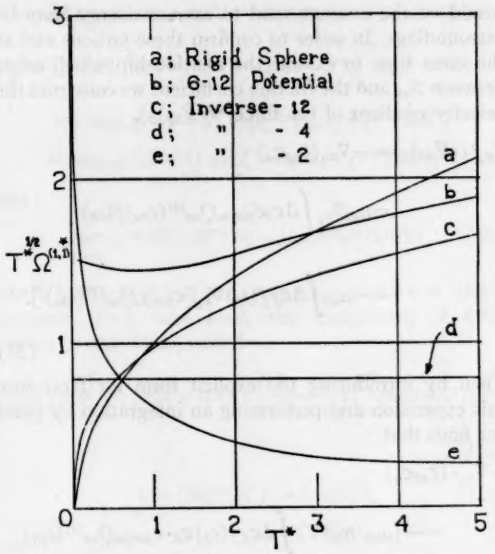

FIG. 2. Temperature dependence of the zero-velocity friction coefficients

$$\zeta_{\alpha\beta}(0)=(8/3)\pi n_\beta\sigma_{\alpha\beta}^2(2\epsilon\mu_{\alpha\beta}/\pi)^{\frac{1}{2}}T_{\alpha\beta}^{*\frac{1}{2}}\Omega_{\alpha\beta}^{(1,1)*}(T_{\alpha\beta}^*)$$

for the 12-6 and several inverse power potentials. The curve for the inverse-2 potential is based on an estimated value of $A^{(1)}(2)$.

is the collisional rate of change of kinetic energy, which analogously to (7) may be expressed in the form

$$\langle(d/dt)[(m_\alpha/2)c_\alpha^2]\rangle=\sum_{\beta=1}^{\nu}{}^{\alpha}\langle(P_{\alpha\beta})_\tau\rangle=\langle(P_\alpha)_\tau\rangle. \tag{21}$$

Here, ${}^{\alpha}\langle(P_{\alpha\beta})_\tau\rangle$, the power consumption due to moderation by β species molecules, is given by

$${}^{\alpha}\langle(P_{\alpha\beta})_\tau\rangle$$
$$=(m_\alpha/2)\int\mathbf{dc}_\beta\int_0^\infty bdb\int_0^{2\pi}d\phi[(\mathbf{c}_\alpha+(2\mu_{\alpha\beta}/m_\alpha)\mathbf{kk}\cdot\mathbf{c}_{\beta\alpha})^2$$
$$-c_\alpha^2]c_{\beta\alpha}f(c_\beta)$$
$$={}^{\alpha}\langle(\mathbf{F}_{\alpha\beta})_\tau\rangle\cdot\mathbf{c}_\alpha+S_{\alpha\beta}(c_\alpha) \tag{22}$$

and

$$S_{\alpha\beta}(c_\alpha)=(\mu_{\alpha\beta}^2/m_\alpha)\int\mathbf{dc}_\beta c_{\beta\alpha}^3 Q_{\alpha\beta}^{(1)}(c_{\beta\alpha})f(c_\beta). \tag{23}$$

Thus, we see that $\langle(P_\alpha)_\tau\rangle$ is composed of a negative contribution $\langle(\mathbf{F}_\alpha)_\tau\rangle\cdot\mathbf{c}_\alpha$, which represents the power transmitted from the directed motion of the α species molecule to its environment, and a positive term $\sum_\beta S_{\alpha\beta}(c_\alpha)$ associated with the molecule's absorption of thermal energy from its neighbors. One might very well expect that when the initial state of the representative α-specie molecule is highly energetic the first of these two contributions would dominate, but that when the molecule's energy is initially less than $3kT/2$ it

would on the average tend to extract energy from its surroundings. In order to confirm these notions and at the same time to exhibit the relationship which exists between $S_{\alpha\beta}$ and the friction coefficient we construct the velocity gradient of the force ${}^{\alpha}\langle(\mathbf{F}_{\alpha\beta})_{\tau}\rangle$.

$$\nabla_{\mathbf{c}_\alpha}{}^{\alpha}\langle(\mathbf{F}_{\alpha\beta})_{\tau}\rangle=-\nabla_{\mathbf{c}\alpha}(\zeta_{\alpha\beta}\mathbf{c}_\alpha)$$

$$=\mu_{\alpha\beta}\nabla_{\mathbf{c}_\alpha}\int d\mathbf{c}_\beta \mathbf{c}_{\beta\alpha}c_{\beta\alpha}Q_{\alpha\beta}{}^{(1)}(c_{\beta\alpha})f(c_\beta)$$

$$=-\mu_{\alpha\beta}\int d\mathbf{c}_\beta f(c_\beta)\nabla_{\mathbf{c}_\beta}[\mathbf{c}_{\beta\alpha}c_{\beta\alpha}Q_{\alpha\beta}{}^{(1)}(c_{\beta\alpha})]. \tag{24}$$

Then by introducing the explicit form for $f(c_\beta)$ into this expression and performing an integration by parts one finds that

$$-\nabla_{\mathbf{c}_\alpha}\cdot(\zeta_{\alpha\beta}\mathbf{c}_\alpha)$$

$$=-(\mu_{\alpha\beta}/m_\beta kT)\int d\mathbf{c}_\beta f(c_\beta)\,\mathbf{c}_\beta\cdot\mathbf{c}_{\beta\alpha}c_{\beta\alpha}Q_{\alpha\beta}{}^{(1)}(c_{\beta\alpha})$$

$$=(m_\beta\mathbf{c}_\alpha/kT)\cdot(\zeta_{\alpha\beta}\mathbf{c}_\alpha)-[(m_\alpha+m_\beta)/kT]S_{\alpha\beta}(c_\alpha)$$

so that

$$S_{\alpha\beta}(c_\alpha)=\mu_{\alpha\beta}\zeta_{\alpha\beta}c_\alpha{}^2/m_\alpha+[kT/(m_\alpha+m_\beta)](3+\mathbf{c}_\alpha\cdot\nabla_{\mathbf{c}_\alpha})\zeta_{\alpha\beta}, \tag{25}$$

and

$${}^{\alpha}\langle(P_{\alpha\beta})_{\tau}\rangle=[3kT/2-m_\alpha c_\alpha{}^2/2+kTc_\alpha\tfrac{1}{2}(\partial/\partial c_\alpha)]$$
$$\times[2\zeta_{\alpha\beta}/(m_\alpha+m_\beta)]. \tag{26}$$

From this it follows that if the friction coefficients are not strongly dependent upon velocity, the kinetic energy of the representative molecule will relax to a value near $3kT/2$ with the characteristic time given by $\tau(c_\alpha)=[\sum_\beta 2\zeta_{\alpha\beta}/(m_\alpha+m_\beta)]^{-1}$.

Frequently one would like to speak of the average amounts of momentum or energy transferred during a single collisional event. In order to facilitate this undertaking we shall therefore introduce the function

$$Z_{\alpha\beta}(c_\alpha)=\int d\mathbf{c}_\beta f(c_\beta)Q_{\alpha\beta}{}^{(1)}(c_{\beta\alpha})c_{\beta\alpha}, \tag{27}$$

which in the case of rigid sphere molecules (to be considered in detail in the next section) has the physical significance of the average collision rate between an α-specie molecule with the prescribed speed c_α and the β-specie members of its environment. By retaining this same interpretation of $Z_{\alpha\beta}$ for an arbitrary choice of the pair potential we can then identify $-\zeta_{\alpha\beta}(c_\alpha)/m_\alpha Z_{\alpha\beta}(c_\alpha)$ and $2{}^{\alpha}\langle(P_{\alpha\beta})_{\tau}\rangle/m_\alpha c_\alpha{}^2 Z_{\alpha\beta}(c_\alpha)$ as the average fractional increments of velocity and kinetic energy which accrue to an α-specie molecule with velocity c_α upon each of its collisions with a β-specie neighbor. The quantities obtained by adding unity to each of these increments are precisely analogous to Jean's "persistence" and do for the case of rigid spheres reduce correctly to his result.[4] For an arbitrary choice of the pair potential the "collisional rate" $Z_{\alpha\beta}$ may be expressed as

$$Z_{\alpha\beta}(c_\alpha)=2n_\beta(m_\beta/2\pi kT)^{\frac{1}{2}}c_\alpha{}^{-1}$$

$$\times\exp(-m_\beta c_\alpha{}^2/2kT)\int_0^\infty dg g^2 Q_{\alpha\beta}{}^{(1)}(g)$$

$$\times\exp(-m_\beta g^2/2kT)\sinh(m_\beta c_\alpha g/kT)$$

$$=4n_\beta\exp(-W_{\alpha\beta}{}^2)\sum_{s=0}^{\infty}\frac{2^{2s+1}\Omega_{\alpha\beta}{}^{(1,s)}(T_{\alpha\beta})}{(2s+1)!}W_{\alpha\beta}{}^{2s} \tag{28}$$

and

$$Z_{\alpha\beta}(0)=4\pi n_\beta\sigma_{\alpha\beta}{}^2(kT/2\pi m_\beta)^{\frac{1}{2}}\Omega_{\alpha\beta}{}^{(1,0)*}(T_{\alpha\beta}{}^*). \tag{29}$$

By manipulations of the same sort that were used to establish the relationship of $\zeta_{\alpha\beta}$ to $S_{\alpha\beta}$ it can be shown that

$$\zeta_{\alpha\beta}(c_\alpha)=\mu_{\alpha\beta}[1+(kT/m_\beta c_\alpha)(\partial/\partial c_\alpha)]Z_{\alpha\beta}(c_\alpha) \tag{30}$$

and so,

$$S_{\alpha\beta}(c_\alpha)=(\mu_{\alpha\beta}{}^2/m_\alpha)[\mathbf{c}_\alpha+(kT/m_\beta)\nabla_{\mathbf{c}_\alpha}]^2 Z_{\alpha\beta}(c_\alpha). \tag{31}$$

In terms of $Z_{\alpha\beta}$ a velocity dependent free path length may be defined by $\lambda_\alpha(c_\alpha)=c_\alpha/\sum_\beta Z_{\alpha\beta}(c_\alpha)$ and the logical generalization of Maxwell's path length[9] is given by

$$\lambda_\alpha=2n_\alpha(2kT/\pi m_\alpha)^{\frac{1}{2}}\Big/\int dc_\alpha f(c_\alpha)\sum_\beta Z_{\alpha\beta}(c_\alpha)$$

$$=(2kT/\pi m_\alpha)^{\frac{1}{2}}/4\sum_\beta n_\beta\Omega_{\alpha\beta}{}^{(1,0)}(T). \tag{32}$$

It is of more than passing interest that the $\Omega^{(1,0)}$ integral should happen to appear in these formulas for the collision rate and free path length. Thus, one will recall that $\Omega^{(1,0)}$ is the only member of the set of Ω integrals which plays no role in the Chapman-Enskog theory of gas transport phenomena, and that in that theory reference is made neither to the collision rate nor to the concept of free path length. These observations suggest that the approach adopted in the present investigation may provide a direct link between the early free path methods and the more modern versions of the kinetic theory. It is not surprising to discover that the velocity dependent free path length for soft interaction potentials increases steadily with molecular velocity, for at very high velocities only a rigid core can produce a significant distortion of the molecular trajectories.

To facilitate the comparison of our results with those obtained by other methods and also for future application to transport theory we now introduce the "average

friction coefficient,"

$$ {}^{\alpha}\langle\zeta_{\alpha\beta}\rangle = n_\alpha^{-1}\int dc_\alpha f(c_\alpha)\zeta_{\alpha\beta}(c_\alpha) $$

$$ = 8n_\beta m_\alpha\left[\Omega_{\alpha\beta}^{(1,0)}(T) - \frac{M_\alpha}{2M_\beta^{\frac{1}{2}}}\int_{M_\alpha}^{1}\frac{\Omega_{\alpha\beta}^{(1,0)}(Ts)ds}{(s-M_\alpha)^{\frac{1}{2}}}\right] \tag{33} $$

corresponding to an equilibrium distribution of the α-specie molecules. Here, $M_\alpha = m_\alpha/(m_\alpha+m_\beta)$ and $M_\beta = m_\beta/(m_\alpha+m_\beta)$.

IV. SAMPLE CALCULATIONS

In this section we shall apply the formulas previously derived to the calculation of friction coefficients for several specific choices of the pair interaction potential.

(a) Rigid Elastic Spheres

In this case $Q_{\alpha\beta}^{(1)} = \pi\sigma_{\alpha\beta}^2$, where $\sigma_{\alpha\beta}$ represents the range of the impulsive interaction. Consequently $Q^{(1)*}$ and the reduced integrals $\Omega^{(1,s)*}$ are all equal to unity. The integration of (13) can then be accomplished in a straightforward manner to yield

$$ \zeta^*(W) = \tfrac{3}{4}\{[(4W^2)^{-1}+\tfrac{1}{2}]\exp(-W^2) $$

$$ -[(4W^3)^{-1}-W^{-1}-W]\int_0^W \exp(-x^2)dx\}, \tag{34} $$

$$ \lim_{W\to\infty}\{\zeta^*(W)/W\} = 3(\pi)^{\frac{1}{2}}/8. \tag{35} $$

Aside from notational differences (34) is identical to the result obtained by Collins and Raffel.[3] The persistence calculated from this formula and the velocity dependent free path length are of course the same as those given by Jeans.[4] The average friction coefficient is found to be

$$ {}^{\alpha}\langle\zeta_{\alpha\beta}\rangle = \pi\sigma_{\alpha\beta}^2 n_\beta\mu_{\alpha\beta}(2kT/\pi\mu_{\alpha\beta})^{\frac{1}{2}} $$

$$ \times\left(1+\frac{1}{M_\beta}-\frac{M_\alpha^2}{M_\beta^{\frac{1}{2}}}\ln\frac{1+M_\beta^{\frac{1}{2}}}{M_\alpha^{\frac{1}{2}}}\right), \tag{36} $$

a result which agrees with that reported in footnote reference (3).

(b) Inverse Power Law

For the potential $\phi_{\alpha\beta}(r) = \epsilon_{\alpha\beta}(\sigma_{\alpha\beta}/r)^\delta$ the cross section and reduced integrals are given by

$$ Q_{\alpha\beta}^{(l)}(g) = 2\pi(2\epsilon_{\alpha\beta}\delta/\mu_{\alpha\beta})^{2/\delta}\sigma_{\alpha\beta}^2 A^{(l)}(\delta)g^{-4/\delta} \tag{37} $$

and

$$ \Omega_{\alpha\beta}^{(1,s)*}(T_{\alpha\beta}^*) $$

$$ = 2(\delta/T_{\alpha\beta}^*)^{2/\delta}\Gamma(s+2-2/\delta)A^{(l)}(\delta)/(s+1)!, \tag{38} $$

where the quantities $A^{(l)}(\delta)$ are numerical constants with values all near unity.[11] It can then be shown that

$$ \zeta_{\alpha\beta}^* = [3(2kT/m_\beta)^{2/\delta}/4\Gamma(3-2/\delta)]c_\alpha^{-3}\int_0^\infty dg g^{2-4/\delta} $$

$$ \times\{(m_\beta c_\alpha g/kT+1)\exp[-m_\beta(c_\alpha+g)^2/2kT] $$

$$ +(m_\beta c_\alpha g/kT-1)\exp[-m_\beta(c_\alpha-g)^2/2kT]\} \tag{39} $$

and

$$ \lim_{W\to\infty}\{\zeta^*(W)/W^{2\lambda-1}\} = 3(\pi)^{\frac{1}{2}}/4\Gamma(\lambda+2), \tag{40} $$

where $\lambda = 1-2/\delta$. For the three choices of $\delta=\infty$ (rigid spheres), $\delta=2$, and $\delta=4$, the integration of (39) proves trivial. Thus, with $\delta=2$

$$ \zeta^*(W) = \tfrac{3}{4}\left[\frac{1}{W^2}\exp(-W^2) - \left(\frac{1}{W^3}-\frac{2}{W}\right)\int_0^W \exp(-x^2)dx\right], \tag{41a} $$

$$ \lim_{W\to\infty}\{W\zeta^*(W)\} = 3(\pi)^{\frac{1}{2}}/4, \tag{41b} $$

and

$$ Z_{\alpha\beta}(c_\alpha) = Z_{\alpha\beta}(0)W_{\alpha\beta}^{-1}\int_0^{W_{\alpha\beta}}\exp(-x^2)dx. \tag{42} $$

For the choice $\delta=4$ one finds that $\zeta_{\alpha\beta}^*=1$ and so the velocity and temperature independent friction coefficient for "Maxwell molecules" is given by

$$ \zeta_{\alpha\beta} = \mu_{\alpha\beta}Z_{\alpha\beta} = 4\pi n_\beta\sigma_{\alpha\beta}^2(2\mu_{\alpha\beta}\epsilon_{\alpha\beta})^{\frac{1}{2}}A^{(1)}(4). \tag{43} $$

If $\delta = 2/(1-\lambda)$ is set equal to some integer other than 2 or 4, then we must employ the power series representation for $\zeta_{\alpha\beta}^*$ given by (18) where the coefficients are

$$ h_s = \frac{3s\Gamma(\lambda+s+1)}{(2s+1)!\Gamma(\lambda+2)}2^{2s-1}. \tag{44} $$

Values of these coefficients through $s=7$ are given in Table I for the two choices of $\delta=6$ and $\delta=12$. The friction coefficients for various inverse power potentials are summarized in Table II and shown graphically in Fig. 3. As predicted by (40), ζ^* tends asymptotically to zero for $\delta<4$ and to infinity for $\delta>4$.

(c) More Realistic Interactions

For more realistic choices of the pair potential than those considered above a thorough examination of the velocity and temperature dependence of the friction coefficient would require the numerical evaluation of the integral appearing on the right-hand side of (13). In principle one could circumvent this calculation by employing the series representation for ζ given by (18). However, the principal disadvantage of this procedure is that a sufficient number of the omega integrals have been evaluated only for the Lennard-Jones 12–6

[11] M. A. Eliason, D. E. Stogryn, and J. O. Hirschfelder, Proc. Natl. Acad. Sci. U.S. **42**, 546 (1956). Also, see footnote reference 8, p. 548.

TABLE I. The coefficients $h_l = 3l(l+1)\,l!2^{2l-3}\Omega^{(1,l)*}/(2l+1)\,!\Omega^{(1,1)*}$ for the inverse power potentials with $\delta=6$ and $\delta=12$, the Lennard-Jones 12-6 potential, and the exponential-6 potential with $\alpha=12$. [Calculations based upon the omega (and Z) integrals tabulated in footnote references 12–14.]

T^*	h_2	$h_3\times10^1$	$h_4\times10^1$	$h_5\times10^2$	$h_6\times10^2$	$h_7\times10^3$
			Exponential-6 potential			
0.3	1.01556	5.0207	1.6352	3.9890	0.77929	1.2755
0.5	0.98059	4.7750	1.5630	3.8829	0.77944	1.3137
0.8	0.97811	4.8604	1.6364	4.1732	0.85513	1.4626
1.0	0.98883	4.9923	1.7045	4.3897	0.90575	1.5555
2.0	1.04510	5.5129	1.9346	5.0662	1.05592	1.8263
5.0	1.09866	5.9232	2.0984	5.5156	1.14984	1.9902
10.0	1.10907	5.9818	2.1145	5.5433	1.15339	1.9889
100.0	1.10570	5.9553	2.1068	5.5388	1.15671	2.0025
			12-6 potential			
0.3	1.0170	5.0540	1.6618	4.0812	0.80368	1.3276
0.5	0.9903	4.8723	1.6107	4.0381	0.81698	1.3828
0.8	0.9916	4.9855	1.6938	4.3510	0.89925	1.5526
1.0	1.0040	5.1274	1.7631	4.5775	0.94756	1.6329
2.0	1.0605	5.6560	2.0045	5.2981	1.11029	1.9327
5.0	1.1181	6.1146	2.1921	5.8197	1.22653	2.1381
10.0	1.1336	6.2207	2.2358	5.9459	1.25174	2.1822
			Inverse-6			
	1.06667	5.58730	1.93141	4.97485	1.02048	1.73860
			Inverse-12			
	1.13333	6.20635	2.22203	5.89175	1.23877	2.01540

potential,[12,13]

$$\phi(r)=4\epsilon[(\sigma/r)^{12}-(\sigma/r)^{6}], \tag{45}$$

and for the exponential-6 potential,[13,14]

$$\phi(r)=\frac{\epsilon}{1-6/\alpha}\{(6/\alpha)\exp[\alpha(1-\sigma/r)]-(\sigma/r)^{6}\}. \tag{46}$$

Even for these special cases the number of omega integrals available is only great enough to permit the accurate calculation of $\zeta^*(W)$ up to about $W=2$. In Table I are collected a few values of the first seven coefficients, h_s, for these two potentials. The behavior at low velocities of the friction coefficient for the exponential-6 potential is presented in Table II and illustrated in Fig. 3. It appears very likely that the general characteristics of the friction coefficient for this potential will be shared by all interactions which combine an attractive long range with a repulsive short range contribution.

(d) Molecules with Internal Degrees of Freedom (Rough Spheres)

Although it is not our intention to include within this paper a detailed study of friction coefficients for molecules with internal degrees of freedom, we shall consider briefly the especially simple case of perfectly rough spheres. In addition to its mass m_i and translational velocity $\mathbf{c}_i$, a rough sphere molecule is characterized by an inertial moment, I_i, diameter σ_i, and rotational velocity $\boldsymbol{\omega}_i$. The collision increments of linear and angular velocity are given by[15]

$$\Delta\mathbf{c}_\alpha=[2\mu_{\alpha\beta}/m_\alpha(\nu_{\alpha\beta}+1)](\nu_{\alpha\beta}\mathbf{V}+\mathbf{k}\mathbf{k}\cdot\mathbf{V}) \tag{47a}$$

and

$$\Delta\boldsymbol{\omega}_\alpha=[\mu_{\alpha\beta}\sigma_\alpha\nu_{\alpha\beta}/I_\alpha(\nu_{\alpha\beta}+1)]\mathbf{k}\times\mathbf{V}, \tag{47b}$$

where $(\nu_{\alpha\beta}\mu_{\alpha\beta})^{-1}=(\kappa_\alpha m_\alpha)^{-1}+(\kappa_\beta m_\beta)^{-1}$, $\kappa_i=4I_i/m_i\sigma_i^2$, $Q_{\alpha\beta}^{(1)}=\pi(\sigma_\alpha+\sigma_\beta)^2/4$, and

$$\mathbf{V}=\mathbf{c}_{\beta\alpha}+(\sigma_\beta\mathbf{k}\times\boldsymbol{\omega}_\beta+\sigma_\alpha\mathbf{k}\times\boldsymbol{\omega}_\alpha)/2. \tag{48}$$

Besides the frictional force, ${}^\alpha\langle(\mathbf{F}_{\alpha\beta})_\tau\rangle$, and translational energy dissipation, ${}^\alpha\langle(P_{\alpha\beta})_\tau\rangle_{\mathrm{tr}}$, we are now also concerned with the frictional torque

$${}^\alpha\langle(\mathbf{G}_{\alpha\beta})_\tau\rangle$$

$$=-\int d\mathbf{c}_\beta\int d\boldsymbol{\omega}_\beta\int_{\{\mathbf{k}\cdot\mathbf{c}_{\beta\alpha}<0\}}d\mathbf{k}\mathbf{k}\cdot\mathbf{c}_{\beta\alpha}\sigma_{\alpha\beta}^2\Delta(I_\alpha\boldsymbol{\omega}_\alpha)\times f(\mathbf{c}_\beta,\boldsymbol{\omega}_\beta) \tag{49}$$

[12] Footnote reference 8, p. 1126.
[13] E. A. Mason, J. Chem. Phys. **27**, 782 (1957).
[14] Footnote reference 8, p. 1164.
[15] S. Chapman, T. G. Cowling, *The Mathematical Theory of Non-Uniform Gases* (Cambridge University Press, New York, 1939), p. 200.

and the rotational energy dissipation

$$^{\alpha}\langle(P_{\alpha\beta})_{\tau}\rangle_{\rm rot} = -\int d\mathbf{c}_{\beta}\int d\omega_{\beta} \int_{\{\mathbf{k}\cdot\mathbf{c}_{\beta\alpha}<0\}} dk k c_{\beta\alpha} \cdot\sigma_{\alpha\beta}^{2}\Delta(I_{\alpha}\omega_{\alpha}^{2}/2)f(\mathbf{c}_{\beta},\omega_{\beta}). \quad (50)$$

By means of a combination of the techniques employed in Secs. II and III these functions can be expressed as

$$^{\alpha}\langle(\mathbf{F}_{\alpha\beta})_{\tau}\rangle = -\{1+[\nu_{\alpha\beta}/(\nu_{\alpha\beta}+1)]\}\zeta_{\alpha\beta}^{(s.s.)}(c_{\alpha})\mathbf{c}_{\alpha} - \tfrac{2}{3}n_{\beta}\mu_{\alpha\beta}\sigma_{\alpha}[\nu_{\alpha\beta}/(\nu_{\alpha\beta}+1)]Q_{\alpha\beta}^{(1)}\omega_{\alpha}\times\mathbf{c}_{\alpha} \quad (51)$$

$$^{\alpha}\langle(\mathbf{G}_{\alpha\beta})_{\tau}\rangle = -[\sigma_{\alpha\beta}^{2}\nu_{\alpha\beta}/2(\nu_{\alpha\beta}+1)]\{\omega_{\alpha}\mu_{\alpha\beta}Z_{\alpha\beta}^{(s.s.)}(c_{\alpha}) - \tfrac{1}{4}\omega_{\alpha}\cdot\nabla_{\mathbf{c}_{\alpha}}[\mathbf{c}_{\alpha}\zeta_{\alpha\beta}^{(s.s.)}(c_{\alpha})]\} \quad (52)$$

$$^{\alpha}\langle(P_{\alpha\beta})_{\tau}\rangle_{tr} = {}^{\alpha}\langle(\mathbf{F}_{\alpha\beta})_{\tau}\rangle\cdot\mathbf{c}_{\alpha} + \{1+[\nu_{\alpha\beta}/(\nu_{\alpha\beta}+1)]^{2}\}S_{\alpha\beta}^{(s.s.)}(c_{\alpha}) + [2\nu_{\alpha\beta}/(\nu_{\alpha\beta}+1)]^{2}kTM_{\alpha}M_{\beta}Z_{\alpha\beta}^{(s.s.)}(c_{\alpha})\kappa_{\beta}^{-1} - M_{\beta}[\nu_{\alpha\beta}/(\nu_{\alpha\beta}+1)]^{\alpha}\langle(\mathbf{G}_{\alpha\beta})_{\tau}\rangle\cdot\omega_{\alpha} \quad (53)$$

and

$$^{\alpha}\langle(P_{\alpha\beta})_{\tau}\rangle_{\rm rot} = \{1-M_{\beta}\kappa_{\alpha}[\nu_{\alpha\beta}/(\nu_{\alpha\beta}+1)]\}{}^{\alpha}\langle(\mathbf{G}_{\alpha\beta})_{\tau}\rangle\cdot\omega_{\alpha} + \kappa_{\alpha}[\nu_{\alpha\beta}/(\nu_{\alpha\beta}+1)]^{2}S_{\alpha\beta}^{(s.s.)}(c_{\alpha}) + M_{\alpha}M_{\beta}kT\kappa_{\alpha}\kappa_{\beta}^{-1}[2\nu_{\alpha\beta}/(\nu_{\alpha\beta}+1)]^{2}Z_{\alpha\beta}^{(s.s.)}(c_{\alpha}), \quad (54)$$

where quantities labeled with superscripts s.s. refer to the *smooth sphere* coefficients calculated in Sec. IV(a). Those terms of (51)–(54) involving $Z_{\alpha\beta}$ and $Q_{\alpha\beta}^{(1)}$ arise from the transference of energy or momentum between the rotational and translational degrees of freedom.

TABLE II. Reduced friction coefficient $\zeta^{*}(W)$ for several inverse power potentials and for the exponential-6 potential with $\alpha=12$.

Exponential-6 potential					
T^{*}	0.5	0.7	1.0	1.5	2.0
0.3	1.003	1.005	1.004	0.983	0.862+(0.03)
1.0	0.998	0.997	0.998	1.006	0.931+(0.04)
2.0	1.012	1.023	1.050	1.105	1.057+(0.04)
10.0	1.027	1.051	1.099	1.188	1.150+(0.04)
100.0	1.026	1.050	1.097	1.181	1.150+(0.04)
Inverse-2					
	0.953	0.911	0.836	0.701	0.582
Inverse-6					
	1.016	1.031	1.060	1.118	1.158+(0.03)
Inverse-12					
	1.033	1.062	1.122	1.243	1.295+(0.04)
Rigid sphere					
	1.049	1.095	1.187	1.392	1.641

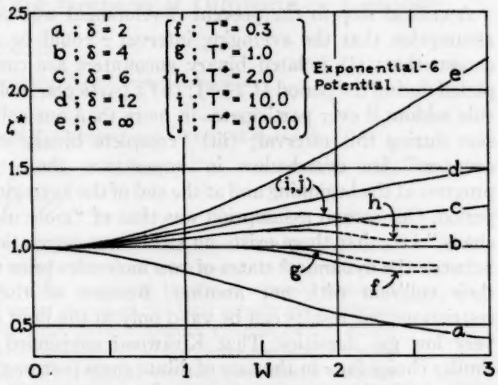

FIG. 3. Velocity dependence of the reduced friction coefficient for various inverse power potentials (δ) and for the exponential-6 potential at several reduced temperatures. The broken portions of the curves indicate more unreliable results obtained by extrapolation.

From (51) we see that the frictional force upon the rough molecule is greater by an amount $1+\nu_{\alpha\beta}/(\nu_{\alpha\beta}+1)$ than that on a smooth sphere with the same size and velocity. Furthermore, when the molecule is rotating it experiences an additional force directed normal to the plane of ω_{α} and $\mathbf{c}_{\alpha}$. According to (52) the velocity dependent rotational relaxation time for $\alpha-\beta$ collisions is equal to $m_{\alpha}\kappa_{\alpha}(\nu_{\alpha\beta}+1)/2\mu_{\alpha\beta}\nu_{\alpha\beta}Z_{\alpha\beta}^{(s.s.)}(c_{\alpha})$. The corresponding average relaxation time can be written as

$$m_{\alpha}\kappa_{\alpha}\tau_{\alpha\beta}(\nu_{\alpha\beta}+1)/2\mu_{\alpha\beta}\nu_{\alpha\beta},$$

where

$$\tau_{\alpha\beta} = n_{\alpha}/\int d\mathbf{c}_{\alpha} f(c_{\alpha})Z_{\alpha\beta}^{(s.s.)}(c_{\alpha})$$

is the mean interval between the collisions an α molecule suffers with β-specie members of its environment.

V. CONCLUDING REMARKS

The formulas which we have presented in this communication reduce the task of calculating the various molecular friction coefficients for a dilute gas to the evaluation of certain definite integrals, which bear a close relationship to those commonly encountered in the theory of gas transport phenomena. Although an exhaustive study of the friction coefficient for realistic intermolecular forces has not been attempted, the low velocity behavior has been charted for the exponential-6 and 12–6 potentials. Furthermore, the results obtained for rigid spheres and for the inverse second power potential provide limits within which the coefficient for virtually any reasonable choice of the pair interaction must be bounded.

A critical step in the prevent development was our assumption that the averaging interval τ could be so chosen that: (i) isolated binary encounters are completed during the period $(t, t+\tau)$; (ii) a particular molecule seldom if ever participates in more than one collision during this interval; (iii) "complete binary encounters" far overshadow in importance those in progress at the beginning and at the end of the averaging period. Our second assumption was that of "molecular chaos," i.e., that there exists no significant correlation between the dynamical states of two molecules prior to their collision with one another. Because of these restrictions our results can be valid only in the limit of very low gas densities. That Kirkwood envisioned a similar choice for τ in the case of dilute gases is strongly suggested by his statement,[16] ". . .using binary collision analysis we find that ζ_i does indeed have a plateau value (a value independent of τ) for values of τ long relative to the representative *duration of a molecular collision*." Thus, it is somewhat surprising to find that, although the averaging intervals in the two developments are apparently identical, our formula for the friction coefficient differs markedly from that of Kirkwood. To locate the origin of this dilemma we must remember that Kirkwood's derivation of the formula

$$\zeta_\alpha^K(c_\alpha) = (3kT\tau)^{-1}\iiint_0^\tau \int_0^s \mathbf{F}_\alpha(t+s) \cdot \mathbf{F}_\alpha(t+s') f^{(N/1)}(\mathbf{C}, \mathbf{Q}/\mathbf{c}_\alpha, \mathbf{r}_\alpha) ds' ds \mathbf{dCdQ}, \quad (55)$$

placed reliance upon the phenomenological theory of Brownian motion in order to estimate and subsequently neglect various terms which involved velocity and force correlations.[17] Therefore, we should expect this formula to be valid only if the averaging interval is comparable in magnitude to that used in the theory of Brownian motion, i.e., much longer than the mean time which elapses *between* the successive collisional encounters suffered by a particular molecule.[18] In liquids there is no possibility of resolving the time between collisions from the duration of a single encounter and so this Brownian motion interval" would indeed seem to be the only meaningful choice for τ. However, in a dilute gas this resolution can be effected and τ chosen equal to the "free path transit time" in just the manner illustrated by our development. The distinction between these two different averaging intervals implies that our approach is more closely applied in spirit to the persistence calculations of Jeans than to the calculation of fluid friction coefficients according to Kirkwood's formula (55). In fact it appears that (55) can be applied to dilute gases only if we are willing (and able) to follow the dynamical trajectory of a representative molecule as it progresses through the long chain of collisional events which would ensue if τ were chosen to be much larger than it has in the present investigation.

As a final step we shall simply disregard these matters of consistency and calculate the friction coefficient defined by (55) with the "free path transit time" choice for the averaging interval. Thus, it follows that

$$\zeta_\alpha^K(c_\alpha) = (3kT)^{-1}\sum_{\beta=1}^{\nu} \int \mathbf{dc}_\beta \int_0^\infty bdb \int_0^{2\pi} d\phi c_{\beta\alpha} f(c_\beta) \times \int_0^\tau ds \int_0^s ds' \mathbf{F}_{\alpha\beta}(t+s) \cdot \mathbf{F}_{\alpha\beta}(t+s'), \quad (56)$$

where

$$\int_0^\tau ds \int_0^s ds' F_{\alpha\beta}(t+s) \cdot F_{\alpha\beta}(t+s') = m_\alpha^2 \int_0^\tau ds \frac{dc_\alpha(t+s)}{ds} \cdot [c_\alpha(t+s) - c_\alpha(t)] = m_\alpha[\tfrac{1}{2} m_\alpha (\Delta c_\alpha)^2]. \quad (57)$$

The coefficient ζ_α^K is therefore related to the energy dissipation functions $S_{\alpha\beta}$ and to our coefficients $\zeta_{\alpha\beta}$ by the formulas

$$\zeta_\alpha^K(c_\alpha) = (m_\alpha/3kT)\sum_{\beta=1}^{\nu} S_{\alpha\beta}(c_\alpha) = \sum_{\beta=1}^{\nu} \{\zeta_{\alpha\beta}(c_\alpha) + (2\mu_{\alpha\beta}/3m_\alpha kT)[\tfrac{1}{2}(m_\alpha c_\alpha^2) - \tfrac{1}{2}(3kT)]\zeta_{\alpha\beta}(c_\alpha) + (\mu_{\alpha\beta}/3m_\beta) c_\alpha (\partial/\partial c_\alpha)\zeta_{\alpha\beta}(c_\alpha)\}. \quad (58)$$

[16] Footnote reference 1, p. 199.

[17] Footnote reference 1, p. 189. See F. C. Collins [Advances in Chem. Phys. **1**, 135 (1958)] for a more detailed exposition of this approximation.

[18] For a discussion of this point see p. 23 of S. Chandrasekhar, Revs. Modern Phys. **15**, 1 (1943).

THE JOURNAL OF CHEMICAL PHYSICS VOLUME 33, NUMBER 5 NOVEMBER, 1960

Flow Equations and Frames of Reference for Isothermal Diffusion in Liquids*

JOHN G. KIRKWOOD,

Sterling Chemistry Laboratory, Yale University, New Haven, Connecticut

AND

ROBERT L. BALDWIN,† PETER J. DUNLOP,‡ LOUIS J. GOSTING, AND GERSON KEGELES§

Departments of Chemistry, Biochemistry, and Dairy and Food Industries, University of Wisconsin, Madison, Wisconsin

(Received May 13, 1960)

Equations for testing Onsager's reciprocal relations for isothermal diffusion depend on the frame of reference chosen for the flows. This subject is considered for certain frames of reference, as is the problem of measuring diffusion coefficients when there is a change of volume on mixing. Frames of reference discussed are those moving with the local center of mass, the local center of volume, the local velocity of the solvent (or of any single component), and that fixed on the diffusion cell. Multicomponent systems, both of strong electrolytes and nonelectrolytes, are considered. An expression is derived which relates the flow of a component in the cell-fixed frame of reference to the flows in any other frame of reference when there is a change of volume on mixing. This relation is used to show that a flow relative to the cell becomes identical to that in the volume-fixed frame as the initial differences in concentration within the diffusion cell are made sufficiently small. Throughout this article a special effort has been made to present derivations and final equations in a form well adapted for use in experimental work.

I. INTRODUCTION

IN experimental studies of multicomponent isothermal diffusion it is customary to describe the transport of matter by means of flow equations which are extensions of Fick's first law. These equations express the flow or current J_i of component i as a sum of concentration gradients each multiplied by a diffusion coefficient D_{ij} of one type. In theoretical work the corresponding phenomenological equations are usually written as sums of forces (negative gradients of chemical potentials) each multiplied by a diffusion coefficient Ω_{ij} of another type. We will refer to the D_{ij} as *practical diffusion coefficients* and to the Ω_{ij} as *fundamental diffusion coefficients*. Although either type of flow equations has the same form for any choice of reference frame within a certain class,[1-5] the values of both the practical and the fundamental diffusion coefficients depend on the frame of reference selected. Onsager's reciprocal relations[6-9] hold between certain of the Ω_{ij}, and the testing of these relations by using data for the D_{ij}, together with certain thermodynamic data, is currently an important application of experimental results from studies of diffusion in multicomponent systems. Correct tests of the Onsager relations require proper specification of the reference frames, and in this paper we derive equations which are convenient to use in one route of testing these reciprocal relations.

It is shown in Sec. II of this article that the existence of reciprocal relations between the Ω_{ij} for the mass-fixed frame (when chemical potential gradients of all components are included in the flow equations) requires that there be reciprocal relations between the Ω_{ij} for the solvent-fixed frame (when the chemical potential gradient of the solvent is eliminated from the flow equations). Explicit equations are obtained for computing the Ω_{ij} from the D_{ij} for the solvent-fixed frame and then for evaluating these D_{ij} from those for the volume-fixed frame. The volume-fixed frame is important to the experimentalist because the D_{ij} for this frame may be determined directly from experi-

* This article resulted from discussions with Professor Kirkwood which began when he visited the University of Wisconsin during the summer of 1956. It contains equations used for some recent tests (footnote references 26, 29, and 30) of the Onsager reciprocal relations for isothermal diffusion. Because this manuscript was not completed until after Professor Kirkwood's death, its final draft has not had the benefit of his helpful suggestions. The remaining authors regret that they have not been in a position to develop fully certain topics which he hoped could be included, particularly an extension of the theory so that it would contain terms in the pressure gradient generally associated with nonsteady state diffusion (see footnote reference 15).

Support for this study was provided in part by the National Science Foundation and by the U. S. Public Health Service.

† Present address: Department of Biochemistry, School of Medicine, Stanford University, Palo Alto, California.

‡ Present address: Department of Physical and Inorganic Chemistry, The University of Adelaide, Adelaide, South Australia.

§ Department of Chemistry, Clark University, Worcester, Massachusetts.

[1] Any reference frame for which the flows are connected by a simple linear relation is a member of this class (see, for example, Secs. 2 and 4 of footnote reference 5). Although the problem of frames of reference for the flows arises in both theoretical and experimental investigations, it frequently has not received adequate attention, especially in experimental work. Different aspects of this problem have been considered by a number of previous workers. Representative references, in addition to footnote references 2–5, include: (a) L. G. Longsworth, Ann. N. Y. Acad. Sci. **46**, 211 (1945); (b) G. S. Hartley and J. Crank, Trans. Faraday Soc. **45**, 801 (1949); (c) S. R. de Groot, *Thermodynamics of Irreversible Processes* (Interscience Publishers, Inc., New York, 1951); (d) R. B. Bird, C. F. Curtiss, and J. O. Hirschfelder, Chem. Eng. Prog. Symposium Ser., No. 16, **51**, 69 (1955); (e) O. Lamm, Acta Chem. Scand. **11**, 362 (1957).

[2] I. Prigogine, Bull. classe sci. Acad. roy. Belg. **34**, 930 (1948).

[3] G. J. Hooyman, H. Holtan, Jr., P. Mazur, and S. R. de Groot, Physica **19**, 1095 (1953).

[4] G. J. Hooyman and S. R. de Groot, Physica **21**, 73 (1955).

[5] G. J. Hooyman, Physica **22**, 751 (1956).

[6] L. Onsager, Phys. Rev. **37**, 405 (1931).

[7] L. Onsager, Phys. Rev. **38**, 2265 (1931).

[8] L. Onsager and R. M. Fuoss, J. Phys. Chem. **36**, 2689 (1932).

[9] L. Onsager, Ann. N. Y. Acad. Sci. **46**, 241 (1945).

mental measurements of diffusion; for the solvent-fixed or mass-fixed frames some auxiliary data, such as partial specific volumes, are required for determination of practical diffusion coefficients. Reciprocal relations are discussed both for solutions of nonelectrolytes and of strong electrolytes.

In Sec. III we consider the problem of how to measure practical diffusion coefficients correctly when the partial specific volumes are dependent on concentration and the solutions therefore exhibit a change of volume on mixing. For this case a reference frame fixed on the diffusion cell is not a member of the class[1] for which simple flow equations may be written. Equations for the J_i relative to the cell must contain a term to describe the hydrodynamic, or bulk, flow of liquid in addition to the usual terms which describe the relative motion of the components. An expression for this bulk flow term is derived.

Definition of Terms

We consider diffusion in an isothermal liquid system containing $q+1$ components numbered $0, \cdots, q$; the solvent is denoted arbitrarily by 0. For simplicity it is assumed that no chemical reactions occur between the components, and, except in the subsection devoted specifically to strong electrolytes, the components are considered to be nonelectrolytes. The equations are restricted to one-dimensional diffusion in the x direction, and external fields (such as the earth's gravitational field) are neglected. In this isothermal system we do not consider any flow of heat which may be produced by the flows of matter (Dufour effect).

Throughout this paper J_i will denote the (local) flow of component i expressed as g/sec crossing an area of one cm^2 normal to x, and c_i will denote the (local) concentration of this component in g/cm^3. The flow $(J_i)_R$, of component i measured relative to some frame of reference R, is related to the flow $(J_i)_S$, of this component relative to another frame of reference S, by the equation

$$(J_i)_R=(J_i)_S+c_i u_{SR}. \tag{1}$$

Here u_{SR} is the velocity of frame S relative to frame R at the position and time considered.[10]

The four kinds of reference frames to be considered in this paper will be denoted by the subscripts M, 0, V, and C. Accordingly M denotes a mass-fixed frame of reference, i.e., one moving with the local center of mass. At each time and each level in the cell this frame has a velocity such that no net flow of mass occurs across a plane attached perpendicular to, and moving with, the x coordinate of this frame. The several flows $(J_i)_M$ measured relative to this frame of reference are therefore subject to the relation

$$\sum_{i=0}^{q}(J_i)_M=0. \tag{2}$$

The subscript 0 denotes a solvent-fixed frame[11] moving locally so that the net flow of solvent relative to it is zero,

$$(J_0)_0=0. \tag{3}$$

Similarly the letter V represents a volume-fixed frame moving locally so that no net flow of volume occurs relative to this frame at the time and level in question, i.e.,

$$\sum_{i=0}^{q}\bar{v}_i(J_i)_V=0, \tag{4}$$

wherein $\bar{v}_i$ is the partial specific volume of component i expressed as cm^3/g. Finally,[12] C is used to denote a coordinate system fixed on the cell in which diffusion occurs.

The meanings of the first three frames of reference may be further clarified from the standpoint of experiment by writing their velocities relative to the cell in terms of flows relative to the cell. To obtain these expressions we require the equation for the solution density, ρ, in g/cm^3,

$$\rho=\sum_{i=0}^{q}c_i, \tag{5}$$

and also the relation

$$\sum_{i=0}^{q}\bar{v}_i c_i=1. \tag{6}$$

Then, by replacing R by C and S by M in Eq. (1), summing over all components, and applying Eqs. (2) and (5), an expression is obtained for the velocity of the mass-fixed frame relative to the cell,

$$u_{MC}=(1/\rho)\sum_{i=0}^{q}(J_i)_C. \tag{7}$$

The velocity of the solvent-fixed frame relative to the

[10] The velocity u_{SR} may be described in terms of the velocity, u_{SC}, of frame S relative to the diffusion cell and the velocity, u_{RC}, of frame R relative to the cell by

$$u_{SR}=u_{SC}-u_{RC}. \tag{1a}$$

The velocity of a given frame of reference relative to the cell will, in general, vary both with position and time. For example, a reference frame (or coordinate system) fixed relative to the local center of mass in one part of the cell will in general be moving with respect to a reference frame fixed relative to the local center of mass in another part of the cell. However, the same unit of length is used everywhere in the system to measure distances for every frame of reference considered.

[11] Although we let 0 denote solvent throughout this paper, all the flow equations are still applicable if instead 0 denotes one of the solutes.

[12] The number-fixed reference frame, N,

$$[\text{defined by } \sum_{i=0}^{q}(J_i)_N/M_i=0]$$

is not considered here because it does not seem particularly useful in studies of liquids. This frame is encountered in studies of gases; it should be noted that for ideal gases the volume-fixed and number-fixed frames are identical.

cell is derived by writing Eq. (1) for component 0 and for frames C and 0, and then applying Eq. (3),

$$u_{0C}=(J_0)_C/c_0. \tag{8}$$

To obtain the velocity of the volume-fixed frame relative to the cell, Eq. (1) is written for frames C and V, multiplied by $\bar{v}_i$, and summed over all components; application of Eqs. (4) and (6) leads to the desired expression

$$u_{VC}=\sum_{i=0}^{q}\bar{v}_i(J_i)_C. \tag{9}$$

In regions where all the concentration gradients are zero, these three velocities become identical[13] and equal to the bulk velocity of the liquid relative to the cell. Where concentration gradients are present, so that the several components are moving relative to each other, the velocities of these three frames of reference relative to the cell are in general different. Then some convention must be adopted in order to define a hydrodynamic, or bulk, velocity in these nonuniform parts of the system (see Sec. III); Onsager and Fuoss[8] and Onsager[9] defined u_{VC}, Eq. (9), to be the bulk velocity.

II. DIFFUSION COEFFICIENTS AND TESTS OF THE ONSAGER RECIPROCAL RELATIONS

Here we consider one route of testing the Onsager reciprocal relations for isothermal diffusion, and we derive equations which are convenient for making the necessary conversions of diffusion coefficients. The case of electrolytic solutions is considered at the end of this section. It is hoped that the material in this section and in Sec. III will stimulate improved tests of the Onsager relations and will help to clarify the relation of reference frames to experimental investigations of diffusion.

Mass-Fixed Frame of Reference

We begin with a set of fundamental flow equations written for the mass-fixed frame, M,

$$(J_i)_M=\sum_{j=0}^{q}(\Omega_{ij})_M X_j \quad (i=0,\cdots,q). \tag{10}$$

For an exact description of nonsteady-state diffusion, including inertial effects,[14a,b] a general expression must be used for each force, X_j. Included in this expression should be a term describing the force associated with the acceleration of component j; for consistency, terms in the associated pressure gradient should be retained in many of the subsequent equations.[15] Although such terms may be important in some experimental cases, they become negligible for the small concentration gradients usually encountered in experiments designed to measure diffusion coefficients. We will neglect such terms in the remainder of this article and write X_j in the familiar form

$$X_j=-\partial\mu_j/\partial x. \tag{11}$$

The derivative $\partial\mu_j/\partial x$ (the chemical potential gradient for the one-dimensional case considered here) is taken with time constant; temperature and pressure are assumed to be constant. Throughout this article μ_j denotes the chemical potential *per gram* of component j. Equation (10) now becomes

$$(J_i)_M=-\sum_{j=0}^{q}(\Omega_{ij})_M(\partial\mu_j/\partial x) \quad (i=0,\cdots,q). \tag{12}$$

[13] This may be shown by substituting into Eqs. (7)–(9) the relation $(J_i)_C=c_i(u_i)_C$, where $(u_i)_C$ denotes the local velocity of component i relative to the cell. Because $(u_i)_C$ must be the same for every component when all the concentration gradients are zero, the equations are readily simplified by using Eqs. (5) and (6) and lead to $u_{MC}=u_{0C}=u_{VC}=(u_i)_C$.

[14] (a) R. J. Bearman and J. G. Kirkwood, J. Chem. Phys. **28**, 136 (1958); (b) R. J. Bearman, *ibid.* **31**, 751 (1959).

[15] Professor Kirkwood expressed considerable interest in this pressure gradient and suggested that in some experiments with large concentration gradients (perhaps in certain cases of diffusion through membranes) it may be of practical importance. He wanted to expand Secs. II and III to include terms in the pressure gradient and in the acceleration term $(1/c_j)[\partial(J_j)_C/\partial t]$ in each force. Because the remaining authors are not in a position to complete this extension as he visualized it, we omit these terms in this article and emphasize that the development given here should be applied only to the conventional type of experiment in which these additional terms are exceedingly small. It seems worthwhile, however, to indicate that by using for X_j the relation [see Eq. (5.13) of footnote reference 14(a) or Eq. (12) of footnote reference 14(b)],

$$X_j=-\{(\partial\mu_j/\partial x)_T+(1/c_j)[\partial(J_j)_C/\partial t]\} \tag{11a}$$

instead of Eq. (11), and by following the derivation outlined in Eqs. (10)–(22), reciprocal relations between the $(\Omega_{ij})_M$ in Eqs. (10) still lead to reciprocal relations between the $(\Omega_{ij})_0$ for the solvent-fixed frame. Equations (14)–(17) remain unchanged except that the X_j defined by Eq. (11a) appear in Eq. (15) instead of $-\partial\mu_j/\partial x$ (the subscript T on $\partial\mu_j/\partial x$ in Eq. (11a) indicates that these new derivatives are taken at constant temperature but not at constant pressure). To eliminate X_0 from this revised Eq. (15) the generalized form of Eq. (18) (with the pressure term retained),

$$\sum_{j=0}^{q}c_j(\partial\mu_j/\partial x)_T=\partial P/dx, \tag{11b}$$

is used to eliminate $(\partial\mu_0/\partial x)_T$, and the derivative of Eq. (7) with respect to time

$$\partial(\rho u_{MC})/\partial t=\sum_{j=0}^{q}\partial(J_j)_C/\partial t \tag{11c}$$

is used to eliminate $(1/c_0)[\partial(J_0)_C/\partial t]$. These substitutions lead to a form of Eq. (19) in which $-\partial\mu_j/\partial x$ is replaced by X_j from Eq. (11a) and there appears the addition term

$$-[(\bar{\Omega}_{i0})_0/c_0]\{(\partial P/\partial x)+[\partial(\rho u_{MC})/\partial t]\}.$$

According to the equation of motion,

$$(\partial P/\partial x)+[\partial(\rho u_{MC})/\partial t]=-\partial[\rho(u_{MC})^2]/\partial x, \tag{11d}$$

the term in braces may be replaced by $-\partial[\rho(u_{MC})^2]/\partial x$. However, this term may be neglected because a term of order $(u_{MC})^2$ corresponds to force terms of order higher than the first power; such terms have already been neglected in writing the linear phenomenological relations, Eqs. (10). Therefore it is found that Eqs. (20)–(22) remain unchanged. Equation (11d) may also be used to show that the pressure gradient from inertial effects is very small in the usual experiments for measuring diffusion coefficients.

As a result of considerations by Onsager of microscopic reversibility,[6,7] the $(q+1)^2$ fundamental diffusion coefficients in Eqs. (12) may be specified so that they are subject to the $\frac{1}{2}q(q+1)$ reciprocal relations,[16]

$$(\Omega_{ij})_M=(\Omega_{ji})_M. \tag{13}$$

Solvent-Fixed Frame of Reference

We now show that if flow equations for the solvent-fixed frame contain terms only in the chemical potential gradients of the *solutes*, the fundamental diffusion coefficients in these equations are subject to reciprocal relations as a consequence of Eq. (13). Flows relative to the solvent-fixed frame, 0, may be expressed in terms of those for the mass-fixed frame by starting with Eq. (1) written for frames 0 and M, $(J_i)_0=(J_i)_M+c_iu_{M0}$. Then the velocity u_{M0} in this relation is replaced by $u_{M0}=-(J_0)_M/c_0$ [obtained by setting $i=0$ and applying Eq. (3)]. Thus one obtains

$$(J_i)_0=(J_i)_M-(c_i/c_0)(J_0)_M. \tag{14}$$

Use of Eq. (12) to express $(J_i)_M$ and $(J_0)_M$ in terms of the chemical potential gradients leads to the flow equations

$$(J_i)_0=-\sum_{j=0}^{q}(\tilde{\Omega}_{ij})_0(\partial\mu_j/\partial x), \qquad (i=0,\cdots,q) \tag{15}$$

wherein the new fundamental diffusion coefficients are related to those in Eq. (12) by

$$(\tilde{\Omega}_{ij})_0=(\Omega_{ij})_M-(c_i/c_0)(\Omega_{0j})_M. \tag{16}$$

It should be noted that in general these coefficients are not subject to reciprocal relations, i.e.,

$$(\tilde{\Omega}_{ij})_0\neq(\tilde{\Omega}_{ji})_0. \tag{17}$$

Next, the chemical potential gradient of component 0 is eliminated from Eq. (15) by means of the Gibbs-Duhem equation written for constant temperature and pressure,

$$\sum_{j=0}^{q}c_j(\partial\mu_j/\partial x)=0. \tag{18}$$

Solution of Eq. (18) for $\partial\mu_0/\partial x$ and substitution into Eq. (15) leads to the set of flow equations,

$$(J_i)_0=-\sum_{j=1}^{q}(\Omega_{ij})_0(\partial\mu_j/\partial x) \qquad (i=1,\cdots,q), \tag{19}$$

where

$$(\Omega_{ij})_0=(\tilde{\Omega}_{ij})_0-(c_j/c_0)(\tilde{\Omega}_{i0})_0, \tag{20}$$

or, after substituting Eq. (16),

$$(\Omega_{ij})_0=(\Omega_{ij})_M-(c_i/c_0)(\Omega_{0j})_M-(c_j/c_0)(\Omega_{i0})_M+(c_ic_j/c_0^2)(\Omega_{00})_M. \tag{21}$$

Application of Eq. (13) to Eq. (21) leads to the reciprocal relations[17,18]

$$(\Omega_{ij})_0=(\Omega_{ji})_0 \tag{22}$$

between these q^2 fundamental diffusion coefficients. No information is lost by omitting a flow equation corresponding to $i=0$ from Eqs. (19), because $(J_0)_0=0$ from Eq. (3) and all $(\Omega_{0j})_0=0$ from Eq. (21).

Equations (19) are converted to flow equations containing practical diffusion coefficients for the solvent frame of reference by expressing the chemical potential gradients in terms of concentration gradients. Because there are q independent concentrations in a single-phase system of $q+1$ components at constant temperature and pressure, the chemical potential gradient of any solute, j, may be written

$$\partial\mu_j/\partial x=\sum_{k=1}^{q}(\partial\mu_j/\partial c_k)(\partial c_k/\partial x) \qquad (j=1,\cdots,q). \tag{23}$$

The derivatives $(\partial\mu_j/\partial c_k)$ and $(\partial c_k/\partial x)$ are taken at constant temperature and pressure; for $(\partial\mu_j/\partial c_k)$ all

---

[16] Because terms for all components are included in Eqs. (12), neither the forces nor the flows are independent. Consequently Eqs. (12) do not uniquely define the $(\Omega_{ij})_M$ without auxiliary relations, and whether the $(\Omega_{ij})_M$ satisfy Eq. (13) depends on the choice of auxiliary relations. Suppose that to describe diffusion in a given system one uses for the $(\Omega_{ij})_M$ a set of permissible numerical values which satisfy the reciprocal relations, Eq. (13). If to each Eq. (12) is then added [see Eq. (18)] the sum

$$\sigma_i=-K_i\sum_{j=0}^{q}c_j(\partial\mu_j/\partial x)=0,$$

where each K_i is a constant, a new set of fundamental diffusion coefficients, $(\hat{\Omega}_{ij})_M=(\Omega_{ij})_M+K_ic_j$, is obtained; these new coefficients are not subject to reciprocal relations (except perhaps for special values of the K_i). This does not imply that the Onsager reciprocal relations are entirely arbitrary. For a ternary system Eqs. (13) provide three restrictions on the $(\Omega_{ij})_M$. One restriction on the set of $(\Omega_{ij})_M$ for this system is required by Onsager's considerations of microscopic reversibility; the other two are simply convenient definitions, such as may be achieved by adjusting the K_i. In this paper we need not consider the auxiliary relations required to define completely the $(\Omega_{ij})_M$ in Eqs. (12); it is sufficient that such relations *may* be specified in a way so that Eqs. (13) are satisfied (see footnote references 4 and 18).

[17] Reciprocal relations also hold between the new fundamental diffusion coefficients in Eqs. (19) when each $(J_i)_0$ is expressed as moles/cm²/sec, and each μ_j as the chemical potential per mole.

[18] This is in agreement with Eq. (4.12.7) of Onsager and Fuoss (footnote reference 8), and Eq. (19) of Hooyman (footnote reference 5). Note that for the $(\Omega_{ij})_0$ to satisfy Eq. (22) it is not *necessary* for the $(\Omega_{ij})_M$ to be defined so that they satisfy Eq. (13); it is sufficient that they *may* be defined so that Eq. (13) is satisfied. This may be shown by starting with the $(\Omega_{ij})_M$ defined so that they satisfy Eq. (13) and then adding σ_i (footnote 16) to each Eq. (12), using values of K_i such that the $(\hat{\Omega}_{ij})_M$ do not exhibit reciprocal relations. After repeating the derivation with these $(\hat{\Omega}_{ij})_M$ one finds that in the equation corresponding to Eq. (21) the coefficients of K_i and K_0 are zero, again giving Eq. (22) as a consequence of $(\Omega_{ij})_M=(\Omega_{ji})_M$.

concentrations are held constant except c_k and c_0.[19] Substitution of Eq. (23) into Eq. (19) leads to flow equations containing the practical diffusion coefficients, $(D_{ik})_0$, for this frame of reference,

$$(J_i)_0 = -\sum_{k=1}^{q}(D_{ik})_0(\partial c_k/\partial x), \quad (i=1, \cdots, q), \quad (24)$$

where[20]

$$(D_{ik})_0 = \sum_{j=1}^{q}(\Omega_{ij})_0(\partial \mu_j/\partial c_k). \quad (25)$$

Equations for computing values of the $(\Omega_{ij})_0$ from known values of $(D_{ik})_0$ are obtained by solving Eqs. (25) with the use of determinants. The result for the general case may be written formally as

$$(\Omega_{ij})_0 = |\,\partial\mu/\partial c\,|_{ik}/|\,\partial\mu/\partial c\,|, \quad (26)$$

where $|\,\partial\mu/\partial c\,|$ represents the determinant of the matrix of $(\partial\mu_j/\partial c_k)$, and $|\,\partial\mu/\partial c\,|_{ik}$ denotes the sum of its appropriate minors multiplied by the corresponding $(D_{ik})_0$. For the case of $q=2$ (the only case sufficiently simple for routine experimental investigation at the present time) one obtains:

$$(\Omega_{11})_0 = [(D_{11})_0(\partial\mu_2/\partial c_2) - (D_{12})_0(\partial\mu_2/\partial c_1)]/S \quad (26a)$$

$$(\Omega_{12})_0 = [(D_{12})_0(\partial\mu_1/\partial c_1) - (D_{11})_0(\partial\mu_1/\partial c_2)]/S \quad (26b)$$

$$(\Omega_{21})_0 = [(D_{21})_0(\partial\mu_2/\partial c_2) - (D_{22})_0(\partial\mu_2/\partial c_1)]/S \quad (26c)$$

$$(\Omega_{22})_0 = [(D_{22})_0(\partial\mu_1/\partial c_1) - (D_{21})_0(\partial\mu_1/\partial c_2)]/S, \quad (26d)$$

in which

$$S = (\partial\mu_1/\partial c_1)(\partial\mu_2/\partial c_2) - (\partial\mu_1/\partial c_2)(\partial\mu_2/\partial c_1). \quad (26e)$$

Volume-Fixed Frame of Reference

Relations will now be derived for computing practical diffusion coefficients for the solvent-fixed frame from those which may be determined by experiment for the volume-fixed frame. An expression for the velocity, u_{0V}, of the solvent-fixed frame relative to the volume-fixed frame is obtained by writing Eq. (1) for frames V and 0, multiplying this equation by $\bar{v}_i$, summing over all components, and applying Eq. (4),

$$u_{0V} = -\sum_{j=1}^{q}\bar{v}_j(J_j)_0. \quad (27)$$

The sum is written from $j=1$ to q because $(J_0)_0=0$. Substitution of Eq. (27) into Eq. (1), written for frames V and 0, yields this relation between flows relative to these two frames of reference,

$$(J_i)_V = (J_i)_0 - c_i\sum_{j=1}^{q}\bar{v}_j(J_j)_0. \quad (28)$$

Substitution of Eq. (24) into Eq. (28) then gives the set of flow equations

$$(J_i)_V = -\sum_{k=1}^{q}(D_{ik})_V(\partial c_k/\partial x) \quad (i=1, \cdots, q), \quad (29)$$

in which the q^2 practical diffusion coefficients are related to the $(D_{ik})_0$ by[21]

$$(D_{ik})_V = (D_{ik})_0 - c_i\sum_{j=1}^{q}\bar{v}_j(D_{jk})_0 \quad \begin{pmatrix} i=1, \cdots, q \\ k=1, \cdots, q \end{pmatrix}. \quad (30)$$

Values of the four $(D_{ik})_V$ for a ternary system may be obtained by procedures[22–26] developed recently for analyzing optical data for free diffusion (see Sec. III). Onsager[9] proposed a set of $(q+1)^2$ practical diffusion coefficients for the volume-fixed frame of reference; for ternary systems equations have been derived[27,28] for calculating his nine coefficients from values of the four $(D_{ik})_V$.

To calculate the $(D_{ik})_0$ from measured values of the $(D_{ik})_V$ it is convenient to have an inverted form of Eq. (30). This is obtained by multiplying Eq. (30) by $\bar{v}_i$, summing from $i=1$ to q, utilizing Eq. (6), and then using Eq. (30) once more to give

$$(D_{ik})_0 = (D_{ik})_V + (c_i/c_0\bar{v}_0)\sum_{j=1}^{q}\bar{v}_j(D_{jk})_V \quad \begin{pmatrix} i=1, \cdots, q \\ k=1, \cdots, q \end{pmatrix}. \quad (31)$$

Equations (26) and (31) may be used to test Onsager's reciprocal relations for isothermal diffusion at a given composition of a system containing three or more components. The data required are values of the $(D_{ik})_V$, $\bar{v}_j$, c_i, and $\partial\mu_j/\partial c_k$. Values of the $(D_{ik})_0$ are first

[19] It will be recalled that for nonelectrolytes the chemical potential per g, μ_j, of component j can be expressed in terms of the concentration, c_j, and molecular weight, M_j, of that component and an activity coefficient, y_j, (which may be a function of all solute concentrations)

$$\mu_j = \mu_j^\circ + (RT/M_j)\ln y_j c_j. \quad (23a)$$

Here R is the gas constant per mole and T is the absolute temperature. This activity coefficient, y_j, is identical with the activity coefficient associated with the molarity scale of concentration; it is customary to let each y_j approach unity as *all* the solute concentrations approach zero. For a given solvent each reference chemical potential, μ_j°, is a function only of temperature and pressure. By differentiation of Eq. (23a) we see that

$$\partial\mu_j/\partial c_k = (RT/M_j)/(\partial\ln y_j/\partial c_k) \quad (j\neq k) \quad (23b)$$

and

$$\partial\mu_j/\partial c_j = (RT/M_j c_j)[1+(\partial\ln y_j/\partial\ln c_j)]. \quad (23c)$$

[20] See Eq. (18) of footnote reference 5.

[21] Our Eq. (30) may be shown to be consistent with Eqs. (30) and (31) of footnote reference 5 by substituting appropriate weight factors into the latter equations.

[22] R. L. Baldwin, P. J. Dunlop, and L. J. Gosting, J. Am. Chem. Soc. **77**, 5235 (1955).

[23] P. J. Dunlop and L. J. Gosting, J. Am. Chem. Soc. **77**, 5238 (1955).

[24] H. Fujita and L. J. Gosting, J. Am. Chem. Soc. **78**, 1099 (1956).

[25] P. J. Dunlop, J. Phys. Chem. **61**, 994 (1957).

[26] H. Fujita and L. J. Gosting, J. Phys. Chem. (to be published).

[27] M. Dole, J. Chem. Phys. **25**, 1082 (1956).

[28] F. E. Weir and M. Dole, J. Am. Chem. Soc. **80**, 302 (1958).

calculated from Eqs. (31); then the $(\Omega_{ij})_0$ are obtained by using Eqs. (26) [or (26a)–(26e)]. If these coefficients are found to satisfy Eq. (22), Onsager's relations are confirmed. This procedure has been applied recently[26,29,30] to data for several compositions of the system NaCl-KCl-H_2O by defining the electrolyte components as indicated in the next subsection; within experimental error $(\Omega_{12})_0$ was found to equal $(\Omega_{21})_0$. One advantage of this procedure for testing Onsager's reciprocal relations is that the $(D_{ik})_0$ and $(\Omega_{ij})_0$ are clearly defined diffusion coefficients in flow equations of simple form; their numerical values may be useful in other types of investigations.

Another route of testing the Onsager reciprocal relations has been developed by Miller.[31–33] He defined a set of fundamental diffusion coefficients for the volume-fixed frame in such a way that they exhibit reciprocal relations; this required the use of composite forces (linear combinations of the chemical potential gradients) instead of a single chemical potential gradient as in Eq. (11).

Reciprocal Relations for Solutions of Strong Electrolytes

Here we begin with a set of equations connecting forces and flows for ionic species. We use the reciprocal relations between coefficients in those equations to show that reciprocal relations exist between fundamental diffusion coefficients in certain flow equations for electrically neutral components.[34,35] It is assumed that no external electric field is applied, so that the net electric current is zero. For simplicity the following derivation is restricted to systems containing an un-ionized solvent (denoted by zero) and a total of s ionic species in solution; conclusions regarding the reciprocal relations are not altered if other un-ionized components are present in addition to the solvent. Furthermore, the only neutral components made of ions (salts) considered here will be those composed of only two kinds of ions. A total of $(s-1)$ such salts should be considered when describing diffusion in these systems because the ionic concentrations are in general restricted only by the condition of electroneutrality. For electrolytic solutions, unlike solutions of nonelectrolytes free from chemical reactions, there may be some arbitrariness in the choice of the salt components as a consequence of dissociation.[36] For example, in a system containing the ionic species Na^+, K^+, Cl^-, and Br^- in addition to the un-ionized solvent, any three of the four neutral solute components NaCl, NaBr, KCl, and KBr may be used to describe diffusion in the system. However, some choices may be less convenient than others if they lead to negative amounts of a salt. It is also possible to consider a neutral component composed of two ionic species of like charge, e.g., one mole of K^+ ions and minus one mole of Na^+ ions; terms corresponding to such components are included for generality in the first steps of the following derivation, but they are subsequently eliminated by defining the concentrations of such components to be zero [i.e., by choosing other components for the required $(s-1)$ salts].

We begin with a set of equations[37] expressing each

[29] P. J. Dunlop and L. J. Gosting, J. Phys. Chem. **63**, 86 (1959).
[30] P. J. Dunlop, J. Phys. Chem. **63**, 612 (1959).
[31] D. G. Miller, J. Phys. Chem. **62**, 767 (1958).
[32] D. G. Miller, J. Phys. Chem. **63**, 570 (1959).
[33] D. G. Miller, Chem. Revs. **60**, 15 (1960).
[34] For ternary solutions of electrolytes, a conversion of equations which describe diffusion in terms of ionic species to equations in terms of neutral components has been made by Miller, who considered these transformations for the equation giving the entropy production (see Appendix I of footnote reference 32).
[35] A different description of diffusion of electrolytes (including consideration of electric currents) has been given by B. R. Sundheim, J. Chem. Phys. **27**, 791 (1957).

[36] There is no problem for $s=2$ and for $s=3$; the neutral solutes are considered to be, respectively, a single salt and two salts with a common ion. For $s=4$ two cases may be encountered. If three of the four ionic species have electric charges of the same sign, the neutral solutes are considered to be three salts with a common ion. If two positive and two negative ionic species are present some arbitrariness exists as indicated in the text, where a solution is considered containing ionic species Na^+, K^+, Cl^-, and Br^-. The arbitrariness is generally greater for larger values of s, except when all of the salts have a common ionic species.

[37] Equations expressing forces in terms of flows, instead of flows in terms of forces, are encountered frequently in the literature, and they seem more convenient for the present derivation. Equation (5.13) of footnote reference 14(a) is of this type. Our Eqs. (32) and (33) are identical with equations which have been given by Onsager and Fuoss [see footnote reference 8, Eqs. (4.12.8), (4.12.9), (4.14.1), and (4.15.4), and pp. 2762 and 2763].

By a derivation somewhat similar to that used to obtain Eq. (19) from (12), Eq. (32) may be obtained from the following expression containing flows of all ionic species and of the solvent relative to the mass-fixed frame,

$$-\partial\bar{\mu}_i/\partial x=\sum_{j=0}^{s}(R_{ij})_M(J_j)_M \qquad (i=0,\cdots,s). \quad (32a)$$

To express the $(J_j)_M$ in terms of flows for the solvent-fixed frame, first Eq. (1) is written for frames M and 0. Then terms in this relation are summed over all components and Eq. (2) applied to obtain u_{0M}. Substitution of this expression back into Eq. (1) for frames M and 0 gives the relation

$$(J_j)_M=\sum_{k=0}^{s}[\delta_{jk}-(c_j/\rho)](J_k)_0. \quad (32b)$$

Here δ_{jk} is the Kronecker delta ($\delta_{jk}=1$ if $j=k$ and $\delta_{jk}=0$ if $j\neq k$). Substitution of Eq. (32b) into (32a) gives

$$-\partial\bar{\mu}_i/\partial x=\sum_{k=0}^{s}(R_{ik})_0(J_k)_0 \qquad (i=0,\cdots,s), \quad (32c)$$

in which

$$(R_{ik})_0=(R_{ik})_M-(1/\rho)\sum_{j=0}^{s}c_j(R_{ij})_M. \quad (32d)$$

Because $(J_0)_0=0$ [Eq. (3)], Eqs. (32c) for the ionic species are seen to be identical with Eqs. (32). If a restriction proposed by Onsager [see Eq. (7b) of footnote reference 9] may be applied to the $(R_{ij})_M$ in the form

$$\sum_{j=0}^{s}c_j(R_{ij})_M=0, \quad (32e)$$

it follows from Eq. (32d) that $(R_{ik})_M=(R_{ik})_0$. Then the subscripts 0 and M could be omitted from the R_{ik} and reciprocal relations for the $(R_{ik})_M$ would correspond directly to Eq. (33). To avoid any uncertainty the subscripts 0 are retained on the R_{ik} in the text.

ionic force in terms of ionic flows for the solvent-fixed frame,

$$-\partial\bar{\mu}_i/\partial x=\sum_{k=1}^{s}(R_{ik})_0(J_k)_0 \qquad (i=1,\cdots,s), \quad (32)$$

in which the coefficients are subject to the reciprocal relations

$$(R_{ik})_0=(R_{ki})_0. \quad (33)$$

Here $\bar{\mu}_i$ denotes the electrochemical potential per gram of ionic species i (i.e., its chemical potential per gram plus the product of its charge per gram times the local electrostatic potential).

By use of the principal of conservation of mass, each ionic flow may be expressed in terms of the flows of neutral components,

$$(J_k)_0=M_k\sum_{l=1}^{s}\frac{z_l(J_{kl})_0}{(z_lM_k-z_kM_l)} \qquad (k=1,\cdots,s). \quad (34)$$

Here symbols M_k, M_l, z_k, and z_l denote the ionic weights and electrochemical valences (with sign) of ionic species k and l, and $(J_{kl})_0$ is the flow in g/cm²/sec of neutral component kl. Each component kl is composed of ionic species k and l in relative amounts such that kl is electrically neutral. For generality the sum in Eq. (34) is taken from 1 through s, though in practice only the $(J_{kl})_0$ corresponding to the chosen $(s-1)$ neutral components may be nonzero. Obviously the flow of component kk (a hypothetical neutral "component" formed from one mole of ionic species k and minus one mole of the same ionic species) is zero. Furthermore, the flows of possible neutral components composed of two different ionic species with the same sign of charge are defined to be zero. For use later it should be noted that $(J_{kl})_0\equiv(J_{lk})_0$.

An expression for the chemical potential per gram, μ_{ij}, of neutral component ij is obtained by first writing its chemical potential per mole as a sum of the electrochemical potentials per mole of ionic species i and j, each multiplied by the number of moles of that species in the component. In terms of chemical potentials and electrochemical potentials per gram that expression becomes

$$\mu_{ij}=\frac{(z_jM_i\bar{\mu}_i-z_iM_j\bar{\mu}_j)}{(z_jM_i-z_iM_j)} \qquad \begin{pmatrix}i=1,\cdots,s\\ j=1,\cdots,s\end{pmatrix}. \quad (35)$$

Differentiation of Eq. (35) with respect to x and substitution of Eqs. (32) for the electrochemical potential gradients gives

$$-\partial\mu_{ij}/\partial x=\sum_{k=1}^{s}\frac{[z_jM_i(R_{ik})_0-z_iM_j(R_{jk})_0]}{(z_jM_i-z_iM_j)}(J_k)_0. \quad (36)$$

Use of Eq. (34) to replace the ionic flows by flows of neutral solute components yields the relations

$$-\partial\mu_{ij}/\partial x$$
$$=\sum_{k=1}^{s}\sum_{l=1}^{s}\left\{\frac{z_lM_k[z_jM_i(R_{ik})_0-z_iM_j(R_{jk})_0]}{(z_jM_i-z_iM_j)(z_lM_k-z_kM_l)}\right\}(J_{kl})_0. \quad (37)$$

The trivial terms corresponding to $k=l$ may be omitted by writing the double sum as

$$[\sum_{k=1}^{l-1}\sum_{l=2}^{s}\{\quad\}(J_{kl})_0+\sum_{k=l+1}^{s}\sum_{l=1}^{s-1}\{\quad\}(J_{kl})_0].$$

Because the terms in the second of these double sums are identical to those in the first, except that the values of k and l are interchanged, we may use the knowledge that $(J_{kl})_0\equiv(J_{lk})_0$ and that $\mu_{ij}\equiv\mu_{ji}$, to write Eq. (37) in the desired form:

$$-(\partial\mu_{ij}/\partial x)_{i<j}$$
$$=\sum_{k=1}^{l-1}\sum_{l=2}^{s}(R_{ijkl})_0(J_{kl})_0 \qquad \begin{pmatrix}i=1,\cdots,j-1\\ j=2,\cdots,s\end{pmatrix}, \quad (38)$$

where

$$(R_{ijkl})_0=\frac{z_lM_k[z_jM_i(R_{ik})_0-z_iM_j(R_{jk})_0]+z_kM_l[z_iM_j(R_{jl})_0-z_jM_i(R_{il})_0]}{(z_jM_i-z_iM_j)(z_lM_k-z_kM_l)}. \quad (39)$$

As a consequence of Eq. (33) it can be readily shown that these coefficients are subject to the reciprocal relations

$$(R_{ijkl})_0=(R_{klij})_0. \quad (40)$$

Equations (38) are still unnecessarily complex; they represent $\frac{1}{2}s(s-1)$ relations each containing the flows of $\frac{1}{2}s(s-1)$ neutral solute components. They may be simplified by retaining only those terms corresponding to the $(s-1)$ salts which are selected as independent solute components: the flows of other possible neutral solute components are set equal to zero and the equations for the corresponding forces are omitted. This in no way disturbs the reciprocal relations, Eqs. (40), for the remaining coefficients.

These expressions, for independent forces in terms of independent flows, for the $(s-1)$ salt components may be solved easily by determinants to obtain equations for the flows in terms of the forces. The resulting $(s-1)$ relations become identical with Eqs. 19 if the salt components are renumbered 1, $\cdots$, $s-1$. Furthermore, the coefficients of the force terms (the fundamental diffusion coefficients) in these equations may readily be shown to exhibit reciprocal relations as a consequence of Eqs. (40). Therefore Eqs. (19) and (22) may be applied to solutions of electrolytes if the flows and

chemical potentials are properly identified with neutral salt components as indicated in this subsection.

III. FLOWS RELATIVE TO THE CELL WHEN THE VOLUME CHANGES ON MIXING

If the partial specific volumes of the components depend on concentration, a volume change will generally occur during diffusion. The resulting hydrodynamic, or bulk, flow has no effect on flow equations for reference frames M, 0, and V [e.g., Eqs. (12), (15), (19), (24), and (29)], or on corresponding flow equations for other frames in the same class.[1] A term describing this bulk flow must, however, be included in correct expressions for the flows $(J_i)_C$ relative to the cell-fixed frame, the one generally associated with experimental studies. Consider, for example, a diffusion cell that is closed at the bottom and open at the top, and in which two homogeneous solutions of different composition are placed initially, one above the other, with a sharp boundary between them. During diffusion the liquid at every level in and above the region of the diffusing boundary is subjected to a hydrodynamic flow created by the volume changes occurring below that level. This hydrodynamic flow is in general a function of height in the cell and of time. Above the boundary region the concentration gradients are zero during free diffusion; here the velocities of reference frames M, 0, and V (and of other frames in this class)[1] are identical and equal to the hydrodynamic velocity, which may be observed experimentally as the velocity of the air-liquid meniscus at the top of the solution column. Therefore it is evident that a sum of products of diffusion coefficients times concentration gradients (or chemical potential gradients), which was adequate to describe flows for the reference frames considered in Sec. II, is not adequate to describe flows relative to the cell; without the additional term describing bulk flow such an expression would erroneously predict that $(J_i)_C=0$ in this region where all the concentration gradients are zero. Within the region of the diffusing boundary the velocities u_{MC}, u_{0C}, and u_{VC} are generally not equal, which indicates that the term "bulk velocity" may be defined in a somewhat arbitrary way; a common definition is[8,9] u_{VC}.

In this section we derive equations for $(J_i)_C$ and use them in considering how to measure practical diffusion coefficients correctly when the partial specific volumes depend on composition. First the velocity, u_{RC}, of an arbitrary frame of reference R is expressed in terms of the partial specific volumes, their variation with distance, and the flows in this frame of reference. (Reference frame R will be identified subsequently with frames 0 and V, respectively.) The desired equations for $(J_i)_C$ are then obtained by substituting this expression for u_{RC} into Eq. (1) written in the form

$$(J_i)_C=(J_i)_R+c_iu_{RC} \qquad (i=0,\cdots,q). \quad (41)$$

Some relations for describing diffusion in binary systems when there is a volume change on mixing have been presented by Prager[38] and Crank[39]; their considerations emphasized Fick's second law. In the following derivation the equations are applicable to multicomponent systems, and the term describing bulk flow appears directly as part of the flow equations which are generalizations of Fick's first law.

Velocity of an Arbitrary Frame of Reference R Relative to the Cell

By differentiating Eq. (41) with respect to x at constant time, multiplying by $\bar{v}_i$, and summing over all components, one obtains

$$\sum_{i=0}^{q}\bar{v}_i\left[\frac{\partial(J_i)_C}{\partial x}\right]_t=\sum_{i=0}^{q}\bar{v}_i\left[\frac{\partial(J_i)_R}{\partial x}\right]_t+\left(\frac{\partial u_{RC}}{\partial x}\right)_t\sum_{i=0}^{q}\bar{v}_ic_i$$
$$+u_{RC}\sum_{i=0}^{q}\bar{v}_i\left(\frac{\partial c_i}{\partial x}\right)_t. \quad (42)$$

The third term on the right is zero because

$$\sum_{i=0}^{q}\bar{v}_i(\partial c_i/\partial x)_t=-\sum_{i=0}^{q}c_i(\partial\bar{v}_i/\partial x)_t=0, \quad (43)$$

where the first equality is obtained by differentiation of Eq. (6) with respect to x, and the second equality is a consequence (when temperature and pressure are constant) of the relation[40] for partial specific volumes analogous to the Gibbs-Duhem equation. That the term on the left of Eq. (42) is also zero may be shown by substitution of the continuity equation which, when written for the cell coordinate system, has the form

$$(\partial c_i/\partial t)_x=-[\partial(J_i)_C/\partial x]_t. \quad (44)$$

The resulting sum, $-\sum\bar{v}_i(\partial c_i/\partial t)_x$, can be shown to be zero by a route analogous to the derivation of Eq. (43). Thus Eq. (42) reduces, after application of Eq. (6) and changing the subscripts from i to j, to

$$(\partial u_{RC}/\partial x)_t=-\sum_{j=0}^{q}\bar{v}_j[\partial(J_j)_R/\partial x]_t. \quad (45)$$

An expression for u_{RC} may be obtained by integrating Eq. (45) by parts. Because some boundary conditions must be assumed in order to obtain a usable relation, we consider here the familiar case of free diffusion in a rectangular cell which is closed at the bottom and open at the top; then, if the positive direction of x is downward, as $x\to+\infty$ we have $u_{RC}\to0$ and every $J_i\to0$. Integration subject to these boundary conditions leads to the result

$$u_{RC}=-\sum_{j=0}^{q}\bar{v}_j(J_j)_R+\int_{+\infty}^{x}\sum_{j=0}^{q}(J_j)_R(\partial\bar{v}_j/\partial x)_t\,dx. \quad (46)$$

Similar expressions corresponding to other boundary conditions are readily obtained if desired. One can see

[38] S. Prager, J. Chem. Phys. **21**, 1344 (1953).

[39] J. Crank, *The Mathematics of Diffusion* (Oxford University Press, New York, 1956), p. 236 ff.

[40] See, for example, K. Denbigh, *The Principles of Chemical Equilibrium* (Cambridge University Press, New York, 1955), Eq. (2.114).

from Eqs. (46) and (4) that $u_{VC}=0$ if the $\bar{v}_j$ are constants; this has been pointed out previously.[3,9]

Equations for Flows Relative to the Cell

A general relation for $(J_i)_C$ in terms of flows relative to the arbitrary frame of reference R is obtained by using Eq. (46) to eliminate u_{RC} from Eq. (41). In writing this result it is possible to express the derivatives $(\partial\bar{v}_j/\partial x)_t$ in terms of concentration gradients of the solutes because at constant temperature and pressure, the $\bar{v}_j$ are functions only of the q solute concentrations

$$(J_i)_C=(J_i)_R-c_i\sum_{j=0}^{q}\bar{v}_j(J_j)_R$$
$$+c_i\int_{+\infty}^{x}\sum_{j=0}^{q}(J_j)_R\sum_{l=1}^{q}(\partial\bar{v}_j/\partial c_l)_{c_{m\neq l}}(\partial c_l/\partial x)dx. \quad (47)$$

Here the subscript $c_{m\neq l}$ on $(\partial\bar{v}_j/\partial c_l)$ indicates that all concentrations except c_l and c_0 are held constant during the differentiation. Before Eq. (47) may be used in connection with experimental studies, flows relative to frame R must be replaced by terms containing concentration gradients and practical diffusion coefficients; this will be done here only for frames 0 and V, although it may be done also for other frames in this class.[1]

To consider the solvent-fixed frame, Eqs. (3) and (24) are introduced into Eq. (47) after changing the subscripts R to 0. This leads to the relation

$$(J_i)_C=-\sum_{k=1}^{q}[(D_{ik})_0-c_i\sum_{j=1}^{q}\bar{v}_j(D_{jk})_0](\partial c_k/\partial x)$$
$$-c_i\int_{+\infty}^{x}\sum_{j=1}^{q}\sum_{k=1}^{q}\sum_{l=1}^{q}(\partial\bar{v}_j/\partial c_l)(D_{jk})_0(\partial c_k/\partial x)(\partial c_l/\partial x)dx, \quad (48)$$

where for brevity the subscript $c_{m\neq l}$ has been omitted on $(\partial\bar{v}_j/\partial c_l)$. One can see from Eq. (30) that the term in brackets equals $(D_{ik})_V$.

An expression for $(J_i)_C$ which contains diffusion coefficients for the volume-fixed frame of reference is obtained by applying Eqs. (30) and (31)–(48),

$$(J_i)_C=-\sum_{k=1}^{q}(D_{ik})_V(\partial c_k/\partial x)$$
$$-c_i\int_{+\infty}^{x}\sum_{j=1}^{q}\sum_{k=1}^{q}\sum_{l=1}^{q}(\partial\bar{v}_j/\partial c_l)[(D_{jk})_V$$
$$+(c_j/c_0\bar{v}_0)\sum_{m=1}^{q}\bar{v}_m(D_{mk})_V](\partial c_k/\partial x)(\partial c_l/\partial x)dx. \quad (49)$$

This equation could have been obtained directly from Eqs. (41) and (46) by letting R denote the volume-fixed frame and applying Eqs. (4), (29), and (43).

To simplify discussion of these equations and their characteristics we write them for binary systems in the form

$$(J_1)_C=-(1-c_1\bar{v}_1)(D)_0(\partial c_1/\partial x)$$
$$-c_1\int_{+\infty}^{x}(\partial\bar{v}_1/\partial c_1)(D)_0(\partial c_1/\partial x)^2dx \quad (50)$$

and

$$(J_1)_C=-(D)_V(\partial c_1/\partial x)-c_1\int_{+\infty}^{x}\frac{\partial\bar{v}_1}{\partial c_1}\frac{(D)_V}{(1-c_1\bar{v}_1)}\left(\frac{\partial c_1}{\partial x}\right)^2dx. \quad (51)$$

Here $(D)_0\equiv(D_{11})_0$ denotes the diffusion coefficient of the solute for the solvent-fixed frame, and $(D)_V\equiv(D_{11})_V$ denotes the mutual diffusion coefficient (which is the same for both components)[9,41,42] for the volume-fixed frame.

The integrals in Eqs. (48) and (49) [or (50) and (51)] are identical, as can be seen by referring to Eq. (31). That the negative of the integral in Eq. (49) equals the bulk velocity u_{VC} may be shown by applying Eqs. (4), (29), and (43) to Eq. (46); the last term in Eqs. (48)–(51) is therefore the bulk flow c_iu_{VC} of component i. The integrals in these equations obviously are zero if the partial specific volumes of the solutes are constant, in agreement with some previous[3,9] considerations of the mean volume velocity or bulk velocity. However, the terms containing these integrals also may be neglected if the partial specific volumes depend on the concentrations, provided that each Δc_k (the concentration difference of solute k between the two solutions used to form the initial boundary) is made sufficiently small. One can readily see this from Eqs. (50) and (51) for the case of binary systems, for which $\partial c_1/\partial x$ is to a first approximation proportional to Δc_1 for a given position and time. Because the first terms of Eqs. (50) and (51) are of order Δc_1, the integral terms, which are of order $(\Delta c_1)^2$, may be neglected for small Δc_1. Therefore if either (a) $\bar{v}_1$ is constant, or (b) Δc_1 is sufficiently small, Eq. (51) reduces to the classical form of Fick's first law, which has been basic to development of procedures for obtaining practical diffusion coefficients from studies of diffusion. Equations (50) and (51) show that such experimental procedures yield directly values of $(D)_V$ [rather than, for example, $(D)_0$]. If each solute in a multicomponent system is subject to restriction (a) or (b), it may be shown similarly that Eqs. (49) reduce to extensions[22,23] of Fick's first law which (for free diffusion in ternary systems) have been used to derive procedures[22–26] for obtaining practical diffusion coefficients. Equations (48) and (49) show that such procedures yield directly values of $(D_{ik})_V$ [not $(D_{ik})_0$]. For experiments in which the $\bar{v}_j$ depend on concentration and the Δc_k are not small, Eqs. (48)–(51) may be used as starting equations from which to develop new procedures for the correct determination of practical diffusion coefficients when there is an appreciable change of volume on mixing.

[41] R. P. Wendt and L. J. Gosting, J. Phys. Chem. **63**, 1287 (1959).

[42] See p. 219 ff. of footnote reference 39.

Microwave Spectrum, Structure, and Dipole Moment of Propane

DAVID R. LIDE, JR.*

National Bureau of Standards, Washington 25, D. C.

(Received May 23, 1960)

The microwave spectrum of ordinary propane and five isotopic species have been measured and analyzed. The rotational constants of C_3H_8 are 29 207.36, 8446.07, and 7458.98 Mc, and the dipole moment is 0.083± 0.001*D*. In its equilibrium configuration the molecule has C_{2v} symmetry, with both CH_3 groups staggered with respect to the CH_2 group. The complete structure has been determined by the substitution method. Important parameters are: $r(CC)=1.526\pm0.002$ A, $\angle CCC=112.4°\pm0.2°$; in the CH_2 group, $r(CH)=1.096\pm0.002$ A, $\angle HCH=106.1°\pm0.2°$; in the CH_3 groups, $r(CH)=1.091\pm0.010$ A, $\angle HCH=107.7°\pm1.0°$. The influence of zero-point effects on the structure determination is discussed; these are found to be particularly bad for the CH_3 group, probably because of its large vibrational amplitude.

INTRODUCTION

ALTHOUGH saturated hydrocarbons are commonly considered to be "nonpolar," there is clearly a possibility of finite permanent dipole moments in all but the most symmetric molecules. Recently, the microwave spectrum of isobutane[1,2] has been observed, and its dipole moment was determined to be 0.132 *D*. This suggested that other saturated hydrocarbons might be amenable to study. It has now been found that the dipole moment of propane is large enough for microwave absorption to be detected. The spectrum of ordinary propane has been measured and analyzed. Five isotopic species have also been studied, and the structure of the propane molecule has been completely determined.

EXPERIMENTAL

The propane spectrum was observed with an 80 kc Stark-modulation spectrograph.[3] Field strengths up to 8000 v/cm were used. All measurements were made at −70°C.

Research grade propane from two different sources was used in the measurements. Samples of $C^{13}H_3CH_2CH_3$ and $CH_3C^{13}H_2CH_3$ in approximately 50% abundance were very kindly provided by Dr. D. P. Stevenson of Shell Development Company. The deuterated samples were prepared by Dr. Max Hellman of the National Bureau of Standards.

NATURE OF THE SPECTRUM

A search for the spectrum of ordinary propane revealed only six lines in the 20–34 kmc region. Each of these was quite sharp and showed a very slow Stark effect. The lines fitted quite naturally into a rigid-rotor series of the type $J_{0J}\rightarrow J_{1,J-1}$ with J ranging from 1 to 6. If absorption coefficient were the only criterion, many additional lines of greater intensity would be expected in the same region. However, the very low dipole moment of propane leads to a rather unusual situation. Calculations show that the ability to achieve sufficient Stark modulation, rather than the intrinsic intensity of the transitions, sets the limit of detectability. The $J_{0J}\rightarrow J_{1,J-1}$ transitions are particularly favorable, since the Stark coefficients tend to be large and, more important, the component with the largest Stark shift ($M=J$) is the most intense one. Even in these transitions it was necessary to depend on one, or at best two components for modulation (in the $J=3$ line the $M=2$ component was partially resolved). One other transition in the accessible frequency range, $0_{00}\rightarrow 1_{11}$, was predicted to have a feasible Stark shift, and this line was detected at 36 666 Mc. No transitions of the type $\Delta J=+1$, $\Delta K=-1$ could be detected with the maximum Stark field available, even when accurate predictions of frequency could be made. Calculations on the most favorable of these transitions showed that the Stark shifts were indeed too small for adequate modulation.

The same considerations apply to the isotopic species of propane. The same transitions were observed here, with the exception of $1_{01}\rightarrow 1_{10}$ which was too weak to be measured. The observed frequencies of all species are listed in Table I.

Although the frequencies follow a rigid-rotor formula sufficiently closely to leave no doubt about the assignment, small centrifugal distortion contributions are present. It was found that a precise fit could be obtained by including a term of the form $k\,J^2(J+1)^2$ in the frequency of the $J_{01}\rightarrow J_{1,J-1}$ transitions. When this term was included, the average deviation between observed and calculated frequencies was about 0.03 Mc for the isotopic species and rather less for ordinary propane. The rotational constants determined in this way are given in Table I.

Some objection might be raised to the introduction of a $J^2(J+1)^2$ centrifugal distortion term without the inclusion of a term in $J(J+1)$. If only a $J(J+1)$

* A part of this research was conducted while the author held a National Science Foundation Senior Postdoctoral Fellowship at the Department of Chemistry, University College London.

[1] D. R. Lide and D. E. Mann, J. Chem. Phys. **29**, 914 (1958).

[2] A. A. Maryott and G. Birnbaum, J. Chem. Phys. **24**, 1022 (1956).

[3] D. R. Lide, D. E. Mann, and R. M. Fristrom, J. Chem. Phys. **26**, 734 (1957).

TABLE I. Observed frequencies and rotational constants (in Mc) for propane and its isotopic species.

Transition	$CH_3CH_2CH_3$	$C^{13}H_3CH_2CH_3$	$CH_3C^{13}H_2CH_3$	CH_2CHDCH_3	$CH_2DCH_2CH_3$ *sym*	$CH_2DCH_2CH_3$ *asy*
$1_{01}\rightarrow 1_{10}$	21 748.37	...	...	...	...	...
$2_{02}\rightarrow 2_{11}$	22 769.74	22 788.80	22 299.03	19 670.78	22 938.16	20 616.12
$3_{03}\rightarrow 3_{12}$	24 365.47	24 315.01	23 961.76	21 445.48	24 324.96	22 137.98
$4_{04}\rightarrow 4_{13}$	26 609.24	26 456.74	26 306.35	23 971.76	26 262.62	24 283.11
$5_{05}\rightarrow 5_{14}$	29 592.51	29 298.58	29 432.48	27 370.09	28 822.23	27 141.90
$6_{06}\rightarrow 6_{15}$	33 414.72	32 933.58	33 446.47	31 759.70	32 083.91	30 811.32
$0_{00}\rightarrow 1_{11}$	36 666.33	36 373.78	36 083.69	33 112.93	35 989.76	34 014.10
a	29 207.36	29 092.05	28 660.50	25 829.94	29 017.79	26 828.97
b	8446.07	8228.77	8447.11	8358.76	7838.32	8123.10
c	7458.98	7281.73	7423.19	7283.00	6971.96	7185.14
k	−0.00228	−0.00155	−0.00317	−0.00225	−0.00188	−0.00319

The uncertainty in the $\Delta J=0$ lines is about 0.03 Mc for ordinary propane and 0.06 Mc for the isotopic species. Because of incomplete modulation, the uncertainty in the $0_{00}\rightarrow 1_{11}$ lines is about twice as large. The rotational constants a, b, c are believed to be accurate to 0.05 Mc for ordinary propane and 0.10 Mc for the isotopic species.

term is used, the fit is poorer and the coefficient turns out abnormally large. The use of both a $J(J+1)$ and $J^2(J+1)^2$ term would obviously permit a better fit than is possible with either term alone, but the improvement would be meaningless because of the limited amount of data. Therefore, it seemed preferable to use a single adjustable parameter and to choose a functional form which gave the best representation of the data. The constant k should thus be regarded as an empirical term which lumps together the effect of several distortion constants.

The manner of handling centrifugal distortion is important only in its possible effect on the rotational constants of propane. If a $J(J+1)$ term is present, its coefficient (D_{JK} in the usual notation) is unlikely to exceed 0.05 Mc. Such a term would alter the rotational constants by a maximum of 0.20 Mc. While this change is larger than the experimental uncertainty, its magnitude should be roughly the same for all isotopic species, so that the isotope shifts, which are important in the structure determination, should not be significantly affected.

STARK EFFECT AND DIPOLE MOMENT

Although the Stark shifts in propane are very small, it was possible to make reasonably good measurements on the $M=J$ components of several lines. Maximum shifts of 2 to 3 Mc were obtained. The observed Stark coefficients are compared with calculated values in Table II; the agreement is quite satisfactory. From this calculation the dipole moment is determined to be

$$\mu=0.083\pm0.001D.$$

INTERNAL ROTATION

The failure to observe a fine structure on the lines in the propane spectrum allows a lower limit of about 2700 cal/mole to be placed on the barrier to internal rotation of a methyl group. This is consistent with the value of 3200 cal/mole obtained by thermodynamic means.[4] It is probable that resolvable splittings occur in the first excited torsional states of propane, and these would permit a precise determination of the barrier height. However, no lines could be detected which might be reasonably assigned as vibrational satellites. The intensities of the torsional satellites are expected to be down by about a factor of 10 from the ground state (if splittings are resolved), and this unfortunately places them just at the threshold of detectability.

EQUILIBRIUM CONFIGURATION OF PROPANE

While there is little doubt about the general configuration of the propane molecule, the arrangement of the methyl groups is not entirely obvious. In principle there are several possible configurations which would lead to different point groups for the complete molecule. The correct choice can be made quite unambiguously from the microwave spectrum of the $CH_2DCH_2CH_3$ species. If the point group is C_{2v}, there will be two distinct substitution points for the D atom, one in the CCC plane and the other out of plane. The spectrum will thus show two rigid-rotor species with statistical weights 1:2. If the point group is C_2 (methyl groups rotated by equal amounts from the C_{2v} position), there will be three distinct species with equal weights. On the other hand the methyl groups might be staggered with respect to each other, giving a C_s

TABLE II. Stark effect of ordinary propane.

Transition	M	$\Delta\nu/\mathcal{E}^2$ [Mc(kv/cm)$^{-2}$] Observed	Calculated[a]
$1_{01}\rightarrow 1_{10}$	1	0.040 ±0.003	0.0425
$2_{02}\rightarrow 2_{11}$	2	0.0485±0.0010	0.0479
$3_{03}\rightarrow 3_{12}$	3	0.0459±0.0015	0.0464

[a] Calculated with $\mu=0.0830D$.

[4] G. B. Kistiakowsky and W. W. Rice, J. Chem. Phys. 8, 610 (1940).

structure. Here one would expect four species with weights 1:2:2:1. More species would result if the symmetry were even lower.

The observed spectrum of $CH_2DCH_2CH_3$ proves that the correct point group is C_{2v}. The two rigid-rotor species which are observed will be designated as *sym* (D atom in CCC plane) and *asy* (out of plane). There are, of course, two arrangements which would result in a C_{2v} structure. From an examination of the actual moments of inertia of the *sym* and *asy* species, it is readily seen that the correct equilibrium configuration is one in which the in-plane H atom on each methyl group is staggered with respect to the methylene CH_2 triangle (i.e., the out-of-plane H atoms of one CH_3 group are eclipsed with respect to the corresponding atoms of the other CH_3 group).[5]

This result has some bearing on the problem of barriers to internal rotation. If there were no interactions between the two CH_3 groups in propane, one would indeed expect, by analogy with ethane and its derivatives, the C_{2v} configuration which has been found here. A strong repulsion between H atoms on different CH_3 groups would tend to force a rotation of the CH_3 groups and thus promote a C_2 structure. If this methyl-methyl repulsion were completely dominant, it would presumably lead to a C_s structure. Since no tendency for the CH_3 groups to rotate from the C_{2v} position is found, one can conclude that methyl-methyl interactions are of minor importance in propane, and that the barrier to internal rotation results principally from interactions between bonds which are only once removed. This conclusion is supported by work on isobutane and other C_{3v} molecules[1], where the methyl-methyl interaction term is found by direct measurement to contribute only a small amount to the barrier.

STRUCTURE

The principal moments of inertia of all isotopic species of propane are collected in Table III. Before discussing the calculation of the structure from these moments, it is worthwhile to inquire into the validity of the rigid-rotor approximation for propane. In the last column of Table III is tabulated the quantity $I_a+I_b-I_c$, which should be invariant to an isotopic substitution in the CCC plane. The observed change in this quantity is small (though experimentally significant) for substitution on either C atom, but is appreciably larger (0.020 amu A^2) for substitution on the *sym* (in-plane) H atom. This rather large change is probably associated with the torsional oscillation of the methyl groups, which leads to unusually large vibrational amplitudes for the methyl H atoms. One can make a rough estimate of this effect in the following way. The sum $I_a+I_b-I_c$ can be regarded as an approximate measure of $\sum m_i\langle z_i^2\rangle$, where z is the coodinate perpendicular to the CCC plane, and the average is taken over the vibrational motion. If we consider only the torsional mode and take this as a harmonic oscillation with a frequency of 250 cm^{-1}, we find that $m\langle z^2\rangle$ is about 0.03 amu A^2 for the in-plane H atom. When deuterium is substituted at this position, $m\langle z^2\rangle$ will increase by about 0.02 amu A^2 (after taking into account the reduced amplitude). While this calculation is very crude, it does show that the observed change in $I_a+I_b-I_c$ has the expected sign and order of magnitude. This effect should be much smaller in the case of carbon substitution because of the smaller vibrational amplitudes. Indeed, the observed change in $I_a+I_b-I_c$ is here negative, as is usually found in planar molecules.

TABLE III. Principal moments of inertia (in amu A^2).

Species	I_a	I_b	I_c	$I_a+I_b-I_c$[a]
$CH_3CH_2CH_3$	17.3083	59.8540	67.7748	9.3875
$C^{13}H_3CH_2CH_3$	17.3769	61.4346	69.4246	9.3869
$CH_3C^{13}H_2CH_3$	17.6386	59.8466	68.1016	9.3836
CH_3CHDCH_3	19.5715	60.4792	69.4125	10.6382
$CH_2DCH_2CH_3$ (*sym*)	17.4214	64.4948	72.5092	9.4070
$CH_2DCH_2CH_3$ (*asy*)	18.8427	62.2337	70.3578	10.7186

[a] Experimental uncertainty in $I_a+I_b-I_c$ is about 0.0010.

[5] We cannot exclude the possibility of a small potential hump in the planar position. However, a significant potential maximum would probably show up in the spectrum in other ways.

The structure of the propane molecule is described by nine independent parameters, after taking advantage of the known C_{2v} symmetry. A total of 18 moments of inertia are available for the various isotopic species, but only 13 of these are independent if the rigid-rotor conditions are invoked. One might attempt to fit the 13 moments to the nine parameters by a least-squares procedure. However, experience has shown that such a calculation is likely to give a rather poorly defined solution. Moreover, there are numerous ways in which the rigid-rotor conditions can be introduced, and each combination will give a different solution because of zero-point effects. A more satisfactory way of carrying out the structure calculation has been proposed by Kraitchman[6] and analyzed in detail by Costain.[7] This "substitution" method uses the isotope shifts in the moments to determine the structural parameters, while making no attempt to fit the actual values of the moments. Although the precise interpretation of the substitution parameters is not yet clear, the method has the great advantage of being straightforward and less subject to arbitrary choices in handling the data. Consequently, the substitution method has been used for propane.

It was pointed out by Kraitchman[6] that isotopic substitution of a single atom in a rigid molecule yields directly the Cartesian coordinates of that atom in the principal axis system of the original molecule. The results can be written as follows for the completely

[6] J. Kraitchman, Am. J. Phys. **21**, 17 (1953).
[7] C. C. Costain, J. Chem. Phys. **29**, 864 (1958).

general case

$$x^2=\mu^{-1}\Delta P_x\{1+[\Delta P_y/(I_z-I_y)]\}\{1+[\Delta P_z/(I_z-I_z)]\}, \quad (1)$$

where

$$\Delta P_x=\tfrac{1}{2}(-\Delta I_x+\Delta I_y+\Delta I_z). \quad (2)$$

Here ΔI_x, ΔI_y, ΔI_z are isotope shifts in the respective moments; I_x, I_y, I_z are moments of the original molecule; and $\mu=M\Delta m/(M+\Delta m)$. The expressions for y^2 and z^2 and for ΔP_y and ΔP_z are obtained by cyclic permutation of x, y, z in Eqs. (1) and (2).

In discussing the propane structure, we shall identify the coordinates x, y, z in Eq. (1) with the principal axes a, b, c, respectively. The y axis is thus the twofold symmetry axis and the xy plane contains the three carbon atoms. H_s refers to the methyl hydrogen atom which lies in the xy plane and H_a to one of the out-of-plane methyl hydrogens. The "original" molecule is ordinary propane, $C^{12}{}_3H_8$.

A straightforward application of Eq. (1) gives the coordinates which are listed in Table IV. The interatomic distances and angles obtained from this set of coordinates are given in the "I_x, I_y, I_z" column of Table V. Now in this calculation *all* experimental isotope shifts were used, even those which should be zero in the rigid-rotor approximation. However, if the rigid-rotor invariants are assumed to apply, most of the atoms can be located without using the full data. For an atom in the xy plane we need only two experimental ΔI's plus the relation $\Delta I_x+\Delta I_y-\Delta I_z=0$, and similarly for an atom in the yz plane. Thus the symmetry elements of propane introduce an ambiguity into the structure calculation, but in this case a rather useful ambiguity, since it provides a check on the consistency of the substitution method.

TABLE IV. Substitution coordinates for propane.[a]

Atom	x	y	z
C_1	1.2682	0.2698	0
C_2	0	−0.5819	0
$H(CH_2)$	0	−1.2381	0.8757
$H_s(CH_2)$	2.1664	−0.3412	0
$H_a(CH_2)$	1.2976	0.9172	0.8809

[a] Where an atom is known to be in a plane of symmetry, the out of plane coordinate has been assumed zero.

In Table V the interatomic distances and angles computed from the various pairs of moments are compared with the structure (I_x, I_y, I_z) obtained by direct application of Eq. (1). The agreement of the four solutions is very good for the carbon-carbon and methylene parameters, where the bond distances vary over a range of less than 0.003 A. A much larger variation occurs with the methyl group; values of the CH_s distance cover a range of almost 0.02 A and the CCH_s angle varies by 1.5°. The greater spread of the methyl parameters is, of course, a consequence of the large zero-point effects in the $CH_2DCH_2CH_3$ species, which have already been discussed. This uncertainty is probably quite general and may well place a fundamental limitation on the precision with which CH_3 structures in this type of molecule can be determined by existing methods. Indeed, it has already been pointed out that the large differences in CH_3 structures reported for various molecules are open to suspicion.[8]

TABLE V. Propane structures calculated from various combinations of moments.

	I_x, I_y, I_z	I_x, I_y	I_y, I_z	I_x, I_z
r(CC)	1.5277 A	1.5263	1.5252	1.5256
∠CCC	112.24°	112.36°	112.50°	112.48°
CH_2 group:				
r(CH)	1.0943	1.0952	1.0971	1.0963
∠HCH	106.32°	106.16°	105.90°	106.04°
CH_3 group:				
$r(CH_s)$	1.0863	1.0970	1.0799	1.0930
∠CCH_s	111.90°	111.36°	112.81°	111.28°

It is difficult to find arguments for preferring any one of the structures in Table V to the other sets. In order to select a "best" structure for propane, we have averaged the four values and extended the limits of error to include all individual values. The final recommended structure is given in Table VI. It should be emphasized that the uncertainties quoted here refer to the self-consistency of the structure as determined by the substitution method. No direct measure can be obtained for the uncertainty in the parameters which involve the H_a atom; however, it is probably comparable to that found for the analogous H_s parameters. The strictly experimental uncertainties are in all cases much smaller than the limits of error given in Table VI.

The moments of ordinary propane which are calculated from the coordinates in Table IV are 17.205, 59.542, and 67.397 amu A². The percentage differences

TABLE VI. Best structure for propane.

r(CC)	=1.526±0.002 A	
∠CCC	=112.4°±0.2°	
CH_2 group:		
r(CH)	=1.096±0.002	
∠HCH	=106.1°±0.2°	
CH_3 group:		
$r(CH_s)$	=1.089±0.009	Av. r(CH)=1.091±0.010
$r(CH_a)$	=1.094	
∠H_aCH_a	=107.3°	Av. ∠HCH=107.7°±1.0°
∠H_aCH_s	=108.1°	
∠CCH_s	=111.8°±1.0°	
∠CCH_a	=110.6°	

[8] V. W. Laurie, J. Chem. Phys. **28**, 704 (1958).

between observed and calculated moments are 0.60, 0.52, and 0.56% for I_a, I_b, and I_c, respectively. Therefore, if we expand the distances in Table VI by a factor of 1.003, the absolute values of the moments of all species can be reproduced to a fairly high accuracy (about 0.03 amu A^2). However, this procedure is quite arbitrary, and it seems preferable to retain the actual substitution distances until the nature of the vibration-rotation interactions is better understood.

DISCUSSION

The CC distance in propane is essentially identical with that found in isobutane (1.525 A) by the substitution method.[9] However, recent electron diffraction measurements[10] on the normal hydrocarbons from C_4H_{10} to C_7H_{16} have given CC distances in the range 1.531–1.534 A, with a stated uncertainty of 0.002 A (although a different determination[11] on C_4H_{10} yielded 1.539±0.003 A). The difference between the microwave and electron diffraction results appears to be well outside the stated limits of error of either method; this point is discussed in the succeeding paper.[9] The CCC angles in the higher normal paraffins fall in the range 111.9°–112.9°, in satisfactory agreement with the propane angle of 112.4°.

The structure of the methylene group in propane is very well determined. The CH distance is close to the accepted value for methane[12] (1.094 A). It is interesting to note that the HCH angle is 3.4° smaller than the tetrahedral value, while the CCC angle is 2.9° larger than tetrahedral; this behavior may be explained on the basis of changes in the hybridization of the carbon orbitals.[13]

The CH_3 group in propane is not so well defined as the rest of the molecule. The apparent difference in the H_s and H_a parameters could easily be due to the large zero-point effects. Since there is no real evidence for asymmetry in the CH_3 group, we have given in Table VI average values for the CH distance and HCH angle. In spite of the larger uncertainties here, there seems little doubt that the HCH angle is smaller than tetrahedral.

The near-symmetry of the CH_3 group can be demonstrated by computing the two distinct H–H distances, which are found to be 1.762 and 1.765 A. The orientation of the symmetry axis of the CH_3 group is of some interest. Using the coordinates in Table IV, one finds that the line joining the center of the H_3 triangle to atom C_1 makes an angle of 1.4° with the C_1—C_2 bond (the axis is tilted such that the out-of-plane atoms of one CH_3 group are brought closer to the corresponding atoms of the other CH_3 group). Furthermore, the CC bond lies only 0.7° from the perpendicular to the plane defined by the three H atoms. Since we have seen that zero-point effects cause an uncertainty of about 1° in the angles defining the CH_3 group, these figures are not very significant. However, it does appear that we can safely rule out a deviation of more than 2° or 3° between the methyl axis and the CC bond.

[9] D. R. Lide, J. Chem. Phys. **33**, 1519 (1960).
[10] R. A. Bonham, L. S. Bartell, and D. A. Kohl, J. Am. Chem. Soc. **81**, 4765 (1959).
[11] K. Kuchitsu, Bull. Chem. Soc. Japan **32**, 748 (1959).
[12] G. Herzberg, *Infrared and Raman Spectra* (D. Van Nostrand Company, Inc., Princeton, New Jersey, 1945), p. 439.
[13] C. A. Coulson, *Valence* (Oxford University Press, London, 1953), pp. 194–196.

THE JOURNAL OF CHEMICAL PHYSICS VOLUME 33, NUMBER 5 NOVEMBER, 1960

Structure of the Isobutane Molecule; Change of Dipole Moment on Isotopic Substitution

DAVID R. LIDE, JR.

National Bureau of Standards, Washington 25, D. C.

(Received May 23, 1960)

The microwave spectra of 5 isotopic species of isobutane have been measured and analyzed. The isobutane molecule is shown to belong to point group C_{3v}. The structural parameters determined by the substitution method are $r(CC)=1.525$ A, $\angle CCC=111.15°$, $r(CH)=1.108$ A (tertiary), $r(CH)=1.09-1.10$ A (methyl), $\angle HCH=107.5°-109.5°$. The structure is compared with that of other hydrocarbons, and it is suggested that a small systematic difference exists between CC distances determined by microwave and electron diffraction methods. Accurate Stark measurements show that the dipole moment of $(CH_3)_3CD$ is $6.5\%\pm0.9\%$ higher than that of $(CH_3)_3CH$.

THE microwave spectrum of the common isotopic species of isobutane has been previously reported from this laboratory.[1] Since this species is a symmetric rotor, only one moment of inertia could be experimentally determined, so that little information was obtained on the structure of the molecule. Measurements have now been carried out on 5 additional isotopic species, and the resulting moments of inertia permit an essentially complete structure determination.

The spectra were observed on a Stark-modulation spectrometer with a minimum detectable absorption coefficient of about 10^{-9} cm^{-1}. All measurements were made at -70°C. The C^{13} species were studied in samples enriched to about 50%.

Only the $J=1\rightarrow2$ transitions were measured in the isotopic species; the $J=0\rightarrow1$ line has been observed for the common species,[1] but is too weak for accurate measurement in the isotopic samples. The $(CH_3)_3C^{13}H$ and $(CH_3)_3CD$ species are symmetric rotors and therefore show a single $J=1\rightarrow2$ line, similar to that of the common species.[2] The other isotopic species are asymmetric rotors, but are near the oblate symmetric limit. The $J=1\rightarrow2$ pattern consists of three lines (type-c selection rule), which are readily identified by their characteristic Stark effects.

The observed frequencies and rotational constants for all species are listed in Tables I and II. In calculating the rotational constants it has been assumed for all species that $D_J=0.011$ Mc, the value found in the common species.[1] D_{JK} has been assumed zero. The experimental uncertainties given for the rotational constants do not include the effect of possible isotopic changes in the centrifugal distortion coefficients; however, errors from this source should have a negligible influence on the structure determination.

EQUILIBRIUM CONFIGURATION

It has already been shown[1] that $(CH_3)_3CH$ has a threefold symmetry axis; i.e., the molecule belongs either to point group C_3 or C_{3v}. The exact point group depends on the equilibrium position of the methyl groups, which may be determined by a study of the $(CH_2D)(CH_3)_2CH$ species. If the point group is C_3, there are 3 distinct substitution points on the methyl group, and the spectrum of $(CH_2D)(CH_3)_2CH$ will show 3 distinct rigid-rotor species. For a C_{3v} model there are only 2 distinct rotational species, a *sym* one with D atom located in a symmetry plane and an *asy* one with the D atom out of plane. The spectrum of the *asy* species will be twice as intense as that of the *sym* species because of the two equivalent out-of-plane positions.

The observed spectrum of $(CH_2D)(CH_3)_2CH$ shows unambiguously that the correct point group is C_{3v}. Furthermore, we can conclude from the actual moments of inertia of the *sym* and *asy* species that each methyl group is oriented such that one CH bond is staggered with respect to the two CC bonds opposite it. Thus the repulsion between H atoms on different methyl groups is not strong enough to force the methyl groups out of the C_{3v} configuration.[3] This conclusion is consistent with the study of torsional satellites in isobutane,[1] where it was found that terms in the internal potential function which represent interactions among the methyl groups were relatively small.

STRUCTURE

In discussing the structure of isobutane the carbon atom which is located on the threefold symmetry axis will be designated as C_2, and one of the off-axis carbons as C_1. The tertiary hydrogen atom, H_t, is attached to C_2; one of the methyl hydrogens, H_s, lies in a symmetry plane of the molecule, while the other two, designated jointly by H_a, lie at equal distances on each side of the symmetry plane. We define a coordinate system xyz with origin at the center of mass of the common species, $(CH_3)_3CH$. The z axis coincides with

[1] D. R. Lide and D. E. Mann, J. Chem. Phys. **29**, 914 (1958).
[2] Under normal modulation conditions only the $K=1\rightarrow1$ transition is observed.
[3] This is contrary to the conclusion of Wilmshurst and Bernstein, Can. J. Chem. **35**, 969 (1957), who assigned the vibrational spectrum of isobutane on the basis of a C_3 model. A part of their assignment now requires revision.

TABLE I. Frequencies and constants for symmetric-rotor species (in Mc).

	$(CH_3)_3CH$[a]	$(CH_3)_3C^{13}H$	$(CH_3)_3CD$
$\nu(J=1\rightarrow2)$	31 157.46±0.03	31 095.18±0.10	30 162.95±0.05
b	7789.45±0.01	7773.88±0.03	7540.82±0.01

[a] From footnote reference 1.

TABLE II. Frequencies and constants for asymmetric-rotor species (in Mc).

	$(C^{13}H_3)(CH_3)_2CH$	*sym* $(CH_2D)(CH_3)_2CH$	*asy* $CH_2D(CH_3)_2CH$
$\nu(1_{01}\rightarrow2_{11})$	30 426.24±0.10	29 765.6 ±1	29 560.45±0.05
$\nu(1_{10}\rightarrow2_{20})$	30 682.00±0.10	30 031.28±0.10	30 147.92±0.05
$\nu(1_{11}\rightarrow2_{21})$	30 910.58±0.10	30 266.06±0.20	30 607.11±0.05
a	7788.28±0.05	7629.15±0.2	7782.70±0.03
b	7546.10±0.05	7378.95±0.4	7259.37±0.03
c	4431 ±45	4466 ±140	4319 ±7

the threefold symmetry axis and has the sense $C_2\rightarrow H_t$, and the xz plane is defined by the atoms C_1, C_2, H_t.

The moments of inertia of the various isobutane species are collected in Table III. These moments have been used to calculate a structure by the "substitution" method, as described by Kraitchman[4] and Costain.[5] In this method the coordinates of each atom (in the xyz frame) are determined from the isotope shifts in the moments of the species which is substituted at that point. The expressions for the coordinates have been given by Kraitchman.[4]

The coordinates obtained in this way are listed in Table IV. Actually, the structure is not completely fixed, since in a symmetric rotor molecule one can obtain (with a single substitution) only the distance of the atom from the symmetry axis, $(x^2+y^2)^{\frac{1}{2}}$, and not x and y separately. The y coordinates of all atoms except H_a are zero by definition, but some further assumption is necessary in order to locate H_a. We have assumed that the three H atoms of a CH_3 group form an equilateral triangle,[6] a condition which is very nearly satisfied in the propane molecule.[7]

The interatomic distances and angles may be readily calculated from these coordinates, and they are listed in Table V. The possible errors resulting from strictly experimental uncertainties in the moments of inertia are included in Table V. However, it is probable that nonrigidity effects introduce somewhat larger uncertainties. In a similar study of propane[7] the structure calculation was overdetermined, and it was possible to estimate the magnitude of these nonrigidity effects. The CC distance was found to be uncertain by about ±0.002 A and the CCC angle by ±0.2°. The methyl group was not as well determined, with an uncertainty of ±0.01 A in the CH distance and ±1° in the HCH angle. Although the geometry of the two molecules is quite different, it is reasonable to expect uncertainties of at least this magnitude in the isobutane structure. The tertiary CH distance in isobutane should be as well determined as the CC distance.

It is usually found that moments of inertia calculated from substitution coordinates are somewhat less than the observed I^0. The coordinates in Table IV yield $I_b=64.521$ and $I_c=111.283$ for $(CH_3)_3CH$. The calculated I_b is thus about 0.6% less than the observed, while the calculated I_c is 0.7 to 1.1% smaller. This is rather similar to the situation with propane, where all three calculated moments were in the range 0.5–0.6% less than the observed.

DISCUSSION OF STRUCTURE

The isobutane structure provides interesting comparisons with other simple hydrocarbons. The comparison with propane[7] is at present the most reliable one, since the two structures were obtained by the same method. The CC distances in propane and isobutane (1.526 A and 1.525 A, respectively) are identical within the estimated precision of 0.002 A. The most accurate spectroscopic structure for ethane comes from the infrared study of Allen and Plyler.[8] However, the result given by them is not a true substitution structure, since only two isotopic species, C_2H_6 and C_2D_6, were available. The isotope shift in I_b fixes the quantity $z^2+\frac{1}{2}y^2$ for the H atoms, where z is measured along the threefold symmetry axis and y is perpendicular to this axis. The value of this quantity (1.8657 A^2) may be regarded as a valid substitution parameter. Now it has been pointed out that the moments calculated from the substitution parameters of propane and isobutane are all about 0.6% smaller than the observed ground-state moments. If we assume that the same ratio applies to ethane, then

[4] J. Kraitchman, Am. J. Phys. **21**, 17 (1953).
[5] C. C. Costain, J. Chem. Phys. **29**, 864 (1958).
[6] If we make the equally reasonable assumption that the CH_t and CH_a distances are identical, the H_aCH_a and H_aCH_t angles become 109.8° and 107.8°, respectively.
[7] D. R. Lide, J. Chem. Phys. **33**, 1514 (1960).
[8] H. C. Allen and E. K. Plyler, J. Chem. Phys. **31**, 1062 (1959).

we predict that the calculated $I_b^s = I_b^0 \div 1.006 = 25.255$ amu A^2 for C_2H_6. This I_b^s and the value of $z^2 + \frac{1}{2}y^2$ fix the substitution CC distance at 1.526 A, in excellent agreement with the values for propane and isobutane.

There is no theoretical justification for the above assumption, and the agreement may be fortuitous. However, if we tentatively accept the results of this calculation as the best available estimate for the substitution structure of ethane, then we may conclude that the substitution CC distance is quite constant at 1.526±0.002 A in the simple paraffin hydrocarbons. On the other hand, recent electron diffraction measurements[9] on the normal paraffins from C_4H_{10} to C_7H_{16} have yielded CC distances in the range 1.531–1.534 A, and an electron diffraction value of 1.536 A has been reported[10] for ethane itself. There is a strong suggestion, then, of a systematic difference of 0.005–0.010 A between CC distances determined by isotopic substitution and diffraction methods. It is not surprising, of course, that a difference should exist, in view of the different nature of the averaging over vibrational motions. It will be interesting to see whether a similar effect is found with other interatomic distances.

TABLE III. Moments of inertia (in amu A^2).

Species	I_a	I_b	I_c
$(CH_3)_3CH$		64.8994	(112.3)[a]
$(CH_3)_3C^{13}H$		65.0294	
$(CH_3)_3CD$		67.0392	
$(C^{13}H_3)(CH_3)_2CH$	64.9092	66.9924	114.1
$(CH_2D)(CH_3)_2CH$ (*sym*)	66.2631	68.5099	113.2
$(CH_2D)(CH_3)_2CH$ (*asy*)	64.9557	69.6384	117.05

[a] Calculated from $I_a - I_b + I_c$ of asymmetric-rotor species.

The CCC angle of 111.15° in isobutane may be compared with 112.4° in propane. The difference is quite real, and there is no obvious explanation.

The tertiary CH distance in isobutane, 1.108 A, compares with 1.096 A in the CH_2 group of propane. Both of these distances are well determined, and there is little doubt of the experimental significance of the 0.012 A difference. A tendency toward long carbon-halogen bonds in tertiary butyl halides has also been noticed.[1] The methyl group in isobutane is not well determined, and we can conclude only that it has a fairly normal structure, with CH distance in the range 1.09–1.10 A and HCH angle of 107.5–109.5°. No information has been obtained on the orientation of the CH_3 axis with respect to the CC bond.

DIPOLE MOMENT OF $(CH_3)_3CD$

The dipole moment of the common isotopic species of isobutane has been previously determined[1] from the Stark effect of the $J=1\rightarrow2$, $K=1\rightarrow1$, $M=1\rightarrow1$ transition. A dipole-moment measurement has now been carried out on $(CH_3)_3CD$. The measurement took the form of a direct comparison between the Stark shifts of the same transition in the two isotopic species. The first-order Stark effect of this transition is given by

$$\Delta\nu_{\pm} = \pm(1/3)\mu\mathcal{E},$$

where μ is the dipole moment and $\mathcal{E}$ the electric field strength. For measurements made on the two species at the same field strength we have

$$\mu_D/\mu_H = (\Delta\nu_+ - \Delta\nu_-)_D \div (\Delta\nu_+ - \Delta\nu_-)_H,$$

where subscripts H and D refer to $(CH_3)_3CH$ and $(CH_3)_3CD$, respectively. In this form the measurement is not influenced by the second-order Stark effect and is not, of course, dependent on an absolute calibration of the field strength.

Measurements were carried out by admitting $(CH_3)_3CH$ and $(CH_3)_3CD$ alternately to the same waveguide cell and observing the frequency of the positive and negative Stark components at a given applied voltage. Zero-based square-wave modulation was used, and the applied voltage was measured with a peak-reading voltmeter. The accuracy of the measurement of μ_D/μ_H depends only on the precision of the frequency measurements and the accuracy with which the applied voltage could be reset to a given value over short time intervals.

The results of a series of measurements at several voltages are given in Table VI. The ratio μ_D/μ_H is found to be 1.065±0.009, and using the previous value[1] of 0.132 D for μ_H, we have $\mu_D - \mu_H = 0.0086 \pm 0.0012$ D.

TABLE IV. Coordinates of atoms in $(CH_3)_3CH$.

Atom	x	y	z
C_1	1.4529 A	0	−0.1018
C_2	0	0	0.3630
H_t	0	0	1.4706
H	1.4850	0	−1.2015
H_a	(1.9853)[a]	(0.8863)[a]	0.2500

[a] Calculated on the assumption that the H atoms of a CH_3 group form an equilateral triangle. The experimentally determined quantity is $(x^2+y^2)^{\frac{1}{2}} = 2.1742$ A.

TABLE V. Structure of isobutane.

Parameter	Value	Expt. uncert.[a]
r(CC)	1.525 A	±0.001 A
∠CCC	111.15°	±0.10°
$r(CH_t)$	1.108	±0.001
$r(CH_a)$	1.100	±0.003
∠CCH_a	109.4°	±0.3°
$r(CH_a)$	(1.092)[b]	
∠H_aCH_a	(108.5°)[b]	
∠H_aCH_a	(107.9°)[b]	

[a] Does not include nonrigidity effects; see text.
[b] Based on assumption that H atoms form equilateral triangle.

[9] R. A. Bonham, L. S. Bartell, and D. A. Kohl, J. Am. Chem. Soc. **81**, 4765 (1959).
[10] A. Almenningen and O. Bastiansen, Acta Chem. Scand. **9**, 815 (1955).

TABLE VI. Stark effect of $(CH_3)_3CH$ and $(CH_3)_3CD$.

Stark voltage[a]	$(CH_3)_3CH$ $\Delta\nu_+$	$(CH_3)_3CH$ $\Delta\nu_-$	$(CH_3)_3CD$ $\Delta\nu_+$	$(CH_3)_3CD$ $\Delta\nu_-$	$(\Delta\nu_+-\Delta\nu_-)_D \div (\Delta\nu_+-\Delta\nu_-)_H$
147 V	7.86 Mc	−7.84	8.31	−8.41	1.065
199	10.59	−10.66	11.45	−11.29	1.070
200	10.65	−10.69	11.50	−11.35	1.071
300	16.20	−16.03	17.09	−17.17	1.063
350	18.94	−18.86	19.95	−19.95	1.056
					Av 1.065

[a] Stark electrode spacing was 0.412 cm.

Small changes in dipole moment have been reported for a few other deuterated molecules, but the present result on isobutane appears to be the most accurate measurement which has been made so far. The interpretation of these isotopic changes has been discussed by Bell and Coop[11] and by Halevi.[12] For a diatomic molecule we have as a first approximation

$$\mu_D-\mu_H=(\partial\mu/\partial r)(\bar{r}_D-\bar{r}_H),$$

where $\bar{r}$ is the average internuclear distance in a particular state and $\partial\mu/\partial r$ is evaluated at the equilibrium distance. Here μ is understood to mean the absolute magnitude of the dipole-moment vector. This expression should be applicable to isobutane, since (in this approximation) the C—H stretching mode is expected to make the chief contribution to the dipole-moment change. Since the observed value of $\mu_D-\mu_H$ is positive, and there is little doubt that $\bar{r}_D-\bar{r}_H$ is negative, we conclude that $\partial\mu/\partial r$ is negative.

It is more difficult to make quantitative deductions from the change of dipole moment. Infrared intensity measurements on methane lead to a value of about 0.7 debye/A (sign undetermined) for $\partial\mu_{CH}/\partial r$ in that molecule.[13] If this *bond moment* derivative can be transferred to isobutane as a total dipole derivative, we obtain $\bar{r}_D-\bar{r}_H=0.01_2$ A. This value appears rather high; for example, spectroscopic data on the diatomic CH and CD molecules lead to a difference[11] of 0.004–0.005 A. However, this calculation is very crude,[14] and the agreement is probably as good as can be expected. It would be interesting to have infrared intensity measurements on isobutane itself to compare with the dipole-moment results.

ACKNOWLEDGMENTS

The author is grateful to Dr. D. P. Stevenson of Shell Development Company for providing the enriched carbon-13 samples and to Dr. Max Hellman of this Bureau for preparing the deuterated compounds. He also wishes to thank the National Science Foundation for a Senior Postdoctoral Fellowship under which a portion of this work was done.

[11] R. P. Bell and I. E. Coop, Trans. Faraday Soc. **34**, 1209 (1938).

[12] E. A. Halevi, Trans. Faraday Soc. **54**, 1441 (1958).

[13] I. M. Mills, Mol. Phys. **1**, 107 (1958).

[14] Higher terms in the dipole-moment expansion, particularly the second derivative of μ with respect to the bending coordinate, may make a significant contribution to $\mu_D-\mu_H$.

THE JOURNAL OF CHEMICAL PHYSICS VOLUME 33, NUMBER 5 NOVEMBER, 1960

A Theory for the Triplet-Triplet Absorption Spectra of Porphyrins

MARTIN GOUTERMAN

Conant Chemical Laboratory, Harvard University, Cambridge, Massachusetts

(Received February 5, 1960)

The triplet excited states of porphin are classified as either singly or doubly excited electron configurations. The latter are discussed in detail in terms of a circular box model with electron interaction plus a perturbation due to the actual molecular shape. The energy and intensity of the triplet-triplet transitions from the lowest triplet to these doubly excited states are predicted to consist of: (1) transitions to a pair of states of energy $\sim$25 000 cm^{-1}; (2) transitions to a group of four states of energy $\sim$20 000 cm^{-1}; and a transition to a state of energy $\sim$18 000 cm^{-1}. The first two groups are predicted to share equally an intensity half that of the porphin Soret band, while the last transition is weakly forbidden. The predictions compare reasonably well with experiment. In addition, a metastable molecular quintet is predicted, with a transition energy to the lowest triplet state slightly smaller than any observed triplet-triplet transition.

I. INTRODUCTION

RECENTLY, Linschitz *et al.*,[1] using improved flash excitation techniques, have measured absorption spectra initiating from the metastable excited state of porphyrin molecules. These spectra were attributed to triplet-triplet transitions. Similar spectra have been taken by other workers.[2] This paper proposes a theory for these transitions for symmetrical porphyrins (e.g., Mg porphin or Zn tetraphenyl porphin), based on an extension of ideas developed in a previous paper.[3]

Section II of this paper discusses the model to be used in our treatment but presents only the qualitative results. Section III gives the detailed mathematical treatment, exposes all its assumptions, and shows the limits to the validity of statements made in Sec. II. Section IV compares the predicted spectrum with experiment.

II. PROPOSED MODEL

Singlet-Singlet Model

The discussions in the author's previous paper[3] have shown that naive molecular orbital (MO) theory is inadequate to explain the singlet-singlet spectra of porphins. Successful predictions required that naive MO theory be modified by ideas initially proposed by Simpson[4] and further developed by Platt.[5] In this section we shall summarize these ideas in a form that is general enough to extend to the interpretation of the triplet-triplet spectra.

Naive MO calculations on porphin yield two top filled orbitals a_{2u} and a_{1u} of different energy.[6] The ground state is the electron configuration $(a_{2u})^2(a_{1u})^2$, i.e., two electrons in each. (The notation leaves out any electrons in orbitals of lower energy.) The lowest empty orbitals are a degenerate pair e_g. Thus the lowest excited states would arise from the electron configurations $(a_{2u})^2a_{1u}e_g$ and $(a_{1u})^2a_{2u}e_g$. The chief fault of the naive theory is its neglect of the electron interaction energy, e^2/r_{ij}, where r_{ij} is the distance between electrons i and j.

A simple way to patch up the naive theory is to identify the porphin orbitals with those of a circular box free electron model, for in the latter the effects of electronic interaction are easier to appreciate. A circular box is described by a radial coordinate r and an angular coordinate θ. Orbitals are written $f(r)\exp(\pm im\theta)$. It has been shown[3] that the orbital pair $(a_{2u}\pm ia_{1u})/\sqrt{2}$ can be identified with the degenerate pair of circular box orbitals $f(r)\exp(\pm i4\theta)$, while the lowest empty e_g orbitals can be identified with $f(r)\exp(\pm i5\theta)$. The first pair is said to have z components of angular momentum $\lambda_z=\pm4$ and angular momentum $\lambda=4$; the second pair, $\lambda_z=\pm5$ and $\lambda=5$.

To see the effects of electron interaction in a circular box, we first construct the molecular states. These may be characterized by a value of total angular momentum along the z axis Λ_z, which is given by the sum of the λ_z for each electron. In the porphin ground state in the circular box model, the orbital pair with $\lambda=4$ are filled with four electrons; this configuration is denoted $(4)^4$ and has $\Lambda_z=0$. The first excited configurations arise by exciting a $\lambda=4$ electron to an orbital with $\lambda=5$, denoted $(4)^35$. This configuration gives rise to degenerate pairs of states with $\Lambda_z=\pm1$ and with $\Lambda_z=\pm9$. The singlet states of different $|\Lambda_z|$ will differ by energy stemming from electron interaction, the pair of lower $|\Lambda_z|$ being at higher energy (Hund's rule). A selection rule says that $\Delta\Lambda_z=\pm1$. Thus the higher energy pair is allowed, the lower energy pair forbidden. The allowed pair is identified with the intense Soret bands of porphin in the near ultraviolet and the forbidden pair with the weak visible bands.

The relation of the circular box model to the naive MO model is the following. If the orbitals a_{2u} and a_{1u}

[1] H. Linschitz and K. Sarkanen, J. Am. Chem. Soc. **80**, 4826 (1958); H. Linschitz and L. Pekkarinen, J. Am. Chem. Soc. **82**, 2407 (1960).

[2] R. Livingston and E. Fujimori, J. Am. Chem. Soc. **80**, 5610 (1958); S. Claesson, L. Lundquist, and B. Holmström, Nature **183**, 661 (1959).

[3] M. Gouterman, J. Chem. Phys. **30**, 1139 (1959).

[4] W. T. Simpson, J. Chem. Phys. **17**, 1218 (1949).

[5] J. R. Platt, *Radiation Biology*, A. Hollaender, editor (McGraw-Hill Book Company, Inc., New York, 1956), Vol. III, Chap. 2.

[6] G. R. Seely, J. Chem. Phys. **27**, 125 (1957).

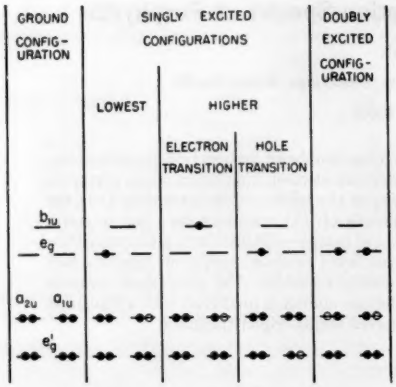

FIG. 1. Electron configurations for the circular box model of porphin. The solid circles show electrons; the empty circles show holes. In the first panel the symmetries of the MO's are indicated.

should differ in energy by an amount small compared to the energy splitting the states of different $|\Lambda_z|$, then it may be shown[3] that the circular box states are the better description of porphin; these are, in fact, 50-50 mixtures of the two lowest excited naive MO states. If a_{2u} and a_{1u} differ by an energy large compared to that splitting the circular box states, then the naive MO states are a better description. Previous work[3] has shown that the circular box model predicts unsuccessfully the observed singlet-singlet spectra of porphin. For this reason and because of its great convenience, we shall use it as a basis for the following discussion of the triplet-triplet spectra.

Triplet-Triplet Model

The electron configuration $(4)^3 5$ gives rise to both singlet and triplet states. The triplets will be separated from the singlets by energy stemming from electron interaction and will lie at lower energy (Hund's rule). Triplet-triplet transitions from this configuration can occur in two ways: transitions to higher singly excited configurations or transitions to a doubly excited configuration. (See Fig. 1.)

We shall not attempt a quantitative estimation of the energies of the higher singly excited states. Such an estimate could not be accurate because of a problem mentioned in the foregoing; namely, the circular box model, which assumes the a_{2u} and a_{1u} orbitals have nearly the same energy, is successful in predicting singlet-singlet spectra, yet naive MO theory predicts a large energy difference. The resolution of this disagreement awaits the application to porphin of a consistent treatment of nitrogen atoms in aromatic rings. Until then, MO theory cannot be relied on for orbital energy differences.

Theory can, however, give some interesting qualitative results on these singly excited configurations. These results follow simply from Fig. 19 of work cited in footnote 3, which shows the orbitals predicted by MO theory, labeled with circular box quantum numbers. If consideration is confined to the orbitals labeled *top filled* and *lowest empty*, there is one set of possible hole transitions (a_{2u}, $a_{1u} \rightarrow e_g'$) and one set of possible electron transitions ($e_g \rightarrow b_{1u}$). (These are indicated in Fig. 1; we have omitted transitions of even parity.) Although the transitions are allowed in porphin, the quantum numbers given in Fig. 19 show that, in the circular box, they are forbidden. Thus we may expect that transitions to higher singly excited configurations will be relatively weak, if they occur in the region of interest.

A further question about singly excited triplet states is of interest, namely how do they return to the unexcited condition; that is, how do they relax. Direct phosphorescence emission of higher excited triplets to the ground state is, in general, unlikely.[7] It is especially so here, as the process is forbidden by symmetry. Relaxation should therefore occur via either a fluorescence or a radiationless transition back to the lowest excited triplet. However both fluorescence and radiationless transitions are fast, and so singly excited states would not appear to be particularly long-lived.

For the doubly excited configuration, attention will be limited to $(4)^2(5)^2$. (See Fig. 1.) This is reasonable since $(4)^3(5)$ is the lowest singly excited configuration and no other is observed down to $\lambda \sim 350$ mμ.[8]

To determine the states that arise from this configuration we shall treat the circular box quantum numbers Λ_z as good. (Even if Λ_z is not rigorously defined, the method will still generate the proper number of states.) Then it can be shown that the following Λ_z values and multiplicities arise from $(4)^2(5)^2$: for $\Lambda_z=0$ there are 2 singlets, 3 triplets, and 1 quintet; for $\Lambda_z=\pm 2$ there is one singlet for each state; for $\Lambda_z=\pm 8$ there is one singlet and one triplet for each state and likewise for $\Lambda_z=\pm 10$; for $\Lambda_z=\pm 18$ there is one singlet for each state. Thus the configuration $(4)^2(5)^2$ gives rise to seven triplet states, three with $\Lambda_z=0$ and one for each the Λ_z values ± 8 and ± 10. The average energy for the states arising from these configurations should be roughly twice as far above the ground state as the average energy of the states $(4)^3(5)$. The state energies will be split by electron interaction terms, which will be evaluated in detail in Sec. III.

The major correction to the circular box model is due to the actual shape of the porphin skeleton. In Sec. III this correction is treated as a one-electron perturbation. It will be shown that such a perturbation will have little effect on the triplets arising from the configuration $(4)^2(5)^2$. It will, however, strongly affect the triplets arising from $(4)^3 5$. These turn out to be accidentally degenerate in the circular box model; the effect of the actual porphin shape is to lift this degeneracy. The

[7] M. Kasha, Discussions Faraday Soc. **9**, 14 (1950).
[8] C. Rimington, S. F. Mason, and O. Kennard, Spectrochim. Acta **12**, 65 (1958).

TABLE I. Excited states and energies of porphin (circular box model).

Configuration	Orbitals occupied	Λ_z	S	Diagonal energy	Approximate diagonal energy[a]	Approximate diagonal energy[a] cm^{-1}
$(4)^4$	$44\bar{4}\bar{4}$	0	0	W_0	0	0
$(4)^35$	$44\bar{4}\bar{5}$	±9	1	W_1	Δ	14 700
	$444\bar{5}$		0	$W_1 \quad 2K_{4\bar{5}}$	$\Delta \quad +2K$	17 700
	$\bar{4}\bar{4}45$	±1	1	W_1	Δ	14 700
	$44\bar{4}5$		0	$W_1 \quad +2K_{45}$	$\Delta+2K_{45}$	25 100
$(4)^2(5)^2$	4455	±18	0	$W_2+K_{4\bar{4}}+2K_{4\bar{5}}+K_{5\bar{5}}$	$2\Delta \quad +2K$	32 400
	$\bar{4}\bar{4}\bar{5}\bar{5}$					
	$4\bar{4}55$	±10	1	$W_2+K_{4\bar{4}}+K_{45}+K_{4\bar{5}}$	$2\Delta+K_{45}$	34 600
	$44\bar{5}\bar{5}$		0	$W_2+3K_{4\bar{4}}+K_{45}+K_{4\bar{5}}$	$2\Delta+K_{45}+2K$	37 600
	$44\bar{5}5$	±8	1	$W_2+K_{45}+K_{4\bar{5}}+K_{5\bar{5}}$	$2\Delta+K_{45}$	34 600
	$4\bar{4}55$		0	$W_2+K_{45}+K_{4\bar{5}}+3K_{5\bar{5}}$	$2\Delta+K_{45}+2K$	37 600
	$\bar{4}\bar{4}55$	±2	0	$W_2+K_{4\bar{4}}+2K_{45}+K_{5\bar{5}}$	$2\Delta+2K_{45}$	39 800
	$44\bar{5}\bar{5}$					
	$4\bar{4}5\bar{5}$	0	2	W_2	$2\Delta \quad -2K$	26 400
			1(a)	$W_2 \quad +2K_{45}+2K_{4\bar{5}}$	$2\Delta+2K_{45}$	39 800
			1(b)	$W_2+K_{4\bar{4}}+2K_{4\bar{5}}+K_{5\bar{4}}$	$2\Delta \quad +2K$	32 400
			1(c)	$W_2+K_{4\bar{4}}+2K_{45}+K_{5\bar{5}}$	$2\Delta+2K_{45}$	39 800
			0(f)	$W_2+2K_{4\bar{4}}+K_{45}+K_{4\bar{5}}+2K_{5\bar{5}}$	$2\Delta+K_{45}+3K$	39 100
			0(g)	$W_2 \quad +3K_{45}+3K_{4\bar{5}}$	$2\Delta+3K_{45}+K$	46 500

Mixing terms	Energy	Approximate energy	Approximate energy cm^{-1}	Definitions
$(\Psi_b \mid H \mid \Psi_c)$	$K_{4\bar{4}}-K_{5\bar{5}}$	0	0	$W_0 \equiv E_0+6J_{44}-2K_{4\bar{4}}$
				$W_1 \equiv E_0+\Delta\epsilon+3J_{44}+3J_{45}-K_{4\bar{4}}-K_{45}-K_{4\bar{5}}$
$(\Psi_f \mid H \mid \Psi_g)$	$\sqrt{3}(K_{45}-K_{4\bar{5}})$	$\sqrt{3}(K_{45}-K)$	6400	$W_2=E_0+2\Delta\epsilon+J_{44}+4J_{45}+J_{55}-K_{4\bar{4}}-2K_{45}-2K_{4\bar{5}}-K_{5\bar{5}}$

[a] The energy of the ground configuration was subtracted out.

resultant states will be 50-50 mixtures of the two lowest triplets of different $|\Lambda_z|$. The selection rule $\Delta\Lambda_z=\pm1$ is, accordingly, weakened. Nonetheless, it will be shown that the total intensity of the triplet-triplet transitions to the doubly excited states is just half that of the total singlet-singlet transition intensity; the intensity will divide evenly between transitions to states with $\Lambda_z=0$ and to those with $\Lambda_z=\pm8$ and ±10.

It is of interest to ask how these doubly excited triplet states relax. It would be expected that as happens in other cases, these states will relax by radiationless transition to the lowest doubly excited state of the same multiplicity. As with the higher singly excited configurations, the doubly excited ones are not expected to phosphoresce to the ground state, but fluorescence back to the lowest triplet could occur. Conversion between the doubly excited configurations and the singly excited ones is another possibility, since they can mix with one another by electron interaction terms. In addition, one may conceivably have spin intercombination to the quintet state.

III. DETAILED THEORY OF THE CONFIGURATION $(4)^2(5)^2$

Circular Box Model

We shall proceed on the basis of the following assumptions. We shall assume that the electrons in the orbitals with $\lambda=4$ or $\lambda=5$, (i.e., the top four electrons) move in a one-electron effective potential set up by the nuclei and the remaining electrons. In addition, these four electrons will be assumed to interact with one another by electron interaction e^2/r_{ij}, but we shall neglect interconfiguration interaction,[9] i.e., electron interaction terms connecting states arising from different electron configurations. We shall treat the circular box quantum numbers as rigorous, so there is no interaction between states with different Λ_z. Our wave function will be taken as Slater determinants that are eigen functions of total spin S. Later in this section, some further assumptions will be required to evaluate the energy terms obtained by this treatment.

The following definitions will be needed. We define E_0 as the ground state energy, except for the electron interaction terms of the top four electrons. We define ϵ_4 and ϵ_5 as the MO energy of the orbitals with $\lambda=4$ and $\lambda=5$ in the one-electron potential. We shall set

$$\Delta\epsilon \equiv \epsilon_5-\epsilon_4. \tag{1}$$

We shall also need the usual Coulomb and exchange

[9] W. Moffitt, J. Chem. Phys. **22**, 320, 1820 (1954).

integrals

$$\text{(i) } J_{\alpha\beta}=e^2\int\frac{\psi_\alpha^*(1)\psi_\beta^*(2)\psi_\alpha(1)\psi_\beta(2)dv_1dv_2}{r_{12}}$$

$$\text{(ii) } K_{\alpha\beta}=e^2\int\frac{\psi_\alpha^*(1)\psi_\beta^*(2)\psi_\beta(1)\psi_\alpha(2)dv_1dv_2}{r_{12}}, \quad (2)$$

where 1 and 2 refer to the position coordinates of electrons 1 and 2, ψ_α and ψ_β are two orbitals, and the star indicates complex conjugate. It can then be shown that our problem will involve three distinct Coulomb integrals and four distinct exchange integrals, namely J_{44}, J_{45}, J_{55}, $K_{4\bar{4}}$, K_{45}, $K_{4\bar{5}}$, $K_{5\bar{5}}$, where the numbers refer to the λ_z values of the orbitals ($\bar{4}\equiv-4$).

Table I shows the states arising from the configurations $(4)^4$, $(4)^35$, and $(4)^2(5)^2$. The Λ_z and S values are enough to determine all states in Table I uniquely, except those states with lower case letters in parentheses after their spin value. These states are particular linear combinations of Slater determinants with different spin assignments to the orbitals $4\bar{4}5\bar{5}$. To indicate these combinations we shall, for simplicity, let a symbol such as $\beta\alpha\alpha\alpha$ refer to a Slater determinant constructed out of orbitals $4^{\beta}\bar{4}^{\alpha}5^{\alpha}\bar{5}^{\alpha}$. Then the combinations chosen are

$$\Psi_a\equiv\tfrac{1}{2}[\beta\alpha\alpha\alpha+\alpha\beta\alpha\alpha-\alpha\alpha\beta\alpha-\alpha\alpha\alpha\beta]$$

$$\Psi_b\equiv\tfrac{1}{2}[\beta\alpha\alpha\alpha-\alpha\beta\alpha\alpha+\alpha\alpha\beta\alpha-\alpha\alpha\alpha\beta]$$

$$\Psi_c\equiv\tfrac{1}{2}[\beta\alpha\alpha\alpha-\alpha\beta\alpha\alpha-\alpha\alpha\beta\alpha+\alpha\alpha\alpha\beta]$$

$$\Psi_f\equiv\tfrac{1}{2}[\alpha\beta\alpha\beta-\alpha\beta\beta\alpha-\beta\alpha\alpha\beta+\beta\alpha\beta\alpha]$$

$$\Psi_g\equiv\{[\alpha\alpha\beta\beta+\beta\beta\alpha\alpha]-\tfrac{1}{2}[\alpha\beta\alpha\beta+\alpha\beta\beta\alpha+\beta\alpha\alpha\beta+\beta\alpha\beta\alpha]\}/\sqrt{3}. \quad (3)$$

The state Ψ_a turns out to be an energy eigen function, but there are interaction terms between Ψ_b and Ψ_c and between Ψ_f and Ψ_g. These are also listed in the Table I.

The energy values listed in Table I depend on $\Delta\epsilon$, $3J$ integrals, and $4K$ integrals which need to be evaluated. However, the spirit of this treament is not such as would require elaborate procedures, such as the Pariser and Parr method,[10] to evaluate the electron interaction integrals. We shall instead make some additional assumptions which allow for empirical estimation of their values. In the circular box model, the orbitals of interest have the forms

$$\psi_{\pm4}=f(r)\exp(\pm i4\theta)$$

$$\psi_{\pm5}=f(r)\exp(\pm i5\theta). \quad (4)$$

It then follows that $\psi_\alpha^*\psi_\alpha$ are identical for all the orbitals. Thus

$$J_{44}=J_{45}=J_{55}=\int\frac{f^2(r_1)f^2(r_2)dv}{r_{12}}\equiv J. \quad (5)$$

[10] R. Pariser and R. G. Parr, J. Chem. Phys. **24**, 250 (1956).

For the K values we obtain

$$K_{4\bar{4}}=e^2\int\frac{f^2(r_1)f^2(r_2)}{r_{12}}\exp[-8i(\theta_1-\theta_2)]dv$$

$$K_{45}=e^2\int\frac{f^2(r_1)f^2(r_2)}{r_{12}}\exp[i(\theta_1-\theta_2)]dv$$

$$K_{4\bar{5}}=e^2\int\frac{f^2(r_1)f^2(r_2)}{r_{12}}\exp[-9i(\theta_1-\theta_2)]dv$$

$$K_{5\bar{5}}=e^2\int\frac{f^2(r_1)f^2(r_2)}{r_{12}}\exp-10i(\theta_1-\theta_2)]dv. \quad (6)$$

We may express $r_{12}^{-1}=[r_1^2+r_2^2-2r_1r_2(\theta_1-\theta_2)]^{-\frac{1}{2}}$. We plot this in Fig. 2 for $r_1=2a_H$ (a_H is the Bohr radius) and $r_2=6a_H$ and different values of $(\theta_1-\theta_2)$. Since this is an even function of $(\theta_1-\theta_2)$, the imaginary parts of the K integrals vanish. Thus the function $f^2(r_1)f(r_2)^2/r_{12}$ is weighted by $\cos(\theta_1-\theta_2)$, $\cos8(\theta_1-\theta_2)$, $\cos9(\theta_1-\theta_2)$, and $\cos10(\theta_1-\theta_2)$ in K_{45}, $K_{4\bar{4}}$, $K_{4\bar{5}}$, and $K_{5\bar{5}}$, respectively. One may use Fig. 2 as a basis for presuming the first to be considerably larger than the others, for in this case the negative values of the cosine dependence occur at the smallest values of $1/r_{12}$.

We can now begin to evaluate some of the integrals in Table I. First we note that in all transition energies the term E_0 and all J integrals will cancel out. We define

$$\Delta\equiv\Delta\epsilon+K_{4\bar{4}}-K_{45}-K_{4\bar{5}}. \quad (7)$$

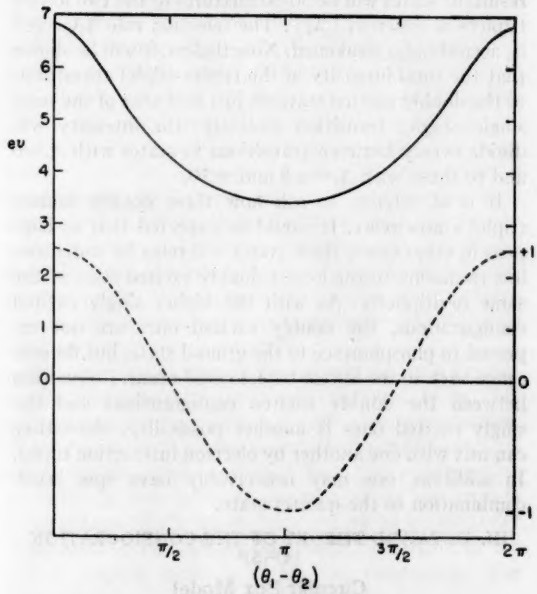

FIG. 2. The function $e^2[r_1^2+r_2^2-2r_1r_2\cos(\theta_1-\theta_2)]^{-\frac{1}{2}}$ (ev) plotted against $(\theta_1-\theta_2)$, shown as solid line for $r_1=2a_H$, $r_2=6a_H$. The dotted line shows $\cos(\theta_1-\theta_2)$.

For Cu Etioporphyrin II,[11] the Soret band occurs at 25 100 cm^{-1} and the visible band at 17 750 cm^{-1}; the phosphorescence[12] occurs at 14 700 cm^{-1}. If we identify these three bands with transition from the gound state to the states of the configuration $(4)^3(5)$ with $\Lambda_z=\pm1$, $S=0$; $\Lambda_z=\pm9$, $S=0$ and $S=1$ states, respectively, then we find

$$\Delta=14\,700\ cm^{-1}$$
$$K_{45}=5200\ cm^{-1}$$
$$K_{4\bar{5}}=1500\ cm^{-1}. \quad (8)$$

We find, as anticipated, that K_{45} is considerably larger than $K_{4\bar{5}}$.

To construct the energy levels for the doubly excited configurations we still need $K_{4\bar{4}}$ and $K_{5\bar{5}}$. For lack of a better procedure and since we have shown they are all small compared to K_{45}, we shall set

$$K_{4\bar{4}}=K_{4\bar{5}}=K_{5\bar{5}}\equiv K. \quad (9)$$

The last column of Table I shows the values of the state energies (with the ground taken as zero energy) in terms of Δ, K_{45}, and K. Using the empirical values of Eq. 8, the energies are plotted in Fig. 3.

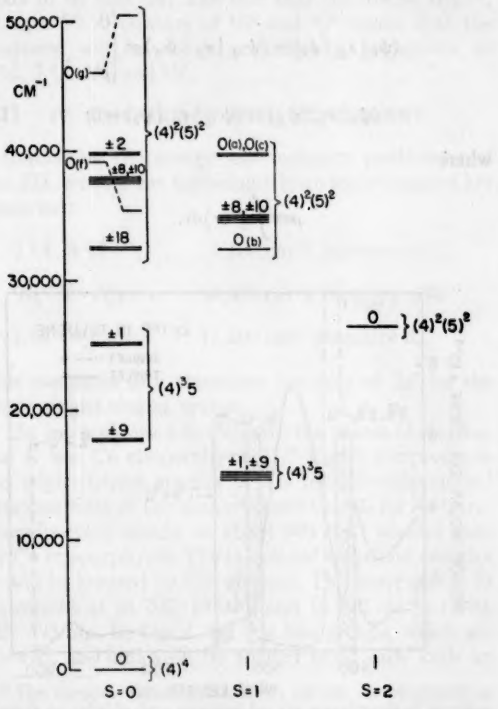

FIG. 3. Porphin energy levels for circular box model of the electron configurations $(4)^4$, $(4)^3(5)$, and $(4)^2(5)^2$. S is the spin. The numbers on the levels are Λ_z values. The levels of $0(f)$ and $0(g)$ show energy before and after inclusion of $(\Psi_f \mid H \mid \Psi_g)$.

[11] J. G. Erdman and A. H. Corwin, J. Am. Chem. Soc. **68**, 1885 (1946).

[12] R. S. Becker and M. Kasha, J. Am. Chem. Soc. **77**, 3669 (1955).

TABLE II. Representations in D_{4h} group of $\pi\rightarrow\pi^*$ states of various angular dependences.

Representation in D_{4h}	Angular dependence
A_{1g}	$\cos 0\theta\equiv1$, $\cos 4\theta$, $\cos 8\theta\cdots$
A_{2g}	$\sin 4\theta$, $\sin 8\theta$, $\sin 12\theta\cdots$
B_{1g}	$\cos 2\theta$, $\cos 6\theta$, $\cos 10\theta\cdots$
B_{2g}	$\sin 2\theta$, $\sin 6\theta$, $\sin 10\theta\cdots$
E_u	$\{\exp(\pm i\theta)$, $\exp(\pm i3\theta)$, $\exp(\pm i5\theta)\cdots$

Nomenclature

For the remaining discussion in this paper, as well as for future reference in experimental work, a systematic nomenclature for these porphin states should be useful. Previously,[3,13] the ground state has been referred to as ^1A; the states derived from $(4)^35$ with $\Lambda_z=\pm1$ and ±9, have been called $^1B^0$, $^3B^0$ and $^1Q^0$, $^3Q^0$, respectively. Names are now needed for the doubly excited triplet and quintet configurations. The following names are consistent with the general nomenclature for aromatic molecules developed by Platt[13] and with a slight revision in preparation[14]: for the states with $\Lambda_z=0$, $^3\dot{A}$ and $^5\dot{A}$; for the states with $\Lambda_z=\pm8$ and ±10, $^3\dot{K}$ and $^3\dot{M}$, respectively. We shall, in conformity with general spectroscopic notation, indicate the different $^3\dot{A}$ states as $1\ ^3A$, $2\ ^3\dot{A}$, $3\ ^3\dot{A}$, in order of increasing energy. We have introduced the dot above the letter name as a symbol indicating the state is doubly excited.

Lifting Accidental Degeneracies

Figure 3 shows degeneracies between the states $2\ ^3A$ and $3\ ^3\dot{A}$; states $^3\dot{K}$ and $^3\dot{M}$; and between states $^3B^0$ and $^3Q^0$. Table I shows that the degeneracy of the first two pairs is spurious and derives from the approximation of Eq. (9) that sets the three small K integrals as equal. These degeneracies are probably split by 500 to 1000 cm^{-1}. Thus there is only one rigorous accidental degeneracy in the circular box model, that between $^3B^0$ and $^3Q^0$.

Table II enables us to consider the effect of the actual D_{4h} symmetry of the porphin skeleton on the states of the circular box. It shows that one might expect the states $^3\dot{K}$ and $^3\dot{M}$ to split into states of symmetry A_{1g}, A_{2g} and B_{1g} and B_{2g}, respectively. Further, the states $^3B^0$ and $^3Q^0$ may mix.

We shall treat the effect of D_{4h} symmetry as a one-electron perturbation.[2,10] Thus, if h_0 is the one-electron circular box potential of the nuclei and the buried elec-

[13] J. R. Platt, J. Opt. Soc. Am. **43**, 252 (1953).

[14] M. Kasha and J. R. Platt (private communication).

TABLE III. Allowed transitions.

Initial		Final	
Λ_z	Configuration	Configuration	Λ_z
0	$4^\alpha 4^\beta \bar{4}^\alpha \bar{4}^\beta$	$4^\alpha \bar{5}^\beta \bar{4}^\alpha \bar{4}^\beta$	-1
		$4^\alpha 4^\beta \bar{5}^\alpha \bar{4}^\beta$	-1
		$4^\alpha 5^\beta \bar{4}^\alpha \bar{5}^\beta$	$+1$
		$5^\alpha 4^\beta \bar{4}^\alpha \bar{5}^\beta$	$+1$
$+1$	$\bar{4}^\alpha \bar{4}^\beta 4^\alpha 5^\alpha$	$\bar{4}^\alpha \bar{5}^\beta 4^\alpha 5^\alpha$	0
		$\bar{5}^\alpha \bar{4}^\beta 4^\alpha 5^\alpha$	0
-1	$4^\alpha 4^\beta \bar{4}^\alpha \bar{5}^\alpha$	$4^\alpha 5^\beta \bar{4}^\alpha \bar{5}^\alpha$	0
		$5^\alpha 4^\beta \bar{4}^\alpha \bar{5}^\alpha$	0
$+9$	$4^\alpha 4^\beta \bar{4}^\alpha 5^\alpha$	$4^\alpha 4^\beta \bar{5}^\alpha 5^\alpha$	$+8$
		$4^\alpha 5^\beta \bar{4}^\alpha 5^\alpha$	$+10$
-9	$\bar{4}^\alpha \bar{4}^\beta 4^\alpha 5^\alpha$	$\bar{4}^\alpha \bar{4}^\beta 5^\alpha \bar{5}^\alpha$	-8
		$\bar{4}^\alpha \bar{5}^\beta 4^\alpha \bar{5}^\alpha$	-10

trons, we had supposed that

$$h_0\psi_{\pm 4}=\epsilon_4\psi_{\pm 4}$$
$$h_0\psi_{\pm 5}=\epsilon_5\psi_{\pm 5}. \tag{10}$$

We now let $h_0 \rightarrow h=h_0+p$, where p is a one-electron perturbation, which changes the potential from $D_{\infty h}$ to D_{4h}. The effect of this is twofold. It modifies $\Delta\epsilon$; however, as this was chosen empirically, it does not affect our results. In addition, it introduces a term connecting the orbitals ψ_4 and $\psi_{\bar{4}}$. If we set (as mentioned in Sec. II)

$$\psi_{\pm 4}=(a_{2u}\pm ia_{1u})/\sqrt{2}, \tag{11}$$

it follows that

$$(\psi_{\bar{4}}\,|\,p\,|\,\psi_4)=\tfrac{1}{2}\{(a_{2u}\,|\,h\,|\,a_{2u})-(a_{1u}\,|\,h\,|\,a_{1u})\}. \tag{12}$$

This term arises from the fact that the a_{2u} and a_{1u} orbitals are not degenerate in D_{4h} porphin, and it is equal to half their energy difference. Treating the reduction to D_{4h} symmetry as a one-electron perturbation means that all splittings must stem from this term.

It may be shown that the one-electron perturbation term of Eq. (12) acts by introducing this term as a matrix element connecting two wave functions that differ by a single orbital, which in the one is ψ_4 and in the other $\psi_{\bar{4}}$. Table I shows that for the states arising from $(4)^2(\bar{5})^2$ such an element will only enter between the ${}^3\dot{A}$ states and the states ${}^3\dot{K}$. However, as these states differ in energy in the circular box model, the effect of such perturbation elements is small. Since there are no first order elements that split the ${}^3\dot{K}$ and ${}^3\dot{M}$ states, these near degeneracies should not be significantly affected.

A rather different result occurs for the triplets arising from $(4)^3 5$. For it follows from what was said above that the ${}^3B^0$ state will have an interaction element with ${}^3Q^0$ of $(\psi_{\bar{4}}\,|\,p\,|\,\psi_4)$. This interaction appeared in the previous treatment of metal porphins[3] and was found to vary over values of less than 100 cm^{-1} to about 2000 cm^{-1}. The result will be that the lowest triplets are 50-50 mixtures of states with $\Lambda_z=\pm 1$ and $\Lambda_z=\pm 9$. We shall refer to the higher energy pair as ${}^3B$, the lower energy pair as ${}^3Q$. (It is to be borne in mind that in this case, since the states are 50-50 mixtures, they no longer have nodal properties.)[15]

A further approximation would consider the effect of the D_{4h} symmetry on the $J_{\alpha\beta}$ and $K_{\alpha\beta}$ integrals. However, this correction means, in essence, abandoning the circular box model completely, since the purpose of the model was to handle electron interaction in a simple way.

Intensities

The 50-50 mixing of the lowest triplets with different $|\Lambda_z|$ values would lead to the idea that little can be said about intensity. Actually, the model gives some interesting predictions which we shall now explore.

Intensity in a circular box is more conveniently estimated from the one electron operators $r_\pm=r\exp(\pm i\theta)$ than from the usual dipole operators (x, y, z). If we use the orbitals of Eq. (4), it follows that:

$$(\psi_4\,|\,r_\pm\,|\,\psi_5)=(\psi_{\bar{4}}\,|\,r_\pm\,|\,\psi_{\bar{5}})=\begin{cases}0\\ \rho\end{cases}$$
$$(\psi_4\,|\,r_\pm\,|\,\psi_{\bar{5}})=(\psi_{\bar{4}}\,|\,r_\pm\,|\,\psi_5)=0, \tag{13}$$

where

$$\rho\equiv\int rf^2(r)\,dv.$$

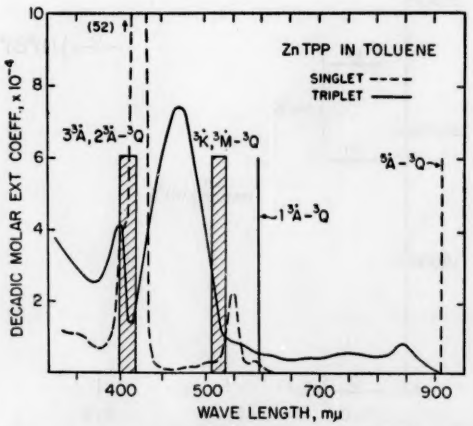

FIG. 4. The observed singlet-singlet and triplet-triplet spectra of Zn tetraphenylporphin (footnote 1). Superposed are the predicted transitions shown as shaded bars of a size proportional to the predicted intensity.

[15] The fact that the observed lowest excited triplets are not fourfold degenerate as shown in Fig. 3 means, of course, that the procedure used to evaluate K_{45} and $K_{4\bar{5}}$ is somewhat oversimplified. A more accurate treatment must take this into account.

Thus, only the transitions $4 \rightarrow 5$ and $\bar{4} \rightarrow \bar{5}$ are allowed. Such transition can be shown to have dipole strengths of $\rho^2/2$.

Table III shows all the allowed transitions from the ground configuration. There are four of them, and the sum of their dipole strengths is therefore $2\rho^2$. This quantity represents the total intensity for all singlet-singlet transitions from the configuration $(4)^4$ to $4^3 5$. For a circular box this intensity appears entirely in the transitions to the singlets with $\Lambda_z = \pm 1$. Table III also shows the transitions possible from the triplets of $(4)^3 5$ (z component of spin $S_z = 1$) to the configuration $(4)^2(5)^2$. Only two transitions are possible from each; thus the total dipole strength is ρ^2. If the lowest triplet were $^3B^0$, all this intensity appears in transitions to the states $n\,^3\dot{A}$. However, a curious feature is that this intensity divides equally between transitions to the states $2\,^3\dot{A}$ and $3\,^3\dot{A}$ (Ψ_a and Ψ_c). Transitions to $1\,^3\dot{A}$ (Ψ_b) are forbidden. (This result follows from Eqs. (3) and the rules for exchanging rows and columns of Slater determinants.) If the lowest triplet were $^3Q^0$, the intensity of ρ^2 would be equally divided between transitions to $^3\dot{K}$ and $^3\dot{M}$. The fact that the lowest triplet, ^3Q, is a 50-50 mixture of $^3B^0$ and $^3Q^0$ means that the intensity will be shared equally by transitions to $2\,^3\dot{A}$, $3\,^3\dot{A}$, $^3\dot{K}$, and $^3\dot{M}$.

IV. COMPARISON WITH EXPERIMENT

Combining the energy and intensity predictions of Sec. III, we find the following triplet-triplet spectra are predicted:

$2\,^3\dot{A}$, $3\,^3\dot{A} - {}^3Q$:	25,100 cm^{-1}, intensity $\rho^2/2$
$^3\dot{K}$, $^3\dot{M} - {}^3Q$:	19,900 cm^{-1}, intensity $\rho^2/2$
$1\,^3\dot{A} - {}^3Q$:	17,700 cm^{-1} intensity 0.

This compares to a transition intensity of $2\rho^2$ for the whole singlet-singlet system.

The molecule used to estimate the values of $\Delta\epsilon$, K_{45}, and K was Cu etioporphyrin II.[16] Figure 4 reproduces the triplet-triplet spectra of Zn tetraphenylprophin.[1] Previous work of the author[3] shows that $\Delta\epsilon$ for Zn tetraphenylporphin should be about 900 cm^{-1} smaller than for Cu etioporphyrin. The calculated transition energies should be lowered by this amount. This corresponds to transitions at 24 200; 19 000; and 16 800 cm^{-1} or 410, 525, 595 mμ. In Fig. 4 the first two groups, which are allowed, are indicated by shaded bars, each with an integrated absorption intensity one quarter that of the Soret bands. The forbidden transition is indicated by a line.

The observed spectrum correlates reasonably well with the predictions. The strong peak at $\lambda \sim 400$ mμ relates to the highest energy allowed pair; that at $\lambda \sim 480$ mμ to the second allowed pair; one of the shoulders to the red could be $1\,^3\dot{A} - {}^3Q$. The other peaks to the red would then correspond to the higher singly excited states.

V. CONCLUSIONS

The theoretical discussion began by pointing out that the upper state of the triplet-triplet spectra could be built either from singly excited configurations or a doubly excited one. The detailed theory on the doubly excited configuration predicted two allowed groups of states in the region 400–500 mμ. The two groups are predicted to have equal intensity, and the total intensity should be half that of the singlet-singlet spectrum. In addition, a weakly forbidden band further to the red is predicted. The predictions correspond reasonably well to certain observed peaks. The remaining peaks, especially those to the red of, say, 700 mμ would then be assigned to transitions to higher singly excited configurations.

Several tests of the theory are possible. First one might attempt to resolve the strong bands into the predicted components. A more indirect test will be possible after spectra of several different metal porphins are available. The hope would be that the observed spectral variations could be derived from the theory by perturbation techniques.

The molecular quintet state predicted in the paper may produce some interesting phenomena. Table I gives it an energy 11 700 cm^{-1} higher than the lowest triplet states. If $\Delta\epsilon$ is corrected by 900 cm^{-1} as before, this is reduced to 10 800 cm^{-1}, a transition of $\lambda = 925$ mμ, which is shown as a dotted line in Fig. 4. It lies slightly to the red of the peaks we have interpreted as higher singly excited states. It is interesting to speculate whether the quintet can be populated and observed as a long-lived phosphorescence.

ACKNOWLEDGMENTS

I should like to express my appreciation to Professor Henry Linschitz of Brandeis University for suggesting the investigation reported in this paper. The author is also indebted to Professor John R. Platt of the University of Chicago for the suggestion that the singly excited states may be weakly forbidden. Professor Platt and Professor M. Kasha are both thanked for advice on systematizing the nomenclature.

[16] The energies were not calculated for the Zn compound as there is no reliable data reported for the wavelength of its phosphorescence.

THE JOURNAL OF CHEMICAL PHYSICS VOLUME 33, NUMBER 5 NOVEMBER, 1960

Spectrum of ReF_6

J. C. EISENSTEIN

National Bureau of Standards, Washington, D. C.

(Received February 22, 1960)

The value of the spin-orbit coupling constant, ζ, for Re^{6+} in ReF_6 is discussed in this paper. Moffitt *et al.* have tentatively assigned a value 3500 cm^{-1} to ζ for the series of compounds from ReF_6 to PtF_6. However, a detailed analysis of the OsF_6 and IrF_6 spectra indicates that ζ has values near 3200 and 3700 cm^{-1} for these two compounds. Since ζ increase in the sequence Re, Os, Ir, it is probably smaller than 3000 cm^{-1} in ReF_6. If one assumes that there is a Jahn-Teller distortion of the fluorine octahedron, the optical absorption data on ReF_6 can be reconciled with this smaller value of ζ.

MOFFITT, Goodman, Fred, and Weinstock[1] have recently published data on the absorption spectra of ReF_7, OsF_7, IrF_7, and PtF_7. Their theoretical analysis is based on the assumption that the odd electrons responsible for the absorption move in a ligand field of octahedral symmetry. They give the value 32 000 cm^{-1} for the ligand-field splitting of the t_2 and e orbitals, and the value 3500 cm^{-1} for the spin-orbit coupling constant ζ.

The point of this note is to suggest that, at least for ReF_6, the value 3500 cm^{-1} for ζ may be a substantial overestimate. It is derived in the following way:

The ligand field of octahedral symmetry plus the spin-orbit coupling partially remove the degeneracy associated with the five possible orbital states and two possible spin states of a single d electron which moves in a spherically symmetric field. The new energy levels are given by

$$\tfrac{1}{2}\{V-\tfrac{1}{2}\zeta-[(V+\tfrac{1}{2}\zeta)^2+6\zeta^2]^{\frac{1}{2}}\}$$

$$\zeta$$

$$\tfrac{1}{2}\{V-\tfrac{1}{2}\zeta+[(V+\tfrac{1}{2}\zeta)^2+6\zeta^2]^{\frac{1}{2}}\}.$$

By taking $V=30\,000$ cm^{-1}, $\zeta=3200$ cm^{-1} one obtains energy levels at 5279 and 32 558 cm^{-1}. The observed levels are at approximately 5280 and 32 400 cm^{-1}, the precise locations being somewhat uncertain because of the resolved vibrational fine structure.

Even this reduced value of 3200 cm^{-1} for ζ is probably too large. It is reasonable to expect that the spin-orbit coupling constant for the metal ion will be larger in OsF_6 than in ReF_6, and still larger in IrF_6. In OsF_6 the lowest orbital level is split by the spin-orbit interaction into three levels whose total separation (in a zero-order approximation) is $3\zeta/2$. Since the observed splitting is 4400 cm^{-1} it follows that ζ for OsF_6 is about 3000 cm^{-1}. A complete calculation,[2] inclusive of configuration interaction, indicates that ζ may be as high as 3200 cm^{-1}. A similar calculation for IrF_6 indicates that ζ is about 3700 cm^{-1} in this compound. It follows that ζ for ReF_6 is probably below 3000 cm^{-1}.

[1] W. Moffitt, G. Goodman, M. Fred, and B. Weinstock, Mol. Phys. **2**, 109 (1959).

[2] J. C. Eisenstein (to be published).

In the absence of other effects such a low value for ζ in ReF_6 would be incompatible with the observed absorption spectrum. However, there is an alternative way to account for the spectrum which does not require use of an unreasonably large ζ. Due to the operation of the Jahn-Teller effect, the two-fold orbital degeneracy of the ground state of ReF_6 may be removed by a spontaneous distortion of the fluorine octahedron. This distortion, in hydrated salts of $3d$ compounds, is believed to have predominantly axial symmetry about a threefold axis of the octahedron of water molecules which surround the metal ion. Let us assume that the ReF_6 molecule is similarly distorted. We can take the perturbing field V' due to the distortion to be proportional to $Y_2^0(\theta, \phi)$, where the angles refer to the trigonal axes,

$$V'=42(5)^{-\frac{1}{2}}Gr^2Y_2^0(\theta, \phi).$$

The numerical factors are introduced for convenience.

The energy levels of ReF_6 corresponding to various values of V, ζ, and G can be calculated. The results of such calculations for selected values of the parameters are given in Table I, where the results are expressed in terms of the radial integral

$$A=G\int_0^\infty r^2 \mid R(r) \mid^2 r^2 dr.$$

$R(r)$ is the radial wave function.

It is apparent from Table I that the values of the spin-orbit coupling constant and the strength of the trigonal field required to fit the experimental spectrum are not independent of one another.

It is possible that a fourth-order term is also present in the perturbing field. Qualitatively, its effect would be the same as that of the second-order term. A similar remark applies to a tetragonal distortion.

The calculations have been based on the assumption of a static Jahn-Teller distortion, because definite results can then be obtained for the positions of the energy levels. It is somewhat more likely that the distortion, if it exists, is due to the dynamical Jahn-Teller effect and arises from the interaction of electronic and vibrational motion. Since both the static and the dynamical Jahn-Teller effects result in lowering

the ground state, the general conclusion of this paper regarding ζ in ReF_6 is not affected by the details of the interaction.

If a distortion of the complex actually exists, it should have two effects on the low-frequency spectrum. In the first place, one might expect to find an absorption peak at the energy E_1. According to Gaunt,[3] there are no peaks below 5000 cm^{-1} which cannot be ascribed to vibrational transitions. However, in view of the uncertainty concerning ζ and the nature of the distortion one does not know exactly where to look for the peak at E_1. It may very well be indistinguishable from a peak in the vibrational spectrum. There is also a possibility that the transition probability from the ground state to the state whose energy is E_1 is too low for an absorption peak to appear in the observed spectrum. Secondly, one would expect the vibrational frequencies to be somewhat different from those in similar molecules where the Jahn-Teller effect is not present. According to Claassen,[4] the vibrational frequencies of the molecules from WF_6 to PtF_6 do not form regular sequences, but it is not clear that the departures from regularity indicate a distortion of the ReF_6 molecule.

TABLE I. Ligand field, trigonal field, and energy levels of ReF_6 as a function of spin-orbit coupling constant. All numbers are energies in cm^{-1}.

ζ	V	A	E_1	E_2	E_3	E_4
2500	29 559	187	1531	5280	32 287	32 513
2600	29 570	167	1419	5280	32 295	32 505
2700	29 590	145	1276	5280	32 305	32 495
2800	29 621	121	1098	5280	32 318	32 482
2900	29 661	95	883	5280	32 334	32 466
3000	29 711	66	629	5280	32 353	32 447
3100	29 770	34	333	5280	32 375	32 425

It would seem that more data are required before the existence of the fields of low symmetry is proved or disproved. Magnetic susceptibility and electron-spin resonance experiments on ReF_6 would be helpful in clarifying the situation.

I am indebted to Miss Irene Stegun and Miss Ruth Zucker, who did the numerical calculations for me.

[3] J. Gaunt, Trans. Faraday Soc. **50**, 209 (1954).
[4] H. H. Claassen, J. Chem. Phys. **30**, 968 (1959).

Emission Spectrum of Trivalent Holmium in the Scheelite Structure

L. G. VAN UITERT AND R. R. SODEN

Bell Telephone Laboratories, Inc., Murray Hill, New Jersey

(Received April 20, 1960)

Fluorescent emission due to holmium can be readily observed in a calcium tungstate host lattice under 3660 A excitation. There are at least eight excited states of holmium which fluoresce in the visible range due to transitions to the $^5I_8$ ground state. These emission peaks show concentration quenching effects which appear to be due to the development of exchange coupling.

A number of emission peaks due to holmium represent transitions which do not correspond to known absorption bands. These peaks are particularly prominent in the emission spectra at high concentrations of holmium.

INTRODUCTION

THE absorption spectrum of trivalent holmium has been examined in detail by Prandtl and Scheiner,[1] Gobrecht,[2] and Severin.[3] However, little has been said concerning the fluorescent emission of this ion. In 1957 Dieke and Hall[4] pointed out that the fluorescence of Ho^{3+} in samples examined to that date was too weak to be studied. Since this time, Keller[5,6] has reported on the emission spectrum of strontium sulfide samples containing 0.04% of holmium. However, considering the weak emission characteristic of holmium as compared to others of the rare earths and the results reported herein, it is questionable as to which part of the previously reported spectra was due to holmium and which part was due to other sources. The only agreement of the previous with the present work is the presence of an emission group at about 5500 A.

MATERIALS

Crystals having the scheelite structure and the compositions $Ca_{1-2x}Na_xHo_xWO_4$, where $x=0.5$, 10^{-1}, 10^{-2}, 10^{-3}, and 10^{-4}, were prepared employing a $Na_2W_2O_7$ flux as previously described.[7] Samples of $CaWO_4$ to which no rare earths were added showed no detectable line emission due to impurities when prepared under these conditions. Examination of crystals of this series by R. Poppalardo of these Laboratories has shown only optical absorptions corresponding to those for holmium[1] to be present. The holmium oxide employed was obtained from the Michigan Chemical Company as a 99.9+% pure grade.

MEASUREMENTS

Measurements were made at room temperature employing a Gaertner high-dispersion spectrometer adapted with an AMINCO photomultiplier microphotometer using a 1P22 tube. Ten-micron slit widths were employed at the entrance and exit to the spectrometer. The system was calibrated against a tungsten lamp to give relative values of brightness of the emitting surface in units of power per unit wavelength range.

Emission was excited by illuminating a sample 1 in. long by $\frac{1}{2}$ in. wide by $\frac{1}{4}$ in. deep with a 3660 A rich H4 spotlight through a Corning 5860 filter. All of the intensity measurements are relative to 100 for the 5450. A peak of a comparable sample of $Na_{0.5}Tb_{0.5}WO_4$, in keeping with previous intensity measurements.[8–10]

Owing to the low level of brightness of the emission from trivalent holmium, it was found to be necessary to use long-wave excitation rather than short-wave excitation to avoid interference from the broad-band lattice emission of calcium tungstate. Under 2537 A excitation, the spectrum observed consists principally of the broad-band emission of calcium tungstate modified by absorption bands due to holmium at wavelengths shorter than 5000 A and by the stronger emission line groups of holmium wavelengths greater than 5000 A.

DISCUSSION

The photomultiplier response to the emission of $Ca_{0.98}Na_{0.01}Ho_{0.01}WO_4$ vs wavelength is shown in Fig. 1. The absorption bands found for the aqueous solution of holmium chloride in the visible region by Prandtl and Scheiner are indicated as blocked out areas below the curve in this figure. The majority of emission peaks observed correspond to known absorption states; in fact, emission lines are observed corresponding to each of the absorption states in the visible region. Since the lowest energy absorption band (corresponding to the $^5I_7$ state) lies about 5100 cm^{-1} above the $^5I_8$ ground state, all of the foregoing absorption transitions are considered to originate in the ground state[2,4]; hence, it is reasonable to expect that the corresponding emission peaks represent transitions from excited states to the ground state. A number of the emission peaks shown in

[1] W. Prandtl and K. Scheiner, Z. anorg. Chem. **220**, 170 (1934).
[2] H. Gobrecht, Ann. Physik (5) **28**, 637 (1937).
[3] H. Severin, Z. Physik **125**, 455 (1947).
[4] G. H. Dieke and L. A. Hall, J. Chem. Phys. **27**, 465 (1957).
[5] S. Keller, J. Chem. Phys. **29**, 180 (1958).
[6] S. P. Keller and G. D. Pettit, J. Chem. Phys. **30**, 434 (1959).
[7] L. G. Van Uitert and R. R. Soden, J. Appl. Phys. **31**, 328 (1960).
[8] L. G. Van Uitert and R. R. Soden, J. Chem. Phys. **32**, 1161 (1960).
[9] L. G. Van Uitert and R. R. Soden, J. Chem. Phys. **32**, 1687 (1960).
[10] L. G. Van Uitert and R. R. Soden, J. Chem. Phys. **33**, 567 (1960).

Fig. 1 do not correspond to absorption bands of holmium; most prominent among these is the one at 5830 A.

The relative strengths of the emission lines vary markedly with composition for holmium concentrations greater than one percent. Figure 2 shows the dependencies of intensity upon concentration for a number of these peaks. The curves are similar to those obtained for the emission from the higher energy excited states of terbium: and europium,[9] the visible emission of dysprosium[11] and the room temperature emission from the excited states of erbium.[10]

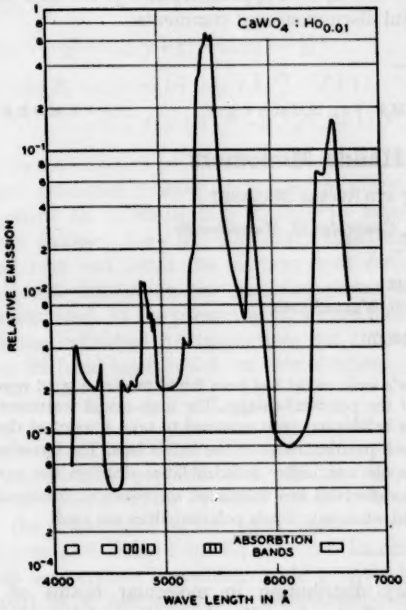

FIG. 1. Intensity of emission plotted on a logarithmic scale vs wavelength for $CaWO_4$ containing one formula per cent of holmium, excited by 3660 A radiation.

The holmium spectra behave like those of erbium in that enhancement of emission from one state by energy transfer from a higher state appears to be limited to relatively small energy separations. The peaks corresponding to the close lying absorption bands between 4600 and 4900 A and between 5350 and 5500 A show this behavior by the progressively increased concentrations of holmium at which they obtain their maxima in brightness while giving no comparable indication of energy transfer between the two major groups. Such a behavior would be suggested by the group at the shorter wavelengths having their maxima in brightness at considerably lower holmium contents than the other, as occurs in the cases of europium and terbium.[8,9]

[11] L. G. Van Uitert, J. Electrochemical Soc. (to be published).

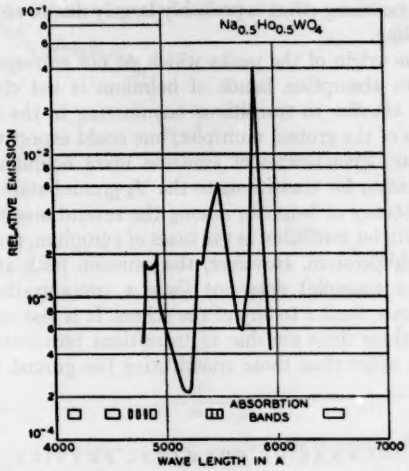

FIG. 2. Intensity of emission plotted on a logarithmic scale vs wavelength for members of the series $Ca_{1-3x}Na_xHo_xWO_4$.

The emission peaks at 4930 and 5830 A and others which do not correspond to absorption bands do not show as rapid a decrease in brightness at the higher concentrations of holmium as the others. In $Na_{0.5}Ho_{0.5}WO_4$, they are dominant features of the emission spectrum, as shown in Fig. 3. A similar emergence of a second set of emission peaks at high concentrations was observed in the case of erbium.[10] However, in the latter case the peaks that were largely quenched by concentration effects at room temperature increased markedly in brightness and became the dominant emission pattern when the temperature was reduced to 77°K. This indicates that vibronic interactions play an important role in quenching emission from excited states of erbium. In contrast holmium is similar to europium, terbium, and dysprosium in that the emission of concentration quenched states shows little tendency to brighten at low temperatures. Here

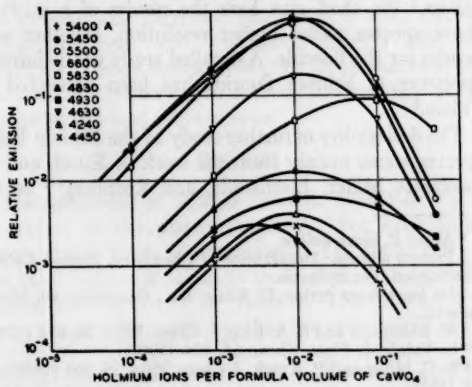

FIG. 3. Intensity of emission plotted on a logarithmic scale vs wavelength for $Na_{0.5}Ho_{0.5}WO_4$ excited by 3660 A radiation.

the quenching effect is probably largely due to exchange coupling.

The origin of the peaks which do not correspond to known absorption bands of holmium is not clear. If they are due to transitions terminating in the higher levels of the ground multiplet, one could expect to find similar dependencies of emission upon holmium concentration for transitions to the $^5I_8$ ground state. Such consistency of behavior among the several members of a multiplet is notable in the cases of europium, terbium, and dysprosium. However, the emission peak at 5830 A (for example) does not show a concentration dependence similar to any of the others. It is also possible that these lines are due to transitions terminating at levels other than those constituting the ground multiplet. If this is the case, the differences in the dependence of quenching effects upon composition may reflect differences in the influence of exchange coupling upon the oscillation strengths for transitions from a common level to terminal states in different multiplets. There is also a possibility that these peaks correspond to very narrow absorption bands that have escaped detection. In this case the higher concentrations at which they obtain their maxima in brightness could be due to energy transfer from higher levels.

ACKNOWLEDGMENTS

The authors are indebted to C. G. B. Garrett, D. L. Wood, R. Pappalardo, and J. H. Scaff for their helpful discussions and comments.

THE JOURNAL OF CHEMICAL PHYSICS VOLUME 33, NUMBER 5 NOVEMBER, 1960

Infrared Spectra of Lithium Halide Monomers

WILLIAM KLEMPERER,* W. G. NORRIS,† AND ALFRED BÜCHLER‡

Department of Chemistry, Harvard University, Cambridge 38, Massachusetts

AND

ALFRED G. EMSLIE

Arthur D. Little, Inc., Cambridge 40, Massachusetts

(Received May 23, 1960)

The infrared spectra of the lithium halides have been reexamined. The vibrational constants of the diatomic molecules are

LiCl	$\omega_e=641\pm3$	$\omega_e x_e=4.2\pm0.3$	
LiBr	$\omega_e=563.2\pm0.2$	$\omega_e x_e=3.53\pm0.15$	$\omega_e y_e=0.02\pm0.03$
LiI	$\omega_e=498.2\pm0.2$	$\omega_e x_e=3.39\pm0.15$	$\omega_e y_e=0.08\pm0.03$.

The first five coefficients of the Dunham expansion of the potential energy have been obtained for lithium bromide and iodide. Rittner's ionic model has been found to give a good representation of the potential energy. The ionic-model treatment of the lithium halides has been extended to take account of the higher multipole polarizabilities of the halide ions. The introduction of quadrupole and higher polarizabilities destroys the agreement between observed and calculated spectroscopic constants which is found when only dipole polarizabilities are used.

I. VIBRATIONAL CONSTANTS OF THE DIATOMIC LITHIUM HALIDES

THE infrared spectra of the lithium halides, with the exception of lithium fluoride, have been reported earlier.[1] We shall give here the results of a study of these spectra under higher resolution, together with results for the fluoride. A detailed study of the infrared spectrum of lithium fluoride has been presented by Vidale.[2]

The desirability of further study of the lithium halide spectra stems mainly from the work of Kusch and his associates Miller, Eisenstadt, and Rothberg[3,4] on the velocity distribution in molecular beams of alkali halides effusing from Knudsen cells, and from the mass-spectrometric analysis of such beams by Friedman and others.[5–7] These studies proved that alkali halide vapors in thermodynamic equilibrium with the corresponding condensed phases consist of both monomeric and polymeric species. The degree of polymerization is highest in the lithium halides. In our earlier work,[1,8] in which prism optics were used, only one absorption band was observed for each compound, and was attributed to the diatomic monomer. The present work, in which a grating spectrometer was used, confirms our earlier assignments and yields several vibrational constants for each diatomic species. Together with the rotational constants of Honig, Mandel, Stitch, and Townes[9] the

* Alfred P. Sloan Fellow.

† Present address: Department of Chemistry, Juniata College, Huntingdon, Pennsylvania.

‡ On leave from Arthur D. Little, Inc., Cambridge 40, Massachusetts.

[1] W. Klemperer and S. A. Rice, J. Chem. Phys. **26**, 618 (1957).

[2] G. Vidale, J. Phys. Chem. **64**, 314 (1960).

[3] R. C. Miller and P. Kusch, J. Chem. Phys. **25**, 860 (1956); **27**, 981 (1957).

[4] M. Eisenstadt, G. M. Rothberg, and P. Kusch, J. Chem. Phys. **29**, 797 (1958).

[5] L. Friedman, J. Chem. Phys. **23**, 477 (1955).

[6] J. Berkowitz and W. A. Chupka, J. Chem. Phys. **29**, 653 (1958).

[7] R. F. Porter and R. C. Schoonmaker, J. Chem. Phys. **29**, 1070 (1958).

[8] S. A. Rice and W. Klemperer, J. Chem. Phys. **27**, 573 (1957).

[9] A. Honig, M. Mandel, M. L. Stitch, and C. H. Townes, Phys. Rev. **96**, 629 (1954).

vibrational constants permit the construction of the potential energy curve of the lithium halides over a considerable region of displacement about the internuclear distance.

Absorption bands due to the polymeric lithium halides have also been observed in the course of the present work. They will be discussed in a subsequent paper.

Theory

To the accuracy required here, the rotation-vibration energy of a diatomic molecule in a $^1\Sigma$ electronic state is given in terms of the usual spectroscopic constants by

$$E_{v,J}=\omega_e(v+\tfrac{1}{2})-\omega_e x_e(v+\tfrac{1}{2})^2+\omega_e y_e(v+\tfrac{1}{2})^3 +[B_e-\alpha_e(v+\tfrac{1}{2})+\gamma_e(v+\tfrac{1}{2})^2]J(J+1) -D_v[J(J+1)]^2+H_v[J(J+1)]^3. \quad (1)$$

In the transitions with which we are concerned, the vibrational quantum number increases by unity ($v\rightarrow v+1$), with an accompanying change in rotational quantum number $J\rightarrow J\pm1$. The exact appearance of the spectrum and hence the features most useful for analysis will depend on the resolving power of the instrument used. In the present work we are unable to resolve the individual rotational lines but can readily observe the band heads which are formed when

$$\Delta[E_{v+1,J+1}-E_{v,J}]/\Delta J=0. \quad (2)$$

At the temperatures involved in the experiments there is an appreciable population in several vibrational levels, so that a series of band heads is observed. From the frequencies of the band heads, the vibrational constants defined by Eq. (1) can be obtained through an iterative procedure, made possible by the fact that as a rule successive vibrational constants differ from each other by two orders of magnitude. For LiBr and LiI the rotational constants B_e, α_e, and γ_e are known from the microwave spectra of the molecules.[9] The higher rotational constants may be approximated by

$$D_v=D_e-\beta(v+\tfrac{1}{2}), \quad (3)$$

where

$$D_e=(4B_e^3/\omega_e^2), \quad (4)$$

$$\beta=-(4B_e^3/\omega_e^3)[5\alpha_e\omega_e+8\omega_e x_e+(1/24)(\alpha_e\omega_e)^2/B_e^3], \quad (5)$$

and

$$H_v\cong H_e=(16B_e^5/\omega_e^4)[2-(\alpha_e\omega_e/6B_e^2)]. \quad (6)$$

Thus three vibrational constants, ω_e, $\omega_e x_e$, and $\omega_e y_e$ may be determined.

Experimental

The instrument used to obtain the spectrograms is a small grating spectrometer which has been described earlier.[10] Two gratings were used, both in first order: a Bausch & Lomb 72-line/mm grating above 750 cm^{-1}, and an N. P. L. Merton Process 40-line/mm grating below that frequency. Higher-order radiation was eliminated by Eastman Kodak infrared filters and selective crystal light choppers. The slit widths used were approximately 1.5 cm^{-1}. These large slit widths were necessary because of the decrease in aperture of the optical system when the 5-ft-long furnace was used as sample cell. Since the resolving power of the optical system was similar to that of a double-passed prism instrument with a 4-in. sample cell, the frequency calibration was based on prism standards.[11]

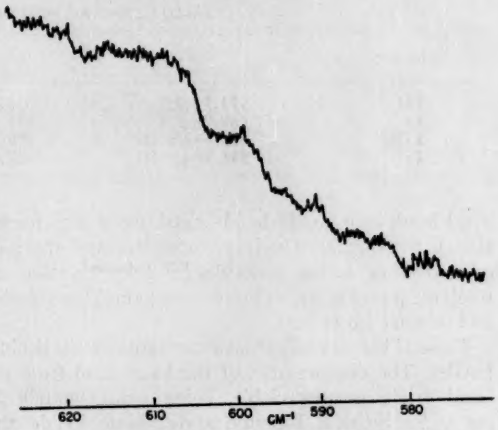

FIG. 1. The infrared absorption spectrum of gaseous lithium bromide.

Commercial samples of the lithium halides were used. They were dried under vacuum at 200°C for 12 hours or more and then placed in the cell, where they were further vacuum-dried at approximately 500°C. The relatively high vapor pressure of these compounds, with the exception of the fluoride, permits the use of a steel tube as the sample cell. In the case of lithium fluoride it is necessary to work above the melting point of steel; the sample was therefore placed in a molybdenum combustion boat and introduced directly into the zirconium dioxide furnace core. In all instances argon was used as a buffer gas to prevent condensation of the vapors on the cold cell windows.

Results

The spectrum of lithium bromide shown in Fig. 1 is typical of the observed spectra. For each halide several band heads are prominent. The frequencies of the band heads are taken as those of the half-intensity points, and are listed in Table I. This procedure is correct under the condition that the true profile of the

[10] T. C. James, W. G. Norris, and W. Klemperer, J. Chem. Phys. 32, 728 (1960).

[11] A. R. Downie, M. C. Magoon, T. Purcell, and B. Crawford, Jr., J. Opt. Soc. Am. 43, 941 (1953).

TABLE I. Observed band head location band and head in cm^{-1}.

Substance	0–1	1–2	2–3	3–4
LiF	973.7±0.1	956.3±0.1	939.8±0.1	
LiCl	689.2±0.4	679.7±0.4	670.4±0.3	
LiBr	604.59±0.15	597.15±0.15	589.72±0.17	582.52±0.17
LiI	534.28±0.16	527.82±0.12	521.78±0.12	516.20±0.20

band head, as it would be observed under high resolution, is rectangular. The frequencies observed are those corresponding to the molecules $Li^7 X^{chemical}$, since our resolving power is not sufficient to separate the chlorine and bromine isotopes.

Table II lists the vibrational constants for the lithium halides. The displacement of the band head from the band origin is appreciable, being approximately 50 cm^{-1}. For lithium bromide and lithium iodide this displacement can be readily calculated from the rotational constants of Honig, Mandel, Stitch, and Townes.[9] Thus the calculations introduce virtually no error into the vibrational constants. For lithium chloride rotational constants have to be estimated. The internuclear distance and therefore the rotational constant of LiCl may be reasonably well estimated from ionic radii[9] as $r_e=2.02\pm0.02$ A giving $B_e=0.707$ cm^{-1}. The rotation-vibration coupling constant is estimated on the assumption that the Dunham constant $a_1=2.70$, the value extrapolated from LiBr and LiI (see Table III). These estimates, together with estimates for the higher terms entering Eq. (1) result in some uncertainty in the vibrational constants above that due to the experimental error in the frequencies of the band heads.

For lithium fluoride no microwave data exist. Vidale[2] has resolved rotational structure in the rotation-vibration spectrum of this molecule; we list his vibrational constants in Table II.

Discussion

There can be little doubt that the carriers of the spectra reported here are diatomic molecules. Thus this work confirms our earlier interpretation of the infrared spectra of the lithium halides[1] (and, by implication, that of the other alkali halide spectra[8]) as far as the assignment of the observed absorption bands to molecular species is concerned. Further corroboration of the assignment to monomers exists in the case of potassium chloride, for which the $J=0\rightarrow J=1$[12] and $J=12\rightarrow J=13$[13] rotational transitions have been measured with high precision. The centrifugal distortion coefficient of KCl calculated from these measurements yields a vibrational frequency of $\omega_e=285.2\pm1.8$ as compared with the infrared value[8] of 281 ± 6 cm^{-1}.

TABLE II. Vibrational constants of the lithium halides.

	ω_e	$\omega_e x_e$	$\omega_e y_e$
LiF[a]	906.2±1.4	7.90±0.010	
LiCl	641.1±3	4.2±0.3	
LiBr	563.16±0.20	3.53±0.15	0.02±0.03
LiI	498.16±0.20	3.39±0.15	0.08±0.03

[a] Reference 2.

The spectroscopic constants are most readily related to potential energy curves by means of Dunham's expression[14] for the energy of a vibrator-rotator. The potential energy is obtained in the form of a power series in the reduced displacement $\xi=(r-r_e)/r_e$ about the equilibrium internuclear separation

$$V(\xi)=a_0\xi^2[1+\sum_{n=1}^{\infty}a_n\xi^n]. \quad (7)$$

The relations between the spectroscopic constants and the potential constants a_n have been given by Dunham. Table III lists the potential constants for LiBr and LiI, together with the corresponding constants calculated from Rittner's model[15] of the alkali halides following the procedure of Honig, Mandel, Stitch and Townes.[9] We shall defer discussion of the calculated values until the end of the following section.

Gaydon[16] has discussed the problem of obtaining the dissociation energies of ionic molecules by the use of a linear Birge-Sponer extrapolation. For all molecules the energetically lowest separated-atom system is that of the ground state atoms. It might be expected that extrapolation from the lower vibrational levels might lead to a separate-atom system consisting of ions and, therefore, to too high a value of the dissociation energy. In fact, in the most clear-cut example available to Gaydon, that of the thallous halides, the dissociation energy given by the linear Birge-Sponer extrapolation was actually too low. The experimental and the linear-Birge-Sponer dissociation energies for the lithium halides, calculated from our vibrational data, are shown in Table IV. There is absolutely no agreement between the two sets of values, the observed dissociation energies being almost twice those obtained by extrapolation.

[12] C. A. Lee, B. P. Fabricand, R. O. Carlson, and I. I. Rabi, Phys. Rev. **86**, 607A (1953); **91**, 1395 (1953).
[13] A. K. Garrison and W. Gordy, Phys. Rev. **108**, 899 (1957).
[14] J. L. Dunham, Phys. Rev. **41**, 721 (1932).
[15] E. S. Rittner, J. Chem. Phys. **19**, 1030 (1951).
[16] A. G. Gaydon, *Dissociation Energies* (Chapman and Hall, Ltd., London, 1953), 2nd ed.

TABLE III. Dunham expansion coefficients for lithium bromide and iodide.

Method	Substance	r_eA	$a_0 10^5$ cm^{-1}	a_1	a_2	a_3	a_4
Experimental	LiBr	2.1704±0.0001	1.4289±0.002	−2.7170±0.002	5.0±0.2	7.3±1.3	11±20
	LiI	2.3919±0.0001	1.3998±0.002	−2.7289±0.002	4.2±0.2	2.1±0.5	0±10
Rittner	LiBr			2.5507	3.946	4.00	1.93
	LiI			2.659	4.24	4.61	2.82

II. IONIC MODEL CALCULATIONS

For a number of years, models consisting of polarizable ions have been used with considerable success to predict[15] and correlate[1,8,9] the spectroscopic constants of the alkali halides. Earlier tests of the ionic model,[9,15] however, were hampered by the fact that the vibrational constants were only poorly known. Furthermore, in the treatments referred to only the dipole polarizabilities of the ions involved were included. Berry[17] has pointed out the importance of induced quadrupole interactions in the calculation of the bending force constants of the group II halides from an ionic model. Even more recently, Burns[18] has included quadrupole, octupole, and hexadecapole polarizabilities in the calculation of antishielding factors for the purpose of evaluating quadrupole coupling constants in gaseous alkali halides.[19] We have therefore reexamined the ionic-model treatment of the lithium halides in order to determine in a particularly simple case the effect of higher polarizabilities on the calculated spectroscopic constants. We shall describe our methods in some detail, since we shall have occasion to use them again in connection with the somewhat more complex problem of the group II dihalides.[20]

Theory

We shall write the potential energy of the gaseous lithium halides as the sum of the electrostatic energy of interaction between the lithium and halide ions ϕ and of an exponential repulsion term, $A \exp -r/\rho$, where A and ρ are constants:

$$W=\phi+A \exp -r/\rho. \tag{8}$$

The dissociation energy implied in Eq. (8) will be that to the free ions. To obtain ϕ, we recall that the dipole polarizability of a spherical conductor is given by the cube of its radius. The key to the treatment to be discussed is the recognition that the observed dipole polarizabilities of halide ions correspond to those of spherical conductors whose radii are of the order of, and in each case somewhat smaller than, the conventional ionic radii. Since the lithium ion is very nearly a point charge, we can obtain ϕ for the lithium halides on the basis of a model consisting of a positive point charge and a negatively charged spherical conductor (Fig. 2). The electrostatic energy of this system can be obtained in a closed-form expression whose expansion yields the individual charge-multipole contributions. In turn, the resulting series can be rewritten in a form which gives ϕ in terms of arbitrary isotropic multipole polarizabilities for the halide ions. It must be pointed out, however, that this treatment still neglects the possibility of the variation of each multipole polarizability with field strength.

TABLE IV. Dissociation energies of the lithium halides (ev).

	LiF	LiCl	LiBr	LiI
Experiment	5.95[a]	4.85[a]	4.35[b]	3.5[b]
Linear Birge Sponer	3.16	2.99	2.75	2.24

[a] W. H. Evans, National Bureau of Standards, private communication.
[b] G. Herzberg, *Molecular Spectra. I. The Spectra of Diatomic Molecules* (D. Van Nostrand Company, Inc., Princeton, New Jersey, 1950), 2nd ed.

[17] R. S. Berry, J. Chem. Phys. **30**, 286, 1104 (1959).
[18] G. Burns, Phys. Rev. **115**, 357 (1959).
[19] M. F. C. Ladd and W. H. Lee, J. Inorg. Nuclear Chem. **11**, 264 (1959), have considered quadrupole terms in the calculation of lattice energies of ionic crystals.
[20] A. Büchler, W. Klemperer, and A. G. Emslie (to be published).

Evaluation of the electrostatic energy

Consider a positive point charge e located at P at a distance r from the center O of a spherical conductor of radius a and carrying a negative charge $-e$ (Fig. 2). The energy of a system of charges and charged con-

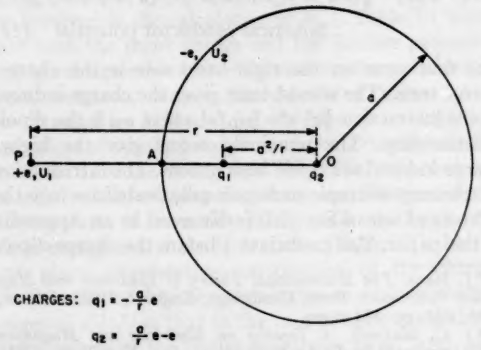

FIG. 2. Electrostatic model for lithium halides.

TABLE V. Data for lithium halide calculations.

	μ Debye	B_e, cm^{-1}	$a^3=\alpha_D(X^-)$ A^3	$E(X)$, ev
LiF	6.421[a]	1.378	0.497	3.62[d]
LiCl	7.144[b]	0.7053	2.17	3.82[d]
LiBr	6.19[c]	0.5548	4.15	3.54[d]
LiI	6.25[c]	0.4432	6.24	3.24[d]

Li: First ionization potential = 5.37 ev[e]

[a] R. Braunstein and J. W. Trischka, Phys. Rev. **98**, 1092 (1955).
[b] J. W. Trischka and D. T. F. Marple, Phys. Rev. **103**, 597 (1956).
[c] Reference 9.
[d] H. O. Pritchard, Chem. Revs. **52**, 529 (1953), Table 10.
[e] R. F. Bacher and S. Goudsmit, Atomic Energy States (McGraw-Hill Book Company, Inc., New York, 1932).

ductors is given by[21]

$$\phi=\tfrac{1}{2}\sum_i q_i U_i, \tag{9}$$

where U_i is the potential at the location of the charge q_i. In the present case, we obtain

$$\phi=\tfrac{1}{2}[eU_1+(-e)U_2], \tag{10}$$

where U_1 is the potential at P and U_2 the potential at the surface of the spherical conductor conveniently evaluated at A. To calculate U_1 and U_2 we use the method of electrostatic images. In the absence of the charge at P, the potential at the surface of and outside the conductor is obtained by replacing the latter by a point charge $-e$ located at its center. To take account of the polarization of the conductor by the positive point charge, we replace the conductor by the image charge q_1 at a distance a^2/r from O and the charge q_2 at O (Fig. 2). The values of U_1 and U_2 are then obtained by calculating the potential at P due to q_1 and q_2 and the potential at A due to q_2. The potentials due to the point charge and its image q_1 cancel at the surface of the sphere. One thus obtains, leaving out a constant term e^2/a,

$$\phi=(-e^2/r)-\tfrac{1}{2}e^2a[1/(r^2-a^2)-(1/r^2)], \tag{11}$$

a result already given by Maxwell.[22] Expanded, Eq. (11) gives

$$\phi=(-e^2/r)-\tfrac{1}{2}(e^2a^3/r^4)[1+(a^2/r^2)+(a^4/r^4)+\cdots]. \tag{12}$$

Spherical conductor potential

The first term on the right-hand side is the charge-charge term. The second term gives the charge-induced dipole interaction $\frac{1}{2}a^3/r^4=\frac{1}{2}\alpha_D/r^4$ where α_D is the dipole polarizability. The remaining terms give the higher charge-induced multipole interactions. The introduction of arbitrary isotropic multipole polarizabilities into the right-hand side of Eq. (12) is discussed in an Appendix to this paper. The coefficient $\frac{1}{2}$ before the charge-dipole and charge-multipole terms, which is usually referred to as due to the "quasi-elastic energy" of the induced moments, arises naturally in the present treatment.

[21] J. Jeans, *The Mathematical Theory of Electricity and Magnetism* (University Press, Cambridge, England, 1925), 5th ed., p. 94; *ibid.*, pp. 184 et seq.
[22] J. C. Maxwell, *A Treatise on Electricity and Magnetism* (1891; reprinted by Dover Publications, Inc., New York, 1954), 3rd ed., Vol. I, p. 251.

Evaluation of the spectroscopic constants

We follow the procedure used in earlier papers.[1,8] The observed (or, in the case of LiCl, estimated) internuclear distance r_e and the vibrational frequency ω_e are used to fix the values of the repulsion parameters A and ρ. The resulting potential function is then used to calculate the dissociation energy to the free ions W_e and the Dunham constant a_1. The latter is related to the vibration-rotation constant α_e through the equation

$$\alpha_e=(-B_e^2/\omega_e)6(1-a_1). \tag{13}$$

Results

1. Data

Primary data for the lithium halide calculation, and the sources from which they were obtained, are listed in Table V. We also give there the values of the ionization potentials $E(X)$ and the electron affinity which were used to convert the dissociation energies D_0^0 of Table IV into the dissociation energies W_e. The vibrational frequencies used are those of Table II. The dipole moments of LiF and LiCl were obtained from the observed values of μ^2A where A is the moment of inertia calculated from the internuclear distances given.

The dipole polarizabilities of the halide ions were calculated from the equation

$$\mu=er_e-(e\alpha_D/r_e^2) \tag{14}$$

in which it is assumed that the difference between the observed molecular dipole and that corresponding to a molecular model consisting of two point charges is due solely to the polarization of the halide ions. From α_D, the radius of the corresponding spherical conductor, $a=\alpha_D^{\frac{1}{3}}$, was obtained.

2. Potential Functions

Three forms of the electrostatic potential were used. The first of these is the "spherical-conductor" potential of Eq. (11), which includes the effect of all induced multipoles. Its use assumes that the higher polarizabilities of the halide ions can be adequately represented by those of a spherical conductor of radius a, where a has been obtained in the manner described in the preceding paragraph. Comparison with various calculations and estimates[17,18,23] of quadrupole and higher polarizabilities shows that the spherical-conductor values are reasonable and indeed conservative.

The second form of the electrostatic potential includes only the charge-charge and charge-dipole terms

[23] R. M. Sternheimer, Phys. Rev. **96**, 951 (1954); **107**, 1565 (1957).

TABLE VI. Ionic model calculations for lithium halides.

	LiF				LiCl			
	Exptl	Spherical conductor potential	Rittner potential	Point-charge potential	Exptl	Spherical conductor potential	Rittner potential	Point-charge potential
W_e, ev[a]	−7.6	−7.95	−7.89	−7.76	−6.4	−6.53	−6.35	−6.12
a_1	−2.567[b]	−2.146	−2.354	−2.485	...	−1.654	−2.619	−2.888
μ, Debye[a]	6.42	exptl	exptl	7.42	7.14	exptl	exptl	9.70
ρ, A	...	0.257	0.269	0.259	...	0.282	0.318	0.286
a^2/r^2 [(cf. Eq. (12)]	...	0.26	...	...	...	0.41	...	...
Electrostatic energy terms+derivatives	ϕ/e^2[d] A^{-1}	ϕ'/e^2 A^{-2}	ϕ''/e^2 A^{-3}	ϕ'''/e^2 A^{-4}	ϕ/e^2[d] A^{-1}	ϕ'/e^2 A^{-2}	ϕ''/e^2 A^{-3}	ϕ'''/e^2 A^{-4}
Charge-charge	−0.647	0.42	−0.54	1.05	−0.495	0.25	−0.24	0.36
Charge-dipole	−0.044	0.11	−0.37	1.42	−0.065	0.13	−0.32	0.95
Charge-multipole	−0.016	0.07	−0.35	2.12	−0.046	0.17	−0.75	4.01

	LiBr				LiI			
	Exptl	Spherical conductor potential	Rittner potential	Point-charge potential	Exptl	Spherical conductor potential	Rittner potential	Point-charge potential
W_e, ev[a]	−6.4	−6.63	−6.07	−5.73	−5.7	−6.31	−5.61	−5.24
a_1	−2.7170[c]	+2.3274	−2.578	−2.987	−2.7289[c]	5.1551	−2.6641	−3.139
μ, Debye[a]	6.19	exptl	exptl	10.4	6.52	exptl	exptl	11.5
ρ, A	...	0.251	0.343	0.296	...	0.251	0.371	0.308
a^2/r^2 [cf. Eq. (12)]	...	0.51	...	...	...	0.59	...	...
Electrostatic energy terms+derivatives	ϕ/e^2[d] A^{-1}	ϕ'/e^2 A^{-2}	ϕ''/e^2 A^{-3}	ϕ'''/e^2 A^{-4}	ϕ/e^2[d] A^{-1}	ϕ'/e^2 A^{-2}	ϕ''/e^2 A^{-3}	ϕ'''/e^2 A^{-4}
Charge-charge	−0.461	0.21	−0.20	0.27	−0.418	0.17	−0.15	0.18
Charge-dipole	−0.094	0.17	−0.40	1.10	−0.095	0.16	−0.33	0.84
Charge-multipole	−0.114	0.44	−2.18	13.4	−0.139	0.50	−2.48	15.2

[a] Cf. Table V.
[b] Reference 2.
[c] Reference 9.
[d] To convert to ev, multiply by 14.40.

in the expansion given by Eq. (12):

$$\phi=(-e^2/r)-(e^2\alpha_D/r^4). \quad \text{Rittner potential} \quad (15)$$

With ϕ in this form, W corresponds very closely to the Rittner potential as we have used it earlier.[1,8]

For the final calculation the molecule was considered as made up of two point charges, so that the electrostatic potential reduces to

$$\phi=-e^2/r. \quad \text{Point-charge potential} \quad (16)$$

3. *Numerical Results and Discussion*

Table VI gives the experimental values of W_e and a_1 together with the values calculated by substituting the three expressions for ϕ in Eq. (8). A number of the parameters involved in the calculations are also given, as well as the dipole moments calculated on the basis of the point-charge model.

A number of conclusions can be drawn from the figures given in Table VI. For the lithium halides, all three ionic-model calculations give adequate agreement between the calculated and observed energy, the latter itself being in every case uncertain to an order of ±0.2 ev. For each molecule an increase in polarization produces increased stabilization, and the effect is more marked as the value of a^2/r_e^2 [cf. Eq. (12)] increases. It should be noted that since the terms due to the induced moments are all of the same sign, the effect of adding higher moments will be in the same direction as that of increasing the magnitude of the polarizabilities.

The potential constant a_1 provides a more sensitive test of the model, since it involves the third derivative of the potential (only the first and second derivatives are involved in the calculation of W_e). Table VI shows that both the point charge and the Rittner potentials give good agreement. An increase of the polarization term, however, makes the calculated values more positive and for LiBr and LiI the effect is so large that the values of a_1 calculated from the spherical-conductor potential have the wrong sign. What has happened can be seen from an examination of the contributions of the various terms of the multipole expansion to the electrostatic energy ϕ and its derivatives (Table VI). In the first place, the relative contribution of the charge-quadrupole and higher terms increases with increasing values of a^2/r_e^2, so that in the case of LiBr and LiI the contributions of the higher multipoles to ϕ''' and, to a lesser extent, to ϕ'', completely swamp that of the

lower terms, while for ϕ itself and for ϕ' the contribution of the multipole terms remains of the same order as that of the other terms.

For LiBr and LiI we have used Rittner's model to calculate also the higher Dunham constants. The results have already been given in Table III. In this set of calculations, account was taken of the finite dipole polarizability of the lithium ion (0.03×10^{-24} cm^3); the polarizabilities of the halide ions were adjusted accordingly. The agreement between calculated and experimental constants is quite startlingly good. Only for a_4, which involves the sixth derivative of the potential function, is there significant disagreement.

We are thus faced with a dilemma. The point-charge model (as we have used it) certainly permits adequate prediction of the spectroscopic constants W_e and a_1 for the lithium halides. Its most serious defect is in the molecular dipole moments, the predicted values of which are uniformly too high (Table VI). This is, of course, the reason why dipole polarizabilities are introduced into the calculations. Once this is done, however, consistency requires the inclusion of the higher multipole polarizabilities, with the consequent destruction of the agreement between the observed and calculated values of a_1. Several causes of this behavior may be proposed. The model ignores the variation of polarizabilities with field strength, and uses an approximate repulsion function whose form is not readily derivable from theory. In any case, the examples of lithium bromide and lithium iodide show that the Rittner model, even regarded as a purely empirical expression, gives an excellent representation of the potential energy curve of these molecules. The problem which remains is why, in view of its apparent physical inconsistency, this model works so well.

APPENDIX

Transformation to arbitrary polarizabilities

It is first necessary to define the multipole polarizabilities in terms of the induced moments, and of the electric field and its derivatives. For the dipole, μ_{ind}, quadrupole, Q_{ind}, and 2^n pole, $p_{\text{ind}}^{(n)}$, induced by a positive unit charge at a distance r, we write:

$$\mu_{\text{ind}}=\alpha_D E=\alpha_D/r^2, \tag{A1}$$

$$Q_{\text{ind}}=\alpha_Q(\partial E/\partial r)=-2\alpha_Q/r^3, \tag{A2}$$

$$p_{\text{ind}}^{(n)}=\alpha_n(\partial^{n-1}E/\partial r^{n-1})=(-1)^{n-1}[(n-1)!\alpha_n/r^{n+1}]. \tag{A3}$$

We now consider the spherical conductor of Fig. 2 to be uncharged, and place a unit positive charge at P. The potential at P due to the moments induced in the conductor is then given by

$$V=-\sum_n(a^{2n+1}/r^{2n+2}) \tag{A4}$$

[cf. Eq. (12)].
In terms of the standard multipole expansion,[24]

$$V=\sum_n[p^{(n)}P_n(\cos\theta/r^{n+1}], \tag{A5}$$

where $P_n(\cos\theta)$ is the Legendre polynomial of order n. Since the direction of the induced dipole, octupole, and higher 2^{2n-1} poles is opposite to the direction OP, $\theta=180°$, so that

$$P_n(\cos\theta)=(-1)^n. \tag{A6}$$

Substituting Eqs (A3) and (A6) in (A5), we obtain

$$V=-\sum_n[(n-1)!\alpha_n/r^{2n-2}], \tag{A7}$$

which, on comparison with Equation (A4), yields

$$\alpha_n=a^{2n-1}/(n-1)! \tag{A8}$$

Substituting this relation in Eq. (12), we obtain

$$\phi=(-e^2/r)-\tfrac{1}{2}e^2\sum_n[(n-1)!\alpha_n/r^{2n+2}] \tag{A9}$$

as the electrostatic energy of the system of Fig. 2 in terms of arbitrary isotropic multipole polarizabilities.

ACKNOWLEDGMENTS

We wish to thank the Research Corporation and the National Science Foundation for their support of this work. Some of the numerical calculations were carried out at Arthur D. Little, Inc., under a contract monitored by the Office of Ordnance Research U.S. Army for the Advanced Research Projects Agency.

---

[24] W. K. H. Panofsky and M. Phillips, *Classical Electricity and Magnetism* (Addison-Wesley Publishing Company, Inc., Reading, Massachusetts, 1955), pp. 12–3. Cf. also H. Margenau and G. M. Murphy, *The Mathematics of Physics and Chemistry* (D. Van Nostrand Company, Inc., Princeton, New Jersey, 1943), 2nd ed., pp. 221–3.

THE JOURNAL OF CHEMICAL PHYSICS VOLUME 33, NUMBER 5 NOVEMBER, 1960

Dissociation Energies of Diatomic Molecules*

G. R. SOMAYAJULU†
Department of Chemistry, University of North Carolina, Chapel Hill, North Carolina

(Received April 1, 1960)

Force constant, dissociation energy, and equilibrium internuclear distance in a sequence of similar diatomic molecules have been found to be related by the expression $k_e r_e/D_0 = \text{const}$. The applicability of this relationship has been shown for eighteen sequences of similar molecules. With the help of this relationship, the dissociation energies of several important diatomic molecules have been determined. Evidence has been adduced in favor of the value 170 kcal for the heat of sublimation of graphite.

1. INTRODUCTION

THE heats of dissociation of several important diatomic molecules have been the topics of great controversy for several decades. A wide variety of experiments including spectroscopic, photochemical, thermochemical, and electron impact appearance potential measurements, are in conflict in several cases. In spectroscopic work, it is often difficult to determine the dissociation limit and the dissociation products. An accurate value for the dissociation limit can be obtained if a convergence limit of bands with its adjoining continuum is observed in absorption. In many cases, however, no band convergence is observed and in such cases, Birge and Sponer[1] have suggested an extrapolation to the position of the convergence limit from the observed bands. The limits obtained by such a method depend on the number of vibrational quanta observed and how the extrapolation is made. The merits and shortcomings of such extrapolation methods have been discussed by Herzberg[2] in his book on the spectra of diatomic molecules and by Gaydon[3] in his book on dissociation energies. The great uncertainty associated with the determination of the dissociation limit and the dissociation products has led to a great deal of speculation and laborious experimentation in the last few decades. We have found an accurate relationship between force constant, dissociation energy and equilibrium internuclear distance applicable for similar molecules in the same electronic state; this may aid in resolving some of the controversies currently existing in this field.

2. RELATIONSHIP BETWEEN FORCE CONSTANT, DISSOCIATION ENERGY AND EQUILIBRIUM INTERNUCLEAR DISTANCE

In a sequence of molecules with constant bond type such as O_2, S_2, Se_2, and Te_2, Pauling[4] showed that the dissociation energy (D_0) is inversely proportional to the equilibium internuclear distance (r_e). From this we have

$$D_0 r_e = \text{const} \tag{1}$$

for a sequence of similar molecules. We shall refer to this as Rule I. This, according to Pauling, may be inferred from the coulombic nature of the potential energy terms in the Hamiltonian function.

Several workers[5–9] have shown that in a sequence of similar molecules, the force constant for infinitesimal amplitudes (k_e) is inversely proportional to the square of the equilibrium internuclear distance. This result is equivalent to the assumption that the potential energy curve near the minimum (which is parabolic in nature) for similar molecules is represented by the function

$$U = a[(r - r_e)/r_e]^2, \tag{2}$$

where a is a constant.[10] From this we have

$$(d^2U/dr^2)_{r=r_e} = 2a/r_e^2 = k_e, \tag{3}$$

which may be written as

$$k_e r_e^2 = \text{const}. \tag{4}$$

We shall refer to this as Rule II.

While Pauling confines his relationship to homopolar molecules of one column of the Periodic Table, Smyth[9] extends Rule II to include heteropolar molecules of the same column. We, however, do not consider these rules to be exact, for there are a number of sequences which do not obey them. We consider these rules to have exact validity only when the condition that the molecules are of constant bond type is rigorously satisfied. This condition is not usually satisfied either in homopolar molecules of one column or in heteropolar molecules, primarily because of changes in the bonding orbitals through hybridization and differences in the valence shell and inner shell repulsions from one mole-

* Work supported by the Office of Ordnance Research, U. S. Army.

† Present address: Lawrence Radiation Laboratory, Department of Chemistry, University of California, Berkeley 4, California.

[1] R. T. Birge and H. Sponer, Phys. Rev. **28**, 259 (1926).

[2] G. Herzberg, *Molecular Spectra and Molecular Structure. I. Spectra of Diatomic Molecules* (D. Van Nostrand Company, Inc., Princeton, New Jersey, 1950).

[3] A. G. Gaydon, *Dissociation Energies* (Chapman and Hall, Ltd., London, England, 1953).

[4] L. Pauling, J. Phys. Chem. **58**, 662 (1954).

[5] A. Kratzer, Z. Physik **3**, 289 (1920).

[6] S. Glasstone, *Recent Advances in Physical Chemistry* (P. Blakiston's Son & Co., Inc., Philadelphia, 1936), 3rd ed. p. 206.

[7] M. Davies, J. Chem. Phys. **17**, 374 (1949).

[8] D. F. Heath, J. W. Linnett, and P. J. Wheatley, Trans. Faraday Soc. **46**, 137 (1950).

[9] R. P. Smyth, J. Phys. Chem. **60**, 1293 (1956).

[10] There is no obvious reason for supposing a to be constant.

TABLE I. Oxides of the alkaline earth metals.[a]

Molecule	k_e	r_e	D_0	S	$k_e r_e^2$	$D_e r_e$	D_0 (Literature)
BeO[b]	7.51	1.331	Excepted				5.4±0.7(G)
MgO	3.484	1.749	4.48	1.36	10.66	7.84	4.5±0.7(G);4.35[c]
CaO	2.84	1.882	3.93	1.36	10.06	7.40	4.0±0.5[d]
SrO	3.4	1.921	4.8	1.36	12.55	9.22	4.82[c]
BaO	3.786	1.94	5.4	1.36	14.25	10.48	5.4±0.5(G)

[a] See Sec. 3 on data and procedure.
[b] BeO constitutes an exception. It may have the dissociation energy recommended by Gaydon.
[c] I. V. Veits and L. V. Gurvich, Optics and Spectroscopy, **1**, 22 (1956). The work of R. F. Porter, W. A. Chupka, and M. G. Inghram, J. Chem. Phys. **23**, 1347 (1955), however, shows that the dissociation energy of MgO is probably below 3.9 ev.
[d] L. Brewer and A. W. Searcy, Ann. Rev. Phys. Chem. **7**, 259 (1956).

cule to another, as postulated by Pitzer.[11] It has been found, however, that effects which would influence the bond type would also induce corresponding effects in the force constants, dissociation energies and internuclear distances, such that the ratio

$$k_e r_e/D_0 = \text{const}, \tag{5}$$

either for a sequence of diatoms belonging to one column or when one of the atoms comes from one particular column and the other from another specified column of the Periodic Table. We shall refer to this as Rule III, and denote the constant by S and call it the sequence constant.

We choose the oxides of the alkaline-earth metals to demonstrate the preceding point. In this sequence, we expect the force constant and dissociation energy to decrease and the internuclear distance to increase as we pass from BeO to BaO. While the internuclear distance increases, the force constant and dissociation energy do not decrease as required by Rules I and II. It is clear that this sequence does not obey Rules I and II but, rather, has been found to obey Rule III as shown in Table I. The values of k_e and r_e for BeO are doubtful; if they prove to be correct then BeO would constitute an exception. The first members of some sequences do seem to constitute exceptions. The anomalous behavior of the first members may be explained in terms of valence shell and inner shell repulsions postulated by Pitzer.[11] The low dissociation energy of F_2 when compared with the dissociation energy of Cl_2 is a famous example of such behavior. There are also a number of sequences within which no member constitutes an exception.

A suitable potential function satisfying the conditions

$$U(r)-U(\infty)=-D_e \tag{6.1}$$

$$(dU/dr)_{r=r_e}=0 \tag{6.2}$$

and

$$(d^2U/dr^2)_{r=r_e}=k_e, \tag{6.3}$$

might be expected to lead to Rule III. It appears, however, that the potential functions so far proposed[12] do not lead to this result. For example, the function

$$U=ar^{-m}-br^{-n} \tag{7}$$

as shown by Sutherland[13] leads to the result

$$k_e r_e^2=mn. \tag{8}$$

Equation (8) has been found by Sutherland to be inapplicable to similar molecules and this has led him to suggest[14] the use of effective internuclear distance (r_e-d) in place of r_e in Eq. (8). Linnett's function[15]

$$U=ar^{-m}-be^{-nr} \tag{9}$$

on the other hand, leads to the result

$$k_e r_e/D_e=mn[1+1/(m-nr_e)]. \tag{10}$$

Assuming both a and m to be constant and b and n to be adjustable for each individual excited state of a given molecule, Linnett found that his potential function leads to a better representation of the interrelation of the constants k_e, r_e, ω_e, and $\omega_e x_e$ than does the Morse function. According to Rule III the right-hand side of Eq. (10) should be constant for similar molecules. The constancy obviously depends on how the constants m and n vary from molecule to molecule.

3. DATA AND PROCEDURE

The k_e values expressed in md/A are those calculated from the molecular data given in footnote reference 2 if not indicated otherwise.

The r_e values (in A) are taken from the *Tables of Interatomic Distances and Configuration of Molecules and Ions* (The Chemical Society, London, England, 1958). The r_e values in parentheses are those estimated by us (if not indicated otherwise) and by others.[16–19] The maximum deviation that would occur in the estimated r_e values is considered to be 0.1 A.

[11] K. S. Pitzer, J. Am. Chem. Soc. **70**, 2140 (1948); J. Chem. Phys. **23**, 1735 (1955).
[12] See Y. P. Varshni, Revs. Modern Phys. **29**, 664 (1957).
[13] G. B. B. M. Sutherland, Proc. Indian Acad. Sci. **8**, 341 (1938).
[14] G. B. B. M. Sutherland, J. Chem. Phys. **8**, 161 (1940).
[15] J. W. Linnett, Trans. Faraday Soc. **36**, 1123 (1940); **38**, 1 (1942).
[16] K. M. Guggenheimer, Proc. Phys. Soc. (London) **58**, 456 (1946).
[17] V. Schomaker and D. P. Stevenson, J. Am. Chem. Soc. **63**, 37 (1941).
[18] R. K. Sheline, J. Chem. Phys. **18**, 927 (1950).
[19] Y. P. Varshni, J. Chem. Phys. **28**, 1081 (1958).

The D_0 or D values which refer to 0°K in electron volts are from footnote reference 2 if they are followed by H in parentheses and from footnote reference 3 if they are followed by G in parentheses.

The following abbreviations have been used: LBS-Linear Birge-Sponer extrapolation; LBSX-Linear Birge-Sponer extrapolation for the levels of the ground state; GBS-Graphical Birge-Sponer extrapolation; and GBSX-Graphical Birge-Sponer extrapolation for the vibrational levels of the ground state. Other abbreviations and symbols used in this paper conform to their usage by spectroscopists.

The general procedure adopted in verifying our rule is to select a reference compound whose k_e, r_e, and D_0 values are known accurately and to estimate the sequence constant. The first member is usually not considered as the reference compound. Then with the help of k_e, r_e, and S, the D_0 values of the other members of the sequence are estimated and compared with their D_0 values in literature. In case of disagreement, the D_0 values in literature have been revised assuming different products of dissociation for the upper states. Since the k_e and r_e values are supposed to be known very accurately, the D_0 values calculated by using the above procedure are considered fairly reliable. For halogens and halides, and also for a few other molecules, the D_0 values estimated by using the above procedure are, however, reliable to within 0.2 ev or less. When approximate values for r_e are used, it would be safer to accept our values with somewhat wider limits, but in any case not exceeding 0.25 ev, unless otherwise some type of strong interaction affects the dissociation energy. The limits vary from sequence to sequence. For example, the dissociation energy of SnS varies by 0.2 ev for a variation of 0.1 A in the estimated value of its r_e while the dissociation energy of NaK varies only by 0.02 ev for a deviation of 0.1 A in the estimated value of its r_e. In cases where a sequence constant is difficult to find, the sequence constant has been estimated as the average of the S values of several members of the sequence.

4. RESULTS AND DISCUSSION

Results have been presented for eighteen sequences of similar molecules. The dissociation limits and other relevant spectroscopic data used in this section have been taken from footnote references 2 and 3 if not indicated otherwise.

4.1. O_2-Type Molecules

The dissociation energy of O_2 is well established to be 5.1148±0.002 ev.[20] Taking O_2 as the reference compound, we have obtained the values 3.37, 2.8, 2.2, 4.26, 3.76, and 3.46 for the dissociation energies of S_2, Se_2, Te_2, SO, SeO, and TeO, respectively. These values can all be derived in a simple way from the dissociation limits or the predissociation limits of these molecules.

[20] P. Brix and G. Herzberg, Can. J. Phys. **32**, 110 (1954).

TABLE II. O_2-type molecules. $S=2.208$ if $D(SO)=5.358$ ev.

Molecule	k_e	r_e	D_0	D_0 (Literature)
O_2	11.765	1.2074	Excepted	5.1148±0.002[a]
S_2	4.959	1.889	4.243	3.3, 3.6 or 4.4 (G)
Se_2	3.612	2.152	3.52	2.8±0.1(G); $D\leq 3.55$(H)
Te_2	2.37	2.59	2.78	2.3±0.2(G); $D\leq 3.18$(H)
SO	7.921	1.4933	5.358	4.212 or 5.358[b]
SeO	6.44	(1.62)	4.725	3.5±1.0(G); 5.4?(H)
TeO	5.304	(1.82)	4.372	2.728 or 3.453(H)

[a] See footnote reference 20.
[b] See footnote reference 21.

However, the general consensus now in the literature is that the above values for S_2 and SO are not correct and should be 4.4 and 5.358 ev, respectively. The value 5.358 ev for $D(SO)$ can be obtained by assuming the predissociation limit at 5.358 ev in the upper state[21] to correspond to dissociation into normal products. The value 4.4 ev for $D(S_2)$ is consistent[22] with the value 5.358 ev for $D(SO)$, and the value −15.3 kcal[23] for $\Delta H_f(SO; g)$. Chemiluminiscence studies by Walsh[24] also favor the higher values for $D(S_2)$ and $D(SO)$. Also, the thermochemistry of SO_2 lends support to the above values.[25] There is also some thermochemical evidence[26] to show that the above values for Se_2 and Te_2 are not correct. Because of these considerations we have felt that O_2, in analogy with F_2, constitutes an exception as a first member. We have, therefore, calculated the dissociation energies of S_2, Se_2, Te_2, SeO, and TeO compatible with the value 5.358 ev for $D(SO)$ and presented them in Table II. The values thus obtained can be supported as shown below.

S_2

LBS of the ground state gives limit at 5.7 ev. If we assume that this value would be 20% higher than the true value, we would obtain 4.5 ev as the dissociation energy of S_2. The weak predissociation in the upper state at 4.4 ev, shows that $D(S_2)\leq 4.4$ ev. GBS of the upper state gives limit at 5.5 ev. If the dissociation products of the upper state are $S(^3P_2)+S(^1D)$ then $D''=4.4$ ev, a value which agrees with the onset of weak predissociation. Our value 4.24 ev lends support to the value 4.4 ev. The other spectroscopic possibilities, viz., 3.3 and 3.6 ev are probably not correct.

[21] R. G. W. Norrish and G. A. Oldershaw, Proc. Roy. Soc. (London) **A249**, 498 (1959).
[22] L. Brewer, J. Chem. Phys. **31**, 1143 (1959).
[23] E. W. Dewing and F. D. Richardson, Trans. Faraday Soc. **54**, 679 (1958).
[24] A. D. Walsh, *Proceedings of the Conference on Chemical Aeronomy in Cambridge, Massachusetts*, 1956 (Pergamon Press, New York, 1957).
[25] D. G. H. Marsden, J. Chem. Phys. **31**, 1144 (1959).
[26] F. R. Bichowsky and F. D. Rossini, *The Thermochemistry of Chemical Substances* (Reinhold Publishing Corporation, New York, 1936).

TABLE III. OH-type radicals ($S=1.569$ if $D(SH)=3.59$ ev.

Radical	k_e	r_e	D_0	D_0 (Literature)
OH	7.791	0.971	Excepted	4.393±0.013[c]
SH	4.195	1.34[b]	3.59	$4.02>D(SH)>2.88$[b]
SeH	(3.18)[c]	(1.47)	2.99	Unknown
TeH	(2.53)[a]	(1.67)	2.70	Unknown

[a] See footnote reference 18.
[b] See footnote reference 30.
[c] See footnote reference 29.

Se_2

LBS of the ground state gives limit at 4.5 ev and if we assume that this value would be 20% higher than the true value, the dissociation energy of Se_2 would be 3.6 ev, a value which is in good agreement with the onset of predissociation in the upper state at 3.55 ev. The upper state gives limit at 3.9 ev and if the dissociation products of this state are $Se(^3P_0)+Se(^3P_2)$, then $D''=3.58$ ev. Our value 3.52 ev lends support to the above assumptions and we would take the value as 3.55 ev. Gaydon derives the value 2.8 ev, assuming that the upper state dissociates into $Se(^3P_2)+Se(^1D)$. Bichowsky and Rossini[26] have estimated the dissociation energy of Se_2 to be 4 ev which, as they note, is in good agreement with that estimated by von Wartenberg from vapor density data. Although this value is quite high, it is closer to 3.55 ev than to 2.8 ev and may be taken to support the value 3.55 ev.

Te_2

LBS of the ground state gives limit at 3.5 ev and, with the usual assumption that this value would be 20% higher than the true value, we obtain the value 2.8 ev for the dissociation energy of Te_2. The upper state gives limit around 3.6 ev. If we assume that the dissociation products of the upper state are $Te(^3P_0)+Te(^3P_2)$ then $D''=3.0$ ev. There is a predissociation above $v'=20$ at 3.18 ev and also an accidental predissociation of the vibrational type at $v'=14$ at 3.07 ev or at $v'=16$ at 3.1 ev.[27] The value which we have obtained from the dissociation limit of the upper state is in satisfactory agreement with the onset of weak predissociation at 3.07 ev. In analogy with S_2 and Se_2, the dissociation energy of Te_2 may be taken to correspond to the predissociation limit. Our value is 2.78 ev and shows that the dissociation energy is around 3.0 ev. Assuming that the upper state dissociates into $Te(^1D)+Te(^3P)$, Gaydon[3] obtains the value 2.3 ev for $D(Te_2)$. Von Wartenberg[28] estimated, from vapor density measurements, the value to be 3.6 ev which is probably much too high. We would take the value to be 3.1 ev.

[27] R. Migeotte and B. Rosen, Bull. soc. roy. sci. Liège **13**, 248 (1944).
[28] von Wartenberg, Z. anorg. u. allgem. Chem. **56**, 320 (1907).

SeO

LBSX value for this molecule is 5.3 ev and with our usual assumption that the LBSX value would be 20% higher than the true value, we obtain the value 4.2 ev for the dissociation energy of SeO. This value agrees with the onset of predissociation above $v=2$ at 4.2 ev. The most likely value for the dissociation energy of this molecule appears to be 4.2 ev. Our value is 4.73 ev and is probably a good deal too high. Gaydon gives 3.5±1.0 ev.

TeO

The levels of the upper state converge to a limit at 4.0 ev. There is evidence of predissociation at 3.9 ev and because of the predissociation we would assume that the upper state dissociates into normal products, giving $D(TeO)=4.0$ ev. Depending on whether the products are $Te(^1D)+O(^3P)$ or $Te(^3P_0)+O(^3P)$, Herzberg gives $D''=2.728$ or 3.453 ev. Our value is 4.37 ev and it may be taken to support the value 4.0 ev.

It can be seen from the foregoing discussion that our results are quite satisfactory for S_2, Se_2, and Te_2 and less satisfactory in the case of SeO and TeO. It may be worthwhile to obtain the dissociation energies of SeO and TeO by thermochemical methods.

4.2. OH-Type Radicals

There was considerable discussion about the dissociation energy of the OH radical. The values proposed range from 4.34 to 4.8 ev. From a careful spectroscopic analysis Barrow[29] has recently concluded that the dissociation energy of OH is 101.3±0.3 kcals (4.393± 0.013 ev). Making certain reasonable assumptions about the dissociation limit of the upper state, Ramsay[30] has estimated the dissociation energy of the SH radical to be 3.59 ev. This value leads to a value of 34.84 kcal for $\Delta H_f(SH; g)$ which compares favorably with that estimated by Franklin and Lumpkin[31] and by Sehon and Darwent.[32] However, it has been found that the above value for $D(SH)$ is not compatible with the dissociation energy of the OH radical. This shows that OH as the first member constitutes an exception in this sequence. No data are available for SeH and TeH radicals. However, based on approximate values for their k_e and r_e, we have estimated their dissociation energies, which are compatible with the dissociation energy of SH, and recorded them in Table III. Although our values for SeH and TeH are approximate, they appear to be the most probable from the standpoint of the thermochemistry of H_2Se and H_2Te and hybridization as shown by the following.

In H_2X type molecules (where X is O, S, Se or Te) it is known that X uses $s-p$ hybrid orbitals for bonding

[29] R. F. Barrow, Arkiv Fysik **11**, 281 (1956).
[30] D. A. Ramsay, J. Chem. Phys. **20**, 1920 (1952).
[31] J. L. Franklin and H. E. Lumpkin, J. Am. Chem. Soc. **74**, 1023 (1952).
[32] A. H. Sehon and B. de B. Darwent, J. Am. Chem. Soc. **76**, 4806 (1954).

and presumably pure p-orbital in XH. Consequently, there should be some difference between the dissociation energies of the first and second XH bonds of H_2X. In the case of H_2O, the values of D(H–OH) and D(OH) are 118 and 101.3 kcal, respectively. Then the value for D(H–OH) $-D$(OH) $=16.7$ kcal. It is also known that the percentage s character in the hybrid orbital of X in H_2X decreases in the order: O>S>Se>Te. Consequently, we should expect the difference between the dissociation energies of the first and second XH bonds of H_2X to decrease in the order: OH>SH>SeH>TeH. That this is so, is shown by the following.

The heat of atomization of H_2S, taking $D(S_2)=4.4$ ev, $\Delta H_f(S_2; g)=30.81$ kcal;[33] $\Delta H_f(H_2S)=-3.91$ kcal, and $D(H_2)=103.24$ kcal, is 173.28 kcal. Since D(SH) has been taken by us to be 3.59 ev (82.78 kcal) the value of D(H–SH) would be 90.5 kcal, a value indicated by both pyrolytic and electron impact methods. The value of D(H–SH) $-D$(SH) $=7.72$ kcal.

If we take the dissociation energy of Se_2 to be 3.55 ev (81.86 kcal), $\Delta H_f(Se_2; g)=33.61$ kcal,[34] and $\Delta H_f(H_2Se; g)=21.5$ kcal, then the heat of atomization of H_2Se would be 139.47 kcal. Our value for D(SeH) $=2.99$ ev (68.95 kcal) and this leads to a value of 70.52 kcal for D(H–SeH). Then, the value of D(H–SeH) $-D$(SeH) would be 1.57 kcal.

The heat of atomization of H_2Te, taking $D(Te_2)=3.1$ ev (71.49 ev), $\Delta H_f(Te_2; g)=41$ kcal,[34] and $\Delta H_f(H_2Te; g)=34$ kcal,[35] is 125.49 kcal. Then taking the value for D(TeH) as 2.70 ev (62.26 kcal), we would obtain the value 63.23 kcal for D(H–TeH) and 0.97 kcal for D(H–TeH) $-D$(TeH).

We have presented in Table IIIa the values of D(H–XH), referred to as D_1, D(XH), referred to as D_2, and D_1-D_2. We have also presented some structural data for these molecules and the values estimated by Pauling[35] for the percentage s character in the hybrid orbital of X in H_2X. These values for the percentage s character do not, however, appear to be unique. For example, Bird and Townes[36] have reported that the interpretation of the nuclear quadrupole coupling data requires about 14.6% s character in the hybrid orbital of S in H_2S. Interpretation of the dipole moments of these molecules also requires somewhat higher percentages of s character than the values suggested by Pauling. Estimates of percentage s character seem to vary with the property under consideration and also to depend on our fundamental assumptions, but they show a general trend, viz., a decrease in the order: O>S>Se>Te. The D_1-D_2 values recorded in Table IIIa also show a similar trend.

TABLE IIIa. Structural and other data for H_2O, H_2S, H_2Se, and H_2Te.

H_2X	D(H-XH)	D(XH)	D_1-D_2	Bond angle	$\mu(D)$	% s-character[b]
H_2O	118	101.3	16.7	104.45°	1.85	6
H_2S	90.5	82.78	7.72	92.2°	0.92	3.6
H_2Se	70.52	68.95	1.57	91.0°	0.24[a]	2.6
H_2Te	63.23	62.26	0.97	89.5°	...	2

[a] A. W. Jache, P. W. Moser, and W. Gordy, J. Chem. Phys. 25, 209 (1956).
[b] See footnote reference 35, p. 123.

TABLE IV. Alkali metals. $S=0.697$ if $D(Na_2)=0.76$ ev.

Molecule	k_e	r_e	D_0	D_0 (Literature)
Li_2	0.255	2.672	0.98	1.03(H); 1.10±0.05(G)
Na_2	0.172	3.078	0.76	0.75±0.03(G)
K_2	0.0985	3.923	0.555	0.51±0.05(G); 0.56±0.04[a]
Rb_2	0.082	4.19	0.493	0.49(H); 0.47±0.05(G)
Cs_2	0.069	4.57	0.453	0.45(H); 0.45±0.04(G)
NaK	0.13	(3.5)	0.65	0.62±0.03(G)
NaRb	0.121	(3.59)	0.62	0.57±0.04(G)
NaCs	0.108	(3.76)	0.58	Unknown

[a] See footnote reference 37.

4.3. Alkali Metals

Fairly reliable values for the dissociation energies of Na_2, Rb_2, and Cs_2 are known. In the case of Na_2, GBS of the upper state almost to convergence limit gives 0.76 ev for its dissociation energy. Vapor pressure data also indicate a value around this. We have, therefore, taken $D(Na_2)=0.76$ ev and estimated the dissociation energies of the other members of this sequence. The results are reported in Table IV.

In the case of Rb_2, GBS for the upper state of blue system and GBS for the upper state of the violet system gives 0.49 ev which agrees very well with our value 0.493 ev. In the case of Cs_2, GBS for the ground state and GBS for the upper state give 0.45 ev, a value in excellent agreement with that obtained by us. The spectroscopic value for K_2 is 0.51 ev, while the molecular beam method gives a value around 0.56 ev.[37] Our value, 0.555 ev, is consistent with the latter value.

The values obtained by us for NaK and NaRb are in agreement with the approximate values suggested by Gaydon. Because of the uncertainty in the estimated values of r_e for NaK, NaRb and NaCs, we would consider our values accurate to within 0.02 ev.

Li_2, however, constitutes an exception. For this molecule, GBS for the upper state gives 1.12±0.03 ev and the molecular beam method gives 1.03 ev. Our value is 0.98 ev. It is known that for some excited states of homonuclear molecules, dipole-dipole interactions may lead to small potential maxima and the true dissociation energy of this molecule may be below the apparent convergence limits. It is therefore possible

[33] D. R. Stull and G. C. Sinke, Advances in Chem. Ser. No. 18, 1956.
[34] F. D. Rossini *et al.*, Natl. Bur. Standards (U. S.) Circ. No. 500 (1952).
[35] L. Pauling, *The Nature of the Chemical Bond* (Cornell University Press, Ithaca, New York, 1960), 3rd ed., p. 123.
[36] G. R. Bird and C. H. Townes, Phys. Rev. 94, 1203 (1954).
[37] F. W. Loomis and R. E. Nausbaum, Phys. Rev. 39, 89 (1932).

TABLE V. Hydrides of the alkali metals. $S=0.6738$ if $D(\text{LiH})=2.429$ ev.

Molecule	k_e	r_e	D_0	D_0 (Literature)
LiH	1.026	1.5954	2.429	2.429[a]
NaH	0.789	1.8873	2.187	2.05±0.02(G)
KH	0.561	2.244	1.868	1.86±0.15(G)
RbH	0.515	2.367	1.809	1.7±0.2(G)
CsH	0.467	2.494	1.728	1.8±0.3(G)

[a] See footnote reference 38.

for us to explain a low value for Li_2. However, there is also a possibility that the first member of a sequence may constitute an exception to our rule. We are, therefore, inclined to suggest that the true dissociation energy of Li_2 may be around 1.03 ev.

4.4. Hydrides of the Alkali Metals

Velasco[38] has recently determined the dissociation energy of LiH to be 2.429 ev. This value has been found to be quite suitable for obtaining the sequence constant and the dissociation energies of the other members of this sequence. The results are presented in Table V.

In the case of NaH, LBS for the ground state gives 2.18 and GBS for the A state gives 2.0±0.2 ev. Gaydon gives 2.05±0.2 ev. Our value is 2.187 ev and appears to be highly probable. The dissociation limit of the A state of KH assuming $K(^2P)+H(^2S)$ leads to $D''=1.86$ ev. Our value 1.868 ev, supports this value. LBS for the ground state gives 1.86 ev for RbH and our value is 1.809 ev, Gaydon gives 1.7±0.2 ev. We consider our value 1.809 ev to be quite reasonable. In the case of CsH, the vibrational levels for the ground state known only up to $v=2$ would extrapolate linearly to give limit at 1.9 ev. Gaydon gives 1.8±0.3 ev. Our value is 1.728 ev.

4.5. Halogens and Interhalogens

Presumably because of the valence shell repulsion postulated by Pitzer,[11] F_2 behaves anomalously among halogens. All the other members of this sequence obey our rule satisfactorily (see Table VI) and the calculated and experimental values for the dissociation energies are only at a slight variance, the maximum deviation being 0.15 ev.

TABLE VI. Halogens and interhalogens ($S=2.73$).

Molecule	k_e	r_e	D_0	D_0 (Literature)	Deviation
F_2	4.453	1.418	2.313	1.609±0.037[b]	
Cl_2	3.286	1.988	2.393	2.475	−0.082
Br_2	2.458	2.284	2.056	1.971	0.085
I_2	1.721	2.667	1.681	1.5434[c]	0.138
FCl	4.56	1.628	2.719	2.616	0.103
FBr	4.1[a]	1.756	2.637	2.6	0.037
FI	3.64	(2.05)	2.73	2.87	−0.140
BrCl	2.717	2.138	2.128	2.26	−0.132
ICl	2.383	2.321	2.026	2.153	−0.127
IBr	2.064	2.434	1.84	1.817	0.023

[a] R. A. Durie, Proc. Roy. Soc. (London) **A207**, 388 (1951).
[b] A. L. G. Rees, J. Chem. Phys. **26**, 1567 (1957).
[c] R. D. Verma, J. Chem. Phys. **32**, 738 (1960).

[38] R. Velasco, Can. J. Phys. **35**, 1204 (1957).

There has been some controversy about the dissociation energy of BrF and the suggested values are 2.16, 2.384,[39] and 2.6 ev. Our rule gives 2.637 and this may be taken to support the value 2.6 ev. Similarly in the case of FI, two values, viz., 1.98 and 2.87 ev have been suggested. Using an estimated value for its r_e, we have found its dissociation energy to be 2.73 ev which lends support to the higher value. According to our rule, the value for F_2, comes out to be 2.3 which is in agreement with the value 2.17±0.2 ev suggested by Barrow and Caunt,[40] but the evidence in favor of the value 1.61±0.04 ev is so very overwhelming that it is hardly possible to consider any value other than 1.61±0.04 ev. Although F_2, constitutes an exception among halogens, fluorides do not seem to constitute exceptions among halides. The values obtained for fluorides agree with the lower limits of the literature values and hence we are in favor of suggesting the value 1.57 ev for the dissociation energy of F_2.

TABLE VII. Hydrogen halides ($S=1.55$).

Molecule	k_e	r_e	D_0	D_0 (Literature)
HF	9.655	0.9171	5.713	5.8±0.1
HCl	5.157	1.2749	4.242	4.431(G)
HBr	4.116	1.4138	3.754	3.754(H)
HI	3.141	1.6041	3.251	3.06±0.01(G)

4.6. Hydrogen Halides

The dissociation energies of HCl, HBr, and HI are known very accurately; they are the thermochemical values. Taking HBr as our reference compound, we have estimated the dissociation energies of the hydrogen halides and recorded them in Table VII. The estimated values for HCl and HI deviate from the experimental values by 0.2 ev, the value for HCl being less and the value for HI being greater than the experimental value. Our rule, in general, predicts slightly lower values for chlorides and slightly higher values for iodides when the bromides are taken as the standards. This trend is repeated in all the halide sequences we have studied. The value 5.71 ev obtained by us for HF suggests that the value of $D(F_2)$ is 1.57 ev.

4.7. Hydrides of the Alkali Metals

The dissociation energies of the alkali metal halides determined by atomic fluorescence, thermochemical and spectroscopic methods have been summarized by Gaydon. Although halogens obey our rule somewhat

[39] P. H. Brodersen and J. E. Sicre, Z. Physik **141**, 515 (1955).
[40] A. D. Caunt and R. F. Barrow, Nature **164**, 753 (1949).

approximately, the alkali halides obey our rule very satisfactorily. The sequence constant has been found by averaging the S values of some of these halides. The dissociation energies calculated by this method have been presented in Table VIII. The force constants of LiF and NaF are not known and the values recorded in the table are those estimated by using the present rule. Two values (0.55 and 0.77 md/A) available in the literature for the force constant of CsI appear to be inaccurate. Using our rule, we have estimated its value to be 0.665 md/A. It is interesting to note that the first members LiCl, LiBr, and LiI do not constitute exceptions to our rule. The values obtained in all these cases may be accurate to within 0.1 ev. We shall take the values for chlorides as 0.1 ev greater and the values for iodides as 0.1 ev less than the values indicated by our rule.

TABLE VIII. Alkali metal halides ($S=0.63$).

Molecule	k_e	r_e	D_0	D_0 (Literature)
LiF	(2.36)[a]	(1.59)	5.95	5.95±0.2(G)
LiCl	1.499[b]	(2.02)	4.8	5.0±0.3(G)
LiBr	1.248[b]	2.17	4.3	4.35±0.3(G)
LiI	0.973[b]	2.392	3.69	3.5±0.2(G)
NaF	(1.465)[a]	(2.0)	4.65	4.65±0.2(G)
NaCl	1.1[b]	2.361	4.12	4.24±0.05(G)
NaBr	0.959[b]	2.502	3.81	3.80±0.1(G)
NaI	0.763[b]	2.712	3.28	3.07±0.1(G)
KF	1.24[c]	(2.55)	5.0	5.0±0.25(G)
KCl	1.02[c]	2.667	4.32	4.4±0.05(G)
KBr	0.83[c]	2.821	3.72	3.94±0.05(G)
KI	0.70[c]	3.048	3.39	3.32±0.05(G)
RbF	1.39[c]	(2.3)	5.1	5.35±0.2(G)
RbCl	1.076[c]	2.787	4.76	4.50±0.2(G)
RbBr	0.80[c]	2.945	3.74	4.0±0.25(G)
RbI	0.66	3.177	3.33	3.35±0.1(G)
CsF	1.451[c]	2.345	5.4	5.5±0.2(G)
CsCl	0.95[c]	2.906	4.38	4.6±0.2(G)
CsBr	0.86[c]	3.072	4.19	4.1±0.25(G)
CsI	(0.665)[a]	3.315	3.5	3.4±0.1(G)

[a] A rough value estimated by using the present rule.
[b] S. A. Rice and W. Klemperer, J. Chem. Phys. 27, 643 (1957).
[c] R. F. Barrow and A. D. Caunt, Proc. Roy. Soc. (London) A219, 120 (1953).

4.8. Monohalides of B, Al, Ga, In, and Tl

For many of these molecules, Birge-Sponer extrapolation for the levels of the ground states give quite low values. Higher values are obtained from the extrapolation for the excited $^1\Pi$ state, these values have been found to be in agreement with those obtained by thermochemical and atomic fluorescence methods. In this sequence, BF, BCl, and BBr (and probably BI) form a subgroup and obey our rule with a different sequence constant. The value of S applicable for these molecules is 1.194. All the other members of this sequence form another group and obey our rule with the sequence constant 1.015. The results obtained by us (see Table IX) for all these molecules excepting AlCl, GaCl, and InCl are very satisfactory. For InCl, predissociation sets limit between 4.4 and 4.68 ev; Gaydon gives 4.5±0.1 ev. Our value is 3.76 ev; even if this value is low, as it usually is in the case of chlorides, the conspicuous difference of 0.6 ev between the predissociation limit and our value suggests that the predissociation probably occurs into $In(^2P_{\frac{1}{2}})+Cl(^2P_{\frac{1}{2}})$ giving $D''=4.02$ ev. In the case of GaCl, LBS for the ground state gives only 3.7 ev, while GBS for the excited $^1\Pi$ assuming $Ga(^2P_{\frac{1}{2}})+Cl(^2P_{\frac{1}{2}})$ gives 4.9 ev. This is in utter disagreement with our value, 3.96 ev. Our value is, however, close to the LBSX value. Similarly, for AlCl value, 4.38 ev is nearer to the LBSX value.

TABLE IX. Monohalides of B, Al, Ga, In, and Tl. $S=1.194$ for BF, BCl, BBr, and BI and 1.015 for the other members of this sequence.

Molecule	k_e	r_e	D_0	D_0 (Literature)
BF	8.043	1.262	8.5	8.5±0.5(G)
BCl	3.473	1.716	5.0	5.1±0.4(G)
BBr	2.665	1.887	4.21	4.2±0.2(G)
BI	(1.86)[a]	(2.1)	3.3	Unknown
AlF	4.191[b]	1.654	6.83	6.7±0.3(G)
AlCl	2.078	2.138	4.38	5.0±0.2(G)
AlBr	1.692	2.295	3.83	4.3±0.3(G)
AlI	1.31	(2.54)	3.3	3.7±0.7[d]
GaF	3.41[e]	1.775	5.96	6.2±0.03[e]
GaCl	1.821	2.208	3.96	3.7?(H); 4.99±0.02(G)
GaBr	1.516	(2.34)	3.5	3.5±0.8(G)
GaI	1.233	(2.5)	3.0	2.9±0.2(G)
InF	2.74[e]	1.985	5.36	5.41(G)
InCl	1.591	2.401	3.76	4.5±0.1(G)
InBr	1.366	2.541	3.42	3.4±0.2(G)
InI	1.114	(2.72)	3.0	2.8±0.2(G)
TlF	2.31	2.084	4.74	4.75±0.2(G)
TlCl	1.453	2.541	3.64	3.8±0.2(G)
		2.485	3.56	
TlBr	1.26	2.618	3.25	3.2±0.1(G)
TlI	1.038	2.814	2.88	2.8±0.25[d]

[a] Estimated value. See footnote reference 19.
[b] S. M. Naude and T. J. Hugo, J. Chem. Phys. 33, 573 (1955).
[c] R. F. Barrow *et al.*, Proc. Phys. Soc. (London) A70, 34 (1957).
[d] L. Brewer *et al.*, Natl. Nuclear Energy Ser. 19B, 000 (1950).
[e] R. F. Barrow *et al.*, Proc. Phys. Soc. (London) A67, 528 (1955).

4.9. N_2-Type Molecules

The dissociation energies of N_2, P_2, and As_2 are known almost definitely to be 9.76, 5.03, and 3.96 ev, respectively. Recently Huffman *et al.*[41] from vapor pres-

TABLE X. N_2-type molecules. $S=2.136$ if $D(As_2)=3.96$ ev.

Molecule	k_e	r_e	D_0	D_0 (Literature)
N_2	22.962	1.0976	11.8	9.762
P_2	5.556	1.8943	4.93	4.12 or 5.03
As_2	4.069	2.08	3.96	3.96(H)
Sb_2	2.611	2.48	3.03	3.0±0.5(G)
Bi_2	1.836	2.68	2.3	1.7 or 2.2(H)
PN	10.16	1.491	7.09	7.1±0.05[a]
AsN	7.926	(1.59)	5.9	5.0±1.0(G)
SbN	6.564	(1.79)	5.5	5.5[b]
SbBi	2.193	(2.58)	2.65	3.0±2.0(G)

[a] Huffman *et al.*, J. Am. Chem. Soc. 76, 6239 (1954).
[b] Assuming the limit of the upper state correlates with $Sb(^2D)+N(^4S)$.

[41] E. O. Huffman *et al.*, J. Am. Chem. Soc. 76, 6239 (1954).

TABLE XI. CN-type molecules. $S=2.251$ if $D(CN)=8.48$ ev.

Molecule	k_e	r_e	D_0	D_0 (Literature)
CN	16.29	1.1718	8.48	8.48
CP	7.83	1.562	5.43[a]	5.0±1.0(G)
SiN	7.29	1.572	5.09	4.5±0.5(G); 5.2 (GBS of $B\,^2\Sigma^+$)

[a] In analogy with the oxides, nitrides may form a separate group in this sequence. In that case, the value for CP would be much higher than 5.43 ev. See Sec. 4.13 for a discussion of the anomalous behavior of oxides.

[b] Assuming the predissociation in the $J^2\Delta$ state at 68 420 cm^{-1} is genuine. (see footnote reference 43) If $D(CN)$ is 8.2 ev then the dissociation energies of CP and SiN would be 5.25 and 4.92 ev, respectively.

sure measurements and assuming $D(N_2)=9.76$ and $D(P_2)=5.03$ ev, have estimated the dissociation energy of PN to be 7.1±0.05 ev. The values 1.7 and 2.2 are possible for $D(Bi_2)$. For Sb_2, AsN, SbN, and SbBi, the values are not known accurately.

It has been found that N_2 constitutes an exception in this sequence. The sequence constant has been, therefore, calculated using the k_e, r_e, and D_0 values of As_2. The results for the other members of this sequence are presented in Table X. Our value 4.93 ev for $D(P_2)$ indicates that the dissociation energy of P_2 is 5.03 ev, but not 4.12 ev as was thought at one time. Our value, 2.3 ev for $D(Bi_2)$ shows that the dissociation products of the B state are $Bi(^4S)+Bi(^2D_{\frac{3}{2}})$ giving $D''=2.2$ ev. The value 7.09 ev obtained for PN lends strong support to the value obtained by Huffman *et al.* This also shows that $D(N_2)=9.76$ and $D(P_2)=5.03$ ev. The values obtained by us for Sb_2, AsN, and SbBi are in agreement with the approximate values suggested by Gaydon. In the case of SbN, LBS of the upper state gives a limit around 7.8 ev. Gaydon showed that if this state is $^1\Pi$ it must correlate with $Sb(^2D)+N(^2D)$ giving D'' around 3.1 ev. He has, however, mentioned that if this state is not $^1\Pi$ then other correlations would be possible. Our value is 5.5 ev and this shows that the upper state correlates with $Sb(^2D)+N(^4S)$ giving $D''=5.48$ ev in agreement with our value.

It is interesting to note that our rule predicts the value for $D(N_2)$ as 11.8 ev, a value considered at one time to be very probable. Glockler[42] finds that this value fits various empirical correlations. There may be some hidden significance for this value, which we are unable to appreciate at present.

4.10. CN-Type Molecules

Some data are available only for the molecules CN, CP, and SiN of this sequence. Assuming $L(C)=170$ kcal and $D(N_2)=9.76$ ev, Gaydon suggested the value 8.2 ev for the dissociation energy of CN. No definite spectroscopic evidence was so far produced to support this value. Carroll[43] has, however, suggested that the fading of the structure of the (3−0) band of the $J^2\Delta\rightarrow A\,^2\Pi$ system at 68 420 cm^{-1} might be due to a predissociation occuring into $C(^3P)+N(^4S)$. The presence of the (4−0) band presents certain difficulties in the interpretation of the predissociation. The predissociation can, however, be assumed to be either weak or forbidden. If this predissociation is genuine, then $D(CN)$ would be 8.48 ev, a value which finds good support from our rule. A linear Birge-Sponer extrapolation for the levels of the $J\,^2\Delta$ state gives a limit at 87 500 cm^{-1}. If we assume that this limit corresponds to $C(^3P)+N(^2D)$, then $D''=8.46$ ev. Adopting the value 8.48 ev for $D(CN)$ we have calculated the dissociation energies of CP and SiN and presented them in Table XI.

In the case of SiN, LBS for the ground state gives 6.2 ev. If we assume that this value is 20% higher than the true value then $D(SiN)=5.0$ ev. Also GBS for the $B\,^2\Sigma^+$ state gives limit at 5.2 ev. If we assume that this limit corresponds to $Si(^3P)+N(^4S)$, then $D''=5.2$ ev. Our value is 5.09 ev; Gaydon, however, assumes that this limit is to $Si(^1D)$ and suggests the value 4.4 ev for $D(SiN)$. We are, however, in favor of a value around 5.0 ev.

For CP, LBS for the ground state gives 6.9 ev. LBS for $A\,^2\Pi$ and also $B\,^2\Sigma$ favor a similar value. If we assume that the LBSX value is 20% higher than the true value then $D(CP)=5.5$ ev. This agrees very well with our value 5.43 ev. However, there is a possibility that the value for $D(CP)$ might be higher than 5.5 ev if the nitrides behave differently from the phosphides, arsenides, etc.

4.11. NO-Type Molecules

The dissociation energy of NO is known to be 6.503 ev, but this molecule has been found to constitute an exception in this sequence. From the data available for PO and AsO we have estimated the sequence constant to be around 2.47. The dissociation energies of these molecules are presented in Table XII.

PO

Assuming that the predissociation in the E state occurs into $P(^2D)+O(^3P)$, Dressler[44] reported the dissociation energy of PO to be 5.4±0.1 ev. Our value is 5.52 ev. From chemiluminiscence data, Walsh[24] has

TABLE XII. NO-type molecules ($S=2.47$).

Molecule	k_e	r_e	D_0	D_0 (Literature)
NO	15.94	1.1503	7.42	6.503
PO	9.409	1.449	5.52	5.4±0.1[a]
AsO	7.226	(1.64)	4.8	4.9±0.1(G)
SbO	5.561	(1.84)	4.14	3.8(H)
BiO	4.314	(1.94)	3.39	4.0±1.0(G)
NS	8.537	1.496	5.17	5.0±0.1(G)

[a] See footnote reference 44.

[42] G. Glockler, J. Chem. Phys. **19**, 124 (1951).
[43] P. K. Carroll, Can. J. Phys. **34**, 83 (1956).
[44] K. Dressler, Helv. Phys. Acta **28**, 563 (1955).

estimated the dissociation energy of PO to be almost exactly 5.4 ev. On the basis of the aforementioned results we recommend the value 5.4 ev for D(PO).

AsO

There is a predissociation in the upper state below $v=1$ at 4.95 ev. Gaydon gives 4.95±0.1 ev for the dissociation energy of this molecule. Using an estimated value for its r_e, we have estimated its dissociation energy to be 4.8 ev; this lends support to the value suggested by Gaydon.

SbO

LBS for the ground state gives 3.8 ev and our value using an estimated value for its r_e is 4.14 ev.

BiO

Scari[45] has recently reported that a linear extrapolation for the vibrational levels of the ground state gives limit at 3.7±0.9 ev. LBS of the lower state of the C and D systems gives 5.7 ev. If this corresponds to Bi($^2D_{5/2}$)+O(^3P), then the dissociation energy of BiO would be around 3.5 ev. Our value of 3.4 ev lends support to the above assumption.

NS

LBS for the ground state gives limit at 6 ev; Gaydon gives 5±1 ev. Our value is 5.17 ev; however, there is a possibility that the sequence constant applicable for the oxides may not be applicable to the sulphides, selenides and tellurides. In such a case, the dissociation energy of NS would be much higher than 5.17 ev and possibly a little less than the LBSX value.

4.12. NH-Type Radicals

The dissociation energy of BiH is known to be 2.5±0.3 ev. Data are not adequate for any other radical of this sequence. Assuming that the dissociation energy of BiH is 2.2 ev, we have estimated the dissociation energies of the other radicals of this sequence and presented them in Table XIII. These values are, however, approximate, based on approximate values for k_e and r_e.

The true dissociation energy of NH has not been determined but a value around 3.7 ev has been suggested by Gaydon and others as the most probable value. Our value is 4.45 ev; this shows that NH constitutes an exception.

Our value for D(PH) is 3.3 ev (76 kcal). Some support can be given to this value by assuming that there is only a little s character in the bonding orbitals of P in PH_3 and consequently very little difference between the values of $D(PH_2\text{–}H)$, D(PH–H), and D(P–H). The most likely value for comparison with that obtained by us for D(P–H) would be the P—H bond energy obtained from the heat of atomization of PH_3. From relevant thermochemical data, the P—H bond energy is 77 kcal.

[45] O. Scari, Acta Phys. Hung. **6**, 73 (1956).

TABLE XIII. NH-type radicals ($S=1.404$).

Radical	k_e	r_e	D_0	D_0 (Literature)
NH	(6.02)	1.038	4.45	3.7±0.5(G)
PH	(3.26)	(1.43)	3.32	Unknown
AsH	(2.43)	(1.51)	2.61	Unknown
SbH	(2.05)	(1.71)	2.5	Unknown
BiH	1.708	1.809	2.2	2.5±0.3(G)

Similarly, our value for D(As–H) is 2.6 ev (60 kcal), while the As—H bond energy from the heat of atomization of AsH_3 is around 59 kcal.

By choice of a proper sequence constant and with the accurate values for k_e and r_e, we can probably estimate the dissociation energies of these radicals much more precisely.

4.13. CO-Type Molecules

Most of the molecules of this sequence were studied spectroscopically by Barrow and his coworkers.[46–53] They find that the convergence for the E state is rapid and leads to a limit agreeing in general with that obtained by linear Birge-Sponer extrapolation for the vibrational levels of the ground state. Consequently, they assume that the ground and E states both dissociate into ground-state atoms. They consider the E state to be singlet state ($^1\Sigma^+$) arising from the normal ^3P components in most cases and from the excited ^3P components in a few cases. For a number of these molecules, the dissociation limits were not observed by direct observation. It was assumed that the true dissociation energy of the E state is a constant fraction (0.456±0.08) of the linearly extrapolated value. For a few of these molecules the thermochemical values are also available; and, they generally agree with the values suggested by Barrow and his co-workers.

Our attempts to correlate the dissociation energies of these molecules showed that the oxides behave quite differently from the rest of the molecules of this sequence. This is probably a consequence of the anomalous behavior of O_2 in its family. With the exception of CO, the other oxides of this sequence form a group and

[46] (a) E. E. Vago and R. F. Barrow, Proc. Phys. Soc. (London) **58**, 538 (1946); (b) **58**, 707 (1946).

[47] E. E. Vago and R. F. Barrow, *Victor Henri Commemorative Volume* (Maison Desoeur, Liége, Belgium, 1948).

[48] G. Drummond and R. F. Barrow, Proc. Phys. Soc. (London) **A65**, 148, 277 (1952).

[49] R. F. Barrow, G. Drummond, and H. C. Rowlinson, Proc. Phys. Soc. (London) **A66**, 885 (1953).

[50] A. Lagerqvist, G. Nihelden, and R. F. Barrow, Proc. Phys. Soc. (London) **A65**, 419 (1952).

[51] R. F. Barrow and H. C. Rowlinson, Proc. Roy. Soc. (London) **A224**, 374 (1954).

[52] S. J. Q. Robinson and R. F. Barrow, Proc. Phys. Soc. (London) **A67**, 95 (1954).

[53] A. Lagerqvist, H. Westerlund, C. V. Wright, and R. F. Barrow, Arkiv Fysik **14**, 387 (1958).

TABLE XIV. CO-type molecules. $S=1.726$ for SiO, GeO, SnO, and PbO, 1.647 for all the molecules headed by CS.

Molecule	k_e	r_e	D_0	D_0 (Literature)
CO	19.02	1.1282	11.11	11.11(G)
SiO	9.247	1.510	8.09	8.09±0.27[b]
GeO	7.525	1.6507	7.20	6.75±0.23[b]
SnO	5.615	1.838	5.98	5.9[c]
PbO	4.557	1.922	5.07	4.3(H)
CS	8.488	1.534	7.90	7.9[c]
SiS	4.937	1.9288	5.78	6.39±0.14[d]
GeS	4.358	(2.06)	5.45	5.66±0.13(G)
SnS	3.536	(2.26)	4.85	4.81±0.28[e]
PbS	2.992	2.395	4.35	4.6[f]
CSe	6.585	1.669	6.67	6.8(H)
SiSe	4.094	(2.14)	5.32	5.8(H)
GeSe	3.743	(2.19)	5.02	4.98±0.25(G)
SnSe	3.066	(2.39)	4.45	4.54[g]
PbSe	2.595	(2.53)	3.98	4.27[f]
CTe	(4.945)[a]	(1.95)	5.85	Unknown
SiTe	3.130	(2.34)	4.44	5.3±0.4(G)
GeTe	2.902	(2.39)	4.13	4.1±0.4(G)
SnTe	2.439	(2.57)	3.81	4.1[g]
PbTe	2.086	(2.73)	3.46	3.5(H)

[a] B. Rosen, *Donnes Spectroscopiques Concernant les Molecules Diatomiques* (Herman & Cie, Paris, France, 1951).
[b] See footnote reference 51.
[c] Thermochemical value.
[d] See footnote reference 52.
[e] See footnote reference 49.
[f] See footnote reference 47.
[g] See footnote reference 46(a).

obey our rule. The sulphides, selenides and tellurides headed by CS also form a separate group and obey our rule with a different sequence constant.

The dissociation energy of CO is now well established to be 11.11 ev. However, CO as the first member constitutes an exception among the oxides. In the case of SiO, both thermochemical and spectroscopic evidences are in favor of a value around 8.1 ev. This is about the value one would obtain if the heat of vaporiza- of silicon is taken to be 105 kcal[54] and $\Delta H_f(\mathrm{SiO}; g)$ to be -21.4 ± 0.6 kcal.[55] Although the true dissociation limit was not observed, Barrow and Rowlinson[51] under reasonable assumptions have found that the E state of this molecule gives a limit at 8.09 ± 0.27 ev. On the basis of the value 8.09 ev for $D(\mathrm{SiO})$ we have estimated the dissociation energies of GeO, SnO, and PbO and recorded them in Table XIV. These results are now discussed.

GeO

Baughan[56] has estimated the heat of vaporization of germanium to be 89 ± 4 kcal. Combining this value with -10.5 kcal[57] for $\Delta H_f(\mathrm{GeO}; g)$ and 58.98 kcal for $\Delta H_f(\mathrm{O}; g)$ we obtain the value 158.5 ± 4 kcal for the dissociation energy of GeO. Assuming that the E state dissociates into ground state atoms, Barrow and Rowlinson[51] have obtained the value 6.75 ± 0.23 ev for the dissociation energy of GeO. LBS of the ground gives a limit at 6.9 ev. Our value is 7.2 ev and is probably a little high. We consider a value around 7 ev as highly justifiable for this molecule. Our result also indicate that the heat of vaporization of germanium to be 93 kcal.

SnO

Searcy and Freeman[58] have obtained the value 71.9 ± 2 kcal for the heat of vaporization of tin. Based on the value 70 kcal for the heat of vaporization of tin, Brewer and Mastick[59] have deduced the value of 132 kcal for the dissociation energy of SnO. With Searcy and Freeman's value for the heat of vaporization of tin, this value would become 134 ± 2 kcal. Drummond and Barrow[48] have found that the E state of this molecule gives limit at 5.678 ev. Our value for this molecule is 5.98 ev (138 kcal). On the basis of the thermochemical value and of our value, we suggest the value 5.9 ev for the dissociation energy of this molecule. Accordingly, the heat of vaporization of tin would be 74 kcal.

PbO

LBS for the ground state and also a thermochemical calculation based on the value 46.5 kcals for the heat of vaporization of lead give 4.3 ev for $D(\mathrm{PbO})$. Our value is 5.07 ev, this shows that the heat of vaporization of lead is around 63 kcals. According to Cottrell,[60] the value of 46.5 kcal for the heat of vaporization of lead is not well founded. It will be shown in the next section that the thermochemistry of PbS also leads to a value around 63 kcal for the heat of vaporization of lead.

Sulphides, Selenides, and Tellurides

Headed by CS, there are 15 molecules in this sequence and all of them have been found to obey our rule. Schäfer and Wiedemer[61] have recently reported the value 60 ± 6 kcal for the heat of formation of CS. Combining this value with 170 kcal for the heat of sublimation of graphite and 66 kcal for $\Delta H_f(\mathrm{S}; g)$ we obtain the value 176 ± 6 kcal for the dissociation energy of CS. LBS for the ground state of CS gives[53] a limit at 181 kcal. LBS for the $A\ ^1\Pi$ state gives a limit around 8.2 ev. Barrow and his coworkers[53] suggest the value 175 ± 7 kcal for the dissociation energy of this molecule. We have found the value 7.9 ev (182 kcal) to be quite satisfactory. Taking $D(\mathrm{CS})=7.9$ ev, we have calculated the dissociation energies of the other members of this sequence and presented the results in Table XIV. These results are now discussed.

[54] R. E. Honig, J. Chem. Phys. **22**, 1610 (1954).
[55] L. Brewer and R. K. Edwards, J. Phys. Chem. **58**, 351 (1954).
[56] E. C. Baughan, Quart. Revs. (London) **7**, 103 (1953).
[57] W. L. Jolly and W. M. Mortimer, J. Am. Chem. Soc. **74**, 5757 (1952).
[58] A. W. Searcy and R. D. Freeman, J. Am. Chem. Soc. **76**, 5229 (1954).
[59] L. Brewer and D. F. Mastick, J. Chem. Phys. **19**, 834 (1951).
[60] T. L. Cottrell, *The Strengths of the Chemical Bonds*, (Butterworths Scientific Publications, Ltd., London, 1958) 2nd ed.
[61] H. Schäfer and H. Wiedemer, Z. anorg. u. allgem. Chem. **296**, 241 (1958).

SiS

A short extrapolation for the E state gives limit at 148.6 kcal.[52] If the products of the E state are assumed be be $Si(^3P_2)+S(^3P_0)$ then $D''=147.4$ kcal. Robinson and Barrow[52] give the final value to be 147.4 ± 3 kcal (6.39 ± 0.14 ev). Gaydon gives 6.4 ± 0.4 ev. Our value is 5.78 ev; we take $D(SiS)=6$ ev.

SnS

A fairly short extrapolation for the E state gives limit at 4.8 ev.[49] Our value is 4.85 ev. Based on the value 65 kcal for the heat of vaporization of tin and 4.4 ev for $D(S_2)$, Barrow, Drummond, and Rowlinson deduced[49] the value 97 kcal for $D(SnS)$. If we use 74 kcal instead of 65 kcal for the heat of vaporization of tin, the thermochemical value for $D(SnS)$ would be 106 kcal (4.6 ev). If we assume the products of the E state to be $Sn(^3P_1)+S(^3P_2)$ then $D''=4.6$ ev which is in agreement with the thermochemical value. A value around 4.8 ev appears to be quite safe.

GeS

LBS of the ground state gives limit at 5.6 ev. The levels of the E state converge to a limit at 5.79 ev. If we assume that the dissociation products of the E state are $Ge(^3P_2)+S(^3P_0)$ then $D''=5.54$ ev. Our value is 5.45 ev; Gaydon gives $5.66+0.13$ ev; we suggest the value 5.54 ev.

PbS

Based on the convergence limit of the upper state, Vago and Barrow[47] give 4.6 ev. Our value is 4.35 ev. A thermochemical value based on 46.5 kcal for $L(Pb)$ and 4.4 ev for $D(S_2)$ is 3.25 ev. If our new value, 63 kcal, is used instead of 46.5 kcal for $L(Pb)$ then the thermochemical value for $D(PbS)$ would be 4.0 ev. A value around 4.3 ev is suggested.

CSe

LBS for the ground state gives limit at 6.8 ev, our value is 6.67 ev. On this basis, we suggest the value 6.7 ± 0.1 ev for the dissociation energy of this molecule.

SiSe

LBS for the ground state gives limit at 5.8 ev. LBS for the upper state and also GBS for the E state give limit at 5.7 ev. Our value is 5.32 ev. If we assume the dissociation products of the E state to be $Si(^3P_2)+Se(^3P_0)$ then $D''=5.36$ ev in agreement with our value. Hence we suggest the value 5.36 ev for $D(SiSe)$.

GeSe

The levels of the E state converge to a limit at 5.23 ev. Our value is 5.02 ev. If we assume the dissociation products of the E state to be $Ge(^3P_2)+Se(^3P_2)$ then $D(SiSe)=5.05$ ev in agreement with our value. However, if we assume that the E state dissociates into ground-state atoms then $D(SiSe)=5.23$ ev. A value around 5.1 ev appears to be quite safe to us.

SnSe

LBS for the ground state gives limit at 4.6 ev; GBS for the E state gives limit at 4.54 ev; our value is 4.45 ev. On this basis we suggest the value 4.5 ev for $D(SnSe)$.

PbSe

Based on the convergence limit for the upper state, Vago and Barrow[47] give 4.27 ev for $D(PbSe)$; our value is 3.98 ev. If we assume that the upper state dissociates into $Pb(^3P_0)+Se(^3P_2)$ then $D''=3.96$ ev in good agreement with our value.

CTe

It appears no one has yet studied this molecule. Based on approximate values for its r_e and k_e, we have estimated its dissociation energy to be 5.85 ev.

SiTe

GBS for the D state gives limit at 5.0 ev (5.64 ev with Vago and Barrow's[46b] formula); LBS for the ground state gives 5.5 ev; Gaydon gives 5.3 ± 0.4 ev. Our value is 4.44 ev. If we assume that the D state dissociates into $Si(^3P_2)+Te(^3P_0)$ and take the dissociation limit of the D state as 5.0 ev, then $D''=4.39$ ev in agreement with our value.

SnTe

Upper states B, D and E converge to limits at 3.3, 4.07 and 4.9 ev, respectively. Vago and Barrow[46b] adopt 4.1 ev for $D(SnTe)$. Our value is 3.81 ev. If we assume that the E state dissociates into $Sn(^3P_2)+Te(^3P_0)$ then $D''=3.88$ ev in agreement with our value. We recommend the value 3.88 ev.

PbTe

LBS for the upper state gives limit at 3.8 ev; Herzberg[2] gives 3.5 ev; Gaydon gives 3.5 ± 1.0 ev. Our value is 3.46 ev which is in good agreement with the value suggested by Herzberg.

The above results for these molecules show that the E state is a singlet state arising in most cases from the excited ^3P components instead of from the normal ^3P components as assumed by Vago and Barrow.[47] They also confirm the anomalous behavior of the oxides. Our results are consistent with the values of 170, 105, 93, 74, and 63 kcal, respectively, for the heats of formation of gaseous C, Si, Ge, Sn, and Pb atoms. Our results for the sulphides indicate that the dissociation energy of S_2 is 4.4 ev.

TABLE XV. BeH-type radicals ($S=1.119$).

Radical	k_e	r_e	D_0	D_0 (Literature)
BeH	2.263	1.343	2.72	2.3±0.3(G)
MgH	1.275	1.731	1.97	2.0±0.5(G)
CaH	0.977	2.002	1.75	1.7(G)
SrH	0.854	2.1456	1.64	1.65±0.1(G)
BaH	0.809	2.232	1.61	1.8±0.1(G)

4.15. BeH-Type Radicals

The results for this sequence are presented in Table XV. Our values for MgH, CaH, SrH, and BaH appear to be reliable to within 0.05 ev. BeH probably constitutes an exception. The results are as follows.

BeH

GBS for the ground state gives limit at 2.5 ev; the dissociation limit of the $^2\Pi$ state assuming Be(^3P) leads to $D''=2.2$ ev; Gaydon gives 2.3±0.3 ev. Our value of 2.72 ev appears to be slightly high. BeH probably constitutes an exception.

MgH

GBS for the ground state gives 2.0 ev and our value of 1.97 ev is in good agreement with this.

CaH

Predissociation in the C state assuming Ca(^3P) gives 1.70 ev. Our value, 1.75 ev, lends support to the above assumption.

SrH

Predissociation in the C state gives 1.66 ev and this is in good agreement with our value of 1.64 ev.

BaH

Predissociation in the C state gives $D''\leq 1.82$ ev. Our value is 1.61 ev.

4.16. BH-Type Radicals

The results for the radicals of this sequence are presented in Table XVI. Our results are very satisfactory for AlH, InH, and TlH. BH constitutes an exception. Based on approximate values for its r_e and k_e, we have suggested an approximate value for the dissociation energy of GaH.

TABLE XVI. BH-type radicals ($S=0.98$).

Radical	k_e	r_e	D_0	D_0 (Literature)
BH	(3.03)	1.233	3.8	3.0±0.4(G)
AlH	1.62	1.646	2.72	2.9±0.2(G)
GaH	(1.42)[a]	(1.72)[a]	2.49	Unknown
InH	1.28	1.838	2.4	2.5±0.1(G)
TlH	1.142	1.87	2.18	2.18(H)

[a] Estimated values. See footnote reference 18.

4.17. CuH-Type Molecules

The results for CuH, AgH, and AuH are presented in Table XVII and discussed as follows.

CuH

LBS for the ground state gives 2.9 ev. Gaydon gives 2.7±0.3 ev; flame photometry, by Sugden's method, gives 2.87 ev.[62] Our value is 2.77 ev. Based on this, we suggest 2.8 ev for D(CuH).

AgH

For AgH, the vibrational levels of the ground state known up to $v=11$ would extrapolate to give a limit at 2.3 ev; Gaydon gives 2.3±0.1 ev. By comparison of the rates of evaporation of silver in helium or nitrogen, and in hydrogen, Farkas[63] has deduced the value 2.5 ev for D(AgH). Our value, 2.53 ev, is in good agreement with the thermochemical value.

TABLE XVII. CuH-type molecules ($S=1.16$).

Molecule	k_e	r_e	D_0	D_0 (Literature)
CuH	2.2	1.4631	2.77	2.7±0.3(G); 2.87[a]
AgH	1.817	1.6174	2.53	2.3±0.1(G); 2.5[b]
AuH	3.138	1.5237	4.12	3.1(H); 4.1[c]

[a] See footnote reference 62.

[b] See footnote reference 60.

[c] The upper state gives limit at 4.1 ev. If this state is assumed to be $^1\Sigma^+$ then it correlates with normal products and gives $D''=4.1$ ev. Both Gaydon and Herzberg assume that this state is $^3\Pi_{0^+}$ and correlate it with Au($^2D_{5/2}$)+H(^2S). Then its dissociation energy would be 3 ev in agreement with a thermochemical value of around 3.1 ev.

AuH

In the case of AuH, LBS for the ground state gives 3.6 ev and GBS for the upper state gives limit at 4.1 ev. Assuming the upper state to be $^3\Pi_{0^+}$ and that it dissociates into Au($^2D_{5/2}$)+H(^2S), both Gaydon and Herzberg give 3.0 ev for the dissociation energy of this molecule. This agrees very well with the thermochemical value of 3.1 ev deduced by Farkas.[63] However, if the upper state is $^1\Sigma^+$ then it correlates with normal products giving $D''=4.1$ ev. This value is in excellent agreement with the value of 4.12 ev obtained by us. If this value is correct, then it would predict that the volatility of gold would be increased by many orders of magnitude by passing hydrogen over it. Further work is required before we can conclude that AuH constitutes an exception to our rule. Tentatively we suggest 4.1 ev for D(AuH).

4.18. CH-Type Radicals

The dissociation energies of any of these radicals is not known definitely. Two values have been suggested

[62] E. M. Bulewicz and T. M. Sugden, Trans. Faraday Soc. 52, 1475 (1956).

[63] A. Farkas, Z. physik. Chem. B5, 467 (1929).

TABLE XVIII. CH-type radicals. $S=1.3026$ if $D(\mathrm{PbH})=2.04$ ev.

Radical	k_e	r_e	D_0	D_0 (Literature)
CH	4.484	1.12	3.86	3.47?(G)
SiH	2.39[a]	1.521[a]	2.79	3.19±0.25[a]
GeH	(1.87)	(1.591)	2.28	Unknown
SnH	(1.47)	(1.822)	2.06	2.13[b]
PbH	1.445	1.839	2.04	D″≤2.04(G); 1.59(H)

[a] See footnote reference 64.
[b] Assuming that the predissociation at 3.2 ev occurs into $\mathrm{Sn}(^1D)+\mathrm{H}(^2S)$.

for the dissociation energy of PbH. The weak predissociation in the upper state shows that $D(\mathrm{PbH})\leq 2.04$ ev. From the predissociation in the B state at 20 550 cm^{-1} Herzberg gives 1.59 ev for $D(\mathrm{PbH})$; Gaydon gives the value as 1.8±0.2 ev presumably assuming that either 2.04 or 1.59 ev would be the correct value. We have found the value 2.04 to be satisfactory. Based on this value for PbH, we have calculated the dissociation energies of the other radicals of this sequence and presented them in Table XVIII. The results are now discussed.

SnH

There is a predissociation at 3.2 ev, and if this is assumed to occur into $\mathrm{Sn}(^1D)+\mathrm{H}(^2S)$ then $D''=2.13$ ev. Our value of 2.06 ev lends support to the above assumption.

GeH

No data are available for this radical. Using estimated values for its r_e and k_e, we have estimated its dissociation energy to be 2.28 ev.

SiH

There is no direct observation of the dissociation limit for this molecule. GBS for the $^2\Delta$ states gives a limit around 4 ev. Assuming that this state dissociates into $\mathrm{Si}(^1D)+\mathrm{H}(^2S)$ Douglas[64] obtained the value 3.19±0.25 ev for the dissociation energy of this molecule. Our value is 2.79 ev. Since, as Douglas pointed out, the $^2\Delta$ state is a shallow state, the value may be around 2.8 ev.

CH

The usually quoted value for the dissociation energy of this radical is 3.47 ev. Our value is 3.86 ev. CH probably constitutes an exception in this sequence. However, it should be pointed out that Gerö and Schmid[65] have found a number of breaking-off points in the upper state indicating predissociation; our value may correspond to one of them.

5. CONCLUSION

Our results show that the first member, as a rule, constitutes an exception. There are, however, a few sequences such as the hydrogen halides, hydrides of the alkali metals, etc., in which the first member does not constitute an exception. Although F_2 constitutes an exception among the halogens, the fluorides do not constitute exceptions among halides. There is, however, evidence to show that the oxides behave anomalously from the sulphides, selenides and tellurides. Data are not adequate to make any such conclusions about the behavior of the nitrides.

There are not enough data to treat several other diatomic molecules in the above way; but, as more and more data become available, it may be fruitful to test the accuracy of their dissociation energy values by using this rule. It would be advisable to take into consideration any available thermochemical evidence before a particular value is assigned to a given molecule.

It might be also profitable to extend this rule to similar bonds in polyatomic molecules but, at present, there do not seem to be any reliable data on bond energies and bond stretching force constants. Also, the bond stretching force constants available in the literature are based on several types of assumptions and are not compatible with each other. On the strength of the results presented in this paper, we can, however, anticipate that this rule will find application for similar bonds in polyatomic molecules.

ACKNOWLEDGMENTS

I am very greatly indebted to Professor Oscar K. Rice for several helpful discussions on this subject and for various helpful suggestions in the preparation of the manuscript. My thanks are also due Professor Leo Brewer and the referee of this paper for suggestions concerning the dissociation energies of S_2, SO, SiO, and CS. This work was supported by the Office of Ordnance Research of the U.S. Army, to which I offer my grateful thanks.

[64] A. E. Douglas, Can. J. Phys. **35**, 71 (1957).

[65] L. Gerö and R. Schmid, Z. Physik **118**, 210 (1941).

Derivation of Thermodynamic Relations for Three-Dimensional Systems

FRANCIS S. MANNING
Chemical Engineering Department, Carnegie Institute of Technology, Pittsburgh, Pennsylvania
AND
WILLIAM P. MANNING
Merck & Co. Inc., Rahway, New Jersey

(Received April 4, 1960)

The relations between the first-order derivatives of the thermodynamic properties of three-dimensional systems have been evaluated. The method of Jacobians which was used previously for simple or two-dimensional systems has been extended, and the results presented in tabular form.

INTRODUCTION

THE use of Jacobians for deriving thermodynamic relations between the properties of simple systems, i.e., those which may be fully described by two intensive variables, was first expounded by Shaw.[1] Compact tables enabling all first- and second-order partial derivatives to be expressed as ratios of reference Jacobians were presented. Crawford[2,3] extended the theory to n-variable systems for both unrestricted and polyphase, polycomponent systems. A method of expressing any desired first-order partial derivative in terms of the elements of a fundamental n-dimensional reference Jacobian was indicated.

The present work extends Shaw's table of the partial, first-order derivatives of thermodynamic properties to include systems undergoing such irreversible processes as permit the definition of an entropy in terms of the conventional thermodynamic parameters, in particular, systems undergoing chemical reaction. This development is restricted to three-dimensional systems, i.e., those for which the additional effect may be quantitatively expressed by one pair of variables. The method of de Donder, Prigogine, and Defay[4] was used to describe the irreversibility when due to chemical reaction. The greatly increased range of application made possible by this extension warrants the preparation of such tables.

TABLE I. Reference Jacobians.

No.	Name	Letter
1	$J(P, V, T)$	a
2	$J(P, V, S)$	b
3	$J(P, V, A)$	c
4	$J(P, V, \xi)$	d
5	$J(P, T, S)$	e
6	$J(P, T, A)$	f
7	$J(P, T, \xi)$	g
8	$J(P, S, A)$	h
9	$J(P, S, \xi)$	i
10	$J(P, A, \xi)$	e
11	$J(V, T, S)$	j
12	$J(V, T, A)$	k
13	$J(V, T, \xi)$	l
14	$J(V, S, A)$	m
15	$J(V, S, \xi)$	n
16	$J(V, A, \xi)$	j
17	$J(T, S, A)$	c
18	$J(T, S, \xi)$	d
19	$J(T, A, \xi)$	−a
20	$J(S, A, \xi)$	−b

SYSTEM CHARACTERIZATION

Systems undergoing chemical reaction may be expressed in terms of the variables pressure, P; volume, V; temperature, T; entropy, S; affinity, A; and extent of reactions, ξ. The four thermodynamic potential functions are defined as:

$$dU = TdS - PdV - Ad\xi, \tag{1}$$

$$dH = TdS + VdP - Ad\xi, \tag{2}$$

$$dF = -SdT - PdV - Ad\xi, \tag{3}$$

$$dG = -SdT + VdP - Ad\xi. \tag{4}$$

These equations are applicable to polycomponent systems as the occurring changes can be represented by one reaction coordinate.

PROPERTIES OF JACOBIANS

Any three-dimensional Jacobian $J(x, y, z)$ is defined in terms of three arbitrary reference variables, α, β, γ,

$$J(x, y, z/\alpha, \beta, \gamma) = \begin{vmatrix} \partial x/\partial\alpha & \partial y/\partial\alpha & \partial z/\partial\alpha \\ \partial x/\partial\beta & \partial y/\partial\beta & \partial z/\partial\beta \\ \partial x/\partial\gamma & \partial y/\partial\gamma & \partial z/\partial\gamma \end{vmatrix}. \tag{5}$$

The use of Jacobians in relating first-order partial derivatives depends on the following fundamental characteristics:

1. Any first-order partial derivative may be written as a ratio of two Jacobians which must be expressed in terms of the same reference variables,

$$(\partial p/\partial q)_{x,y} = J(p, x, y)/J(q, x, y). \tag{6}$$

2. Repetition of any variable results in a value of zero,

$$J(x, x, y) = 0. \tag{7}$$

[1] A. N. Shaw, Phil. Trans. Roy. Soc. (London) **A234**, 299 (1935).
[2] F. H. Crawford, Proc. Am. Acad. Arts & Sci. **78**, 165 (1950).
[3] F. H. Crawford, Proc. Am. Acad. Arts & Sci. **83**, 191 (1955).
[4] I. Prigogine and R. Defay, *Chemical Thermodynamics*, translated by D. H. Everett (Longman's, Green and Company, New York, 1954).

TABLE II. Nonzero Jacobians.

Jacobian	Value in terms of reference Jacobians
$J(P, V, T)$	a
$J(P, V, S)$	b
$J(P, V, A)$	c
$J(P, V, \xi)$	d
$J(P, V, U)$	Tb−Ad
$J(P, V, H)$	Tb−Ad
$J(P, V, F)$	−Ad−Sa
$J(P, V, G)$	−Ad−Sa
$J(P, V, Q)$	Tb
$J(P, V, W)$	O
$J(P, T, S)$	e
$J(P, T, A)$	f
$J(P, T, \xi)$	g
$J(P, T, U)$	Pa+Te−Ag
$J(P, T, H)$	Te−Ag
$J(P, T, F)$	Pa−Ag
$J(P, T, G)$	−Ag
$J(P, T, Q)$	Te
$J(P, T, W)$	−Pa
$J(P, S, A)$	h
$J(P, S, \xi)$	i
$J(P, S, U)$	Pa−Ai
$J(P, S, H)$	−Ai
$J(P, S, F)$	Pb+Se−Ai
$J(P, S, G)$	Se−Ai
$J(P, S, Q)$	O
$J(P, S, W)$	−Pb
$J(P, A, \xi)$	e
$J(P, A, U)$	Pc−Ae−Th
$J(P, A, H)$	−Ae−Th
$J(P, A, F)$	Pc+Sf−Ae
$J(P, A, G)$	Sf−Ae
$J(P, A, Q)$	−Th
$J(P, A, W)$	−Pc
$J(P, \xi, U)$	Pd−Ti
$J(P, \xi, H)$	−Ti
$J(P, \xi, F)$	Pd+Sg
$J(P, \xi, G)$	Sg
$J(P, \xi, Q)$	−Ti
$J(P, \xi, W)$	−Pd
$J(P, U, H)$	APd−PTb
$J(P, U, F)$	PSa+PTb+STe−ASg−ATi
$J(P, U, G)$	APd+PSa+STe−ASg−ATi
$J(P, U, Q)$	ATi−PTb
$J(P, U, W)$	APd−PTb
$J(P, H, F)$	PTb+STe−APd−ASg−ATi
$J(P, H, G)$	STe−ASg−ATi
$J(P, H, Q)$	ATi
$J(P, H, W)$	APd−PTb
$J(P, F, G)$	APd+PSa
$J(P, F, Q)$	ATi−PTb−STe
$J(P, F, W)$	APd+PSa
$J(P, G, Q)$	ATi−STe
$J(P, G, W)$	APd+PSa
$J(P, Q, W)$	−PTb
$J(V, T, S)$	j
$J(V, T, A)$	k
$J(V, T, \xi)$	l
$J(V, T, U)$	Tj−Al
$J(V, T, H)$	Tj+Va−Al
$J(V, T, F)$	−Al
$J(V, T, G)$	Va−Al
$J(V, T, Q)$	Tj
$J(V, T, W)$	O
$J(V, S, A)$	m
$J(V, S, \xi)$	n
$J(V, S, U)$	−An
$J(V, S, H)$	Vb−An
$J(V, S, F)$	Sj−An
$J(V, S, G)$	Sj+Vb−An
$J(V, S, Q)$	O
$J(V, S, W)$	O
$J(V, A, \xi)$	j
$J(V, A, U)$	−Aj−Tm
$J(V, A, H)$	Vc−Aj−Tm
$J(V, A, F)$	Sk−Aj
$J(V, A, G)$	Sk+Vc−Aj
$J(V, A, Q)$	−Tm
$J(V, A, W)$	O
$J(V, \xi, U)$	−Tn
$J(V, \xi, H)$	Vd−Tn
$J(V, \xi, F)$	Sl
$J(V, \xi, G)$	Sl+Vd
$J(V, \xi, Q)$	−Tn
$J(V, \xi, W)$	O
$J(V, U, H)$	TVb−AVd
$J(V, U, F)$	STj−ASl−ATn
$J(V, U, G)$	STj+TVb−ASl−ATn−AVd
$J(V, U, Q)$	ATn
$J(V, U, W)$	O
$J(V, H, F)$	AVd+STj+SVa−ASl−ATn
$J(V, H, G)$	STj+SVa+TVb−ASl−ATn
$J(V, H, Q)$	ATn−TVb
$J(V, H, W)$	O
$J(V, F, G)$	−AVd−SVa
$J(V, F, Q)$	ATn−STj
$J(V, F, W)$	O
$J(V, G, Q)$	ATn−STj−TVb
$J(V, G, W)$	O
$J(V, Q, W)$	O
$J(T, S, A)$	c
$J(T, S, \xi)$	d
$J(T, S, U)$	−Ad−Pj
$J(T, S, H)$	Ve−Ad
$J(T, S, F)$	−Ad−Pj
$J(T, S, G)$	Ve−Ad
$J(T, S, Q)$	O
$J(T, S, W)$	Pj
$J(T, A, \xi)$	−a
$J(T, A, U)$	Aa−Tc−Pk
$J(T, A, H)$	Aa+Vf−Tc
$J(T, A, F)$	Aa−Pk
$J(T, A, G)$	Aa+Vf
$J(T, A, Q)$	−Tc
$J(T, A, W)$	Pk
$J(T, \xi, U)$	−Pl−Td
$J(T, \xi, H)$	Vg−Td
$J(T, \xi, F)$	−Pl
$J(T, \xi, G)$	Vg
$J(T, \xi, Q)$	−Td
$J(T, \xi, W)$	Pl
$J(T, U, H)$	PTj+PVa+TVe−APl−AVg
$J(T, U, F)$	−ATd−PTj
$J(T, U, G)$	PVa+TVe−APl−ATd−AVg
$J(T, U, Q)$	ATd+PTj
$J(T, U, W)$	PTj−APl
$J(T, H, F)$	APl+AVg−ATd−PTj−PVa
$J(T, H, G)$	TVe−ATd
$J(T, H, Q)$	ATd−TVe
$J(T, H, W)$	PTj+PVa−APl
$J(T, F, G)$	PVa−APl−AVg
$J(T, F, Q)$	ATd+PTj
$J(T, F, W)$	−APl
$J(T, G, Q)$	ATd−TVe
$J(T, G, W)$	PVa−APl
$J(T, Q, W)$	PTj
$J(S, A, \xi)$	−b
$J(S, A, U)$	Ab−Pm
$J(S, A, H)$	Ab+Vh
$J(S, A, F)$	Ab−Pm−Sc
$J(S, A, G)$	Ab+Vh−Sc
$J(S, A, Q)$	O
$J(S, A, W)$	Pm
$J(S, \xi, U)$	−Pn
$J(S, \xi, H)$	Vi
$J(S, \xi, F)$	−Pn−Sd

TABLE II.—*Continued.*

Jacobian	Value in terms of reference Jacobians
$J(S, \xi, G)$	Vi−Sd
$J(S, \xi, Q)$	O
$J(S, \xi, W)$	Pn
$J(S, U, H)$	PVb−APn−AVi
$J(S, U, F)$	ASd+PSj
$J(S, U, G)$	ASd+PSj+PVb−APn−AVi
$J(S, U, Q)$	O
$J(S, U, W)$	−APn
$J(S, H, F)$	APn+ASd+AVi−PVb−SVe
$J(S, H, G)$	ASd−SVe
$J(S, H, Q)$	O
$J(S, H, W)$	PVb−APn
$J(S, F, G)$	PSj+PVb+SVe−APn−AVi
$J(S, F, Q)$	O
$J(S, F, W)$	PSj−APn
$J(S, G, Q)$	O
$J(S, G, W)$	PSj+PVb−APn
$J(S, Q, W)$	O
$J(A, \xi, U)$	−Pj−Tb
$J(A, \xi, H)$	Ve−Tb
$J(A, \xi, F)$	Sa−Pj
$J(A, \xi, G)$	Sa+Ve
$J(A, \xi, Q)$	−Tb
$J(A, \xi, W)$	Pj
$J(A, U, H)$	PVc−APj−AVe−PTm−TVh
$J(A, U, F)$	PSk+PTm+STc−ASa−ATb
$J(A, U, G)$	PSk+PVc+STc−APj−ASa−ATb−AVe−TVh
$J(A, U, Q)$	ATb−PTm
$J(A, U, W)$	−APj−PTm
$J(A, H, F)$	APj+AVe+PTm+STc−ASa−ATb−PVc−SVf
$J(A, H, G)$	STc−ASa−ATb−TVh−SVf
$J(A, H, Q)$	ATb+TVh
$J(A, H, W)$	PVc−APj−PTm
$J(A, F, G)$	PSk+PVc+SVf−APj−AVe
$J(A, F, Q)$	ATb−PTm−STc
$J(A, F, W)$	PSk−APj
$J(A, G, Q)$	ATb+TVh−STc
$J(A, G, W)$	PSk+PVc−APj
$J(A, Q, W)$	−PTm
$J(\xi, U, H)$	PVd−PTn−TVi
$J(\xi, U, F)$	PSl+PTn+STd
$J(\xi, U, G)$	PSl+PVd+STd−TVi
$J(\xi, U, Q)$	−PTn
$J(\xi, U, W)$	−PTn
$J(\xi, H, F)$	PTn+STd−PVd−SVg
$J(\xi, H, G)$	STd−SVg−TVi
$J(\xi, H, Q)$	TVi
$J(\xi, H, W)$	PVd−PTn
$J(\xi, F, G)$	PSl+PVd+SVg
$J(\xi, F, Q)$	−PTn−STd
$J(\xi, F, W)$	PSl
$J(\xi, G, Q)$	TVi−STd
$J(\xi, G, W)$	PSl+PVd
$J(\xi, Q, W)$	−PTn
$J(U, H, F)$	APSl+APTn+ASVg+ATVi−PSTj−PSVa−PTVb−STVe
$J(U, H, G)$	APSl+APTn+ASVg+ATVi+PTVb−PSTj−PSVa−STVe
$J(U, H, Q)$	PTVb−APTn−ATVi
$J(U, H, W)$	PTVb−APVd
$J(U, F, G)$	PSTj+PSVa+PVTb+SVTe−APSl−APTn−ASVg−ATVi
$J(U, F, Q)$	ASTd+PSTj
$J(U, F, W)$	PSTj−APSl−APTn
$J(U, G, Q)$	ASTd+PSTj+PTVb−APTn−ATVi
$J(U, G, W)$	PSTj+PTVb−APSl−APTn−APVd
$J(U, Q, W)$	APTn
$J(H, F, G)$	PSTj+PSVa+PTVb+STVe−APSl−APTn−ASVg−ATVi
$J(H, F, Q)$	APTn+ASTd+ATVi−PTVb−STVe
$J(H, F, W)$	APVd+PSTj+PSVa−APSl−APTn
$J(H, G, Q)$	ASTd−STVe
$J(H, G, W)$	PSTj+PSVa+PTVb−APSl−APTn
$J(H, Q, W)$	APTn+PTVb
$J(F, G, Q)$	PSTj+PTVb+STVe−APTn−ATVi
$J(F, G, W)$	−APVd−PSVa
$J(F, Q, W)$	APTn−PSTj
$J(G, Q, W)$	APTn−PSTj−PTVb

3. Changing the cyclic order of the variables changes the sign,

$$J(x, y, z) = J(y, z, x) = J(z, x, y) = -J(x, z, y) = -J(y, x, z) = -J(z, y, x). \quad (8)$$

The six properties used to define the four thermodynamic potentials may be used to form 120 (i.e., 6·5·4) nonzero three-dimensional Jacobians. Application of the symmetry relationships stated in Eq. (8) leaves 20 Jacobians that differ by more than a change in sign. These are listed in Table I. In addition, for the sake of compactness, each Jacobian has been given a characteristic letter.

THERMODYNAMIC RELATIONSHIPS

No use has been made yet of the mathematical properties of the four thermodynamic potentials.

1. Maxwell Equations

The thermodynamic potentials are state functions and therefore their differentials are exact. For a three-dimensional system, six relationships between the first-order partial derivatives of the corresponding Jacobians are obtained. Mathematically, if

$$dM = Xdx + Ydy + Zdz,$$

then

$$(\partial X/\partial y)_{z,x} = (\partial Y/\partial x)_{y,z},$$

or

$$J(X, z, x,) = J(Y, y, z). \quad (9)$$

These six Maxwellian relations, which are shown in Table I by representing two Jacobians by the same letter, reduce the number of different Jacobians from 20 to 14.

2. Expansion Equations

In a three-dimensional system, any state property is a function of any other three independent variables, mathematically,

$$dM = (\partial M/\partial x)_{y,z}dx + (\partial M/\partial y)_{z,x}dy + (\partial M/\partial z)_{x,y}dz, \quad (10)$$

or

$$(\partial M/\partial x)_{p,q}=(\partial M/\partial x)_{y,z}+(\partial M/\partial y)_{z,x}(\partial y/\partial x)_{p,q}$$
$$+(\partial M/\partial z)_{x,y}(\partial z/\partial x)_{p,q}. \quad (11)$$

Transforming Eq. (11) into Jacobian form,

$$J(M, p, q)\cdot J(x, y, z)=J(M, y, z)\cdot J(x, p, q)$$
$$+J(M, z, x)\cdot J(y, p, q)+J(M, x, y)\cdot J(z, p, q). \quad (12)$$

Four independent expansion equations are obtained using this method:

$$-a\cdot b+j\cdot e-n\cdot f+m\cdot g=0, \quad (13)$$

$$a\cdot b+j\cdot e-k\cdot i+l\cdot h=0, \quad (14)$$

$$d\cdot c+j\cdot e-n\cdot f+l\cdot h=0, \quad (15)$$

$$d\cdot c-a\cdot b-n\cdot f+i\cdot k=0. \quad (16)$$

All nonzero Jacobians $J(x, y, z)$ where x, y, z may be any of $P, V, T, S, A, \xi, U, H, F, G, Q, W$ may now be expressed in terms of the reference Jacobians. The results are listed in Table II.

USES

Table II permits the rapid and systematic derivation of any relationship involving the first-order partial derivatives of three-dimensional systems.

NOMENCLATURE

A	affinity
F	Helmholtz work function
G	Gibbs' free energy
H	enthalpy
J	three-dimensional Jacobian, Eq. (5)
M, p, q, x, y, z	arbitrary state functions
P	pressure
Q	reversible heat effect, $dQ=TdS$
S	entropy
T	temperature
U	internal energy
V	volume
W	reversible work effect, $dW=PdV$
X	$(\partial M/\partial x)y, z$
Y	$(\partial M/\partial y)z, x$
Z	$(\partial M/\partial z)x, y$
α, β, γ	arbitrary reference variables
ξ	extent of reaction.

THE JOURNAL OF CHEMICAL PHYSICS VOLUME 33, NUMBER 5 NOVEMBER, 1960

Normal Vibrations of the Polymer Molecules of Helical Configuration

HIROYUKI TADOKORO

Department of Polymer Science, Faculty of Science, Osaka University, Nakanoshima, Kitaku, Osaka, Japan

(Received April 4, 1960)

A method suitable for numerical calculations of the normal vibrations of helical molecules is derived by the use of *GF*-matrix method. The method is described for the case of the isolated infinite helical molecule in which the one-dimensional crystallographic repeat unit contains n chemical units and m turns (one chemical unit contains p atoms). It is shown that the optically active fundamental frequencies of such molecules can be obtained by solving the secular equations for A, B, E_1, and E_2 species, the maximum orders of which are $3p-2$, $3p$, $3p-1$, and $3p$, respectively. This method can be also applied to the cases of infinitely extended planar zigzag chains such as polyethylene and cyclic molecules such as trioxane, etc., as special cases. As examples of application of this method, calculations of the skeletal vibrations of a simple model of polyoxymethylene molecule under the group $D(10\pi/9)$ and of the planar zigzag chain of carbon atoms are given.

INTRODUCTION

THERE are known many high polymer molecules having helical structures, such as those in crystalline isotactic polymers, polyoxymethylene, polyethylene glycol, polytetrafluoroethylene, polypeptides, etc. As to the method of crystal structure analysis of such helical high polymers, there has already appeared an excellent general treatment by Cochran *et al.*[1] It is highly desirable to calculate the normal vibrations of these polymers from the point of view of infrared spectroscopy, but no such numerical calculations have been reported, except for the cases of planar zigzag chain,[2] which is a special case of a helix as shown below. Although a general theory of the vibrations of helical molecules has been already reported by Higgs,[8] he applied his results only to a special simple model. We have derived independently a method for the calculation of the normal vibrations of a helical molecule, which is suitable for numerical calculations. In this paper we should like to describe the outline of this method, and the results of its application to a simple model of polyoxymethylene and to a planar zigzag chain of carbon atoms as an extreme case.

FACTOR GROUP OF ONE-DIMENSIONAL SPACE GROUP

Let us consider an isolated infinite helical molecule in which the one-dimensional crystallographic repeat unit (unit cell) contains n chemical units and m turns (one chemical unit contains p atoms). For example, the polyoxymethylene molecule in the crystalline state has been reported to contain nine chemical units —CH_2O— and five turns in the unit cell length 17.3 A. One chemical unit contains four atoms ($n=9$, $m=5$, and $p=4$).[9] In the case of the planar zigzag chain of polyethylene, in which the chemical unit is —CH_2—, $n=2$, $m=1$, and $p=3$. The symmetry of a helical polymer molecule may be described by a one-dimensional space group. It has been shown that only the normal modes in which all the unit cells vibrate in phase may be active in the infrared and Raman spectra.[10] In other words, it is sufficient spectroscopically to study a factor group with translational subgroup as unit element. The factor group in question may be denoted in terms of $C(2m\pi/n)$,[7] which is isomorphous with the point group C_n. The character table, numbers of normal modes, and selection rules (A: active, F: forbidden) for the helical polymer molecules under the group $C(2m\pi/n)$ are shown in Table I. In the table the symmetry operation C^1 is a rotation of $2m\pi/n$ about the axis of the helix followed by a translation along the axis of $1/n$ of the unit cell length. The symmetry operation C^k signifies that the symmetry operation C^1 is performed k times in succession. N is the number of total normal modes under each irreducible

[1] W. Cochran, F. H. C. Crick, and V. Vand, Acta Cryst. **5**, 581 (1952).

[2] Polyethylene[3-5] and polytetrafluoroethylene.[6,7] The latter possesses a helical configuration, but the distortion of its molecular configuration from a planar zigzag is relatively small, so the calculation of the normal frequencies have been approximated with a planar zigzag model by these authors.

[3] S. E. Whitcomb, H. H. Nielsen and L. H. Thomas, J. Chem. Phys. **8**, 143 (1940).

[4] L. Kellner, Proc. Phys. Soc. (London) **A64**, 521 (1951).

[5] T. Shimanouchi and S. Mizushima, J. Chem. Phys. **17**, 1102 (1949).

[6] T. Shimanouchi, J. Chem. Phys. **17**, 245, 734, 848 (1949).

[7] C. Y. Liang and S. Krimm, J. Chem. Phys. **25**, 563 (1956).

[8] P. W. Higgs, Proc. Roy. Soc. (London) **A220**, 472 (1953).

[9] Although Sauter[10] has assumed the model with $m=4$, Huggins[11] has inferred $m=5$ from the consideration of bond distance and bond angles. We have recently found by x-ray analysis that Huggins' model ($m=5$) is adequate.[12]

[10] E. Sauter, Z. physik. Chem. (Leipzig) **B21**, 161 (1933).

[11] M. L. Huggins, J. Chem. Phys. **13**, 37 (1945).

[12] H. Tadokoro, T. Yasumoto, S. Murahashi, and I. Nitta, J. Polymer Sci. **44**, 266 (1960).

[13] For example, S. Bhagavantam and T. Venkatarayudu, *Theory of Groups and Its Application to Physical Problems* (Andhra University, Waltair, India, 1951); M. C. Tobin, J. Chem. Phys. **23**, 891 (1955); C. Y. Liang, J. Mol. Spectroscopy **1**, 61 (1957).

TABLE I. Character table, numbers of normal modes and selection rules (A: active, F: forbidden) for the helical polymer molecule under the group $C(2m\pi/n)$.[a]

n = odd

		E	C^1	C^2	...	C^{n-1}	N	Infrared	Raman
A		1	1	1	...	1	$3p$ (T_z, R_z)	A	A
E_1	{	1	ϵ	ϵ^2	...	ϵ^{n-1}	$3p$ (T_x)	A	A
	{	1	ϵ^{-1}	ϵ^{-2}	...	$\epsilon^{-(n-1)}$	$3p$ (T_y)	A	A
E_2	{	1	ϵ^2	ϵ^4	...	$\epsilon^{2(n-1)}$	$3p$	F	A
	{	1	ϵ^{-2}	ϵ^{-4}	...	$\epsilon^{-2(n-1)}$	$3p$	F	A
E_3	{	1	ϵ^3	ϵ^6	...	$\epsilon^{3(n-1)}$	$3p$	F	F
	{	1	ϵ^{-3}	ϵ^{-6}	...	$\epsilon^{-3(n-1)}$	$3p$	F	F
.		.	.	.	...	.	.	.	.
.		.	.	.	...	.	.	.	.
$E_{(n-1)/2}$	{	1	$\epsilon^{(n-1)/2}$	$\epsilon^{[(n-1)/2]2}$	...	$\epsilon^{[(n-1)/2](n-1)}$	$3p$	F	F
	{	1	$\epsilon^{-(n-1)/2}$	$\epsilon^{-[(n-1)/2]2}$	...	$\epsilon^{-[(n-1)/2](n-1)}$	$3p$	F	F

n = even

		E	C^1	C^2	...	C^{n-1}	N	Infrared	Raman
A		1	1	1	...	1	$3p$ (T_z, R_z)	A	A
B		1	-1	1	...	-1	$3p$	F	A
E_1	{	1	ϵ	ϵ^2	...	$\epsilon^{(n-1)}$	$3p$ (T_x)	A	A
	{	1	ϵ^{-1}	ϵ^{-2}	...	$\epsilon^{-(n-1)}$	$3p$ (T_y)	A	A
E_2	{	1	ϵ^2	ϵ^4	...	$\epsilon^{2(n-1)}$	$3p$	F	A
	{	1	ϵ^{-2}	ϵ^{-4}	...	$\epsilon^{-2(n-1)}$	$3p$	F	A
E_3	{	1	ϵ^3	ϵ^6	...	$\epsilon^{3(n-1)}$	$3p$	F	F
	{	1	ϵ^{-3}	ϵ^{-6}	...	$\epsilon^{-3(n-1)}$	$3p$	F	F
.		.	.	.	...	.	.	.	.
.		.	.	.	...	.	.	.	.
$E_{[(n/2)-1]}$	{	1	$\epsilon^{[(n/2)-1]}$	$\epsilon^{[(n/2)-1]2}$	...	$\epsilon^{[(n/2)-1](n-1)}$	$3p$	F	F
	{	1	$\epsilon^{-[(n/2)-1]}$	$\epsilon^{-[(n/2)-1]2}$	...	$\epsilon^{-[(n/2)-1](n-1)}$	$3p$	F	F

[a] $\epsilon = \exp i(2m\pi/n)$.

representation, and T_z and T_σ are pure translations parallel and perpendicular to the helix axis, respectively, and R_z pure rotation about the axis.

CONSTRUCTION OF G AND F MATRICES

In this calculation we use the GF-matrix method.[14] It is sufficient for our present purpose to carry out the calculation on the unit cell for which the G and F matrices would be constructed as follows:

$$\mathbf{G}\ (\text{or } \mathbf{F}) = \begin{vmatrix} G_{11} & G_{12} & G_{13} & \cdots & G_{1n} \\ G_{21} & G_{22} & G_{23} & \cdots & G_{2n} \\ G_{31} & G_{32} & G_{33} & \cdots & G_{3n} \\ \cdots & \cdots & \cdots & \cdots & \cdots \\ G_{n1} & G_{n2} & G_{n3} & \cdots & G_{nn} \end{vmatrix}, \quad (1)$$

[14] E. B. Wilson, Jr., J. C. Decius, and P. C. Cross, *Molecular Vibrations* (McGraw-Hill Book Company, Inc., New York, 1955).

where $\mathbf{G}_{ij}$ denotes the G (or F) matrices related to the internal coordinates of the ith and the jth chemical units. The order of these submatrices is equal to the number of the internal coordinates of one chemical unit. This matrix can be rewritten as follows, neglecting the interactions between the chemical units far apart:

$$\mathbf{G}\ (\text{or } \mathbf{F}) = \begin{pmatrix} \alpha & \beta' & \gamma' & \delta' & 0 & 0 & \delta & \gamma & \beta \\ \beta & \alpha & \beta' & \gamma' & \delta' & 0 & 0 & \delta & \gamma \\ \gamma & \beta & \alpha & \beta' & \gamma' & \delta' & 0 & 0 & \delta \\ \delta & \gamma & \beta & \alpha & \beta' & \gamma' & \delta' & 0 & 0 \\ 0 & \delta & \gamma & \beta & \alpha & \beta' & \gamma' & \delta' & 0 \\ 0 & 0 & \delta & \gamma & \beta & \alpha & \beta' & \gamma' & \delta' \\ \delta' & 0 & 0 & \delta & \gamma & \beta & \alpha & \beta' & \gamma' \\ \gamma' & \delta' & 0 & 0 & \delta & \gamma & \beta & \alpha & \beta' \\ \beta' & \gamma' & \delta' & 0 & 0 & \delta & \gamma & \beta & \alpha \end{pmatrix}. \quad (2)$$

This matrix is written for an example of the case of $n=9$. Here α denotes the G and F matrices for the internal coordinates of one chemical unit, β for those related to the internal coordinates of any neighboring chemical units. γ (and δ) represents the interaction between the internal coordinates related to the second (and third) neighboring chemical units. β', γ', and δ' are the transposed matrices of β, γ, and δ, respectively. The interactions between the chemical units separated further apart can be taken into account if needed.

Now it is shown that the matrix (2) can be diagonalized by the unitary transformation using the following matrix (3):

$$\mathbf{U} = (1/n)^{\frac{1}{2}} \begin{pmatrix} 1 & 1 & 1 & \cdots & 1 \\ 1 & \epsilon & \epsilon^2 & \cdots & \epsilon^{n-1} \\ 1 & \epsilon^2 & \epsilon^4 & \cdots & \epsilon^{2(n-1)} \\ \cdots & \cdots & \cdots & \cdots & \cdots \\ 1 & \epsilon^{n-1} & \epsilon^{(n-1)2} & \cdots & \epsilon^{(n-1)(n-1)} \end{pmatrix} \times \mathbf{E}, \quad (3)$$

where $(1/n)^{\frac{1}{2}}$ is normalization factor, $\epsilon = e^{i\omega}$, $\omega = 2m\pi/n$, and $\mathbf{E}$ a unit matrix the order of which is the same as that of the submatrices α, β, etc. in Eq. (2), and $\times$ denotes the direct product.

The diagonal matrix obtained by the transformation is shown as follows:

$\mathbf{UGU}\dagger =$ 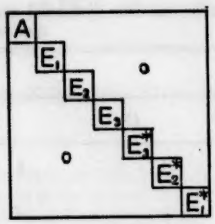

for $n=$odd ($n=7$), (4)

or

$\mathbf{UGU}\dagger =$ 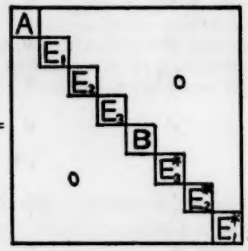

for $n=$even ($n=8$), (5)

where

$$\mathbf{A} = \alpha + (\beta+\beta') + (\gamma+\gamma') + (\delta+\delta'),$$
$$\mathbf{E}_k = \alpha + \beta\epsilon^k + \beta'\epsilon^{-k} + \gamma\epsilon^{2k} + \gamma'\epsilon^{-2k} + \delta\epsilon^{3k} + \delta'\epsilon^{-3k},$$
$$\mathbf{B} = \alpha - (\beta+\beta') + (\gamma+\gamma') - (\delta+\delta'),$$
$$\mathbf{E}_k{}^* = \alpha + \beta\epsilon^{-k} + \beta'\epsilon^k + \gamma\epsilon^{-2k} + \gamma'\epsilon^{2k} + \delta\epsilon^{-3k} + \delta'\epsilon^{3k},$$
$$k = 1, 2, 3, \cdots. \quad (6)$$

$\mathbf{U}\dagger$ is the transposed and complex conjugate matrix of $\mathbf{U}$.

Thus we can reduce the G (or F) matrices (2) into the forms shown in Eqs. (4) and (5) by the general procedure of the unitary transformation. But it is more desirable to use the real matrices than the complex matrices from the point of view of the ease of computation. Here we will show a more convenient method of reduction using real matrices only for an example. The G (or F) matrix (2) can be reduced by the orthogonal transformation as follows:

$\mathbf{U}_1\mathbf{GU}_1' =$ 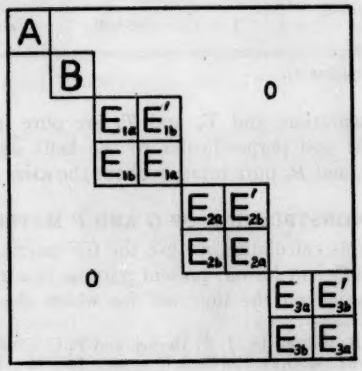

for $n=8$, (7)

where

$$\mathbf{U}_1=(2/n)^{\frac{1}{2}}\begin{vmatrix} (\frac{1}{2})^{\frac{1}{2}} & (\frac{1}{2})^{\frac{1}{2}} & (\frac{1}{2})^{\frac{1}{2}} & \cdots & (\frac{1}{2})^{\frac{1}{2}} \\ 1 & \cos\omega & \cos 2\omega & \cdots & \cos(n-1)\omega \\ 0 & \sin\omega & \sin 2\omega & \cdots & \sin(n-1)\omega \\ 1 & \cos 2\omega & \cos 4\omega & \cdots & \cos 2(n-1)\omega \\ 0 & \sin 2\omega & \cos 4\omega & \cdots & \sin 2(n-1)\omega \\ \cdots & \cdots & \cdots & \cdots & \cdots \\ 1 & \cos[\tfrac{1}{2}(n-1)]\omega & \cos[\tfrac{1}{2}(n-1)]2\omega & \cdots & \cos[\tfrac{1}{2}(n-1)](n-1)\omega \\ 0 & \sin[\tfrac{1}{2}(n-1)]\omega & \sin[\tfrac{1}{2}(n-1)]2\omega & \cdots & \sin[\tfrac{1}{2}(n-1)](n-1)\omega \end{vmatrix} \times \mathbf{E} \quad \text{for } n=\text{odd}, \tag{8}$$

$$\mathbf{U}_1=(2/n)^{\frac{1}{2}}\begin{vmatrix} (\frac{1}{2})^{\frac{1}{2}} & (\frac{1}{2})^{\frac{1}{2}} & (\frac{1}{2})^{\frac{1}{2}} & \cdots & (\frac{1}{2})^{\frac{1}{2}} \\ (\frac{1}{2})^{\frac{1}{2}} & -(\frac{1}{2})^{\frac{1}{2}} & (\frac{1}{2})^{\frac{1}{2}} & \cdots & -(\frac{1}{2})^{\frac{1}{2}} \\ 1 & \cos\omega & \cos 2\omega & \cdots & \cos(n-1)\omega \\ 0 & \sin\omega & \sin 2\omega & \cdots & \sin(n-1)\omega \\ 1 & \cos 2\omega & \cos 4\omega & \cdots & \cos 2(n-1)\omega \\ 0 & \sin 2\omega & \sin 4\omega & \cdots & \sin 2(n-1)\omega \\ \cdots & \cdots & \cdots & \cdots & \cdots \\ 1 & \cos[(n/2)-1]\omega & \cos[(n/2)-1]2\omega & \cdots & \cos[(n/2)-1](n-1)\omega \\ 0 & \sin[(n/2)-1]\omega & \sin[(n/2)-1]2\omega & \cdots & \sin[(n/2)-1](n-1)\omega \end{vmatrix} \times \mathbf{E} \quad \text{for } n=\text{even}. \tag{9}$$

$$\mathbf{A}=\alpha+(\beta+\beta')+(\gamma+\gamma')+(\delta+\delta'),$$

$$\mathbf{B}=\alpha-(\beta+\beta')+(\gamma+\gamma')-(\delta+\delta'),$$

$$\mathbf{E}_{ka}=\alpha+(\beta+\beta')\cos k\omega+(\gamma+\gamma')\cos 2k\omega+(\delta+\delta')\cos 3k\omega,$$

$$\mathbf{E}_{kb}=(\beta-\beta')\sin k\omega+(\gamma-\gamma')\sin 2k\omega+(\delta-\delta')\sin 3k\omega,$$

$$k=1, 2, 3, \cdots. \tag{10}$$

In Eqs. (8) and (9) $\mathbf{E}$ is a unit matrix, the order of which is the same as that of the submatrices α, β, etc. and $\times$ denotes the direct product. The submatrices

$$\left(\begin{array}{c|c} \mathbf{E}_{ka} & \mathbf{E}_{kb'} \\ \hline \mathbf{E}_{kb} & \mathbf{E}_{ka} \end{array}\right)$$

can be further factored into the following form by the suitable orthogonal transformation[15]:

$$\mathbf{U}_{2k}\left(\begin{array}{c|c} \mathbf{E}_{ka} & \mathbf{E}_{kb'} \\ \hline \mathbf{E}_{kb} & \mathbf{E}_{ka} \end{array}\right)\mathbf{U}_{2k}'=\left(\begin{array}{c|c} \mathbf{E}_k & \mathbf{0} \\ \hline \mathbf{0} & \mathbf{E}_k \end{array}\right). \tag{11}$$

We will show an example of the matrix $\mathbf{U}_{2k}$ in a later section.

The matrices $\mathbf{A}$, $\mathbf{E}_k$ (and $\mathbf{E}_k^*$), and $\mathbf{B}$ in these matrices (4), (5), (7), and (11) correspond to the symmetry species of the same notations in Table I, respectively. The vibrations for the species A are ones in which the motions in all chemical units are in phase, and are active in both infrared and Raman spectra. The transition moments of these modes are parallel to the main axis. The vibrations for E_k are ones in which motions in neighboring chemical units generally differ in phase by $\pm 2mk\pi/n$. The E_1 modes are active in both infrared and Raman spectra, and the transition

[15] It may be noticed that $\mathbf{U}_0(=\mathbf{U}_2\mathbf{U}_1)$ is the ordinary transformation matrix from the internal coordinates to the symmetry coordinates. Here $\mathbf{U}_2$ is a matrix containing $\mathbf{U}_{2k}$ as the diagonal elements.

TABLE II. Character table, numbers of normal modes and selection rules (A: active, F: forbidden) for the model of polyoxymethylene molecule under the group $D(10\pi/9)$.[a]

	E	$2C^1$	$2C^2$	$2C^3$	$2C^4$	$9C_2$	N	Infrared	Raman
A_1	1	1	1	1	1	1	2	F	A
A_2	1	1	1	1	1	−1	4 (T_x, R_z)	A	F
E_1	2	$2\cos\omega$	$2\cos2\omega$	$2\cos3\omega$	$2\cos4\omega$	0	12 ($T_z\times2$)	A	A
E_2	2	$2\cos2\omega$	$2\cos4\omega$	$2\cos6\omega$	$2\cos8\omega$	0	12	F	A
E_3	2	$2\cos3\omega$	$2\cos6\omega$	$2\cos9\omega$	$2\cos12\omega$	0	12	F	F
E_4	2	$2\cos4\omega$	$2\cos8\omega$	$2\cos12\omega$	$2\cos16\omega$	0	12	F	F

[a] $\omega=10\pi/9$.

moments of these vibrations are perpendicular to the main axis. The E_2 modes are forbidden in the infrared spectrum but active in the Raman spectrum. Those for E_3, E_4, ··· are forbidden in both spectra, and so we do not need to take account of them. The B species are active only in Raman spectrum. Thus the equations to be solved for the normal vibrations active in infrared and Raman spectra are

$$|\mathbf{GF}-\lambda\mathbf{E}|=0, \tag{12}$$

for the A, B, E_1, and E_2 species, where λ is $4\pi^2\nu^2$ and $\mathbf{E}$ the unit matrix.

ORDER OF *GF* MATRICES

Now the submatrices in the matrices (4) and (5) should be transformed into ones related to the symmetry coordinates of the chemical unit. The order of the matrices to be solved would be decreased to $3p-2$ for the A species, $3p-1$ for the E_1 species, and $3p$ for the E_2 species by elimination of the redundant coordinates through suitable transformations. When there are any symmetry elements in the chemical unit, the order of the matrices $\mathbf{A}$ and $\mathbf{B}$ will be decreased by reduction due to the symmetry of the chemical unit. For example, the symmetry species A of the matrices (4) and (5) can be reduced to two species A_1 and A_2 in the cases of $D(2m\pi/n)$[7] which possesses twofold symmetry axes in the plane perpendicular to the principal axis. The whole symmetry obtained here is equal to the direct product of the aforementioned factor group and the group of the symmetry of the chemical unit. Furthermore, the order of the matrices will be decreased by splitting of the high and low frequency vibrations. Thus we can calculate the normal vibrations of the helical (or planar zigzag) polymer molecules by solving the GF matrices of maximum order of $3p-1$ for the purpose of infrared spectroscopy.

EXAMPLE OF METHOD USING REAL MATRICES ONLY: SKELETAL VIBRATIONS OF POLYOXYMETHYLENE MOLECULE

In this section we will show the method using real matrices only for the example of the calculations of the skeletal vibrations of a simplified model of polyoxymethylene molecule. For this model, $n=9$, $m=5$, and $p=2$, if we consider the methylene group as a united atom with the atomic weight of CH_2. This "methylene atom" will be denoted with M hereafter. The character table, numbers of normal modes, and selection rules for this model under the group $D(10\pi/9)$ are shown in Table II. A part of the helix is illustrated in Fig. 1, in order to make clear the meaning of the following four internal coordinates:

$$\begin{aligned} &R_h(M_h-O_h=R_0),\\ &R_h'(O_h-M_{h+1}=R_0),\\ &\Theta_h(\angle O_{h-1}M_hO_h=\Theta_0),\\ &\Theta_h'(\angle M_hO_hM_{h+1}=\Theta_0). \end{aligned} \tag{13}$$

Here R_0 and Θ_0 in parentheses denote the equilibrium values which are taken as $R_0=1.43$ A, and $\Theta_0=109°28'$, respectively.[16] The suffix h can change from 1 to 9. In this calculation we omitted the torsional coordinates for simplicity.

Neglecting the interaction between atoms far apart, we express the potential energy[18] related to the unit cell of the one-dimensional crystal as

$$V=\sum_{h=1}^{9}V_h, \tag{14}$$

where

$$\begin{aligned} V_h=&\sum_{R,R'}[K_R'R_0(\Delta R_h)+\tfrac{1}{2}K_R(\Delta R_h)^2]\\ &+\sum_{\Theta,\Theta'}[H_\Theta'R_0^2(\Delta\Theta_h)+\tfrac{1}{2}H_\Theta(R_0\Delta\Theta_h)^2]\\ &+\sum_{Q,Q'}[F_Q'Q_0(\Delta Q_h)+\tfrac{1}{2}F_Q(\Delta Q_h)^2]. \end{aligned}$$

Here Q_h and Q_h' denote the following interatomic distances not bonded directly with equilibrium values

[16] By use of the equations derived by Shimanouchi *et al.*,[17] we obtained the values of the bond angle $\Theta_0=110°53'$ and the internal rotation angle $\tau=77°23'$, assuming that $R_0=1.43$ A, $m=5$, and identity period=17.3 A. But we adopted here the values of $\Theta_0=109°28'$ and $\tau=78°$ for simplicity.

[17] T. Shimanouchi and S. Mizushima, J. Chem. Phys. **23**, 707 (1955).

[18] We used Urey-Bradley force field.[6,19]

[19] H. C. Urey and C. A. Bradley, Phys. Rev. **38**, 1969 (1931).

shown in parentheses,

$$Q_h(O_{h-1}-O_h=Q_0),$$
$$Q_h'(M_h-M_{h+1}=Q_0). \qquad (15)$$

These can be expressed in terms of the bond lengths and bond angles of Eq. (13).

The G and F matrices related to the internal coordinates in the form of matrix (2) are constructed as follows:

$$\alpha = \begin{array}{c|cccc} & \Delta R_1 & \Delta R_1' & \Delta\textcircled{H}_1 & \Delta\textcircled{H}_1' \\ \hline \Delta R_1 & a & b & e & f \\ \Delta R_1' & b & a & e_0 & f \\ \Delta\textcircled{H}_1 & e & e_0 & c & g \\ \Delta\textcircled{H}_1' & f & f & g & d \end{array}$$

$$\beta = \begin{array}{c|cccc} & \Delta R_2 & \Delta R_2' & \Delta\textcircled{H}_2 & \Delta\textcircled{H}_2' \\ \hline \Delta R_2 & o & b_0 & o & f_0 \\ \Delta R_2' & o & o & o & o \\ \Delta\textcircled{H}_2 & e_0 & e & c_0 & g \\ \Delta\textcircled{H}_2' & o & f_0 & o & d_0 \end{array} \qquad (16)$$

$$\gamma = \delta = 0,$$

where for the elements of the G matrix

$a=\mu_C+\mu_O$,

$b=-\mu_O/3$,

$b_0=-\mu_C/3$,

$c=2\rho_0^2\mu_O+\frac{8}{3}\rho_0^2\mu_C$,

$c_0=(\frac{4}{3}\cos^2\tau-1)\rho_0^2\mu_O$,

$d=2\rho_0^2\mu_C+\frac{8}{3}\rho_0^2\mu_O$,

$d_0=(\frac{4}{3}\cos^2\tau-1)\rho_0^2\mu_C$,

$e=-(2\sqrt{2}/3)\rho_0\mu_C$,

$e_0=(2\sqrt{2}/3)\rho_0\mu_O\cos\tau$,

$f=-(2\sqrt{2}/3)\rho_0\mu_O$,

$f_0=(2\sqrt{2}/3)\rho_0\mu_C\cos\tau$,

$g=-\frac{4}{3}\rho_0^2\cos\tau(\mu_C+\mu_O)$,

μ_C = reciprocal mass of the "methylene atom,"

μ_O = reciprocal mass of the oxygen atom,

ρ_0 = reciprocal interatomic distance C—O,

τ = internal rotation angle,

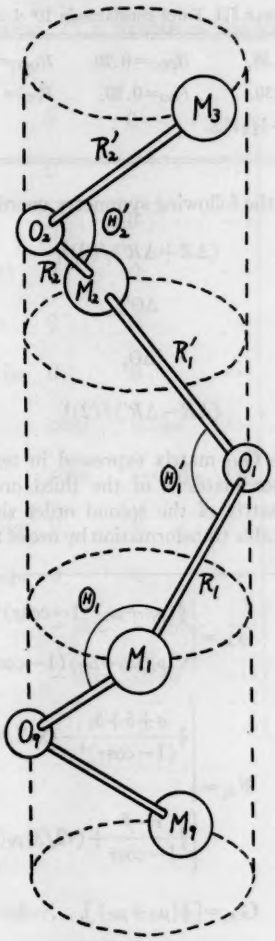

FIG. 1. The model of the polyoxymethylene molecule.

for the elements of the F matrix

$a=K_{CO}+\frac{1}{3}(F_{CC}'+F_{OO}')+\frac{2}{3}(F_{CC}+F_{OO})$,

$b=-\frac{1}{3}F_{CC}'+\frac{2}{3}F_{CC}$,

$b_0=-\frac{1}{3}F_{OO}'+\frac{2}{3}F_{OO}$,

$c=(H_{OCO}-\frac{2}{3}F_{OO}'+\frac{1}{3}F_{OO})R_0^2$,

$d=(H_{COC}-\frac{2}{3}F_{CC}'+\frac{1}{3}F_{CC})R_0^2$,

$e=(\sqrt{2}/3)(F_{OO}'+F_{OO})R_0$,

$f=(\sqrt{2}/3)(F_{CC}'+F_{CC})R_0$,

$c_0=d_0=e_0=f_0=g=0$.

Taking into account the symmetry of the helix $D(10\pi/9)$, the matrix for the A species can be split into two matrices corresponding to the species A_1 and

TABLE III. Force constants in 10^5 d/cm.

$K_{CO}=4.38$,	$H_{COC}=0.20$,	$H_{OCO}=0.50$,
$F_{CC}=0.30$,	$F_{OO}=0.50$,	$F_{CC}'=-\frac{1}{10}F_{CC}$,
$F_{OO}'=-\frac{1}{10}F_{OO}$.		

TABLE IV. The calculated and the observed frequencies (cm^{-1}).

	Calculated freq.	Observed freq. (dichroism)
A_1	903 470	} inactive in Infrared.
A_2	1146	1099 (‖)
E_1	1028	936 (⊥)
	616	630 (⊥)
	439	455 (⊥)
	1075	1094 (⊥)

A_2 by use of the following symmetry coordinates:

$$(\Delta R+\Delta R')/(2)^{\frac{1}{2}},$$

$$\Delta\Theta',$$

$$\Delta\Theta,$$

$$(\Delta R-\Delta R')/(2)^{\frac{1}{2}}. \tag{17}$$

Although the $\mathbf{G}_{A1}$ matrix expressed in terms of these symmetry coordinates is of the third order, we can obtain the matrix of the second order shown below, through a suitable transformation by use of the following matrix:

$$\begin{pmatrix} (1-\cos\tau)/2 & -R_0/2 & -R_0/2 \\ 2(1-\cos\tau) & R_0 & R_0 \\ 0 & (\frac{1}{2})^{\frac{1}{2}} & (\frac{1}{2})^{\frac{1}{2}} \end{pmatrix}. \tag{18}$$

The one remaining root of the secular equation is zero. Thus we have

$$\mathbf{G}_{A_1}=\begin{pmatrix} \frac{3}{2}(\mu_O+\mu_C)(1-\cos\tau)^2, & \sqrt{2}\rho_0(\mu_O-\mu_C)(1-\cos^2\tau) \\ \sqrt{2}\rho_0(\mu_O-\mu_C)(1-\cos^2\tau), & \frac{4}{3}\rho_0^2(\mu_O+\mu_C)(1+\cos\tau)^2 \end{pmatrix},$$

$$\mathbf{F}_{A_1}=\begin{pmatrix} \frac{4}{9}\dfrac{a+b+b_0}{(1-\cos\tau)^2}-(8\sqrt{2}/9)\rho_0\dfrac{e+f}{1-\cos\tau}+\frac{4}{9}\rho_0^2(c+d), & \frac{2}{3}\dfrac{e-f}{1-\cos\tau}+(\sqrt{2}/3)\rho_0(d-c) \\ \frac{2}{3}\dfrac{e-f}{1-\cos\tau}+(\sqrt{2}/3)\rho_0(d-c), & \frac{1}{2}(c+d) \end{pmatrix},$$

$$\mathbf{G}_{A_2}=[\tfrac{4}{3}(\mu_O+\mu_C)],$$

$$\mathbf{F}_{A_2}=[a-b-b_0]. \tag{19}$$

The next problem is the factoring (11) of the block for the $\mathbf{G}_{E_1}$ (and $\mathbf{F}_{E_1}$) matrix in Eq. (7). We may use the following transformation matrix for this purpose:

$$\mathbf{U}_{21}=(\tfrac{1}{2})^{\frac{1}{2}}\begin{pmatrix} \cos\frac{1}{4}\omega & \cos\frac{3}{4}\omega & 0 & 0 & -\sin\frac{1}{4}\omega & -\sin\frac{3}{4}\omega & 0 & 0 \\ \sin\frac{1}{4}\omega & -\sin\frac{3}{4}\omega & 0 & 0 & \cos\frac{1}{4}\omega & -\cos\frac{3}{4}\omega & 0 & 0 \\ 0 & 0 & 1 & \cos\frac{1}{2}\omega & 0 & 0 & 0 & -\sin\frac{1}{2}\omega \\ 0 & 0 & 1 & -\cos\frac{1}{2}\omega & 0 & 0 & 0 & \sin\frac{1}{2}\omega \\ -\sin\frac{1}{4}\omega & -\sin\frac{3}{4}\omega & 0 & 0 & -\cos\frac{1}{4}\omega & -\cos\frac{3}{4}\omega & 0 & 0 \\ \cos\frac{1}{4}\omega & -\cos\frac{3}{4}\omega & 0 & 0 & -\sin\frac{1}{4}\omega & \sin\frac{3}{4}\omega & 0 & 0 \\ 0 & 0 & 0 & -\sin\frac{1}{2}\omega & 0 & 0 & -1 & -\cos\frac{1}{2}\omega \\ 0 & 0 & 0 & \sin\frac{1}{2}\omega & 0 & 0 & -1 & \cos\frac{1}{2}\omega \end{pmatrix}. \tag{20}$$

In this case the transformation matrix $U_0(=U_2U_1)$ in footnote reference 15 is written as the following from (of the 9×4th order):

$$U_0=(\tfrac{1}{6})^{\frac{1}{2}}\begin{vmatrix}
(\frac{1}{2})^{\frac{1}{2}} & (\frac{1}{2})^{\frac{1}{2}} & 0 & 0 & (\frac{1}{2})^{\frac{1}{2}} & (\frac{1}{2})^{\frac{1}{2}} & 0 & 0 & \cdots\\
0 & 0 & 0 & 1 & 0 & 0 & 0 & 1 & \cdots\\
0 & 0 & 1 & 0 & 0 & 0 & 1 & 0 & \cdots\\
(\frac{1}{2})^{\frac{1}{2}} & -(\frac{1}{2})^{\frac{1}{2}} & 0 & 0 & (\frac{1}{2})^{\frac{1}{2}} & (-\frac{1}{2})^{\frac{1}{2}} & 0 & 0 & \cdots\\
\cos\frac{1}{4}\omega & \cos\frac{3}{4}\omega & 0 & 0 & \cos\frac{5}{4}\omega & \cos\frac{7}{4}\omega & 0 & 0 & \cdots\\
\sin\frac{1}{4}\omega & -\sin\frac{3}{4}\omega & 0 & 0 & \sin\frac{5}{4}\omega & -\sin\frac{7}{4}\omega & 0 & 0 & \cdots\\
0 & 0 & 1 & \cos\frac{1}{2}\omega & 0 & 0 & \cos\omega & \cos\frac{3}{2}\omega & \cdots\\
0 & 0 & 1 & -\cos\frac{1}{2}\omega & 0 & 0 & \cos\omega & -\cos\frac{3}{2}\omega & \cdots\\
-\sin\frac{1}{4}\omega & -\sin\frac{3}{4}\omega & 0 & 0 & -\sin\frac{5}{4}\omega & -\sin\frac{7}{4}\omega & 0 & 0 & \cdots\\
\cos\frac{1}{4}\omega & -\cos\frac{3}{4}\omega & 0 & 0 & \cos\frac{5}{4}\omega & -\cos\frac{7}{4}\omega & 0 & 0 & \cdots\\
0 & 0 & 0 & -\sin\frac{1}{2}\omega & 0 & 0 & -\sin\omega & -\sin\frac{3}{2}\omega & \cdots\\
0 & 0 & 0 & \sin\frac{1}{2}\omega & 0 & 0 & -\sin\omega & \sin\frac{3}{2}\omega & \cdots\\
\cdots & \cdots & \cdots & \cdots & \cdots & \cdots & \cdots & \cdots & \cdots\\
\cdots & \cdots & \cdots & \cdots & \cdots & \cdots & \cdots & \cdots & \cdots
\end{vmatrix}. \tag{21}$$

Then we have

$$G_{E_1}=\begin{vmatrix}
(\mu_O+\mu_C)(1-\frac{1}{3}\cos\frac{1}{2}\omega), & \frac{1}{3}(\mu_O-\mu_C)\sin\frac{1}{2}\omega,\\
\frac{1}{3}(\mu_O-\mu_C)\sin\frac{1}{2}\omega, & (\mu_O+\mu_C)(1+\frac{1}{3}\cos\frac{1}{2}\omega),\\
(2\sqrt{2}/3)\rho_0(\mu_O+\mu_C)(-\cos\frac{1}{4}\omega+\cos\tau\cos\frac{3}{4}\omega), & (2\sqrt{2}/3)\rho_0(\mu_O-\mu_C)(\sin\frac{1}{4}\omega-\cos\tau\sin\frac{3}{4}\omega),\\
(2\sqrt{2}/3)\rho_0(\mu_O-\mu_C)(\cos\frac{1}{4}\omega+\cos\tau\cos\frac{3}{4}\omega), & -(2\sqrt{2}/3)\rho_0(\mu_O+\mu_C)(\sin\frac{1}{4}\omega+\cos\tau\sin\frac{3}{4}\omega),\\
(2\sqrt{2}/3)\rho_0(\mu_O+\mu_C)(-\cos\frac{1}{4}\omega+\cos\tau\cos\frac{3}{4}\omega), & (2\sqrt{2}/3)\rho_0(\mu_O-\mu_C)(\cos\frac{1}{4}\omega+\cos\tau\cos\frac{3}{4}\omega)\\
(2\sqrt{2}/3)\rho_0(\mu_O-\mu_C)(\sin\frac{1}{4}\omega-\cos\tau\sin\frac{3}{4}\omega), & -(2\sqrt{2}/3)\rho_0(\mu_O+\mu_C)(\sin\frac{1}{4}\omega+\cos\tau\sin\frac{3}{4}\omega)\\
\frac{1}{3}(\mu_O+\mu_C)\rho_0^2\{7-8\cos\tau\cos\frac{1}{2}\omega+(4\cos^2\tau-3)\cos\omega\}, & \frac{1}{3}\rho_0^2(\mu_O-\mu_C)\{(4\cos^2\tau-3)\cos\omega-1\}\\
\frac{1}{3}\rho_0^2(\mu_O-\mu_C)\{(4\cos^2\tau-3)\cos\omega-1\}, & \frac{1}{3}\rho_0^2(\mu_O+\mu_C)\{7+8\cos\tau\cos\frac{1}{2}\omega+(4\cos^2\tau-3)\cos\omega\}
\end{vmatrix},$$

$$F_{E_1}=\begin{vmatrix}
a+(b+b_0)\cos\frac{1}{2}\omega, & (-b+b_0)\sin\frac{1}{2}\omega, & (e+f)\cos\frac{1}{4}\omega, & (e-f)\cos\frac{1}{4}\omega\\
(-b+b_0)\sin\frac{1}{2}\omega, & a-(b+b_0)\cos\frac{1}{2}\omega, & (e-f)\sin\frac{1}{4}\omega, & (e+f)\sin\frac{1}{4}\omega\\
(e+f)\cos\frac{1}{4}\omega, & (e-f)\sin\frac{1}{4}\omega, & \frac{1}{2}(c+d) & \frac{1}{2}(c-d)\\
(e-f)\cos\frac{1}{4}\omega, & (e+f)\sin\frac{1}{4}\omega, & \frac{1}{2}(c-d), & \frac{1}{2}(c+d)
\end{vmatrix}. \tag{22}$$

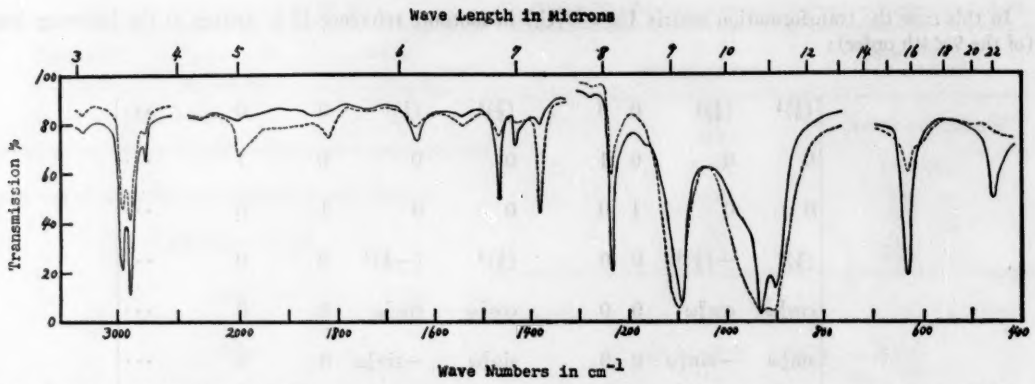

FIG. 2. Polarized infrared spectra of polyoxymethylene (footnote reference 22). —— electric vector perpendicular to stretched direction. ------ electric vector parallel to stretched direction.

The numerical values of force constants used in this calculation are shown in Table III. These values were chosen referring to the paper on the normal vibrations of ethyl ether.[20] The calculated and observed frequencies for A_1, A_2, and E_1 species are shown in Table IV.[21] The values of frequencies as well as the dichroism are found to be in good agreement with the observed ones irrespective of the simplicity of the model taken here. In Fig. 2 the polarized infrared spectra of polyoxymethylene (Delrin-acetal resin of du Pont Corporation) are reproduced from our previous paper.[22]

The remaining discordance between the observed and the calculated values may be due to the following reasons:

(1) Neglect of the hydrogen atoms. The coupling of the C—O—C stretching and the CH_2 rocking vibrations appears to be considerable according to our calculations on the more accurate model.

(2) Omitting the torsional displacement coordinates.

(3) Neglect of the intramolecular interaction between the subsequent turns of the helix and the intermolecular interactions between the neighboring chains.

The detailed calculations on the more accurate model of the polyoxymethylene molecule are now being made; they will be reported in the near future.

SKELETAL VIBRATIONS OF THE PLANAR ZIGZAG CHAIN OF CARBON ATOMS

As another example we will show here that the calculation of the skeletal vibrations of the planar zigzag chain of carbon atoms, reported already by several authors,[23–25] can be carried out in a more simple and systematic way by using our method. In this model, $n=2$, $m=1$, and $p=1$. Since the number of chain atoms in one chemical unit is equal to one, γ should be taken into account of the second neighbor interactions. Then, matrix (2) is constructed as follows:

$$
\begin{array}{c|cc}
 & \Delta R_1 & \Delta\theta_1 \\
\Delta R_1 & a & c \\
\Delta\theta_1 & c & b \\
\Delta R_2 & a_0 & c_0 \\
\Delta\theta_2 & c & b_0 \\
\Delta R_3 & 0 & 0 \\
\Delta\theta_3 & c_0 & b_1
\end{array}
\qquad \delta = 0, \tag{23}
$$

where for the elements of the G matrix,

$a=2\mu$,

$a_0=-\mu/3$,

$b=\frac{14}{3}\rho^2\mu$,

$b_0=\frac{8}{3}\rho^2\mu$,

$b_1=\frac{1}{3}\rho^2\mu$,

$c=-(2\sqrt{2}/3)\rho\mu$,

$c_0=-(2\sqrt{2}/3)\rho\mu$,

μ = reciprocal mass of carbon atom,

ρ = reciprocal interatomic distance,

for the elements of the F matrix,[26]

[20] M. Hayashi, J. Chem. Soc. Japan, Pure Chem. Sec. **78**, 222 (1957).

[21] The calculation using the complex matrices [Eq. (6)] gives exactly the same values as those in Table IV.

[22] H. Tadokoro, T. Yasumoto, G. Morimoto, and S. Murahashi, Chem. High Polymers (Tokyo) **17**, 95 (1960).

[23] J. G. Kirkwood, J. Chem. Phys. **7**, 506 (1939).

[24] K. S. Pitzer, J. Chem. Phys. **8**, 711 (1940).

[25] C. Y. Liang, S. Krimm, and G. B. B. M. Sutherland, J. Chem. Phys. **25**, 543 (1956).

[26] Here we used the valence force field after Liang *et al.*[25]

$a=K_{CC}$=stretching force constant of the C—C bond,

$b=H_{CCC}/\rho^2$=(deformation force constant of the C—C—C angle)$/\rho^2$,

$a_0=b_0=b_1=c=c_0=0$.

Then using Eq. (6), we have

$$G_A=(12\mu),$$
$$F_A=[(a+8\rho^2 b)/9],$$
$$G_B=(8\mu/3),$$
$$F_B=(a). \qquad (24)$$

Assuming $K_{CC}=3.43\times10^5$ dynes/cm and $H_{CCC}=0.34\times10^5$ d/cm, which are the values used by Liang *et al.*,[25] we obtain

$\nu=1077$ cm^{-1} for A species,

$\nu=1138$ cm^{-1} for B species.

FURTHER PROPOSED APPLICATIONS TO SOME SPECIAL CASES

This method may also be applied to a cyclic structure, which is a limiting case as the identity period along the main axis is zero. For an example, we may give the case of the trioxane molecule ($n=3$, $m=1$ and $p=4$).

ACKNOWLEDGMENTS

The author expresses his sincere thanks to Professor T. Shimanouchi of the University of Tokyo for his invaluable advice and criticism, and to Professor I. Nitta, Professor S. Murahashi, and Professor S. Seki of this faculty for their continuous encouragement through this investigation. The author is also indebted to Dr. K. Nakamura of Dai-nippon Pharmaceutical Industries Company, Ltd., and Assistant Professor T. Miyazawa of the Protein Research Institute of this University for their helpful discussions, and to G. Morimoto for his help in part of the numerical calculations.

THE JOURNAL OF CHEMICAL PHYSICS VOLUME 33, NUMBER 5 NOVEMBER, 1960

Approximate Electronic Energy Surfaces from Cuspless Wave Functions*

CARL E. WULFMAN

The Defiance College, Defiance, Ohio, and The Carnegie Institute of Technology, Pittsburgh, Pennsylvania

(Received May 23, 1960)

The eigenfunctions of a molecular Hamiltonian in which all Coulomb potentials have been replaced by Hooke's law potentials are easily determined. Their electronic parts are essentially single-particle single-center harmonic oscillator, or Gaussian wave functions originating at the center of nuclear charge. An investigation is made to determine the feasibility of using these cuspless base functions in variational calculations of relative molecular electronic energies. It is found that:

A. Addition of Coulombic or delta-function singularities to the Hooke's law potentials leads to the formation of rigid molecular systems.

B. The Coulomb potentials in 21–26 electron triatomics can be treated as a perturbation upon quadratic potentials.

In agreement with experiment it is noted that:

C. Approximately homonuclear (i.e., nonhydride) 8-, 20-, and 40-electron polyatomics are configurationally unstable.

D. The molecules CO_2^+, CO_2, N_2O, NCO^-, BO_2^-, N_3^-, and NO_2^+ should all be linear.

E. The molecules NO_2^-, O_3, FNO, F_2O, and a number of excited states of the molecules (D) should all be nonlinear.

F. The stable form of nitrous oxide should be N—N—O rather than N—O—N.

A number of general features of the treatment are discussed and several of its limitations are pointed out. A tabulation of coefficients required in Clebsch-Gordan expansions of products of Hermite polynomials is given.

I. INTRODUCTION

ONE of the major difficulties in calculating molecular energies arises because of the difficulty of developing cusps in electronic wave functions at nuclei. Recently, for example, Howell and Shull found in a one-center expansion of the wave function of H_2^+ that convergence was very poor for just this reason.[1] The very lack of improvement brought about by the inclusion of additional terms in their series augurs well, however, for the success of calculations in which "relative" rather than "absolute" molecular energies

* Research supported by a research grant from the National Science Foundation to Carnegie Institute of Technology and by a grant from The Research Corporation to The Defiance College.

[1] K. M. Howell, and H. Shull, J. Chem. Phys. **30**, 627 (1959).

are of interest. This is usually the case in problems confronting chemists.

The cusps in electronic wave functions at nuclei are largely due to atomic inner-shell electrons—primarily, in fact, to 1s electrons. Since these are not affected by most molecular transformations one suspects that it may be possible to obtain qualitatively correct relative energy values from wave functions that lack these cusps.

With these observations in mind, Gaussian functions are here considered as base functions in a variational calculation of the energy of a number of triatomic molecules and no attempt is made to develop cusps in the resulting wave functions.

Each molecular system is viewed as an assemblage of nuclei capable of adiabatic movement in an electron cloud containing all the electrons of the molecule.

It is advantageous to build the electron cloud from eigenfunctions of a known Hamiltonian. Consequently in Sec. II we begin with a study of a quasi-molecular system—a system of nuclei and electrons interacting by Hooke's rather than Coulomb's law. The Schrödinger equation for such a system may be solved exactly. Its salient properties are outlined for the case of homonuclear molecules. The electronic wave functions are found to be nothing but Slater determinants of one-electron single-center Gaussians.

In Sec. III these cuspless electronic functions are used as basis functions in a variational treatment designed to locate the extrema of electronic potential energy surfaces. Criteria are developed which help one to choose a reasonable set of basis functions and help one to determine whether a given configuration can yield an extremum in the electronic energy.

In Sec. IV this approach is applied to 20-26 electron triatomics. It is noted that the nonexistence of 20 electron triatomics implies the practical validity of a perturbation treatment of these systems. This perturbation-perturbation treatment in every case correctly indicates the linearity or nonlinearity of the known molecules.

II. ZERO-ORDER PROBLEM

Let $\mathbf{r}_i$ be the vector from the origin of an inertial coordinate system to particle i of charge e_i. Then to every multiparticle Coulomb's law potential,

$$V_e=\sum_{i<j} e_i e_j \mid \mathbf{r}_i-\mathbf{r}_j \mid^{-1} \tag{1a}$$

there is a corresponding Hooke's law potential,

$$V_h=\sum_{i<j} k_{ij}(\mathbf{r}_i-\mathbf{r}_j)^2+d_{ij}. \tag{1b}$$

If each force constant k_{ij} is opposite in sign to $e_i e_j$, then the individual potentials are correspondingly attractive or repulsive in each case. The d_{ij} adjust the origin from which the energy is measured.

Because of the correspondence $V_e \rightleftharpoons V_h$ there must be a correspondence between the Schrödinger equations,

$$\mathfrak{H}_e\psi_e=E_e\psi_e \tag{2a}$$

$$\mathfrak{H}_h\psi_h=E_h\psi_h, \tag{2b}$$

where, if m_i is the mass of particle i and $\mathfrak{p}_i$ its momentum vector, the quantum-mechanical operators $\mathfrak{H}$ correspond to the classical Hamiltonians,

$$H_e=T+V_e=\sum_i(\mathfrak{p}_i)^2/2m_i+V_e \tag{2c}$$

$$H_h=T+V_h=\sum_i(\mathfrak{p}_i)^2/2m_i+V_h. \tag{2d}$$

We wish to investigate some aspects of this correspondence.

The mathematical form of the solutions for the Coulomb case is generally unknown, though its physical consequences are apparent to all. On the other hand, the mathematical form of the solutions for the Hooke case is easily discovered, though it has no direct physical consequences. It is convenient therefore to proceed by comparing the known properties of molecules with the properties of the solutions of (2b).

Normal Mode Analysis

H_h is factorable by the usual normal mode analysis. Transforming to mass weighted coordinates, $\mathfrak{g}_i=\mathbf{r}_i m_i^{\frac{1}{2}}$ and $\mathfrak{g}_i'=(d\mathfrak{g}_i/dt)$, one has

$$H_h=\tfrac{1}{2}\sum_i(\mathfrak{g}_i')^2+\tfrac{1}{2}\sum_{i,j} f_{ij}\mathfrak{g}_i\cdot\mathfrak{g}_j+D \tag{3a}$$

$$f_{ij}=(m_i m_j)^{-\frac{1}{2}}k_{ij}; \quad (i\neq j); \qquad f_{ii}=m_i^{-1}\sum_j k_{ij} \tag{3b}$$

$$D=\sum_{i<j} d_{ij}. \tag{3c}$$

In the homonuclear case there are only two different masses, m_+, m_- and two different charges, e_+, e_- giving rise to only three different force constants, k_{++}, k_{+-}, k_{--}. The problem is formally similar to a nuclear problem treated by Bloch and Hseih.[2] By comparison with their work one finds that if there are Z nuclei and N electrons, the roots λ and eigenvectors $\mathbf{q}$ of the secular determinant of the normal mode analysis are

$$\lambda_0=0 \tag{4a}$$

$$\mathbf{q}_0=(\textstyle\sum m_i^{\frac{1}{2}}\mathfrak{g}_i)(\sum m_i)^{-\frac{1}{2}} \tag{4b}$$

$$\lambda_{+-}=(m_+m_-)^{-1}(Nm_-+Zm_+)k_{+-} \tag{4c}$$

$$\mathbf{q}_{+-}=(Nm_-^{\frac{1}{2}}\sum_1^Z\mathfrak{g}_+-Zm_+^{\frac{1}{2}}\sum_1^N\mathfrak{g}_-)(NZ[Nm_-+Zm_+])^{-\frac{1}{2}} \tag{4d}$$

$$\lambda_+=m_+^{-1}(Zk_{++}+Nk_{+-}) \tag{4e}$$

$$\lambda_-=m_-^{-1}(Nk_{--}+Zk_{+-}). \tag{4f}$$

[2] Y. C. Hsieh and I. Bloch, Phys. Rev. **101**, 205 (1956).

The roots, (4e), (4f), may be considered to be nondegenerate, their corresponding eigenvectors then being collective coordinates describing the motions of the nuclei and the electrons, respectively. It is more natural, however, to consider (4e) to be $(Z-1)$-fold degenerate, (4f) to be $(N-1)$-fold degenerate. In this case the corresponding normal coordinates are highly arbitrary. It is only necessary that each of them be orthonormal to the others of its kind and that the sum of the coefficients of the $\mathbf{g}$'s in each vanish.

The factored Hamiltonian may be written in the form

$$H_h=H_0+H_{+-}+H_++H_-+D \tag{5a}$$

where

$$H_+=\sum_{b=1}^{Z-1}H_{b+}, \qquad H_-=\sum_{a=1}^{N-1}H_{a-} \tag{5b}$$

and in general,

$$H_V=\tfrac{1}{2}(\mathbf{q}_V')^2+\tfrac{1}{2}\lambda_V(\mathbf{q}_V)^2. \tag{5c}$$

Since λ_{+-} is the sum of the attractive parts of λ_+ and λ_-, it is clear that it is much greater in magnitude than either. Because of the way the electronic and nuclear mass enter into λ_+ and λ_-, it is also clear that λ_- is roughly 10^3 times as large as λ_+. The vector $\mathbf{q}_0$ is a vector to the center of mass of the system. The vector $\mathbf{q}_{+-}$ increases monotonically with the difference between the center of mass (or charge) of the electrons and the center of mass (or charge) of the nuclei.

Eigenfunction of the Zero-Order Hamiltonian

The solutions of the Schrödinger equation (2b) obtained using (5) are of the form

$$\psi_h=\phi_0\cdot\phi_{+-}\cdot\phi_+\cdot\phi_-; \qquad \phi_+=\prod_{b=1}^{Z-1}\phi_{b+}; \qquad \phi_-=\prod_{a=1}^{N-1}\phi_{a-} \tag{6a}$$

$$E_h=\omega_0+\omega_{+-}+\omega_++\omega_-+D;$$

$$\omega_+=\sum_{b=1}^{Z-1}\omega_{b+}; \qquad \omega_-=\sum_{a=1}^{N-1}\omega_{a-}, \tag{6b}$$

where the ϕ's and ω's are such that

$$\mathcal{H}_V\phi_V=\omega_V\phi_V. \tag{6c}$$

ϕ_0 is a three-dimensional plane-wave function describing the free motion of the center of mass of the system, and ω_0 is its kinetic energy. The other functions can be given the following expressions.

In Cartesian coordinates:

$$\phi_V\equiv\phi_{lmn}(\lambda^{\frac{1}{4}}\mathbf{q}_V)=\phi_l(x_{qV})\cdot\phi_m(y_{qV})\cdot\phi_n(z_{qV}), \tag{7a}$$

x_{qV} is the x component of $\lambda^{\frac{1}{4}}\mathbf{q}_V$

$$\omega_V=\omega_{xV}+\omega_{yV}+\omega_{zV} \tag{7b}$$

$$\phi_n(\beta^{\frac{1}{2}}z)=(\beta/\pi)^{\frac{1}{4}}(2^n n!)^{-\frac{1}{2}}H_n(\beta^{\frac{1}{2}}x)\exp[-(\beta/2)x^2]. \tag{7c}$$

The H_n are Hermite polynomials.

$$\omega z_{qV}\equiv\omega_{nV}=(n+\tfrac{1}{2})\hbar\lambda^{\frac{1}{2}}$$

$$\beta=\lambda^{\frac{1}{2}}/\hbar. \tag{7d}$$

In polar coordinates,[3]

$$\phi_V=\phi_{\nu\lambda\mu}(\mathbf{q}_V)=R_{\nu\lambda}(r_{qV})\cdot Y_{\lambda\mu}(\theta_{qV},\phi_{qV}). \tag{7e}$$

The $Y_{\lambda\mu}$ are normalized surface spherical harmonics, and

$$\int_0^\infty R_{\nu\lambda}{}^2r^2dr=1 \tag{7f}$$

$$\omega_V\equiv\omega_{\nu V}=(\nu+\tfrac{3}{2})\hbar\lambda^{\frac{1}{2}}. \tag{7g}$$

The first few functions $R_{\nu\lambda}$ are

$$R_{0s}=\beta^{3/4}[4/(\pi)^{\frac{1}{2}}]^{\frac{1}{2}}\exp[-(\beta/2)r^2]$$

$$R_{1p}=\beta^{3/4}[4/(\pi)^{\frac{1}{2}}]^{\frac{1}{2}}\exp[-(\beta/2)r^2]\times(\tfrac{2}{3})^{\frac{1}{2}}\beta^{\frac{1}{2}}r$$

$$R_{2s}=\beta^{3/4}[4/(\pi)^{\frac{1}{2}}]^{\frac{1}{2}}\exp[-(\beta/2)r^2]\times(\tfrac{2}{3})^{\frac{1}{2}}(\tfrac{3}{2}-\beta^{\frac{1}{2}}r)$$

$$R_{2d}=\beta^{3/4}[4/(\pi)^{\frac{1}{2}}]^{\frac{1}{2}}\exp[-(\beta/2)r^2]\times(\tfrac{4}{15})^{\frac{1}{2}}\beta r^2$$

$$R_{3p}=\beta^{3/4}[4/(\pi)^{\frac{1}{2}}]^{\frac{1}{2}}\exp[-(\beta/2)r^2]\times(\tfrac{4}{15})^{\frac{1}{2}}(\beta^{\frac{5}{2}}r-\beta^{\frac{1}{2}}r^3)$$

$$R_{3f}=\beta^{3/4}[4/(\pi)^{\frac{1}{2}}]^{\frac{1}{2}}\exp[-(\beta/2)r^2]\times(\tfrac{8}{105})^{\frac{1}{2}}\beta^{\frac{1}{2}}r^3. \tag{8}$$

Exchange Symmetry

Since $\mathbf{q}_0$ and $\mathbf{q}_{+-}$ are always symmetric under exchange of identical particles, the corresponding wave functions have the same symmetry. The wave functions involving $\mathbf{q}_+$ and $\mathbf{q}_-$, however, do not necessarily have the proper behavior under particle exchange. This may be corrected and spin taken into account in the manner proposed by Bloch and Hsieh.[2] By taking linear combinations of the set of $(Z-1)$ or $(N-1)$ degenerate normal coordinates (our $\mathbf{q}_+$ or $\mathbf{q}_-$), they construct a new set of Z or N linearly dependent coordinates, say $\mathbf{Q}_+$ or $\mathbf{Q}_-$. Each of these can be so taken as to represent the motion of one of the group of identical particles (nuclei or electrons) with respect to the center of mass of the assemblage of all similar particles. They then show that Hermite functions of these coordinates may be multiplied by spin functions and antisymmetrized in the ordinary way, and that the resulting ground and first excited state functions of a given spin are eigenfunctions of the H_+ and H_- part of (5a).

Thus in these cases, even though the Hamiltonian contains interelectronic and internuclear repulsion terms, the identical particles move "independently" of one another in essentially the same sense as they do in antisymmetrized independent particle models. That is, the major dependence is that usually considered due to antisymmetrization. The only difference is, that in

[3] Note the use of λ here as a quantum number rather than as a root of the secular determinant of the normal coordinate treatment.

this case, the motions must be measured with respect to the center of mass of the identical particles, while in the usual problem they are measured with respect to the center of mass of the molecule.

Born-Oppenheimer Approximation

This difference is not a crucial one. As pointed out earlier we may expect λ_{+-} to be much the largest λ. As a consequence the separation of the ground and first excited levels, ω_{+-} must be large compared with the separation of the levels ω_{+} or the levels ω_{-}. The center of mass, hence the center of charge, of the electrons must be strongly bound to that of the nuclei. In fact, the Born-Oppenheimer approximation that the cross derivatives $(\partial/\partial\mathbf{r}_{+})(\partial/\partial\mathbf{r}_{-})$ vanish, requires that the separation of the levels ω_{+-} is extremely great and that ϕ_{+-} approximates a delta function. We shall therefore suppose that the center of nuclear charge and the center of electronic charge coincide in the cases of interest to us—harmonic oscillator systems that correspond to stable molecular systems. The coordinates of the particles will henceforth all be supposed measured from the center of mass (charge) of the system. For ground and first excited states the internal wave function Υ is therefore assumed to be of the form

$$\Upsilon=\Omega'(\lambda_{+};\varrho_{1+},\varrho_{2+}\cdots\varrho_{z+})\cdot\Omega(\lambda_{-};\varrho_{1-},\varrho_{2-}\cdots\varrho_{N-}). \tag{9}$$

Here Ω' and Ω are nuclear and electronic antisymmetric spin-dependent functions. In general they are linear combinations of Slater determinants. The wave function Ω is a function of λ_{-} but not of λ_{+}, while the converse is true of Ω'. For convenience it shall henceforth be supposed that λ_{-} and λ_{+} or, equivalently, β and β' are to be the independent parameters of the treatment. The k's are thus relegated to the limbo of arbitrary and unused variable constants.

The function Ω is identical with the function one would obtain by applying the usual independent particle "aufbau" procedure to a single-center isotropic harmonic oscillator system in its ground or first excited state of a given spin.

Particle Distribution

The harmonic oscillator system itself is a nebulous approximation to an actual molecule. If Ω' is nondegenerate, the nuclear distribution has complete spherical symmetry, and has only radial extrema. If it is degenerate, no one distribution of less than spherical symmetry is preferred over any other, and spherical symmetry is always possible. The same statements apply to the electronic distribution. In other words, the distribution of a set of particles interacting as isotropic harmonic oscillators is itself isotropic.

The steric rigidity one associates with actual molecules can hence not be accounted for by the quadratic potentials of the harmonic oscillator treatment. It does however arise as soon as one includes singularities at the origins of the potentials. A delta-function singularity supplementing the quadratic potentials is effective in this respect.[4]

The lack of any steric rigidity in the harmonic oscillator system makes it "operationally" meaningless to apply the usual static nucleus approximation to the wave function (9). The approximation only becomes consequential when applied in concert with a Hamiltonian capable of developing this rigidity. This fact need not here concern us further as we shall henceforth be solely concerned with Ω, the eigenfunction of the H_{-} portion of H_{h}.

III. VARIATION TREATMENT

We wish now to consider the actual, physically meaningful, solutions of the Schrödinger equation (2a). It is simplest to begin by making the static nucleus approximation, supposing that the nuclei are of infinite mass. Then the electronic portion of the wave function, ψ_e, is a parametric function of the nuclear positions $\mathbf{s}_i$, describing the nuclear configuration S of the system. More specifically,

$$(\mathfrak{I}_e+\mathfrak{V}_e)\psi_e=E_e\psi_e \tag{10a}$$

where

$$T_e=\sum_{i=1}^{N}(\varrho_i)^2/2m_i;\qquad V_e=\sum_{i<j}^{N}\frac{e_{-}^{2}}{|\mathbf{r}_i-\mathbf{r}_j|}+\sum_{i,j}^{N,Z}\frac{e_{-}e_{+}}{|\mathbf{r}_i-\mathbf{s}_j|}. \tag{10b}$$

With this supposition one may expand $\psi_e(S)$ as

$$\psi_e=\sum c_n(S)\Omega_n(\beta). \tag{11}$$

This expansion will be assumed subject to the center of charge condition [(12d) following]. By making use of the variational theorem the parameters in this expansion may now be fixed in the usual way. We require:

$$(\partial/\partial c_n)\langle\psi_e\,|\,\mathfrak{IC}_e\,|\,\psi_e\rangle=0:\qquad n=1,2,3\cdots \tag{12a}$$

$$(\partial/\partial\beta)\langle\psi_e(\beta)\,|\,\mathfrak{IC}_e\,|\,\psi_e(\beta)\rangle=0 \tag{12b}$$

$$(\partial/\partial\mathbf{s}_j)\langle\psi_e\,|\,\mathfrak{IC}_e\,|\,\psi_e\rangle=0:\qquad j=1,2,\cdots z. \tag{12c}$$

$$\sum_j e_{+}\mathbf{s}_j=\langle\psi_e\,|\,\sum_i e_{-}\mathbf{r}_i\,|\,\psi_e\rangle=0. \tag{12d}$$

Equation (12a) leads in the well-known manner to the secular equations,

$$\sum c_n\langle\Omega_n\,|\,\mathfrak{IC}_e\,|\,\Omega_{n'}\rangle-E\delta_{n,n'}=0;\qquad n=1,2,3\cdots \tag{13}$$

By a standard dimensional analysis Eq. (12b) may be rewritten

$$\beta^{\natural}=-\tfrac{1}{2}\langle\psi_e(1)\,|\,\mathfrak{V}_e'\psi_e(1)\rangle\div\langle\psi_e(1)\,|\,\mathfrak{I}_e\,|\,\psi_e(1)\rangle, \tag{14}$$

[4] In this case, the condition that the system be configurationally stable is easily shown to be that each nucleus simply be at a maximum in the electronic distribution (cf. the following). There is no difficulty in developing the required maxima, for the delta-function singularities can often remove the degeneracies of the zero-order distribution.

where

$$\mathcal{V}_e' = \sum e_- e_- / |\mathbf{r}_i - \mathbf{r}_j| + \sum e_- e_+ / |\mathbf{r}_i - \beta^{\frac{1}{2}}\mathbf{r}_j| \tag{14a}$$

The $\beta^{\frac{1}{2}}$ in the Coulomb operator may be eliminated with the aid of (12c) which requires that $\beta^{\frac{1}{2}}\mathbf{s}_j = \mathbf{t}_j$, a constant vector independent of β. Equation (12c) may be rewritten as

$$0 = (\partial/\partial \mathbf{s}_j) \langle \psi(\mathbf{r}_i) \mid \sum (e_+ e_- / |\mathbf{r}_i - \mathbf{s}_j|) \mid \psi(\mathbf{r}_i) \rangle$$

$$= \int \sum (e_+ e_- / |\mathbf{r}_i|)(\partial/\partial \mathbf{s}_j) \mid \psi(\mathbf{r}_i + \mathbf{s}_j)^2 \mid d\tau$$

$$= \int N^{-1} \sum (e_+ e_- / |\mathbf{r}_i|)(\partial/\partial \mathbf{r}_i) \mid \psi(\mathbf{r}_i + \mathbf{s}_j)^2 \mid d\tau$$

$$= N^{-1} \int \sum (e_+ e_- / |\mathbf{r}_i - \mathbf{s}_j|)(\partial/\partial \mathbf{r}_i) \mid \psi(\mathbf{r}_i)^2 \mid d\tau. \tag{15}$$

Since the major contribution to this last integral comes from the regions near $\mathbf{r}_i = \mathbf{s}_j$, it is clear that the vanishing of the derivative of the electronic distribution at this point is approximately sufficient for (15) to hold. This criterion is, practically, of little value if exact wave functions are being used, and it is just as useless if base functions such as LCAO functions are used in the variational expansion, as these functions have cusps at the nuclei.

When the nuclear and electronic distributions have some symmetry, it is possible to make this analysis more precise and useful. By taking symmetry determined linear combinations of Eqs. (15), and noting that the potential and the molecule must have the same symmetry, it is not difficult to show that the nuclei must be at extrema of the electronic distribution with respect to nontotally symmetric nuclear displacements. This is the burden of the recent paper by Clinton and Rice on the relationship between the Helmann-Feynman theorem and the Jahn-Teller theorem.[5]

It is also helpful to keep in mind the result as given by Jahn and Teller that except in linear systems a nuclear distribution cannot be configurationally stable if it gives rise to a degenerate electronic wave function.[6]

Choice of a Starting Set of Basis Functions

In order for the harmonic oscillator approach given here to be useful, it is necessary that relatively few basis functions must suffice to give reasonably accurate results. Now a minimal set of these functions can be determined with the aid of the noncrossing rule, LCAO theory, and the nearly united-atom theories recently proposed by Werner Bingel[7] and the author.[8] To choose the set of basis functions one first picks a particular nuclear configuration S_a. A totally symmetric displacement will on the one hand carry this into a nearly-united-atom configuration, and on the other hand into a completely separated-atom configuration. The orbitals in these configurations can be correlated one with another in the manner of footnote reference 8, and the orbital occupancy can be determined as a function of molecular size. By correlating the harmonic oscillator functions with, say the nearly united-atom functions, one can determine which harmonic oscillator functions are likely to be important to the problem at hand. This selection procedure can be repeated for all pertinent nuclear configurations S. The set of orbitals so obtained we shall term a "minimal" set. The membership of this set is not a function of β though of course its usefulness is. Howell and Shull have in fact noted in a similar problem that a proper choice of a starting set greatly minimizes the dependence of the energy of the system upon a parameter such as β.[1]

Evaluation of Matrix Elements

Once a "minimal" set has been settled upon, one needs to evaluate the matrix elements between the members of this set. These may be expressed in two different ways:

$$\langle \Omega_n \mid \mathfrak{IC}_e \mid \Omega_n' \rangle \equiv \langle n \mid \mathfrak{IC} \mid n' \rangle = \langle n \mid \sum \mathfrak{IC}_{a-} \mid n' \rangle + \langle n \mid \mathcal{V}_e - \sum_a \tfrac{1}{2}\lambda_{a-} \mathbf{Q}_{a-}^2 \mid n' \rangle$$

$$= \sum_a \omega_{a-} \delta_{n,n'} + \langle n \mid \mathcal{V}_e - \sum_a \tfrac{1}{2}\lambda_{a-} \mathbf{Q}_{a-}^2 \mid n' \rangle, \tag{16a}$$

and

$$\langle n \mid \mathfrak{IC} \mid n' \rangle = \langle n \mid \mathfrak{I}_e \mid n' \rangle + \langle n \mid \mathcal{V}_e \mid n' \rangle = \tfrac{1}{2} \langle n \mid \sum \mathfrak{IC}_{a-} \mid n' \rangle + \langle n \mid \mathcal{V}_e \mid n' \rangle. \tag{16b}$$

When the matrix elements are written in this last form the theory may be seen to bear a close relationship to the free-electron theory of Platt.[9] In both, the zero-order problem simply determines a zero-order electronic distribution, its kinetic energy, and consequent degeneracies. To determine the molecules that can arise from this distribution, the nuclei are allowed to perturb it and organize themselves into distributions of minimal potential energy. The major difference between the approaches is that in the harmonic oscillator approach the degeneracies are not the same as in the free-electron theory and they are considered to be removed directly by the action of the nuclei rather than indirectly through boundary value restrictions appropriate to the nuclear distribution. Furthermore, in the harmonic oscillator theory, only when $n = n'$ or Ω_n, Ω_n' are of opposite

[5] W. L. Clinton, and B. Rice, J. Chem. Phys. **30**, 542 (1959).
[6] H. A. Jahn and E. Teller, Proc. Roy. Soc. (London) **A161**, 220 (1937).
[7] Werner Bingel, J. Chem. Phys. **30**, 1254 (1959).
[8] Carl E. Wulfman, J. Chem. Phys. **31**, 381 (1959).
[9] J. R. Platt, J. Chem. Phys. **22**, 1448 (1954); Colloques intern. centre natl. recherche sci. Paris, No. 82 (1959).

parity is it true that:

$$\langle n \mid \mathcal{H}_e \mid n' \rangle = \langle n \mid \mathcal{V}_e \mid n' \rangle + \text{constant} \times \omega_0 \delta_{n,n'}$$

(the constant here is $\frac{1}{2}$). (16c)

The matrix elements of formulas (16) can be reduced to sums of integrals with the aid of the relations of Condon and Shortley.[10] The results are exactly like those obtained in other single-particle treatments. Thus, for example, if σ is a spin function, one obtains when the Ω are each single determinants:

$$\langle n \mid \sum_i (e_+ e_-/(\mathbf{r}_i - \mathbf{s}_j) \mid n' \rangle$$

$$= \pm \langle (\sigma\phi)_{a1} \mid (e_+ e_-/\mid \mathbf{r}_1 - \mathbf{s}_j \mid) \mid (\sigma\phi)_{a'1} \rangle \equiv \pm \langle a \mid \mathcal{V}_j \mid a' \rangle$$

if $n \neq n'$ and only $a \neq a'$. (17a)

$$= \sum_{a,b}^{\text{occ.}} \langle a \mid \mathcal{V}_j \mid b \rangle \qquad \text{if } n = n'. \tag{17b}$$

$$= 0 \text{ otherwise.} \tag{17c}$$

The integrals required may be evaluated in Cartesian or polar coordinates. In Cartesian coordinates one may expand the one-dimensional densities, $\phi_l(x)\phi_l'(x)$ in a Clebsch-Gordan series;

$$\phi_l(x)\phi_l(x) = \sum_{L=0}^{l+l'} (lLl')\phi_L(2^{\frac{1}{2}}x). \tag{18}$$

Explicit expressions for the coefficients (lLl') are given in Appendix I.

In an analogous way one may obtain eigenfunction expansions for the potentials:

$$\mid \mathbf{r} - \mathbf{s} \mid^{-1} = \sum_{L,M,N} U_{LMN}(\mathbf{s})\phi_L(2^{\frac{1}{2}}x)\phi_M(2^{\frac{1}{2}}y)\phi_N(2^{\frac{1}{2}}z) \tag{19}$$

$$\mid \mathbf{r}_1 - \mathbf{r}_2 \mid^{-1} = \sum_{I,J,K,L,M,N} V_{IJK}{}^{LMN}\phi_I(1)\phi_J(1)\phi_K(1) \times \phi_L(2)\phi_M(2)\phi_N(2). \tag{20}$$

As Boys[11] noted some time ago, the coefficients required in these expansions can easily be evaluated by differentiation of the error integral.

On using the expansions one has:

$$\langle a \mid V_j \mid a' \rangle \equiv \langle lmn \mid V_j \mid l'm'n' \rangle = \sum_{L,M,N} (lLl')(mMm')(nNn')U_{LMN} \tag{21}$$

$$\langle ab \mid a'b' \rangle = \sum_{I,J,K,L,M,N} (iIi')(jJj')(kKk')(lLl') \times (mMm')(nNn')V_{LMN}{}^{IJK}. \tag{22}$$

For the discussion of Sec. IV of this paper it is simplest to carry out the integrations in polar coordinates. One has, for example, (cf. reference footnote 8):

$$\langle \phi_{\nu\lambda\mu} \mid\mid \mathbf{r} - \mathbf{s} \mid^{-1} \mid \phi_{\nu'\lambda'\mu'} \rangle = \sum_k s^k \left\{ \int_0^\infty R_{\nu\lambda} R_{\nu'\lambda'} \mathbf{r}^{1-k} d\mathbf{r} + \int_0^s R_{\nu\lambda} R_{\nu'\lambda'} [(\mathbf{r}^{k+2}/s^{2k+1}) - \mathbf{r}^{1-k}] d\mathbf{r} \right\} \times 2^{\frac{1}{2}}\pi(2k+1)^{-\frac{1}{2}} c^k(\lambda\mu;\lambda'\mu') Y_{k,\mu-\mu'}(\theta_s, \phi_s). \tag{23}$$

The c^k coefficients are tabulated in Condon and Shortley's book.[10] The radial integrals are most simply evaluated by reducing them to sums of integrals of the form:

$$A_n(t) \equiv \int_0^t r^n \exp -r^2 dr. \tag{24}$$

These may be expanded in rapidly converging power series in the region $(t \leq 1)$ of interest.

IV. APPLICATION TO 20-26 ELECTRON SYSTEMS

The triatomics composed of second-row atoms are the simplest interesting systems for which an extensive junction with experiment is possible. Great regularity has been observed in their properties.[12] The systems offer a particularly simple test of the ideas advanced here if one proceeds by considering the stability of linear systems. In linear systems some of the conditions (12c) are automatically satisfied since the energy of a linear system is necessarily an extremum with respect to bending motions of the nuclei. The problem is thus reduced to one of determining radial distributions of the nuclei such that the remaining conditions (12) are satisfied. Once this has been done it is only necessary to determine whether these nuclear configurations correspond to maxima or to minima in the electronic energy surface.

The united-atom separated-atom correlation diagrams given in reference 8 indicate that one should include $2d$, $3p$, $3f$, and $5p$ harmonic oscillator functions in a consideration of 20–26 electron triatomics. This conclusion is not altered if electron repulsion effects are taken into account. However there is evidence to indicate that this set is much larger than is required in a treatment of stable systems. A 20-electron harmonic oscillator system is a closed-shell system. It has a nondegenerate distribution function with no angular extrema and with its only radial extremum at the origin. It can only develop the extrema required by (12c) through the mixing-in of excited states. If a choice of β which minimizes the energy of the system widely separates these states from the ground state this mixing will be difficult. That this is in fact the case is evidenced by the total nonexistence of 20 electron triatomics.

Apparently the stability of systems containing a few more than 20 electrons arises from the possibility

[10] E. U. Condon and G. H. Shortley, *Theory of Atomic Spectra* (Cambridge University Press, New York, 1953).

[11] S. F. Boys, Proc. Roy. Soc. (London) **A200**, 542 (1950).

[12] Irving Langmuir, J. Am. Chem. Soc. **41**, 1543 (1919); A. D. Walsh, J. Chem. Soc. **1953**, 2260 *et seq.*

of the last electrons developing the extrema required by (12c). All this suggests that one can here at least treat the difference between the harmonic oscillator and Coulomb potentials as a perturbation. If this is true, then, in the neighborhood of their minima, the potential energy surfaces of these triatomics should be obtainable from a perturbation treatment based upon degenerate $3p$, and $3f$ zero-order harmonic oscillator functions.

Let us therefore consider these triatomics in this way, and suppose them derived from a 20 electron homonuclear system by successive additions of electrons, followed when necessary by alterations in nuclear charges. The 20 electron closed-shell function gives rise to the electronic distribution plotted in cross section in Fig. 1. It is to be compared with the distribution in Fig. 1 in which the Os^2 contribution does not appear. As additional electrons are added they must go into the fourth harmonic oscillator shell, containing the degenerate p and f orbitals. Their radial distribution is shown in cross section in Fig. 2. With the aid of the

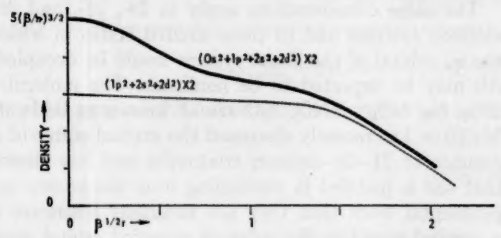

ELECTRON DENSITY CROSS SECTIONS ALONG THE Z AXIS

FIG. 1.

p or f orbitals it is possible to develop additional radial extrema in the electron distribution, as shown in Fig. 3. Angular extrema can be developed with the aid of either the p or f orbitals and in considerable variety. The possibilities may in general be investigated most simply with the aid of the work of Bethe.[13] Here, however, his symmetry considerations are unnecessary and it is only necessary to determine how the Coulombic interactions split the degeneracies in the various orbitals appropriate to a linear configuration.

It is simplest to begin by considering $D_{\infty h}$ configurations, supposing at first that the energy of the system is only a function of the common internuclear distance. When the three nuclei are united in the center of the distribution, the p orbitals are much lower in energy than the f orbitals; the Coulombic attraction of the central nucleus preferentially lowers the energy of the p orbitals and Coulombic repulsions between electrons preferentially raise the energy of the f orbitals. This splitting is large, for the f functions correlate with united atom $4f$ orbitals while the p functions correlate with united atom $2p$ orbitals.

[13] H. Bethe, Ann. Physik (5) **3**, 133 (1929).

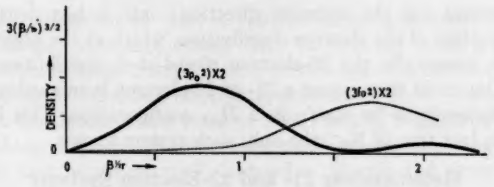

ELECTRON DENSITY CROSS SECTIONS ALONG THE Z AXIS

FIG. 2.

As the nuclei are slightly separated, the degeneracy among the p orbitals is removed. If the z axis is considered to pass through the three nuclei, then the p_0 orbital is lowest in energy because the terminal nuclei move into regions of higher electron density in it, while remaining on nodes of the p_{+1} and p_{-1} orbitals. Sometime after the nuclei pass the shoulder in the 20 electron distribution function, the electron repulsions and nuclear attractions begin to have opposite effects on the energy separation of the p_0 and f_0 functions. However, the f_0 can never cross the p_0 because both are of the same symmetry in the group $D_{\infty h}$.

Stability of $D_{\infty h}$ Configurations

The implications of these observations are fairly clear. In a 21 or 22 electron system the electronic energy can be at a minimum with respect to totally symmetric nuclear displacements only if the terminal nuclei are near radial maxima in the distribution function, and this requires that the 21st and 22nd electrons occupy a σ_u orbital which is predominately p_0 but which inevitably contains some admixture of f_0. Though in this approximation the hybrid distribution function does not develop a complete radial maximum at the origin, this is not necessary for radial stability because the central nucleus cannot move toward either of the terminal nuclei without violating the center of charge restriction so long as the terminal nuclei remain at their respective maxima in the electronic distribution.

The system is also stable with regard to bending. During a bending motion subject to the center of charge restriction the terminal nuclei move into less dense portions of the σ_u orbital while the central nucleus also

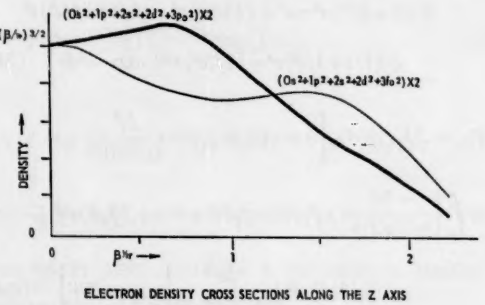

ELECTRON DENSITY CROSS SECTIONS ALONG THE Z AXIS

FIG. 3.

moves (in the opposite direction) into a less dense portion of the electron distribution, which at the origin is essentially the 20-electron closed-shell distribution. One must thus expect a 21- or 22-electron homonuclear molecule to be stable in a $D_{\infty h}$ configuration. This is in fact true of N_3^-, the only such system known.

Heteronuclear 21- and 22-Electron Systems

In systems that are moderately heteronuclear the perturbation approximation might also be expected to hold. It is then simplest to consider the heteronuclear molecules as derived from homonuclear ones by a rearrangement of nuclear charge. In this case one easily discovers that small increments or decrements in the charge of the central nucleus do not alter the conclusions reached for N_3^-. Thus CO_2^+, CO_2, BO_2^-, and NO_2^+ are all linear molecules.

Again if one considers alterations in nuclear charges which make the terminal nuclei inequivalent the arguments go through as before except that, to satisfy the center of charge restriction, the central nucleus is no longer to be put at the center of the system. Again the 21 and 22 electron systems are linear as in NCO^- and N_2O.

Finally it is to be noted that when all the nuclei are not identical the molecule will be most stable if the nuclei with greatest nuclear charge are put in the terminal positions, since here the greatest electron density is developed in the zero-order problem. Thus one has O—C—O not C—O—O, and perhaps more surprisingly, N—N—O rather than N—O—N. However N—O—N should be metastable and one suspects that it may be isolable at low temperatures.

23- to 26-Electron Systems

When a further electron is added to a 22-electron $D_{\infty h}$ system, it is conceivable that it might enter either a $\sigma_u(f_0)$ or a $\pi_u(p_1)$ orbital. The energy ordering of these is not symmetry determined and a numerical investigation is required to decide it. Evaluation of the interaction potentials between a nucleus and the f_0 and p_1 distribution gives

$$V_{p_1}=\tfrac{32}{15}(2\beta)^{\frac{1}{2}}e_+\Big[\tfrac{9}{8}-\tfrac{13}{48}t^2+\int_0^t\{\tfrac{5}{4}r-(\tfrac{25}{4}+t^2)r^3 +(5+t^2/5)r^5-r^7+(25/4t)r^4-(5/t+5/4t^3)r^6 +(1/t+1/t^3)r^8-(1/5t^3)r^{10}\}\exp-r^2dr\Big] \quad (24a)$$

$$V_{f_0}=\tfrac{64}{105}(2\beta)^{\frac{1}{2}}e_+\Big[3+\tfrac{4}{15}t^2+\tfrac{2}{11}t^4+\frac{5t^6}{4(7361)^{\frac{1}{2}}} +\int_0^t\Big\{\frac{-5t^6}{2(7361)^{\frac{1}{2}}}r-\tfrac{2}{11}t^4r^3-\tfrac{4}{15}t^2r^5+r^8/t+(\tfrac{4}{15}t^3)r^{10} +(2/11t^5)r^{12}+\frac{5r^{14}}{2(7361)^{\frac{1}{2}}t^7}\Big\}\exp-r^2dr\Big]. \quad (24b)$$

At $t=\beta^{\frac{1}{2}}s=2^{\frac{1}{2}}/2$, the position of the maximum in the p_0 distribution, one finds that $V_{p_1}/V_{f_0}\simeq 5/4$. Consequently, even neglecting the presence of the central nucleus and even neglecting electron repulsion effects, the p_1 orbitals are lower in energy than the f_0 orbital. In a linear system crossing of these two only takes place at an internuclear distance far greater than that which yields a radially stable molecule. Consequently, on adding an electron to a 22-electron triatomic it enters a π_u orbital.

However, the moment this happens the central nucleus ceases to be at a saddle point in the electronic distribution and is at an absolute minimum instead. It therefore has a great tendency to move off in a direction perpendicular to the axis of the molecule. Because of the center of charge restriction it may do this only if the terminal nuclei may move in the opposite direction. This they may easily do as replacement of the f_0 component of the σ_u orbital by a $f_{\pm 2}$ component enables the electron density maximum to follow the terminal nuclei.

The same considerations apply to 24-, 25-, and 26-electron systems and to those excited states in which the π_u orbital of the linear system would be occupied. All may be expected to be nonlinear. The molecules NO_2, O_3, NO_2^-, FNO, F_2O are all known to be bent. Mulliken has recently discussed the excited states of a number of 21–26-electron triatomics and has shown that one is justified in concluding from the known experimental work that they are nonlinear whenever a π_u orbital would be the topmost occupied orbital were they linear.[14]

There are no known 27- or 28-electron triatomics.

Conclusion

The general view expressed here is that in problems of theoretical stereochemistry it is profitable to consider nuclei as constrained by an electron cloud *belonging to the whole molecule*. From this point of view one is able to rationalize observations like those of Walsh[12] which clearly imply that it is the topmost occupied orbitals that determine the shape of simple molecular systems. Moreover, from this point of view, it is not difficult to determine when and how to employ cuspless single-center wave functions to advantage. When such singularity-free functions can be used it is possible to avoid many of the problems due to the singularity of the Coulomb potential. The fault in the cuspless function becomes a virtue because it enables the use of simple criteria for configurational stability. Cuspless wave functions do not eliminate the orbital following problem but they can greatly alleviate it.

Despite the many obvious limitations of the exploratory treatment given here, it is apparent that the harmonic oscillator approach can be both valid and simple, and it would appear that the Gaussian expan-

[14] R. S. Mulliken, Can. J. Chem. **36**, 10 (1959).

sions used by a number of authors[15] bear further investigation. Some idea of the range of usefulness of the treatment can be obtained by considering the stability of systems other than 20-electron triatomics which correspond to harmonic oscillator closed shells. Among these there are no stable 8-electron molecules known. The closest known approach to a stable homonuclear 40-electron triatomic is the reactive intermediate dichlorocarbene. Its nuclear charges differ by a factor of nearly 3:1 and there is much evidence to indicate that the shape of carbenes in general is very easily altered.[16] No 8-, 20-, or 40-electron tetratomics are known but there are stable 20-electron diatomics. Though the homonuclear Ne_2 is not one of them, by a minor transformation it yields the stable NaF. During this transformation the electronic distribution remains essentially unaltered and it is clear that the failure of the harmonic oscillator perturbation treatment is associated with a great electronic rearrangement brought about by the comparatively large charges of the original Ne_2. In general the harmonic oscillator approach is more likely to be valid in systems of many moderately charged vibrating nuclei than in systems with few nuclei of large charge. In the former systems the force on each individual electron approximates more closely to the Hooke's law force it would feel in a uniformly charged sphere. The harmonic oscillator approach may in fact be meaningfully termed a "distributed atom" approach.

ACKNOWLEDGMENT

The author wishes to express his appreciation to Professor Robert G. Parr for many helpful discussions and kindnesses which have made this work possible.

APPENDIX I. HERMITE CLEBSCH-GORDAN COEFFICIENTS[17]

We wish to determine the coefficients (lNm) in the expansion:

$$\phi_l{}^1\phi_m{}^1=\sum(lNm)\phi_N{}^2 \tag{1}$$

where

$$\phi_k{}^a\equiv\phi_k(\alpha^{\frac{1}{2}}x)=[(\alpha/\pi)^{\frac{1}{4}}(2^k k!)^{-1}]^{\frac{1}{2}}H_k(\alpha^{\frac{1}{2}}x)\exp-(\alpha/2)x^2. \tag{2}$$

For this purpose the following two identities are useful:

$$(lNm)=\int_{-\infty}^{+\infty}\phi_l{}^1\phi_N{}^2\phi_m{}^1dx \tag{3}$$

$$H_k(x)=(\partial/\partial t)_0{}^k\exp(-t^2+2tx)_{t=0}\equiv(\partial/\partial t)_0{}^k\exp(-t^2+2tx). \tag{4}$$

The first of these is a direct consequence of the orthonormality of the functions ϕ. Equation (4) is simply the statement that the exponential given is the generating function for the Hermite polynomials.

On thrice substituting (4) into (3) one obtains:

$$(lNm)=(\pi/2)^{1/4}(2^{l+m-N}l!m!N!)^{-\frac{1}{2}}I_{lNm}, \tag{5}$$

where

$$I\equiv(2/\pi)^{\frac{1}{2}}(\partial/\partial t)_0{}^l(\partial/\partial v)_0{}^N(\partial/\partial u)_0{}^m\int\exp[-t^2+2tx-u^2+2ux-v^2+2v\sqrt{2}x-2x^2]dx \tag{6}$$

$$=(\partial/\partial t)_0{}^l(\partial/\partial v)_0{}^N(\partial/\partial u)_0{}^m\{\exp[-\tfrac{1}{2}(t-u)^2+\sqrt{2}v(t+u)]. \tag{7}$$

On making use of Leibnitz's rule for the differentiation of a product, this becomes

$$(\partial/\partial v)_0{}^N(\partial/\partial u)_0{}^m\sum_{p=0}^{l}\binom{l}{p}[(\partial/\partial t)_0{}^p\exp-\tfrac{1}{2}(t-u)^2]\cdot[(\sqrt{2}v)^{l-p}\exp[[vu], \tag{8}$$

and, again,

$$(\partial/\partial v)_0{}^N\sum_{p=0}^{l}\sum_{q=0}^{m}\binom{l}{p}\binom{m}{q}[(\partial/\partial u)_0{}^q(\partial/\partial t)_0{}^p\exp-\tfrac{1}{2}(t-u)^2]\cdot[(\sqrt{2}v)^{l-p+m-q}]. \tag{9}$$

But,

$$[(\partial/\partial u)_0{}^q\exp-\tfrac{1}{2}(t-u)^2]_{t=0}=(-1)^q[(\partial/\partial t)_0{}^q\exp-\tfrac{1}{2}(t-u)^2]_{u=0}=(-1)^q(\partial/\partial r)_0{}^q\exp-\tfrac{1}{2}r^2, \tag{10}$$

[15] Cf., e.g. S. F. Boys, footnote reference 11; R. McWeeny, Nature **166**, 21 (1950); Acta Cryst. **6**, 631 (1953); A. Meckler, J. Chem. Phys. **21**, 1750 (1953); G. E. Kimble and G. F. Neumark, *ibid.* **26**, 1285 (1957).

[16] P. S. Skell, "Bi-valent carbon," Cleveland Meeting of the American Chemical Society, April, 1960.

[17] To avoid confusion of primes and factorials the symbolism in this Appendix differs from that in the body of the paper.

so

$$I=(\partial/\partial v)_0{}^N\sum\sum\binom{l}{p}\binom{m}{q}[(-1)^q(\partial/\partial r)_0{}^{p+q}\exp-\tfrac{1}{2}r^2]\cdot[(\sqrt{2}v)^{l+m-(p+q)}] \tag{11}$$

$$=\sum\sum\binom{l}{p}\binom{m}{q}[(-1)^q(\partial/\partial r)_0{}^{p+q}\exp-\tfrac{1}{2}r^2]\cdot 2^{N/2}N!\delta_{N,[l+m-(p+q)]}. \tag{12}$$

Now

$$(\partial/\partial r)_0{}^a\exp-\tfrac{1}{2}r^2=\begin{cases}0; & a\text{ odd}\\ (-1)^{a/2}a!/2^{a/2}(a/2)!; & a\text{ even.}\end{cases} \tag{13}$$

Hence

$$I=\sum\sum\binom{l}{p}\binom{m}{q}(-1)^q\frac{(-1)^{\frac{1}{2}(p+q)}(p+q)!}{2^{\frac{1}{2}(p+q)}[\frac{1}{2}(p+q)]!}N!2^{N/2}\delta_{N,[l+m-(p+q)]} \tag{14}$$

$$=\sum\sum\frac{l!m!(-1)^q(-\frac{1}{2})^{\frac{1}{2}(p+q)}(p+q)!2^{N/2}N!\delta_{N,[l+m-(p+q)]}}{p!(l-p)!q!(m-q)![\frac{1}{2}(p+q)]!} \tag{15}$$

$$=(-1)^{\frac{1}{2}(l+m-N)}2^{-\frac{1}{2}(l+m-2N)}\left\{\frac{(l+m-N)!}{[(l+m-N)/2]!}\right\}N!l!m!\sum_p\frac{(-1)^p}{(l-p)!p!(N+p-l)!(l+m-N-p)!}. \tag{16}$$

Thus, since $l+m-N$ is an even number ($l+m-N=p+q=a$),

$$I=(-1)^{(l+m-N)/2}2^{N-[(l+m)/2]}N!l!m!\left\{\frac{(l+m-N)!}{[(l+m-N)/2]!}\right\}\sum_p\frac{(-1)^p}{(l-p)!p!(N+p-l)!(l+m-N-p)!}. \tag{17}$$

As a consequence one finds, after some straightforward algebra,

$$(lNm)=\left[\frac{l!m!N!}{(2\pi)^{\frac{1}{2}}2^{2l+2m-N}}\right]^{\frac{1}{2}}(-1)^{(l+m-N)/2}\left[\frac{(l+m-N)!}{[(l+m-N)/2]!}\right]\sum_p\frac{(-1)^p}{(l-p)!p!(N+p-l)!(l+m-N-p)!}. \tag{18}$$

The summation is to be carried out over all positive values of p for which all of the factorials have nonnegative arguments. It is easily seen that (lNm) vanishes unless $l+m-N$ or $l+m+N$ is an even number. It also vanishes, unless

$$N\leq l+m. \tag{19}$$

A number of the coefficients will be found in Table I.

TABLE I. Hermite Clebsch-Gordan coefficients.

l	l'	$L=0$	1	2	3	4	5	6
0	0	1						
1	0		$(1/2)^{\frac{1}{2}}$					
1	1	$(1/4)^{\frac{1}{2}}$		$(1/2)^{\frac{1}{2}}$				
2	0	$-(1/8)^{\frac{1}{2}}$		$(1/4)^{\frac{1}{2}}$				
2	1		$(1/16)^{\frac{1}{2}}$		$(3/8)^{\frac{1}{2}}$			
2	2	$(9/64)^{\frac{1}{2}}$		$(1/8)^{\frac{1}{2}}$		$(3/8)^{\frac{1}{2}}$		
3	0		$-(3/16)^{\frac{1}{2}}$		$(1/8)^{\frac{1}{2}}$			
3	1	$-(3/32)^{\frac{1}{2}}$		0		$(1/4)^{\frac{1}{2}}$		
3	2		$(3/128)^{\frac{1}{2}}$		$(1/16)^{\frac{1}{2}}$		$(5/16)^{\frac{1}{2}}$	
3	3	$(25/16^2)^{\frac{1}{2}}$		$(9/128)^{\frac{1}{2}}$		$(3/32)^{\frac{1}{2}}$		$(5/16)^{\frac{1}{2}}$

(lLl') is $(1/2\pi)^{1/4}\times$the value tabulated. Thus: $(231)=(1/2\pi)^{1/4}(3/8)^{\frac{1}{2}}$.

Letters to the Editor

THE Letters to the Editor section is subdivided into three parts entitled Communications, Comments and Errata, and Notes. These three sections are all subject to the same limitations on length. The textual material of each Letter is limited to a number of words equal to 950 minus the following; (a) 200 words for each average-sized figure: (b) 50 words for each displayed equation: (c) 7 words for each line of table including headings and horizontal rulings. No proof will be sent to the authors of "Communications" and "Comments and Errata." Proof will be sent to the authors of "Notes." The publication charge for Letters is $30 per page, with a minimum of $30 per Letter. If honored, the Institution will be entitled to 100 reprints without covers. See issues of May–September, 1957, for descriptions of categories.

Communications

First Excited $^1\Sigma_g^+$ State of H_2. A Double-Minimum Problem*

ERNEST R. DAVIDSON

Chemistry Department, Indiana University, Bloomington, Indiana

(Received August 22, 1960)

COMPUTATIONAL techniques with electronic computers now make feasible the direct computation of term levels of a number of simple molecular systems. The excited states of the H_2 molecule are a fruitful area for this type of work since the spectra are complex, showing many irregularities,[1] while the electronic problem is relatively simple, involving only two electrons. The present work was also undertaken as a practicable example of the use of the excited-state variation theorem of Shull and Lowdin[2] which permits computation of an accurate excited-state function without the formal requirement that it be orthogonal to the true ground-state eigenfunction.

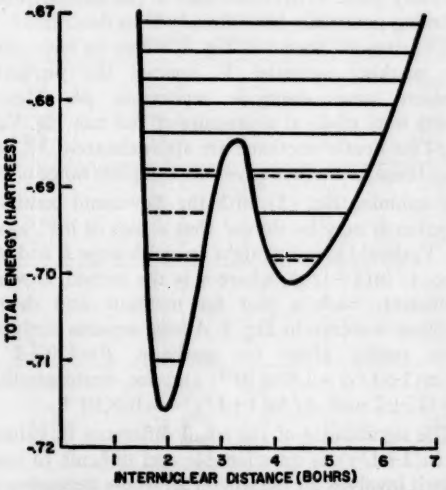

FIG. 1. The potential curve and vibrational levels for the first excited $^1\Sigma_g^+$ state of the hydrogen molecule. The term levels are indicated by solid lines in regions in which the probability density is large.

The potential curve for the first excited $^1\Sigma_g^+$ state has been calculated by the linear variation method using a 20-term expansion in elliptical coordinates without explicit r_{12} dependence. As Fig. 1 shows, the potential curve computed from this expansion is characterized by two deep minima. Since the wave function is largely covalent at the inner minimum, this minimum can be identified with the state characterized by experimentalists as $1s2s\ ^1\Sigma_g^+$.[3] At the outer minimum, however, the wave function is largely ionic in nature and seems to correspond to the experimental $(2p\sigma)^2\ ^1\Sigma_g^+$ state.[4]

It has been common practice, heretofore, to compare the theoretical potential curve with one derived by a best fit to experimental term levels. It seems practicably and esthetically more desirable, however, to calculate directly the rotational-vibrational eigenfunctions of the theoretical potential curve. This has been done by a numerical integration technique for the potential curve of Fig. 1. Although the potential energy curve itself is in absolute error by about 800 cm^{-1} over the entire distance range, the relative spacing of the term levels agrees to about 20 cm^{-1} with experiment. The calculation shows, however, two new vibrational levels, with probability density largely in the outer minimum, which have not been experimentally identified. These are predicted to be near 101 600 cm^{-1} and 102 700 cm^{-1} for the $K=0$ levels. The computed B value for both these levels is about 6 cm^{-1}, although the lower one is perturbed somewhat by the nearby level with probability density largely in the inner minimum.

The double minimum in this state arises from the H^+H^- separated atom level, which lies between $1s4s$ and $1s5s$ at $R=\infty$. This level "crosses" all the $1sns$ levels below it (except $1s^2$) to form the outer minimum. Two or more minima are therefore predicted for the second, third, and the fourth excited $^1\Sigma_g^+$ levels also. Our calculations have already demonstrated the presence of a double minimum in the second excited state. It is likely that some of the unassigned levels in the H_2 spectrum, hitherto surmised to belong to doubly excited states, do instead arise from these double minima.

Further calculations are in progress, both for these higher states and for other isotopic species to permit a complete theoretical analysis of the H_2 spectrum.

* Supported in part by a contract between the AF OSR and Indiana University and by a grant from the National Science Foundation. The calculations reported were carried out in the Indiana University Research Computing Center.

[1] G. H. Dieke, J. Mol. Spectroscopy **2**, 494 (1958).

[2] H. Shull and P.-O. Lowdin, Phys. Rev. **110**, 1466 (1958).

[3] G. Herzberg (see material on the E state), *Spectra of Diatomic Molecules* (D. Van Nostrand Company, Inc., Princeton, New Jersey, 1950), 2nd ed.; reference 1 (material on the $2A$ state).

[4] G. Herzberg, material on the F state (reference 3), or Dieke, material on the $2K$ state (reference 1).

Comments and Errata

Electric Strength of Methane and Deuteromethane

J. C. Devins and R. W. Crowe*

General Electric Research Laboratory, Schenectady, New York

(Received September 8, 1960)

RECENT interpretations of the dependence of electric strength of hydrocarbon gases on molecular structure[1] have been based upon the following equation[2] for the Townsend ionization coefficient

$$\alpha/p = AE/p \exp(-Bp/E). \quad (1)$$

Here E is the applied electric field, p is the pressure, and A and B are constants, characteristic of the gas. In the development of this equation it was assumed that the only important electron energy losses in collision with molecules were by electronic excitation and ionization. While quantitative considerations permit the neglect of losses due to elastic collision in the region of E/p of interest to this work, energy losses to vibration and rotation are insufficiently understood to treat them similarly. Bailey,[3] working at very low E/p where electronic excitation was negligible, concluded that energy losses were many times those attributable to elastic collisions. More recent theoretical treatments,[4] however, have not completely explained these results.

In an effort to assess the importance of vibrational and rotational losses to electrical breakdown we have measured the sparking potentials of methane and deuteromethane. It is to be expected that electronic losses will be similar for these molecules, while vibrational and rotational loses will be considerably different. Hall,[5] for example, has observed that the energy loss per electron collision in hydrogen was twice that for deuterium at low E/p (1–10 v cm^{-1} mm Hg^{-1}), although the total collision cross section was identical in the two gases. Huxley,[6] in an interpretation of this work, has concluded that a major fraction of this energy loss is due to rotational excitation.

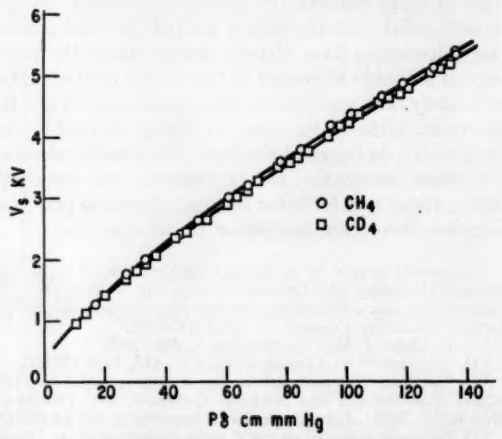

FIG. 1. Sparking potentials for methane and deuteromethane.

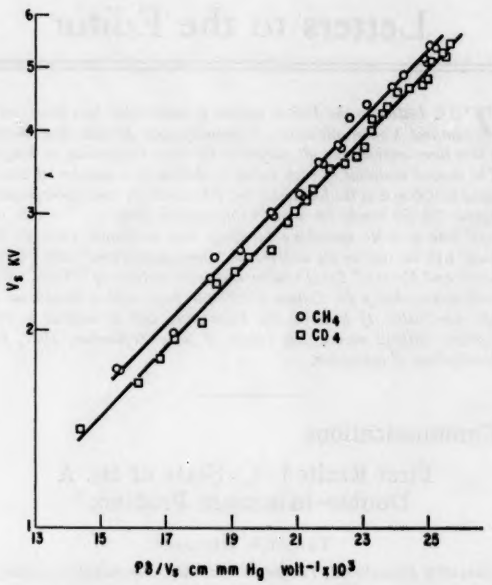

FIG. 2. Dependence of the sparking potential on the ratio $P\delta/V_s$.

The methane used in this work was labeled greater than 99% pure. The deuteromethane was supplied by Tracerlab and was said to be greater than 95% isotopically pure. Techniques used in the measurement of sparking potentials have already been described.[1]

The data are shown in Fig. 1, where we have plotted the sparking potential V_s against the product of pressure times electrode separation $p\delta$. Measurements were made at a pressure of 265 mm Hg. Values of $p\delta$ for deuteromethane are approximately 3% lower than those for methane over the complete range of $p\delta$.

Combining Eq. (1) with the Townsend breakdown criterion it may be shown[1] that a plot of $\ln V_s$ against $P\delta/V_s$ should give a straight line with slope B and intercept $A/\ln(1+1/\gamma)$, where γ is the second Townsend coefficient. Such a plot for methane and deuteromethane is shown in Fig. 2. A least-squares analysis of these results gives: for methane, $B=120\pm2$ and $A/\ln(1+1/\gamma)=3.80\times10^{-3}$; and for deuteromethane, $B=121\pm2$ and $A/\ln(1+1/\gamma)=4.16\times10^{-3}$.

The significance of the small difference in values of $A/\ln(1+1/\gamma)$ is questionable and difficult to assess, since it involves the parameter A, whose dependence on molecular structure has not been evaluated, and γ, which is dependent upon the nature of the cathode surface as well as the nature of the gas. The quantity B,

which has been correlated with molecular structure, shows no isotope effect. It may be concluded, therefore, that excitation of vibrational and rotational losses probably does not provide an important energy loss mechanism in the range of E/p considered in our earlier work on the breakdown of hydrocarbon gases.

* Present address: Thomas A. Edison Research Laboratory, West Orange, New Jersey.

[1] J. C. Devins and R. W. Crowe, J. Chem. Phys. **25**, 1053 (1956).
[2] R. W. Crowe, J. K. Bragg, and J. C. Devins, J. Appl. Phys. **26**, 1121 (1955).
[3] V. A. Bailey, Phil. Mag. **13**, 993 (1932).
[4] E. Gerjouy and S. Stein, Phys. Rev. **98**, 1848 (1955), and references (in this paper) to earlier work.
[5] B. I. H. Hall, Australian J. Phys. **8**, 468 (1955).
[6] L. G. H. Huxley, Australian J. Phys. **9**, 44 (1956).

Erratum: Lattice Energies of the Alkali Halides and the Electron Affinities of the Halogens

[J. Chem. Phys. **31**, 1646 (1959)]

DANIEL CUBICCIOTTI

Stanford Research Institute, Menlo Park, California

(Received August 17, 1960)

THE author is indebted to Dr. Robert Baron (University of Chicago) for pointing out that a wrong value (8) was used for the number of next nearest neighbors in the rock-salt structure (correct value = 12).

Correcting that mistake had the following effect. The values of k (Table III) should be multiplied by 1.5 for all salts with rock-salt structure. Footnote 5 no longer applies. The values for ρ should be about 1% larger. Such a change in ρ has a negligible effect on the final results; so the values of ρ averaged were used unchanged in this recalculation. The revised set of r_+ and r_- are: Li 0.580; Na 0.946; K 1.246; Rb 1.376; Cs 1.517; F 1.057; Cl 1.447; Br 1.569; I 1.752. These changes affect only the overlap repulsion terms and the final lattice energy of Table V. The revised values are given in the table below. Only three lattice energies are more than 0.5 kcal different from the original values (LiF, NaF, NaCl). The average electron affinity for F becomes 81.5 kcal/mole (essentially the same as values from direct experiment) while those of the other halogens are increased by 0.1 to 0.2 kcal/mole.

Revised values (kcal/mole).

	Overlap repulsion			
	Plus, minus	Minus, minus	Plus, plus	−Lattice energy
LiF	35.6	6.2	0.8	248.4
LiCl	21.5	6.3	0.1	203.1
LiBr	18.6	6.4	0.0	191.7
LiI	15.9	7.0	0.0	177.7
NaF	31.3	1.6	1.3	219.7
NaCl	22.5	2.1	0.2	186.6
NaBr	20.1	2.3	0.1	177.3
NaI	17.0	2.6	0.0	165.9
KF	26.4	0.3	1.7	195.2
KCl	20.7	0.5	0.2	169.9
KBr	19.4	0.6	0.1	162.8
KI	17.2	0.7	0.1	153.4
RbF	25.5	0.2	2.1	186.6
RbCl	19.8	0.3	0.3	164.4
RbBr	18.5	0.3	0.2	157.8
RbI	17.0	0.4	0.1	149.0
CsF	21.9	0.1	2.2	179.3
CsCl	17.0	0.7	1.8	156.1
CsBr	16.4	0.9	1.1	151.3
CsI	14.5	1.3	0.5	143.8

Notes

Rapid Determination of Gaseous Diffusion Coefficients by Means of Gas Chromatography Apparatus

J. CALVIN GIDDINGS AND SPENCER L. SEAGER

Department of Chemistry, University of Utah, Salt Lake City 12, Utah

(Received August 3, 1960)

CURRENT methods[1–3] used to determine binary diffusion coefficients in gases require many individual measurements for a single evaluation of the diffusion coefficient. We are investigating what promises to be a rapid, accurate method for determining these coefficients in a single experimental run. A conventional gas chromatographic apparatus has been used in preliminary work, but there are indications that some modification is desired in order to decrease the effect of the detector volume. The packed column is replaced by an empty tube of circular cross section. The theory of gaseous diffusion in such columns has been worked out exactly, notably by Taylor.[4]

The height equivalent to a theoretical plate for a circular tube is

$$H=(2D_{1,2}/v)+(vr_0^2/24D_{1,2}), \qquad (1)$$

where $D_{1,2}$ is the binary diffusion coefficient, v the average gas velocity, and r_0 the tube radius. The first term on the RHS represents spreading due to axial diffusion while the second term on the RHS represents a spreading due to lateral nonequilibrium[5] introduced by the viscous nature of the flow. If the tube geometry and

flow velocity are such as to require significant pressure gradients, known correction factors[6] must be applied to each of the terms in (1). The quantity H is obtained by means of the equation $H=L\tau^2/t^2$, where L is the tube length, t is the passage time, and τ is the rms deviation in passage time of a single peak which is injected as a δ function. All quantities discussed are easily and accurately measured by conventional means, leaving $D_{1,2}$ as the sole quantity to be determined. It is assumed in this analysis that (1) the flow is laminar, (2) the effect of tube bending is negligible,[7] and (3) the contribution of the detector and of the finite sample size to the peak spreading is negligible. The latter assumption is improved by using long tubes and detectors of very low volume (which have just recently become available). The effects of the conventional detector used in this laboratory, plus the effect of finite sample size and any end effects, were allowed for by taking measurements on both a long and a short column and subtracting τ^2, t, and L of the latter from the former. This is done, in practice, by obtaining a calibration curve of τ^2 values for the short tube.

The diffusion of hydrogen peaks into a nitrogen carrier have been investigated on a Perkin Elmer model 154-C instrument at 293°K and atmospheric pressure, which, at this location is about 640 mm Hg. A long 30-M column and a short 1-M column, both with $r_0=$ 0.244 cm, were used. A plot of $D_{H2,N2}$ against velocity yields a curve with two distinct regions. Up to $v=16$ cm/sec the points lie on a line that is straight and very nearly horizontal, as predicted. Beyond $v=16$ cm/sec, at which velocity the Reynolds number is 53, the curve swings up into another nearly straight-line portion. The reason for the latter trend is under investigation.

Twenty-one determinations obtained from the first portion of the curve yield an average diffusion coefficient (corrected to 1 atm) of 0.7975 cm²/sec at 293°K. The precision is 1.9% and the deviation of the average from a currently accepted value[8] is 4.7%.

While the method has not been entirely refined, it shows a number of potentially interesting advantages. If the influence of the detector volume and finite sample size on peak spreading can be eliminated, the data necessary for one determination of the diffusion coefficient should require less than a minute to obtain. Several new types of detectors,[9,10] only some of them measuring thermal conductivity,[10] can be applied to this end. A trace of the minor component is all that is required for analysis. While we used a sample size of 0.04 cm³ or about 10^{-6} moles, ionization detectors are capable of detecting much smaller samples of some substances, and smaller tube diameters can be used, also, to reduce sample size. The basic apparatus for these measurements is readily available, including a choice of detector, and injection device, and a carefully thermostated cabinet. The possibility exists also of extending this method to the rapid measurement of diffusion coefficients in liquids.

This investigation was supported by a research grant from the National Science Foundation.

[1] L. E. Boardman and N. E. Wild, Proc. Roy. Soc. (London) **A162,** 511 (1932).
[2] C. A. Boyd, N. Stein, V. Steingrimsson, and W. F. Rumpel, J. Chem. Phys. **19,** 548 (1951).
[3] R. E. Walker and A. A. Westenberg, J. Chem. Phys. **29,** 1139 (1958); **32,** 1314 (1960).
[4] Sir Geoffrey Taylor, Proc. Roy. Soc. (London) **A219,** 186 (1953).
[5] J. C. Giddings, J. Chromatography (to be published).
[6] J. C. Giddings, S. L. Seager, L. R. Stucki, and G. H. Stewart, Anal. Chem. **32,** 867 (1960).
[7] J. C. Giddings, J. Chromatography **3,** 520 (1960).
[8] R. C. Reid and T. K. Sherwood, *Properties of Gases and Liquids* (McGraw-Hill Book Company, Inc., New York, 1958), pp. 273–277.
[9] G. R. Primavesi, G. F. Oldham, and R. J. Thomson in *Gas Chromatography* 1958, edited by D. H. Desty (Butterworth's Scientific Publications, Ltd., London, 1958), p. 165.
[10] N. Sasaki, K. Tominago, and M. Aoyagi, Nature **309,** 186 (1960).

Preparation and Crystal Structures of RuC and OsC

CHARLES P. KEMPTER AND M. R. NADLER

Los Alamos Scientific Laboratory, University of California, Los Alamos, New Mexico

(Received July 14, 1960)

IN a previous study[1] of solidus temperatures in refractory metal-carbon systems, we observed the appearance of weak unidentified lines in the Ru—C and Os—C systems. A thorough literature survey indicated that no carbide of osmium had been reported and that no carbide of ruthenium had been characterized. McLennan, Allen, and Wilhelm[2] measured the electrical conductivity of two "ruthenium carbide" specimens prepared by fusing mixtures of "Ru_2O_3" and graphite. The authors assumed compound formation.

Proceeding on the premise that the unidentified lines were metal carbide lines, equimolar metal-graphite mixtures were prepared and pressed into $\frac{1}{16}$-in.-diam pellets in a steel die. The pellets were prepared for firing by insertion in a $\frac{1}{16}$-in.-diam hole drilled axially in a $\frac{1}{2}$-in.-diam spectro-grade graphite rod, $\frac{3}{4}$ in. long. A $\frac{1}{16}$-in-diam graphite rod was placed over the top of the pellets, and the assembly was inductively heated in one atm of helium. The temperature was read optically in a 0.040-in.-diam hole drilled in the top of the graphite cylinder. The Ru—C pellets were heated at 2200, 2500, and 3000°C for 15, 60, and 3 min, respectively. Examination of the reacted mixtures by x-ray powder diffraction revealed ruthenium, graphite, and a hexagonal phase isomorphous with WC. The 2200°C sample contained very little of this phase. The Os—C pellets

were heated at 2800°C for 15 min and at 3000°C for 3 min. The first sample showed osmium, graphite, and a hexagonal phase isomorphous with WC; the second sample showed only osmium and graphite. Since unreacted metal was found to be the major phase in all five specimens, additional specimens were made up using 1:3 and 1:10 metal:graphite molar ratios. The best yields of the hexagonal WC-type phases were obtained using the latter ratio and heating for 2600°C for 4 hr. Therefore, larger pellets ($\frac{1}{2}$-in.-diam) of Ru: 10C were prepared and heated in the same manner at 2600°C for 4 hr, and 2600°C for 8 hr. In the first case, a hard area of the hexagonal phase formed at the bottom surface of the pellet, but in the second case there was no evidence of the presence of a carbide. It would appear that the best preparative method should involve formation under pressure to prevent vaporization and/or dissociation of the carbide.

TABLE I. X-ray powder data for RuC and OsC.

	RuC		OsC	
hkl	*d*, A	I_{rel}	*d*, A	I_{rel}
001	2.83	60	2.81	60
100	2.52	90	2.50	65
101	1.882	95	1.875	70
110	1.453	30	1.450	40
002	1.418	10	1.416	40
111	1.293	60	1.291	50
200	1.258	30	1.257	30
102	1.236	50	1.235	40
201	1.152	30	1.152	30
112	1.015	40	1.015	50
210	0.9510	40	0.9510	50
202	0.9462	10	0.9456	20
003	0.9418	40	0.9413	50
211	0.9019	100	0.9019	100

X-ray powder-diffraction data for RuC and OsC are shown in Table I. The patterns were taken at 25°C with a 114.59 mm Debye-Scherrer camera using Fe filtered Co radiation. The materials were also examined at 25°C in a 120-mm, symmetrical-back reflection-focusing camera. The lattice constants and their standard deviations were determined on an IBM 704 computer,[3] assuming systematic errors in $\Delta a_0/a_0$ directly proportional to $\phi \tan\phi$, where ϕ is the complement of the Bragg angle. The values obtained were $a_0=2.90775\pm0.00004$ A, $c_0=2.82176\pm0.00010$ A, and $c_0/a_0=0.9704$ for RuC; and $a_0=2.90752\pm0.00007$ A, $c_0=2.82166\pm0.00019$ A, and $c_0/a_0=0.9705$ for OsC. The standard deviations express the precision, not the accuracy of the measurement. Correcting for refraction in iron-filtered cobalt radiation, these values become $a_0=2.90785$ A and $c_0=2.82186$ A for RuC and $a_0=2.90769$ A and $c_0=2.82182$ A for OsC, with the same axial ratios. For 1 Mc per unit cell, the theoretical densities at 25°C are 9.088 g/cc and 16.25 g/cc, respectively. The microstructures of the two carbides were examined by C. G. Hoffman of this Laboratory, who found the microhardnesses (DPH) to be 3480 and 2000 kg/mm², respectively, using a 100-g load. Therefore, RuC is the hardest known metallic carbide.

Spectrographic analyses of the Ru (American Platinum Works) showed 0.001–0.01% Mg, Si, and Mn as the major impurities, and of the Os (J. A. Samuel Company), 0.001–0.01% Al, Si, K, Fe, Pd, Ir, Pt, and Au.

The authors thank O. R. Simi and J. A. Mariner for the spectrographic analyses, Miss D. L. Cooper for the IBM 704 fits, L. A. Wahman for the x-ray-film reading, and C. G. Hoffman for the metallographic examinations.

[1] M. R. Nadler and C. P. Kempter, J. Phys. Chem. (to be published).
[2] J. C. McLennan, J. F. Allen, and J. O. Wilhelm, Trans. Roy. Soc. Can. **25** (3), 13 (1931).
[3] R. E. Vogel and C. P. Kempter, Los Alamos Scientific Laboratory Rept. LA-2317 (April, 1959).

Proton Resonance in Diphenyl Picryl Hydrazyl*

M. E. ANDERSON AND G. E. PAKE
Department of Physics, Stanford University, Stanford, California
AND
T. R. TUTTLE, JR.
Department of Chemistry, Stanford University, Stanford, California

(Received July 7, 1960)

ATTEMPTS to resolve different Knight shifts associated with various proton-hyperfine couplings in crystalline α,α-diphenyl-β-picryl hydrazyl (DPPH) have been reported,[1,2] but even at 77°K the experiments have provided only a hint of resolution in the proton resonance, leaving the number of shifted components and the magnitude of their shifts in doubt. This note reports experiments in the temperature range between 4.2°K and 1.4°K, in which a number of components are clearly resolved and the $1/T$ dependence of these shifts is clearly exhibited. In addition, the first of a series of deuterium-substitution experiments has permitted explicit identification of one of the shifted components.

Figure 1(a) presents the 4.2°K proton resonance absorption spectrum of a polycrystalline sample of the 1:1 DPPH-benzene complex[3] as measured at 22.8 Mc. The large central component is principally due to the benzene protons present in the crystal as has been shown by recrystallizing the sample in hexadeuterobenzene [Fig. 1(b)]. Diamagnetic impurities are probably responsible for the residual central com-

ponent visible in Fig. 1(b). Both upfield- and downfield-shifted components are evident, providing a striking illustration of the existence of spin densities of both signs at proton sites in the molcules.[4]

Deuterium substitution for the protons in the DPPH picryl group has been carried out by one of us (TRT), and the resulting spectrum [Fig. 1(c)] shows a sharp reduction in intensity of the component with the largest downfield shift (this identification has been further confirmed by another deuteration involving all DPPH protons *except* the pair on the picryl group.) Coupled with the fact that both upfield and downfield shifts are actually observed, this explicit identification lends credence, at least in a qualitative sense, to the theoretical treatment of Gutoswky, *et al.*[1] In a broader sense these data are the confirmation of ideas[4] which have grown out of the calculation on triphenyl methyl by Brovetto and Ferroni.[5]

Although the spectrum of Fig. 1 is moderately well resolved, interpretation of the position of each resonance peak is open to some doubt because of the possible existence of anisotropic hyperfine coupling which could lead to asymmetric line shapes for our polycrystalline sample. Preliminary experiments at 4.2°K on a single crystal of DPPH-benzene in various positions about an arbitrary rotation axis exhibited up to 15% anisotropy for those lines which could be followed through rotation steps of 10 deg. The single-crystal spectrum is highly complex, containing as many as 15 resolvable peaks in certain orientations, and not all lines can be followed through such large rotation steps. Nevertheless, since both the single-crystal experiment and theoretical conjecture[6] suggest that the isotropic contact term dominates the hyperfine interaction, it may be useful to estimate isotropic hyperfine coupling constants associated with the various resonance peaks

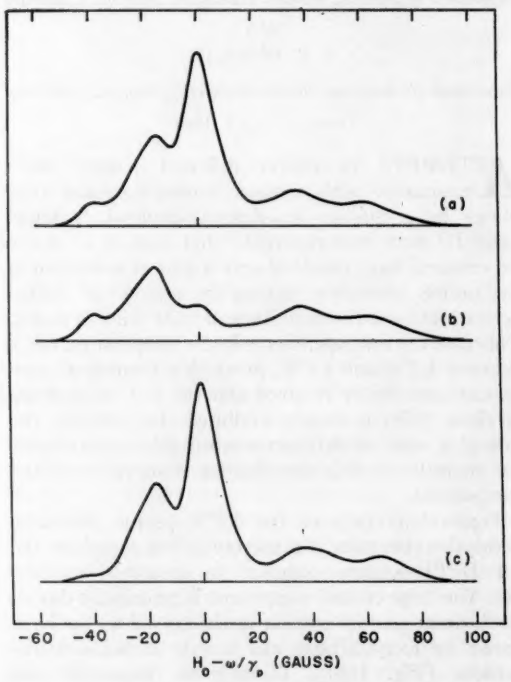

FIG. 1.

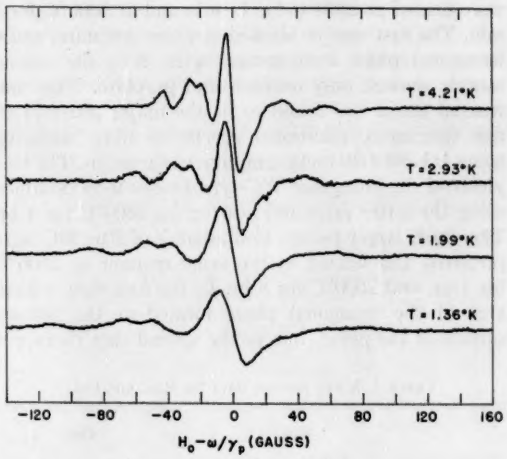

FIG. 2.

TABLE I. Experimental proton resonance shifts and hyperfine coupling constants for DPPH at 22.8 Mc and 4.2°K.

Δ_H	a_H
−39 gauss	+1.4 gauss
−17	+0.6
+37	−1.3
+62	−2.2

observed in the polycrystalline sample. Supposing these shifts to arise from the exchange-narrowed hyperfine interaction with the average polarization of the electron spin obeying Boltzmann statistics, it is readily shown that the shift is

$$\Delta H = H_0 - (\omega/\gamma_p) = -a_H(\gamma_e/\gamma_p)(\gamma_e\hbar/4kT)(\omega/\gamma_p), \quad (1)$$

where a_H is the electron resonance splitting measured in gauss and the other symbols have their usual significance. Table I is constructed from Fig. 1(b) using Eq. (1). Values of a_H deduced from Eq. 1 are generally somewhat smaller than those predicted theoretically.[1] They are not inconsistent with the EPR proton hyperfine splitting of DPPH in solution recently observed by Deguchi.[7]

Figure 2 shows the derivative of the DPPH spectrum at several temperatures. The shifts have a $1/T$

dependence within the limit of observation, giving weight to the assumptions implicit in Eq. (1).

* Supported in part by the U. S. Air Force through the Air Force Office of Scientific Research.

[1] H. S. Gutowsky, Hazime Kusumoto, T. H. Brown, and D. H. Anderson, J. Chem. Phys. **30**, 860 (1959).
[2] M. E. Anderson, T. R. Tuttle, Jr., and G. E. Pake, Bull. Am. Phys. Soc. **4**, 251 (1959).
[3] J. A. Lyons and W. F. Watson, J. Polymer Sci. **18**, 141 (1955).
[4] H. M. McConnell and D. B. Chesnut, J. Chem. Phys. **27**, 984 (1957); J. Chem. Phys. **28**, 107 (1958).
[5] P. Brovetto and S. Ferroni, Nuovo Cimento **5**, 142 (1957).
[6] T. H. Brown, D. H. Anderson, and H. S. Gutowsky, J. Chem. Phys. **33**, 720 (1960).
[7] Yasuo Deguchi, J. Chem. Phys. **32**, 1584 (1960).

NMR Analysis of CF_3CF_2CFICl: Example of an Unexpected Spin-Coupling Constant

L. M. Crapo and C. H. Sederholm

Department of Chemistry, University of California, Berkeley 4, California

(Received June 22, 1960)

An NMR analysis of CF_3CF_2CFICl yielded, upon examination at 56 Mecs, three distinct fluorine resonances. The CF group appeared at low field, separated from the CF_2 group by 2120 cps and from the CF_3 group by 114 cps. The three fluorines of the CF_3 group appear to be equivalent, whereas the two fluorines of the CF_2 group are nonequivalent.[1] Therefore, CF_3CF_2CFICl can be treated as an AB_3XY molecule.

The CF_2 group is a quartet, each member being further split into a doublet. This, in addition to the CF_3 part of the spectrum, implies that $J_{BX}=J_{BY}=0\pm0.3$ cps. Hence, this portion may be treated as the XY part of an AXY spectrum. Such a treatment yields $|J_{XY}|=270.4\pm0.5$ cps, $|J_{AX}|=14.6\pm0.1$ cps, $|J_{AY}|=13.4\pm0.1$ cps, and $\nu_X-\nu_Y=270.4\pm0.5$ cps, $\nu_X-\nu_A=2255\pm3$ cps.

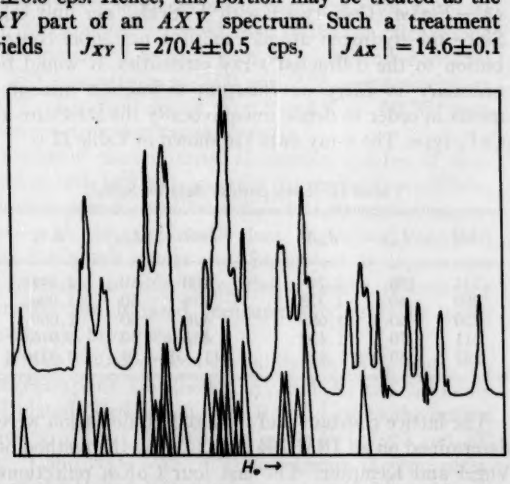

Fig. 1. Observed and calculated NMR fluorine spectrum of the —CFICl group in CF_3CF_2CFICl.

The spectrum of the CF_3 group is a doublet, each line being about 1 cps wide. Interpretation of this portion of the spectrum treating it as the B_3 part of an AB_3 group yields $|J_{AB}|=10.8\pm0.1$ cps.

With the above data, and assigning $\nu_B-\nu_A=114\pm0.5$ cps, the spectrum of the CF group was calculated by first-order perturbation theory, applying the perturbation $H'=J_{AX}I_A\cdot I_X+J_{AY}I_A\cdot I_Y$ to the exact solution for the AB_3 case. The observed and calculated spectra are compared in Fig. 1. Combination bands are not shown, but were observed at spectral positions predicted by the theoretical calculations. The close correlation supports our assignment of coupling constants. The additional lines in the observed spectrum in Fig. 1 were assigned to impurities in the sample. The sample was prepared by the gas-phase light-catalyzed reaction between $CFCl=CF_2$ and CF_3I, as outlined by Hazeldine.[2] This method of preparation yielded a very impure sample. Attempts at purification by fractional distillation were not totally successful. Therefore, the sample contained some impurities, including a sizable amount of $CFIClCF_2CFClCF_2CF_3$. The fluorines in these impurities would be expected to have absorption bands in the same regions as the sample. These were not troublesome in most areas of the spectrum as they were much smaller in intensity than the sample bands. However, in the portion of the spectrum recorded in Fig. 1, the absorption due to the compound under consideration is very small, and therefore the impurity bands appear nearly as large as the sample bands.

The nearly zero coupling constant between the CF_3 and CF_2 groups, $J(CF_3CF_2)$, prompted a search of the literature for other such cases. Saika and Gutowsky[3] reported $J(CF_3CF_2)=0$ in $(CF_3)_2NCF_2CF_3$. Van Dyke Tiers[4] implied that $J(CF_3CF_2)$ is very small in $CF_3CF_2CF_2H(D)$. Reilly[5] has reported a small coupling constant in CF_3CF_2COOH, $J(CF_3CF_2)=1.48$ cps.

The high-resolution spectrum of $CF_3CF_2CF_2COOH$ consists[6] of a triplet corresponding to the CF_3 group, a quartet corresponding to one CF_2 group, and a singlet corresponding to the other CF_2 group. To maintain consistency with the other cases presented here, we assert that $J(CF_3CF_2)\approx0$, and that the splitting is due to the $\alpha-CF_2$ group interacting with the CF_3 group.

The cause of these small coupling constants is not readily apparent. Their widespread occurrence implies that there is a more fundamental reason behind them than pure chance. Variation of the electron withdrawing power of the attached groups does not seem to enhance these small coupling constants, as can be seen from the cases sighted above. It is felt that the cause of this effect must be connected with the hindered rotation about the carbon-carbon bond. On the basis of the

above examples, we suggest that the coupling constant between the two groups of fluorines in the $—CF_2—CF_2—$ group is nearly zero if the minima in the potential energy as a function of rotation about the carbon-carbon bond correspond to the staggered positions and is nonzero otherwise. Further investigation of this hypothesis is now in progress.

[1] J. N. Shoolery and Bryce Crawford, Jr., J. Mol. Spectroscopy **1**, 270 (1957).
[2] R. N. Haszeldine and B. R. Steele, J. Chem. Soc. **1953**, 1592.
[3] A. Saika and H. S. Gutowsky, J. Am. Chem. Soc. **78**, 4818 (1956).
[4] George Van Dyke Tiers, J. Am. Chem. Soc. **79**, 5585 (1957).
[5] C. A. Reilly, J. Chem. Phys. **25**, 604 (1956).
[6] C. H. Sederholm (to be published).

Preparation and Properties of Scandium Dihydride

JOSEPH C. MCGUIRE AND CHARLES P. KEMPTER

Los Alamos Scientific Laboratory, University of California, Los Alamos, New Mexico

(Received July 14, 1960)

A THOROUGH literature search revealed no references to scandium hydrides. For the Y—H system, Lundin[1] has reported YH_2 (face-centered cubic, isotypic with CaF_2, $a=5.201$ A, $\rho=4.293$ g/cc) and YH_3 (hexagonal, $a=3.674$ A, $c=6.599$ A, $c/a=1.796$, $\rho=3.958$ g/cc). For the La—H system, Holley, *et al*[2] have reported LaH_2 (CaF_2—type, $a=5.667\pm0.001$ A, $\rho=5.14$ g/cc), and Stalinski[3] has reported LaH_3 (face-centered cubic, BiF_3-type, $a=5.60$ A).

The scandium used for this investigation was obtained from the St. Eloi Corporation; a spectrographic analysis showed 0.5% Al and 0.2% Y as the major metallic impurities. The hydrogen used in the reaction was purified by passage through a Deoxo unit, barium oxide, and hot uranium chips. The scandium was outgassed at 800°C in a silica tube heated by a resistance furnace. The tube was then cooled to room temperature and connected to a series of calibrated volumes containing hydrogen at slightly below atmospheric pressure. Pressures were indicated on a mercury monometer read by a cathetometer to the nearest 0.05 mm. The metal was heated slowly until reaction was indicated by a drop in the manometer reading. At 450°C reaction was observed, and the run was held at this temperature for 16 hr. The metal was then slowly cooled to room temperature to promote any additional metal-hydrogen reaction; none was observed. At this point, sufficient hydrogen had reacted to correspond to $ScH_{2.027}$. The possibility had been considered that a ScH_3, similar to YH_3, might be formed at lower temperatures; however, two repetitions of the process, yielded very little additional reaction. It is possible that ScH_3 is formed at higher hydrogen pressures.

The vapor pressure data for scandium dihydride are shown in Table I.

TABLE I. Vapor pressure data for ScH_2.

Temp. °C	p, mm Hg	Temp, °C	p, mm Hg
300	6.80	620	33.40
340	9.00	660	41.40
380	10.50	700	55.10
420	12.80	740	76.80
460	15.80	780	105.20
500	20.80	820	140.60
540	24.90	860	188.20
580	30.70	900	262.20

A van't Hoff plot ($\log p$ vs $1/T$, where $T=$°K) was made of these data. From 300 to about 650°C, the IBM 704 linear least-squares equation is $\log p=(2.788\pm0.069)-(1137\pm49)/T$, and from about 650° to 900°C, $\log p=(5.484\pm0.103)-(3632\pm107)/T$. If one assumes that the latter linear fit represents a two-phase ($Sc+ScH_2$) region, then the calculated enthalpy change for the absorption of 1 mole of gaseous hydrogen is $-16\,620\pm490$ cal. If one compares this value with corresponding thermodynamic data for the lanthanide dihydrides given by Gschneider,[4] this value seems low, and therefore the above assumption may not be realistic.

The silica reaction tube was transferred to an inert-atmosphere glove box, and this coarse gray powder crushed to pass through a 200-mesh screen. A -325 mesh specimen was taken for x-ray examination and sealed in a Lindemann glass capillary (using a hot platinum wire within the glove box). A Debye-Scherrer pattern was taken with iron-filtered cobalt radiation, and the ScH_2 lattice was found to be face-centered cubic. It is probable that the lattice has space group O_h^5-Fm3m (CaF_2-type) with 4 (ScH_2) per unit cell. Since the hydrogen atoms exhibit a negligible contribution to the diffracted x-ray intensities, it would be necessary to carry out neutron diffraction measurements in order to define unequivocally the structure as CaF_2-type. The x-ray data are shown in Table II.

TABLE II. X-ray powder data for ScH_2.

hkl	I_{rel}	d, A	hkl	I_{rel}	d, A
111	100	2.74	400	10	1.194
200	40	2.378	331	50	1.096
220	60	1.685	420	50	1.069
311	70	1.439	422	50	0.9763
222	30	1.378	511, 333	50	0.9210

The lattice constant and its standard deviation were determined on an IBM 704 computer by the method of Vogel and Kempter.[5] The last four $CoK\alpha_1$ reflections were used and all systematic errors in $\Delta a_0/a_0$ assumed directly proportional to the Nelson-Riley function,

after correction for shrinkage. The lattice constant obtained was $a_0=4.78309\pm0.00047$ A at 25°C. Correcting for refraction this becomes $a_0=4.78315$ A. For 4 (ScH_2) per unit cell, the theoretical density is 2.851 g/cc, and the Sc—8H bond distance is 2.0712 A. Subtracting the metallic radius of α—Sc for Sc—8 Sc (1.596 A), one obtains 0.475 A for the tetrahedral radius of hydrogen. ScH_2 contains 7.31×10^{22} hydrogen atoms/cm³, and therefore may be useful as a high-temperature neutron moderator.

The authors thank O. R. Simi for the spectrographic analysis, C. I. Fairchild, D. D. Bowdish, and A. D. Zielinski for preparative help, L. A. Wahman for x-ray film reading, and Dorothy L. Cooper for IBM 704 fits.

[1] C. E. Lundin, "Rare Earth Metal Phase Diagrams," presented at ASM Rare Earth Symposium, Chicago (November, 1959).
[2] C. E. Holley, Jr., R. N. R. Mulford, F. H. Ellinger, W. C. Koehler, and W. H. Zachariasen, J. Phys. Chem. **59**, 1226 (1955).
[3] B. Stalinski, Met. Abstr. **23**, 894 (1956).
[4] K. A. Gschneidner, Jr., *Rare Earth Alloys* (to be published).
[5] R. E. Vogel and C. P. Kempter, Los Alamos Scientific Laboratory, Report LA-2317 (April, 1959).

Equilibrium Constant for Isotope Exchange in Ammonia from Infrared Spectra*

LLEWELLYN H. JONES

Los Alamos Scientific Laboratory, University of California, Los Alamos, New Mexico

(Received July 5, 1960)

ALL isotopic-exchange equilibria among the H and D ammonias can be derived from $K_1(NH_3+NHD_2=2NH_2D)$ and $K_2(ND_3+NH_2D=2NHD_2)$.

At high temperature, $K_1=K_2=3$, as determined by the symmetry numbers of the various species. Kimball and Stockmayer[1] reported that statistical calculations from spectroscopic data give $K_1=2.94$ and $K_2=2.90$ at 25°C, increasing to 3.00 and 2.98, respectively, at 300°C. Kemball[2] found $K_1=K_2=2.9$ at 248°C from mass-spectrometer measurements.

Stedman[3] used infrared absorption spectra of mixtures of NH_3 and ND_3 to study the exchange equilibria. His data give $K_1=0.62$ and $K_2=1.31$, in gross disagreement with the calculated values. Bigeleisen[4] suggested that Stedman's results must be subject to large errors. As outlined in this note, the apparent discrepancy between the infrared measurements and the other results has been resolved.

If the initial and the equilibrium NH_3 and ND_3 concentrations are known, K_1 and K_2 can be easily calculated. Stedman applied Beer's Law to the optical density of the Q branches of ν_2 for NH_3 (967 and 932 cm^{-1}) and ND_3 (745 cm^{-1}) to measure the concentrations of NH_3 and ND_3 in mixtures prepared from known amounts of pure NH_3 and ND_3. This procedure appeared justified, as he previously had determined that the NH_3 and ND_3 peaks he used obeyed Beer's Law in the pressure range of interest (at constant path length). However, as discussed below, this apparent obedience to Beer's Law is a result of mutual cancellation of two marked deviations from the Lambert-Beer Law.

There are two effects we have observed which clarify the situation: (A) Slit width effect at constant pressure: If the peaks in question did obey the Lambert-Beer Law, the absorption coefficient $\alpha=OD/Pt$ should be a constant as path length t is varied at constant pressure P. However, in the pure species at constant pressure of 15 mm, α for the Q branches increased nearly linearly by a factor of 2.2 for NH_3 and 1.7 for ND_3 as t was decreased from 10 cm to 1.25 cm. Thus, by working at constant pressure to eliminate variation in pressure broadening, we are confronted with serious deviation from the Lambert Law. (B) Pressure broadening: A 10-cm cell was filled with 15-mms pressure of NH_3. It was found that with this constant partial pressure of ammonia at constant path length, α for the NH_3 Q branches doubled when about 45 mm of N_2 (or H_2) was added. More foreign gas increased α steadily until it reached a maximum (another doubling) at about 1 atm of N_2 (or H_2). A similar effect is noted for ND_3, though it is not as large.

It is easy to show that both of these effects are to be expected for absorption bands much narrower than the effective spectrometer slit width. The apparent obedience to Beer's Law when the pressure of pure NH_3 (or ND_3) is varied at constant path length evidently results from a fortuitous mutual cancellation of effects (A) and (B).

To avoid the above difficulties, we used *apparent absorption coefficients determined on path lengths of the pure species at the same total pressure as in the exchange experiment and giving the same optical density for the peak measured as in the experiment.* For example, in a mixture of NH_3, ND_3, NH_2D, and NHD_2 at a *total ammonia pressure of* P_t (and no foreign gas) the concentration of NH_3 was determined as follows. The optical density of the Q branch of ν_2 was recorded from cells of four different path lengths, ranging from 1.25 to 10 cm, all containing pure NH_3 *at fixed pressure* P_t. This optical density then was plotted vs α_{NH_3}. The four points gave a smooth curve. Then, in our experiment with mixed species at the same total pressure P_t, we observed the optical density of the NH_3 band, read α_{NH_3} from the $OD-\alpha_{NH_3}$ plot, and calculated the partial pressure of NH_3. The ND_3 was determined in the same way.

Using the above method on 50-50 mixtures of NH_3 and ND_3, we arrived at values for K_1 and K_2 of 3 ± 0.5. Part of the uncertainty arises because the NH_2D and NHD_2 P and R branches overlap the NH_3 and ND_3 Q branches to some extent, and this must be

allowed for. Also, the equilibrium constants are quite sensitive to small errors in the NH_3 and ND_3 concentrations. No doubt a large number of experiments could reduce the uncertainty considerably by sheer force of statistics. However, it is doubtful that the result would be as accurate as the values calculated by Kimball and Stockmayer.[1]

Infrared spectra can be used successfully to analyze for the various isotopic ammonias, provided one uses the proper "apparent absorption coefficient," as discussed previously. For the equilibrium constants K_1 and K_2 at room temperature, one can feel quite secure using the calculated values of about 2.9. For the analogous constants in NH_3—NT_3 or ND_3—NT_3 equilibria one could also feel secure using 2.9.

* This work was sponsored by the U. S. Atomic Energy Commission.

[1] G. E. Kimball and W. H. Stockmayer, SAM Rept. 100X_4-1657, Oct. 14, 1942, quoted in "Physical Properties of Heavy Water" by Kirschenbaum, NNES III-4A.
[2] C. Kemball, Trans. Faraday Soc. **48**, 254 (1952).
[3] D. F. Stedman, J. Chem. Phys. **20**, 718 (1952).
[4] J. Bigeleisen, J. Chem. Phys. **20**, 1495 (1952).

Absorption Spectra of Photo-Oxide of Mesonaphthodianthrene

HARUO KURODA*

Division of Pure Chemistry, National Research Council, Ottawa, Canada

(Received August 4, 1960)

IN the previous note[1] we have shown that the electrical conductivity of an evaporated film of mesonaphthodianthrene increases remarkably as a result of oxygen adsorption. This suggests that a charge transfer is taking place between adsorbed oxygen molecules and the surface of the hydrocarbon film. This is in accord with the evidence found by Matsunaga,[2] using the electron spin resonance of mesonaphthodianthrene powder, that new spin centers are created when the powder is placed in contact with air. The change of the electrical conductivity in oxygen is a slow process. It was observed that this change can be accelerated if the film is illuminated with visible light, which suggests that some kind of photooxidation is taking place on the surface of the film. Accordingly, the reaction between oxygen and mesonaphthodianthrene in benzene solution was investigated by observing the changes in absorption spectra.

The hydrocarbon was purified by vacuum sublimation and sealed in a glass tube in vacuum. Benzene was distilled twice under an atmosphere of nitrogen to remove oxygen. The solution was made by breaking under benzene the glass tube containing the hydrocarbon powder. The resulting solution was divided into two parts; one part was kept in nitrogen, and oxygen was bubbled into the other part. Both solutions were illuminated with visible light. Small quantities of the solutions were taken out from time to time to determine the changes of their absorption spectras. Absorption spectra were measured with a Cary Recording Quartz Spectrometer, model 11M.

The absorption spectra of the oxygen-containing solution changed gradually with time, while that of the oxygen-free solution remained unchanged. The results are shown in Fig. 1. Curve (1) is the spectrum of the oxygen-free solution. The three peaks observed in the wavelength region of 500–700 mμ, have been attributed to the p band by Clar.[3] The intensity of these peaks decreases with time when the oxygen-containing solution is illuminated with light. At the same time, the absorption intensity increases in the region where the wavelength is shorter than 400 mμ. It seems obvious that this change is due to a reaction with oxygen, since it is observed only with the oxygen-containing solution.

Using the molecular orbital method, Pullman[4] has shown that the free valency of the two mesopositions of the mesonaphthodianthrene molecule are very high. Hence, we should expect high reactivity toward oxygen. On the other hand, however, an oxygen molecule cannot bridge between the two reactive positions, since they are too far apart. This situation is unfavorable for the formation of a stable oxygen addition compound. Savage[5] attempted to isolate the photo-oxide, but was unable to do so. Evidently the oxygen molecule is combined loosely with mesonaphthodianthrene.

The absorption spectrum of the benzene solution of mesonaphthodianthrene also changes remarkably when a small amount of iodine is added to it. In this case again, the p band disappears as shown in Fig. 1 [curve (4)]. Iodine is known to form charge-transfer complexes with various polycyclic aromatic hydrocarbons.[6] Thus, the change in the absorption spectra of mesonaphthodianthrene caused by the addition of iodine is almost

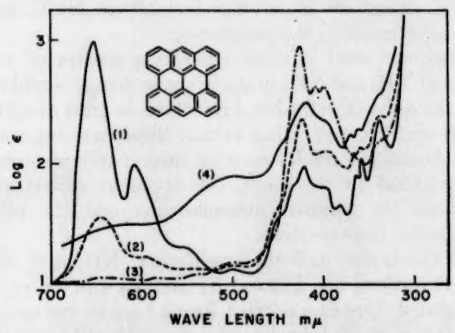

FIG. 1. Absorption spectra of mesonaphthodianthrene. (1) oxygen-free solution; (2) (3) oxygen-containing solution after illumination for ½ hr and 2 hr, respectively; (4) iodine complex (saturated solution).

certainly due to the formation of a charge-transfer complex.

The similarity found between the change in spectra resulting from reactions with oxygen and iodine, respectively, suggests that the interaction between oxygen and mesonaphthodianthrene is also due to a charge-transfer force.

I wish to thank Dr. E. A. Flood for his interest and encouragement.

* National Research Council Postdoctorate Fellow. Present address: Department of Chemistry, Faculty of Science, University of Tokyo, Tokyo, Japan.

[1] H. Kuroda and E. A. Flood, J. Chem. Phys. **33**, 952 (1960).
[2] Y. Matsunaga, Can. J. Chem. **38**, 323 (1960).
[3] E. Clar, Chem. Ber. **82**, 55 (1949).
[4] B. Pullman, Proc. Third Carbon Conference, (1958), p. 3.
[5] M. G. Sauvage, Compt. rend. **225**, 247 (1947).
[6] R. S. Mulliken, J. Am. Chem. Soc. **72**, 600 (1950); L. T. Andrews, Chem. Rev. **54**, 713 (1956).

The Diffusion Theory of Chemical Reaction

J. L. Wood

Department of Chemistry, Imperial College, London, S.W.7., England

(Received March 14, 1960)

Montroll and Shuler[1] have obtained an exact equation for the relaxation of a set of harmonic oscillators contained in a constant-temperature heat bath. If the process of chemical reaction is represented by a model in which all oscillators reaching the Nth level are removed from the assembly, i.e., as "product" of the reaction, they show that after a sufficient time τ the number of oscillators in the assembly falls by the usual exponential decay law, with a rate constant

$$K=[\sum_{n=0}^{N-1} t_{n,N}\chi_n(\tau)]/[\sum_{n=0}^{N-1}\chi_n(\tau)],$$

where $t_{n,N}$ is the induced transition probability for a change from the nth to the Nth level, and $\chi_n(\tau)$ is the number of oscillators in this level at time τ.

This result may be compared with that obtained from the classical kinetic theory of liquids in the following way.

If the oscillators are immersed in a liquid, the induced transition probability $t_{n,N}$ is determined by the component of frequency $\nu_0(h\nu_0=E_N-E_n)$ in the random fluctuating force $\mathfrak{F}$ acting on the oscillator. With the use of a result of Rice,[2] the relation is

$$t_{nN}=A_{nN}\int_0^\infty \langle \mathfrak{F}(t)\mathfrak{F}(t+\tau)\rangle_{Av}\cos 2\pi\nu_0\tau d\tau, \quad (1)$$

where A_{nN} is a parameter independent of the statistical characteristics of the fluctuating force and determined by the form of the interaction between the oscillator and the liquid. $\langle\ \rangle_{Av}$ indicates an average over the oscillators. The fluctuating force $\mathfrak{F}$ is related to the friction constant by[3]

$$\beta=\lim_{\tau_1\to\infty}(kT)^{-1}\int_0^{\tau_1}\langle \mathfrak{F}(t)\mathfrak{F}(t+\tau)\rangle_{Av}d\tau. \quad (2)$$

If a white spectrum for $\mathfrak{F}$ is assumed,[4] the spectral density is $4\beta kT$, and $t_{nN}=4A_{nN}\beta kT$. Consequently, Montroll and Shuler's method leads to

$$k=[4\beta kT\sum_{n=0}^{N-1}A_{nN}\chi_n(\tau)]/[\sum_{n=0}^{N-1}\chi_n(\tau)]. \quad (3)$$

Approaching the problem from the classical kinetic theory of liquids, the reaction may be represented by a steady-state flow in momentum space, systems considered to have "reacted" when they attain a momentum mu_c. When an equilibrium exists in coordinate space the Planck-Fokker equation reduces to

$$(\partial W/\partial t)=\mathrm{div}_u\{\beta(Wu)+(\beta kT/m)\ \mathrm{grad}_u W\}, \quad (4)$$

and the steady-state flow j in momentum space is

$$j=\beta(Wu)+(\beta kT/m)\ \mathrm{grad}_u W,\ =\ \text{constant}. \quad (5)$$

The symbols are as used by Chandrasekhar.[5] From this equation the rate constant obtained is

$$k=\beta(2kT/\pi m)^{\frac{1}{2}}\left(\int_{u=0}^{u=u_c}\exp(mu^2/2kT)du\right)^{-1}, \quad (6)$$

which shows exactly the same dependence on β as (3).

Thus a model in which chemical reaction is represented by a flow in energy or momentum space gives a rate constant directly proportional to the friction constant β, whether one starts from a quantum or classical viewpoint.

However, in the treatment of chemical reaction by the diffusion theory,[6-8] the model that has been used represents the reaction by a flow in position space, and in that case, when β is large, the rate obtained is *inversely* proportional to β, and when β is small, it is independent of β.

I feel that in most cases the rate is determined by the acquisition of energy, and that the first model is the better one.

[1] E. W. Montroll and K. E. Shuler, *The Application of the Theory of Stochastic Processes to Chemical Kinetics*, (University of Maryland Press, 1957).
[2] S. O. Rice, reprinted in *Noise and Stochastic Processes* (Dover Publications, New York, 1954), p. 133.
[3] J. G. Kirkwood, J. Chem. Phys. **14**, 180, 1946.
[4] R. Eisenschitz, *Statistical Theory of Irreversible Processes* (Oxford University Press, New York, 1958), p. 68.
[5] S. Chandrasekhar, Revs. Modern Physics **15**, 1, 1943.
[6] H. A. Kramers, Physica **7**, 248, 1940.
[7] H. C. Brinkman, Physica **22**, 29, 149, 1956.
[8] J. L. Wood and A. Suddaby, Trans. Faraday Soc. **53**, 1437, 1957.

Paramagnetic Studies of Radiation Damage in Silica Gel

HAROLD W. KOHN

Oak Ridge National Laboratory, Oak Ridge, Tennessee*

(Received July 5, 1960)

THE effects of penetrating radiations on solids are most readily noted by changes in physical characteristics such as color, hardness, magnetic properties, electrical conductivity, dielectric properties, and crystallinity.[1] Such observations are not always feasible or even possible in studies of gels, which present special problems because of their lack of crystallinity and high state of subdivision. Hence, the PMR spectrometer is a useful tool for studying radiation damage in gels. We have now recorded, in addition to the purple color center previously treated in irradiated silica gel,[2] several paramagnetic resonances and a new color center.

Irradiations were carried out in a Co^{60} γ source of about 700 curies strength. Paramagnetic resonance measurements were made using a simple paramagnetic resonance spectrometer with a rectangular transmission cavity operating in the TE_{101} mode with direct oscilloscope presentation of the spectrum. Changes in the strength of the resonance were estimated from signal-to-noise ratios. Numbers of centers were estimated by comparison with a diphenyl picryl hydrazyl crystal. The measurements were made by Henry Zeldes of this Laboratory.

At the ambient irradiation temperatures of $\sim$50°C, gamma or reactor irradiation of silica gel samples previously evacuated at 500°C or above produces a very sharp paramagnetic resonance at a spectroscopic splitting factor of $g=2.0005+0.0005$. This paramagnetic resonance is only a few (best estimate, 1.5–2) gauss wide, displays some g anisotropy seen as a slight shoulder on the low-field side, is easily saturated at low power, and is not greatly changed by cooling to −196°C. Samples of differing aluminum content (0.001–0.1%) have not shown correspondingly different intensities of this paramagnetic resonance. The physical characteristics of this line in silica gel are similar to those of two resonances induced in quartz and fused silica.[3] The maximum radiation yield for production of this line is roughly 0.1 center/100 ev absorbed.

Under ordinary conditions, the line is stable for months at room temperature, but it can be destroyed by heating to 250°C, by irradiating with ultraviolet light, or by adding O_2, Hg vapor, or H_2O.[4] The addition of hydrogen to irradiated samples does not destroy the line, but makes it more susceptible to annealing. In such samples most of the resonance disappears after 6 hr at 75°C.

Irradiation of degassed silica gels at −196°C produces a second, somewhat broader line immediately on the low-field side of the first line. This line could not be saturated with microwave power and, as long as the sample is kept cold, is unaffected by added gases such as O_2, H_2, and N_2. Brief warming of the sample destroys this second line. Addition of oxygen to gels irradiated at −196°C causes the slow appearance of an orange color, but leaves the paramagnetic resonance spectrum unaffected. If, however, oxygen is present during the low-temperature irradiation, both a marked reddish-orange color and a third, very strong, broad resonance at $g=2.0061\pm0.001$ are developed. The radiation yield G is very roughly 0.3 centers/100 ev absorbed. Brief warming of the sample will cause the color to disappear, but the resonance remains unless more extensive annealing, such as removal of the sample from the nitrogen bath for 3–5 min, is used. Once annealed, this line cannot be produced by recooling. Samples irradiated in the presence of nitrogen have a faint orange cast, but show no resonances different from those irradiated *in vacuo*. Samples irradiated in the presence of hydrogen show the two-line spectrum characteristic of those irradiated *in vacuo* plus the resonances characteristic of atomic hydrogen.

The sharp resonance at $g=2.0005$ probably arises from an electron trapped at an oxygen vacancy, either at the surface or in the lattice.[3] Its disappearance upon oxygen adsorption at 25°C substantiates this picture, and strengthens the postulate of a surface rather than a lattice defect. From its manner of formation, the reddish-orange color appears to be due to the reaction of oxygen (at −196°C), with defects produced in the gel by radiation which are not observable by the PMR spectrometer. The very broad resonance at $g=2.0061$ appears to be a radiolysis product of a condensed oxygen phase stabilized by adsorption on the gel at −196°C.

* Operated by the Union Carbide Corporation for the U. S. Atomic Energy Commission.

[1] G. J. Dienes and G. H. Vineyard, *Radiation Effects in Solids* (Interscience Publishers, Inc., New York, 1957).

[2] H. W. Kohn, Nature **184**, 630 (1959).

[3] R. A. Weeks and C. M. Nelson, J. Am. Ceram. Soc. (to be published).

[4] Samples degassed at 300° or less show no resonance.

Optical Transparency and Resistance to Flash Heating*

W. F. LIBBY

Department of Chemistry, University of California, Los Angeles

(Received April 14, 1960)

OPTICAL transparency when combined with low thermal conductivity, as is the case for silica or clear plastics, allows very high-temperature gradients to be maintained. Thus, the surfaces of such solids can be very hot while the bulk solid a short distance away

is unperturbed. In this way high-temperature evaporation, which consumes more energy by breaking chemical bonds to form smaller molecules, radicals and even atoms, becomes possible, so heats of vaporization rivaling those of the highest-boiling solids can be achieved.

Of course, with optical transparency goes low emission efficiency, so the radiation heat sink is reduced in importance for these materials. This reduction in cooling power can be compensated, however, by the evaporative cooling. In more detail, one would expect that the vapor generated at the surface of such a solid would have a composition corresponding to its temperature. Thus, close to the surface of an organic plastic, the monomer probably would predominate, while farther out the monomer would be broken into radicals and atoms, some of which might be carried away in the air and thus serve as a heat sink.

In contrast, in the case of an opaque body such as graphite the heat spreads rapidly throughout the mass, destroying the system by spalling due to thermal stress. The hot surface skin of a nonconductive optically transparent solid is not thick enough to spall even though the thermal gradient is very large.

It seems likely that applications of these principles can be made in the ballistic-missile nose-cone problem[1(a),(b)] and in the use of plastic paints to resist flash heating.[2] According to these principles the surface underlying the plastic or silica layer should have a mirror finish to reflect the light, and some attention should be paid in design to the matter of optics in order to avoid trapping of the light.

* This research was supported by the United States Air Force through the Air Force Office of Scientific Research of the Air Research and Development Command.

[1] (a) M. C. Adams and E. Scala, "The Interaction of High Temperature Air with Materials During Re-entry," Proceedings of an International Symposium on High Temperature Technology, arranged by Stanford Research Institute, Menlo Park, California (McGraw-Hill Book Company, Inc., New York, 1960), pp. 54–60.
(b) M. C. Adams, Jet Propulsion **29**, 625 (1959).

[2] "New Plastic Coat Shrugs off Heat," Chem. Eng. News **38**, 54 (1960).

Satellite Lines in Paramagnetic Resonance Spectra

A. VAN ROGGEN

Polychemicals Department, E. I. du Pont de Nemours & Company, Du Pont Experimental Station, Wilmington, Delaware

(Received June 22, 1960)

THE paramagnetic resonance (PMR) spectrum of *p*-benzosemiquinone[1–3] in dilute solution shows hyperfine structure (hfs) resulting from coupling of the unpaired electron spin to the nuclear spins of the four equivalent protons in the free radical. The five lines are well resolved, since the spacing (6.64 Mc sec^{-1}) is much larger than the linewidth (<0.2 Mc sec^{-1}). The line width in PMR spectra is dependent on instrumental factors and on solvent and temperature.[4] The effect of instrumental factors was eliminated by using homogeneous magnetic fields, low microwave power, and small modulation amplitudes. At room temperature, better resolution was obtained in 2-methoxyethanol than in ethanol. Each of the spectral lines was found to have two small satellite lines displaced symmetrically from the main line. These satellites are always found under conditions of high resolution and sensitivity, independent of the sample source. Since the satellites are always present in spectra from pure samples of different origin and have a g factor identical to that of the main free radical, they appear to be inherent in the spectrum. Impurity lines have been observed in other, less pure samples, but these lines have a different g factor and vary with solution concentration. The satellite lines are interpreted as a 10-line spectrum from *p*-benzosemiquinone in which one C^{12} isotope is replaced by C^{13}. The 10 lines arise from a proton quintet splitting ($a_1=6.64$ Mc sec^{-1}), identical to that of the main quintet, and from an additional doublet splitting ($a_2=1.54$ Mc sec^{-1}) from C^{13}. Additional lines are expected from molecules with two or more C^{13} nuclei. The latter molecules are present in concentrations two orders of magnitude lower than those with only one C^{13}, and thus give hfs lines indetectably weak.

Consider molecules with one C^{13} nucleus. If the hfs splitting constant is dependent on ring position, two pairs of satellite lines can arise, one pair from C^{13} in position 1 or 4, the other pair from C^{13} in position 2, 3, 5, or 6. The amplitude ratio of satellite line to main line will be 1.1 and 2.2%, respectively, for the two pairs. However, when the two splitting constants differ only slightly, or when the splitting is independent of ring position, the two pairs of satellites will overlap, and only one pair may be observed with amplitude ratio 3.3%. Furthermore, the C^{13} coupling in positions 1 and 4, or that in positions 2, 3, 5, and 6 may be such that the resultant satellite lines are not resolved from the main quintet. This too would lead to one pair of observed satellites with amplitude ratios of 2.2 and 1.1%, respectively. Although the sensitivity during several runs was high enough to detect lines with one-tenth the intensity of the observed satellites, further satellite pairs were not detected. The experimental amplitude ratio was found to be 2.5%, but the accuracy of measurements is insufficient to determine unequivocally whether the observed splitting constant is that of the 1 and 4 position or that of the 2, 3, 5, and 6 position.

Unexplained satellite lines were reported[3] in samples of 2, 3, 5, 6-tetramethyl-p-benzosemiquinone. Here, two satellite doublets were found, the inner doublet with coupling constant $a_2=1.90$ Mc sec^{-1}, and the outer

doublet with $a_1=3.81$ Mc sec^{-1}. These sets may arise from C^{13} in the ring and methyl groups. Measurements on C^{13}-enriched materials are needed to verify these conclusions.

[1] J. E. Wertz and J. L. Vivo, J. Chem. Phys. **23**, 2441 (1955).
[2] M. Adams, *et al.*, J. Chem. Phys. **28**, 774 (1958).
[3] B. Venkataraman, *et al.*, J. Chem. Phys. **30**, 1006 (1959).
[4] K. H. Hausser, Z. Naturforsch. **14a**, 425 (1959).

Fragmentation Patterns of Halogenated Pentaboranes

I. SHAPIRO* AND H. LANDESMAN†

Research Laboratory, Olin Mathieson Chemical Corporation, Pasadena, California

(Received July 28, 1960)

As part of the spectral study of the boron hydrides and their derivatives[1] the monoisotopic mass spectra of pentaborane and several of its monohalogenated derivatives were examined. Chloro-, bromo-, and iodo-pentaboranes were prepared by direct halogenation of pentaborane in the presence of aluminum chloride in a carbon disulfide medium. Elemental analysis of the iodopentaborane (mp 53-54.5°) yielded 4.27% H and 66.8% I. Calculation for B_5H_8I: 4.26% H, 67.1% I. Although there was no difficulty in preparing and purifying the bromo- and iodo-derivatives, the chloropentaborane could be prepared only in microquantities and was contaminated by carbon tetrachloride. Attempts to prepare larger quantities of chloropentaborane resulted in explosions.

The B^{11}-NMR spectra of bromo- and iodopentaboranes indicated that the halogen replaced the hydrogen atom at the apex-boron position of the pyramidal pentaborane molecule.[2] The relative NMR shifts in these spectra have been reported previously.[3]

The mass spectra were obtained with a Consolidated Model 21-103 mass spectrometer operating at an ionizing potential of 70 v. In order to compare the fragmentation patterns, the polyisotopic spectra were reduced to monoisotopic spectra and the species reported as shown in Fig. 1. For the isotopic reduction the following isotopic abundances were used: 20% B^{10}, 80% B^{11};[4] 50.57% Br^{79}, 49.43% Br^{81}. In the case of chloropentaborane, the monoisotopic spectrum was similar to that of bromopentaborane after the spectrum was corrected for the presence of carbon tetrachloride and carbon disulfide.

An examination of the fragmentation patterns in Fig. 1 reveals: (1) the relative ease of fragmentation of an iodine atom from the pentaborane nucleus; (2) the loss of a bromine (or chlorine) atom results in the rupture of the pentaborane nucleus, i.e., loss of a BBr(Cl) group; (3) the general distribution of species in the fragmentation pattern of iodopentaborane is similar to that in pentaborane,[5] viz., prevalent loss of

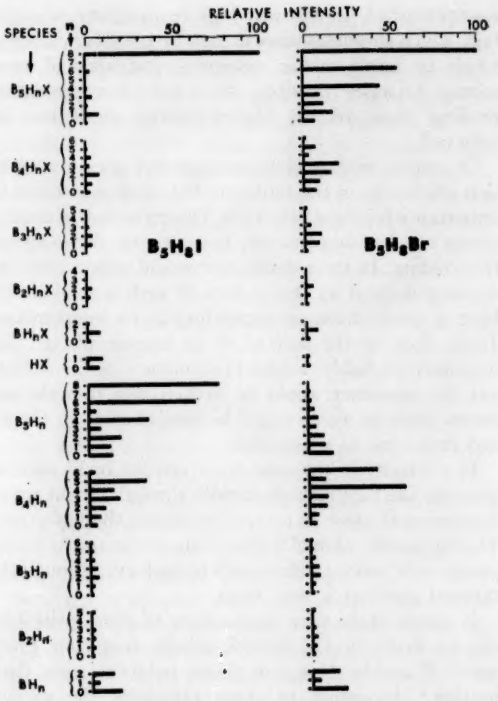

FIG. 1. Monoisotopic mass spectra of monohalogenpentaboranes.

hydrogen atoms in pairs, etc.; (4) the loss of hydrogen atoms from the parent peak group of bromopentaborane also occurs predominantly in pairs. From these observations it appears possible to arrange an order of relative ease of breaking certain bonds in these compounds, viz., BI>BH>BB>BBr(Cl). Apparently this order does not bear the same relation to CH and CX bond energies observed in the mono-halogenated benzene series since the reported BH and BX bond energies are in the order BI<BBr<BH<BCl<BF.[6,7] In the halogenated benzene compounds the fragmentation patterns for chloro-, bromo-, and iodobenzenes were reported[8] to be similar to each other but different from the patterns of fluorobenzene and benzene. The latter two patterns also are reported to be similar to each other. The differences in the patterns were correlated with the CH and CX bond energies, viz., $\Phi I < \Phi Br < \Phi Cl < \Phi H < \Phi F$.

Two considerations are offered to account for the apparent discrepancy in the order of breaking certain bonds in halogenated pentaboranes and the reported order of bond energies. First, the bond energies were derived from the boron trihalides. Second, the inductive effect of the halogen on the pentaborane nucleus may be of greater importance than the resonance effect. It is observed in the NMR spectra that the substitution of iodine for hydrogen in pentaborane

induces a greater electron density at the apex-boron site,[3] while bromine produces an opposite effect and shifts the apex-boron peak to lower magnetic field.[3]

* Present address: Hughes Tool Company, Aircraft Division, Culver City, California.

† Present address: National Engineering Science Company, Pasadena, California.

[1] Reviews on mass spectra and infrared spectra presented by I. Shapiro, J. Ditter, C. O. Wilson, and W. J. Lehmann at the 133rd Meeting of the American Chemical Society, San Francisco, April 1958, will appear shortly in the *Advances in Chemistry Series* under the title *From Borax to Boranes*. Also see list of references in S. G. Gibbins and I. Shapiro, J. Chem. Phys. **30**, 1483 (1959).

[2] R. Schaeffer, J. N. Shoolery, and R. Jones, J. Am. Chem. Soc. **80**, 2670 (1958).

[3] T. P. Onak, H. Landesman, R. E. Williams, and I. Shapiro, J. Phys. Chem. **63**, 1533 (1959).

[4] See discussion relative to B^{10}/B^{11} ratio in I. Shapiro and J. F. Ditter, J. Chem. Phys. **26**, 798 (1957).

[5] V. H. Dibeler, F. Mohler, L. Williamson, and R. Reese, J. Research Natl. Bur. Standards **43**, 97 (1949).

[6] D. D. Wagman, T. R. Munson, and W. H. Evans, Natl. Bur. Standards Tech. Rept. No. 3456.

[7] W. S. Koski, J. J. Kaufman, and C. F. Pachucki, Abstracts 134th Am. Chem. Soc. Meeting, Chicago (Sept. 1958), 26N.

[8] J. Momigny, Bull. Soc. Chim. Belg. **64**, 144 (1955).

Proton Resonance Shifts in Pyrene Mononegative Ion at 4.2°K

M. E. Anderson

Department of Physics, Stanford University, Stanford, California

AND

P. J. Zandstra and T. R. Tuttle, Jr.

Department of Chemistry and Chemical Engineering, Stanford University, Stanford, California

(Received August 5, 1960)

PROTON resonance shifts measured on solid potassium pyrenide[1] at 4.2°K provide evidence for both positive and negative hyperfine coupling constants (see Fig. 1). Values for the constants calculated[2] from these shifts may be compared with the isotropic couplings determined by Hoijtink, Townsend, and Weissman[3] from the analysis of the ESR absorption spectrum of this hydrocarbon ion in dilute solution (see Table I). We assume a correspondence between the two sets of results which is suggested by the magnitudes of the constants, Although the proton resonances are not completely resolved, the areas under the absorption curves have been estimated and are consistent with this assumption. From this, it appears that the positive coupling constant must be attributed to protons 2 and 7 and the negative ones to the other protons.

While our experimental data are precise enough so that the magnitudes may be deduced within about 5%, and inverse proportionality between shifts and temperature persists down to 1.9°K, some doubt remains as to the meaning of constants so deduced. These doubts arise from uncertain factors, among which are the

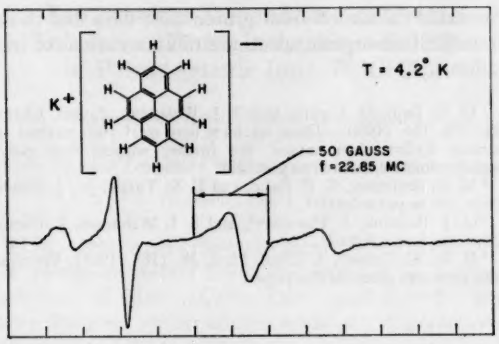

Fig. 1. Proton magnetic resonance spectrum of potassium pyrenide at 4.2°K. The supporting solvent was tetrahydrofuran-d_8. Derivative of absorption is plotted vs magnetic field increasing from left to right. Progressing to higher fields, the second line is unshifted. Shifts were measured between absorption maxima.

contributions of anisotropic interactions and the effect of residence in the crystal lattice on the molecular wave functions. Considering these uncertainties, we conclude that the best analysis of isotropic hyperfine interaction in pyrene mononegative ion with the available data is a combination of our signs and the magnitudes given by Hoijtink, Townsend, and Weissman.[3]

Table I. Proton-electron hyperfine couplings (in gauss).

a	b	$a-b$
+1.24	(+)1.09	+0.15
−2.81	(−)2.06	−0.75
−4.98	(−)4.70	−0.29

[a] Proton-electron coupling constants calculated from proton resonance shifts at 4.2°K.[2]

[b] Isotropic proton-electron coupling constants from Hoijtink, Townsend, and Weissman.[3]

It is interesting to consider briefly some possible sources for the differences between the two sets of data. If our signs are assumed to apply to the spin resonance data, then the differences all have signs the same as the corresponding coupling constants (see Table I). This fact suggests that these differences arise at least in part from the same type of interaction responsible for the presence of isotropic proton-electron coupling.[4] For example, changes in unpaired π-electron distribution in an ion resulting from its lattice surroundings would be accompanied by corresponding changes in the $\pi-\sigma$ exchange responsible for isotropic hyperfine interaction.[4] It is also clear that the proton resonance lines are somewhat anisotropic (see Fig. 1). This anisotropy could also account for some part of the differences. We plan to extend our experimental studies to other free radicals in order to determine the signs of coupling constants and to learn more about the effects which cause the discrepancies between coupling

constants calculated from proton shift data and those from ESR absorption spectra of dilute solutions of free radicals.

[1] D. E. Paul, D. Lipkin, and S. I. Weissman, J. Am. Chem. Soc. **78**, 116 (1956). These authors first used this method of naming hydrocarbon anions. We further suggest that polynegative ions be suffixed as polyides.
[2] M. E. Anderson, G. E. Pake, and T. R. Tuttle, Jr., J. Chem. Phys. (to be published).
[3] G. J. Hoijtink, J. Townsend, and S. I. Weissman, J. Chem. Phys. (to be published).
[4] H. M. McConnell, J. Chem. Phys. **28**, 1188 (1958). Previous references are given in this paper.

Equilibrium in the Exchange of Tritium Between Ammonia and Hydrogen and the Zero-Point Energy Difference Between NH_3 and NH_2T† *

JOEL R. GUTMANN AND MAX WOLFSBERG‡

Department of Isotope Research, Weizmann Institute of Science, Rehovoth, Israel

AND

Chemistry Department, Brookhaven National Laboratory, Upton, New York

(Received July 18, 1960)

THE equilibrium in the exchange of deuterium between ammonia and hydrogen has been measured over a wide temperature range. Perlman, *et al.*[1] used the data to calculate the difference in zero-point energy between the NH_3 and NH_2D molecules.

The corresponding equilibrium in the exchange reaction involving tritium, $NH_3(g)+HT(g)=NH_2T(g)+H_2(g)$, was determined in a kinetic investigation performed on this reaction.[2] The zero-point energy difference between NH_3 and NH_2T may then be obtained.

An iron catalyst was used to equilibrate ammonia and hydrogen with respect to their isotopic composition. Ammonia and hydrogen were separately labeled with tritium by liberating ammonia from a solution of ammonium chloride in tritiated water and by zinc reduction of tritiated water vapor, respectively. Their specific activities were determined, to 2% accuracy, by gas counting of a measured amount of the appropriate gas in a small G-M glass counter, with the addition of a standard argon-alcohol mixture. Measurement of the hydrogen activity is a straightforward procedure; introduction of ammonia into the counter, however, results in too low a counting rate, due to absorption of ammonia on the counter wall. The magnitude of the correction was estimated from the effect on the counting rate, of the addition of normal ammonia.

The equilibrium distribution of tritium between hydrogen and ammonia was measured at 516°K, 538°K, and 623°K. At the lower temperatures equilibrium is reached slowly. In this case the most reliable method for obtaining $K=(NH_2T)(H_2)/(NH_3)\ (HT)$, the equilibrium constant, is the comparison of the tritium transfer rates in the forward and backward direction of the reaction in nonequilibrium mixtures. It has been shown[2,3] that the ratio of the rates $R(\rightarrow)$ and $R(\leftarrow)$ as defined below approaches K when the labeling isotope is present in trace concentrations. Labeled hydrogen and inactive ammonia were mixed and introduced into the catalyst chamber. The change in the specific activity of the hydrogen gas with time was measured by extracting samples of the reaction mixture, freezing out the ammonia, and determining the hydrogen activity. The rate of decrease of the specific activity of the hydrogen at the start of the experiment was obtained from the measurements by standard methods.[4] The transfer rate $R(\rightarrow)$ of T from the hydrogen to the ammonia (expressed in terms of atom fraction per min) is then obtained by dividing by the initial specific activity of the hydrogen reactant. The results[2] were $R(\rightarrow)_{516}=(6.5\pm0.3)\ 10^{-3}\ min^{-1}$ and $R(\rightarrow)_{538}=(1.50\pm0.03)\ 10^{-2}\ min^{-1}$. The rates of T transfer from NH_2T to hydrogen $R(\leftarrow)_{516}=(1.8\pm0.1)\ 10^{-3}\ min^{-1}$ and $R(\leftarrow)_{538}=(4.4\pm0.2)\ 10^{-3}\ min^{-1}$ were obtained in an analogous fashion from the rate of increase of the specific activity of the hydrogen divided by the initial specific activity of the ammonia in an experiment where labeled ammonia is interacted with normal hydrogen under identical experimental conditions. Then $K_{516}=3.6\pm0.25$ and $K_{538}=3.4\pm0.2$.

At 623°K the exchange is so fast that the rate cannot be measured accurately. A conventional method for determining K, i.e., measurement of the specific activity of both hydrogen and ammonia at equilibrium, was used. Because of the difficulties in the direct determination of ammonia activity, the results were checked by a material balance calculation based on the activity of hydrogen in the equilibrated and unequilibrated mixtures. Both methods gave results in agreement within the experimental errors. Six separate determinations at 623°K gave a value of $K_{623}=2.9\pm0.1$.

Theoretically, K is given by

$$f(NH_2T/NH_3)/f(HT/H_2);$$

f is the function of Bigeleisen and Mayer.[5] For the pertinent temperature range $f(HT/H_2)$ has been calculated[6]: $f(HT/H_2)=1.633\ \exp(555.9/T)$. For calculating $f(NH_2T/NH_3)$, one needs, besides symmetry numbers, (a) the ratio of products of the frequencies of NH_2T and NH_3, (b) the vibrational excitation functions $[1-\exp(-h\nu c/kT)]^{-1}$, and (c) the zero-point energy difference $[\Delta E_0(NH_2T)]$ between NH_3 and NH_2T. Factor (a) is calculated by the Teller-Redlich product rule to be 0.425; the product of moments of inertia[7] is obtained from the structural data.[8] Contribution from (b), including a small correction for the splitting of ν_2, is evaluated from the tabulation

(calculated) of Morgan, *et al.*[9] of the vibrational frequencies of NH_3 and NH_2T. Their numbers do not represent harmonic frequencies, but are calculated values for the first vibrational transitions, taking into account anharmonicities; they are therefore quite suitable for our purpose. The calculated excitation factor [1.046–1.073 (over the temperatures concerned), adequately represented by $1.213\ \exp(76.5/T)$] is sufficiently small so that small errors in the frequencies are not very important compared to errors in the K measurements. The only unknown is $\Delta E_0(NH_2T)$, which we now obtain by a comparison between the experimental value and the theoretical expression for K. We find

$$K_{538}=3.4\pm0.2=0.817\ \exp[hc/kT(\Delta E_0(NH_2T)-\Delta E_0(HT)]=0.291\ \exp(hc\Delta E_0(NH_2T)/kT),$$

and hence

$$\Delta E_{0(\text{exp})}(NH_2T)=919\pm21\ \text{cm}^{-1}.$$

The resulting expression $K=0.947\ \exp(689.6/T)$ can be used to calculate the expected values of K at other temperatures. $K_{516(\text{calc})}=3.60$; $K_{623(\text{calc})}=2.86$. The good agreement with the experimental values is in part fortuitous, considering the magnitude of the experimental error.

$\Delta E_{0(\text{exp})}(NH_2T)$ may be compared with the value $\Delta E_{0(\text{Morgan})}(NH_2T)=885\ \text{cm}^{-1}$, half the difference between NH_3 and NH_2T "frequencies" as given by Morgan, *et al.*,[9] although this difference should not precisely give a zero-point energy difference for the reason pointed out above. Perlman *et al.*[1] found $\Delta E_0(NH_2D)=635\ \text{cm}^{-1}$ while $\Delta E_{0(\text{Morgan})}(NH_2D)=613\ \text{cm}^{-1}$. It is interesting that $\Delta E_{0(\text{Morgan})}(NH_2T)$ may be obtained from $\Delta E_{0(\text{Morgan})}(NH_2D)$ by assuming that one is dealing with only one frequency, which involves a hydrogen vibrating against a heavy mass [i.e., $\Delta E_0(T)=(1-1/\sqrt{3})/(1-1/\sqrt{2})\,\Delta E_0(D)$]. With the same reasoning one obtains $\Delta E_0(NH_2T)=916\ \text{cm}^{-1}$ from the result of Perlman *et al.*, in good agreement with the value found here. Conversation with Dr. J. Bigeleisen is thankfully acknowledged.

† Research carried out in part at Brookhaven National Laboratory under the auspices of the U. S. Atomic Energy Commission.

* The experimental work was performed by Joel R. Gutmann; the theoretical work is the joint effort of both the authors.

‡ Most of this work was carried out while Max Wolfsberg was a visitor at the Weizmann Institute. He is very grateful to the Institute for its hospitality.

[1] M. Perlman, J. Bigeleisen, and N. Elliott, J. Chem. Phys. **21**, 70 (1953).
[2] J. R. Gutmann, J. Appl. Radiation and Isotopes **7**, 186 (1960).
[3] L. Melander, Arkiv Kemi **7**, 287 (1955).
[4] J. R. Gutmann, J. Phys. Chem. **59**, 478 (1955).
[5] J. Bigeleisen and M. G. Mayer, J. Chem. Phys. **15**, 261 (1947).
[6] J. Bigeleisen, F. S. Klein, R. Weston, and M. Wolfsberg, J. Chem. Phys. **30**, 1340 (1959).
[7] J. Hirschfelder, J. Chem. Phys. **8**, 431 (1940).
[8] W. S. Benedict and E. K. Plyler, Can. J. Phys. **35**, 1235 (1957).
[9] W. Morgan, P. A. Staats, and J. H. Goldstein, ORNL-2430 Phys. Div. Semiannual Rept. (1958), p. 96.

Temperature Dependence of Proton Relaxation Times in Aqueous Solution of Paramagnetic Ions. II. $CrCl_3$†

THOMAS H. BROWN,* ROBERT A. BERNHEIM,‡ AND H. S. GUTOWSKY

Noyes Chemical Laboratory, University of Illinois, Urbana, Illinois

(Received July 1, 1960)

IN a recent paper,[1] the temperature dependence of the proton relaxation times was reported for aqueous solutions of Mn^{++}, Co^{++}, Cu^{++}, and Gd^{+++}. This note describes similar studies made of $CrCl_3$ solutions. Our results differ from the less extensive, previous work of Hausser and Laukien[2] in that, in addition to the time dependence they report for the relaxation times in the "green" modification, we find the relaxation times of the "blue" modification of the $CrCl_3$ solution to depend upon its thermal history. In order for the solution to exhibit such thermal hysteresis, the "structure" of the solvated species must change with temperature. Also, the rate at which the solution regains thermodynamic equilibrium after a temperature change must be slower than the time scale of the experiment.[3]

There are at least two sets of reactions and chemical equilibria associated with the thermal hysteresis effects, One, above room temperature, involves times on the order of days, while the other, at lower temperatures, occurs on the order of minutes. The complexity and time scales involved have discouraged us from attempting a complete study. However, a report of the

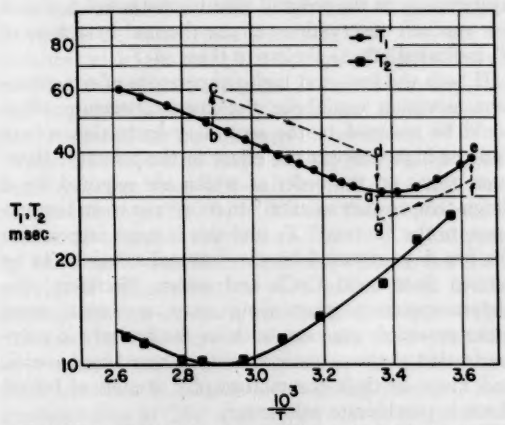

FIG. 1. Log T_1 and log T_2 measured as a function of reciprocal temperature and thermal history for protons at a magnetic resonance frequency of 20 Mc/sec in an aqueous solution containing 3×10^{18} $CrCl_3$ molecules/cm³. The points are "normal" values representing the thermodynamic state of the solution at room temperature a. The vertical lines are the changes observed in T_1 upon holding the "normal solution" at a fixed temperature for times relatively long compared to the time scales of the other temperature-dependence studies. The change $b\rightarrow c$ took 3 hr; $d\rightarrow a$ was on the order of weeks; while the times required for $e\rightarrow f$ and $g\rightarrow a$ were on the order of minutes, but a time less than $a\rightarrow e$ and $f\rightarrow g$.

results obtained may serve as a guide to braver men. Moreover, although the Cr^{+++} solutions are perhaps an extreme case, their properties prompt the suggestion that temperature-dependent equilibria may affect T_1 and T_2 in other solutions.

The equipment and methods for measuring T_1 and T_2 have been described in I. The solutions used were prepared from commercially available cp-grade $CrCl_3$. In Fig. 1 we give typical results. The time required for Cr^{+++} solution to attain thermodynamic equilibrium at room temperature depends upon its previous thermal treatment and may be days or weeks. However, once the solution is equilibrated at room temperature, quite reproducible results, as shown by the points in Fig. 1, can be obtained for the temperature dependence of T_1 and T_2. These "normal" results represent, or at least reflect, the thermodynamic equilibrium of the solution at room temperature.

If a solution having initially a "normal" T_1 is kept at a given elevated temperature for several hours, the T_1 value changes and approaches a limiting value as much as 20–30% larger. This suggests that the concentrations of the species in solution have changed and attained thermodynamic equilibrium at the higher temperature. When the T_1 of this "high-temperature solution" is measured rapidly at lower temperatures, the values are systematically larger than those of the "normal solution," as shown schematically in Fig. 1. The magnitude of this effect depends upon the temperature as well as the duration of the high-temperature treatment. The T_1 of a "low-temperature solution" is less than that of the "normal," and the time scale of the hysteresis is on the order of minutes instead of hours. A few random observations of the thermal hysteresis of T_2 indicated effects similar to those of T_1.

If both the low- and high-temperature effects represent solvation equilibria, the low-temperature effect could be assigned to the secondary hydration sphere and the high temperature effect to the primary. However, times on the order of weeks are required for a "high-temperature solution" to recover at room temperature to the "normal" T_1, and this is much larger than the few days required for the "normal solution" to be formed from solid $CrCl_3$ and water. Therefore, the high-temperature phenomena may represent some other reversible reaction, such as the hydrolytic polymerization of the cationic species, as noted by Laswick and Plane in their chromatographic studies of boiled chromic perchlorate solutions.[4]

The results for the "normal solution" of Cr^{+++} are similar to those reported in I for Mn^{++}. However, for Cr^{+++} the T_2 values are mainly on the low-temperature side of the minimum, and T_1 also exhibits a minimum. The latter can hardly come from the dipolar contribution, since τ_c is ordinarily much shorter in liquids than the 10^{-8} sec required. Also, the hysteresis effects are in the wrong direction to contribute to the T_1 minimum. In the formalism of I, they would give a p which increased with decreasing temperature. This leaves the temperature dependence of the exchange correlation time τ_e, which includes the electron-spin relaxation time τ_s and the chemical lifetime of the hydration sphere τ_h. However, a better understanding of the thermal hysteresis and of τ_s is needed before the various effects can be separated quantitatively.

† This research was supported in part by the Office of Naval Research and by a grant from the National Science Foundation.

* Now at the Union Carbide Research Institute, Tuxedo, New York.

‡ Now at the Department of Chemistry, Columbia University, New York.

[1] R. A. Bernheim, T. H. Brown, H. S. Gutowsky, and D. E. Woessner, J. Chem. Phys. **30**, 950 (1959); hereafter referred to as I.

[2] R. Hausser and G. Laukien, Arch. sci. (Geneva) **11**, 252 (facs. spec.) (1958).

[3] For studies of the solvation of the Cr^{+++} ion by other methods, see R. A. Plane and Henry Taube, J. Phys. Chem. **56**, 33 (1952); J. P. Hunt and R. A. Plane, J. Am. Chem. Soc. **76**, 5960 (1954); and subsequent work of these authors.

[4] J. A. Laswick and R. A. Plane, J. Am. Chem. Soc. **81**, 3564 (1959).

Transient Species in the Radiolytic Polymerization of Cyanogen

C. E. Melton and P. S. Rudolph

*Chemistry Division, Oak Ridge National Laboratory, Oak Ridge, Tennessee**

(Received July 8, 1960)

PREVIOUS investigators[1–3] have shown that the rates of radiolytic polymerization are, in general, increased by the admixing of noble gases. This increase is approximately proportional to the stopping power of the noble gas. In most systems studied, the rare gases had higher ionization potentials than the reactant gases, and the increased rates of reaction were explained on the basis of charge transfer.[4] However, in the $(CN)_2$+Xe system charge transfer to the reactant is not energetically possible, since Xe has the lower ionization potential (13.6 and 12.1). Thus, in this system charge transfer would result in a decreased reaction rate. It was found,[2] however, that Xe increased rather than diminished the yield of polymerization of cyanogen. The observed increase in yield was proportional to the energy absorbed by the Xe, all of which appeared to be utilized in the polymerization reaction.

Because of this anomaly, Dr. S. C. Lind suggested that we investigate the transient species produced in the $(CN)_2$ and $(CN)_2$+Xe systems. The reactant gas was irradiated by 135-ev electrons at a pressure of 1 mm in the ionization chamber of our research mass spectrometer.[5,6] Pure $(CN)_2$ and various mixtures of $(CN)_2$+Xe were investigated.

The observed transient polymer species produced in the electron-induced radiolysis of $(CN)_2$ as well as

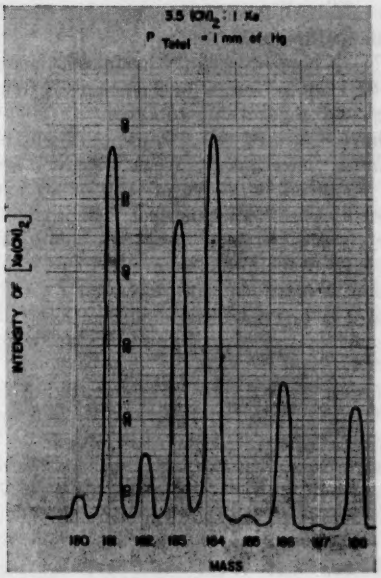

FIG. 1. The isotopic pattern of $[Xe(CN)_2]^+$ observed in a 3.5 $(CN)_2$ to 1 Xe mixture at 1 mm pressure.

the absolute intensity for each species are given in Table I.[7] When Xe was admixed with $(CN)_2$, the total intensity of negative ions was markedly increased. For example, in a 9 Xe:1$(CN)_2$ mixture the intensity of $(CN)^-$ was increased about twenty fold. This increase in negative-ion intensity is attributed to two processes: (1) ionization by secondary electrons from Xe, and (2) a reaction of metastable Xe* ($5p^56s$) with $(CN)_2$ to form ·CN radicals, which are subsequently ionized.

TABLE I. Polymer-ion mass spectra of $(CN)_2$ at 1 mm.

		Intensity[a] (ions/sec)	
M/e	Formula	Pos. ions × 10^{-3}	Neg. ions
26	CN	2.5×10^{3}	2.4×10^{3}
52	$(CN)_2$	9.0×10^{9}	1.9×10^{7}
78	$(CN)_3$	1.6×10^{8}	1.3×10^{5}
104	$(CN)_4$	5.2×10^{10}	2.0×10^{6}
130	$(CN)_5$	6.0×10^{5}	4.5×10^{5}
156	$(CN)_6$	1.2×10^{6}	3.1×10^{5}
182	$(CN)_7$	4.7×10^{3}	5.4×10^{4}
208	$(CN)_8$	1.1×10^{3}	3.7×10^{3}
234	$(CN)_9$	1.0×10	3
260	$(CN)_{10}$	2.2×10	5

[a] Intensities higher than 1×10^{3} were calculated from the integrated ion currents.

In addition to the increased polymerization due to negative ions in the $(CN)_2$+Xe mixtures, the addition complex, $[Xe(CN)_2]^+$, postulated by Eyring[8] was observed (see Fig. 1). He further postulated that this complex would lead to additional polymerization.

We believe that the increased rate of polymerization of $(CN)_2$ upon the admixture of Xe observed by previous workers[1-3] can now be explained on the basis of the reactive addition complex $[Xe(CN)_2]^+$ and the increased intensity of negative-ion polymers observed in this study.

* Operated for the U. S. Atomic Energy Commission by the Union Carbide Corporation.

[1] S. C. Lind, D. C. Bardwell, and J. H. Perry, J. Am. Chem. Soc. **48**, 1556 (1926).
[2] S. C. Lind and D. C. Bardwell, J. Am. Chem. Soc. **48**, 1575 (1926).
[3] D. C. Bardwell and D. K. Naylor, Radiation Research **11**, 432 (1959).
[4] S. C. Lind and D. C. Bardwell, Science, **62**, 593 (1925).
[5] P. S. Rudolph and C. E. Melton, J. Chem. Phys. **32**, 586 (1960).
[6] C. E. Melton, J. Chem. Phys. **33**, 647 (1960).
[7] Only integral multiplicities of CN are reported therein. Other transient species, both positive and negative, of varying proportions of C to N were observed and will be reported in a subsequent paper.
[8] Henry Eyring, J. Chem. Phys. **7**, 792 (1939).

Mass Spectrum and Appearance Potentials of Tetrafluorohydrazine*

JOHN T. HERRON AND VERNON H. DIBELER

Mass Spectrometry Section, National Bureau of Standards, Washington, D. C.

(Received July 15, 1960)

RECENTLY, two brief communications have reported the mass spectrum[1,2] and appearance potentials of the NF^+ and NF_2^+ ions[2] of tetrafluorohydrazine. As these reports include data that are at variance with results of a study of light-element fluorides currently in progress in this laboratory, we wish to present a preliminary report and a brief discussion of some of our experimental observations.

Measurements were made on two samples of tetrafluorohydrazine from different sources. The first was obtained through Dr. D. E. Mann. The second was a portion of a sample supplied to Dr. G. T. Armstrong by the Rohm and Haas Company. These materials were used without further purification. Most of the measurements were made on the first sample, which contained several percent nitric oxide and probably some nitrous oxide. The only other impurities were small amounts of fluorocarbons giving principal ions corresponding to CF_3^+ and $C_2F_5^+$.

Mass spectra were obtained with a conventional 60° sector field, 30-cm radius of curvature mass spectrometer at constant ion accelerating voltage.

The ion source was designed for free radical studies and was more "open" than conventional sources. It operated at about 200°C. Ion currents were measured with a 16-stage electron multiplier and a vibrating-reed electrometer. Appearance potentials were measured by techniques described previously.[3]

Column 3 of Table I summarizes relative abundances of the principal ions observed in tetrafluorohydrazine. Previously reported spectra[1,2] include no ions containing two nitrogen atoms, with the exception of the N_2^+ ion. The accompanying spectrum of silicon tetrafluoride and the isotopic compositions of nitrogen and silicon obviate any misassignment of the m/e 47, 66, 85, and 104 ions in the N_2F_4 spectrum due to the possible impurity, silicon tetrafluoride.

TABLE I. Partial mass spectra of tetrafluorohydrazine and silicon tetrafluoride.

	N_2F_4		SiF_4	
m/e	Ion	Rel. abundance (%) (70-v electrons)	Ion	Rel. abundance (%) (70-v electrons)
19	F^+	0.8	F^+	0.4
33	NF^+	28.0	SiF_2^{++}	2.1
47	N_2F^+	3.7	SiF^+	1.6
52	NF_2^+	100.0	...	...
66	$N_2F_2^+$	4.5	SiF_2^+	0.3
67	$N_2F_2^+$	0.04	SiF_2^+	0.02
85	$N_2F_3^+$	4.5	SiF_3^+	100.0
86	$N_2F_3^+$	0.04	SiF_3^+	5.0
87	...	...	SiF_3^+	3.3
104	$N_2F_4^+$	2.1	SiF_4^+	2.0
105	$N_2F_4^+$	0.01	SiF_4^+	0.1
106	...	...	SiF_4^+	0.07

Mass spectra obtained at constant magnetic field and under various other conditions of focus, ion-repeller voltage, and pressure were essentially identical to that given in Table I. A spectrum obtained on a 180° instrument with a closed ion source operating at 250°C was similar, except that the most abundant peak was the NF^+ ion. This suggests that under certain conditions of temperature and residence time within the ion source, N_2F_4 undergoes dissociation to NF_2.

We have measured the ionization potential of N_2F_4 and of SiF_4 and find marked differences: $I(N_2F_4) = 12.04 \pm 0.10$ ev and $I(SiF_4) = 15.4 \pm 0.4$ ev. This gives further support to the identity of the $N_2F_4^+$ ion.

Loughran and Mader[2] report $A(NF_2^+) = 11.8 \pm 0.2$ ev and $A(NF^+) = 15.0 \pm 0.2$ ev. Using these values and their value for $A(NF_2^+)$ from NF_3, together with estimates of N—F bond energies and $I(NF)$ by Reese and Dibeler,[4] they conclude that the process leading to the formation of NF_2^+ is $N_2F_4 \rightarrow NF_2^+ + NF + F^-$, and that the N—N bond energy in N_2F_4 is 1.3 ev (30.0 kcal).

The heat of formation of tetrafluorohydrazine has recently been measured[5] as $\Delta H_f(g)_{298} = -2.0 \pm 2.5$ kcal/mole. This value, together with the necessary data on NF_3 reported by Reese and Dibeler[4] and by Armstrong, Marantz, and Coyle,[6] permits a calculation of $D(F_2N-NF_2)$ from the relations $\Delta H_f(NF_2) = \Delta H_f(NF_3) + D(NF_2-F) - \Delta H_f(F)$, and $D(F_2N-NF_2) = 2\Delta H_f(NF_2) - \Delta H_f(N_2F_4)$. Thus, $D(F_2N-NF_2) = 53$ kcal. This can be compared with $D(H_2N-NH_2) = 59$ kcal as calculated from the analogous relationships for ammonia and hydrazine.

The N—N bond energy in N_2F_4 is also estimated to be about 62 kcal by means of Fineman's[7] extension of Pauling's electronegativity concepts.

We have measured the appearance potential of the NF_2^+ and F^- ions of N_2F_4. We find $A(NF_2^+) = 12.7 \pm 0.2$ ev. However, the shape of the semilog ionization efficiency curve differs somewhat from that of $N_2F_4^+$ and Ar^+, so that it is probable that more than one process leads to the formation of NF_2^+ ions.

A dissociative attachment process for F^- is observed at about 2 ev and there is some indication of onset of an ion-pair process of very low probability at about 13 ev.

The lowest energetic process leading to the formation of NF_2^+ from N_2F_4 is that suggested by Loughran and Mader, i.e., $N_2F_4 \rightarrow NF_2^+ + NF + F^-$. Assuming no excess kinetic energy in the ionization and dissociation process, $A(NF_2^+)$ can be calculated from $A(NF_2^+) = D(F_2N-NF_2) + I(NF_2) + D(FN-F) - EA(F)$. Using $D(F_2N-NF_2) = 2.3$ ev, $I(NF_2) = 11.0$ ev,[4] $D(FN-F) = 2.9$ ev,[6] and $EA(F) = 3.6$ ev,[8] we calculate $A(NF_2^+) = 12.6$ ev., in substantial agreement with our measured value.

The low value for $A(NF_2^+) = 11.8$ ev reported by Loughran and Mader, together with the absence of heavier ions and the presence of a rather long tail on the probability curve near threshold, again suggests decomposition of the N_2F_4 and the direct observation of NF_2 radicals.

* This work was supported in part by the National Bureau of Standards Free Radical Research Program supported by the Department of the Army.

[1] C. B. Colburn and A. Kennedy, J. Am. Chem. Soc. **80**, 5004 (1958).
[2] E. D. Loughran and Charles Mader, J. Chem. Phys. **32**, 1578 (1960).
[3] J. T. Herron and V. H. Dibeler, J. Am. Chem. Soc. **82**, 1555 (1960).
[4] R. M. Reese and V. H. Dibeler, J. Chem. Phys. **24**, 1175 (1956).
[5] G. T. Armstrong, Thermodynamics Section, National Bureau of Standards (private communication).
[6] G. T. Armstrong, S. Marantz, and C. F. Coyle, J. Am. Chem. Soc. **81**, 3798 (1959).
[7] M. A. Fineman, J. Phys. Chem. **62**, 947 (1958).
[8] H. O. Pritchard, Chem. Revs. **52**, 537 (1953).

Lowest Triplet States of Ethylene*

ROBERT S. MULLIKEN

Laboratory of Molecular Structure and Spectra, Department of Physics, University of Chicago, Chicago 37, Illinois

(Received July 22, 1960)

WRITING the ground state (N) of ethylene as $\cdots(\pi_x+\pi_x)^2$, $^1A_{1g}$, where $\pi_x+\pi_x$ describes the π_x-electron bonding MO in LCAO approximation, the experimentally known first excited singlet states are a Rydberg state (R), probably $\cdots(\pi_x+\pi_x)(3s)$, $^1B_{3u}$ and

a V state $\cdots(\pi_z+\pi_z)(\pi_z-\pi_z)$, $^1B_{1u}$. The vertical energies of these two states are, respectively, 7.1 and 7.6 ev.

The location of the corresponding triplet state (T), $\cdots(\pi_z+\pi_z)(\pi_z-\pi_z)$, $^3B_{1u}$ has been uncertain until recently. In the methylated ethylenes, absorption bands very much weaker than the $R\leftarrow N$ and $V\leftarrow N$ systems, and at somewhat longer wave lengths (2100–2500 A) and distinct from the latter, have long been known.[1] With a decrease in the number of methyl groups, these come closer to the singlet bands, and in ethylene itself they cannot be seen, presumably being covered up by the much stronger, long-wavelength tail of the $V\leftarrow N$ bands.

However, extrapolation from the methylated ethylenes to the case of zero methyl groups indicates a location of the triplet upper level of these bands in ethylene itself at a vertical energy of about 6.4 ev, that is, 1.2 ev below the V state. This location has been generally accepted as that of the T state of ethylene, although very few people realize that the value was obtained in the manner just described.

In 1950 Reid[2] examined the absorption spectrum of a 1.4-m path in liquid ethylene and found a series of bands extending from about 3.8 to 4.6 ev, merging into much stronger absorption at higher frequencies. He attributed the bands to the long-wavelength tail of the $T\leftarrow N$ bands, and the stronger absorption to the $V\leftarrow N$ tail, but concluded that the maximum of the $T\leftarrow N$ bands is covered by the stronger $V\leftarrow N$ tail, so that the vertical energy of the T state could not be determined. Although Reid did not say so, he may have implied that the vertical energy of the T state could be at the previously concluded location.

D. F. Evans[3] has thrown new light on the question by his oxygen-intensification technique, with which he confirmed in gaseous ethylene the $T\leftarrow N$ bands found by Reid. He further concluded (although the basis for this conclusion is perhaps not made absolutely clear in his paper) that these have an intensity maximum corresponding to a vertical energy of 4.6 ev for the T state. Evans also pointed out that the Reid-Evans bands show a vibrational frequency interval (doubtless for C—C stretching) of about 1000 cm^{-1}, comparable to that (about 850 cm^{-1}) for the V state,[4] whereas the 2100–2500 A bands (in the methylated ethylenes) show much larger intervals[1] (about 1400 cm^{-1}). For these reasons, there seems to be little doubt that the $T\leftarrow N$ bands have now been correctly located.

What, however, then becomes of the bands formerly supposed to be $T\leftarrow N$? It is notable that their vibrational intervals of about 1400 cm^{-1} agree well with the 1375 cm^{-1} spacing found in the $R\leftarrow N$ bands.[4] It then seems highly probable that the bands previously identified as $T\leftarrow N$ have as their upper state the expected $^3B_{3u}$ state of the same electron configuration as the $^1B_{3u}$ state R. Let us call this the T_R state. The smaller energy separation $R-T_R$ (7.1−6.4=0.7 ev) as compared with $V-T$ (7.6−4.6=3.0 ev) is entirely reasonable, since the exchange interaction of the $(\pi_z+\pi_z)$ MO with the large (3s?) Rydberg MO in state T_R *should* be much smaller than that with the $(\pi_z-\pi_z)$ MO in state T.

As Evans has pointed out, the newly established location of state T agrees with semiempirical, self-consistent-field LCAO-MO calculations, such as those of Pariser and Parr and Pople, much better than did the formerly accepted location.

* This work was assisted by the Office of Naval Research in conjunction with the University of Chicago.

[1] Cf. W. J. Potts, J. Chem. Phys. **23,** 65 (1955).
[2] C. Reid, J. Chem. Phys. **18,** 1299 (1950).
[3] D. F. Evans, J. Chem. Soc. **1960,** 1735.
[4] Cf. P. G. Wilkinson and R. S. Mulliken, J. Chem. Phys. **23,** 1895 (1955).

C^{13} Chemical Shifts in CO and CO_2

RAYMOND ETTINGER, PHILIP BLUME, AND ANDREW PATTERSON, JR.
Department of Chemistry, Yale University, New Haven, Connecticut
AND
PAUL C. LAUTERBUR
Mellon Institute, Pittsburgh, Pennsylvania

(Received July 21, 1960)

THE carbon-13 nuclear magnetic resonance spectra of various compounds have been previously reported.[1–3] These compounds were usually observed as pure liquids or concentrated solutions under "rapid-passage" sweep conditions in the dispersion mode, such conditions complementing the large rf fields required (normally 3 to 20 mgauss) and the moderately long relaxation times of the C^{13} nuclei. Although the spectrum of liquid CO_2, containing C^{13} in natural abundance, has been observed and measured[4] at room temperature, that of CO has not. Because of the importance of these simple linear molecules to the theory of chemical shifts, gas-phase measurements have now been made on C^{13}-enriched samples.

Approximately 5 mmoles of 61% enriched $C^{13}O_2$, generated from enriched $BaC^{13}O_3$ with benzenesulfonic acid, were passed slowly by Toepler pumping over an 80-mesh zinc column heated to 300–400°C. in a micro-analytical combustion oven. The system was evacuated prior to the reduction to preclude oxygen contamination of the sample, the latter being checked mass spectrometrically. The collected gases were passed into an evacuated 15-mm-o.d. Pyrex NMR cell, cooled to liquid nitrogen temperature, and the cell was sealed off. Conversion to the monoxide, about 80%, was sufficiently high so that the CO, although not condensable, would still be present in the cell in significant percentage. It was desirable to have CO_2 present as an internal reference, since its chemical shift in the gas phase had been established in experiments on the

enriched gas under high pressure.[6] Within experimental error, the latter shift is identical with that found for liquid CO_2, and for enriched CO_2 dissolved in neutral and alkaline aqueous media.[5,6]

Because of the very short relaxation times in the gas phase, the resulting signals were of the "slow-passage" dispersion type although they were recorded under conditions[1,3] normally suitable for the "rapid-passage" dispersion spectra of liquid samples. The shift of CO_2 being known, the low-field signal was identified as that of carbon monoxide by employing the substitution method[3] with a sample of CS_2 whose spectrum was modulated at 720 cps. The separation of the CO_2 and CO peaks, determined from the average of seven measurements in both increasing and decreasing sweep fields, was 57.1 ± 0.3 ppm, and from the known shift of carbon dioxide

$$\delta_e(CO_2) = 68.6 \text{ ppm}$$

$$\delta_e(CO) = 11.5$$

$$\delta_e(CS_2) = 0 \text{ (reference)}.$$

Because the partial pressure of each oxide was of the order of an atm, the signals were very weak. For future experiments, methods have been devised for the preparation of pure enriched CO NMR samples under 10 or more atm pressure. The preparation of enriched carbonyl sulfide, OCS, is also being undertaken.

A satisfactory approach to the theoretical calculation of C^{13} shifts, even in the simple linear molecules just cited, has yet to be formulated, although a variational approach[7] would appear to hold some promise. Within the class of compounds in which carbon has approximately sp hybridization, the shifts will range from $\delta i = 120$ ppm in acetylenes[4] to $\delta i = -15$ ppm in $Fe(CO)_5$[4], about one-third the entire C^{13} spectrum.

[1] P. C. Lauterbur, J. Chem. Phys. **26**, 217 (1957).
[2] C. H. Holm, J. Chem. Phys. **26**, 707 (1957).
[3] P. C. Lauterbur, Ann. N. Y. Acad. Sci. **70**(4), 841 (1958).
[4] P. C. Lauterbur, unpublished work.
[5] A. Patterson, Jr. and R. Ettinger, Z. Elektrochem. **64**, 98 (1960).
[6] R. Ettinger, P. C. Lauterbur, and A. Patterson, Jr. (to be published).
[7] M. J. Stephen, Proc. Roy. Soc. (London), **A243**, 264 (1957).